CRETACEOUS OF POLAND

and of adjacent areas

FIELD TRIP GUIDES

Edited by: Ireneusz Walaszczyk and Jordan P. Todes

FACULTY OF GEOLOGY, UNIVERSITY OF WARSAW
Warsaw 2022

11TH INTERNATIONAL
CRETACEOUS
SYMPOSIUM
Warsaw, Poland, 2022

CRETACEOUS OF POLAND

and of adjacent areas

FIELD TRIP GUIDES

Edited by:
Ireneusz Walaszczyk and Jordan P. Todes

FACULTY OF GEOLOGY, UNIVERSITY OF WARSAW
Warsaw, 2022

Copyright © 2022 by Faculty of Geology, University of Warsaw

All rights reserved All characters and company names appearing in the text are registered trademarks or trademarks their owners.

www.cretaceous2022.com

ISBN 978-83-944813-5-3

Publication date:
August 2022

Adress:
Faculty of Geology, University of Warsaw, Poland,
Żwirki i Wigury 93, 02-089 Warszawa, Poland
Phone: + 48 22 554 00 00

Layout: Aleksandra Szmielew

Cover design: Łucja Stachurska

Printed by:
GIMPO-PRINT BARTŁOMIEJ POHL
Transportowców 11, 02-858 Warszawa, Poland

TABLE OF CONTENTS

PREFACE

INTRODUCTORY ACCOUNTS

FIELD-TRIP GUIDES

11TH INTERNATIONAL
CRETACEOUS
SYMPOSIUM
Warsaw, Poland, 2022

Preface

THE CRETACEOUS OF POLAND: Field Guides to excursions accompanying the 11th International Cretaceous Symposium (Warsaw, Poland, August 22nd–26th, 2022)

Ireunesz Walaszczyk[1]| Jordan P. Todes[2]

1| Faculty of Geology, University of Warsaw, 93 Żwirki i Wigury, 02-089 Warszawa, Poland; e-mail: i.walaszczyk@uw.edu.pl

2| Department of the Geophysical Sciences, University of Chicago, 5734 S Ellis Ave, Chicago, IL USA; e-mail: jtodes@uchicago.edu

The Cretaceous Period had a profound effect on the structure and shape of the territory of present-day Poland. Southernmost Poland belonged to the Carpathian portion of the northern Tethys, with numerous sedimentary basins with highly varied environments controlled by tectonics, eustasy, and climatic variations. As early as the mid-Cretaceous, the Tatra Mountains arose, and somewhat later in the Cretaceous the Pieniny Klippen Belt developed. Further to the north, basins accumulated deep, flysch-type sediments that would eventually form the Outer Carpathians; in the Cretaceous, these basins were still expanding and recording all of the significant pan-Tethyan events. This sedimentary basin system transformed into an orogenic system at the end of the Paleogene. In the Miocene, the fold-and-thrust belt of the Outer Carpathians, pushed tens of kilometres north onto its foreland, formed.

However, most of present-day Poland was part of the vast European platform, with the Precambrian basement in the northeast and Paleozoic in the center and southwest, with an extensive sedimentary basin stretching over much of its extent. This basin, part of the Central European Basin System and typically referred to as the Polish Basin, formed in the Late Permian and remained active throughout the entire Mesozoic. The long, Late Permian–Mesozoic history of the basin came to an end starting in the Late Cretaceous (and continuing through the early Paleogene), when its axial, most subsiding part – the so-called Polish-Danish Trough – underwent tectonic inversion.

The series of field trips presented in this volume cover a diverse variety of topics related to the Polish Cretaceous. While the Cretaceous is richly represented throughout much of the Carpathians, in extra-Carpathian Poland outcrops are restricted to southern Poland. In western Poland, this includes the Sudetes (Outer- and Inner-Sudetes) and the Opole Trough. In central and eastern Poland, patches of the Cretaceous occur throughout the Southern Polish Upland, which comprises the Silesian, Małopolska, and Lublin Uplands. The latter includes the famous Middle Vistula River Gorge, a series of Middle Albian through Maastrichtian (and even Danian) exposures along the Vistula River, between Zawichost in the south and Puławy in the north (about 150 km south of Warsaw).

The excursion guides presented in this volume are preceded by two introductory chapters by *Krzywiec et al.* and *Leszczyński*, collectively framing the tectonic, paleogeographic, and paleoenvironmental context of the extra-Carpathian Polish Cretaceous.

Krzywiec et al. offer a brief understanding on the nature of inversion tectonics at large. Using this framework, they illustrate Late Cretaceous inversion structures and associated depositional systems in the Polish Basin, including exceptional examples of processes operating both perpendicular and parallel to the axis of inversion. As noted by the authors, their contribution serves as a synopsis of several high-resolution seismic surveys taken over the past decade, and so serves as a tantalizing introduction to a promised series of detailed seismostratigraphic studies.

Leszczyński provides a succinct paleogeographic portrait of the Polish Cretaceous, illustrating depositional evolution from a system bound within the subsiding Mid-Polish Trough in the Early Cretaceous, to widespread deposition following the great mid-Cretaceous transgression, and ultimately the development of a complex – but overall-shallowing – facies pattern associated with the inversion of the Mid-Polish Trough. Importantly, the work presented by Leszczyński represents the synthesis of over sixty years of subsurface exploration by the Polish geological community.

The excursion guides cover a diversity of regions within the Southern Polish Upland, the Opole Trough, and the Sudetes of extra-Carpathian Poland, and all three main tectonic units of the Carpathians – the Outer (Flysch) Carpathians, the Pieniny Klippen Belt, and the Tatras (Inner or Central Carpathians) (Fig. 1).

The first excursion guide, by *Machalski et al.,* provides an extensive paleoenvironmental, palaeobiological, and event stratigraphic overview of the Cretaceous–Paleogene boundary succession in the Lublin Upland, which captures a diversity of fossils, the youngest ammonites in Poland, and the geochemical and lithological indicators characteristic of the K-Pg boundary. In this expansive chapter, the historical context, lithostratigraphic development, and biostratigraphy, paleontology and ichnology of the Maastrichtian and Danian strata between the Vistula River and Lublin are discussed, with a particular focus on the development of bioturbation (and associated pseudobrecciation), condensation, and hardground formation in the highest Maastrichtian.

Remin et al. discusses the Late Cretaceous inversion of the southeastern part of the Polish Basin as inferred from syn-depositional tectonics, facies distribution and bathymetric changes. As generally realized, the inversion of the Mid-Polish Trough into the present-day Mid-Polish Anticlinorium fundamentally controls the modern distribution of the Cretaceous in Poland. However, the timing of the start of inversion is still controversial, with two broad interpretations: that (i) the inversion initiated during the latest Maastrichtian and Paleogene, and (ii) that inversion begun during the Coniacian or Santonian. In their contribution, *Remin et al.* provide an integrated sedimentary, paleoenvironmental, and seismostratigraphic perspective on the southeastern portion of the Polish Basin, unequivocally demonstrating that inversion must have commenced in the Coniacian or latest Turonian. Crucially, the presence of mid-Campanian deltaic deposits in the Roztocze Hills indicates that the Mid-Polish Trough in the present-day San Anticlinorium must have been emergent by the Campanian. These findings have also considerable implications for our understanding of the bathymetric context of Late Cretaceous lithofacies.

Jurkowska et al. illustrates the biogeochemical silica cycle in a Late Cretaceous marine environment in the Miechów Trough. One of the most distinctive features of the Cretaceous System is the prevalence of chalk deposits: indeed, the *Terrain Crétacé* was named after the extensive chalk beds in the Paris Basin, and the word Cretaceous is derived from the Latin *creta* (= "chalk"). In Poland, a unique twist on the chalk paradigm is provided by *opoka,* a Polish term traditionally used to describe Cretaceous chalks substantially harder than classical chalk. Recent work incorporating a variety of modern analytical techniques has formalized the definition of opoka, demonstrating that it essentially is composed of chalk with a considerable biogenic silica component. In this framework, *Jurkowska et al.* use the distribution of opoka and other silica-bearing rocks (e.g., chert nodules, gaizes) to track the evolution of the Late Cretaceous biogeochemical silica cycle in the Cretaceous Central European Basin System. Their field excursion, in conjunction with microfacies, SEM, and XRD analyses, highlights the major regional and diagenetic controls on silica distribution within the Polish Cretaceous Basin, which in turn is expressed by the forma-

tion of thick opoka successions and diverse, abundant siliceous sponge assemblages.

In Opole, *Jagt-Yazykova et al.* deliver an overview of the eponymous Opole Trough, an erosional remnant of widespread Late Cretaceous cover linked to the Bohemian Cretaceous Basin. Intriguingly, they include a historical summary of the Opole Cretaceous, covering its intimate links to the local cement industry and to the development of Opole. A palaeobiological overview of the highly diverse fauna is provided, including numerous invertebrate taxa, rarer vertebrate taxa, various plant fossils, and rich microfauna. Importantly, new stratigraphic information on inoceramid and microfaunal biostratigraphy and chemostratigraphy is presented, representing an insightful glance into the stratigraphic revision and correlative relevance of this important Turonian–Coniacian succession.

West of the Opole Trough stretches the Sudetes, where Cretaceous strata are mainly found in two regions: the North- and Intra-Sudetic synclinoria.

Wojewoda et al. document the Late Cretaceous stratigraphic, sedimentologic, paleogeographic, and paleoenvironmental evolution of the Intra-Sudetic Basin and Upper Nysa Kłodzka Trough, both extensional synsedimentary tectonic units bound by deep marginal faults, providing a clear record of syndepositional geodynamic activity. Collectively, they represented the main depositional areas in the Sudetes during the Cretaceous and capture a characteristic littoral-to-shelf succession with a large range of lithologic variation: these include remarkable accumulation terraces (with >15 m subaqueous dunes!) resulting from tectonically generated escarpments. *Wojewoda et al.* observe that the stratigraphic succession observed in their study area is broadly comparable to the main Bohemian Cretaceous Basin, but differs in important regional aspects, illustrating the important of global eustatic, local tectonic, and regional paleogeographic controls on shaping stratigraphic architecture.

Continuing in the Sudetes, *Leszczyński et al.* chronicle the stratigraphic, sedimentologic, and paleoenvironmental development of the North Sudetic Cretaceous, which during the Cenomanian to Santonian formed a narrow strait at the northern periphery of the Bohemian Massif. Within their rigorous stratigraphic framework, these authors contextualize the paleoenvironmental framework of the palaeontological, paleobotanical, and ichnological studies conducted within the North Sudetic Synclinorium, which collectively have contributed a great deal to understanding Cretaceous paleobiology. Finally, a comprehensive overview of the natural resources hosted within the North Sudetic Synclinorium Cretaceous is provided, illustrating the economic importance of this succession for fields as diverse as masonry and ceramic production.

The Western Carpathians capture a diverse range of sedimentary and tectonic environments. They consist of the Inner Carpathians and the Flysch Carpathians, separated by the chaotic tectonic mélange of the Pieniny Klippen Belt. Each range contains several tectonic nappes and domains, encompassing a variety of shallow- to deep-marine Tethyan deposits – including, but not limited to, pelagic carbonates, hemipelagic marlstones, flysch-type terrigenous sediments, and *Urgonian*-type platform carbonates. The first contribution by *Grabowski et al.* illustrates an expansive field excursion through the highlights of the Jurassic and Cretaceous Polish Carpathian successions. Primary emphasis is placed on the variable stratigraphic development of Late Jurassic – Early Cretaceous strata in different depositional settings recorded within the Polish Carpathians, in particular during the Tithonian – Berriasian boundary interval (see also the second contribution by *Grabowski et al.*).

Despite the complexities of working in the Flysch Carpathians, they have long constituted a classic region for investigations on turbiditic sedimentology, flysch deposit paleogeography, deep-sea ichnology, and agglutinated benthic foraminifera. In the volume, *Uchman and Szczęch* provide an overview of the Cretaceous deposits in the various Flysch Carpathian nappes, and visit a series of localities that collectively illustrate the stratigraphic and ichnological development of Cretaceous flysch-type deposits. There is a pronounced emphasis on the secular evolution of the ichnofacies, which the authors link (i) the progressive (if protracted and dynamic) of the Cretaceous seafloor and (ii) the evolution, dispersal, and exclusion of trace-making biota.

The final chapter, by *Grabowski et al.*, is focused on the Jurassic–Cretaceous transition in the Western Carpathians of Slovakia and Hungary.

The Cretaceous is the final Phanerozoic system without a formally defined lower boundary, in part due to the fact that differences between Upper Jurassic and Lower Cretaceous strata and fauna are quite subtle. Over the past two decades, the nature and formal definition of the Tithonian–Berriasian boundary – and more broadly, the Jurassic–Cretaceous boundary – has been the subject of vigorous investigation, discussion, and debate among Mesozoic geologists. In collaboration with the 11th International Congress on the Jurassic System (Budapest, 2022), the second contribution by *Grabowski et al.* presents a cross-border, cross-boundary perspective on the Jurassic–Cretaceous boundary question. A series of sections in the Pieniny Klippen Belt (Slovakia) and Transdanubian Range (Hungary), which collectively illustrate the regional expression of Jurassic–Cretaceous boundary biotic events and paleoenvironmental evolution, are presented, collectively providing a rich body of data insightful for the ultimate designation of a Berriasian (and, potentially, Cretaceous) GSSP.

11TH INTERNATIONAL
CRETACEOUS
SYMPOSIUM
Warsaw, Poland, 2022

THE LATE CRETACEOUS INVERSION OF THE POLISH BASIN AND SURROUNDING AREAS – A CURRENT PERSPECTIVE BASED ON SEISMIC DATA

Piotr Krzywiec[1]| Aleksandra Stachowska[1]| Łukasz Grzybowski[2]| Quang Nguyen[3]| Łukasz Słonka[1]| Michał Malinowski[3]| Regina Kramarska[4]| Niklas Ahlrichs[5]| Christian Hübscher[5]

1| Institute of Geological Sciences, Polish Academy of Sciences, Warsaw, Poland; e-mails: piotr.krzywiec@twarda.pan.pl; aleksandra.stachowska@twarda.pan.pl; lukasz.slonka@twarda.pan.pl

2| Institute of Geology, Adam Mickiewicz University, Poznań, Poland; e-mail: lukasz.grzybowski@amu.edu.pl

3| Institute of Geophysics, Polish Academy of Sciences, Warsaw, Poland; e-mails: qnguyen@igf.edu.pl; michalm@igf.edu.pl

4| Polish Geological Institute, Gdańsk, Poland; e-mail: regina.kramarska@gmail.com

5| Institute of Geophysics, University of Hamburg, Hamburg, Germany; e-mails: Niklas.Ahlrichs@uni-hamburg.de; Christian.Huebscher@uni-hamburg.de

ABSTRACT

Inversion of sedimentary basins leads to uplift of basement blocks and significant reduction of accommodation space. As a result, syn-tectonic growth strata, deposited in vicinity of such blocks, are characterized by thickness reductions and localized unconformities. Uplifted inversion structures, including also compressionaly reactivated salt diapirs, could also focus contourite currents and, as a result, contourites could develop in their vicinity. High quality offshore and onshore seismic data illustrate such sedimentary features in different segments of the Permo-Mesozoic Polish Basin, which underwent complete inversion during the Late Cretaceous/Palaeogene.

INTRODUCTION

The term "inversion tectonics" was coined in the early 1980s, when an inversion model for a simple tectonic half-graben bounded by master faults rooted in crystalline basement was first formulated (Glennie and Boegner 1981; Bally 1984; cf. Kley 2018; Tari et al. 2020; Krzywiec et al. 2022a). Since then, numerous papers – and three dedicated volumes – focused on the geometry and evolution of inversion structures in different geodynamic settings have been published (Cooper and Williams 1989; Buchanan and Buchanan 1995; Krzywiec et al. 2022b).

Some researchers regard inversion tectonics as a generalized suite of phenomena, collectively leading to the reduction of accommodation space and, eventually, the closure and cessation of the entire sedimentary basin (cf. Dewey 1989; see also Kley 2018; Krzywiec et al. 2018). However, recent consensus has largely restricted the term "inversion tectonics" to the scenario depicted by the classic Bally (1984) model: that is, assuming (1) the formation of a sedimentary basin bounded by normal fault(s) during regional extension, and (2) the compressional reactivation of basin-bounding fault(s) and the uplift of sedimentary infill deposited during the extensional phase (cf. also Cooper et al. 1989; Williams et al. 1989; Cooper and Warren 2010, 2020; Tari et al. 2020; Fig. 1A). In this model, a master fault that controls the evolution of a sedimentary basin is rooted in the crystalline basement, so its reactivation under regional compression can be regarded as "thick-skinned inversion tectonics" (cf. Brun and Nalpas 1996). Alternatively, the master fault may also be rooted within the pre-extensional sedi-

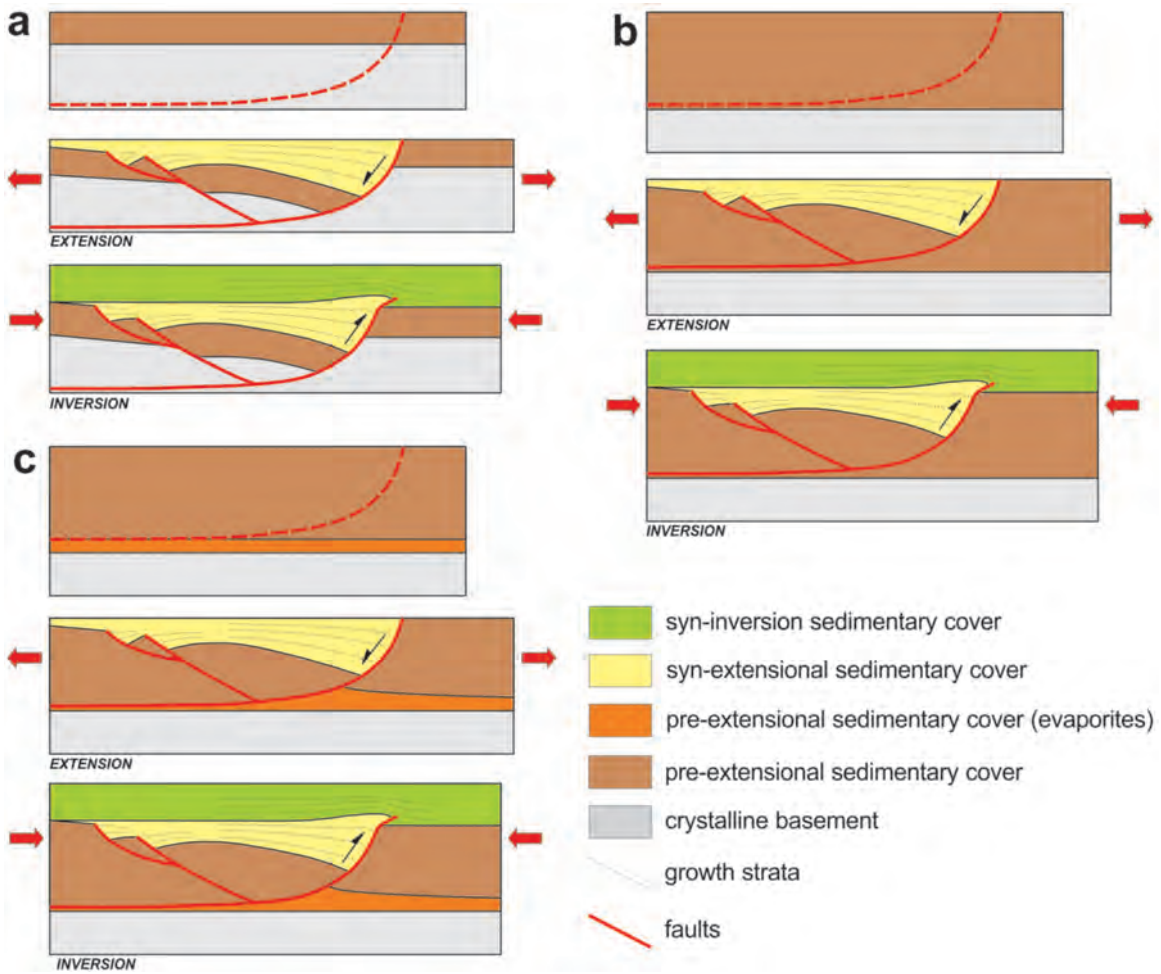

Fig. 1. Comparison of various inversion tectonic models (from Krzywiec et al. 2022a). A – The classic thick-skinned inversion model of a half-graben, with the master listric fault rooted within the crystalline basement; based on Bally (1984); see also Cooper and Warren (2010, 2020), and Tari et al. (2020). B – A thin-skinned inversion model of a half-graben, with the master listric fault rooted within a thick pre-extensional sedimentary cover. C – A thin-skinned inversion model of a half-graben, with the master listric fault detached above pre-extensional evaporites. Note that all three models, despite their different structural characteristics at depth, have the same shallow tectono-sedimentary expression, with identical key elements of an inverted extensional system such as an inversion anticline and syn-inversion growth strata.

mentary cover; for example, within a more ductile shaly interval entrained within thick sandstones, or within evaporites (Fig. 1B, C; e.g., Brun and Nalpas 1996; Krzywiec 2006a; Jackson and Larsen 2008; Jackson et al. 2013; Dooley and Hudec 2020; Hansen et al. 2021; Krzywiec et al. 2022a). Despite their different structural characteristics at depth, the same shallow tectono-sedimentary expression, including key elements of the inverted extensional system such as an inversion anticline and syn-inversion growth strata, can be observed in each case.

Inversion tectonics invariably leads to the uplift of various basement blocks. As a result, those areas subject to the most intense subsidence and sedimentation during extension are characterized by significantly reduced accommodation space, resulting in the deposition of syn-inversion growth strata that, locally, have decreased thicknesses relative to contemporaneous strata (Fig. 2A). In fortuitous situations with high relative sea level and limited uplift, the preservation of the syn-inversion succession is possible, and can thus be used to precisely constrain and date inversion tectonics (cf. Hardy et al. 1996). In cases, however, of more substantial post-inversion erosion driven by significant uplift and/or relative sea-

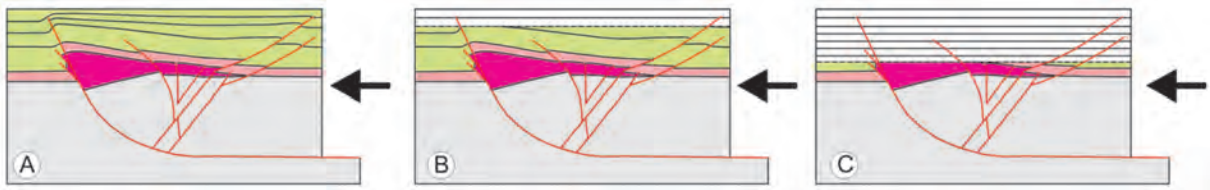

Fig. 2. Model of listric fault inversion (after McClay 1995, cf. Krzywiec 2009a, 2015). A – No or minimal post-inversion erosion, with syn-inversion growth strata almost fully preserved and usable for dating inversion tectonics. B – After moderate post-inversion erosion that partly removed syn-inversion strata. C – After deep erosion that removed most of the syn-inversion strata. Color scheme: gray – basement, purple – syn-extensional strata, pink – post-extension, pre-inversion strata, green – syn-inversion strata characterized by localized thinning within the inversion anticline hinge, formed above the tip of the inverted fault.

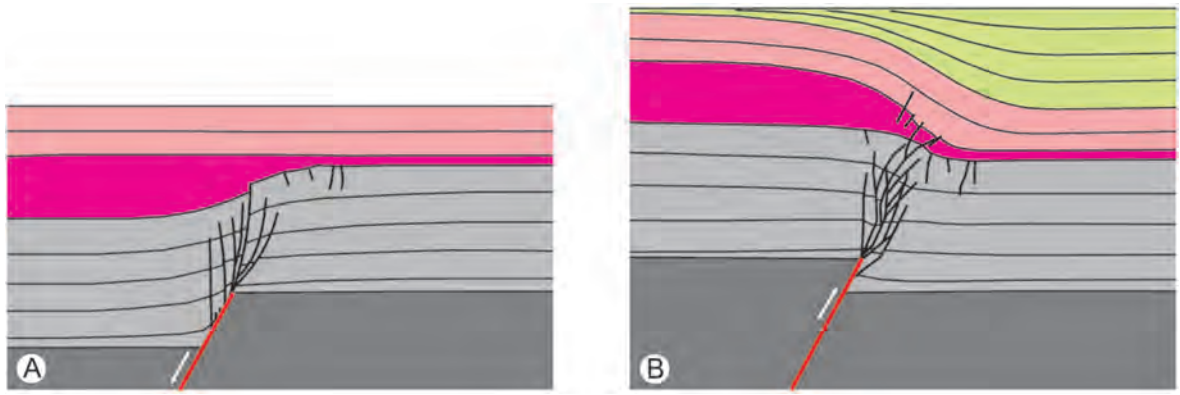

Fig. 3. Model of syn-inversion strata formation (cf. Krzywiec et al. 2009); see text for further explanation. Color scheme: gray – basement, purple – syn-extensional strata of increased thickness above the hanging wall block, pink – post-extension, pre-inversion strata of constant thickness, green – syn-inversion strata characterized by localized thinning towards the uplifted hanging wall block.

level drop, syn-inversion growth strata may be partly (Fig. 2B) or fully removed (Fig. 2C) (cf. Hardy et al. 1996).

The depositional architecture of syn-extensional and syn-inversion successions fundamentally differ. Increased subsidence caused by basement faulting leads to an increase of accommodation space and the deposition of thicker syn-extensional infill (Fig. 3A). Compressional reactivation of the master fault, in turn, results in the uplift of the previous basin center, which then forms the axis of inversion (Fig. 3B). Above this uplifted block, accommodation space is reduced, and localized erosion provides detritus that is then transported towards the flanks of the basin (Fig. 3B). In short: the gross polarity of depositional systems during (i) extension and subsidence and (ii) compression and inversion are reversed.

Along the edges of crustal blocks uplifted during inversion, coarse-grained deposits can be formed (cf. Voigt et al. 2004, 2008), similar to syn-kinematic deposits formed along the trailing edges of fold-and-thrust belts (e.g., Yonkee and Weil 2015). As recently illustrated by numerical modelling studies, substantial block uplift during sedimentary basin inversion might lead to the down-bending of its flanks and related flexural subsidence, comparable to the nature of flexural subsidence within foreland basins (cf. Sinclair 2012; Hindle and Kley 2021).

Finally, the uplift of basement blocks within relatively deep sedimentary basins – such as, for example, the Late Cretaceous European epicontinental basin – can create local bathymetric highs that focus contour currents and, as a result, led to the formation of contourites and similar deposits. Excellent examples of this phenomena, imaged on seismic data, include Upper Cretaceous contourites developed along major inversion axes, including the Sorgenfrei–Tornquist Zone in Denmark (Lykke-Andersen and Surlyk 2004; Esmerode et al. 2007; Surlyk and Lykke-Andersen 2007), the northwest Teisseyre–Tornquist Zone in Germany (Hübscher et al. 2019), and the

southeast Teisseyre–Tornquist Zone in Poland (Krzywiec et al. 2009, 2018).

GENERAL GEOLOGICAL SETTING

The Polish Basin formed due to regional subsidence and sedimentation within an extensive Permo-Mesozoic basin covering a considerable part of Europe (Ziegler 1990; van Wees et al. 2000; Scheck-Wenderoth et al. 2008; Doornenbal and Stevenson 2010; Pharaoh et al. 2010). The Polish Basin – including its axial, most rapidly subsiding portion, the Mid-Polish Trough – was located within the easternmost segment of this vast sedimentary basin (Ziegler 1990; Dadlez et al. 1995; Stephenson et al. 2003). It underwent long-term Mesozoic thermal subsidence, punctuated by three major pulses of accelerated tectonic subsidence: the late Permian to Early Triassic, the Late Jurassic (Oxfordian to Kimmeridgian), and the early Cenomanian (Dadlez et al. 1995; Stephenson et al. 2003). The earliest Cenomanian (c. 97 Ma) event has been tentatively linked by Dadlez et al. (1995) with regional compression, rather than to the extension and flexural behavior of the lithosphere, and may possibly include the reactivation of pre-existing crustal discontinuities. As such, it has been interpreted as a precursor to larger-scale compressional deformation during the latest Cretaceous basinal inversion (Dadlez et al. 1995; Stephenson et al. 2003).

The evolution of the northwest and central segments of the Polish Basin, where thick Zechstein (Wuchiapingian to Changhsingian) evaporites were deposited (Wagner 1994, 1998; Krzywiec et al. 2017), was characterized by regional mechanical decoupling between the sub-Zechstein Rotliegend and older substratum, and the Mesozoic supra-Zechstein cover, both during subsidence and during inversion and uplift (cf. Krzywiec 2006a, b; Krzywiec et al. 2022a). The Zechstein evaporites are overlain by a Triassic to Cretaceous clastic – carbonate sedimentary succession (cf. Ziegler 1990; Dadlez and Marek 1997; Krzywiec 2006a).

The inversion of the Polish Basin occurred during the Late Cretaceous–Paleogene (Dadlez et al. 1995; Krzywiec 2002b, 2006b; Resak et al. 2008; Krzywiec et al. 2009), associated with a widespread inversion of the European foreland triggered by the Alpine–Carpathian collision and Iberia–Europe convergence (cf. Mazur et al. 2005; Kley and Voigt 2008; Kley 2018; Voigt et al. 2021). This inversion led to the substantial uplift and erosion of the axial part of the Polish Basin – that is, the Mid-Polish Trough – which subsequently was transformed into the Mid-Polish Swell (Anticlinorium), outlined by the subcropping of Lower Cretaceous and older strata (Fig. 4A). Inversion of the Polish Basin commenced in the late Turonian, and lasted until the Maastrichtian–Paleocene (e.g., Krzywiec 2002a, 2006b; Resak et al. 2008; Krzywiec et al. 2009, 2018; Remin et al. 2022). At present, the Upper Cretaceous succession is preserved only along the flanks of the Mid-Polish Swell (Fig. 4B). Increased Late Cretaceous subsidence along these flanks, caused by their flexural bending combined with high eustatic sea level during the Cretaceous, created relatively abundant accommodation space filled by mostly syn-kinematic Upper Cretaceous strata. On the other hand, the progressive growth of individual inversion structures, including compressionally-reactivated salt diapirs, led to the localized reduction of accommodation space and associated erosion, in conjunction with the formation of growth strata characterized by reduced thickness, progressive unconformities, and facies changes (Krzywiec 2002a, b, 2006b, 2012; Leszczyński 2002, 2012; Krzywiec et al. 2009; 2018; Krzywiec and Stachowska 2016). All of these processes have been recorded in the extra-Carpathian Polish Upper Cretaceous sedimentary succession, and can now be precisely deciphered using high-quality seismic data acquired throughout the basin, both offshore and onshore.

LATE CRETACEOUS INVERSION TECTONICS AND ITS CONTROL ON DEPOSITIONAL SYSTEMS – AN OVERVIEW

The combination of relatively high Cretaceous eustatic sea level and the moderate uplift of various inversion structures within the Polish Basin – excluding the Mid-Polish Swell, where the entire Cretaceous has been removed by erosion (Fig. 4A, B) – led to the preservation of most of the syn-inversion sedimentary cover, which often includes the entire Upper

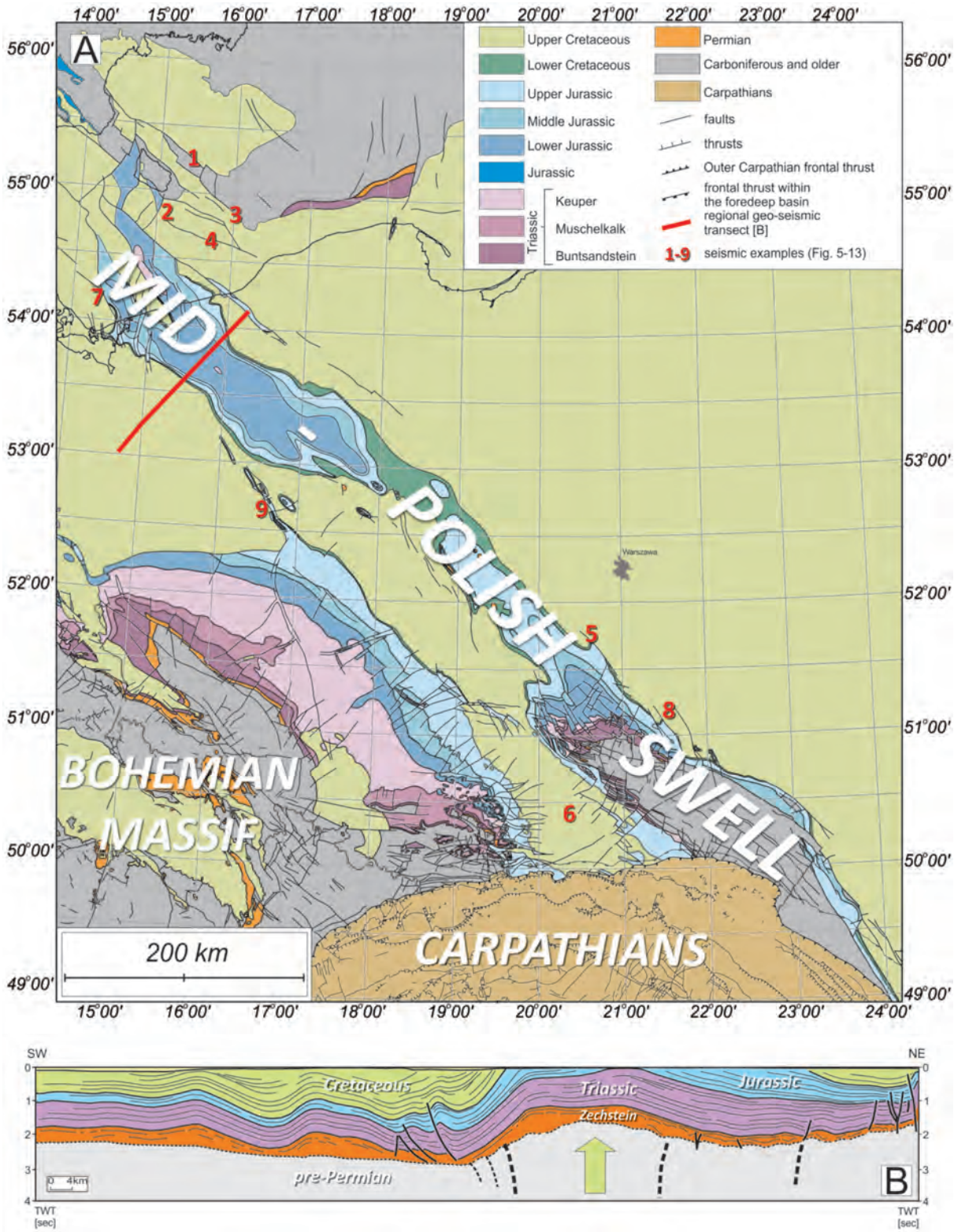

Fig. 4. A – Geological map of Poland and surrounding areas, without Cenozoic strata (compiled and simplified after Pożaryski 1979; Vejbæk 1985; Vejbæk et al. 1994; Kramarska et al. 1999; Dadlez et al. 2000); B – Regional geo-seismic cross-section across the Mid-Polish Swell (Anticlinorium) (based on Krzywiec 2006b; Scheck-Wenderoth et al. 2008). Green arrow indicates Late Cretaceous inversion focused within the axial part of the basin, leading to the formation of the Mid-Polish Swell (Anticlinorium).

Cretaceous (Cenomanian–Maastrichtian) succession. In this chapter, we present seismic examples that illustrate inversion tectonics within the Polish Basin. Emphasis has been placed on depositional systems and their relationship with active tectonic processes during the inversion of the Polish Basin. Two main categories of gross depositional processes have been distinguished: [1] those generally perpendicular to the main inversion axis i.e. the Mid-Polish Swell: that is, characterized by gross sedimentary transport towards the northeast or the southwest and [2] those generally parallel to the Mid-Polish Swell or other inversion-related structures, such as compressionally-reactivated salt diapirs.

A variety of seismic data were available for this study. Inversion structures within the southern Baltic Sea were studied using a regional high-resolution seismic survey acquired in 2016 by the BalTec German-Polish-Swedish research project (cf. Hübscher et al. 2016; Krzywiec et al. 2021). The BalTec seismic survey covered a region within the transition zone between the East European Craton and the Paleozoic Platform, was processed up to Kirchhoff pre-stack time migration, and provided excellent imaging for both shallow depth intervals – i.e., the first few hundred meters, which is often strongly contaminated by multiples in standard industry data – and for deep depth intervals, often reaching down to the top of the Precambrian basement. Additional shallow seismic data recorded in 1997 and 1998 down to 0.6 sec (Kramarska et al. 1999) were employed. For the onshore portions of the study area, various seismic data acquired over decades of hydrocarbon exploration were used. In combination, this data yielded exceptional portraits of Late Cretaceous inversion structures and related depositional systems. Below, an overview of the main findings is provided. The present synopsis will be followed at a later date by separate papers devoted to detailed analyses of particular structures and areas.

Depositional systems perpendicular to the main inversion axis

The subsurface structure of the southwest Baltic Sea – that is, of the sector located roughly south and southwest of Bornholm Island, is characterized by the presence of numerous basement blocks and fault zones active in the Paleozoic and Mesozoic (Fig. 4A; e.g., Vejbæk 1985; Dadlez 1990; Vejbæk et al. 1994; Krzywiec et al. 2003; Mazur et al. 2005; Pokorski 2010; Seidel et al. 2018). The Late Cretaceous inversion was the final major regional tectonic event, locking in the local crustal structure. During inversion, numerous blocks were uplifted and eroded. In several cases, this uplift was syn-depositional, as recorded by syn-inversion depositional systems (cf. Krzywiec et al. 2003).

Four seismic examples from the BalTec seismic survey provided detailed insight into these syn-depositional Late Cretaceous tectonics. The first, shown on Fig. 5, is located east of Bornholm, along the eastern boundary of the Christiansø High (Block), where pre-Cretaceous (here, Silurian) rocks outcrop beneath a thin veneer of Cenozoic deposits (Fig. 4A; see Vejbæk 1985; Vejbæk et al. 1994; Sopher and Juhlin 2013 for detailed nomenclature of particular tectonic elements in this part of the Baltic Sea). It illustrates a substantially uplifted basement block composed of Silurian (and older) rocks, flanked by a marginal trough mostly filled by an Upper Cretaceous succession, and possibly underlain by a very thin Lower Cretaceous (Albian) and Triassic–Jurassic cover resting above Paleozoic rocks (cf. Pan et al. submitted). This marginal trough forms the southeastern part of the Hanö Bay Basin (Sopher and Juhlin 2013; Pan et al. submitted). Its Upper Cretaceous infill is characterized by an overall progradational pattern towards the east, above a basal unconformity. Additionally, some of the seismically defined packages thicken westwards: that is, towards the Christiansø High. This general geometry quite closely resembles the sedimentary infill geometry in a classic foreland basin (Sinclair 2012; Yonkee and Weil 2015). This suggests that, in this area, Late Cretaceous subsidence was driven by the flexure of the pre-Cretaceous basement caused by the uplift of the Christiansø High along a deeply rooted reverse fault.

A different scenario is presented in seismic example [2], located south of Bornholm (Fig. 4A). In this area, the pre-Cretaceous basement is not uplifted along a discrete reverse fault; instead, regional inclination of the

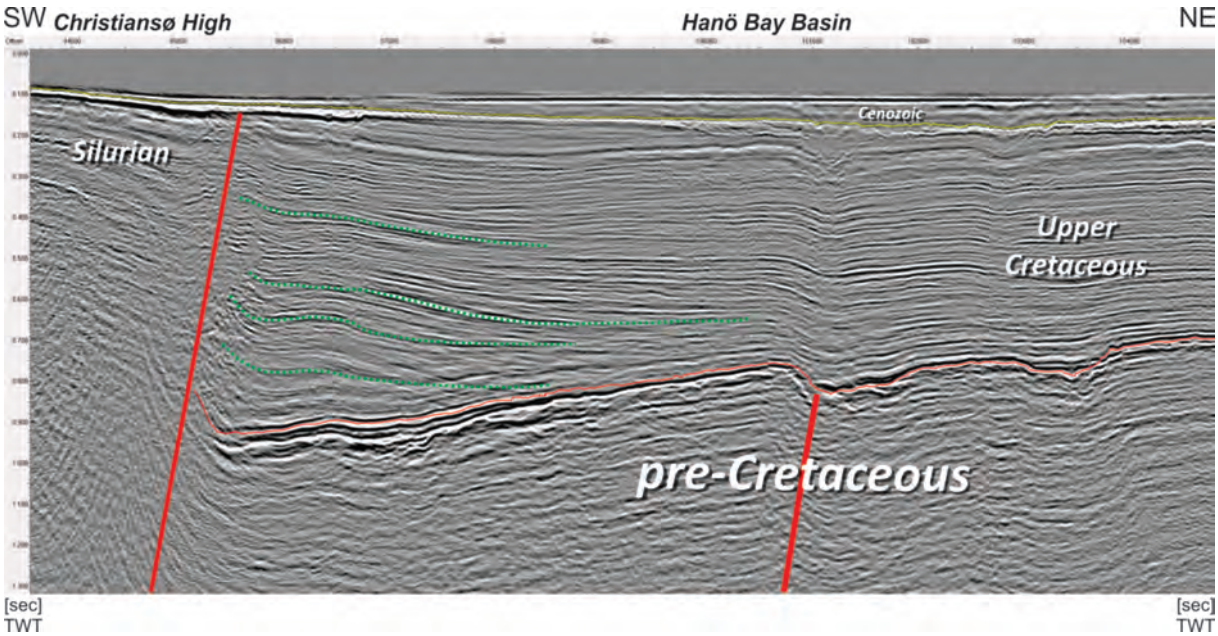

Fig. 5. Seismic example [1] (part of seismic profile BGR16-256) from the Baltic Sea, illustrating how uplift of the basement block led to the deposition of syn-inversion Upper Cretaceous strata characterized by a geometry partly resembling the depositional system of a flexural foreland basin. For location, see Fig. 4A. Horizontal offset in [m].

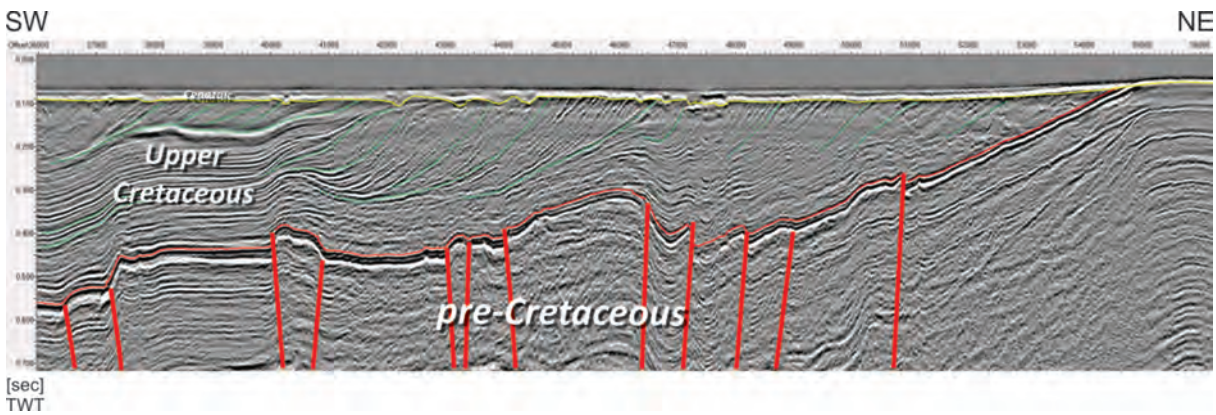

Fig. 6. Seismic example [2] (part of seismic profile BGR16-256) from the Baltic Sea, illustrating an Upper Cretaceous progradational system (cf. also Krzywiec et al. 2003). Subsequent erosion removed most of its topsets. For location, see Fig. 4A. Horizontal offset in [m].

pre-Cretaceous strata is observed as it eventually reaches the sub-Cenozoic surface (Fig. 6). Within the Upper Cretaceous syn-inversion cover complex, a progradational system delivered sediments towards the flank of this basement high – that is, towards the southwest. Subsequently, erosion removed most topsets in this system. The lack of a discrete reverse fault resulted in the corresponding absence of clear flexural subsidence, in contrast to seismic example [1].

Seismic example [3] illustrates that a vast area within the Polish offshore presently devoid of Mesozoic sediments – the Ustka and Słupsk Blocks (cf. Pokorski 2010) – was uplifted in the Late Cretaceous, and forms a part of a large, regional inversion system (Fig. 7). Intra-Upper Cretaceous and sub-Cenozoic unconformities document a two-staged uplift process, at odds with a previously published model that assumed that this uplift was much older (late Caledonian) and that the Cretaceous veneer

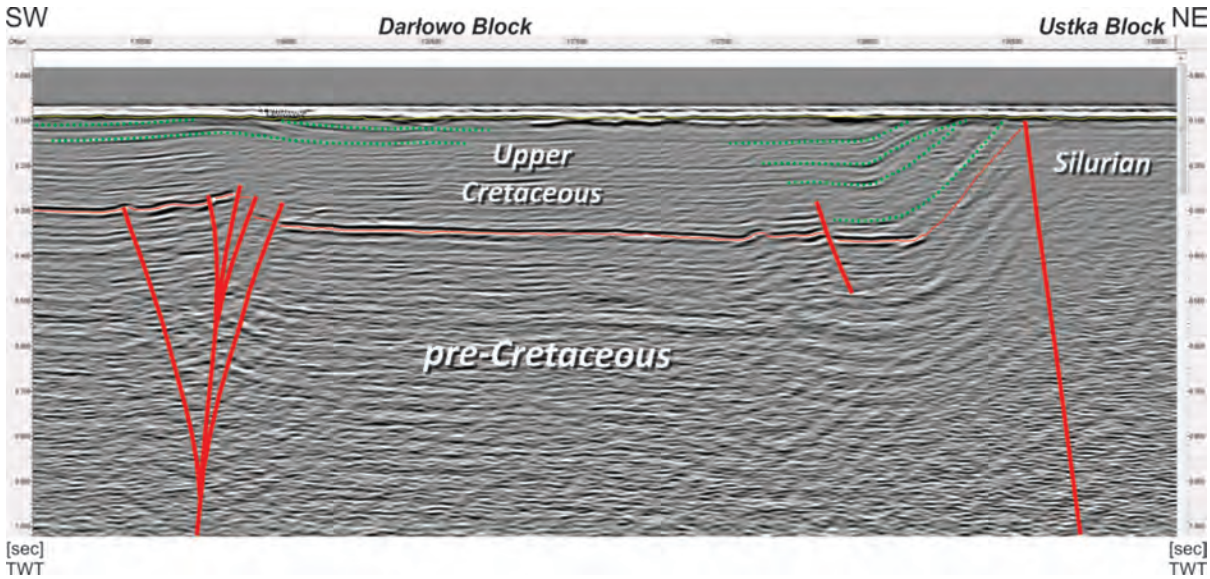

Fig. 7. Seismic example [3] (part of seismic profile BGR16-212) from the Baltic Sea, illustrating the latest Cretaceous uplift of the Ustka and Słupsk Blocks and strike-slip movements within the Darłowo Block (cf. Krzywiec et al. 2003; Pokorski 2010). For location, see Fig. 4A. Horizontal offset in [m].

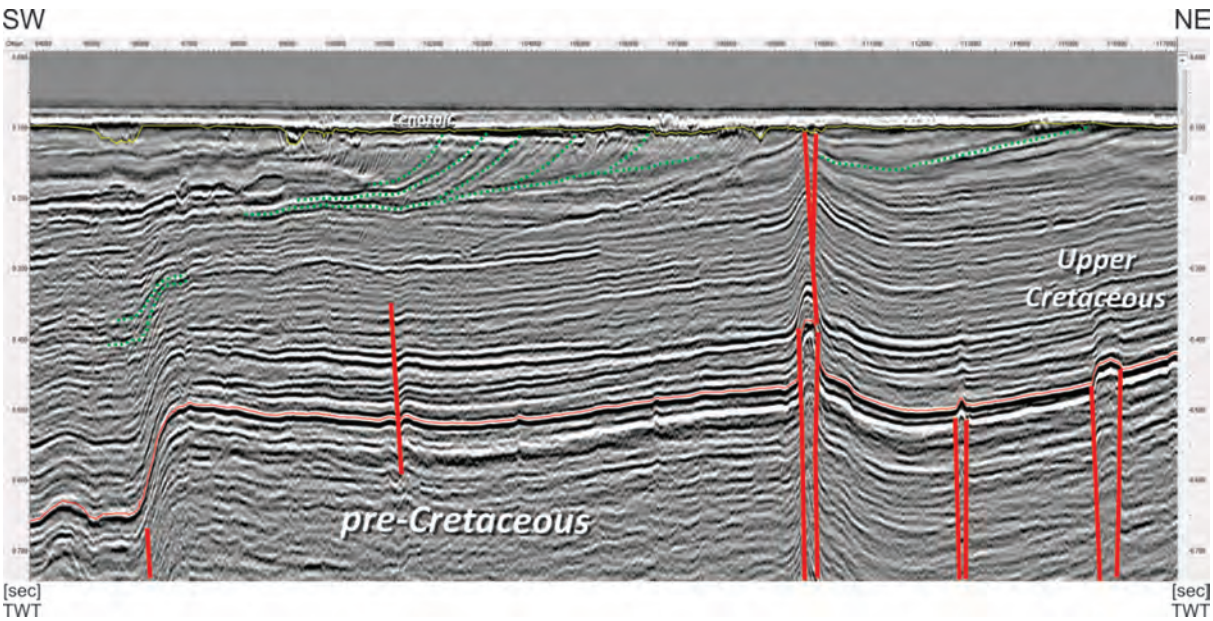

Fig. 8. Seismic example [4] (part of seismic profile BGR16-212) from the Baltic Sea, illustrating an Upper Cretaceous progradational system. Subsequent erosion removed most of its topsets. It also demonstrates the important role of strike-slip movements, which formed a positive flower structure that deformed the entire preserved Upper Cretaceous succession (cf. also Krzywiec et al. 2003). For location, see Fig. 4A. Horizontal offset in [m].

unconformably covered uplifted Paleozoic rocks (Jaworowski et al. 2010). This seismic example also illustrates that latest Cretaceous strike-slip movements affected the Darłowo Block, as demonstrated by a deeply rooted positive flower structure deforming the entire Upper Cretaceous cover (cf. Krzywiec et al. 2003).

An Upper Cretaceous progradational system within the Darłowo Block, with associated strike-slip movements, is precisely delineated by seismic example [4] (Fig. 8). Reductions in

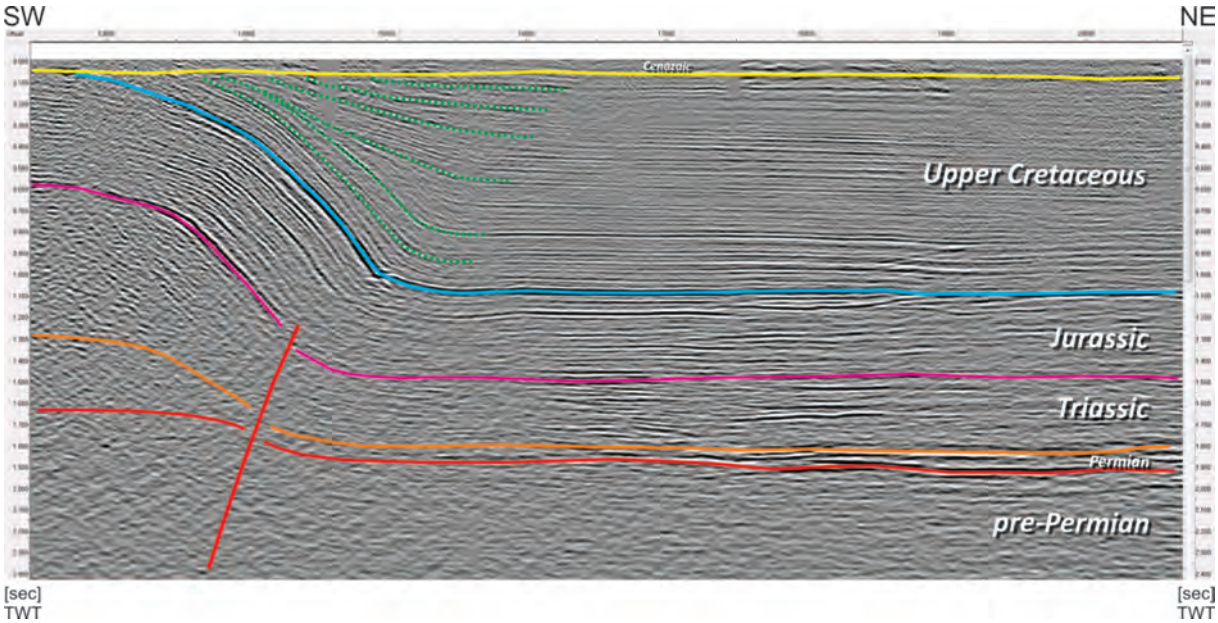

Fig. 9. Seismic example [5] from central Poland, illustrating how Upper Cretaceous strata recorded progressive uplift along the northeast edge of the Mid-Polish Swell (cf. also Krzywiec 2009b). For location, see Fig. 4A. Horizontal offset in [m].

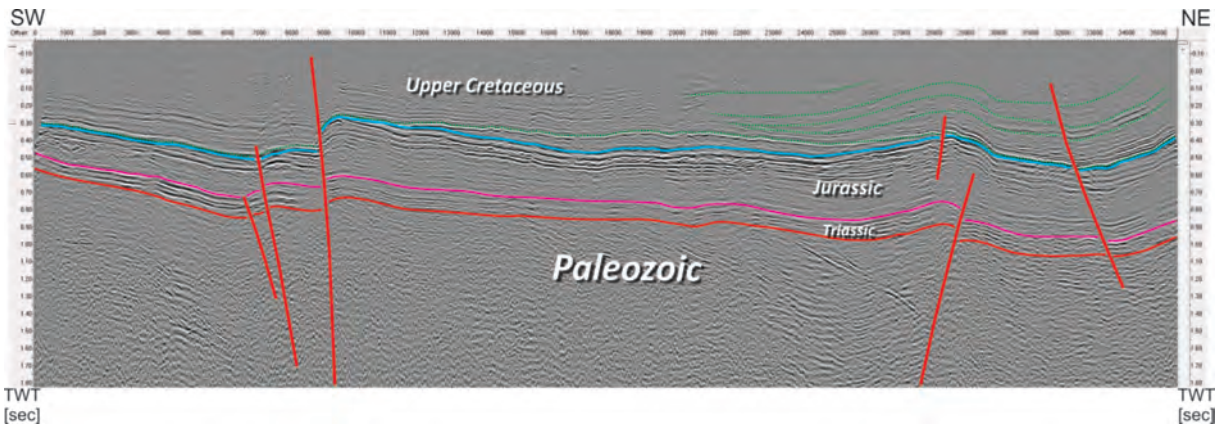

Fig. 10. Seismic example [6] from the Miechów Trough (Syncline) in southern Poland, where key basement faults remained active as normal faults and controlled localized subsidence during most of the Late Cretaceous, as evidenced by locally thickening Upper Cretaceous strata. In this area, inversion tectonics initiated in the latest Cretaceous – Paleogene. For location, see Fig. 4A. Horizontal offset in [m].

thickness above the fold, developed above a deeply rooted reverse fault visible in the left part of this seismic profile, demonstrate that uplift along this fault was syn-depositional. As such, even the lower part of the Upper Cretaceous succession here may be regarded as syn-tectonic (cf. Krzywiec et al. 2003).

Seismic data document the syn-depositional Late Cretaceous uplift of basement blocks across several different segments of the Mid-Polish Swell. Seismic example [5] (Fig. 9), for instance, is located south of Warsaw (in central Poland), and illustrates progressive uplift along the northeast edge of the Mid-Polish Swell, as recorded by Upper Cretaceous strata. This inversion-induced uplift lasted almost the entire Late Cretaceous (cf. also Krzywiec 2009b), as evidenced by thinning of the Upper Cretaceous strata and intra-Upper Cretaceous unconformities, comparable to the model presented in Fig. 3B.

Seismic example [6] (Fig. 10) is from the Miechów Trough (Synclinorium) of southern Poland, which is filled by a complete Cenomanian–Maastrichtian succession (e.g., Jurkowska 2016, and references therein). In this area, inversion tectonics developed following a slightly different scenario than elsewhere in the basin. As illustrated by the localized increase in thickness of the Upper Cretaceous succession above several main basement faults, extension and subsidence prevailed throughout much of the Late Cretaceous. The basement faults within the axial part of the Miechów Trough (Synclinorium) inverted in the latest Cretaceous–Paleogene, as inversion-induced faulting and folding includes some Maastrichtian strata.

Depositional systems parallel to the main inversion axis

Those depositional systems that were approximately perpendicular to the Mid-Polish Swell supplied sediments from areas uplifted during inversion into surrounding lows, as illustrated by local thinning or unconformities within the Upper Cretaceous inversion-related succession that are clearly visible on seismic data (see also Remin et al. 2022). Apart from these "classic" inversion-related depositional systems, another class of depositional systems can be distinguished – those that ran parallel to the Mid-Polish Swell. While they are more difficult to identify on seismic data, they are nonetheless important; they, too, attest to the presence of inversion-related, Late Cretaceous bathymetry. Their formation was related to contour currents along the edges of inversion structures (cf. Krzywiec et al. 2009; Remin et al. 2016). As a result, contourites formed within the Upper Cretaceous succession, and can be identified on seismic data. Classically, contourites are defined as deposits formed by deep-water bottom currents, in turn resulting from oceanic thermohaline circulation (Faugères et al. 1999; Rebesco et al. 2014). Contourite drifts are most easily recognized when they have an along-slope, elongated mound shape and an adjacent concave moat (Rebesco et al. 2014). To remain stable, contour currents require some sort of slope, so the identification of ancient contourites unequivocally indicates that a slope must have existed during their deposition. Of course, the most obvious setting for contourite formation would be on passive margins, along which global-scale contour currents could flow. Within an inverting basin, positive morphological features at the basin's bottom related to uplifted blocks are often observed. Along their edges, contour currents can flow, potentially resulting in the formation of contourites. Indeed, contourites of this nature have already been identified in the Danish and German parts of the epicontinental Late Cretaceous European basin (Lykke-Andersen and Surlyk 2004; Esmerode et al. 2007; Surlyk and Lykke-Andersen 2007; Hübscher et al. 2019).

Seismic example [7] is located in the southwestern Baltic Sea (Fig. 11). It illustrates contourites developed along the southwestern edge of the Gryfice Block, in the offshore segment of the Mid-Polish Swell (Fig. 4A; cf. Dadlez et al. 2000; Mazur et al. 2005). They belong to the same Maastrichtian contourite system identified by Hübscher et al. (2019; their figures 6 and 7).

Contourites have been precisely imaged in southeastern Poland along the northeastern edge of the Mid-Polish Swell, as illustrated by seismic example [8] (Fig. 12; cf. Krzywiec et al. 2009). Here, the Upper Cretaceous succession on the northeastern flank of the Mid-Polish Swell is characterized by a low-angle progradational complex directed towards the northeast, away from the regional inversion axis (Krzywiec et al. 2009; Remin et al. 2022). The Upper Cretaceous succession thins to the southwest – towards the Mid-Polish Swell – which testifies to the role of gradual syn-depositional uplift during basin inversion. Within the Campanian part of the succession, contourites have been identified, produced by contour currents that flowed along the slope formed by the Mid-Polish Swell as it was progressively uplifted during the Late Cretaceous (Krzywiec et al. 2009). The upsection migration of contourites away from the inversion axis resulted from the progressive uplift of the Mid-Polish Swell, and the associated shift of major depositional zones.

Seismic examples [7] and [8] (Figs 11 and 12) illustrate parallel contourite depositional systems developed along the edges of the Mid-Polish Swell, which must have formed large morphological barriers at the bottom of the

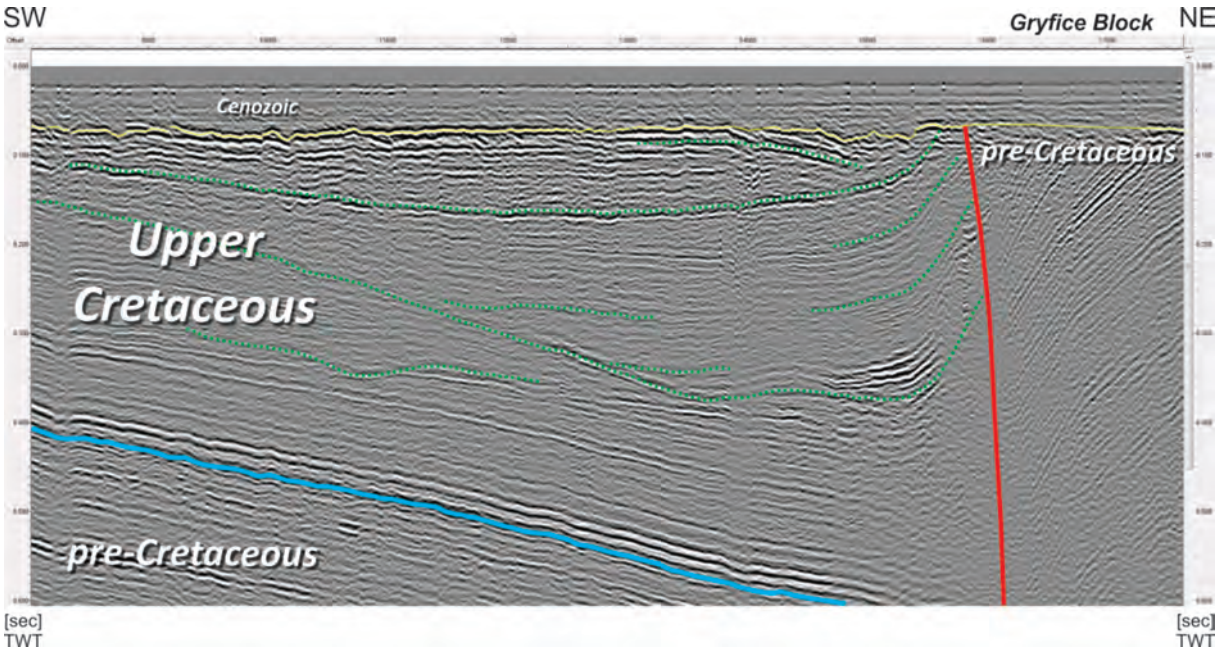

Fig. 11. Seismic example [7] (part of seismic profile TNO 3A-97; cf. Kramarska et al. 1999) from the southwest Baltic Sea, illustrating contourites along the southwestern edge of the Gryfice Block (cf. Hübscher et al. 2019). For location, see Fig. 4A. Horizontal offset in [m].

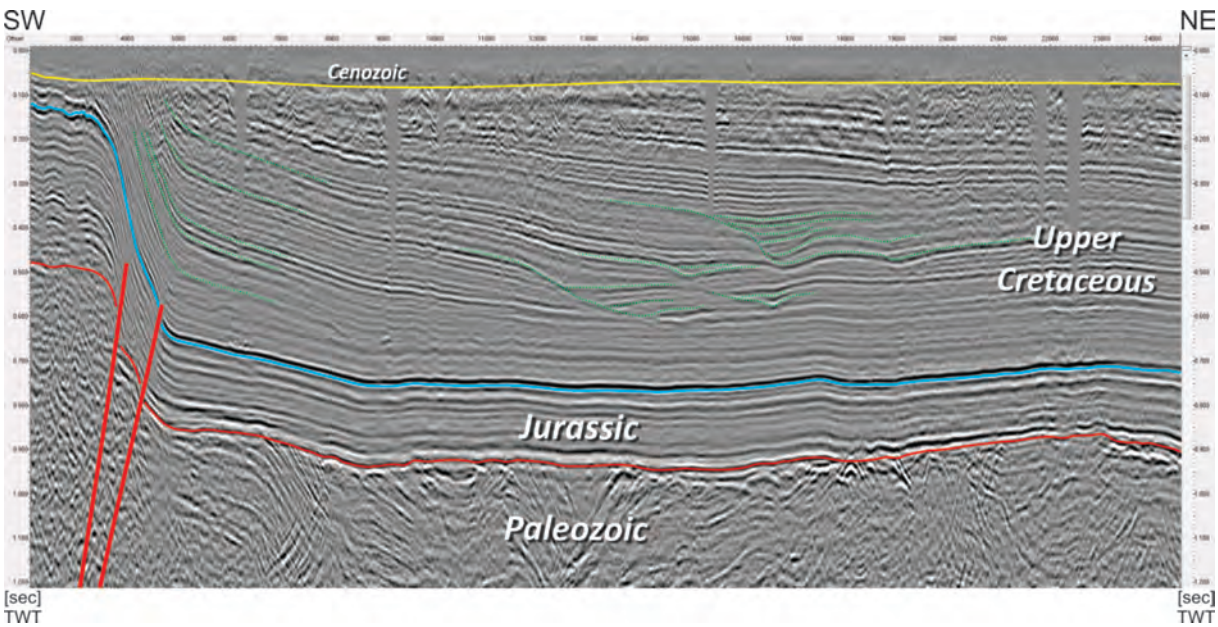

Fig. 12. Seismic example [8] from southeast Poland, illustrating contourites formed along the edge of the Mid-Polish Swell (cf. Krzywiec et al. 2009, 2018). Note, also, the significant thinning of the Upper Cretaceous succession towards the uplifted edge of the Mid-Polish Swell, which documents progressive uplift in the Late Cretaceous (cf. Fig. 3). For location, see Fig. 4A. Horizontal offset in [m].

basin. However, more localized barriers also existed, mostly related to compressionally-reactivated, uplifted salt diapirs (cf. Krzywiec 2012; Krzywiec and Stachowska 2016). They also apparently focused contour currents, leading to the depositions of contourites. Seismic example [9] from northwest Poland illustrates contourites formed along the south-

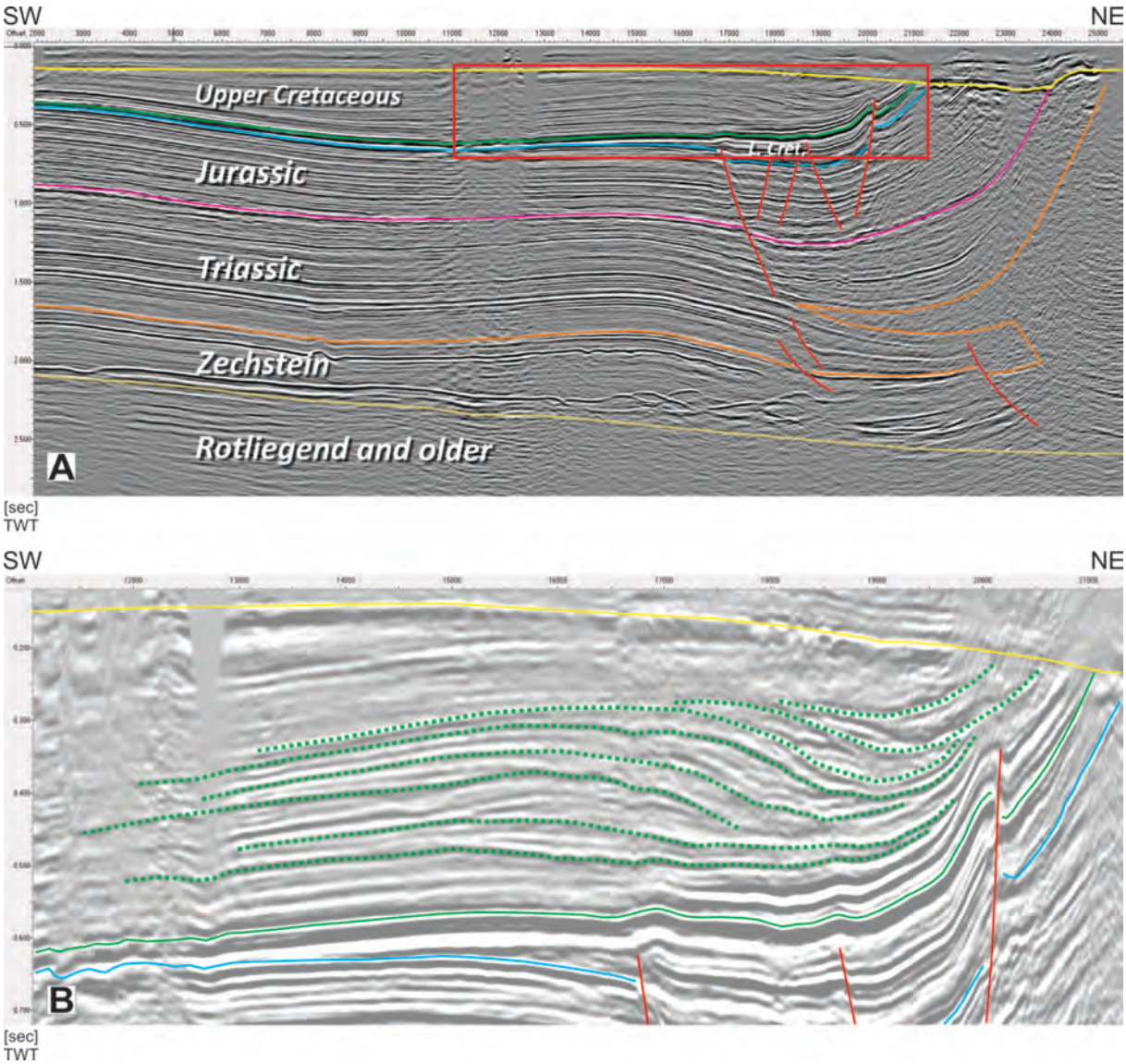

Fig. 13. Seismic example [9] from northwestern Poland, illustrating contourites formed along the Szamotuły salt diapir. For location, see Fig. 4A. Horizontal offset in [m].

western edge of the Szamotuły salt diapir (Fig. 13). Their formation might have been controlled by processes similar to those operating in the vicinity of the recently pierced diapir in the Santos Basin of offshore Brazil (Schattner et al. 2018).

ACKNOWLEDGEMENTS

The analysis of the seismic data that formed the foundation of this overview paper was supported by NCN grants 2017/27/B/ST10/02316 (offshore) and 2018/29/B/ST10/02947 (southeast Poland). PGNiG is thanked for providing onshore seismic data, and IHS Kingdom for providing their seismic interpretation software.

REFERENCES

Bally, A.W. 1984. Tectogenese et sesmique reflexion. Bulletin la Société Géologique de France, S7-XXVI (2), 279–285.

Brun, J.-P. and Nalpas, T. 1996. Graben inversion in nature and experiments. Tectonics, 15, 677–687.

Buchanan, J.G. and Buchanan, P.G. (Eds) 1995. Basin Inversion. Geological Society, London, Special Publications, 88, 1–596.

Cooper, M.A. and Williams, G.D. (Eds) 1989. Inversion tectonics. Geological Society, London, Special Publications, 44, 1–375.

Cooper, M. and Warren, M.J. 2010. The geometric characteristics, genesis and petroleum significance of inversion structures. Geological Society, London, Special Publications, 335, 827–846.

Cooper, M. and Warren, M.J. 2020. Inverted fault systems and inversion tectonic settings. In: Scarselli, N., Adam, J., Chiarella, D., Roberts, D.G. and Bally, A. (Eds), Regional Geology and Tectonics: Principles of Geologic Analysis, 169–204. Elsevier; Amsterdam, The Netherlands.

Cooper, M.A., Williams, G.D., de Graciansky, P.C., Murphy, R.W., Needham, T., de Paor, D., Stoneley, R., Todd, S. P., Turner, J.P. and Ziegler, P.A. 1989. Inversion tectonics – a discussion. Geological Society, London, Special Publications, 44, 335–347.

Dadlez, R. 1990. Tectonics of the Southern Baltic. Geological Quarterly, 34, 1–20.

Dadlez, R. and Marek, S. 1997. Development of the Permian and Mesozoic basins. Prace Instytutu Geologicznego, 153, 403–409. [In Polish with English summary]

Dadlez, R., Narkiewicz, M., Stephenson, R.A., Visser, M.T.M. and van Wees, J.D. 1995. Tectonic evolution of the Mid-Polish Trough: Modelling implications and significance for central European geology. Tectonophysics, 252, 179–195.

Dadlez, R., Marek, S. and Pokorski, J. (Eds) 2000. Geological map of Poland without Cainozoic deposits, 1:1000000. Państwowy Instytut Geoleologiczny; Warszawa.

Dewey, J.F. 1989. Kinematics and dynamics of basin inversion. Geological Society, London, Special Publications, 44, 1–352.

Dooley, T.P. and Hudec, M.R. 2020. Extension and inversion of salt-bearing rift systems. Solid Earth, 11, 1187–1204.

Doornenbal, H. and Stevenson, A. (Eds) 2010. Petroleum Geological Atlas of the Southern Permian Basin Area, 342 pp. EAGE Publications BV; Houten, The Netherlands.

Esmerode, E.V., Lykke-Andersen, H. and Surlyk, F. 2007. Ridge and valley systems in the Upper Cretaceous chalk of the Danish Basin: contourites in an epeiric sea. Geological Society, London, Special Publications, 276, 265–282.

Faugères, J.-C., Stow, D.A.V., Imbert, P. and Viana, A. 1999. Seismic features diagnostic of contourite drifts. Marine Geology, 162, 1–38.

Glennie, K.W. and Boegner, P.L.E. 1981. Sole Pit inversion tectonics. In: Illing, L.V. and Hobson, G.D. (Eds), Petroleum Geology of the Continental Shelf of Northwest Europe, 110–120. Institute of Petroleum; London.

Hansen, T.H., Clausen, O.R. and Andresen, K.J. 2021. Thick- and thin-skinned basin inversion in the Danish Central Graben, North Sea – the role of deep evaporites and basement kinematics. Solid Earth, 12, 1719–1747.

Hardy, S., Poblet, S., McClay K. and Waltham D. 1996. Mathematical modelling of growth strata associated with fault-related fold structures. Geological Society, London, Special Publications, 99, 265–282.

Hindle, D. and Kley, J. 2021. The Subhercynian Basin: An example of an intraplate foreland basin due to a broken plate. Solid Earth, 12, 2425–2438.

Hübscher, C., Niklas, N., Allum, G., Behrens, T., Bülow, J., Krawczyk, C., Damm, V., Demir, Ü., Engels, M., Frahm, L. Grzyb, J., Hahn, B., Heyde, I., Juhlin, C., Knevels, K., Lange, G., Lydersen, I.B., Lange, G., Malinowski, M., Noack, V., Preine, J., Rampersad, K., Schnabel, M., Seidel, E., Sopher, D., Stakemann, J.M. and Stakemann, J. 2017. BalTec – Cruise No. MSM52 – March 1 – March 28, 2016 – Rostock (Germany) – Kiel (Germany).

Hübscher, C., Al Hseinat, M., Schneider, M. and Betzler, C. 2019. Evolution of contourite systems in the late Cretaceous Chalk Sea along the Tornquist Zone. Sedimentology, 66, 1341–1360.

Jackson, C.A.L. and Larsen, E. 2008. Temporal constraints on basin inversion provided by 3D seismic and well data: a case study from the South Viking Graben, offshore Norway. Basin Research, 20, 397–417.

Jackson, C.A.L., Chua, S.-T., Bell, R. and Magee, C. 2013. Structural style and early stage growth of inversion structures: 3D seismic insights from the Egersund Basin, offshore Norway. Journal of Structural Geology, 46, 167–185.

Jaworowski, K., Wagner, R., Modlinski, Z., Pokorski, J., Sokołowski A. and Sokołowski J. 2010. Marine ecogeology in semi-closed basin: case study on a threat of geogenic pollution of the southern Baltic Sea (Polish Exclusive Economic Zone). Geological Quarterly. Geological Quarterly, 54, 267–288.

Jurkowska, A. 2016. Inoceramid stratigraphy and depositional architecture of the Campanian and Maastrichtian of the Miechów Synclinorium (southern Poland). Acta Geologica Polonica, 66, 59–84.

Kley, J. 2018. Timing and spatial patterns of Cretaceous and Cenozoic inversion in the Southern Permian Basin. Geological Society, London, Special Publications, 469, 19–31.

Kley, J. and Voigt, T. 2008. Late Cretaceous intraplate thrusting in central Europe: Effect of Africa–Iberia–Europe convergence, not Alpine collision. Geology, 36, 839–842.

Kramarska, R., Krzywiec, P. and Dadlez, R. 1999. Geo-

logical map of the Baltic Sea bottom without Quaternary Deposits. Wydawnictwo Kartograficzne Polskiej Agencji Ekologicznej; Gdańsk – Warszawa.

Krzywiec, P. 2002a. Mid-Polish Trough inversion – seismic examples, main mechanisms, and its relationship to the Alpine-Carpathian collision. EGU Stephan Mueller Special Publication Series, 1, 151–165.

Krzywiec, P. 2002b. Oświno structure (NW Mid-Polish Trough) – salt diapir or inversion-related compressional structure? Geological Quarterly, 46, 337–346.

Krzywiec, P. 2006a. Triassic–Jurassic evolution of the Pomeranian segment of the Mid-Polish Trough – Basement tectonics and subsidence patterns. Geological Quarterly, 50, 139–150.

Krzywiec, P. 2006b. Structural inversion of the Pomeranian and Kuiavian segments of the Mid-Polish Trough – Lateral variations in timing and structural style. Geological Quarterly, 50, 151–168.

Krzywiec, P. 2009a. Devonian–Cretaceous repeated subsidence and uplift along the Tornquist–Teisseyre Zone in SE Poland – insight from seismic data interpretation. Tectonophysics, 475, 142–159.

Krzywiec, P. 2009b. Structure and Mesozoic – Cenozoic evolution of the Grójec strike-slip fault zone: results of seismic data interpretation. Geologia–Kwartalnik AGH Geologia, 35, 377–386. [In Polish with English abstract]

Krzywiec, P. 2012. Mesozoic and Cenozoic evolution of salt structures within the Polish basin: An overview. Geological Society, London, Special Publications, 363, 381–394. https://doi.org/10.1144/SP363.17.

Krzywiec, P. 2015. Late Cretaceous inversion along the NE Permo-Mesozoic rim of the Holy Cross Mountains – results of seismic data interpretation. In: Skompski, S. and Mizerski, W. (Eds), 84 Zjazd Naukowy Polskiego Towarzystwa Geologicznego. Ekstensja i Inwersja powaryscyjskich basenów sedymentacyjnych, Chęciny, 9–11 September 2015, Abstracts & Field Guide, 51–58. Państwowy Instytut Geologiczny – Państwowy Instytut Badawczy; Warszawa. [In Polish]

Krzywiec, P. and Stachowska, A. 2016. Late Cretaceous inversion of the NW segment of the Mid-Polish Trough – how marginal trough was formed, and does it matter at all? Zeitschrift der Deutschen Gesellschaft für Geowissenschaften, 167, 107–119.

Krzywiec, P., Kramarska, R. and Zientara, P. 2003. Strike-slip tectonics within the SW Baltic Sea and its relationship to the inversion of the Mid-Polish Trough – evidence from high-resolution seismic data. Tectonophysics, 373, 93–105.

Krzywiec, P., Gutowski, J., Walaszczyk, I., Wróbel, G. and Wybraniec, S. 2009. Tectonostratigraphic model of the Late Cretaceous inversion along the Nowe Miasto–Zawichost Fault Zone, SE Mid-Polish Trough. Geological Quarterly, 53, 27–48.

Krzywiec, P., Peryt, T.M., Kiersnowski, H., Pomianowski, P., Czapowski, G. and Kwolek, K. 2017. Permo-Triassic evaporites of the Polish Basin and their bearing on the tectonic evolution and hydrocarbon system, an overview. In: Soto, J. I., Flinch, J. F. and Tari, G. (Eds), Permo-Triassic Salt Provinces of Europe, North Africa and the Central Atlantic: Tectonics and Hydrocarbon Potential, 243–261. Elsevier; Amsterdam.

Krzywiec, P., Stachowska, A. and Stypa, A. 2018. The only way is up – on Mesozoic uplifts and basin inversion events in SE Poland. Geological Society, London, Special Publications, 469, 33–57.

Krzywiec, P., Słonka, Ł., Nguyen, Q., Malinowski, M., Kufrasa, M., Stachowska, A., Huebscher, C. and Kramarska, R. 2021. Late Cretaceous – Cenozoic history of the transition zone between the East European Craton and the Paleozoic Platform, Polish sector of the Baltic Sea, revealed by new offshore regional seismic data. In: EGU General Assembly, Vienna, Austria, 19–30.04.2021, EGU21-13383.

Krzywiec, P., Kufrasa, M., Poprawa, P., Mazur, S., Koperska, M. and Ślemp, P. 2022a. Together but separate: decoupled Variscan (late Carboniferous) and Alpine (Late Cretaceous – Paleogene) inversion tectonics in NW Poland. Solid Earth, 13, 639–658.

Krzywiec, P., Kley, J. and Buiter, S. (Eds) 2022b. Inversion tectonics – 30 years later. Solid Earth Special Issue, https://se.copernicus.org/articles/special_issue1047.html.

Leszczyński, K. 2002. Late Cretaceous inversion and salt tectonics in the Koszalin–Chojnice and Drawno–Człopa–Szamotuły zones, Pomeranian sector of the Mid-Polish Trough. Geological Quarterly, 46, 347–362.

Leszczyński, K. 2012. The internal geometry and lithofacies pattern of the Upper Cretaceous–Danian sequence in the Polish Lowlands. Geological Quarterly, 56, 363–386.

Lykke-Andersen, H. and Surlyk, F. 2004. The Cretaceous–Palaeogene boundary at Stevns Klint, Denmark: Inversion tectonics or sea-floor topography? Journal of the Geological Society, 47, 343–352.

Mazur, S., Scheck-Wenderoth, M. and Krzywiec, P. 2005. Different modes of the Late Cretaceous–Early Tertiary inversion in the North German and Polish basins. International Journal of Earth Sciences, 94, 782–798.

McClay, K.R. 1995. The geometries and kinematics of inverted fault systems: a review of analogue model studies. Geological Society, London, Special Publications, 88, 97–118.

Pan, Y., Seidel, E., Juhlin, C., Hübscher, C. and Sopher, D. (submitted). Inversion tectonics in the Sorgenfrei–Tornquist Zone: insight from new marine seismic images at the Bornholm Gat, SW Baltic Sea. Geologiska Föreningens Förhandlingar.

Pharaoh, T.C., Dusar, M., Geluk, M., Kockel, F., Krawczyk, C.M., Krzywiec, P., Scheck-Wenderoth, M., Thybo, H., Vejbaek, O. and Van Wees, J.D. 2010. Tectonic

evolution. In: Doornenbal, J.C. and Stevenson, A.A. (Eds), Petroleum geological atlas of the Southern Permian Basin area, 25–57. European Association of Geoscientists and Engineers (EAGE); Houten, The Netherlands.

Pokorski, J. 2010. Geological section through the lower Paleozoic strata of the Polish part of the Baltic region. Geological Quarterly, 54, 123–130.

Pożaryski, W. (Ed.) 1979. Geological map of Poland and surrounding countries without Cenozoic (Carpathians without Quaternary), 1:1000000. Wydawnictwa Geologiczne; Warszawa.

Rebesco, M., Hernández-Molina, F.J., Van Rooij, D. and Wåhlin, A. 2014. Contourites and associated sediments controlled by deep-water circulation processes: State-of-the-art and future considerations. Marine Geology, 352, 111–154.

Remin, Z., Gruszczyński, M. and Marshal, J.D. 2016. Changes in paleo-circulation and the distribution of ammonite faunas at the Coniacian–Santonian transition in central Poland and western Ukraine. Acta Geologica Polonica, 66, 107–124.

Remin, Z., Cyglicki, M. and Niechwedowicz, M. 2022. Deep vs. shallow – two contrasting theories? A tectonically activated Late Cretaceous deltaic system in the axial part of the Mid-Polish Trough: a case study from southeast Poland. Solid Earth, 13, 681–703.

Resak, M., Narkiewicz, M. and Littke, R. 2008. New basin modelling results from the Polish part of the Central European Basin system: implications for the Late Cretaceous–Early Paleogene structural inversion. International Journal of Earth Sciences, 97, 955–972.

Schattner, U., Lobo, F.J., García, M., Kanari M., Ramos, R.B. and Michaelovitch de Mahiques, M. 2018. A detailed look at diapir piercement onto the ocean floor: New evidence from Santos Basin, offshore Brazil. Marine Geology, 406, 98–108.

Scheck-Wenderoth, M., Krzywiec, P., Zuhlke, R., Maystrenko, Y. and Froitzheim, N. 2008. Permian to Cretaceous tectonics. In: McCann, T. (Ed.), The Geology of Central Europe Volume 2: Mesozoic and Cenozoic, 999–1030. The Geological Society of London; London.

Seidel, E., Meschede, M. and Obst, K. 2018. The Wiek Fault System east of Rügen Island: origin, tectonic phases and its relationship to the Trans-European Suture Zone. Geological Society, London, Special Publications, 469, 59–82.

Sinclair, H. 2012. Thrust wedge/foreland basin systems. In: Busby, C. and Azor, A. (Eds), Tectonics of Sedimentary Basins: Recent Advances, 522–537. Blackwell Publishing Ltd.

Sopher, D. and Juhlin, C. 2013. Processing and interpretation of vintage 2D marine seismic data from the outer Hanö Bay area, Baltic Sea. Journal of Applied Geophysics, 95, 1–15.

Stephenson, R.A., Narkiewicz, M., Dadlez, R., van Wees, J.-D. and Andriessen, P. 2003. Tectonic subsidence modelling of the Polish Basin in the light of new data on crustal structure and magnitude of inversion. Sedimentary Geology, 156, 59–70.

Surlyk, F. and Lykke-Andersen, H. 2007. Contourite drifts, moats and channels in the Upper Cretaceous chalk of the Danish Basin. Sedimentology, 54, 405–422.

Tari, G., Arbouille, D., Schléder, Z. and Tóth, T. 2020. Inversion tectonics: A brief petroleum industry perspective. Solid Earth, 11, 1865–1889.

Vejbæk, O.W. 1985. Seismic stratigraphy and Tectonics of Sedimentary Basins around Bornholm. Geology Survey of Denmark DGU Serie A, 8, 1–30.

Vejbæk, O.W., Stouge, S. and Poulsen, K.D. 1994. Paleozoic tectonic and sedimentary evolution and hydrocarbon prospectivity in the Bornholm area. Geological Survey of Denmark, DGU Serie A, 34, 1–23.

Voigt, T., von Eynatten, H. and Franzke, H.-J. 2004. Late Cretaceous unconformities in the Subhercynian Cretaceous Basin (Germany). Acta Geologica Polonica, 54, 675–696.

Voigt, T., Reicherter, K., von Eynatten, H., Littke, R., Voigt, S. and Kley, J. 2008. Sedimentation during basin inversion. In: Littke, R., Bayer, U., Gajewski, D. and Nelskamp, S. (Eds), Dynamics of Complex Intracontinental Basins – The Central European Basin System, 211–232. Springer-Verlag; Berlin, Heidelberg.

Voigt, T., Kley, J. and Voigt, S. 2021. Dawn and dusk of Late Cretaceous basin inversion in central Europe. Solid Earth, 12, 1443–1471.

Wagner, R. 1994. Stratigraphy and evolution of the Zechstein basin in the Polish Lowlands. Prace Państwowego Instytutu Geologicznego, 146, 1–71. [In Polish with English summary]

Wagner, R. 1998. Zechstein. In: Dadlez, R., Marek, S. and Pokorski, J. (Eds), Paleogeographic atlas of epicontinental Permian and Mesozoic in Poland, 1:2500000. Państwowy Instytut Geologiczny; Warszawa, Poland.

van Wees, J.-D., Stephenson, R., Ziegler, P., Bayer, U., McCann, T., Dadlez, R., Gaupp, R., Narkiewicz, M., Bitzer, F. and Scheck, M. 2000. On the origin of the Southern Permian Basin, Central Europe. Marine and Petroleum Geology, 17, 43–59.

Williams, G.D., Powell, C.M. and Cooper, M.A. 1989. Geometry and kinematics of inversion tectonics. Geological Society, London, Special Publications, 44, 3–15.

Yonkee, W.A. and Weil, A.B. 2015. Tectonic evolution of the Sevier and Laramide belts within the North American Cordillera orogenic system. Earth-Science Reviews, 150, 531–593.

Ziegler, P. A. 1990. Geological Atlas of Western and Central Europe, 2nd Edition, 239 pp. Shell Internationale Petroleum Maatschappij; The Hague. Geological Society; London.

11TH INTERNATIONAL
CRETACEOUS
SYMPOSIUM
Warsaw, Poland, 2022

AN OUTLINE OF THE PALAEOGEOGRAPHY AND LITHOFACIES EVOLUTION OF THE CRETACEOUS BASINS IN EXTRA-CARPATHIAN POLAND

Krzysztof Leszczyński

Polish Geological Institute – National Research Institute, 4 Rakowiecka Str.; 00-975 Warsaw, Poland;
e-mail: krzysztof.leszczynski@pgi.gov.pl

ABSTRACT

The palaeogeographical and lithofacies evolution of the Cretaceous basins of the extra-Carpathian Poland, is presented. These basins represented the easternmost part the Central European Basin system, and were the main seaways, particularly during the Late Cretaceous. The main tectonic feature of this basin system, controlling the facies distribution, palaeogeography and tectonic evolution was the Mid-Polish Trough stretching across the territory of Poland.

INTRODUCTION

The Cretaceous basins of extra-Carpathian Poland were part of the Central European Basin system, in which up to 10 km of Permian to Cenozoic deposits accumulated beneath epicontinental seaways. A prominent feature of this system was the Mid-Polish Trough, which stretched across Poland from the north-west to the south-east (Fig. 1). Its location was controlled by the Teisseyre–Tornquist Zone, the boundary between the East European Craton and the Palaeozoic Platform (e.g., Dadlez et al. 1995). The earliest foundations of the sedimentary basins in the Mid-Polish Trough date back to the early Permian, when continental rocks were first deposited, followed by the accumulation of the thick Zechstein salt series. The evolution of the late Permian to Danian epicontinental basin was impacted by both tectonic and eustatic factors, and furthermore strongly influenced by salt movements. Following Permian rifting, the basins experienced long-term thermal subsidence throughout the Mesozoic. Three stages of increased tectonic subsidence have been distinguished: in the late Permian–Early Triassic, Late Jurassic, and Cenomanian (Dadlez et al. 1995; Stephenson et al. 2003). The last led to the deposition of a thick Cenomanian to Danian succession of predominantly open-marine carbonate and carbonate-siliceous rocks. The final stage of the entire Late Cretaceous–Danian sedimentary megacycle was the Early Paleocene (Danian) relict basin. The axial zone of the Mid-Polish Trough ultimately inverted into the present-day Mid-Polish Anticlinorium: inversion processes initiated in the late Turonian and continued into the early Paleogene (e.g., Leszczyński 2002a, b, 2012; Krzywiec 2006). The palaeogeographic and lithofacies interpretations presented in this contribution are based chiefly on subsurface data from numerous boreholes.

EARLY CRETACEOUS

Palaeogeography

The Early Cretaceous epicontinental marine basin of Poland developed within the subsident Mid-Polish Trough (Fig. 1) during several transgressive-regressive cycles; however, marine conditions periodically expanded slightly outside the trough towards both the north-east and south-west (Marek 1988). In the Early Cretaceous, the Mid-Polish Trough was

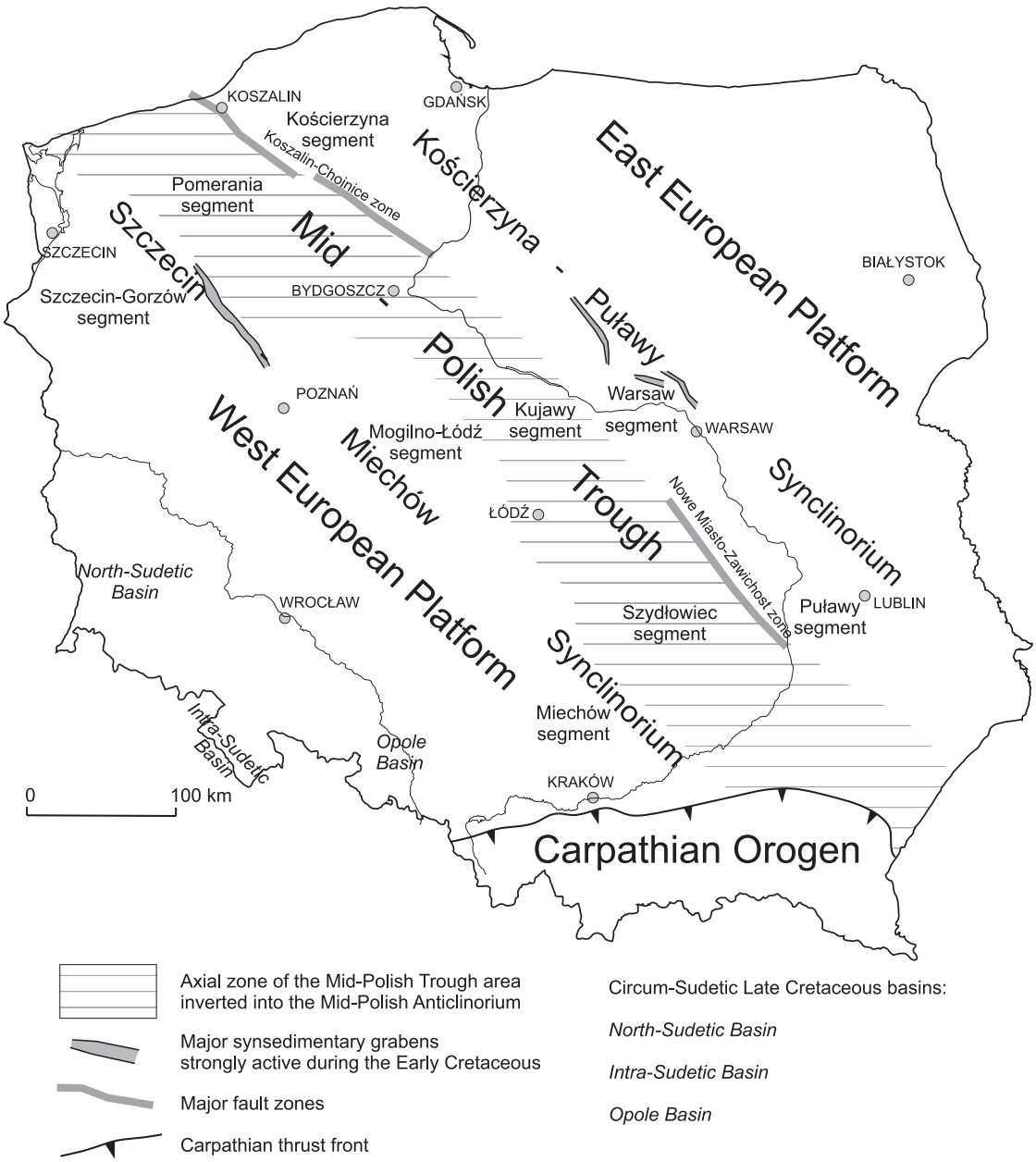

Fig. 1. Tectonic megaunits of Poland and position of the axial zone of the Mid-Polish Trough (based on Dadlez et al. 1998 and Żelaźniewicz et al. 2011, modified).

a narrow basin influenced by the Tethys and northern Boreal oceans, as well as by freshwater from surrounding land areas to the north-east and south-west (Marek 1997). Subsidence rates were highest in the central part (Kujawy segment) of the Mid-Polish Trough, resulting in Lower Cretaceous deposits that locally exceeded 700 m thickness (Vejbaek et al. 2010). The Kujawy segment also featured the most intense activity of low-amplitude salt movements during the Berriasian, Late Valanginian, Valanginian/Hauterivian transition, Barremian, and early Albian (Marek 1988). Near the borders of the Mid-Polish Trough, synsedimentary grabens were active during the Early Cretaceous, and are characterized by more complete and thicker sections compared to adjacent areas [the location of some major synsedimentary grabens are shown in Fig. 1]. As described below, these grabens were later subject to tec-

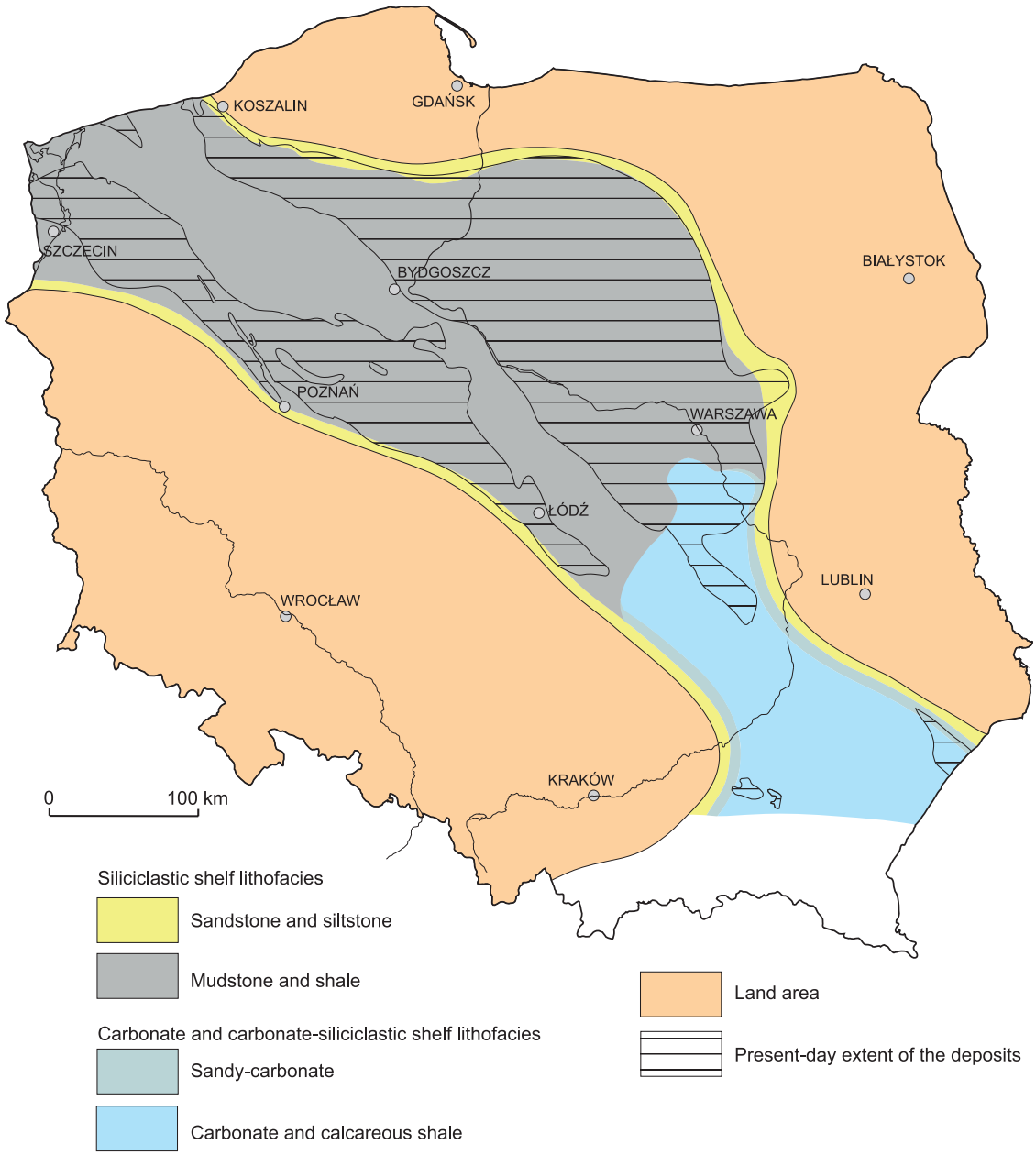

Fig. 2. Hauterivian lithofacies and palaeogeography.

tonic inversion in the Late Cretaceous. The Early Cretaceous basin is largely filled by siliciclastic lithofacies, although carbonate-marly lithofacies developed predominantly in the southeast. The biostratigraphy of Lower Cretaceous deposits in the Polish Basin is primarily based on ammonites; however, other groups – such as ostracods, bivalves, foraminifera, and selected other taxa – have considerable significance as well (Marek and Raczyńska 1979; Marek 1997).

Lithofacies development

The earliest Cretaceous basin (early Berriasian) represents the continuation and terminal stage of the Late Jurassic basin, with shallow-marine carbonate-sulphate (the latter, predominantly anhydrites) and shale-marly deposition with frequent coquina layers (Kcynia Formation) (Niemczycka and Brochwicz-Lewiński 1988), passing into limestones to the south-east

(Urbaniec et al. 2010; Pacześna and Sobień 2015).

A transgression initiated in the middle–late Berriasian led to the widespread high-stand deposition of upper Berriasian–lower lower Valanginian black shales (Rogoźno Formation) on a deeper-marine shelf, followed by a series of upper lower Valanginian shallow-marine (probably also deltaic? alluvial?) coarser-grained lithofacies – predominantly sandstones (Bodzanowo Formation). The next marine transgression, in conjunction with the expansion and widening of the basin, led to the accumulation of finer-grained lithofacies (Włocławek Formation) in the late Valanginian – and even widespread black shales in the Hauterivian (Fig. 2). These rocks contain siderites and iron ores that currently are of non-economic significance (Osika 1964). In the south-east, carbonate deposition continued throughout this interval.

The overlying series is mainly represented by Barremian–middle Albian sandstones, albeit it remains poorly documented biostratigraphically (Raczyńska 1979). These are relatively thick deposits (Mogilno Formation), exceeding 150 m in some areas, and locally provide thermal water at temperatures of up to 70°C (Sowiżdżał et al. 2020). In some deeper-marine zones of the basin, the middle part of this sequence is represented by a thin series of finer-grained mudstones and clay shales of presumed Aptian age (Raczyńska 1979). The late Albian was a interval of comparatively rapid relative sea level rise, resulting in a great transgression successively inundating coastal regions, representing the commencement of the Late Cretaceous megacycle (Marcinowski 1974). This transgressive event is marked with a basal sandstone layer containing abundant glauconite and phosphatic concretions. The Albian phosphorite deposits are well documented and were once mined in Poland, predominantly along the north-eastern margin of the Holy Cross Mountains, but currently the deposits are considered to be non-economic (Szuflicki et al. 2021). In the axial zone of the Mid-Polish Trough, sandy deposits grade into marls followed by limestones, demonstrating the (i) deepening of the marine basin and (ii) increasing distance from land (e.g., Jaskowiak-Schoeneichowa and Krassowska 1988).

LATE CRETACEOUS

Palaeogeography

The Late Cretaceous was an interval of high eustatic sea level and widespread carbonate deposition at a global scale (e.g., Hancock and Kauffman 1979). Increased subsidence rates in the NW-SE-trending Mid-Polish Trough (Fig. 1) resulted in the deposition of a thick marine succession of mainly carbonate and carbonate-siliceous rocks, which in some areas exceeded 2500 m (Vejbaek et al. 2010; Leszczyński 2012). Connections to the Boreal and Tethyan seas were unrestricted (Jaskowiak-Schoeneichowa and Krassowska 1988; Krassowska 1997). Small islands probably existed in southern Poland.

Tectonic inversion processes in the axial part of the Mid-Polish Trough most likely began in the late Turonian, activating (i) salt movements, to form salt structures, and (ii) pre-existing faults, as reverse faults (e.g., Leszczyński 2002a, b, 2012; Krzywiec 2006). Synsedimentary grabens (cf. Fig. 1), active zones of subsidence in the Early Cretaceous, also inverted: their Upper Cretaceous infills are thinner than in the surrounding depositional settings. Palaeogeographic reconstructions and basin modelling suggest that inversion resulted in the removal of some 1 to >2 km of Upper Cretaceous deposits in the Mid-Polish Anticlinorium; in the Kujawy segment, in particular, the basal Zechstein was elevated by 4 km (Dadlez et al. 1997; Dadlez 2001; Wagner et al. 2002; Resak et al. 2008).

The withdrawal of Zechstein salt deposits from synclinal areas was active throughout the Cretaceous, but intensified from the late Turonian–Coniacian onwards, due to ongoing tectonic inversion (Cieśliński and Jaskowiak 1973; Leszczyński 2000). In turn, this withdrawal significantly influenced sea-floor topography and basin bathymetry, resulting in the development of both deeper and shallower zones within the basin. Deeply rooted fault systems in north-west and central Poland – that is, in the Koszalin–Chojnice, Drawno–Człopa–Szamotuły, and Gopło–Ponętów–Wartkowice zones – were active during sedimentation and played a significant role in lithofacies distribution (Dadlez and Marek 1974; Jaskowiak-Schoeneichowa 1976; Leszczyński 2002a, b). Faults influential in Late Cretaceous sedimen-

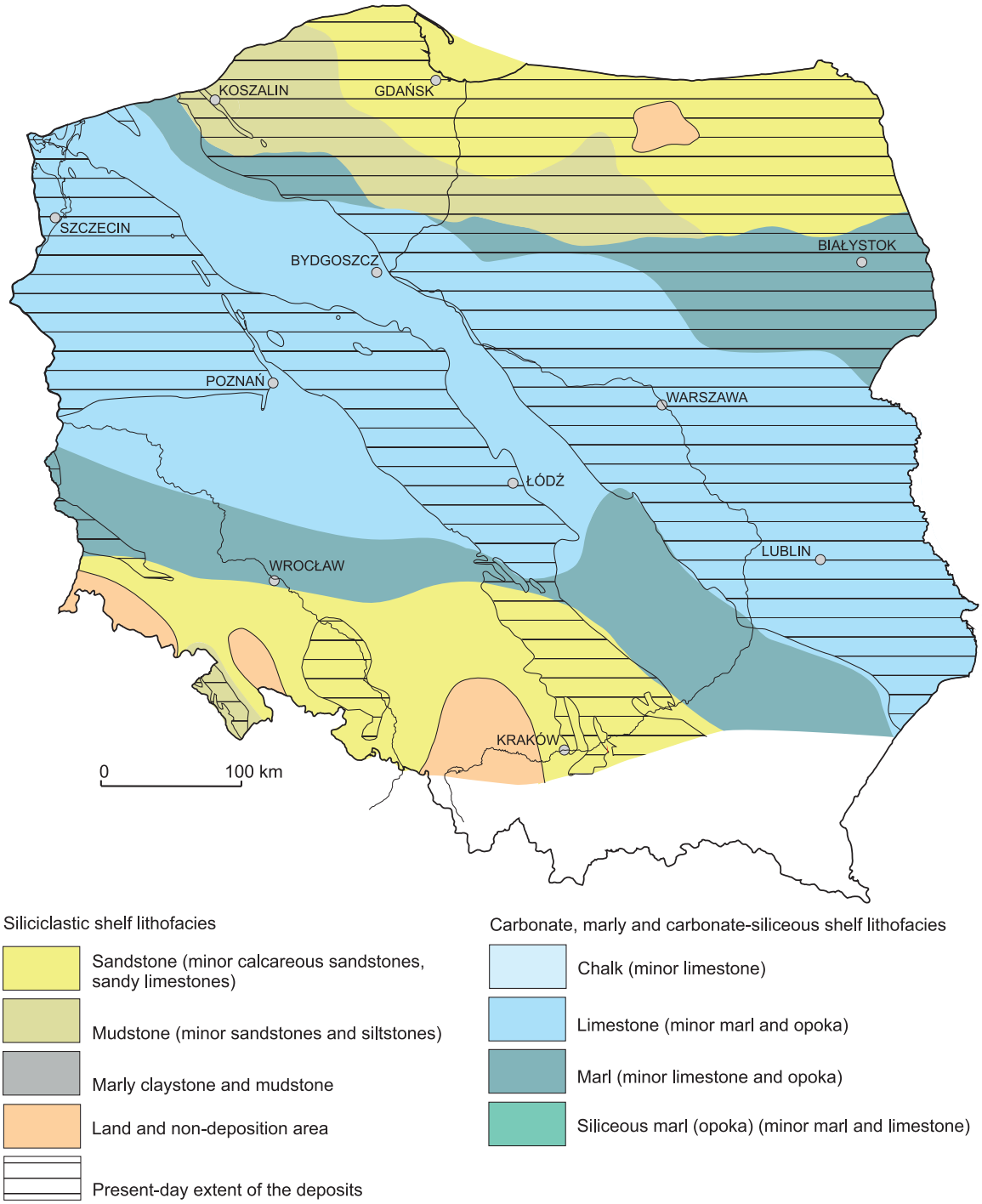

Fig. 3. Cenomanian lithofacies and palaeogeography.

tation patterns have also been identified within the basement of the Holy Cross Mountains and of the Lublin area in south-east Poland (Hakenberg and Świdrowska 1998; Świdrowska 2007).

Lithofacies development

Overall, the lithofacies pattern of the Upper Cretaceous succession exhibits (i) a general trend of continuous carbonate/chalk sedimen-

tation in north-western and eastern Poland, (ii) carbonate deposition, later replaced largely by carbonate-siliciclastic lithofacies in the Mid-Polish Trough, and (iii) siliciclastic-dominated lithofacies extending to the north. The greatest variety of lithofacies styles are present in the latter: here, the lithofacies pattern is constrained by both inversion processes and the supply of Scandinavian clastic material, due to its proximity to the emergent Baltic Shield.

In the south, shallow shelf marly deposition was predominant in the Opole Basin, an erosional relic of an originally larger depositional area connected to the Mid-Polish Trough marine basin. Marly and siliciclastic lithofacies exist in the other circum-Sudetic basins.

In the Late Cretaceous, nearshore, shallow shelf environments in the Polish Basin exhibited siliciclastic and siliciclastic-carbonate (marly) lithofacies. In deeper, more distal shelf areas, carbonate deposition (including both chalks and limestones) prevailed. It appears that the deposition of carbonate-siliceous (opoka) strata – which first became prominent during the Turonian and was the dominant lithology in the Polish Lowlands until the Maastrichtian and Danian – and marls could occur in both shallow (if a greater-than-average quantity of terrigenous material was present) and deeper shelf environments (Jaskowiak-Schoeneichowa and Krassowska 1988; Krassowska 1997; Leszczyński 1997, 2010). Along the flanks of the Mid-Polish Anticlinorium, which progressively uplifted during the Late Cretaceous, inversion-related contour current deposits have been interpreted (Krzywiec et al. 2018). Local sand bodies near rising anticline crests and the uplifting Mid-Polish Anticlinorium have also been interpreted as gravity flow deposits forming submarine fan-type bodies within the open-marine carbonate-siliceous deposits typical of deeper marine environments in the Santonian and Campanian (Jaskowiak-Schoeneichowa 1977; Leszczyński 2000, 2002a). Similar submarine slides and/or fans are also observed on seismic profiles within the Campanian–Maastrichtian succession in the Nowe Miasto–Zawichost Fault Zone (Krzywiec et al. 2009).

A characteristic feature of carbonate-dominated sequences in the Late Cretaceous Polish Basin is the existence of gradual transitions between individual lithologies: that is, chalk → marly chalk → chalk-like limestone → limestone → marly limestone → marl → opoka (siliceous carbonates) → gaize (a fine-grained, carbonate-siliceous lithology of sedimentary origin, which is porous due to the presence of abundant sponge spicules).

Late Cretaceous lithofacies development in the Mid-Polish Basin was strongly influenced by eustatic and tectonic processes, the latter predominantly inversion-related, in combination with halotectonic activity. These, predictably, influenced the creation, stability, and destruction of accommodation space, carbonate productivity, the supply of clastic material derived from land and rising salt structures, and the location and timing of sedimentary gaps and hardgrounds at a regional scale (Leszczyński 2017). In the Upper Cretaceous carbonate succession, hardground surfaces have been identified in many regions throughout the Polish Basin. They developed due to regressive events related to eustatic sea-level fall and the uplift of salt-cored anticlines, reflecting – to a certain extent – depositional cyclicity in the basin (Krassowska 1973, 1986; Marcinowski 1974; Jaskowiak-Schoeneichowa 1979, 1981; Jaskowiak-Schoeneichowa and Krassowska 1983; Walaszczyk 1992; Olszewska-Nejbert 2004; Leszczyński 2017). Increased bottom sea current activity may have also played an important role in hardground formation. However, the main factors controlling sedimentation and lithofacies were the distance from the shoreline, the topography of both emergent land and the seafloor, and climate, which in the Late Cretaceous was relatively stable with low-magnitude variability due to the existence of extensive epicontinental seas.

As described above, the transgressive Albian seaway expanded considerably beyond the Mid-Polish Trough. Marine transgression continued during the Cenomanian, leading to the deposition of carbonates (limestones) in a wide belt stretching east to west across the Polish Lowlands (Fig. 3). Its northern and southern flanks were marked by a marly depositional zone. Even further to the north (to the east of Koszalin) and south, siliciclastic (sandstones, mudstones) and siliciclastic-carbonate (mainly calcareous sandstones and sandy limestones, with gaize locally) lithofacies constitute the entire Cenomanian section. In the north, clastic material was most likely derived from the emergent Baltic Shield. Chalk lithofacies are

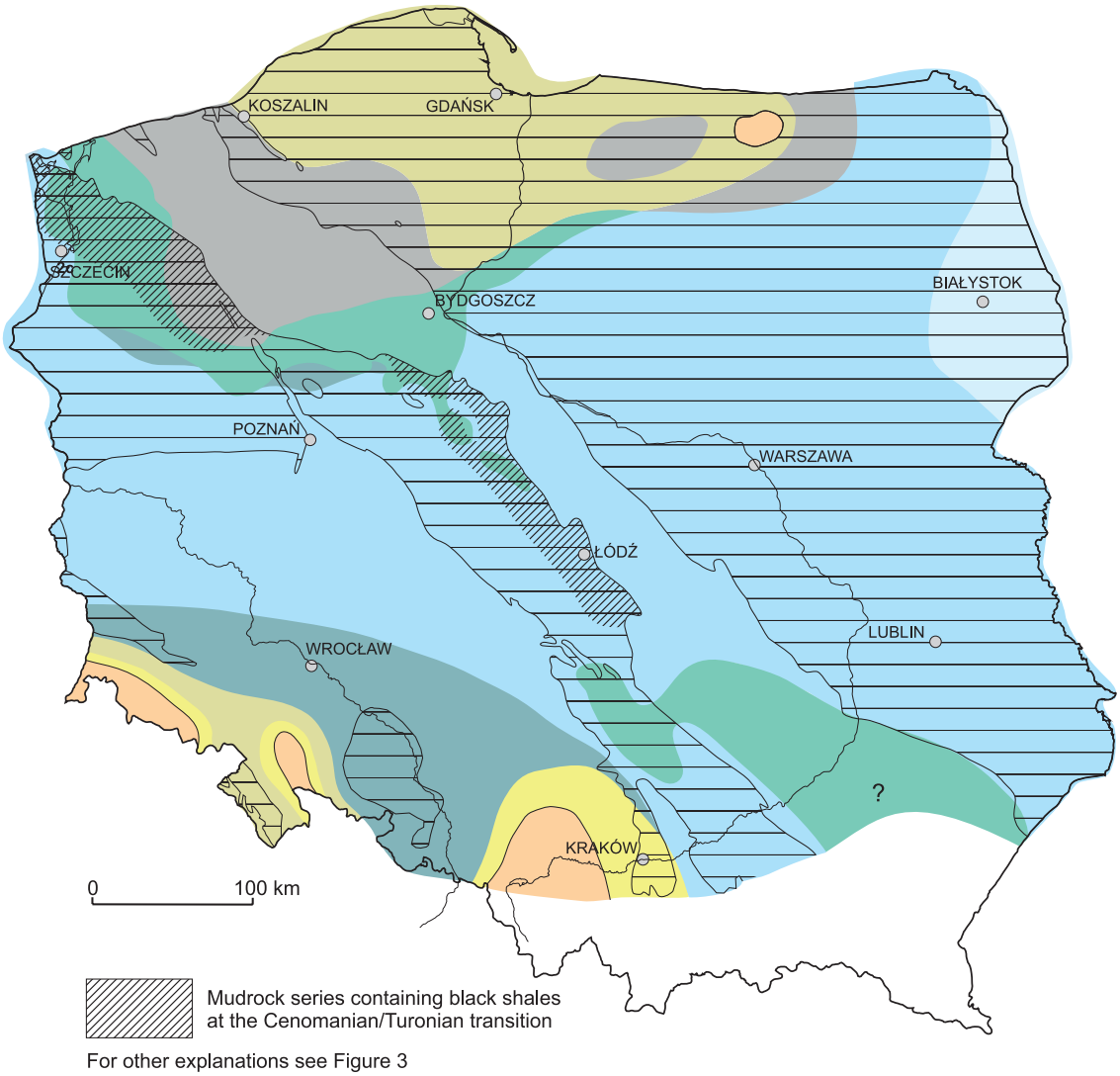

Fig. 4. Early Turonian lithofacies and palaeogeography.

observed only in the Wolin Island region, in the north-western extreme of Poland. In the southern areas, the most common lithofacies are various styles of sandstones, frequently containing calcium carbonate to a more-or-less extensive degree. In general, the vertical Upper Albian–Cenomanian succession represents a continuously expanding and deepening sedimentary basin, progressing from shallow shelf siliciclastic and siliciclastic-carbonate deposition to open-marine carbonate deposition on a deeper shelf.

In the Turonian, the retreat of siliciclastic lithofacies and their successive replacement by carbonate and chalk lithofacies is observed in north-eastern Poland (Białystok region; Fig. 4). Concurrently, in the late Turonian and Coniacian the development of carbonate-siliceous lithofacies (opoka) occurred, most notably in north-west and central Poland (e.g., Jaskowiak-Schoeneichowa and Krassowska 1988; Leszczyński 2012) and further to the south-east along the slope of the present-day Mid-Polish Anticlinorium (e.g., Walaszczyk 1992). In the Pomerania segment of the Mid-Polish Trough, clay-marly and muddy-marly sedimentation prevailed. Muddy-marly and muddy-sandy-marly lithofacies are dominant towards the north-east (Kościerzyna segment of the Kościerzyna–Puławy Synclinorium), with

a higher proportion of sand and sandy-glauconitic lithofacies (Jaskowiak-Schoeneichowa 1976). The Koszalin–Chojnice tectonic zone, an important palaeotectonic and palaeogeographic element, served as a barrier to the expansion of the siliciclastic facies from the Łeba Elevation and Peribaltic Syneclise, which were both especially well pronounced during the Coniacian and Santonian (Fig. 1). However, the dominant lithofacies across the Polish Lowlands remained open-marine carbonates (organogenic, organodetrital, and pelitic limestones), often accompanied by marls (Jaskowiak-Schoeneichowa 1972, 1977; Leszczyński 2002b).

Eastern and north-eastern Poland were areas of calm, open-marine pelagic chalk and chalk-like limestone sedimentation, especially from the late Turonian onwards (Krassowska 1986, 1997). Carbonate and marly deposition expanded southwards, encompassing most of the Opole and North-Sudetic basins (e.g., Milewicz 1979; Walaszczyk 1992). The siliciclastic deposition of mudstones and sandstones (e.g., the Quader Sandstone), locally accompanied by marls, continued in the Intra-Sudetic Basin (e.g., Radwański 1975). Over a large expanse of the Szczecin–Miechów Synclinorium – close to the slope of the present-day Mid-Polish Anticlinorium – thin black shale layers are observed within a mudrock series at the Cenomanian/Turonian boundary (Jaskowiak-Schoeneichowa 1972, 1977, 1987; Leszczyński 2002a, 2012). These rocks show depositional features suggestive of preferentially hypoxic accumulation, and are potentially correlative with Oceanic Anoxic Event 2, also referred to as the Bonarelli Event (e.g., Schlanger and Jenkyns 1976; Jenkyns 1980; Arthur et al. 1987).

The carbonate-siliceous lithofacies (opoka – see Jaskowiak-Schoeneichowa 1981; Jurkowska 2022) is very common in the upper Turonian and Coniacian, covering large portions of the Mid-Polish Trough Basin. To the south-west and east of the carbonate-siliceous zone, marly and carbonate (limestone) lithofacies are dominant, passing further east into chalk on the East European Craton (Jaskowiak-Schoeneichowa 1979; Leszczyński 2010, 2012). Intriguingly, siliciclastic lithofacies occur close to the south-western slope of the present-day Mid-Polish Anticlinorium, deposited as a consequence of the uplifting Mid-Polish Anticlinorium and rising salt-cored anticline crests (Jaskowiak-Schoeneichowa 1972, 1977, 1987; Leszczyński 2012). On both salt-cored (Jaskowiak-Schoeneichowa 1972, 1981) and some non-salt structures (Jaskowiak-Schoeneichowa 1976; Leszczyński 2002b), stratigraphic gaps are observed in Upper Cretaceous sections. North of the Koszalin–Chojnice Zone, there is a transition to muddy-marly and sandy lithofacies that extend as far north-east as the Vistula Lagoon (Leszczyński 2002b). In south-western Poland, clayey marls and mudstones predominate in the Opole Basin (Walaszczyk 1992), marls passing southwards into siliciclastic (even sandy) deposits are reported from the North-Sudetic Basin (e.g., Milewicz 1979), and a thick series of siliciclastic rocks (predominantly sandstones) occurs in the Intra-Sudetic Basin (e.g., Radwański 1975). All of these basins represent deposition close to the emergent Sudetic islands.

A similar lithofacies distribution pattern is observed in the Santonian; locally, however, marly lithofacies are more common. Siliciclastic lithofacies in north-western Poland, along the south-western slope of the present-day Mid-Polish Anticlinorium (the transition from the Szczecin–Gorzów to the Pomerania segment), are separated from the siliciclastic deposits of the Kościerzyna segment by a belt of carbonate-siliciclastic lithofacies stretching to the south-west of the Koszalin–Chojnice Zone. A similar situation reappears once more in the Campanian, and is suggestive of different clastic sources to these areas.

A large non-depositional area has been interpreted east of Olsztyn, in north-east Poland (Jaskowiak-Schoeneichowa and Krassowska 1988; Leszczyński 2012). Sedimentary and/or erosional gaps are recorded on salt-cored anticlines in the central part of the Mid-Polish Trough (Jaskowiak-Schoeneichowa 1977, 1981; Leszczyński 2002b), and in the Koszalin-Chojnice Zone (Jaskowiak-Schoeneichowa 1976; Leszczyński 2002b).

During the Santonian, marine conditions progressively retreated from the circum-Sudetic basins in south-western Poland. In the North-Sudetic Basin, the Santonian is represented by local siliciclastic deposits containing thin coal beds (Milewicz 1985, 2006).

The general lithofacies distribution pat-

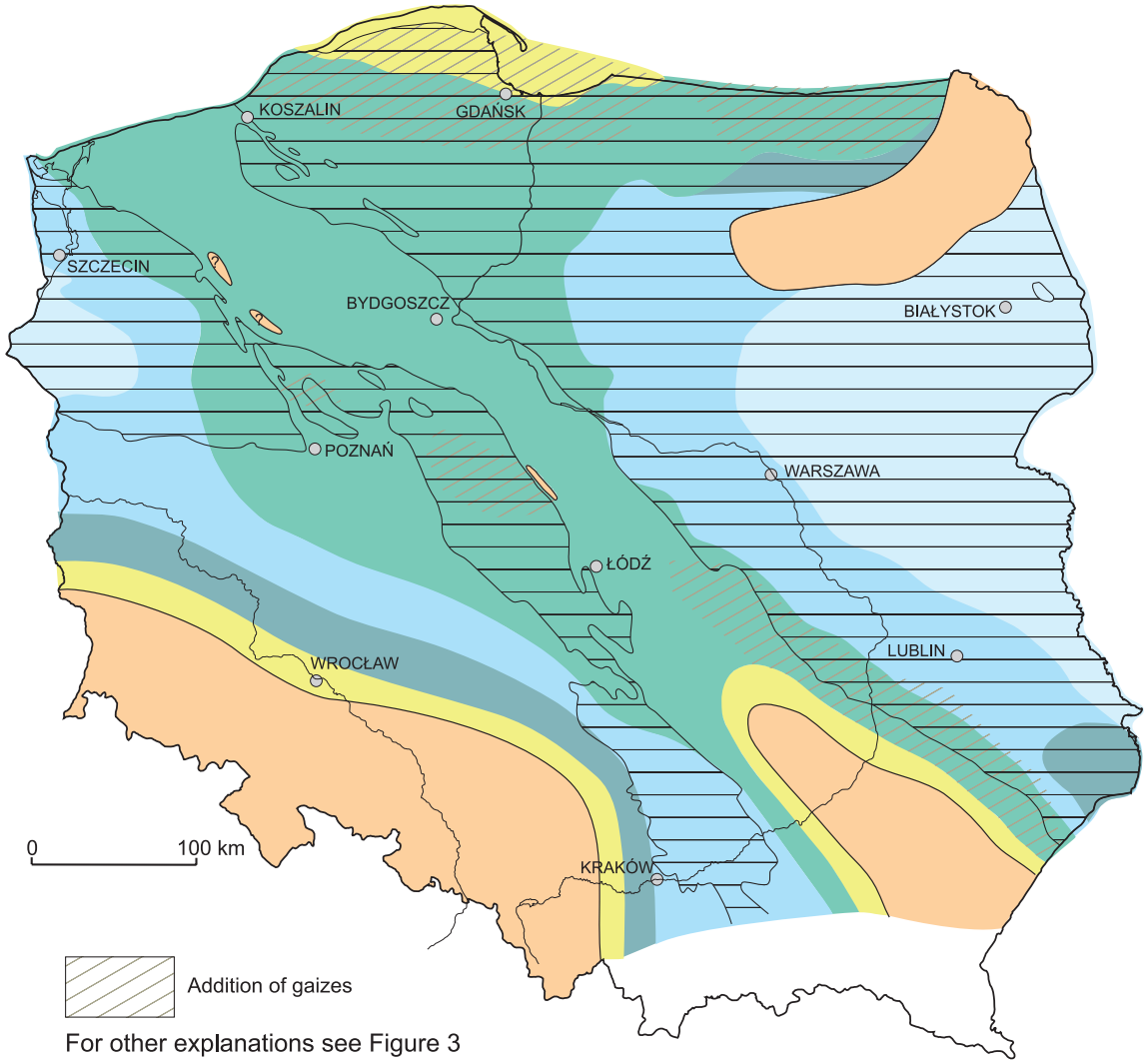

Fig. 5. Campanian lithofacies and palaeogeography.

tern in the Campanian is also roughly similar to the late Turonian–Santonian (Fig. 5). A characteristic distinguishing feature, however, is the higher proportion of carbonates at the expense of carbonate-siliceous rocks, and the smaller extent of siliciclastic deposition in northern Poland, where carbonate-siliceous and, locally, marly lithofacies predominate. Carbonate-siliceous lithofacies stretch in a wide belt along the Mid-Polish Trough and adjoining areas from the Baltic coast towards the Szydłowiec (Holy Cross Mountains) segment of the Mid-Polish Trough. Chalk, accompanied by limestones, appears in north-western Poland. Carbonate and predominantly chalk lithofacies occupy a wide expanse, from Olsztyn and Białystok through Mazowsze to the north-east Lublin region, and further east towards the Ukrainian and Belarusian border. The carbonate-siliceous lithofacies of the Pomeranian segment grade north-eastwards to sandy lithofacies (Jaskowiak-Schoeneichowa 1976). A land area possibly existed in south-eastern Poland in the axial part of the Mid-Polish Trough, where Remin et al. (2022), remarkably, report the presence of a tectonically activated deltaic system in the Lublin Trough.

A particularly important lithological component of Campanian deposits is gaize – including calcareous and sandy variations – which is present predominantly in northern Poland. Local sandstone bodies occur in some areas

within the Mid-Polish Trough, particularly along the south-western slope of the present-day Mid-Polish Anticlinorium near rising salt diapirs (Jaskowiak-Schoeneichowa 1977, 1981; Leszczyński 2000, 2002a).

The non-depositional area in north-east Poland, previously observed in the Santonian, shrank slightly and moved towards the south (Jaskowiak-Schoeneichowa and Krassowska 1988). Local sedimentary gaps are observed in the Koszalin–Chojnice Zone (Jaskowiak-Schoeneichowa 1976; Leszczyński 2002b). The maximum subsidence rates and thickest deposits were located in the Mogilno–Łódź segment of the Szczecin–Miechów Synclinorium.

Strata assigned to the Maastrichtian occupy a smaller area than in previous ages, and sections are commonly incomplete due to Cenozoic erosion. They demonstrate greater lithofacies variability, both vertically and laterally, due to oscillatory sea-level changes manifested in repeated transgressions and regressions (Jaskowiak-Schoeneichowa and Krassowska 1988). In central Poland and further north towards the Gulf of Gdańsk, deposits largely consist of a dominant carbonate-siliceous (opoka) lithofacies. The Maastrichtian of Poland also stretches to the south-east in the Mid-Polish Trough, where sandy and carbonate-sandy lithofacies also play an important role. The carbonate-siliceous lithofacies is fringed to the east and west by carbonate and chalk lithofacies, as in the Campanian (Fig. 5). Carbonate-sandy (calcareous sandstones, sandy limestones, and sandy marls with interbedded gaize) and siliciclastic deposits are the predominant lithofacies in Pomerania. Gaizes are very common throughout the basin, especially in north-eastern Poland, where marly deposition is also the most widespread. To the north and north-west of Warsaw (the Warsaw segment of the Kościerzyna–Puławy Synclinorium), an unconformity separating Campanian deposits from the overlying upper Maastrichtian has been identified in seismic sections (Stachowska and Krzywiec 2021) with a gap, probably spanning the uppermost Campanian–lower Maastrichtian. A hardground close to the unconformity has been reported from this area (Jaskowiak-Schoeneichowa and Krassowska 1983; Leszczyński 2017). The zone of maximum subsidence was in the Puławy segment and the south-eastern part of the Warsaw segment of the Kościerzyna–Puławy Synclinorium (Krassowska 1997; Świdrowska et al. 2008).

Lower Paleocene (Danian) deposits (mainly carbonate-siliceous and marly lithofacies) in the Polish Lowlands are only known to the northeast of the Mid-Polish Anticlinorium. In most areas, they are separated from the Upper Cretaceous by a distinct stratigraphic gap (Popiel 1977; Krassowska 1986; Jaskowiak-Schoeneichowa and Krassowska 1988). The Maastrichtian/Danian boundary is locally manifested as a hardground (e.g., Popiel 1977) or an erosional-omission surface (Machalski 1998). In the Lublin region, Maastrichtian deposits locally pass into the Danian without any sedimentary breaks (Krassowska 1986; Racki et al. 2011).

REFERENCES

Arthur, M.A., Schlanger, S.O. and Jenkyns H.C. 1987. The Cenomanian/Turonian Oceanic Anoxic Event, II. Palaeoceanographic controls on organic-matter production and preservation. Geological Society, London, Special Publication, 26, 401–420.

Dadlez, R. 2001. Mid-Polish Trough – geological cross-sections. Państwowy Instytut Geologiczny Warszawa. [In Polish]

Dadlez, R. and Marek, S. 1974. General outline of the tectonics of the Zechstein-Mesozoic complex in central and northwestern Poland. Biuletyn Instytutu Geologicznego, 274, 111–148. [In Polish]

Dadlez, R., Narkiewicz, M, Stephenson, R.A., Visser, M.T. and Van Wees, J.-D. 1995. Tectonic evolution of the Mid-Polish Trough: modelling implications and significance for central European geology. Tectonophysics, 252, 179–195.

Dadlez, R., Jóźwiak, W. and Młynarski, S. 1997. Subsidence and inversion in the western part of Polish basin – data from seismic velocities. Geological Quarterly, 41, 197–208.

Dadlez, R., Iwanow, A., Leszczyński, K. and Marek, S. 1998. Tectonic map of the Zechstein-Mesozoic complex, 1:500 000. Państwowy Instytut Geologiczny. Warszawa

Hakenberg, M. and Świdrowska, J. 1998. Evolution of the Holy Cross segment of the Mid-Polish Trough during the Cretaceous. Geological Quarterly, 42, 239–262.

Hancock, J.M. and Kauffman, E.G. 1979. The great transgressions of the Late Cretaceous. Journal of the Geological Society, 136, 175–186.

Jaskowiak-Schoeneichowa, M. 1972. The Upper Cretaceous in the Mogilno-Łódź Trough. Kwartalnik Geologiczny, 16, 315–329. [In Polish]

Jaskowiak-Schoeneichowa, M. 1976. Kreda górna (łącznie z albem górnym i paleocenem dolnym). In: Dadlez, R. (Ed.), Permian and Mesozoic of the Pomerania Trough, Prace Instytutu Geologicznego, 79, 94–105.

Jaskowiak-Schoeneichowa, M. 1977. Kreda górna. In: Marek, S. (Ed.), Geological structure of the eastern part of the Mogilno-Łódź Trough (Gopło–Ponętów–Pabianice Zone), Prace Instytutu Geologicznego, 80, 99–112.

Jaskowiak-Schoeneichowa, M. 1979. Upper Cretaceous (including Upper Albian). In: Jaskowiak-Schoeneichowa, M. (Ed.), The geological structure of the Szczecin Trough and Gorzów Block, Prace Instytutu Geologicznego, 96, 77–90. [In Polish]

Jaskowiak-Schoeneichowa, M. 1981. Upper Cretaceous sedimentation and stratigraphy in north-western Poland. Prace Instytutu Geologicznego, 98, 91 pp. [In Polish]

Jaskowiak-Schoeneichowa, M. 1987. Kreda górna. In: Raczyńska, A. (Ed.), Geological structure of the Pomeranian Swell and its basement. Prace Instytutu Geologicznego, 119, 140–151.

Jaskowiak-Schoeneichowa, M. and Krassowska, A. 1983. Kreda górna. In: Marek, S. (Ed.), The geological structure of the Warsaw (Płock) Trough and its basement. Prace Instytutu Geologicznego, 103, 177–197.

Jaskowiak-Schoeneichowa, M. and Krassowska, A. 1988. Palaeothickness, lithofacies and palaeotectonics of the epicontinental Upper Cretaceous in Poland. Kwartalnik Geologiczny, 32, 177–198. [In Polish]

Jenkyns, H. C. 1980. Cretaceous anoxic events: from continents to oceans. Journal of the Geological Society, 137, 171–188.

Jurkowska, A. 2022. The biotic-abiotic control of Si burial in marine carbonate systems of the pre-Eocene Si cycle. Global Biogeochemical Cycles, 36, 1–20.

Krassowska, A. 1973. Alb górny, kreda górna i paleocen. In: Krassowska, A. (Ed.), Profile Głębokich Otworów Wiertniczych Instytutu Geologicznego. Magnuszew IG 1, 4, 165–182.

Krassowska, A. 1986. The Upper Cretaceous and Lower Paleocene in the vicinity of Lublin. Kwartalnik Geologiczny, 30, 559–574. [In Polish]

Krassowska, A. 1997. Kreda górna. Sedymentacja, paleogeografia i paleotektonika. In: Marek, S. and Pajchlowa, M. (Eds), Epicontinental Permian and Mesozoic in Poland, Prace Instytutu Geologicznego, 153, 386–402. [In Polish]

Krzywiec, P. 2006. Structural inversion of the Pomeranian and Kuiavian segments of the Mid-Polish Trough – lateral variations in timing and structural style. Geological Quarterly, 51, 151–168.

Krzywiec, P., Gutowski, J., Walaszczyk, I., Wróbel, G. and Wybraniec, S. 2009. Tectonostratigraphic model of the Late Cretaceous inversion along the Nowe Miasto–Zawichost Fault Zone, SE Mid-Polish Trough. Geological Quarterly, 53, 27–48.

Krzywiec, P., Stachowska, A., Schattner, U. and Popiela, A. 2018. Inversion-related Upper Cretaceous contourites within the Polish Basin – their seismic expression and geodynamic significance. 18th International SEISMIX Symposium "Seismology between the Poles" 17–22.06.2018, Cracow

Leszczyński, K. 1997. The Upper Cretaceous carbonate-dominated sequences of the Polish Lowlands. Geological Quarterly, 41, 521–532.

Leszczyński, K. 2000. The Late Cretaceous sedimentation and subsidence south-west of the Kłodawa Salt Diapir, central Poland. Geological Quarterly, 44, 167–174.

Leszczyński, K. 2002a. The Cretaceous evolution of the Ponętów–Wartkowice Zone (in Polish). Prace Państwowego Instytutu Geologicznego, 176, 96 pp. [In Polish]

Leszczyński, K. 2002b. The Late Cretaceous inversion and salt tectonics in the Koszalin–Chojnice and Drawno–Człopa–Szamotuły Zones, Pomeranian segment of the Mid-Polish Trough. Geological Quarterly, 46, 347–362.

Leszczyński, K. 2010. Lithofacies evolution of the Late Cretaceous basin in the Polish Lowlands. Biuletyn Państwowego Instytutu Geologicznego, 443, 33–54. [In Polish]

Leszczyński, K. 2012. The internal geometry and lithofacies pattern of the Upper Cretaceous–Danian sequence in the Polish Lowlands. Geological Quarterly, 56, 363–386.

Leszczyński, K. 2017. The significance of Upper Cretaceous hardgrounds and other discontinuity surfaces for basin-wide correlations, based on drillcore data from boreholes in northern Poland. Geological Quarterly, 61, 825–844.

Machalski, M. 1998. The Cretaceous–Tertiary boundary in Central Poland. Przegląd Geologiczny, 46, 1153–1161. [In Polish]

Marcinowski, R. 1974. The transgressive Cretaceous (Upper Albian through Turonian) deposits of the Polish Jura Chain. Acta Geologica Polonica, 24, 117–217.

Marek, S. 1988. Palaeothickness, lithofacies and palaeotectonics of the epicontinental Lower Cretaceous in Poland. Kwartalnik Geologiczny, 32, 157–174. [In Polish]

Marek, S. 1997. Kreda dolna (berias-alb górny). Sedymentacja, paleogeografia i paleotektonika. In: Marek, S. and Pajchlowa, M. (Eds), Epicontinental Permian and Mesozoic in Poland, Prace Instytutu Geologicznego, 153, 362–366. [In Polish]

Marek, S. and Raczyńska, A. 1979. Lithostratigraphic subdivision of epicontinental Lower Cretaceous in Poland and proposals for its rearrangement. Kwartalnik Geologiczny, 23, 631–637.

Milewicz, J. 1979. Distribution of Cretaceous rocks in the

North-Sudetic Basin. Kwartalnik Geologiczny, 23, 819–826. [In Polish]

Milewicz, J. 1985. A proposal of formal stratigraphic subdivision of the infill of the North Sudetic Depression. Przegląd Geologiczny, 33, 385–390. [In Polish]

Milewicz, J. 2006. On Santonian deposits within the North Sudetic Basin. Przegląd Geologiczny, 54, 693–694. [In Polish]

Niemczycka, T. and Brochwicz-Lewiński, W. 1988. Evolution of the Upper Jurassic sedimentary basin in the Polish Lowland. Kwartalnik Geologiczny, 32, 137–155. [In Polish]

Olszewska-Nejbert, D. 2004. Development of the Turonian/Coniacian hardground boundary in the Cracow Swell area (Wielkanoc quarry, Southern Poland). Geological Quarterly, 48, 159–170.

Osika, R. 1964. Prospects in search for iron ore deposits in the Mesozoic formations of Poland. *Kwartalnik Geologiczny,* 8, 559–572. [In Polish]

Pacześna, J. and Sobień, K. (Eds) 2015. Profile Głębokich Otworów Wiertniczych – Narol IG1 1, Narol PIG 2, 143. Warszawa.

Popiel, J. S. 1977. Lithology and stratigraphy of the uppermost Maastrichtian deposits from the Lublin and Chełm areas. Kwartalnik Geologiczny, 21, 515–526. [In Polish]

Racki, G., Machalski, M., Koeberl, C. and Harasimiuk, M. 2011. The weathering-modified iridium record of a new Cretaceous–Palaeogene site at Lechówka near Chełm, SE Poland, and its palaeobiologic implications. Acta Palaeontologica Polonica, 56, 205–215.

Raczyńska, A. 1979. Kreda dolna (bez albu górnego). In: Jaskowiak-Schoeneichowa, M. (Ed.), The geological structure of the Szczecin Trough and Gorzów Block, Prace Instytutu Geologicznego, 96, 69–77. [In Polish]

Radwański, S. 1975. Cretaceous of the Central Sudety Mountains in the light of results of new boreholes. Biuletyn Instytutu Geologicznego, 187, 5–59. [In Polish]

Remin, Z., Cyglicki, M. and Niechwedowicz, M. 2022. Deep vs. shallow – two contrasting theories? A tectonically activated Late Cretaceous deltaic system in the axial part of the Mid-Polish Trough: a case study from southeast Poland. Solid Earth, 13, 681–703. https://doi.org/10.5194/se-13-681–2022

Resak, M., Narkiewicz, M. and Littke, R. 2008. New basin modelling results from the Polish part of the Central European Basin system: implications for the Late Cretaceous–Early Paleogene structural inversion. International Journal of Earth Sciences, 97, 955–972.

Schlanger, S. O. and Jenkyns, H. C. 1976. Cretaceous oceanic anoxic events: causes and consequences. Geologie en Mijnbouw, 55, 179–184.

Sowiżdżał, A., Hajto, M. and Hałaj, E. 2020. Thermal waters of central Poland: a case study from Mogilno-Łódź Trough, Poland. Environmental Earth Sciences, 79, 112. https://doi.org/10.1007/s12665-020-8855-2

Stachowska, A. and Krzywiec, P. 2021. Depositional architecture of the Upper Cretaceous succession in central Poland (Grudziądz-Polik area) based on regional seismic data. Geological Quarterly, 65, 21.

Stephenson, R. A., Narkiewicz, M., Dadlez, R., Van Wees, J.-D. and Andriessen, P. 2003. Tectonic subsidence modelling of the Polish Basin in the light of new data on crustal structure and magnitude of inversion. Sedimentary Geology, 156, 59–79.

Szuflicki, M., Malon, A. and Tymiński, M. (Eds) 2021. The Balance of Mineral Resources Deposits in Poland as of 31 XII 2020. Państwowy Instytut Geologiczny, Warszawa. [In Polish]

Świdrowska, J. 2007. Cretaceous in Lublin area – sedimentation and tectonic conditions. Biuletyn Państwowego Instytutu Geologicznego, 422, 63–78. [In Polish]

Świdrowska, J., Hakenberg, M., Poluhtovič, B., Seghedi, A. and Višnâkov, I. 2008. Evolution of the Mesozoic basins on the southwestern edge of the East European Craton (Poland, Ukraine, Moldavia, Romania). Studia Geologica Polonica, 130, 3–130.

Urbaniec, A., Bobrek, L. and Świetlik, B. 2010. Lithostratigraphy and micropalaeontological characteristic of Lower Cretaceous strata in central part of the Carpathian Foreland. Przegląd Geologiczny, 58, 1161–1175. [In Polish]

Vejbaek, O.V., Andersen, C., Dusar, M., Herngreen, G.F.W., Krabbe, H., Leszczyński, K., Lott, G.K., Mutterlose, J. and Van Der Molen, A.S. 2010. Cretaceous. In: Doornenbal, J.C. and Stevenson, A.G. (Eds), Petroleum Geological Atlas of the Southern Permian Basin Area. EAGE Publications b.v. Houten), 195–209.

Wagner, R., Leszczyński, K., Pokorski, J. and Gumulak, K. 2002. Paleotectonic cross-sections through the Mid-Polish Trough. Geological Quarterly, 46, 293–306.

Walaszczyk, I. 1992. Turonian through Santonian deposits of the Central Polish Uplands; their facies development, inoceramid paleontology and stratigraphy. Acta Geologica Polonica, 42, 1–122.

Żelaźniewicz, A., Aleksandrowski, P., Buła, Z., Konon, A., Oszczypko, N., Ślączka, A., Żaba, J. and Żytko, K. 2011. Regionalizacja tektoniczna Polski. Komitet Nauk Geologicznych PAN, Drukarnia KID.

11TH INTERNATIONAL
CRETACEOUS
SYMPOSIUM
Warsaw, Poland, 2022

THE END OF AN ERA: A RECORD OF EVENTS ACROSS THE CRETACEOUS–PALEOGENE BOUNDARY IN POLAND

Marcin Machalski[1]| Ewa Świerczewska-Gładysz[2]| Danuta Olszewska-Nejbert[3]

1| Institute of Paleobiology, Polish Academy of Sciences, ul. Twarda 51/55, 00-818 Warszawa, Poland; e-mail: mach@twarda.pan.pl

2| Department of Geology and Geomorphology, Faculty of Geographical Sciences, University of Łódź, ul. Narutowicza 88, 90-139 Łódź; Poland; e-mail: ewa.swierczewska@geo.uni.lodz.pl

3| Faculty of Geology, University of Warsaw, ul. Żwirki i Wigury 93, 02-089 Warszawa; Poland; e-mail: don@uw.edu.pl

ABSTRACT

The west-east trending outcrop belt in the Lublin Upland, Poland, permits a preliminary assessment of regional patterns in facies development, fossil content, stratigraphic completness, and depositional history across the Cretaceous–Paleogene (K-Pg) boundary. The observed patterns are interpreted in the context of regional palaeogeography, synsedimentary tectonics, and relative sea-level change. One of the most important features of the regional K-Pg succession is a heavily burrowed surface that truncates Maastrichtian or lowermost Danian strata, and is overlain by condensed glauconite-rich deposits of Danian age. This discontinuity is interpreted as the transgressive surface of the early, but not earliest, Danian sedimentary cycle. The history of research on the Maastrichtian and Danian strata in the Lublin Upland, their significance for local communities, geoheritage, and geotouristics, and selected lithofacies and fossils are also described.

INTRODUCTION

(*Marcin Machalski*)

The aim of this chapter is to present a geological and palaeontological record of environments, biotic communities, and events across the Cretaceous–Paleogene (K-Pg) boundary in central and eastern Poland (Fig. 1a–c). Geographically, this area lies within the Lublin Upland and extends between Kazimierz Dolny, Lublin, and Chełm (Fig. 1b). Structurally, this area is located in the Kościerzyna–Puławy Synclinorium, which borders the Mid-Polish Anticlinorium to the south-west (Fig. 1a). The anticlinorium originated through a multi-phase inversion of the former Mid-Polish Trough during the Late Cretaceous and earliest Paleogene (Krzywiec et al. 2018; Remin et al. 2022).

During the late late Maastrichtian, the north-eastern part of present-day Poland, including the Lublin Upland, was covered by a relatively shallow epicontinental sea with predominant carbonate-siliceous sedimentation, particularly of the opoka facies, and a distinct regressive tendency (Pożaryski 1962; Machalski and Malchyk 2019). The shoreline was approximately parallel to the axis of the Mid-Polish Swell (Fig. 2a). After the final stages of inversion of the Mid-Polish Swell near the Maastrichtian–Danian transition (the Laramide phase of the Alpine Orogeny), the shoreline moved farther eastwards (Fig. 2b) and the uplifted area started to deliver significant amounts of siliciclastic material to the nearshore parts of Danian sea, including the western Lublin Upland (Pożaryski 1962). For an overview of the Upper Cretaceous setting of Poland, the reader is referred to Voigt et al. (2008).

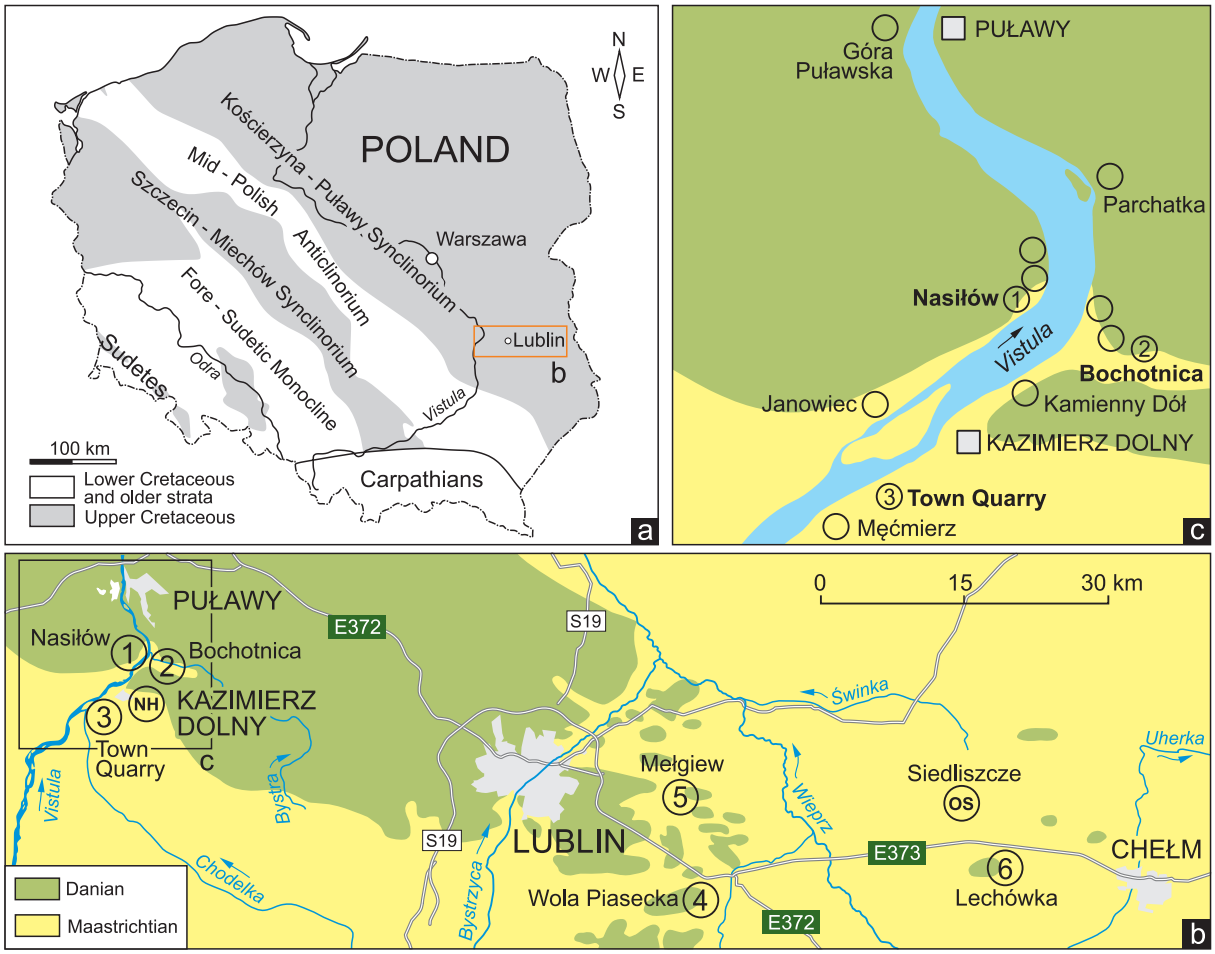

Fig. 1. **a** – geological sketch-map of Poland without the Cenozoic (after various sources); **b** – geological map of the northern Lublin Upland (the extent of the Danian modified from Harasimiuk 1984, fig. 1); **c** – the northern Middle Vistula River section near Kazimierz Dolny. 1–6 – key outcrops of upper Maastrichtian and Danian strata described in the excursion chapter, circles mark important outcrops; NH – Natural History Museum, Kazimierz Dolny; OS – Open-air Museum, Siedliszcze.

Kazimierz Dolny is located in the northern part of the classical Middle Vistula River section, a homoclinally arranged succession of Albian through Danian strata exposed along the banks of the Vistula River (Walaszczyk et al. 2016). The sections near Kazimierz Dolny (Fig. 1c) have been intensively studied, and are of key importance for understanding the stratigraphy and depositional evolution of the Maastrichtian–Danian succession of the Lublin Upland.

Historical background

The famous Polish-German scholar Georg Gottlieb Pusch (born 1790, deceased 1846) was amongst the first students of Cretaceous strata in the Lublin Upland (Pusch 1833–1836). In his monograph *Polens Paläontologie*, he described several fossils from the environs of Kazimierz Dolny, spelled by him as Kazimirz or Kadzimirz (Pusch 1837). However, the first correct stratigraphic interpretation of the Cretaceous–Paleogene succession along the banks of the Vistula was published by the Russian geologist Nikolay J. Krischtafovitsch (born 1866, deceased 1941). This ex-army officer, self-taught without formal degrees (Maruszczak 2003; Woroncowa-Marcinowska 2016), worked from 1894–1914 at the Institute of Farming and Forestry at Nowo Aleksandria (today Puławy). Krischtafovitsch (1897, 1899) presented an elegant stratigraphical interpretation of the Vistula section, proposing a ho-

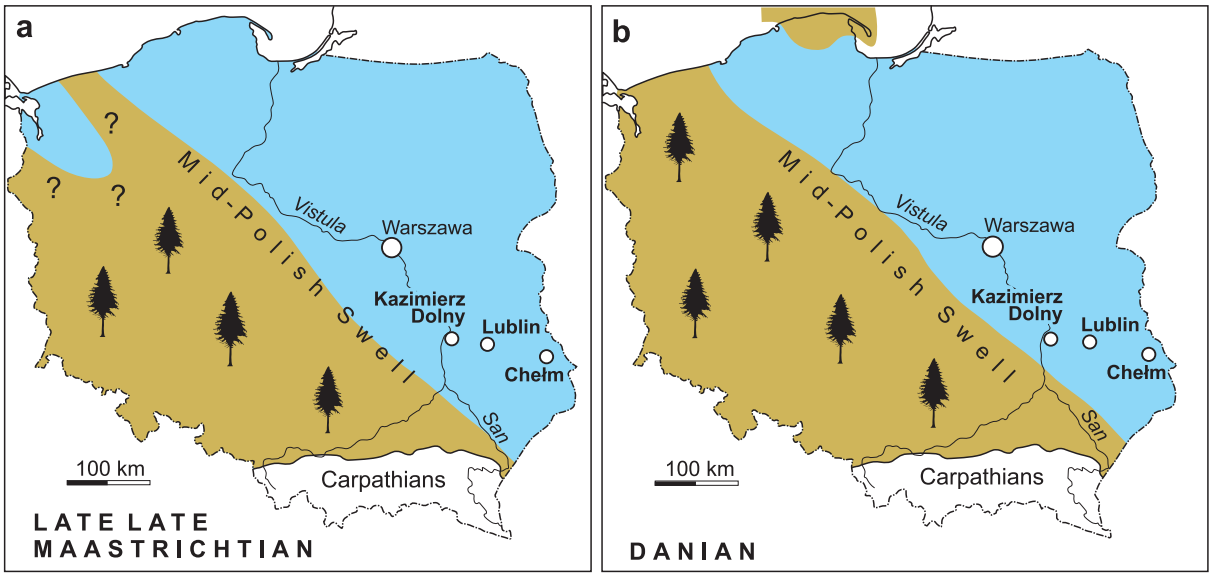

Fig. 2. Palaeogeography of Poland during the (**a**) late late Maastrichtian and (**b**) Danian (after Pożaryski 1962, facies maps for the upper part of the upper Maastrichtian and Danian–Paleocene, and Cieśliński and Jaskowiak 1973, fig. 196).

moclinal structure with progressively younger strata exposed to the north. Notably, this was a reversal of the stratigraphy adopted by earlier authors, who assumed older strata were gradually exposed towards the north.

In the vicinity of Kazimierz Dolny, Krischtafovitsch (1897, 1899) distinguished two stratigraphic "zones". The higher zone, Cr 4/s, was composed of sandy-limy marls with limestone nodules; he considered it to represent the highest levels of the Cretaceous (these deposits are termed the Siwak, which in current interpretation is of Danian age). To his lower zone, Cr 3/s, Krischtafovitsch assigned the yellow-white opokas (the Kazimierz Opoka in current definition) with sandy-glauconitic intercalations and nests of fossils at the top. The latter is, indeed, the K-Pg boundary interval, which as described below encompasses an indurated opoka bed with glauconite-filled burrows at the top of the Kazimierz Opoka and an overlying sandy-glauconitic unit (referred to here as the Greensand). This was the first description of the K-Pg boundary interval, as presently recognized, in the Middle Vistula River section, and more broadly in Poland, although Krischtafovitsch regarded the whole succession as Cretaceous. The renowned Polish geologist and palaeontologist Józef Siemiradzki (born 1858, deceased 1933) was the first to correlate the Cr 4/s zone with the *Etage Danien* and *calcaire pisolitique* and the Cr 3/s zone with the *Etage Maestrichtien* (Siemiradzki, 1901, 1905; see Głowniak 2007 for a bibliography of J. Siemiradzki).

Several subsequent contributions have dealt with the stratigraphy, sedimentology, and palaeontology of Maastrichtian–Danian strata near Kazimierz Dolny. These include Kongiel (1935), Kongiel and Matwiejewówna (1937), Pożaryski (1938, 1956), Putzer (1942), Pożaryska (1952, 1965, 1967), Krach (1974, 1981), Błaszkiewicz (1980), Hansen et al. (1989), Machalski and Walaszczyk (1987), Żarski et al. (1998), Machalski (1998, 2007), Świerczewska-Gładysz and Olszewska-Nejbert (2006), Dubicka and Peryt (2012), Machalski and Jagt (2018), and Remin et al. (2021). As far as "pure" palaeontology is concerned, early studies were summarised by Abdel-Gawad (1986) in his excellent monograph on Maastrichtian non-cephalopod mollusks. More recently, papers by Geys and Machalski (1992), Radwańska and Radwański (1994), Radwański (1996), Machalski et al. (2003), Machalski and Robaszewska (2003), Machalski (2005a, b, 2021), Świerczewska-Gładysz (2006), Keutgen et al. (2017), Malchyk (2018), and Fraaije et al. (2018) are of considerable merit.

Several fossils were first described from the Kazimierz Dolny area and, indeed, owe their Linnean names to this site. These include the large gastropod *Volutispina kasimiri*, the

bivalves *Pholadomya kasimiri* and *Pinna kasimirensis* and – last but not least – the belemnite *Belemnella kazimiroviensis*, the index taxon for the highest belemnite zone of the Boreal Maastrichtian in Europe (Abdel-Gawad 1986; Keutgen et al. 2017).

The upper Maastrichtian and Danian strata in the central and eastern Lublin Upland – that is, near Lublin and Chełm, respectively (Fig. 1c) – have not been studied as thoroughly (Pożaryski 1956; Popiel 1977; Wyrwicka 1977; Harasimiuk and Henkiel 1981; Harasimiuk 1984; Harasimiuk and Rutkowski 1984; Machalski 2005a; Jagt and Kin 2010). Of special importance is Pożaryski (1956), which provided a wealth of data on upper Maastrichtian–Danian stratigraphy and lateral facies changes along a west-east transect across the Lublin Upland. Recently, a section at Lechówka, near Chełm, has yielded a distal record of the Chixculub impact, including the K-Pg boundary clay, the associated Ir-anomaly, and spherules and meteorite remnants (Racki et al. 2011; Brachaniec et al. 2014; Machalski et al. 2016; Szopa et al. 2017). This enables a linkage of the Polish K-Pg transition to global hypotheses of the Chixculub impact and, to some extent, Deccan volcanism. It should be also noted that the sections at Nasiłów, Bochotnica, Mełgiew and Lechówka yielded important insights on ammonite extinction (Landman et al. 2014, 2015).

Papers on regional biostratigraphy, based on calcareous nannoplankton (Gaździcka 1978), ammonites (Błaszkiewicz 1980; Machalski 2005a, b), and foraminifers (Dubicka and Peryt 2012), form the background for understanding the K-Pg boundary succession of the Lublin Upland.

Outcrops, quarries, and building stones

In the past, the upper Maastrichtian and, to a lesser extent, Danian strata were subjected to opencast mining activities across the Lublin Upland (Fig. 3). Several large quarries were active along the Vistula banks, each with exposed rock-faces up to several hundred metres long. The best known are the quarries at Nasiłów, the so-called Town Quarry south of Kazimierz Dolny, and Góra Puławska near Puławy (Fig. 1c). There, Maastrichtian and Danian rocks were mined for regulation of the banks of the Vistula (Pożaryska and Pożaryski 1951; Pożaryska 1952; Bąk and Szeląg 2013; Bąk and Radwanek-Bąk 2020). The former pit at Góra Puławska no longer exists, but those at Nasiłów (Fig. 3a) and Kazimierz Dolny (Fig. 3c) are still accessible.

Several small rural quarries existed in the Kazimierz Dolny and Lublin regions, where upper Maastrichtian opoka was excavated as a local building stone (Pinińska 2007; Bąk and Szeląg 2013; Bąk and Radwanek-Bąk 2020). The façades of many residential and historic buildings in the Kazimierz Dolny area are composed of opoka, with the ruins of the castle towering over Kazimierz Dolny perhaps the most famous example (Fig. 3f). In the village of Bochotnica, upper Maastrichtian opoka was worked in several underground quarries (Fig. 3b) by hand; an indurated limestone at the top of the Maastrichtian served as a natural roof of exploration galleries (Pożaryska and Pożaryski 1951; Bąk and Szeląg 2013; Bąk and Radwanek-Bąk 2020). Today, most of these quarries are covered with rubble, overgrown, or difficult to access due to the construction of new houses in their immediate vicinity.

A number of former small peasant quarries to the south and east of Lublin once exposed the K-Pg boundary interval (Pożaryski 1956). However, they are currently unavailable, and many local successions are accessible only by excavation, as exemplified by trenches excavated by MM in search of the youngest Polish ammonites at Mełgiew, east of Lublin (Fig. 3e; Machalski 2005a). A large, currently inactive upper Maastrichtian opoka quarry still exists at the village of Wola Piasecka, with the K-Pg interval present at the top of the exposure (Fig. 3d). Farther east, there are no good K-Pg outcrops at all. The only exception is a former opencast mine of decalcified opoka at Lechówka, where the K-Pg boundary clay was first identified by Racki et al. (2011).

Not only science

The geological sites of the Lublin Upland are valuable not only for science, but serve as remarkable resources for education, geoconservation, and geotourism as well (Pożaryska and Pożaryski 1951; Radwański 1985; Walaszczyk et al. 1999; Pinińska 2007; Bąk and Szeląg 2013; Bąk and Radwanek-Bąk 2020). This is primarily, although not exclusively, true for the western

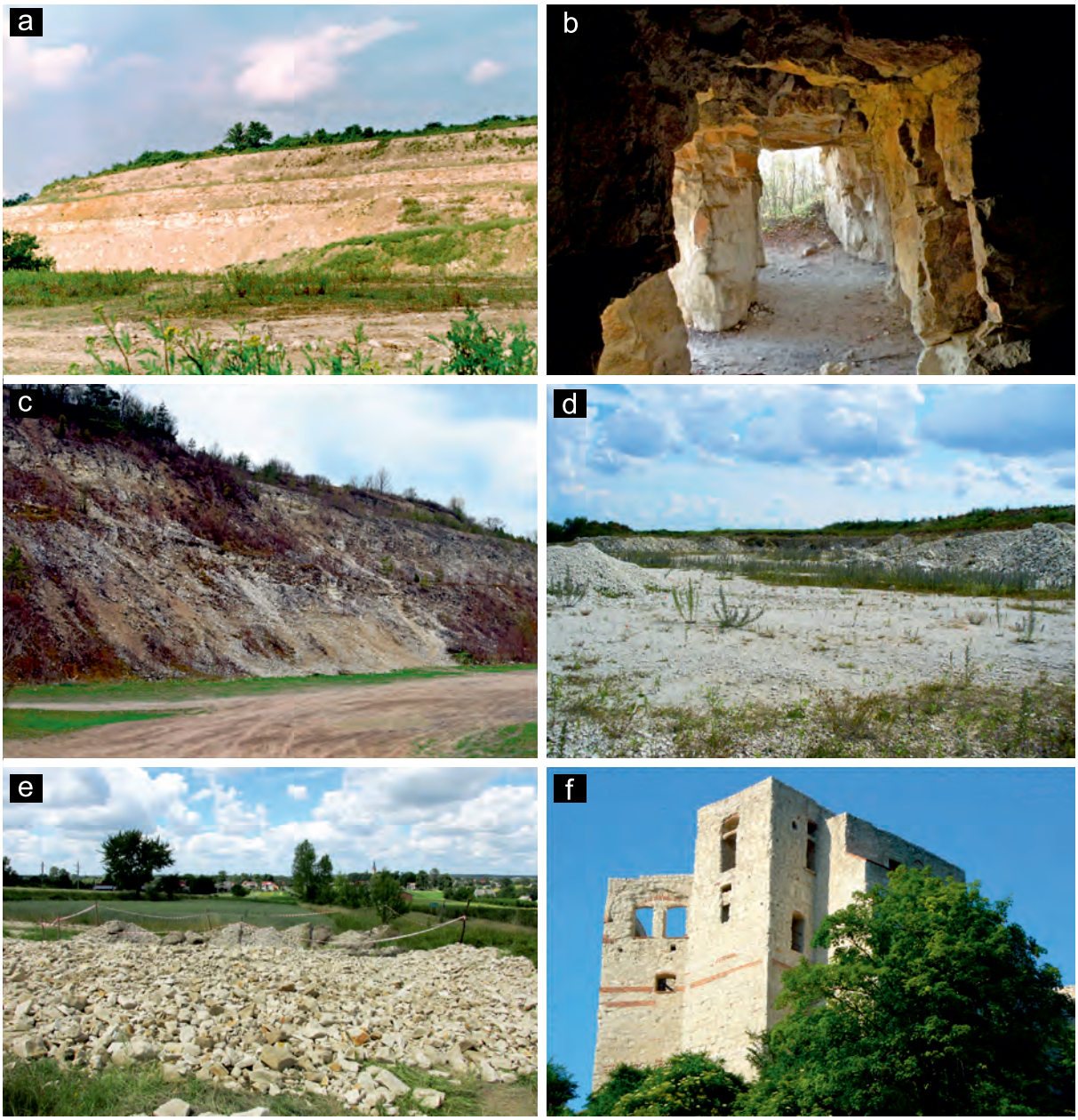

Fig. 3. Outcrops, mining, and building stone application of the upper Maastrichtian and Danian rocks in the Lublin Upland: **a** – Nasiłów Quarry (Locality 1; early 1990s, courtesy of J. Szkuat); **b** – underground opoka mine at Bochotnica (site "Ścianka Krystyny i Władysława Pożaryskich", photo courtesy of J. Szkuat); **c** – present view of the Town Quarry south of Kazimierz Dolny (Locality 3); **d** – quarry at Wola Piasecka (Locality 4); **e** – temporary trench excavated in 2019 by MM at Mełgiew, with opoka heaps in foreground (Locality 5); **f** – medieval castle in Kazimierz Dolny constructed from upper Maastrichtian opoka.

part of the upland near Kazimierz Dolny. This part of the Vistula valley forms the northern part of the proposed Małopolska Gap of the Vistula River geopark (Harasimiuk et al. 2011) which, regrettably, did not go beyond the planning phase.

A documentation site was established in 1992 in one of the abandoned quarries in Bochotnica that preserves the K-Pg interval and a spectacular system of old, underground opoka mining-galleries. It is named the "Krystyna and Władysław Pożaryski Wall"

to commemorate this Polish scientist couple (Dybkowska 1993). Unfortunately, the educational value of the site has been diminished by the creation of a bat refuge in the former mine. Plans to protect the K-Pg site at Lechówka were presented by Machalski et al. (2019).

The Natural History Museum in Kazimierz Dolny is the best place to see regional geological, palaeontological, and biological exhibits. It was established in 1982 as one of the four branches of the Nadwiślańskie Museum, and is located in a picturesque 16th century granary (Kowalczyk 2004). The museum serves approximately 30,000 visitors per year; its collections comprise over 12,000 geological, palaeontological, zoological, and botanical items. There are four permanent exhibitions at the museum: one, "The secrets of the extinct world", provides an excellent overview of local Maastrichtian and Danian fossils (Szkuat and Piskorek 2009). The Natural History Museum has long cooperated with Polish and foreign scientific institutions; in 2001, it hosted a travelling international exhibit entitled "Dinosaurs, ammonites and asteroids. Life and Death in the Maastrichtian" (Graaf et al. 1999; Schulp et al. 1999). This exhibit was prepared in cooperation with the Institute of Paleobiology of Polish Academy of Sciences, Warsaw, the Natural History Museum Maastricht, the Netherlands, and other foreign institutions.

DEPOSITIONAL SUCCESSION

(*Marcin Machalski, Ewa Świerczewska-Gładysz, Danuta Olszewska-Nejbert*)

No formal lithostratigraphical scheme for the upper Maastrichtian and Danian succession in the excursion area has been proposed. As such, we have used the traditional, informal lithostratigraphical terminology: that is, the Kazimierz Opoka, the Greensand, and the Siwak (review in Machalski 1998). These names stem from research in the vicinity of Kazimierz Dolny, where the K-Pg succession was first recognised and extensively studied. The regional dip is 1–3° NE, leading to increasingly younger strata occuring downstream on the Vistula River.

The most detailed composite section of the Kazimierz Dolny succession was provided by Pożaryska (1952) and Pożaryski (1956), based on surface outcrops along the Vistula River and a borehole log at Góra Puławska near Puławy (Fig. 4). It is described below and compared to eastern equivalents to highlight the lateral facies variation of Maastrichtian and Danian strata across the Lublin Upland.

Kazimierz Opoka

The Kazmierz Opoka is a c. 50 m thick opoka unit that overlies upper Maastrichtian marls exposed farther to the south at Męćmierz (Figs 1c, 4). The Kazimierz Opoka comprises the x and y horizons in the regional subdivision of the Middle Vistula River section by Pożaryski (1938; Table 1). It consists of rather massive, porous opoka beds, with thin intercalations of indurated opoka and marly beds (Figs 4, 5a). The Kazimierz Opoka is terminated by a distinctive level of hard opoka cemented by calcium carbonate. This indurated limestone bed (described as a "hardground") is riddled with burrows, largely of decapod crustacean origin, filled with sandy-glauconitic sediment piped down from the overlying Greensand. The Kazimierz Opoka may be subdivided into two parts (Fig. 4). The lower, which possesses two distinctive marl layers near the top, is exposed in the Town Quarry south of Kazimierz Dolny (Fig. 5a). The upper, composed of a more marly opoka, is exposed in the Nasiłów and Bochotnica quarries.

Microfacies. The Kazimierz Opoka is composed of wackestones and packstones (Fig. 6a–c) with predominant sponge spicules (up to 30–35%), visible mainly as voids left after dissolution, and foraminifera bioclasts. Other bioclasts, largely of echinoderm, bryozoan, bivalve, and brachiopod origin, are subordinate. Furthermore, the Kazimierz Opoka contains an admixture of rare, small (up to 50 μm in size), angular detrital quartz grains, rare euhedral authigenic quartz, and even rarer, very small (20–60 μm) authigenic glauconite grains (see also Sujkowski 1931; Pożaryska 1952). The quartz and glauconite content in the Kazimierz Opoka is ~0.5–1.0% for each mineral, and slightly rises through the section (Pożaryski 1938; Machalski and Malchyk 2019).

Fossil assemblages. The Kazimierz Opoka hosts rich fossil assemblages, composed of

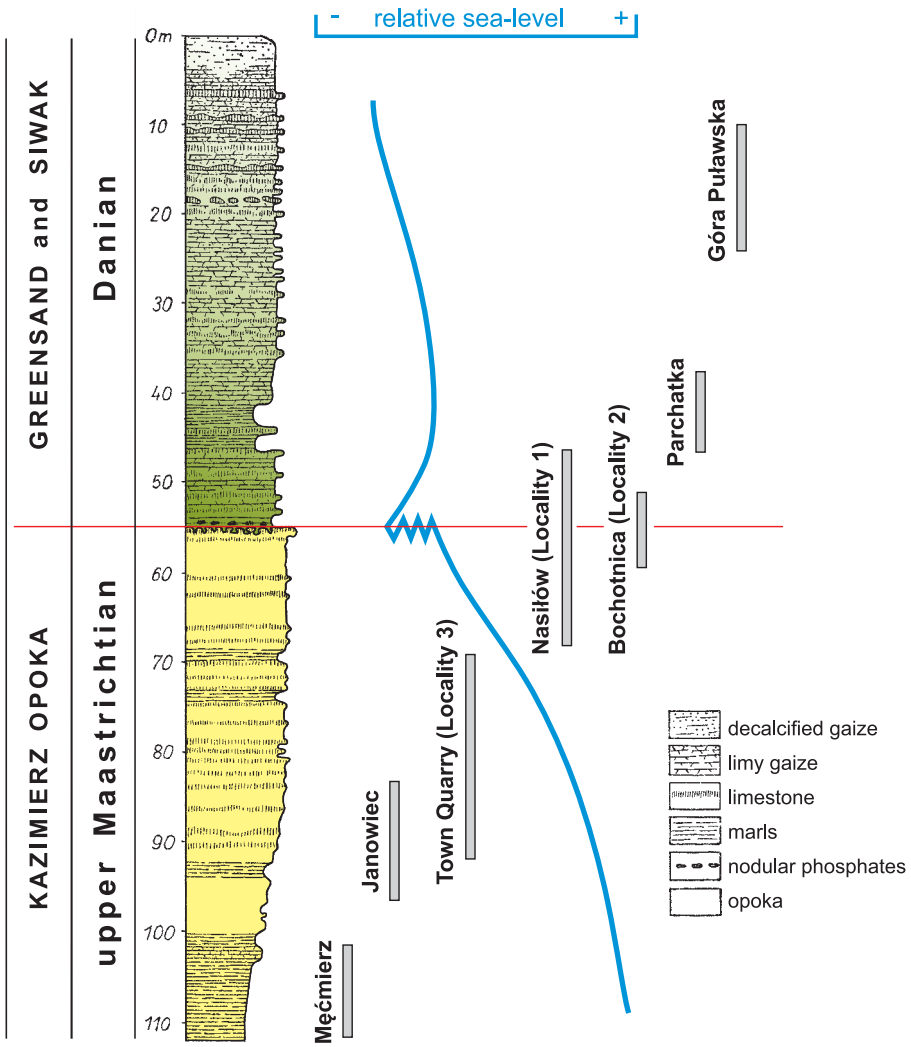

Fig. 4. The Cretaceous–Paleogene succession in the Middle Vistula River section. Lithological log based on Góra Puławska borehole, after Pożaryski (1956, fig. 6) with updated stratigraphy, ranges of the surface sections described in the text, and a generalised curve of relative sea-level.

mass occuring sponges, solitary corals, serpulids, terebratulid and rhynchonellid brachiopods, non-cephalopod (gastropods, bivalves, and scaphopods) and cephalopod mollusks (ammonites, nautiloids, and belemnites), and rare echinoids (see Abdel-Gawad 1986 for an overview of the invertebrate faunas). Vertebrates are not common; those present include fish scales and vertebrae, shark teeth, and extremely rare mosasaur teeth (Machalski et al. 2003). Rare, land-swept conifer twig remains have been also recorded (Halamski 2013). Selected fossils from the Kazimierz Opoka are illustrated in Figs 7–8. Calcitic shells are well preserved, while originally aragonitic shells are dissolved throughout the unit, leaving only moulds (Fig. 7c,d; Abdel-Gawad 1986; Machalski 2021). Except for some storm-generated tabular and lens-like fossil accumulations (Machalski and Malchyk 2019), fossil assemblages from the Kazimierz Opoka are broadly autochtonic and parautochtonic remnants of the indigenous Late Cretaceous biotic communities (Abdel-Gawad 1986; Świerczewska-Gładysz 2006).

Biostratigraphy. The Kazimierz Opoka in the Middle Vistula River section represents the upper, but not uppermost Maastrichtian, belonging to the highest standard belemnite

Fig. 5. The upper Maastrichtian opoka of the Lublin Upland: **a** – opoka outcrop in a valley north of the Town Quarry (Locality 3) near Kazimierz Dolny, with the lower marl layer marked by an arrow; **b** – typical appearance of opoka at Wola Piasecka (Locality 4); **c** – block of opoka with remains of hexactinellid sponges (*Pleurostoma dichotoma* to the left and *Rhizopoterion cribrosum* to the right) at Wola Piasecka (Locality 4); **d** – a façade of an old building in Kazimierz Dolny, with an intensely weathered surface of opoka derived from the upper, marly portion of the Kazimierz Opoka (calcitic bivalve shells jut out from the rock, with the scallop *Dhondtichlamys acuteplicata* marked by an arrow).

Belemnella kazimiroviensis Zone, the tegulated inoceramid *Tenuipteria argentea* Zone, and the scaphitid ammonite *Hoploscaphites constrictus crassus* Zone (Błaszkiewicz 1980; Abdel-Gawad 1986; Machalski 1996, 2005a, b, 2012; Walaszczyk et al. 2016). The upper portion of the Kazimierz Opoka, as exposed at Nasiłów, belongs to the highest pachydiscid ammonite *Menuites terminus* Zone (Machalski and Jagt 1998). In terms of microfossil zonation, the Kazimierz Opoka is assigned to the coccolith *Nephrolithus frequens* Zone, the planktic foraminiferal *Guembelitria cretacea* Zone (*sensu* Peryt 1980) and to the regional X–XII foraminiferal zones (see Gaździcka 1978; Peryt 1980; Dubicka and Peryt 2012, respectively; see also Walaszczyk et al. 2016). The reader is referred to Tables 1 and 2 for the stratigraphic zonations used in the present work.

Environment. Physical and palaeontological evidence suggests that deposition occured in a relatively shallow epicontinental setting with normal salinity and clear waters, located far from terrigenous source areas. Changes in the composition of foraminiferal (Dubicka and Peryt 2012), siliceous sponge (Świerczewska-Gładysz 2006), gastropod, and bivalve assemblages (Abdel-Gawad 1986), and increases in belemnite abundance (Machalski and Malchyk 2019) are documented upwards in the Kazimierz Opoka. Distal tempestites composed of shell and sponge fragments occur in the upper portion of the unit (Machalski and

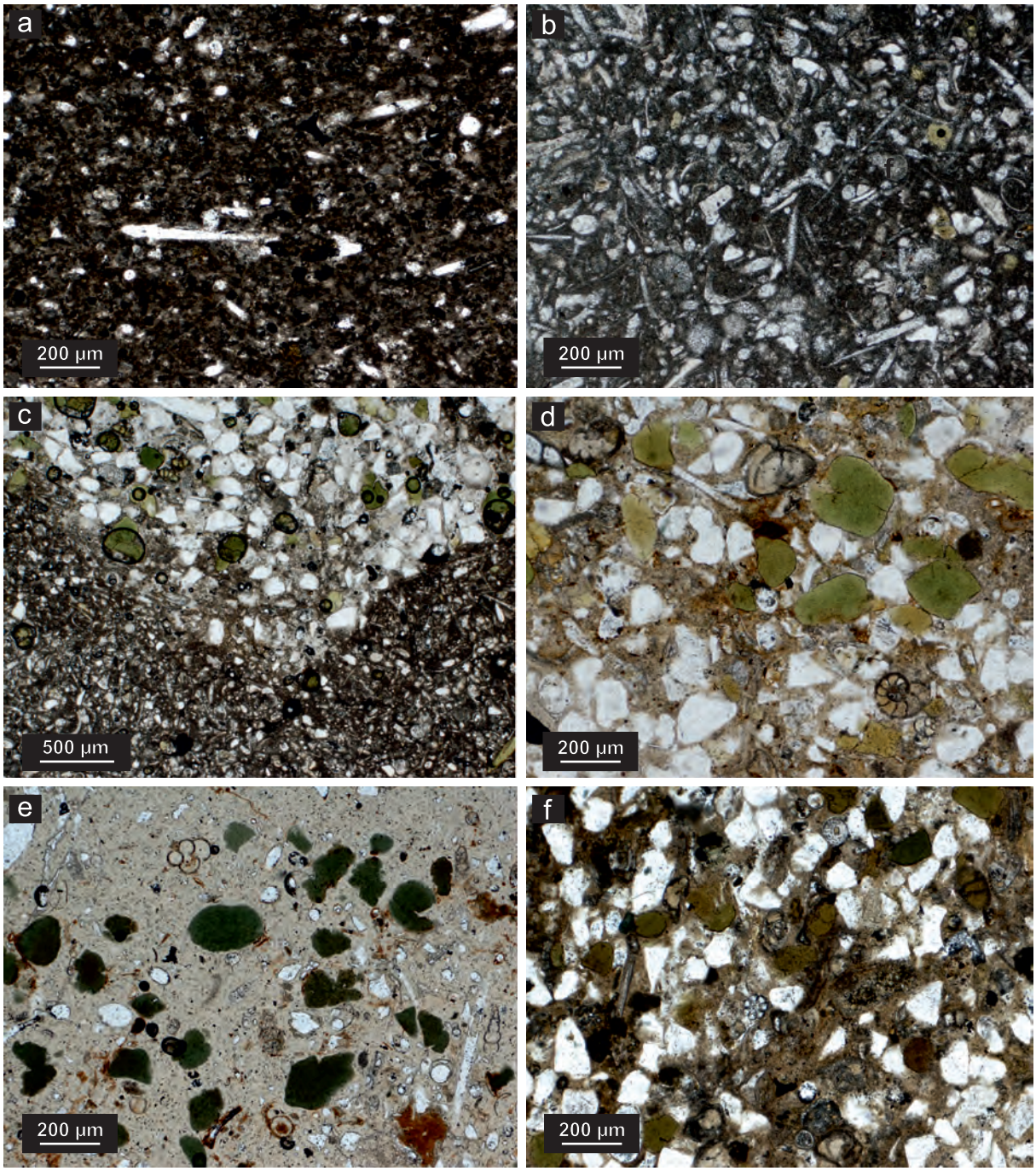

Fig. 6. Major microfacies types in the Cretaceous–Paleogene boundary succession in the Middle Vistula River section: **a** – porous opoka (calcareous wackestone) with dominant voids after dissolved sponge spicules, upper Maastrichtian, Nasiłów (Locality 1); **b** – hard opoka (calcareous packstone) with voids after spicules filled by sparite and an admixture of fine detrital quartz, glauconite, and foraminifera, upper Maastrichtian, Nasiłów (Locality 1); **c** – junction between hard opoka below and quartz-glauconitic sandstone above, upper Maastrichtian–Danian, Kamienny Dół, Kazimierz Dolny; **d** – quartz-glauconitic sandstone with subangular and subrounded quartz grains and pelloid glauconite, with an admixture of benthic foraminifera, Danian, Kamienny Dół, Kazimierz Dolny; **e** – phosphatised opoka with abundant glauconite, voids after dissolved sponge spicules and foraminifera; the beige matrix is composed of phosphate minerals; an example of a late Maastrichtian nodular phosphate incorporated into the Danian Greensand, Nasiłów (Locality 1); **f** – gaize composed of fine detrital angular and subangular quartz grains, glauconite, sponge spicules, echinoderm bioclasts, and benthic foraminifera, Danian, Kamienny Dół, Kazimierz Dolny.

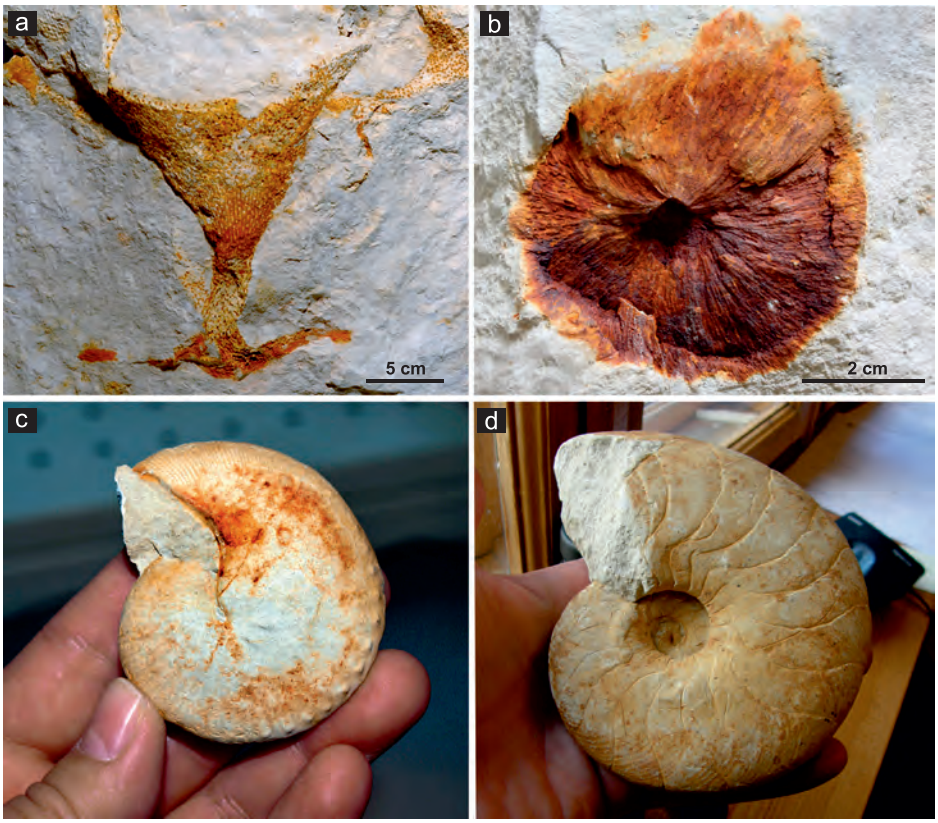

Fig. 7. Selected fossils from upper Maastrichtian opokas: **a** – *Rhizopoterion cribrosum*, the most common lychniscosid sponge species, Town Quarry near Kazimierz Dolny (Locality 3); **b** – *Geodiopsis* sp., a rare example of a bodily preserved non-rigid demosponge, Town Quarry (Locality 3); **c** – *Hoploscaphites constrictus crassus*, a scaphitid ammonite with mouldic preservation, Nasiłów (Locality 1); **d** – *Cymatoceras intrasiphonatum*, a nautiloid with mouldic preservation, Nasiłów (Locality 1).

This work	POŻARYSKI (1938)	BŁASZKIEWICZ (1980)		ABDEL-GAWAD (1986)	PERYT (1980)	GAŹDZICKA (1978)
Danian	z	Danian-Montian	D-M	*Belemnella kazimiroviensis* - *Tenuipteria argentea*	Danian	Danian
upper Maastrichtian	y	*Hoploscaphites constrictus crassus*	Mg_2		*Guembelitria cretacea*	*Nephrolithus frequens*
	x					
	w	*Belemnitella junior*	Mg_1	*Belemnitella junior*		
lower Maastr.	v	*Belemnella occidentalis*	Md_2	*Belemnella occidentalis*	*Rugoglobigerina pennyi*	*Lithraphidites quadratus*
upper Campanian	u	*Belemnella lanceolata lanceolata*	Md_1	*Belemnella lanceolata*	*Globigerinelloides multispinus*	*Tetralithus aculeus*
	t					
	s	*Nostoceras pozaryskii*	Kg_4	*Nostoceras pozaryskii*		
	r	*Didymoceras donezianum*	Kg_3	*Didymoceras donezianum*		
	p					

Table 1. Stratigraphic subdivision of the upper Campanian to Danian in the Middle Vistula River section (modified from Abdel-Gawad 1986, table 2). The Kazimierz Opoka is in yellow, the overlying Greensand in green (the Siwak is not included).

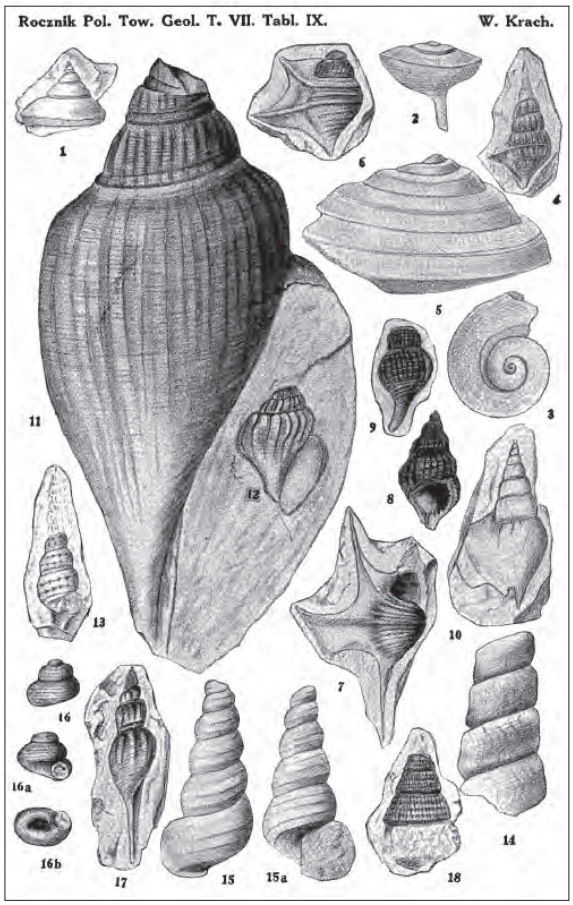

Fig. 8. Gastropods from the upper Campanian and Maastrichtian opokas of the Middle Vistula River section, refigured from Table IX in Krach (1931). Specimen 11 is *Volutispina kasimiri* from the upper Maastrichtian Kazimierz Opoka, exposed in the Town Quarry south of Kazimierz Dolny (Locality 3).

Malchyk 2019). The above observations suggest a distinct shallowing, regressive trend during the sedimentation of the Kazimierz Opoka (Fig. 4), which was already inferred by Krischtafovitsch (1897, 1898) and Pożaryski (1938). The lower Kazimierz Opoka may have been deposited in outer shelf environments below the storm wave-base, and the upper in a progressively shallowing middle shelf setting slightly above the storm wave-base.

Greensand

This is a thin, c. 50 cm thick glauconitic sandstone layer sandwiched between the Kazimierz Opoka and the Siwak (Fig. 4; local horizon x in Pożaryski 1938, see Table 1). It is a poorly to well cemented, olive-green, marly, glauconitic-quartz sandstone. A more or less distinct layer of nodular phosphates and fossils occurs in what is conventionally regarded as the upper Greensand (the so-called "phosphorite layer"). Finer phosphatic fractions occur throughout the unit, including burrow infillings that pipe down into the underlying opoka. The entire Greensand is mottled by burrowing animals, as evidenced by ichnofabrics discernible on polished slabs and quarry walls. The best Greensand outcrops are at Bochotnica and Nasiłów; at Kazimierz Dolny rather poor exposures exist. The lower Greensand boundary is sharp, marked by a strongly burrowed, irregular junction with the underlying Kazimierz Opoka, while the Greensand gradually passes into the Siwak gaizes above (Fig. 9).

Microfacies. As seen in thin section, the Greensand may be classified as a hybrid arenite or, more accurately, as a hybrid wacke because the matrix content exceeds 15% (Fig. 6c, d). The grain support is composed of detrital quartz (c. 25–35%), mainly authigenic glauconite (c. 8–15%), tiny phosphate grains (c. 5%), and feldspar (up to 1%); the bioclasts are represented by rare sponge spicules, echinoderm fragments, foraminifera, and bryozoans (see also Pożaryska 1952). Rare heavy mineral grains are also present in the sandstone (Morawski 1970). The grain sizes of both quartz (100–200 μm) and glauconite (200–300 μm) are significantly greater than in the underlying opoka. Unlike those in opoka, the quartz grains are usually subangular to rounded, while the glauconite grains are dark green, peloidal, and sometimes crushed (Fig. 6c, d). The matrix is composed of micrite, with an admixture of clay minerals and silica.

Nodular phosphates. The phosphates are grey, beige to dark-brown, and range from a few mm to dm in size. They contain 22.1–26.05% P_2O_5 (Morawiecki 1925). Many phosphates are bodily preserved sponges (Świerczewska-Gładysz and Olszewska-Nejbert 2006), while other phosphates are moulds after other invertebrate groups, mostly bivalves and gastropods; many belemnite alveoles are also infilled by phosphatised material (Fig. 10c – 1, 3, 5, 6; Machalski and Walaszczyk 1987; Machalski 1998; Machalski and Jagt 2018). In thin section, the phosphates reveal various

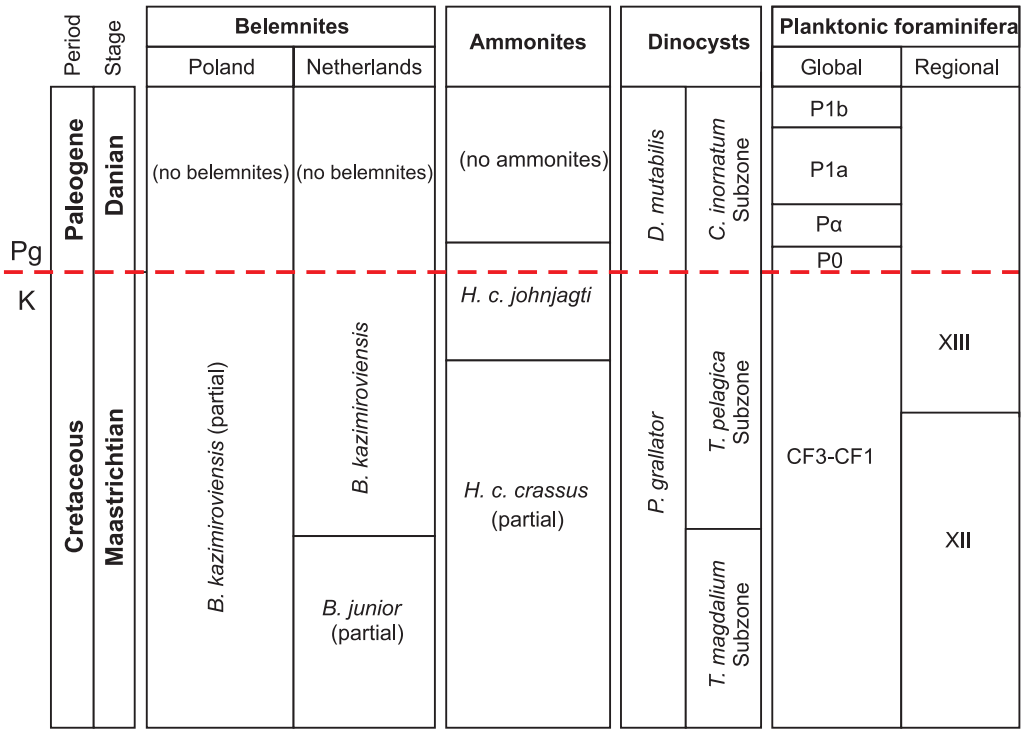

Table 2. Selected biostratigraphic zonations used in this work, modified from Machalski et al. (2016, table 1). See text for full names of the index taxa.

microfacies types, including phosphatised opoka, phosphatised opoka with an admixture of large glauconite grains (Fig. 6e), and a phosphatised glauconitic sandstone identical to the surrounding non-phosphatised sediment (Machalski and Walaszczyk 1987; Świerczewska-Gładysz and Olszewska-Nejbert 2006; Machalski and Jagt 2018).

Fossil assemblages. The Greensand is extremely fossiliferous and yields specimens in a wide spectrum of preservation states, ages, and inferred provenances (Fig. 10a–c). The phosphorite layer is particularly fossiliferous, although both phosphates and fossils also occur in burrows descending into the topmost levels of the Kazimierz Opoka. Amongst the Greensand fossils, there are specimens derived from the underlying opoka (e.g., Fig. 10a), phosphatised late Maastrichtian fossils (Fig. 10c – 1, 3, 5, 6) partially derived from a now-missing glauconitic opoka unit, and abundant remains of indigenous Danian bivalves and gastropods preserved as moulds in the same lithology as the surrounding sediment (Fig. 10b; Krach 1974, 1981; Machalski and Walaszczyk 1987; Machalski 1998; Żarski et al. 1998; Świerczewska-Gładysz and Olszewska-Nejbert 2006; Machalski and Jagt 2018). The most striking Greensand fossils are dissociated valves of the late Maastrichtian scallop *Dhondtichlamys acuteplicata*, oyster shells, belemnite rostra, and phosphatised sponge fragments. Echinoid spines occur in masses, and shark teeth are not uncommon. As far as ammonites are concerned, only two fragmentary specimens of *Hoploscaphites constrictus* subsp. indet., both in phosphatic mould preservation, have been reported from Nasiłów (Machalski and Walaszczyk 1988).

Biostratigraphy, age, and environments. The age of the Greensand and its depositional history have been the subject of considerable controversy, mostly due to the fact that late Maastrichtian and Danian fossils are intermixed in this unit (for review, see Machalski 1998). Krach (1981) assigned a Paleocene (in his view, Montian) age to those mollusks predominantly preserved as glauconitic sandstone moulds in Greensand. Żarski et al. (1998) reported on the occurrence of Danian mollusks in the Greensand exposed in Kamienny Dół at Kazimierz Dolny. Hansen et al. (1989)

Fig. 9. The Cretaceous–Paleogene interval exposed at Bochotnica behind the old watermill (Locality 2): **a** – the burrowed top of the upper Maastrichtian Kazimierz Opoka, represented by indurated opoka (unit 2) and brecciated soft opoka (unit 3), is overlain by the Danian glauconitic sandstone of the Greensand (unit 4), which passes gradually into Danian gaizes of the Siwak (unit 5, see also left side of Fig. 25); **b** – the same interval in another part of the outcrop.

assigned the Greensand from Nasiłów to the dinoflagellate *Senoniasphaera inornata* (formerly *Chiropteridium inornatum*) Subzone within the Danian *Danea mutabilis* Zone; the dinocyst results of Słodkowska (2003) are compatible with this assessment. Pożaryska (1965, 1967) described a rich assemblage of Danian (Dano-Montian in her view) benthonic and planktonic foraminifera from the Greensand, noting the occurrence of the Danian planktonic foraminifera *Globoconusa daubjergensis* in the sandy-glauconitic infillings of burrows

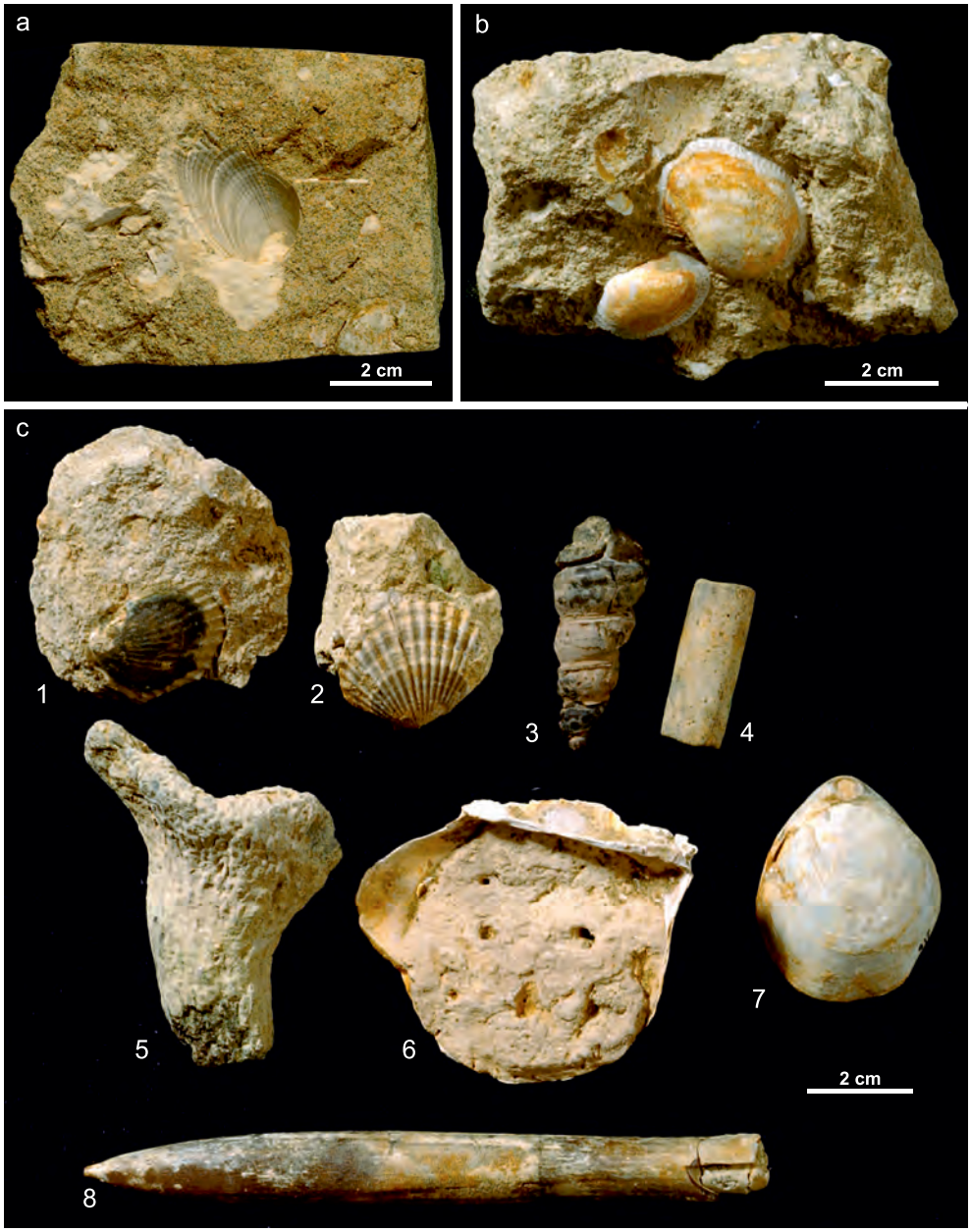

Fig. 10. Fossils of the Greensand: **a** – late Maastrichtian bivalve *Limatula* sp., with attached soft opoka piece; **b** – Danian bivalve *Cucullaea volgensis*, **c** – late Maastrichtian fossils (1,3,5, and 6 in phosphatic preservation): 1 and 2 – *Dhondtichlamys acuteplicata*; 3 – gastropod, probably *Turritella plana*; 4 – fragmentary and worn belemnite rostrum; 5 – fragment of the sponge *Rhizopoterion cribrosum*; 6 – oyster *Pycnodonte vesicularis*; 7 – brachiopod *Neoliothyrina obesa*; 8 – belemnite *Belemnella kazimiroviensis*. Specimens from Nasiłów and Bochotnica.

descending deep into the Maastrichtian opoka at Bochotnica. Żarski et al. (1998) assigned the Greensand at Kamienny Dół to the *Subbotina triloculinoides–Globigerina compressa* Zone: that is, to the P1b Zone in the standard planktonic foraminiferal zonation (compare Tables 1 and 2). In contrast, Remin et al. (2021) proposed a different interpretation of the microfossil record from Greensand, arguing for an entirely late Maastrichtian age of this unit. However, as elaborated below, the Danian position of Greensand is firmly supported here, and the Cretaceous–Paleogene boundary is drawn at its base. The facies development of

the Greensand and its complex depositional, phosphatisation, and reworking history, inferred from the fossils and phosphates, indicate that this unit originated in a turbulent, shallow water marine milieu under a low net sedimentation rate regime (Fig. 4; Machalski 1998; Świerczewska-Gładysz and Olszewska-Nejbert 2006; Machalski and Jagt 2018).

Siwak

The Greensand passes upwards into a c. 50 m thick series of gaizes with rhythmic limestone intercalations, traditionally termed the Siwak (Fig. 11), with a dark marly interval in the middle (formerly exposed at Parchatka, see Machalski 1988; Fig. 4). Macroscopically, the Siwak gaizes are grey to olive-green microporous rocks, either friable or well-cemented by calcium carbonate to form hard nodular limestone intercalations.The lithology of the Siwak was described in detail by Sujkowski (1931) and Pożaryska (1952).

Fig. 11. The Siwak, displaying characteristic rhythmic limestone intercalations, Nasiłów (Locality 1).

Microfacies. In thin section, the Siwak is a quartz-glauconite calcareous wacke (Fig. 6f). According to our data from the lowermost part of the succession, the grain support is composed of detrital quartz (up to 15%), glauconite (up to 7%), sponge spicules or voids left after their dissolution (up to 10%), foraminifera (up to 4%), echinoid bioclasts (2%), and rare calcispheres and other unidentifiable calcareous bioclasts (Fig. 6f). The detrital quartz and glauconite content in higher parts of the succession is variable, but is always much higher than in the opoka: for quartz, it ranges from 5–19%, and for glauconite, 5–25% (Pożaryska 1952). The angular and subangular quartz grains, typically beetween 80–150 μm, are usually finer than those from the Greensand, but significanly larger than those from the Kazimierz Opoka (Fig. 6). The peloidal glauconite grains in the Siwak range from 60 μm to 150 μm, clearly smaller than their equivalents in the Greensand (Pożaryska 1952, and observations by EŚ-G and DO-N).

Fossil assemblages. In contrast to the underlying units, the Siwak is poorly fossiliferous, except for the oyster "banks" formerly exposed at Parchatka (Machalski 1988). The Siwak fauna is fully marine throughout the section. It is predominatly composed of minute bivalves and gastropods (Krach 1981); irregular echinoid tests are not uncommon (Kongiel 1949), and minute cidaroid spines occur in masses. Examples of the Siwak fossils are illustrated in Fig. 12. Only loose siliceous sponge spicules are recognisable in Siwak (Pożaryska 1952). Notably, a fragmentary skeleton of the marine crocodile *Thoracosurus* was found alongside a driftwood concentration near the bottom of the Siwak, at Kamienny Dół in Kazimierz Dolny (Machalski 1998; Żarski et al. 1998).

Biostratigraphy. Historically, the Siwak has been assigned to various ages – Danian, Montian, Palaeocene, and even Eocene (Krach 1974; Machalski 1998). At present, there is a consensus that it falls within the Danian. Specifically, the lower part of this unit, as exposed at Nasiłów, was assigned by Hansen et al. (1989) to the dinoflagellate *Senoniasphaera inornata* (formerly *Chiropteridium inornatum*) Subzone within the Danian *Danea mutabilis* Zone. Planktonic foraminifera from the lower Siwak at Kamienny Dół document the Danian P1b Zone (Żarski et al. 1998). Gaździcka (1978) assigned the Siwak to the Danian coccolith *Fasciculithus tympaniformis* Zone. The upper Siwak, which was formerly accesible at Góra Puławska, yielded the same echinoid, bivalve, and gastropod taxa known from the lower portions of the unit (Kongiel 1949; Krach 1981). Therefore, the upper Siwak is also regarded here as Danian, although the presence of higher microfossil zones cannot be excluded.

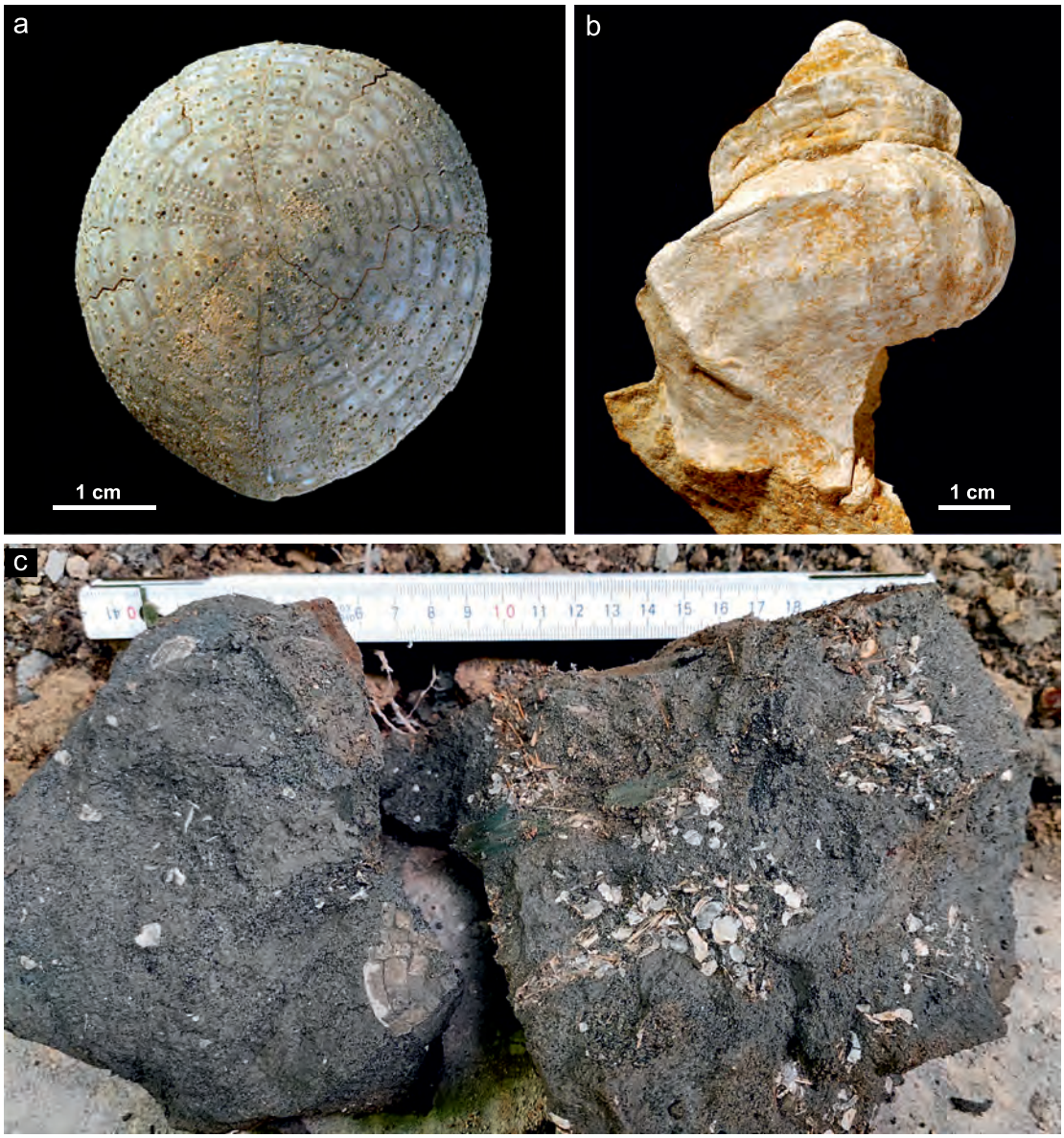

Fig. 12. Fossils from the Siwak: **a** – *Echinocorys* sp., Parchatka; **b** – gastropod with mouldic preservation, Bochotnica; **c** – accumulation of biotic remains, including bivalves with remnants of their original aragonitic shells and an echinoid test, from the dark marly Siwak exposed at Parchatka.

Environment. The Siwak fauna commonly occurs in layers and lenses of storm and/or bioturbational origin, composed of dissociated shell hash; hard limestone intercalations are occasionally associated with *Thalassinoides* burrow systems (observations by MM at Nasiłów). Significant detrital quartz concentrations are consistent with strong terrigenous input to a shallow water basin of normal salinity, probably within the upper middle and inner shelf zones. The only sponges represented are the non-rigid demosponges, which tolerate shallow water conditions better than other siliceous sponge groups (Hooper and van Soest 2002). This remarkable impoverishment of sponge fauna points to a shallower setting for the Siwak in comparison to the Kazimierz Opoka (Fig. 4). The driftwood concentration near the base of the Siwak at Kamienny Dół, and the development of a dark marly facies upsection at Parchatka, point to a gradual increase in basin depth through the duration

of the Siwak, reflecting the progress of the Danian transgression (Fig. 4).

Lateral facies changes

The lateral equivalents of the Kazimierz Opoka, Greensand, and Siwak may be traced in exposures throughout the Lublin Upland, all the way to the environs of Chełm (e.g., Krischtafovitsch 1897, 1899; Pożaryski 1956; Popiel 1977; Machalski et al. 2016). In the central upland, the Kazimierz Opoka equivalents exhibit the same facies development as, and similar fossil assemblages to, the upper portion of the Kazimierz Opoka on the Vistula River (Fig. 5b, c), implying that they share the same age and depositional environments. The upper Maastrichtian opokas and their faunas were examined by MM near the villages of Mętów, Biedaczów, Kolonia Prawiedniki, Klimusin, and Wola Piasecka, all to the south and east of Lublin. In each of these localities, the index taxa of the belemnite *Belemnella kazimiroviensis*, inoceramid *Tenuipteria argentea*, and scaphitid *Hoploscaphites constrictus crassus* Zones are present. Only an outcrop near Mełgiew, east of Lublin, exposed a different style of opoka, with fossils testifying to the younger scaphitid *Hoploscaphites constrictus johnjagti* Zone (Machalski 2005a, b, 2012) and the XIII regional foraminiferal zone of Dubicka and Peryt (2012) (compare Tables 1 and 2). A similar biostratigraphic position, albeit with a degree of uncertainity in view of the preservational state (that is, the partial decalcification of the section), has been proposed for the upper levels of the Maastrichtian at Lechówka (Machalski et al. 2016).

In contrast to the Maastrichtian opokas, lateral equivalents of the Greensand and Siwak reveal significant facies changes towards the east. In general, both units become less quartzose and more opoka-like east of Kazimierz Dolny, suggesting a more off-shore, distal location relative to the terrigenous source area (Krischtafovitsch 1897, 1899; Pożaryski 1956). The equivalents of the Greensand and Siwak at Wola Piasecka and Mełgiew near Lublin express the development of an opoka-like facies, with abundant glauconite near the base. The same holds true for the Greensand and Siwak equivalents near Chełm (glauconitites from this area were described by Popiel 1977, Gazda et al. 1992, and Racki et al. 2011). Gazda et al. (1992) described the occurence of glauconitites in several sites around Chełm, but most of these outcrops are inaccesible at present (observations by MM). At Lechówka, the succession is more complete, given the presence, below the glauconitite level, of the boundary clay marking the K-Pg boundary and (decalcified) remnants of a thin white unit, tentatively interpreted as an equivalent of the Danish Cerithium Limestone (Racki et al. 2011; Machalski et al. 2016; see below). A clay layer similar to that from Lechówka was recorded at Zawadówka near Chełm (Harasimiuk and Rutkowski 1984).

The higher portions of the Siwak, developed as soft, occasionally slightly glauconitic gaizes and opokas with limestone intercalations, have been examined by MM in outcrops at Wąwolnica and Nałęczów (small towns between Kazimierz Dolny and Lublin), in the Tatary neighbourhood of Lublin, in the environs of Mełgiew, in temporary sections along the reconstructed S19 route south of Lublin, and at Stawska Góra and Lechówka near Chełm. Dark pyrite-bearing marly gaizes and clays recorded several dozen metres above the top of the Maastrichtian in the Żuków borehole, c. 30 km south-east of Lublin (Harasimiuk 1984), are probably correlatable with the dark middle Siwak marls at Parchatka. These deposits may have been deposited in a deeper-water environment that those below and above.

The Greensand and Siwak equivalents in the central and eastern Lublin Upland contain Danian fossil assemblages (mainly minute bivalves and gastropods) that are taxonomically very similar to, but not quite as abundant as, those from the Middle Vistula River section (Krach 1981). This also holds true for the basal glauconite-rich deposits at Wola Piasecka and Lechówka (observations by MM). The basal glauconitites additionally contain reworked late Maastrichtian fossils, although their abundance and preservation diminish eastwards. The nodular phosphates characteristic of the Greensand near Kazimierz Dolny are only represented by tiny grains at Wola Piasecka, and are absent farther east. As described below, burrow diversity, size, density, and burrowing depth also decrease eastwards along the prominent burrowed surface cutting through the upper Maastrichtian and lower-

most Danian deposits. In summary, physical and palaeontological evidence suggests a gentle eastward sloping of the seafloor and calmer, deeper, more offshore environments during the deposition of the Greensand and lower Siwak equivalents in the central and eastern Lublin Upland.

Only a single modern microfossil-based biostratigraphic assessment is available for the Greensand and Siwak equivalents east of Kazimierz Dolny. The site at Lechówka places both units as lower, but not lowermost, Danian (Machalski et al. 2016), which is consistent with the chronostratigraphy of the Greensand and the lower Siwak in the Kamienny Dół succession at Kazimierz Dolny (Żarski et al. 1998). The foramnifera quoted by Harasimiuk (1984) from boreholes near Lublin seem to be compatible with these datings.

According to borehole data, Siwak equivalents with basal glauconite-rich deposits lie discordantly on various upper Maastrichtian units in the central Lublin Upland (Wyrwicka 1980). This is compatible with the biostratigraphic differences of the topmost opoka units at Wola Piasecka and Mełgiew, as demonstrated by Machalski (2005a). Harasimiuk and Henkiel (1981) and Harasimiuk (1984) reported an angular disconformity between the Cretaceous and Paleogene strata in some locations. Generally, the thickness and facies patterns of the Maastrichtian strata were influenced by synsedimentary tectonics throughout the whole Maastrichtian, particularly near the Maastrichtian–Danian boundary (Wyrwicka 1977). This tectonic activity was related to the Laramide movements that led to the uplift and inversion of the Mid-Polish Anticlinorium (Swell) west of the outcrop area (Krzywiec et al. 2018).

OPOKA AND SPONGES

(*Ewa Świerczewska-Gładysz, Danuta Olszewska-Nejbert, Marcin Machalski*)

Definition of opoka

The term "opoka" was first used in the geological literature by Pusch (1833–1836), and literally translates to "foundation stone" (see Jurkowska et al. 2019 for a history of investigation). Since historically the recognition of opoka has been essentially restricted to the Polish literature, it is discussed below in more detail, along with the characteristics of the siliceous sponges that significantly contributed to the origin of this lithofacies.

Opoka is a carbonate siliceous rock, grey, white-grey or creamy yellow in colour, and is typically microporous and rather hard. The petrographic definition of opoka has been the subject of considerable debate (Sujkowski 1931; Pożaryska 1952; Jurkowska et al. 2019). A distinctive feature of opoka is that it does not disintegrate when treated with hydrochloric acid (Sujkowski 1931; Pożaryska 1952; Jurkowska et al. 2019). Recently, Jurkowska (2022, p. 9) proposed the following definition of opoka: "a carbonate rock composed of calcite (38–90%) and an insoluble residue (10–62%) whose main component is authigenic opal-CT (4–46%), forming networks consisting of adjoining lepispheres". This characteristic opal-CT framework distinguishes opoka from white chalk. Only a minor terrigenous contribution is present in opoka, in contrast to gaize, which contains a significant amount of detrital quartz (Jurkowska 2022).

Sponge spicules, mainly derived from the disintegration of non-rigid demosponges, are the main source of silica in opokas. The mass occurrence of siliceous spicules of non-rigid sponges – and/or voids after their dissolution – in opoka was first noted in Campanian opoka of the Middle Vistula River section (Świerczewska-Gładysz 2012). Further studies demonstrated that non-rigid sponge spicules were the main silica source in Campanian and lower Maastrichtian opokas (Jurkowska et al. 2019; Jurkowska and Świerczewska-Gładysz 2020); this also holds true in the Kazimierz Opoka (unpublished data of EŚ-G). After burial, sponge spicules, which were originally composed of biogenic silica (opal-A), dissolved, and the dissolved silica saturated porewaters such that opal-CT precipitation was enabled. The calcium carbonate contribution largely reflects primary grains composed of coccolith plates and foraminiferal tests, and a significant number of diagenetic, authigenic grains (Jurkowska et al. 2019; Jurkowska 2022).

The Kazimierz Opoka occurs in two macroscopically distinct varieties. The first – the porous opoka – is white or pale-cream and moderately hard, with dominant voids after dissolved sponge spicules (Fig. 6a). The second – the hard opoka – is light-grey and very

hard, with voids after spicules filled by sparite (Fig. 6b), and forms thin rhythmic intercalations in the Town Quarry section and a distinctive layer at the top of the Kazimierz Opoka. The average specific gravity for porous opoka from Kazimierz Dolny is about 1.46 g/cm^3, whereas that for the hard opoka from the top of the Bochotnica section is over 2.0 g/cm^3 (Pękala and Musiał 2021). The properties of typical opoka render it a good, weathering-resistant building stone, particularly stone from the lower Kazimierz Opoka. The more marly upper part of this unit is less resistant to weathering, as can be observed on the façades of old buildings in Kazimierz Dolny (Fig. 5d). A distinctive unit of brittle opoka at the top of the uppermost Maastrichtian at Mełgiew is even less resistant to weathering. At certain locations, the upper opoka levels were decalcified due to Paleogene weathering (Pożaryski 1951; Racki et al. 2011).

Sponge palaeoecology and taphonomy

Siliceous sponges are among the most important components of the fossil assemblages in the Kazimierz Opoka and its eastern equivalents. Their body fossils are discernible in virtually every larger piece of opoka (Fig. 5c). The sponge specimens are commonly limonitized, and usually their skeletons are completely dissolved. Voids after dissolved spicules are readily visible, in contrast to sponge fossils known from white chalk elsewhere. Bodily preserved sponges from Kazimierz Opoka and its eastern counterparts are almost exclusively from groups with rigid skeletons – that is, abundant hexactinosidan and lychnicosidan sponges (class Hexactinellidae) (Figs 5c, 7a, 13a), and less numerous lithistids (informal group of the class Demospongiae). Root-tuffs of lyssacinosidan sponges (hexactinellids with loose spicules) are very rare. Poorly preserved body remains of non-rigid demosponges are extremely rare (Fig. 7b), although their isolated spicules occur in masses throughout the opoka.

Almost all sponges with rigid skeletons that have been recovered from the Kazimierz Opoka show adaptations to soft bottom colonisation, developing root-like outgrows or rhizoids (Figs 7a, 13a–c) unknown in modern sponges. Lyssacinosidans root-tuffs also confirm the soft nature of the bottom sediment. Some species preferred hard substrata, settling on mollusk shells or the skeletons of dead sponges.

Recent non-rigid and lithistid demosponges inhabit a wide depth spectrum. Only some lithistid genera (unknown from opoka) are noted in extremely shallow seas (Hooper and van Soest 2002). In terms of structure and physiology, all hexactinellid sponges are adapted to live in deeper, calm waters with relatively low sedimentation rates (Leys et al. 2007). Tests of hexactinellid sponges with rigid skeletons from the Kazimierz Opoka show the adapative variability of pertinent morphological characters (Świerczewska-Gładysz 2006). Hexactinellid sponges characterised by very thin walls and regular body shapes (e.g., funnel-like with a thin stalk, less than 10 mm in diameter) are particularly common in the lower Kazimierz Opoka exposed in the Town Quarry, indicating a calm, outer shelf environment. In contrast, the upper Kazimierz Opoka at Nasiłów and Bochotnica is typified by relatively low hexactinellid species diversity, the absence of extremely thin-walled species, and the occurrence, in some species, of an additional siliceous network layer to strengthen the skeleton. All these observations confirm a general shallowing trend during the deposition of the Kazimierz Opoka (Świerczewska-Gładysz 2006).

The phosphatised remains of siliceous sponges are of special interest for the depositional history of the Greensand (Fig. 10c – 5). Only Late Cretaceous taxa have been identified in this unit; no bodily preserved Danian sponges have been identified (Świerczewska-Gładysz 2006; Świerczewska-Gładysz and Olszewska-Nejbert 2006). Świerczewska-Gładysz and Olszewska-Nejbert (2006) analysed the internal sediments preserved in spongocoels, interspicular spaces, and canals within phosphatised sponge skeletons from Nasiłów. Two distinctive assemblages were distinguished. The first comprises specimens infilled by phosphatised opoka, corresponding to the Kazimierz Opoka. Some of these specimens also contain relics of phosphatised opoka enriched in glauconite relative to the Kazimierz Opoka. Specimens of the second assemblage are infilled only by this phosphatised glauconitic opoka. The latter assemblage, therefore, was interpreted to stem from

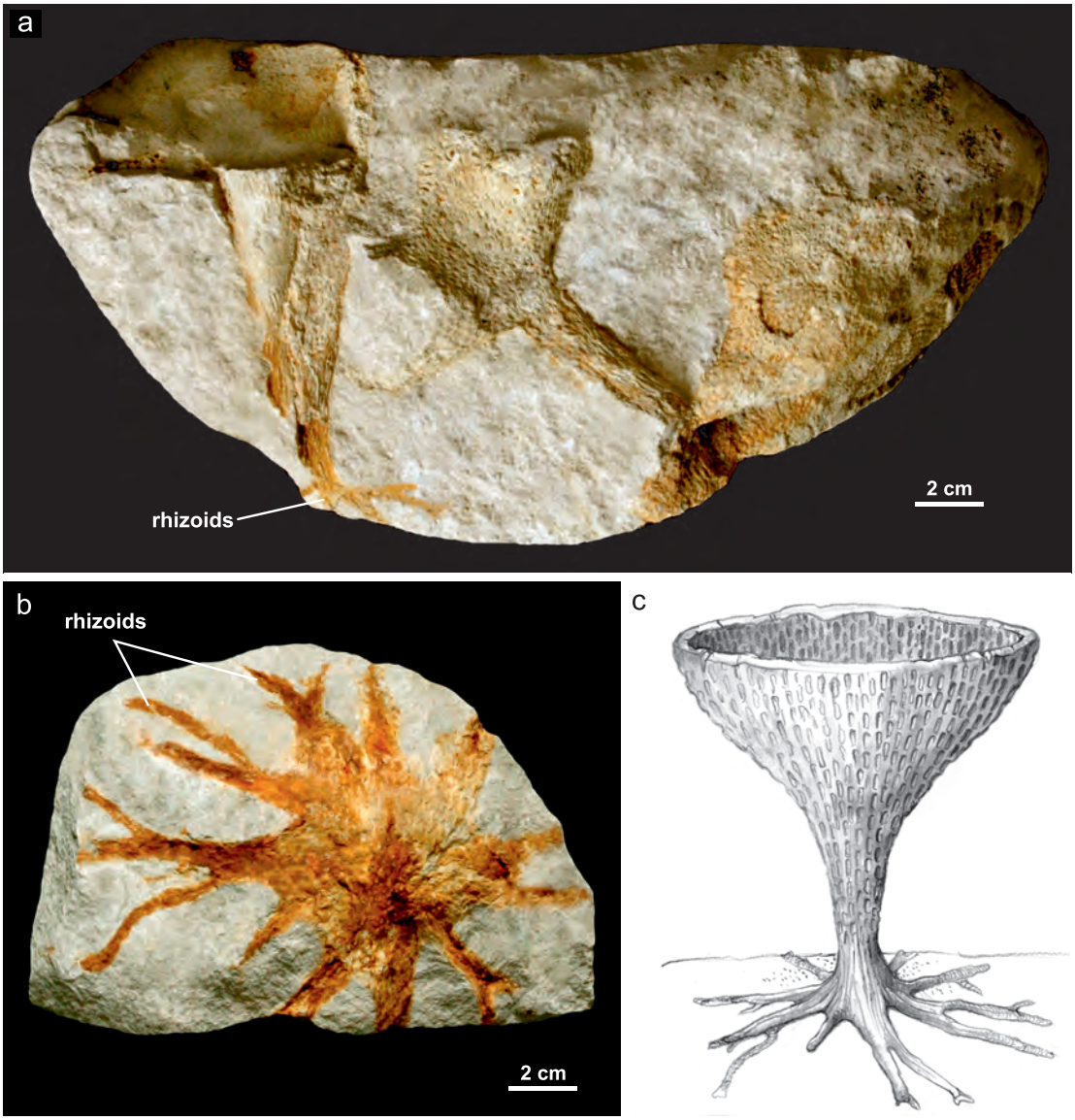

Fig. 13. Ventriculitid sponges (Lychniscosida) with preserved root-like outgrows (rhizoids) from the Kazimierz Opoka: **a** – two specimens of *Rhizopoterion cribrosum* (in the center and left) and *Sporadoscinia decheni* (to the right), Nasiłów (Locality 1); **b** – rhizoids of *Rhizopoterion cribrosum*, Town Quarry south of Kazimierz Dolny (Locality 3); **c** – reconstruction of a living sponge, stabilised on the seafloor by rhizoids.

a glauconitic opoka unit eradicated from the Kazimierz Dolny area *via* erosion (Machalski and Walaszczyk 1987; Hansen et al. 1989; Machalski 1998).

The data presented by Świerczewska-Gładysz and Olszewska-Nejbert (2006) suggest a complex taphonomical scenario. In the earliest stage, sponges originally embedded in opoka were exposed and subsequently buried in the glauconitic opoka sediment along with indigenous specimens. All of these specimens were subsequently exhumed during another erosional event, and afterwards were ultimately buried in the Greensand proper. Their phosphatisation took place under low net accumulation rates, during temporary cover by sediment. As expected, the taxonomic composition of the stratigraphically older sponge group is similar to that of the sponge assemblage from the Kazimierz Opoka. In the younger group, lithistids are more abundant and tax-

onomically diverse, suggesting a continuation of the shallowing trend inferred for the Kazimierz Opoka (Świerczewska-Gładysz and Olszewska-Nejbert 2006).

CRETACEOUS–PALEOGENE BOUNDARY INTERVAL

(*Marcin Machalski*)

A prominent burrowed discontinuity surface that truncates the Maastrichtian deposits near Kazimierz Dolny and Lublin and the lowermost Danian strata near Chełm, as well as the age and genetic interpretation of the overlying glauconite-rich units, are of key importance for understanding the Cretaceous–Paleogene (Maastrichtian–Danian) boundary events in the excursion area. The burrowed surface will be discussed in detail, with a particular focus on its ichnofossils and origin. The dating and genesis of the glauconite-rich units are also discussed, mainly in the context of a recent paper by Remin et al. (2021).

Main burrowed surface

A heavily burrowed surface, referred to as the main burrowed surface further on in this chapter, is strikingly apparent at the top of the Kazimierz Opoka succession. This major regional discontinuity surface has attracted attention since Kongiel (1935), Pożaryski (1938), and Pożaryska (1952, 1965), who classified it as a hardground. However, the cross-cutting relationships of successive burrow generations, filled with sandy-glauconitic sediment from above, demonstrate that the carbonate cementation of the opoka postdated the commencement of Greensand deposition (Machalski 1998). Therefore, the indurated bed at the top of the Kazimierz Opoka cannot be classified as a hardground (Machalski 1998).

An additional argument against a hardground interpretation stems from the fact that the topmost interval of the Kazimierz Opoka, 10–20 cm thick, is not indurated at all, but rather is composed of a very soft marly opoka. At Bochotnica, a gradual transition exists between the soft and hard opoka (Pożaryska 1952; Machalski 1998; Machalski and Jagt 1998), while at Nasiłów the boundary appears more distinct (Remin et al. 2021). There is also no evidence that the top of the indurated zone represents an incipient hardground, as proposed by Machalski and Walaszczyk (1987) and Remin et al. (2021). Incipient hardgrounds are those where the lithification front did not reach the seafloor surface (Kennedy and Garisson 1975a). At Nasiłów and Bochotnica, however, many glauconite-filled burrows present in the indurated opoka start well above this zone – in the soft opoka or in the glauconitic sandstone. Such burrows certainly could not have penetrated the indurated zone if it was already cemented.

The burrows run in various directions, which makes them appear in a variety of cross sections on rock surfaces (Fig. 14a). Moreover, they are commonly obliterated by subsequent burrow generations (Fig. 14c, d). Therefore, the burrows often lack ichnotaxonomically diagnostic characters. The most informative burrow fragments belong to *Thalassinoides saxonicus* (*sensu* Kennedy 1967), *Th. suevicus*, *Th.* isp., *Gyrolithes* isp., and *Chondrites* isp. (Machalski and Walaszczyk 1987; Machalski 1998). The burrows of *Th. saxonicus* are large, reaching up to c. 15 cm in diameter. The corresponding ichnoassemblage contains both the omission and early post-omission suites (see Bromley 1975 for definitions). Similar assemblages are typical for discontinuity surfaces in the epicontinental Jurassic and Cretaceous of Europe (e.g., Kennedy 1967; Fürsich 1974; Bromley 1975). The pre-omission suite below the top of the Kazimierz Opoka includes *Planolites*, *Palaeophycus*, and *Lepidenteron*, and the late post-omission suite in Greensand is represented by *Schaubcylindrichnus* isp. ("*Spongeliomorpha*" *annulata* of Machalski and Walaszczyk 1987) and indeterminate burrows.

The *Thalassinoides* structures have been widely interpreted as burrows of fossorial decapod crustaceans (e.g., Bromley 1975; Carmona et al. 2004). Interpretations that some apparently J-shaped burrows from Nasiłów were produced by counterparts of recent, tidal-flat bound *Ocypode* crabs (Radwański 1985; Abdel-Gawad 1986) have been questioned by Machalski (1998).

The burrows usually do not descend deeper than the indurated opoka, although rare examples are discernible below this zone. As observed by Machalski (1998) and Machalski and Jagt (2018), the crowding of successive

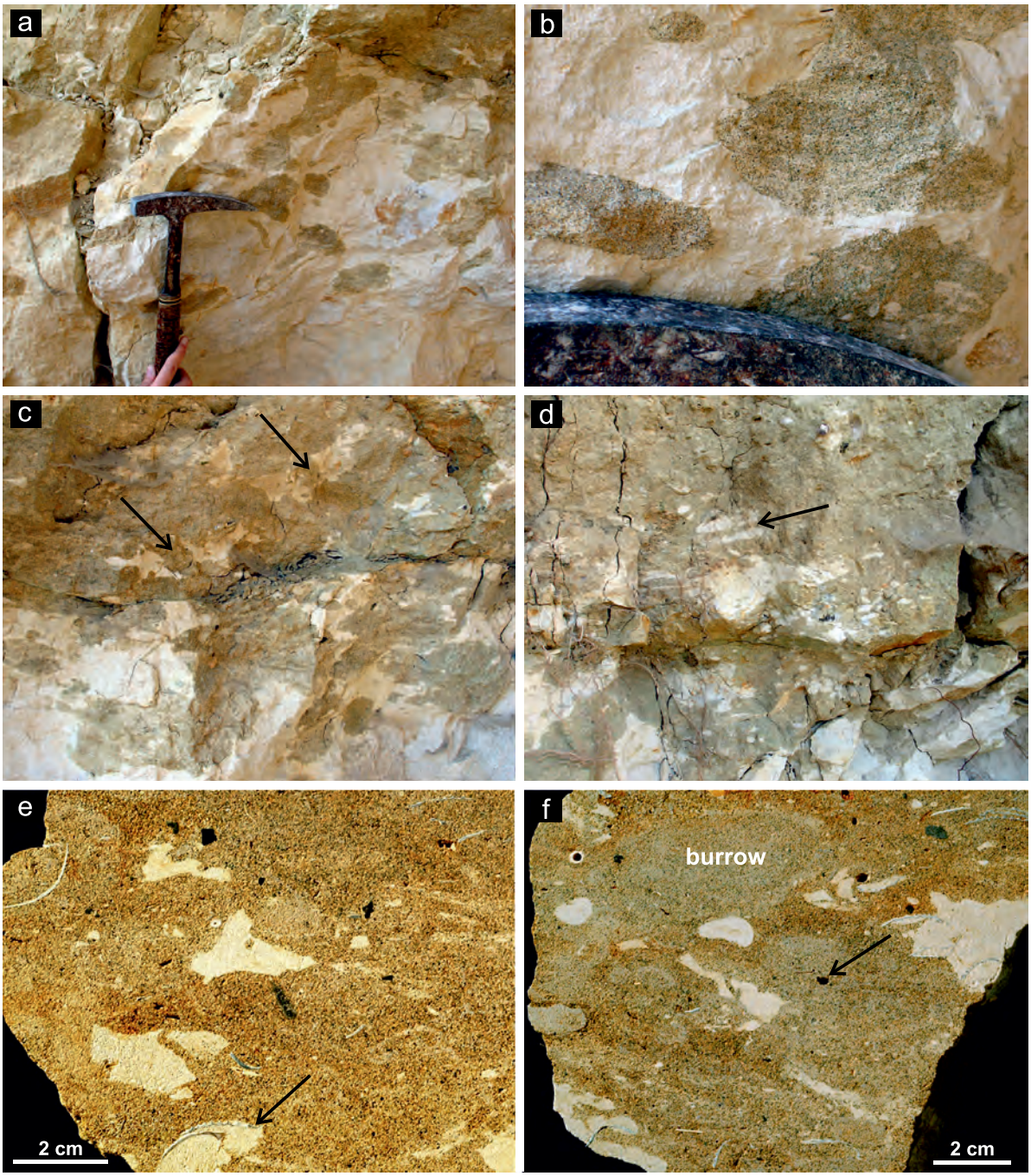

Fig. 14. Details of the Cretaceous–Paleogene interval at Bochotnica (Locality 2): **a** – top of the Kazimierz Opoka, with burrows filled with the overlying glauconitic sandstone of the Danian Greensand; **b** – laminated infill of a burrow; **c** and **d** – pseudobreccia at the top of the Kazimierz Opoka with horizontal parts of the post-omission burrows (marked by arrows) created during sedimentation of the Greensand; **e** and **f** – details of the pseudobreccia zone with a scallop valve (probably *Dhondtichlamys acuteplicata*) marked in e, and a tiny phosphate grain marked in f. Note the mottled ichnofabric of the glauconitic sandstone with cross-sections of the post-omission burrows in f.

generations of omission and post-omission burrows results in a brecciated appearance of the topmost Kazimierz Opoka (Fig. 14c–f). As a result, irregular soft opoka shreds float in the glauconitic sediment mass (the pseudobreccia of Bromley 1975, see also Frey and

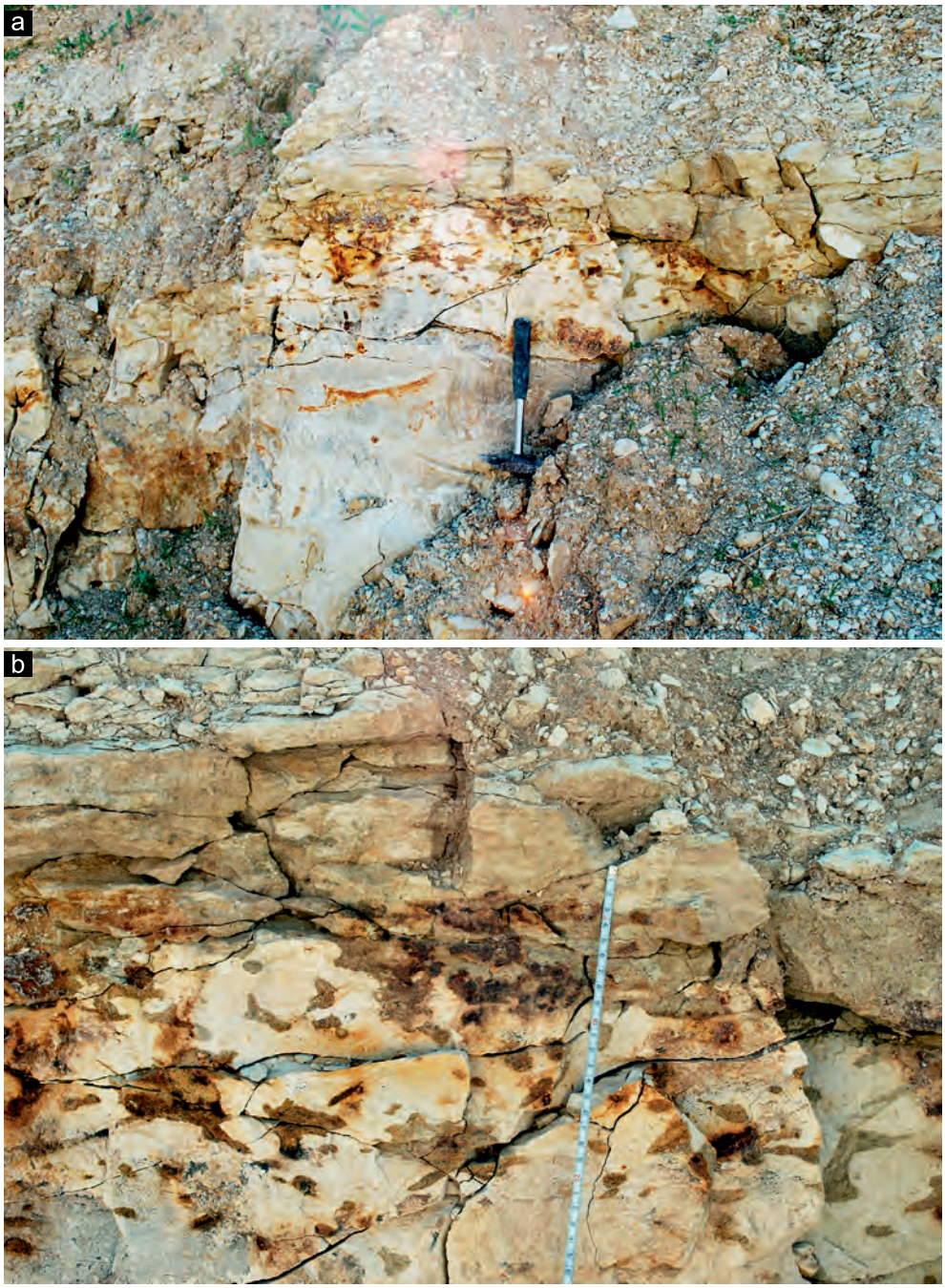

Fig. 15. The Cretaceous–Paleogene interval at Wola Piasecka (Locality 4): **a** – general view, note the strongly burrowed top of the upper Maastrichtian opoka and the overlying glauconitic sediment of Danian age, which also infills the (limonite-stained) burrows piping down into the opoka; **b** – details of a. Photos from 2010, courtesy of M. Duda.

Bromley 1984 and Bottjer 1985). These shreds, which occur up to the phosphorite layer, are so soft and filigree in shape (Fig. 14c–f) that they could not have survived any physical reworking (Machalski and Jagt 2018).

The burrow outlines reveal no deformation, and faint lamination may be seen in some infillings (Fig. 14b). It may be therefore concluded that these were open burrows excavated in a semi-cohesive sediment, a typical

example of the *Glossifungites* ichnofacies (see e.g., MacEachern et al. 2007).

There are significant differences in the composition, burrow morphology, density, and burrowing depth between the burrow assemblages along a lateral transect of the burrowed surface through the Lublin Upland.

At Wola Piasecka (and in other localities near Lublin, except Mełgiew), the trace fossil assemblage is similar in composition and density to that from Nasiłów and Bochotnica. However, the largest burrows, assigned to *Thalassinoides saxonicus*, appear to be rare at Wola Piasecka (Fig. 15a, b). Most of the omission and post-omission burrows at this site represent *Thalassinoides suevicus*. The maximum burrowing depth is the same as at Nasiłów and Bochotnica, but the pseudobreccia is much less prominent at Wola Piasecka (Fig. 15a, b).

At Mełgiew, burrows at the top of the uppermost Maastrichtian opoka are less numerous, and are represented by simple (unnamed) tubes (Machalski 2005a). Typically, they reach 1 to 3 cm in diameter, are straight or gently curved, and pipe down to a level at most 20 cm below the top of the Maastrichtian, but usually shallower. Pseudobreccia is absent at Mełgiew due to the relatively low burrow density.

At Lechówka, burrows also possess simple morphologies, although branching may be observed. These burrows are surrounded by cementation aureoles, are usually around 1 cm in diameter, and reach depths less than 20 cm. The burrow density is somewhat greater at Lechówka relative to Mełgiew, resulting in pseudobreccia formation.

In all studied locations, the burrows descending from the main burrowed surface are filled with glauconite-rich sediments piped down from above. The fundamental difference, however, is that while burrows from almost all of the sites mentioned above penetrate into the underlying Maastrichtian deposits, the Lechówka burrows descend into the possible equivalent of the lower Danian Cerithium Limestone from Denmark (Racki et al. 2011) and the underlying K-Pg boundary clay, which by definition is the lowermost Danian. The implication, then, is that the formation of the main burrowed surface postdates the K-Pg boundary.

In summary, ichnotaxonomic diversity, burrow complexity, burrow size, and burrowing depth generally decrease eastwards along the main burrowed surface. This trend was presumably related to ecological conditions, which seem to have been more favourable for a greater variety (and maximum body size) of burrowing decapods in the west. The observed changes parallel the facies patterns observed in the deposits overlying the burrowed surface, and suggest that it sloped to the east, from shallower to deeper environments. The origin of the burrowed surface relief is presumably tied to the tectonic uplift of the western part of the study area, which may have been related to the final phases of the Mid-Polish Anticlinorium inversion.

Genetically, the formation of this regional discontinuity surface may have been accomplished in three stages. At the first stage, the erosional surface was developed during a sea-level low (or emersion?). During the second, omission stage, the surface was colonised by fossorial decapod crustaceans which produced open burrows. At the third stage, these burrows were filled by the glauconite-rich sediments of the next depositional cycle. In terms of sequence stratigraphy, then, the main burrowed surface may be interpreted as a transgressive surface superimposed on the sequence boundary.

Nature and age of the Greensand and correlative glauconitites

In contrast to the Kazimierz Opoka and the Siwak, the age of the Greensand in the Middle Vistula River section has been subjected to persistent controversy, which has led to divergent placements of the K-Pg boundary (Fig. 16; Machalski 1998; Machalski and Jagt 2018; Remin et al. 2021). As remarked above, a vast majority of recent students agree that the Greensand is Danian in age – and, more precisely, is the basal bed of the Danian depositional cycle. Consequently, the most recent workers place the K-Pg boundary at the top of the Kazimierz Opoka (Fig. 16). This same assessment has been made for Greensand counterparts in the central and eastern Lublin Upland (e.g., Wyrwicka 1977, 1980; Harasimiuk 1984).

Remin et al. (2021) firmly rejected this interpretation, however, based on their study of planktic foraminifera and dinoflagellates from Nasiłów. These authors argued that the

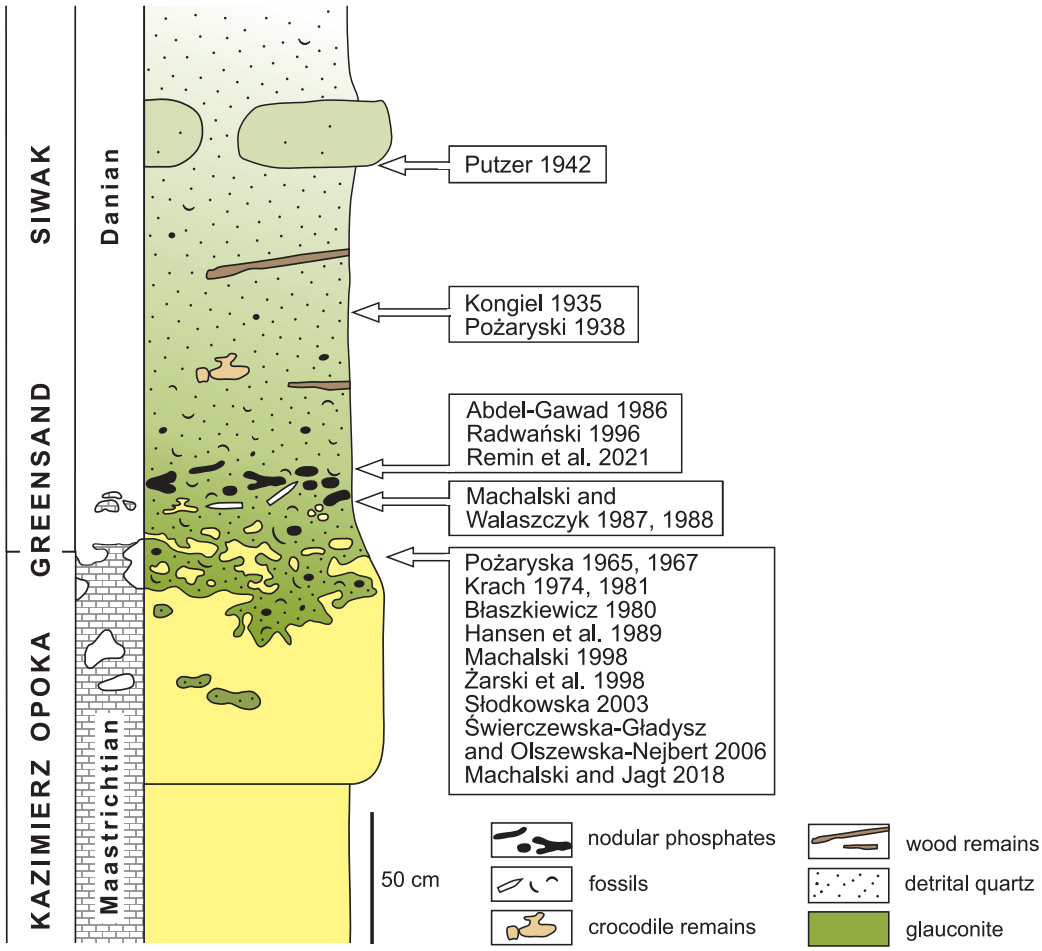

Fig. 16. Placement of the Cretaceous–Paleogene (Maastrichtian–Danian) boundary by various authors on a generalised section of the Kazimierz Dolny area (modified from Machalski 1998, fig. 2). The crocodile and wood remains refer to those described from the Kamienny Dół section by Żarski et al. (1998).

Greensand is a distinctive depositional unit with sharp lower and upper boundaries, and is of "a very terminal Maastrichtian age" (Remin et al. 2021, p. 19). Consequently, they placed the K-Pg boundary above the layer of nodular phosphates and fossils, conventionally regarded as the upper part of the Greensand. There is insufficient space here to discuss all of their data and conclusions. However, some comments are necessary to explain why their interpretation cannot be accepted here:

1) The upper boundary of the Greensand is not sharp, as depicted in Remin et al. (2021, fig. 3) but gradational to the overlying Siwak. As such, the Greensand falls into the category of "base-of-cycle" condensed beds (Type III and IV fossil concentrations in Kidwell 1986, 1991a). This fact, alone, testifies to the genetic linkage of the Greensand and the Siwak, which is of Danian age (Krach 1974; Machalski 1998).

2) A unit above the indurated "hardground" distinguished by Remin et al. (2021) as the "Marly Chalk" is better interpreted as a soft, unlithified opoka passing gradually into the indurated opoka below (Machalski 1998, 2005a; Machalski and Jagt 2018). The soft opoka contains the same macrofossil assemblage as the hard opoka (Machalski 1998, 2005a). This assemblage includes the scaphitid *Hoploscaphites constrictus crassus*, the index fossil for the *H. c. crassus* Zone of Błaszkiewicz (1980) and Machalski (2012), thus casting doubt on the conclusions of Remin et al. (2021) about the latest Maastrichtian age of their Marly Chalk.

3) Remin et al. (2021) proposed a latest Maastrichtian age for the Greensand based on five samples, only one of which did not contain any Danian microfossils; rare specimens of Danian foraminifera and dinoflagellates were reported from the other samples. These Danian records were discarded by Remin et al. (2021) as contamination or material piped down by burrowers. Only at the level above the phosphorite layer did they observe a bloom of Danian planktonic foraminifera and dinoflagellates.

The evidence presented by Remin et al. (2021) is considered here insufficient to overthrow the interpreted Danian age of the Greensand. Masses of phosphatised and unphosphatised Maastrichtian fossils, in various degrees of preservation, are known to occur in the Greensand (Kongiel 1935; Krach 1974; Hansen et al. 1989; Machalski 1998; Świerczewska-Gładysz and Olszewska-Nejbrt 2006). The original provenance of these assemblages can be deciphered based on examinations of fossil infillings, and/or pieces of rock still adhering to their surface (as demonstrated for sponges in the preceding section; see also Figs 10a, c-1,6, 14e). Accordingly, the Maastrichtian fossils – which are represented only by most resistant and insoluble calcitic shells or equally durable "pre-fossilised" phosphatic moulds – have been interpreted as partly derived from the underlying opoka and partly from a glauconitic opoka unit subsequently removed by erosion (these latter fossils thus form a *remanié* assemblage *sensu* Fürsich et al. 1981). To date, no demonstrably *in situ* late Maastrichtian macrofossils have been identified from the Greensand.

Some of the Danian macrofossils from the Greensand are also preserved as phosphatic moulds (Machalski and Jagt 2018), but most commonly they occur as unphosphatised moulds of originally aragonitic bivalves (Fig. 10b) and gastropods. These moulds are lithologically identical to the surrounding glauconitic sandstone, pointing to the indigenous nature of the Danian assemblage. The Danian bivalve and gastropod taxa present in the Greensand usually range to the higher levels of the Siwak (Krach 1974, 1981; Machalski 1998), which again supports a strong link between these units. The co-occurrence of exhumed and indigenous faunal elements in the Greensand enables a classification of this unit as a mixed lag/hiatal fossil concentration *sensu* Kidwell (1991b).

Late Maastrichtian and Danian macrofossils are randomly mixed in the Greensand, as may be best appreciated when studying the section at Bochotnica. In some places, particularly in the phosphorite layer, fossils and nodules of different ages and preservation states are aligned more or less horizontally (Fig. 17a), suggestive of hydrodynamic reworking. Putzer (1942) correctly interpreted the phosphorite level at Nasiłów and Bochotnica as the *Aufarbeitungshorizont*. In other places, the fossils and nodules occur in "nests" composed of specimens in all possible positions (Fig. 17b). Such concentrations are best interpreted as a result of intense biogenic sediment reworking (Machalski and Walaszczyk 1987; Machalski and Jagt 2018). This process, which gently preserves fossils from the soft opoka, may have been dominant prior to the formation of the phosphorite layer. The many "opoka fossils" in the Greensand are only partially exposed on the surface of opoka shreds (Figs 10a, 14e).

In Remin et al. (2021), the term "condensation" is never mentioned. However, the glauconite and phosphate-rich facies, and the inferred complex taphonomic histories of the fossil assemblages, point to a condensed nature of the Greensand. Additionally, the phosphorite layer, although conventionally regarded as the upper portion of the Greensand, is better considered a basal conglomerate. The soft opoka shreds range to the phosphorite level (Fig. 17b), suggesting that the top surface of the Kazimierz Opoka was originally situated at about this level. Subsequently, it was largely replaced by sandy-glauconitic sediment infilling successive burrow generations (Machalski 1998; Machalski and Jagt 2018).

In conclusion, the physical and palaeontological evidence support an interpretation of the Nasiłów and Bochotnica Greensand as the basal, condensed transgressive portion of the Danian sedimentary cycle, with the phosphorite layer forming a basal lag laid down over the underlying burrowed surface at the top of the Kazimierz Opoka. Analogous admixtures of fossils with variable ages, preservation states, and derivations are typical of heavily bioturbated, glauconite- and phosphate-rich condensed transgressive units elsewhere (Kennedy and Garrison 1975b; Fürsich et al.

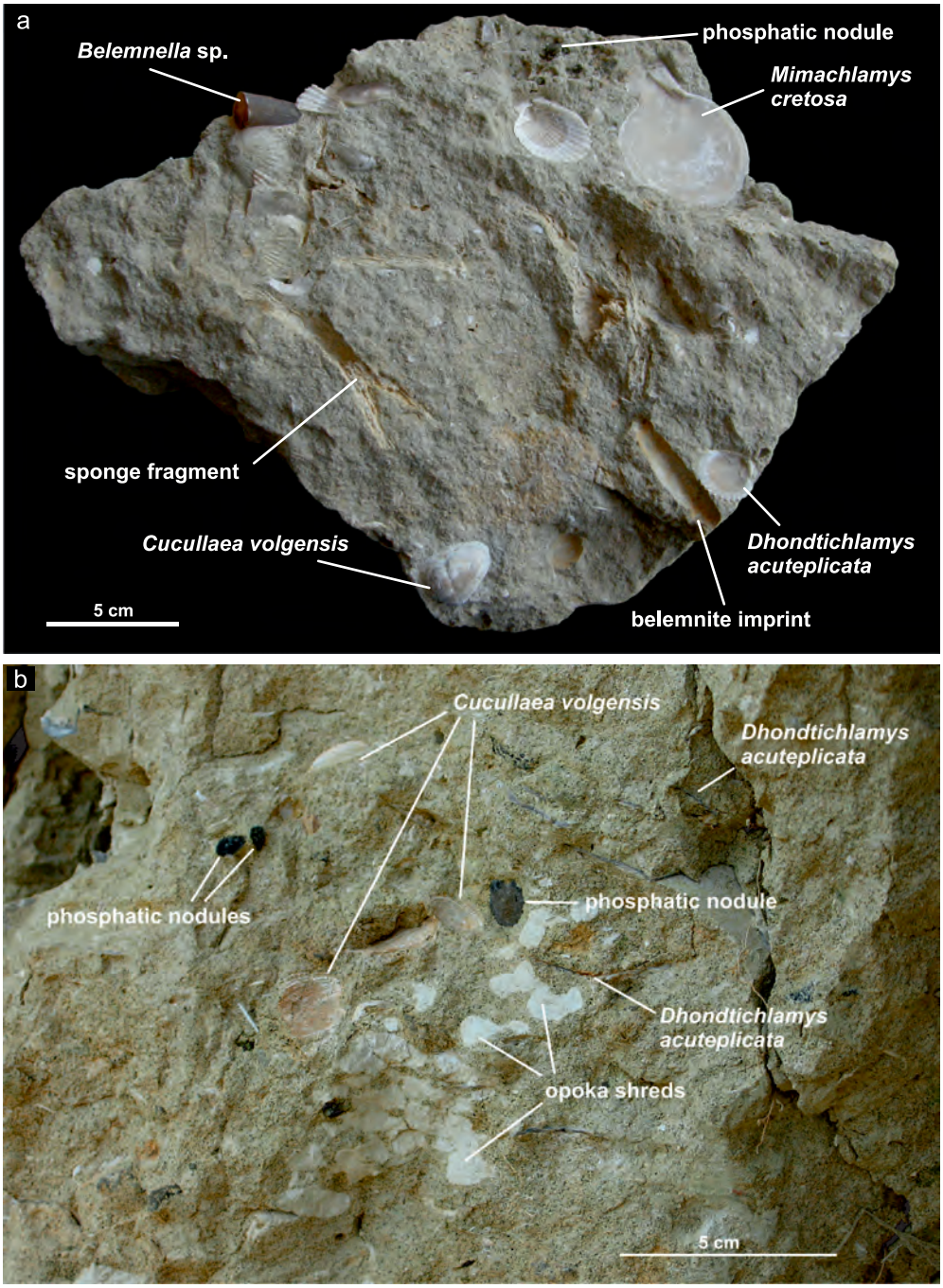

Fig. 17. Fossil concentrations in the Greensand exposed at Bochotnica: **a** – derived Maastrichtian and indigenous Danian (*Cucullaea volgensis*) fossils on a horizontal bedding plane, in a slab collected approximately at the phosphorite level; **b** – vertical section in the upper portion of the Greensand with a mixture of Maastrichtian and Danian fossils, soft opoka shreds, and phosphatic nodules (photo taken at Locality 2).

1981; Bottjer 1985; Kidwell 1991a, b; Wilmsen 2012). There is no contradiction betwen this interpretation and the massive predominance of Maastrichtian microfossils reported by Remin et al. (2021) from the Greensand. Indeed, it may be expected that a basal transgressive unit with abundant macrofossils derived from older deposits would also contain profuse mi-

crofossils of the same derivation. Specifically, the decapods that dug deep burrows in the underlying Maastrichtian soft sediment, also during the early stages of the Greensand sedimentation (post-omission burrows), must have expelled significant amounts of Maastrichtian sediment and microfossils to the Greensand sediment-water interface (in analogy to their recent counterparts, see e.g., Pillay and Branch 2011).

As mentioned earlier, the glauconite-rich lateral equivalents of the Greensand in the central and eastern Lublin Upland contain less diverse fossil assemblages. Late Maastrichtian fossils, demonstrably reworked from the underlying opoka (as evidenced by opoka infillings and adhered pieces of opoka) are common in the glauconite-rich bed at Wola Piasecka. Interestingly, no concentration of glauconite, phosphates, and fossils has been observed at Mełgiew. In the glauconitite level at Lechówka, Maastrichtian fossils are extremely rare (Racki et al. 2011; observations by MM). In contrast, Danian gastropod and bivalve assemblages are well represented in all studied glauconitites. They substantially differ in taxonomic composition from the upper Maastrichtian assemblages known from the underlying opokas (Abdel-Gawad 1986), but are very similar to the assemblages documented from the Siwak (Krach 1981). Danian mollusks have been collected from the glauconite-rich bed at Wola Piasecka (unpublished data of MM). Several Danian gastropod and bivalve taxa were recorded by Racki et al. (2011) from the glauconitite at Lechówka. Together with foraminiferal dating (Machalski et al. 2016), this supports an early, but not earliest, Danian age. The basal Danian glauconite-rich deposits from the central and eastern Lublin Upland are therefore best interpreted as less condensed counterparts of the Danian Greensand from the Middle Vistula River section.

Correlations and event sequence across the K-Pg boundary

The physical and palaeontological evidence presented above enables correlations to be made between the key K-Pg outcrops treated in this excursion. The famous K-Pg section at Stevns Klint (eastern Denmark) serves as the reference section for these correlations (Fig. 18). The Danish succession (Surlyk 1997; Hart et al. 2004, 2005; Rasmussen et al. 2005; Surlyk et al. 2006) is one of the most important and intensely studied on the planet (Alvarez et al. 1980, 1984), and originated in the same basin as the Polish successions discussed. Table 3 presents chrono-, litho- and biostratigraphic subdivisions of the Stevns Klint section.

Discontinuity surfaces and marker beds are selected as primary correlative tools, in combination with the available biostratigraphical data. Amongst the latter, two subdivisions are regarded as paramount. These are:

(1) The regional subdivision of the Boreal upper Maastrichtian in central Europe based on successive temporal subspecies of the scaphitid ammonite *Hoploscaphites constrictus* evolutionary lineage (Fig. 19; Table 2; Machalski 2005a, b, 2012; Walaszczyk et al. 2016; Machalski et al. 2021).

(2) Planktonic foraminiferal biozonation of the upper Maastrichtian and lower Danian (e.g.,

Chrono-stratigraphy		Lithostratigraphy			Foraminiferal zonation
Paleogene	Danian	Chalk Group	Stevns Klint Fm.	Korsnoeb Mb.	P1c
					P1b
			Rødvig Fm.	Cerithium Limestone Mb.	P1a
					Pα
				Fish Clay Mb.	P0
Cretaceous	Maastrichtian		Tor Fm.	Højerup Mb.	*Stensioeina esnehensis*
				Sigerslev Mb.	*Pseudotextularia elegans*

Table 3. Stratigraphy of the Stevns Klint section (modified from Surlyk et al. 2006, fig. 4).

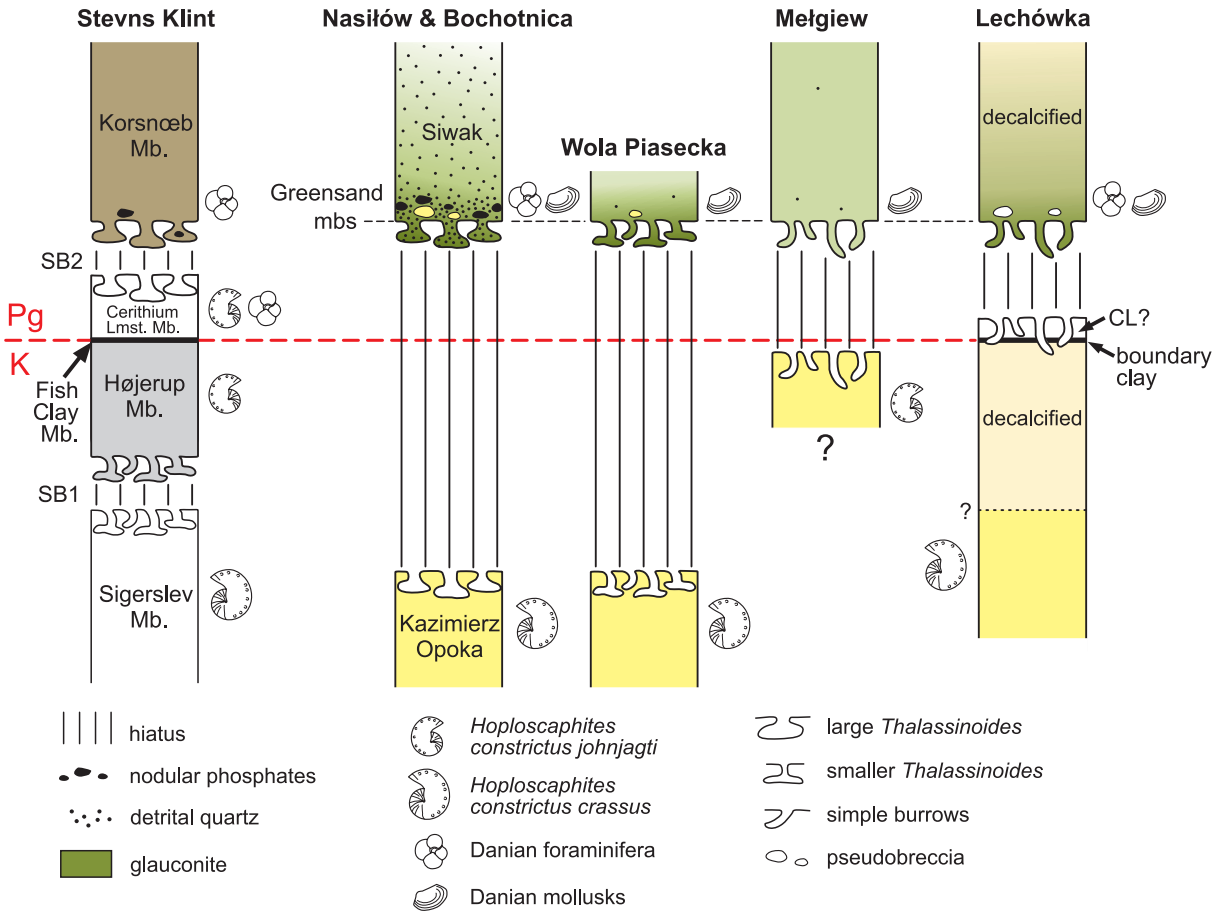

Fig. 18. Correlation between the Stevns Klint section in Denmark and the key Cretaceous–Paleogene sections in the Lublin Upland. CL? – a possible counterpart of the Danish Cerithium Limestone; mbs – main burrowed surface. See text for further explanations.

Keller et al. 1993; Rasmussen et al. 2005; Tables 2 and 3).

There are three principal correlational levels in the Stevns Klint succession (Fig. 18). These are (from bottom to top):

(1) Two superimposed incipient hardgrounds with decapod burrows, which separate the relatively deep water white chalk of the Sigerslev Member (Tor Formation) from the relatively shallow, bioclast rich grey chalk of the Højerup Member (Tor Formation). In terms of sequence stratigraphy, this double hardground represents the sequence boundary SB1, caused by a sea level fall and hiatus between the late and lastest Maastrichtian (Surlyk 1997; see also Lykke-Andersen and Surlyk 2004). Only smaller *Thalassinoides* burrow systems, comparable to *Th. suevicus*, occur at this surface (Surlyk et al. 2006, fig. 8).

(2) A thin clay layer (traditionally called the Fish Clay or Fiskeler; in current nomenclature, the Fish Clay Member of the Rødvig Formation) with an anomalous concentration of iridium and impact ejecta. This clay was rapidly deposited in shallow basins between the crests of the upper Maastrichtian bioherms of the Højerup Member in the direct aftermath of the Chixculub impact (Alvarez et al. 1980; Schulte et al. 2010). The boundary clay, the base of which defines the Cretaceous–Paleogene boundary, passes upwards into the lowermost Danian Cerithium Limestone Member of the Rødvig Formation (e.g., Rasmussen et al. 2005; Surlyk et al. 2006).

(3) A prominent, strongly burrowed hardground with phosphate and glauconite mineralisation, with redeposited phosphatised and glauconitised Maastrichtian fossils on top

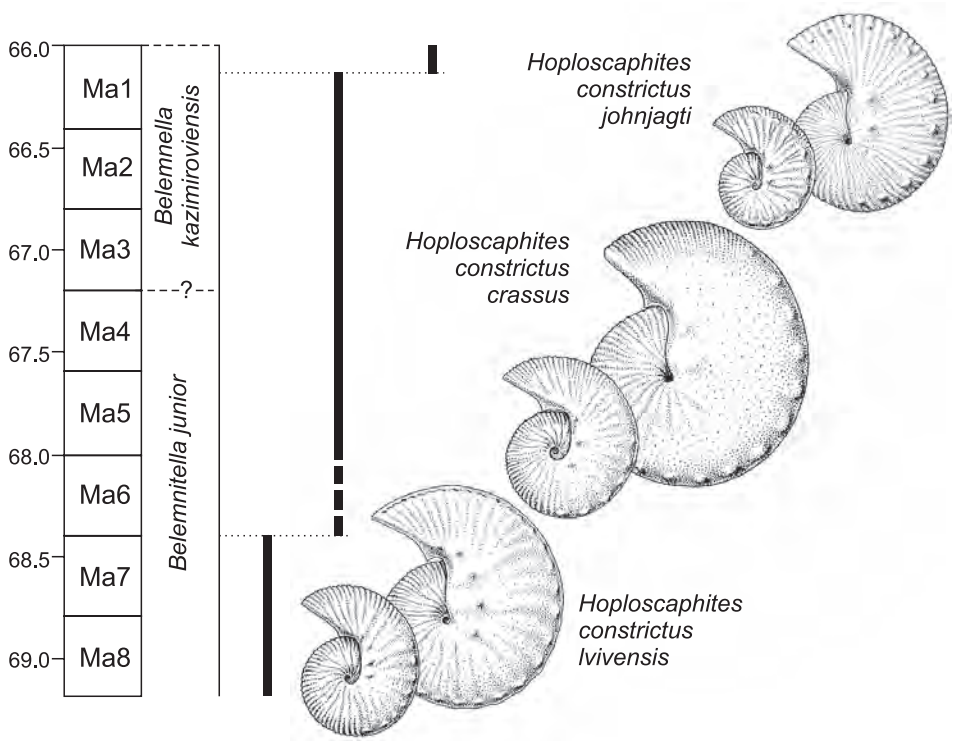

Fig. 19. Evolutionary lineage and subspecies succession of the scaphitid ammonite *Hoploscaphites constrictus* in the upper Maastrichtian of central Europe, plotted against the astronomical and belemnite scales of Keutgen (2018). Modified from Machalski et al. (2021, supplemental fig. 3).

(Rasmussen 1971; Machalski and Heinberg 2005). This hardground truncates both the Cerithium Limestone basins and the intervening Maastrichtian bioherm crests (Alvarez et al. 1984; Surlyk et al. 2006). This is sequence boundary SB2 of Surlyk (1997), separating the lowermost Danian Fish Clay and Cerithium Limestone Members from the lower Danian bryozoan limestones of the Korsnæb Member (Stevens Klint Formation). The origin of this surface has been linked to a major drop in relative sea level (Surlyk 1997). Both large and smaller boxworks of *Thalassinoides* burrows occur along this discontinuity surface (Rasmussen 1971; Bromley 1975).

For correlation with the Lublin Upland sections, the occurrence of *Hoploscaphites constrictus crassus* in the Sigerslev Member and the succeding subspecies, *H. c. johnjagti*, in the overlying Højerup and Cerithium Limestone Members are of first-rate importance (Figs 18, 19; Machalski 2005a, b). These species are the eponymous index taxa of the successive *H. c. crassus* and *H. c. johnjagti* zones (Machalski 2012). The occurrence of planktonic foraminifera belonging to the P1b Zone at the base of the Korsnæb Member is also quite important (Fig. 18; Table 3; Rasmussen et al. 2005; Surlyk et al. 2006).

In Poland, no counterpart of the SB1 hardground at Stevns Klint has been recognised in surface outcrops to date. Some of the nodular phosphates from the Greensand at Nasiłów and Bochotnica seem to represent reworked fragments of a nodular incipient hardground riddled with decapod burrows (Machalski and Walaszczyk 1987). These, perhaps, are the remnants of the SB1 hardground, which was subsequently reworked into the Greensand.

A counterpart of the Fish Clay Member has been recognised in Poland solely at Lechówka (Fig. 20; Racki et al. 2011). The boundary clay provides the strongest correlative link between Poland and Denmark, additionally strengthened by the occurrence of a white burrowed unit above the clay, interpreted as a counterpart to the Cerithium Limestone (Racki et al. 2011). The boundary clay at Lechówka contains

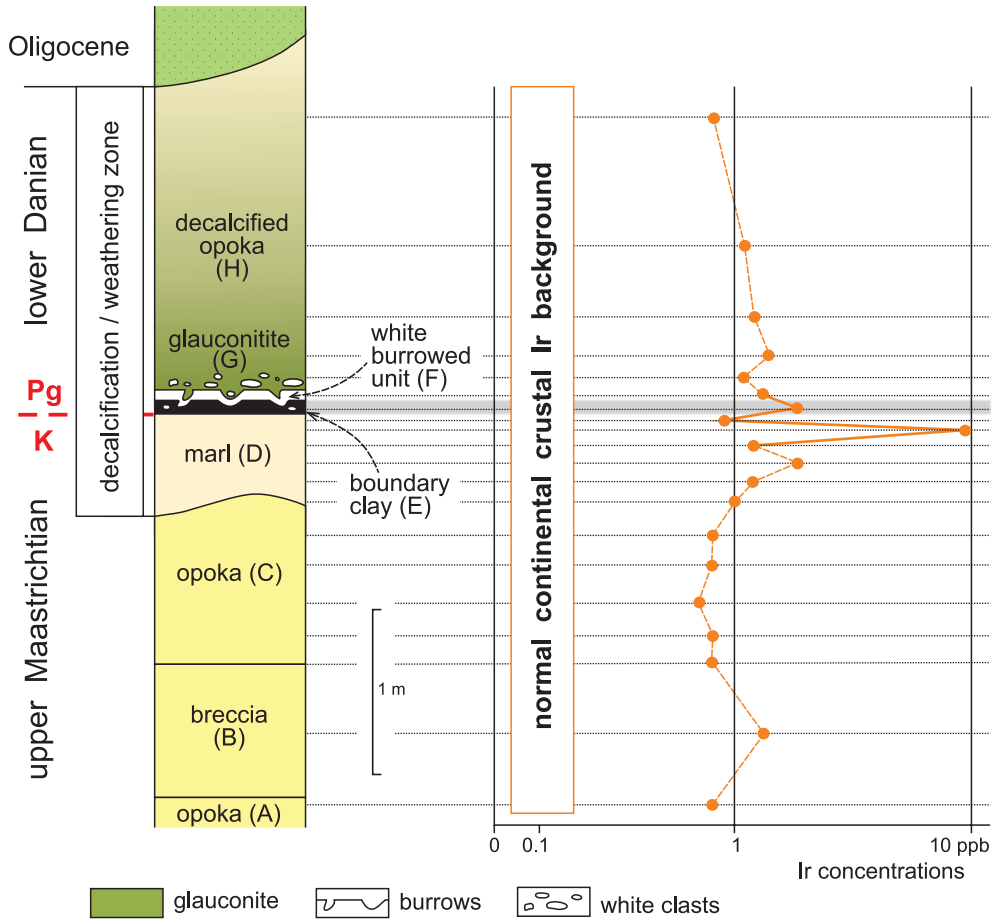

Fig. 20. The iridium (Ir) spike at Lechówka, based on data from Racki et al. (2011). See text for further explanations.

impact ejecta (Racki et al. 2011; Brachaniec et al. 2014; Machalski et al. 2016; Szopa et al. 2017), but the Ir spike typical of K-Pg boundary clays has been secondarily displaced to a level 10 cm below the clay – that is, to the Maastrichtian marls. This anomalous position of the Ir anomaly (Fig. 20) was explained by Racki et al. (2011) as a result of diagenetic mobilisation and re-concentration of impact-derived components by acidic groundwater during Paleogene weathering (cf. Pożaryski 1951). Neither the K-Pg boundary clay nor the Ir anomaly have been documented so far from other parts of the Lublin Upland, although a slight Ir enrinchment in the Greensand samples at Nasiłów suggests that the boundary clay may have also been formerly present in the Kazimierz Dolny area (Hansen et al. 1989).

At Stevns Klint, hardground SB2 truncates the uppermost Maastrichtian and lowermost Danian deposits with *H. c. johnjagti* (Fig. 18; Machalski 2005a, b; Machalski and Heinberg 2005). On the other hand, the bryozoan limestones of the Korsnæb Member, which lie directly above SB2, yield planktonic foraminifera of the P1b Zone (Rasmussen et al. 2005; Surlyk et al. 2006). In Poland, the correlative main burrowed surface lies on upper Maastrichtian deposits of the *H. c. crassus* Zone in the Kazimierz Dolny area and in most outcrops near Lublin. But at Mełgiew, however, this surface truncates the uppermost Maastichtian deposits of the *H. c. johnjagti* Zone. Farther east, at Lechówka, the main burrowed surface is located above the lowermost Danian strata (Fig. 18). It should be noted that the topmost Maastrichtian strata beneath the boundary clay at Lechówka did not yield subspecifically determinable *Hoploscaphites* specimens. However, their dinoflagellate assemblages

suggests that they may correspond to the *H. c. johnjagti* Zone (Machalski et al. 2016). On the other hand, the glauconitite level at Lechówka yields early, but not earliest, Danian planktonic foraminifera (Machalski et al. 2016), matching dating of both the Greensand (Machalski 1998; Żarski et al. 1998) and the basal Korsnæb Member (Rasmussen et al. 2005). These tie points enable tentative correlation of the main burrowed surface with the SB2 hardground at Stevns Klint, and of the overlying glauconite-rich units with the base of the Korsnæb Member (Fig. 18). Additional evidence stems from the occurrence of Danian bivalve and gastropod assemblages (Krach 1981) above the main burrowed surface across the Lublin Upland (Fig. 18). Admittedly, these correlations are somewhat speculative in view of the lack of adequate microfossil sampling of many sections (study in progress by MM and co-workers). Moreover, they are incompatible with Remin et al. (2021), and further research is needed to clarify the situation.

According to Surlyk (1997), the SB2 discontinuity marks a prominent sea-level fall; the overlying Korsnæb Member was deposited during the next (early but not earliest) Danian transgressive sequence (see also Lykke-Andersen and Surlyk 2004, fig. 2). Interestingly, the glauconite-rich Danian deposits of the Geuhelm Member (Houthem Formation) in the Maastrichtian type area (Belgium and the Netherlands), which overlie the prominent Vroenhoven hardground at the top of the Maastricht Formation, also yield P1b Zone foraminifera (Velekoop et al. 2019; see Jagt and Jagt-Yazykova 2012 for overview of the type Maastrichtian). This suggests that similar developments took place in this part of the European basin.

In the light of the above correlations, it is possible to assess the extent of the stratigraphical hiatus across the K-Pg boundary interval in the Lublin Upland (Fig. 18). The hiatal duration decreased towards the east, encompassing the largest duration at Nasiłów and Bochotnica, and possibly in most of the sections near Lublin except for Mełgiew. At the latter locality, the gap seems to extend over a shorter duration, as the opokas immediately beneath the main burrowed surface yield the youngest scaphitids. In the eastern part of the area, at Lechówka, there is no detectable hiatus at the K-Pg boundary. However, the glauconite concentration above the burrowed surface does suggest an intra-Danian gap (Fig. 18).

As noted above, the west-east arrangement of the studied outcrops – from Nasiłów and Bochotnica to Lechówka – approximately corresponds to the deepening trend inferred from physical and palaeontological evidence. Importantly, the successive outcrops seem also to be located at an increasing distance from the possible NW-SE trending shoreline of a landmass that emerged as a consequence of the inversion of the Mid-Polish Anticlinorium (Fig. 2b). The inferred stratigraphical completness pattern near the K-Pg boundary (Fig. 18) seems, therefore, to have been controlled by the position of sections relative to the uplifted zone. The early, but not earliest, Danian transgression entered this topographically differentiated substrate, apparently after the main phase of regional uplift. A tentative model of the initial stages of the Danian transgression onto the older substrate is presented in Fig. 21. The following succession of events around the K-Pg boundary may be suggested for the studied area:

(1) Deposition of the Kazimierz Opoka and its counterparts over the entire studied area during the late, but not latest, Maastrichtian. The "Kazimierz Opoka Sea" gradually shallowed due to the global late Maastrichtian regression.

(2) Deposition of latest Maastrichtian deposits of various facies and faunal compositions in even shallower environments, characterised by sea-level oscillations. At present, these deposits have survived only at Mełgiew and Lechówka.

(3) Deposition of the K-Pg boundary clay as a far-field consequence of the Chixculub impact, followed by the deposition of a (possible) Cerithium Limestone equivalent. These lowermost Danian deposits are preserved only at Lechówka, and possibly at some neighbouring sites.

(4) Formation of the discontinuity surface during the early Danian (Fig. 21). This surface originated during a major relative sea-level low, which led to the erosion of the underlying beds (erosion was more intense to the west). The discontinuity surface truncates the upper Maastrichtian at Nasiłów, Bochotnica, and

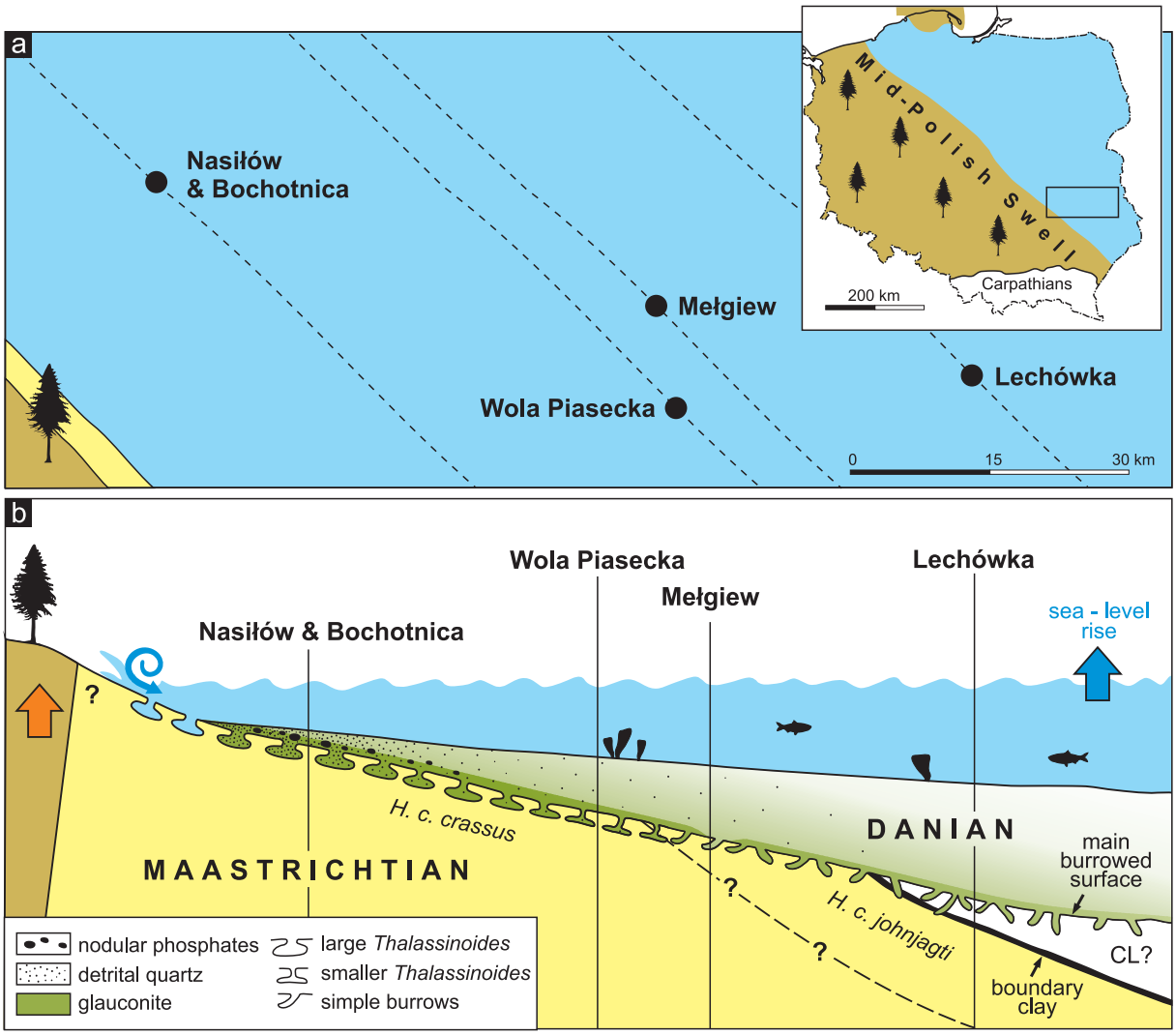

Fig. 21. Early stages of the Danian transgression in the studied part of the Lublin Upland: **a** – position of key sections in relation to the possible shore line of the uplifted Mid-Polish Swell; **b** – facies and stratigraphic relationships along the slope of the main burrowed surface during the Cretaceous–Paleogene interval, not to scale. CL? – a possible counterpart of the Danish Cerithium Limestone. See Fig. 18 for correlations and text for further explanations.

Wola Piasecka, the uppermost Maastrichtian at Mełgiew, and the lowermost Danian at Lechówka (Fig. 21). The sloping of this surface to the east resulted from stronger tectonic uplift of the western Lublin Upland in relation to its central and eastern parts; this uplift occurred after the deposition of the earliest Danian deposits. In the Kazimierz Dolny area, the strongest erosion removed previously deposited Maastrichtian and possibly Danian deposits, leaving only *remanié* fossils and nodular phosphates subsequently incorporated into the Danian Greensand.

(5) Creation of the omission surface after the cessation of erosive processes. Seafloor colonisation by fossorial decapods that produced open burrow systems during the earliest phases of the new, early Danian sedimentary cycle.

(6) Deposition of glauconite-rich condensed units (the Greensand and its correlatives) during the early phases of the Danian transgression, which infilled burrows with sediment. In the west, these glauconite-rich deposits are strongly condensed, but the degree of condensation and time-averaging decreased

eastwards, along with increasing distance from land and growing basin depth. Detrital quartz concentrations, especially in the west, reflect terrigenous input, while glauconite concentrations resulted from lower sedimentation rates. Bioturbational disturbances of the discontinuity surface continued at this stage (post-omission burrows), particularly in the western, shallower part of the Lublin Upland, as denoted by prominent pseudobreccias. Current winnowing lead to the formation of a phosphorite lag above the pseudobreccia. The current-driven, lateral transport of reworked phosphates and fossils from even more westerly sites (not preserved at present) cannot be excluded.

(7) Transition from condensed beds to the overlying gaizes of the Siwak and its equivalents throughout the entire outcrop area, in response to progressively increased sedimentation rates during the early Danian transgression. The later stages of this transgression and the regressive phases of the Paleogene sedimentary cycle are beyond the scope of the present guidebook.

FIELD STOPS (*Marcin Machalski*)

Stop 1: Nasiłów

Village on the left bank of the Vistula River, opposite of Kazimierz Dolny, and part of the Middle Vistula River section. A large abandoned quarry (51° 20' 38.126'' N, 21° 57' 34.749'' E) on the Vistula escarpment east of the village.

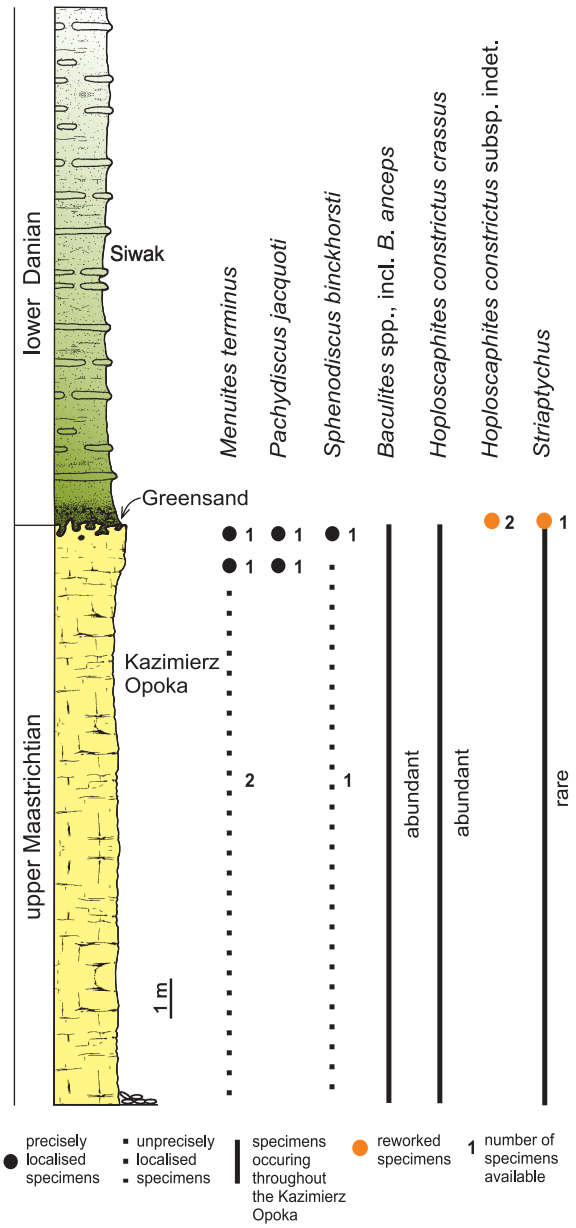

Fig. 22. The section exposed at Nasiłów (Locality 1), with ranges of the late Maastrichtian ammonites (and a scaphitid aptychus) recovered from the Kazimierz Opoka and the Danian Greensand (modified from Machalski 2005a, fig. 3).

Section, stratigraphy, and significance. The section at Nasiłów (Fig. 22) exposes c. 14 m of the Kazimierz Opoka and c. 12 m of the Siwak (including the Greensand at the base). The quarry wall is divided into three exploitation levels. The Kazimierz Opoka at Nasiłów represents the upper, more marly part of this unit. When the quarry was active, it provided excellent opportunities to collect rich Maastrichtian fauna, dominated by sponges (Świerczewska-Gładysz 2006), non-cephalopod mollusks (Abdel-Gawad 1986), and cephalopods (Machalski 1996, 2005a, b). The most important ammonite finds recovered from the Kazimierz Opoka at Nasiłów are summarised in Fig. 22. The presence of numerous *Hoploscaphites constrictus crassus* specimens throughout the opoka points to the *H. c. crassus* Zone of Błaszkiewicz (1980) and Machalski (2012) (see Fig. 19). Today, large parts of the section are overgrown by vegetation and/or covered by scree. However, fossil collecting may be conducted at small pits produced by amateur fossil collectors.

For the purposes of the present excursion, the K-Pg interval has been exposed in the mid-

Fig. 23. The Cretaceous–Paleogene boundary interval along the wall of the middle exploitation level at Nasiłów (Locality 1). Jakub Jabłoński is standing with his hand placed on the Maastrichtian–Danian boundary at the top of the Kazimierz Opoka.

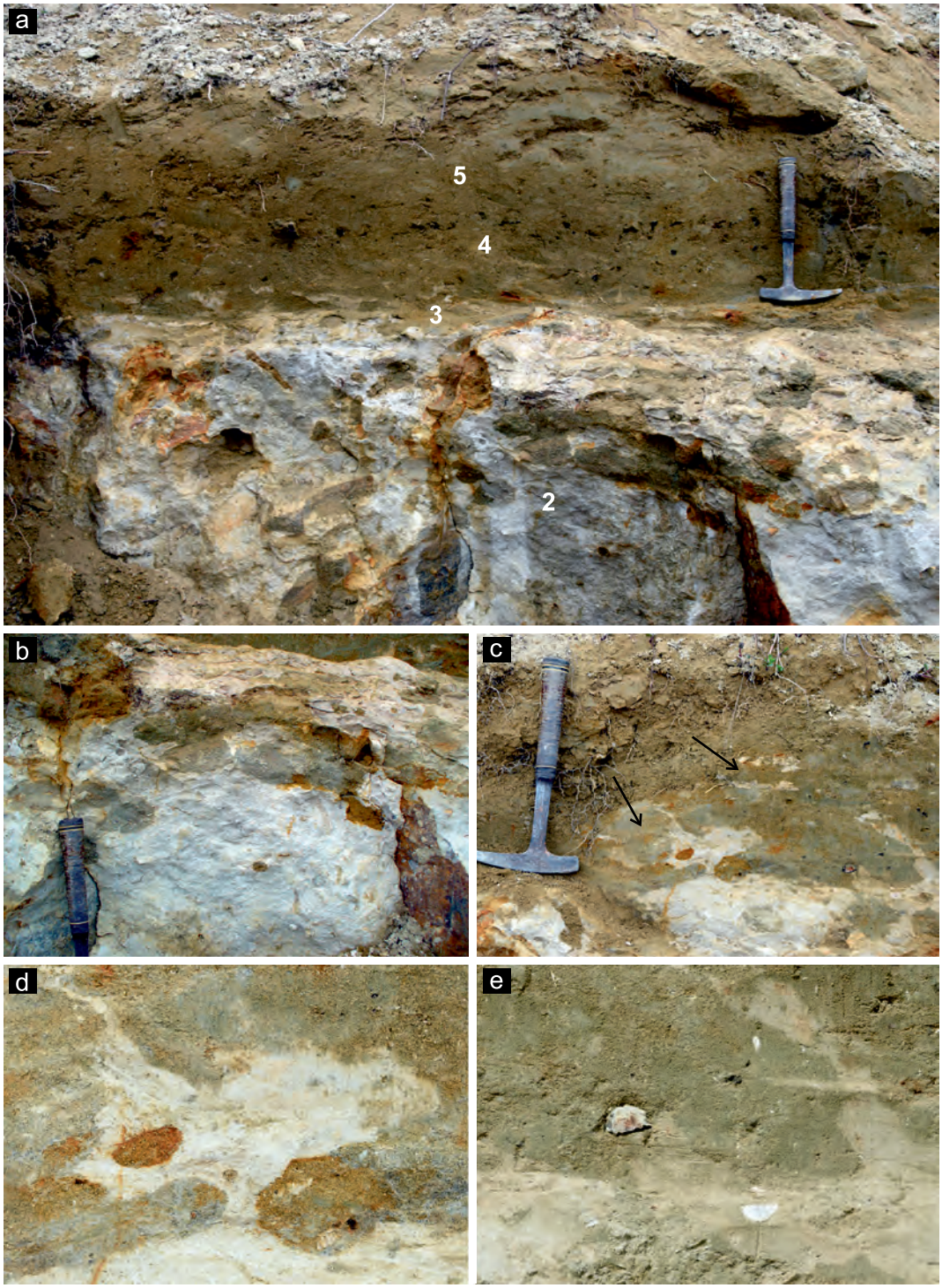

Fig. 24. Details of the Cretaceous–Paleogene boundary interval at Nasiłów shown in Fig. 23: **a** – top of the Kazimierz Opoka, composed of indurated opoka (unit 2) and the pseudobreccia zone (unit 3), followed above by the Danian Greensand with a phosphatic, fossil-rich level (unit 4) and the lowermost portion of the Danian Siwak (unit 5); **b** – decapod burrows filled with glauconitic sandstone in the indurated opoka bed; **c** – details of the convoluted top surface of the Kazimierz Opoka, with post-omission burrows (arrows) penetrating through the bosses of soft opoka; **d** – details of the soft opoka boss from c; **e** – another opoka boss from c. Both bosses are rooted in the underlying soft opoka, pointing to their *in situ* creation by burrowing decapods. Many apparently isolated opoka shreds in this part of the Greensand are actually entrenched in the underlying opoka, which may be demonstrated by serial vertical sectioning of the outcrop walls, both at Nasiłów and Bochotnica.

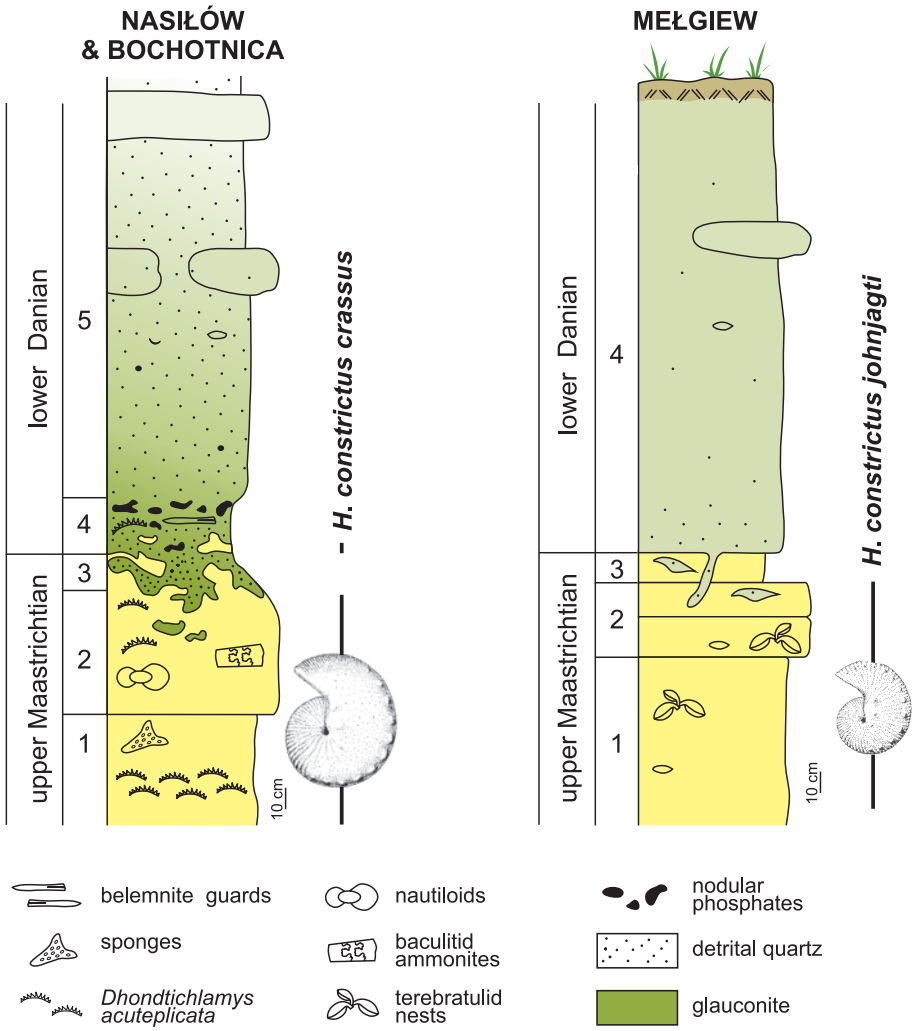

Fig. 25. The Cretaceous–Paleogene boundary interval in the combined Nasiłów and Bochotnica section compared to that at Mełgiew, with ranges of the late Maastrichtian scaphitid subspecies *Hoploscaphites constrictus crassus* and *H. c. johnjagti*, modified from Machalski (2005a, fig. 2). Units in the left section: 1 – soft opoka; 2 – indurated opoka; 3 – pseudobreccia zone; 4 – Greensand; 5 – Siwak. Units in the right section: 1 – brittle marly opoka; 2 – indurated opoka; 3 – soft marl; 4 – less sandy equivalent of the Siwak. See text for further explanation.

dle exploitation level (Figs 23, 24a). It consists of the indurated, strongly burrowed opoka bed at the top of the Kazimierz Opoka overlain by the Greensand layer, which passes gradually into the gaizes and limestones of the Siwak (units 2–5 in Fig. 25). The K-Pg interval at Nasiłów formed the basis for the study by Remin et al. (2021). However, it should be noted that the K-Pg section at Nasiłów is not as well preserved as at Bochotnica on the opposite bank of the Vistula (Locality 2), which renders precise observation of the K-Pg boundary more difficult (compare Figs 9, 14 with Fig. 24). This difference is probably due to more intense weathering of the Vistula escarpment at Nasiłów. In any case, the section at Nasiłów allows us to study the burrows and soft pseudobreccia at the top of the Kazimierz Opoka as well as the overlying Danian units: the Greensand, with a well developed phosphorite layer (Fig. 24), and the Siwak (Fig. 11). The reader is referred to the earlier parts of this text for detailed descriptions and interpretations of the age, facies development, and palaeontological content of these units. Loose blocks of opoka, glauconitic sandstones, and gaizes on the exploitation terraces will allow us to collect samples and specimens representative of each unit.

Stop 2: Bochotnica

Village on the right bank of the Vistula River, north of Kazimierz Dolny, and part of the Middle Vistula River section. An abandoned peasant quarry behind the old watermill (51° 20' 18.953" N, 22° 0' 13.785" E) in the eastern part of the village; another quarry exposing the same succession is located c. 100 m east.

Section, stratigraphy, and significance. The section behind the old watermill (Fig. 26) has been known for a considerable time (Kongiel 1935; Machalski and Jagt 2018). Currently, this is the best section to study the K-Pg boundary interval at Bochotnica, as most of the other sections in this village mentioned and/or decribed by earlier authors are inaccessible today. The section exposes a 5–6 m thick succession across the K-Pg boundary, including the indurated bed at the top of the Kazimierz Opoka (upper Maastrichtian), overlain by the Danian Greensand and the Siwak (Figs 25, 26). The reader is referred to the earlier parts of this text for detailed descriptions and interpretations of the age, facies development, and palaeontological content of these units.

The well lithified, rain-washed walls of the Bochotnica outcrop provide excellent opportunities to examine the details of the K-Pg interval (units 1–5 in Figs 9a, 25). These include the main burrowed surface with the pseudobreccia (unit 3), the omission and post-omission *Thalassinoides* burrows, and the Greensand with phosphatic nodules and fossils discernible on quarry walls (Figs 9, 14, 17b). (Caution: helmets are necessary when inspecting the quarry walls, given the danger of falling rocks!).

Fig. 26. General view of the quarry behind the old watermill at Bochotnica (Locality 2), with the Kazimierz Opoka below and the Greensand and Siwak above. Note the gradual character of the Greensand to Siwak transition, enabling a treatment of the Greensand as a basal bed of the Siwak succession. An entrance to a subterranean opoka mine is visible, with the indurated bed at the top of the Kazimierz Opoka forming a roof.

Entrances to the underground opoka mines are visible at a level below the hard opoka (Fig. 26). Subterranean opoka mining was once commonplace in Bochotnica; the excavated stone was mainly used for local building purposes (Bąk and Szeląg 2013; Bąk and Radwanek-Bąk 2020).

Stop 3: Kazimierz Dolny (Town Quarry)

Southern outskirts of Kazimierz Dolny, Middle Vistula River section. A large abandoned quarry (51° 18' 56.346'' N, 21° 55' 22.507'' E) on the Vistula escarpment.

Section, stratigraphy, and significance. This huge quarry exposes a 30 m thick succession of the lower portion of the upper Maastrichtian Kazimierz Opoka (Fig. 3c). The section is composed of porous opoka, forming massive beds particularly in its lower part, with several thin intercalations of hard opoka and two distinctive marly beds near the top (Fig. 4). The reader is referred to Abdel-Gawad (1986, fig. 5) for the quarry log, with ranges of the most important fossils.

In general, the fauna of the lower Kazimierz Opoka, as exposed in the Town Quarry, is much less abundant than that from the upper part of the unit at Nasiłów. Nevertheless, in the past this site was a source of many interesting and spectacular Maastrichtian macrofossils (e.g., Krach 1931; Abdel-Gawad 1986; Świerczewska-Gładysz 2006). The presence of relatively common *Hoploscaphites constrictus crassus* individuals is diagnostic of the scaphitid *H. c. crassus* Zone of Błaszkiewicz (1980) and Machalski (2012). Interestingly, belemnites – of the *Belemnella kazimiroviensis* group – are extremely rare throughout the section; they are relatively common only in the upper marl at the top of the section. The still well-exposed

Maastrichtian opoka in this deserted quarry will allow us to collect typical fossils and assess the lithology of the Kazimierz Opoka.

Stop 4: Wola Piasecka

Village near Piaski, southeast of Lublin. A large, currently inactive quarry (51° 7' 34.642'' N, 22° 48' 6.098'' E) in the southeastern part of the village.

Section, stratigraphy, and significance. The bulk of the Wola Piasecka succession (Fig. 3d) is composed of a c. 15 m thick upper Maastrichtian opoka, which in terms of facies and faunal content is identical to the Kazimierz Opoka in the Middle Vistula River section. Like the latter, the opoka of Wola Piasecka belongs to the highest standard belemnite *Belemnella kazimiroviensis* Zone, the tegulated inoceramid *Tenuipteria argentea* Zone, and the scaphitid ammonite *Hoploscaphites constrictus crassus* Zone (Błaszkiewicz 1980; Abdel-Gawad 1986; Machalski 1996, 2005a, b, 2012). The index fossils of these zones have been recently identified by MM throughout the section (except for Machalski and Malchyk 2019, the stratigraphy of the Wola Piasecka outcrop had not been dealt with in any publications).

The higher 5–7 m thick portion of the opoka succession, as exposed in the major area of the quarry, is strongly reminiscent in lithology and faunal content to the upper Kazimierz Opoka from Nasiłów and Bochotnica. Recent investigations have revealed the presence of interesting fossil accumulations in this part of the section. These include layers of fragmented fossils interpreted as tempestites as well as spectacular "nests" composed of nautiloid specimens (Machalski and Malchyk 2019, fig. 2a and b respectively).

The lower part of the opoka succession at Wola Piasecka is only exposed in a deep side-pit at the western corner of the quarry. Its facies development, in combination with a relatively meagre fossil content, is reminiscent of the lower Kazimierz Opoka (e.g., the Town Quarry succession). Exposures of the upper Maastrichtian opoka along the quarry walls provide good opportunities for observations and fossil collecting. Typical examples of late Maastrichtian macro- and ichnofossils are displayed in Fig. 27a–f.

The top of the upper Maastrichtian opoka is preserved only in the eastern part of the quarry. It is developed as a hard opoka bed, similar in many ways to the indurated opoka bed that terminates the Kazimierz Opoka. Like the latter unit, the top of the opoka at Wola Piasecka is riddled by decapod burrows, mostly *Thalassinoids suevicus* (Figs 15, 28a–c). These burrows are easily discernible on the bright opoka surfaces due to their infilling by a darker, olive-green glauconitic deposit, heralding the next sedimentary cycle (Fig. 15).

The higher portion of the Wola Piasecka succession has been preserved only in the easternmost part of the quarry. There, it is represented by a marly opoka succession, up to 2 m thick, with high glauconite content in the lower part (Fig. 15). The junction with the underlying Maastrichtian opoka is sharp, and there is a pseudobreccia at the contact zone, analogous to that seen in the K-Pg interval of the Middle Vistula River (Fig. 28d). Unlike in the previous sections, however, the deposit above the burrowed surface is a glauconite-rich marly opoka, not glauconitic sandstone. Glauconite grains are chaotically dispersed throughout this deposit and frequently occur in spots, reflecting sediment mottling by burrowing fauna (Fig. 28d–f). Another difference from the Vistula sections is that at Wola Piasecka the phosphates are represented only by minute fragments, 1–2 mm in diameter (Fig. 28f).

Fossils are frequent in the basal glauconite-rich deposit. The Maastrichtian fossils, representing the calcitic fraction of assemblages present in the underlying opoka, are the most eye-catching faunal elements. The most common are the scallop *Dhondtichlamys acuteplicata*, the oyster *Pycnodonte vesicularis*, terebratulid brachiopods, and the belemnite *Belemnella kazimiroviensis* (Fig. 28e). Many of these fossils are clearly reworked from the underlying opoka by burrowers, as demonstrated by their association with pieces of pseudobreccia. No Maastrichtian fossils have been found in the Wola Piasecka glauconitite that can be interpreted as indigenous faunal remains. This is fully analogous with the Greensand in the Middle Vistula River section.

Intermixed with the Maastrichtian *ex situ* fossils are remains of minute, originally ara-

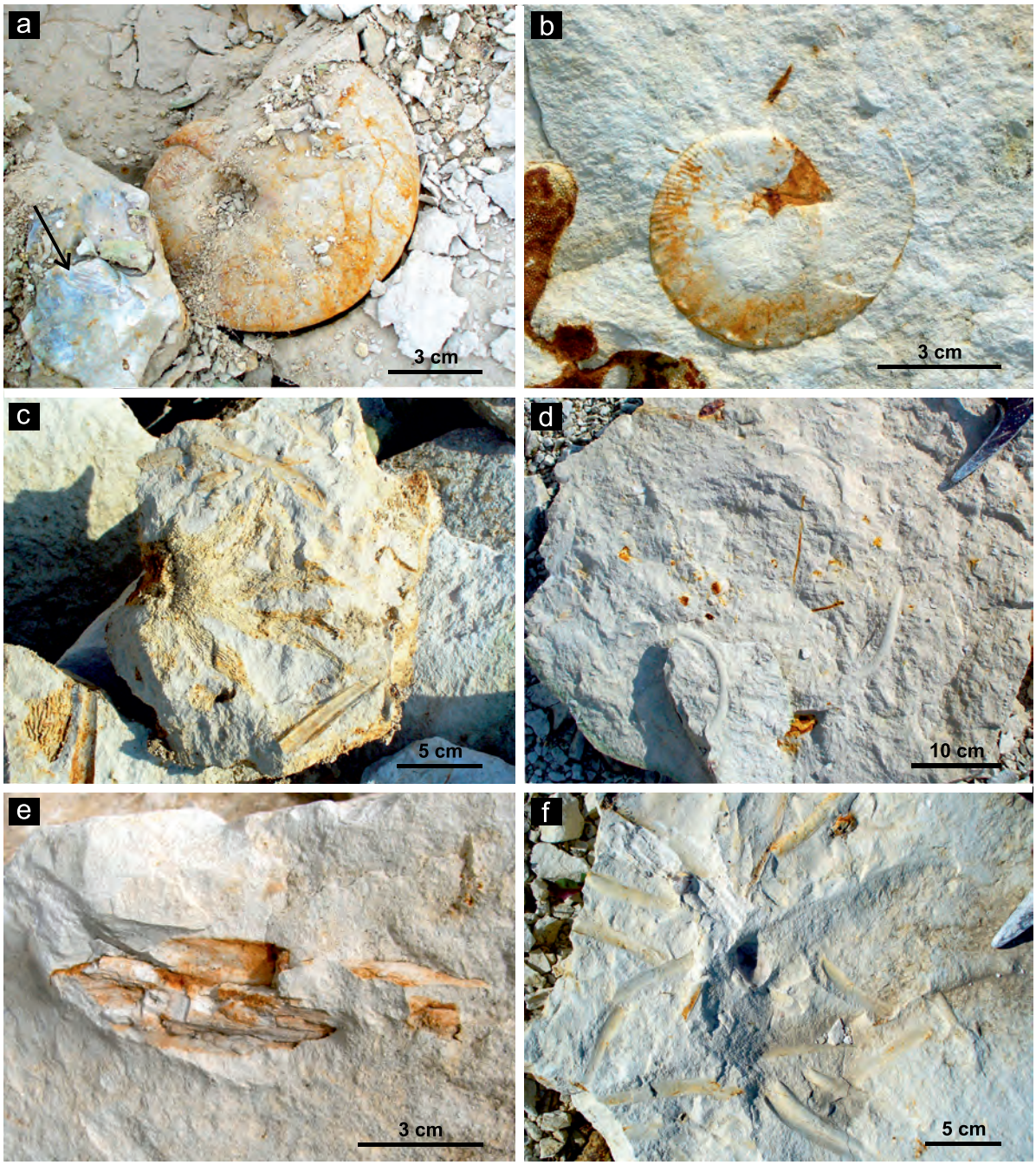

Fig. 27. Fossils from the upper Maastrichtian opoka exposed at Wola Piasecka (Locality 4): **a** – nautiloid *Cymatoceras intrasiphonatum* with mouldic preservation associated with oyster *Pycnodonte vesicularis* with original calcitic shell preservation (arrow); **b** – scaphitid *Hoploscaphites constrictus crassus* with mouldic preservation; **c** – root-like outgrows of the sponge *Rhizopoterion cribrosum* associated with other fauna; **d** – burrows *Planolites* isp.; **e** – driftwood preserved as an imprint; **f** – concentration of *Gervillia solenoides* specimens, probably reflecting the pseudoplanktonic mode of life of these bysally-attached bivalves.

gonitic bivalves and gastropods (Fig. 28d–f). They represent an assemblage similar to that described from the Siwak by Krach (1981). These fossils may be interpreted as indigenous Danian fauna, again analogous to the Greensand. In summary, the glauconite-rich basal deposit overlying the burrowed surface is best interpreted as a "diluted" age and ge-

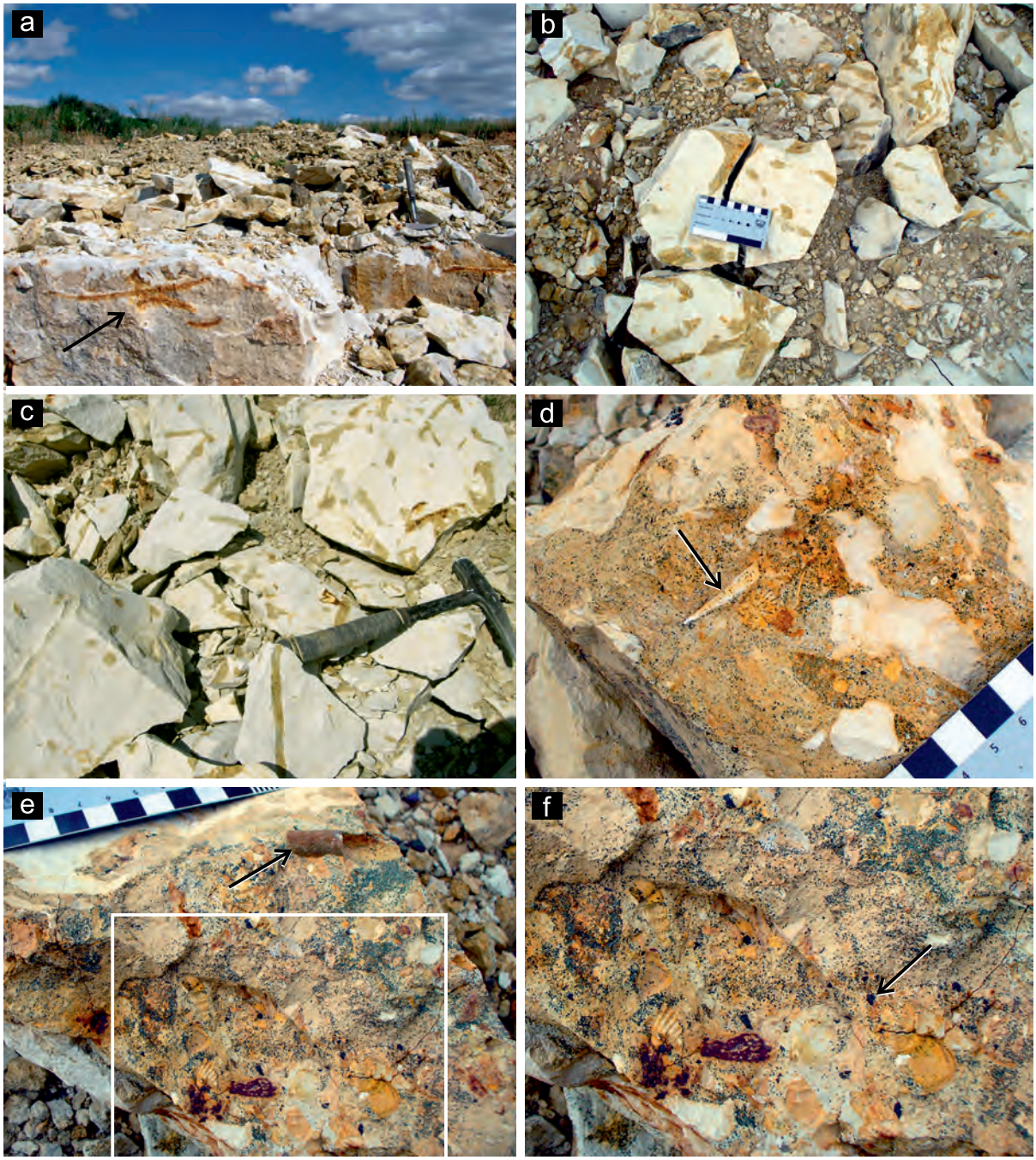

Fig. 28. Details of the Cretaceous–Paleogene boundary interval at Wola Piasecka (Locality 4): **a** – top of the upper Maastrichtian opoka with decapod burrows (arrow); **b** and **c** – pieces of the upper Maastrichtian opoka with decapod burrows infilled with glauconitic sediment from the overlying Danian unit; **d** – bedding plane at the pseudobreccia level, with a gastropod imprint (arrowed) in glauconitic opoka of Danian age; **e** and **f** – bedding plane from a slightly higher level with mixed Maastrichtian (belemnite arrowed in e) and Danian fossils and minute phosphate grains (arrowed in f).

netic counterpart of the Danian Greensand from the Middle Vistula River section.

The K-Pg interval at Wola Piasecka has not been studied previously, and all data presented above are the unpublished data of MM. A newly exposed K-Pg interval at this site was recently sampled by MM for the purposes of this excursion and planned work.

Stop 5: Mełgiew

Village east of Świdnik and Lublin. A temporary outcrop (51° 13' 23.88'' N, 22° 47' 29.327'' E) on a hill east of the northern end of the village.

Section, stratigraphy, and significance. The section exposed by Machalski (2005a) comprised over 1 m of upper Maastrichtian opoka and limestone, and ca. 1.7 m of Danian marly gaize or sandy opoka with a limestone intercalation at the top (Figs 25, 29a). In terms of facies, the Maastrichtian part of the succession (units 1 and 2) is similar to its counterparts in Nasiłów and Bochotnica (Fig. 29e), albeit the "hardground" (unit 2 in Fig. 25) is more brittle and marly in Mełgiew than in Nasiłów and

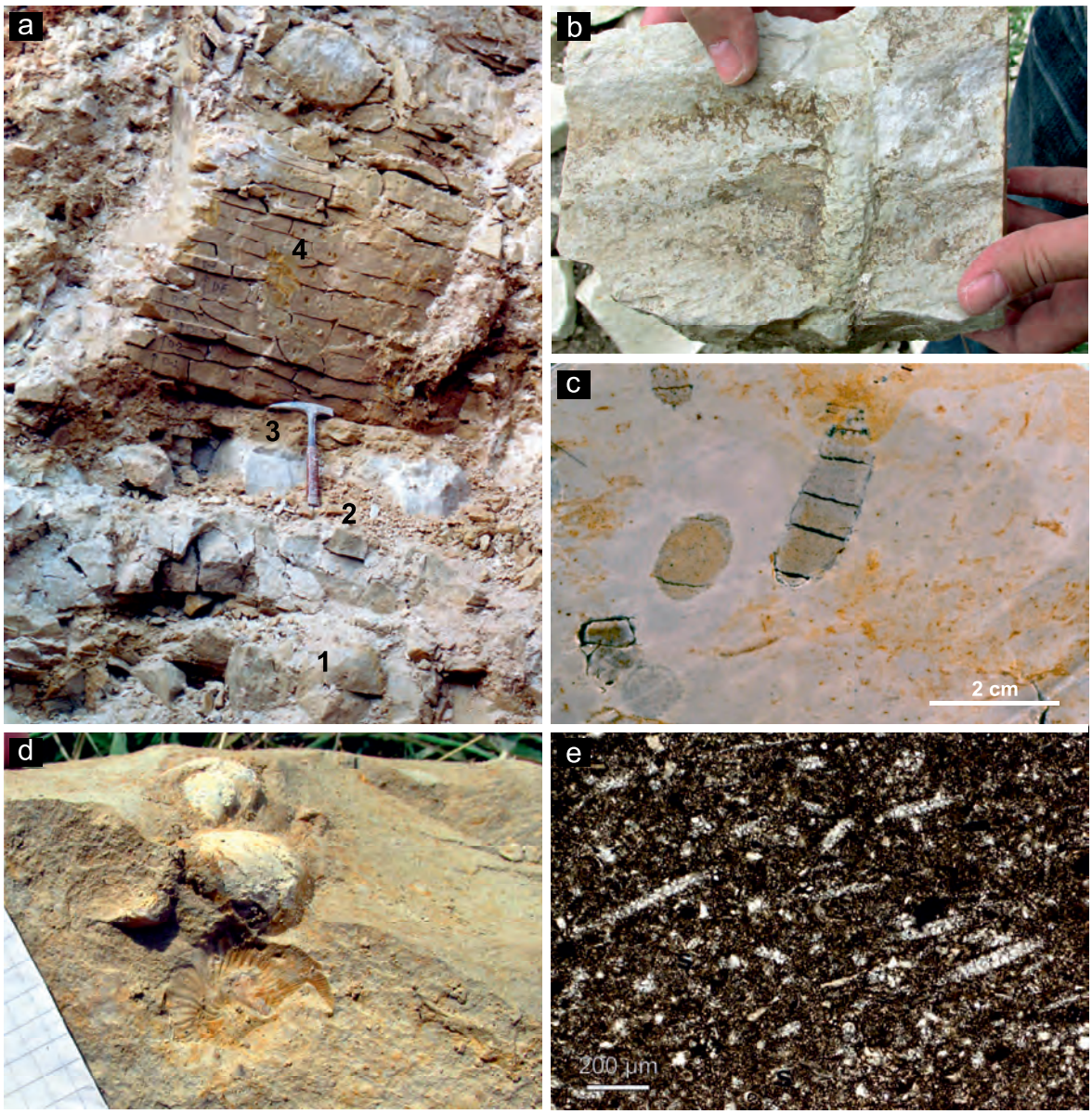

Fig. 29. The Cretaceous–Paleogene boundary interval exposed at Mełgiew (Locality 5): **a** – temporary section exposed in 2003, with units 1–4 corresponding to those on the right side of Fig. 25; **b** – burrow *Ophiomorpha* isp. from the uppermost Maastrichtian opoka; **c** – simple burrows at the top of the uppermost Maastrichtian opoka, infilled with fine glauconitic sediment from above; **d** – terebratulid brachiopods associated with the scaphitid ammonite *Hoploscaphites constrictus johnjagti* (the brachiopods probably settled on the shell of the dead ammonite); **e** – thin section of the opoka from unit 2 (calcareous wackestone), with numerous voids after sponge spicules filled by sparite, and admixture of rare, very fine detrital quartz grains.

Bochotnica, and is overlain by a thin, continuous layer of soft marl (unit 3). Burrows at the top of the opoka are less numerous than in the Middle Vistula River sections, and have simple morphologies (Fig. 29c).

As noted earlier, the relatively low burrow density results in the absence of the pseudobreccia phenomenon at the top of the Maastrichtian succession. The soft marl (unit 3 in Fig. 25) is barren; it is assigned to the Maastrichtian on the basis of lithology. The underlying units 1 and 2 contain scarce late Maastrichtian fauna dominated by small bivalves, mostly nuculids and oysters. In contrast to the sections near Kazimierz Dolny, *Dhondtichlamys acuteplicata* is absent from this assemblage. Units 1 and 2 also contain brachiopods, gastropods, scaphopods, and quite abundant scaphitids assigned to *Hoploscaphites constrictus johnjagti* (Machalski 2005a, b). The latter are commonly covered with oyster spat. Nests of the terebratulid brachiopod *Neoliothyrina* sp., each composed of several specimens, are not uncommon, and are often associated with ammonite specimens that they apparently settled on (Fig. 29d). Their preservation attests to a calmer, deeper environment with higher depositional rates than during the deposition of the Kazimierz Opoka, and to the soupy nature of the sea bottom, which forced sedentary animals to exploit all available hard substrates. The occurrence of rare *Ophiomorpha* burrows additionally supports the existence of soft bottom conditions (Fig. 29b). A marly gaize or sandy opoka (unit 4 in Figs 25, 29a) follows, with a sharp break on top of the Maastrichtian succession; this same sediment is also piped down into the opoka via burrows. There is no concentration of glauconite, fossils, or phosphorites at Mełgiew (Figs 25, 29a).

The importance of the Mełgiew section lies in the fact that it yields scaphitid ammonites characteristic of the highest Maastrichtian scaphitid zone *Hoploscaphites constrictus johnjagti* – the only site in Poland where this zone has been recovered (Machalski 2005a, b, 2012). In terms of the regional foraminiferal zonation of Dubicka and Peryt (2012), the Maastrichtian part of the Mełgiew section represents their topmost Maastrichtian XIII zone (see Table 2).

There is no outcrop at Mełgiew at present. Prior to the excursion, a trench will be excavated near the top of the hill to demonstrate the section.

Stop 6: Lechówka

Environs of the village of Lechówka, south of the main road between Lublin and Chełm. An abandoned quarry (51° 10' 07.0'' N, 23° 14' 24.5''E) located on a small hilltop at the edge of a forest, 1.2 km south of this road.

Section, stratigraphy, and significance. The Lechówka section was studied by Popiel (1977), Racki et al. (2011), and Machalski et al. (2016). The study by Racki et al. (2011) is of prime importance due to the recognition – for the first time in Poland – of the K-Pg boundary clay and associated iridium anomaly (Figs 20, 30).

The section studied by Racki et al. (2011) was over 4 m thick, and consisted of eight lithological units (units A–H in Fig. 20). These are, in ascending order: A – opoka, 10 cm; B – a tectonic or karstic breccia, ca. 70 cm thick, composed of irregular soft opoka pieces; C – opoka layer, ca. 100 cm thick, with a sharp lower boundary, a diffuse, undulating top, and a decalcified cover passing continuously into the overlying sediments; D – marl layer, c. 30 cm thick, with bioturbation at the top; E – clay unit, c. 10 cm thick, with a rusty layer at the base (Fig. 30b); F – white burrowed unit, c. 10–15 cm thick, with irregular lower and upper boundaries, composed of a bright decalcified deposit with numerous burrows, which are filled with sediment from the overlying glauconitite and surrounded by white cemented aureoles in their parts penetrating through the clay (Fig. 30b, c); G – glauconitite layer, c. 40 cm thick, with bioturbational, spotty concentrations of glauconite grains and clasts derived from the underlying white layer (Fig. 30d); H – decalcified opoka, c. 150 cm thick, with faint remnants of original limestone intercalations analogous to those occuring in Siwak from the Middle Vistula River section. At Lechówka, the top of the K–Pg succession is locally truncated by glauconite sands with gravel, conventionally assigned to the Oligocene. The upper part of the succession is decalcified due to Paleogene weathering (Fig. 20; Racki et al. 2011). A similar section in

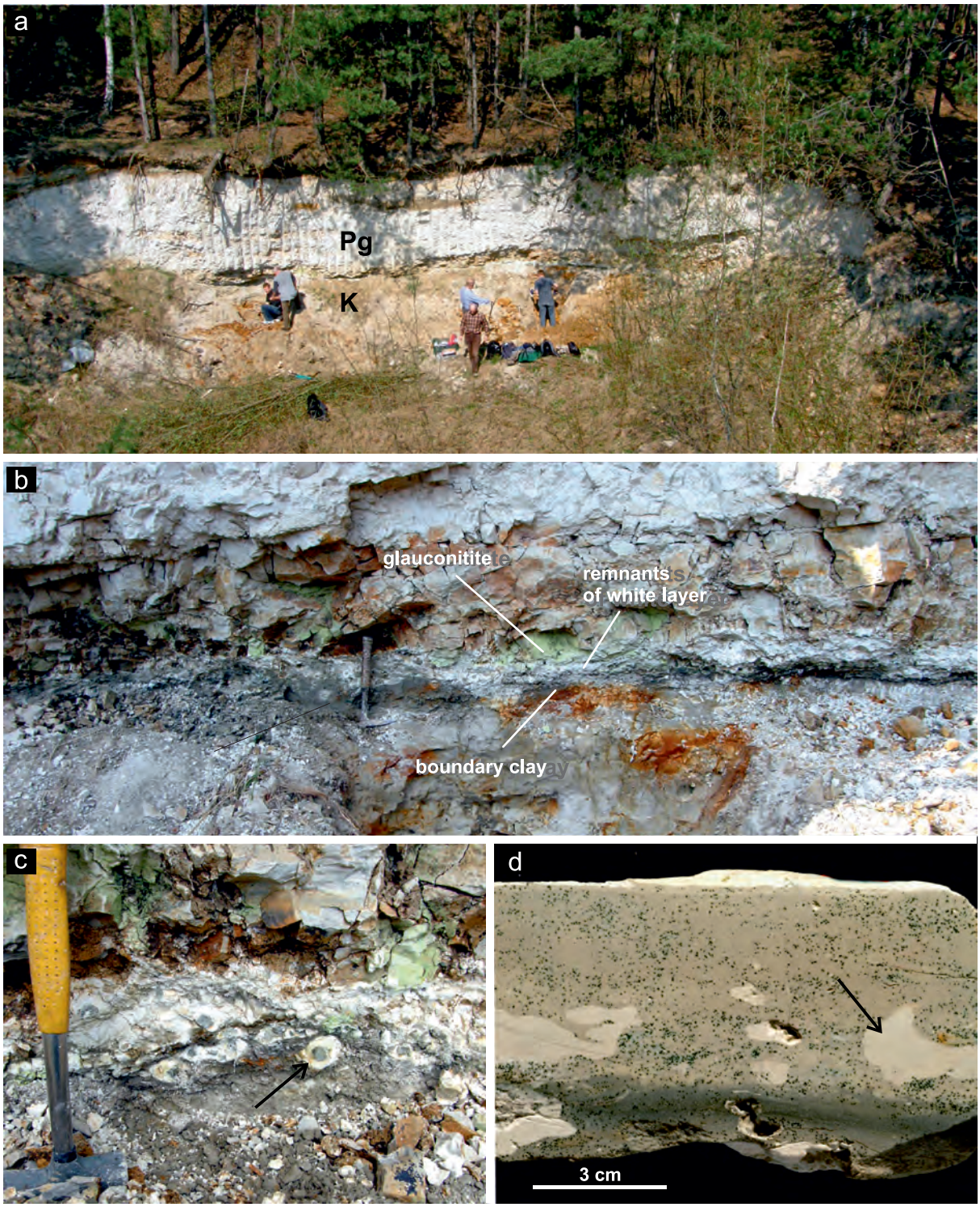

Fig. 30. The Cretaceous–Paleogene boundary interval at Lechówka (Locality 6): **a** – general view of the outcrop, with white decalcified Danian opoka in the upper part and partially decalcified Maastrichtian strata in the lower part (photo taken in 2009); **b** – the middle portion of the section with the K-Pg boundary clay, remnants of a white layer (probably an equivalent of the lower Danian Cerithium Limestone in Denmark), and the glauconitite bed from which burrows descend into the underlying deposits; **c** – burrows filled with glauconitic sediment and surrounded by white cementation aureoles, penetrating through the boundary clay; **d** – glauconitite with mottled ichnofabric and pseudobreccia composed of white clasts.

another part of the exposure was described by Machalski et al. (2016), and formed the basis for a more detailed study based on foraminifera, dinoflagellates, and macrofauna (Machalski et al. 2016, fig. 2).

The most important features of the Lechówka section are (1) the clay layer, interpreted by Racki et al. (2011) as the K-Pg boundary clay, and (2) the remnants of a white unit, tentatively interpreted as the equivalent of the Cerithium Limestone at Stevns Klint (Figs 18, 20, 21). The Ir spike, which usually occurs globally at the base of the boundary clay, has been displaced downsection (Fig. 20) due to the secondary remoblisation of the impact products by acidic weathering processes during the Paleogene (Racki et al. 2011). The reader is referred to Racki et al. (2011) for detailed geochemical data and resultant interpretations. Despite the displacement of the Ir anomaly below the clay layer, the significance of the latter unit as a true K-Pg boundary clay is confirmed by the presence of other extraterrestrial impact phenomena (i.e., the spherules and meteorite remnants described by Brachaniec et al. 2014 and Szopa et al. 2017). The glauconitite bed at Lechówka (unit G), with burrows descending into the underlying E and F layers (Fig. 20), is regarded to be a correlative equivalent of the Greensand and other glauconite-rich units in the areas west of Lechówka.

The palaeontological evidence gathered by Racki et al. (2011) and Machalski et al. (2016) supports the above conclusions, although the fossil record at Lechówka is spoiled by decalcification of the upper portion of the section. Beds A–C contain fossils typical of the Kazimierz Opoka elsewhere, including the index taxon of the *Hoploscaphites constrictus crassus* Zone of Machalski (2012). The overlying unit D yielded a sparse fauna, but one still clearly of late Maastrichtian character, including subspecifically indeterminate *H. constrictus*. However, the predominance of the dinocyst marker taxon *Palynodinium grallator* in this part of the section suggests the presence of the uppermost Maastrichtian *Thalassiphora pelagica* Subzone of the *P. grallator* Zone, which is correlatable with the *H. c. johnjagti* Zone (Table 2). In addition, the planktonic foraminiferal assemblage from unit D is coeval with that from the *H. c. johnjagti* Zone, as well (zone XIII of Dubicka and Peryt 2012). Notably, a reduction in test size among calcareous epifaunal benthic foraminifera was noted at a level 50 cm below the K-Pg boundary, which has been interpreted as being related to the environmental stress associated with Deccan volcanism prior to the Chixculub impact (Machalski et al. 2016). The glauconite-rich unit G contains a sparse fauna of minute bivalves and gastropods in mouldic preservation, similar in taxonomic composition to that known from the Danian Siwak in the Middle Vistula River section (Racki et al. 2011). In agreement with the macrofossil record, microfossil sampling of the glauconitite unit yielded some poorly preserved early, but not earliest, Danian foraminifera (Machalski et al. 2016). In brief, then, the section may be regarded as the most complete Cretaceous–Paleogene interval in Poland (Racki et al. 2011).

The Lechówka section has experienced heavy deterioration since the completion of the above studies, especially due to heavy, vegetative overgrowth of the pit and covering of the quarry slopes by weathered material from above. It will be cleared and re-excavated prior to this excursion.

ACKNOWLEDGEMENTS

Hieronim Zonik, the mayor of Siedliszcze, is acknowledged for his help with clearing the Lechówka outcrop. Piotr Kondraciuk, head of the Nadwiślańskie Museum at Kazimierz Dolny, and Joanna Szkuat, head of the Natural History Museum (branch of the Nadwiślańskie Museum) are thanked for help and assistance, especially in clearing the Bochotnica outcrop. Magdalena Wójcik, the head of the Mełgiew commune, is thanked for help in fieldwork. Special thanks go to Marek Młynarczyk (Mełgiew) and Dariusz Pawlak (Bochotnica) for allowing access and work in their land. Maciej Duda is warmly thanked for photos of the K-Pg interval at Wola Piasecka. Amongst the staff of the Institute of Paleobiology, Polish Academy of Sciences, special thanks go to: Michał Andziak, Jakub Jabłoński and Adam Zaremba for assistance in fieldwork; Grażyna Dziewińska and Marian Dziewiński for specimen photography; and Aleksandra Hołda-Michalska and Agnieszka Kapuścińska for digitizing figures. Jordan Todes is thanked for linguistic help. The Institute of Paleobiology is acknowledged for financial support of fieldwork. Unless stated otherwise, photos were taken by the authors or their teams as part of their professional duties.

REFERENCES

Abdel-Gawad, G.I. 1986. Maastrichtian non-cephalopod mollusks (Scaphopoda, Gastropoda and Bivalvia) of the Middle Vistula Valley, Central Poland. Acta Geologica Polonica, 36, 69–224.

Alvarez, L.W., Alvarez,W., Asaro, F. and Michel, H. V. 1980. Extraterrestrial cause for the Cretaceous–Tertiary extinction. Science, 208, 1095–1108.

Alvarez, W. Kauffman, E.G., Surlyk, F., Alvarez, L.W., Asaro, F. and Michel, H.V. 1984. Impact theory of mass extinctions and the invertebrate fossil record. Science, 223, 1135–1141.

Bąk, B. and Szeląg, A. 2013. Opoki i gezy – zapomniane kopaliny Lubelszczyzny. Górnictwo Odkrywkowe, 2, 107–116.

Bąk, B. and Radwanek-Bąk, B. 2020. Oto opoka, a na niej zbudowano – Kazimierz Dolny. Górnictwo Odkrywkowe, 1, 55–63.

Błaszkiewicz, A. 1980. Campanian and Maastrichtian ammonites of the Middle Vistula River Valley, Poland; A stratigraphic-palaeontological study. Prace Instytutu Geologicznego, 42, 1–63.

Bottjer, D.J. 1985. Trace fossils and paleoenvironments of two Arkansas Upper Cretaceous discontinuity surfaces. Journal of Paleontology, 59 (2), 282–298.

Brachaniec, T., Karwowski, Ł. and Szopa, K. 2014. Spherules associated with the Cretaceous–Paleogene boundary in Poland. Acta Geologica Polonica, 64, 99–108.

Bromley, R.G. 1975. Trace fossils at omission surfaces. In: Frey, R.W. (Ed.), The study of Trace Fossils, 399–428. Springer; New York.

Carmona, N.B., Buatois, L.A. and Mángano, M.G. 2004. The trace fossil record of burrowing decapod crustaceans: evaluating evolutionary radiations and behavioural convergence. Fossils and Strata, 51, 141–153.

Cieśliński, S. and Jaskowiak, M. 1973. Paleogeografia. Kreda górna. In: Cieśliński, S. and Czermiński, J. (Eds), Budowa Geologiczna Polski, Stratygrafia, 2, Mezozoik, 709–716. Wydawnictwa Geologiczne; Warszawa.

Dubicka, Z. and Peryt, D. 2012. Latest Campanian and Maastrichtian palaeoenvironmental changes: implications from an epicontinental sea (SE Poland and western Ukraine). Cretaceous Research, 37, 272–284.

Dybkowska, M. 1993. The Krystyna and Władysław Pożaryski Wall at Bochotnica near town of Kazimierz Dolny as a site of geological documentation. Chrońmy Przyrodę Ojczystą, 49, 1, 30–38. [In Polish with English abstract]

Fraaije, R.H.B., Jagt, J.W.M., Van Bakel, B.W.M. and Tshudy, D.M. 2018. New lobsters (Decapoda, Nephropoidea) from the Cretaceous–Paleogene section of the Middle Vistula valley, east-central Poland. Acta Geologica Polonica, 68, 503–509.

Frey, R.W. and Bromley, R.G. 1985. Ichnology of American chalks: the Selma Group (Upper Cretaceous), western Alabama. Canadian Journal of Earth Sciences, 22, 801–828.

Fürsich, F.T. 1974. Corallian (Upper Jurassic) trace fossils from England and Normandy. Stuttgarter Beiträge zur Naturkunde, B13, 1–52.

Fürsich, F.T., Kennedy, W.J. and Palmer, T. 1981. Trace fossils at a regional discontinuity surface: the Austin/Taylor (Upper Cretaceous) contact in central Texas. Journal of Paleontology, 55, 537–551.

Gazda, L., Harasimiuk, M. and Krzowski, Z. 1992. Litogeneza warstw z glaukonitem w górnej kredzie i paleocenie Pagórów Chełmskich (Wyżyna Lubelska, E Polska). Annales Universitatis Mariae Curie–Skłodowska, Sectio B Geographia, Geologia, Mineralogia et Petrographia, 47, 1–24.

Gaździcka, E. 1978. Calcareous nannoplankton from the uppermost Cretaceous and Paleogene deposits of the Lublin Upland. Acta Geologica Polonica, 28, 335–375.

Geys, J.F. and Machalski, M. 1992. A new salenioid echinoid, *Salenia sigillata pozaryskae* subsp. n. from the uppermost Maastrichtian of the Middle Vistula Valley, Central Poland. Acta Geologica Polonica, 42, 135–139.

Głowniak, E. 2007. Biography of Józef Siemiradzki. Volumina Jurassica, 5, 3–26.

Graaf, D.Th., Jagt, J.W.M., Schulp, A.S. and Machalski, M. 1999. Wielkie jaszczury, amonity i planetoidy – Sto pięćdziesiąta rocznica ustanowienia piętra mastrychckiego. Przegląd Geologiczny, 47, 608–609.

Halamski, A.T. 2013. Latest Cretaceous leaf floras from southern Poland and western Ukraine. Acta Palaeontologica Polonica, 58, 407–443.

Hansen, H.J., Rasmussen, K.L., Gwoździ, R., Hansen, J.M. and Radwański, A. 1989. The Cretaceous/Tertiary boundary in Central Poland. Acta Geologica Polonica, 39, 1–12.

Harasimiuk, M. 1984. Osady najniższego trzeciorzędu Wyżyny Lubelskiej. Annales Universitatis Mariae Curie-Skłodowska, Lublin – Polonia, 39, 1–13.

Harasimiuk, M. and Henkiel, A. 1981. Utwory pogranicza kredy i trzeciorzędu w okolicy Lublina. Annales Universitatis Mariae Curie-Skłodowska Lublin – Polonia, 35/36, Sectio B, 1–12.

Harasimiuk, M. and Rutkowski, J. 1984. Osady pogranicza kredy i trzeciorzędu rejonu Chełma i Rejowca (Staw). In: Harasimiuk, M. (Ed.), Przewodnik LVI Zjazdu Polskiego Towarzystwa Geologicznego, 6–8 września 1984, Lublin, 157–163. Wydawnictwa Geologiczne; Warszawa.

Harasimiuk, M., Domonik, A., Machalski, M., Pinińska, J., Warowna, J. and Szymkowiak, A. 2011. Małopolska Gap of Vistula River – projected geopark. Przegląd Geologiczny, 59, 405–416. [in Polish with English Abstract]

Hart, M.B., Feist, S.E., Price, G.D. and Leng, M.J. 2004. Reappraisal of the K-T boundary succession at Stevns Klint, Denmark. Journal of the Geological Society London, 161, 1–8.

Hart, M.B., Feist, S. E., Håkansson, E., Heinberg, C., Price, G.D., Leng, M.J. and Watkinson, M.P. 2005. The Cretaceous–Palaeogene boundary succession at Stevns Klint, Denmark: foraminifers and stable isotope stratigraphy. Palaeogeography, Palaeoclimatology, Palaeoecology, 224, 6–26.

Hooper, J.N.A. and van Soest, R.W.M. 2002. Systema Porifera. Guide to the supraspecific classification of sponges and spongiomorphs (Porifera). Plenum, New York, 1706 p.

Jagt, J.W.M. and Jagt-Yazykova, E. 2012. Stratigraphy of the type Maastrichtian–a synthesis. Scripta Geologica. Special Issue, 8, 5–32.

Jagt, J.W.M. and Kin, A. 2010. The phymosomatid echinoid *Trochalosoma taeniatum* from the Maastrichtian (Upper Cretaceous) of southeast Poland. Acta Geologica Polonica, 60, 429–435.

Jaskowiak-Schoeneichowa, M. and Krassowska, A. 1988. Paleomiąższości, litofacje i paleotektonika epikontynentalnej kredy górnej w Polsce. Kwartalnik Geologiczny, 32, 177–198.

Jurkowska, A. 2022. The biotic-abiotic control of Si burial in marine carbonate systems of the pre-Eocene Si cycle. Global Biogeochemical Cycles, 36, e2021GB007079.

Jurkowska, A. and Świerczewska-Gładysz, E. 2020. The new model of Si balance in Late Cretaceous European Basin. Global and Planetary Change, 186, 103–108.

Jurkowska, A., Świerczewska-Gładysz, E., Bąk, M. and Okoński, S. 2019. The role of biogenic silica in formation of Upper Cretaceous pelagic carbonates and its paleoecological implications. Cretaceous Research, 93, 170–187.

Keller, G., Barrera, E., Schmitz, B. and Mattson, E. 1993. Gradual mass extinction, species survivorship, and long-term environmental changes across the Cretaceous–Tertiary boundary in high latitudes. Geological Society of America Bulletin, 105, 979–997.

Kennedy, W.J. 1967. Burrows and surface traces from the Lower Chalk of Southern England. Bulletin of the British Museum (Natural History), Geology, 15, 14–167.

Kennedy, W.J. and Garisson, R. 1975a. Morphology and genesis of nodular chalks and hardgrounds in the Upper Cretaceous of southern England. Sedimentology, 22, 311–386.

Kennedy, W.J. and Garrison, R. 1975b. Morphology and genesis of nodular phosphates in the Cenomanian Glauconitic Marl of south-east England. Lethaia, 8, 339–360.

Keutgen, N. 2018. A bioclast-based astronomical timescale for the Maastrichtian in the type area (southeast Netherlands, northeast Belgium) and stratigraphic implications: the legacy of P.J. Felder. Netherlands Journal of Geoscience/Geologie en Mijnbouw, 97, 229–260.

Keutgen, N., Remin, Z. and Jagt, J.W.M. 2017. The late Maastrichtian *Belemnella kazimiroviensis* group (Cephalopoda, Coleoidea) in the Middle Vistula valley (Poland) and the Maastricht area (the Netherlands, Belgium) – taxonomy and palaeobiological implications. Palaeontologia Electronica, 20.2.38A, 1–29.

Kidwell. S.M. 1986. Models for fossil concentrations: paleobiologic implications. Paleobiology, 12, 6–24.

Kidwell, S.M. 1991a. Condensed deposits in siliciclastic sequences: Expected and observed features. In: Einsele, G., Ricken, W., Seilacher, A. (Eds), Cycles and Events in Stratigraphy, 682–695. Springer; Berlin, Heidelberg, New York.

Kidwell, S.M. 1991b. The stratigraphy of shell concentrations. In: Allison, P.A. and Briggs, D.E.G. (Eds), Taphonomy: Releasing the data locked in the fossil record. Topics in Geobiology, 9, 211–290. Plenum Press; New York.

Kongiel, R. 1935. Contribution à l'étude du "siwak" dans les environs de Puławy (plateau de Lublin). Prace Towarzystwa Przyjaciół Nauk w Wilnie, Wydział nauk matematycznych i przyrodniczych, 9. Prace Zakładów Geologicznego i Geograficznego, Uniwersytetu St. Batorego w Wilnie, 19, 1–59. [In Polish with French summary]

Kongiel, R. 1949. Les Echinocorys [sic] du Danien de Danemark, du Suède et de Pologne. Prace Państwowego Instytutu Geologicznego, 5, 1–89.

Kongiel, R. and Matwiejewówna, L. 1937. Matériaux fauniques de la Craie supérieure des environs de Puławy. Prace Towarzystwa Przyjaciół Nauk w Wilnie, Wydział nauk matematycznych i przyrodniczych, 11. Prace Zakładu Geologicznego, Uniwersytetu St. Batorego w Wilnie, nowa serja, 1, 1–34. [In Polish with French summary]

Kowalczyk, W. 2004. Przewodnik po wystawach. Muzeum Przyrodnicze Oddział Muzeum Nadwiślańskiego w Kazimierzu Dolnym, 1–43. [In Polish with English and German summary]

Krach, W. 1931. Niektóre małże i ślimaki kredowe z Kazimierza nad Wisłą i z okolicy. Roczniki Polskiego Towarzystwa Geologicznego, 7, 355–392. [In Polish with German summary]

Krach, W. 1974. Biostratigraphy of the Paleogene in the Middle Vistula region on the basis of molluscan macrofauna. Biuletyn Instytutu Geologicznego, 281, 49–58. [In Polish with English Summary]

Krach, W. 1981. Paleocene fauna and stratigraphy of the Middle Vistula River, Poland. Studia Geologica Polonica, 71, 1–80. [In Polish with English summary]

Krischtafovitsch, N.J. 1897. Short lecture on the investigations of Cretaceous deposits in the governorates of Lublin and Radom. Materials for geology of Russia, 18, 159–170. St. Petersburg. [In Russian]

Krischtafovitsch, N.J. 1899. Lithological character, fauna, stratigraphy and age of Cretaceous deposits on the territory of Lublin and Radom governorates. Materials for geology of Russia, 19, 1–19. St. Petersburg. [In Russian]

Krzywiec, P., Stachowska, A. and Stypa, A. 2018. The only way is up – on Mesozoic uplifts and basin inversion events in SE Poland. In: Kilhams, B., Kukla, P.A., Mazur, S., McKie, T., Mijnlieff, H.F. and Van Ojik, K. (Eds), Mesozoic Resource Potential in the Southern Permian Basin. Geological Society, London, Special Publications, 469, 33–57.

Landman, N.H, Goolaerts, S., Jagt, J.W.M. Jagt-Yazykova, E.A., Machalski, M. and Yacobucci, M. 2014. Ammonite extinction and Nautilid survival at the end of the Cretaceous. Geology, 42, 8, 707–710.

Landman, N.H., Goolaerts, S., Jagt, J.W.M., Jagt-Yazykova, E.A. and Machalski, M. 2015. Ammonites on the brink of extinction: diversity, abundance, and geographic range of the Order Ammonoidea at the Cretaceous–Paleogene (K/Pg) boundary. In: C. Klug et al. (Eds), Ammonoid Paleobiology: From macroevolution to paleogeography, Topics in Geobiology, 44, 497–553.

Leszczyński, K. 2012. The internal geometry and lithofacies pattern of the Upper Cretaceous–Danian sequence in the Polish Lowlands. Geological Quarterly, 56, 363–386.

Leys, S.P., Mackie, G.O. and Reiswig, H.M. 2007. Biology of glass sponges. Advances in Marine Biology, 52, 1–145.

Lykke-Andersen, H. and Surlyk, F. 2004. The Cretaceous–Palaeogene boundary at Stevns Klint, Denmark: inversion tectonics or sea-floor topography? Journal of the Geological Society, London, 161, 343–352.

MacEachern, J.A., Gingras, M.K., Bann, K.L., Pemberton, S.G. and Dafoe, L.T. 2007. Applications of ichnology to high-resolution genetic stratigraphic paradigms, In: MacEachern, J.A., Bann, K.L., Gingras, M.K. and Pemberton, S.G. (Eds), Applied Ichnology, SEPM Short Course Notes, 52, 95–129.

Machalski, M. 1988. Redescription of a Danian oyster *Pycnodonte simile* (Pusch, 1837) from Poland. Acta Palaeontologica Polonica, 33, 73–83.

Machalski, M. 1996. Scaphitid ammonite correlation of the Late Maastrichtian deposits in Poland and Denmark. Acta Palaeontologica Polonica, 41, 369–383.

Machalski, M. 1998. The Cretaceous–Tertiary boundary in the Vistula valley. Przegląd Geologiczny, 46, 1153–1161. [In Polish with English abstract]

Machalski, M. 2005a. The youngest Maastrichtian ammonite faunas from Poland and their dating by scaphitids. Cretaceous Research, 26, 813–836.

Machalski, M. 2005b. Late Maastrichtian and earliest Danian scaphitid ammonites in central Europe: taxonomy, evolution, and extinction. Acta Palaeontologica Polonica, 50, 653–696.

Machalski, M. 2007. Wydarzenia na granicy kreda-paleogen w Małopolskim Przełomie Wisły. In: Harasimiuk, M., Brzezińska-Wójcik, T., Dobrowolski, R., Mroczek, P. and Warowna, J. (Eds), Budowa geologiczna regionu lubelskiego i problemy ochrony litosfery, 229–234. Wydawnictwo Uniwersytetu Marii Curie-Skłodowskiej; Lublin. [In Polish with English abstract]

Machalski, M. 2012. A new ammonite zonation for the Maastrichtian Stage in Poland. In: Jagt, J.W.M. and Jagt-Yazykova, E.A. (Eds), The Maastrichtian stage; the current concept, Natuurhistorisch Museum Maastricht/Centre Ceramique 6–8 September 2012, Workshop programme, abstracts and field guide, 40–44. Natuurhistorisch Museum Maastricht; The Netherlands.

Machalski, M. 2021. Correlation of shell and aptychus growth provides insights into the palaeobiology of a scaphitid ammonite. Palaeontology, 64, 225–247.

Machalski, M. and Heinberg, C. 2005. Evidence for ammonite survival into the Danian (Paleogene) from the Cerithium Limestone at Stevns Klint, Denmark. Bulletin of the Geological Society of Denmark, 52, 97–111.

Machalski, M. and Jagt, J.W.M. 1998. Latest Maastrichtian pachydiscid ammonites from the Netherlands and Poland. Acta Geologica Polonica, 48, 121–133.

Machalski, M. and Jagt, J.W.M. 2018. A new Danian echinoid assemblage from the Greensand in the Kazimierz Dolny area, central Poland: taxonomy, taphonomy and sedimentological implications. Acta Geologica Polonica, 68, 571–596.

Machalski, M., Jagt, J.W.M., Dortangs, R.W., Mulder, E.W.A. and Radwański, A. 2003. Campanian and Maastrichtian mosasaurid reptiles from central Poland. Acta Palaeontologica Polonica, 48, 397–408.

Machalski, M. and Malchyk, O. 2019. Relative bathymetric position of opoka and chalk in the Late Cretaceous European Basin. Cretaceous Research, 102, 30–36.

Machalski, M. and Robaszewska, E. 2003. Large pycnodonteine oysters in the Upper Maastrichtian of Poland. Neues Jahrbuch für Geologie und Paläontologie, Monatshefte, 2003, 50–64.

Machalski, M., Owocki, K., Dubicka, Z., Malchyk, O. and Wierny, W. 2021. Stable isotopes and predation marks shed new light on ammonoid habitat depth preferences. Scientific Reports, 11, 22730.

Machalski, M., Stróżyk, K. and Grabarczyk, A. 2019. The Cretaceous–Paleogene (K-Pg) Boundary Site at Lechówka – a New Point on the Geoheritage Map of Southeastern Poland. Geoheritage, 1–9. Topical Collection on Geoheritage and Conservation: Modern Approaches and Applications Towards the 2030 Agenda, IX ProGEO Symposium, Poland, 25–28th June, 2018.

Machalski, M., Vellekoop, J., Dubicka, Z., Peryt, D. and Harasimiuk, M. 2016. Late Maastrichtian cephalo-

pods, dinoflagellate cysts and foraminifera from the Cretaceous–Paleogene succession at Lechówka, southeast Poland: stratigraphic and environmental implications. Cretaceous Research, 57, 208–227.

Machalski, M. and Walaszczyk, I. 1987. Faunal condensation and mixing in the uppermost Maastrichtian/Danian Greensand (Middle Vistula Valley, central Poland). Acta Geologica Polonica, 37, 75–91.

Machalski, M. and Walaszczyk, I. 1988. The youngest (uppermost Maastrichtian) ammonites in the Middle Vistula Valley, Central Poland. Bulletin of the Polish Academy of Sciences, Earth Sciences, 36, 67–70.

Malchyk, O. 2018. Late Cretaceous and early Paleogene nautilids from Poland and western Ukraie. In: El Hassani, Ah., Becker, R.T., Hartenfels, S. and Lüddecke, F. (Eds), 10th International Symposium 'Cephalopods – Present and Past' Fes, 26th March – 3rd April 2018, Program and Abstracts. Münstersche Forschungen zur Geologie und Paläontologie, 110, 79–80. Münster.

Maruszczak, H. 2003. Pierwsza monografia geologiczna Wyżyny Lubelskiej i jej autor Nikołaj I. Krisztafowicz (1866–1941). Kwartalnik Historii Nauki i Techniki, 48, 109–121.

Morawiecki, A. 1925. Fosforyty okolic Kazimierza nad Wisłą. Archiwum Pracowni Mineralogicznej Towarzystwa Naukowego Warszawskiego, 1, 142–150.

Morawski, J. 1970. Charakterystyka piasku glaukonitowo-kwarcowego znad twardego dna w Bochotnicy. Annales Universitatis Mariae Curie-Skłodowska, Lublin – Polonia, 25, 95–107.

Peryt, D. 1980. Planktonic foraminifera zonation of the Upper Cretaceous in the Middle Vistula River Valley, Poland. Palaeontologia Polonica, 41, 3–101.

Pękala, A. and Musiał, M. 2021. Modelling the leachability of Strontium and Barium from stone building materials. Materials, 14, 3403.

Pillay, D. and Branch, G.M. 2011. Bioengineering effects of burrowing thalassinidean shrimps on marine soft-bottom ecosystems. Oceanography and Marine Biology: An Annual Review, 49, 137–192.

Pinińska, J. 2007. Rock mining industry – the geological contribution to cultural heritage of Lublin region. Biuletyn Państwowego Instytutu Geologicznego, 422, 97–112. [in Polish with English abstract]

Popiel, J.S. 1977. Litologia i stratygrafia osadów najwyższego mastrychtu w okolicy Lublina i Chełma. Kwartalnik Geologiczny, 21, 515–526.

Pożaryska, K. 1952. The sedimentological problems of the Maastrichtian and Danian of the environment of Puławy. Biuletyn Państwowego Instytutu Geologicznego, 81, 1–104. [In Polish]

Pożaryska, K. 1965. Foraminifera and biostratigraphy of the Danian and Montian in Poland. Palaeontologia Polonica, 14, 1–156.

Pożaryska, K. 1967. The Upper Cretaceous and the Lower Paleogene in Central Poland. Instytut Geologiczny, Biuletyn, 5, 41–68.

Pożaryska, K. and Pożaryski, W. 1951. Przewodnik geologiczny po Kazimierzu i okolicy. Wydawnictwo Muzeum Ziemi, Warszawa, 101 pp.

Pożaryski, W. 1938. Senons Stratigraphie im Durchbruch der Weichsel zwischen Rachów und Puławy in Mittelpolen. Biuletyn Państwowego Instytutu Geologicznego, 6, 1–94. [In Polish with extended German Summary]

Pożaryski, W. 1951. Odwapnione utwory kredowe na północno–wschodnim przedpolu Gór Świętokrzyskich. Biuletyn Państwowego Instytutu Geologicznego, 75, 1–70.

Pożaryski, W. 1956. Kreda. In: Książkiewicz, M. and Dżułyński, S. (Eds), Regionalna Geologia Polski, Tom II. Region Lubelski, 14–56, Polskie Towarzystwo Geologiczne; Kraków.

Pożaryski, W. 1962. Kreda. In: Atlas geologiczny Polski. Zagadnienia stratygraficzno-facjalne, 10, Instytut Geologiczny; Warszawa.

Pusch, G.G. 1833–1836. Geognostische Beschreibung von Polen so wie der übrigen Nordkarpathen-Länder, 338 pp. J.G. Cotta'schen Buchhandlung; Stuttgart und Tübingen.

Pusch, G.G. 1837. Polens Paläontologie oder Abbildung und Beschreibung der vorzüglichsten und der noch unbeschriebenen Petrefakten aus den Gebirgsformationen in Polen, Volhynien und den Karpathen, nebst einigen algemeinen Beiträgen zur Petrefaktenkunde und einem Versuch zur Vervollständigung der Geschichte des Europäischen Auer-Ochsen, 214 pp. E. Schweizerbart's Verlagshandlung; Stuttgart.

Putzer, H. 1942. Die oberste Kreide bei Bochotnica a.d. mittleren Weichsel. Zentralblatt für Mineralogie, Geologie und Paläontologie, B12, 361–377.

Racki, G., Machalski, M., Koeberl, C. and Harasimiuk, M. 2011. The weathering-modified iridium record of a new Cretaceous–Palaeogene site at Lechówka near Chełm, SE Poland, and its palaeobiologic implications. Acta Palaeontologica Polonica, 56, 205–215.

Radwańska, U. and Radwański, A. 1994. The topmost Cretaceous discinisсian brachiopods, *Discinisca* (*Arquinisca* subgen. n.) *vistulae* sp. n. from the Middle Vistula valley, Central Poland. Acta Geologica Polonica, 44, 251–260.

Radwański, A. 1985. Cretaceous. In: Bełka, Z., Matyja, B.A. and Radwański, A. (Eds), Field-guide to the Geological Excursion to Poland, 1, 71–78. Institute of Geology, University of Warszawa; Warszawa.

Radwański, A. 1996. The predation upon, and the extinction of, the latest Maastrichtian populations of the ammonite species *Hoploscaphites constrictus* (J. Sowerby, 1817) from the Middle Vistula Valley, Central Poland. Acta Geologica Polonica, 46, 117–135.

Rasmussen, H.W. 1971. Echinoid and crustacean burrows and their diagenetic significance in the Maastrichtian–Danian of Stevns Klint, Denmark. Lethaia, 4, 191–216.

Rasmussen, J.A., Heinberg, C. and Håkansson, E. 2005. Planktonic foraminifers, biostratigraphy and the diachronous nature of the lowermost Danian Cerithium Limestone at Stevns Klint, Denmark. Bulletin of the Geological Society of Denmark, 52, 113–131.

Remin, Z., Cyglicki, M., Barski, M., Dubicka, Z. and Roszkowska-Remin, J. 2021. The K-Pg boundary section at Nasiłów, Poland: stratigraphic reassessment based on foraminifers, dinoflagellate cysts and palaeomagnetism. Geological Quarterly, 65, 1–21.

Remin, Z., Cyglicki, M. and Niechwedowicz, M. 2022. Deep vs. shallow – two contrasting theories? A tectonically activated Late Cretaceous deltaic system in the axial part of the Mid-Polish Trough: a case study from southeast Poland, Solid Earth, 13, 681–703.

Schulp, A.S., Graaf, D.Th., Jagt, J.W.M., Jianu, C.M., Machalski, M., Boekschoten, B. and Weishampel, D.B. 1999. Dinosaurs, ammonites and asteroids. Life and Death in the Maastrichtian, 1–47. Maastricht. Guide to the international paleontology exhibition in Maastricht, July 10, 1999.

Schulte, P., Alegret, L., Arenillas, I., Arz, J.A., Barton, P.J., Bown, P. R., et al. 2010. The Chicxulub asteroid impact and mass extinction at the Cretaceous–Paleogene boundary. Science, 327, 1214–1218.

Słodkowska, B. 2003. Preliminary data of the phytoplankton researches in Kamienny Dół outcrop (near Kazimierz Dolny). Przegląd Geologiczny, 51, 1075–1078. [In Polish with English Abstract]

Sujkowski, Z. 1931. Petrografia kredy Polski. Kreda z głębokiego wiercenia w Lublinie w porównaniu z kredą niektórych innych obszarów Polski. Sprawozdania Państwowego Instytutu Geologicznego, 6, 483–615.

Surlyk, F. 1997. A cool–water carbonate ramp with bryozoan mounds; Late Cretaceous–Danian of the Danish Basin. In: James, N.P. and Clarke, J.A.D. (Eds), Cool-water carbonates. Society of Economic Paleontologists and Mineralogists Special Publication, 56, 293–307.

Surlyk, F., Damholt, T. and Bjerager, M. 2006. Stevns Klint, Denmark: uppermost Maastrichtian chalk, Cretaceous–Tertiary boundary, and lower Danian bryozoan mound complex. Bulletin of the Geological Society of Denmark, 54, 1–48.

Szkuat, J. and Piskorek, W. 2009. Tajemnice wymarłego świata. Muzeum Przyrodnicze, Oddział Muzeum nadwiślańskiego w Kazimierzu Dolnym. Kazimierz Dolny.

Szopa, K., Brachaniec, T., Karwowski, Ł. and Krzykawski, T. 2017. Remnants of altered meteorite in the Cretaceous–Paleogene clay boundary in Poland. Meteoritics & Planetary Science, 52, 612–622.

Siemiradzki J. 1901. Die stratigraphischen Verhältnisse der oberen Kreide in Polen. Annuaire géologique et minéralogique de la Russie, 5, 20–27.

Siemiradzki J. 1905. O utworach górnokredowych w Polsce (Note sur les dépôts crétacés supérieurs en Pologne). Kosmos, 30, 471–492.

Świerczewska-Gładysz, E. 2006. Late Cretaceous siliceous sponges from the Middle Vistula River Valley (Central Poland) and their palaeoecological significance. Annales Societatis Geologorum Poloniae, 76, 227–296.

Świerczewska-Gładysz, E. 2012. Hexactinellid sponge assemblages across the Campanian–Maastrichtian boundary in the Middle Vistula River section, central Poland. Acta Geologica Polonica, 62, 561–580.

Świerczewska-Gładysz, E. and Olszewska-Nejbert, D. 2006. The origin of phosphatized sponges from the Danian glauconitic sandstone from Nasiłów (central Poland, Vistula River valley). Przegląd Geologiczny, 54, 710–719. [In Polish]

Vellekoop, J., van Tilborgh, K.H.V., Knippenberg, P.V., Jagt, J.W.M., Stassen, P., Goolaerts, S. and Speijer, R.P. 2019. Maastrichtian gastropod faunas show rapid ecosystem recovery following the Cretaceous–Palaeogene boundary catastrophe. Palaeontology, 63, 349–367.

Voigt, S., Wagreich, M., Surlyk, F., Walaszczyk, I., Uličný, D., Čech, S., Voigt, T., Wiese, F., Wilmsen, M., Niebuhr, B., Reich, M., Funk, H., Michalík, J., Jagt, J.W.M., Felder, P.J. and Schulp, A.S. 2008. Cretaceous. In: McCann, T. (Ed.), Geology of Central Europe. Mesozoic and Cenozoic, Volume 2, 923–997. The Geological Society; London.

Walaszczyk, I., Cieśliński, S. and Sylwestrzak, H. 1999. Selected geosites of Cretaceous deposits in Central and Eastern Poland. Polish Geological Institute Special Papers, 2, 71–76.

Walaszczyk, I., Dubicka, Z., Olszewska-Nejbert, D. and Remin, Z. 2016. Integrated biostratigraphy of the Santonian through Maastrichtian (Upper Cretaceous) of extra-Carpathian Poland. Acta Geologica Polonica, 66, 313–350.

Wilmsen, M. 2012. Origin and significance of Late Cretaceous bioevents: examples from the Cenomanian. Acta Palaeontologica Polonica, 57, 759–771.

Woroncowa-Marcinowska, T. 2016. Russian geologists in Poland at the turn of the XIX and XX century. Biuletyn Państwowego Instytutu Geologicznego, 466, 377–387. [In Polish with English Summary]

Wyrwicka, K. 1977. Wykształcenie litologiczne i węglanowe surowce skalne mastrychtu lubelskiego. Biuletyn Instytutu Geologicznego, 299, 1–98.

Wyrwicka, K. 1980. Stratygrafia, facje i tektonika mastrychtu zachodniej części Wyżyny Lubelskiej. Kwartalnik Geologiczny, 24, 805–819.

Żarski, M., Jakubowski, G. and Gawor-Biedowa, E. 1998. The first Polish find of a Lower Paleocene crocodile *Thoracosaurus* Leidy, 1852; geological and palaeontological description. Geological Quarterly, 42, 141–160.

11TH INTERNATIONAL
CRETACEOUS
SYMPOSIUM
Warsaw, Poland, 2022

THE LATE CRETACEOUS INVERSION OF THE SOUTHEASTERN PART OF THE POLISH BASIN – SYN-DEPOSITIONAL TECTONICS, FACIES DISTRIBUTION AND BATHYMETRIC CHANGES

Zbyszek Remin[1]| Piotr Krzywiec[2]| Aleksandra Stachowska[2]

1| Faculty of Geology, University of Warsaw, Al. Żwirki i Wigury 93, PL-02-089 Warsaw, Poland; e-mail: zremin@uw.edu.pl

2| Institute of Geological Sciences, Polish Academy of Science, ul. Twarda 51/55, PL-00-818, Warsaw, Poland; e-mails: piotr.krzywiec@twarda.pan.pl; aleksandra.stachowska@twarda.pan.pl

ABSTRACT

The Polish Basin formed the eastern part of the Central European Basin System. During the Late Cretaceous, its axial, most subsiding part – the Mid-Polish Trough – underwent uplift, which consequently resulted in its inversion and transformation into the Mid-Polish Anticlinorium, with two adjacent synclinoria: the Kościerzyn–Puławy Synclinorium towards the northeast, and the Szczecin–Łódź–Miechów Synclinorium towards the southwest. The timing of the onset of the inversion tectonics in the southeast segment of the Mid-Polish Trough is still controversial. Based on sedimentary, environmental, and facies data from selected localities northeast of the present Mid-Polish Anticlinorium, and on high-resolution seismic data covering the entire area, we propose that the inversion of the southeastern part of the Mid-Polish Trough had already initiated in the Coniacian, or even in the latest Turonian.

INTRODUCTION

Starting in the mid-Late Cretaceous, central Europe was impacted by compressional tectonics, the results of which (that is, basement uplift and inversion) are recorded across the entire Central European Basin System. Material eroded from the uplifted structures was deposited in newly formed flexural basins (e.g., Ziegler 1990; Nielsen and Hansen 2000; Krzywiec 2006; Kley and Voigt 2008; Krzywiec and Stachowska 2016; Voigt et al. 2021). Late Cretaceous inversion tectonics also induced marked changes in palaeogeography and facies architecture, particularly in a belt along the margin of the East European Craton (Figs 1, 2).

The Polish Basin (Fig. 2), the easternmost part of the Central European Basin System, records these processes (for review compare: Krzywiec 2002; Krzywiec et al. 2009, 2018). Its palaeotectonic evolution has been intensely debated in the Polish geological literature for more than a century, and the evolution and timing of the tectonic inversion of the Mid-Polish Trough, representing its axial, most rapidly subsiding part, is still an area of active research (see reviews in Krzywiec et al. 2009; Walaszczyk and Remin 2015; Krzywiec et al. 2018; Remin et al. 2022).

Broadly speaking, two concepts exist regarding the onset of Mid-Polish Trough inversion tectonics and its subsequent transformation into the Mid Polish-Anticlinorium (for a thorough review, see: Krzywiec et al. 2009, 2018; Walaszczyk and Remin 2015; Remin et al. 2022).

The first concept, which in our opinion is only of historical interest, argues that the inversion of the Mid-Polish Trough initiated during the Late Maastrichtian and Paleogene. Accordingly, the southeastern edge of the

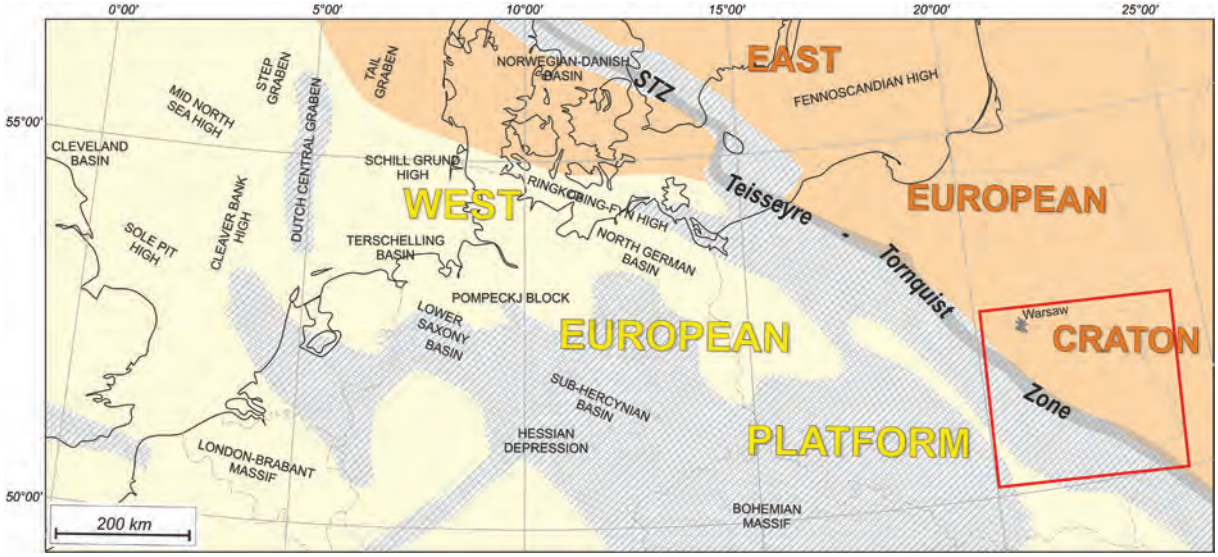

Fig. 1. Regional schematic map of western and central Europe (after Krzywiec et al. 2018, with further references), with extent of the Late Cretaceous - Paleocene inversion (stippled area); red rectangle – studied area.

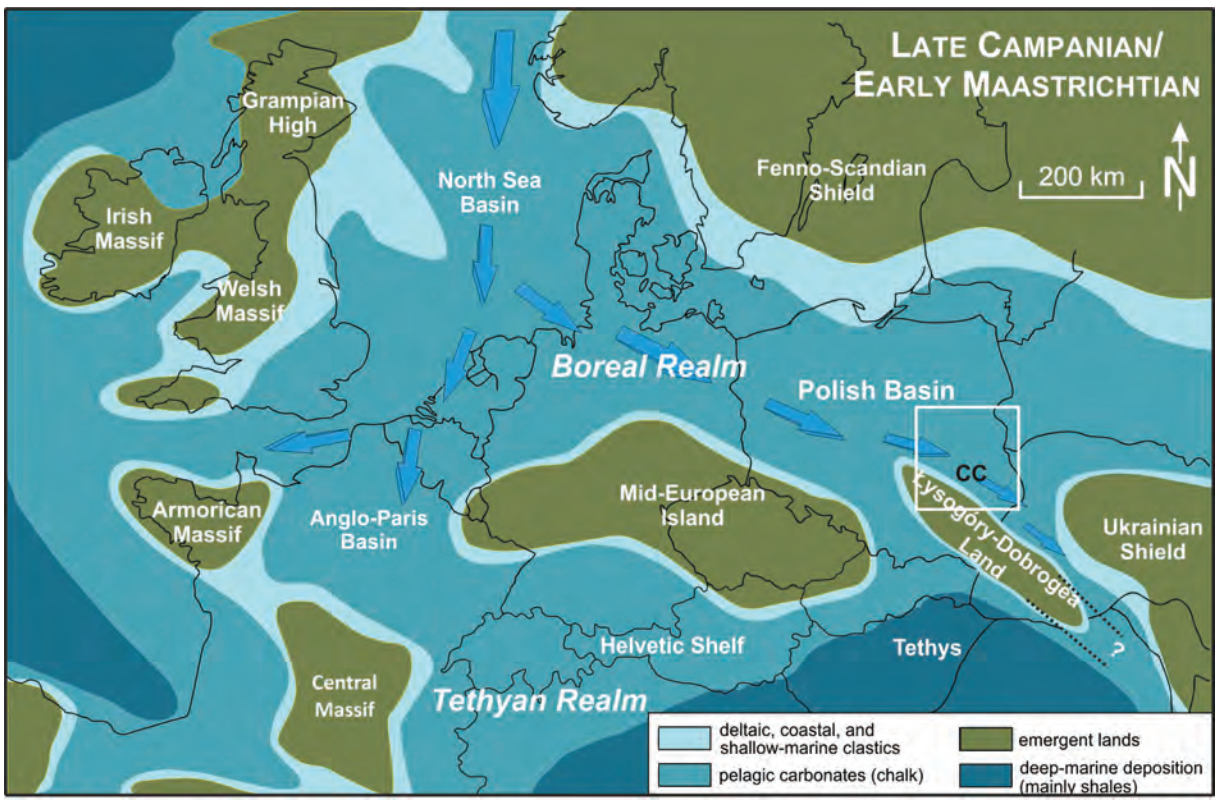

Fig. 2. Schematic paleogeographic map (compiled from Ziegler 1990; Dadlez et al. 1998) and location of studied sections in southeastern Poland (white rectangle). Ocean current flows are based on Remin et al. (2016) and Remin (2018); the presence of contourite currents (CC) follows Krzywiec et al. (2009, 2018); adapted from Remin et al. (2022).

Mid-Polish Trough (Figs 3, 4), which currently is almost devoid of Mesozoic overburden (Figs 3–5), represented the axial part of the Polish Basin and, so, the deepest, most subsiding sedimentary environments during the Late Cretaceous (e.g., Kutek and Głazek

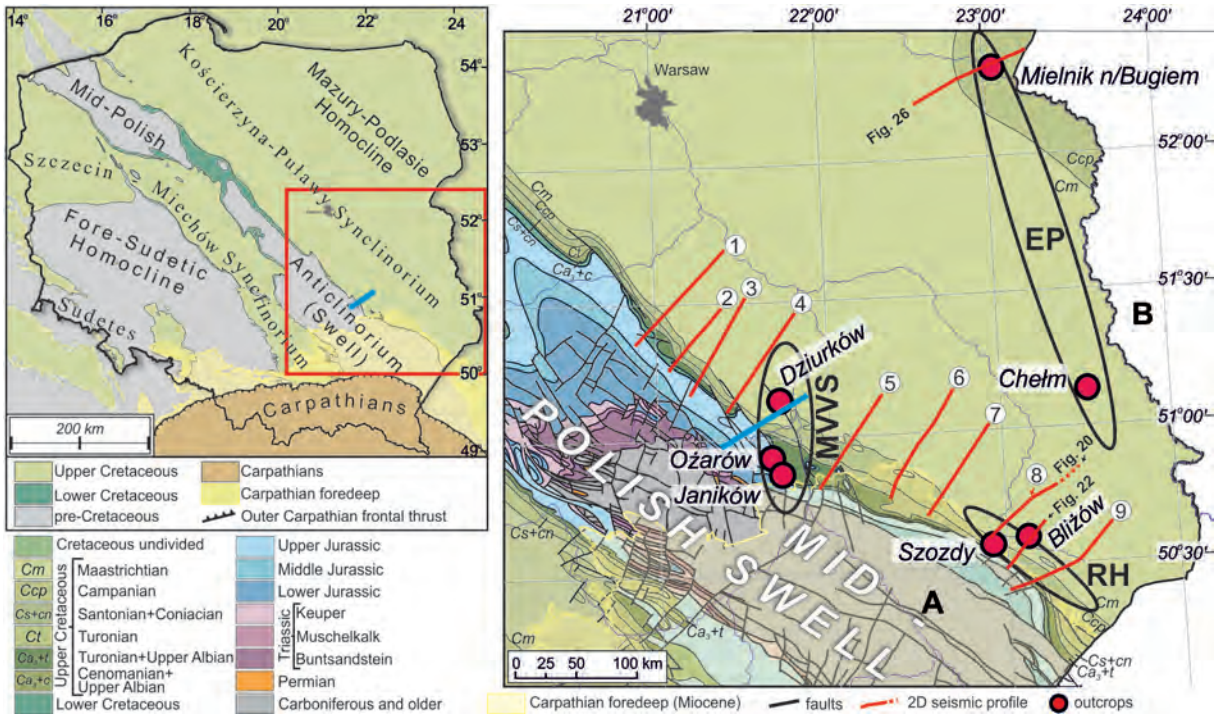

Fig. 3. General position of the analyzed area (left) against the geological map of extra-Carpathian Poland, excluding Cenozoic deposits, except for the modern extension of the Carpathian Foredeep (transparent yellow); adapted from Dadlez et al. (2000); tectonic units after Żelaźniewicz et al. (2011). The analyzed area is subdivided into three regions – MVVS = the Middle Vistula Valley Section; RH = the Roztocze Hills; EP = Eastern Poland. Close-up location (right) of the presented surface outcrops. 1-9: seismic profiles shown in Krzywiec et al. (2018), profiles 3-4 are shown on Figs 10-12 (cf. Krzywiec et al. 2009). The blue line indicates the approximate position of the cross-section provided in Fig. 9.

1972; Hakenberg and Świdrowska 1998, 2001; Świdrowska and Hakenberg 1999; Świdrowska 2007; Świdrowska et al. 2008). This also implies that the area currently devoid of Mesozoic remnants (Figs 3–5) was deeply buried by those deposits. In turn, this paleotectonic model constituted the basis for facies and bathymetric interpretations. It suggests sediments deposited close to the axial part of the Polish Basin (i.e., within the Mid-Polish Trough), such as those in the Middle Vistula Valley and the Roztocze Hills (southeast Poland) constitute the deepest facies.

The second, and at present more widely accepted, concept argues that inversion tectonics started much earlier – during the Coniacian and/or Santonian, or perhaps even in the Late Turonian (e.g., Pożaryski 1960, 1962; Jaskowiak-Schoeneichowa and Krassowska 1988; Walaszczyk 1992; Leszczyński and Dadlez 1999; Krzywiec et al. 2009, 2018; Leszczyński 2010, 2012; Walaszczyk and Remin 2015; Remin et al. 2016, 2022; Remin 2018; Łuszczak et al. 2020).

Recent studies have shown that by the Coniacian and Santonian (and possibly even in the latest Turonian), the axial part of the Polish Basin (i.e., the Mid-Polish Trough) should be already considered to be an emergent landmass or paleomorphological barrier, rather than the deepest part of the basin; this is especially true in southeastern Poland (e.g., Krzywiec et al. 2009, 2018; Remin et al. 2015a, 2016, 2022; Walaszczyk and Remin 2015; Remin 2018). According to this model (Fig. 4), deposits adjacent to the area of epigenetic erosion represent the shallowest facies, passing into deeper facies towards the northeast (Fig. 4) (Remin et al. 2022 for an overview).

This interpretation is supported by the presence of clearly shallow-water facies locally developed along the northeastern edge of the southeastern part of the present-day Mid-Polish Anticlinorium – in the area where the deepest facies should be expected according to the first model. These include the Turonian Janików Limestone (sandy limestone), char-

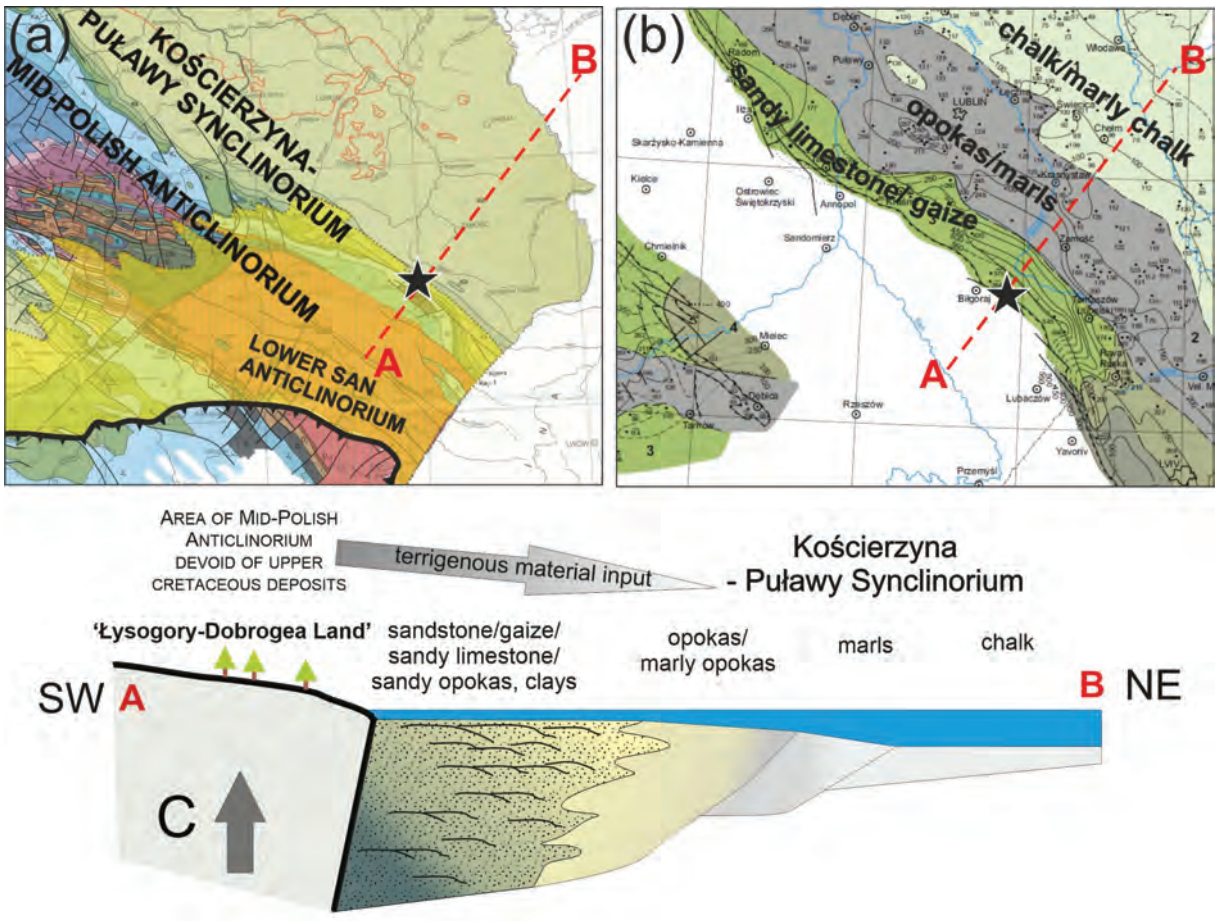

Fig. 4. (**a**) A detailed view of the analyzed area, relative to the position of the Holy Cross Mountains and the Lower San Anticlinorium – the most southeastern part of the Mid-Polish Anticlinorium; (**b**) The general distribution of Campanian lithofacies in southeast Poland (adapted from Świdrowska 2007); **(c)** the depositional, structural, and environmental interpretation of facies and bathymetry in a cross-section perpendicular to the axis of the Mid-Polish Anticlinorium (adapted from Remin et al. 2015a, 2022; Walaszczyk and Remin 2015).

acterized by a progradational sedimentary pattern and a transport direction northeast towards the flank of the basin (Walaszczyk 1992 and unpublished data), and deltaic, sand-rich sedimentation in the Roztocze Hills during the Campanian and possibly Maastrichtian (Remin et al. 2022). It is worth noting that the sandy facies of the Roztocze Hills have been mentioned by several authors (e.g., Kamieński 1925; Jaskowiak-Schoeneichowa and Krassowska 1988; Świdrowska et al. 2007; Leszczyński 2010, 2012; and literature therein), but this prominent terrigenous input has never been explored sedimentologically to reveal possible depositional environments, paleobathymetry, and source area.

Additionally, the above interpretation is supported by new sedimentological and biotic data (Remin et al. 2015a, 2016, 2022; Niechwedowicz et al. 2016, 2021; Cyglicki and Remin 2017, 2018; Remin 2018). Close proximity to land is also suggested by extraordinarily preserved plant debris, including complete compound leaves (Halamski 2013) and characteristic shallow-marine palynofacies (Remin et al. 2022).

The discovery of the Szozdy deltaic system in the Roztocze Hills (Remin et al. 2022) pro-

Fig. 5. Different palaeogeographic interpretations based on the distribution of lithofacies, palaeothickeness maps, and the present-day thickness of Campanian strata ; (**a**) Świdrowska and Hakenberg (1999); (**b**) Jaskowiak-Schoeneichowa and Krassowska (1988); (**c**) Świdrowska et al. (2008). →

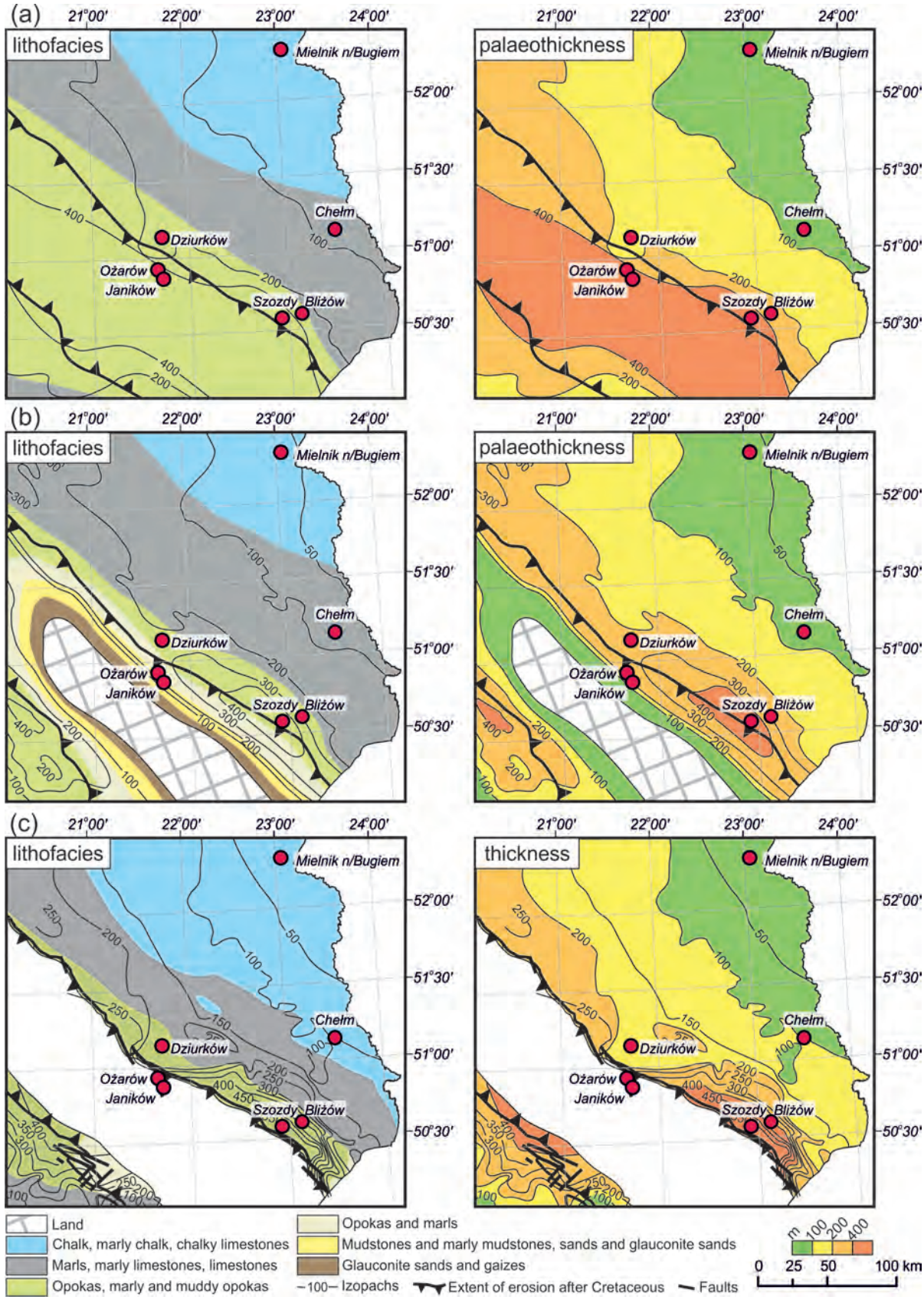
(a)
lithofacies
palaeothickness
(b)
lithofacies
palaeothickness
(c)
lithofacies
thickness
21°00'
22°00'
23°00'
24°00'
52°00'
51°30'
51°00'
50°30'
Mielnik n/Bugiem
Chełm
Dziurków
Ożarów
Janików
Szozdy
Bliżów
Land
Chalk, marly chalk, chalky limestones
Marls, marly limestones, limestones
Opokas, marly and muddy opokas
Opokas and marls
Mudstones and marly mudstones, sands and glauconite sands
Glauconite sands and gaizes
–100– Izopachs
Extent of erosion after Cretaceous
Faults
m
100
200
400
0
25
50
100 km

vides a fresh perspective into interpretations of different facies along the northeast edge of the Mid-Polish Anticlinorium. It also emphasized the need for a revision to the existing paleotectonic model of the southeastern part of the Polish Basin, driving the adoption of a new facies and bathymetric model (Fig. 4) for several Late Cretaceous facies (discussion in: Krzywiec et al. 2009, 2018; Remin et al. 2015a, 2022; Walaszczyk and Remin 2015). According to Remin et al. (2022), the source area for the deltaic facies was located to the southwest, in the area now devoid of Mezosoic remnants (Fig. 4).

These arguments (discussion in Remin et al. 2022), provide the foundation for the first direct sedimentological, petrographic, and palynofacies evidence for the presence of an emerged landmass – the Łysogóry–Dobrogea Land – in an area now devoid of Mesozoic cover (Figs 3, 4). These data, at least in part, confirm the earlier proposals of Krzywiec et al. (2009, 2018) based on subsurface seismic data.

Intriguingly, ours is not a novel interpretation. Up to the 1960s (e.g., Rogala 1909; Nowak 1907, 1908; Kamieński 1925; Samsonowicz 1925; Pożaryski 1960, 1962), and even later, the area of southeast Poland was interpreted as an emerged landmass during the Late Cretaceous. The following names have been utilized for this landmass: the "Łysogóry–Dobrogea Land" of Samsonowicz (1925) and Jurkowska et al. (2019a); the "Maastrichtian Island" of Jurkowska and Barski (2017); the "Krukienic Island" of Pasternak (1959), Pasternak et al. (1968, 1987), Walaszczyk (1992), and Dubicka et al. (2014); and the "Świętokrzyski Land" or "Małopolska Land" of Pożaryski (1960, 1962) and Jaskowiak-Schoeneichowa and Krassowska (1988), among others.

The rationale of this review is to show the Late Cretaceous facies development of the Polish Basin in the context of syndepositional inversion tectonics. The dynamic tectonic regime – inversion processes (uplift) of the axial part of the Polish Basin on the one hand and rapid subsidence on the other – coupled with possible wave and/or bottom current transport processes and significant terrigenous/terrestrial input (at least in some areas), were the main driver of the bathymetrical and facies changes observed in cross-sections perpendicular to the uplifting Mid-Polish Trough. Special emphasis is put on the Campanian and Maastrichtian successions present in three analyzed regions.

REGIONAL SETTING

General remarks on the sedimentary infill of the Polish Basin

In the Permian, the Polish Basin represented the eastern part of the so-called Southern Permian Basin (e.g., Kiersnowski et al. 1995; Krzywiec et al. 2017). In general, during the Permian and Mesozoic, the Polish Basin constituted the eastern part of the Central European Basin System, part of the western and central European epicontinental basins (e.g., Pharaoh et al. 2010). The Mid-Polish Trough represented its most subsiding, axial part.

During the Permian to early Late Cretaceous, the Polish Basin experienced long-term subsidence (e.g., Dadlez et al. 1995), resulting in its filling by up to c. 8000 m of Permian and Mesozoic deposits. In particular, the highest thicknesses are especially located along the NW-SE trending Mid-Polish Trough (e.g., Dadlez et al. 1998) that constituted the central and axial part of the basin.

After this episode of long-term Mesozoic subsidence, the Polish Basin (particularly its axial part – the Mid-Polish Trough) underwent inversion and uplift, particularly during the late Late Cretaceous. Inversion tectonics, as exemplified both in facies changes and seismic images, started sometime in the Late Turonian and lasted until the end of the Maastrichtian (or even post-Maastrichtian) (e.g., Krzywiec 2000, 2002, 2006, 2009; Resak et al. 2008; Krzywiec et al. 2009, 2018; Remin et al. 2022).

The Permo-Mesozoic sedimentary cover differs significantly within the Polish Basin. While in the western and central part of the basin thick Permian, Triassic, Jurassic, and Cretaceous strata were deposited, the southeastern part is devoid during many intervals. Here, only Middle/Upper Jurassic and Cretaceous deposits are well-documented (e.g., Świdrowska et al. 2008 for an overview); the missing part of the succession has been attributed to denudation.

During inversion tectonics, the axial part of the basin – the Mid-Polish Trough – was

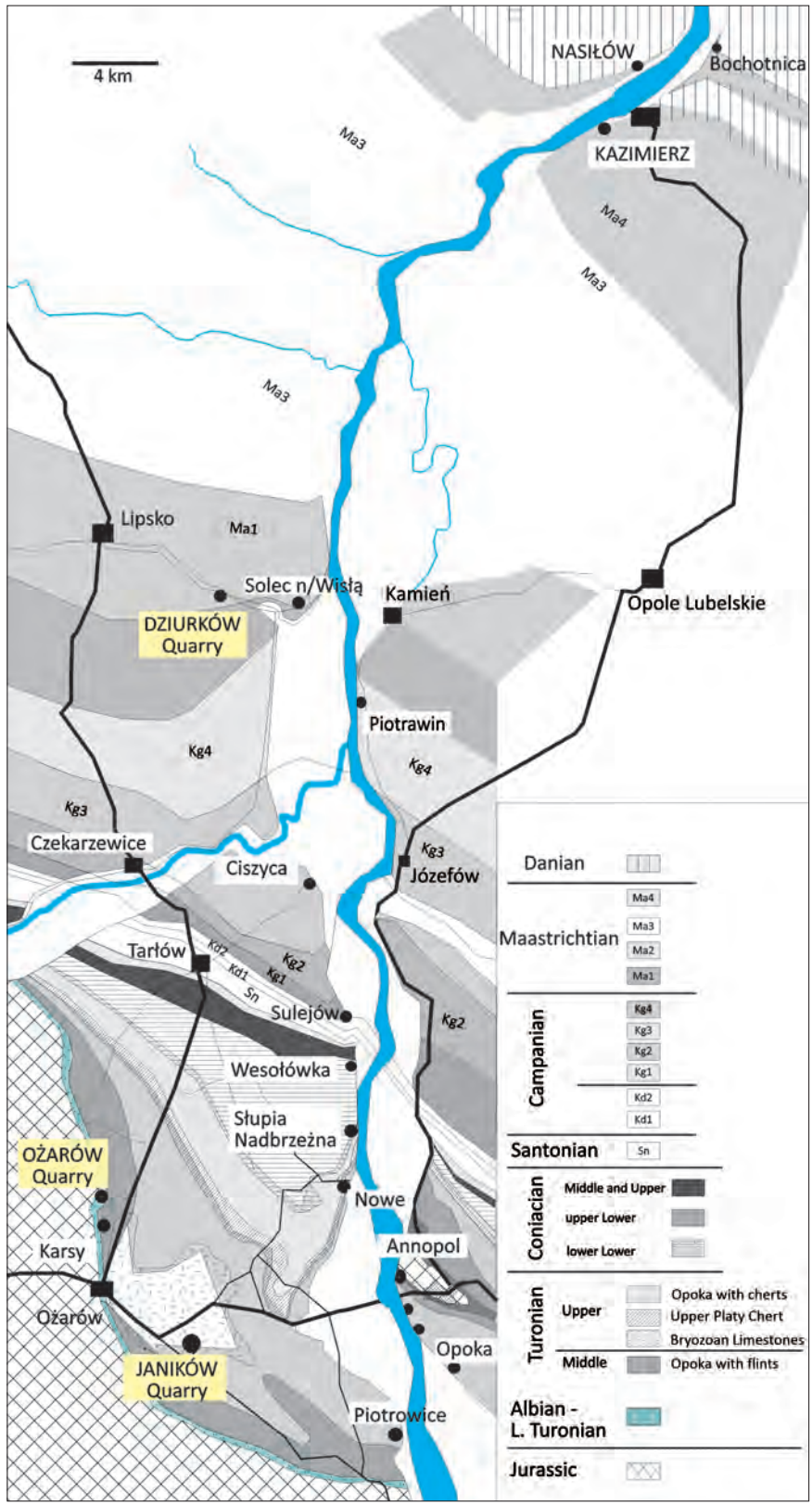

Fig. 6. Geological sketch-map and main localities of the Middle Vistula River composite section; the homoclinal structure of the area yields progressively younger beds towards the north; adapted from Walaszczyk et al. (2016).

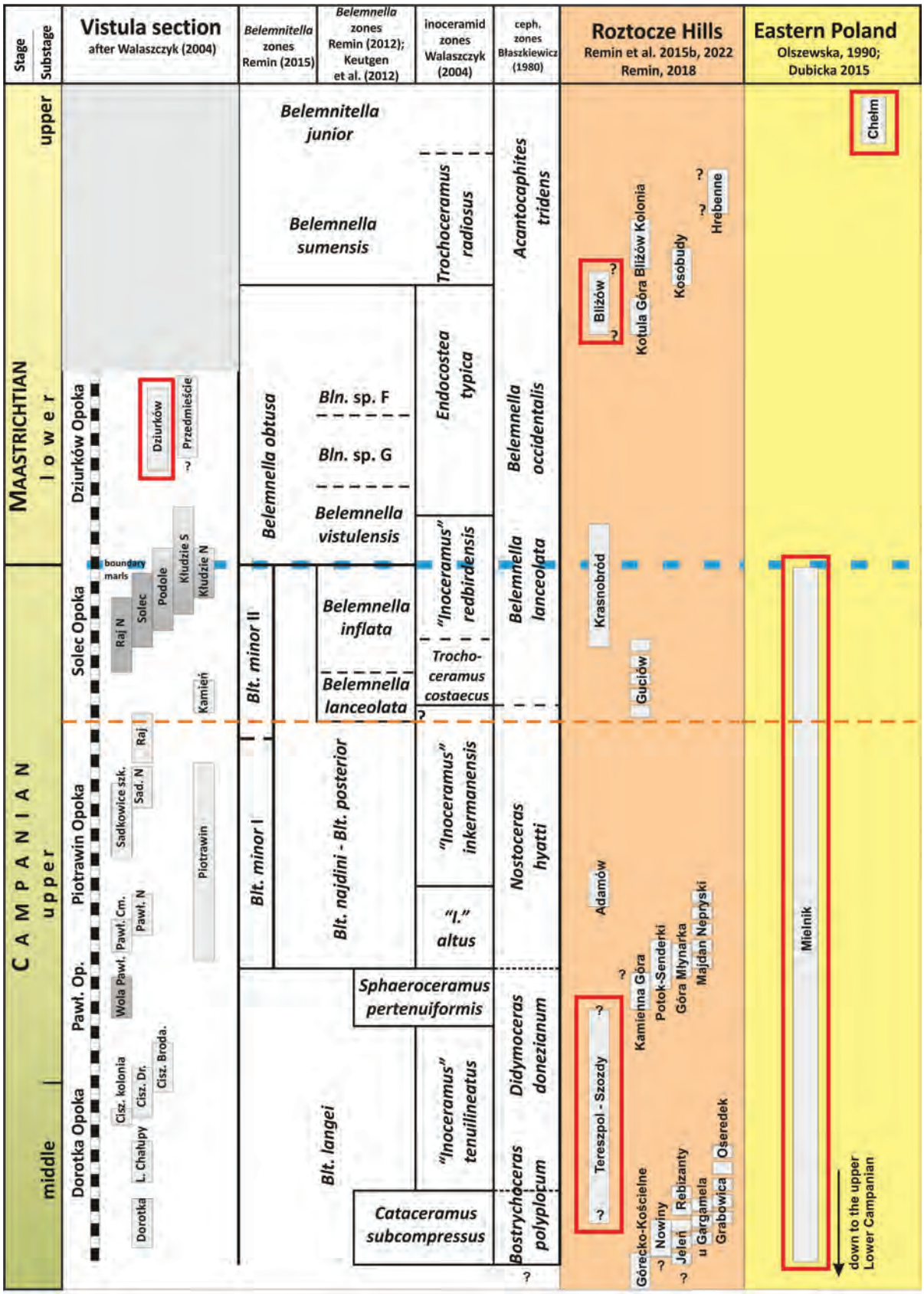
Stage
Substage
Vistula section
after Walaszczyk (2004)
Belemnitella zones Remin (2015)
Belemnella zones Remin (2012); Keutgen et al. (2012)
inoceramid zones Walaszczyk (2004)
ceph. zones Błaszkiewicz (1980)
Roztocze Hills
Remin et al. 2015b, 2022
Remin, 2018
Eastern Poland
Olszewska, 1990; Dubicka 2015
MAASTRICHTIAN
lower
upper
CAMPANIAN
middle
upper
Dziurków Opoka
Solec Opoka
Piotrawin Opoka
Pawł. Op.
Dorotka Opoka
boundary marls
Dziurków
Przedmieście
Kłudzie N
Kłudzie S
Podole
Solec
Raj N
Kamień
Raj
Sad. N
Sadkowice szk.
Pawł. N
Pawł. Cm.
Wola Pawł.
Piotrawin
Cisz. Broda.
Cisz. Dr.
Cisz. kolonia
L. Chałupy
Dorotka
Belemnitella junior
Belemnella sumensis
Belemnella obtusa
Belemnella vistulensis
Belemnella inflata
Belemnella lanceolata
Blt. minor II
Blt. minor I
Blt. najdini - Blt. posterior
Blt. langei
Bln. sp. F
Bln. sp. G
Trochoceramus costaecus
Sphaeroceramus pertenuiformis
Cataceramus subcompressus
Trochoceramus radiosus
Endocostea typica
"Inoceramus" redbirdensis
"Inoceramus" inkermanensis
"I." altus
"Inoceramus" tenuilineatus
Acantocaphites tridens
Belemnella occidentalis
Belemnella lanceolata
Nostoceras hyatti
Didymoceras donezianum
Bostrychoceras polyplocum
Bliżów
Krasnobród
Guciów
Adamów
Tereszpol - Szozdy
Górecko-Kościelne
Nowiny
Jeleń
Rebizanty
u Gargamela
Grabowica
Oseredek
Kamienna Góra
Potok-Senderki
Góra Młynarka
Majdan Nepryski
Kołtuła Góra
Bliżów Kolonia
Kosobudy
Hrebenne
Chełm
Mielnik
down to the upper Lower Campanian

transformed into a prominent structural unit – the Mid-Polish Anticlinorium (Fig. 3). Simultaneously, two marginal troughs were formed: the Kościerzyna–Puławy Synclinorium to the northeast and the Szczecin–Miechów Synclinorium to the southwest (Fig. 3), both fed at least partially by the elevated (uplifted) and eroding areas of the Mid-Polish Anticlinorium. As a result of the inversion, Upper Cretaceous deposits are currently preserved only along the flanks of the Mid-Polish Anticlinorium (Figs 3–5).

The Middle Vistula Valley section

The Middle Vistula Valley, in southeastern Poland, is a unique section within the whole of Europe and constitutes the reference section for the Cretaceous of extra-Carpathian Poland. It is located in the border zone between the inverted Mid-Polish Anticlinorium and the Kościerzyna–Puławy Synclinorium (Fig. 3). The area gives direct insight into the sedimentary record of the Albian and the entire Late Cretaceous, including the K-Pg boundary (Samsonowicz 1925, 1934; Pożaryski 1938, 1948; Marcinowski and Radwański 1983; Walaszczyk in Voigt et al. 2008a; Remin et al. 2021). Flowing to the north, the Vistula River crosses the homoclinal structure, passing through successively younger depositional belts (Figs 3, 6) between Annopol and Kazimierz Dolny.

The whole interval is accessible in a series of natural and artificial exposures along both banks of the Vistula River. During recent years, this section has been extensively studied for a variety of purposes, especially for biostratigraphic subdivision (overview in Walaszczyk et al. 2016). Special emphasis has been placed on the Campanian–Maastrichtian transition (compare Fig. 7 with additional references).

The Roztocze Hills region

The Roztocze Hills constitute a prominent range between the cities of Kraśnik (southeast Poland) and Lviv in western Ukraine (Fig. 4). They are located along the elevated Mid-Polish Anticlinorium with the Kościerzyna–Puławy Synclinorium to the north (southeast Poland) (Figs 3, 4), covering an area of approximately 185 by 25 km.

In their Polish part, the Roztocze Hills are composed of Campanian and Maastrichtian deposits dipping gently to the northeast. The older part of the Late Cretaceous succession is not exposed. The Roztocze Hills provides access to various Late Cretaceous facies: calcareous sandstones, calcareous mudstones, argillaceous mudstone or clays, various opoka facies (siliceous chalk/limestone with a variable admixture of biogenic silica), and gaizes (siliceous limestone with a considerable admixture of detrital quartz, glaucony, and clay). Usually, the hills are topped by unconformably lying Miocene deposits (e.g., Pożaryski 1956).

The southwestern edge of the present-day Roztocze Hills forms a prominent (50–80 m high) escarpment. Structurally, this well-visible escarpment forms the border of the subsurface northern part of the San Anticlinorium (the most southeastern part of the Mid-Polish Anticlinorium). The latter is covered by Miocene deposits of the present-day Carpathian Foredeep (Fig. 4) (e.g., Dziadzio et al. 2006 for further references). The subsurface San Anticlinorium (southeastern part of the Mid-Polish Anticlinorium) is represented by Neoproterozoic and Cambrian flysch-type deposits; they are markedly tectonized and slightly metamorphosed, and their thickness is unknown (e.g., Dziadzio and Jachowicz 1996; Buła et al. 2008; Żelaźniewicz et al. 2009; Buła and Habryń 2011).

It is generally considered that this tectonic line, which delineates the Roztocze Hills to the southwest, is based in crustally-rooted fault zones (review in Narkiewicz et al. 2015; Narkiewicz and Petecki 2017). These fault zones were repeatedly reactivated as reverse faults during Late Cretaceous inversion tectonics (Krzywiec 1999; Krzywiec et al. 2009); they were also active during the Carpathian

← Fig. 7. The stratigraphic position of Campanian and Maastrichtian sections in the three regions examined in this chapter (rectangled in red). The scale bar (= 2 m) is only valid for the Middle Vistula Valley section. For the Roztocze Hills and Eastern Poland, the chronostratigraphic positions of particular sections are relative to the Middle Vistula Valley section. The biostratigraphic subdivision follows Błaszkiewicz (1980), Olszewska (1990), Walaszczyk (2004), Machalski (2012); Remin (2012, 2015, 2018), Keutgen et al. (2012), Dubicka (2015), Remin et al. (2015b, 2022), and Walaszczyk et al. (2016). Blue line = the Campanian/Maastrichtian boundary according to the Tercis definition (GSSP); orange line = the traditional Campanian/Maastrichtian boundary based on the entrance of the genus *Belemnella*.

movements in the Miocene (Kowalska et al. 2000; Buła et al. 2008; Buła and Habryń 2011).

Eastern Poland

In this region, our focus is centered on two sections representing both Campanian and Maastrichtian deposits (Fig. 3). The sections of Chełm and Mielnik are located, respectively, in the Kościerzyna–Puławy Synclinorium and the Mazury–Podlasie Homocline (Fig. 3). In contrast to the Middle Vistula River section and the Roztocze Hills, where several (natural and artificial) outcrops are available for study – enabling the construction of composite Late Cretaceous sections – Eastern Poland has considerably fewer surface outcrops due to considerable Quaternary cover.

It is worth noting that the facies development of Upper Cretaceous strata in Eastern Poland differs significantly from those observed in the Middle Vistula River section and the Roztocze Hills: they are predominantly composed of chalk facies deposited through almost the entire late Cretaceous (Fig. 5). Additionally, the thickness pattern is also different, although uniform – Upper Cretaceous strata in Eastern Poland are characterized by markedly reduced thicknesses in comparison to the aforementioned regions. For instance, the whole Upper Cretaceous succession in Mielnik (from the Cenomanian to the Campanian/Maastrichtian boundary) is c. 200 m, whereas in the Roztocze Hills region the Campanian strata alone exceed 500 m (compare Fig. 5), and the entire Cretaceous reaches c. 1000–1200 m.

The sections at Chełm and Mielnik, as those most distant from the inverting Mid-Polish Trough, occupy the most offshore, and most likely deepest, zones (Figs 4, 5). As this area was located furthest from the Łysogóry–Dobrogea Land, it did not receive a significant terrigenous supply. As such, the chalk facies – especially in Mielnik – are composed of nearly 98% $CaCO_3$.

STRATIGRAPHIC OVERVIEW

In southeastern Poland, the Middle/Upper Albian and the whole Upper Cretaceous succession comprise c. 1000–1200 m, deposited in a rather shallow epicontinental basin (e.g., Jaskowiak-Schoeneichowa and Krassowska 1988). Outcrops and well data enable precise biostratigraphic subdivisions based on inoceramids, ammonites, belemnites, echinoids, foraminifera, and to a lesser extent other groups (for overview, compare Walaszczyk et al. 2016). The Upper Cretaceous succession is best exposed in the northeastern peripheries of the elevated Mid-Polish Anticlinorium, where it is accessible in a series of natural and artificial exposures: that is, in the Middle Vistula Valley Section and the Roztocze Hills area (Fig. 3), and to a lesser extent in Eastern Poland. Starting in the Cenomanian until the Maastrichtian, marine deposits cover most of southeastern Poland, and are mostly ascribed to a siliciclastic-carbonate shelf system (e.g., Leszczyński 1997, 2010, 2012).

Syn-depositional tectonics – a clue for understanding Late Cretaceous facies distribution

The very existence of clearly shallow water ephemeral facies in the heart of the inverting Mid-Polish Trough – that is, the Turonian Janików Limestone/Sandstone in the Middle Vistula Valley Section and Campanian deltaic deposits in the Roztocze Hills – shed new light on the understanding of at least some Late Cretaceous facies. This concern mainly terrigenous-rich deposits, opoka, and chalk, and their spatial and bathymetric relationships (Fig. 4).

The adopted paleotectonic and paleofacies model (Fig. 4) for the Roztocze Hills area, in close proximity to the Łysogóry–Dobrogea Land (see discussion in Remin et al. 2022), points to a rather shallow depositional environment for the opoka facies (or its variants), which seems to be true for both ephemeral facies mentioned above. This paleoenvironmental model proposed in 2015 (Remin et al. 2015a; Walaszczyk and Remin 2015) has been recently advocated by Jurkowska et al. (2019a, b) and Machalski and Malchyk (2019).

Accordingly, during the Late Cretaceous the Łysogóry–Dobrogea Land (the recent-day San Anticlinorium) was a source area for the siliciclastics and argillaceous clays of the Roztocze Hills. The Szozdy delta system, rich in terrestrially-sourced material, passes northeast to gaize and opoka facies. The interfingering of deltaically influenced sedimentation with

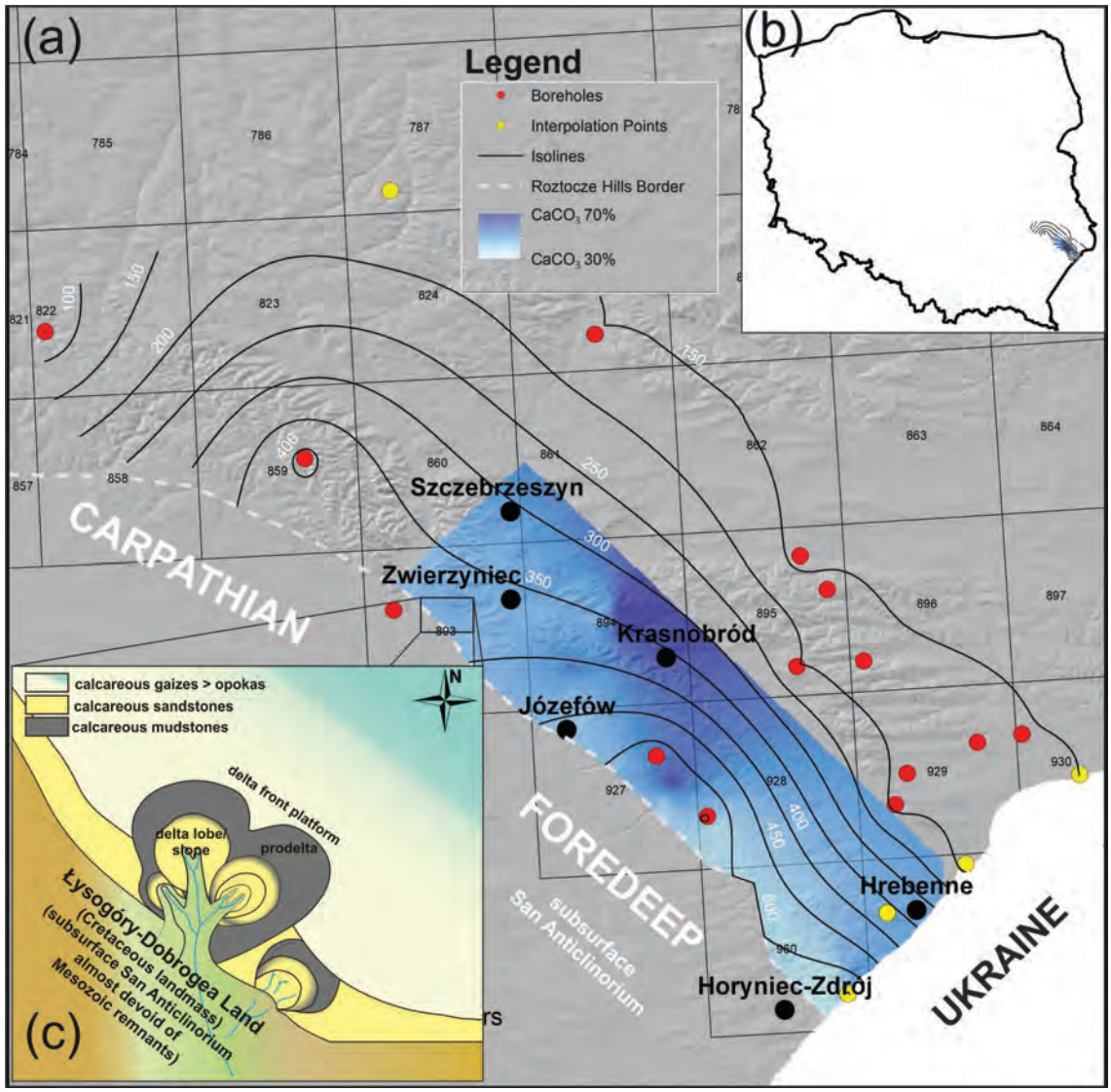

Fig. 8. **(a)** $CaCO_3$ distribution pattern (blue area) against isolines of Campanian deposit thickness. Red dots = boreholes; yellow dots = interpolation points; **(b)** General map of Poland with study area; **(c)** Subaerial view of the Szozdy deltaic environment in relation to the distribution pattern of bordering facies – not to scale. Squares with numbers represent the associated geological map sheets (www.geologia.pgi.gov.pl); adapted from Remin et al. (2022).

gaize and opoka suggests that opoka should be linked to shallow-water environments, in contradiction to previous conceptions that suggested a deep origination for the opoka facies. In general, the further northeast from the Łysogóry–Dobrogea Land, the more carbonate-rich deposits occur. This phenomenon is visible even in the Roztocze Hills, where most terrigenous-rich sediments occur along the southwestern edge of the Roztocze Hills (Fig. 8): that is, close to the source area. In a wider context, the passage to carbonate sedimentation is best exemplified by the chalk deposits of Eastern Poland, where pure chalk sedimentation took place in the more offshore, deeper zones of the basin (Figs 3, 4 and discussion in Remin et al. 2022). Confirmation of the presence of deeper zones and a regional submarine slope to the northeast, alongside the Łysogóry–Dobrogea Land itself (Fig. 2), is provided by contourites discovered by Krzywiec et al. (2009, 2018).

A similar facies and paleotectonic model has been described for Coniacian to Campa-

nian strata of the Subhercynian Cretaceous Basin. Here, most of the sandy and marly material was derived from the elevated Harz Mountains, which acted as a source area during Late Cretaceous inversion tectonics (Voigt et al. 2004, 2006, 2008; von Eynatten et al. 2008). Indeed, the Harz Mountains were inverted and uplifted at the same time as the axial part of the Polish Basin.

Until recently, understanding of the spatial distribution of Late Cretaceous facies within the Polish Basin was markedly influenced by the existing paleotectonic model (Kutek and Głazek 1972). In this framework, the axial part of the Polish Basin was *a priori* synonymized with its deepest, most subsiding part. Consequently, the sediments deposited in the Mid-Polish Trough were simply considered to be the deepest. In this respect, the opokas of the Middle Vistula Valley Section and, especially, the Roztocze Hills (adjacent to areas now devoid of Mesozoic cover; Fig. 4) were considered to be deposited in the deepest sedimentary environments. One can easily conclude that such environmental interpretations of facies distribution were fit to the adopted paleotectonic model, rather than *vice versa* (see discussion in Remin et al. 2022).

Even though the deposits of the Roztocze Hills, where the opoka facies was predominant (especially during the Campanian and Maastrichtian), are markedly enriched in terrestrially-sourced material (Remin et al. 2022), the notion that opoka was of deep-water origin was accepted for decades (e.g., Hakenberg and Świdrowska 1998, 2001; Świdrowska and Hakenberg 1999; Świdrowska 2007; Świdrowska et al. 2008; Świerczewska-Gładysz 2006; Leszczyński 2010, 2012). It is worth acknowledging, however, that the opoka facies eludes easy environmental interpretations. In this respect, the former paleoenvironmental (bathymetrical) model and spatial distribution of particular facies were not supported by any relevant sedimentological or biological indicators.

In the light of new data, especially the presence of some ephemeral, clearly shallow-water (coastal) facies developed in the heart of the inverting Mid-Polish Trough, the conception that the opoka facies originated in deep-waters cannot be upheld (compare Remin et al. 2022).

Paleocirculation, contourite currents, and the redistribution of terrigenous material along the inverting Łysogóry–Dobrogea Land

Without doubt, the uplift of the Łysogóry–Dobrogea Land due to Late Cretaceous inversion tectonics markedly rearranged the paleogeographic architecture of the Polish Basin and its surroundings. An obvious consequence of the appearance of a paleogeographic barrier in the axial part of the basin was changes in paleocirculation. Remin et al. (2016) suggested that ocean currents flowing from the north along the inverting Mid-Polish Trough, possibly an emerged landmass by the Coniacian and Santonian, influenced paleotemperatures (based on oxygen isotopes) and the spatial distribution of ammonites within the Polish Basin. Similarly, the distribution of belemnite fauna during the Lower Maastrichtian also suggested the presence of a paleogeographic barrier in the location of the present-day Mid-Polish Anticlinorium (Remin 2018).

Further support for such a paleocirculation model (Fig. 2) is provided by contourites, present due to contourite currents flowing parallel to the strike of the Łysogóry–Dobrogea Land during the Campanian. Indeed, contourites were revealed by Krzywiec et al. (2009, 2018) based on seismic cross-sections perpendicular to the landmass (compare the seismic overview below).

The presence of contourites has fundamental importance for understanding seafloor morphology. Their appearance within basins is usually connected with changes in oceanographic and bathymetric conditions which, in turn, might be caused by enhanced tectonic activity (e.g., inversion) that will regulate the morphology of the seafloor (e.g., Rebesco et al. 2014). The presence of contourites within the Polish Basin (e.g., Krzywiec et al. 2009, 2018) and Danish Basin (e.g., Surlyk and Lykke-Andersen 2007) provides additional confirmation of our proposed paleocirculation model (Fig. 2).

In a wider context, the appearance of contourites during the Campanian indicates the development of a regional seafloor submarine slope (an effect of the inversion of the axial part of the basin) located parallel and to the northeast of the shoreline of the emerging Łysogóry–Dobrogea Land. This, in turn, might have some impact on the redistribution

of (mainly) the finest terrigenous material (e.g., from the Szozdy deltaic system), pushing it towards the southeast (Figs 2, 8). A potential manifestation of the current-driven redistribution of the finest terrigenous material may be pure clay deposits, of approximately the same age, located southeast of the Szozdy delta system – that is, in the Horyniec Zdrój area (Fig. 8).

Inversion-related sedimentation along the northeast edge of the Mid-Polish Swell (Anticlinorium) – an overview based on seismic data

Seismic data across the entire Polish Basin demonstrate that inversion of the epicontinental Permo-Mesozoic basin and formation of the Mid-Polish Swell (Anticlinorium) commenced in the Turonian and lasted until the Maastrichtian–Paleogene (e.g., Krzywiec 2006; Krzywiec et al. 2009, 2018; Krzywiec and Stachowska 2016). The significant role played by reverse faulting, and the associated uplift of deeper basement blocks, had already been postulated by Pożaryski in the mid-20th century (Pożaryski 1948). This paper, published well before modern sedimentary basin inversion concepts had been established, presented a conceptual geological cross-section based on detailed field mapping and shallow cartographic wells that showed a system of reverse (i.e., inversion related) faults dissecting both the Palaeozoic basement and the Mesozoic sedimentary cover (Fig. 9).

The conceptual model proposed by Pożaryski in 1948 has been fully confirmed by mod-

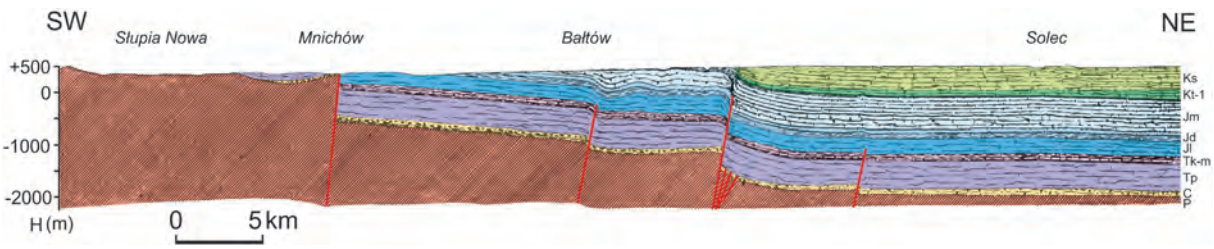

Fig. 9. Geological cross-section across the northeastern boundary of the southeast segment of the Mid-Polish Swell, based only on shallow wells and outcrops (Pożaryski 1948, from Krzywiec et al. 2009). Note reverse fault system, clearly indicating late–post-Cretaceous inversion tectonics in this area; P: Old Paleozoicum, C: Zechstein, Tp: Trias-Bunter, Tk-m: Trias-Keuper and Muschelkalk, Jl: Lower Jurassic, Jd: Middle Jurassic, Jm: Upper Jurassic, Kt-1: Cretaceous–Turonian–Albian, Ks: Cretaceous–Senonian (original explanations of Pożaryski 1948).

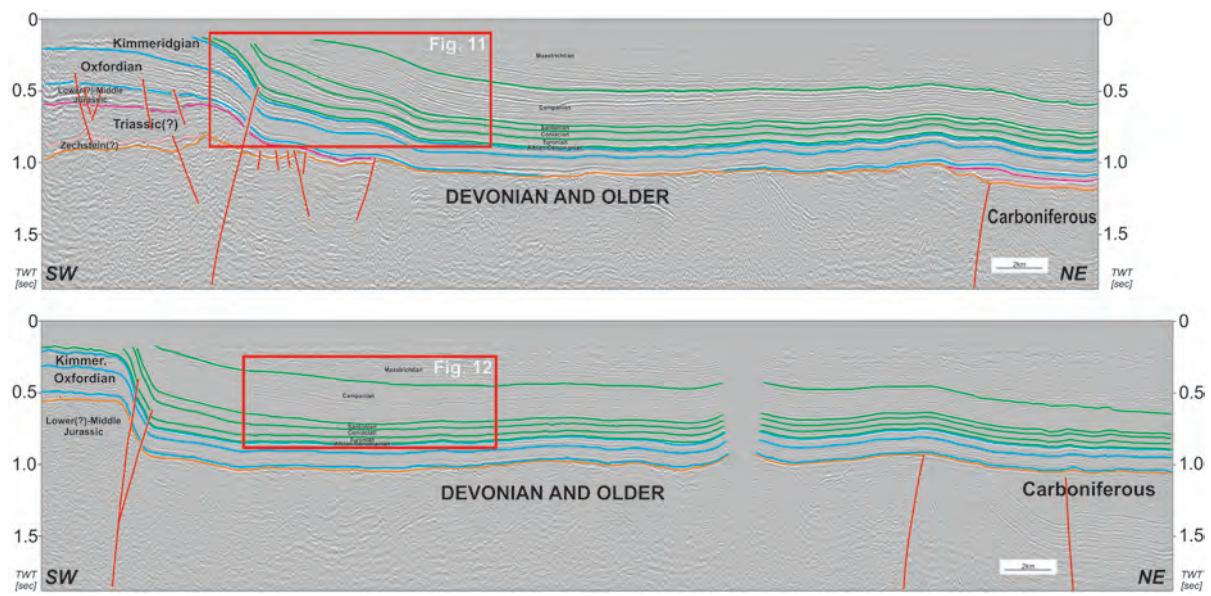

Fig. 10. Interpreted seismic profiles located above the northeast boundary zone of the southeast segment of the Mid-Polish Swell (Mid-Polish Anticlinorium) (Krzywiec et al. 2009); see Fig. 3 for geographic location of the seismic profile.

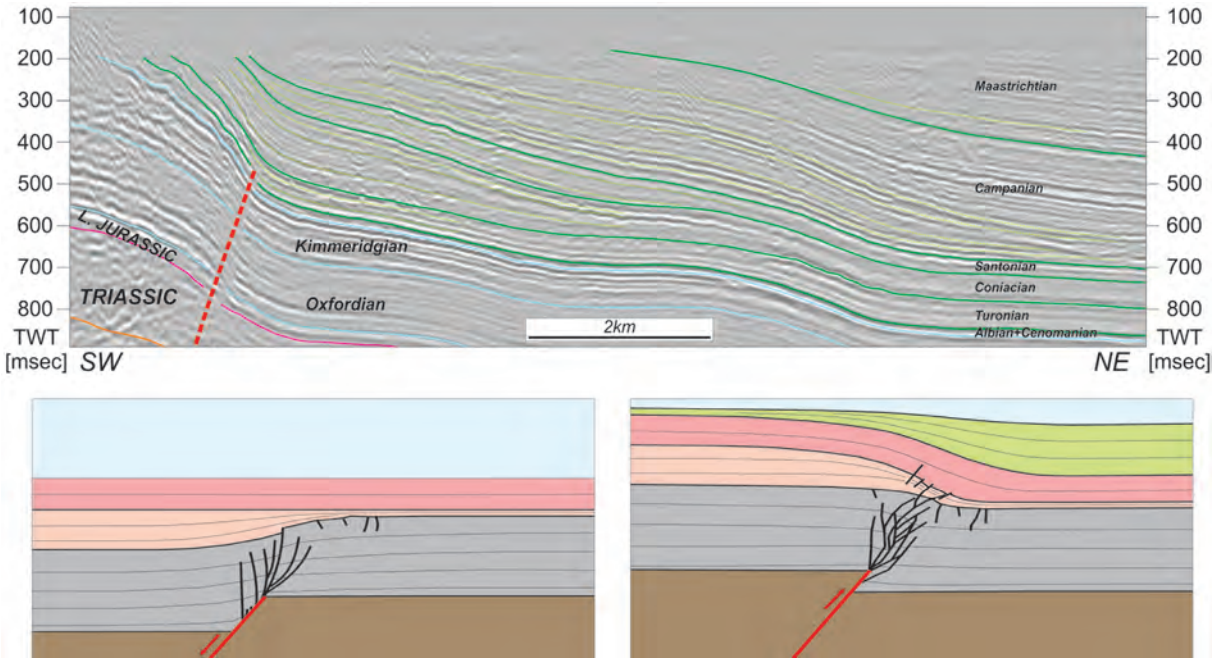

Fig. 11. Upper panel: enlarged part of the upper seismic profile from Fig. 10 showing reductions in thickness within the Turonian(?) – Maastrichtian towards the southwest and northeast, due to the inversion and uplift of the Mid-Polish Swell (Krzywiec et al. 2009); see Fig. 3 for geographic location of the seismic profile. Lower panel: model of transition from basin subsidence to basin inversion; green succession: syn-inversion growth strata (based on Krzywiec et al. 2018).

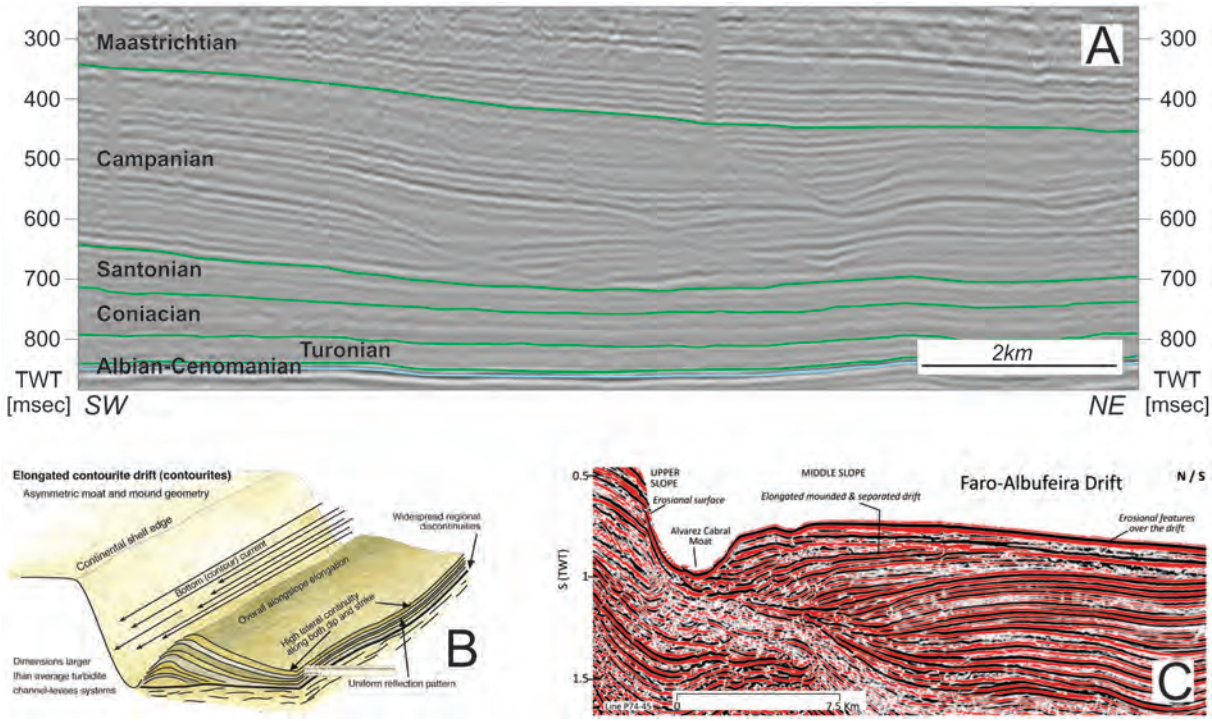

Fig. 12. A) Enlarged part of the lower seismic profile from Fig. 10 showing an Upper Cretaceous (Campanian) contourite drift formed along the uplifted northeastern edge of the southeast segment of the Mid-Polish Swell (Anticlinorium) (Krzywiec et al. 2009); see Fig. 3 for geographic location of the seismic profile. B) Schematic model showing ideal contourite drifts (Rebesco et al. 2014). C) Faro-Albufeira drift, Gulf of Cádiz (Rebesco et al. 2014).

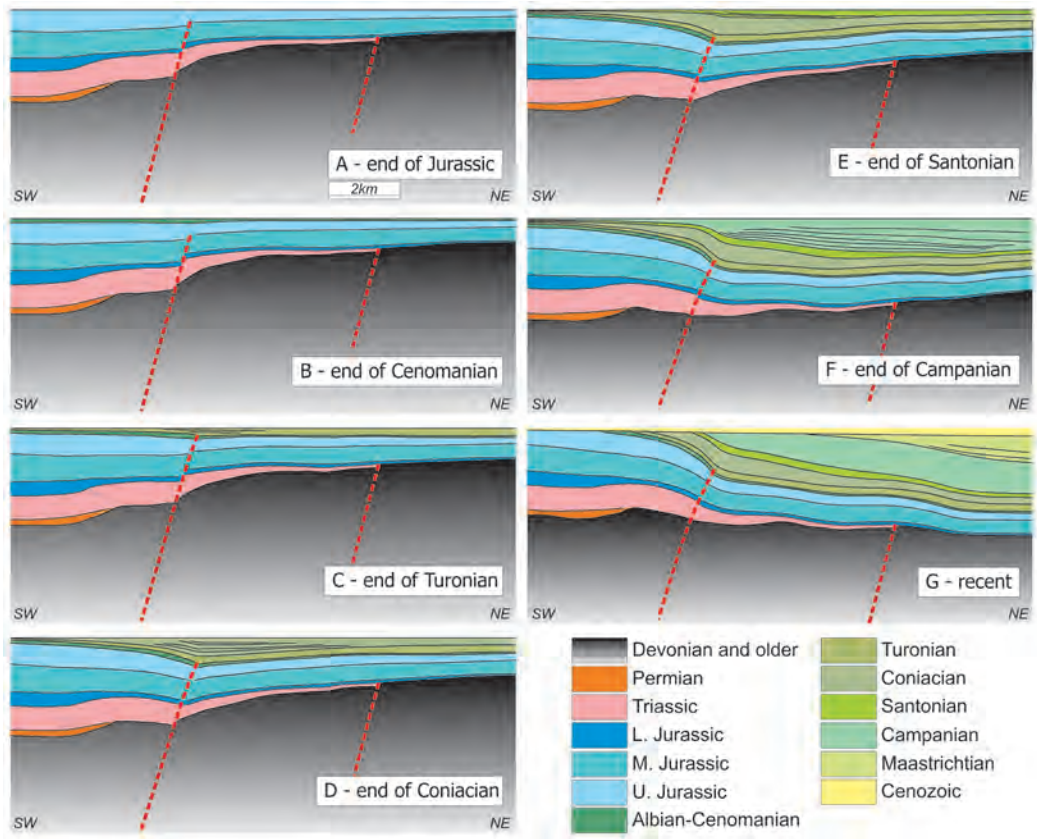

Fig. 13. Model of transition from Jurassic extension and subsidence to Late Cretaceous inversion and uplift along the northeastern edge of the Mid-Polish Swell (Anticlinorium) in southeast Poland based on seismic data (cf. Fig. 11). Vertical scale approximately equals horizontal scale (from Krzywiec et al. 2009).

ern seismic data (Fig. 10; compare also Krzywiec 2002, 2009; Krzywiec et al. 2009). In seismic profiles, pre-Cretaceous to Cenomanian sedimentary cover is characterized by increased thickness towards the southwest, towards the Mid-Polish Swell. This is indicative of a subsidence stage within the axial part of the basin, accompanied by the deposition of thick sedimentary cover above the hanging wall block. However, almost the entire preserved Upper Cretaceous succession is characterized by a different pattern – seismic packages thin both towards the southwest and towards the northeast (Figs 10, 11).

Seismic data also revealed Upper Cretaceous contourites – bottom current deposits (Fig. 12; cf. Rebesco et al. 2014). The formation of contourites during certain stages of sedimentary basin development points to the intensification of bottom currents triggered, potentially, by certain oceanographic, bathymetric, and tectonic conditions. Seismic data from southeastern Poland hints to the formation of a coupled drift-moat contourite deposit succession over a relatively flat seafloor. Their initiation may have been influenced by regional basin inversion tectonics that led to the formation of various morphological highs at the sea bottom – that is, barriers that focused the bottom current flow along localized routes. The presence of contourite deposits in different parts of the basin suggests that strong ocean bottom currents prevailed across the basin, providing independent evidence for paleo-circulation within the Polish Basin during the Late Cretaceous and thus supporting the reconstruction proposed by Remin et al. (2016) and Remin (2018).

Dense seismic coverage along the northeastern edge of the Mid-Polish Swell (Anticlinorium) enabled the construction of a generalized Late Cretaceous depositional model that illustrates progressive inversion-related growth of the Mid-Polish Anticlinorium and related syn-inversion sedimentation (Fig. 13).

FIELD STOPS

Linking surface and seismic data – selected examples

Stop 1: Dziurków

Abandoned quarry on the western bank of the Vistula River, between Lipsko and Solec nad Wisłą [51° 8' 17.86" N; 21° 42' 54.87" E]; Lower Maastrichtian (Figs 3, 14).

An about 12 m thick succession of light yellow brittle opoka (the Dziurków Opoka of Walaszczyk 2004) is exposed in the eastern wall of the quarry (Fig. 14). It is fossiliferous, with common bivalves, gastropods, ammonites, belemnites, and sponges. Brown spots around fossils are characteristic. Biostratigraphic zones based on inoceramids, belemnites, and ammonites are recognized in the succession (Fig. 7). The section is located in the lower *Endocostea typica* inoceramid Zone (Walaszczyk 2004), the *Belemnella obtusa* belemnite Zone (*Bln*. sp. *G* and *Bln*. sp. *F* belemnite Subzones) (Remin 2012, 2015), and yields already *Pachydiscus neubergicus* Hauer (Machalski 2012) (for a review compare Walaszczyk et al. 2016).

Stop 2: Ożarów Quarry

Working cement plant quarry, with readily accessible basal part of the mid-Cretaceous transgressive sequence of the former Mid-Polish Trough, inverted subsequently into the Mid-Polish Anticlinorium. [50° 55' 41.39" N; 21° 39' 46.10" E]; Middle Albian–Middle Turonian (Figs 3, 15, 16).

Ożarów Quarry, located about 3 km north of the town of Ożarów, offers easy access to the Middle Albian through Middle Turonian of the Middle Vistula River succession. The succession captures middle Albian–Cenomanian siliciclastic transgressive sequence, with an incipient hardground at its top. This part of the succession is followed by a carbonate sequence, dated in the quarry as lower – basal middle Turonian (Fig. 16). This carbonate succession serves as the main component of the rest of the Upper Cretaceous in the Middle Vistula Valley region, and in general in the whole of southeastern Poland.

The transgressive sequence is characterized by a series of phosphatic horizons, hardgrounds, and associated stratigraphic gaps, typical for deposition on a swell area. This swell area is referred to as the Vistula Swell, the Mesozoic paleotectonic element running perpendicular to the axis of the Danish–Polish Trough (see Cieśliński 1976).

The section embraces the Albian through Cenomanian transgression and the lower part of the overlying Turonian carbonate succession, overlying Jurassic (Kimmeridgian) limestones (Fig. 16).

The Cretaceous succession starts with

Fig. 14. General view on the southeast wall of the Dziurków quarry, exposing ca. 12 meters of white, yellowish opoka facies.

Fig. 15. General view of the eastern wall of Ożarów quarry, exposing the initial stages of the mid/Late Cretaceous transgression in the Polish Basin; compare also Fig. 16.

glauconitic sands with an indistinct basal conglomerate, composed of large pebbles derived from the underlying Jurassic limestones (Fig. 16). About 2.5 m above the top of the Jurassic, two thin phosphorite horizons (units 3 and 5) occur, followed by a relatively thin glauconitic sandstone series (unit 6) and a thick unit of irregularly bedded siliceous sandstone with extremely sparse macrofauna (unit 7). These are overlain by a 5.6 m thick series of poorly cemented marly sandstone (units 8 and 9), grading upwards into sandy-glauconitic marl and sandy limestone (unit 10) containing relatively common phosphatized and unphosphatized fauna, including stratigraphically important ammonites and belemnites indicative of an early to early middle Cenomanian age. The marls are capped by an incipient hardground horizon (unit 11), with a planar upper surface and weak phosphatization. The overlying limestone with glauconite and numerous inoceramids is late early Turonian in age. The exposed succession continues up into the lower middle Turonian (compare Walaszczyk 1992; Fig. 16).

The Cenomanian–Turonian boundary interval is missing; a stratigraphic gap spanning the upper middle Cenomanian through the lowermost Turonian is associated with the boundary hardground (Fig. 16). The gap is partly due to original omission, and partly due to secondary erosion, as indicated by the presence of late Cenomanian and early Turonian foraminifers within the hardground-associated omission burrows.

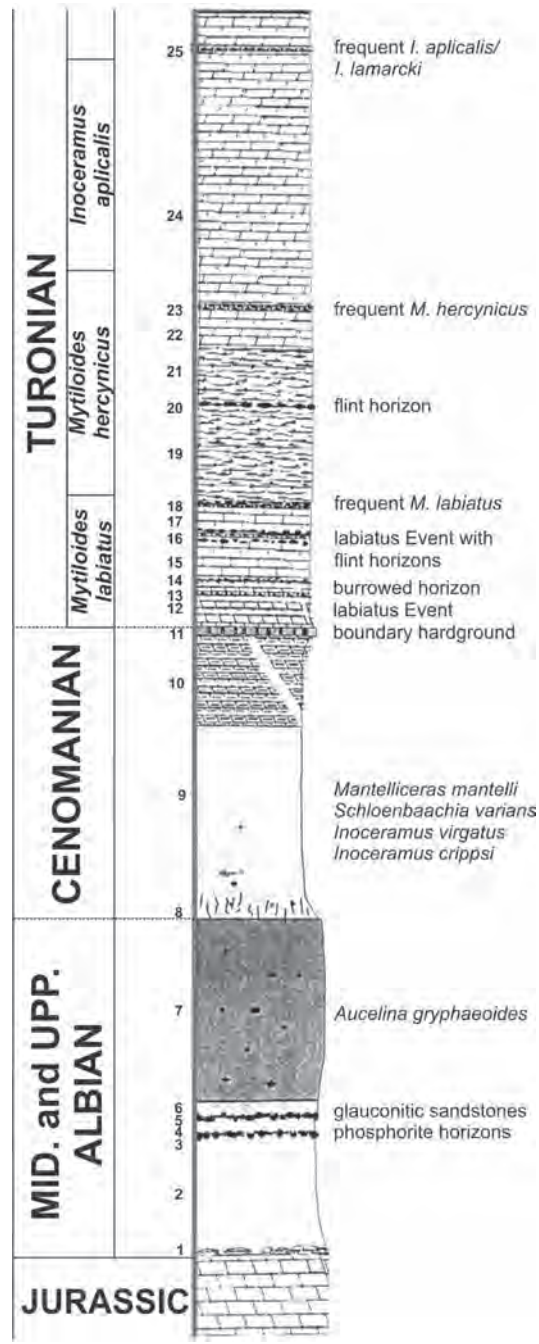

Fig. 16. Lithologic column of the succession exposed in Ożarów quarry (adapted from Walaszczyk 1992), representing the initial stages of the mid/Late Cretaceous transgression. Marker horizons and biostratigraphic zonation of the Middle Albian – Middle Turonian are labelled.

Stop 3: Janików Quarry

A series of small quarries east of Janików, south of Ożarów. [50° 52' 1.35" N; 21° 42' 48.76" E]; basal Upper Turonian (Figs 3, 17).

The Janików Limestone represents one of the early Late Cretaceous shallow-marine, ephemeral facies (Łuniewski 1923; Walaszczyk 1992; Walaszczyk and Remin 2015) more-or-less developed in the axial part of the Polish Basin (i.e., within the former Mid-Polish Trough), and now located in the northeast part of the Middle Polish Anticlinorium.

The Janików Limestone is represented by thick-bedded (0.5–2 m) calcarenites composed of calcareous grains, represented mostly by badly preserved bryozoan and crinoid fragments (approximately 40%). The entire sequence represents an upward-coarsening succession dominated by bryozoan detritus at

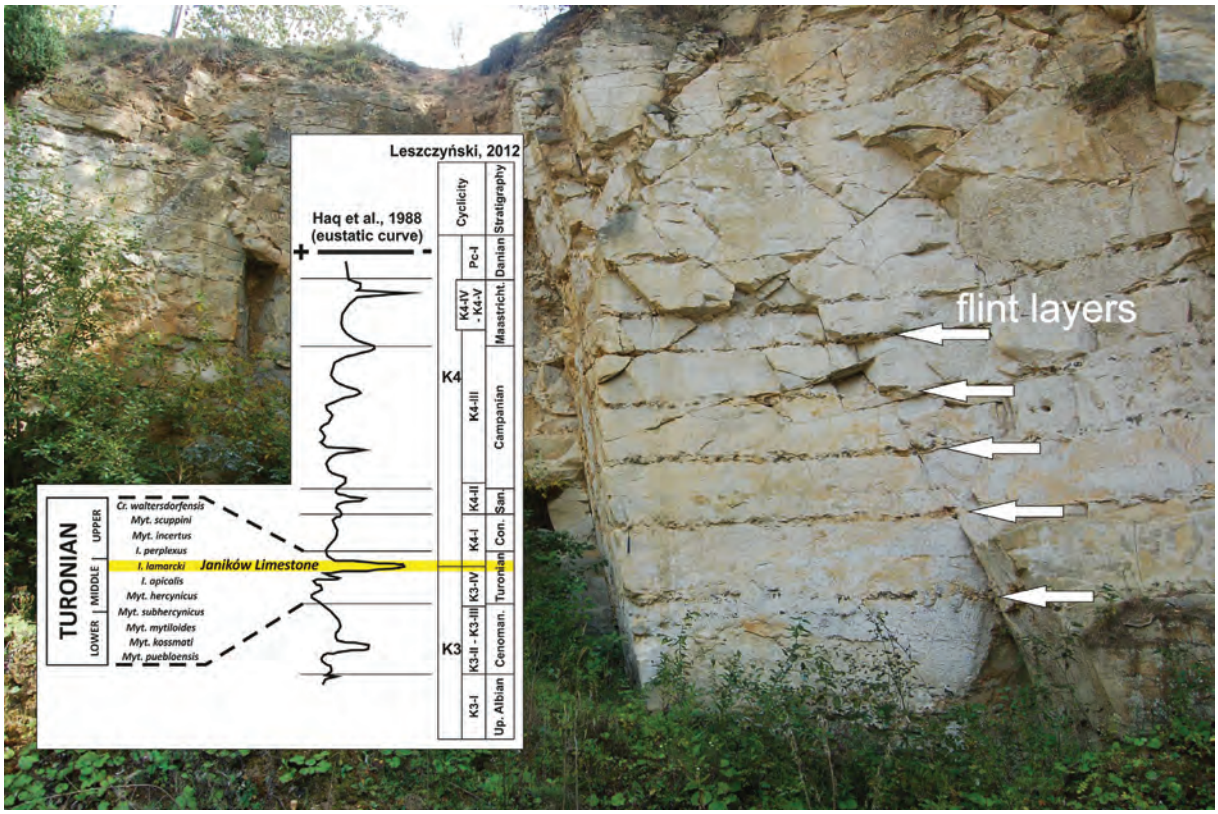

Fig. 17. General view of a quarry which expose the Janików Limestone; successive beds (approximately 0.5-0.7 m) are underlined by flint layers, as easily visible in the central part of the photo. The yellow line indicates the age of the Janików Limestone, which aligns well with a global eustatic lowstand (Haq et al., 1988); link between the eustatic curve of Haq et al. (1988), stratigraphy and recognized cyclicity after Leszczyński (2012).

the base, transitioning to crinoid-dominated detritus at the top of the available succession (Walaszczyk 1992). Bedding planes are underlined by numerous flint horizons (Fig. 17). Macrofossils are extremely rare.

Initially, the Janików Limestone was interpreted as a record of a fossil bryozoan reef (Pożaryski 1948, 1956). However, a detrital nature had already been suggested earlier by Łuniewski (1923). More recently, the unit has been regarded as deposits originating from the destruction of a bryozoan reef (review in Cieśliński 1976; and in Walaszczyk and Remin 2015).

The stratigraphic position of the Janików Limestone is based on foraminifera, extremely rare inoceramids, and well-dated opokas interfingering with the Janków Limestone towards the northeast; the Janków Limestone spans the topmost middle and the lower upper Turonian (Alexandrowicz 1978; Walaszczyk 1992; see also Walaszczyk and Remin 2015). Microfacies analysis indicates the Janików Limestone was deposited between normal and storm wave base, which is confirmed, for instance, by large-scale cross-bedding (unpublished data). The original bryozoan reef structure was located south of Janików, as confirmed by measurements of transport direction (unpublished data).

Stop 4: Szozdy section

Railroad cut of the Broad Gauge Metallurgical Railway Line near Szozdy, 4 km southwest of Zwierzyniec. [50° 34' 45.22" N; 22° 54' 56.25" E]; middle Campanian (Figs 3, 18, 19).

The most prominent feature of the Szozdy section is the presence of tripartite cyclothems. Individual cyclothems consist of three units:

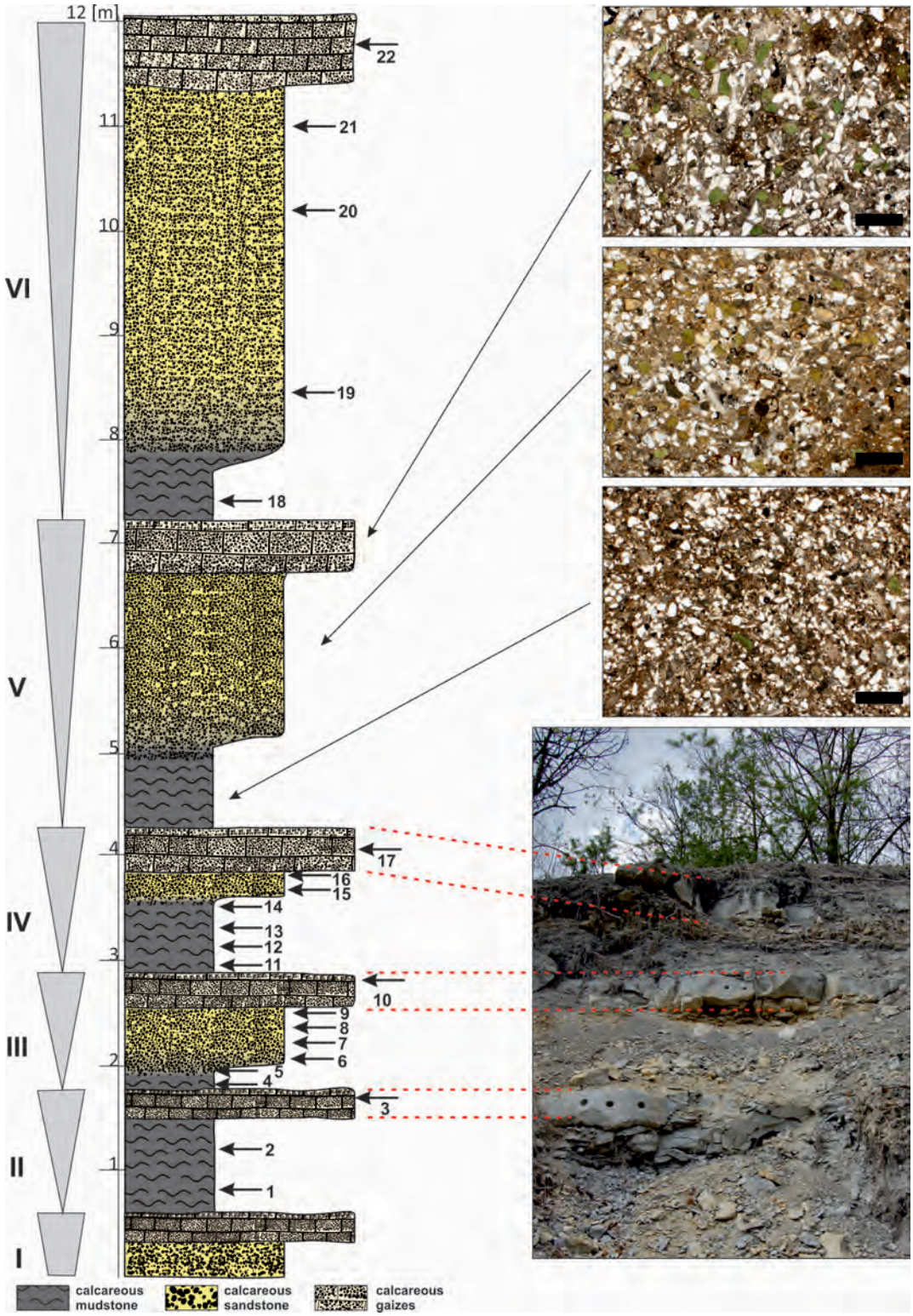

Fig. 18. Lithological column of the Szozdy section. Triangles on the left side of the column indicate coarsening-upward cyclothems. Top right: typical thin sections from successive lithofacies of a single cyclothem; scale bar = 500 µm; most of the white particles represent quartz grains. Bottom right: field photo of a part of the secession with prominent calcareous gaize layers, indicated on the section by red dashed lines. The horizontal scale represents relative resistance to weathering of particular units; adapted from Remin et al. (2022).

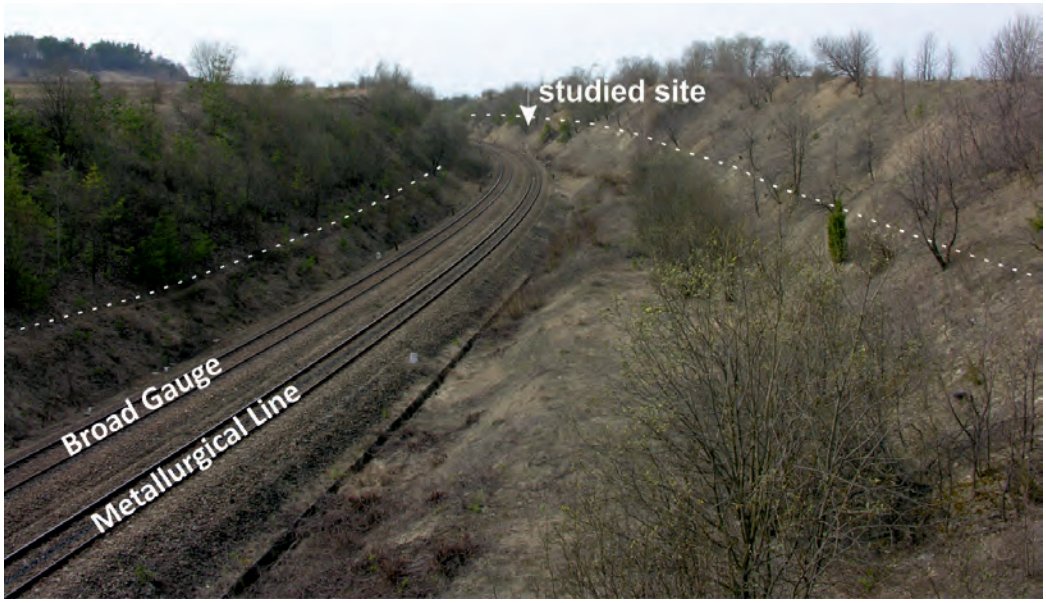

Fig. 19. General view of the Szozdy section – the exposures (white dashed lines) extend along both sides of the railroad cut over approximately 800 m showing tripartite cyclothems (compare Fig. 18).

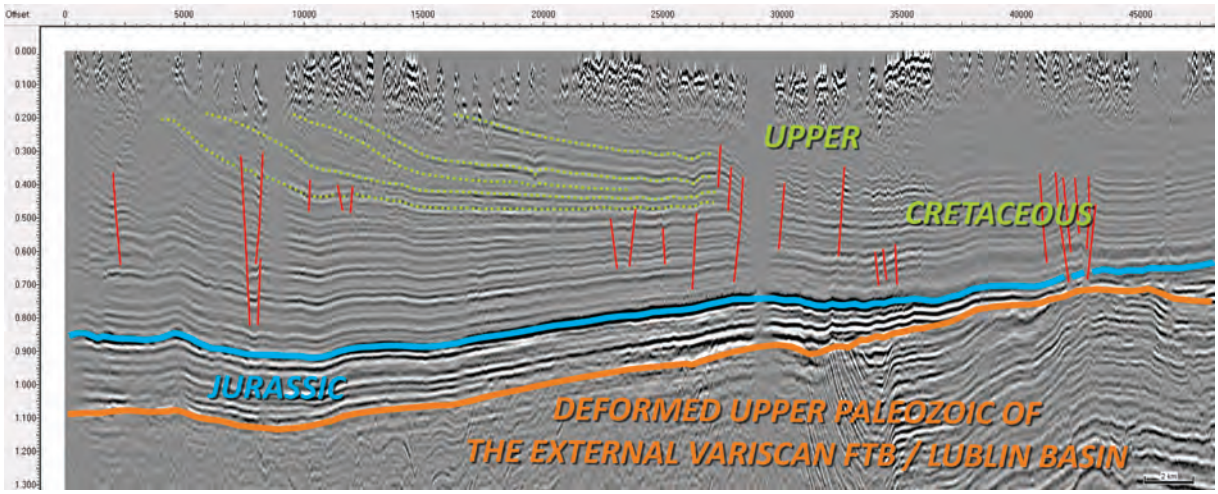

Fig. 20. Seismic profile located near Szozdy stop that shows syn-inversion Upper Cretaceous succession (dotted green lines) (cf. Krzywiec et al. 2018). Vertical scale in seconds TWT; see Fig. 3 for geographic location of the seismic profile.

from bottom to top, calcareous mudstone, calcareous sandstone, and calcareous gaize (Fig. 18). The cyclothems are sometimes incomplete, lacking, for instance, the calcareous sandstone unit (Fig. 18; compare Remin et al. 2022).

The total thickness of the Szozdy delta system cannot be estimated – neither the lower nor upper limit of this succession is known. The sole exposure of this special facies is available in the railroad cut near the village of Szozdy, giving access to c. 30–35 m of the cyclic succession (Fig. 19). It is available over a distance of nearly 800 m. There are no other exposures in close proximity to the railroad cut. Nearby well-log data from are also absent, precluding any firm conclusions. A 12-meter-thick interval consisting of six cycles, including both complete and incomplete ones, is shown in Fig. 18.

The studied interval has yielded a rich fossil assemblage, comprising ammonites, belemnites, inoceramid and non-inoceramid bivalves, echinoids, diverse gastropods, and

a suite of microfossils (Remin et al. 2015a, b; Remin et al. 2022) in addition to partially carbonized plant debris such as leaves or boughs.

This fossil assemblage defines a middle Campanian age for the Szozdy section (Fig. 7; Remin et al. 2015a, 2018, 2022). In general, the surface outcrops in the Roztocze Hills may be easily correlated with the Middle Vistula River Valley composite section (Fig. 7), which constitutes a reference section for the Upper Cretaceous of extra-Carpathian Poland (e.g., Walaszczyk 2004; Walaszczyk et al. 2016 and references therein).

A seismic profile located slightly northwest from the Szozdy stop imaged Upper Cretaceous succession deposited during the inversion of this segment of the Polish Basin and the gradual uplift of the Mid-Polish Swell (Anticlinorium); it is characterized by an overall progradational pattern from the southwest towards the northeast (Fig. 20).

Stop 5: Bliżów

Small quarry in the village of Bliżów, Roztocze, southeast Poland. [50° 36' 5.96" N; 23° 7' 38.36" E]; Lower Maastrichtian (Figs 3, 21).

The section (Fig. 21) is situated within the border zone of the structurally elevated Mid-Polish Anticlinorium and the southeastern part of the Kościerzyna–Puławy Synclinorium (Fig. 3). An about 16 m thick succession of light yellow brittle opoka is exposed in the northern wall of the quarry. It is fossiliferous, with common bivalves, gastropods, ammonites, belemnites, and sponges in addition to plant

Fig. 21. Section at Bliżów, Roztocze Region, southeastern Poland.

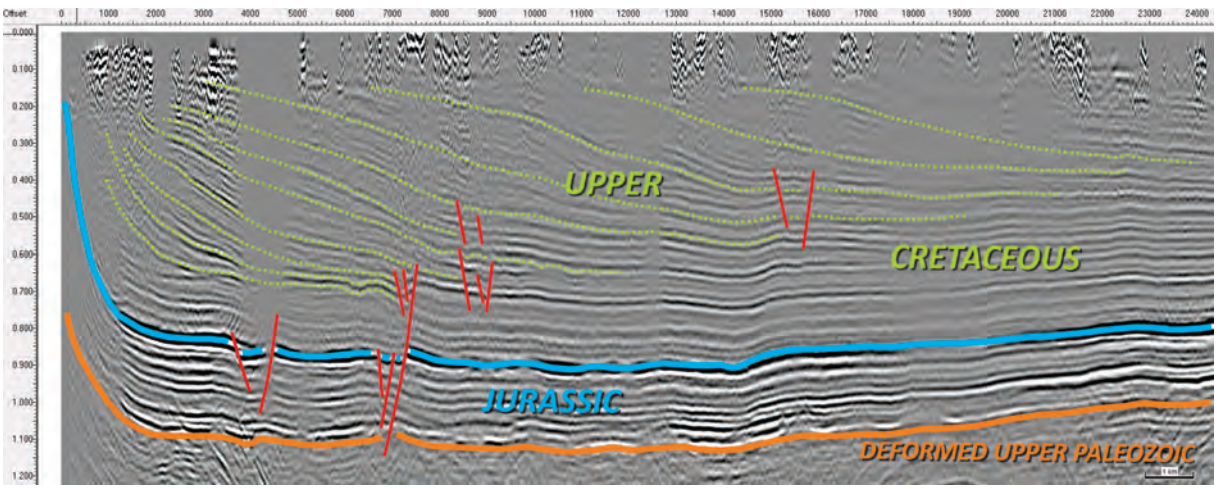

Fig. 22. Seismic profile located near the Bliżow stop that shows the syn-inversional Upper Cretaceous succession (dotted green lines). Vertical scale in seconds TWT; see Fig. 3 for geographic location of the seismic profile.

debris. Several biostratigraphic zones based on inoceramids, belemnites, and ammonites have been recognized in the succession. The section is located in the *Endocostea typica* inoceramid Zone of Walaszczyk (2004), and the *Belemnella obtusa* belemnite Zone (Remin 2012, 2015, 2018) (for a review, compare Walaszczyk et al. 2016).

A seismic profile located in the immediate vicinity of the Bliżów stop provided excellent images of syn-inversion Upper Cretaceous growth strata characterized by an overall progradational pattern from the southwest to the northeast: that is, from the inversion axis (the gradually rising Mid-Polish Swell) towards the flank of the basin (Fig. 22). Within this syn-kinematic succession, the clear migration of the progradational pattern upsection towards the northeast is visible, which conforms very well with progressive uplift of the Mid-Polish Swell during the Late Cretaceous.

Stop 6: Chełm

Huge working quarry of the Chełm Cement Plant in Chełm, northeast of the Roztocze region, southeast Poland. [51° 8' 13.35" N; 23° 30' 47.65" E]; basal Upper Maastrichtian (Figs 3, 7, 23).

The Chełm quarry provides access to lower Upper Maastrichtian pure white to grey chalk facies, very similar to that exposed in Mielnik (next stop); see the description of the Mielnik stop.

Stop 7: Mielnik quarry

Working quarry in Mielnik, eastern Poland. [52° 19' 51.77" N; 23° 3' 11.66" E]; upper Lower Campanian–Lower Maastrichtian (Figs 3, 24, 25).

The Mielnik section is located in the southeast part of the Mazury–Podlasie Homocline of eastern Poland (for structural details, see Żelaźniewicz et al. 2011). In this area, the entire thickness of the Cretaceous is approximately 200 m (Cieśliński and Jaskowiak 1973), covering an interval spanning the Albian to the Lower Maastrichtian. The available succession is exposed in a working quarry in Mielnik, comprising c. 30 m (Figs 24, 25) of Campanian and Maastrichtian white chalk (see also Olszewska 1990; Olszewska-Nejbert and Świerczewska-Gładysz 2011; Jurkowska et al. 2015; Dubicka 2015).

Fig. 23. Satellite image of the Chełm Quarry in the town of Chełm; according to Google Maps.

Fig. 24. General view of the Mielnik Quarry, exposing c. 30 m of chalk facies.

The Campanian part of the succession is terminated by a hardground (Figs 24, 25). The associated stratigraphic gap comprises part of the upper Campanian and lower Maastrichtian. The deposits below the hardground are intensely bioturbated; the burrows are filled with glauconitic chalk, which is distinctly visible in the field.

Biostratigraphically, the succession exposed in Mielnik represents the upper part of the Lower Campanian (belemnite species *Goniotheutis gracilis* and *Belemnellocamax mammillatus*), the upper Campanian (*Belemniella mucronata*), and the Lower Maastrichtian, as traditionally defined by the entrance of the genus *Belemnella* (e.g., Olszewska 1990).

The horizontal, tectonically undisturbed position of the succession is underlined by two well-developed flint horizons below the Campanian/Maastrichtian hardground. The layer-cake geometry of the entire Upper Cretaceous succession is clearly visible on

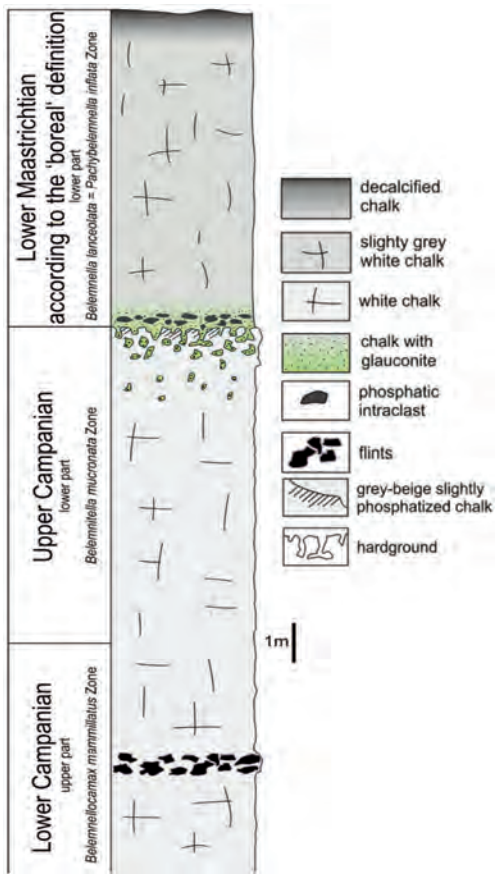

Fig. 25 Lithologic column, stratigraphy and sedimentary phenomena in the section exposed in the Mielnik quarry (adapted from Olszewska-Nejbert and Świerczewska Gładysz 2011).

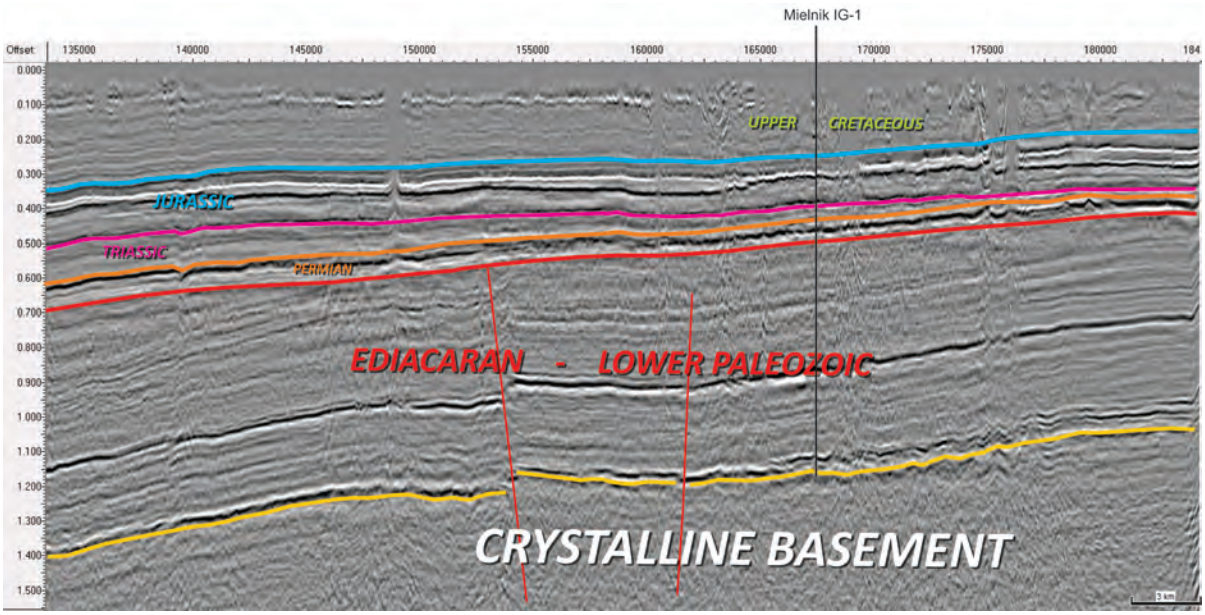

Fig. 26. Seismic profile located near the Mielnik outcrop, demonstrating the layer-cake Upper Cretaceous succession deposited above the cratonic edge. Vertical scale in seconds TWT.

seismic data acquired in the immediate vicinity of Mielnik (Fig. 26).

ACKNOWLEDGEMENTS

This research has been supported by the Polish National Science Centre [Narodowe Centrum Nauki, Polska], grant number – UMO-2018/29/B/ST10/02947; "*Late Cretaceous tectonic evolution of the SE part of the Danish-Polish Trough; revision of the facial architecture and implication for the paleo- and paleobiogeography of Europe*".

REFERENCES

Alexandrowicz, S.W. 1978. Foraminifera from the Janikow Limestones (The Turonian of central Poland). Bulletin de l'Académie Polonaise des Sciences. Série des Sciences de la Terre, 26, 5–14.

Błaszkiewicz, A. 1980. Campanian and Maastrichtian ammonites of the Middle Vistula River valley, Poland: a stratigraphic and paleontological study. Prace Instytutu Geologicznego, 92, 1–63.

Buła, Z. and Habryn, R. 2011. Precambrian and Palaeozoic basement of the Carpathian Foredeep and the adjacent Outer Carpathians (SE Poland and western Ukraine). Annales Societatis Geologorum Poloniae, 81, 221–239.

Buła, Z., Byś, I., Florek, R., Habryn, R., Jachowicz, M., Kwarciński, J., Laskowicz, R., Liszka, B., Madej, K., Maksym, A., Markowiak, M., Pietrusiak, M., Probulski, J., Ryłko, W., Salwa, S., Sikora, R., Staryszak, G., Tabol-Wójcik, P., Tomaś, A. and Zacharski, J. 2008. Geological-structural atlas of the Palaeozoic basement of the Outer Carpathians and Carpathian Foredeep. Polish Ministry of Environment, Warszawa, 104, 775–796.

Cieśliński, S. 1976. Rozwój bruzdy duńsko-polskiej na obszarze świętokrzyskim w albie, cenomanie i turonie dolnym. Biuletyn Instytutu Geologicznego, 295, 249–271.

Cieśliński, S. and Jaskowiak, M. 1973. Kreda. In: Sokołowski S. (Ed.), Budowa Geologiczna Polski. T. 1. Stratygrafia. Część 2, 603–615. Wydawnictwo Geologiczne; Warszawa.

Cyglicki, M. and Remin, Z. 2017. Provenance of heavy minerals in the middle Campanian (Cretaceous) siliciclastic deposits of the Roztocze Hills, SE Poland. In: Żylińska, A. (Ed.), 10th Baltic Stratigraphic Conference, Chęciny, 12–14 September 2017, Abstracts & Field Guide, 28–29. Faculty of Geology, University of Warsaw; Warsaw.

Cyglicki, M. and Remin, Z. 2018. HRHMA (high-resolution heavy mineral analysis) zastosowana dla górnokampańskich skał silikoklastycznych krawędziowej części Roztocza Środkowego, SE Polska. In: Kędzierski, M. and Gradziński, M. (Eds), Polska Konferencja Sedymentologiczna POKOS 7, Góra Św. Anny, 4–7 June 2018, Abstracts & Field Guide, 67. Polskie Towarzystwo Geologiczne; Kraków.

Dadlez, R., Narkiewicz, M., Stephenson, R.A. Visser, M.T.M. and van Wess, J.D. 1995. Tectonic evolution of the Mid-Polish Trough: modelling implications and significance for central European geology. Tectonophysics, 252, 179–195.

Dadlez, R., Marek, S. and Pokorski, J. (Eds) 1998. Palaeogeographical Atlas of the Epicontinental Permian and Mesozoic in Poland. Polish Geological Institute; Warszawa. [In Polish with English summary]

Dadlez, R., Marek, S. and Pokorski, J. (Eds) 2000. Geological map of Poland without Cenozoic deposits at 1:1 000 000 scale. Polish Geological Institute; Warszawa.

Dubicka, Z. 2015. Benthic foraminiferal biostratigraphy of the lower and middle Campanian of the Polish Lowlands and its application for interregional correlation. Cretaceous Research, 56, 491–503.

Dubicka, Z. Peryt, D. and Szuszkiewicz, M. 2014. Foraminiferal evidence for paleogeographic and paleoenvironmental changes across the Coniacian–Santonian boundary in western Ukraine. Palaeogeography, Palaeoclimatology, Palaeoecology, 401, 43–56.

Dziadzio, P. and Jachowicz, M. 1996. Budowa podłoża utworów mioceńskich na SW od wyniesienia Lubaczowa. Przegląd Geologiczny, 44, 1124–1130.

Dziadzio, P., Maksym, A. and Olszewska, B. 2006. Miocene deposition in the eastern part of the Carpathian Foredeep in Poland. Przegląd Geologiczny, 54, 413–420. [In Polish with English summary]

von Eynatten, H., Voigt, T., Meier, A., Franzke, H.-J. and Gaupp, R. 2008. Provenance of the clastic Cretaceous Subhercynian Basin fill: constraints to exhumation of the Harz Mountains and the timing of inversion tectonics in the Central European Basin. International Journal of Earth Sciences, 97, 1315–1330.

Hakenberg, M. and Świdrowska, J. 1998. Evolution of the Holy Cross segment of the Mid-Polish Trough during the Cretaceous. Geological Quarterly, 42, 239–262.

Hakenberg, M. and Świdrowska, J. 2001. Cretaceous basin evolution in the Lublin area along the Teisseyre–Tornquist Zone (SE Poland). Annales Societatis Geologorum Poloniae, 71, 1–20.

Halamski, A.T. 2013. Latest Cretaceous leaf floras from Southern Poland and Western Ukraine. Acta Palaeontologica Polonica, 58, 407–433.

Haq, B.U., Hardenbol, J. and Vail, P.R. 1988. Mesozoic and Cenozoic chronostratigraphy and cycles of sea-level change. In: Wilgus, C.K., Kendall, C.G.St.C., Posamentier, H.W., Ross, C.A. and Van Wagoner, J.C. (Eds), Sea Level Changes – An Integrated Approach: Tulsa, Society of Economic Paleontologists and Mineralogists Special Publication 42, 71–108.

Jaskowiak-Schoeneichowa, M. and Krassowska, A. 1988. Paleomiąższości, litofacje i paleotektonika epikontynentalnej kredy górnej w Polsce. Geological Quarterly, 32, 177–198.

Jurkowska, A., Świerczewska-Gładysz, E., Dubicka, Z. and Olszewska-Nejbert, D. 2015. *Porosphaera globularis* (Phillips, 1829) (Porifera, Calcarea) in the Campanian (Upper Cretaceous) of extra-Carpathian Poland. Acta Geologica Polonica, 65, 121–139.

Jurkowska, A. and Barski, M. 2017. Maastrichtian island in the Central European Basin – new data inferred from palynofacies analysis and inoceramid stratigraphy. Facies, 63, 1–20.

Jurkowska, A., Barski, M. and Worobiec, E. 2019a. The relation of a coastal environment to early diagenetic clinoptilolite (zeolite) formation – New data from the Late Cretaceous European Basin. Palaeogeography, Palaeoclimatology, Palaeoecology, 524, 166–182.

Jurkowska, A., Świerczewska-Gładysz, E., Bąk, M. and Kowalik, S. 2019b. The role of biogenic silica in the formation of Upper Cretaceous pelagic carbonates and its palaeoecological implications. Cretaceous Research, 93, 170–187.

Kamieński, M. 1925. Przyczynek do znajomości kredy żurawieńskiej. Contribution a'la connaissance du facies Sablonneux des cauches cre'tace'es de Żurawno (Pologne). Kosmos, 50, 1408–1425.

Keutgen, N., Walaszczyk, I. and Remin, Z. 2012. Early representatives of the belemnite genus *Belemnella* (Cephalopoda) from the uppermost Campanian–Lower Maastrichtian of the Middle Vistula River section, central Poland. Acta Geologica Polonica, 62, 535–559.

Kiersnowski, H., Paul, J., Peryt, T.M. and Smith, D.B. 1995. Facies, paleogeography, and sedimentary history of the Southern Permian Basin in Europe. In: Scholle, P., Peryt, T.M. and Ulmer-Scholle, D. (Eds), The Permian of Northern Pangea. Volume 2: Sedimentary Basins and Economic Resources, 119–136. Springer; Berlin.

Kley, J. and Voigt, T. 2008. Late Cretaceous intraplate thrusting in Central Europe: Effect of Africa–Iberia–Europe convergence, not Alpine collision. Geology, 36, 839–842.

Kowalska, S., Kranc, A., Maksym, A. and Śmist, P. 2000. Geology of the north-eastern part of the Carpathian Foredeep basement, the Lubaczów–Biszcza Region. Nafta-Gaz, 54, 158–178. [In Polish]

Krzywiec, P. 1999. Miocene tectonic evolution of the Eastern Carpathian Foredeep Basin (Przemyśl–Lubaczów) in light of seismic data interpretation. Prace Państwowego Instytutu Geologicznego, 168, 249–276. [In Polish]

Krzywiec, P. 2000. On mechanism of the Mid-Polish Trough inversion. Biuletyn Państwowego Instytutu Geologicznego, 393, 135–166. [In Polish with English summary]

Krzywiec, P. 2002. Mid-Polish Trough inversion – Seismic examples, main mechanisms and its relationship to the Alpine–Carpathian collision. In: Bertotti, G., Schulmann, K. and Cloetingh, S. (Eds), Continental

Collision and the Tectonosedimentary Evolution of Forelands. European Geosciences Union, Stephan Mueller Special Publication Series, 1, 151–165.

Krzywiec, P. 2006. Structural inversion of the Pomeranian and Kuiavian segments of the Mid-Polish Trough–lateral variations in timing and structural style. Geological Quarterly, 50, 151–168.

Krzywiec, P. 2009. Devonian–Cretaceous repeated subsidence and uplift along the Teisseyre–Tornquist zone in SE Poland – Insight from seismic data interpretation. Tectonophysics, 475, 142–159.

Krzywiec, P. and Stachowska, A. 2016. Late Cretaceous inversion of the NW segment of the Mid-Polish Trough – how marginal troughs were formed, and does it matter at all? Zeitschrift der Deutschen Gesellschaft für Geowissenschaften, 167, 107–119.

Krzywiec, P., Gutkowski, J., Walaszczyk, I., Wróbel, G. and Wybraniec, S. 2009. Tectonostratigraphic model of the Late Cretaceous-inversion along the Nowe Miasto–Zawichost fault zone, SE Mid-Polish Trough. Geological Quarterly, 53, 27–48.

Krzywiec, P., Peryt, T.M., Kiersnowski, H., Pomianowski, P., Czapowski, G. and Kwolek, K. 2017. Permo-Triassic evaporites of the Polish Basin and their bearing on the tectonic evolution and hydrocarbon system, an overview. In: Soto, J.I., Flinch, J.F. and Tari, G. (Eds), Permo-Triassic Salt Provinces of Europe, North Africa and the Central Atlantic: Tectonics and Hydrocarbon Potential, 243–261. Elsevier; Amsterdam.

Krzywiec P., Stachowska A. and Stypa A. 2018. The only way is up – on Mesozoic uplifts and basin inversion events in SE Poland. In: Kilhams, B., Kukla, P.A., Mazur, S., McKie, T., Mijnlieff, H.F. and van Ojik, K. (Eds), Mesozoic Resource Potential in the Southern Permian Basin. Geological Society, London, Special Publications, 469, 33–57.

Kutek, J. and Głazek, J. 1972. The Holy Cross area, Central Poland, in the Alpine cycle. Acta Geologica Polonica, 22, 603–652.

Leszczyński, K. 1997. The Upper Cretaceous carbonate-dominated sequences of the Polish Lowlands. Geological Quarterly, 41, 521–532.

Leszczyński, K. 2010. Lithofacies evolution of the Late Cretaceous basin in the Polish Lowlands, Biuletyn Państwowego Instytutu Geologicznego, 443, 33–54. [In Polish with English summary]

Leszczyński, K. 2012. The internal geometry and lithofacies pattern of the Upper Cretaceous–Danian sequence in the Polish Lowlands. Geological Quarterly, 56, 363–386.

Leszczyński, K. and Dadlez, R. 1999. Subsidence and the problem of incipient inversion in the Mid-Polish Trough based on thickness maps and Cretaceous lithofacies analysis – discussion. Przegląd Geologiczny, 47, 625–628. [In Polish with English summary]

Łuniewski, A. 1923. Z geologii okolic Zawichosta. Sprawozdania z Polskiego Instytutu Geologicznego, 2, 49–72.

Łuszczak, K., Wyglądała, M., Śmigielski, M., Waliczek, M., Matyja, B.A., Konon, A. and Ludwiniak, M. 2020. How to deal with missing overburden – Investigating exhumation of the fragment of the Mid-Polish Anticlinorium by a multi-proxy approach. Marine and Petroleum Geology, 114, 104–229.

Machalski, M. 2012. Stratigraphically important ammonites from the Campanian–Maastrichtian boundary interval of the Middle Vistula River section, central Poland. Acta Geologica Polonica, 62, 91–116.

Machalski, M. and Malchyk, O. 2019. Relative bathymetric position of the opoka and chalk in the Late Cretaceous European Basin. Cretaceous Research, 102, 30–36.

Marcinowski, R. and Radwański, A. 1983. The mid-Cretaceous transgression onto the Central Polish Uplands (marginal part of the Central European Basin). Zitteliana, 10, 65–96.

Narkiewicz, M. and Petecki, Z. 2017. Basement structure of the Paleozoic Platform in Poland. Geological Quarterly, 61, 502–520.

Narkiewicz, M., Maksym, A., Malinowski, M., Grad, M., Guterch, A., Petecki, Z., Probulski, J., Janik, T., Majdański, M., Środa, P. Czuba, W., Gaczyński, E. and Jankowski, L. 2015. Transcurrent nature of the Teisseyre–Tornquist Zone in Central Europe: results of the POLCRUST-01 deep reflection seismic profile. International Journal of Earth Sciences, 104, 775–796.

Niechwedowicz, M., Cyglicki, M. and Remin, Z. 2016. Zmiany zespołów cyst dinoflagellata z osadów deltowych środkowego kampanu Roztocza, SE Polska – implikacje środowiskowe. In: Wojewoda, J. (Ed.), III Polski Kongres Geologiczny, Wrocław, 14–19 September 2016, Abstracts, 267–268. Wrocław.

Niechwedowicz, M., Walaszczyk, I. and Barski, M. 2021. Phytoplankton response to palaeoenvironmental changes across the Campanian–Maastrichtian (Upper Cretaceous) boundary interval of the Middle Vistula River section, central Poland. Palaeogeography, Palaeoclimatology, Palaeoecology, 577, 110558.

Nielsen, S.B. and Hansen, D.L. 2000. Physical explanation of the formation and evolution of inversion zones and marginal troughs. Geology, 28, 875–878.

Nowak, J. 1907. Przyczynek do znajomości kredy Lwowsko-Rawskiego Roztocza. Kosmos, 32, 160–169.

Nowak, J. 1908. Spostrzeżenia w sprawie wieku kredy zachodniego Podola. Kosmos, 33, 279–285.

Olszewska, D. 1990. Belemnites from the Upper Cretaceous chalk of Mielnik (eastern Poland). Acta Geologica Polonica, 40, 111–110.

Olszewska-Nejbert, D. and Świerczewska-Gładysz, E. 2011. Campanian (Late Cretaceous) hexactinellid sponges from the white chalk of Mielnik (Eastern Poland). Acta Geologica Polonica, 61, 383–417.

Pasternak, S.I. 1959. Biostratygrafiya kreydovykh vid-

kladiv Volyno-Podilskoi plyty, 3–98. Akademia Nauk Ukrainskoi RSR; Kiev.

Pasternak, S.I., Gavrylyshyn, V.I., Ginda, V.A., Kotsyubinsky, S.P. and Senkovskyi, Y.M. 1968. Stratygrafia i fauna kredowych vidkladiv zachodu Ukrainy, 1–272. Naukova Dumka; Kiev.

Pasternak, S.I., Senkovskyi, Y.M. and Gavrylyshyn, V.I. 1987. Volyno-Podillya u kreydovomu periodi, 3–258. Naukova Dumka; Kiev.

Pharaoh, T.C., Dusar, M., Geluk, M., Kockel, F., Krawczyk, C.M., Krzywiec, P., Scheck-Wenderoth, M., Thybo, H., Vejbaek, O. and Van Wees, J.D. 2010. Tectonic evolution. In: Doornenbal, J.C. and Stevenson, A.A. (Eds), Petroleum geological atlas of the Southern Permian Basin area, 25–57. European Association of Geoscientists and Engineers (EAGE); Houten, The Netherlands.

Pożaryski, W. 1938. Stratygrafia senonu w przełomie Wisły między Rachowem i Puławami. Biuletyn Państwowego Instytutu Geologicznego, 6, 1–94.

Pożaryski, W. 1948. Jurassic and Cretaceous between Radom, Zawichost and Kraśnik (Central Poland). Biuletyn Państwowego Instytutu Geologicznego, 46, 1–141. [In Polish with English summary]

Pożaryski, W. 1956. Kreda. In: Książkiewicz, M. and Dżułyński, S. (Eds), Regionalna geologia Polski, T. 2, 14–62. Polskie Towarzystwo Geologiczne, Państwowe Wydawnictwo Naukowe; Kraków.

Pożaryski, W. 1960. Zarys stratygrafii i paleogeografii na Niżu Polskim. Prace Instytutu Geologicznego, 30, 377–418.

Pożaryski, W. 1962. Atlas geologiczny Polski. Zagadnienia stratygraficzno-facjalne, z. 10 – Kreda. Instytut Geologiczny; Warszawa.

Rebesco, M., Hernández-Molina, F.J, Van Rooij, D. and Wåhlin, A. 2014. Contourites and associated sediments controlled by deep-water circulation processes: state-of-the-art and future considerations. Marine Geology, 352, 111–154.

Remin, Z. 2012. The *Belemnella* stratigraphy of the Campanian–Maastrichtian boundary; a new methodological and taxonomic approach. Acta Geologica Polonica, 62, 495–533.

Remin, Z. 2015. The *Belemnitella* stratigraphy of the Upper Campanian–basal Maastrichtian of the Middle Vistula section, central Poland. Geological Quarterly, 59, 783–813.

Remin, Z. 2018. Understanding coleoid migration patterns between eastern and western Europe – belemnite faunas from the upper lower Maastrichtian of Hrebenne, southeast Poland. Cretaceous Research, 87, 368–384.

Remin, Z., Cyglicki, M., Cybula, M. and Roszkowska-Remin, J. 2015a. Deep versus shallow? Deltaically influenced sedimentation and new transport directions – case study from the Upper Campanian of the Roztocze Hills, SE Poland. In: 31st IAS Meeting of Sedimentology held in Kraków, Poland, 22–25 June 2015, Abstracts, 438. Polish Geological Society; Kraków.

Remin, Z., Machalski, M. and Jagt, J.W.M. 2015b. The stratigraphically earliest record of Diplomoceras cylindraceum (heteromorph ammonite) – implications for Campanian/Maastrichtian boundary definition. Geological Quarterly, 59, 843–848.

Remin, Z., Gruszczyński M. and Marshall J.D. 2016. Changes in paleo-circulation and the distribution of ammonite faunas at the Coniacian–Santonian transition in central Poland and Western Ukraine. Acta Geologica Polonica, 66, 107–124.

Remin, Z., Cyglicki, M., Barski, M., Dubicka, Z. and Roszkowska-Remin, J. 2021. The K-Pg boundary section at Nasiłów, Poland: stratigraphic reassessment based on foraminifers, dinoflagellate cysts and palaeomagnetism. Geological Quarterly, 65, 1–21.

Remin, Z., Cyglicki, M. and Niechwedowicz, M. 2022. Deep vs. shallow – two contrasting theories? A tectonically activated Late Cretaceous deltaic system in the axial part of the Mid-Polish Trough: a case study from southeast Poland. Solid Earth, 13, 681–703.

Resak, M., Narkiewicz, M. and Littke, R. 2008. New basin modelling results from the Polish part of the Central European Basin system: implications for the Late Cretaceous–Early Paleogene structural inversion. International Journal of Earth Sciences, 97, 955–972.

Rogala, W. 1909. O stratygrafii utworów kredowych Podola. Kosmos, 34, 1160–1164.

Samsonowicz, J. 1925. Szkic geologiczny okolic Rachowa nad Wisłą. Sprawozdania Państwowego Instytutu Geologicznego, 3, 45–118.

Samsonowicz J. 1934. Objaśnienia arkusza Opatów. Ogólna mapa geologiczna Polski w skali 1 : 100.000. Państwowy Instytut Geologiczny; Warszawa.

Surlyk, F. and Lykke-Anderson, H. 2007. Contourite drifts, moats and channels in the Upper Cretaceous chalk of the Danish Basin. Sedimentology, 54, 405–422.

Świdrowska, J. 2007. Kreda w regionie lubelskim – sedymentacja i jej tektoniczne uwarunkowania. Biuletyn Instytutu Geologicznego, 422, 63–78.

Świdrowska, J. and Hakenberg, M. 1999. Subsydencja i początki inwersji bruzdy śródpolskiej na podstawie analizy map miąższości i litofacji osadów górnokredowych. Przegląd Geologiczny, 47, 61–68.

Świdrowska, J., Hakenberg, M., Poluhtovič, B., Seghedi, A. and Višnâkov, I. 2008. Evolution of the Mesozoic basins on the southwestern edge of the East European Craton (Poland, Ukraine, Moldova, Romania). Studia Geologica Polonica, 130, 3–130.

Świerczewska-Gładysz, E. 2006. Late Cretaceous siliceous sponges from the Middle Vistula River Valley (Central Poland) and their palaeoecological significance. Annales Societatis Geologorum Poloniae, 76, 227–296.

Voigt, T., von Eynatten, H. and Franzke, H.-J. 2004. Late Cretaceous unconformities in the Subhercynian

Cretaceous Basin (Germany). Acta Geologica Polonica, 54, 675–696.

Voigt, T., Wiese, F., von Eynatten, H., Franzke, H.-J. and Gaupp, R. 2006. Facies evolution of syntectonic Upper Cretaceous Deposits in the Subhercynian Cretaceous Basin and adjoining areas (Germany). Zeitschrift der Deutschen Gesellschaft für Geowissenschaften, 157, 203–244.

Voigt, S., Wagreich, M., Surlyk, F., Walaszczyk, I., Uličný, D., Čech, S., Voigt, T., Wiese, F., Wilmsen, M., Niebuhr, B., Reich, M., Funk, H., Michalík, J., Jagt, J.W.M., Felder, P.J. and Schulp, A.S. 2008a. Cretaceous. In: McCann, T. (Ed.), Geology of Central Europe. Volume 2: Mesozoic and Cenozoic, 923–998. Geological Society; London.

Voigt, T., Reicherter, K., von Eynatten, H., Littke, R. Voigt, S. and Kley, J. 2008b. Sedimentation during basin inversion, In: Littke, R., Bayer, U., Gajewski, D. and Nelskamp, S. (Eds), Dynamics of complex sedimentary basins. The example of the Central European Basin System, 211–232. Springer-Verlag; Berlin–Heidelberg.

Voigt, T., Kley, J. and Voigt, S. 2021. Dawn and Dusk of Late Cretaceous Basin Inversion in Central Europe. Solid Earth, 12, 1443–1471.

Walaszczyk, I. 1992. Turonian through Santonian deposits of the Central Polish Upland; their facies development, inoceramid paleontology and stratigraphy. Acta Geologica Polonica, 42, 1–122.

Walaszczyk, I. 2004. Inoceramids and inoceramid biostratigraphy of the Upper Campanian to basal Maastrichtian of the Middle Vistula River section, central Poland. Acta Geologica Polonica, 54, 95–168.

Walaszczyk, I. and Remin, Z. 2015. Kreda obrzeżenia Gór Świętokrzyskich. In: Skompski, S. and Mizerski, W. (Eds), LXXXIV Zjazd Naukowy Polskiego Towarzystwa Geologicznego. Ekstensja i Inwersja powaryscyjskich basenów sedymentacyjnych, Chęciny, 9–11 September 2015, Abstracts & Field Guide, 41–50. Państwowy Instytut Geologiczny – Państwowy Instytut Badawczy; Warszawa.

Walaszczyk, I., Dubicka, Z., Olszewska-Nejbert, D. and Remin, Z. 2016. Integrated biostratigraphy of the Santonian through Maastrichtian (Upper Cretaceous) of extra-Carpathian Poland. Acta Geologica Polonica, 66, 313–350.

Ziegler, P.A. 1990. Geological Atlas of Western and Central Europe, 2nd Edition, 239 pp. Shell Internationale Petroleum Maatschappij; The Hague. Geological Society; London.

Żelaźniewicz, A., Buła, Z., Fanning, M., Seghedi, A. and Żaba, J. 2009. More evidence on Neoproterozoic terranes in southern Poland and southeastern Romania. Geological Quarterly, 53, 93–124.

Żelaźniewicz, A., Aleksandrowski, P., Buła, Z., Karnkowski, P., Konon, A., Oszczypko, N., Ślączka, A., Żaba, J. and Żytko, K. 2011. Regionalizacja tektoniczna Polski, 60 pp. Komitet Nauk Geologicznych; Wrocław.

Central Geological Database: www.geologia.pgi.gov.pl

11TH INTERNATIONAL
CRETACEOUS
SYMPOSIUM
Warsaw, Poland, 2022

TRACING THE BIOGEOCHEMICAL SILICA CYCLE IN A LATE CRETACEOUS MARINE ENVIRONMENT: THE GEOLOGICAL AND PETROGRAPHIC RECORD OF THE UPPER CRETACEOUS IN THE MIECHÓW TROUGH, SOUTHERN POLAND

Agata Jurkowska[1]| Ewa Świerczewska-Gładysz[2]| Aleksandra Kasztelewicz[1,3]| Szymon Kowalik[4]

1| AGH University of Science and Technology, ul. Mickiewicza 30; 30-059 Kraków, Poland; e-mail: jurkowska.a@gmail.com

2| Faculty of Geographical Sciences, University of Łódź, ul. Narutowicza 88; 90-139 Łódź, Poland; e-mail: ewa.swierczewska@geo.uni.lodz.pl

3| Mineral and Energy Economy Research Institute, Polish Academy of Sciences, ul. Wybickiego 7a, 31-261 Kraków, Poland; e-mails: kasztelewicz@meeri.pl

4| e-mail: pl; szymon.kowalik@10g.pl

ABSTRACT

The process of early diagenetic silica precipitation led to a significant silica burial flux, expressed in the geological record by the formation of thick opoka successions. The mineralogical composition of silica-bearing rocks, comprising opoka, chert nodules, and marly intercalations, is presented in various Upper Cretaceous localities of the Miechów Synclinorium of southern Poland.

INTRODUCTION TO THE GEOLOGY OF THE MIECHÓW SYNCLINORIUM

The Miechów Synclinorium, which forms the southeastern segment of the Szczecin–Łódź–Miechów Synclinorium (Fig. 1A), is largely built of upper Albian–lower Maastrichtian strata. These rocks unconformably overlie the Jurassic substrate; in the central and southern synclinorium, they are covered by Miocene strata of the Carpathian Foredeep (Kowalski 1948; Aleksandrowicz 1954; Cieśliński and Pożaryski 1970; Pożaryski 1974) (Fig. 1B). Campanian–Maastrichtian deposits are exposed in the middle of the synclinorium, while Albian–Santonian deposits are best preserved on the synclinorium flanks (Fig. 1B).

In the south-west, the Cretaceous succession of the Miechów Synclinorium is lithostratigraphically bipartite, subdivided into a highly condensed upper Albian–Santonian succession with numerous hiatuses and gaps (Sujkowski 1926; Alexandrowicz 1954; Walaszczyk 1992) and an upper Campanian–Maastrichtian succession of largely continuous carbonate strata, with distinctive glauconitic horizons (Rutkowski 1965).

The upper Albian–Santonian succession was deposited during a transgression that, in extra-Carpathian Poland, began in the middle Albian gradually inundating the present-day Miechów Synclinorium (Marcinowski and Radwański 1983). It is composed of siliciclastic rocks (glauconitic sands, conglomerates) that passes upwards to carbonates (limestones, opoka, marls). In the central and southwestern Miechów Synclinorium, these deposits are relatively thin (a few meters), but to the northeast their thickness increases up to 100 m (Walaszczyk 1992).

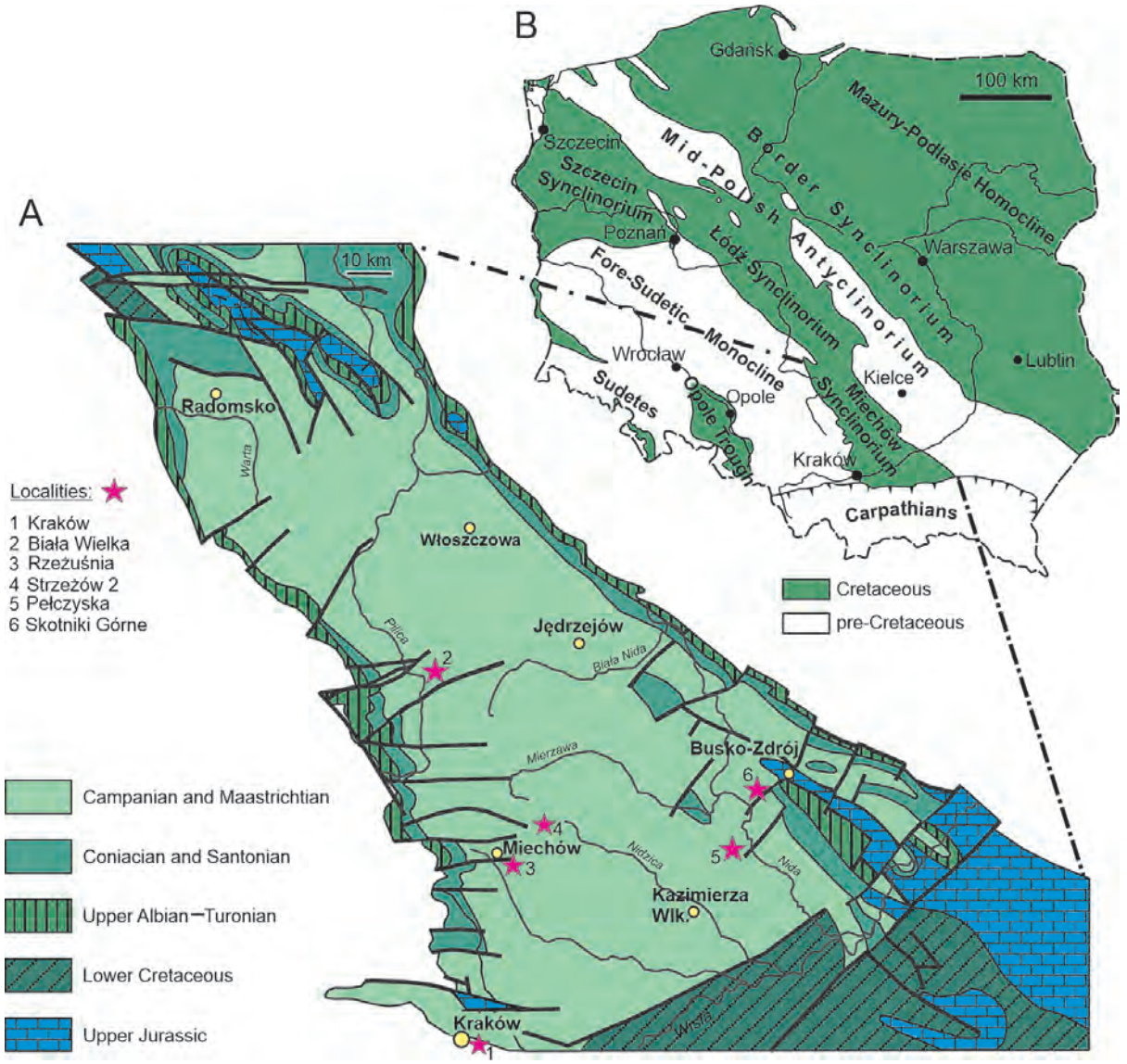

Fig. 1. A. Tectonic sketch map of Poland, without Cenozoic cover (after Pożaryski 1974; Żelaźniewicz et al. 2011). B. Geological map of the Miechów Synclinorium (modified after Dadlez et al. 2000) with localities.

During the Campanian and early Maastrichtian, almost the entirety of the present-day Miechów Synclinorium was covered by an epicontinental sea associated with the Central European Basin. In the Campanian, pelagic carbonate sedimentation prevailed, with only an insignificant terrigenous influx. Conversely, by the early Maastrichtian, significant detrital input (quartz/clays) is noted in both open-sea areas and in the vicinity of the Łysogóry-Dobrogea Archipelago (Zuber 1902; Jurkowska and Barski 2017; Remin 2017; Jurkowska et al. 2019a). As such, the thick (up to 500 m; Heller and Moryc 1984; Jurkowska 2016) Campanian–lower Maastrichtian succession of the Miechów Synclinorium is composed of marls, overlain by opoka with chert horizons and marly intercalations, and ultimately capped by argillaceous opoka and gaize in the lower Maastrichtian.

The Campanian–lower Maastrichtian succession is continuous and has a high-resolution, inoceramid-based biostratigraphic zonation (Jurkowska 2016).

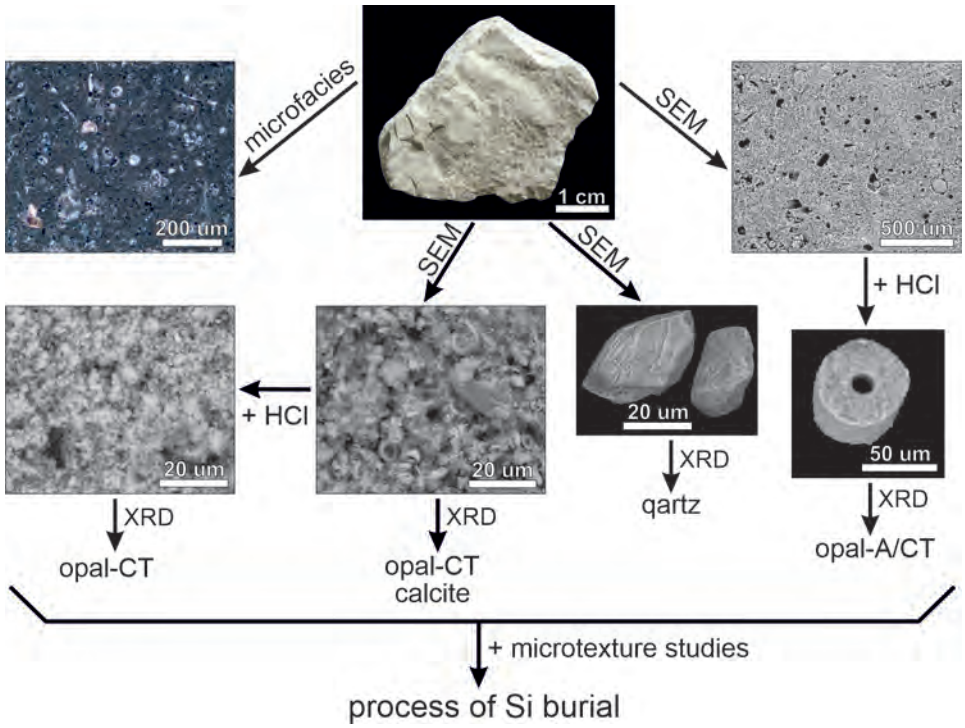

Fig. 2. Research methods used for the determination of mineralogical composition and the recognition of sedimentary Si burial mechanisms.

SILICA BALANCE IN THE EPICONTINENTAL CAMPANIAN–MAASTRICHTIAN CENTRAL EUROPEAN BASIN

During the Late Cretaceous, considerable epicontinental areas were flooded due to brisk mid-ocean ridge spreading rates, leading to the formation of large epicontinental seaways. In general, Late Cretaceous seawater was characterized by elevated dissolved silicon (DSi) concentrations (~40 ppm, 4x higher than at present; Siever 1991; Racki and Cordey 2000; Conley et al. 2017), with siliceous sponges among the dominant silicifiers. In the Central European Basin, seawater DSi was extensively utilized by siliceous sponges, which occur in abundance in certain portions of the basin. After sponge death, biogenic silica spicules (opal-A) dissolved in the seabed mud, saturating the porewater with respect to DSi. In due course, precipitation of silica from DSi-rich porewater within the sediment column occurred under thermodynamically favorable conditions, driven by microbial activity during organic matter decomposition (Clayton 1984; Zijlstra 1994; Jurkowska et al. 2019b; Jurkowska 2022). This process of early diagenetic silica precipitation led to a significant silica burial flux, expressed in the geological record by the formation of thick opoka successions (Jurkowska and Świerczewska-Gładysz 2020a, b) (Fig. 2).

FIELD STOPS

Stop 1:
Biała Wielka and Rzeżuśnia sections: Carbonate pelagic sedimentation

In the Central European Basin, pelagic Campanian deposits form thick carbonate successions composed of chalk and opoka. ***Opoka*** is a Polish term (Pusch 1836) traditionally used to describe Cretaceous chalks that are substantially harder than classical chalk; this feature has enabled their use in architecture and construction. Historically, the absence of analytical techniques to recognise silica polymorphs (Sujkowski 1931; Pożaryska 1952; Rutkowski 1965) precluded the usage of opoka in the international geological literature, although the term was retained by regional geologists. However, recent work incorporating XRD analyses and SEM observations has enabled a formal definition of opoka (Jurkowska et al. 2019b; Jurkowska and Świerczewska-Gładysz 2020a). In this context, ***opoka*** is a carbonate rock composed of calcite (38–90%) and an insoluble residue (10–62%), whose main component is authigenic opal-CT (4–46%) forming networks consisting of adjoining lepispheres (Jurkowska 2022). The presence of authigenic silica polymorphs in opoka is related to the abundant occurrence of siliceous spicules derived from non-rigid demosponges (Jurkowska et al. 2019b), which delivered DSi to the seafloor sediments. The geographically restricted occurrence of abundant, non-rigid demosponge assemblages in the Central European Basin was putatively controlled by DSi-rich oceanic currents, which delivered DSi from volcanic and/or hydrothermal sources linked with oceanic ridges (Fig. 2) (Jurkowska and Świerczewska-Gładysz 2020a). In portions of the Central European Basin where non-siliceous chalk was deposited, porewater DSi concentrations were much lower (<10 ppm) relative to areas with opoka deposition (Jurkowska et al. 2019b).

Monotonous pelagic carbonate sedimentation was repeatedly interrupted by siliceous, nodular chert and flint horizons in opoka and chalk, respectively. Pale to dark grey chert nodules are abundant in the lower–middle Campanian opoka succession. Although their mineralogical composition is similar to opoka, they can be distinguished by higher opal-CT (57.27%) and lower calcite (31.9%) concentrations, along with the presence of authigenic nano-α-quartz (10.9%) (Jurkowska and Świerczewska-Gładysz 2020b). The compositional difference between the chert nodules and flints is linked to variations in the variety of authigenic silica polymorph present. The main component of flints is authigenic nano-α-quartz+moganite (92.18%), with only a minor contribution from opal-CT (6.29%) (Jurkowska and Świerczewska-Gładysz 2020b).

The formation of siliceous nodule horizons – cherts and flints in opoka and chalk, respectively – reflects repeated, rapid spikes in elevated porewater DSi concentrations. These events, in turn, were likely related to oceanic DSi influxes, but siliceous nodule formation ultimately took place by abiotic silica precipitation within the sedimentary column (Jurkowska and Świerczewska-Gładysz 2020b).

During this part of the excursion, we will focus on the mineralogical composition of silica-bearing rocks, comprising opoka, chert nodules, and marly intercalations.

Stop 2:
Biała Wielka section: lower Campanian opoka, marls, and siliceous nodule horizons

Biała Wielka is a temporarily active quarry located in the southern part of the eponymous village (GPS: N 50°41′17.19″; E 19°39′42.52″). In the quarry, a 10 m section of lower Campanian (*Sphaeroceramus sarumensis/Cataceramus dariensis* inoceramid zones) opoka with chert nodule horizons and marly intercalations is visible. The cherts are 10–15 cm in size and light to dark gray in color, while the marly intercalations are 15–20 cm thick. In opoka, cherts, and marls, fossils are relatively common and mainly represented by cephalopods and echinoids. Siliceous sponges, although less numerous than in Rzeżuśnia, are dominated by

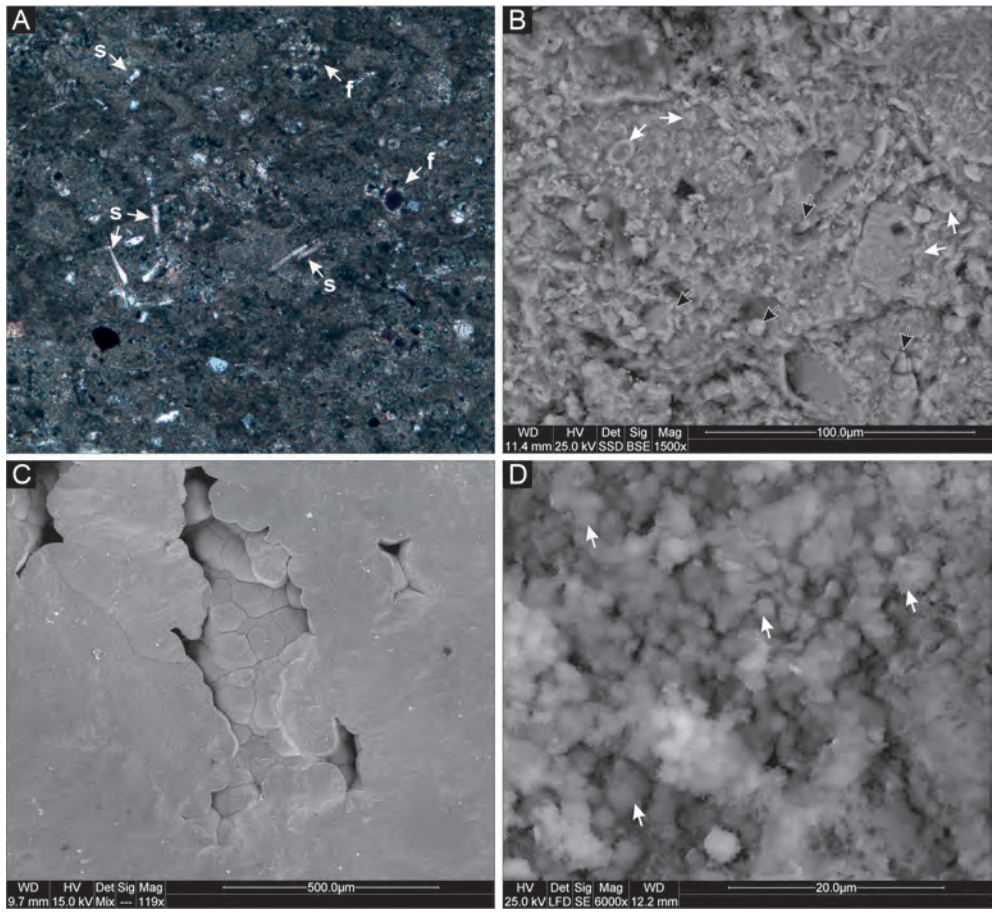

Fig. 3. Biała Wielka section. A. Thin section of opoka-bioclastic wackestone with foraminifera (f) and rare voids after spicule dissolution, with secondary spicule infilling by opal-A/CT (s). B. Carbonate matrix with visible micrite components: coccoliths (white arrow), pseudomicrite diagenetic rounded grains, and euhedral sparite (black arrow). C. Microtexture of opal-CT lepispheres in chert nodule visible as aggregates of large lepispheres (50–100 µm) composed of sharply bladed opal-CT crystals. D. Microtexture of opal-CT lepispheres in chert nodule visible as small (1–2 µm) lepispheres (white arrow), which are incorporated between carbonate grains and form a porous structural network.

Aphrocallistes and *Leptophragma* (hexactinosidan) and *Rhizpoterion* (lychniscosidan) species. Only one lithistid species (*Verruculina miliaris*) is known. Root tufts derived from lyssacinosidan sponges are also found.

In Biała Wielka, the opoka is a bioclastic packstone (Fig. 3A). The main component of this opoka is calcite (56.43%), with some contribution from opal-CT (27.46%) and insignificant detrital quartz (5.4%) and clays (10.6%) contributions (Jurkowska and Świerczewska-Gładysz 2020a; Jurkowska 2022). Compared to Rzeżuśnia, the opoka in Biała Wielka contains more opal-CT and less calcite. In the Biała Wielka section, the carbonate matrix is porous and mostly composed of single coccoliths, detached individual coccolith crystals, and their spines (Fig. 3A). Other matrix components are (i) small (< 4 µm), rounded, rhombic calcium carbonate grains and (ii) rare pseudosparite grains (> 4 µm) of euhedral calcite crystals (Fig. 3B). Opal-CT occurs as lepisphere networks that represent early forms of small (0.5–1 µm), sharply bladed lepispheres (terminology following Lynne et al. 2007). The quartz and clays (the latter mostly mixed-layer illite-smectite) are of detrital origin.

The mineralogical composition of the marly intercalations from Biała Wielka are similar to those from Rzeżuśnia, as described below. However, in Biała Wielka, coarse (0.8–0.9 mm), rounded quartz grains have been documented

in addition to the more typical medium (0.3–0.6 mm), sharply edged quartz grains.

The chert nodules in Biała Wielka are composed of opal-CT (54.92%), calcite (36.83%), and nano-α-quartz (4.52%). In thin section, they appear as siliceous rocks with an opal-CT matrix and sponge spicules infilled by chalcedony. There are two distinct opal-CT lepisphere microtextures: (1) aggregates of large lepispheres (50–100 μm) composed of sharply bladed opal-CT crystals, which can fuse into homogenous masses with visible relicts of primary rounded structures, and (2) small (1–2 μm) lepispheres incorporated between carbonate grains that form a porous structural network easily visible after calcium carbonate dissolution (3C–D). Voids after spicule dissolution are not well preserved in this section (Jurkowska and Świerczewska-Gładysz 2020a).

Stop 3: Rzeżuśnia section: middle Campanian opoka, marls, and siliceous nodule horizons

An abandoned quarry in the village of Rzeżuśnia (GPS: N 50°20′9.98″; E 19°58′15.53″) captures a 13 m thick opoka succession of middle Campanian age ('*Inoceramus*' *azerbaydjanensis*/'*Inoceramus*' *vorhelmensis* inoceramid zones; Jagt et al. 2004, Jurkowska 2016) (Fig. 4A). In the lower part of the section, chaotically distributed, irregularly shaped, 3–10 cm gray chert nodules have been documented (Fig. 4B). In the upper part of the section, chert nodules become less abundant and 15–20 cm thick marly intercalations occur. Siliceous sponges are represented mainly by those with rigid skeletons – including very abundant and taxonomically diverse Hexactinosida and Lychniscosida and uncommon lithistid sponges, the latter mainly from the family Pleromidae. Lyssacinosida (hexactinellid sponges without a rigid skeleton) are relatively numerous, but usually only their root tufts are preserved (Świerczewska-Gładysz and Jurkowska 2013). Ammonites, echinoids, bivalves, and belemnites are abundant throughout the whole section and occur in opoka, marly intercalations, and chert nodules. In the middle part of the section, a single, 30–40 cm thick opoka horizon contains a mass occurrence of ammonites (with dense *Chondrites* ichnofabric on the lower side) and inoceramids with green glauconitic coatings (Jurkowska et al. 2017). Several horizons with chaotically distributed ammonites – *Baculites* sp. – have been documented.

The opoka from Rzeżuśnia, in thin section, is a packstone with foraminifera and siliceous sponge spicules, the latter preserved as voids or filled by secondary opal-CT (Fig. 4C). Abundant monaxonid spicules of non-rigid demosponges and rare loose hexactines of lyssacinosidan sponges have been noted (Świerczewska-Gładysz and Jurkowska 2013). Mineralogically, the opoka from Rzeżuśnia constitutes an intermediate style of opoka (Jurkowska 2022), containing a significant amount of calcite (75.23%) and opal-CT (11.2%), and to a lesser degree detrital clays (7.2%) and quartz (3.25%). Relative to Biała Wielka, the opoka from Rzeżuśnia contains less opal-CT and more calcite. The micrite (< 4 μm) is composed of coccoliths and calcite grains, and euhedral pseudosparite crystals (> 4 μm) are also present. Small (~1 μm) opal-CT lepispheres form a densely packed siliceous network. The quartz and clays are of detrital origin.

The presence of a fossiliferous, glauconitic horizon within a glauconite-poor opoka succession is putatively caused by the activity of the *Chondrites* tracemaker, which induced geochemical reactions within the seabed sediments and thus drove glauconite formation (Jurkowska et al. 2017).

The marly intercalations are composed of calcite (69.9%), quartz (6.2 %), opal-CT (8.13%), and clays (17.43%) (Jurkowska 2022), and are broadly similar to those in the Biała Wielka section. The calcite is comprised of coccolith fragments, diagenetic, rounded micrite grains, and euhedral sparite crystals (> 4 μm). In marls, the opal-CT framework is composed of small, densely packed lepispheres (< 1 μm) with smooth blades (Fig. 4D). This is an embryonic, immature opal-CT, as evidenced by the distinctive fuzzy microtexture and significant Mg^{2+} concentrations (Kastner et al. 1977; Jurkowska 2022). The lepispheres are usually overgrown by authigenic clays with honeycomb morphologies. The detrital clays, which probably dominate in the marls, have flaky morphologies. The quartz grains are uniformly medium-grained (0.3–0.6 mm) and angular.

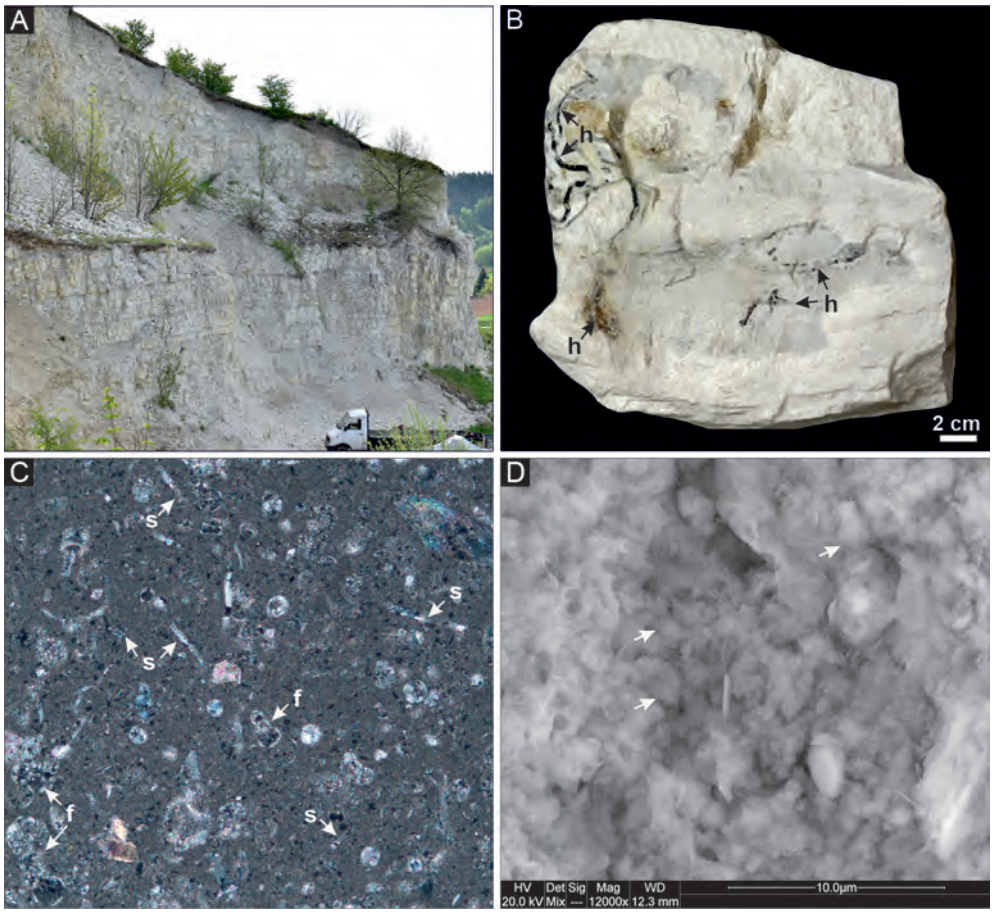

Fig. 4. Rzeżuśnia section. A. General view of Rzeżuśnia section. B. Chert nodule (gray) with fragments of bodily preserved hexactinellid sponges (h). C. Thin section of opoka-packstone, with foraminifera and voids left after siliceous sponge spicules infilled by secondary opal-A/CT (s). D. Siliceous network of opal-CT lepispheres in opoka.

The mineralogical composition of the chert nodules is identical to those from Biała Wielka.

Stop 4:
Strzeżów 2 and Pełczyska sections: Detrital quartz and clay influx

The lower Maastrichtian deposits of the Miechów Synclinorium are largely represented by argillaceous opoka, transitioning upward into gaize. Argillaceous opoka has all of the primary features of opoka (that is, a siliceous opal-CT lepisphere framework), but additionally contains significant amounts of detrital grains (quartz, clays, muscovite, kaolinite) and authigenic clinoptilolite (Jurkowska et al. 2019a). The term ***gaize*** originates from France, and was introduced to the geological literature by Cayeux (1929) for sedimentary carbonates that contain both biogenic silica and abundant detrital quartz, glauconite grains, and clays. Recent work has clarified that the biogenic silica in Cayuex's original definition describes opal-CT lepispheres with a similar morphology to those in opoka (Jurkowska 2022). In the Miechów Synclinorium, the mineralogical composition of gaizes reflects a relatively high proportion of detrital components – namely, quartz (~20%) and clays (~10%).

Stop 5:
Strzeżów 2 section: Lower Maastrichtian gaize

Strzeżów 2 is an abandoned quarry located on a hilltop (GPS: N 50°22′56.6″; E 20°25′7.34″)

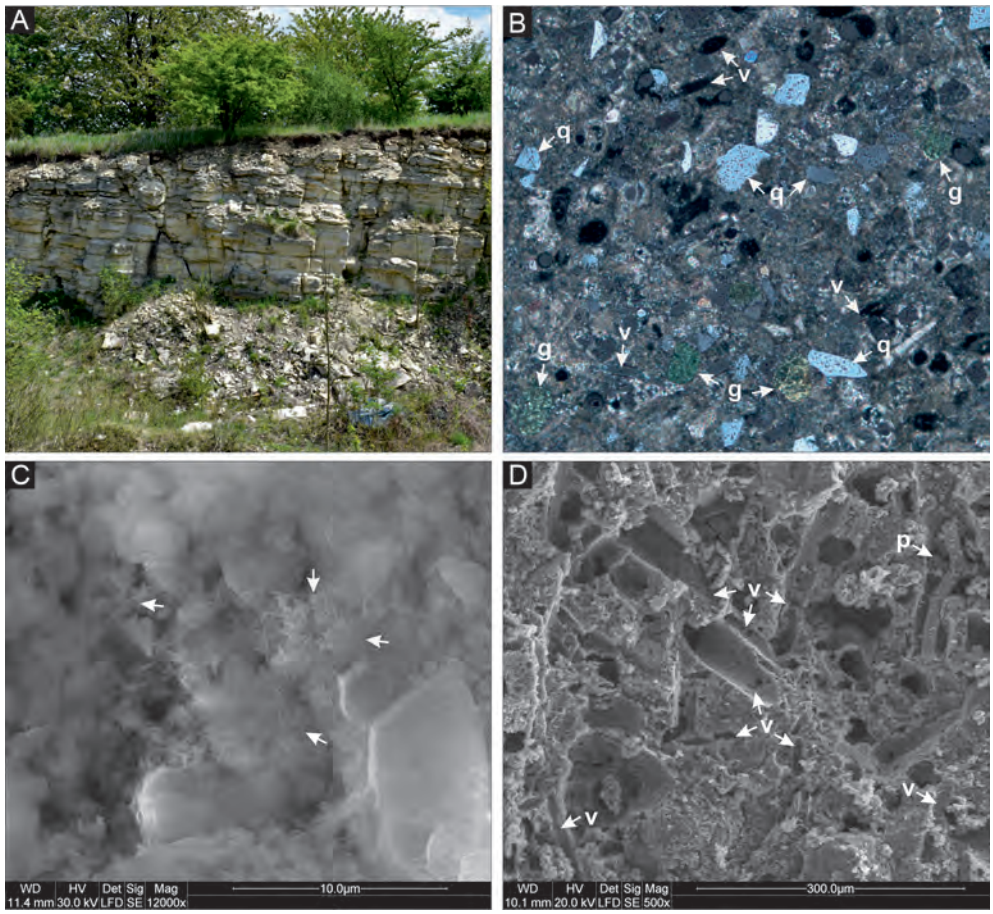

Fig. 5. Strzeżów 2 section. A. General view of Strzeżów 2 section. B. Thin section of gaize – bioclastic packstone with quartz (q) and glauconite (g) grains and poorly visible voids left after dissolved monaxonid spicules (v). C. Densely packed opal-CT lepispheres (white arrows). D. Abundant voids left after dissolved, variably sized monaxonid (v) and protriaene (p) spicules.

in the village of Strzeżów. On the southeast wall of the quarry, a 4 m section of lower Maastrichtian (*Trochoceramus radiosus* inoceramid Zone) gaize with marly intercalations can be observed (Fig. 5A). Fossils are very rare, represented mainly by bivalves (*Lucina* sp.) and ichnofossils (*Thalassinoides* sp.). Sponge body fossils have not been reported.

In the Strzeżów 2 section, the gaize is a bioclastic packstone with quartz and glauconite grains (Fig. 5B). The detrital quartz grains are medium-grained (0.3–0.6 mm) and sharply-edged (Fig. 5B). The average mineralogical composition of gaize consists of calcite (40.4%), opal-CT (26.7%), and a significant detrital component: quartz (18.63%), clays (11.43%), microcline (0.73%), and clinoptilolite (2.0%) (Jurkowska 2022). Relative to lower–middle Campanian opoka, the Strzeżów 2 gaize contains a greater detrital contribution, especially with regards to quartz (5% vs. 18%). The micrite is a diagenetic pseudomicrite, in turn comprised of small (< 1 µm) rounded grains, disintegrated individual coccoliths, and detached coccolith crystal elements. Larger (~4 µm) sparite grains of rombic sub-/euhedral morphologies are abundant. An authigenic opal-CT network also occurs in the gaizes, composed of 1–3 µm lepispheres with sharp-edged blades. The lepispheres are densely packed and adjoined, and show a distinctive crisscross structural pattern characteristic of mature opal-CT forms (Lynne et al. 2007) (Fig. 5C). The clays include smectite and mixed-layer illite/smectite of both detrital and authigenic origin. The detrital clays are characterized by flaky morphologies and are the dominant contributor to gaize clay mineralogy; authigenic clays can be recognized by a typical rose-like/

honeycomb texture and have a patchy distribution. The quartz, muscovite, and feldspar grains are of detrital origin. In particular, the quartz grains have sharply-edged crystals and conspicuous surficial abrasion marks. Although body preservation of siliceous sponges has not been documented in the field, abundant voids left after dissolved monaxonid (mainly oxeas) and rare protriaene spicules are visible under SEM (Fig. 5D). The sponge assemblage noted in gaize differs than those from opoka facies, consisting of only non-rigid demosponges: this is probably linked to environmental conditions – potentially, fast sedimentation rates and elevated water-column energy.

Stop 6:
Pełczyska section: lower Maastrichtian argillaceous opoka (shoreface sedimentation)

The section is a natural outcrop in the northern part of a hill located in the archeologically famous Pełczyska village (GPS: N 50°21′34.58″; E 20°33′40.14″). The section comprises 12.3 m of alternating gray (highly bioturbated) and white (weakly bioturbated) clayey opoka (= argillaceous opoka) of lower Maastrichtian age (*Endocostea typica* inoceramid Zone) (Jurkowska 2016; Jurkowska et al. 2019a). Poorly preserved macrofossils include numerous sponges (mainly Hexactinellida), bivalves, echinoids, ammonites, and ichnofossils. Hexactinosidan and lychniscosidan sponge specimens are fragmented and highly corroded, with signs of surficial mechanical damage.

Palynological and palynofacies analysis conducted in this section revealed that the argillaceous opoka was deposited in a coastal environment, under the influence of weak currents delivering substantial amounts of sponge spicules (biogenic opal) from offshore. Terrestrial input was provided by rivers sourced from the neighboring Łysogóry–Dobrogea Archipelago (Jurkowska et al. 2019a).

Mineralogically, the argillaceous opoka is composed of calcite (61.5%), opal-CT (16.2%), clays (7.1%), muscovite (5.6%), and clinoptilolite (3.1%). The Pełczyska opoka differs from the lower–middle Campanian opoka in that it contains significant amounts of detrital muscovite and authigenic clinoptilolite (Jurkowska et al. 2019a). The main calcite components are fragmented coccolith shields and spines (allomicrite). The pseudomicrite is composed of small, subrounded-to-rounded subhedral calcite grains (< 1 μm) and rare euhedral calcite crystals (< 4 μm). Opal-CT is present as lepispheres (1–2 μm) with visible crisscross structures (Fig. 6A). The lepispheres usually occupy the inter- and intra- particle voids between calcite grains. After removing the calcium carbonate, opal-CT forms a siliceous rock framework composed of adjoining lepispheres (Jurkowska et al. 2019a) (Fig. 6A). The quartz is silty to very finely grained (20–100 μm) and angular/subangular with high/medium relief, with rare subrounded grains with abundant mechanical abrasion features: it is of

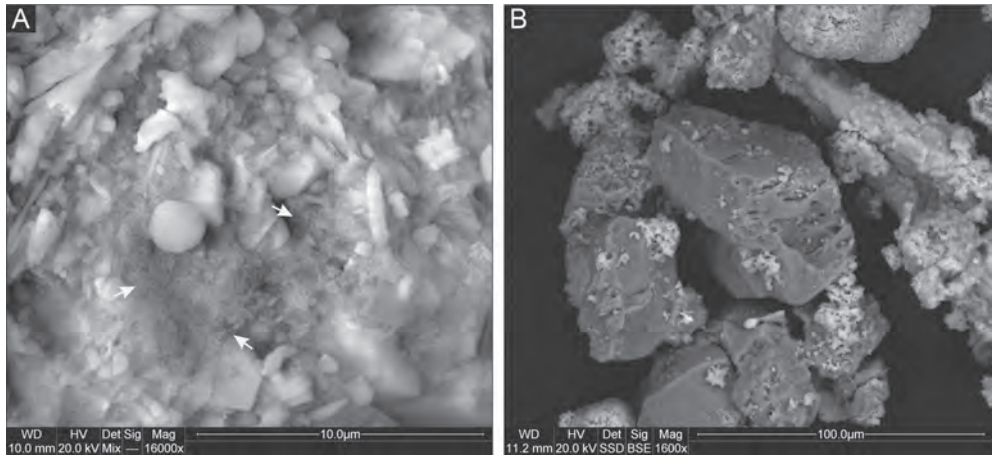

Fig. 6. Pełczyska section. A. Siliceous petrographic framework of adjoining opal-CT lepispheres (white arrows). B. Angular to subangular quartz grains (20–100 μm).

detrital origin (Jurkowska et al. 2019a) (Fig. 6B). The clays are dominated by smectitic group minerals, are slightly crenulated, and display flaky morphologies. The muscovite occurs as large flakes (20–30 μm) incorporated into the matrix. The quartz grains, clays, and muscovite are of terrestrial origin and were transported to the coastal zone by rivers from the emergent Łysogóry–Dobrogea Archipelago (Jurkowska et al. 2019a). The clinoptilolite (zeolite) is of authigenic origin, precipitated during early diagenesis from porewaters enriched with silica and aluminum, due to the dynamic silica concentration equilibrium modulated by opal-CT crystallization (Jurkowska et al. 2019a). Intriguingly, clinoptilolite is usually derived from rhyolitic glass alteration. In this case, the unusual formation of authigenic clinoptilolite is linked to atypical paleoenvironmental conditions, in which the coastal depositional setting was influenced by both terrestrial and offshore marine input, delivering sufficient dissolved aluminum and DSi to the porewaters to promote zeolite growth (Jurkowska et al. 2019a).

Casts after dissolved, non-rigid demosponge monaxonid spicules are empty or infilled by sparite. These voids are often aligned in parallel, suggestive of spicule transport.

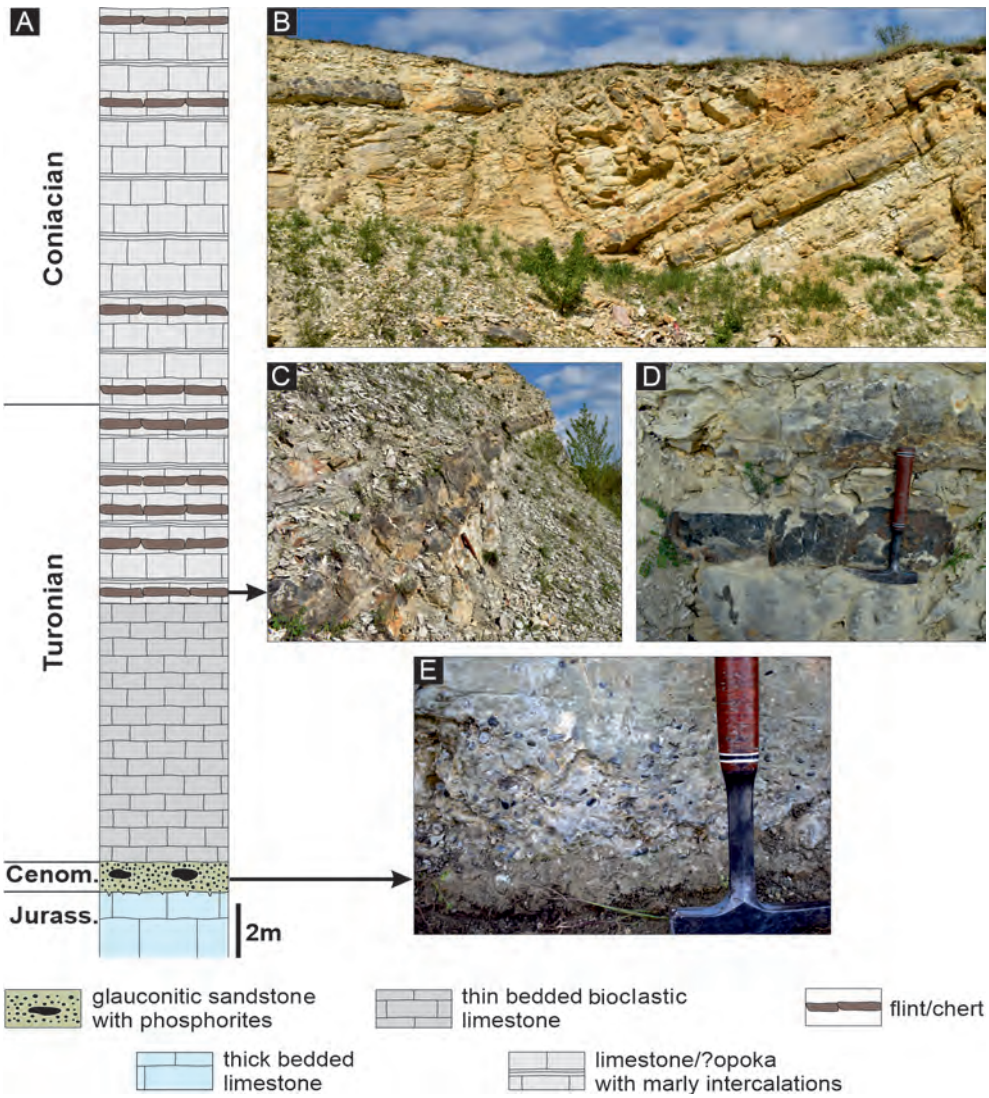

Fig. 7. Zajęcza Góra quarry. A. Lithological column of the Zajęcza Góra quarry in Skotniki Duże (modified and simplified after Walaszczyk, 1992). B. General view of the Turonian-Coniacian deposits. C. Flint horizon. D. Close-up of flint nodules in the flint horizon. E. Glauconitic sandstone with phosphorites.

Stop 7: Zajęcza Góra Quarry, Skotniki Duże: Cenomanian–Coniacian sedimentation

The inactive Zajęcza Góra Quarry is located in the Skotniki Duże village (GPS: N 50°25′30.24″ E 20°39′17.49″). In the west part of the quarry, thickly bedded Kimmerdigian limestone is exposed (Radwański and Górka 2012) (Fig. 7), overlain by 2 m of lower/lower middle Cenomanian glauconitic sandstones with phosphorite concretions and detrital quartz (Walaszczyk 1992). A hardground occurs between the Cenomanian–Turonian boundary. Above, the marls are covered by (i) lower or low-middle Turonian thin bedded bioclastic limestones and (ii) upper Turonian limestones/?opoka with 20–30 cm flint and marly intercalation horizons (Walaszczyk 1992). Lower–middle Coniacian strata are largely a continuation of late Turonian sedimentation, represented by marls and limestones/?opoka with crinoid and crinoidal-inoceramid tempestite intercalations. Generally, fossils from the Zajęcza Góra quarry are rare, and those present are dominated by inoceramids. Body fossils of sponges have not been observed, although voids after spicules are noted in limestones/?opoka (Walaszczyk 1992). The abrasional upper surface of the Upper Cretaceous strata is covered by Badenian basal conglomerates, with patches of organic limestones (Radwański 1969).

This work was supported by the National Science Centre of Poland (Grant No. 677 2016/23/D/ST10/01526).

REFERENCES

Alexandrowicz, S. 1954. Turon południowej części Wyżyny Krakowskiej. Acta Geologica Polonica, 4, 361–390.

Cayeux, L. 1929. Les roches siliceuses. Mémoire pour servir á l'explication de la carte géologique détaillée de la France, p. 774. Imprimerie Nationale; Paris.

Cieśliński, S. and Pożaryski, W. 1970. Cretaceous. Prace Państwowego Instytutu Geologicznego, 56, 185–232. [In Polish with English summary]

Clayton, C.J. 1986. The chemical environment of flint formation in Upper Cretaceous Chalks. In: Sieveking, G. and Hart, M.B. (Eds), The scientific study of flint and chert. Proceedings of the Fourth International Flint Symposium Held at Brighton Polytechnic. 10–15 April 1983, 43–54. Cambridge University Press.

Conley, D.J., Frings, P.J., Fontorbe, G., Clymans, W., Stadmark, J. and Hendry, K.R. 2017. Biosilicification drives a decline of dissolved Si in the oceans through geologic time. Frontiers of Marine Sciences, 4, 397.

Dadlez, R., Marek, S. and Pokorski, J. 1998. Paleogeographical Atlas of the Epicontinental Permian and Mesozoic in Poland, 1:2 500 000. Państwowy Instytut Geologiczny; Warszawa. [In Polish]

Heller, I. and Moryc, W. 1984. Stratigraphy of the Upper Cretaceous deposits in the Carpathian Foreland. Biuletyn Instytutu Geologicznego, 346, 63–108. [In Polish with English summary]

Jagt, J.W.M., Walaszczyk, I., Yazykova, E.A. and Zatoń, M. 2004. Linking southern Poland and northern Germany: Campanian cephalopods, inoceramid bivalves and echinoids. Acta Geologica Polonica, 54, 573–586.

Jurkowska, A. 2016. Inoceramid stratigraphy and depositional architecture of the Miechów Synclinorium (southern Poland). Acta Geologica Polonica, 66, 59–84.

Jurkowska, A. 2022. The biotic-abiotic control of Si burial in marine carbonate systems of the pre-Eocene Si cycle. Global Biogeochemical Cycles, 36, e2021GB007079.

Jurkowska, A. and Barski, M. 2017. Maastrichtian island in the Central European Basin – new data inferred from palynofacies analysis and inoceramid stratigraphy. Facies, 63, 26.

Jurkowska, A., Barski, M. and Worobiec, E. 2019a. The relation of a coastal environment to early diagenetic clinoptilolite (zeolite) formation – New data from the Late Cretaceous European Basin. Palaeogeography, Palaeoclimatology, Palaeoecology, 524, 166–182.

Jurkowska, A., Świerczewska-Gładysz, E., Bąk, M. and Okoński, S. 2019b. The role of biogenic silica in formation of Upper Cretaceous pelagic carbonates and its paleoecological implications. Cretaceous Research, 93, 170–187.

Jurkowska, A. and Świerczewska-Gładysz, E. 2020a. New model of Si balance in the Late Cretaceous epicontinental European Basin. Global and Planetary Change, 186, 103–108.

Jurkowska, A. and Świerczewska-Gładysz, E. 2020b. Evolution of Late Cretaceous Si cycling reflected in the formation of siliceous nodules (flints and cherts). Global and Planetary Change, 195, 103–334.

Jurkowska, A., Uchman, A. and Banaś, M. 2017. Life beneath ammonite shells – A unique Late Cretaceous habitat for the trace maker of *Chondrites* and its impact on taphonomy of the shells. Cretaceous Research, 72, 151–160.

Kastner, M., Keene, J.B. and Gieskes, J.M. 1977. Diagenesis of siliceous oozes. I. Chemical controls on the rate of opal-A to opal-CT transformation an experimental study. Geochimica et Cosmochimica Acta, 41, 1041–1059.

Kowalski, W.C. 1948. Geological outline of Cretaceous deposits in the environs of Solec. Biuletyn Państwowego Instytutu Geologicznego, 51, 5–53. [In Polish with English summary]

Lynne, B.Y., Campbell, K.A., James, B.J., Browne, P.R.L. and Moore, J. 2007. Tracking crystallinity in siliceous hot-spring deposits. American Journal of Science, 307, 612–641.

Marcinowski, R. and Radwański, A. 1983. The mid-Cretaceous transgression onto the Central Polish Uplands (marginal part of the Central European Basin. Zitteliana, 10, 65–95.

Pożaryska, K. 1952. The sedimentological problems of Upper Maastrichtian and Danian of the Puławy Environment (Middle Vistula). Biuletyn Państwowego Instytutu Geologicznego, 81, 1–104. [In Polish with English summary]

Pożaryski, W. 1974. Tectonics. Part 1. Polish Lowlands. In: Pożaryski, W. (Ed.), Geology of Poland IV, pp. 2–34. Wydawnictwa Geologiczne; Warszawa.

Pusch, G.G. 1836. Geognostische Beschreibung von Polen so wie der übrigen Nordkarpathen-Länder, zweiter Theil, 695 pp. J.G. Cotta'schen Buchhandlung; Stuttgart–Tübingen.

Racki, G. and Cordey, F. 2000. Radiolarian palaeoecology and radiolarites: Is the present the key to the past? Earth-Science Review, 52, 83–120.

Radwański, A. 1969. Lower Tortonian transgression onto the sothern slopes of the Holy Cross Mts. Acta Geologica Polonica, 19, 1–176. [In Polish with English summary]

Radwański, A. 1973. Lower Tortonian transgression onto the south-eastern and eastern slopes of the Holy Cross Mts. Acta Geologica Polonica, 23, 375–434. [In Polish with English summary]

Radwański, A. and Górka, M. 2012. Wybrzeże morza mioceńskiego – Korytnica, Lubania i głazowisko klifowe w Skotnikach. In: Skompski, S. (Ed.), Góry Świętokrzyskie: 25 najważniejszych odsłonięć geologicznych, 160 pp. Uniwersytet Warszawski, Wydział Geologii; Warszawa.

Remin, Z. 2017. Understanding coleoid migration patterns between eastern and western Europe – belemnite faunas from the upper lower Maastrichtian of Hrebenne, southeast Poland. Cretaceous Research, 87, 368–384.

Rutkowski, J. 1965. Senonian in the area of Miechów, southern Poland. Rocznik Polskiego Towarzystwa Geologicznego, 35, 3–53. [In Polish with English summary]

Siever, R. 1991. Silica in the oceans: Biological-geochemical interplay. In: Schneider, S.H and Boston, P.J. (Eds), Scientists on Gaia, 287–295. MIT Press; Cambridge MA.

Sujkowski, Z. 1926. Sur le Jurassique, le Cretace, et le Quaternaire des environs de Wolbrom. Sprawozdania Polskiego Instytutu Geologicznego, 3, 382–467.

Sujkowski, Z. 1931. Petrografia kredy Polski. Kreda z głębokiego wiercenia w Lublinie w porównaniu z kredą niektórych innych obszarów Polski. Sprawozdania Państwowego Instytutu Geologicznego, 6, 485–628.

Świerczewska-Gładysz, E. and Jurkowska, A. 2013. Occurrence and paleontological significance of lyssacinosid sponges in the Upper Cretaceous deposits of southern Poland. Facies, 59, 773–777.

Walaszczyk, I. 1992. Turonian through Santonian deposits of the Central Polish Uplands; their facies development, inoceramid paleontology and stratigraphy. Acta Geologica Polonica, 42, 1–122.

Zijlstra, J.J.P. 1994. Sedimentology of the Late Cretaceous and Early Tertiary (tuffaceous) Chalk of Northwest Europe. Geologica Ultraiectina, 119, 1–192.

Żelaźniewicz, A., Aleksandrowski, P., Buła, Z., Karnkowski, P. H., Konon, A., Oszczypko, N., Ślączka A., Żaba, J. and Żytko. K. 2011. Regionalizacja tektoniczna Polski, 60 p. Komitet Nauk Geologicznych PAN; Wrocław.

11TH INTERNATIONAL
CRETACEOUS
SYMPOSIUM
Warsaw, Poland, 2022

PALAEOENVIRONMENTS AND BIOTA OF THE OPOLE CRETACEOUS

Elena Jagt-Yazykova[1]| Dawid Mazurek[1]| Mariusz Kędzierski[2]| John W.M. Jagt[3]| Jordan P. Todes[4]

1| Instytut Biologii/European Centre of Palaeontology, Uniwersytet Opolski, Opole, Poland; e-mails: eyazykova@uni.opole.pl; dawid.mazurek@uni.opole.pl

2| Faculty of Geography and Geology, Jagiellonian University, Kraków, Poland; e-mail: mariusz.kedzierski@uj.edu.pl

3| Natuurhistorisch Museum Maastricht, Maastricht, the Netherlands; e-mail: john.jagt@maastricht.nl

4| Department of the Geophysical Sciences, University of Chicago, Chicago, Illinois, USA; e-mail: jtodes@uchicago.edu

ABSTRACT

From the early 19th century, Opole has become an important centre of cement production: underneath a thin soil cover, Cretaceous marls and limestones proved to be ideal raw material for this process. Today, there are only two active quarries in the vicinity of Opole: Odra Nowa and Folwark. Turonian–lower Coniacian carbonates are characterised by a highly diverse fossil composition, with numerous invertebrate taxa, rarer vertebrate taxa, various plants, and rich microfossils. The latter include calcareous nannofossils, planktic and benthic foraminifera, and dinoflagellates, all illustrating a diverse marine ecosystem. New chemostratigraphic data for the succession complement the picture.

INTRODUCTION

The first studies of Cretaceous strata in Opole (Fig. 1A, B) are closely linked to the development of the local cement industry, beginning with the invention of the earliest Portland Cement in the early 19th century. Opole rapidly became an important centre of cement production: underneath a thin soil cover, Cretaceous marls and limestones proved to be ideal raw material for such production. While the entire Opole region is rich in carbonate rocks – mainly Triassic limestones quarried at Górażdże, Strzelce Opolskie and Tarnów Opolski, and previously in numerous other places, including Gogolin, Kamień Śląski and Szymiszów – these rocks are not as suitable for cement production as they require the addition of clay (for example, the clay once mined at Krasiejów).

The first cement plant in Opole, Portland Zementwerke, was built near what is now Struga Street in the mid-19th century (Bereszyński 2007). Friedrich Wilhelm Grundmann, a pioneer of industrialisation and responsible for developing the village of Katowice into a city, was a shareholder in this enterprise. He quickly became the sole owner of the cement plant by buying his partners' shares. In the first year the plant was fully operational, it produced 900 tonnes of cement. In 1867, the Universal Exhibition of All Nations was held in Paris; there, the Grundmann cement plant delighted visitors with a cement replica of a Roman statue, which later returned to Opole and was placed in the park on Wyspa Pasieka. Unsurprisingly, more entrepreneurs rapidly followed suite. In 1865, Heymann Prinsheim built a cement plant near what is now Marka z Jemielnica Street. A third cement plant followed at Groszowice in 1871. Soon, other cement plants rapidly proliferated near Zakrzów (the ancestor of the present Odra cement

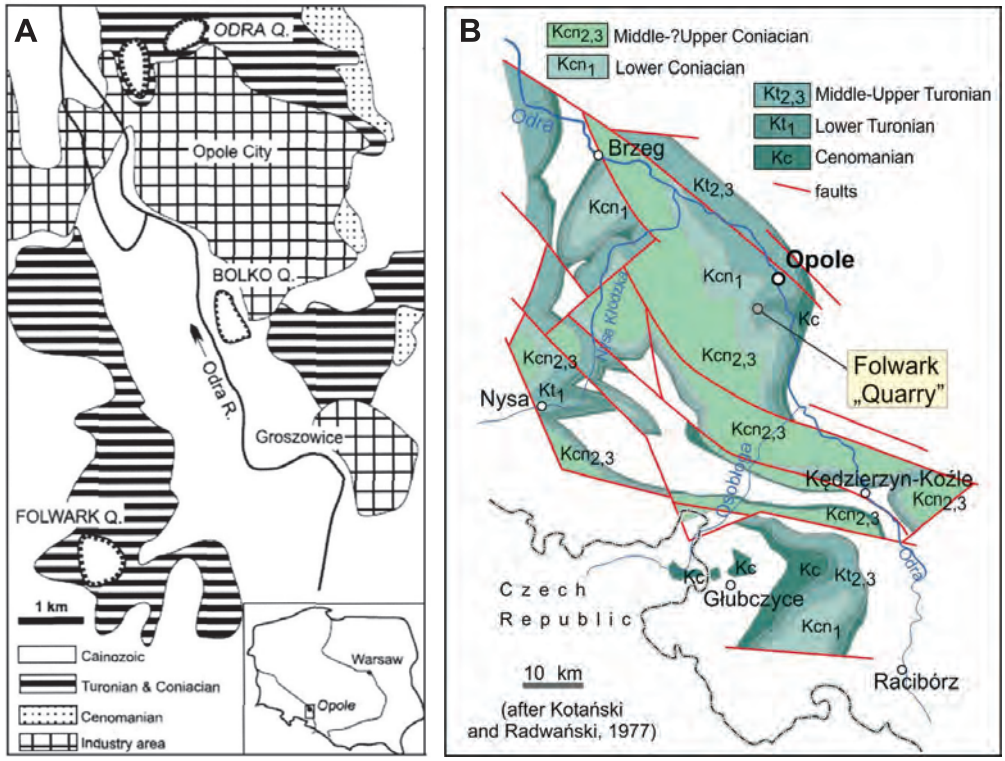

Fig. 1. A – Map of the Opole area (southwest Poland), showing the Odra (both disused and currently exploited), Bolko (disused/flooded) and Folwark quarries (from Mazurek, 2008). B – Geological map of the Opole Trough Cretaceous (from Kędzierski and Uchman 2015).

plant), near the railway station at Giesel, at Bolko, and in Nowa Wieś Królewska (then a separate village), Silesia, and Stadt Oppeln (the ancestor of the Piast cement plant).

By the beginning of the 20th century, most Silesian cement plants were located in the immediate vicinity of Opole (Bereszyński 2007). Even by the end of the 19th century, a cement plant syndicate had formed, sparking fights between companies in the competitive cement industry. It was the cement industry that drove Opole's development: engineering advances developed for raw material extraction and production were remarkably innovative, and the resulting cement was highly regarded throughout Europe. For the most part, the cement plants survived the Second World War, but fell into ruin soon after. Throughout the communist era in Poland, however, many plants were reactivated. Despite this, the "Silesia" cement plant could not be rebuilt: the construction of another plant was planned, but later abandoned (Bereszyński 2007). By the end of the 20th century, the strength of the Opole cement industry began to decline: in 1979, Bolko closed; in 2000, Groszowice. These were gradually replaced by plants using the Triassic carbonates located outside Opole: these (mostly) small excavations have an equally long exploitation history comparable to the Opole chalk. In Opole itself, only the Odra cement plant is still active, associated with an abandoned chalk pit (Odra Stara) and a newer, still in operation, chalk pit (Odra Nowa). As of 2022, Folwark quarry is owned and operated by the Górażdże HeidelbergCement Group (www.gorazdze.pl/pl/grupa-gorazdze; in Polish).

In 1841, Friedrich Adolf Roemer was the first geologist to determine the age of the Opole Cretaceous succession correctly, by equating the 'Kreda opolska' (that is, the Opole Cretaceous) with the Chalk Marl of Great Britain (F.A. Roemer 1841). Subsequently, he studied and compared fossils from the German Cretaceous with material from the Opole Cretaceous, describing twenty-one species from the so-called 'Scaphite Beds' of Opole (F.A. Roemer 1841, 1864). One of the most in-

fluential papers on the geology and palaeontology of Silesia is *Geologie von Oberschlesien* by Friedrich's brother, Ferdinand (F. Roemer 1870), who outlined the lithostratigraphy of the Opole Cretaceous strata, distinguishing sands and sandstones, calcareous marls and calcareous sandstones with muscovite – that is, a broadly comparable succession to the modern lithostratigraphical standard. A series of German scholars subsequently visited these outcrops, recording various sponge, echinoid and ammonite species. Of particular note was a paper by Leonhard (1898), who illustrated the geology of the region – and, especially, strata of Turonian age – in a particularly professional manner. He was the first to distinguish between the grey, unfossiliferous sandy-marly clays with pyrite nodules, and the marly limestones with *Inoceramus brongniarti* and beds with abundant *Scaphites geinitzi* and/or *Inoceramus cuvieri*. According to Leonhard, the Cenomanian was only developed in a sandy facies: most fossils described by the Roemer brothers had exclusively been recovered from sections in the scaphitid-rich beds. In the upper part of the *Inoceramus brongniarti* interval, he noted two marly layers with the brachiopod *Gyrosoria lata*.

Numerous new boreholes drilled at the beginning of the 20th century enabled a better understanding of the Opole Cretaceous lithostratigraphical succession. Palaeontological studies were resumed by Wegner (1913), who described a few dozen sponge, coral, bryozoan, cephalopod, crinoid and other macrofossil species. Some of the specimens described, however, represent the sole examples of these taxa ever recorded from Opole, which may be a consequence of either improper classification and sampling or of subsequent degradation and loss of outcrops from which this material had been collected.

In 1960, Biernat presented a geological map of the city of Opole. Some macro- and microfossils were also described, and the lithological zonation was corrected. As far as the biostratigraphy of the Turonian was concerned, an *Inoceramus labiatus* Zone (based exclusively on microfossils) was erected, as were the *I. lamarcki* and *Scaphites geinitzi* zones. Other influential papers from this interval include those by Alexandrowicz and Radwan (1973) and Alexandrowicz (1974, 1975).

Tarkowski (1991) attempted to synthesise all available data on the Opole Cretaceous, with the emphasis on macrofauna and biostratigraphy. A more workable biozonation can be found in a subsequent paper (Tarkowski 1996); that being said, the macrofaunal assemblages described in those papers are in need of re-evaluation and additional comments, representing a promising field for future study. An independent biozonation was developed by Walaszczyk (1988, 1992), who presented clear divisions based on well-known inoceramid taxa.

Kędzierski (1995) discussed the nannofauna and detected lower Turonian strata at Odra quarry (see also Kędzierski 2008), while Kędzierski and Uchman (2001) presented an outline of ichnofossil assemblages and ichnofabrics. Olszewska-Nejbert (2007) recorded irregular echinoids from the section exposed at Odra Nowa and Folwark, noting numerous specimens of the spatangoid genus *Micraster* and the holasteroid *Echinocorys*.

GEOLOGICAL HISTORY OF THE OPOLE TROUGH

The Opole Trough is a remnant of a more widespread Upper Cretaceous cover, subsequently eroded during the Cenozoic. The total thickness of Cretaceous deposits in the Opole Trough is ~300 m, spanning the Cenomanian to upper Coniacian (and, quite possibly, Santonian) and resting upon an uneven topography of the Palaeozoic and Triassic basement, and covered to some degree by Miocene and Quaternary strata (Kotański and Radwański 1977). Cretaceous deposits within the Opole Trough dip gently to the west: the oldest (upper Cenomanian) levels are known exclusively in the eastern part (near Opole), whereas the youngest (upper Coniacian–?Santonian) crop out in the west (Kotański and Radwański 1977; Tarkowski 1991; Walaszczyk 1992). That being acknowledged, this general pattern is belied by a complex tectonic structure (Figs 1, 2).

The Opole Trough (Figs 2, 3) lies in a transitional zone between the Tethyan and Boreal realms, bounded by the Bohemian Cretaceous Basin and the Intra-Sudetic Basin (Nysa Trough), which broadly span the same chronostratigraphical range with a comparable facies development. Collectively, during the

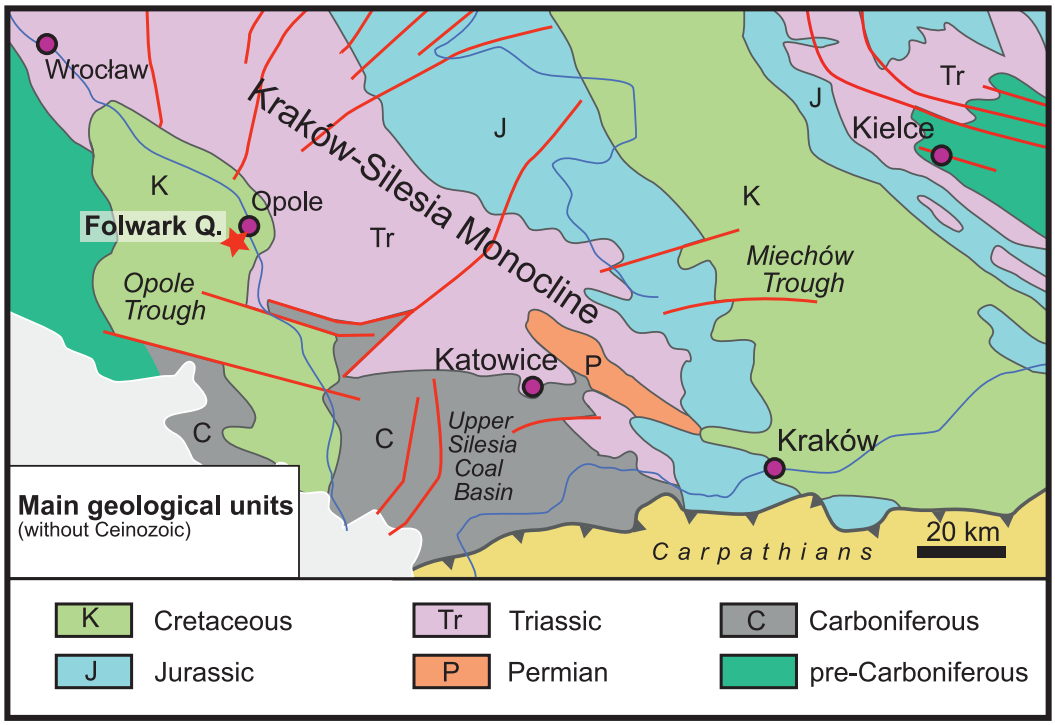

Fig. 2. The main geological units around the Opole Trough (from Kędzierski and Uchman 2015).

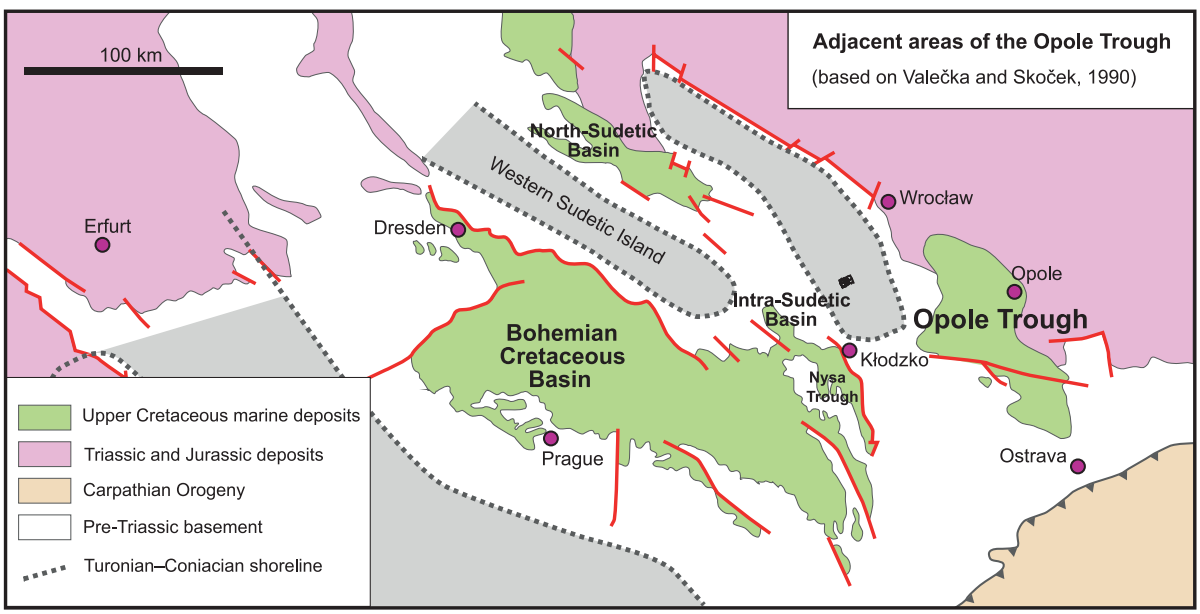

Fig. 3. Areas in Germany and the Czech Republic adjacent to the Opole Trough (from Kędzierski and Uchman 2015).

Cenomanian–Coniacian, these basins were supplied mainly by clastics from the Sudetic Islands. As such, the Opole Trough is regarded to be part of the Circum-Sudetic Trap Basin (*sensu* Walaszczyk 1992).

OPOLE CRETACEOUS – A COMPOSITE SECTION

As outlined extensively by Kędzierski and Uchman (2015), a singular transgression-re-

gression megacycle is developed here, in bedded chalk facies. [The bedded-chalk facies differs from the more typical massive chalk facies in having distinctive bedding planes, caused by varying siliciclastic input; it is typically observed as marlstone-limestone cyclicity. (Wray et al. 1995)]. Lithologically, the sequence exposed is quite monotonous: in general, the calcium carbonate content increases from the bottom of the succession to the Marly Limestones, above which carbonate abundance gradually decreases. There is some alternation of more and less clayey layers throughout the section that are linked to Milankovitch cyclicity, and some levels are highly bioturbated.

On the basis of borehole, core and extensive outcrop analyses, the following informal lithological scheme is widely recognised (Alexandrowicz and Radwan 1973; Fig. 4 here):

1. Sands and sandstones (Cenomanian: not currently exposed, and known primarily from drill core);
2. Lower Clayey Marls Unit (lower–middle Turonian: *Mytiloides* ex gr. *labiatus* to *Inoceramus apicalis* zones);
3. Lower Marls Unit (middle–upper Turonian: *I. lamarcki* to *I. perplexus* zones);
4. Marly Limestones Unit (upper Turonian: *I. perplexus* to *I. incertus* zones);
5. Upper Marls Unit (upper Turonian: *I. incertus* Zone);
6. Upper Clayey Marls Unit (upper Turonian–lower Coniacian: *I. incertus* through *I. kleini* zones).

It should be noted that the lithostratigraphical development presented here is quite comparable to that in the Bohemian Cretaceous Basin, as first outlined by Kędzierski and Uchman (2015). There, the middle Turonian Jizera Formation is composed of strata with elevated carbonate contributions; the overlying and underlying Bílá Hora and Teplice formations, respectively, reflect increasing siliciclastic contributions (Čech et al. 1980). The general trend in long-term accommodation and sedimentation rates – that is, a continued increase from the early Turonian through the early Coniacian, and possibly beyond – is broadly similar to that observed in the Bohemian Cretaceous Basin (Uličny et al. 2009). In this context, Kędzierski and Uchman (2015) suggested that the genetic sequences erected by Uličny et al. (2009) in the Bohemian Cretaceous Basin are also applicable to the Opole Trough.

Note: At Odra Nowa, only units 2–4 are exposed to date. Units 2–6 have been referred to as the Prószków Formation (Alexandrowicz and Radwań 1973), although this nomenclature has not been widely adopted.

ODRA NOWA (ODRA II) AND FOLWARK

At the present time, Odra Nowa and Folwark are the only active Cretaceous quarries in the vicinity of Opole. Odra Nowa (Odra II) is connected subterraneously with the now defunct, partially overgrown Odra Stara (Odra I) quarry. Here, three informal members can be distinguished: from bottom to top, these are the Lower Clayey Marls, the Lower Marls and the Marly Limestones. In general, the changes in lithology reflect progressively (i) increasing carbonate and (ii) decreasing organic matter and pyrite contributions. This has been interpreted as a general deepening trend and greater distances from the shoreline. Higher frequency lithological variation is putatively related to Milankovitch cycles, although this does merit further study. Two notable layers within the sequence are (i) a coquina-style hardground layer at the base of the Lower Marls and (ii) a limestone layer close to the top of the Lower Marls. Along with the Marly Limestones, the upper Turonian to lower Coniacian Upper Marls and Upper Clayey Marls are only represented at the large Folwark quarry: due to this and its excellent, fresh exposures, Folwark has been chosen as the main locality for the this field trip.

Palaeoenvironment and invertebrate macrobiota

The limy, soupy bottom of the Turonian Opole sea has been considered to be an inhospitable environment, deposited beneath storm wave base in a calm-water environment with low to moderate sedimentation rates. Despite this, numerous benthic groups established their presence here, largely due to specialised adaptive morphologies: for instance, the

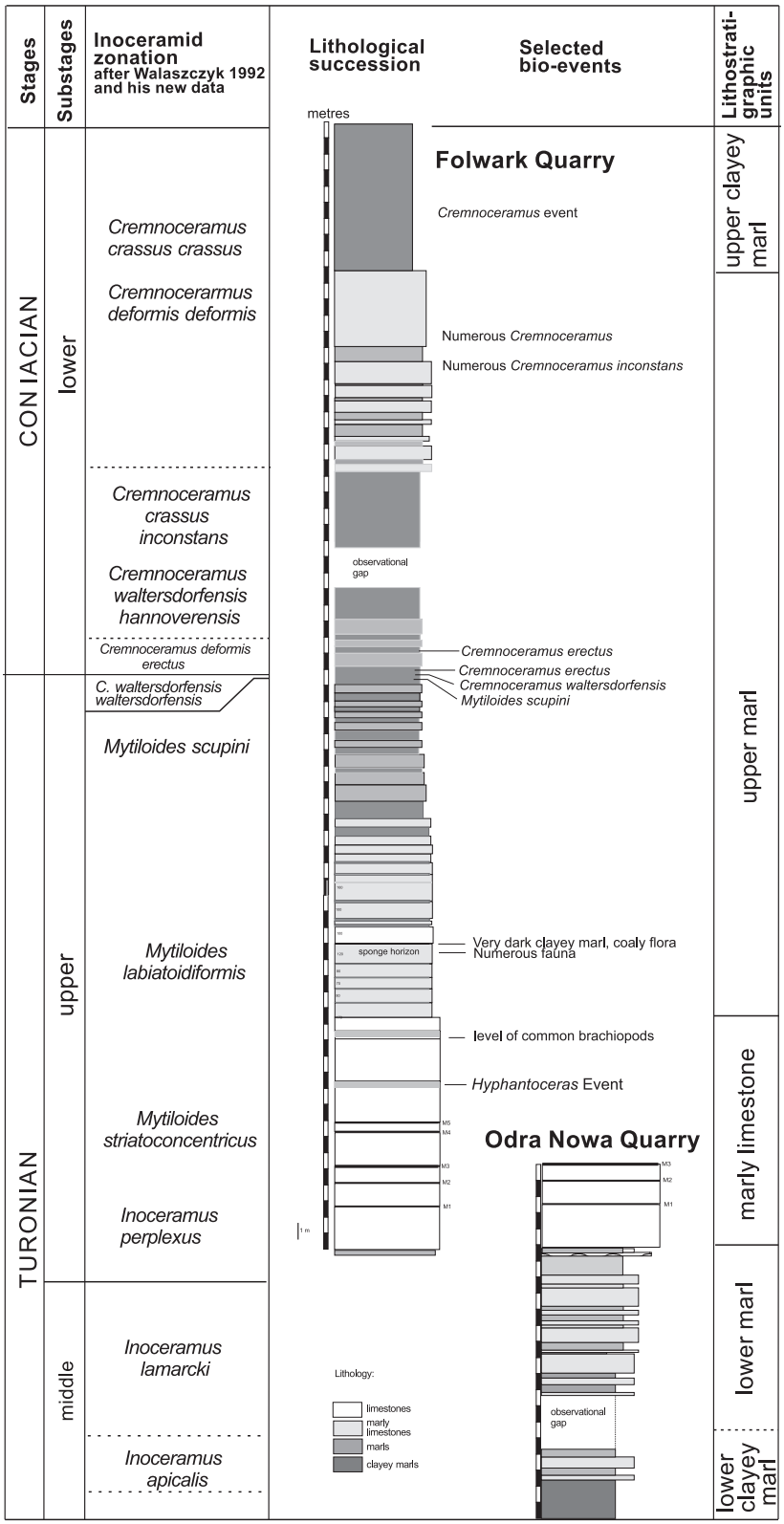

Fig. 4. Lithological succession, lithostratigraphy, inoceramid zonation and selected events of the Turonian–Coniacian succession in the Opole area, as exposed in the Odra Nowa and Folwark quarries; after Walaszczyk (1992) and Walaszczyk and Todes (in preparation); lithological units after Alexandrowicz and Radwan (1973).

sclerobiont habit, the employment of snowshoe and iceberg strategies, the development of root-like systems, and – quite possibly – chemosymbiosis. Since many literature-based identifications are difficult to interpret and verify, the following data are based mainly on newly collected specimens.

Among the most common invertebrate groups are sponges, in particular ventriculitid hexactinellids. The Opole sponge fauna has recently been revised, and dozens of species have now been identified (Świerczewska-Gładysz 2012; Świerczewska-Gładysz and Jurkowska 2013; Świerczewska-Gładysz et al. 2019). Apart from ventriculitids, other Lychniscosida are also known; Lyssacinosida and Sceptrulophora taxa are much rarer. Ventriculitids often possess a root-like system and a calice shape, which allow for firm attachment to the sea floor and elevated, tiered filter feeding. In lyssacinoids, basal spicule tufts 'lift' the sponge body above the soupy sediment-water interface. The Demospongiae are chiefly 'lithistids'. Sponges are preserved mainly in limonite, which in the Opole Cretaceous is a product of pyrite weathering. Clionaid sponge borings (ichnogenus *Entobia*) can often be recognised in inoceramid shells.

Corals are a rare component of the benthos; despite this, both hexacorals, as primitive micrabaciids and caryophyllids, and octocorals, as attachments of bamboo corals (Isididae), are represented.

Bivalves are relatively common in the Opole Cretaceous succession. To date, inoceramids have been the focus of most work, largely on account of their biostratigraphical value (e.g., Walaszczyk 1988; Tarkowski 1991). That being acknowledged, oysters – especially gryphaeids – are equally abundant. Spiny spondylids and wood-boring pholadoids are also reasonably common, and a complete inventory of bivalves from the Opole Cretaceous also includes protobranchs, anomiids, pectinids, mytilids, bakevelliids and radiolitids. A diversity of functional strategies was employed by these bivalves: many were initially cemented to a hard substrate and either remained attached (e.g., many anomiids, some oysters, *Spondylus latus*) or subsequently proceeded to free-living life strategies (oysters, spondylids). Some bivalves were infaunal, and pholadoids are known from their calcite-lined burrows into driftwood. It is possible that some inoceramids may have been able to harbour chemosymbionts. Rare rudists may have been deposited *post mortem*, as float.

Gastropods are represented chiefly by vetigastropods – that is, turbiniform taxa and large sponge-feeding pleurotomariids. These are often preserved as composite moulds or 'ghosts', which occasionally preserve ornamentation in great detail.

Both terebratulid and rhynchonellid brachiopods are common. With regard to terebratulids, small cancellothyridids (*Gyrosoria lata*) do occur *en masse*, and pedicle etching traces of the ichnogenus *Podichnus* can be found on inoceramids. Larger terebratulids are represented by the genus *Gibbithyris*. The rhynchonellid fauna remains poorly studied, but appears to comprise members of the genera *Orbirhynchia*, *Woodwardirhynchia, Cyclothyris* and *Cretirhynchia*.

Apart from some bivalves, common sclerobionts include bryozoans and serpulids. Both cyclostome ('*Stomatopora*', '*Proboscina*' and '*Berenicea*') and cheilostome bryozoans are known to occur; the latter include a primitive electrid (*Herpetopora*) and somewhat more advanced forms, such as *Biaviculigera*. The serpulid fauna is diverse and includes representatives of the genera *Neomicrorbis*, *Dorsoserpula*, *Neovermilia*, *Propomatoceros* and *Spiraserpula*.

The most common echinoderms are spatangoid (micrasterids) and holasteroid (*Plesiocorys* (*Sternotaxis*) *plana*, *Echinocorys*) echinoids (Olszewska-Nejbert 2007). Burrows (ichnotaxa) produced by those taxa (*Scolicia*) can also be found. Regular echinoids are rare and are chiefly (and, in the case of cidaroids, only) known from spines, although there are historical records of complete tests. Smaller-sized tests of the phymosomatid *Gauthieria* and Zeuglopleuridae are also on record. Crinoids are known by isolated elements of stalks, cups and arms (isocrinids) and bourgueticrinid root systems and cups (Jagt and Salamon 2007). Other comatulids are also known, albeit rarely: for the Lower Clayey Marls. Sea stars are represented by pycinasterid and goniasterid 'valvatids', mostly in the form of dissociated marginal ossicles. Ophiuroids are present as well, albeit rarely; to date, only *Ophiotitanos serrata* has been identified at the species level.

Arthropods constitute yet another diverse group: many ichnofossils (e.g., *Thalassinoides*) in the Opole Cretaceous can be ascribed to their activities. Minute podocopid ostracods are common. No crabs are known to date, but lobsters (*Enoploclytia*) have been recorded (Jagt *et al*., 2015). The cirripede fauna, which includes cretiscalpellids, scalpellids and stramentids, is currently under study (Jagt and Mazurek 2010, in prep.).

With regard to nektic invertebrates, nautiloids are rather rare and poorly known taxonomically. For the most part, stratigraphically important Turonian ammonites (i.e., colligoniceratids) are too rare for practical use in biostratigraphy. That being said, the desmoceratoid *Lewesiceras* is common: some shells are known to reach over a metre in diameter. Two problematic specimens have been assigned to the genus *Pachydesmoceras* (Kin and Niedźwiedzki 2012). Heteromorph ammonites are the most diverse group, and comprise common scaphitids and *Allocrioceras*, and rarer nostoceratids (*Hyphantoceras*, *Nostoceras* [*sensu lato*]): the latter are particularly abundant in the *Hyphantoceras* Event Bed.

Inoceramid biostratigraphy

Given the importance of inoceramids for biostratigraphical correlation in the Upper Cretaceous, it is worth delving briefly into the Opole inoceramid succession. Inoceramids form the basis of the Opole Cretaceous biozonation scheme (Walaszczyk 1988; Tarkowski 1996; Fig. 4) – which, while certainly still applicable, is somewhat dated with regard to taxonomic concepts and zonation schemes. As such, a revision of the inoceramid fauna, biostratigraphy and biozonation scheme of the Opole Cretaceous is currently in progress (Walaszczyk and Todes, in prep.).

As observed by Walaszczyk (1988), the Lower Clayey Marls recognised at Odra Nowa quarry lie in the middle Turonian *Inoceramus apicalis* Zone. The *I. lamarcki Z*one is located a few (2–3) metres above the base of the Lower Marls. As of 1988, there was an observational gap between the Folwark and Odra Nowa quarries. However, the progressive expansion of Folwark over the past 3–4 years has enabled precise correlation across the River Odra: at present, the *Hyphantoceras* Event is located 9–10 m above the base of the Folwark Quarry (Fig. 4). The standard inoceramid zonation for the central European upper Turonian – that is, the *I. perplexus, Mytiloides striatoconcentricus, M. labiatoidiformis* and *M. scupini* zones – is applicable to the Opole Cretaceous succession, although additional work is needed to identify the taxa ranges and zonal boundaries precisely (Wiese et al. 2020). Importantly, the inoceramid 'barren zone' characteristic of many central European upper Turonian successions is present in Folwark.

A rapid taxonomic turnover from the late Turonian *Mytiloides*-dominated fauna to the latest Turonian–early Coniacian *Cremnoceramus*-dominated fauna is readily recognised in the middle Upper Marls, with the flood introduction of *Cremnoceramus waltersdorfensis waltersforfensis*, the zonal index of the epynomous zone. Less than a metre above, *C. deformis erectus,* which by definition marks the base of the Coniacian (Walaszczyk et al., 2022), appears. The standard early Coniacian inoceramid biozonation – that is, the *C. deformis erectus*, *C. w. hannovrensis*, *C. crassus inconstans* and *C. c. crassus* zones – can be erected at Folwark Quarry; the Upper Marls–Upper Clayey Marls boundary being located within the *C. c. crassus* Zone. In general, the latest Turonian–early Coniacian inoceramid succession in the Opole Trough is easily correlatable with the classic Turonian–Coniacian boundary sections in Salzgitter-Salder and Słupia Nadbrzeżna (Walaszczyk et al. 2010, 2022).

Vertebrates

At the Odra Nowa quarry (Turonian; Figs 5, 6) and other outcrops in the Opole area (for instance, Folwark and Bolko quarries; Cenomanian–Coniacian), fish remains are quite abundant, but usually relatively small, easily overlooked and non-diagnostic; consequently, the ichthyofauna is rather poorly known. Sharks usually occur as isolated teeth or tooth crowns. Teleosts (the most common osteichthyan group) can be collected as isolated teeth, scales or bones, and/or are concentrated in spatial association with trace fossils (in particular, *Lepidenteron lewesiensis*; see Jurkowska and Uchman, 2013; Bieńkowska-Wasiluk *et al*., 2015), burrows (i.e., bottom-cur-

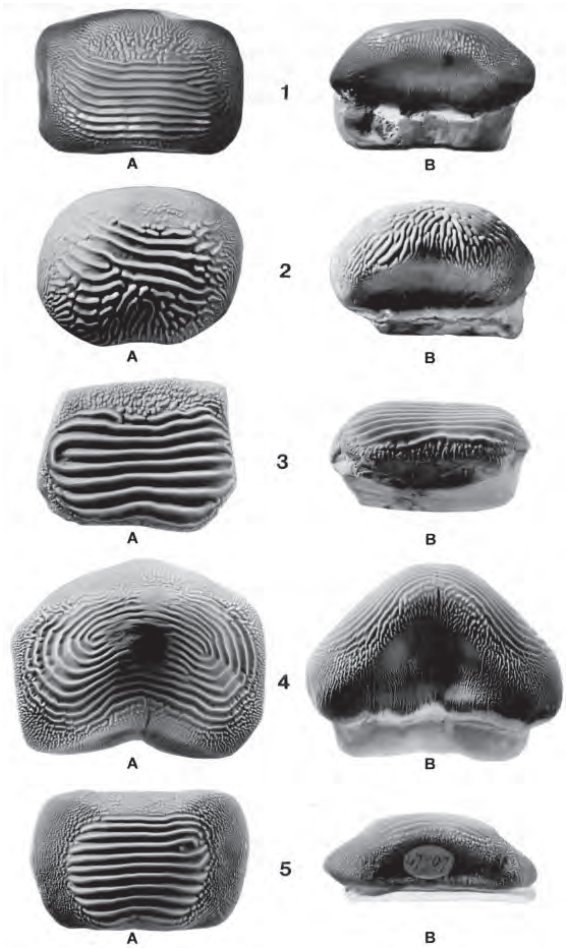

Fig. 5. Ptychodontid shark teeth: *Ptychodus decurrens* (1), *P. oweni* (2), *P. polygyrus* (3), *P. concentricus* (4) and *P. marginalis* (5) (after Longbottom and Patterson 2002).

rent resedimentation), or in the residues and/or regurgitates of piscivorous animals.

Leonhard (1898) described teeth of three shark species, *Hybodus dentatus*, *Notidanus microdon* and *Ptychodus mammillaris*, and several unidentified corprolites and vertebrae. All recorded ganoids are pycnodonts – namely, *Coelodus complanatus*, *Coelodus cretaceus* and *Ganoideorum*? sp. – while teleosts recognised include *Enchodus halocyon*, *Osmeroides lewesiensis*, *Beryx zippei*, *Beryx* sp., *Saurocephalus marginatus* and *Protosphyraena ferox*.

Osteichthyans have remained virtually unrecognised since Leonhard (1898). Niedźwiedzki and Kalina (2003), dealing with sharks from Opole, recorded mainly ptychodontids – for instance, *Ptychodus latissimus*, *Ptychodus polygyrus* and *Ptychodus mammillaris*. Other shark clades are also represented: Niedźwiedzki and Kalina (2003) listed anacoracids (*Squalicorax* sp.), mitsukurinids (*Scapanorhynchus raphiodon)*, alopiids (*Paranomotodon angustidens*) and unidentified cretoxyrhinids.

Ptychodus was a shell-crushing (durophagous) shark (Fig. 5); at Odra Nowa, accumulations of *Ptychodus* teeth occur, albeit rarely. The Lower Marls – and in particular, the lower portion of this informal unit – have mainly yielded teeth of *P. mammillaris*, potentially linked to the contemporaneous occurrence of common small inoceramid taxa and heteromorph ammonites. Higher in the succession, *P. latissimus* and *P. polygyrus* are found in association with their preferred large inoceramid prey. Additional, recent discoveries of shark remains constitute mainly cretoxyrhinid teeth, with numerous other lamniforms. A few unidentifiable shark coprolites (or intestinal fillings; see Hunt *et al*. 2015) have been collected as well; these appear to be fairly common in the Lower Clayey Marls, especially below the two prominent limestone levels (Fig. 4).

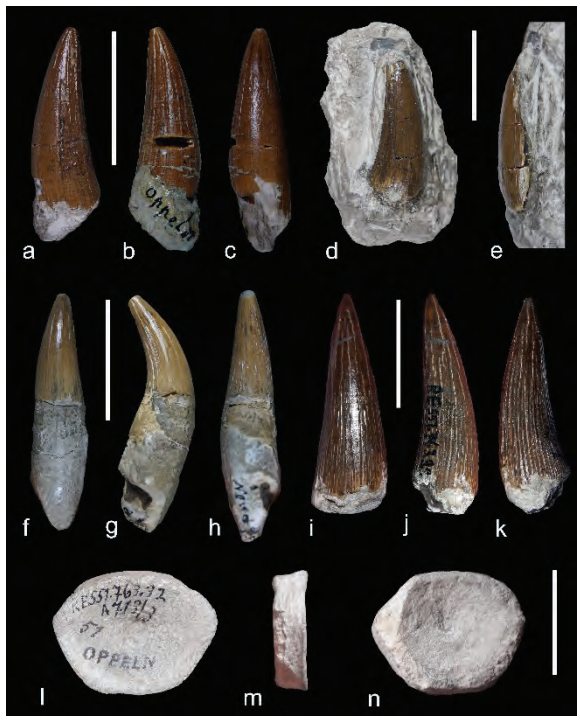

Fig. 6. Teeth and tooth crowns of polycotylid plesiosaurians (a–h) and a purported plesiosaurian limb bone (l–n) (after Sachs et al. 2018).

Recently, Sachs *et al*. (2018) reported on the rediscovery of most of the 19th century reptile material described from Opole by Leonhard (1898), as well as some additional material collected by that author. This collection is composed of teeth belonging to polycotylid plesiosaurians and a russellosaurine mosasauroid and a single purported plesiosaurian limb bone (Fig. 6). In 2009, one of the authors (DM) collected a specimen that may represent sea turtle material.

Flora

Elements of terrestrial flora are very common and include conifers (frenelopsids, *Geinitzia*) and flowering plants (Hellemond 2015, Mazurek et al., in prep.). Most plant fossils are, however, unidentifiable, encompassing carbonised driftwood (often bored by teredinids or pholadoids), debris and burrow infill (*Lepidenteron mantelli*). The spore and pollen record illustrates a diverse florule, with various ferns, conifers and other plants (Płachno *et al.*, 2019).

Ichnofauna

All Cretaceous sedimentary rocks in the Opole area are characterised by a pervasively bioturbated background, resulting in preservation of only the mixed layer. For the most part, all primary sedimentary structures are completely obliterated (Kędzierski and Uchman 2001). Some exceptions to this general paradigm can be recognised in the lowermost part of Odra Nowa Quarry (Lower Clayey Marls) and the uppermost part of Folwark Quarry (siliceous marls within the Upper Clayey Marls), where rare primary lamination is partially preserved. The completely bioturbated portions of the Opole Cretaceous contain numerous ichnofossils, including *Ophiomorpha* isp., *Phycosiphon* isp., *Palaeophycus* isp., *Planolites* isp., *Teichichnus* isp. and *Thalassinoides* isp., assigned to the *Thalassinoides* ichnofabric – a typical representation of the *Cruziana* ichnofacies, indicative of a subtidal, well-oxygenated, soupy substrate between fair-weather and storm-wave base. The ichnofossil *Lepidenteron mantelli* – interpreted as having been produced by a burrowing marine invertebrate (likely a polychaete) that sequestered plant remains – is found in a limited stratigraphical range in the Marly Limestone Unit (Jurkowska et al. 2018). Importantly, there is a colour contrast between the background matrix and trace fossil infillings, which may be a consequence of the decay of abundant organic matter that accumulated during short episodes of sea floor oxygen depletion, followed by bioturbation during times of increased bottom-water ventilation. Moreover, the colour contrast almost disappears in the Marly Limestone Unit, which is reminiscent of the nodular English Chalk and reveals the largest *Thalassinoides* isp. in the entire succession, with tunnels of up to 100 mm in width (Kędzierski and Uchman 2001, 2015).

In those parts of the succession where partially preserved primary lamination is visible, *Chondrites* isp. dominates over *Thalassinoides* isp.; *Trichichnus* isp. is also abundant. This feature is characteristic of the *Chondrites* ichnofabric, which, in turn, is considered indicative of less oxygenated *Thalassinoides* ichnofabric deposits. It is particularly intriguing that this ichnofabric is present in the uppermost part of the section exposed at Folwark quarry (siliceous marls), where exceptionally thick *Trichichnus* isp. occurs. If *Trichichnus* isp. is indeed a remnant of bioelectrical processes of giant, *Thioploca*-like sulphur bacteria, this may be evidence that these marls were deposited under upwelling conditions. Additional support for this premise is provided by the abundant occurrence of radiolarians (Kędzierski and Uchman 2001, 2015; Kędzierski et al. 2015).

Microfauna and geochemistry

Recent microfaunal studies in the Opole Trough have been limited to focused investigations of dinoflagellate cysts and foraminifera in the Turonian–Coniacian boundary interval (Stróżyk et al. 2018). The dinoflagellate cyst record from the Opole succession has not been systematically examined, but appears to be a promising field for future work. Further studies of planktic and benthic foraminifera through the entire Opole succession are currently in progress (Dubicka, in prep.).

A taxonomically rich, well-preserved dinoflagellate fauna has been recovered from the Turonian–Coniacian boundary interval at Folwark Quarry: 67 species have been rec-

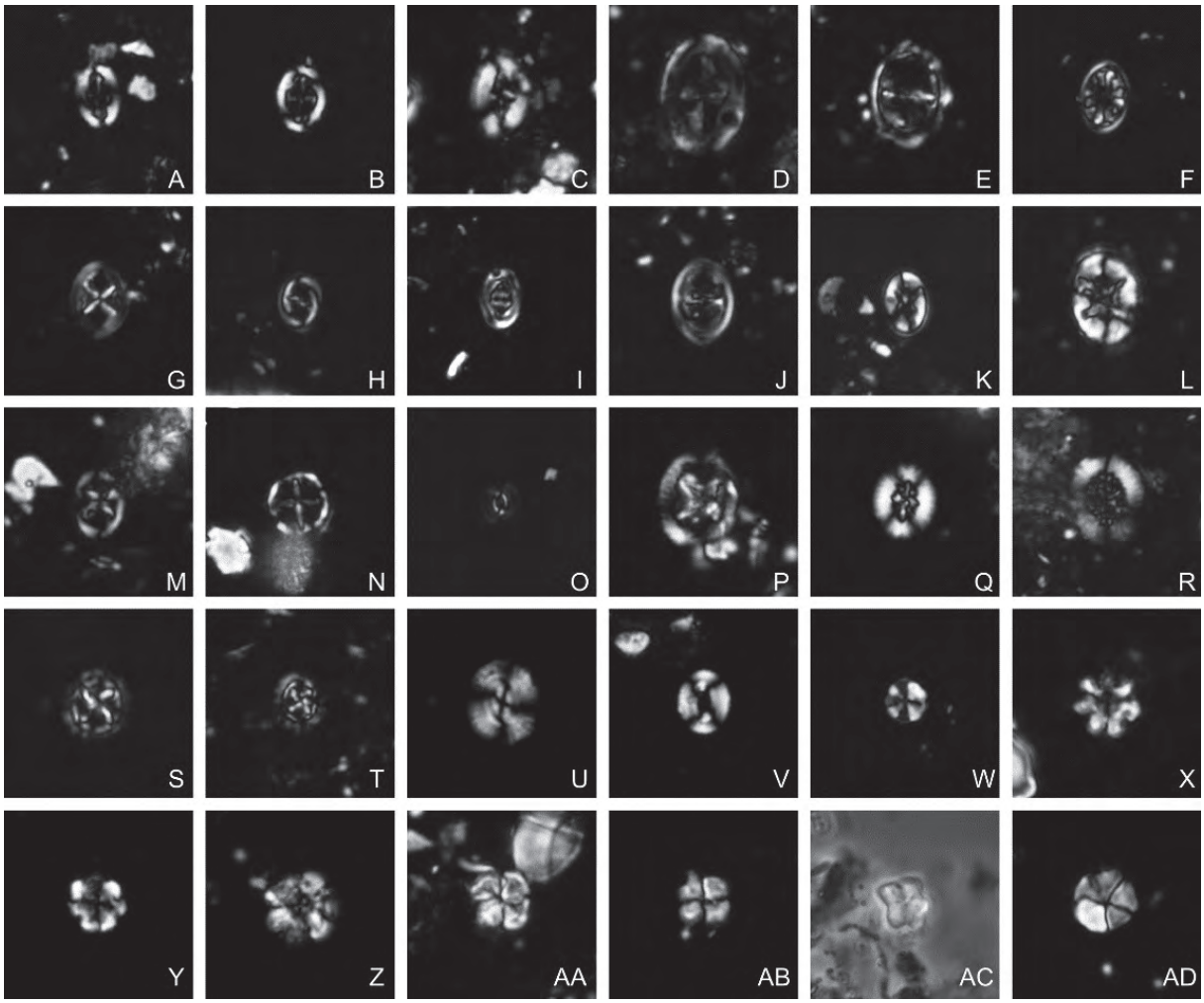

Fig. 7. Selected calcareous nannofossils from the lower–middle Turonian in cross-polarised and phase contrast (P) light: A – *Broinsonia signata*; B – *Broinsonia matalosa*; C – *Broinsonia furtiva*; D – *Gartnerago obliquum*; E – *Gartnerago theta*; F – *Ahmuellerella octoradiata*; G – *Chiastozygus litterarius*; H – *Placozygus fibuliformis*; I – *Zeugrhabdotus bicrescenticus*; J – *Zeugrhabdotus scutula*; K – *Eiffellithus casulus*; L – *Eiffellithus turriseiffelli*; M – *Tegumentum stradneri*; N – *Stoverius achylosus*; O – *Biscutum constans*; P – *Grantharabdus coronadventis*; Q – *Retecapsa angustiforata*; R – *Retecapsa crenulata*; S – *Prediscosphaera ponticula*; T – *Prediscosphaera cretacea*; U – *Watznaueria barnesiae*; V – *Watznaueria fossacincta*; W – *Eprolithus floralis*; X, Y – *Eprolithus moratus*; Z – *Eprolithus octopetalus*; AA, AB – *Quadrum gartneri*; AC – *Quadrum intermedium* (P); AD – *Braarudosphaera* sp.

ognised (Stróżyk et al. 2018). In Opole, the Turonian–Coniacian boundary is approximated by the highest occurrences of *Circulodinium distinctum*, *Stephodinium coronatum*, *Florentinia ferox* and *Senoniasphaera rotundata alveolata,* with an additional acme of *Palaeohystrichophora infusorioides* in the basal Coniacian. Incidentally, many biostratigraphically critical forms are absent, adding to a growing body of evidence indicative of considerable dinocyst assemblage heterogeneity in the Turonian–Coniacian boundary interval. That being said, the dinocyst assemblages are broadly comparable to those recognised in the Bohemian Cretaceous Basin, suggesting comparable palaeoenvironmental controls on dinoflagellate distribution throughout the Circum-Sudetic Trap Basin (Olde et al. 2015).

Both planktic and benthic foraminifera are abundant and well preserved in the Opole Cretaceous succession. In the Turonian–Coniacian boundary interval, planktic foraminiferal assemblages are of low diversity, typically

dominated by long-ranging taxa with limited stratigraphical utility. By contrast, stratigraphically pertinent events within several benthic foraminiferal lineages – namely, transitions in the *Gavelinella vesca–G. praeinfrasantonica*, *G. ammonoides–G. loreiana* and *Protostensioeina* lineages – have been recognised (Stróżyk et al. 2018). Importantly, these events have high correlation potential for recognising the base of the Coniacian Stage. The *Protostensioeina* transitional event, in particular, has been recognised as a precise marker of the Turonian–Coniacian boundary in the Salzgitter-Salder stratotype (Peryt and Dubicka *in* Walaszczyk *et al*. 2022).

Carbon ($\delta^{13}C$) and oxygen ($\delta^{18}O$) chemostratigraphical records have been developed from the succession exposed at Odra Nowa and Folwark quarries (Walaszczyk and Todes, in prep.). Broadly, the major upper Turonian and lower Coniacian carbon isotope events – the upper Turonian Bridgewick $\delta^{13}C$ minimum and subsequent Hitch Wood $\delta^{13}C$ maximum, the Turonian–Coniacian Navigation $\delta^{13}C$ minimum, and the lower Coniacian Beeding $\delta^{13}C$ maximum – are recognised in the Opole succession, although $\delta^{13}C$ values are *c*. 0.5‰ lower than in the English Chalk, and about 1‰ heavier than in the Bohemian Cretaceous Basin (Jarvis et al. 2006, 2015). $\delta^{18}O$ values are relatively stable at *c*. -3.5‰, with minimal stratigraphical variation.

Calcareous nannofossils

Under 1,000x light microscopy, smear slides from the Opole Cretaceous reveal a very diverse, well-preserved nannofossil assemblage; indeed, most visible carbonates are fragmentary or complete nannofossils (Fig. 7). Overall, the assemblage consists of >80 calcareous nannofossil species, dominated by the genus *Watznaueria.* This is comparable to other Turonian–Coniacian deposits, although there are surprising appearances of *Petrarhabdus copulatus* and *Staurolithes imbricatus*, which typically first appear in the Santonian. The occurrence of *Nannoconus* in the Lower Marl Unit may be indicative of a considerable Tethyan influence, in stark contrast to the occurrence of the high-latitude species *Repagulum parvidentatum* in the youngest deposits (Kędzierski 2008). Moreover, the genus *Nannoconus* co-occurs with *Liliasterites angularis*, as is also known from the Bohemian Cretaceous Basin (Kędzierski 2008).

Biostratigraphically, strata at the Odra Nowa and Folwark quarries represent the UC6 through UC10 nannofossil zones of Burnett (1998). These zones are chronostratigraphically correlated with the late early Turonian to the middle Coniacian (Kędzierski 2008).

REFERENCES

Alexandrowicz, S.W. 1974. Kreda opolska. In: Rutkowski, J. (Ed.), Przewodnik XLVI Zjazdu PTG, Opole, 12–14 września 1974, pp. 29–38.

Alexandrowicz S.W. 1975. Margle kredowe w Komprachcicach koło Opola. Przegląd Geologiczny, 22, 66–68.

Alexandrowicz, S.W. and Radwan, D. 1973. Kreda opolska – problematyka stratygraficzna i złożowa. Przegląd Geologiczny, 240, 183–188.

Bereszyński, Z. 2007. Pierwsza opolska cementownia powstała 150 lat temu. Gazeta Wyborcza, March 29, 2007.

Bieńkowska-Wasiluk, M., Uchman, A., Jurkowska, A. and Świerczewska-Gładysz, E. 2015. The trace fossil *Lepidenteron lewesiensis*: a taphonomic window on diversity of Late Cretaceous fishes. Paläontologische Zeitschrift, 89, 795–806.

Biernat, S. 1960. Budowa geologiczna kredy opolskiej. Biuletyn Instytutu Geologicznego, 152, 173–241.

Burnett, J.A. 1998. Upper Cretaceous. In: Bown, P.R. (Ed.), Calcareous nannofossil biostratigraphy, pp. 132–199. Kluwer Academic Publishers, Dordrecht.

Čech, S., Klein, V., Kříž, J. and Valečka, J., 1980. Revision of the Upper Cretaceous stratigraphy of the Bohemian Cretaceous Basin. Věstník Ústředního ústavu geologického, 55, 277–296.

Hellemond, A. 2015. First note on the discovery of a Turonian conifer twig from the Folwark quarry in Opole (Poland). First note on the discovery of a Turonian conifer twig from the Folwark quarry in Opole (Poland) (researchgate.net)

Hunt, A.P., Lucas, S.G., Milàn, J., Lichtig, A.J. and Jagt, J.W.M. 2015. Vertebrate coprolites from Cretaceous chalk in Europe and North America and the shark surplus paradox. In: Sullivan, R.M. and Lucas, S.G. (Eds), Fossil Record 4. New Mexico Museum of Natural History and Science Bulletin, 67, 63–68.

Jagt, J.W.M., Jagt-Yazykova, E.A. and Kijok, R. 2015. Notes on Turonian decapod crustacean body fossils and ichnotaxa from Odra Nowa Quarry, Opole (southwest Poland). Nature Journal, Opole Scientific Society, 43, 117–122.

Jagt, J.W.M. and Mazurek, D. 2010. A calanticid cirripede from the middle Turonian of the Opole Cretaceous

Basin. Nature Journal, Opole Scientific Society, 48, 101–113.

Jagt, J.W.M. and Salamon, M.A. 2007. Late Cretaceous bourgueticrinid crinoids from southern Poland – preliminary observations. Scripta Geologica, 134, 61–76.

Jarvis, I., Gale, A.S., Jenkyns, H.C. and Pearce, M.A. 2006. Secular variation in Late Cretaceous carbon isotopes: a new $\delta^{13}C$ carbonate reference curve for the Cenomanian–Campanian (99.6–70.6 Ma). Geological Magazine, 143, 561–608.

Jarvis, I., Trabucho-Alexandre, J., Gröcke, D.R., Uličný, D. and Laurin, J. 2015. Intercontinental correlation of organic carbon and carbonate stable isotope records: evidence of climate and sea-level change during the Turonian (Cretaceous). The Depositional Record, 1, 53–90.

Jurkowska, A. and Uchman, A. 2013. The trace fossil *Lepidenteron lewesiensis* (Mantell, 1822) from the Upper Cretaceous of southern Poland. Acta Geologica Polonica, 63, 611–623.

Jurkowska, A., Uchman, A. and Świerczewska-Gładysz, E. 2018. A record of sequestration of plant material by marine burrowing animals as a new feeding strategy under oligotrophic conditions evidenced by pyrite microtextures. Palaios, 33, 312–322.

Kędzierski, M. 1995. Stratygrafia turonu i koniaku okolic Opola na podstawie nanoplanktonu wapiennego. Przegląd Geologiczny, 43, 406–408.

Kędzierski, M. 2008. Calcareous nannofossil and inoceramid biostratigraphies of a Middle Turonian to Middle Coniacian section from the Opole Trough of SW Poland. Cretaceous Research, 29, 451–467.

Kędzierski, M. and Uchman, A. 2001. Ichnofabrics of the Upper Cretaceous marlstones in the Opole region, southern Poland. Acta Geologica Polonica, 51, 81–91.

Kędzierski, M. and Uchman, A. 2015. Bedded chalk marls in the Opole Trough: epicratonic deposits of the Late Cretaceous super-greenhouse episode. In: Haczewski, G. (Ed.), Guidebook for field trips accompanying 31st IAS Meeting of Sedimentology held in Kraków on 22nd–25th of June 2015, 145–158. Polish Geological Society, Kraków.

Kędzierski, M., Uchman, A., Sawlowicz, Z. and Briguglio, A. 2015. Fossilized bioelectric wire – the trace fossil Trichichnus. Biogeosciences, 12, 2301–2309.

Kin, A. and Niedźwiedzki, R. 2012. First record of the puzosiine ammonite genus Pachydesmoceras from the Middle and Upper Turonian of Poland. Cretaceous Research, 33, 15–20.

Kotański, Z. and Radwański, S. 1977. Geologia wgłębna opolszczyzny. Biuletyn Instytutu Geologicznego, 303, 91–163.

Leonhard, R. 1898. Die Fauna der Kreideformation in Oberschlesien. Palaeontographica, 44, 11–70.

Longbottom, A.E. and Patterson, C. 2002. Fishes. In: Smith, A.B. and Batten, D.J. (Eds), Fossils of the Chalk. Palaeontological Association, Field Guides to Fossils, no. 2 (second edition, revised and enlarged), pp. 296–324. The Palaeontological Association, London.

Mazurek, D. 2008. Paleoekologia i biostratygrafia utworów turonu (górna kreda) kamieniołomu Odra w Opolu. Uniwersytet Opolski, Wydział Przyrodniczo-Techniczny, Katedra Biosystematyki, Zakład Paleobiologii, Opole (Praca magisterska), 84 p.

Niedźwiedzki, R. and Kalina, M. 2003. Late Cretaceous sharks in the Opole Silesia region (SW Poland). Geologia Sudetica, 35, 13–24.

Olde, K., Jarvis, I., Pearce, M., Uličný, D., Tocher, B., Trabucho-Alexandre, J. and Gröcke, D. 2015. A revised northern European Turonian (Upper Cretaceous) dinoflagellate cyst biostratigraphy: integrating palynology and carbon isotope events. Review of Palaeobotany and Palynology, 213, 1–16.

Olszewska-Nejbert, D. 2007. Late Cretaceous (Turonian–Coniacian) irregular echinoids of western Kazakhstan (Mangyshlak) and southern Poland (Opole). Acta Geologica Polonica, 57, 1–87.

Płachno, B.J., Jurkowska, A., Pacyna, G., Worobiec, E., Gedl, P. and Świerczewska-Gładysz, E. 2018. Plant assemblage from Opole, southern Poland: new data on Late Cretaceous vegetation of the northern part of the European Province. Proceedings of the Geologists' Association, 129, 159–170.

Roemer, F. 1870. Geologie von Oberschlesien, xxiv + 587 pp. Nischkowsky, Breslau.

Roemer, F.A. 1840–1841. Die Versteinerungen des norddeutschen Kreidegebirges, iv + 1–48, pls 1–7 (1840); 49–145, pls 8–16 (1841). Hahn'sche Hofbuchhandlung, Hannover.

Roemer, F.A. 1864. Die Spongitarien des norddeutschen Kreide-Gebirges. Palaeontographica, 13, 1–63.

Sachs, S., Jagt, J.W.M., Niedźwiedzki, R., Kędzierski, M., Jagt-Yazykova, E. and Kear, B.P. 2018. Turonian marine amniotes from the Opole area in southwest Poland. Cretaceous Research, 84, 578–587.

Strózyk, K., Barski, M., Dubicka, Z. and Walaszczyk, I. 2018. Integrated biostratigraphy of the Turonian–Coniacian Boundary Interval in the Folwark Quarry (Opole Trough, SW Poland). 19th Czech–Slovak–Polish Paleontological Conference & MIKRO 2018 workshop. Folia Musei rerum naturalium Bohemiae occidentalis – Geologica et Paleobiologica, Special Volume, p. 82.

Świerczewska-Gładysz, E. 2012. Late Turonian and Early Coniacian ventriculitid sponges (Lychniscosida) from Opole Trough (southern Poland) and their palaeoecological significance. Annales Societatis Geologorum Poloniae, 82, 201–224.

Świerczewska-Gładysz, E. and Jurkowska, A. 2013. Occurrence and paleoecological significance of lyssacinosid sponges in the Upper Cretaceous deposits of southern Poland. Facies, 59, 763–777.

Świerczewska-Gładysz, E., Jurkowska, A. and Niedź-

wiedzki, R. 2019. New data about the Turonian–Coniacian sponge assemblage from Central Europe. Cretaceous Research, 94, 229–258.

Tarkowski, R. 1991. Stratygrafia, makroskamieniosci i paleogeografia utworów górnej kredy niecki opolskiej. Zeszyty Naukowe AGH, Geologia, 51, 1–156.

Tarkowski, R. 1996. Inoceramid biostratigraphy in the Turonian of the Opole Trough (southwestern Poland). In: Spaeth, C. (Ed.), New developments in Cretaceous research topics. Proceedings of the 4th International Cretaceous Symposium, Hamburg 1992. Mitteilungen aus dem Geologisch–Paläontologischen Institut der Universität Hamburg, 77 (J. Wiedmann Memorial Volume), pp. 489–501.

Uličny, D., Laurin, J. and Čech, S. 2009. Controls on clastic sequence geometries in a shallow-marine transtensional basin: the Bohemian Cretaceous Basin, Czech Republic. Sedimentology, 56, 1077–1114.

Walaszczyk, I. 1988. Inoceramid stratigraphy of the Turonian and Coniacian strata in the environs of Opole (southern Poland). Acta Geologica Polonica, 38, 51–61.

Walaszczyk, I. 1992. Turonian through Santonian deposits of the Central Polish Uplands: their facies development, inoceramid paleontology and stratigraphy. Acta Geologica Polonica, 42, 1–122.

Walaszczyk, I., Čech, S., Crampton, J.S., Dubicka, Z., Ifrim, C., Jarvis, I., Kennedy, W.J., Lees, J.A., Lodowski, D., Pearce, M., Peryt, D., Sageman, B.B., Schiøler, P., Todes, J., Uličný, D., Voigt, S. and F. Wiese, with contributions by C. Linnert, T. Püttmann and S. Toshimitsu. 2022. The Global Boundary Stratotype Section and Point (GSSP) for the base of the Coniacian Stage (Salzgitter-Salder, Germany) and its auxiliary sections (Słupia Nadbrzeżna, central Poland; Střeleč, Czech Republic; and El Rosario, NE Mexico). Episodes, 45, 181–220.

Walaszczyk, I., Wood, C.J., Lees, J.A., Peryt, D., Voigt, S. and Wiese, F. 2010. The Salzgitter-Salder Quarry (Lower Saxony, Germany) and Słupia Nadbrzeżna river cliff section (central Poland): a proposed candidate composite Global Boundary Stratotype Section and Point for the Coniacian Stage (Upper Cretaceous). Acta Geologica Polonica, 60, 445–477.

Wegner, R.N. 1913. Tertiaer und umgelagerte Kreide bei Oppeln. Palaeontographica, 60, 175–274.

Wiese, F., Čech, S., Walaszczyk, I. and Košťák, M. 2020. An upper Turonian (Upper Cretaceous) inoceramid zonation and a round-the-world trip with *Mytiloides incertus* (Jimbo, 1894). Zeitschrift der deutschen Gesellschaft für Geowissenschaften, 171, 211–226.

Wray, D.S., Kaplan, U. and Wood, C.J. 1995. Tuff-Vorkommen und ihre Bio- und Eventstratigraphie im Turon des Teutoburger Waldes, der Egge und des Haarstrangs. Geologie und Paläontologie in Westfalen, 37, 1–53.

11TH INTERNATIONAL
CRETACEOUS
SYMPOSIUM
Warsaw, Poland, 2022

CRETACEOUS OF THE NORTH SUDETIC SYNCLINORIUM (SOUTHWESTERN POLAND): STRATIGRAPHY, ORIGIN AND ECONOMIC IMPORTANCE

Stanisław Leszczyński[1]| Alina Chrząstek[2]| Adam T. Halamski[3]| Wojciech Nemec[4]| Jurand Wojewoda[5]

1| Jagiellonian University, Poland; e-mail: stan.leszczynski@uj.edu.pl

2| University of Wrocław, Poland; e-mail: alina.chrzastek@uwr.edu.pl

3| Instituite of Paleobiology, Polish Academy of Sciences, Warszawa, Poland; e-mail: ath@twarda.pan.pl

4| University of Bergen, {miasto}, Norway; e-mail: wojtek.nemec@uib.no

5| University of Wrocław, Poland; e-mail: jurand.wojewoda@uwr.edu.pl

ABSTRACT

The integrated stratigraphy, ichnology, depositional processes, sedimentary environments, and economic importance of the North Sudetic Cretaceous (Cenomanian to Santonian) are presented. The sediments of the North Sudetic Cretaceous were deposited in a narrow, northwest-trending basin at the northern periphery of the Bohemian Massif, between the West Sudetic Island to the southwest and the East Sudetic Island to the northeast. The basin was one of the Central European seaways linking the Boreal and Tethyan marine provinces. The sedimentary succession comprises shallow-marine, lagoonal, fluvio-deltaic, and paludal/lacustrine sediments deposited in response to the bathymetric configuration of the basin and contemporaneous sea-level changes controlled by eustasy and Alpine tectonism.

INTRODUCTION

The Cretaceous of the North Sudetic Synclinorium (NSS) constitutes an important part of the Cretaceous System in Central Europe, both from the point of view of pure geology, especially palaeontology, as well as for applied geology, especially its economic branch. The Cenomanian–Santonian part of the NSS is a mostly siliciclastic succession. The deposits have been explored in many respects and exploited for several hundred years. The first geological description of a small fragment of the area was given by Charpentier (1768), and the earliest, brief geological description of the basin by von Raumer (1819). Research conducted since the nineteenth century, first by German and then by Polish geologists, allowed for the recognition of the stratigraphic architecture of the sedimentary succession and the processes and palaeoenvironmental conditions of its accumulation. Research has provided valuable palaeontological and ichnological data, contributing significantly to the overall understanding of the Cretaceous System. Last, but not least, the NSS Cretaceous is of great regional economic importance because of the natural resources it hosts.

GEOLOGICAL SETTING

The NSS is a tectonic unit situated in the northern foreland of the Variscan Orogen of the Sudetes (Berg 1913; Born 1921), in the northern marginal zone of the Bohemian Massif (Fig. 1A). The unit extends SE-NW along the

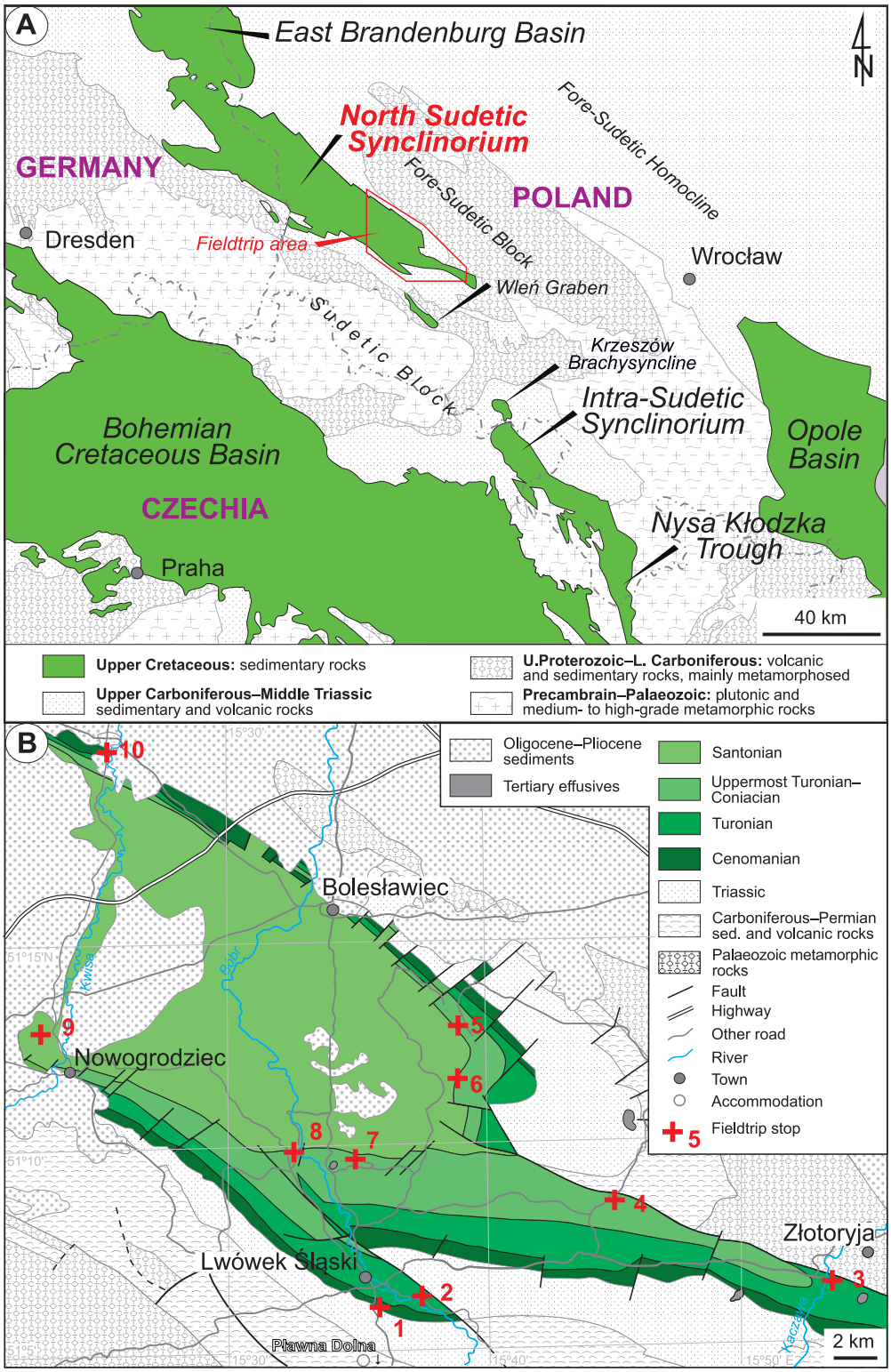

Fig. 1. Geological setting of the fieldtrip area. A – Location of the North Sudetic Synclinorium relative to the northern margin of the Bohemian Massif; geological map without Cenozoic, modified from Pożaryski et al. (1969). B – Geological map of the North-Sudetic Synclinorium and adjacent areas, without Quaternary deposits, compiled from Badura (2005), Cymerman et al. (2005a, b), Kozdrój et al. (2005), Przybylski et al. (2005), Sztromwasser (1995) and Halamski et al. (2020); partly reinterpreted by S. Leszczyński, with the location of fieldtrip stops marked.

Sudetic Boundary Fault and comprises a succession of Late Carboniferous, Permian, Early to Middle Triassic, and Late Cretaceous (Cenomanian–Santonian) strata, mostly siliciclastic sedimentary rocks and Late Palaeozoic volcanics, resting unconformably upon the Variscan basement (Scupin 1910; Oberc 1962; Śliwiński et al. 2003; Chrząstek and Wojewoda 2011). The NSS is bordered to the northeast by the elevated crystalline Fore-Sudetic Block, devoid of Mesozoic deposits, and by its northwestern envelope known as the Żary Pericline, with a Permian to Middle Triassic depositional cover. To the southwest, it is bordered by the elevated Görlitz and Kaczawa fold belts composed of pre-Permian metamorphic rocks (Żelaźniewicz et al. 2011). The complex internal structure of the NSS is due to faulting and inversion related to the multiphase convergence between Africa–Iberia and West-Central Europe (e.g., Kley and Voigt 2008) in the Cretaceous to Paleogene (Solecki 2011), the detailed timing of which is poorly constrained (Sobczyk et al. 2019 and references therein). Faults subdivide the NSS into subordinate units of various scale, most sharing the Cretaceous cover (Scupin 1913; 1931; Milewicz 1968). Only the southeastern part of the NSS Cretaceous crops out at the surface, with the rest hidden under various, mostly terrestrial, Cenozoic sediments and volcanics (Fig. 1B). The stratigraphy and lithofacies of these sediments, as well as the character and age of volcanics, indicate that in the Paleogene–Miocene this area was elevated and subject to peneplanation, basement weathering, and faulting (Oberc 1962; Jahn 1980; Migoń and Lidmar-Bergström 2001; Badura et al. 2004 and references therein). Differential subsidence with widespread terrestrial sedimentation occurred in the Miocene (Oberc, 1962; Dyjor 1995). The present-day relief shows a significant influence of prominent Oligocene–Miocene volcanism (Birkenmajer et al. 1966, 2004; Badura et al. 2005; Ulrych et al. 2011) and various Quaternary processes, particularly Pleistocene glaciation.

The NSS is a well-preserved axial relic of a Late Cretaceous sedimentary basin, called the North Sudetic Basin (NSB), that developed within the area of a former Late Palaeozoic–Jurassic(?) basin. Like the other Late Cretaceous basins of the Bohemian Massif, the NSB was formed at the Central European interface of the Tethyan and Boreal provinces by the regional reactivation of older, mainly Variscan fault zones dissecting the Bohemian Massif and its surroundings (Fig. 2). The initiation of these basins coincided with the worldwide Cenomanian transgression. As a result, a major part of Central Europe, including large areas of the Bohemian Massif, the present-day Sudetes, and their foreland, were flooded (Voigt et al. 2008), forming an island-dotted seaway, the so-called European Archipelago, between the Tethys and the Boreal Ocean (Csiki-Sava et al. 2015). The NSB formed a southeastern extension of the East Brandenburg Basin (Musstow 1968; Voigt et al. 2008) and was at least temporarily connected by hypothetical straits with the adjacent Intra-Sudetic Basin and further with the large Bohemian Basin (Fig. 2; Partsch 1896; Scupin 1910; Leszczyński 2018).

STRATIGRAPHY

The North Sudetic Cretaceous forms an over 1000 m thick sedimentary succession (Milewicz 2006) comprised of sandstones, mudstones, claystones, and marlstones, with subordinate limestone intercalations in the lower part and thin coal intercalations in the upper part. The limestones occur exclusively in the northwestern part of the NSS, and are known only from drill cores. The sediments are known to host a rich assemblage of body and trace fossils, both fauna and flora (Goeppert 1841, 1844; Drescher 1863; Williger 1882; Scupin 1913; Leszczyński 2010, 2018; Chrząstek and Wypych 2018; Halamski et al. 2020, and references therein), which – together with physical sedimentary features – indicate mostly nearshore, paralic, and offshore marine deposition (Beyrich 1849; Drescher 1863; Williger 1882; Partsch 1896; Scupin 1910; Milewicz 1965, 1996; Leszczyński 2010, 2018; Chrząstek and Wypych 2018; Leszczyński and Nemec 2020; Halamski 2020; Kowalski 2021). Outcrops and drill cores demonostrate considerable lateral and vertical variation of these lithofacies assemblages, with siliciclastic sandstone lithosomes dominant to the southeast and pinching out in mudstones and marlstones towards the northwest (Fig. 3).

The lithostratigraphic interpretation of the North Sudetic Cretaceous has evolved with

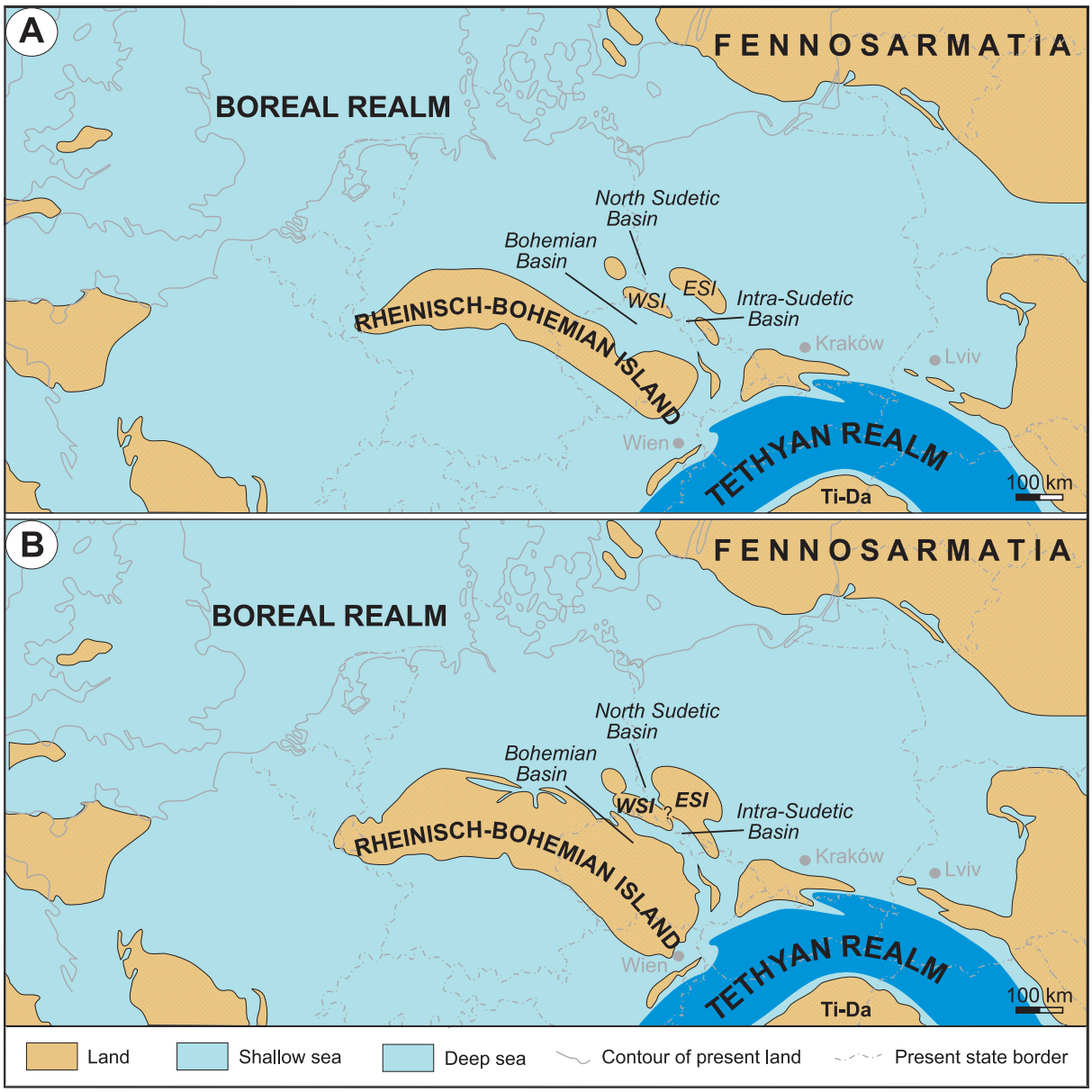

Fig. 2. Palaeogeography of southern Poland and adjacent areas during the Turonian (A) and the middle Coniacian regression (B); based on Ron Blakey from Csiki-Sava et al. (2015) and Kowalski (2021), modified for Poland and neighbouring areas by S. Leszczyński. Abbreviations: ESI – East Sudetic Island(s); WSI – West Sudetic Island(s); Ti-Da – Tisia-Dacia Block.

time (see review by Milewicz 1996). The existing lithostratigraphy (Fig. 3) was proposed by Milewicz (1985), who – based on earlier German and later Polish data – subdivided the succession into three formations. The marine lower half of the succession – dominated by sandstones to the southeast and by mudstones, marlstones, and limestones to the northwest – was designated the Rakowice Wielkie Formation, with its main sandstone lithosomes distinguished as separate members (the Wilków, Chmielno, Dobra, and Żerkowice Members; Fig. 3). The upper half of the succession was divided by Milewicz (1985) into two coeval formations, referred to as the Węgliniec Formation and the Czerna Formation (Fig. 3). The former is marine, ca. 250 m thick, and is composed chiefly of mudstones, whereas the latter to the southeast is paralic, attains a thickness of ca. 500–800 m, and comprises

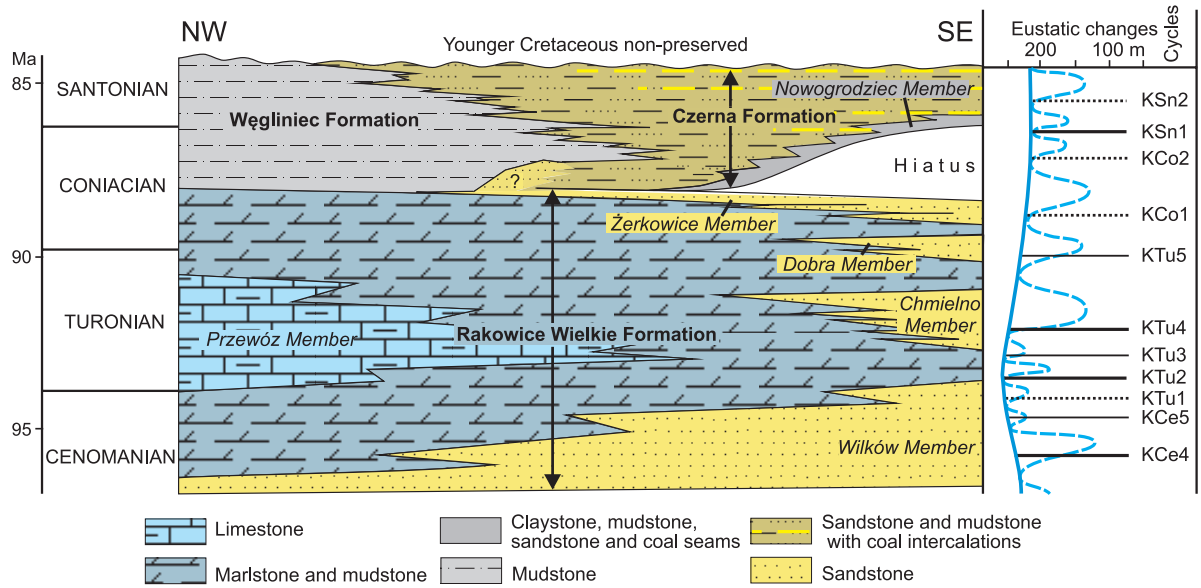

Fig. 3. The Upper Cretaceous stratigraphy of the North Sudetic Synclinorium, shown in axial cross-section. Lithostratigraphy is after Milewicz (1996), chronostratigraphy after Walaszczyk (2008) and Halamski et al. (2020), and numerical ages after Cohen et al. (2013); the corresponding eustatic curve is redrawn from Haq. (2014).

sandstones intercalated with mudstones, claystones, and thin coal seams, and is autochthonous to hypautochthonous (Milewicz 1985, 1996). The mud-dominated limnic lowermost part of the Czerna Formation, rich in coal and 2–50 m thick, was distinguished by Milewicz (1985) as the poorly defined Nowogrodziec Member (Fig. 3).

The first biostratigraphic dating of the sedimentary succession, based by Beyrich (1855) on bivalves and ammonites, indicated a Cenomanian–Senonian age. Milewicz (1958) limited the age of the upper part of the succession to the Santonian, and Krutzsch (1966) specified it further to the early Santonian. Milewicz (1956, 1969) also postulated a late Coniacian (late Emscherian) hiatus between the Rakowice Wielkie Formation and the Czerna Formation in the southeastern part of the North Sudetic Synclinorium, with a decrease in the duration of this stratigraphic gap towards the northwest (Fig. 3).

A more recent biostratigraphic study by Walaszczyk (2008) revised the succession chronostratigraphy. The boundary between the Rakowice Wielkie Formation and the overlying Węgliniec and Czerna Formations was assigned to the middle/late Coniacian transition, with the Coniacian/Santonian boundary in the middle of these latter formations, and the hiatus discussed above corresponding to the late middle Coniacian. Recent palaeobotanical studies by Halamski et al. (2020) speak for a local hiatus such as that indicated by Milewicz (1996). This revised chronostratigraphy is followed in the present guidebook (Fig. 3).

SEDIMENTOLOGICAL CHARACTERISTICS AND ORIGIN

The Rakowice Wielkie Formation

The sedimentary succession of the North Sudetic Cretaceous starts with a 5–40 cm thick pebbly conglomerate or pebbly sandstone resting almost conformably upon Late Carboniferous–Middle Triassic sedimentary and volcanic rocks, which are also found locally as clasts in the basal part of the unit (Fig. 4; see fieldtrip stops 1 and 10). The gravelly deposits pass upwards into very coarse- and medium-grained sandstones, and further into fine-grained sandstones. These are quartzose arenites to poor wackes with a small admixture of lydites and siliceous shists, mainly massive (structureless) or large-scale cross-stratified, and are largely unfossiliferous.

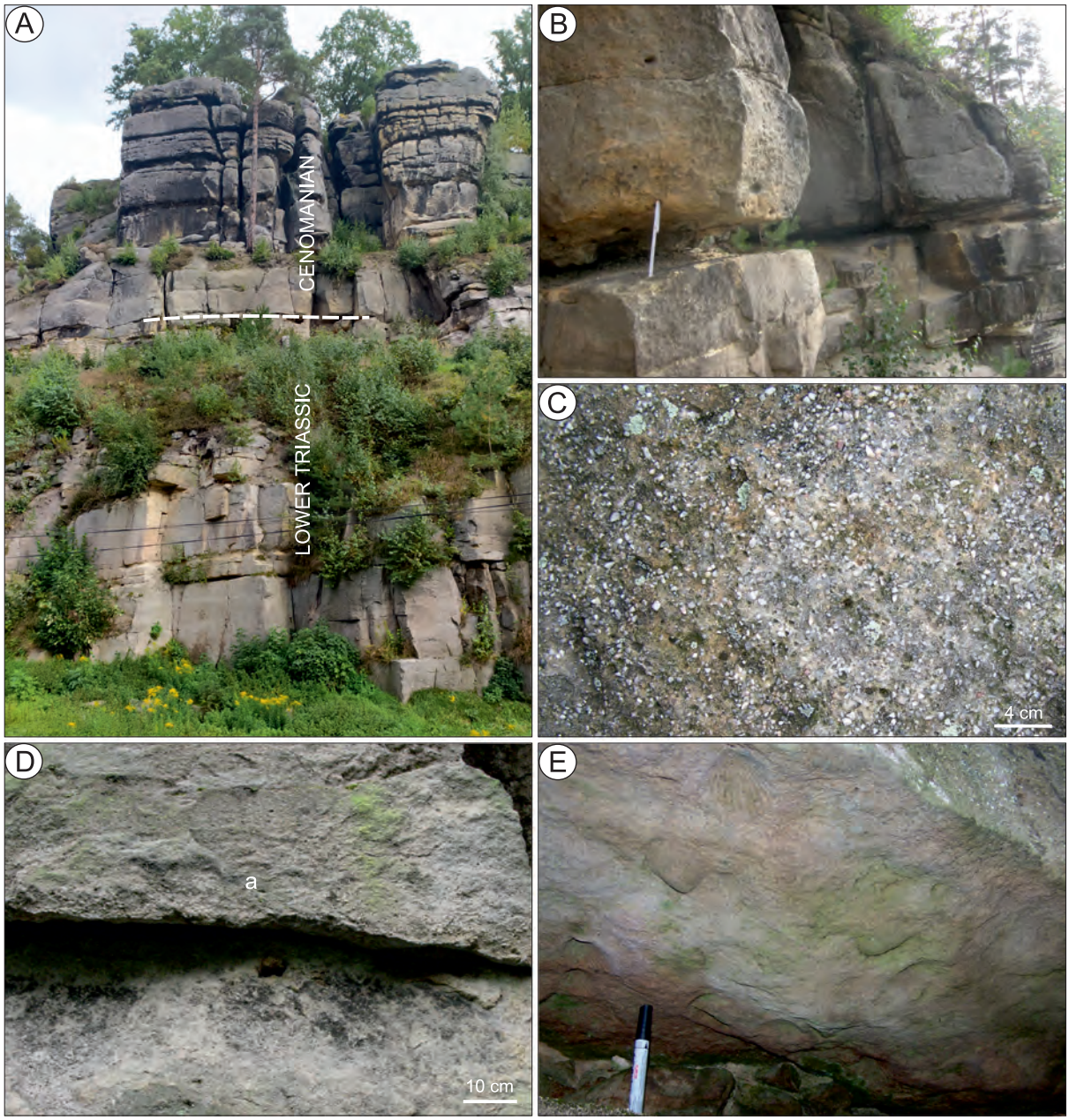

Fig. 4. The Cenomanian Wilków Member and its relationship to the underlying deposits. A – General view of the unit and its relationship to the underlying Early Triassic sandstones of the Radłówka Formation. B – The boundary (ravinement surface) between the Triassic and Cenomanian sediments. Note differences in sediment grain size. C – Texture of structureless Wilków Sandstone. D – Normal grading in structureless sandstone, highlighted by the granule sandstone tempestite located in the basal part of bed (a). E – Molds of bivalve shells at the sole of structureless tempestite sandstone bed. Pictures A to C are from fieldtrip stop 1 (in Lwówek Śląski), D and E are from the Wilków Sandstone in an abandoned quarry between the villages of Niwnice and Kotliska (7.5 km northwest of Lwówek Śląski). All photographs by S. Leszczyński.

The fossils consist of mostly bivalves (*Pecten asper* Lamarck, *P. hispidus* Goldfuss, *Exogyra columba* Lamarck, *Ostrea carinata* Lamarck, *Inoceramus bohemicus* Leonhard, *I. pictus* Sowerby, *Mytiloides hercynicus* (Petrascheck), single cephalopods, brachiopods, and echinoderms; numerous fish bones have been found in the sandstones (Drescher 1863; Scupin 1913; see Milewicz 1996). In the northwestern part of the NSS, the sandstones are calcareous and

glauconitic (Milewicz 1996). The deposits were called the *Unterquader* by German geologists (Scupin 1906, 1913). Milewicz (1985, 1996) distinguished them as the Wilków Sandstone and included them into the Rakowice Wielkie Formation. Their thickness reaches 135 m in the southeastern part of the NSS and decreases to several metres in the northwestern part of the unit (Milewicz 1996). The top part of the unit is locally marked by an iron hydroxide-impregnated layer, up to 30 cm thick.

The Wilków Sandstone is overlain by a succession of fine-grained sediments constituting the sedimentary background of the Rakowice Wielkie Formation. These start with dark-grey sandy and silty marls, marly siltstones, mudstones, and subordinately clayey ironstones, locally rich in various fossils and highly bioturbated (Milewicz 1960, 1996; *Pläner* in the German literature). The sediments become sandier upwards and are virtually sand-dominated to the southeast, where German geologists distinguished the *Pläner Sandstein* (e.g., Scupin 1913; see fieldtrip stop 2). In the northwestern part of the NSS, intercalations of grey to dark-grey, thin- to thick-bedded mudstone and wackestone- to packstone-, dolomitic, glauconite-bearing marly limestones appear in the higher part of succession. The latter subsequently develops into a homogenous limestone unit, up to 110 m thick, transitioning upward into a succession of interbedded, dark-grey to black, clayey, silty and sandy marls and calcareous mudstones (Milewicz 1996). The limestones are known from drillings in the northwestern part of the NSS and disappear to the southeast (Milewicz 1996). Rare fossils, mostly bivalves and brachiopods recorded in limestones from the lower part of the sedimentary succession, include *Inoceramus crippsi* Mantell, *I. pictus* Sowerby, and *Mytiloides hercynicus* (Petrascheck) (Milewicz 1966). Different inoceramids, including *Mytiloides labiatus* (Schlotheim), and *Mytiloides mytiloides* (Mantell), and foraminifers occur in the higher, lower Turonian part of the fine-grained succession (Milewicz 1996). Several inoceramid taxa, including *Inoceramus costellatus* Woods, *I. inaequivalensis modestus* Heinz, and *Cremnoceramus inconstans* (Woods) have been found higher, in the upper Turonian–lower Coniacian part of this succession, and *Volviceramus koeneni* (Müller) and *I. kleini* Müller are reported from its top in the northwestern part of the NSS (Milewicz 1996).

The fine-grained succession of the Rakowice Wielkie Formation thins to the southeast, where it is split by wedges of the Chmielno and Dobra Sandstone Members and topped by an extensive wedge of the Żerkowice Sandstone (Fig. 3).

The Chmielno Sandstone (*Mittelquader* according to Scupin 1913; *Rabendockensandstein* and *Ludwigsdorfer Sandstein* in Scupin 1935; see fieldtrip stop 3) is a unit composed of light-grey and beige, mostly coarse-grained, locally pebbly sandstone that is massive, faintly cross-stratified, and rarely plane-parallel stratified (Figs 5–9); compositionally, it is quartzose with a small admixture of feldspar and a sparse kaolinitic and ferrous cement. Numerous soft-sediment convectional disturbances with characteristic shapes (e.g., folds, helicoidal torsions) occur locally (Figs 6C, 7B, F). In some places, gravelly material is immersed in the underlying sand (drop-shaped load casts; Figs 6, 9B) The unit is up to 90 m thick, splitting to the northwest into two subordinate wedges (tongues). The lower one consists of coarse-grained sandstones in the lower part, whereas the upper shows an opposite vertical grain-size trend (Milewicz 1996). The lower and upper boundary of the unit are sharp. The top surface is covered by a layer of clayey ironstone. The sandstones contain fairly rich fossil fauna, including inoceramids (*M. labiatus*, *M. hercynicus*, *I. lamarcki* Parkinson, *I. costellatus*), other bivalves (*Pinna decussata* Goldfuss, *Lima canalifera* Goldfuss, *Pecten acuminatus* Geinitz, *Pectunculus geinitzi* d'Orbigny, *Cardita geinitzi* d'Orbigny), and some brachiopods, as well as trace fossils (mainly *Ophiomorpha nodosa*).

The Dobra Sandstone is a thinner unit, known from a narrow zone along the northern margin of the NSS southeast to northwest of Bolesławiec. The unit is composed of coarse- to fine-grained quartzose, and is mostly represented by cross-stratified sandstones. Their thickness does not exceed a few dozen metres (Milewicz 1985, 1996).

The Żerkowice Sandstone Member (*Oberquader* in German literature; see fieldtrip stops 4–8) is the uppermost lithostratigraphic division of the Rakowice Wielkie Formation in the southeastern part of the NSS, where this sandy

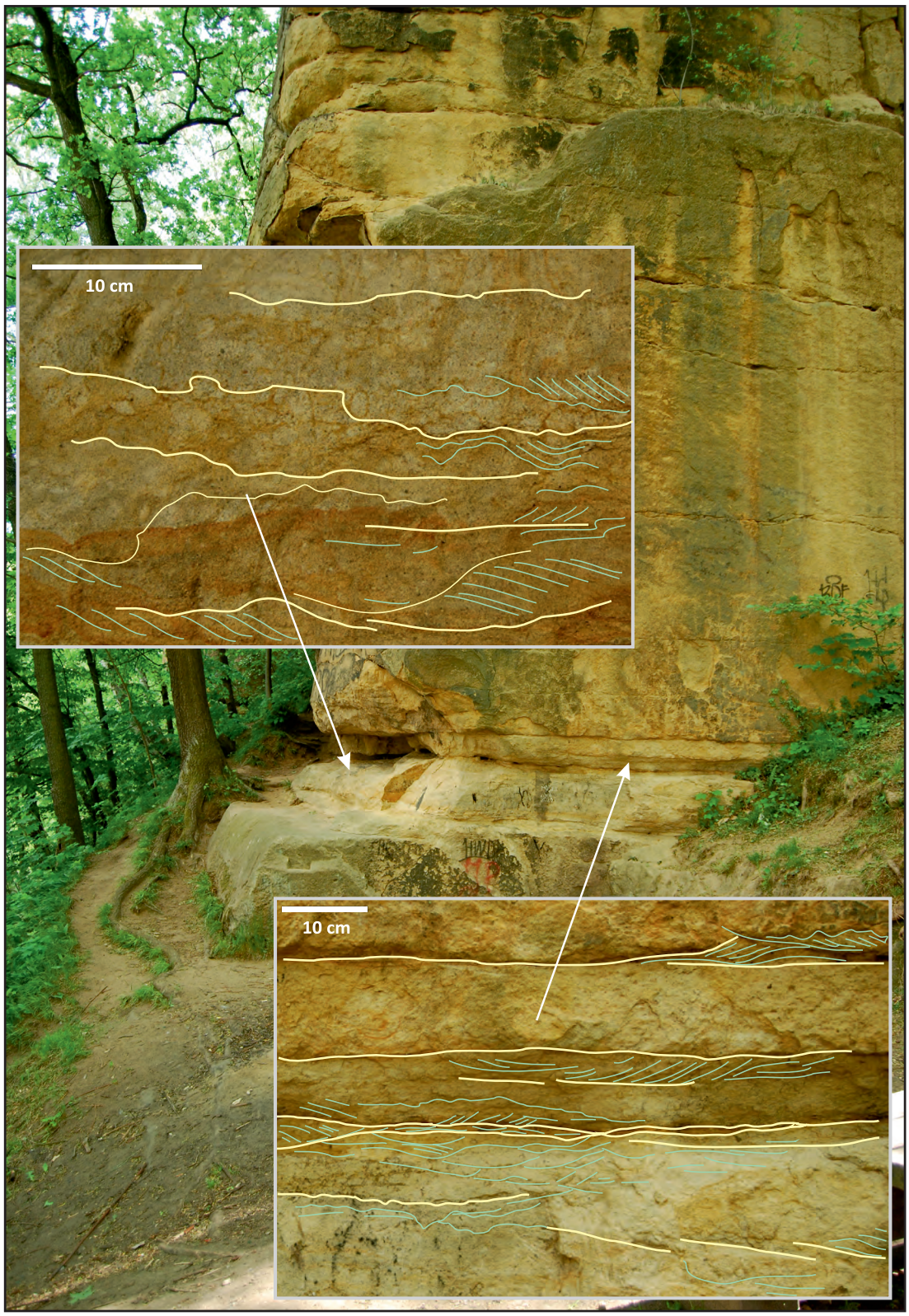

Fig. 5. Sandstones of the Chmielno Member at fieldtrip stop 3, site A (see Figs 1B and 33). Sandstones and gravelly sandstones of the lower part of the profile, mostly cross bedded in large- and small-scale cosets, with conglomeratic layers and highly bioturbed sediments. All photographs by J. Wojewoda.

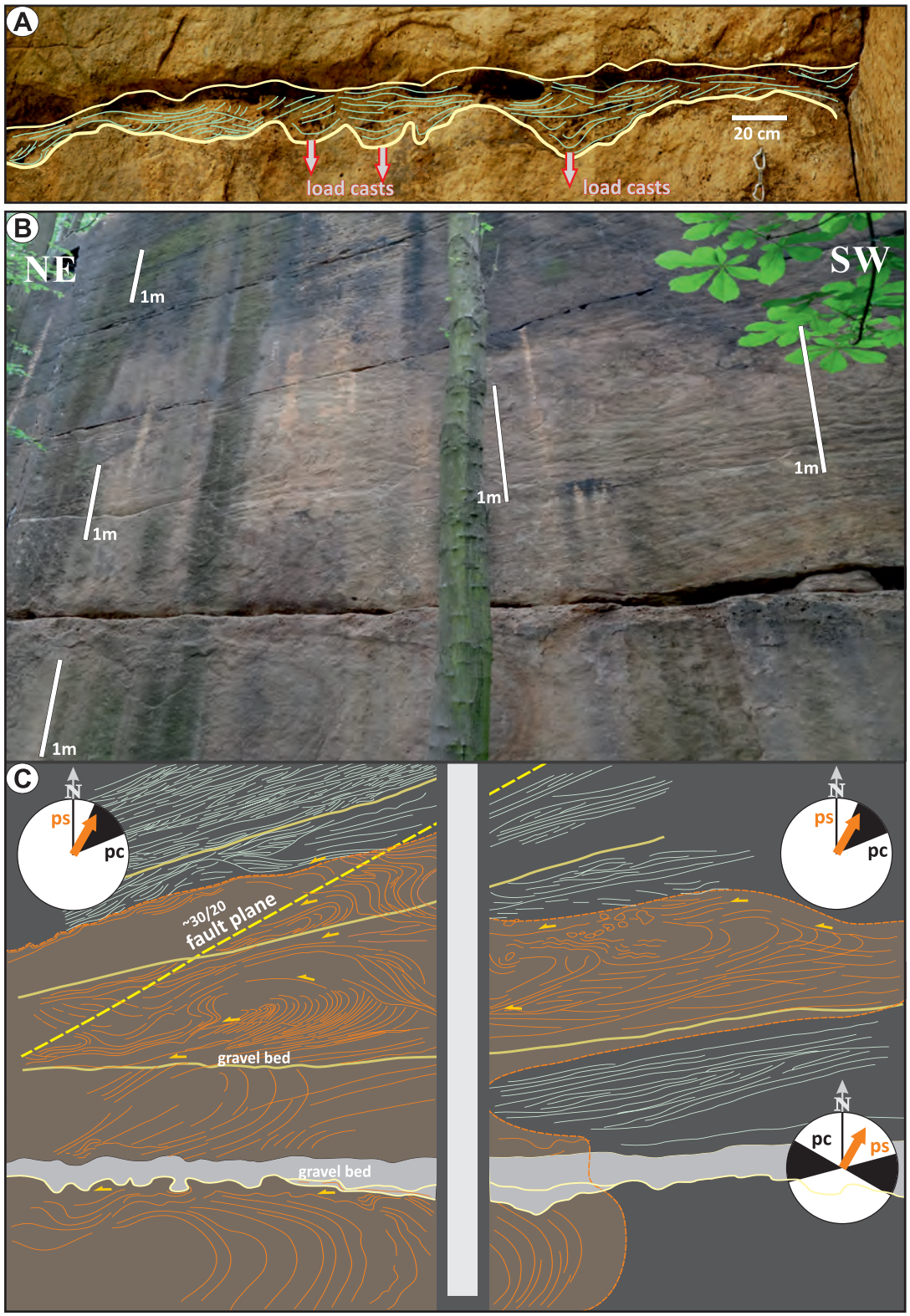

Fig. 6. Large-scale deformations of primary sedimentary structures in sandstones of the Chmielno Member at fieldtrip stop 3. A, B – from site I, C from site J (see Fig. 33); drop-like load structures in the conglomerates of the upper part of the "Krucze Skały" profile (contorsions and sinked gravel ripples?); the cross beddings indicate the dominant palaeocurrent was towards the north. All photographs by J. Wojewoda.

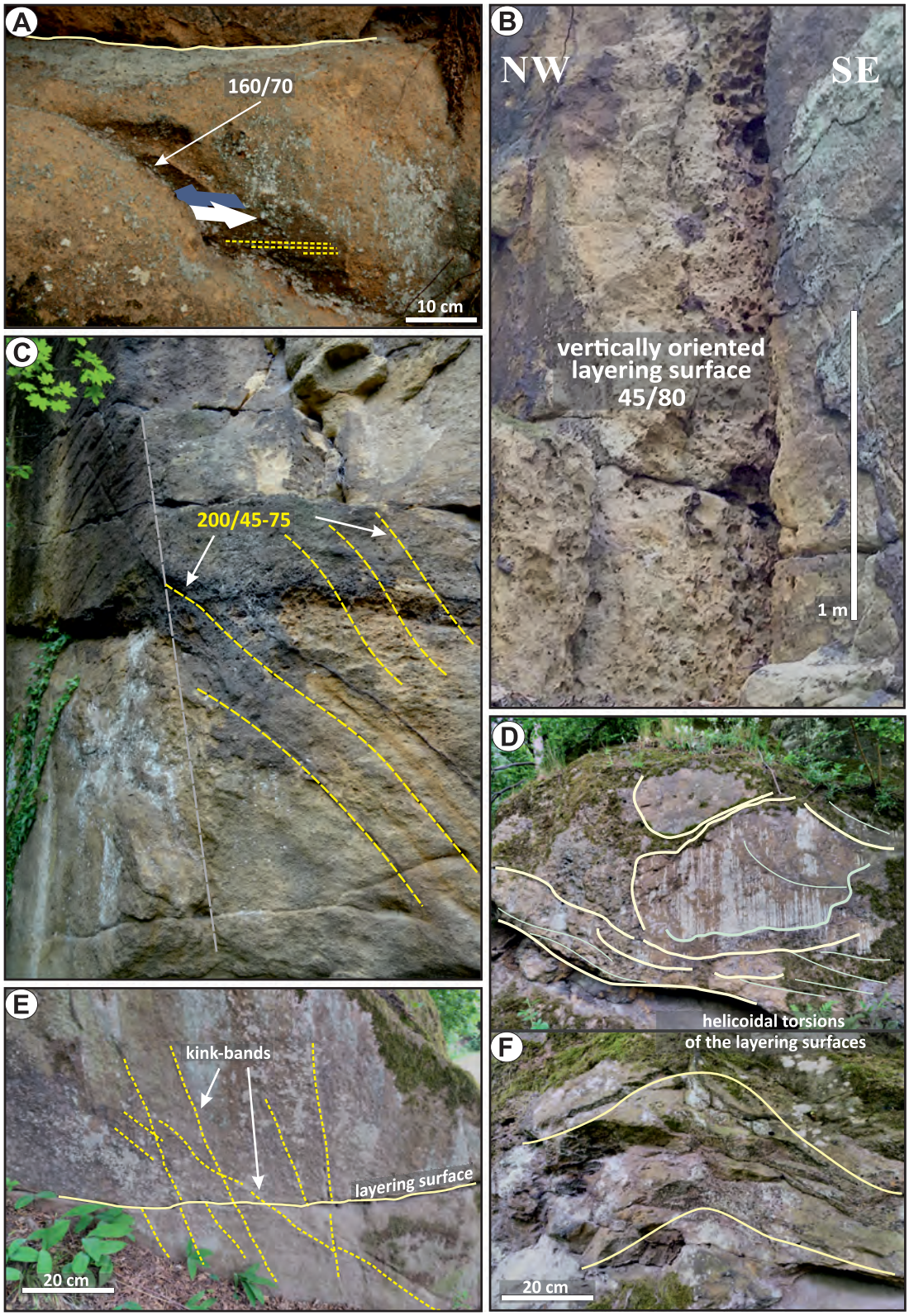

Fig. 7. Sandstones of the Chmielno Member. Examples of deformation structures within nonconsolidated sediments (kink bands, helicoidal torsions) and tectonic deformations (striation on tectonic mirrors, Riedel T-shears); fieldtrip stop 3. A – from site B. B – from site E. C – from site C. D – from site F. E – from site D (see Fig. 33). All photographs by J. Wojewoda.

Fig. 8. Sandstones of the Chmielno Member at fieldtrip stop 3, site K (see Fig. 33), approximately 400 m south of the previous sites, without any signs of deformation. Photograph by J. Wojewoda.

lithosome is exposed and has been subject to open-pit mining for several centuries as a highly valued dimension stone. The lower boundary of the unit is generally distinct, with fine-grained quartzose sandstones conformably overlying a lithosome of dark-grey mudstones, with a silty transition (Fig. 10). The boundary is less distinct and rather controversial in the northern part of the NSS, where the mudstone lithosome pinches out and the sandstones of the Żerkowice Member directly overlie the Dobra Sandstone (cf. Figs 3 and 10; Bossowski 1991). The top of the Żerkowice Member is the upper boundary of the Rakowice Wielkie Formation in the southeastern part of the synclinorium. This boundary is sharp and mainly erosional, with a stratigraphic hiatus (Fig. 3); the sandstones are overlain by a coal-bearing heterolithic unit dominated by mudstones and claystones (the Nowogrodziec Member of the Czerna Formation, *sensu* Milewicz 1985), increasingly ferruginized towards the southeast and containing local patches of ferricrust or ferruginized fossil turf (e.g., at fieldtrip stop 5).

Exploration boreholes show the sandstone lithosome of the Żerkowice Member thickens towards the northwest over 25 km along the synclinorium axis, from 50 m between fieldtrip stops 4 and 5, to 60 m roughly between fieldtrip stops 8 and 9, and up to 100 m ca. 10 km to northwest (Fig. 1B; see Leszczyński and Nemec 2020). Only a few kilometres farther to the northwest, the sandstone lithosome thickens abruptly to >200 m (corrected to >160 m on the account of local tectonic tilt) and virtually pinches out in a nearby borehole. This prominent thickening and abrupt pinch-out of the sandstone lithosome at its northwestern termination is meaningful, as discussed further in the text.

The Żerkowice Member consists of fine- to medium-grained and subordinately coarse-grained quartzose arenitic sandstones that are greyish white in colour, cream-yellow to light orange on weathered outcrop surfaces, and range in hardness from well cemented (mined as building blocks) to nearly soft (mined as glass sand). Mudstone interbeds are minor,

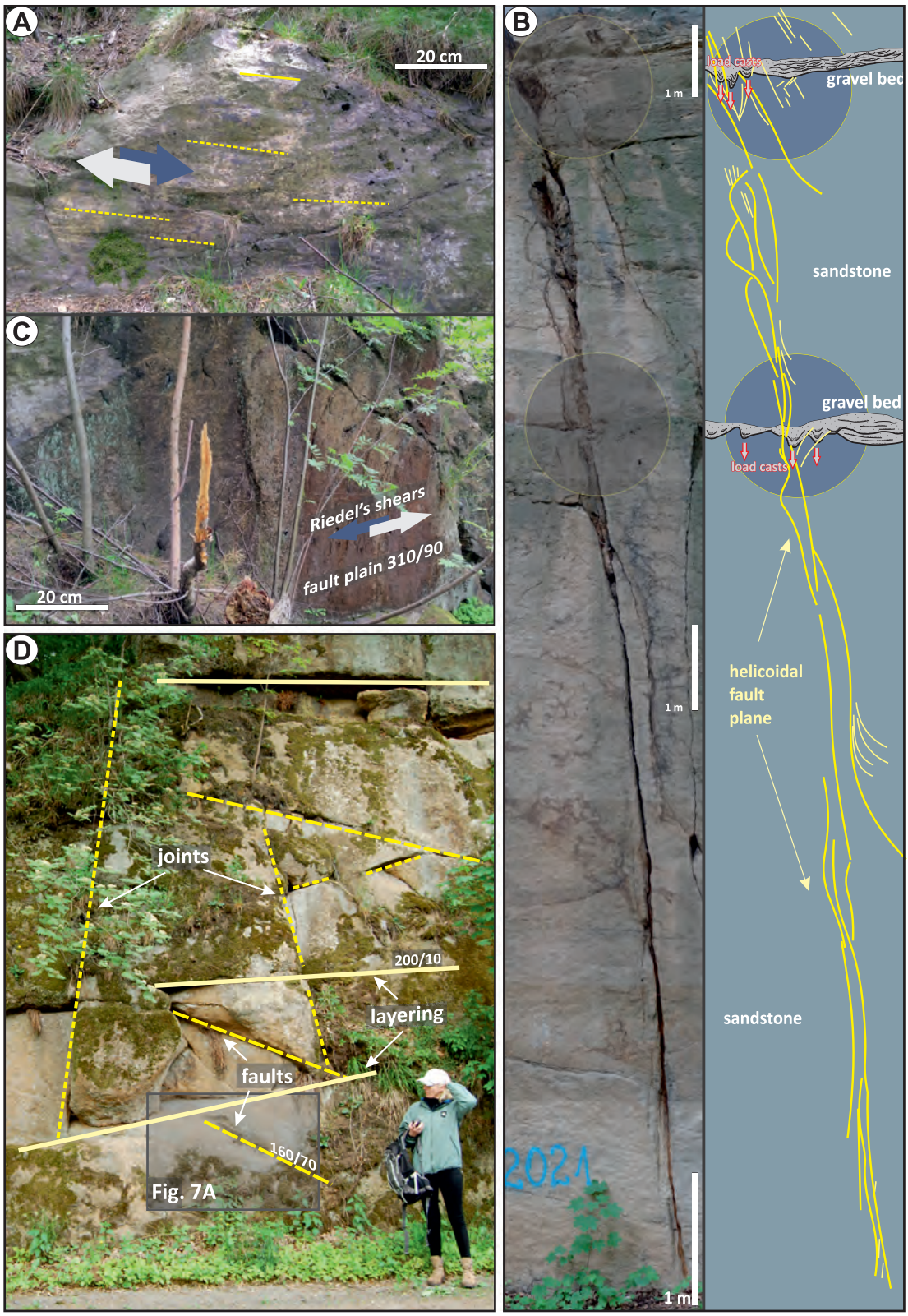

Fig. 9. Sandstones of the Chmielno Member displaying spatial change in interrelationships of stratification, tectonic deformations, and features formed in nonconsolidated sediments as they approach the Jerzmanice Fault. Fieldtrip stop 3. A, C – site G; B – site H; C – site G; D – site A". All photographs by J. Wojewoda.

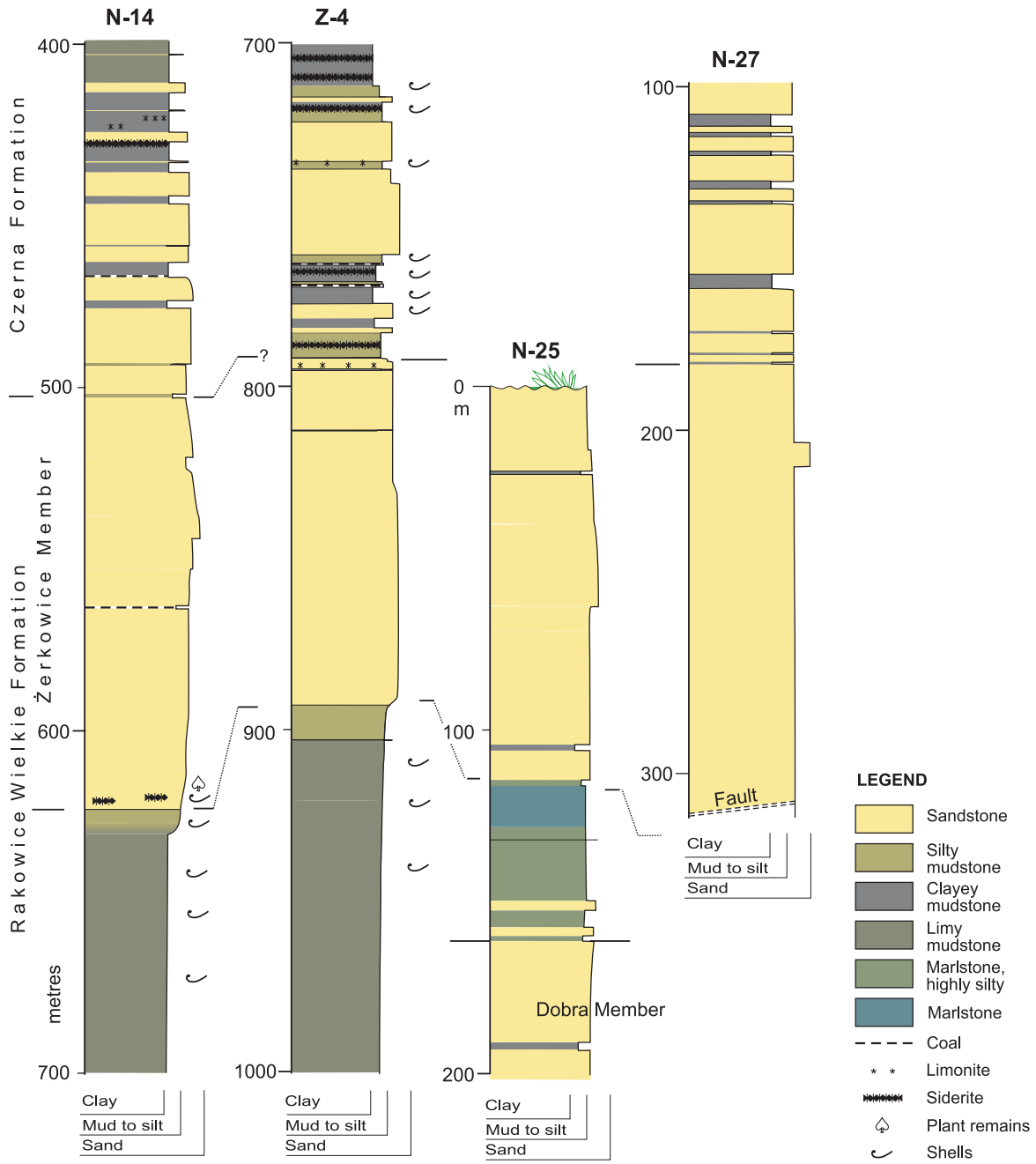

Fig. 10. Borehole logs showing the stratigraphic transition of the Rakowice Wielkie Formation to the Czerna Formation compiled by Leszczyński and Nemec (2020).

thin and laterally discontinuous. The sand is mainly very well sorted, which commonly renders its internal stratification and bed boundaries poorly visible.

The volumetrically dominant lithofacies are sandstones with large-scale planar or trough cross-stratification (lithofacies Sc in Leszczyński and Nemec 2020; Fig. 11A–C). Cross-strata sets range from a decimetre to 3.2 m in thickness, show variable and often bidirectional transport directions, and form laterally extensive cosets up to 15 m thick (Figs 13, 14; legend explained in Fig. 12). Some cross-strata sets show hydroplastic deformation and partial homogenization by liquefaction. Subordinate lithofacies distinguished

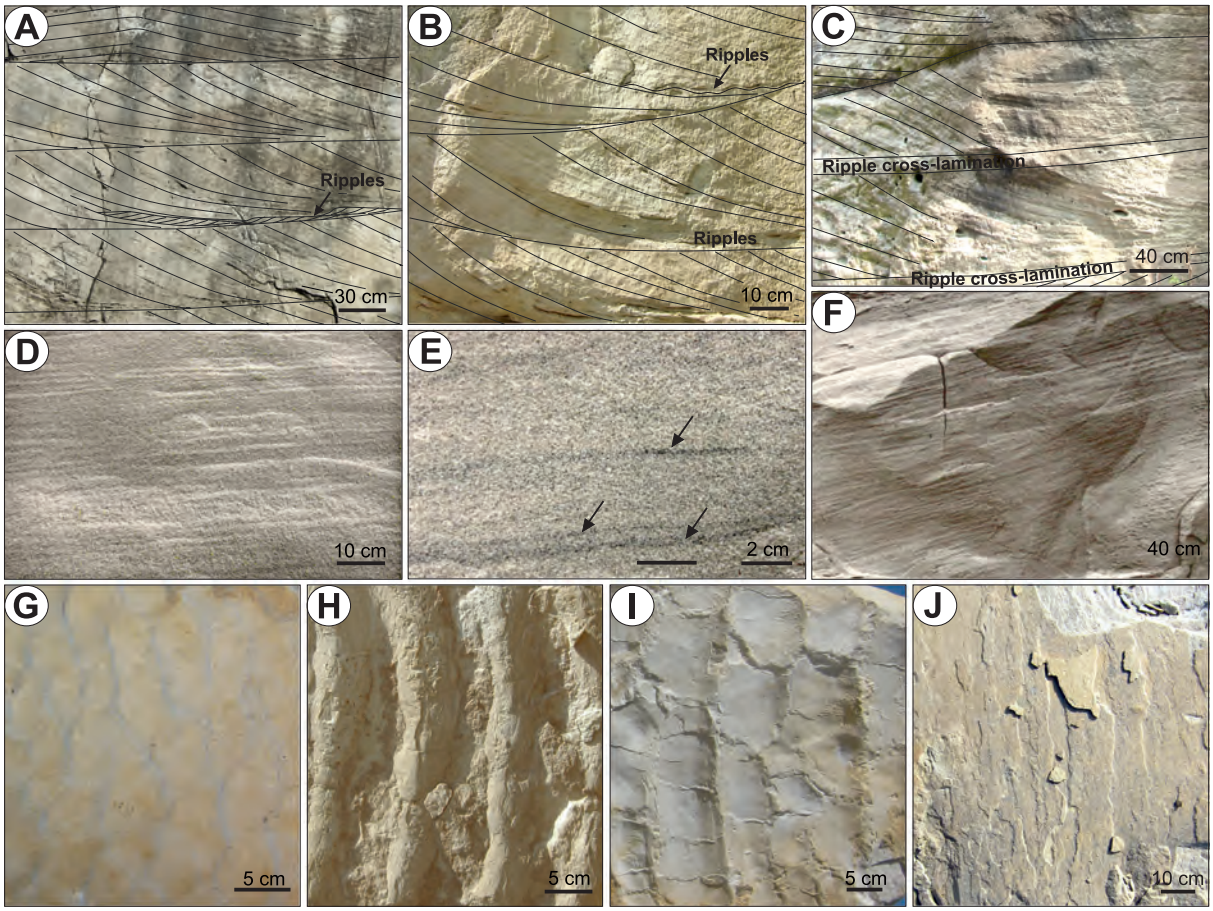

Fig. 11. Lithofacies and ichnofauna of the Żerkowice Member by Leszczyński and Nemec (2020). A – Sandstone with trough cross-stratification (lithofacies Sc) in vertical outcrop; fieldtrip stop 5A; note minor intrasets of reverse-flow ripple cross-lamination; main transport direction to the right, obliquely away from the viewer. B – Sandstone with planar tangential cross-stratification (lithofacies Sc) in vertical outcrop; fieldtrip stop 5A; note minor intrasets of reverse-flow ripple cross-lamination; main transport direction to the right, increasingly away from the viewer upwards. C – Sandstone with planar angular cross-stratification (lithofacies Sc) and interbeds of current ripple cross-lamination (lithofacies Sr) in vertical outcrop; fieldtrip stop 6B; transport direction to the right, obliquely towards the viewer. D – Sandstone with horizontal plane-parallel stratification (lithofacies Sp); vertical outcrop; active glass sand open pit ca. 2 km west of fieldtrip stop 10. E – Plane-parallel swash stratification in lithofacies Sp with dark laminae enriched in heavy minerals (arrows); vertical outcrop, locality as in D. F – Sandstone with gently inclined plane-parallel stratification (lithofacies Sp) in vertical outcrop, locality as in D. G – 3D current ripples exhumed on a bedding plane in sandstone lithofacies Sr; fieldtrip stop 7A. H – Symmetrical 2D wave ripples with rounded crests, exhumed on a bedding plane in sandstone lithofacies Sw; fieldtrip stop 5A. I – Sharp-crested symmetrical 2D wave ripples exhumed on a bedding plane in sandstone lithofacies Sw; fieldtrip stop 5A. J – Parting lineation on bedding surface in a swash-stratified sandstone of lithofacies Sp; fieldtrip stop 5A. All photographs by S. Leszczyński.

by Leszczyński and Nemec (2020) include sandstones with current ripple cross-lamination (lithofacies Sr, Fig. 11A–C, G), wave ripple cross-lamination (lithofacies Sw, Fig. 11H, I) and plane-parallel stratification (lithofacies Sp, Fig. 11D–F). Lithofacies Sr occurs as local intercalations, 5–50 cm thick, within the large-scale cross-strata cosets (Fig. 11C). Lithofacies Sp and Sw commonly alternate with each other, forming units 0.1–4 m thick that split or cap the cross-strata cosets of lithofacies Sc (Fig. 14, top). Lithofacies Sp dominates along the margins of the synclinorium, where it shows a gentle primary basinward inclination of 3–5° and forms basinward wedges up to 10 m thick. Where the inclination is steeper (10–15°, Fig. 11F), the plane-parallel stratification shows primary current lineation (Fig. 11J) and hosts laminae rich in heavy minerals (Fig. 11E). Clayey to silty grey mudstones (lithofacies M) are a minor component. This lithofacies occurs as thin (0.5–2 cm) and laterally

discontinuous drapes between some of the cross-strata sets of sandstone lithofacies Sc. Thicker mudstone units, up to 15 cm, are thinly interlayered with sand and/or silt, forming heterolithic beds (lithofacies H) beneath some of the sandstone cross-strata cosets.

Bioturbation occurs only locally in the sandstones (Milewicz 1965, 1996; Chrząstek and Wypych 2018; Leszczyński 2018). Burrows (Figs 15A–E, 16A–C) are concentrated as patches on the surfaces separating cross-strata cosets, especially where draped with mud, and in the topmost parts (10–15 cm) of cosets, which are often intensely bioturbated with single burrows reaching down nearly 1.5 m. Trace fossils include *Ophiomorpha* isp. (Fig. 15A–C), *Ophiomorpha nodosa* (Figs 15B, C; 16C), *Thalassinoides suevicus* (Fig. 15D), *T. paradoxicus* (Fig. 16B), *Rosarichnoides sudeticus* (Fig. 16A), *Nereites* isp., *Terptichnus* isp. and some small unidentified burrows (Fig. 15E). The trace-fossil assemblages seem to range between a stressed expression of the *Skolithos* Ichnofacies and a proximal expression of the *Cruziana* Ichnofacies (Chrząstek and Wypych 2018; Leszczyński 2018). Body fossils are rare, represented by bivalves (Fig. 16D–G; mainly inoceramids, e.g., Fig. 16D), including *Volviceramus involutus*, *I. percostatus* Müller), gastropods (Fig. 15F), ammonites, and echinoderms (Fig 16H; Milewicz 1965; Walaszczyk 2008). Some patchy shell pavements and discrete horizons rich with imprints and casts of shell debris (Figs 11F, 15F, 16E–G) were found at fieldtrip stops 5 and 6 (Leszczyński 2010, 2018; Chrząstek and Wypych 2018). Scattered wood fragments of various sizes and aggregated imprints of large fishbones are sporadically present at fieldtrip stops 5, 6A and 8. Some large driftwood fragments are preserved solely as clustered *Teredolites*, casts of wood-boring bivalves (Leszczyński 2018).

According to Leszczyński and Nemec (2020), the spatially and genetically related lithofacies of the Żerkowice Member represent several sedimentary systems (environments), reviewed below. Sediment assemblages dominated by the cross-stratified sandstones of lithofacies Sc form mounded elongate sandbodies (longitudinal sand bars) roughly parallel to the synclinorium axis and virtually dominant in the axial zone to the southeast (Figs 13–17). Quarry outcrops show that these sandbodies are 5–15 m

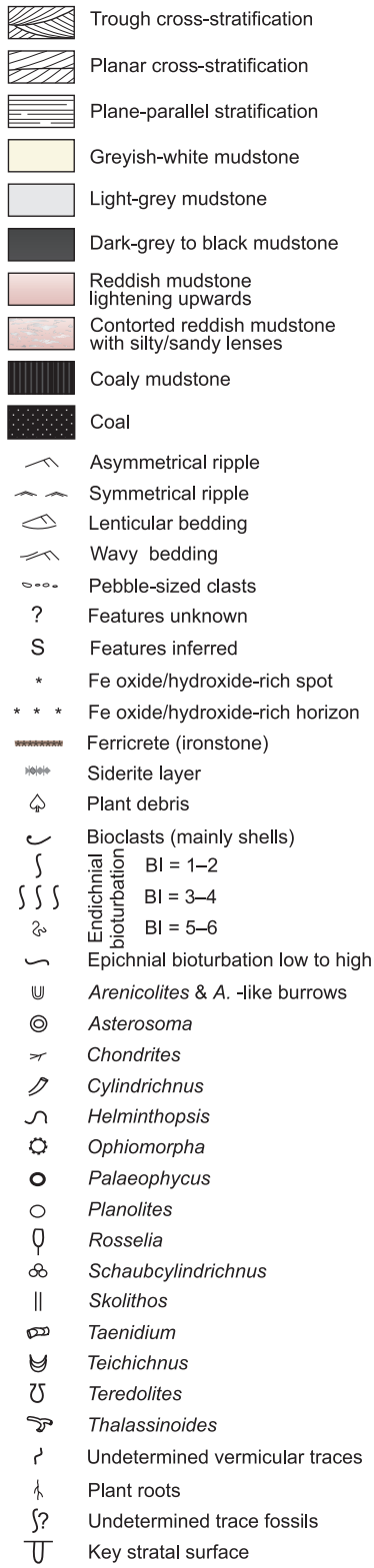

Fig. 12. Review of sedimentological and ichnological features recognized in Coniacian outcrops, given as a legend to the outcrop logs shown farther in this guide (after Leszczyński and Nemec 2020).

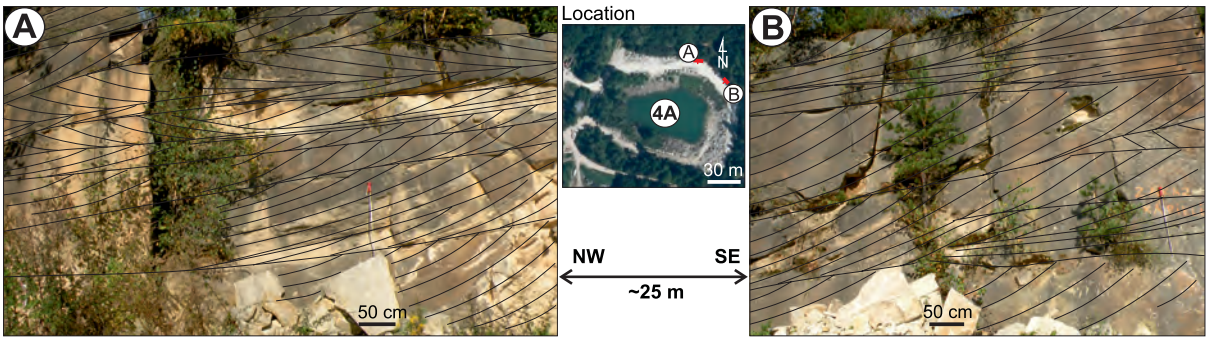

Fig. 13. Succession of vertically stacked, bidirectional dune cross-strata sets (lithofacies Sc) interpreted as a northwest-trending longitudinal tidal bar (sand ridge). Outcrop photographs A and B (by S. Leszczyński) show cliff portions of the abandoned quarry (fieldtrip stop 4A), as indicated in the inset image from Google Earth. From Leszczyński and Nemec (2020).

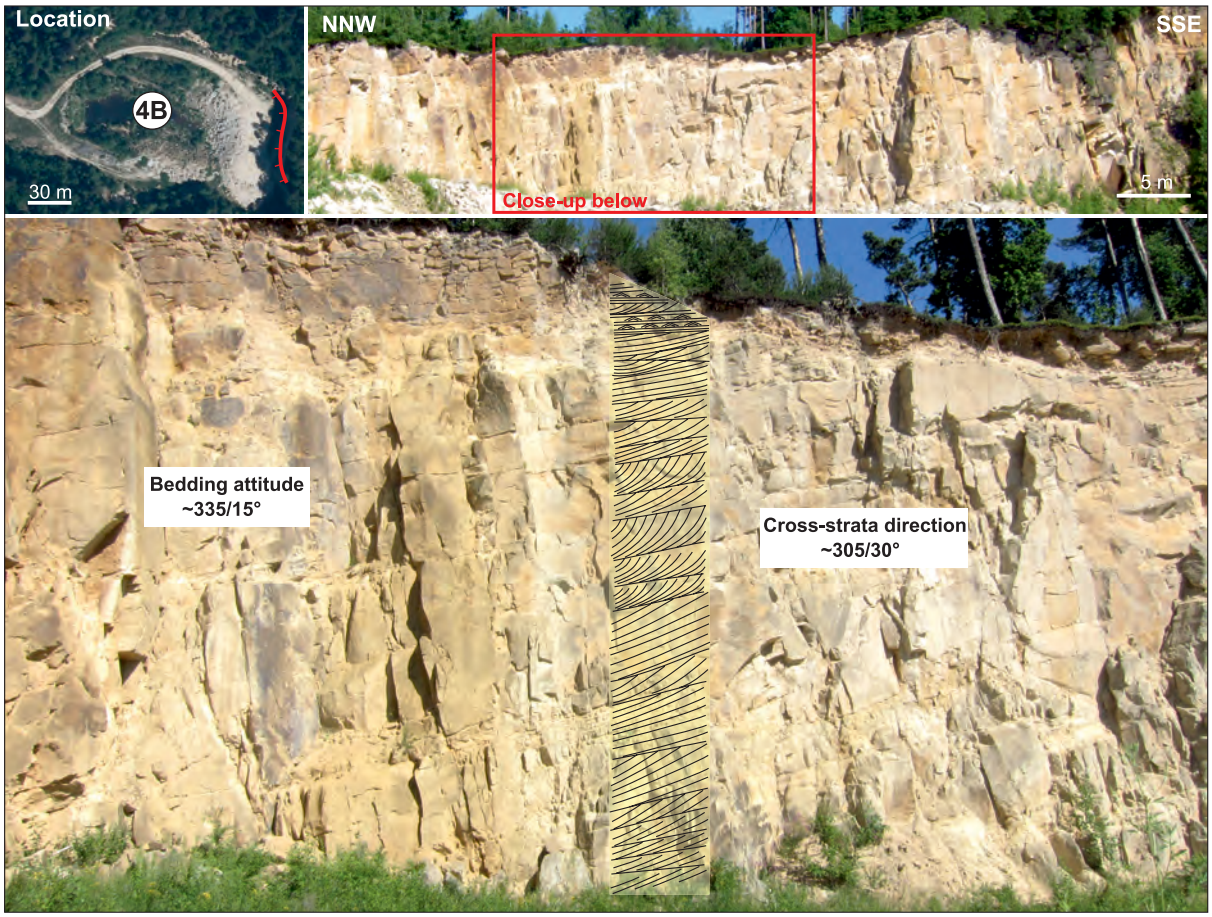

Fig. 14. Succession of vertically stacked dune cross-strata sets (lithofacies Sc) interpreted as a northwest-trending longitudinal tidal bar (sand ridge). The bedding inclination at this locality includes at least 5° of secondary tectonic tilt. Abandoned quarry in Czaple (fieldtrip stop 4B, Fig. 1B); the quarry and cliff location are shown in the inset image from Google Earth. From Leszczyński and Nemec (2020). Phohotographs by S. Leszczyński.

thick and apparently several kilometres long, stacked laterally and vertically into complexes up to 50 m thick. Their internal architecture displays vertically stacked 2D and 3D dune cross-strata sets, with bedding surfaces slightly rising or subhorizontal and gently falling to the northwest (Figs 13, 14). Transport directions to the northwest locally dominate (Fig. 14), but

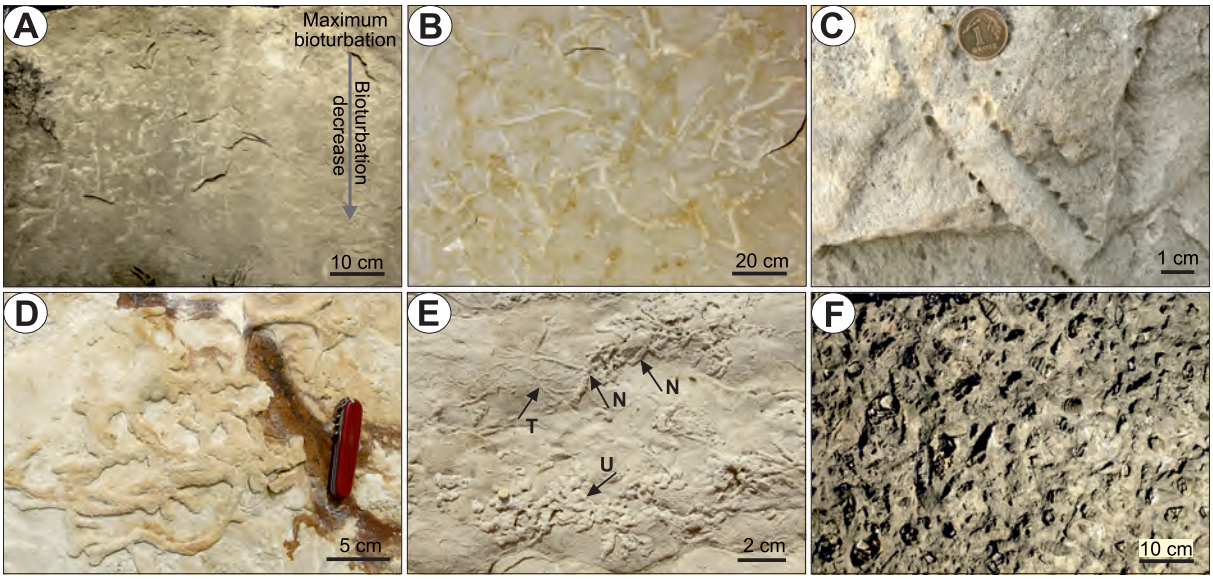

Fig. 15. Trace fossils and body fossils of the Żerkowice Member by Leszczyński and Nemec (2020). A – *Ophiomorpha* with density decreasing downwards in sandstone lithofacies Sc at fieldtrip stop 5A. B – *Ophiomorpha nodosa* network on sandstone bedding surface at fieldtrip stop 5A. C – Subvertical *Ophiomorpha nodosa* in sandstone at fieldtrip stop 6. D – *Thalassinoides suevicus*, slightly flattened by compaction, on sandstone bedding plane at Locality 8 in Leszczyński and Nemec (2020), neighbouring to fieldtrip stop 7. E – ?*Nereites* isp. (N); *Terptichnus* isp. (T) and undetermined burrows (U) on sandstone bedding surface at fieldtrip stop 6A. F – Shell lag (*Nerinea*) on a bedding plane in sandstone lithofacies Sp at fieldtrip stop 6. All photographs by S. Leszczyński.

the dune cross-sets are generally bidirectional (Fig. 13A) and show a wide range of transport directions (see rose diagram in Fig. 17). Some cross-sets are underlain by local drapes of lithofacies M. Interbeds of lithofacies Sw and Sr are minor, with the latter showing mainly reverse flow directions relative to those of the adjacent dune cross-strata (Fig. 11A–C). The basal parts of sand bodies consist of smaller dune cross-sets (Figs 14, 17) and are occasionally underlain by a heterolithic unit of lithofacies H, whereas their top parts are commonly packages of interbedded lithofacies Sp and Sw (Figs 10 and 13). Some of the sandbodies show shallow, isolated palaeochannels at the top (Fig. 18) filled with lithofacies Sc and trending slightly obliquely to the estimated long axis of the sandbody.

The elongate cross-stratified sand bodies are interpreted as longitudinal tidal sand bars (Leszczyński and Nemec 2020), also known as tidal sand ridges (Allen 1982; McBride 2003; Fig. 19A, B). They extend roughly parallel to the direction of tidal currents and grow seawards with a lateral migration component. The component tidal dunes migrate through the bars (lithofacies Sc in Fig. 11A–C), range from 2- to 3-dimensional, commonly grow in thickness by overstepping one another (Fig. 13B), and often show hydroplastic deformation of various origins. Tidal sand ridges are commonly associated with estuaries, tidal inlet deltas, and narrow straits (see Leszczyński and Nemec 2020 and references therein).

The bars interpreted in the Żerkowice Member are often underlain by inter-bar muddy heterolithic lithofacies H (cf. Hein 1986) and show an upward increase in flow energy (dune and grain sizes), indicating aggradational shallowing culminating in reworking by sea waves (Figs 14, 17) after reaching fairweather wave base. The alternation of lithofacies Sw and Sp in bar cappings indicates considerably fluctuating wave orbital velocity (Komar and Miller 1965), possibly including episodic erosion by storm waves (Clifton and Dingler 1984). Isolated palaeochannel features (Fig. 22) are interpreted as tidal conduits cut over the sand-ridge top, probably to accommodate local storm-boosted tidal current flows (cf. Dalrymple 1984).

Based on measurements in the rock tor "Skała z Medalionem" (fieldtrip stop 6B; Fig. 17) and the neighbouring, now abandoned, Żerkowice Quarry, Leszczyński and Nemec (2020) estimated the mean thickness of cross-sets

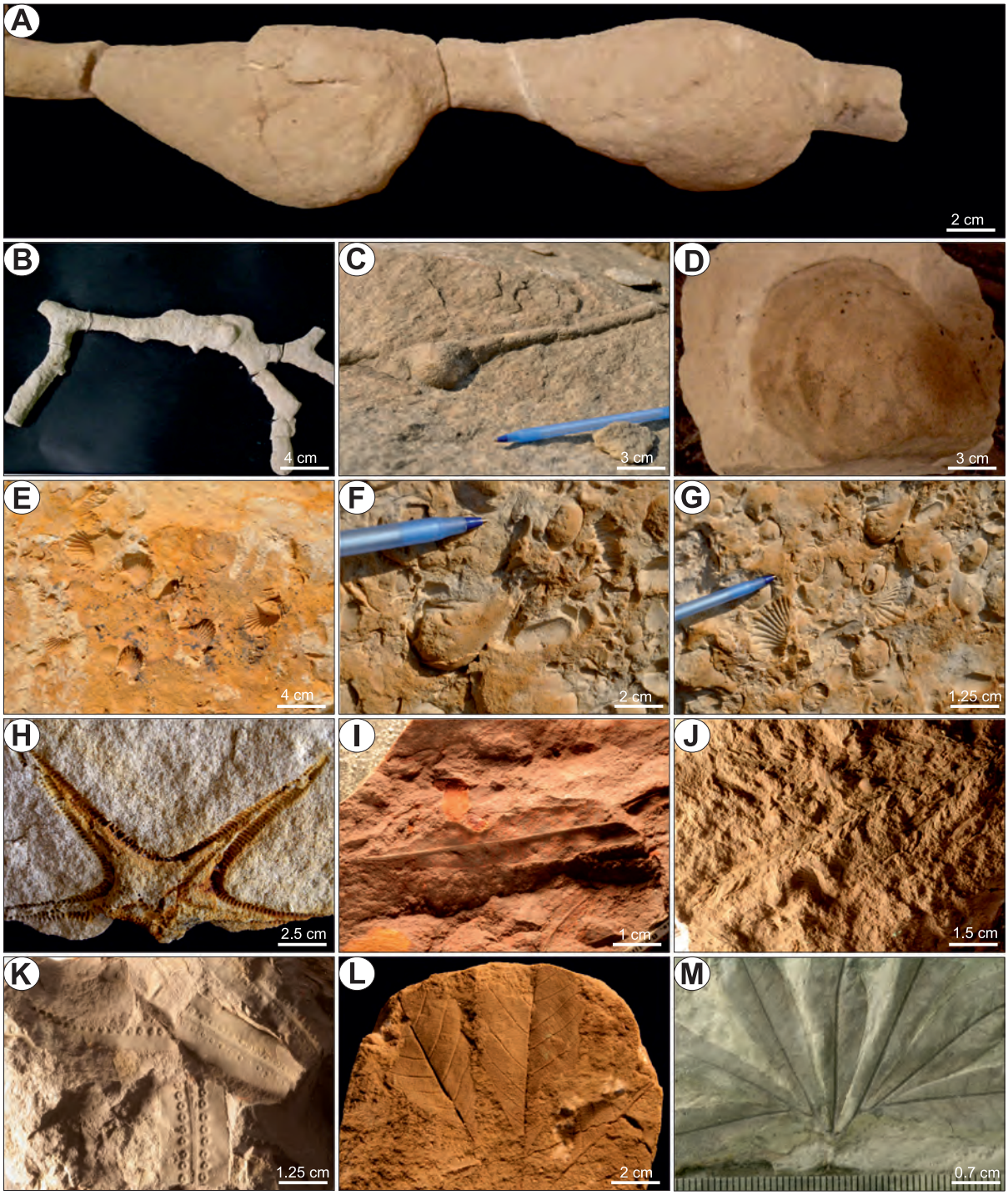

Fig. 16. Plant, macrofaunal body, and trace fossils from the Upper Cretacaeous of the North Sudetic Synclinorium. A–H – Macrofaunal body fossils and trace fossils from the Żerkowice Member. A – Full relief of *Rosarichnoides sudeticus* Chrząstek, Muszer, Solecki, Sroka, 2018 from quarry at fieldtrip stop 4B (Chrząstek et al., 2018). Specimen MGUWr-6650s. B – Full relief of *Thalassinoides paradoxicus* Kennedy, 1967, from the quarry at Żerkowice (ca. 250 m to the north of fieldtrip stop 7; Chrząstek et al., 2018). C – Full relief of *Ophiomorpha nodosa* Lundgren, 1891, in loose block of sandstone at the quarry in Żerkowice (cf. B; Chrząstek and Jewticz, 2019). D – A cast of *Inoceramus* sp. in sandstone of the quarry at fieldtrip stop 4A (Chrząstek et al., 2018). E – Imprints of bivalves *Trigonia glaciana* Stürm, 1901 at bedding surface of sandstone in loose block (quarry at fieldtrip stop 6; Chrząstek and Jewticz, 2019). F – Internal mold of bivalve *Anatina* (*Cercomya*) *lanceolata* Geinitz, 1871–1875 in loose block of sandstone (quarry at fieldtrip stop 6). G – Bivalve shell lag (imprints and internal molds) on a →

in individual tidal bars as ranging from 50 to 66 cm, with a consistent median value of 40 cm. The mean cross-set thicknesses are consistently higher than the median values, which indicates a positively skewed thickness frequency distribution and implies a moderate excess of larger dunes. This is probably an effect of local dune overstepping and thickness amplification (Fig. 13B). The standard deviations of dune cross-set thickness show bar-to-bar differences in the range of 38–69 cm, which is probably an artefact of the derivation of data from different parts of laterally stacked asymmetrical bars.

Based on the approximate equations given by McBride (2003), the maximum bar thicknesses measured in the Żerkowice Member (10–15 m) suggest bar lengths of 12–18 km and widths of 1–1.5 km, with formative water depth of bars at 15–20 m (Fig. 19A). The palaeocurrent data (rose diagram in Fig. 17) are broadly compatible with the flow pattern expected for in-

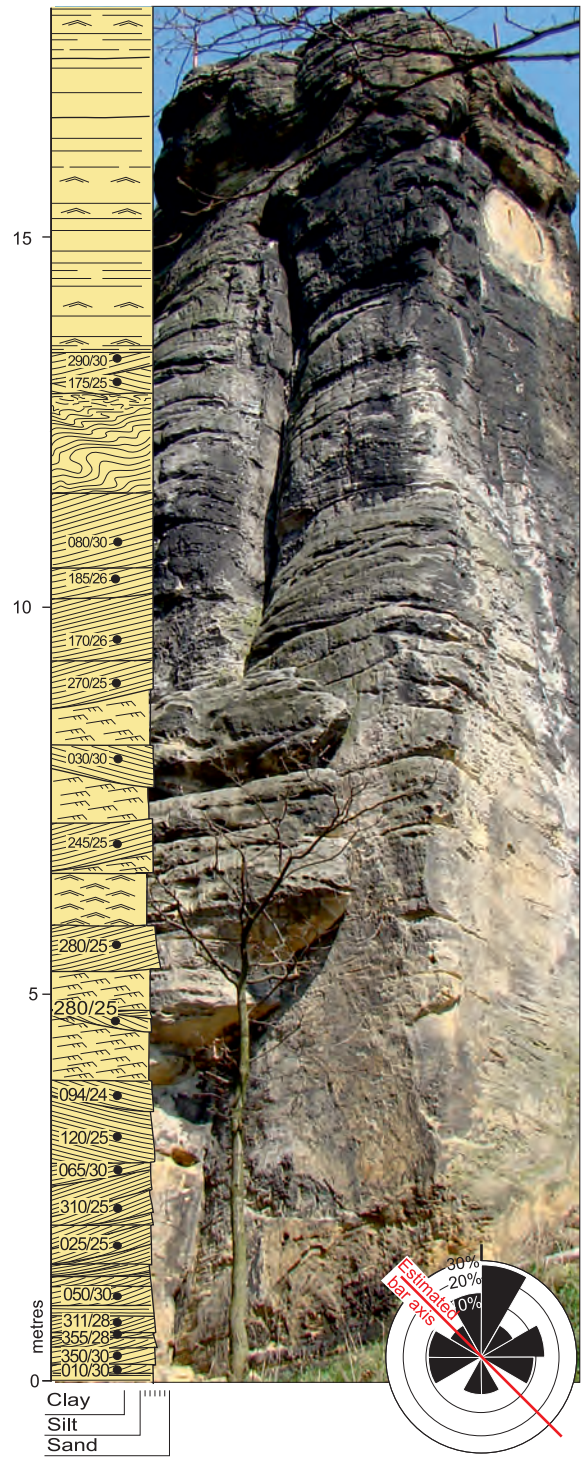

Fig. 17. Succession of vertically stacked dune cross-strata sets of lithofacies Sc with interbeds of current- and wave-ripple cross-laminated lithofacies Sr and SW, increasingly wave worked at the top (lithofacies Sw and Sp). "Skała z Medalionem" tor, fieldtrip stop 7B. The succession is thought to represent a shoaling-upwards bar. The inset rose diagram summarizes cross-strata palaeocurrent directions. From Leszczyński and Nemec (2020).

sandstone bedding plane at fieldtrip stop 6. H – Imprint of the starfish *Lophidiaster scupini* (Andert, 1934), formerly *Astropecten scupini* Andert, 1934, in sandstone (quarry at fieldtrip stop 4B; Chrząstek et al., 2018). I–M – Plant fossils and their assignment to the assemblages distinguished by Halamski et al. (2020). I – Imprint of an isolated leaflet of *Dewalquea haldemiana* Debey ex de Saporta and Marion, 1873. Specimen MB.Pb.2008/320. Rakowice Małe, detailed locality unknown; Nowogrodziec Member, lower part (Assemblage 4), upper Coniacian?–lower Santonian? J – Imprint of a twig of *Geinitzia reichenbachii* (Geinitz, 1842) Hollick and Jeffrey, 1909 (Gymnospermae, Coniferae, family unknown). Specimen MB.Pb.2008/0252. Ołdrzychów, Nowogrodziec Member, upper part (Assemblage 5), upper Coniacian?–lower Santonian? K – Accumulation of imprints of fertile pinnules of *Konijnenburgia* cf. *galleyi* (Miner, 1935) Kvaček and Dašková, 2010 (Filicophyta, Leptosporangiatae, Matoniaceae). Specimen MB.Pb.2008/373.2a. Żerkowice, detailed location unknown; Nowogrodziec Member, lower part (Assemblage 4), upper Coniacian?–lower Santonian? L – Imprint of a trifoliolate leaf of *Dryophyllum westerhausianum* (Richter, 1904) Halamski and Kvaček in Halamski et al., 2020 (Angiospermae, Dictotyledoneae, Fagales). Specimen MB.Pb.2008/346. Ulina, detailed location unknown; Czerna Formation (Assemblage 6), lower–middle Santonian. M – Imprint of a subcomplete compound leaf of *Dewalquea* aff. *gelindenensis* de Saporta and Marion, 1873 (Angiospermae, Dicotyledoneae, Eudicotyledoneae). Bolesławiec (former quarry southeast of the town centre, between Miłosza, Starzyńskiego, and Kosiby Streets). Specimen MGUWr 2880p. Czerna Formation (Assemblage 8), lower–middle Santonian. MB – Museum für Naturkunde, Berlin. MGUWr – Muzeum Geologiczne Uniwersytetu Wrocławskiego, Wrocław. Photographs A – H by A. Chrząstek, I – M by A. Halamski.

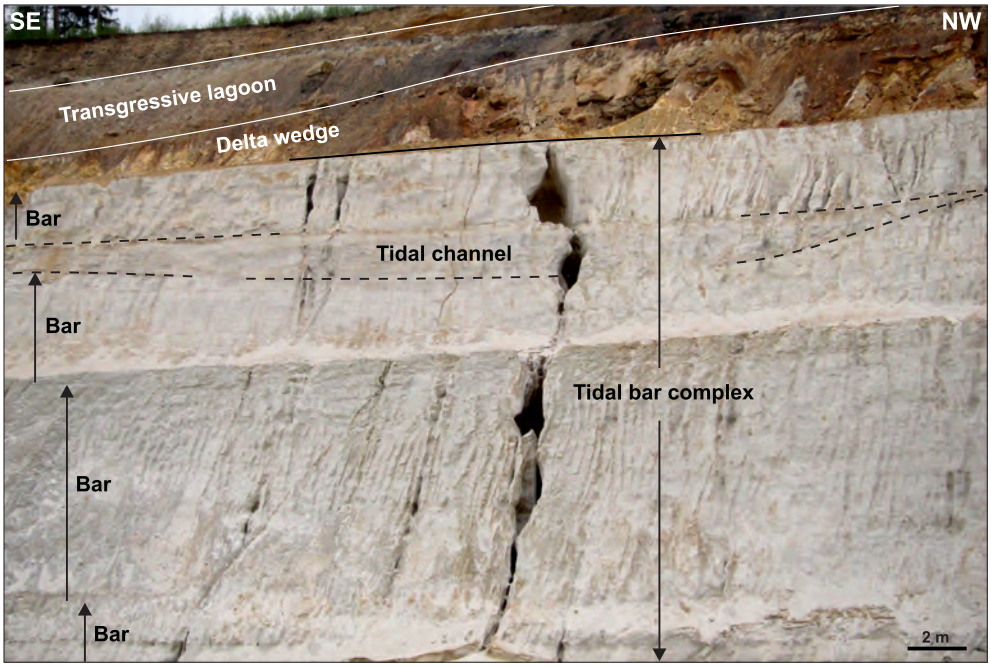

Fig. 18. Portion of outcrop section in active glass sand open pit ca. 2 km west of fieldtrip stop 10 (Fig. 1B). Here, the topmost part of Żerkowice Member comprises a northwest-prograding tidal bar complex with an embedded tidal palaeochannel, overlain by a southwest-advancing basin-margin delta wedge. The overlying basal part of the Czerna Formation consists of transgressive lagoon deposits. From Leszczyński and Nemec (2020).

stantaneous tidal current reversals over a sand ridge (Fig. 19D; cf. Snedden and Dalrymple, 1999; Reynaud et al., 1999), while the lateral and vertical stacking of sand ridges into complexes implies groups of coalescing adjacent coeval bars (Fig. 19C).

The local wedge-shaped sediment assemblages composed of lithofacies Sp, with subordinate intercalations of lithofacies Sr and Sw and sporadic isolated dune cross-sets of lithofacies Sc – which extend from the synclinorium outcrop margins towards its axis, transverse to the inferred tidal sand ridges and effectively interfingering with or onlapping the latter (Figs 20–22) – are interpreted by Leszczyński and Nemec (2020) as basin margin shoal-water deltas (*sensu* Leeder et al. 1988; Postma 1990) or mouth bar-type deltas (*sensu* Dunne and Hempton 1984; Wood and Ethridge 1988). These deltas are dominated by river frictional effluent (lithofacies Sp, Wright, 1966) and fluctuating wave action (lithofacies Sp and Sw; Komar and Miller 1965), with basin-axis tidal current influence (lithofacies Sc; Dalrymple 1984, 2010). The deltaic sandbodies in the Żerkowice Member extend basinwards from both the southwestern (Figs 20, 21) and the northeastern (Figs 22, 23) of the original synclinal basin; near the synclinorium margins, their maximum preserved thicknesses are up to 20 m. Drifted plant fragments are common. Trace fossils are mainly indicative of a shore-proximal expression of the *Cruziana* Ichnofacies (Leszczyński 2018). Advancing deltas apparently impinged sidewise onto the basin-axis tidal bars (Figs 20 to 23). The shore-proximal subaerial parts of the deltas are scarcely preserved, removed by the erosion of the synclinorium flanks (cf. Fig. 22). The outcrop that comes closest to showing a fluvial feeder system is the delta wedge near fieldtrip stop 10 (Fig. 23), where delta-top distributary palaeochannels are recognizable (see the top photograph, Fig. 23), represented by coarser-grained, cross-stratified sandstones (log interval 23–26 m in Fig. 23) and interpreted as fluvial channel-mouth deposits.

The sand wedges with thicknesses of up to 5 m, consisting of gently basinwards inclined (3–5°) deposits of alternating lithofacies Sp and Sw (log interval 6–10 m in Fig. 23; intervals separating tidal bars in log interval 0–20 m in Fig. 23), are interpreted by Leszczyński and

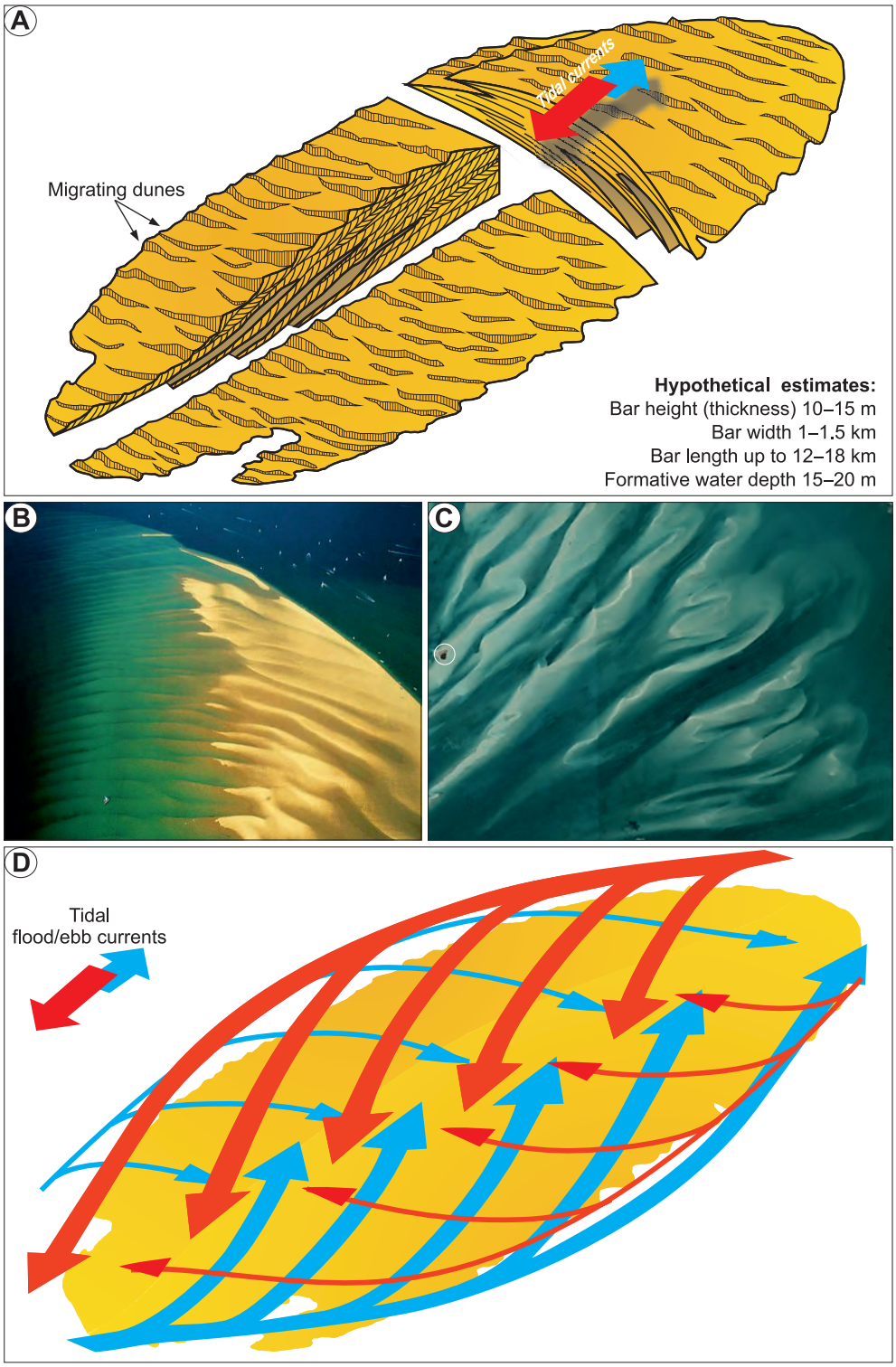

Fig. 19. Longitudinal tidal bar (sand ridge) features and their development. A – Idealized model of a prograding bar with hypothetical estimates of its dimensions and formative water depth pertaining to the Żerkowice Member. B – Modern tidal sand ridge in the southern North Sea; the white spots on the water surface (top right) are wakes of small motorboats. C – An array of coalescing tidal sand ridges, fanning out from a strait in the Bahamas; large cruise ship (encircled) for scale. D – Interpreted pattern of instantaneously reversing tidal currents over a tidal sand ridge inferred from palaeocurrent measurements (e.g., Fig. 17). From Leszczyński and Nemec (2020). Aerial images from Google Earth.

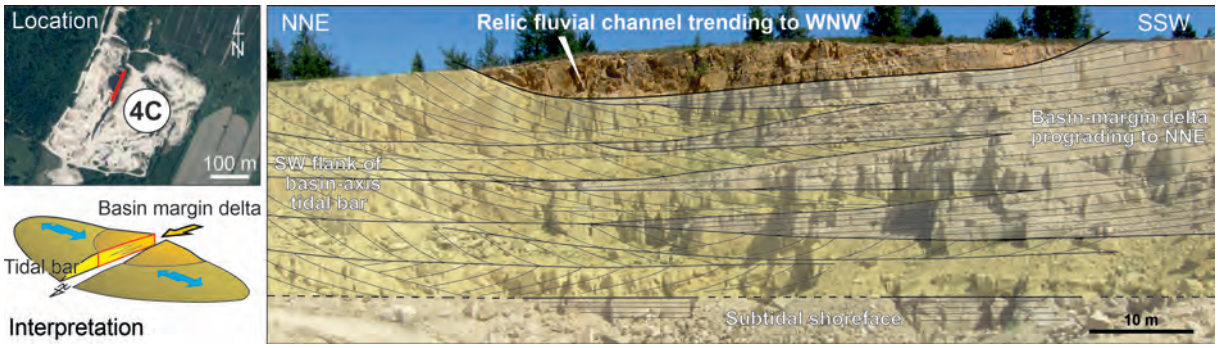

Fig. 20. Outcrop section in the active quarry in Czaple (fieldtrip stop 4C; see Fig. 1B and inset Google Earth image), showing a basin-margin delta interfingering with the southwest flank of a basin-axis tidal sand bar (see inset interpretative diagram). The relic fluvial palaeochannel at the top represents the forced regression that terminated the deposition of the Żerkowice Member. From Leszczyński and Nemec (2020). Photograph by S. Leszczyński.

Fig. 21. Outcrop detail from active quarry in Czaple (fieldtrip stop 4C, Fig. 1B; and inset Google Earth image) from Leszczyński and Nemec (2020), showing a basin-margin shoal-water delta wedge onlapping the southwest flank of basin-axis longitudinal tidal bar. Photograph by S. Leszczyński.

Nemec (2020) as wave-dominated upper shoreface deposits (Komar and Miller, 1965; Clifton and Dingler, 1984) that prograded from both sides of the basin jointly with the basin-margin local river deltas. The sediments commonly display subtle angular unconformities in the form of planar erosional surfaces. The plane-parallel stratification in some units of lithofacies Sp is as steep as 10–15° (Fig. 11F), showing heavy-mineral placers (Fig. 11E) and primary current lineation (Fig. 11J). The sand is nearly pure quartz, very well sorted and poorly cemented. Trace fossils are uncommon, and those present represent an environmentally stressed version of the *Skolithos* Ichnofacies (Leszczyński 2018). Internal planar unconformities are attributed to episodic erosion by storm waves. The advancing shoreface deposits locally interfinger with basin-axis tidal bars (Fig. 23). The more steeply inclined packages of lithofacies Sp, with heavy-mineral placers and parting lineation, are interpreted as fore-

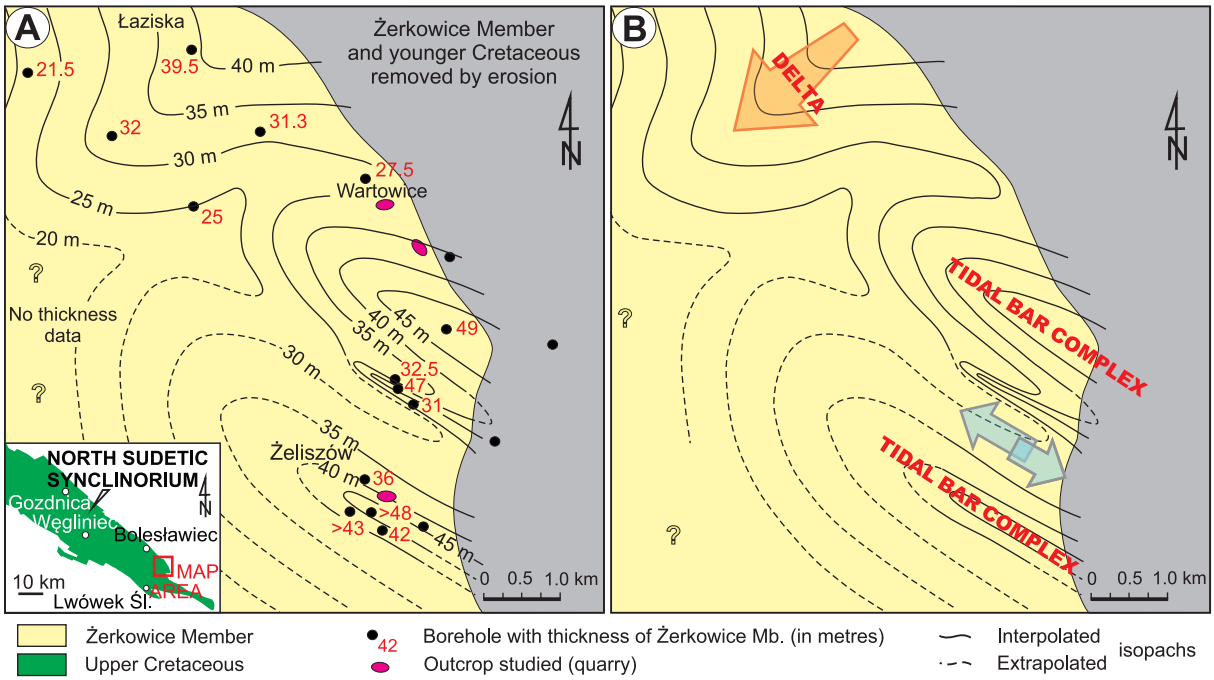

Fig. 22. A – Local sandstone isopach map of the Żerkowice Member (area indicated in the inset map) with the location of boreholes and quarries in Wartowice (fieldtrip stop 5) and Żeliszów (fieldtrip stop 6); see localities in Fig. 1B. Borehole data from Drozdowski et al. (1978). B – Interpretation of the isopach map as a basin-margin delta that interfered with northwest-prograding tidal bar complexes. Note the large extent of basin-fill erosion due to the end-Cretaceous tectonic inversion of the basin. From Leszczyński and Nemec (2020).

shore swash deposits (Allen 1982), implying local encroachment of the basin shoreline (e.g., Fig. 23, log interval 9.5–10 m).

The Czerna Formation

The Czerna Formation begins with a prominent mudstone distinguished by Leszczyński and Nemec (2020; Figs 10, 23–25). It forms units up to a few metres thick, ranging in colour from maroon and orange, with ferricrete (ironstone) concretions or bands up to 5 cm thick, to greenish and dark grey with local siderite interlayers up to 6 cm thick. Some mudstone units are densely interspersed with sand and/or silt streaks and thin interlayers, forming the heterolithic lithofacies H that is often strongly bioturbated and occurs as units up to a few metres thick (Figs 23B, 26K–O). The mudstones are also intercalated with claystone lithofacies CL (Figs 23B, 26J) that forms 0.1–1.2 m thick units, ranging in colour from maroon and orange with clayey ironstone interlayers to greenish and dark grey or subordinately black (coaly). Another new facies are the coal beds of lithofacies C, up to 25 cm thick and ranging from autochthonous, underlain by seat-earth, to hypautochthonous (Figs 23D, 25, 26D). Fine-grained, ripple cross-laminated sandstone beds of lithofacies Sr and Sw, 10–25 cm thick, occur as sheet-like intercalations in lithofacies H or are overlain by the planar parallel-stratified sandstones of lithofacies Sp as upwards coarsening couplets 0.5–2 m thick (Figs 23A, 25, 26E, F). Many sandstone beds are variably homogenized by bioturbation. The cross-stratified sandstones of lithofacies Sc are commonly medium- to coarse-grained, with an admixture of granules and small pebbles. This lithofacies occurs solely as the infill of local palaeochannels, each a few metres deep and less than 100 m wide, trending to the northwest and dominated by trough (3D dune) cross-stratification (Figs 25, top, 26G).

Trace fossils abound, including rhizoliths, rhizocretions (Fig. 26A), and densely plant root-penetrated palaeosols (Fig. 26B, C), classified as vertisol to histosol (cf. Retallack 2001). Only some of the palaeosol horizons are actual seat-earths to coal beds (Fig. 25). Common

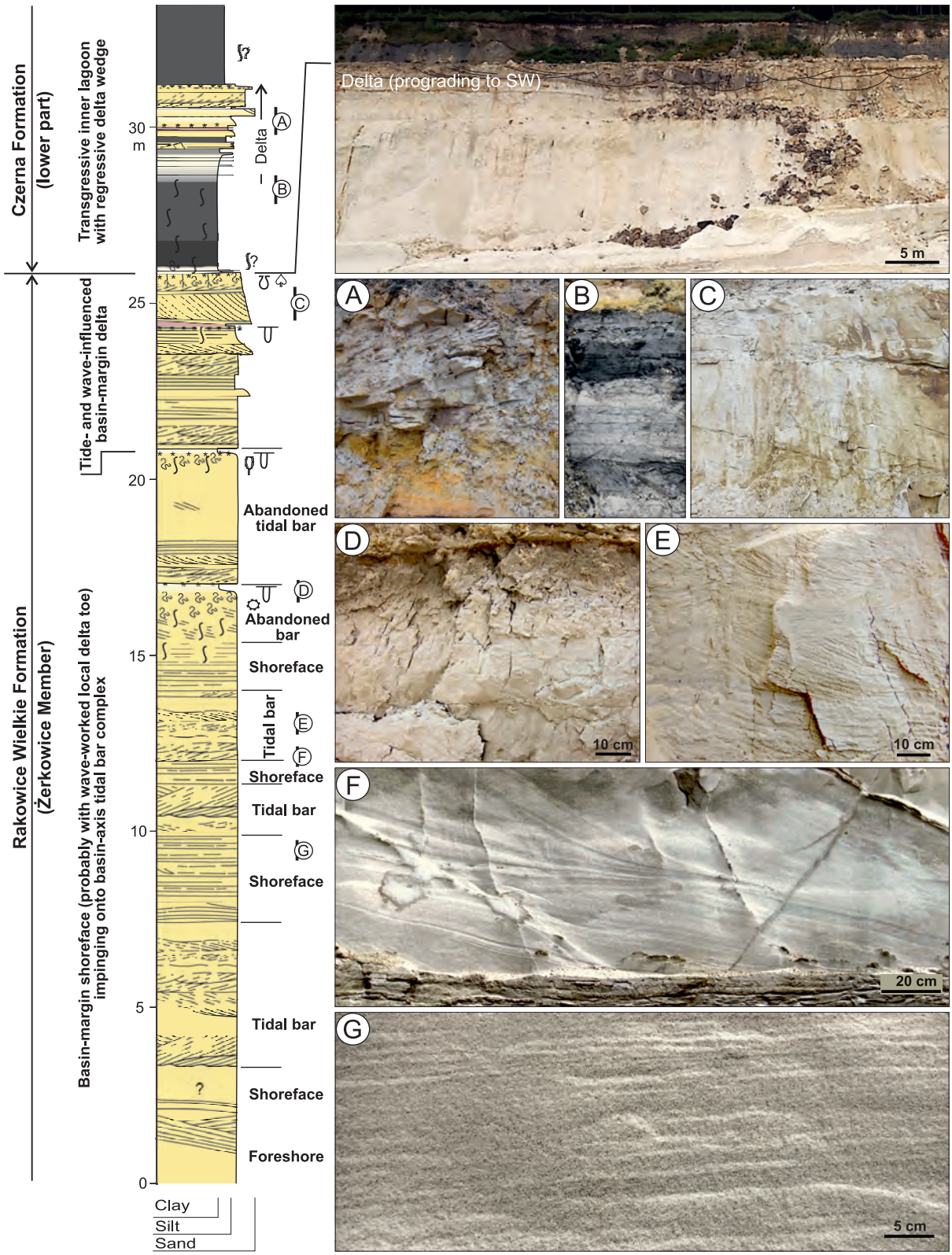

Fig. 23. Sedimentological log and corresponding outcrop photograph (top) of the upper part of Żerkowice Member and the lowermost Czerna Formation in the glass sand pit at Osiecznica (~2 km west of fieldtrip stop 10, Fig. 1B). From Leszczyński and Nemec (2020). Note the basin-margin delta wedge impinged sidewise onto the basin-axis tidal system at the top of the →

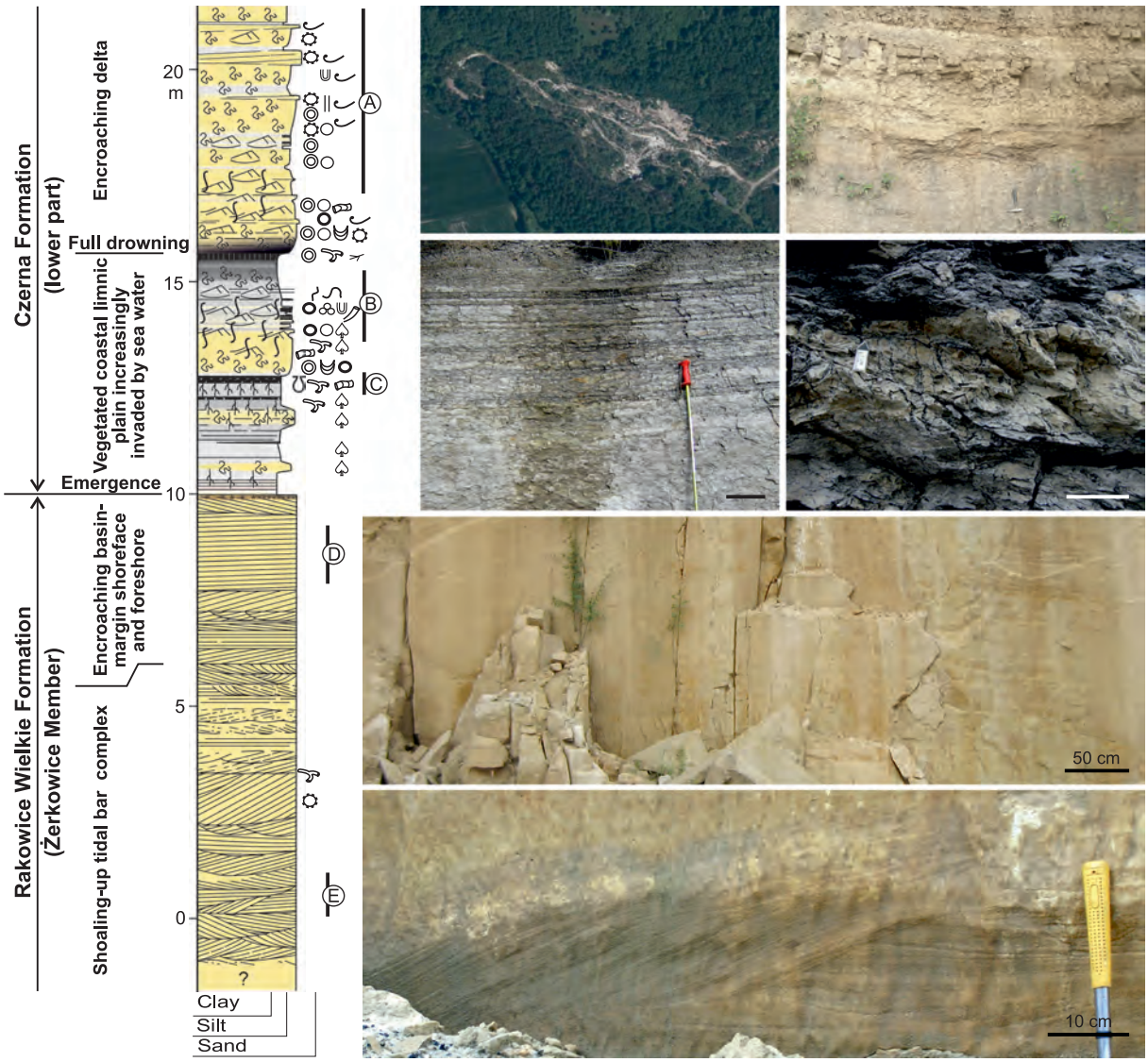

Fig. 24. Sedimentological log of the uppermost Żerkowice Member and lower Czerna Formation at the Rakowiczki quarry (fieldtrip stop 8, Fig. 1B), from Leszczyński and Nemec (2020). The tidal sand bar complex here was covered by a regressive sandy wedge of basin-margin shoreface to foreshore deposits prior to emergence. The overlying paralic deposits indicate gradual marine inundation and eventual full flooding, followed by encroachment of a basin-margin wedge of prodelta deposits. For log legend, see Fig. 12. Outcrop details (indicated at the log margin and in the inset Google Earth image). A – Coarsening-upwards packages of bioturbated progradational prodelta deposits of lithofacies Sr. B – Thin-bedded, bioturbated lagoonal deposits of lithofacies H. C – Paludal deposits of lithofacies M with horizons of plant-root traces and brackish marine burrows in the coal bed. D – Wave-worked upper shoreface sandstone of planar parallel-stratified lithofacies Sp. E – Dune cross-stratified sandstone of lithofacies Sc. All photographs by S. Leszczyński.

Żerkowice Member and the overlying transgressive lagoon deposits of the basal Czerna Formation, split by the minor delta re-advance. For log legend, see Fig. 12. Outcrop details (indicated at the log margin): A – Sandy mouth bar of the coarsening-upwards minor deltaic wedge. B – Muddy lagoonal deposits directly below deltaic wedge. C – Sandy mouth bar of the main delta wedge. D – Bioturbated top of quasi-abandoned tidal bar. E – Bidirectional dune cross-stratification in tidal bar. F – Gently northwest-descending tangential cross-strata sets in lower part of prograding tidal bar. G – Plane-parallel stratification in wave-worked upper part of tidal bar. All photographs by S. Leszczyński.

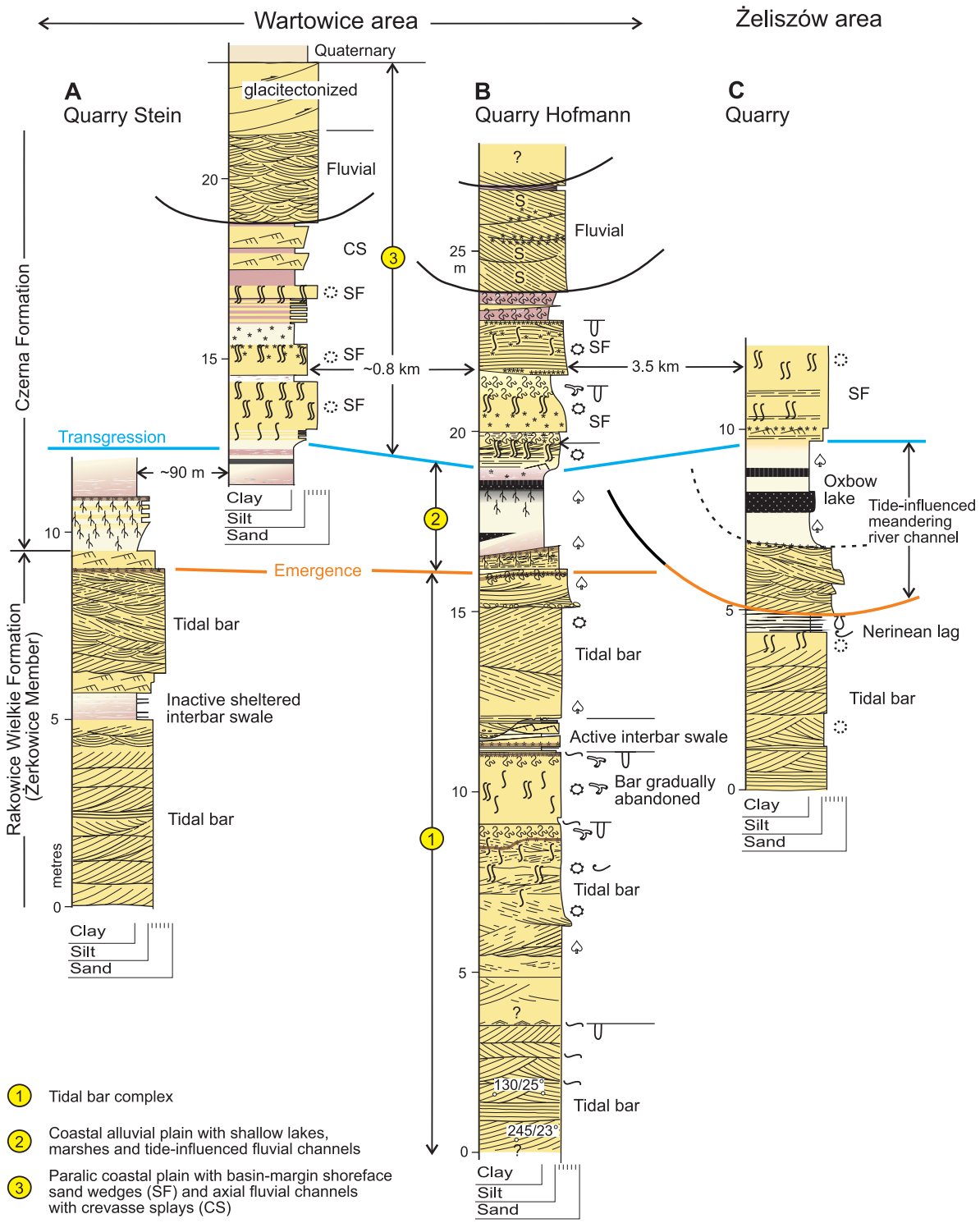

Fig. 25. Sedimentological logs from quarries at fieldtrip stops 5C (A), 5A (B) and 6 (C) (see Fig. 1B), showing the upward passage of the Żerkowice Member of the Rakowice Wielkie Formation to the Czerna Formation. From Leszczyński and Nemec (2020). Note that the deposition of Żerkowice Member was terminated by emergence, with the tide-influenced fluvial palaeochannel probably a time-equivalent of the fluvial palaeochannel at fieldtrip stop 4 (Fig. 20). The deposition of the Czerna Formation in this area commenced in a peat-forming coastal-plain environment, which was eventually flooded by marine transgression. The subsequent highstand normal regression involved rapid advances of the basin-margin shoreface, culminating in the expansion of a basin-margin fluvio-deltaic system.

animal traces include *Ophiomorpha* (Fig. 26I), *Palaeophycus* (Fig. 26L), *Arenicolites* (Fig. 26M), *Thalassinoides* and *Asterosoma* (Fig. 26N). Leszczyński (2010, 2018) reported in detail the rich ichnofauna assemblages in the quarry associated with fieldtrip stop 8 (Fig. 1B), while pointing to the sparse bioturbation at some other localities, such as the rare, taxonomically undetermined ichnofossils at the glass sand pit in Osiecznica (ca. 2 km west of fieldtrip stop 10; Figs 1B and 23). Leszczyński (2010) also reported on scattered mollusc shells, some buried in life position, and on shell lags preserved solely as imprints. Sporadic horizons with brackish-water bivalve and gastropod shells were described earlier by Drescher (1863) and Milewicz (1965, 1996).

The sedimentary succession of the Czerna Formation, which roughly corresponds to that distinguished as the *Überquader* by Beyrich (1855), rests upon the Rakowice Wielkie Formation in the southeastern part of the NSS, with a stratigraphic hiatus (Fig. 3) composed of an erosional unconformity that decreases in duration to the northwest along the basin axis and passes seawards into a correlative conformity (Milewicz 1956, 1969; Walaszczyk 2008). This erosional boundary demarcates a dramatic change in the sedimentary facies and depositional environment of the Coniacian North Sudetic Basin (Figs 3 and 23–25).

The lower boundary of the Czerna Formation, a subaerial unconformity surface, is locally incised by northwest-trending isolated fluvial palaeochannels filled with lithofacies Sc (Fig. 20), some tidally-influenced before abandonment (Fig. 25C). These palaeochannels are interpreted as representing an incised fluvial drainage system directed along the basin axis towards the northwest and frontally influenced by marine tides. The incision of fluvial channels directly in littoral deposits (Figs 20 and 21C) strongly supports the idea of a forced marine regression (Leszczyński and Nemec 2020).

The overlying sedimentary succession of the Czerna Formation commences with a widespread unit of fined-grained deposits, 2–5 m thick, dominated by lithofacies M, CL, and H with subordinate intercalations of sandstone lithofacies Sr and autochthonous or hypautochthonous coal beds of lithofacies C (Figs 23–25; fieldtrip stops 5, 6, 8). Brackish shelly fauna and ichnofauna accompany palaeosols and accumulations of plant debris in this unit, locally even directly at its base and within the same depositional bed. This unit of coal-bearing muddy deposits is presumably the poorly defined Nowogrodziec Member of Milewicz (1985) (Fig. 3).

The short-distance lateral variation in the thickness of this unit and the relative proportion of its component lithofacies is noteworthy (cf. Figs 23–25; Leszczyński and Nemec 2020). In the glass sand pit 2 km west of fieldtrip stop 10, this muddy unit is at least 9 m thick and split in the middle by a coarsening-upwards sandstone wedge, 2–4 m thick, composed of lithofacies Sr, Sp, and Sc (Fig. 23, top). The nearby boreholes N-14 and N-26 (Fig. 10; see Leszczyński and Nemec 2020) show that the unit pinches out abruptly towards the northwest by interfingering with a coeval, few dozen metre thick prominent sandbody that rests directly on the sandstones of the Żerkowice Member. This thick sandstone body, earlier considered to be part of the Żerkowice Member, is interpreted by Leszczyński and Nemec (2020) as an integral part of the lowermost Czerna Formation (see below).

According to Leszczyński and Nemec (2020), the coal-bearing muddy basal unit of the Czerna Formation (i.e., the Nowogrodziec Member of Milewicz, 1985), with its brackish/marine fauna, represents a paralic environment comprising extensive shallow lakes with peat-forming mires and small stream deltas. The thick, muddy deposits at the glass sand pit in Osiecznica (near fieldtrip stop 10; Fig. 23, top) are considered to represent a transgressive lagoon intruded sidewise by a southwest-prograding basin-margin sandy delta wedge. The lagoon was apparently sheltered from the open sea by the thick and narrow sandbody mentioned above and recognized in boreholes N-14 and N-26 (Fig. 10), interpreted by Leszczyński and Nemec (2020) as a cross-basinal transgressive coastal sand barrier. The formation and in-place growth of this barrier would have blocked the earlier fluvial drainage of the emerged southeastern part of the basin and turned this area into a peat-forming paralic lacustrine plain with local stream deltas. The eventual in-place drowning of the barrier (cf. Sanders and Kumar 1965; Rampino and Sanders 1981) would then bring about another change to the basin environment.

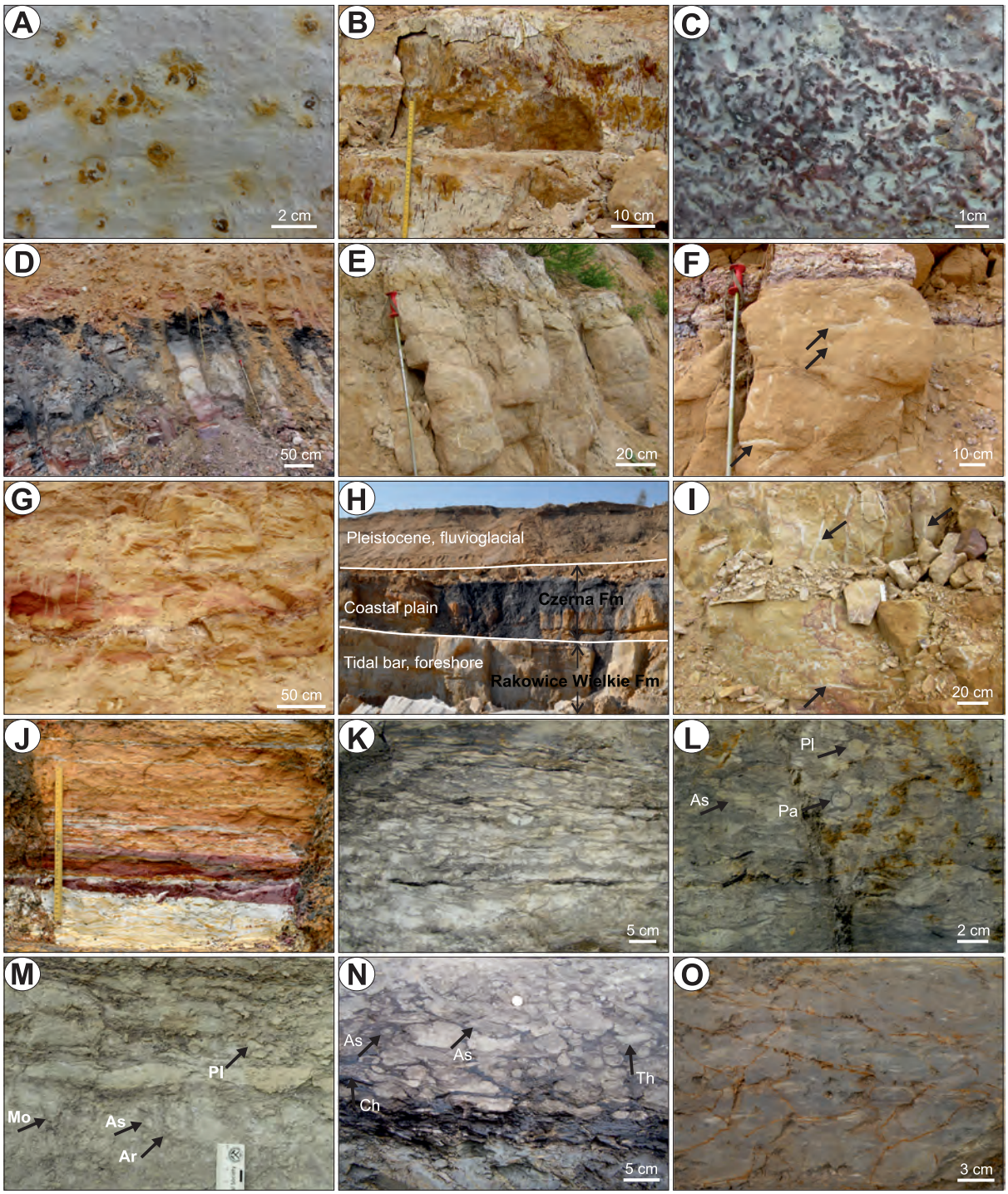

Fig. 26. Lithofacies and ichnofauna of the lower Czerna Formation according to Leszczyński and Nemec (2020). A – Rhizocretions, and in B, C – denser plant-root penetration structures at the formation base at fieldtrip stop 5A (cf. Fig. 25A). D – Dark-grey claystone of lithofacies CL overlain by autochthonous coal of lithofacies C in the basal part of the formation at fieldtrip stop 5A (Fig. 25B). E, F – The overlying shoreface lithofacies Sp at fieldtrip stop 5A (Fig. 25B), showing a variable degree of bioturbation with Ophiomorpha (two fragments are indicated by arrows). G – Cross-stratified fluvial sandstone of lithofacies Sc in the top part of outcrop at the same locality (Fig. 25B). H – Tidally influenced fluvial palaeochannel incised in the underlying formation at fieldtrip stop 6 (Fig. 25C). I – Ophiomorpha burrows (three cases indicated by arrows) in shoreface lithofacies Sp in the uppermost part of outcrop at fieldtrip stop 6 (Fig. 25C). J – Light-grey to reddish claystone with ferricrete (lithofacies CL) passing upwards into iron oxyhydroxide-stained yellowish mudstone (lithofacies M) in the basal part of the formation at fieldtrip stop 8. →

The overlying deposits – ca. 10 m thick (Figs 23–25), in the lower part of the Czerna Formation, consisting of muddy heterolithic lithofacies H intercalated with sheets of sandstone lithofacies Sr, Sp and minor Sw forming coarsening-upwards or sporadically fining-upwards packages, 0.5–1.5 m thick (Figs 23, 25) and variably bioturbated – are thought to represent a marine offshore-transition environment that underwent rapid shallowing by the spasmodic encroachment of basin-margin shoreface and prodelta sand wedges (Leszczyński and Nemec, 2020). The uppermost exposed cross-stratified deposits (lithofacies Sc; Fig. 25, top) are interpreted to be laterally and vertically stacked palaeochannels, 3–4 m deep and 100–120 m wide. These channels record the shallowing of the marine environment and expansion of the basin-margin alluvial plain with small shoal-water deltas, fluvial channels, and associated crevasse-splays (Fig. 25, top).

The remaining, major part of the Czerna Formation, up to 500 m thick, is almost exclusively comprised of siliciclastic deposits, predominantly sandy (from nearly loose sands to sandstones), muddy, and clayey (partly plastic), subordinately gravely, with thin intercalations of coal, ironstone, and siderite (Scupin 1913; Milewicz 1996). The relative proportion of the individual lithologies, their features, and their vertical arrangement vary both laterally and vertically in the sedimentary succession. Its lower part consists mainly of grey to dark grey fine-grained deposits, locally with red-brown or cherry colouration and with frequent thin xylite-rich coal interlayers (Górniak 1991), coalified wood fragments, and numerous mollusc fossils. In the upper part, the fine-grained deposits show lighter colouration, mostly light grey to whitish towards the top, and lack fossil fauna (Górniak 1991). The fine-grained sediments contain predominantly detrital-like kaolinite and up to 20% mica group minerals (illite, muscovite; Górniak 1991, 1996).

The sandy and gravelly sediments in the Czerna Formation (Fig. 27, fieldtrip stop 9; Górniak 1991) are whitish, drab to cream-yellow, locally orange, brown or cherry red in colour. Sandstones are mainly fine- to medium-grained, quartzose, with kaolinite matrix and cement. Weathered feldspars, micas, halloysite-goethite-hematite-siliceous impregnation (ironstone, ferruginous silcrete), and coalified plant remains (leaf fragments, wood; Górniak 1996) are present as accessorary constituents. The sandstones occur as thin to several metre thick beds, massive (structureless) or with planar or cross-stratification, plant-root horizons, and casts or molds of fossil fauna (Górniak 1991; Milewicz 1996). Pebble admixtures and thin pebbly conglomerate layers/lenses occur in the basal parts of sandy trough cross-strata sets, particularly in the uppermost preserved part of the Czerna Formation (fieldtrip stop 9; Fig. 27; Górniak 1991).

In the Santonian, coarse-grained sediments (mainly sandstone or sands) prevail in the eastern part of the NSS (see Górniak 1996, fig. 1). Towards the west and northwest, they form two leading divisions – one in the lower part of the Santonian succession and the other at the top (Milewicz 2006). These divisions are separated by a wedge of almost exclusively fine-grained, dark coloured, muddy and clayey sediments, poorly calcareous to non-calcareous, defining the Węgliniec Formation. The thickness of this fine-grained wedge grows to the northwest, associated with the wedging out of the lower coarser-grained division. The thickness of the upper coarser-grained division grows towards the basin centre and further decreases towards the northwest, ultimately pinching-out (Milewicz, 2006). Fossil fauna, almost exclusively brackish molluscs (bivalves and gastropods, e.g., *Cucullaea zimmermanni* Andert, *Cyrena lischkei* Andert, *Cytherea kruschi* Andert, *Ceromya cretacea* Müller, *Natica geinitzi* Holzapf, *Mytilus rackwitzensis* Scupin, *Cerithium dressleri* Scupin, *Turitella acanthophora* Müller; see Williger 1882; Milewicz 1996 and references therein), occur in the lower coarser-grained division and in the lower part of the overlying fine-grained wedge.

K–M – Lagoonal heterolithic deposits of lithofacies H, highly to totally bioturbated, enclosing ichnogenera *Arenicolites* (Ar), *Asterosoma* (As), *Monocraterion*? (Mo), and Palaeophycus (Pa) at fieldtrip stop 8. N – Prodelta heterolithic sediments of lithofacies H, highly bioturbated, including ichnogenera *Asterosoma* (As), *Chondrites* (Ch) and Thalassinoides (Th) at fieldtrip stop 8. O – Offshore-transition lithofacies H with interlayers of fine-sand lithofacies Sw heavily obliterated by bioturbation at fieldtrip stop 8. Fieldtrip stop numbers as in Fig. 1B. Photographs A–G and I–O by S. Leszczyński, and H by A. Chrząstek.

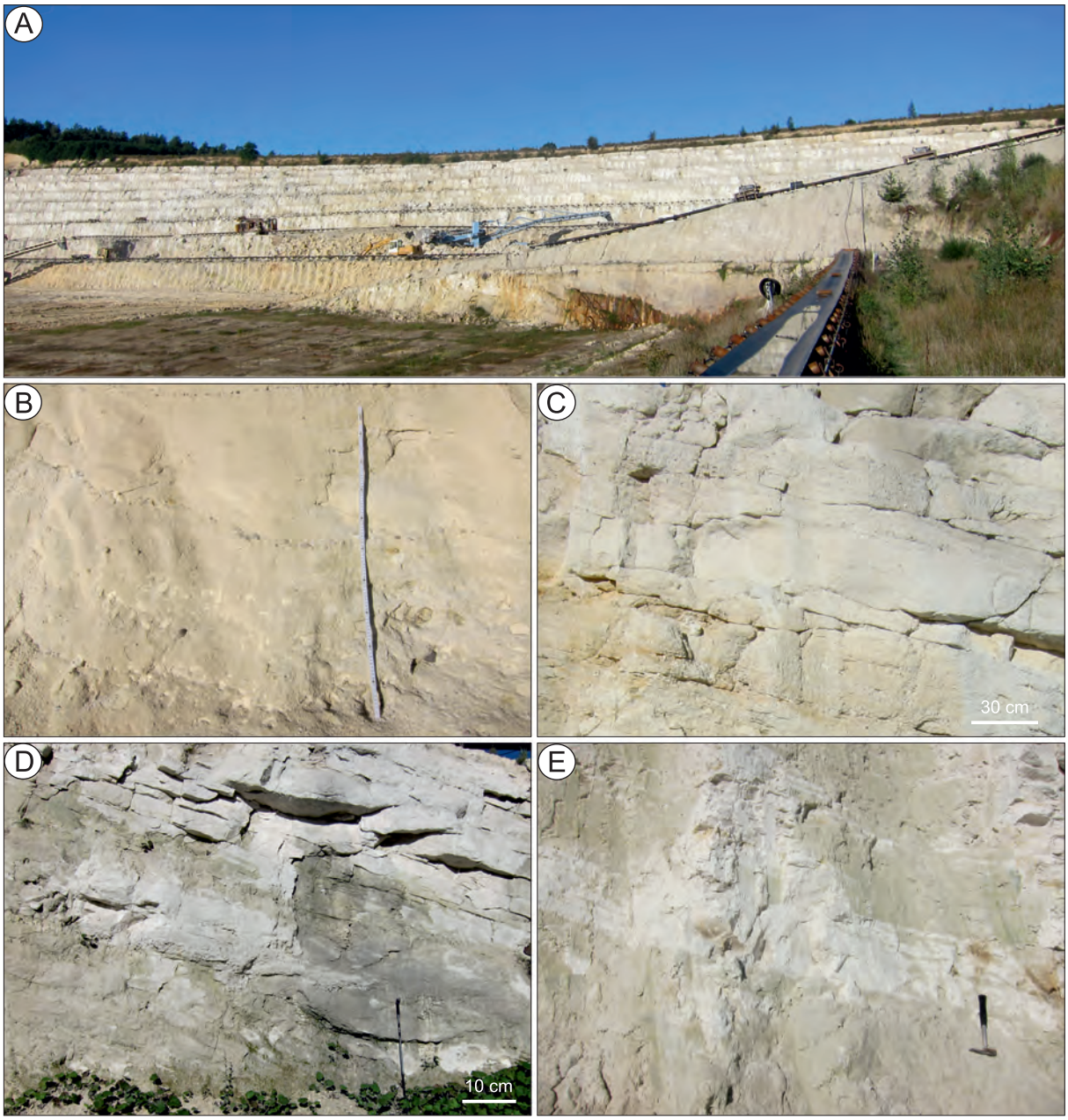

Fig. 27. The Czerna Formation in the kaolin open pit of the Kopalnie Surowców Mineralnych Surmin-Kaolin S.A. in Nowogrodziec (fieldtrip stop 9, Fig. 1B). A – general view of the western pit wall. Note the homoclinal dipping of the sedimentary succession to the right (northeast) B – Agglomeration of claystone intraclasts, small quartz pebble stringers and crudely stratified coarse-grained sandstone of a channel fill. C – Conglomerate of quartz pebbles and claystone intraclasts (cream-yellow) overlain by high-angle and low-angle cross-stratified fine sandy conglomerate. D – Package of lenses, irregular bodies and tabular beds of small-pebble conglomerate, sandstone and siltstone; the walking stick (scale) is 1 m. E – Plane-parallel stratified siltstone with fine-grained sandstone stringers and thin layers; the hammer (scale) is 35 cm. All photographs by S. Leszczyński.

The lithofacies are indicative of a marine to terrestrial, generally deltaic and prodeltaic origin of these deposits. The coarse-grained divisions are delta-front deposits, while the others represent delta-plain palaeochannels and inter-channel zones with swamps and ponds (Williger 1882; Scupin 1913; Milewicz 1996, 2006; Górniak 1991, 1996).

Rich kaolinite occurrences in both fine-grained and sandy sediments render them an

important raw material for the ceramics industry; indeed, the kaolin has been exploited for several centuries.

PALAEOBOTANY

The Upper Cretaceous of the NSS has yielded a moderately diverse fossil flora (Fig. 161–M) that has only recently received a modern comprehensive analysis. The megaflora, microflora, and palaeoecology were treated by Halamski et al. (2020). Fern tree stem casts were described by Greguš et al. (2013) and the mesoflora by Heřmanová et al. (2019, 2020). An exceptional specimen of an angiosperm leaf overgrown by marine bryozoans was described by Halamski and Taylor (2022). The historical aspects of collections were discussed by Mohr (2009), whereas short overviews of all Polish Cretaceous palaeofloras, including extensive reference lists, may be found in Halamski (2020) and Barbacka et al. (in press).

The Late Cretaceous palaeoflora from the NSS, like others from Central and Northern Europe, is preserved in marine and marginal marine strata, which means the plant remains were washed out from land and are dispersed within the sections. No "plant beds" have been found. From a methodological point of view, this means the systematic revision of megafloras is conducted mostly on the basis of ancient collections, assembled over many years when numerous small local quarries were active. In contrast, the biostratigraphy, taphonomy, mesoflora, and microflora are studied based on new observations and newly collected material.

The palaeoflora of the North Sudetic Basin is composed of 29 megafloral taxa, 9 mesofloral taxa, and >126 microfloral taxa (Halamski et al. 2020; Heřmanová et al. 2020). It is worth mentioning that the microflora from strata overlying the Nowogrodziec Member (*sensu* Milewicz 1985; Fig. 3) was studied for decades by the Polish palaeobotanist Jadwiga Raniecka-Bobrowska, but her voluminous memoir (with several hundred taxa) unfortunately remains at a preliminary stage and unpublished. Moreover, the exact location and stratigraphy of boreholes from which the palynomorphs were extracted remains unclear.

The mega- and mesoflora are dominated by angiosperms, while the most common microfloral elements are ferns. The plant palaeocommunities may thus be interpreted as generally intermediate between those pre-dating the Cretaceous Terrestrial Revolution and modern, angiosperm-dominated vegetation (Halamski et al. 2020).

The megaflora was grouped by Halamski et al. (2020) into eight assemblages, consisting of localities grouped by their similar stratigraphy and floral content. Assemblages 1–3 belong to the Rakowice Wielkie Formation, Assemblages 4 and 5 to the Nowogrodziec Member of the Czerna Formation, and Assemblages 6–8 to the part of the Czerna Formation overlying the Nowogrodziec Member. Assemblage 3 contains fern tree stems preserved as casts (Greguš et al. 2013). Assemblage 6 (sandstones of the higher Czerna Formation) contains mainly the fagalean angiosperm *Dryophyllum westerhausianum*. Assemblage 8 (ceramic clays in the Bolesławiec area and other localities) is relatively diversified, including, in particular, the trifoliolate platanoid *Platanites willigeri*. Further descriptions of Assembleges 4 and 5 are provided below.

Plant palaeocommunities interpreted on the basis of the fossil mega-, meso- and microflora to have grown on the East Sudetic Islands include: (i) back-swamp forests dominated by the conifer *Geinitzia*, with ferns; (ii) several varieties of angiosperm-dominated riparian and alluvial-plain forests with *Dryophyllum* and platanoids; (iii) fern savanna with patches of *Pinus* woodlands; (iv) dunes; (v) halophytic vegetation (mangroves) with *Frenelopsis*: a single grain of *Spinizonocolpites* sp. suggests *Nypa* is a part of this community, but requires confirmation; and (vi) pioneer vegetation with lycophytes and ferns (Halamski et al. 2020).

Finally, it should be mentioned that the palaeobiogeographic patterns identified on the basis of fossil flora are in striking contrast to those based on palaeofauna (Csiki-Sava et al. 2015). While faunal reconstructions indicate the Cretaceous European Archipelago was a highly endemic zone, with strong differentiation among individual islands, the plant cover of the same area and interval is mainly comprised of widely distributed species, some of which were similar or possibly identical to those found in North America.

DEVELOPMENT OF SEDIMENTATION

Palaeontological data collected over nearly two centuries indicate that Cretaceous sedimentation in the North Sudetic Basin commenced in the Cenomanian and proceeded until at least the middle Santonian (Walaszczyk 2008). Scupin (1910) suggested that the basin, which he referred to as the *Löwenberger Becken*, was situated between two elevated island areas: one to the northeast, which he called the *Ostsudetische Landmasse* (East Sudetic Landmass), and the other to the southwest named the *Riesengebirgsinsel* (West Sudetic Island; Fig. 2A). The notion that the Late Cretaceous basin lied between two Sudetic landmasses was supported by Andert (1934), although he postulated that the East Sudetic Landmass was much smaller, limited only to an area in the southeastern part of that suggested by Scupin. Recently, two islands have been shown to exist both southwest and northeast of the North Sudetic Basin, and in its southeastern prolongation (Wilmsen et al. 2014; Kowalski 2021). It is generally accepted that the size and relief of the islands changed during their existence (Scupin 1936), due to the influence of eustasy and Alpine tectonism. Therefore, the exact location of the basin coastlines remains a subject of controversy (Biernacka and Józefiak 2009; Biernacka 2012). It is worth noting that Scupin (1913) correctly recognized the northwesterly transition of sandy deposits into mudstones and marlstones (cf. Fig. 3) as the longitudinal direction of bathymetric deepening of the basin.

According to Leszczyński (2018), the two islands mentioned above existed as separate landmasses until the middle Coniacian (Fig. 28A, B). The mid-Coniacian forced regression resulted in a retreat of the sea to the northwest, which merged the two islands and drove the formation of an erosional hiatus in the southeastern part of the basin (Milewicz 1956; Figs 3 and 28B, C). Consequently, the late Coniacian transgression occurred in an embayment open to the northwest, ca. 35 km long and 15 km wide (Leszczyński 2018; Fig. 28D–F), with sedimentation persisting until the final retreat of the sea around the middle Santonian or later.

Palaeogeographic reconstructions suggest that the North Sudetic Basin, in its southern prolongation, had at least two narrow linking straits: one near the town of Złotoryja (which closed in the mid-Coniacian) and another preserved as a relic in the Wleń Graben (Fig. 1B; Kowalski 2021). The latter author has suggested that marine sedimentation in the Wleń strait persisted long after the mid-Coniacian closure of the Złotoryja strait. However, this opinion is questionable, because the youngest Cretaceous deposits in the Wleń Graben are poorly dated and, given their carbonate content, seem to correspond to those documented as predating the mid-Coniacian regression in other areas of the NSS; hence, they may be older than the Żerkowice Member in the excursion area (Fig. 3).

According to Leszczyński and Nemec (2020), the Cretaceous North Sudetic Basin formed as an early, synclinal side effect of the Alpine orogeny, in combination with eustatic forces; crucial stages of basin evolution occurred in the Coniacian. In the early Coniacian, the basin was a long and narrow shallow-marine embayment with the hypothetical (non-preserved) Złotoryja bayhead strait funnelling tidal currents. Input from Wleń strait is unrecognizable in the basin – additionally, the the timespan of this strait's activity is uncertain. Coalescing tidal sand ridges extending from the Złotoryja strait formed a littoral platform that prograded from the bayhead zone along the basin axis, laterally impinged on by the basin-margin shoreface and local river deltas. A mid-Coniacian forced marine regression and closure of the bayhead strait, attributed to Alpine tectonism combined with eustasy, brought about a dramatic change in the ba-

Fig. 28. Schematic interpretative reconstruction of the Coniacian palaeogeography and sedimentation pattern in the inner, southeastern part of the North Sudetic Basin; after Leszczyński and Nemec (2020). A – The littoral system of coalescing tidal sand ridges of the Żerkowice Member (Fig. 3) progrades to the northwest, impinged on laterally by the basin-margin nearshore and deltaic sandy systems. B – This tide-driven littoral sand platform reaches its maximum basinward extent, terminated by the closure of the basin bayhead tidal strait and a forced marine regression. C – The emerged former littoral sand platform is denudated and incised by river channels, with the coastal area of paralic sedimentation shrinking basinwards; this stage of development marks the top of the Żerkowice Member. D – The onset of subsequent eustatic sea-level rise creates a transgressive, aggrading coastal sand barrier at the outer edge of the former littoral sand platform, with a barrier-sheltered →

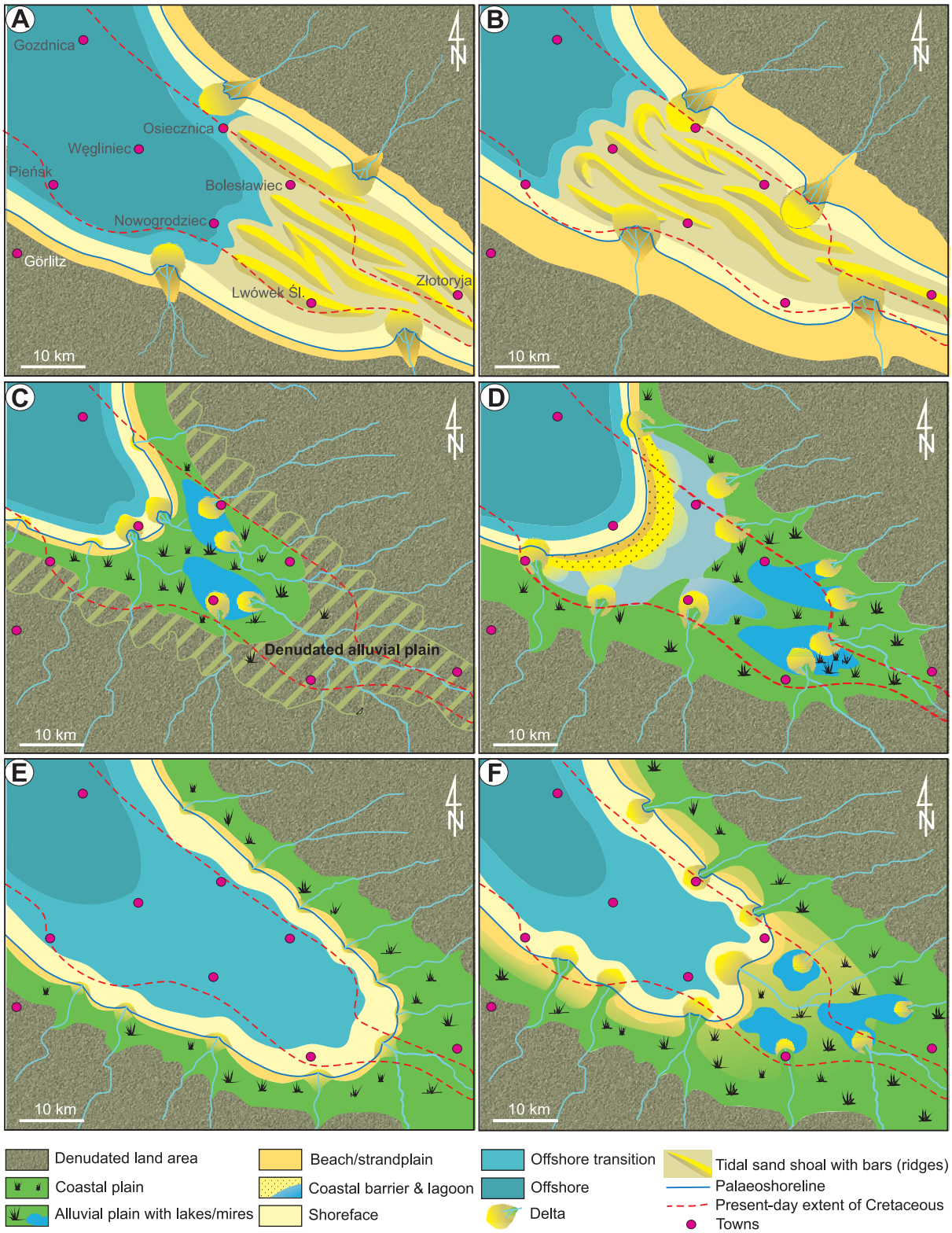

lagoonal to paralic bayhead alluvial plain. E – The aggrading coastal sand barrier is eventually drowned by the sea, whereby the bayhead paralic plain briefly becomes an offshore-transition marine zone. F – The rebounding sediment yield from the elevated margins of the basin causes rapid shallowing by the lateral encroachment of nearshore and fluvio-deltaic systems; the diagram portrays the beginning of the late Coniacian normal-regressive advance of the Czerna Formation (cf. Fig. 3).

sin, through which the basin-wide littoral sand platform emerged and briefly turned into a denudated coastal plain. The late Coniacian eustatic transgression formed an in-place, growing coastal sand barrier at the outer edge of the former littoral platform, sheltering a paralic limno-lagoonal plain with peat-forming mires (the Nowogrodziec Member of Milewicz (1997). The coastal barrier was eventually drowned and maximum marine flooding occurred, followed by a normal regression recorded as a rapidly upward-shallowing succession of offshore-transition to fluvio-deltaic deposits. The sedimentation pattern in an palaeogeographically evolving, tectonically controlled marine embayment contributes to existing models for estuarine sedimentary environments.

Sequence stratigraphy

According to Walaszczyk (2008), the Cretaceous of the NSS represents a single sedimentary cycle including two or three poorly regressive cycles. The Coniacian–Santonian part of the sedimentary succession was interpreted by Milewicz (1997) as representing the latest regressive phase of a transgressive-regressive (T-R) cycle and the earliest transgressive phase of the next T-R cycle. His recognition of a hiatus between the Rakowice Wielkie Formation and the Czerna Formation in the southeastern part of the basin, which he attributed to a northwesterly retreat of the sea from a large inner part of the basin and terrestrial erosion in this emerged area, was particularly important. Walaszczyk (2008) dated this event to the late mid-Coniacian, and Leszczyński (2018) translated it as a forced regression in the parlance of sequence stratigraphy. Leszczyński (2010) interpreted the Żerkowice Member of the Rakowice Wielkie Formation as a regressive systems tract formed at the culmination of the regressive phase and separated by a hiatus from the overlying transgressive systems tract of a 3rd-order eustatic cycle. Later, Leszczyński (2018) attributed the deposition of the Żerkowice Member to the KCo1 eustatic sea-level fall (Haq 2014).

More recently, Leszczyński and Nemec (2020) interpreted the Żerkowice Member as representing a normal-regressive highstand systems tract (Fig. 28A, B) that ended in a forced regression (Fig. 28C) caused by a combination of regional tectonics and eustatic sea-level fall (cf. curve in Fig. 3). The resulting erosional hiatus in the southeastern part of the basin predictably passes into a correlative, normal-regressive deltaic lowstand systems tract in the unexposed northwestern part of the basin (Fig. 29). The forced-regressive unconformity is overlain by a transgressive systems tract represented by the Nowogrodziec Member of Milewicz (1985), including the hypothetical, grown in-place transgressive coastal sand barrier (Figs 28D, 29). Maximum marine flooding occurred during the in-place drowning of the barrier (Figs 25, 28E). The overlying exposed deposits of the lower Czerna Formation (Fig. 25, upper part) are considered by Leszczyński and Nemec (2020) as representing a normal-regressive highstand systems tract (Figs 28F, 29). The thick and narrow sandbody found in boreholes N-14 and N-27 (Fig. 10) is interpreted as an in-place drowned transgressive coastal sand barrier (Fig. 29), stratigraphically belonging to the lowest part of the Czerna Formation as a lateral equivalent of the Nowogrodziec Member of Milewicz (1985).

Leszczyński and Nemec (2020) further observed that the Late Cretaceous pattern of marine transgression and regression in the North Sudetic Basin correlates well with eustatic sea-level changes (Fig. 3), and in particular coincides with the mid-Coniacian pulse of regional Alpine tectonism that critically amplified the eustatic impact on the basin. As such, this Late Cretaceous sequence-stratigraphic record from the northern, outer part of the Central European Boreal–Tethys seaway differs from that in the large, intermediately-located Bohemian Basin (Fig. 1A; Voigt et al. 2008; Mitchell et al. 2010; Nádaskay and Uličný 2014), where the eustatic signal may have been obscured by complicated palaeogeography and local Alpine tectonism.

Apart from regional stratigraphic debates, the Cretaceous seaway eventually retreated from the North Sudetic Basin and the other basins surrounding the Bohemian Massif around the latest Cretaceous to early Palaeogene(?) (Kley and Voigt 2008; Voigt et al. 2021), as evidenced by the shallowing-upward top part of the sedimentary succession and the cessation of marine sedimentation. The retreat resulted from the ultimate Alpine uplift of the region, documented through the deformation of Cretaceous strata and as distinct basement

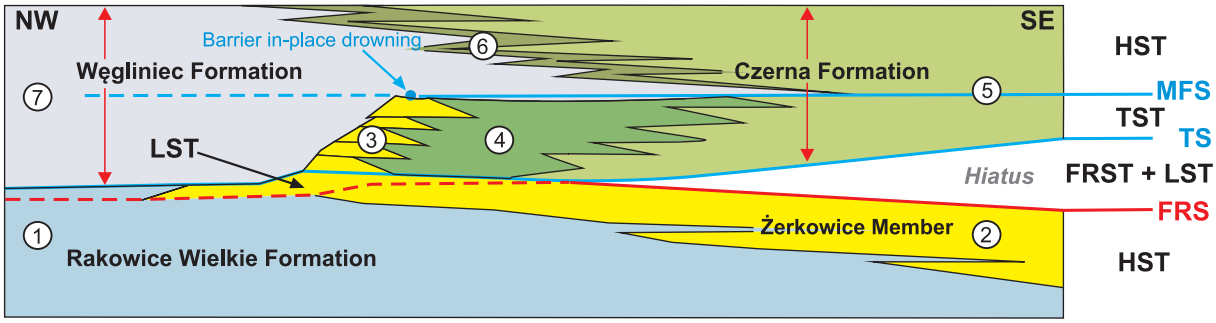

Main sedimentary environments of the Coniacian–Santonian succession:

1. Carbonate-rich, distal muddy offshore zone
2. Subtidal sand platform with laterally impinging deltas and shoreface to beach zone
3. Hypothetical transgressive sand barrier complex (unexposed, inferred from boreholes)
4. Lagoonal zone with sand supply by barrier washover and fluvio-deltaic processes
5. Paralic alluvial plain with rivers, lakes, lacustrine deltas and peat-forming mires
6. Shoreface with shoal-water deltas and prodelta zone
7. Carbonate-poor, distal muddy offshore zone

Sequence-stratigraphy code:

FRS – Forced-regression surface
MFS – Maximum-flooding surface
TS – Transgression surface
FRST – Forced-regressive systems tract
HST – Highstand systems tract
LST – Lowstand systems tract
TST – Transgressive systems tract

Fig. 29. Sequence-stratigraphic interpretation of the Coniacian–early Santonian sedimentary succession in the southeastern part of the North Sudetic Basin, displayed as a basin longitudinal cross-section (schematic, not to scale); slightly modified from Leszczyński and Nemec (2020). The hypothetical notion of an in-place aggrading transgressive coastal sand barrier (unexposed) is based on the great thickness of sandstones in borehole N-27 and their apparent absence in borehole J-1 located ~9 km farther northwest relative to the basin axis.

cooling recorded by thermochronological data (Skoček and Valečka 1983; Jarmołowicz-Szulc 1984; Ziegler 1986; Milewicz 1996; Wojewoda 1996; Uličný 2001; Aramowicz et al. 2006; Ventura et al. 2009; Danisik et al. 2010; Botor et al. 2019). According to Kley and Voigt (2008), this uplift was caused by compression and transpression induced by the Europe–Iberia–Africa plate convergence.

NATURAL RESOURCES

The Cretaceous of the NSS is known for its various natural resources, including, in particular, building stones, ceramic clays, and glass sands. The first consist of sandstones that have been quarried for several hundred years as dimension and carving stones. The oldest mentions of their extraction come from the 12th century (Walendowski 2001). They are highly valued due to their excellent workability and high resistance to weathering. In stone masonry, they were previously used as ashlar, but later and recently have mostly served as veneer. Several quarries between the towns of Lwówek and Bolesławiec are currently active, and some others are ready to begin mining operations.

The early recognition of the value of these sandstones as building and decoration material is documented in the old local architecture, which is richly preserved in Lwówek Śląski and Bolesławiec. The early Coniacian fine-grained sandstones from the top part of the Żerkowice Member south and southeast of Bolesławiec (fieldtrip stops 4–8) are particularly valuable. Farther to the northwest, their quality decreases due to declines in rock strength. The exploited sandstones are divided into several categories differing in colour and texture, and are named after their extraction localities. These sandstones, and coeval sandstones from the Intra-Sudetic Synclinorium, are still considered to be some of the most important building sandstones in Germany (Ehling 2006). They were the dominant natural stone in Berlin's architecture for many decades (1880–1942), and were also used in other German and European cities during that period. After World War II, and especially after the fall of communist regime, they also became important dimension stones in Poland, where recently they have been used mainly as the veneer material of important, official, and exclusive buildings. A renaissance in their use in Germany occurred in 1990 (Ehling 2006). They are still highly prized for their high

degree of homogeneity and attractive physical properties.

Ceramic clay deposits occur in the lower part of the Santonian Czerna Formation, in a ca. 200 m thick succession that abounds in beds and lenses of clay-rich sandstones, kaolinitic white-firing clays, stoneware clays, and refractory clays (Milewicz 1964; Galos 2010). These clay lenses and beds have thickness of 0.2–3.0 m, and constitute ca. 25% of the whole succession. Originally, white-firing clays were extracted from clay beds and lenses. Later, they were extracted by washing from the bulk sediment, if it contained more than 20% good quality clay minerals (Nieć and Ratajczak 2004).The deposits contain diagenetic and secondary kaolin, redeposited to streams and lakes (oxbow lakes) on a delta plain due to the erosion of residual deposits.

White-firing and stoneware clay deposits are recognized mainly in the southern limb of the NSS, in the vicinity of Węgliniec and Nowogrodziec, as well as between Bolesławiec and Lwówek Śląski. Since the Middle Ages, they have been extracted here in open pits; in some intervals in the 20th century, they were also exploited in underground mines. The sediments display differentiated mineralogical composition, with the percentage of grains coarser than 0.063 mm exceeding, in some cases, 50%. The main components are well-ordered kaolinite, illite, and muscovite, although the quartz content varies from 15 to 80% (Stoch 1962; Galos 2010). Due to their large lithological and mineralogical variability, numerous varieties have been distinguished, according to bending strength after drying, >0.063 mm grain content, water absorption, and whiteness after firing (Nieć and Ratajczak, 2004). Kaolin extracted here (e.g., from the Maria III deposit exploited by the Surmin Kaolin plant in Nowogrodziec; fieldtrip stop 9) is used in the ceramic industry for the production of fine pottery products, as well as in the refractory, paper, glass, and cement industries.

White-firing clay resources are currently recognized in six deposits in the Bolesławiec area. The total estimate reservoir of this raw material amounts to ca. 59.6 million t, but a total of ca. 1.1 million t of pure clays in seams and lenses are recognized in three abandoned deposits. In the other three deposits (Janina I, Nowe Jaroszowice, and Ocice), a total of ca. 58.6 million t of sandy-clayey raw material, used for the production of white-firing clay by washing, have been recognized, enabling the production of ca. 16.2 million t of raw white-firing clayey material. Some white firing clay varieties occur in the two nearby, undeveloped stoneware clay deposits (Anna-Włodzice Małe and Ocice II), with total resources estimated as ca. 11.5 million t (see Galos 2010 and references therein). Moreover, the adjacent Czerwona Woda sandy-clayey deposit, recognized previously as a natural foundry sand, has recently started to be used for the production of raw white-firing clayey material, with ca. 5.0 million t available (Galos 2010 and references therein). Prospective areas between Bolesławiec and Nowogrodziec that have tentatively considered for industrial exploration have total estimated resources of ca. 132 million t sandy-clayey sediment, which might allow the production of ca. 40 million t of raw white-firing clay (Galos 2010).

Due to the Cretaceous ceramic clay deposits and local usage, Bolesławiec has been known since the Middle Ages as a town of pottery industry. Unique, stamp-ornamented Bolesławiec ceramic products attract collectors from all over the world.

Another major regional resource are glass sand deposits, which occur in the Coniacian, and subordinately in the Santonian, succession of the Bolesławiec area. They are the second most-important sand glass deposits in Poland (Burkowicz et al. 2020). Top-quality glass sand is mined at the plant Kopalnia i Zakład Przeróbczy Piasków Szklarskich Osiecznica sp. z o.o. (which, since 1995, has belonged to the Quarzwerke GmbH group), and is sold both within the country and abroad. Glass sand of slightly lower quality, spoiled by colouring oxides, is also obtained as a by-product from the processing of kaolinitic sandstone in the plant Kopalnie Surowców Mineralnych Surmin Kaolin S.A. in Nowogrodziec (since 1998, in the Quarzwerke GmbH group). The mining sites between the Osiecznica and Nowogrodziec are particularly famous for the production of glass sands and fine ceramic clays.

Natural resources of subordinate significance in the NSS Cretaceous include foundry sands, which have been documented within the Czerna Formation in the village of Czerwona Woda, northwest of Bolesławiec.

FIELD STOPS

Stop 1:

Rock tors "Szwajcaria Lwówecka" (German *Löwenberger Schweiz,* English *Switzerland of Lwówek*) in Lwówek Śląski (German *Löwenberg in Schlesien*) (Fig. 30);

51° 6' 6.4'' N, 15° 35' 37.4'' E; A rocky, wooded ridge on the southern outskirts of Lwówek Śląski between the Bóbr River and the main road to the town of Jelenia Góra, rising up to 40 m above the bottom of surrounding valleys, limited by a cliff from the west and featuring numerous tors, each several metres high (Fig. 4A).

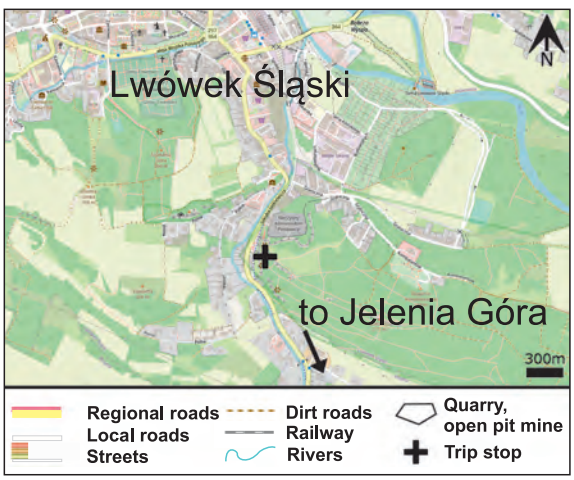

Fig. 30. Location of fieldtrip stop 1.

Structure and stratigraphy: Lwówek Syncline; Radłówka Formation (Lower Triassic Buntsandstein) and the Wilków Member (upper Cenomanian) of the Rakowice Wielkie Formation

Subject: Stratigraphy (Triassic–Cretaceous contact) and sedimentology (lithofacies record of the Cenomanian transgression)

Remarks: Thick- and medium-bedded, pinkish and light grey, quartzose and arkosic sandstones, medium- to coarse-grained with admixture of granules and small pebbles, plane-parallel stratified and cross-stratified, overlain almost conformably by light grey and drab sandstones with quartz pebbles, 0.3 to 0.8 cm in size, scattered in the sandy groundmass (Fig. 4C). The first lithology represents the Early Triassic Radłówka Sandstone Formation, whereas the second belongs to the late Cenomanian Wilków Member of the Rakowice Wielkie Formation. The boundary between the two lithostratigraphic units is a sharp surface overlain by pebbly sandstone (ravinement surface; Fig. 4B). The individual beds of the Wilków Sandstone are 0.5 to 1.5 m thick, structureless, occasionally normally graded, crudely plane-parallel and cross-stratified.

Genesis: Deposition by longshore currents and mass settling from storm-derived suspension clouds in the upper shoreface zone of a high energy coast. Episodic local sediment homogenization by benthic fauna.

Stop 2:

Former quarry on the eastern side of the road from Lwówek Śląski to the village of Sobota (German *Zobten am Bober*), 1.8 km from the intersection of Złotoryjska and Widokowa Streets, towards the village of Sobota (Fig. 31); 51° 6' 20'' N, 15° 37' 19.4'' E; Land depression in the woods, bounded by a rock cliff to the north, below a small cave called Zimna Dziura (in English, cold hole).

Structure and stratigraphy: Lwówek Syncline; Chmielno Member (?) and overlying part of the Rakowice Wielkie Formation (Turonian)

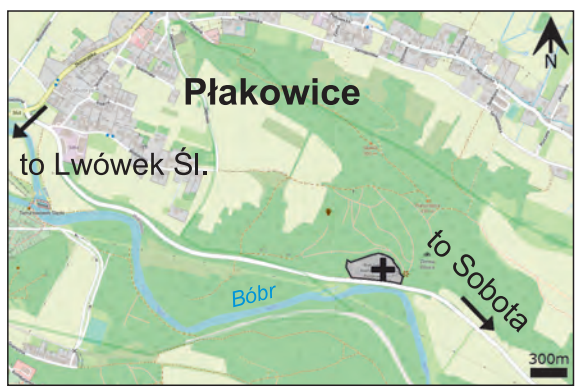

Fig. 31. Location of stop 2. For explanation of symbols see Fig. 30.

Subject: Stratigraphy and sedimentology; features of the top part of the Chmielno Sandstone and the overlying fine-grained sediments of the Rakowice Wielkie Formation, with focus on the appearance of the boundary between two lithostratigraphic units.

Remarks: Ca. 12 m thick portion of the uppermost Chmielno Sandstone, composed of structureless or faintly cross-stratified, medium- to coarse-grained, noncalcareous sandstone with small pebbles, friable in the higher part, delimited at the top by a 20 cm thick transition zone to the overlying grey, brittle, silty to sandy marlstones, crudely thin-bedded, strongly to totally bioturbated with frequent, poorly preserved, deformed macrofossils. Sandstone cross-stratification occurs in 30–50 cm thick sets, with strata dipping to the northeast.

Genesis: Sandstone of shoreface origin (basin margin nearshore sedimentation by longshore currents and reworking by waves) overlain by lower shoreface to upper offshore marly sediments.

Stop 3:

Rock tors "Krucze Skały" (English *Raven's Rocks*; German *Rabenfelsen*) in Jerzmanice Zdrój (German *Hermsdorf*; Fig. 32); 51° 6' 46.1'' N, 15° 53' 30.5'' E; Sandstone bluff up to 25 m high, marking the eastern bank of the Kaczawa River valley, near the train station in the village of Jerzmanice Zdrój.

Structure and stratigraphy: Leszczyna half-graben; Chmielno Member (middle Turonian, Inoceramus lamarcki horizon) of the Rakowice Wielkie Formation; so-called "Middle Jointed Sandstone" (German Mittel Quadersandstein).

Subject: Sedimentological features; ichnofossils and sedimentary environment; depositional and post-depositional processes; large scale seismotectonic deformations; soft-sediment shears and kink-bands.

Remarks: The sand and gravel rocks in the vicinity of Jerzmanice Zdrój were first stratigraphically classified by Scupin (1910, 1913) as Lower Turonian. In later studies and on subsequent geological maps (Jerzmański 1955; Śliwiński et al. 2003; Chrząstek and Wojewoda

Fig. 32. Location of 3. For explanation of symbols see Fig. 30.

2011), it was included into the Middle Turonian, what is probably justified as its petrography and sedimentological features are same to those of the paleontologically well-documented Radków Bluff Sandstones in the Intra-Sudetic Basin, which belong to the Inoceramus lamarcki horizon (Wojewoda 1997, 2020).

The sedimentary succession is bipartite. Its lower part (Fig. 5) consists of strongly homogenized conglomeratic sandstone units, which locally show relics of low-angle and large-scale cross-bedding (sediments of lateral accretion of nearshore bars (?)). Layers reach up to 4 m thickness and mostly consist of sand size material, with admixture of scattered pebbles up to 6 cm in size. Usually near the bottom of layers, the grains are visibly coarser and sediment shows relics of swaley and hummocky cross stratification. Primary sedimentary structures are largely oblitered, mostly due to locally high trace fossil concentrations, dominantly of the Ophiomorpha type. The layer at the base of the quarry shows large-scale trough cross-stratification resulting from the migration of large current-formed bedforms (paleocurrent direction is bimodal 175–225°) on the shoreface bar slopes.

The sandstone layers are separated by layers of pebbly conglomerate with thicknesses of up to 0.5 m. The bottom surfaces of these layers are usually irregular. Within them, relics of the stratification characteristic of wave-generated bedforms are present (Fig. 6A). In the lowest part of the Chmielno Member succession, which only outcrops in the tectonically disturbed zone at the Jerzmanice Fault in the north, these conglomeratic beds can reach

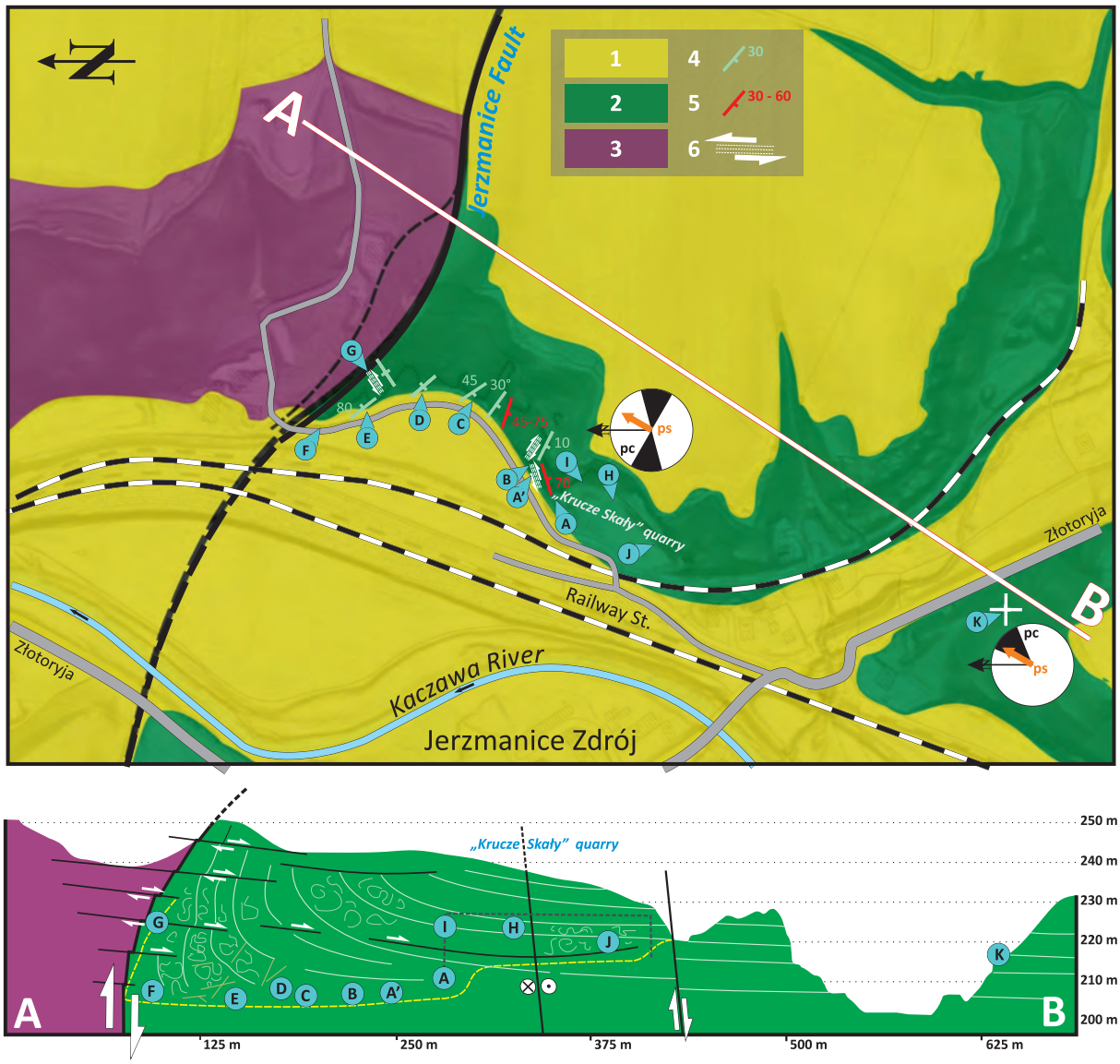

Fig. 33. Schematic map and cross-section illustrating the geological structure of the "Krucze Skały" geosite in Jerzmanice Zdrój. Explanation: 1 – unseparated Neogene deposits, 2 – Cretaceous, 3 – metamorphic rocks of the Kaczawa Complex, 3 – layering, 4 – local fault surfaces, 5 – vertical or steeply inclined surfaces of horizontal shearing; rose diagrams: pc – palaeocurrent, ps – paleoslope; black lines: solid – certain faults, dashed – suspected faults; X – X': geological cross-section: lines – continuous white (layering surfaces), dashed yellow (trip route), explaned sites from A to K.

thicknesses of up to 1.5 m (cf. Fig. 7E, F). No escape trace fossils were found on these areas of rapid sediment accretion. The upper part of the succession consists of cosets of large-scale tabular and trough cross-stratification. Transport directions to the northeast predominate here (Figs 6C, 8).

In summary, the clastic material of the Chmielno Member sandstones and conglomerates was deposited close to storm wave base, not far from shore, in an area with relatively slow sediment accumulation rates. At the same time, this area was dominated by offshore (longshore?) currents towards the north and northeast, which excludes the present-day Jerzmanice Fault as a zone delimiting the contemporaneous shoreline of the basin.

A significant proportion of sediments inside the layers in the lower part of the succession, as well as within the cosets of the upper

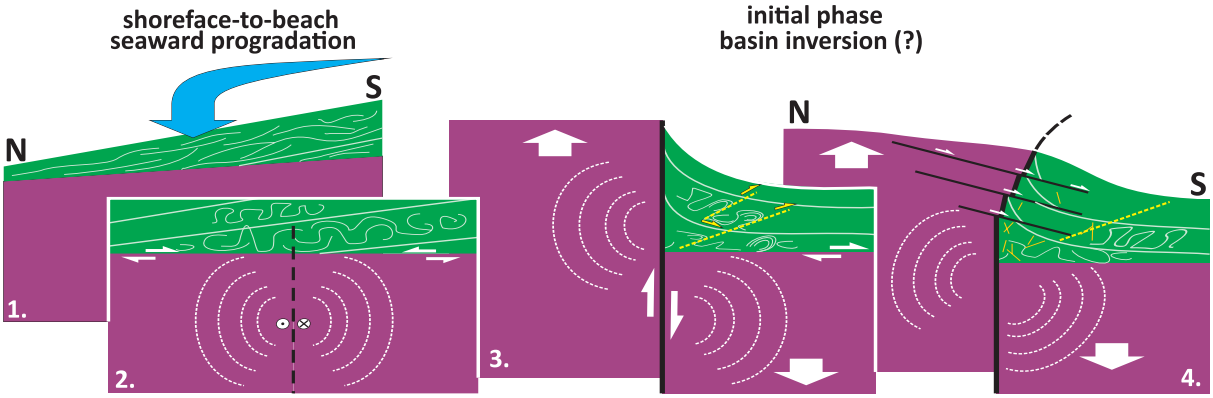

Fig. 34. Diagram explaining the probable sequence of sedimentation (1–2) and geodynamic (3–4) phenomena at Krucze Skały.

part of the unit, exhibit numerous soft-sediment convectional disturbances with characteristic shapes (e.g., folds, helicoidal torsions) (Figs 6C; 7B, F). In some places, the gravel material are immersed in the underlying sand (drop-shaped load casts) (Figs 6A; 9B). All of these deformations, especially in the upper part of the Chmielno Member, gradually disappear towards the southwest (cf. Fig. 6), where they have not been documented in natural exposures to date. Most of the deformations show a clear northward vergence, which is in accordance with the direction of local sedimentary redeposition, as well as the direction of the local palaeoslope during sedimentation. This, in turn, places the Late Cretaceous North-Sudetic Basin shoreline to the south or southwest of the sites discussed here. Some of the nearly vertical faults observed also have soft sediment features (helicodal torsions and shears, complementary kink bands) (Figs 7C, E, F; 9B). Probably some of these faulted zones were later reactivated as typical tectonic deformations of Cretaceous rocks during the regional inversion of the sedimentary basin.

As we approach the Jerzmanice Fault zone, the sediments of the Chmielno Member dip progressively steeper towards the south-southwest (cf. Figs 33, 7B, 9D). Close to the fault zone, the conglomerate and conglomeratic sandstone layers are vertically oriented and even inverted. In the latter, there are autobreccias – that is, deformations typical of local *in situ* redeposition or tectonic destruction of still unlithified sediment. Some fractures, especially low-angle, coupled shear surfaces of the R type (Riedel's shears), and kink-bands surfaces have features typical of incompletely lithified sediment (Figs 7C, E; cf. Solecki, 2011). In addition, numerous subhorizontal, inclined, and vertical surfaces have typical indicators of fault surfaces including lineation and slickenside features, and/or are covered with recrystallization slickenfibres, which indicate a generally oblique and overthrusting movement direction of approximately 190–170° (Figs 9A, D). Interestingly, the majority of horizontally oriented layers have boundaries and/or subhorizontal tectonic surfaces within them – classic signs of overthrust slides – which allows for a slightly different interpretation of the "inversional" nature of the Jerzmanice Fault than would appear from the cartographic image (see Fig. 34).

Genesis: Sand-gravely deposits of the shelf and shoreface, forming cyclic layers with slightly coarsening upwards grains, partially obliterated primary sedimentary structures, and storm-induced gravel accumulations. Numerous soft sediment deformation structures (convectional, helicoidal torsions, load casts) indicate high synsedimentary seismotectonic activity of the Jerzmanice Fault.

Stop 4:

Kopka Hill (German *Hockenberg*) between the villages of Czaple (German *Hockenau*) and Nowa Wieś Grodziska (German *Neudorf am Groditzberg*) (Fig. 35); **Stop 4A**: 51° 8' 40.5'' N, 15° 44' 53'' E; **Stop 4B**: 51° 8' 32.4'' N, 15° 45' 9.9'' E; **Stop 4C**: 51° 45' 9.9'' N, 15° 45' 9.8'' E;

Fig. 35. Location of stop 4. For explanation of symbols see Fig. 30.

Stop 4A: Abandoned quarry at the western foot of Kopka Hill, by the road from the village of Czaple to the village of Nowa Wieś Grodziska. Stop 4B: Abandoned quarry on the southwestern slope of the hill. Stop 4C: Active quarry at the top part of the hill. All quarries are operated by the Polish company "Kamieniarz", Tadeusz Modliński, Kielce.

Structure and stratigraphy: Leszczyna half-graben; Żerkowice Member (lower Coniacian). The sub-stops (individual quarries) are labelled in stratigraphic order, with stop 4A showing the lowest part of the Żerkowice Member and stop 4C its top part. Relics of the basal Czerna Formation (lower Santonian) seem to occur at stop 4C.

Subject: Sedimentological features; depositional processes; ichnofossils and depositional environment; normal-regression deposits; economic importance.

Remarks: A sedimentary succession composed of mostly medium-grained, quartzose, noncalcareous, moderately to weakly cemented sandstones with dune-scale, bidirectional planar and trough cross-stratification (lithofacies Sc of Leszczyński and Nemec 2020) is exposed at stops 4A–C (Figs 13, 14, 20, 21). Some admixture of coarse sand and granules occurs at stop 4C. Cross-strata sets are up to 1.5 m thick with foreset dip mostly towards the northwest (ca. 330°), and less often towards the southeast. Intercalations of plane-parallel stratified and ripple cross-laminated sandstone are subordinate (e.g., in the quarry at stop 4B; Fig. 14) The local bedding inclination includes at least 5° of secondary tectonic tilt. The top part of the sedimentary succession exposed in the eastern quarry wall at stop 4C shows a sandstone lens, ca. 50 m wide and 4 m thick, incised in the substrate (Fig. 20). In contrast, the topmost western wall of the quarry at stop 4C used to show a ca. 4 m thick succession comprised of pinkish-red clayey mudstone overlain by two cross-stratified sandstone bodies separated by a white mudstone layer (Leszczyński observation from 2010). The prominent variegated mudstones with sandstone interbeds suggest a basal relic of the Czerna Formation, as exposed at stop 5.

No trace fossils and only a few body fossils (*Inoceramus* sp., Fig. 16D; *Inoceramus kleini* Müller, 1888; Chrząstek et al. 2018) have been found in the quarry at stop 4A. Rare trace fossils occur at stop 4B, including vertical Ophiomorpha nodosa shafts, *Rosarichnoides sudeticus* (Chrząstek et al. 2018), *Thalassinoides suevicus*, *T. paradoxicus*, *Phycodes* cf. *palmatus*, and *Gyrochorte* isp.; additionally, body fossils of the starfish *Lophidiaster scupini* Andert, 1934 (formerly *Astropecten scupini* Andert 1934; Fig. 16H) have been recovered (Chrząstek and Wypych 2018). Intense bioturbation occurs at stop 4C, with bedding surfaces densely covered with burrows such as *Gyrochorte* isp., *Ophiomorpha nodosa*, *Phycodes* cf. *curvipalmatum*, *Phycodes* isp., *Planolites* cf. *beverleyensis*, and ?*Thalassinoides–Phycodes* compound burrows (Chrząstek and Wyoych 2018; Chrząstek et al. 2018).

The presence of the starfish Lophidiaster scupini Andert, 1934 (formerly Astropecten scupini; Fig. 16H) suggests a shallow-marine setting (shoreface). These fossils used to occur in abundance down to a water depth of usually 30–50 m (Beddingfield and McClintock 1993; Villier et al. 2004). They are well-adapted to soft-bottom substrates, as detrivores and predators of gastropods, bivalves, and crustaceans (Caregnato et al. 2009; Blake and Guensburg 2016). Inoceramids are very common and cosmopolitan in Upper Cretaceous marine shelf environments and had broad ecological tolerances (Harries and Ozanne 1998).

The sandstones at the Kopka hill have been exploited since the Middle Ages as valuable dimension stones.

Genesis: The sediment packages mainly composed of dune-scale cross-stratified sandstones are interpreted as longitudinal tidal bars, up to 10–15 m thick, with complexes of vertically and laterally stacked bars reaching several dozen metres. The planar cross-strata sets were deposited as 2D dunes, and the trough cross-strata sets as 3D dunes. Both indicate transport mainly to the northwest, and evidence for opposite transport directions supports the existence of tidal flows. The top part of the sedimentary succession exposed at stop 4C shows a basin-margin delta prograding to the north-northeast and interfingering with the southwest flank of a tidal sand bar. The incised sandstone lens at the succession top is a fluvial palaeochannel formed during the forced regression that terminated the deposition of the Żerkowice Member. The relic, topmost part of the succession in the western quarry wall at stop 4C comprises lacustrine clayey mudstone and fluvial channel sandstones.

Stop 5:

Quarries south of the village of Wartowice (German *Warthau*) (Fig. 36); **Stop 5A**: 51° 12' 45.3'' N, 15° 39' 12'' E; **Stop 5B**: 51° 12' 53.6'' N, 15° 39' 2.8'' E; **Stop 5C**: 51° 18' 37.5'' N, 15° 45' 42'' E; all stops are active quarries; Stop 5A: Quarry currently operated by Hofmann Natursteinwerke Polen Sp. z o.o., Kraków; Stop 5B: Quarry currently operated by Geiger Stein- und Schotterwerke GmBH, Kinding, Germany; Stop 5C: Quarry currently operated by ATS-Stein Sp. z o.o. Kopalnie piaskowca, Bolesławiec.

Structure and stratigraphy: Bolesławiec (Grodziec) Syncline; Upper part of the Żerkowice Member (lower Coniacian) of the Rakowice Wielkie Formation and lower part of the Czerna Formation with Nowogrodziec Member (lower Santonian)

Subject: Sedimentological features; lateral change of the succession; depositional processes; body fossils and ichnofossils; palaeosols and depositional environment; normal regression and transgressive deposits; economic importance.

Remarks: The lower part of the sedimentary succession exposed in all three quarries shows the uppermost part of the Żerkowice

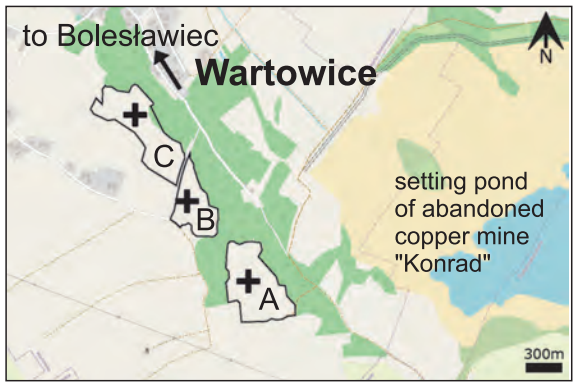

Fig. 36. Location of stop 5. For explanation of symbols see Fig. 30.

Sandstone Member, exploited here as valuable dimension stone. The upper part of the succession represents the lower part of the overlying Czerna Formation (Fig. 25A, B, 37).

The Żerkowice Member exposed at the visited quarries is up to ca. 17 m thick at stop 5A, 7 m at stop 5B, and 9 m at stop 5C. The general appearance of the succession varies with the nature of the exposure. On the surfaces of older natural joints, portions of the succession with thicknesses of several metres look massive, divided into two sandstone beds as much as 4 m thick, separated from each other by a flat to highly irregular discontinuity surface (e.g., in the quarry at stop 5B; Fig. 37B). Elsewhere, a packet of heterolithic sediment occurs, up to 1 m thick (lithofacies H in Leszczyński and Nemec 2020; quarries at stops 5A and 5C; Fig. 37A, D). Weathered surfaces tend to show thinner bedding, tabular and lenticular in vertical section, with beds up to 1.5 m thick (Fig. 37A left side of photo). On closer inspection, one can see dune-scale cross-stratification (lithofacies Sc of Leszczyński and Nemec 2020; Fig. 11A, B), plane-parallel stratification (lithofacies Sp in Leszczyński and Nemec 2020), and rarely ripple cross-lamination, besides the massive structure. Cross-stratification occurs as 30–95 cm thick sets. The thinner sets are bounded either by discontinuity surfaces or by laterally discontinuous siltstone or mudstone drapes 0.5–2 cm thick (lithofacies M in Leszczyński and Nemec 2020). The sandstone is mostly fine- to medium-grained, arenitic, quartzose, noncalcareous with kaolinitic and generally ferrous-poor cement. An admixture

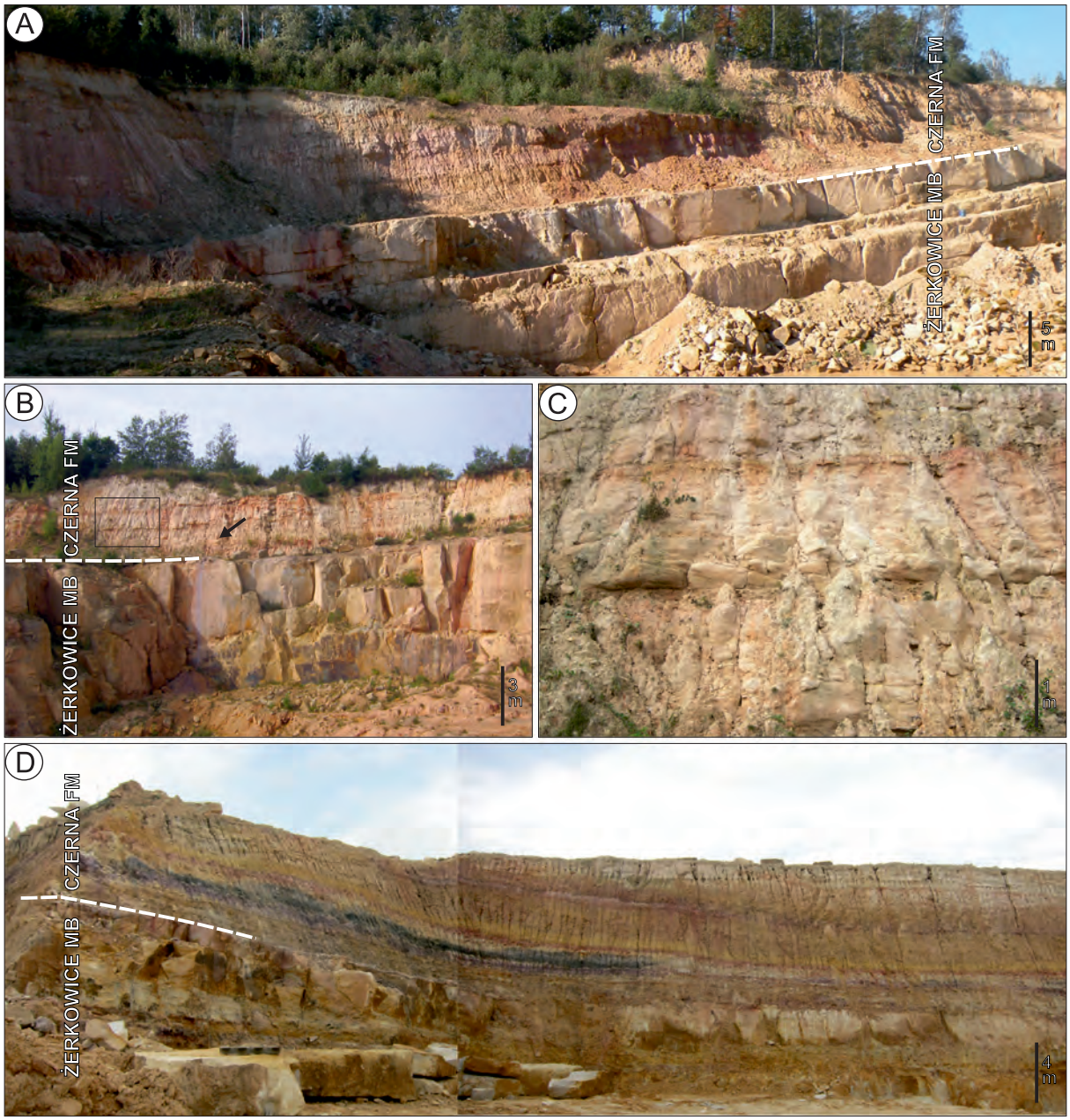

Fig. 37. General appearance of outcrops at stop 5. A – View of fieldstop 5A on October 10, 2010. B – View of fieldstop 5B view September 29, 2021. The arrow indicates location of numerous *Ophiomorpha nodosa*. The black rectangle indicates close-up in C. C – Portion of the Czerna Formation at fieldstop 5B on September 29, 2010. D – View of fieldstop 5C on September 29, 2021.

of coarser grains up to small quartz pebbles (1 cm in size) occurs in the highest bed.

Isolated and clustered fishbones (Leszczyński 2018, fig. 11F) as well as single imprints of driftwood fragments with clustered casts of wood boring bivalves (*Teredolites clavatus*) were found in the sandstones at stop 5A (Leszczyński 2018, fig. 12B). Claystone intraclasts occur in the fills of large gutters. The bedding surfaces of sandstone, particularly the scoop-shaped surfaces bounding trough cross-strata sets, are covered with wave or combined-flow ripple marks (Fig. 11H, I), bioturbation structures (Fig. 15A, B), and rarely molds and casts of body fossils, mostly bivalves (Leszczyński 2018, fig. 11A). The bioturbation structures include trace

fossils ranging between a stressed expression of the *Skolithos* Ichnofacies and a proximal expression of the *Cruziana* Ichnofacies (Leszczyński, 2018). Two thick sandstone beds in the top part of the Żerkowice Member at stop 5A show a totally bioturbated, locally ferruginized, sharp top (Fig. 25A, B; Leszczyński 2018, fig. 10A–C). Some bioturbation structures reminisce rhizoliths (Leszczyński 2018, fig. 10B). Moreover, numerous *Ophiomorpha nodosa* occur locally in the lower bed, up to 3 m below its top. At stop 5A, local ferruginization occurs in the two highest thick sandstone beds, at their top and up to ca. 1 m below it. The ferruginized layer is up to 10 cm thick.

In all three quarries, the Czerna Formation begins with a heterolithic unit dominated by mudstones and claystones, locally containing ferricrete or bands up to 5 cm thick and globular to vermicular hematitic concretions (the Nowogrodziec Member of Milewicz 1985). This unit is up to 7 m thick, and its basal part is marked by a packet of mostly greyish white or variegated silty mudstone overlain by very fine sandstone with siltstone interlayers and rhizoliths (Figs 25A, B; 26A–C; Leszczyński 2018; Leszczyński and Nemec 2020). In quarry 5A, the unit contains two coal lenses up to 25 cm thick. The lower one encloses coalified trunks of driftwood with diameters of up to 12 cm. The upper lens rests on a clay layer enclosing plant roots in its top part (Figs 25B; 26D). In quarry 5C, a coal and coaly mudstone lens, ca. 20 m long and up to 1 m thick, has recently been exposed. It occurs approximately 2 m above the base of the Czerna Formation (Fig. 37D). Some mudstone layers therein are densely interspersed with sand and/or silt streaks and thin interlayers, forming the heterolithic lithofacies H of Leszczyński and Nemec (2020), which occurs as beds up to 2 m thick and is often strongly bioturbated (in part abiotically contorted?) in the upper part of the unit (Fig. 25A, B). The heterolithic deposits pass upwards into fine-grained and further medium- to coarse-grained sandstones, mostly homogenized by bioturbation (Fig. 26E, F), locally showing ripple cross-lamination (lithofacies Sr and Sw of Leszczyński and Nemec 2020), up to 2 m thick, variably ferruginized, with local ferricrete at their top. Some sandstone beds have both sharp bases and tops and show plane-parallel stratification and cross-stratification.

The overlying part of the Czerna Formation, up to 8 m thick, is dominated by medium- to coarse-grained sandstones with an admixture of small pebbles, planar-parallel stratified and trough cross-stratified (lithofacies Sp and Sc of Leszczyński and Nemec 2020). They occur as beds up to several metres thick, separated by sheet-like heterolithic units of lithofacies H, 10–25 cm thick. The lowest thick sandstone bed locally captures *Ophiomorpha nodosa* (Fig. 26F).

Genesis: As with the sandstones of the Żerkowice Member at stop 4, the dune-scale cross-stratified sandstones at stop 5 are interpreted as representing longitudinal tidal bars elongated roughly parallel to the basin axis. Their planar cross-strata sets were deposited as 2D dunes, and the trough cross-sets as 3D dunes. Foreset dip directions indicate a dominant transport direction to the northwest, but the cross-sets are generally bidirectional and show a wide range of transport directions (cf. Fig. 19D). The heterolithic interbeds were deposited in inactive, sheltered interbar swales.

The lower part of the Czerna Formation is interpreted as deposits of a coastal alluvial plain with shallow lakes (ponds and oxbow lakes), peat-forming mires, and tide-influenced fluvial channels. The upper part includes deposits of a paralic coastal plain with basin-margin sand wedges and axial fluvial channels with crevasse splays (referred to as minor mouth bars where spread into lacustrine ponds).

Stop 6:

Active quarry near the village of Żeliszów (German *Giersdorf;* Fig. 38); 51° 11' 3'' N, 15° 38' 54.92'' E; Active quarry owned by the company "Kamieniarz", Tadeusz Modliński, Kielce

Structure and stratigraphy: Bolesławiec (Grodziec) Syncline; Żerkowice Member (lower Coniacian) and Nowogrodziec Member (lower Santonian).

Subject: Sedimentological features; depositional processes; ichnofossils and depositional environment; normal- to forced-regressive and transgressive to normal-regressive systems tracts; economic importance.

Fig. 38. Location of stop 6. For explanation of symbols see Fig. 30.

Remarks: The lower part of the sedimentary succession exposed in the quarry is up to ca. 10 m thick and represents the uppermost part of the Żerkowice Member, exploited here as dimension stone. The upper part, up to 7 m thick, represents the lower part of the Czerna Formation (Fig. 25C). The deposits are overlain by a several metre thick succession of fluvioglacial gravels. The Żerkowice Member consists of several beds of fine- to medium-grained, quartzose, noncalcareous, arenitic, cream-yellow sandstone up to 4 m thick, separated from one another by flat to irregular (erosional) discontinuity surfaces (Fig. 26H) or packets of heterolithic sediment up to 0.7 m thick (lithofacies H in Leszczyński and Nemec 2020). The sandstones appear either structureless or show planar and trough bidirectional cross-stratification and plane-parallel stratification. Cross stratification occurs in 15–35 cm thick sets. The top surface of the uppermost bed exhibits a shell lag (Leszczyński and Nemec, fig. 5K) dominated by casts and molds of the gastropod *Nerinea bicincta* and rare trace fossils, mostly *Ophiomorpha nodosa* (Fig. 15C). The latter can also be rarely found in bed cross-sections.

The Czerna Formation begins with a 0.5 m thick heterolithic packet (lithofacies H), with bioturbated greyish-white to yellow claystone and fine-grained sandstone. An imprint of a driftwood fragment with clustered *Teredolites clavatus* (casts of wood-boring bivalves) has been found in the middle part of this packet. The packet is overlain by a ca. 1.8–3 m thick composite bed of fine- to very coarse-grained sandstone, trough cross-stratified, with thin siltstone and mudstone interlayers and rare *Ophiomorpha nodosa*. The cross-strata sets are inclined toward the southwest. The unit in its thinner segment is overlain by a lens of light-grey to orange claystone, sandy mudstone, and two coal beds (0.6 m and 0.25 m thick). The lens has an SE-NW (150–330°) extent of ca. 30 m and is up to ca. 3 m thick. It is overlain by a 0.35 m thick bed of planar-parallel-laminated siltstone passing upwards into ripple cross-laminated, very fine-grained sandstone. The succession is topped with a 2.3 m thick bed of sandstone with clustered occurrences of mostly vertically oriented *Ophiomorpha nodosa* (Fig. 26I), indicating the *Skolithos* Ichnofacies.

Genesis: Similar to the sandstones of the Żerkowice Member at stops 4 and 5, the sandstones at this stop are interpreted as representing a tidal sand bar, with planar cross-strata sets deposited as 2D dunes and the trough cross-sets as 3D dunes. Like in stops 4 and 5, foreset dips indicate a dominant transport direction to the northwest. The top surface of the Żerkowice Member, covered by a shell lag, may represent the shoreface of a retreating sea.

The Czerna Formation sediments are interpreted as deposits of a coastal alluvial plain with shallow lakes (ponds and oxbow lakes) and tide-influenced fluvial channels. The upper part includes deposits of a paralic coastal alluvial plain with basin-margin sand wedges (Fig. 26H).

Stop 7:

Active quarry and a rock tor between the villages of Skała (German *Hohlstein*) **and Żerkowice** (German *Sirgwitz*; Fig. 39); **Stop 7A**: 51° 9' 34.9'' E, 15°3 4' 55.8'' E; **Stop 7B**: 51° 9' 30.6'' E, 15° 34' 33.4'' E; Stop 7A: Active quarry currently owned by Hofmann Natursteinwerke Polen Sp. z o.o., Kraków; Stop 7B: "Skała z Medalionem" tor, 26 m high, in the woods on the southern slope of Wieżyca Hill.

Structure and stratigraphy: Southern outskirts of the Bolesławiec Syncline; Żerkowice Sandstone Member (lower Coniacian).

Subject: Sedimentological features; ichnofossils; depositional processes and environment; economic importance.

Fig. 39. Location of stop 7. For explanation of symbols see Fig. 30.

Remarks: Approximately the same part of the Żerkowice Member is exposed in both sub-stops, which are separated by about 400 m, although the quarry outcrop is stratigraphically less than half the length of the rock tor and corresponds to the upper part of the tor. Both the quarry and the tor expose mostly fine- to medium-grained, quartzose sandstones with planar and trough cross-stratification (lithofacies Sc of Leszczyński and Nemec 2020; Figs 11A–C, 17) as well as planar-parallel stratification (lithofacies Sp of Leszczyński and Nemec 2020; Fig. 17) with surfaces covered by parting lineation (Fig. 11J). Cross-strata sets range from a decimetre to 0.9 m in thickness and show variable and often bidirectional transport directions (Fig. 17). Thinner sets occur in the lower part of the succession, whereas the thickest are characteristic of the middle part (Fig. 17). Sandstones with current ripple cross-lamination (lithofacies Sr of Leszczyński and Nemec 2020; Fig. 17) and wave ripple cross-lamination (lithofacies Sw of Leszczyński and Nemec 2020; Fig. 17) constitute subordinate lithofacies. The top part of the sedimentary succession, best preserved in the tor, shows only faint, bioturbated planar-parallel stratification and ripple-cross lamination. Wave and current ripples (Fig. 11G–I) and bioturbation structures (mainly ichnogenus *Thalassinoides*, rarely *Ophiomorpha*, *Treptichnus*, *Planolites, Nereites*, and other; see Leszczyński 2018; Fig. 15E), are frequently encountered on cross-set bounding surfaces. However, bioturbation is restricted to these bedding surfaces and is rarely visible in vertical bed cross-sections. The trace fossil assemblage represents a proximal expression of the *Cruziana* Ichnofacies. Some cross-strata sets show hydroplastic deformation and partial homogenization by liquefaction (Fig. 17). The sandstone in the quarry is exploited as a building stone.

Genesis: The sedimentary succession at both sub-stops is thought to represent a shoaling-upwards tidal bar, increasingly wave-worked at the top (lithofacies Sw and Sp). The cross-strata sets represent 2D and 3D dunes migrating over an accreting tidal bar, obliquely to its axis (cf. Fig. 19). Plane-parallel stratified and ripple cross-laminated sandstones in the top part of the tor are thought to represent a wave-dominated bar top shoal, probably merged with the upper shoreface environment of the basin shoreline.

Stop 8:

Rakowiczki, abandoned quarry in the village of Rakowice Małe (German *Wenig Rackwitz*) (Fig. 40); 51° 9' 55.6'' E, 15° 32' 33.8'' E; Abandoned quarry now mostly overgrown with young trees. The southern wall, up to 10 m high, shows sandstones. The northern wall, now up to 15 m high, shows sandstones in the lower part, up to 4 m high, and claystones, mudstones, siltstones and sandstones in the upper part (Fig. 24).

Structure and stratigraphy: Southwestern outskirts of the Bolesławiec Syncline; Żerkowice Member of the Rakowice Wielkie Formation (lower Coniacian) and Nowogrodziec Member of the Czerna Formation (lower Santonian; Fig. 24).

Subject: Fully marine to brackish shoreface; lagoonal and paludal sediments; palaeosol; marine regression/transgression record; fossils; bioturbation.

Remarks: Rakowice Małe is one of the main localities for the extraction of Cretaceous sandstones and for studies of North-Sudetic Cretaceous stratigraphy and related historical collections of Cretaceous megaflora. The extraction of sandstone from here lasted several hundred years. Rich floral collections have been collected from this quarry and other outcrops in the area, and palaeobotanical issues

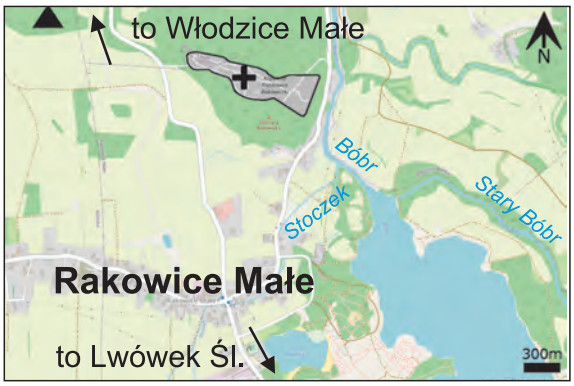

Fig. 40. Location of stop 8. For explanation of symbols see Fig. 30.

are discussed separately at the end of the stop description.

The sedimentary succession in the quarry, particularly the part representing the Czerna Formation, has been described in many papers since the 19th century. The Żerkowice Member below consists predominantly of fine- and medium-grained, cream-yellow to locally orange-brown, moderately hard, non-calcareous quartzose sandstones, plane-parallel and through cross-stratified (lithofacies Sp and Sc of Leszczyński and Nemec, 2020), partly massive-looking and indistinctly bedded (Fig. 24D, E). The massive-looking and planar parallel-stratified lithofacies form the topmost part of the unit. Cross-strata sets range from a decimetre to 1 m thickness and show variable, often bidirectional transport directions. Rare, taxonomically undefined bioturbation structures (ethologically mostly pascichnia) and the ichnogenera *Ophiomorpha* and *Thalassinoides* are encountered on the bedding surfaces (Leszczyński 2010, 2018; Fig. 15D). The upper boundary of the Żerkowice Member is sharp, flat, ferruginized, and covered with ironstone crust. Until 2012, the sandstones of this unit were extracted in this quarry as valuable buildingstone, whetstone, and carvingstone for several hundred years.

The overlying Czerna Formation begins with a layer of cream-yellow, cherry-red, and orange banded, streaked, and mottled muddy claystone, 0.65 m thick (Fig. 26J). The cherry-red variety displays vertically elongate, white-coloured root-like structures. X-ray diffraction analysis revealed that this is a kaolinite-dominated deposit (average kaolinite content 53.9% by weight). The basal layer passes upwards into a 70 cm thick bed of mottled, brown mudstone, with a 15–20 cm thick interlayer of mottled siltstone to fine-grained sandstone in its lower part. The deposits show dispersed coalified plant fragments. The top of the mudstone layer is marked by a level rich in coalified plant fragments, locally forming a shiny coal layer as much as 2 cm thick.

The overlying part of the succession begins with a 37 cm thick bed of grey-brown, mottled to subtly parallel laminated mudstone (with plant roots?) that grades upwards into siltstone and subsequently to an argillaceous sandstone as much as 30 cm thick. The latter grades upwards into a 22 cm thick layer of dark-brown mudstone capped by a 5–10 cm thick coal seam. The sandstone is rich in large coalified plant debris and is cut by plant roots (Fig. 24C). This basal part of the Czerna Formation is tectonically duplexed in the eastern part of the quarry (with only remnants presently visible), whereas small thrusts occur in its western part, now covered by the quarry waste (see Leszczyński 2010, fig. 3).

The coal seam overlying the duplexed part shows burrows reminiscent of the ichnogenus *Thalassinoides*. The coal seam is overlain by a brown mudstone, 33–45 cm thick, showing a mottled structure and locally penetrated by plant roots (Fig. 24C). This mudstone is overlain by a bed of impure coal, up to 20 cm thick (see log height 12.7 m in Fig. 24). Over the duplex structure, this coal seam occurs amalgamated into one bed with the lower-lying seam. The upper coal seam is brittle with sand insertions, similar to the lower-lying seam. The coal shows sand insertions with tortuous shapes and some dish shaped lamellation in cross-section. They resemble structures described by Kamola (1984) as various ichnospecies of *Thalassinoides*. The tortuous ones with lamellae resemble structures shown by Seilacher (1955) as cf. *Phycodes palmatum* Hall (1852), and to some extent *Teichichnus zigzag* Frey and Bromley 1985. Their tortuosity may be in part a result of compaction. The bundles of lens-shaped sand insertions may possibly represent the ichnogenus *Phycodes*. Some lenses showing a striated surface and an obliquely laminated interior in cross section may represent the ichnogenus *Teichichnus*. The branched, rope-sized burrows represent

two *Thalassinoides* isp. Another feature of the coal seam is the occurrence, at its top, of tree trunk fragments containing casts of the wood borings *Teredolites clavatus* Leymerie, 1842 (Leszczyński 2010, fig. 10E, F). Compositionally, this coal bed corresponds to the "log-ground" of Savrda et al. (1993): that is, a ground consisting of a high concentration of allochthonous wood strewn across a depositional surface.

The overlying unit is a highly to completely bioturbated argillaceous sandstone passing upwards into a sandstone-mudstone heterolithic packet (Fig. 24 log, B), showing variable bioturbation intensity (Fig. 26K–M). This whole unit is 165 cm thick. The argillaceous sandstone shows a mottled structure with remnants of flaser and wavy bedding. Trace fossils of the ichnogenera *Asterosoma*, *Palaeophycus*, *Ophiomorpha*, *Thalassinoides*, *Planolites*, and *Taenidium* are the dominant recognizable ichnotaxa (Leszczyński 2010), particularly in the lower part of the muddy-sandstone unit. In places, the sediment fabric seems to show *Asterosoma* and inferred *Cylindrichnus* overprinted by *Thalassinoides* isp., a thickly mud-lined burrow tentatively called *Palaeophycus* isp., *P.* cf. *tubularis* Hall, 1847, and *Planolites* isp. indet. (Fig. 26L). Elsewhere in the lower part of the unit, the ichnofabric is dominated by roughly horizontally winding burrows of the ichnogenus *Ophiomorpha* and *Palaeophycus* (Leszczyński, 2010, fig. 12B). Most burrows in the lower part of the argillaceous sandstone resemble *Ophiomorpha irregulaire* Frey, Howard and Pryor, 1978 (Leszczyński, 2010, fig. 12A, C, D). They are accompanied by rare burrows showing annulations of pelleted mud lining as in *O. annulata* (Książkiewicz 1977; see Leszczyński 2010, fig. 12A, B). Bedding-parallel to oblique burrows, resembling the ichnogenus *Taenidium*, occur locally in the argillaceous sandstone. Specimens of *Taenidium baretti* (Bradshaw,1981) (Leszczyński 2010, fig. 12C, D) and *Taenidium serpentinum* Heer, 1877 (see Leszczyński 2010, fig. 12B) were recorded in the *Ophiomorpha*-dominated division. In total, the trace fossil assemblage appears to represent the *Cruziana* Ichnofacies in the proximal expression of a stressed environment.

The upper part of the heterolithic packet comprises interbedded drab to pale-coloured argillaceous sandstone, arenitic sandstone, and grey to dark-brown sandy mudstone and mudstone. These deposits show variable intensities and styles of bioturbation. The proportion of sandstone relative to mudstone decrease upwards, as the mudstone also becomes more clayey. The less bioturbated divisions show wavy to lenticular bedding. Current ripple lamination with variable and often bidirectional inclination, combined-flow ripples, and wave ripples are recognizable in the poorly bioturbated sand lenses and layers. The icnofabric primarily consists of irregular tan to drab sediment mottles. Distinct trace fossils are represented by several ichnotaxa dominated by 1 mm thick, bedding-parallel to vertical, mud-lined and sand-filled burrows and similarly thick, unlined, mud-filled burrows. Some thin, mud-lined burrows are U-shaped and Y-shaped and resemble *Arenicolites* (Fig. 26M) and *Psilonichnus*. They are analogous with burrows of the polychaete *Capitella* cf. *capitula* described from the upper offshore of Georgia, U.S.A. (Hertweck et al. 2007). The mud-lined burrows showing different orientations to bedding seem to correspond to the trace fossil *Bornichnus tortuosus* Bromley and Uchman (2003) described from the Lower–Middle Jurassic tidal flat deposits of Bornholm (Denmark). Ichnotaxa also include *Schaubcylindrichnus* isp. indet., ?*Phycosiphon* isp. indet., *Planolites* isp. indet. and other taxonomically undetermined forms. Some *Schaubcylindrichnus* specimens resemble the ichnospecies S. *coronus* Frey and Howard, 1981. They tend to occur in bundles of congruent, sand-lined tubes. Some rock parts contain aggregations of taxonomically undetermined sand-filled burrows resembling diminutive *Planolites* in cross-section and small burrows showing concentric structure in cross-section. The trace fossil assemblage would seem to represent a single ecological suite. The forms of structures, the inferred ichnotaxa and the sedimentological and ichnological context of these deposits indicate the *Cruziana* Ichnofacies of a highly stressed environment.

The heterolithic packet passes gradually upwards into a 1 m thick bed composed of grey to greenish-grey and green clayey mudstone sandwiched by several thin clay ironstone (siderite) interbeds and topped by a coaly mudstone layer several centimetres thick (log height 16.0 m in Fig. 24). The latter is

the highest unit in the local sedimentary succession of the Nowogrodziec Member. No distinct bioturbation structures have been found in the mudstone deposit. Examination of three samples from its lower, middle, and upper parts revealed an absence of foraminifers or other microfossils.

The overlying coaly mudstone is highly burrowed in its upper part, where bioturbation obscures its upper boundary and adds to its gradual passage into the overlying sandstone. Bioturbation is dominated by densely packed sand-filled burrows *Asterosoma ludwigae* Schlirf, 2000, accompanied by *Thalassinoides* isp. indet., *Chondrites* isp. indet. (Leszczyński 2010, fig. 14D–F; Fig. 26N) and some other taxonomically undetermined ichnotaxa. *Asterosoma* dominates in the whole bioturbated division, whereas *Thalassinoides* is most densely distributed from 10 to 20 cm above the lower boundary of the mudstone bed and *Chondrites* is recorded only from 5 to 9 cm above this boundary. *Asterosoma* is intersected by *Thalassinoides* isp. Both ichnotaxa cross-cut *Chondrites* isp. Burrowing becomes less distinct upwards, in the drab coloured argillaceous sandstone; however, the mottled appearance of its splitting surfaces suggests profound bioturbation. The ichnofossils are typical of taxonomically impoverished archetypal *Cruziana* Ichnofacies (see MacEachern et al. 2007).

The overlying part of the sedimentary succession (above log height 15.8 m in Fig. 24) consists of two coarsening- to fining-upwards divisions comprising seven lower-order coarsening-upward divisions. The top part of this unit is strongly reworked by Quaternary surficial processes. The whole unit is rather poorly preserved, being strongly jointed, irregularly impregnated with iron oxides, and commonly penetrated by recent plant roots (Fig. 26O). Massive or cross-stratified sandstone deposits are present, and a sand-dominated heterolithic deposit occurs at its top. The heterolithic deposit shows wavy to lenticular bedding and a chaotic structure. The lamination of current ripples, combined-flow ripples, and wave ripples is visible locally. The sandstone deposit is pale to orange and yellowish in colour and shows a generally massive structure. Some of its parts display ripple lamination and medium-scale cross-stratification. It shows sparse to abundant bioturbation. Thorough examination revealed the occurrence of *Asterosoma* isp. indet. (see Leszczyński 2010, fig. 15C, D), *Paleophycus* cf. *tubularis*, *Ophiomorpha* cf. *irregulaire* (see Leszczyński 2010, fig. 15D, E), *O.* cf. *nodosa*, and *Planolites* isp. Argillaceous sandstone shows rich casts and molds of various bivalves (e.g., *Cyrena cretacea*), partly concentrated on bedding surfaces. The sandstone of the lower part of the thickest coarsening-upwards unit shows bivalve shells in life position and fragments of vertical to nearly vertical, cylindrical, smooth-walled burrows resembling *Skolithos linearis* Haldeman, 1840 (see Leszczyński 2010, fig. 16C, D) and *Arenicolites*-like trace fossils. The trace fossils in heterolithic deposits represent the *Cruziana* Ichnofacies in a distal to proximal expression of a stressed environment, whereas the assemblage recorded in massive, poorly bioturbated sandstones seems to represent the *Skolithos* Ichnofacies.

Small thrusts and tectonic duplexing occur in the lower part of the Czerna Formation (Leszczyński 2010, fig. 3), although these former features in the western quarry segment are now covered by the quarry waste, whereas the duplexed body, ca. 13 m in length, has been removed by mining operations.

Palaeobotany of the stop and its surroundings: The Nowogrodziec Member of the Czerna Formation has been the focus of recent palaeobotanical investigations by a joint Polish–Czech–German team (see Halamski et al. 2020 and references therein). The earliest plant fossils have been found directly at the boundary between the Żerkowice Member and the Czerna Formation (see Assemblage 4 in Halamski et al. 2020). This assemblage is dominated by the angiosperm *Dewalquea haldemiana* (Fig. 16I) and the matoniaceous fern *Konijnenburgia* cf. *galleyi* (Fig. 16K). Both have thick coriaceous leaves and may be interpreted as dwellers of xerophytic habitats (dryland and/or fern savannas). The next assemblage (Assemblage 5 in Halamski et al. 2020) comes from about 6–8 m of overlying dark siltstone containing irregular coal intercalations (including, therefore, parts B–C of the lithological column given in Fig. 24) This assemblage is dominated by the conifer *Geinitzia reichenbachii* (Fig. 16J) and clearly corresponds to backswamp forests.

The mesoflora and microflora have been recently studied on the basis of collections from

the upper part of the Nowogrodziec Member (corresponding to the megafloral Assemblage 5, stratigraphy as above). The mesoflora is relatively poor, and recent investigations failed to locate the rich mesofloral level from which the material described by the Czech palaeobotanist Ervín Knobloch was reportedly derived (Knobloch and Mai 1986).

The microflora consists of 126 taxa, including 105 terrestrial palynomorphs (54 bryophyte, lycophyte, and pteridophyte spores, 16 gymnosperms, 35 angiosperms; Halamski et al. 2020). Marine palynomorphs, in particular dinocysts, are extremely infrequent. Therefore, in contrast to initial expectations, the position of the Coniacian–Santonian boundary could not be verified on the basis of microflora.

The microflora from this area had previously been investigated by the pioneering palynologists F. Thiergart and W. Krutzsch. Thiergart (1942) described a characteristic schizeaceous fern spore *Appendicisporites appendicifer*. Krutzsch (1966) distinguished the "Löwenberger Bild" as an informal palynostratigraphic unit within the Cretaceous. Locality data for Krutzsch's samples are not available, but he presumably collected them at Rakowice Małe, the largest quarry in the region. However, his palynofloral list is notably different from the findings of recent authors even at the genus level (see Halamski et al., 2020, p. 858 for details). An interesting direction for future research would be to explore the details and reasons for these differences.

Genesis: The sandstones in the lower part of the sedimentary succession (Żerkowice Member) show features (lithofacies and trace fossils) indicative of a shoaling tidal bar complex overlain by the encroaching basin margin shoreface and foreshore (Fig. 24). In contrast, the lower part of the Czerna Formation (Nowogrodziec Member), indicates sedimentation on a vegetated coastal limnic plain increasingly invaded by seawater. The change of depositional environment recorded by the Czerna Formation is attributed to a separation of the coastal plain from the open sea by a sand barrier formed within the transgressive systems tract (Figs 28D, 29). Siltstones with plant roots and driftwood fragments showing the trace fossil *Teredolites clavatus*, together with coal seams containing *Thalassinoides* isp., are thought to represent a coastal plain with paludal sedimentation and incursions of marine water. The fining-upwards top part of the Nowogrodziec Member – showing an almost archetypal *Cruziana* Ichnofacies suggesting highly stressed brackish conditions – indicates extensive marine drowning and lagoonal sedimentation. The termination of the drowning, marked as a maximum flooding surface (Fig. 29), is indicated by the coaly mudstone at the top of the Nowogrodziec Member. A punctuated normal regression with prograding brackish bay shoreface and deltas is inferred from lithofacies, ichnofossils and body fossils for the deposits overlying the Nowogrodziec Member and topping the examined succession (Fig. 29). The trace fossils indicate *Cruziana* Ichnofacies and *Skolithos* Ichnofacies in an expression of slightly stressed environments.

Stop 9:

Active open pit (Kopalnie Surowców Mineralnych Surmin-Kaolin S.A. in Nowogrodziec; Quarzwerke GmbH group) near the town of Nowogrodziec (German *Naumburg am Queis*; Fig. 41); 51° 12' 45'' N, 15° 22' 31'' E; pit ca. 500×550 m in area, ca. 25 m deep, active, with 10 extraction horizons.

Structure and stratigraphy: Bolesławiec Syncline; Czerna Formation (German *Überquader*), Santonian(?)

Subject: Sedimentological features; origin and economic significance.

Fig. 41. Location of stop 9. For explanation of symbols see Fig. 30.

Remarks: Sedimentary succession composed of lenses and beds of brittle, trough and rarely planar cross-stratified or structureless, very coarse- to fine-grained, greyish-white to white, subordinately orange-brown, quartzose sandstones, minor granule to pebble quartzose conglomerates, and light-grey to white poorly cemented siltstones, mudstones (muds), and claystones (clays). The lenses and beds of the fine-grained sediments are 0.2–3.0 m thick, mostly 0.5–1.5 m, and constitute ca. 25% of the whole succession (Galos 2020). The succession dips homoclinally £12° to the northeast (Fig. 27).

These are typical kaolins. Here, white-firing clay is extracted from both the coarse-grained and fine-grained sediments by washing the crushed output from parts of the succession where the proportion of good quality clay minerals is >20%.

Genesis: The mainly lenticular beds of both coarse- and fine-grained sediments, common cross-stratification of sandy, and erosional gravelly horizons indicate an alluvial origin of the sedimentary succession. The white colour of sediments results from bleaching by highly acidic pore waters (e.g., Rushton et al., 2020 and references therein)

Stop 10:

Osiecznica (German *Wehrau*), **the birthplace of** Abraham Gottlob Werner (1749–1817), the founder of Neptunism theory (Fig. 42); 51° 19' 36.3'' N, 15° 25' 23.3'' E. Rock tors on the left bank of the Kwisa river gorge.

Structure and stratigraphy: Bolesławiec Syncline; upper Cenomanian Wilków Sandstone Member (German *Unterquader*) of the Rakowice Wielkie Formation

Subject: Sedimentological features and origin of late Cenomanian deposits at the norththeastern margin of the North Sudetic Synclinorium; natural resources of the local Cretaceous and their use.

Remarks: The rock tors show diffusely interbedded, structureless to crudely cross-stratified, medium- to coarse-grained quartzose, noncalcareous sandstones and granule to fine pebble conglomerates with poor kaolinitic and ferrous cement and amuddy matrix. The rock colour is whitish grey to drab, zonally orange-brown. Deposits in nearby outcrops are covered by grey, thin-bedded sandy marlstones. The Cenomanian age of these sediments is based on the occurrence of *Pecten asper* Lamarck, found in an old quarry ("Napoleon") south of the Bolesławiec–Kliczków road and in excavations to the north of it (see Przybylski and Ihnatowicz 2012). The sandstones are vertically and horizontally fractured. They used to be mined in quarries a few kilometres to the southeast.

Fig. 42. Location of stop 10. For explanation of symbols see Fig. 30.

The village of Osiecznica is presently the second-largest glass sand pit processing plant in Poland. The Coniacian Żerkowice Sandstone exploited here is an almost loose sand, containing >99% SiO_2. The sedimentological features of these sandy and overlying muddy deposits are described in the main text of the guidebook.

Genesis: The sediments in the tors show features indicative of deposition in a high wave-energy shoreface, dominated by longshore currents and sea storms.

REFERENCES

Alexandrowicz, S.W. 1976. Foraminifera from the brackish Santonian deposits in the North Sudetic Basin (Western Poland). Rocznik PTG, Annales de la Société Géologique de Pologne, 46, 183–195.

Allen, J.R.L. 1982. Sedimentary Structures: Their Character and Physical Basis, Vol. 2. Developments in Sedimentology, 30B, 643 p. Elsevier; Amsterdam.

Allmon, W.D. and Cohen, P.A. 2008. Palaeoecological

significance of turritelline gastropod-dominated assemblages from the mid-Cretaceous (Albian–Cenomanian) of Texas and Oklahoma, USA. Cretaceous Research, 29, 65–77.

Andert, H. 1934. Die Fazies in der sudetischen Kreide unter besonderer Berücksichtigung des Elbsandsteingebirges. Zeitschrift der Deutschen Geologischen Gesellschaft, 86, 616–636.

Aramowicz, A., Anczkiewicz, A.A. and Mazur, S. 2006. Fission-track dating of apatite from the Góry Sowie Massif, Polish Sudetes, NE Bohemian Massif: Implications of post-Variscan denudation and uplift, Neues Jahrbuch für Mineralogie – Abandlungen, 182, 221–229.

Badura, J. 2005. Szczegółowa mapa geologiczna Polski, 1:50 000, arkusz Bolesławiec (621). Wydawnictwa Geologiczne; Warszawa.

Badura, J., Przybylski, B. and Zuchiewicz, W. 2004. Cainozoic evolution of Lower Silesia, SW Poland: A new interpretation in the light of sub-Cainozoic and sub-Quaternary topography, Acta Geodynnamica Geomaterialia, 1 (135), 6–29.

Badura, J., Pécskay, Z., Koszowska, E., Wolska, A., Zuchiewicz, W. and Przybylski, B. 2005. New age and petrological constraints on Lower Silesian basaltoids, SW Poland, Acta Geodynamica et Geomaterialia, 2 (139), 6–15.

Barbacka, M. Pacyna, G. and Halamski, A.T. in press. Achievements of Polish palaeobotany during the last 100 years. Palaeozoic and Mesozoic floras. 3. Mesozoic macrofossils. Annales Societatis Botanicorum Poloniae.

Beddingfield, S.D. and McClintock, J.B. 1993. Feeding behavior of the sea star *Astropecten articulatus* (Echinodermata: Asteroidea): an evaluation of energy-efficient foraging in a soft-bottom predator. Marine Biology, 115, 669–676.

Berg, G. 1913. Beiträge zur Geologie von Niederschlesien mit besonderer Berücksichtigung der Erzlagerstätten. Abhandlungen der Königlich Preußischen Geologischen Landesanstalt. Neue Folge, 64, 1–63.

Berg, G. 1938. Erläuterungen zu Blatt Landeshut, Lieferung 193. Preußische Geologische Landesanstalt, Berlin.

Beyrich, E. 1849. Das Quadersandsteingebirge in Schlesien. Zeitschrift der Deutschen Geologischen Gesellschaft, 1, 390–393.

Beyrich, E. 1855. Ueber die Lagerung der Kreideformation im schlesischen Gebirge. Abhandlungen der Königlichen Akademie der Wissenschaften zu Berlin, 26, 56–80.

Biernacka, J. 2012. Provenance of Upper Cretaceous quartz-rich sandstones from the North Sudetic Synclinorium, SW Poland: Constraints from detrital tourmaline. Geological Quarterly, 56, 315–332.

Biernacka, J. and Józefiak, M. 2009. The Eastern Sudetic Island in the early-to-middle Turonian: Evidence from heavy minerals in the Jerzmanice sandstones, SW Poland. Acta Geologica Polonica, 59, 45–565.

Birkenmajer, K., Jeleńska, M., Kądziałko-Hofmokl, M. and Kruczyk, J. 1966. Age of deep-seated fractures zones in Lower Silesia (Poland), based on K-Ar and paleomagnetic dating of Tertiary basalts. Annales de la Société géologique de Pologne, 46, 545–552.

Birkenmajer, K., Pécskay, Z., Grabowski, J., Lorenc, M.W. and Zagożdżon, P.P. 2004. Radiometric dating of the Tertiary volcanics in Lower Silesia, Poland. IV. Further K-Ar and paleomagnetic data from late Oligocene to early Miocene basaltic rocks of the Fore-Sudetic block. Annales Societatis Geologorum Poloniae, 64, 1–19.

Blake, D.B. and Guensburg, T.E. 2016. An asteroid (Echinodermata) faunule from the Oxfordian Swift Formation (Upper Jurassic) of Montana. Journal of Paleontology, 90, 1160–1168.

Bobiński, W., Gawlikowska, E. and Kłonowski, M. 1999. Important geosites of the Polish Sudetes. Polish Geological Institute Special Papers, 2, 19–26.

Born, A. 1921. Über Jungpaläozoische kontinentale Geosynklinalen Mitteleuropas. Abhandlungen der Senckenberg Gesellschaft für Naturforschung, 360, 506–583.

Bossowski, A. 1991. Wykroty N-14. Profile Głębokich Otworów Wiertniczych Państwowego Instytutu Geologicznego, 62, 1–45.

Botor, D., Anczkiewicz, A.A., Mazur, S. and Siwecki, T. 2019. Post-Variscan thermal history of the Intra-Sudetic Basin (Sudetes, Bohemian Massif) based on apatite fission track analysis. International Journal of Earth Sciences, 108, 2561–2566.

Bradshaw, M.A. 1981. Palaeoenvironmental interpretations and systematics of Devonian trace fossils from the Taylor Group (Lower Beacon Supergroup), Antarctica. New Zealand Journal of Geology and Geophysics, 24, 615–652.

Bromley, R.G. and Uchman, A. 2003. Trace fossils from the Lower and Middle Jurassic marginal marine deposits of the Sorthat Formation, Bornholm, Denmark. Bulletin of the Geological Society of Denmark, 50, 185–208.

Burkowicz, A., Galos, K. and Guzik, K. 2020. The resource base of silica glass sand versus glass industry development: The case of Poland. Resources, 9, 1–20.

Caregnato, F.F., Wiggers, F., Tarasconi, J.C. and Veitenheimer-Mendes, I.L. 2009. Taxonomic composition of mollusks collected from the stomach content of *Astropecten brasiliensis* (Echinodermata: Asteroidea) in Santa Catarina, Brazil. Revista Brasileira de Biociências, 7, 252–259.

Čech, S. 2011. Palaeogeography and Stratigraphy of the Bohemian Cretaceous Basin (Czech Republic) – an overview. Geologické výzkumy na Moravě a ve Slezsku, 1, 18–21.

Charpentier, J.F.W. 1768. Mineralogische Geographie

der Chursächsischen Lande, 432 p. S.L. Crusius; Lepizig.

Chrząstek, A. and Jewticz, S. 2019. Trace fossils and associated mollusc fossils from the Coniacian sandstones (Żeliszów Quarry, Żerkowice Quarry) from the North Sudetic Synclinorium – new palaeoecological and palaeoenvironmental implications. In: Muszer, J., Chrząstek, A. and Niedźwiedzki, R. (Eds), XXIV Konferencja Naukowa Sekcji Paleontologicznej Polskiego Towarzystwa Geologicznego, "Od prekambru do holocenu – zmiany bioróżnorodności zapisane w skałach". Materiały konferencyjne. PTG, UWr, Zakład Geologii Stratygraficznej Instytutu Nauk Geologicznych, Zakład Paleozoologii Instytutu Biologii Środowiskowej, Wrocław 2019, 17–18. [in Polish]

Chrząstek, A., Muszer, J., Solecki, A. and Sroka, A.M. 2018. *Rosarichnoides sudeticus* igen. et isp. nov. and associated fossils from the Coniacian of the North Sudetic Synclinorium (SW Poland). Geological Quarterly, 62, 181–196.

Chrząstek, A. and Wojewoda, J. 2011. Mesozoic of South-Western Poland (The North Sudetic Synclinorium). In: Żelaźniewicz, A., Wojewoda, J. and Ciężkowski, W. (Eds), Mezozoik i Kenozoik Dolnego Śląska [Mesozoic and Cenozoic of the Lower Silesia]. pp. 1–10. WIND; Wrocław. [In Polish with English summary]

Chrząstek, A. and Wypych, M. 2018. Coniacian sandstones from the North Sudetic Synclinorium revisited: palaeoenvironmental and palaeogeographical reconstructions based on trace fossil analysis and associated body fossils. Geologos, 24, 29–53.

Clifton, H.E. and Dingler, J.R. 1984. Wave-formed structures and paleoenvironmental reconstruction. Marine Geology, 60, 165–198.

Cloos, H. 1922. Der Gebirgsbau Schlesiens und die Stellung seiner Bodenschätze, 106 p. Gebrüder Borntraeger; Berlin.

Cohen, K.M., Finney, S.C., Gibbard, P.L. and Fan, J.-X. 2013. The ICS International Chronostratigraphic Chart. Episodes, 36, 199–204.

Csiki-Sava, Z., Buffetaut, E., Ósi, A., Pereda-Suberbiola, X. and Brusatte, S.L. 2015. Island life in the Cretaceous – faunal composition, biogeography, evolution, and extinction of land-living vertebrates on the Late Cretaceous European archipelago. ZooKeys, 469, 1–161.

Cymerman, Z., Ihnatowicz, A., Kozdrój, W. and Przybylski, B. 2005a. Szczegółowa mapa geologiczna Polski, 1:50 000, arkusz Lwówek Śląski (658). Wydawnictwa Geologiczne; Warszawa.

Cymerman, Z., Ihnatowicz, A., Kozdrój, W. and Przybylski, B. 2005b. Szczegółowa mapa geologiczna Polski, 1:50 000, arkusz Lubań (656). Wydawnictwa Geologiczne; Warszawa.

Danišík, M., Migoń, P., Kuhlemann, J., Evans N.J., Dunkl, I. and Frisch, W. 2010. Thermochronological constraints on the long-term erosional history of the Karkonosze Mts., Central Europe. Geomorphology, 116, 68–89.

Dercourt, J., Gaetani, M., Vrielynck, B., Barrier, E., Biju-Duval, B., Brunet, M. F., Cadet, J.P., Crasquin, S. and Snadulescu, M. 2000. Atlas Peri-Tethys, Palaeogeographical Maps. CCGM/CGMW, Paris: 24 maps and explanatory notes, I–XX, 269 pp.

Drescher, R. 1863. Ueber die Kreide-Bildungen der Gegend von Löwenberg. Zeitschrift der Deutschen Geologischen Gesselschaft, 14, 291–366.

Drozdowski, S., Engel, W. and Falecki, W. 1978. Dokumentacja geologiczna złoża rud miedzi Wartowice w kategorii C. Archives, Przedsiębiorstwo Geologiczne; Wrocław.

Dunne, L.A. and Hempton, M.R. 1984. Deltaic sedimentation in the Lake Hazar pull-apart basin, southeastern Turkey. Sedimentology, 31, 401–412.

Dyjor, S. 1995. Young Quaternary and recent crustal movements in Lower Silesia, SW Poland. Folia Quarternaria, 66, 51–58.

Ehling, A. 2006. Eigenschaften, Abbau und Verwendung schlesischer Bausandsteine – ein aktueller Vergleich mit der Historie. Zeitschrift der Deutschen Gesellschaft für Geowissenschaften, 158, 351–360.

Frey, R.W. and Bromley, R.G. 1985. Ichnology of American chalks: the Selma Group (Upper Cretaceous), western Alabama. Canadian Journal of Earth Sciences, 22, 801–828.

Frey, R.W. and Howard, J.D. 1981. Conichnus and Schaubcylindrichnus: redefined trace fossils from the Upper Cretaceous of the Western Interior. Journal of Paleontology, 55, 800–804.

Frey, R.W., Howard, J.D. and Pryor, W.A. 1978. Ophiomorpha: its morphologic, taxonomic and environmental significance. Palaeogeography, Palaeoclimatology, Palaeoecology, 23, 199–229.

Galos, K. 2010. Ball clays for the production of porcelain tiles in Poland. Gospodarka Surowcami Mineralnymi, 26, 21–43.

Goeppert, H.R. 1841. Über die fossile Flora der Quadersandsteinformation in Schlesien, als erster Beitrag zur Flora der Tertiärgebilde. Nova Acta Academiae Caesareae Leopoldinae Naturae Curiosorum, 19, 99–134.

Goeppert, H.R. 1844. Uebersicht der fossilen Flora Schlesiens. In: Wimmer, F. (Ed.), Flora von Schlesien, preussischen und österreichischen Antheils. Zweiter Band, 156–225. Ferdinand Hirt; Breslau.

Górniak, K. 1991. The influence of sedimentary and early diagenetic conditions on the mineral composition of alluvial sediments (an example of sandy-clayey sediments of the North-Sudetic Trough). Prace Geologiczne PAN Oddział w Krakowie, 136, 1–95. [In Polish with English summary]

Górniak, K. 1996. The role of diagenesis in the forma-

tion of kaolinite raw materials in the Santonian sediments of the North-Sudetic Trough (Lower Silesia, Poland). Applied Clay Science, 12, 313–328.

Greguš, J., Kvaček, J. and Halamski, A.T. 2013. Revision of Protopteris and Oncopteris tree fern stem casts from the Late Cretaceous of Central Europe. Acta Musei Nationalis Pragae, Series B – Historia Naturalis, 69, 69–82.

Halamski, A.T. 2020. Upper Cretaceous megafloras of Poland – history of research, collections, and results of taxonomic revisions. In: Skrzyński, G., Badura, M. and Noryśkiewicz, A. (Eds), Sympozjum Sekcji Paleobotanicznej Polskiego Towarzystwa Botanicznego 4.12.2020. pp. 8–13. Polskie Towarzystwo Botaniczne, Warszawa. [In Polish, English summary]

Halamski, A.T., Kvaček, J., Svobodová, M., Durska, E. and Heřmanová, Z. 2020. Late Cretaceous mega-, meso-, and microfloras from Lower Silesia. Acta Palaeontologica Polonica, 65, 811–878.

Halamski, A.T. and Taylor, P.D. 2022. Angiosperm tree leaf as a bryozoan substrate: a case study from the Cretaceous and its taphonomic consequences. Lethaia, 55, 1–7.

Haldeman, S.S. 1840. Supplement to Number One of "A Monograph of the Limniades, or Freshwater Univalve Shells of North America" Containing Descriptions of Apparently New Animals in Different Classes, and the Names and Characters of the Subgenera in Paludina and Anculosa. 3 p. Philadelphia.

Hall, J. 1847. Palaeontology of New York. Volume 1. 338 p., C. Van Benthuysen; Albany.

Hall, J. 1852. Palaeontology of New York. Volume 2, 362 p., C. Van Benthuysen; Albany.

Haq, B.U. 2014. Cretaceous eustasy revisited. Global and Planetary Change, 114, 44–58.

Harries, P.J. and Ozanne, C.R. 1998. General trends in predation and parasitism upon inoceramids. Acta Geologica Polonica, 48, 377–386.

Hein, F.J. 1986. Tidal/littoral offshore shelf deposits – Lower Cambrian Gog Group, Southern Rocky Mountains, Canada. Sedimentary Geology, 52, 155–182.

Heer, O. 1877. Flora fossilis Helvetiae. Die vorweltliche Flora der Schweiz. 182 p. J. Wurster; Zürich.

Heřmanová, Z., Kvaček, J., Halamski, A.T., Zahajská, P. and Šilar, J. 2019. Reinterpretation of fossil reproductive structures *Zlivifructus microtriasseris* (Normapolles complex, Fagales) from the Czech and Polish Late Cretaceous. Review of Palaeobotany and Palynology, 268, 88–94.

Heřmanová, Z., Kvaček, J., Dašková, J. and Halamski, A.T. 2020. Plant reproductive structures and other mesofossils from Coniacian/Santonian of Lower Silesia, Poland. Palaeontologia Electronica, 23, a61.

Hertweck, G., Wehrmann, A. and Liebezeit, G. 2007. Bioturbation structures of polychaetes in modern shallow marine environments and their analogues to Chondrites group traces. Palaeogeography, Palaeoclimatology, Palaeoecology, 245, 382–389.

Jahn, A. 1980. Tertiary relief of the Sudetes. Geographia Polonica, 43, 5–23.

Jarmołowicz-Szulc, K. 1984. Geochronological study of a part of the northern cover of the Karkonosze granite by fission track method. Archiwum Mineralogiczne, 39, 139–183.

Jerzmański, J. 1955. Szczegółowa mapa geologiczna Sudetów w skali 1:25 000, arkusz Złotoryja. Instytut Geologiczny; Warszawa.

Kamola, D.L. 1984. Trace fossils from marginal-marine facies of the Spring Canyon Member, Blackhawk Formation (Upper Cretaceous), East-Central Utah. Journal of Paleontology, 58, 529–541.

Kley, J. and Voigt, T. 2008. Late Cretaceous intraplate thrusting in central Europe: effect of Africa–Iberia–Europe convergence, not Alpine collision. Geology, 36, 839–842.

Knobloch, E. and Mai, D.H. 1986. Monographie der Früchte und Samen in der Kreide von Mitteleuropa. Rozpravy Ústředního ústavu geologického, 47, 1–219.

Komar, P.D. and Miller, M.C. 1965. The initiation of oscillatory ripple marks and the development of planebed at high shear stresses under waves. Journal of Sedimentary Petrology, 45, 696–603.

Kowalski, A. 2021. Late Cretaceous palaeogeography of NE Bohemian Massif: diachronous sedimentary successionsin the Wleń Graben and Krzeszów Brachysyncline (SW Poland). Annales Societetis Geologorum Poloniae, 91, 1–36.

Kozdrój, W., Ihnatowicz, A. and Przybylski, B. 2005. Szczegółowa mapa geologiczna Polski, 1:50 000, arkusz Złotoryja (659). Wydawnictwa Geologiczne; Warszawa.

Krutzsch, W. 1966. Die sporenstratigraphische Gliederung der Oberkreide im nordlichen Mitteleuropa. Abhandlungen des Zentralen Geologischen Institutes, 8, 79–111.

Książkiewicz, M. 1977. Trace fossils in the flysch of the Polish Carpathians. Palaeontologia Polonica, 36, 1–208.

Leeder, M.R., Ord, D.M. and Collier, R. 1988. Development of alluvial fans and fan deltas in neotectonic extensional settings: implications for the interpretation of basin-fills. In: Nemec, W. and Steel, R.J. (Eds), Fan Deltas – Sedimentology and Tectonic Settings, pp. 163–185. Blackie; London.

Leszczyński, S. 2010. Coniacian–?Santonian paralic sedimentation in the Rakowice Małe area of the North Sudetic Basin, SW Poland: sedimentary facies, ichnological record and palaeogeographical reconstruction of an evolving marine embayment. Annales Societatis Geologorum Poloniae, 80, 1–24.

Leszczyński, S. 2018. Integrated sedimentological and ichnological study of the Coniacian sedimenta-

tion in North Sudetic Basin, SW Poland. Geological Quarterly, 62, 666–816.

Leszczyński, S. and Nemec, W. 2020. Sedimentation in a synclinal shallow-marine embayment: Coniacian of the North Sudetic Synclinorium, SW Poland. The Depositional Record, 6, 144–161.

Lewicka E. and Galos K. 2004. Gospodarka iłami ceramicznymi w Polsce. In: Surowce mineralne Polski. Surowce skalne. Surowce ilaste, pp. 341–369. Wydawnictwo Instytutu Gospodarki Surowcami Mineralnymi i EnergetycznymiPolskiej Akademii Nauk; Kraków.

Lorenc, S. and Mroczkowski, J. 1968. The sedimentation and petrography of Zechstein and lowermost Triassic deposits in the vicinity of Kochanow (Intra-Sudetic Trough). Geologia Sudetica, 13, 23–39.

MacEachern, J.A., Bann, K.L., Pemberton, S.G. and Gingras, M.K. 2007. The ichnofacies paradigm: High resolution paleoenvironmental interpretation of the rock record. In: MacEachern, J.A., Bann, K.L., Gingras, M.K. and Pemberton, S.G. (Eds), Applied Ichnology. Society of Economic Paleontologists and Mineralogists, Short Course Notes, 52, 27–64.

McBride, R.A. 2003. Offshore sand banks and linear sand ridges. In Middleton. G.V. (Ed.), Encyclopedia of Sediments and Sedimentary Rocks, pp. 636–639. Kluver Academic Publishers; Dordrecht.

Migoń, P. and Lidmar-Bergström, K. 2001. Weathering mantles and their significance for geomorphological evolution of central and northern Europe since the Mesozoic. Earth Science Reviews, 56, 285–324.

Milewicz, J. 1956. Zaburzenie utworów kredowych w Rakowicach Małych. Przegląd Geologiczny, 4, 361–364.

Milewicz, J. 1958. Podział stratygraficzny osadów kredowych w niecce północno-sudeckiej. Przegląd Geologiczny, 6, 386–388.

Milewicz, J. 1960. The Cretaceous of the Jerzmanice Graben (Sudetes). Biuletyn Instytutu Geologicznego, 239, 36–66. [In Polish with English summary]

Milewicz, J. 1964. Złoża górnokredowych iłów ceramicznych na tle budowy geologicznej depresji północnosudeckiej. Biuletyn Instytutu Geologicznego, 280, 216–259.

Milewicz, J. 1965. Facje górnej kredy wschodniej części niecki północnosudeckiej. Biuletyn Instytutu Geologicznego, 160, 15–80.

Milewicz, J. 1966. Kreda z głębokiego otworu Węgliniec IG 1. Kwartalnik Geologiczny, 10, 1144–1146.

Milewicz, J. 1968. The geological structure of the North-Sudetic Depression. Biuletyn Instytutu Geologicznego, 226, 5–26.

Milewicz, J. 1969. Distribution of Cretaceous Rocks in the North Sudetic Basin. Kwartalnik Geologiczny, 23, 819–825. [In Polish with English summary]

Milewicz, J. 1985. A proposal of formal stratigraphic subdivision of the infill of the North Sudetic Depression. Przegląd Geologiczny, 33, 385–389. [In Polish with English summary]

Milewicz, J. 1988. Makrofauna z osadów kredowych otworu wiertniczego Węgliniec IG 1. Kwartalnik Geologiczny, 32, 389–404.

Milewicz, J. 1996. Upper Cretaceous of the North Sudetic Depression (litho- and biostratigraphy, paleogeography, tectonics and remarks on raw materials). Prace Geologiczno-Mineralogiczne, 61, 1–59.

Milewicz, J. 2006. O osadach santońskich na obszarze basenu północnosudeckiego. Przegląd Geologiczny, 54, 693–694.

Mitura, J., Cieśliński, S. and Milewicz, J. 1969. Inoceramy kredowe z niecki północnosudeckiej. Biuletyn Instytutu Geologicznego, 216, 169–166.

Mohr, B. 2009. A truly European forest: A historic Lower Silesian Palaeobotanical Collection (Late Cretaceous) at the Museum of Natural History (Berlin). Earth Sciences History, 28, 276–292.

Musstow, R. 1968. Beitrag zur Stratigraphie und Paläogeographie der Oberkreide und des Albs in Ostbrandenburg und der östlichen Niederlausitz. Geologie, 16, 1–61.

Nieć, M. and Ratajczak, T. 2004. Złoża kopalin kaolinowych, iłów biało wypalających się i kopalin haloizytowych. In: Ney, R. (Ed.), Surowce Mineralne Polski. Surowce skalne. Surowce ilaste, pp. 31–66. Wydawnictwo Instytutu Gospodarki Surowcami Mineralnym i Eneregetycznymi Polskiej Akademii Nauk; Kraków.

Oberc, J. 1962. Sudety i Obszary Przyległe. In. Pożaryski, W. (Ed.), Budowa Geologiczna Polski, vol. 4, part 2, 306 p. Wydawnictwa Geologiczne; Warszawa.

Partsch, J. 1896. Schlesien. Eine Landeskunde für das deutsche Volk, 1. Teil: Das ganze Land. 420 p. Ferdinand Hirt; Breslau.

Postma, G. 1990. An analysis of the variation in delta architecture. Terra Nova, 2, 124–130.

Pożaryski, W., Brochwicz-Lewiński, W., Brodowicz, Z., Jaskowiak-Szoenejch, M., Milewicz, J., Sawicki, L. and Uberna, T. 1969. Geological Map of Poland and Adjoining Countries (without Cenozoic). Wydawnictwo Geologiczne; Warszawa.

Przybylski, B. and Ihnatowicz, A. 2005. Szczegółowa mapa geologiczna Polski, 1:50 000, arkusz Nowogrodziec (620). Wydawnictwa Geologiczne; Warszawa.

Przybylski, B. and Ihnatowicz, A. 2012. Objaśnienia do szczegółowej mapy geologicznej Polski, 1:50 000, arkuszNowogrodziec (620). 37 p. Wydawnictwa Geologiczne; Warszawa.

Rampino, M.R. and Sanders, J.E. 1981. Evolution of the barrier islands of southern Long Island, New York., Sedimentology, 28, 36–46.

Randhaber, K. 1906. Ein Beitrag zur Kenntniss der Bunzlauer Tone. 65 p. Kaemerer & CO; Halle.

Raumer, K., 1819. Das Gebirge Nieder-Schlesiens, der

Grafschaft Glatz und eines Theils von Böhmen und der Ober-Lausitz, geognostisch dergestellt. 182 p. G. Reimer; Berlin.

Retallack, G.J. 2001. Soils of the Past. 600 p. Blackwell; Oxford.

Reynaud, J.Y., Tessier, B., Proust, J.N., Dalrymple, R., Marsset, T., De Batist, M. and Lericolais, G. 1999. Eustatic and hydrodynamic controls on the architecture of a deep shelf sand bank (Celtic Sea). Sedimentology, 46, 603–621.

Rushton, J.C., Wagner, D., Pearce, J.M., Rochelle, C.A. and Purser, G. 2020. Red-bed bleaching in a CO_2 storage analogue: Insight from Entrada Sandstone fracture-hosted mineralization. Journal of Sedimentary Research, 90, 48–66.

Sanders, J.E. and Kumar, N. 1965. Evidence of shoreface retreat and in-place "drowning" during Holocene submergence of barriers, shelf off Fire Island, New York. Geological Society of America Bulletin, 86, 65–66.

Saul, L.R. and Squires, R.L. 1998. New Cretaceous gastropods from California. Palaeontology, 41, 461–488.

Savrda, C.E., Ozalas, K., Demko, T.H., Hutchinson, T.A. and Scheiwe, T.D. 1993. Log grounds and the ichnofossil *Teredolites* in transgressive deposits of the Clayton Formation (Lower Paleocene), western Alabama. Palaios, 8, 311–324.

Scupin, H. 1910. Über sudetische prätertiäre junge Krustenbewegungen und die Verteilung von Wasser und Land zur Kreidezeit in der Umgebung der Sudeten und des Erzgebirges. Zeitschrift für Naturwissenschaften, 82, 321–344.

Scupin, H. 1913. Die Löwenberger Kreide und ihre Fauna. Palaeontographica-Supplementbände, 6, 1–266.

Scupin, 1935. Die stratigraphischen Beziehungen der mittel- und nordsudetischen Kreide. Zeitschrift der Deutschen Geologischen Gesellschaft, 86, 523–538.

Scupin, H. 1936. Zur palaeographie des Sudetischen Kreidemeeres. Zeitschrift der Deutschen Gessellschaft für Geowissenschaften, 88, 309–325.

Seilacher, A. 1955. Spuren und Fazies im Unterkambrium. In: Schindewolf, O. H. and Seilacher, A. (Eds), Beitrage zur Kenntnis des Kambriums in der Salt Range (Pakistan), pp. 373–399. Akademie der Wissenschaften und Literatur, Mainz.

Skoček, V. and Valečka, J. 1983. Palaeogeography of the Late Cretaceous quadersandstein of central Europe. Palaeogeography Palaeoclimatology Palaeoecology, 44, 61–92.

Snedden, J.W., and Dalrymple, R.W. 1999. Modem shelf sand ridges: from historical perspective to a unified hydrodynamic and evolutionary model. In: Bergman, K.M and Snedden, J.W. (Eds), Isolated Shallow Marine Sand Bodies: Sequence Stratigraphic Analysis and Sedimentological Perspectives. Society for Sedimentary Geology (SEPM) Special Publication, 64, 13–28.

Sobczyk, A., Sobel, E.R. and Georgieva, V. 2019. Meso-Cenozoic cooling and exhumation history of the Orlica-Śnieżnik Dome (Sudetes, NE Bohemian Massif, Central Europe): Insights from apatite fission-track thermochronometry. Terra Nova, 32 (2), 122–133.

Sohl, N.F. 1987. Cretaceous gastropods: contrasts between Tethys and temperate provinces. Journal of Paleontology, 61, 1085–1111.

Sohl, N.F and Kollmann, H.A. 1985. Cretaceous Actaeonellid Gastropods from the Western Hemisphere. US Geological Survey Professional Paper, 1304, 1–97.

Solecki, A. 2011. Structural development of the epi-Variscan cover in the North Sudetic Synclinorium area. In: Żelaźniewicz, A., Wojewoda, J. and Ciężkowski, W. (Eds), Mezozoik i Kenozik Dolnego Śląska, pp. 19–36. WIND; Wrocław [In Polish, with English abstract.]

Sztromwasser, E. 1995. Szczegółowa mapa geologiczna Polski, 1:50 000, arkusz Chojnów (622). Wydawnictwa Geologiczne, Warszawa.

Stoch, L. 1962. Mineralogia glin kaolinitowych okolic Bolesławca. Prace Geologiczne, 6, 1–120.

Śliwiński, W., Raczyński, P. and Wojewoda, J. 2003. Sedimentation of the epi-Variscan cover in the North-Sudetic Basin. In: Ciężkowski, W., Wojewoda, J. and Żelaźniewicz, A. (Eds), Sudety zachodnie od wendu do czwartorzędu, pp. 119–126. Wind, Wrocław. [In Polish with English summary]

Thiergart, F. 1942. Mikropaläobotanische Mitteilungen 1–3. Jahrbuch der Reischsamtes für Bodenforschung, 62, 109–116.

Uličný, D. 2001. Depositional systems and sequence stratigraphy of coarse-grained deltas in a shallow-marine, strike-slip setting: The Bohemian Cretaceous Basin, Czech Republic. Sedimentology, 48, 599–628.

Uličný, D., Čech, S. and Grygar, R. 2003. Tectonics and depositional systems of a shallow marine, intra-continental strike-slip basin: Exposures of the Český Ráj region, Bohemian Cretaceous Basin. Geolines, 16, 133–148.

Uličný, D., L. Špičáková, L., Grygar, R., Svobodová, M., Čech, S. and Laurin, J. 2009. Palaeodrainage systems at the basal unconformity of the Bohemian Cretaceous Basin: Roles of inherited fault systems and basement lithology during the onset of basin filling. Bulletin of Geosciences, 84, 566–610.

Ulrych, J., Dostál, J. Adamovič, J., Jelínek, E., Špaček, P., Hegner, E. and Balogh, K. 2011. Recurrent Cenozoic volcanic activity in the Bohemian Massif (Czech Republic). Lithos, 123, 133–144.

Ventura, B., Lisker, F. and Kopp, J. 2009. Thermal and denudation history of the Lusatian Block (NE Bohemian Massif, Germany) as indicated by apatite fission-track data. The Geological Society, London, Geological Society Special Publications, 324, 181–192.

Villier, L., Kutscher, M. and Mah, C.L. 2004. Systematics and palaeoecology of middle Toarcian Asteroidea (Echinodermata) from the "Seuil du Poitou", Western France. Geobios, 37, 807–825.

Voigt, S., Wagreich, M., Surlyk, F., Walaszczyk, I., Uličný, D., Čech, S., Voigt, T., Wiese, F., Wilmsen, M., Niebuhr, B., Reich, M., Funk, H., Michalík, J., Jagt, J.W.M., Felder, P.J. and Schulp, A.S. 2008. Cretaceous. In: McCann, T. (Ed.), Geology of Central Europe. Volume 2: Mesozoic and Cenozoic, pp. 923–998. Geological Society; London.

Voigt, T., Kley, J. and Voigt, S. 2021. Dawn and Dusk of Late Cretaceous Basin Inversion in Central Europe. Solid Earth, 12, 1443–1461.

Walaszczyk, I. 2008. North Sudetic Basin (Outer Sudetic Cretaceous). In: T. McCann (Ed.), The Geology of Central Europe, 2 (Mesozoic and Cenozoic), pp. 959–960. Geological Society; London.

Walendowski, H. 2001. Piaskowce bolesławieckie w architekturze. Świat Kamienia, 6.

Williger, G. 1882. Die Löwenberger Kreidemulde, mit besonderer Berücksichtigung ihrer Fortsetzung in der preussischen Ober-Lausitz. Jahrbuch der königlichen preussischen geologischen Landesanstalt, 1881, 55–125.

Wilmsen, M., Uličný, D. and Košťák, M. 2014. Cretaceous basins of Central Europe: deciphering effects of global and regional processes – a short introduction. Zeitschrift der Deutschen Gesellschaft für Geowissenschaften, 165, 495–499.

Wilson, K. and Mohrig, D. 2021. Modern coastal tempestite deposition by a non-local storm: Swell-generated transport of sand and boulders on Eleuthera, The Bahamas. Sedimentology, 68, 2043–2068.

Wojewoda, J. 1986. Fault scarp induced shelf sand bodies in Upper Cretaceous of Intrasudetic Basin. In: Teisseyre A.K. (Ed.), 6th IAS Regional Meeting. Excursion Guidebook, Excursion A-1, pp. 31–52. Committee of Geological Sciences, Polish Academy of Sciences, Ossolineum; Wrocław.

Wojewoda, J. 1996. Upper Cretaceous littoral-to-shelf succession in the Intrasudetic Basin and Nysa Trough, Sudety Mts. In: Wojewoda, J. (Ed.), Obszary Źródłowe: Zapis w Osadach, pp. 81–96. WIND; Wrocław.

Wojewoda, J. 2020. Geoatrakcje pogranicza – Góry Stołowe i Broumowskie Ściany. B. Kokot vel Kokociński, Nowa Ruda, 300 p.

Wood, M.L. and Ethridge, F.G. 1988. Sedimentology and architecture of Gilbert- and mouth bar-type fan deltas, Paradox Basin, Colorado. In: Nemec, W. and Steel, R.J. (Eds), Fan Deltas – Sedimentology and Tectonic Settings, pp. 251–263. Blackie; London.

Wright, L.D. 1966. Sediment transport and deposition at river mouths: a synthesis. Geological Society of America Bulletin, 88, 856–868.

Ziegler, P.A. 1986. Late Cretaceous and Cenozoic intraplate compressional deformations in the Alpine foreland. Tectonophysics, 136, 389–420.

Żelaźniewicz, A., Aleksandrowski, P., Buła, Z., Karnkowski P.H., Konon, A., Oszczypko, N., Ślączka, A., Żaba, J. and Żytko, K. 2011. Regionalizacja Tektoniczna Polski. 60 pp. Komitet Nauk Geologicznych Polskiej Akademii Nauk; Wrocław.

11TH INTERNATIONAL
CRETACEOUS
SYMPOSIUM
Warsaw, Poland, 2022

LATE CRETACEOUS GEODYNAMICS IN THE MIDDLE SUDETES AREA (SEDIMENTARY AND ICHNOLOGICAL RECORD)

Jurand Wojewoda[1]| Alina Chrząstek[1]| Dominik Sokalski[1,2]

1| University of Wroclaw, Institute of Geological Sciences, 9 Maksa Borna, 50-204 Wroclaw, Poland; e-mails: jurand.wojewoda@uwr.edu.pl; alina.chrzastek@uwr.edu.pl; dominik.sokalski@uwr.edu.pl

2| KGHM Polska Miedź S.A., 48 Marii Skłodowskiej-Curie, 59-301 Lubin, Poland; e-mail: dominik.sokalski@kghm.com

ABSTRACT

The Intra-Sudetic Basin and Upper Nysa Kłodzka Trough are extensional synsedimentary tectonic units bounded by deep marginal faults. During the Late Cretaceous, they represent the main depositional areas in the Sudetes, capturing a characteristic littoral-to-shelf succession due to the southwesterly progradation of shallow marine depositional systems. Deposition was dominated by permanent alongshore drift and periodic storm events. Tectonic escarpments induced spectacular giant bedforms – accumulation terraces – and related facies association. The Upper Cretaceous sedimentary architecture resulted from superimposed global events and local tectonic activity.

INTRODUCTION

(*Jurand Wojewoda*)

Marine deposits of the Bohemian Cretaceous Basin cover most of northwestern Czechia and extend to south-eastern Germany (Saxony) and southwestern Poland (the Sudetes). An epeiric sea formed when the Variscan platform block of the **Bohemian Massif** and adjacent areas were inundated during the late Cenomanian transgression. Upper Cenomanian to Santonian marine deposition was preceded in the early to mid-Cenomanian by lacustrine and fluvial sedimentation in the basin. The present outline of the **Bohemian Cretaceous Basin** is elongated from northwest to southeast, and is about 300 km long and about 100 km wide. The original extent of this basin is unknown, mostly due to Neogene erosion.

The generally accepted view is that the basin was partly enclosed from the north and northeast by the West and East Sudetic Islands and from the southwest by the Central European Island (cf. Scupin 1935; Valečka 1979). The facies development of the Upper Cretaceous Series of the Bohemian Cretaceous Basin is rather monotonous, and typical for an epicontinental sea. Despite some local variations, two basin lithofacies can be recognized: (1) the sandy lithofacies and (2) the muddy lithofacies, containing various calcareous mudrocks (cf. Klein and Soukup 1966; Valečka 1979, 1989; Klein et al. 1979). Sandstones predominate in some areas, forming widespread bodies, several dozen metres thick, of Turonian and Coniacian age. In some localities – for instance, near Děčin, Česka Lipa, Turnov, Jícín, in the southern neighbourhood of Dresden, Adrspach–Teplice, and in the Góry Stołowe (Table Mountains) – they form picturesque "rock-cities".

A broad spectrum of shallow marine environments is represented by the various sandstone bodies of the Bohemian Cretaceous Basin. Some that are completely encased in marine mudrock show no signs of emergence and were clearly deposited offshore on a shallow shelf. Possible eustatic fluctuations have been suggested by Kauffman (1978), Valečka and Skoček (1991), Voigt (1996), and others. Laurin and Uličný (2004) suggested that Milan-

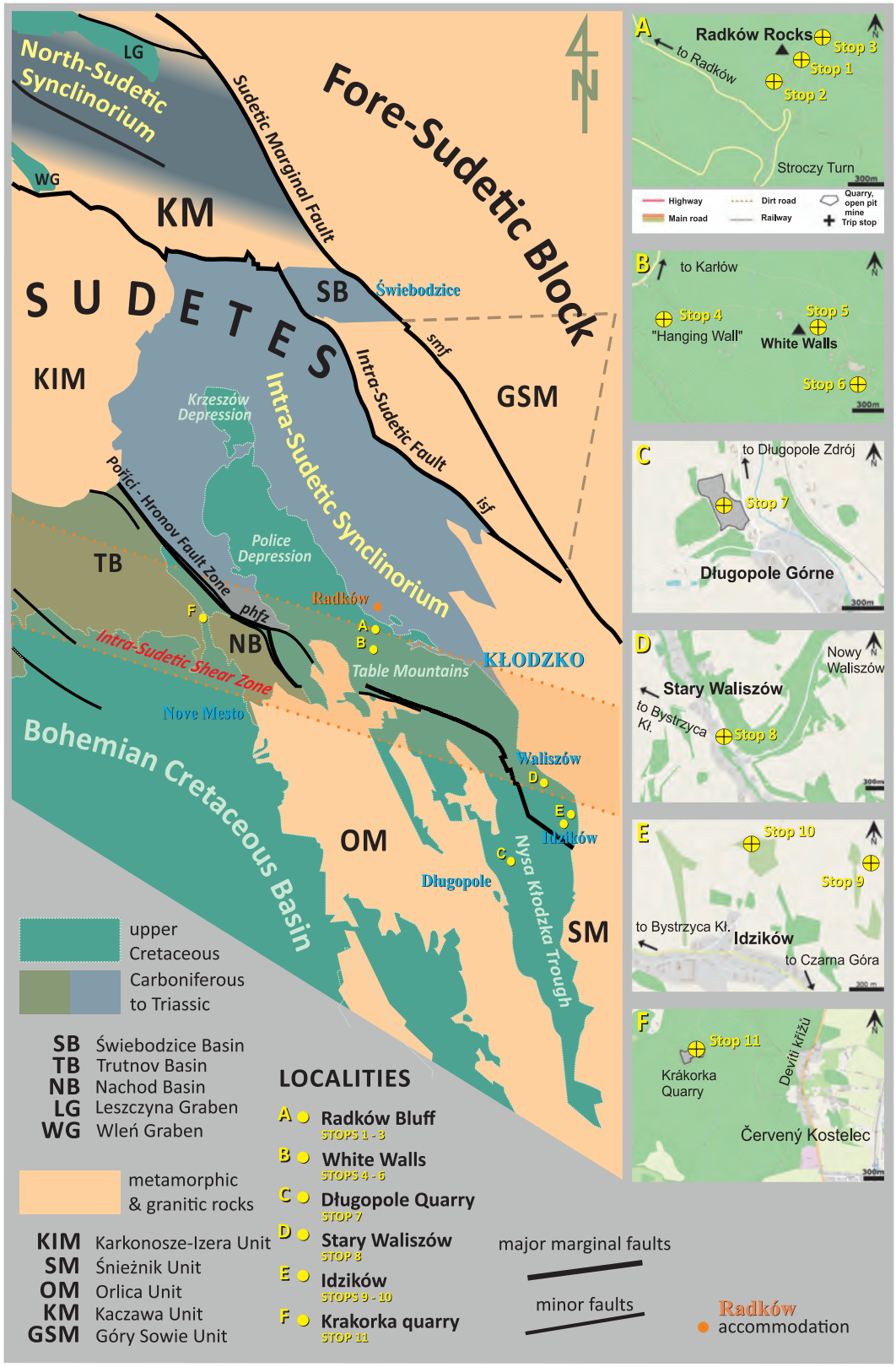

Fig. 1. Schematic geological context of the Cretaceous deposits in the Central Sudetes. The locations of the most important geosite clusters have been marked.

kovitch climatic cycles controlled the late Turonian stacking patterns *via* sediment supply or sea-level fluctuations. The physiography of the faulted basin margin was considered to be an influential factor on stratal geometries by Uličný et al. (2002). The controls on clastic sequence geometries in shallow-marine, transtensional sub-basins within the Bohemian Cretaceous Basin and surrounding areas have been extensively documented (e.g., Jerzykiewicz and Wojewoda 1986; Wojewoda 1986, 1997, 2003; Uličný et al. 2009).

GEOLOGICAL SETTING

(*Jurand Wojewoda*)

The **Intra-Sudetic Synclinorium** is an intramontane depression located at the northeastern periphery of the Bohemian Massif, depositionally active from the early Carboniferous to the Recent (Fig. 1; see also Nemec et al. 1982). The Intra-Sudetic Synclinorium is currently interpreted in terms of a pull-apart model (e.g., Wojewoda and Mastalerz 1989; Lankrejer and Littke 1997; Uličný 1997, 2002, 2004; Wojewoda 1997, 2007, 2009, 2011, 2019; Uličný et al. 2002, 2003, 2009; Wojewoda et al. 2009, 2011, 2016). The major fault zones responsible for the generation of the Intra-Sudetic Synclinorium were the WNW-ESE-trending **Intra-Sudetic Fault** and the **Poříčí-Hronov Fault Zone**.

The **Intra-Sudetic Basin** initiated in the early Carboniferous as a N-S trending deep, narrow fracture that formed on continental crust and underwent rapid subsidence (e.g., Teisseyre 1968, 1973, 1975; Teisseyre and Teisseyre 1969; Tasler 1979; Nemec 1984; Kurowski 1998). The rate of subsidence waned during the late Palaeozoic, as documented by upward decreasing thicknesses of upper Carboniferous and lower Permian sediments and changes in volcanic composition from typically acidic to bimodal (cf. Teisseyre 1966; Dziedzic 1996; Awdankiewicz 1997, 1998; Awdankiewicz et al. 2003). This stage of basin evolution cumulated in the extensive planation of the Sudetes during the early Permian and Triassic, and by contemporaneous/subsequent infilling (e.g., Wołkowicz 1988; Wojewoda and Mastalerz 1989). The next, post-orogenic depositional period continued during the Late Cretaceous and was accompanied by Laramide block tectonics (Jerzykiewicz 1967, 1968b; Radwański 1975; Vejlupek 1986) (Fig. 2).

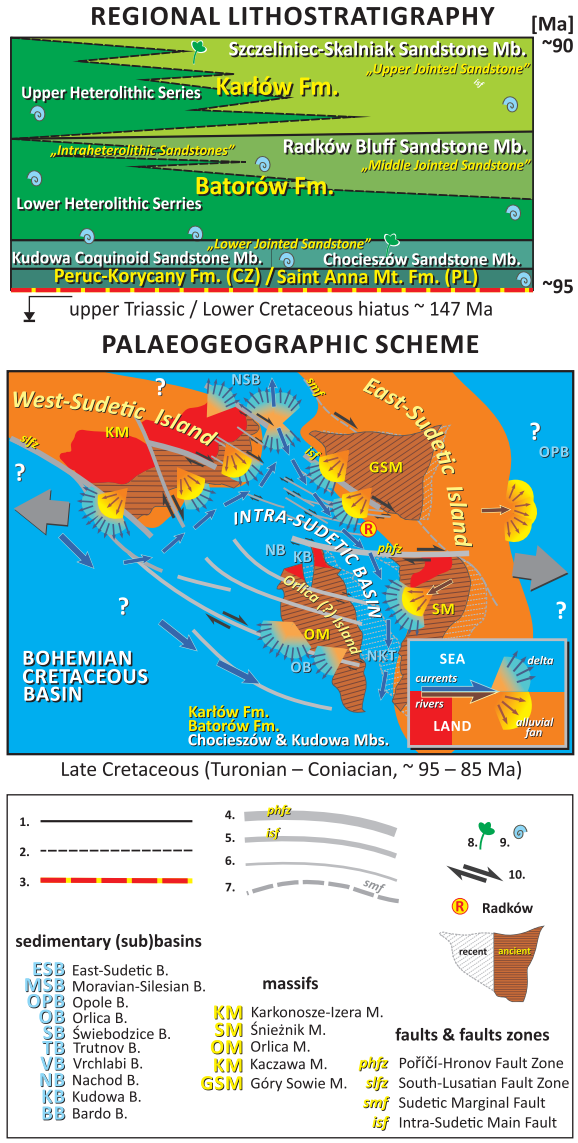

Fig. 2. Stratigraphic succession of the Intra-Sudetic Cretaceous Basin (the Table Mountains area) and its Turonian-Coniacian palaeogeography (after Wojewoda 2011, 2019 and 2020, modified). Explanations to graphics shown in lower box: 1 – isochronic boundaries, 2 – diachronic boundaries, 3 – discordance, 4 – regional fault zones, 5 – regional faults, 6 – local faults, 7 – supposed faults, 8 – fossil plants, 9 – fossil animals, 10 – sense of strike slip.

The **Nysa Kłodzka Trough** is a much younger tectonic structure that came into existence as a sedimentary sub-basin in the middle and late Turonian (Closs 1922; Rode 1936; Pachucki 1957; Don and Don 1960; Komuda and Don 1964; Radwański 1975; Jerzykiewicz 1970, 1971; Don 1996). The Nysa Kłodzka River Trough ap-

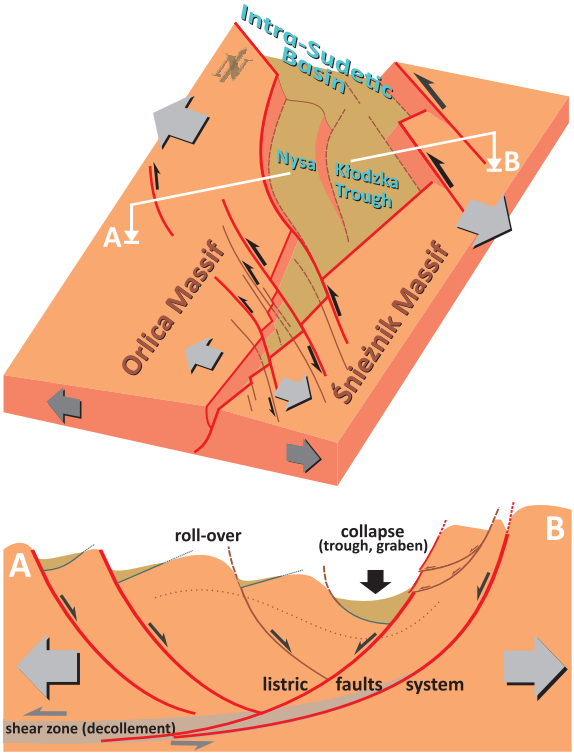

Fig. 3. Structural model of the Upper Nysa Kłodzka Trough, showing its relations to the Intra-Sudetic Basin and neighbouring crystalline massifs. The strongly asymmetrical tectonic trough is interpreted as a rollover-related structure caused by deep listric downfaulting to the east (modified after Wojewoda 1997; Don and Wojewoda 2005).

pears as a strongly asymmetrical graben, interpreted as a *rollover* related structure caused by deep listric down faulting on a fault that now separates the Nysa Kłodzka River Trough from the **Śnieżnik Massif** (Fig. 3) (cf. Naylor et al. 1986; Ellis and McClay 1988; Xiao and Suppe 1992). The Nysa Kłodzka Trough area remains tectonically active, as indicated by the present-day topography capturing hanging river valleys and terrace systems.

Both the Intra-Sudetic Basin and Nysa Kłodzka Trough are extensional tectonic features bound by deep marginal faults; together, they form the largest regional structure in the Sudetes. Starting in the Cretaceous, their joint development controlled the location of marine sedimentation (cf. Fig. 2). This structure played a fundamental role in the later Cenozoic evolution of the Central Sudetes and in the creation of the present-day relief of this area, which largely inherited features from the Cretaceous developmental stage. The geokinematic evolution of the Central Sudetes, starting in the Permian, is essentially extensional (Fig. 2). The stages of regional compression that have been earlier postulated (e.g., Don et al. 2003; Don and Gotowała 2008), including by some authors of supra-regional synthetic and modeling studies, are poorly justified by their referenced field observations, which are rather usually of only local significance (e.g., Badura et al. 2002, 2005; Badura and Rauch 2014; Sobczyk 2019; Sobczyk and Szczygieł 2021). Some models can be considered to be one-sided interpretations (e.g., Sobczyk et al. 2020) or even methodological artifacts (e.g., Sobczyk et al. 2015; Głuszyński and Aleksandrowski 2021). For example, the sections in Fig. 4 show two completely different, but equally possible, interpretations of the regional geological situation from that presented by Sobczyk et al. (2020), although they are all based on the same geochronological data. Moreover, the synthetic cross-sections presented here are almost entirely consistent with field facts, including those that have been selectively presented in some synthetic studies (cf. Wojewoda et al. 2010 and Aleksandrowski and Wojewoda 2010).

It should be emphasized that this area owes its consistently extensional development to the supra-regional tectonic structure – the **Intra-Sudetic Shear Zone** – which seems to be the most important structure on the northern edge of the Bohemian Massif, extending beyond the borders of the Sudetes (cf. Fig. 1). Both the local massifs and sedimentary (sub)basins directly refer to the geokinematic scheme imposed on the Sudetes by the Intra-Sudetic Shear Zone. Both in the past and present, the Intra-Sudetic Shear Zone generally shows a right-lateral strike-slip regime (Wojewoda 2007, 2009, 2011). Of course, this does not exclude the possibility of local transpressional phenomena, especially on the peripheral parts of the Intra-Sudetic Shear Zone (e.g., Wojewoda et al. 2010; Wojewoda and Kowalski 2016). It is worth noting that the geokinematic regime of the Intra-Sudetic Shear Zone is largely in accordance with the well-documented and similarly interpreted areas in the vicinity of the Sudetes, especially to the south (e.g., Uličný 2001, 2004; Grygar and Jelínek 2003; Uličný et al. 2003, 2009a, b).

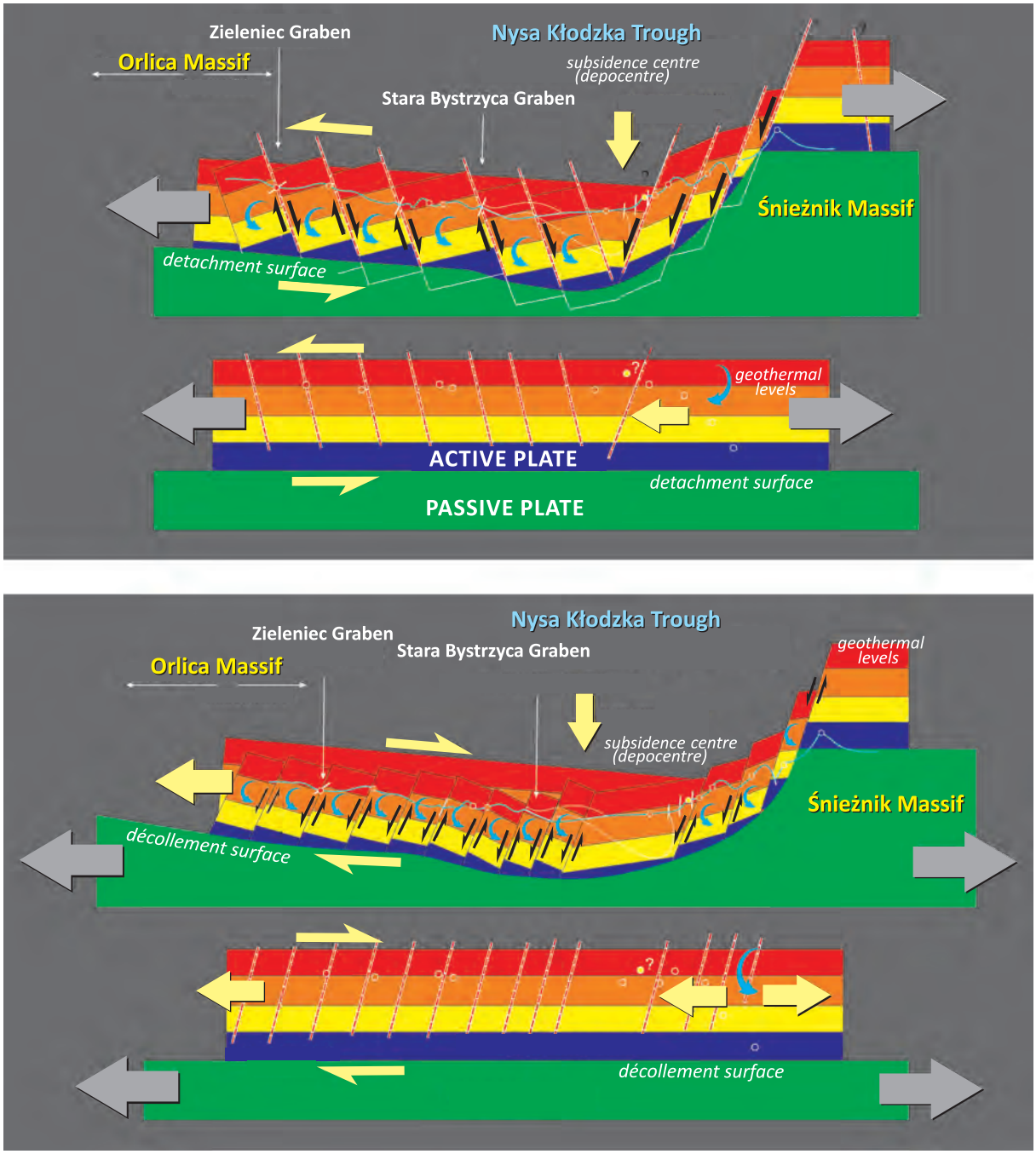

Fig. 4. Two extensional development models of the Upper Nysa Kłodzka Trough, alternatives to the compressional model presented by Sobczyk et al. (2015, 2020) and Sobczyk and Szczygieł (2021). The models proposed here are based on the same regional geological facts and thermo-geochronological data produced and used in the model of the above-mentioned authors.

In the Late Cretaceous, the Intra-Sudetic Basin and Nysa Kłodzka Trough together constituted a peripheral bay in the north and northeast of the Bohemian Cretaceous Basin – the **Intra-Sudetic Cretaceous Basin**. Until the basin was completely filled up during the Coniacian and Santonian, a strait periodically connected it with the shelf basin system of the North Atlantic through the North-Sudetic Cretaceous Basin (e.g., Wojewoda 1986, 1997; Don and Wojewoda 2005; Leszczyński 2010; Leszczyński and Nemec 2020) (cf. Fig. 1).

STRATIGRAPHY

(*Jurand Wojewoda*)

The Cretaceous succession, from west to east, ranges in thickness from 350 m in the Intra-Sudetic Basin (**Krzeszów Depression**, **Police Depression**, and the **Table Mountains**) to over 1,200 m in the **Nysa Kłodzka Trough**, and contains sediments of upper Cenomanian to Santonian age (Fig. 5). The stratigraphy of the succession is essentially based on inoceramid bivalves found in mostly fine grained, heterolithic intervals, partly aided by lithostratigraphic correlations of several mappable sandstone lithosomes with diachronous bases (Fig. 6). Sandstone clinoforms and heterolithic sediments together form specific rock architectures (i.e., cake-like) that gives rise to the characteristic forms of local landscapes (e.g., the Table Mountains) (Figs 7, 8).

Krzeszów Trough

In the oldest proposal for a stratigraphic division of the Cretaceous of the Krzeszów Depression (Berg 1905; Berg and Dathe 1906, 1913, supplemented in 1940; Dathe and Petrascheck 1933), the so-called middle jointing sandstones were included in the Turonian. This first division, however, was based solely on lithological premises. Scupin (1935), basing his scheme on fossils, also placed the **Gorzeszów Jointed Sandstone** in the middle Turonian *Inoceramus lamarcki* Zone. In the most recent stratigraphic subdivision of the Cretaceous in the Krzeszów Depression by Jerzykiewicz (1970–1978), the middle Turonian age of the sandstone was confirmed; this stratigraphy is followed herein (cf. Fig. 5). Jerzykiewicz's division is consistent with micropaleontological results (Teisseyre 1972a).

Table Mountains

The lowermost part of the Table Mountains succession is represented by an upper Cenomanian (*Actinocamax plenus*) glauconitic, poorly sorted, gravelly sandstone that unconformably overlies strongly weathered crystalline basement in the south and lower Permian clastics in the north. This sandstone is overlain by a lower Turonian (*Mytilodies labiatus* Zone) mudstone containing intercalations of spongiolite. Above, the mudstone is gradually replaced by the middle Turonian **Radków Bluff Sandstone**. In the north, the Radków Bluff Sandstone is up to 80 m thick and composes picturesque kilometre-long bluffs. Locally, the Radków Bluff Sandstone can subdivided into three-to-five units by intervening calcareous mudstones and claystones. Fine-grained, mostly calcareous sediments of middle Turonian age (*Inoceramus lamarcki* Zone) rest on the Radków Bluff Sandstone, and gradually pass upwards into the **Skalniak–Szczeliniec Sandstone**. This quartz arenitic sandstone, up to 70 m thick, forms the topographic culminations of the Table Mountains, and is late Turonian (and also supposedly early Coniacian) in age (see also Kodym et al. 1967; Jerzykiewicz 1968a, 1969).

Jerzykiewicz and Wojewoda (1986) proposed the stratigraphic subdivision of the Cretaceous in the Table Mountains, taking into account sedimentological studies and data from available drilling material. In their division, the middle Turonian sandstones occur within the calcareous mudstones and limestones of the *I. lamarcki* Zone (cf. Fig. 5). The stratigraphic succession of the Cretaceous sediments in the Table Mountains presented here is also consistent with micropaleontological results (e.g., Teisseyre 1975).

Nysa Kłodzka Trough

The upper Cenomanian–Turonian sequence of the Nysa Kłodzka River Trough is very similar to that of the Table Mountains. However, the equivalents of the Radków Bluff Sandstone and the Skalniak–Szczeliniec Sandstone lithosomes are represented by glauconitic sandstone and calcareous sandstone, respectively, and show markedly reduced thicknesses. Moreover, wedges of the the Skalniak–Szczeliniec Sandstone successively die out to the southeast. The uppermost Turonian is represented by a siliceous spongiolite member which, in turn, is overlain by the very thick claystone-sandstone alternations of the **Idzików Lower Beds**. This heterolithic Coniacian succession (*Volviceramus involutus* Zone) is, in its upper part, replaced by a gneissic conglomerate forming the **Idzików Upper Beds**. This member wedges entirely out toward the west over a distance of 2 km from the eastern mar-

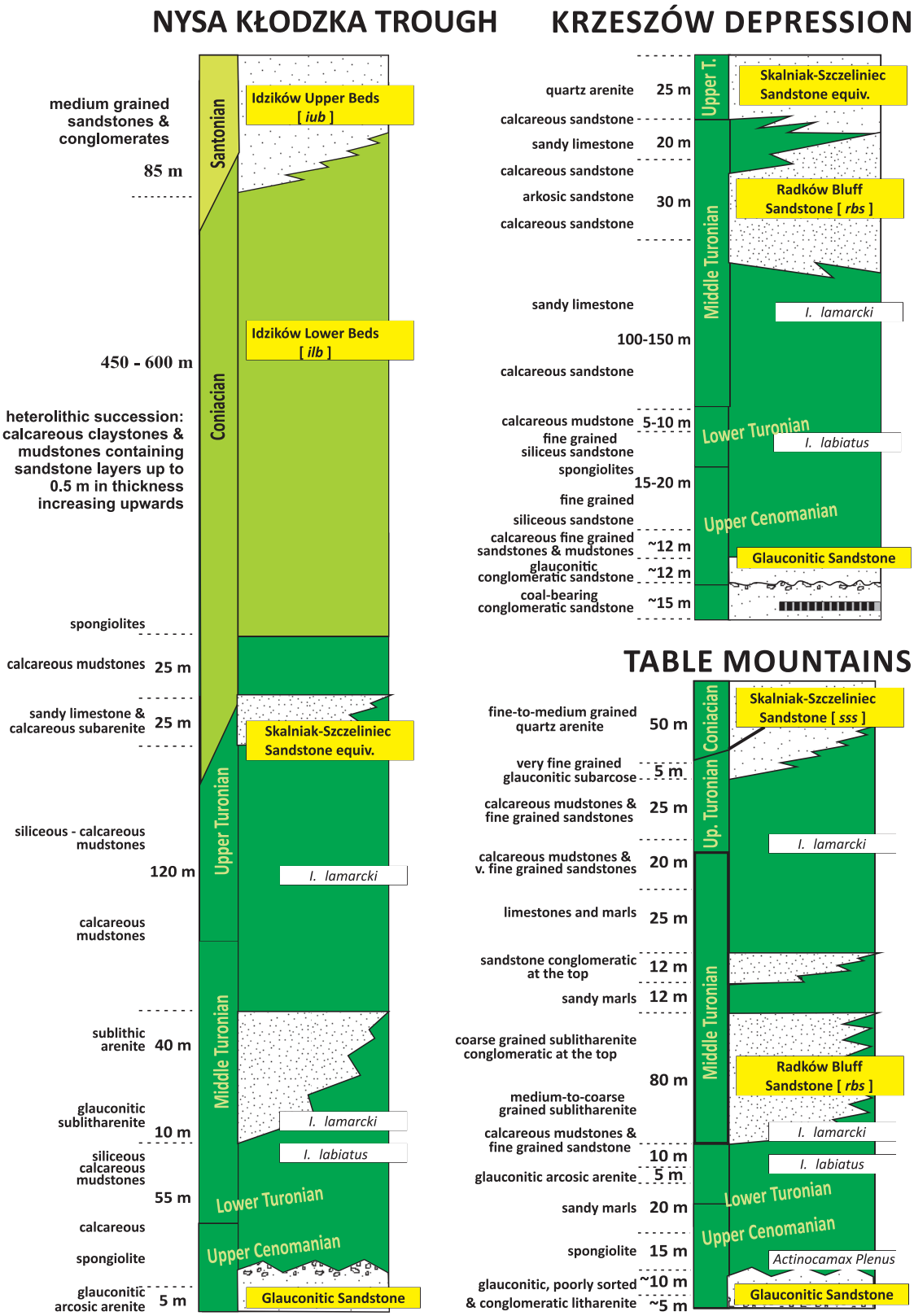

Fig. 5. Cretaceous sedimentary successions of the Upper Nysa Kłodzka Trough, the Table Mountains, and the Krzeszów Depression (modified after Wojewoda 1997).

Fig. 6. The most important and historically significant specimens of the Lower Silesian Cretaceous fauna from the Geological Museum of the University of Wrocław (courtesy of Dr. P. Raczyński).

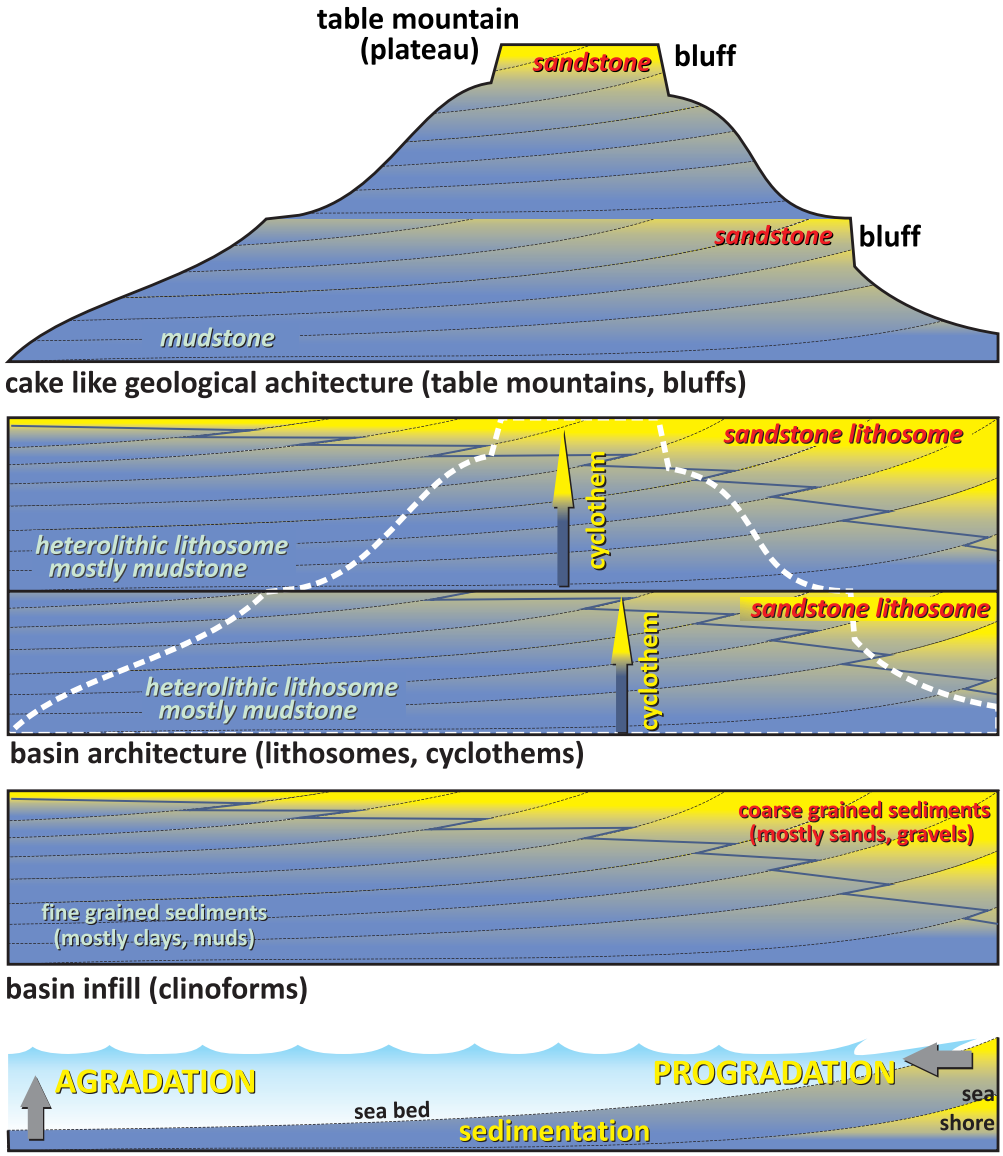

Fig. 7. Diagram showing the relationship between the sedimentation-conditioned architecture of the Cretaceous sedimentary rocks in the Table Mountains (clinoforms, lithosomes), with characteristic features of the terrain (steep bluffs, flat plateaus).

ginal fault of the Nysa Kłodzka Trough (Don and Don 1960; Jerzykiewicz 1971).

The palaeontological and sedimentological studies of Jerzykiewicz (1971) clarified the stratigraphic subdivision of the Cretaceous in the Nysa Kłodzka River Trough. His lithostratigraphic scheme, with slight terminological changes, is adopted herein (cf. Fig. 5) and was confirmed by subsequent micropaleontological studies (Teisseyre 1972b, 1975; Kędzierski 2002). A similar subdivision for the Nysa Kłodzka River Trough succession based on inoceramid bivalves was applied in the Czech part of the trough (Janeček 2015).

SEDIMENT ARCHITECTURE AND BASINS EVOLUTION

(*Jurand Wojewoda*)

Comparison and correlation of the lithostratigraphic columns of the Intra-Sudetic Cretaceous Basin and the Nysa Kłodzka Trough shows that both the Radków Bluff Sandstone and the Skalniak–Szczeliniec Sandstone litho-

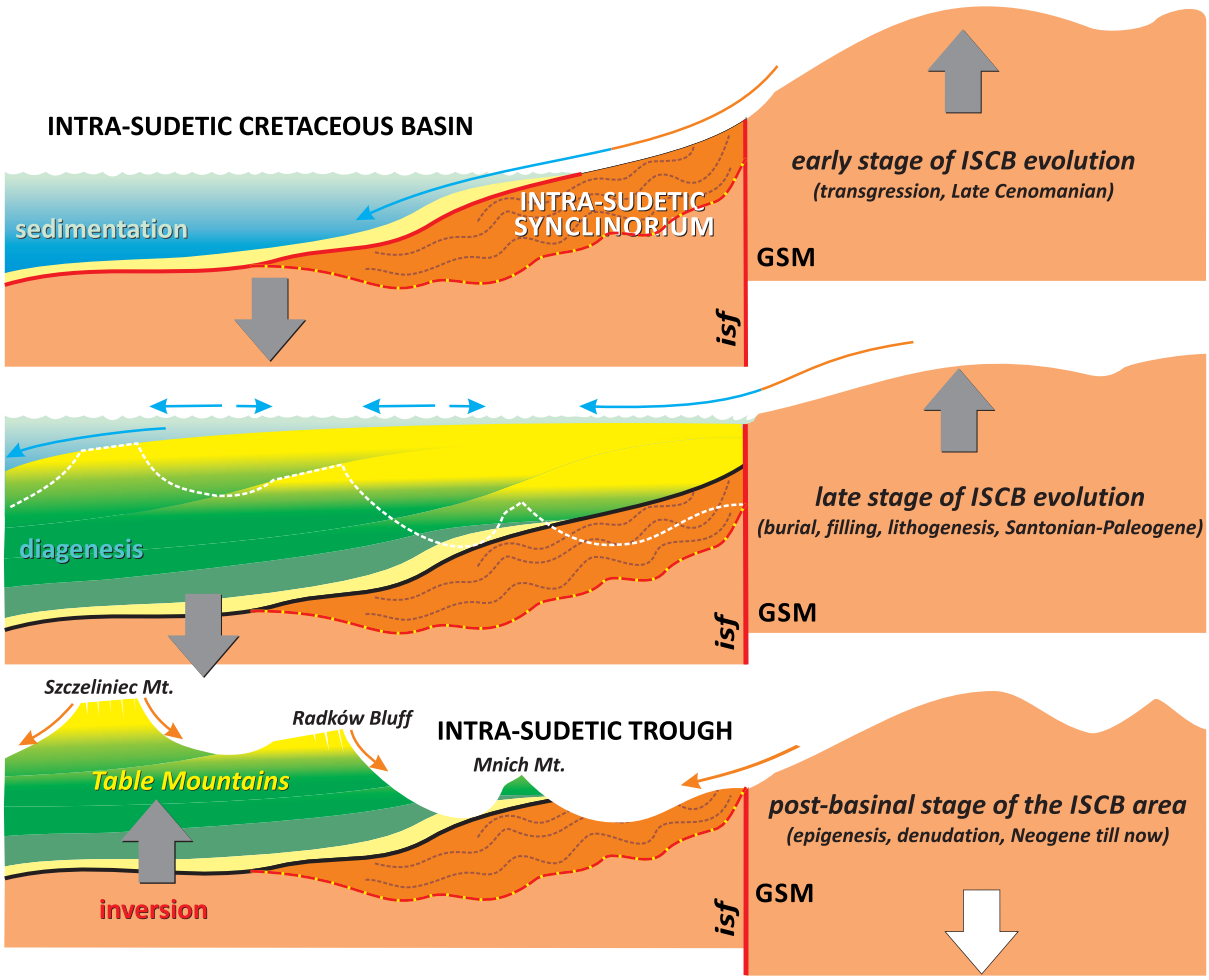

Fig. 8. Chronology of various phenomena and processes in the Intra-Sudetic Synclinorium; isf – Intra-Sudetic Fault; GSM - Góry Sowie Massif.

somes are diachronous (Fig. 9). If the assumed isochrones are correct, at least four stages of basin evolution can be distinguished in the Nysa Kłodzka Trough. These stages coincide remarkably well with both global and regional eustatic events (cf. Kauffman 1978; Valečka and Skoček 1991; Miller et al. 2003, 2005; Laurin and Uličný 2004; Vakarelov et al. 2006; Schlager 2012)

Transgression (Cenomanian–early Turonian)

During the Cenomanian–Turonian transgression, sedimentary conditions were uniform, resulting in a single transgressive sequence recognizable across the entire Intra-Sudetic Cretaceous Basin. The sequence contains glauconitic sandstone at the base, followed by calcareous and siliceous mudstones with spongiolite intercalations near the top. If the sandstone represents nearshore sediments, the spongiolite reflects the greatest palaeodepth, corresponding to the maximum extent of the transgression. The absence of terrestrial material in the spongiolite is perhaps due to the fact that it represents the most distal position relative to the palaeoshoreline in the entire succession, and perhaps reflects marine transgression over nearly the entire Sudetes area and probably (?) most of the Bohemian Massif.

The correlated columns (Fig. 9) are situated along a NW-SE trending line. It is highly probable that the direction of the main facies gradient was perpendicular to it. This supports existing opinions that the transgression proceeded towards the northeast, and suggests that the late Cretaceous sea encroached on a flat and significantly leveled pre-Cenomanian palaeorelief (cf. Don 1996).

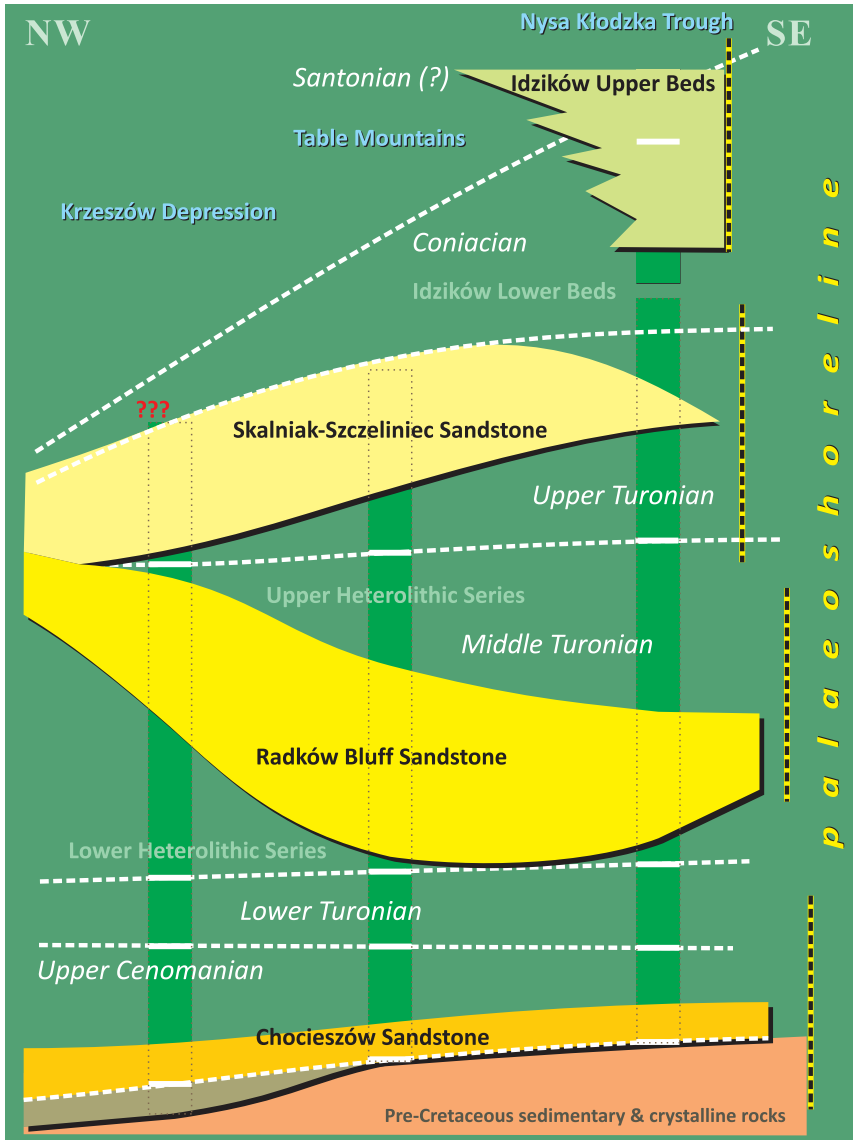

Fig. 9. Spatial and age correlation of the main sandstone lithosomes in the Central Sudetes.

Regression and cyclic filling of the basin (middle–upper Turonian)

Near the end of the early Turonian, an eustatic fall resulted in a landmass along the northeastern periphery of the **Intra-Sudetic Cretaceous Basin** (now the **Sowie Góry Mountains**). This northern part, the **East-Sudetic Cretaceous Island**, became the main source area during the Turonian. In the Intra-Sudetic Basin area, the regression resulted in the southwestern progradation of nearshore and shelf sediments and the formation of asymmetrical, coarsening upwards megacyclothems. Several episodes of rapid subsidence were superimposed on this constant progradational trend, resulting in a twofold radical back-displacement of the facies associations to the northeast (Wojewoda 1986). This stage of basin evolution can be characterized as a syntectonic deposition.

Cycle I (Radków Bluff Sandstone and its lithostratigraphic equivalents)

Lateral facies displacements in the middle Turonian were evidently directed towards the southwest, which implies a permanently inclined basin slope in this direction. The depo-

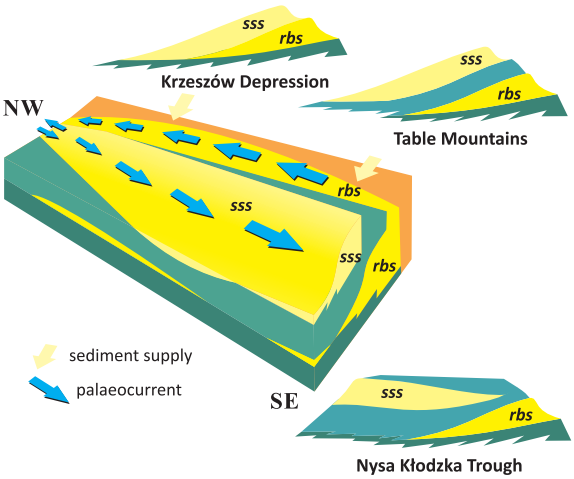

Fig. 10. A spatial model of the regional formation of sandstone lithosomes during the middle and late Turonian (respectively, the Radków Bluff Sandstone (rbs) and the Szczeliniec–Skalniak Sandstone (sss)) forced by two main factors: the inversion of alongshore transport direction and the permanent progradation of sedimentary-environmental zones (modified after Wojewoda 1997).

sition of the Radków Bluff Sandstone first began in the Table Mountains area; much later, it spread over the Krzeszów Depression on the northwestern peripheries of the Intra-Sudetic Cretaceous Basin (Fig. 10). This suggests a successive enlargement of the Radków Bluff Sandstone lithosome to the northwest, as supported by middle Turonian alongshore paleotransport directions toward the northwest (Wojewoda 1986). In the Nysa Kłodzka Trough, the Radków Bluff Sandstone and its lithostratigraphic equivalents are sharply overlain by the fine-grained distal sediments of the next cyclothem, whereas in the Krzeszów Depression they pass gradually and directly into the younger sandstone, the Skalniak–Szczeliniec Sandstone (cf. Figs 9, 10).

Cycle II (Szczeliniec-Skalniak Sandstone and its lithostratigraphic equivalents)

In the Table Mountains, the Szczeliniec–Skalniak Sandstone and its equivalents terminate cycle II. Despite its evidently diachronous nature, the Szczeliniec–Skalniak Sandstone appears to have begun almost synchronously over the entire Intra-Sudetic Cretaceous Basin. However, a southeasterly directed alongshore paleotransport during the late Turonian implies enlargement of the Szczeliniec–Skalniak Sandstone lithosome in this direction (cf. Jerzykiewicz 1967, 1968). The textural and spatial convergence of middle and upper Turonian sandstones towards the northwest suggests that both sandstone lithosomes are non-contemporaneous members of the same progradational system. In this case, the Szczeliniec–Skalniak Sandstone would be an upper Turonian equivalent of the Radków Bluff Sandstone as a result of consistent southwestern progradation (cf. Figs 9, 10).

Transgression and formation of the Upper Nysa Trough (upper Turonian–Coniacian)

Near the end of the late Turonian, the paleodepth and accumulation and accommodation rates in the Nysa Kłodzka Trough increased significantly. This is documented by the deposition of spongiolite and so-called "concretion bearing" beds, which are overlain by the heterolithic, clayey-sandy Idzików Lower Beds, up to 600 meters thick (Don and Don 1960; Jerzykiewicz 1971). This stage resulted from the combination of eustatic transgression and the rapid subsidence that initiated the Nysa Kłodzka Trough as a fault-bounded subbasin. The markedly asymmetrical facies distribution and the easterly increasing thickness of the Idzików Lower Beds suggest that the deepest zone of the basin was aligned N-S, located close to the eastern margin of the basin. During the Coniacian, the dominant sediment source was an area located on the east of the present day Krowiarki and Śnieżnik Massifs, on the eastern part of the East Sudetic Cretaceous Island.

The heterolithic Idzików Lower Beds were interpreted as deep-marine turbidites (Jerzykiewicz 1970, 1971), which influenced some incorrect regional interpretations (e.g., Don 1996). It is clear, however, that the so-called Nysa Graben flysch represents a sequence of distal-to-transitional tempestites, which corresponds well with the regional shallow-marine environmental setting (see, for discussion, Valečka 1984).

Regression and cyclic filling of the Upper Nysa River Trough (Coniacian–?Santonian)

A later stage of the evolution of the Nysa Kłodzka Trough was characterized by gradual

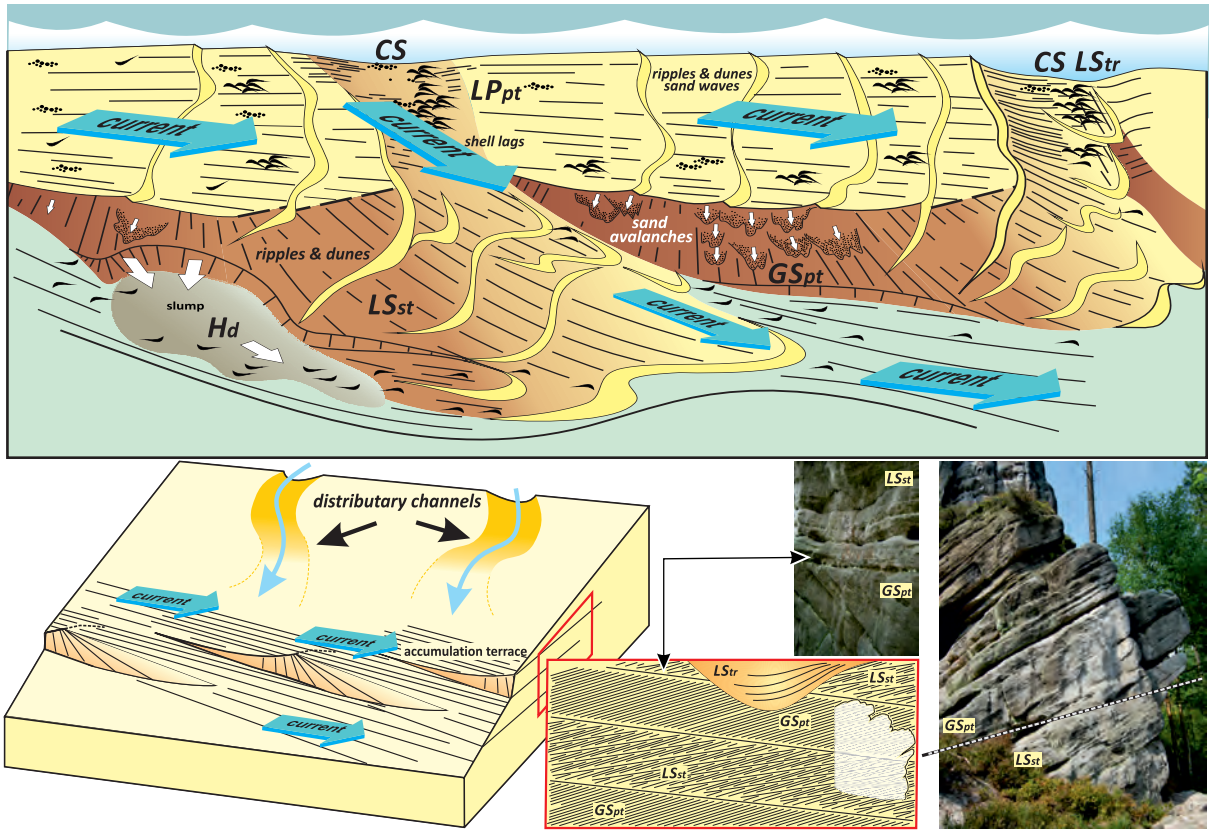

Fig. 11. Presumed appearance of tectonically forced accumulation terraces on the sea floor of the Middle Sudetes area in the late Turonian. Example of an almost complete facies association accompanying the climbing of various terrace slope segements, which occurs in geosites of the famous White Walls location in the Table Mountains (modified after Wojewoda 1986).

regression, accompanied by cyclic downslip activity along the eastern marginal fault. This resulted in the formation of typical, scarp-related fan-delta to nearshore deposits (Idzików Upper Beds) and the cyclic deposition of tempestites (upper part of the heterolithic sequence).

SEDIMENTARY FACIES AND PROCESSES

(*Jurand Wojewoda*)

The Cretaceous sedimentary setting of the Intra-Sudetic Cretaceous Basin was largely typified by shallow-marine processes dominated by wind-driven currents, and intermittently interrupted by storm events (Wojewoda 1986). In the Table Mountains, only the shelf facies are preserved, as much of the record was removed during post-Cretaceous erosion. In the Nysa Kłodzka River Trough, the Cretaceous sediments fill a topographic depression, and now reveal a fully preserved facies tract ranging from a fan delta system near the basin margin to distal outer shelf sediments.

Table Mountains (Góry Stołowe Mountains)

Sandstones form progradational and coarsening-upwards units that mostly consist of various inner shelf deposits. The deposition of sand took place on the basin floor, which had a scarp-like configuration produced by synsedimentary tectonic activity. In turn, this topography induced peculiar depositional conditions in which giant bedforms formed (Fig. 11; Wojewoda 1986). The existence of such bedforms was anticipated by Jerzykiewicz (1968), who termed them **accumulation terraces** and interpreted them as tidally originated ridges. However, this interpretation is untenable on several grounds (Wojewoda 1986; see below).

The progradation of the accumulation terraces left behind a characteristic facies com-

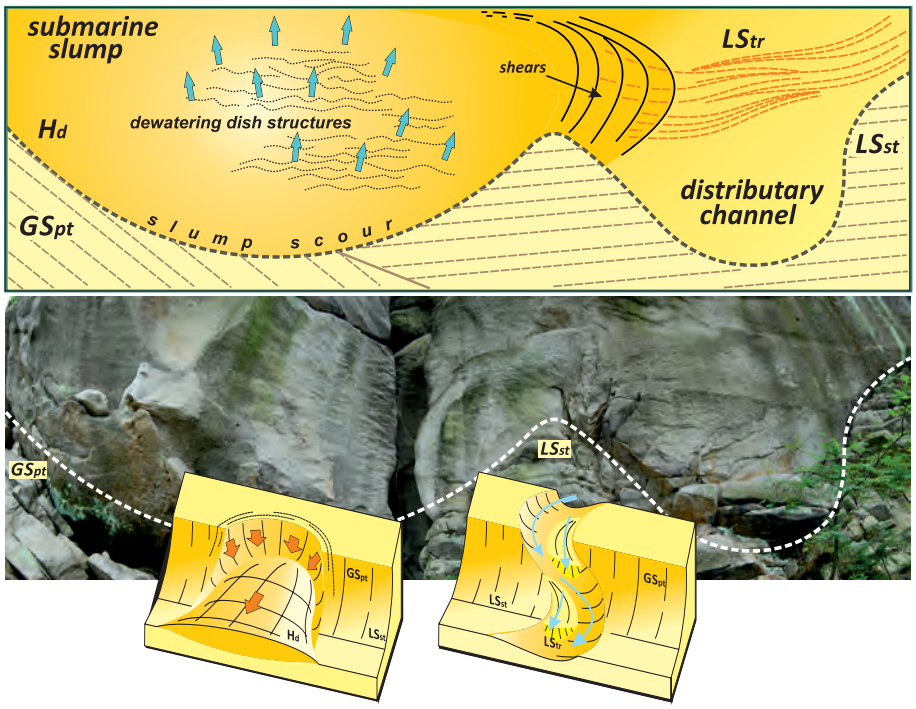

Fig. 12. Two perfectly preserved structures: a sinuous shelf distributary channel and a submarine slump, partially destroying the filling of the previous one. One of the geosites of the White Walls location in the Table Mountains.

plex including, among others, two dominant and distinctive facies. The first facies is giant-scale cross-bedded sandstone (**GS_{pt}** facies), in which individual sets reach up to 18 m (cf. Figs 11, 13A). The second variety are sandstones whose cosets also reach the same thickness as above, and consist of sloping cross-bedded deposits in large-scale tabular sets (**LS_{st}** facies, cf. Fig. 11).

The small scatter of bed inclination in the **GS_{pt}** facies (200–230°/25–40°) implies a constant trend of terrace slope inclinations in both the Radków Bluff Sandstone and Skalniak–Szczeliniec Sandstone lithosomes. This trend closely follows the strike of neighbouring faults. Sediment transport was dominated by permanent alongshelf drift directed towards the northwest and southeast during the formation of the Radków Bluff Sandstone and Skalniak–Szczeliniec Sandstone lithosomes, respectively (Jerzykiewicz and Wojewoda 1986; Wojewoda 1986). However, there is evidence of drift inversion, causing changes in the paleocurrent system. It is unclear whether these changes were only of local significance (that is, only pertinent to the Intra-Sudetic Cretaceous Basin), or whether they concerned the entire Bohemian Cretaceous Basin. Perhaps an indicator of the drivers of palaeotransport direction is the temporal coincidence between the formation of the Skalniak–Szczeliniec Sandstone lithosome and the initiation and/or intensification of tectonic activity in the Nysa Kłodzka Trough in the southeastern part of the Intra-Sudetic Cretaceous Basin.

The **GS_{pt}** facies is, in places, intercalated with a homogenous sandstone (**H_d** facies) that represents various gravity mass-flow deposits ranging from fluidized sediment flows to flux-oturbidites (Fig. 12). This sandstone locally fills southwesterly inclined scours cut in the **GS_{pt}** facies (Fig. 13). In such instances, the **H_d** facies is ungraded and reveals traction carpets, floating shells, and fluid escape systems (e.g., tubes and dishes).

Large trough cross-bedded sandstones (**LS_{tr}** facies) commonly appear in the upper part of sandstone sections as channel fills, 2–4 m deep. This facies represents a nearshore-to-shelf channel distributary system (cf. Figs 11, 12). Storm events resulted in the formation of a proximal coquinoid tempestite (**C_s** facies, Figs 11, 13D). This sediment forms a persistent layer(s), up to 1 m thick, which is underlain by an

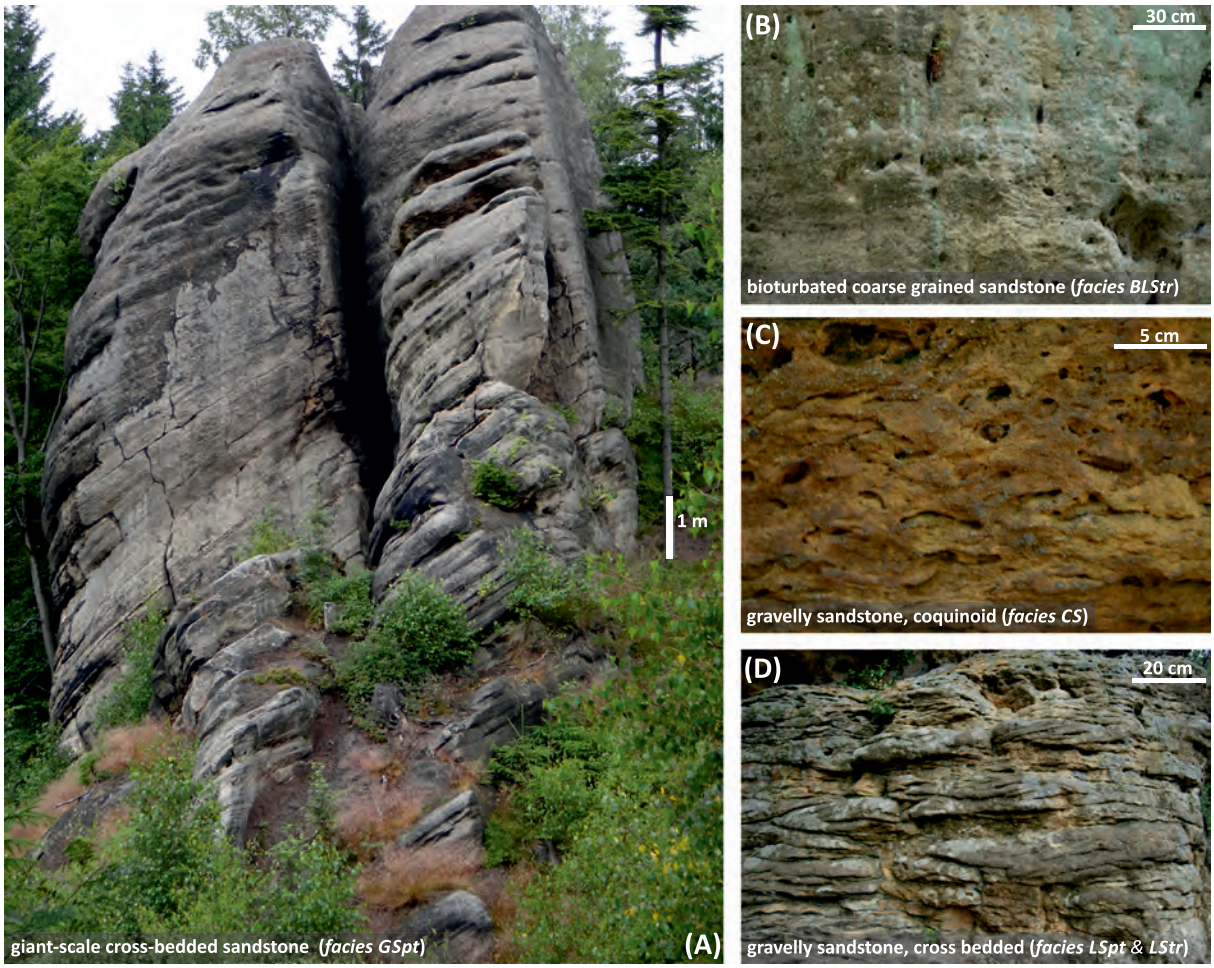

Fig. 13. The most common structural varieties of Cretaceous sandstones in the Table Mountains area: (A) giant-scale cross-bedded sandstones, unique globally (slope deposits of accumulation terraces, GS_{pt} facies); (B) bioturbated, homogeneous sandstones at the top of the Radków Bluff Sandstone (BLS_{pt-tr} facies); (C) conglomeratic coquinoid sandstones (proximal tempestite, C_s facies) and (D) large-scale cross-bedded sandstones (deposits of current induced bedforms migrating on the surfaces and slopes of accumulation terraces, LS_{pt-st} facies) (modified after Wojewoda 1986, 1997).

erosion surface of regional extent. Sand deposition in the Table Mountains area was suddenly interrupted by a rapid subsidence pulse, documented by abrupt contacts with the overlying mudstones. These fine-grained sediments are mostly calcareous mudstones and claystones in which the majority of *Inoceramus* fauna have been found. They represent stratigraphic distal equivalents of the sandstone facies. Two main facies groups can be distinguished in the fine-grained sediment: heterolithic distal tempestites (Rotnicka 1997) and homolithic calcareous micrite, locally silicified or enriched with organic detritus (Ziółkowska et al. 1992).

Seismotectonic structures provide evidence of synsedimentary tectonic activity during the Cretaceous. The most spectacular are synsedimentary faults and shears, which document motion on the neighbouring Guzowata Fault and Radków–Batorów Fault during the deposition of the Radków Bluff Sandstone and the Skalniak–Szczeliniec Sandstone, respectively (Wojewoda 1997). It is believed that these faults were also responsible for the generation of the accumulation terraces. The shear zones developed in unconsolidated sand, and constitute a system of low-angle Riedel's T-shears. Their orientation suggests the predominance of downslip movement during the middle Turonian and strike-slip displacement in the late Turonian. The shears are often accompanied by ball-shaped empty hollows and associated gas

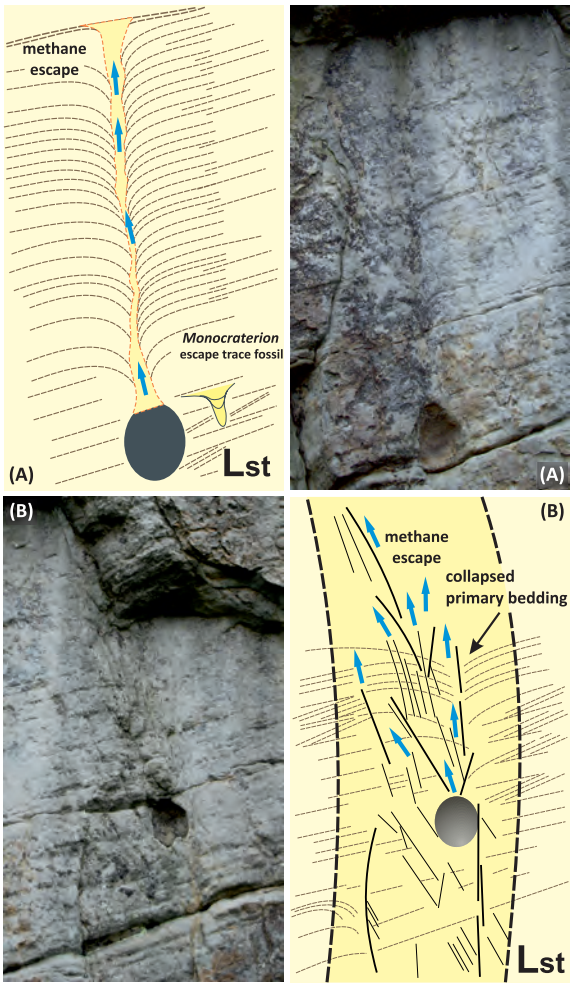

Fig. 14. Unique traces of methane escape from sediment and seismotectonic shears in one of the geosites of the White Walls location in the Table Mountains (after Wojewoda 1986, 1997).

escape pipes (Fig. 14). It is very likely that the rapid progradation of a 20-m tall accumulation terrace onto unconsolidated, freshly deposited muds resulted in gas extraction, squeezing gas from the overloaded substrate and concentrating it in sand. If the seismic shock partly fluidized sediment, the gas bubbles migrated upwards and formed escape structures.

Nysa Kłodzka Trough

The lower part of the Cretaceous succession of the Nysa Kłodzka Trough (Cenomanian–middle Turonian) is very similar to the contemporaneous succession of the Intra-Sudetic Synclinorium (cf. Fig. 5). Although it is characterized by much smaller sandstone lithosome thicknesses, the lithostratigraphic boundaries within fine-grained heterolithic sediments are clearly marked (Fig. 15). The upper part of the succession (Turonian–Coniacian) in the Nysa Kłodzka Trough is clearly bipartite; the lower part consists of heterolithic sediments (Idzików Lower Beds), whereas the upper part is dominated by sandstones and conglomerates (Idzików Upper Beds) (Fig. 16). This is mainly due to the syntectonic activity of the eastern border fault of the Nysa Kłodzka Trough, which significantly narrowed the beach zone. It also caused periodic influxes of river and fan delta sediments into the beach area, where they were redistributed along the steep slopes of the land and basin (Fig. 17).

The heterolithic succession of the Idzików Lower Beds represents distal to transitional

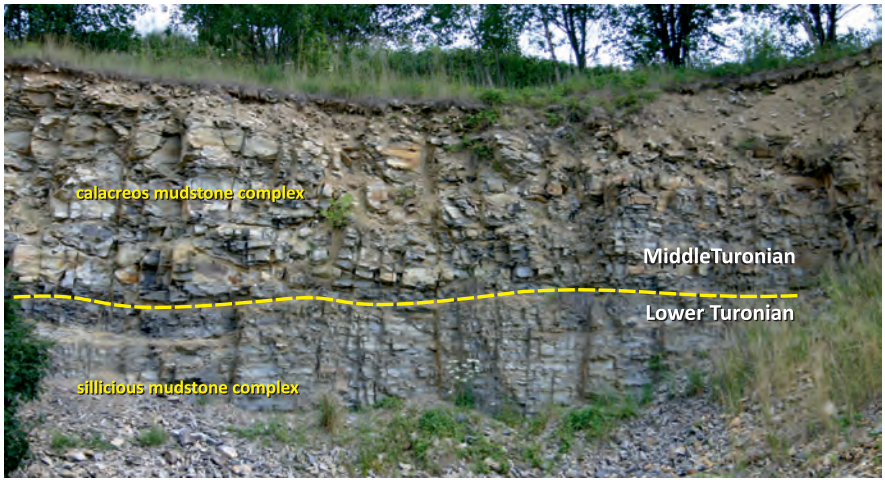

Fig. 15. The lower–middle Turonian boundary between fine-grained sediments, most likely related to changes in seawater oxygenation (Stara Bystrzyca Quarry, Upper Nysa Kłodzka Trough).

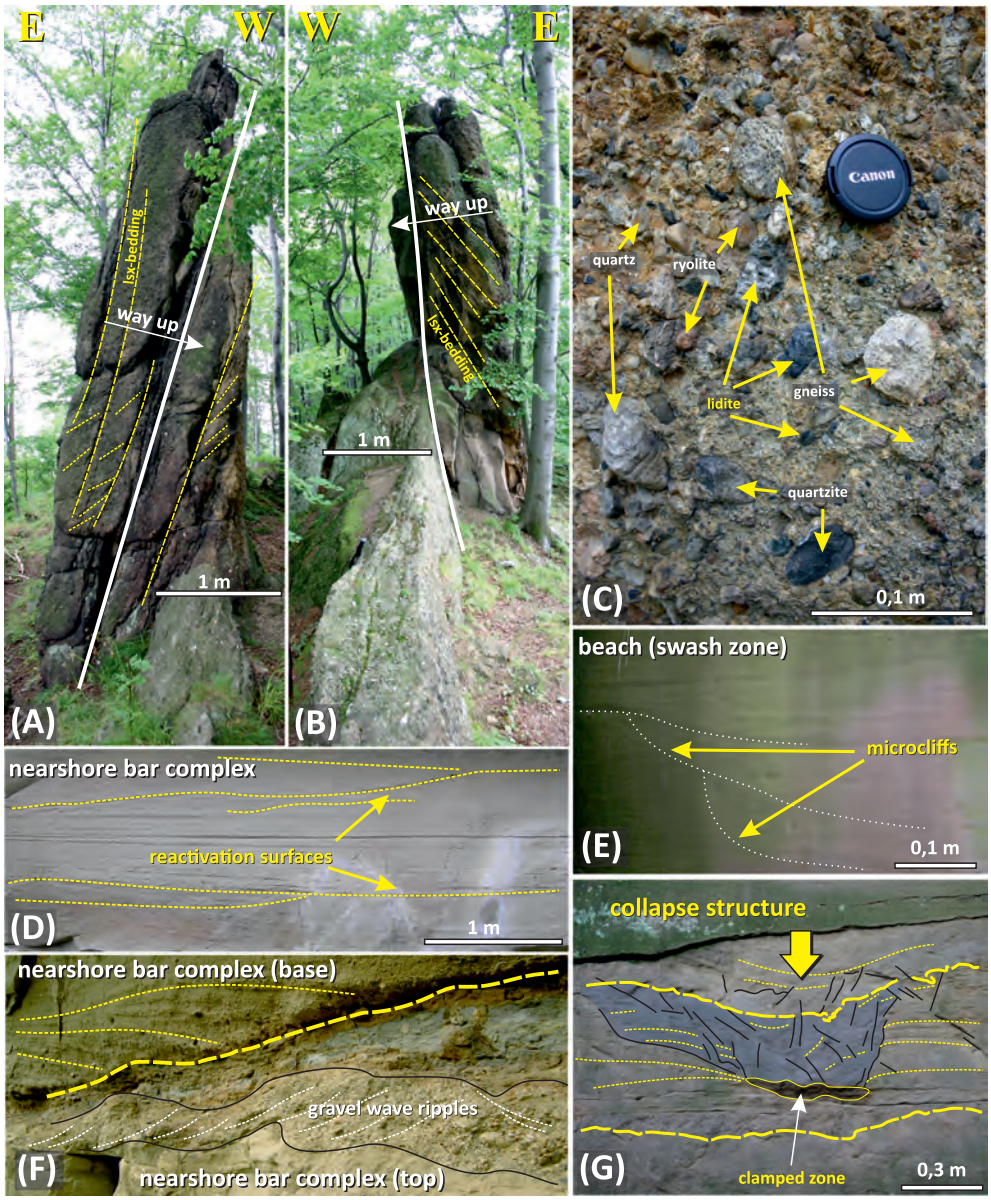

Fig. 16. Dominant sediment types in the Idzików Upper Beds – the youngest preserved Cretaceous sediments in the Central Sudetes: (A) and (B) steeply tectonically inclined polymictic conglomerates (C) in the immediate vicinity of the eastern fault frame of the Nysa Kłodzka Trough (supposedly fan delta sediments, Shepard's Rocks location); (D) nearshore bar sediments with numerous reactivation surfaces, with (E) rarely preserved microcliffs; (F) gravelly wave ripples; (G) a collapse structure of unknown origin. Idzików Quarry (after Wojewoda 1997).

tempestites. The great thickness of this succession was previously regarded as evidence of an extremely deep-water basin setting (cf. Jerzykiewicz 1970, 1971), but it is more likely to reflect high subsidence accompanied by vigorous sediment supply into the basin.

The conglomerates of the Idzików Upper Beds only occur near the eastern margin of the Nysa Kłodzka Trough. They belong to the main fan-delta system established during the late Turonian and Coniacian, and subsequently fed the rest of the basin. The conglomerates show clast imbrication and structures diagnostic of beach and nearshore environments (e.g., microclifs, beach cusps, low-angle inclined bedding, and trace fossils) (cf. Wojewoda 1997; Chrząstek 2020). Additionally, spectacular gravelly wave ripples documenting high-en-

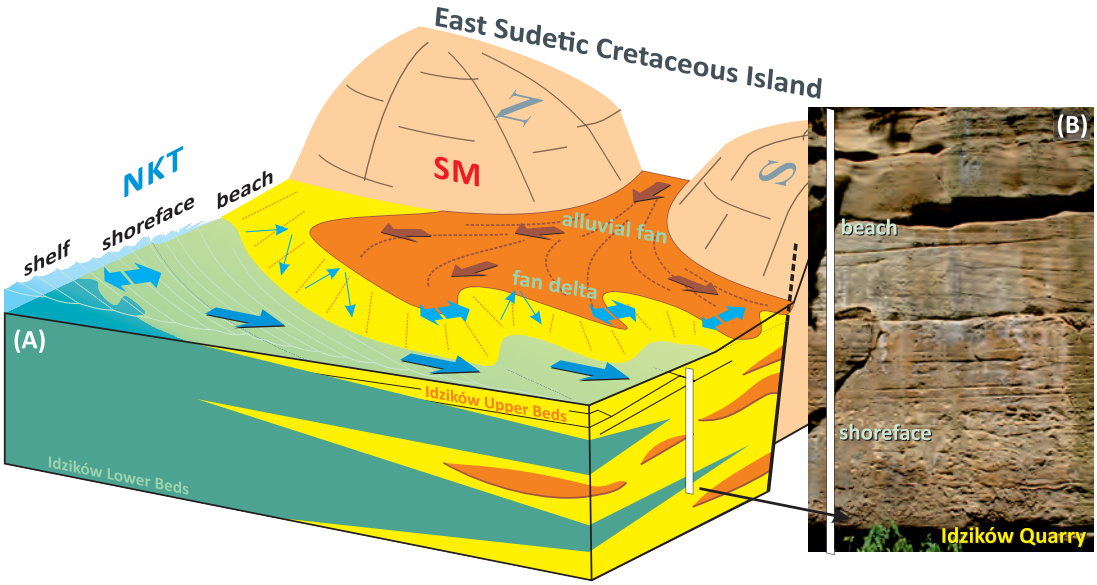

Fig. 17. Palaeogeographic scheme of the eastern coast of the Cretaceous Sea in the Upper Nysa Kłodzka Trough, corresponding to the facies association of the Idzików Upper Beds. Shepard's Rocks and Idzików Quarry.

ergy waves and wave-generated currents are present (Fig. 16). The gravelly sandstones and sandstones of the Idzików Upper Beds form large-scale cross-bedded and compound sedimentary units that resulted from the migration (progradation) of swash zone and nearshore bars (Fig. 16). Both the cross-bedding and numerous reactivation surfaces are inclined to the south, and reflect an alongshore palaeocurrent.

The sandstones usually form multi-story sedimentary units of a proximal-to-transitional tempestitic character (Fig. 16). Their multiple recurrences in the vertical section apparently reflects high subsidence rates and high accumulation potential, characteristic for near fault scarp conditions (cf. Fig. 17).

PALAEOGEOGRAPHY

(*Jurand Wojewoda*)

During the Cenomanian, eustatic sea-level rise affected both the Sudetes and the Fore-Sudetic Block, transgressing from the southwest (**Bohemian Cretaceous Basin**) and the east (**Opole Basin**). In the early Turonian, the mid-Sudetes area was almost entirely drowned. The regression began in the middle Turonian, interrupted by several rapid episodes of increased subsidence. Palaeotransport was directed towards the northwest and south, mostly by alongshore wind drift. Steeply inclined basin slopes favored storm surges and the intense redistribution of littoral material into the open shelf. Very rapid progradation was accompanied by fault tectonics. During the late Turonian, the palaeotransport dramatically reversed: that is, shifting toward the southeast. The storm redistribution of clastic material was no longer as significant as in earlier times, mostly because of the progressive levelling of the basin slopes.

Some short-term paleoflow changes can be rationally explained by wind tides. The river basin faults were still active, but the kinematics style changed from predominately (relatively) vertical to typically strike-slip towards the end of the Turonian. During the Turonian–Coniacian transition, the sea again flooded the Sudetic area. At the same time, in the eastern part of the basin strongly increased subsidence affected the Nysa Kłodzka Trough. A subsequent marine regression continuing throughout the Coniacian resulted in the filling of the basin. Simultaneously, the nearby eastern marginal fault of the Nysa Kłodzka Trough generated a system of fan deltas with a narrow littoral-beach zone. The steep slopes of the Nysa Kłodzka Trough formed a sort of escarpment which, together with a high subsidence rate, resulted in the formation of a thick tempestite succession.

FIELD STOPS

Stop 1:

Radkowskie Baszty (English *Radków Towers*), Table Mountains National Park, Stroczy Zakręt (English *Stroczy Turn*), close to the Radków–Karłów route (Figs 1, 23A); 50° 28' 46'' N, 16° 23' 40'' E; sandstone bluff up to 40 m high, marking the northern limit of the Table Mountains. (*Jurand Wojewoda*)

Structure and stratigraphy: Intra-Sudetic Synclinorium, Intra-Sudetic Cretaceous Basin; Radków Bluff Sandstone (middle Turonian, *Inoceramus lamarcki* Zone) of the Batorów Formation; so-called Middle Jointed Sandstone (German Mittel Quadersandstein).

Subject: Regional context; sandstone lithosomes, clinoforms and cyclothems; facies association of a storm dominated barred shoreface; palaeocurrents and palaeotransport; impact of synsedimentary tectonics on basin floor relief; basin inversion; lithology as a factor in landform development ("rocky towers", "rocky mushrooms") and induced fracturing.

The rocky forms in the Table Mountains are controlled by structural factors. Apart from vertical bluffs, the most picturesque are the rocky "mushrooms", "towers", and "labyrinths", as well as "blocks" separated off the main sandstone lithosomes. Most of these forms formed in areas where intense surface erosion takes place and surficial waters infiltrate deep into the rock massifs (Fig. 18). The infiltration washes out the rock material and, above all, mineral cements out of the rocks, mostly *via* suffosion. However, the dominant control on the shape and distribution of rocky forms is the underlying geological structure of the Table Mountains. While rock formation shape is more influenced by primary sedimentary structure (Figs 13, 18), their distribution and abundance depend mostly on the secondary tectonic structures, for example faulting or fissuring (Fig. 18A). Rocky towers usually develop at the edges of rock plateaus. At Radków Bluff, towers most often appear in groups, creating characteristic bastions and rock labyrinths in places where the scarp is the highest and surface runoff plays a less important role, and where rainwater or melting snow vertically infiltrates into strongly fissured rocks (cf. Fig. 18B). The destruction of rocks is particularly intensive in zones built of coarse-grained material (**C_s facies**), in which the water filters in much faster, and the process of washing out fine material from the rock is very quick (cf. Fig. 18B).

The Radków rocky towers consist of quartz-feldspar sandstone with clay-silica cements (lithic subarkose). In the middle Turonian, the East-Sudetic Cretaceous Island – consisting of Palaeozoic and older sedimentary rocks – supplied the Intra-Sudetic Cretaceous Basin with sedimentary material, deposited in a

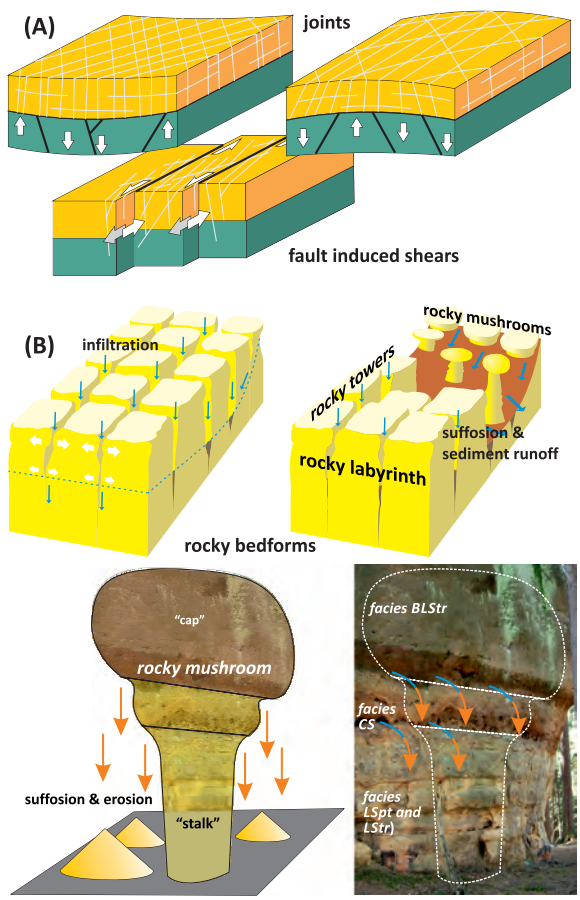

Fig. 18. Influence of filtering water flow, structural phenomena (e.g., joints, fault shears), lithology, and mineral suffosion on the formation and shape of rock forms (e.g., "mushrooms", "towers", "labyrinths").

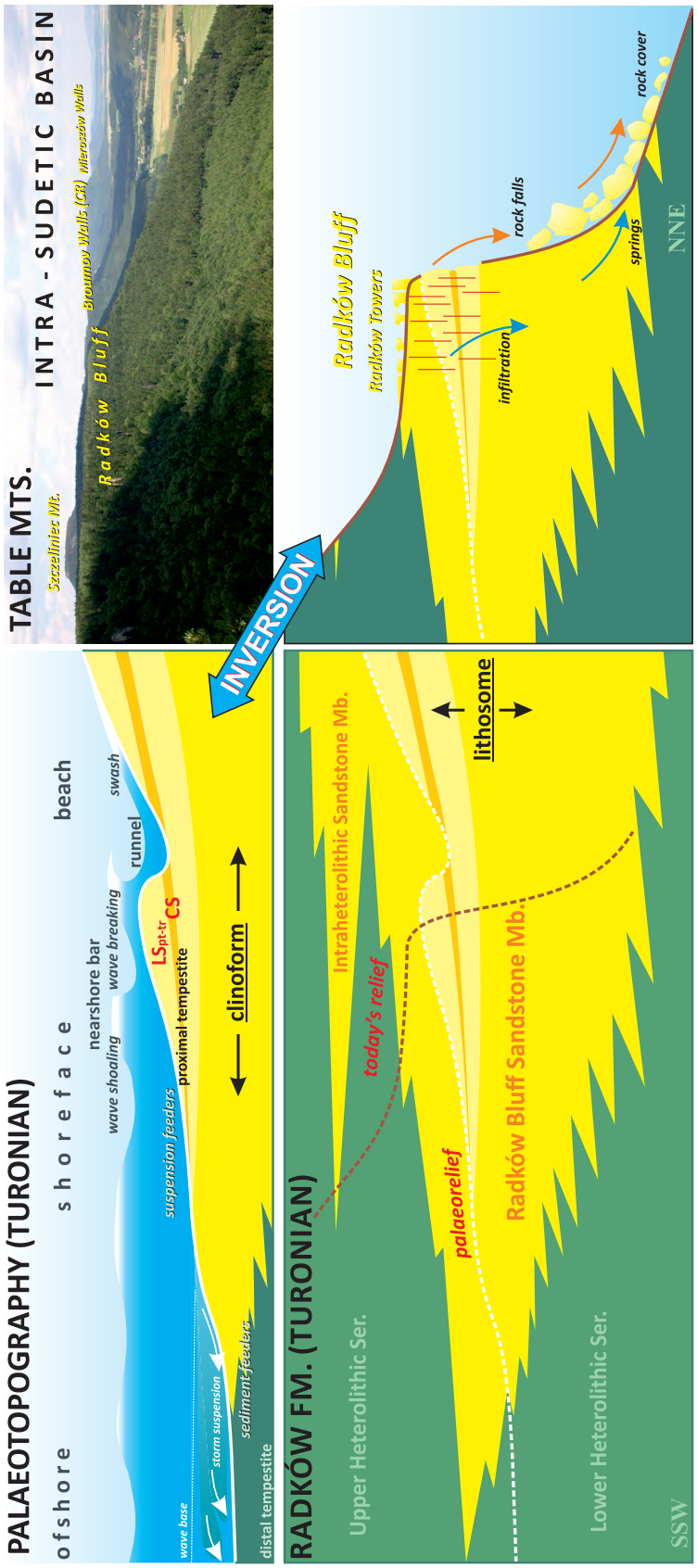

Fig. 19. An example of the influence of the internal facies architecture within sandstone lithosomes on the topographic relief, due to palaeotopographic inversion in the sedimentary basin. Radków Bluff, Table Mountains (Wojewoda et al. 2011).

shallow marine shelf and shoreface environments (cf. Fig. 8).

Seacoast progradation is recorded by a characteristic vertical sequence of sandstone lithosomes (cf. Figs 7, 8). From the bottom, the sequence includes: (1) the shelf-to-shoreface subenvironment, (2) nearshore shoals, (3) coarser grained storm deposits (proximal tempestites), and (4) the beach environment (swell and swash zones) (Fig. 19). In the sandstone clinoform, these zones correspond to the following sediments / sedimentary rocks: below the clinoform and in its lower part, fine-grained claystones and mudstones; in the central part, diagonally layered sandstones (facies **LS_{pt}** and **LS_{tr}**); and in the upper part, coarse-grained conglomeratic sandstones and coquinoids (facies **C_s**). The uppermost part of the sequence consists of the highly homogenized facies **LS_{pt}** and **LS_{tr}**, the **BLS_{pt}** and **BLS_{tr}** facies respectively (Fig. 20A).

The Radków Bluff reflects the exhumation and inversion of relief (during the post-basinal stage) in the Middle Sudetes (cf. Fig. 8). While the area located northeast of the present Table Mountains supplied the Intra-Sudetic Cretaceous Basin during the Cenomanian to Coniacian, the elevated Table Mountains now provide material to the Ścinawa River Valley in the northeast (Fig. 19). It is worth noting that the oldest post-Cretaceous sediments containing Cretaceous material are of late Pliocene age (the lower part of the Gozdnica Formation), placing the start of the Cretaceous denudation in the Neogene. It is also worth emphasising that these sandstones underwent deep residual chemical weathering, as evidenced by kaolinized feldspars. Such material cannot be preserved in a highly energetic sedimentary environment. Residual weathering is commonly documented in the Sudetes and took place during the Oligocene and Miocene, confirming the late exposure of the Cretaceous sedimentary succession and landscape inversion.

Another phenomenon common in the Table Mountains are epigenetically forced fractures, referred to **induced fractures**. The term was originally introduced by Ollier (1978), and then by Wojewoda (2012) and Wojewoda and Ollier (2013). These breaks occur locally on the plateaus of rock massifs disintegrating due to selective weathering. They often accompany rock mushrooms and towers (Fig. 21).

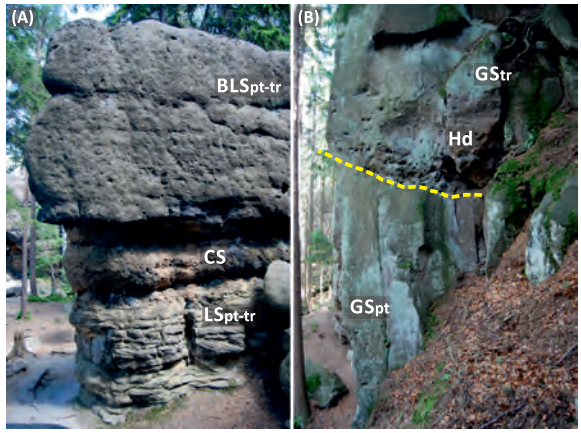

Fig. 20. Sandstones with obliterated primary sedimentary structure due to (A) bioturbation (BLS_{pt-tr} facies) or (B) subaqueous mass redeposition of sediment (GS_{tr} and H_d facies). Radków Bluff (Wojewoda 1986, 1997).

Genesis: Sand-gravely deposits of the shelf and shoreface, forming lithosomes with slightly coarsening-upwards grains and partially obliterated primary sedimentation structures; storm-generated gravel accumulations (proximal tempestites); epigenetically induced fractures.

Stop 2:

Radków Bluff, Table Mountains National Park, Stroczy Zakręt (English *Stroczy Turn*), close to the Radków–Karłów route (Figs 1, 23A); 50° 28' 44'' N, 16° 23' 36'' E; sandstone bluff up to 40 m high, marking the northern limit of the Table Mountains. (*Jurand Wojewoda*)

Structure and stratigraphy: Intra-Sudetic Synclinorium, Intra-Sudetic Basin; Radków Bluff Sandstone (middle Turonian, *Inoceramus lamarcki* Zone) of the Batorów Formation; so-called Middle Jointed Sandstone (German Mittel Quadersandstein)

Subject: Distributary channels and runoff plume tracts, and their position within the architecture of shoreface sediments.

In the central part of the Radków Bluff Sandstone lithosome, numerous scours are filled with coarse-grained homogeneous sediment with features typical of fluxoturbidite-type mass flows (facies **H_d**, Fig. 20B, see also Fig. 12). A characteristic feature of the Hd facies

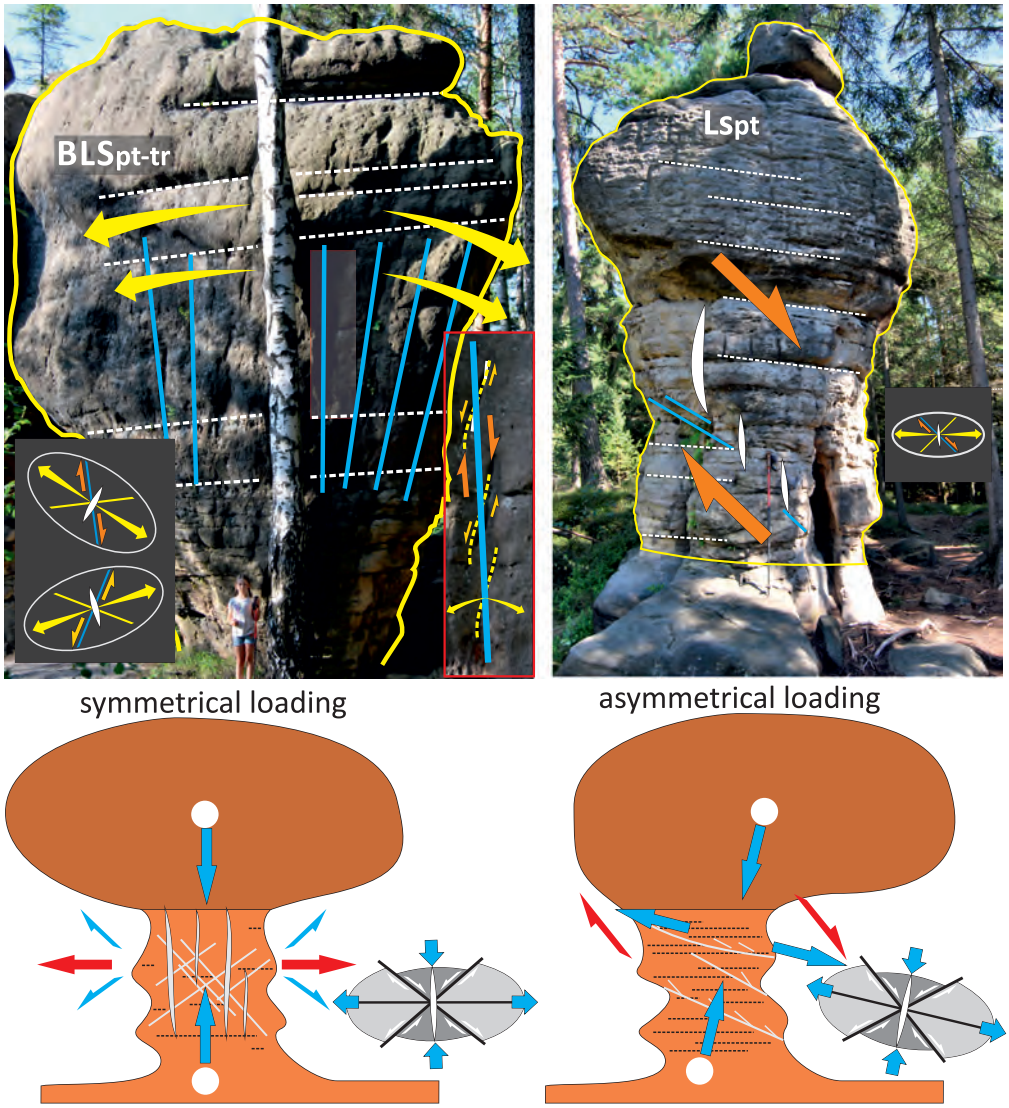

Fig. 21. Development of induced fractures in sandstone rock forms due to lithologically controlled selective erosion and, subsequently, overloading on the rock form bed. Radków Towers. (Ollier 1978; Wojewoda and Ollier 2013).

are concentrations of large shells in the upper parts of mass flow sheets, which may indicate that this material came not only from local redeposition, but additionally contains a significant admixture of detritus from the nearshore zone. The axis of the channel is inclined to the southwest – that is, perpendicular to the supposed palaeoshore of the basin and the edge of the accumulation terrace (cf. Fig. 11). This is supported by the constant slope of layers in the underlying **GS_{pt}** facies (210–240°), cut off by the mass flow runoff.

In this part of the Radków Bluff, over 5 km long, all documented sections show the same facies sequence: **GS_{pt}** (+ **H_d**) – **LS_{pt}** (**LS_{tr}**) – **C_s** –

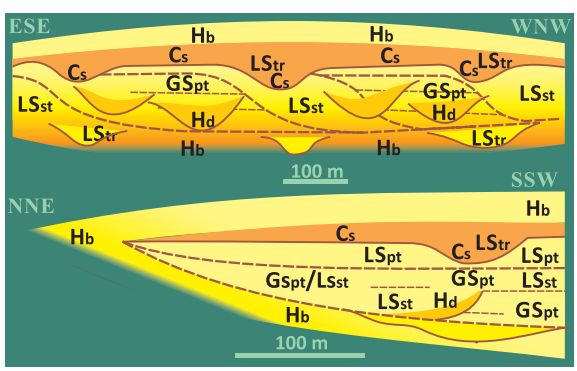

Fig. 22. Facies architecture inside the sandstone lithosomes of the Table Mountains (Wojewoda 1986, 1997).

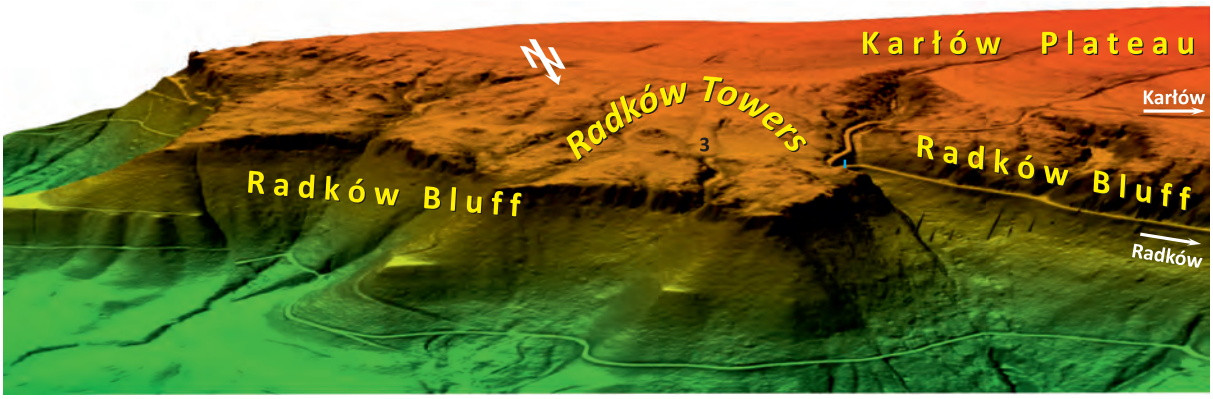

Fig. 23. Radków Towers (Radków Bluff).

BLS$_{pt-tr}$. The shape and spatial interrelations of the facies units in this part of the Radków Bluff exhibit a typical image of the Radków Bluff Sandstone internal architecture (Figs 21A, 22).

Genesis: Sand-gravely deposit redistribution as mass-flow runoff within the nearshore sedimentary system.

Stop 3:

Radków Bluff, Table Mountains National Park, Stroczy Zakręt (English *Stroczy Turn*), close to the Radków–Karłów route (Fig. 1); 50° 28' 50'' N, 16° 23' 47'' E; sandstone bluff up to 40 m high, marking the northern limit of the Table Mountains. (*Jurand Wojewoda, Dominik Sokalski*)

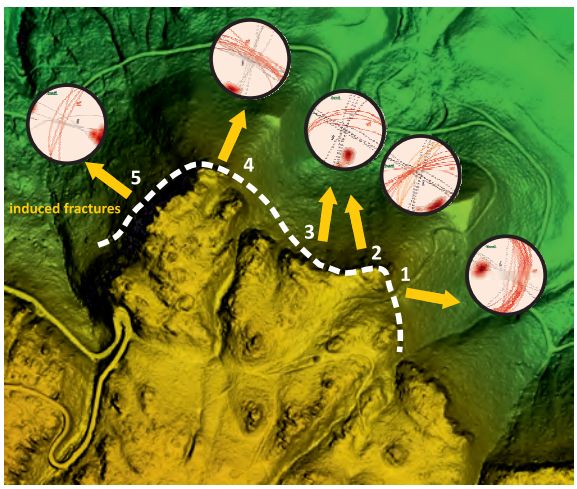

Fig. 24. The orientation of induced fractures at the base of the Radków Bluff, at the Radków Towers locality (modified after Sokalski et al. 2020).

Structure and stratigraphy: Intra-Sudetic Synclinorium, Intra-Sudetic Basin; Radków Bluff Sandstone (middle Turonian, *Inoceramus lamarcki* Zone) of the Batorów Formation; so-called Middle Jointed Sandstone (German Mittel Quadersandstein).

Subject: Induced fracturing near the base of rocky bluffs; physical mechanism of bluff destruction.

At the foot of the escarpment under the Radków Towers, at the end of the rock headland, we can see characteristic damage in the sandstone of the Radków Bluff (Fig. 23). These recently discovered and described fractures show how the basal rock breaks down when it is isolated from the rest of the rock massif. This dense fracture network is created under the pressure of hundreds of tons of weight, illustrating how a block of rock, isolated from the main massif, destroys its own base. These cracks are considered non-tectonic induced fractures (cf. Fig. 21). Their spatial orientation almost exactly aligns with the outline of the rock headland of the Radków Towers (Fig. 24) (Wojewoda and Kowalski 2017, 2018**;** Sokalski et al. 2020).

Genesis: An example of how damage caused by load arises and evolves at the base of high morphological escarpments, mainly within rock blocks separated from the main rock massif.

Stop 4:

Hanging Wall, Table Mountains National Park, Lisia Przełęcz (English *Fox Pass*), close to the Karłów–Kudowa route (Figs 1, 25A, B); 50° 27'

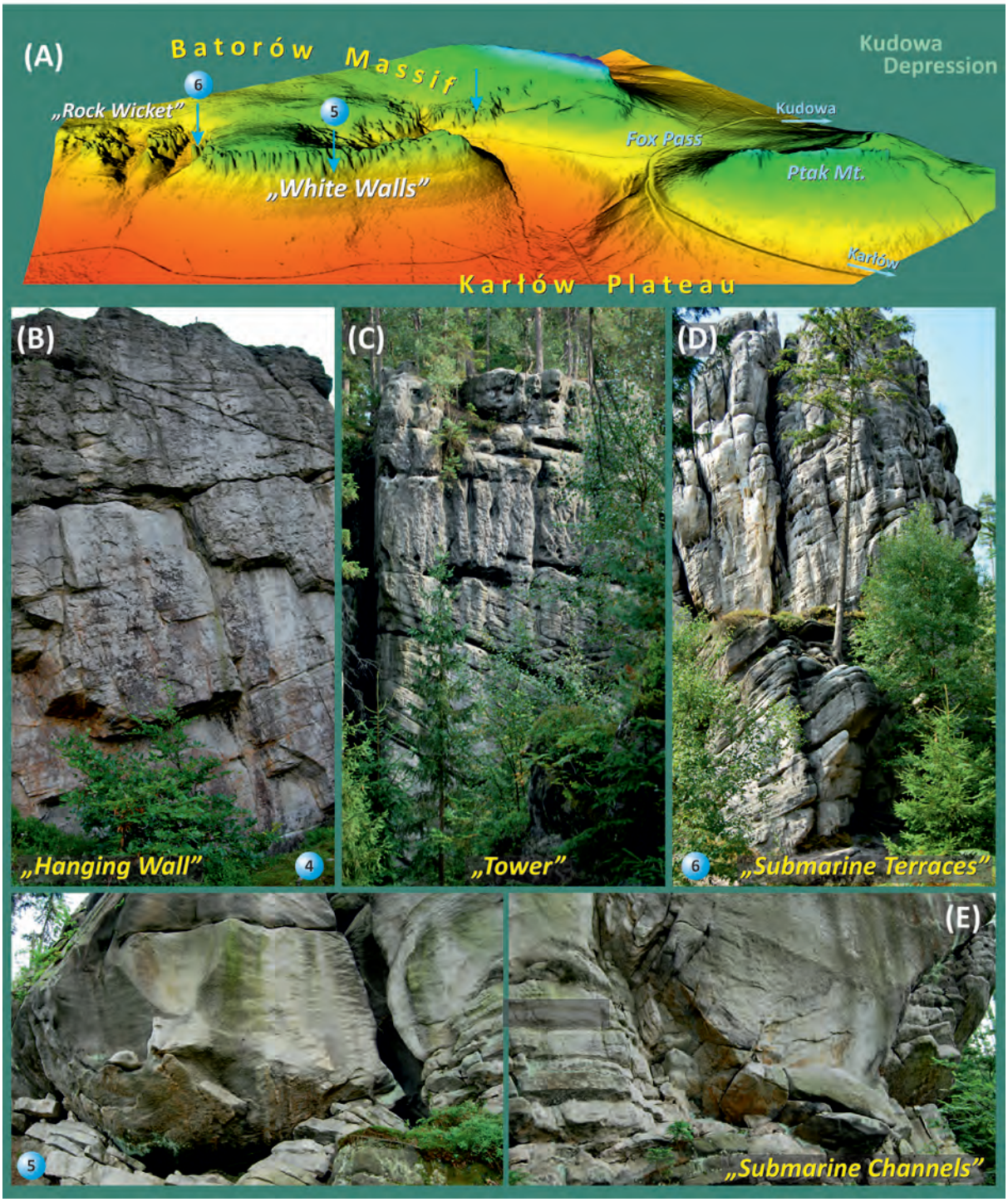

Fig. 25. "White Walls" (the main range of the Table Mountains) with known geosites documenting the unique shallow-sea sedimentation processes during the late Turonian in the Central Sudetes, as well as post-deposition processes in the Szczeliniec Skalniak Sandstone Member (Wojewoda 1986, 1997, 2020; Jerzykiewicz and Wojewoda 1986).

35'' N, 16° 21' 00'' E; sandstone bluff up to 25 m high; main range of the Table Mountains. (*Jurand Wojewoda*)

Structure and stratigraphy: Intra-Sudetic Synclinorium, Intra-Sudetic Cretaceous Basin; Szczeliniec–Skalniak Sandstone Member (up-

per Turonian–?lower Coniacian) of the Karłów Formation; so-called Upper Jointed Sandstone (German Ober Quadersandstein).

Subject: Seismo-tectonically induced structures (gas escape structures, soft sediment shears); ichnofossils (*Monocraterion*, *Ophiomorpha*); accumulation terrace slope deposits (**GS_{pt}** and **LS_{st}** facies).

In both the Szczeliniec and Batorów Massifs, there are characteristic, almost perfectly spherical weathering caverns up to 2 m in diameter in the Szczeliniec–Skalniak Sandstone (cf. Figs 14, 25B). Dumanowski (1961) suggested the caverns formed as a result of the local washing out of material off of less- or non-cemented rocks. He believed that these poorly, or uncemented, zones were saturated with gas (methane) during diagenesis. There is a clear relationship between the spatial distribution of caverns and regional fault zones – for instance, with the **Czerwona Woda Fault** or **Szczeliniec Fault**, both fragments of the **Poříčí-Hronov Fault Zone** (cf. Fig. 1) (Wojewoda 2007).

The caverns are spherical, which shows that the gas accumulated in loose sediment saturated with seawater when the diagenetic conversion of sand to sandstone began. It is only in such circumstances that water saturated with methane accumulates into spherical forms, due to the surface tension at the boundary of solutions with different densities and viscosities. However, this does not determine the genesis of the gas itself, which could have penetrated marine sediments both from below, through a conductive zone, and/or by progressive concentration from the dispersed phase in the sediment mass. This is confirmed by gas escape channels closely related to caverns (Wojewoda 1987, 1997) (cf. Fig. 14). The degassing processes were sudden, even explosive, and most likely caused by seismic events.

There are numerous other phenomena occurring in these sandstones, including seismites and seismotectonites. When seismic events occured in loose sediment, where individual grains or sediment fragments could still move under the influence of pressure or shocks, various types of damage resulted (e.g., shear surfaces, liquefaction, and autobrecciation) (Wojewoda 1987, 1997, 2011).

Genesis: An example of seismically generated phenomena documenting the influence of methane (?) on the diagenesis of sandy deposits and synsedimentary geodynamic activity during deposition.

Stop 5:

Submarine Channels, Table Mountains National Park, Białe Ściany, (English *White Walls*), close to the Karłów–Kudowa route (Figs 1, 25A, E); 50° 27' 40'' N, 16° 21' 35'' E; sandstone bluff up to 30 m high; main range of the Table Mountains. (*Jurand Wojewoda*)

Structure and stratigraphy: Intra-Sudetic Synclinorium, Intra-Sudetic Cretaceous Basin; Szczeliniec–Skalniak Sandstone Member (upper Turonian–?lower Coniacian) of the Karłów Formation; so-called Upper Jointed Sandstone (German Ober Quadersandstein).

Subject: Shoreface-to-shelf distributary channels; homogenized mass-flow deposits and slump scour; soft sediment shears; compaction indicators (**GS_{pt}**, **LS_{st}**, **LS_{tr}**, and **H_d** facies).

The lands surrounding the Intra-Sudetic Cretaceous Basin were denuded and eroding for nearly 10 million years. In the Coniacian, the coasts were almost flat and slightly sloping, and the shoreface areas were shallow and covered with sandy embankments. Accumulation terraces were constantly eroded by waves and currents (e.g., facies **LS_{pt-tr}**). Under such conditions, stronger winds pushed up water onto the shore, flooding large parts of the adjacent lands. After each storm, the water flowed back through channels, including underwater ones, carrying sand from the coast far beyond the seashore to the nearshore and shelf areas. The channels were sinuous, indicating very slightly sloping surfaces. This is shown by the asymmetric cross-section of the distributary channel in this stop; one slope is convex, and the other is concave (Figs 12, 25E).

The shelf of the **Intra-Sudetic Cretaceous Basin** was diversified. Apart from channels, it featured, among other attributes, sand waves (**LS_{pt}** and **LS_{st}** facies), the height of which exceeded 5 m; active faults produced escarpments of even greater heights. These submarine "bluffs" were filled up (accumulation terraces, **GS_{pt}** and **LS_{st}** facies), but often their slopes lost stability; the accumulated sediment moved down through submarine landslides, forming mass run-offs (**H_d** facies). The mate-

rial moving in the landslide/flow was homogenized. New sedimentary structures emerged, caused by the dewatering of the liquefied sand (e.g., water escape dish structures). The liquefied material flowed along a characteristic, symmetrical landslide scour (Figs 12, 25E). The sub-aqeuous stream of fluidized sand was not uniform; the highest flow velocity was in the center of the stream. Towards the limits of the stream, the flow velocity decreased until motion completely ceased in the material surrounding the **H_{st}** facies. The differences in suspension velocity resulted in the formation of co-shaped and circular shear surfaces at the margins of the stream. Away from the axis of the landslide niche, the material around it was less homogenized and more clearly retained its primary structure: in this case, the large-scale trough bedding (**LS_{tr}** facies) is typical of infill within the neighboring distributary channel, which was partially destroyed by a subaqueous mass flow.

Stop 6:

Submarine Terraces, Table Mountains National Park, Lisia Przełęcz (English *Fox Pass*), *Skalna Furta* (Engilsh *Rock Wicket*), close to the Karłów–Kudowa route (Figs 1, 25A, D); 50° 27' 30'' N, 16° 21' 45'' E; sandstone bluff up to 30 m high; main range of the Table Mountains. (*Jurand Wojewoda*)

Structure and stratigaphy: Intra-Sudetic Synclinorium, Intra-Sudetic Cretaceous Basin; Szczeliniec–Skalniak Sandstone Member (upper Turonian–?lower Coniacian) of the Karłów Formation; so-called Upper Jointed Sandstone (German Ober Quadersandstein).

Subject: Accumulation terrace facies; geometry and climbing of various size bedforms; rate of progradation (**GS_{pt}** and **LS_{st}** facies).

In the Turonian to Coniacian, the Sudetes were particularly active geodynamically. This activity manifests most clearly in the alternating occurrence of fine-grained sediments (open sea) and sand clinoforms, which formed under constant regressive conditions, interrupted by episodes of basin deepening (subsidence) (cf. Figs 7, 8). It can be assumed with near certainty that the deepening periods were sudden, short-lived, and geodynamic in nature. It can also be assumed with a great degree of confidence that the tectonic displacements of the basin bottom were localized (fault zones) and did not cover the entire basin.

It was during this period that the characteristic subaqueous bedforms – accumulation terraces (Fig. 11) – were created on the searfloor. These forms were identified and named by Jerzykiewicz and Wojewoda (1986), and then described and interpreted in great detail by Wojewoda (1986, 1997). The impulse for the development of accumulation terraces were the tectonically generated escarpments/slopes that formed north of the present-day Radków Bluff and south of the Czerwona Woda Creek tectonic fault (Wojewoda, 2020) (cf. Fig. 11). The slopes, with a zig-zag course, were buried by sediments supplied from the shore, and thus accumulation terraces formed over time with specific zones – scarp foot, scarp slope, and scarp cap – where different sedimentary processes occurred, and different sediment associations formed (cf. Fig 11). Today we can observe this differentiation in the stratigraphic record, especially in the tripartite profile characteristic of the sandstone lithosomes in the Table Mountains. The lower part of the Skalniak–Szczeliniec Sandstone lithosome profile, corresponding to the scarp foot zone, is composed of highly bioturbated calcareous sandstones with glauconite (mostly **LS_{tr-pt}** facies). The central part of the profile consists of cosets predominantly constructed of the **GS_{pt}**, **LS_{st}** and **H_d** facies. The first two facies formed on more and less inclined slopes, respectively; the third represents redeposited sediment in the form of underwater landslides or mass flows (cf. Fig. 12). At this point, it is worth emphasizing that the **GS_{pt}** facies are remarkably unique. Layered units on this scale (sets up to 18 m thick!) are extremely rare and usually associated with aeolian dune environments. Subaqueous sediments of this type are well-documented only in the Table Mountains, northwest Czechia, Saxony, and 3 other places in the entire world. The upper part of the sandstone lithosome profile is made up of various sediments, previously discussed as nearshore sediments. In this part of the succession, the association of large-scale bedded sandstone facies with conglomeratic and coquinoid sandstones (storm lags (**C_s** facies)) and rip current channel infills (**LS_{tr}** facies) is characteristic (Wojewoda 1986, 1997, 2011).

Stop 7:

Długopole Górne Quarry, close to the Bystrzyca Kłodzka–Międzylesie route (Fig. 1); 50° 13' 42.8'' N, 16° 38' 11.7'' E; individual walls up to 12 metres high. (*Alina Chrząstek and Jurand Wojewoda*)

Structure and stratigraphy: Nysa Kłodzka Trough, Idzików rhomboidal brachysyncline; Sandstone of the middle Turonian (*Inoceramus lamarcki* Zone); so-called Middle Jointed Sandstone (German Mittel Quadersandstein).

Subject: Accumulation terraces; sedimentary and ichnological complex.

The middle Turonian deposits exposed in Długopole Górne Quarry are fine to coarse-grained sandstones with gravel intercalations. They represent the *Quadersandstein* megafacies (see Chrząstek 2013), which appears three times in the Nysa Kłodzka Trough succession: in the Cenomanian, the middle Turonian, and the upper Turonian (Fig. 5). The middle Turonian sandstones are 45 m thick in the vicinity of Bystrzyca Kłodzka, and reach 110 m in the northern and northwestern parts of the Nysa Kłodzka Trough (cf. Chrząstek and Nowicka 2021 and references therein). They pinch out towards the south and southeast (see Chrząstek 2013) and are 70 m thick near Długopole Górne (see also Wroński 1982). The

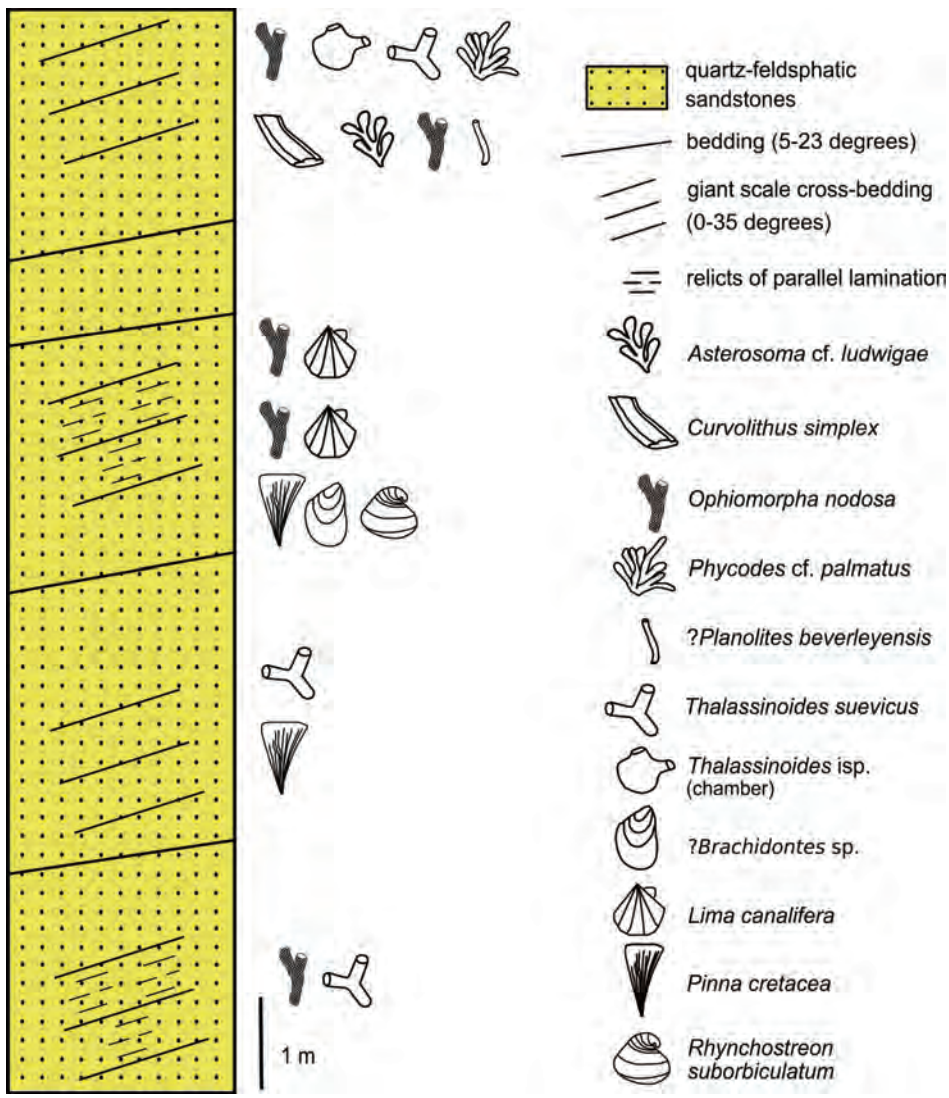

Fig. 26. Lithological section of the middle Turonian sandstones in Długopole Górne Quarry indicating trace fossil distribution (Chrząstek and Nowicka 2021). Bedding and giant scale cross-stratification according to Don and Wojewoda (2004).

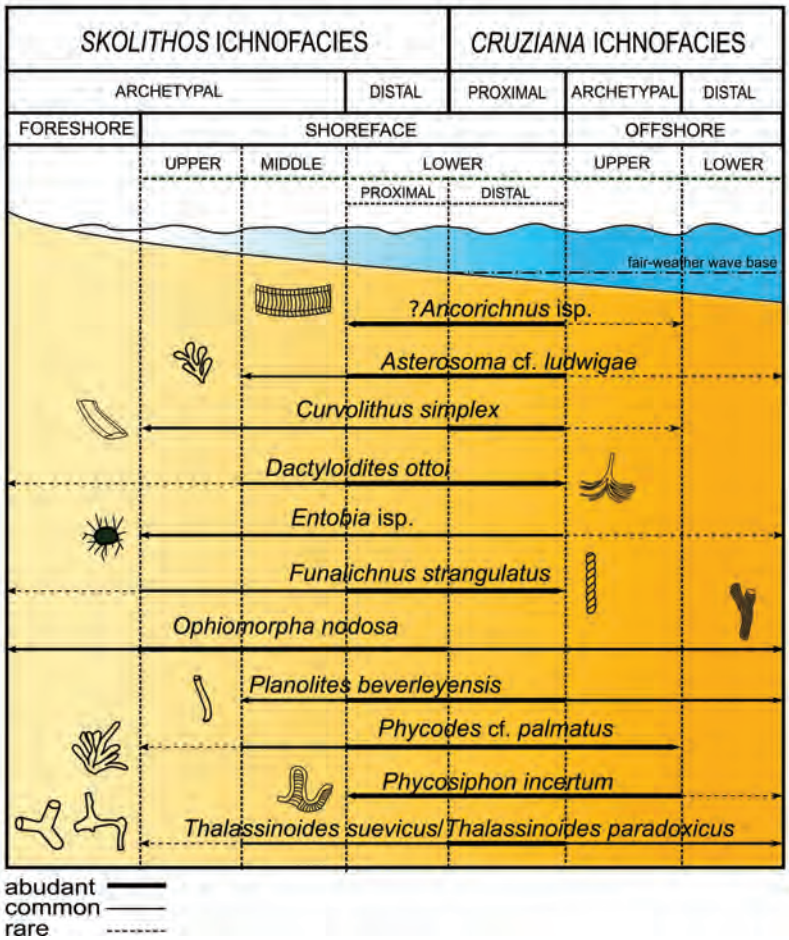

Fig. 27. Environmental distribution of the trace fossil assemblage reported in the middle Turonian sandstones of Długopole Górne Quarry (cf. Chrząstek and Nowicka 2021).

middle Turonian sandstones exposed in the Długopole Górne Quarry represent the middle Turonian *Inoceramus lamarcki* Zone (cf. Chrząstek 2013 and references therein).

The individual beds are 0.5–3.0 m thick, lie almost horizontally (5–23°), and show giant-scale cross-bedding (210–230°) (Don and Wojewoda 2004). They are classified as quartzose-feldspathic sandstones (subarkosic arenite and quartz arenite, cf. Chrząstek 2013 and references therein). The sedimentological structures, including parallel lamination, are poorly visible; these sandstones are mainly structureless. In the lower and middle parts of the Długopole Górne section, the sandstones are yellow-grey; they are dark grey in the uppermost part. They seem to capture a coarsening-upward trend (cf. Chrząstek and Nowicka 2021). Don and Wojewoda (2004) reported the trace fossil *Ophiomorpha*, and the bivalve *Exogyra columba* (now *Rhynchostreon*). A moderately diverse trace fossil assemblage and bivalve body fossils – e.g. ?*Brachidontes* sp., *Lima canalifera*, *Pinna cretacea* (Schlotheim, 1813), and *Rhynchostreon suborbiculatum* (Lamarck, 1801; Figs 26–28) – were recognized by Chrząstek (2013) and Chrząstek and Nowicka (2021). In the Geological Museum of the University of Wrocław, the collections include the bivalve *Lima canalifera* Goldfuss, 1836 (MGUWr-1499s) and rhynchonellids (MGUWr-1883s; compare Chrząstek 2013). The presence of the oyster *Rhynchostreon suborbiculatum* in these deposits is suggestive of a Tethyan influence (cf. Chrząstek and Nowicka 2021).

The recognized trace fossil assemblage comprises abundant burrows: *Ophiomorpha nodosa*, *Ophiomorpha* isp., *Thalassinoides sue-*

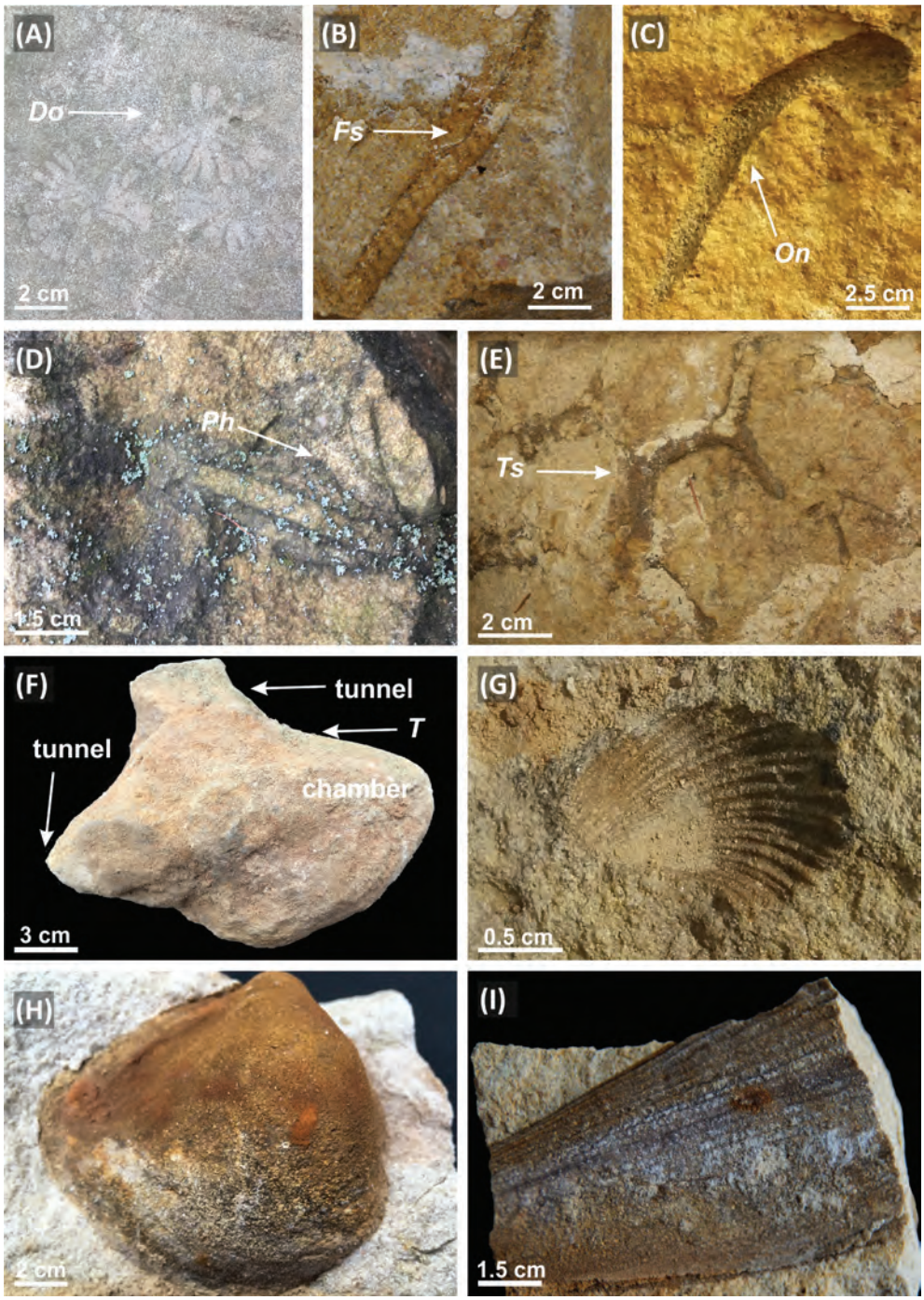

Fig. 28. Trace and body fossils (bivalves) from the middle Turonian sandstones, Długopole Górne Quarry; cf. Chrząstek and Nowicka (2021). Abbreviations: *Do* – *Dactyloidites ottoi*, *Fs* – *Funalichnus strangulatus*, *On* – *Ophiomorpha nodosa*, *Ph* – *Phycodes* cf. *palmatus*, *Ts* – *Thalassinoides suevicus*, *T* – *Thalassinoides* isp. A. *Dactyloidites ottoi*. B. *Funalichnus strangulatus*. C. *Ophiomorpha nodosa*. D. *Phycodes* cf. *palmatus*. E. *Thalassinoides suevicus*. F. *Thalassonides* isp. chamber. G. *Lima canalifera*. H. *Rhynchostreon suborbiculatum*. I. *Pinna cretacea*.

vicus, *Thalassinoides* isp., *Dactyloidites ottoi*, and less commonly *Thalassinoides* cf. *paradoxicus*, ?*Ancorichnus* isp., *Asterosoma* cf. *ludwigae*, *Asterosoma* isp., *Curvolithus simplex*, *Funalichnus strangulatus*, ?*Macaronichnus* isp., *Palaeophycus tubularis*, *Phycodes* cf. *pal-*

matus, cf. *Phycodes*, *Phycosiphon incertum*, ?*Phycosiphon* isp., *Planolites beverleyensis*, and *Entobia* isp. borings (Fig. 26). In the lower part of the succession, *Thalassinoides suevicus* and *Ophiomorpha nodosa* prevail (cf. Chrząstek and Nowicka 2021; Fig 26). In the middle, *Ophiomorpha nodosa* appears (mostly as vertical shafts), together with the bivalves ?*Brachidontes* sp., *Lima canalifera* (Fig. 28G), *Pinna cretacea* (Fig. 28I) and *Rhynchostreon suborbiculatum* (Fig. 28H; Chrząstek and Nowicka 2021). In the upper part of the section, rare *Asterosoma* cf. *ludwigae*, *Curvolithus simplex*, and *Planolites beverleyensis* occur, together with abundant *Ophiomorpha nodosa* (Fig. 28C), ?*Ophiomorpha* isp., *Thalassinoides suevicus* (Fig. 28E) and ?*Thalassinoides* isp. The uppermost part of the succession yielded *Ophiomorpha nodosa*, *Phycodes* cf. *palmatus*, and a large swollen chamber of *Thalassinoides* with tunnels up to 30 cm long (Fig. 28F). Some findings – for instance, *Funalichnus* (Fig. 28B) and *Dactyloidites* (Fig. 28A) – are very rare and/or were described for the first time from the Nysa Kłodzka Trough. These taxa have considerable palaeoenvironmental significance (compare Pemberton et al. 2012). *Dactyloidites ottoi* is a relatively rare form, known from the (?Triassic) Jurassic to Neogene, and usually occurs in shallow-water, nutrient-rich siliciclastic settings, usually between fair-weather and storm wave base (Wilmsen and Niebuhr 2014; Fig. 27). The present record of *Funalichnus strangulatus*, as recently reviewed by Pokorný (2008), is the first report of this taxon from Poland (Chrząstek and Nowicka 2021). This ichnotaxon is known from the upper Cenomanian and the middle–upper Turonian of the Czech Republic (Bohemian Cretaceous Basin, see Pokorný 2008) and Germany (Saxonian and Danubian Basins, see Wilmsen and Niebuhr 2014). The presence of other ichnotaxa – e.g., *Phycodes* (Fig. 28D), *Phycosiphon*, and *Thalassinoides* – constructed by deposit-feeders also suggests sedimentation near fair-weather wave base (Fig. 27). This moderately diverse trace fossil assemblage, representing several ethological categories – domichnia, fodinichnia, repichnia, and pascichnia – indicates a distal *Skolithos* ichnofacies and a proximal *Cruziana* ichnofacies, which characterize proximal and distal lower shoreface settings, respectively (Chrząstek 2013; Chrząstek and Nowicka 2021).

Genesis: The middle Turonian sandstones were deposited in a shallow epicontinental, well-oxygenated, soft-ground, occasionally nutrient-rich basin with normal salinity under low-moderate hydrodynamic conditions, intermittently interrupted by more energetic conditions probably associated with more common or abundant sand supplies. These middle Turonian sandstones might be a part of a giant-scale cross-bedding accumulation terrace (Jerzykiewicz and Wojewoda 1986; Wojewoda 1997; Chrząstek and Nowicka 2021; Fig. 11).

Stop 8:

Stary Waliszów Quarry, at the Bystrzyca Kłodzka–Lądek Zdrój road (Fig. 1); 50° 18' 36.6'' N, 16° 42' 11.2'' E; individual quarry walls are up to 9 m high. (*Alina Chrząstek*)

Structure and stratigraphy: Upper Nysa Kłodzka Trough, Idzików Brachysyncline; middle Coniacian Idzików Lower Beds (*Platyceramus* ex gr. *mantelli* + *Volviceramus koeneni* Zone) (cf. Walaszczyk 2000); *Volvicermaus koeneni*–*Volviceramus involutus* Zone (cf. Walaszczyk and Cobban 2006).

Subject: Middle Coniacian sandstones and mudstones of the Idzików Lower Beds.

The **Idzików Lower Beds**, which crop out in the Stary Waliszów Quarry, consist of calcareous claystones, mudstones, and sandstones (Fig. 29). The total thickness of the member ranges from 450 to 600 m (Wojewoda 1997; Fig. 5). Sandstone intercalations are more common and thicker in the upper part of the unit (see Wojewoda 1997). In Stary Waliszów, the section comprises the uppermost Idzików Lower Beds (compare Raczyński 1997). A complete succession is preserved in the southern part of the Nysa Kłodzka Trough near Międzylesie (cf. Jerzykiewicz 1971). Fossil-bearing calcareous-ferruginous concretions (up to 30 cm in diameter; Jerzykiewicz 1971; Radwański 1966; Don and Gotowała 2008; Trzęsiok et al. 2014), some with well preserved crustaceans (Fig. 30K), are known from the quarry.

The trace fossil assemblage found in the quarry comprises *Arachnostega gastrochaenae* (Fig. 30D), *Archaeonassa fossulata* (Fig. 30E), *Chondrites* isp., *Ophiomorpha nodosa* (Fig. 30C), *Ophiomorpha* isp., *Planolites*-like traces, *Sinusichnus sinuosus* (Fig. 30B), ?*Sinu-*

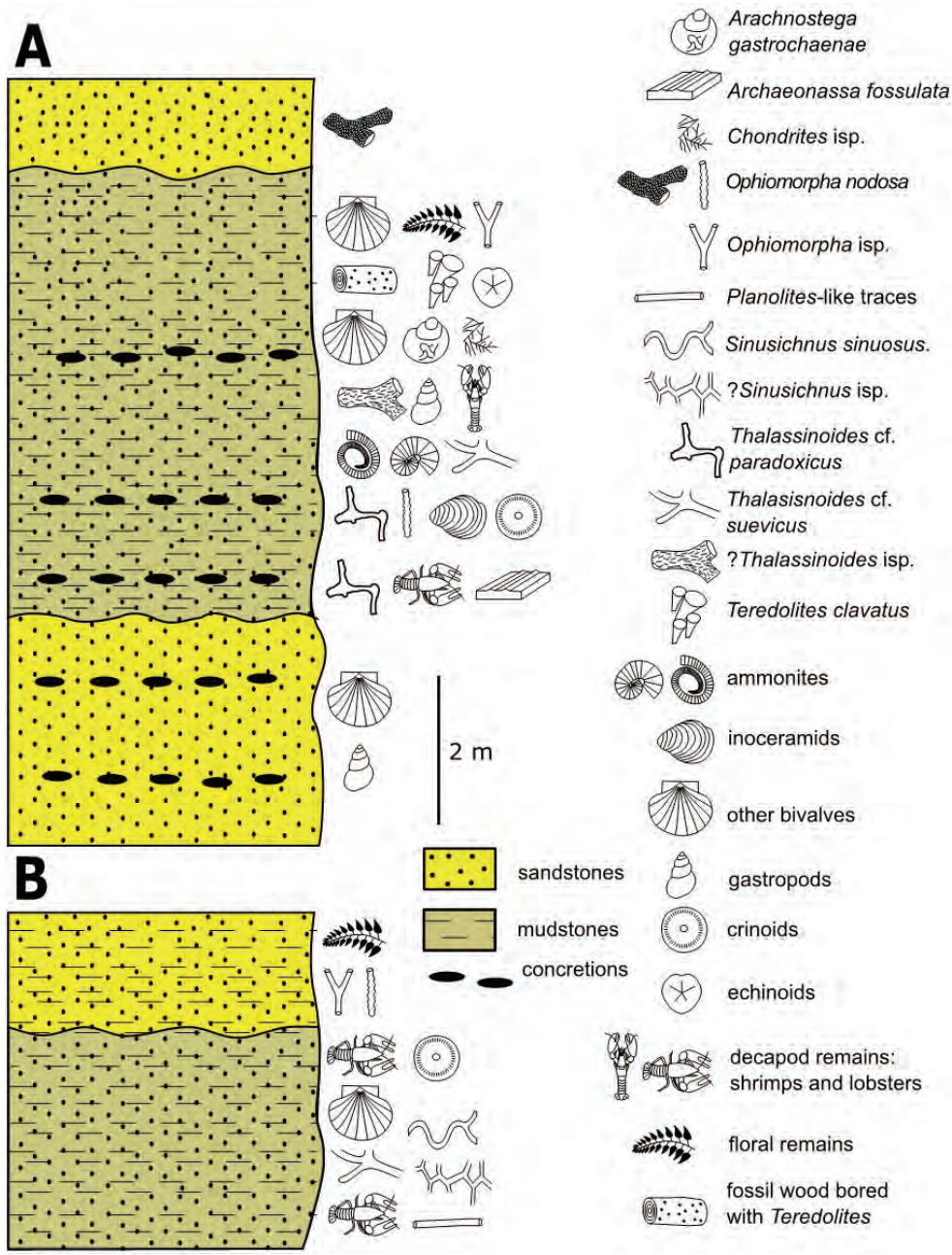

Fig. 29. Lithological section of the Idzików Lower Beds in the Stary Waliszów Quarry, with trace fossils indicated; cf. Chrząstek (in prep.).

sichnus isp., *Thalassinoides* cf. *paradoxicus* (Fig. 30A), *T. suevicus*, ?*Thalassinoides* isp., and *Teredolites clavatus* bivalve wood borings (Fig. 30F). Additionally, the section yielded a rich body fossil assemblage: mollusks (bivalves, gastropods, ammonites), echinoderms (crinoids, echinoids), and crustaceans (lobsters *Haploparia*, shrimps; Fig. 30L). Reported inoceramids (*Volviceramus involutus*, Fig. 30G, and *Platyceramus* ex gr. *mantelli*, Fig. 30H), place the section in the middle–lower upper Coniacian (Chrząstek in preparation). According to Walaszczyk and Cobban (2006), the first appearance of the *Volviceramus–Platyceramus* assemblage marks the base of the middle Coniacian. The Coniacian age assignment is also supported by plants from the Idzików Lower Beds and Idzików Upper Beds

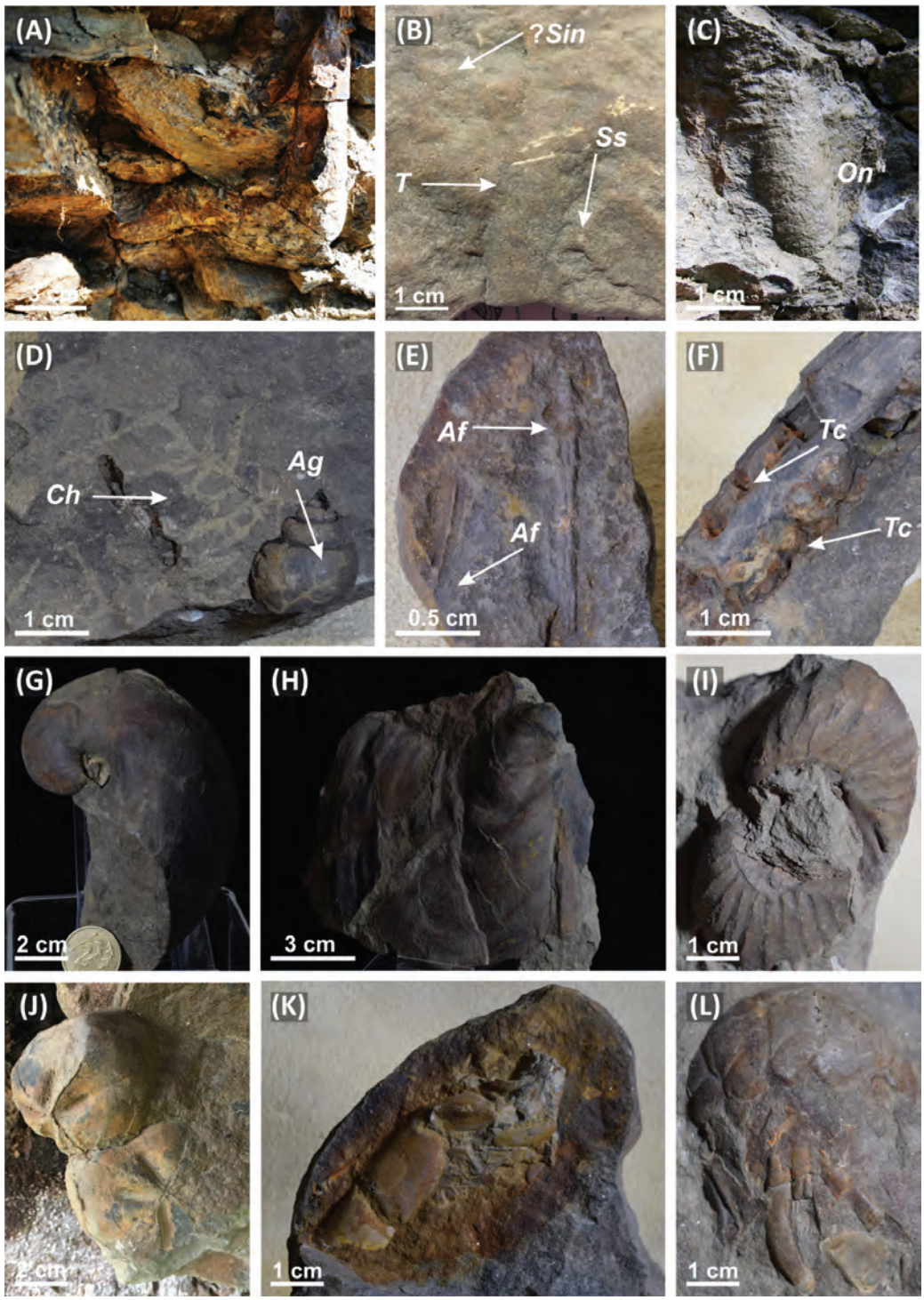

Fig. 30. Trace and body fossils from the middle Coniacian sandstones and mudstones, Stary Waliszów Quarry (Idzików Lower Beds); cf. Chrząstek (in prep.). Abbreviations explained in Figure 28, and additionally: *Ss* – *Sinusichnus sinuosus*, ?*Sin* – ?*Sinusichnus* isp., *Ag* – *Arachnostega gastrochaenae*, *Ch* – *Chondrites* isp., *Af* – *Archaeonassa fossulata*, *Tc* – *Teredolites clavatus*. A. *Thalassinoides* cf. *paradoxicus*. B. *Sinusichnus sinuosus*, ?*Sinusichnus* isp., *Thalassinoides* isp. C. *Ophiomorpha nodosa*. D. *Arachnostega gastrochaenae*, *Chondrites* isp. E. *Archaeonassa fossulata*. F. Bivalve borings *Teredolites clavatus*. G. Inoceramid *Volviceramus involutus*. H. Inoceramid *Platyceramus* ex gr. *mantelli*. I. Bivalves *Trigonia* sp. J. Echinoids ?*Cardiaster* sp. K. Crustacean, probably shrimp ?*Protoccalianassa antiqua* in a siderite concretion. L. Lobster *Haploparia* sp. D–I, K, and L found and photographed by Ireneusz Wójcicki; A found and photographed by Rafał Sołtczerski.

(Kvaček et al. 2015). The Idzików Conglomerate Member is particularly rich in megaflora, yielding common *Dryophyllum geinitzianum* Goeppert, 1848 and *Laurophyllum* sp. (cf. Halamski 2013; Halamski et al. 2020). *Geinitzia reichenbachii* (Geinitz, 1842) Hollick and Jeffrey, 1909, a gymnosperm species, is only known from the Stary Waliszów Quarry (cf. Kvaček et al. 2015). *Geinitzia*, spanning the Turonian through Maastrichtian, was one of the most widespread Late Cretaceous conifers of tropical central European habitats (Halamski et al. 2018 and references therein).

Ichnological analysis shows the presence of a low to moderate diversity trace fossil assemblage, pointing to the distal *Skolithos* and proximal *Cruziana* ichnofacies, typical of the proximal and distal lower shoreface, respectively. The co-occurrence of fodinichnia, agrichnia, and pascichnia produced by deposit-feeders, with subordinate domichnia and equilibrichnia produced by suspension-feeders, suggest sedimentation in a lower part of the shoreface (cf. Pemberton et al. 2012). The trace fossils are filled by siderite cement (*Thalassinoides* cf. *paradoxicus*) or have ferrigenous walls (e.g., *Sinusichnus*, *Planolites*-like traces, *Thalassinoides suevicus* and borings *Teredolites*). The body fossils are well-preserved and weakly fragmented or abraded (compare Trzęsiok et al. 2014; Figs 30I, J).

Genesis: The Idzików Lower Beds were earlier interpreted as deep marine turbidites by Jerzykiewicz (1971). At present, its depositional setting is interpreted as ranging from the upper sublittoral zone (shallow turbidites, Trzęsiok et al. 2014) to a lower shoreface-offshore setting (tempestites, Wojewoda 1997; Chrząstek and Sołczerski 2016). These interpretational differences might be caused by the strong bioturbation of these deposits (cf. Trzęsiok et al. 2014).

Taphonomic studies suggest that sedimentation took place under low energy hydrodynamic conditions in a quiet environment with low sedimentation rate, without long-distance transportation. The presence of articulated bivalves (*Pinna*, *Modiola*, *Trigonia*; Fig. 30I) splayed open on bedding planes supports this interpretation and suggests rapid burial, probably by high-energy storm events (compare Chrząstek in prep.; Trzęsiok et al. 2014). Ichnological studies point to well-oxygenated, nutrient-rich environments with soft substrates near fair-weather wave base (lower shoreface). The presence of stenohaline ammonites, crinoids, and echinoids suggests normal salinity conditions. Integrated ichnological-sedimentological analysis indicates that mudstones were deposited in a low-moderate energy environment interrupted by high energy storm events, during which the sandstones accumulated. Siderite and calcareous concretions (up to 30 cm) were formed during early diagenesis, below the zone of active bioturbation (cf. Trzęsiok et al. 2014).

Stop 9:

Pasterskie Skały (English *Shepherd's Rocks*), Idzików village, close to the Waliszów–Idzików route (Fig. 1); 50° 16' 13'' N, 16° 44' 57'' E; naturally formed sharp rock ridge of the Idzików Upper Beds in the eastern part of the Nysa Kłodzka Trough, along its marginal fault. Individual quarry walls are 8–12 m high. (*Jurand Wojewoda*)

Structure and stratigraphy: Nysa Kłodzka Trough, Idzików Brachysyncline (close to the eastern marginal fault of the Nysa Kłodzka Trough); upper Coniacian (?Santonian).

Subject: Coniacian (?Santonian) conglomerates, regressive deposits of the final stage of the last late Cretaceous regression; fan delta and beach sediment complex; vertically or steeply sloping beds in an inverted stratigraphic position (Figs 16A–C, 18). Distal parts of the conglomerate lithosomes crop out in the Idzików Quarry approximately 700 m east-northeast (Stop 10).

Stop 10:

Idzików Quarry, close to the Bystrzyca Kłodzka–Lądek Zdrój route (Fig. 1); 50° 16' 45.3'' N, 16° 43' 54.7'' E; the quarry is composed of the Idzików Upper Beds and is situated in the eastern part of the Nysa Kłodzka Trough, along its marginal fault. Individual quarry walls up to 12 m high. (*Alina Chrząstek and Jurand Wojewoda*)

Structure and stratigraphy: Nysa Kłodzka Trough, Idzików Brachysyncline; upper Coniacian (?Santonian).

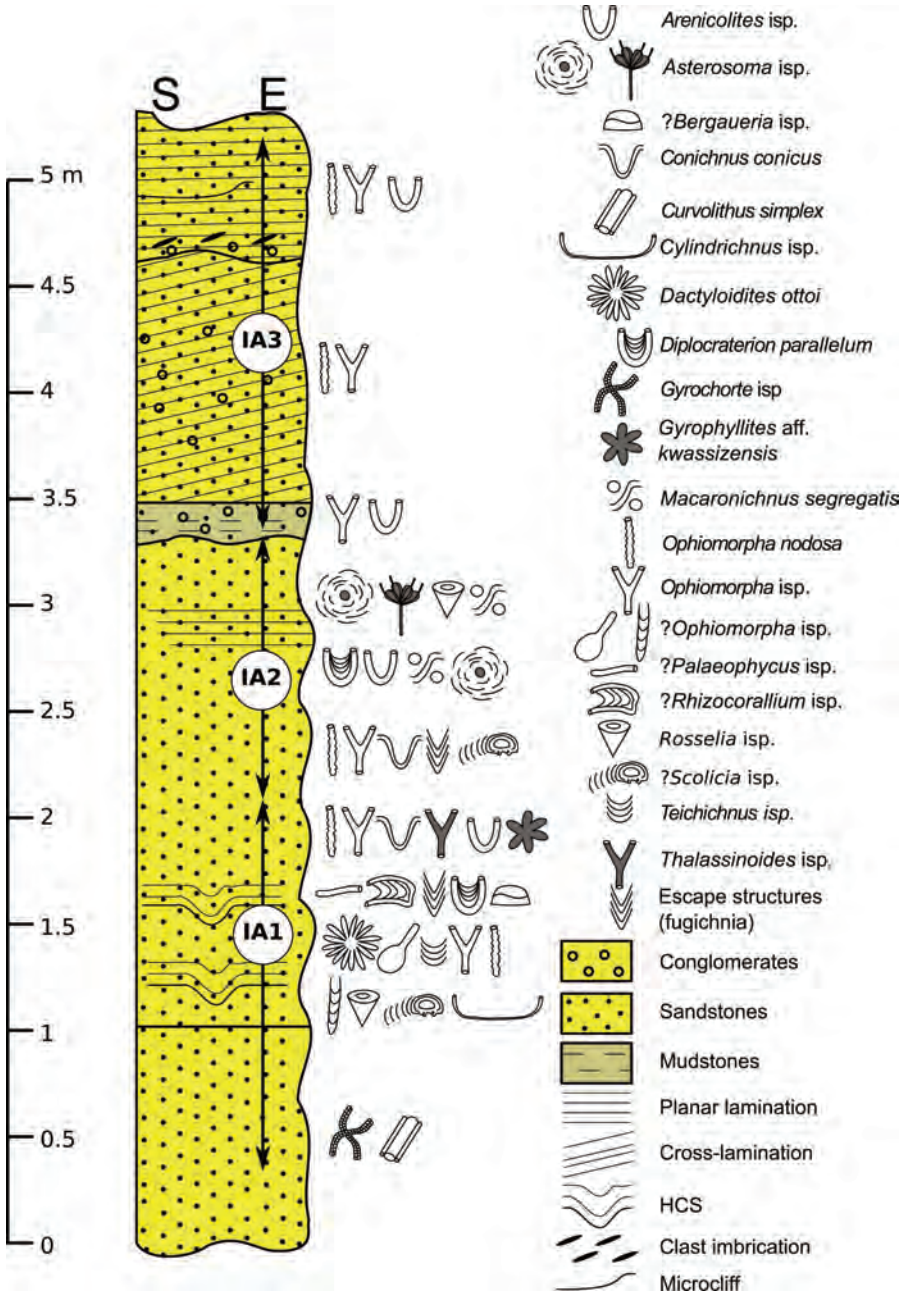

Fig. 31. Lithological section of the Idzików Upper Beds in the Idzików Quarry, with trace fossil assemblages indicated (cf. Chrząstek 2020). IA1 – ichnoassociation *Ophiomorpha–Cylindrichnus*; IA2 – ichnoassociation *Asterosoma–Conichnus*, IA3 – ichnoassociation *Ophiomorpha–Arenicolites.*

Subject: Coniacian sandstones of the Idzików Quarry, regressive deposits of the final stage of the late Cretaceous regression; shoreface to beach complex (transitional-proximal tempestites, beach and bar deposits); **Idzików Upper Beds**.

The Idzików Upper Beds sandstones and conglomerates exposed in the Nysa Kłodzka Trough are 85 m thick (Don and Gotowała 2008) (cf. Fig. 5). According to Don and Don (1960), the conglomerates rest on sandstones. In the lower part of the section, the conglomerates form intercalations, whereas in the middle and upper parts of the section, they form some levels. The studied deposits are fine- to medium-grained, and less frequently coarse-

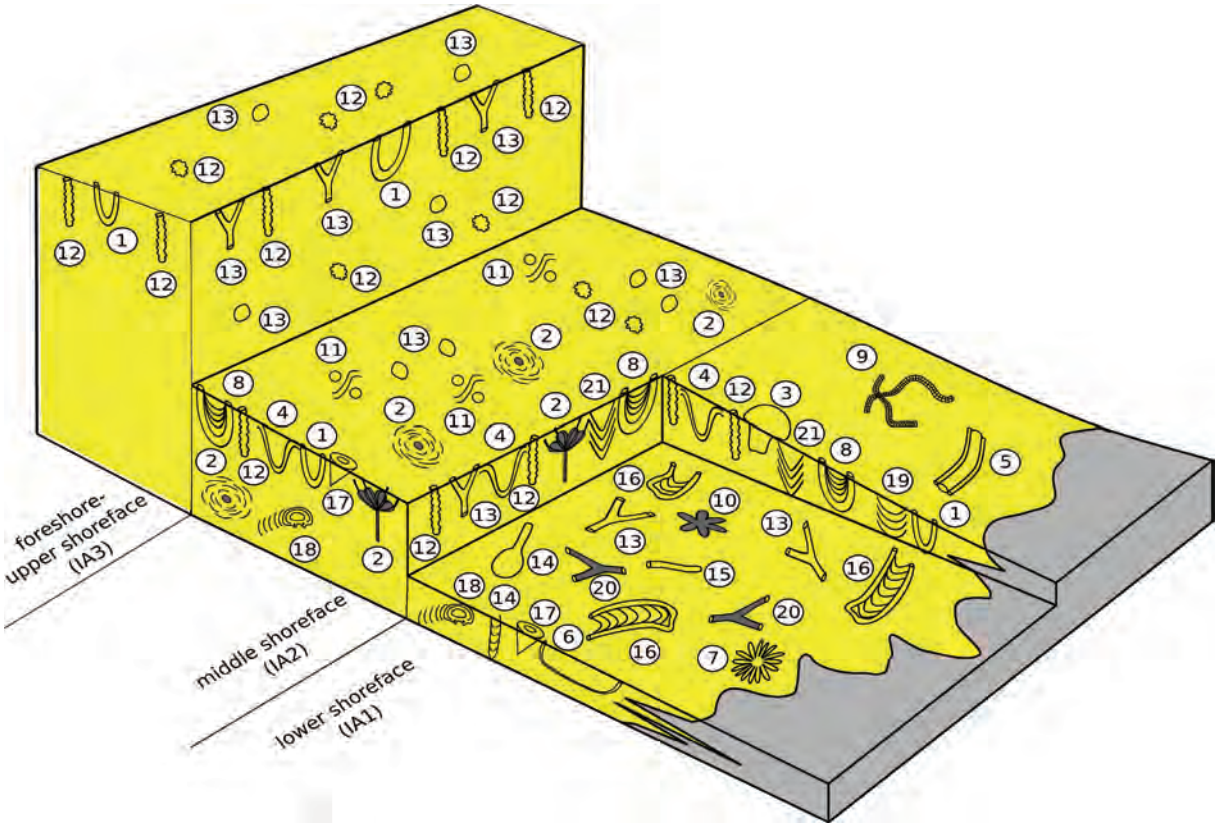

Fig. 32. Block diagram showing trace fossil distribution in ichnoassociations IA1–IA3 (cf. Chrząstek 2020 and references therein). 1 – *Arenicolites*, 2 – *Asterosoma*, 3 – ?*Bergaueria*, 4 – *Conichnus conicus*, 5 – *Curvolithus simplex*, 6 – *Cylindrichnus* isp., 7 – *Dactyloidites ottoi*, 8 – *Diplocraterion parallelum*, 9 – *Gyrochorte* isp., 10 – *Gyrophyllites* aff. *kwassizensis*, 11 – *Macaronichnus segregatis*, 12 – *Ophiomorpha nodosa*, 13 – *Ophiomorpha* isp., 14 – ?*Ophiomorpha* isp., 15 – ?*Palaeophycus*, 16 – ?*Rhizocorallium*, 17 – *Rosselia* isp., 18 – ?*Scolicia* isp., 19 – *Teichichnus*, 20 – *Thalassinoides*, 21 – fugichnia.

grained, sandstones and conglomerates. Their beds are 1–2 m thick and lie almost horizontally. The entire thickness of the succession is up to 12 m. The sandstones contain feldspars, biotite (less so muscovite), and fragments of rocks from the adjacent East Sudetic Cretaceous Island, which was the main source area at that time (cf. Chrząstek, 2020 and references therein). The Idzików Upper Beds were earlier considered Coniacian–Santonian in age (see discussion in Wojewoda 1997; Kvaček et al. 2015). Recent nannoplakton studies (Kędzierski 2002) suggest a late Coniacian age (and a middle Coniacian age for the Idzików Lower Beds).

The lower part of the quarry, built of fine- to medium-grained sandstones, is very rich in trace fossils (Fig. 31), while its upper part, built of pebbly sandstones and conglomerates, is rather poor. The following trace fossils have been found in the sandstones: ?*Arenicolites*, ?*Asterosoma* isp., ?*Bergaueria* isp., *Conichnus conicus*, *Curvolithus simplex*, *Cylindrichnus* isp., *Dactyloidites ottoi*, *Diplocraterion parallelum*, ?*Diplocraterion* isp., *Gyrochorte* isp., *Gyrophyllites* aff. *kwassizensis*, *Macaronichnus segregatis*, *Ophiomorpha nodosa*, *Ophiomorpha* isp., ?*Palaeophycus* isp., ?*Rhizocorallium* isp., *Rosselia* isp., ?*Scolicia* isp., *Teichichnus* isp., *Thalassinoides* isp., fugichnia, and a few unidentified burrows (Figs 32, 33). The associated sedimentary structures consist of hummocky-cross stratification and planar lamination (Chrząstek 2020 and references therein). The pebbly sandstones and conglomerates yield rare *Arenicolites* isp., more abundant *Ophiomorpha nodosa* and, additionally, cross-bedded stratification, ripple-marks, reactivation surfaces, clast imbrication, and microcliffs (Wojewoda 1997; Wojewoda and Raczyński 1997) (cf. Figs 16D–G, 17).

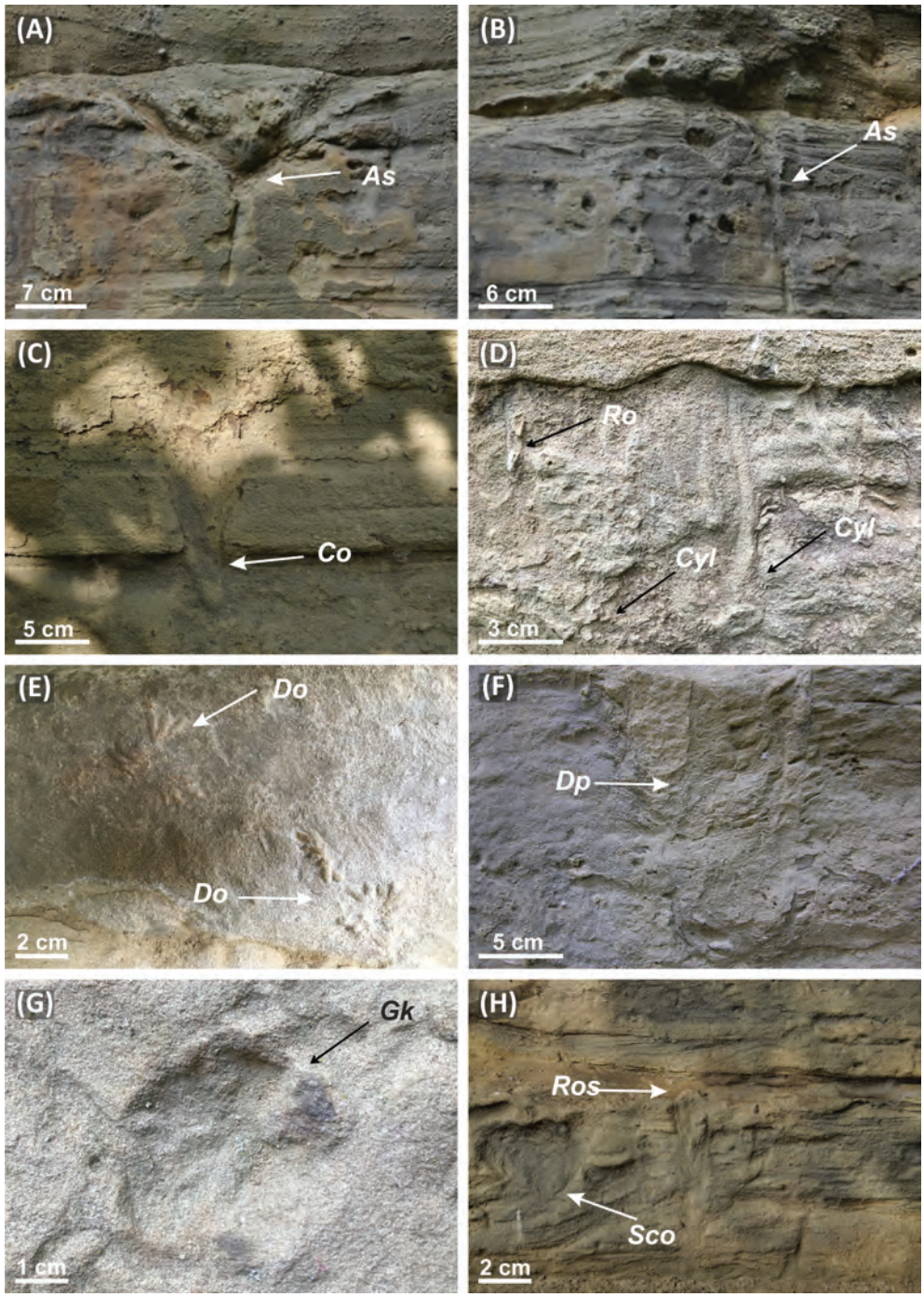

Fig. 33. Trace fossils from the middle Coniacian sandstones, Idzików Quarry (Idzików Upper Beds); cf. Chrząstek (2020). Abbreviations explained in Figs 28 and 30, and furthermore: *As* – *Asterosoma* isp., *Co* – *Conichnus conicus*, *Cyl* – *Cylindrichnus* isp., *Ros* – *Rosselia* isp., *Dp* – *Diplocraterion prallelum*, *Gk* – *Gyrophyllites* aff. *kwassizensis*, ?*Sco* – ?*Scolicia* isp. A, B. *Asterosoma* isp., whole specimens, C. *Conichnus conicus*, D. *Cylindrichnus* isp., *Rosselia* isp., E. *Dactyloidites ottoi*, F. *Diplocraterion parallelum*, G. *Gyrophyllites* aff. *kwassizensis*, H. *Rosselia* isp., *Scolicia* isp.

The moderately diverse trace fossil assemblage represents a wide spectrum of ethological categories produced by deposit-, detritus-, and suspension-feeders and scavengers (domichnia, equilibrichnia, fodinichnia, repichnia, pascichnia, and cubichnia). Detailed ichnological

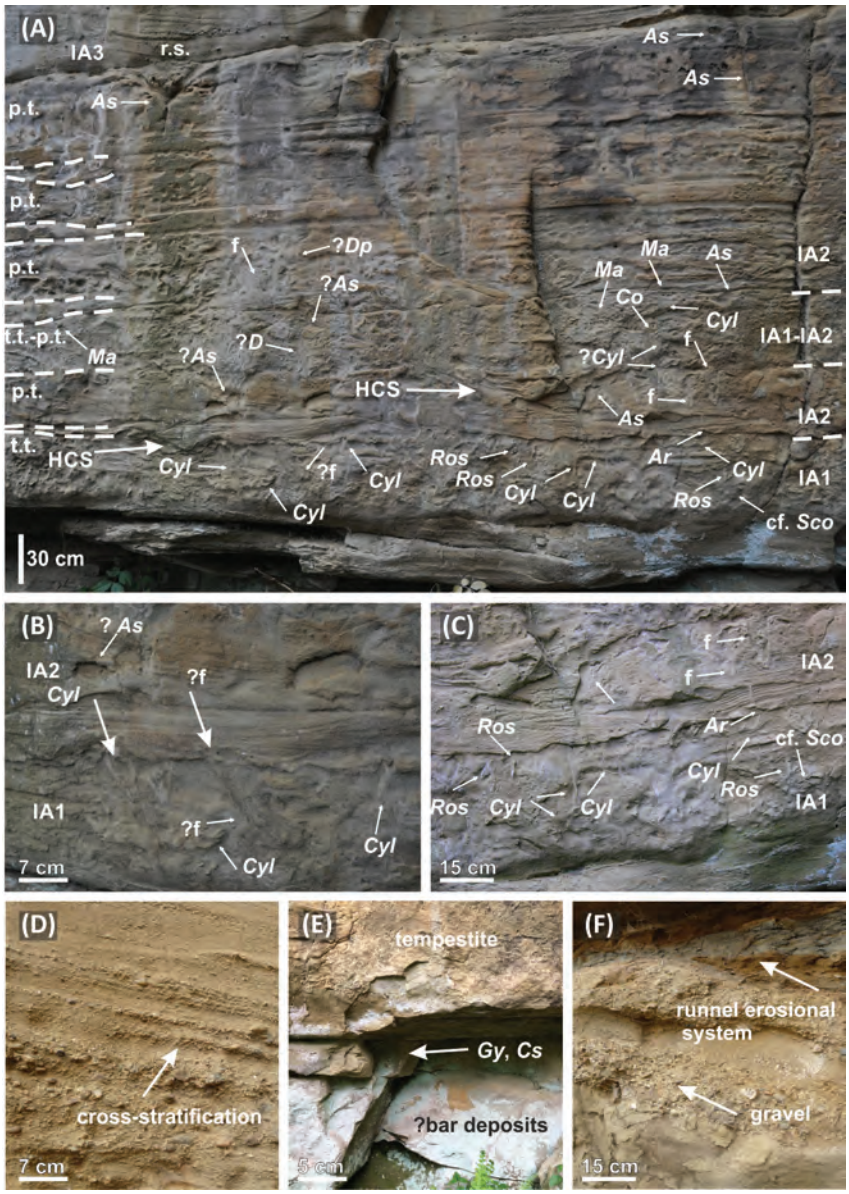

Fig. 34. Trace fossils and sedimentary structures from the Idzików Upper Beds; cf. Chrząstek (2020). Abbreviations as in Figures 28, 30, and 33, and furthermore: ?*As* – ?*Asterosoma* isp., *Ar* – *Arenicolites* isp., ?*Dp* – ?*Diplocraterion parallelum*, ?*D* – ?*Diplocraterion* isp., *Ma* – *Macaronichnus segregatis*, cf. *Sco* – cf. *Scolicia* isp., f – fugichnia, ?f – ?fugichnia, HCS – hummocky cross-stratification, r.s. – reactivation surfaces, p.t. – proximal tempestites, t.t. – transitional tempestites. A–C. Succession of tempestite beds (ichnoassociations IA1–IA2). D. Cross-stratification and reactivation surfaces (IA3). E. The lowermost part of the Idzików Quarry section, arrow marks where *Curvolithus simplex* (*Cs*) and *Gyrochorte* isp. (*Gy*) were found. F. Runnel erosional surface.

analysis of the Idzików Upper Beds indicates the presence of three trace fossils assemblages (IA1–IA3), attributable to the *Skolithos* and the impoverished proximal *Cruziana* ichnofacies (cf. Fig. 32). The IA1 (*Ophiomorpha–Cylindrichnus*) assemblage characterizes the lower shoreface, the IA2 (*Asterosoma–Conichnus*) assemblage is characteristic of the middle shoreface, and the IA3 (*Ophiomorpha–Arenicolites*) assemblage is typical of the foreshore-upper shoreface setting (see Pemberton et al. 2012).

Genesis: Based on sedimentological (hummocky cross-stratification, amalgamated beds) and ichnological evidence, the fine-grained sandstones are recognized as transi-

tional-proximal tempestites. The transitional tempestites mainly occur in the lower part of the succession, while in the middle and upper parts, proximal tempestites dominate (Fig. 34). Moreover, occasionally, transitional and proximal tempestites recur in the lower and middle parts of tempestite beds. Increased energy from the weakly storm-affected shoreface up to the moderately storm-influenced/affected shoreface is presumed (Chrząstek 2020) (cf. Fig. 32).

The coarse-grained sandstones and conglomerates from the upper part of the succession are recognized as littoral-beach and fan-delta deposits (see Wojewoda 1997; Wojewoda and Raczyński 1997). The presence of the latter is also supported by the occurrence of *Ophiomorpha*, which is regarded as the dominant trace fossil in coarse-grained fan-delta systems, and the presence of other ichnotaxa also common in fan-delta deposits, such as *Arenicolites*, *Asterosoma* (Fig. 33A, B), *Curvolithus*, *Cylindrichnus* (Fig. 33D), *Dactyloidites* (Fig. 33E), *Diplocraterion* (Fig. 33F), *Gyrophyllites* (Fig. 33G), ?*Palaeophycus*, *Rosselia* (Fig. 33H), ?*Scolicia*, *Teichichnus*, and *Thalassinoides* (Chrząstek 2020 and references therein).

Stop 11:

Krakorka Quarry, U Devìti křížů area, close to the Červený Kostelec–Úpice route (Figs 1, 35); 50° 29' 27'' N, 16° 3' 23'' E; sandstone quarry, morphological crest, c. 400 m from the parking stop. (*Jurand Wojewoda and Alina Chrząstek*)

Structure and stratigraphy: Červený Kostelec Trough; boundary between the Nachod and the Trutnov Basins (pull-apart units of the Intra-Sudetic Shear Zone) (Figs 35, 36A); Triassic Barchoviny Member, upper Cenomanian, and depositional unit between of unknown age.

Subject: Transgressive sediments; hard bottom; seismites and seismotectonics; trace fossils; transgression of the Intra-Sudetic Cretaceous Sea.

The Triassic and Cretaceous sediments occur on a morphological elevation that subdivides the **Nachod** and **Trutnov Basins**. This area, between Červený Kostelec and Úpice, is known as the "U Devìti křížù" area (Fig. 35). It represents a local structural depression – the **Červený Kostelec Trough** – which to the southwest prolongs into the **Hronov Graben** (Fig. 35). Quartz-kaolinitic sandstones are exploited in the Krákorka Quarry, displaying dense and regular-parting jointing and bedding-parallel split surfaces. Czech geologists traditionally include this area into the Trutnov Basin (cf. Holub 1972; Uličný 2004). Together with the **Mnichovo–Hradiště Basin** (Czech *Mnichovohradišská pánev*), these basins comprise a regional structural-palaeogeographical unit known as the the **Karkonosze Piedmont Basin** (Czech *podkrkonošská pánev*; cf. Tásler 1961; Holub and Tásler 1974). The Nachod Basin represents a separate structural unit with its own architecture and history (Wojewoda 2007d). All of the structural units and basins listed above occur within the Intra-Sudetic Shear Zone, which represents one of the most important tectonic structures in the post-Variscan evolution of the Sudetes (Wojewoda 2007c). The northern boundary of the zone is the **Poříčí–Hronov Fault Zone**, a distinct regional tectonic zone that bounds the Intra-Sudetic Synclinorium from the south (Wojewoda 2008b, 2009b). The **Karkonosze Piedmont Basin** and **Nachod Basin** together constitute the Intra-Sudetic Basin Suite – a set of rhombic-shaped regional structural units. The sedimentary architecture of the basins, and the structure of their boundaries and minor regional units occurring within them, indicate that they mostly represent strike-slip and principally extensional phenomena typical of pull-apart basins (Wojewoda 2007b, c, 2009a; Wojewoda et al. 2016).

Permian, Triassic, and Cretaceous strata are exposed in Krákorka Quarry (Figs 35, 36A) and its close vicinity. The basal part of the quarry, beneath the mining level, is composed of the youngest (Permian) continental deposits in the Sudetes, referred to the Bohuslavice Formation, of Thuringian age (Holub 1972). The formation consists of heterolithic, predominantly conglomeratic, lacustrine and fluvial deposits (e.g., Wojewoda and Mastalerz 1989; Wojewoda 2007c). The uppermost part of the quarry is composed of the Upper Cretaceous marine clastics of the Peruc–Koryčany Formation, dated as early and late Cenomanian (Figs 36, 37). In adjacent areas (e.g., in the Hronov Graben), the Peruc–

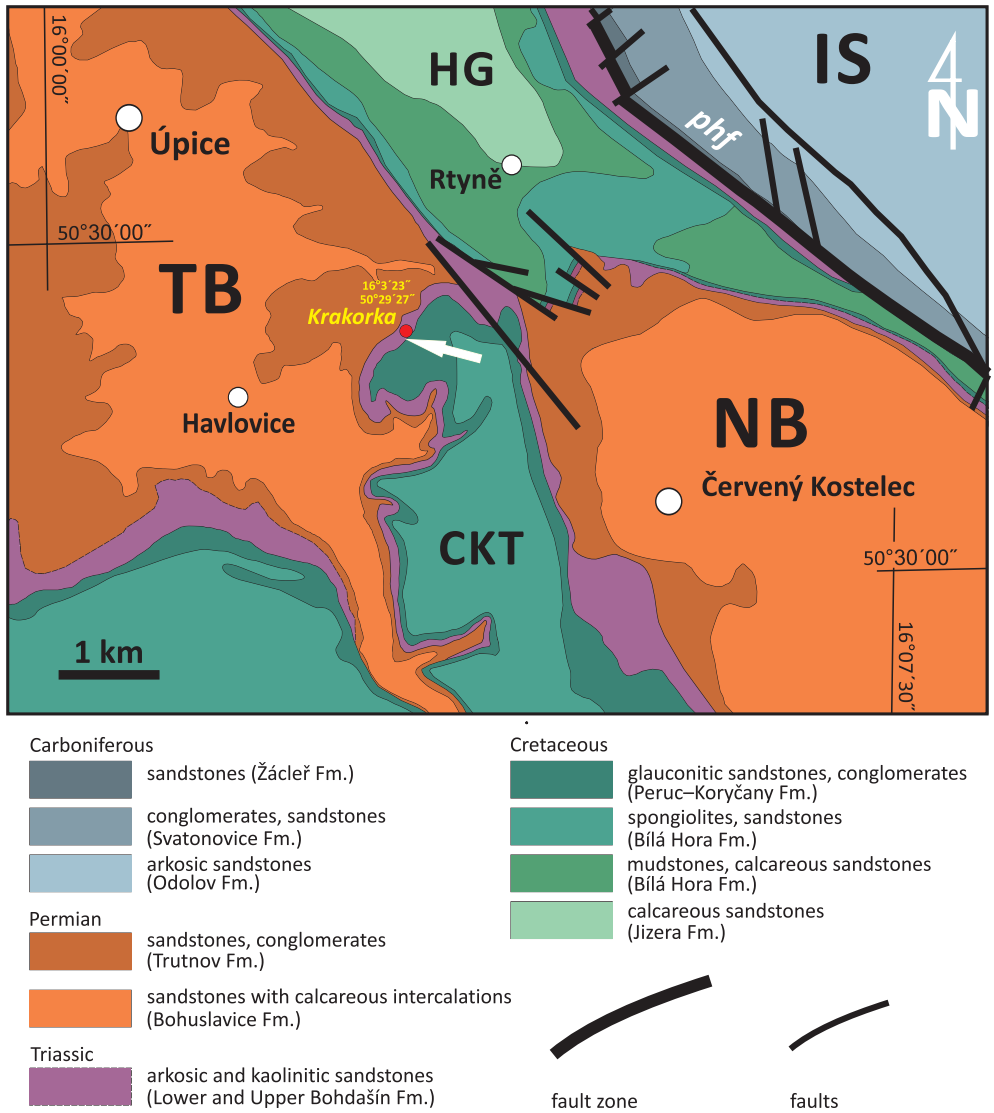

Fig. 35. Geological map of the Červený Kostelec area (Wojewoda et al. 2016). CKT – Červený Kostelec Trough, HG – Hronov Graben, NB – Nachod Basin, ISS – Intra-Sudetic Synclinorium, phfz – Poříčí–Hronov Fault Zone; faults based on Prouza (1988).

Koryčany Formation is overlain by the fine-grained siliceous and calcareous mudstones of the Bílá Hora Formation, of early Turonian age (Tásler 1966).

In Krákorka Quarry, the top of the Triassic sandstones of the Bohdašín Formation does not mark the base of the Cenomanian "transgressive glauconitic conglomerates" in the upper part of the quarry (cf. Fig. 36B, 37A); the discordance surface lies approximately 2 m below (Fig. 37A). This is also evidenced by biogenic structures, including root casts and trace fossils such as *Thalassinoides* and *Arenicolites*, which indicate an extremly shallow-marine, nearshore environment, supposedly of a (?) spit bar sedimentary complex (cf. Mikuláš and Prouza 1999; Uličný et al. 2009).

Trace fossils: Abundant trace fossils, mostly from the recently erected ichnofamily Rosselichnidae (cf. Knaust 2021a), occur in the bioturbated yellowish sandstones of the Krákorka Quarry. These include burrows with thick concentric, spiral, or eccentric internal laminations, for instance *Cylindrichnus cylindricus* Toots in Howard 1966 (Fig. 38A), *Lamellaecylindrica paradoxica* Knaust, 2021 (see Knaust 2021b; Fig. 38B), and ?*Rosselia* isp. (Fig. 38C–E).

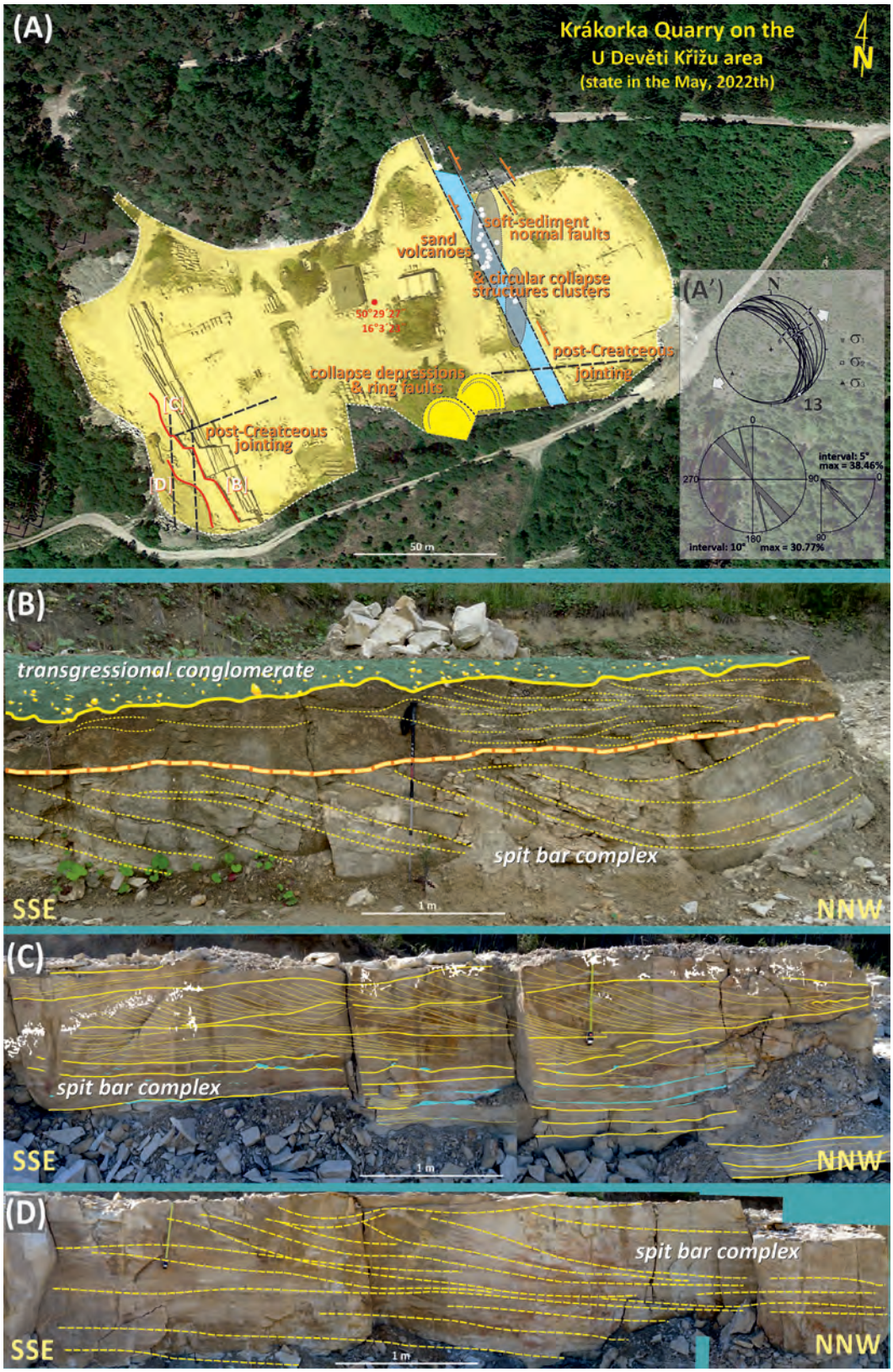

Fig. 36. (A) Krakorka Quarry and upper Cretaceous transgression sediment complex including (B–D) the sediments of a spit bar association (modified after Wojewoda et al. 2016, see text for explanations).

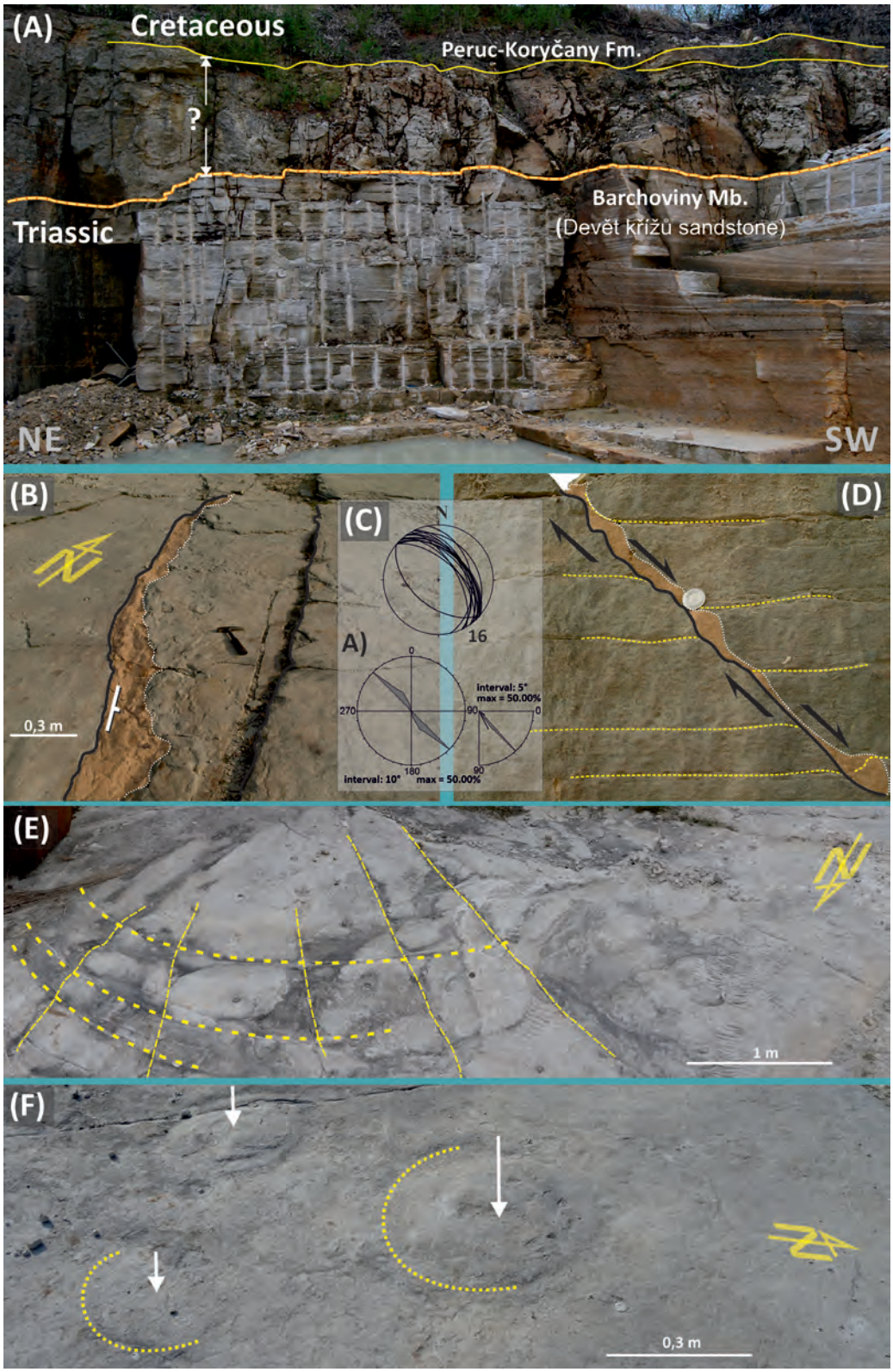

Fig. 37. (A) Discordance between Triassic and Cretaceous sediments in the southern wall of Krákorka Quarry. Sesimic or seismotectonic deformations of unlithified sediment: (B–D) faults, (E) collapse nishes, and (F) sand volcanoes (modifed after Wojewoda et al. 2016).

The most abundant is *Rosselia* isp., which appears both as solitary and crowded specimens (stacked segments and elliptical cross-sections). In some cases, the cross-sections of these burrows are somewhat similar to *Monocraterion* isp. (Fig. 38D; see also Knaust 2021a). This ichnotaxon is regarded ethologically as a domichnion or fodinichnion; equlibrichnion has also been indicated (Chrząstek 2020 and references therein). The trace makers are probably detritus-feeding terebellid polychaetes (Nara 2007). *Rosselia* is widely distributed in shallow-marine settings (Mello et al. 2021). Crowded *Rosselia* ichnofabric (CRI) usually occurs in unstable shoreface settings near fair-weather wave base, with high energy and deposition rates (cf. Bayet-Goll et al. 2021); it is a very useful tool for recognizing storm and transgressive sequences (cf. Nara 2002; Mello et al. 2021). The next most common ichnogenus is *Cylindrichnus* (although, in some cases, assignment to *Rosselia* cannot be excluded), which ethologically is regarded as a domichnion. The trace makers are suspension and surface deposit feeding worm-like organisms, probably polychaetes (Chrząstek 2020 and references therein). This ichnogenus occurrs in middle shoreface to offshore settings, and is most abundant in the lower shoreface (see Chrząstek 2020 and references therein). It is common in storm and transgressive deposits, between fair-weather and storm-wave base (Knaust 2017; Schultz et al. 2020).

Parahaentzschelinia-like traces, most probably bivalve trace fossils, are also common (compare Reynolds and McIlroy 2017; Fig. 38J). These specimens mostly occur as vertical shafts. *Parahaentzschelinia* is interpreted as a feeding or equilibrium burrow constructed by deposit- and detritus-feeders. The possible trace maker is considered to be a worm-like organism or a siphonate tellinid bivalve (cf. Reynolds and McIlroy 2017 and references therein). This ichnotaxon usually occurs in shallow-marine, storm influenced deposits (Luo et al. 2020). Dense *Parahaentzschelinia* populations record the adjustment of trace makers to rapid sedimentation events.

This shallow to deep-tier trace fossil assemblage characterizes both the *Skolithos* and *Cruziana* ichnofacies and is typical of transgressive shallow-marine shoreface deposits, such as those exposed in Krákorka Quarry.

Synsedimentary deformation structures: Numerous features related to tectonic and seismic activity during Triassic and Cretaceous sedimentation are observed in Krákorka Quarry and its immediate surroundings. The most spectacular are circular sand liquefaction zones (Fig. 37). These structures were described as sand volcanoes (Uličný 2004). A detailed description by Wojewoda et al. (2016) does support their injection origin; however, they are not typical sand volcanoes.

Injection structures, circular or irregular in outline, occur on bedding planes, have diameters from several cm to over 0.5 m, and thicknesses from 1 to 6 cm (Fig. 37F). Their architecture resembles small laccolites. They occur in fine- or medium-grained, very well sorted, laminated sand. Within the structures, the sediment is massive and homogeneous. They occur in isolation or form linearly distributed clusters, usually along synsedimentary fissure zones (faults?) (Figs 35A, 37B).

Laccolite structures are probably preserved due to the stabilization of the sediment surface by microbial mats, as evidenced by microbially induced sedimentary structures referred to as wrinkle structures (cf. Prave 2002) or elephant skin (Porada and Bouougri 2007), and perfectly preserved desiccation (syneresis?) cracks, despite the complete lack of pelitic sediments within the sandstones. Increased pore pressure (e.g., due to wave swelling, rising tide, and seismicity) is the main driving factor for the formation of sand volcanoes (cf. Dornbos et al. 2007; Martin-Chivelet et al. 2011; Taj et al. 2014).

The circular collapse structures differ significantly from the sand volcanoes, representing deformations of the top surface of the sediment. Usually, the structures are a series of similarly shaped circular embankments (folds) with wavelengths from 3 to 7 cm and amplitudes up to 1 cm. A single structure is commonly composed of 3 to 5 rings, whose amplitudes gradually decrease outwards (cf. Wojewoda et al. 2016). Some of the collapse structures from the Krákorka Quarry are extensional in character: that is, they represent fragments of decollated beds that form isolated "swimming pillows" on the fluidized sediment (e.g., Moretti et al. 1999; Bureau et al. 2014) (Fig. 37B, F). Diameters of the observed collapse depressions reach 5 m.

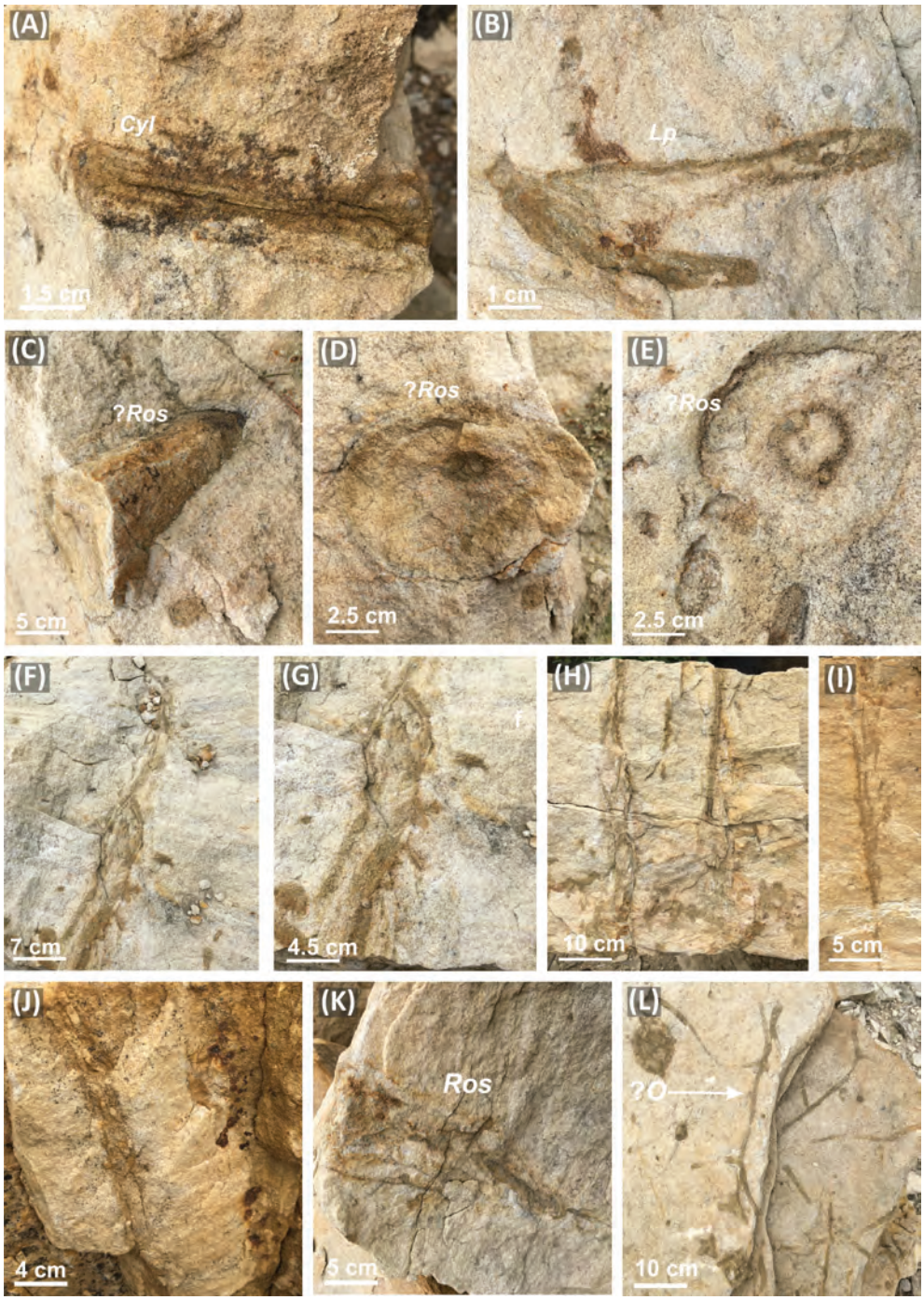

Fig. 38. Trace fossils from the Cenomanian sandstones of the Krákorka Quarry (Czech Republic). Abbreviations: *Cyl* – *Cylindrichnus* isp., *Lp* – *Lamellaecylindrica paradoxica*, *?Ros* – *?Rosselia* isp, *?O* – *?Ophiomorpha* isp., *Ros* – *Rosselia* isp. A. *Cylindrichnus* isp. B. *Lammelaecylindrica paradoxica*. C–E. cross-sections of *?Rosselia* isp.; C,D the same specimen. F-I. bivalve burrows ?Rosselichnidae. J. *Parahaentzschelinia*-like burrows. K. *Rosselia* isp. L. *?Ophiomorpha* isp.

Normal faults, extensional fractures, and joints occur in the Devìt křížù sandstones. The oldest faults were most likely created in a fairly lithified, or even unlithified, sand deposit (cf. Fig. 37B–D). Fault displacements are not significant and do not exceed a few centimetres. The fault surfaces are usually non-planar, but consist of segments dipping

at different angles. Some of the faults that probably developed in the unlithified material display a decreased dip angle trend at the floors of some beds. In some beds, the fault surface is parallel to the floor (cf. Fig. 37B–D). The joint surfaces are almost vertical, with two joint sets, NW-SE and NE-SW, dominating in the quarry (cf. Fig. 35A, A'). The orientation of these two joint sets indicates the presence of orthogonal joint normal faults (cf. Fig. 35A'). The strike directions of the orthogonal joint system are often almost parallel or perpendicular to the dominant strike direction of the younger normal faults (after lithification), which may suggest that the formation of both deformation systems in the Devìt křížù sandstones could be related to similarly oriented tension fields.

Fibrous quartz mineralization on "pre-lithification" fault surfaces was found exclusively on the lowest quarry level. Due to the low solubility of quartz, it seldom fills subsurface fractures. However, it can be transported and precipitated subaerially in unlithified deposits, although the process is regarded to take many decades (cf. Maltman 1994). The oldest normal faults were created in a stress field with NE-SW tension. After lithification of the Devìt křížù deposits, the sandstone beds were cut again by normal faults with features typical of a brittle regime. It seems that the orientation of the stress field did not change, and these younger faults were also formed during NE-SW extension (azimuth N 55°). Consequently, some of the older faults were reactivated.

The U Devìti křížù area is located almost centrally within a structure that was composed, at that time, of the present-day Trutnov and Nachod Basins. This area was the basin depocentre in the Early Triassic (Upper Buntsandstein, Röt), and formed a longitudinally elongated basin that represented land periodically flooded by the Olenekian Sea. The record of this interval points to terrestrial and shallow-marine sedimentation coupled with high tectonic and seismic activity (Fig. 39B). Due to the permanent meridional elongation of the basin, the area began its passive stage of development, becoming first an elevation within the basin (first stage of inversion). At that time, meridional synsedimentary extension (synsedimentary listric faults) was particularly intense. The next stage was

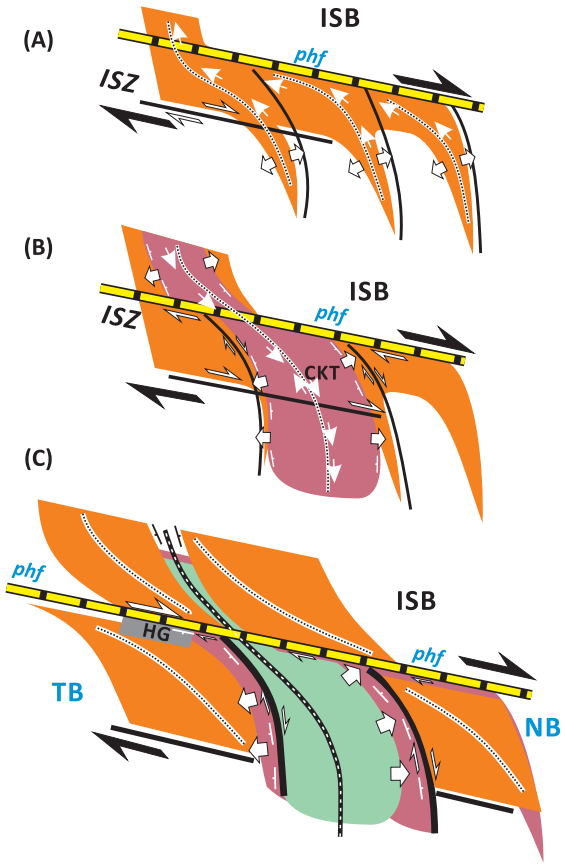

Fig. 39. Schematic evoution of the Červený Kostelec Trough (CKT) and the U Devìti křížù Elevation (DKE): (A) early Permian, (B) Triassic and (C) post-Cretaceous (modified after Wojewoda et al. 2016). Thick arrows show regional palaeokinematic trends, thin arrows indicate the regional palaeotransport of sedimentary material; ISB – Intra-Sudetic Basin, TB – Trutnov Basin, NB – Nachod Basin, HG – Hronov Graben, phfz – Poříčí–Hronov Fault Zone.

the Cretaceous transgression, during which the U Devìti křížù area probably represented a distinct morphological elevation. This is indicated, for instance, by a distinct erosional boundary between the Devìt křížù sandstones and the Peruc–Koryčany Formation. Generations of jointing developed during and after the formation of the Cretaceous cover. In the last stage, most probably during the Miocene, a subsequent inversion took place, and the Nachod and Trutnov Basins were distinctly separated from each other by the U Devìti křížù morphological elevation (Fig. 39C). Listric faults most probably formed in this interval; to a large degree they follow fault traces or use older synsedimentary destruction zones.

ACKNOWLEDGEMENTS

The paper was reviewed by Cliff Ollier (University of Western Australia), who is gratefully acknowledged.

REFERENCES

Aleksandrowski, P. and Wojewoda, J. 2010. Low-angle detachment related to strike-slip faulting in Late Cretaceous mudstones of the Table Mountains (SW Poland). In: 11th Czech–Polish Workshop on Recent Geodynamics of the Sudetes and Adjacent Areas, Třešt, November 4–6th, 2010, Academy of Sciences of the Czech Republic (Institute of Rock Mechanics) and 430 Wrocław University of Environmental Sciences (Institute of Geodesy and Geoinformatics), Abstracts, 30–31.

Audemard, F.A., Gómez, J.C., Taverab, H.J. and Orihuela, N. 2005. Soil liquefaction during the Arequipa Mw 8.4, June 23, 2001 earthquake, southern coastal Peru. Engineering Geology, 78, 237–255.

Awdankiewicz, M. 1997. Transition from calkaline to mildly alkaline volcanisin in a Late Palacozoic intramontane trough: evidence from the Intrasudetic Basin, SW Poland. In: European Union of Geosciences, Strassbourg, 23–27 March 1997, Abstracts, p. 146.

Awdankiewicz, M. 1998. Volcanism in a late Variscan intramontane trough: Carboniferous and Permian volcanic centres of the Intra-Sudetic Basin, SW Poland. Geologia Sudetica, 32, 13–47.

Awdankiewicz, M. Kurowski, L., Mastalerz, K. and Raczyński, P. 2003. The Intra-Sudetic Basin – a Record of Sedimentary and Volcanic Processes in Late – to Post-Orogenic Tectonic Setting. Geolines, 16, 165–183.

Badura, J. and Rauch, M. 2014. Tectonics of the Upper Nysa Kłodzka Graben. Geologia Sudetica, 42, 137–148.

Badura J., Przybylski B., Krzyszkowski D., Zuchiewicz W., Farbisz J. and Sroka J. 2002. Morphotectonic properties of the Sudetic Marginal Fault and Kłodzko Basin faults, SW Poland, in the light of geoelectrical Resistivity studies. In: V. Schenk and Z. Schenkova (Eds) Recent geodynamics of the Sudety Mts. And adjacent areas; Acta Montana, ser. A, Geodynamics, 20, 57–65.

Badura, J., Przybylski, B., Zuchiewicz, W., Farbisz, J., Sroka, W. and Jamroz, O. 2005. Tektonika rowu górnej Nysy Kłodzkiej – sporne problem – dyskusja. Przegląd Geologiczny, 53, 200–205.

Bayet-Goll, A., Knaust, D., Daraei, M., Bahrami, N. and Bagheri, F. 2021. *Rosselia* ichnofabrics from the Lower Ordovician of the Alborz Mountains (northern Iran): palaeoecology, palaeobiology and sedimentology. Palaeobiodiversity and Palaeoenvironments, 102, 103–128.

Berg, G. 1905. Über die geologischen Aufnahmen auf den Blättern Schomberg und Landeshut i. Schles. Jahrbuch der Königlich Preussischen Geologischen Landesanstalt zu Berlin, 26 (1908), 717–730.

Berg, G. and Dathe, E. 1905. Geologische Karte, Blatt Schömberg. Königlich Preussischen Geologischen Landesanstalt zu Berlin.

Berg, G. and Dathe, E. 1913. Geologische Karte, Blatt Landeshut. Königlich Preussischen Geologischen Landesanstalt zu Berlin.

Berg, G. and Dathe, E. 1940. Erläuterungen zu Blatt Landeshut. Rechst. Bodenfor. Berlin.

Bureau, D., Mourgues, R. and Cartwright, J. 2014. Use of a new artificial cohesive material for physical modelling: application to sandstone intrusions and associated fracture networks. Journal of Structural Geology, 66, 223–236.

Chrząstek, A. 2013. Middle Turonian trace fossils from the Bystrzyca and Dlugopole sandstones in the Nysa Kłodzka Graben (Sudetes, SW Poland). Geological Quarterly, 57, 443–466.

Chrząstek, A. 2020. Palaeoenvironmental interpretation of the Late Cretaceous Idzików Conglomerate Member (SW Poland, Sudetes, Idzików Quarry) based on analysis of trace fossils. Annales Societatis Geologorum Poloniae, 90, 149–194.

Chrząstek, A. and Sołczerski, R. 2016. Skamieniałości śladowe skorupiaków z dolnych warstw idzikowskich (Stary Waliszów, rów górnej Nysy Kłodzkiej [Crustacean trace fossils from the Lower Idzików Beds (Stary Waliszów, Upper Nysa Kłodzka Graben]. In: Pawłowska, K. and Pawłowski, D. (Eds), XXIII Konferencja Naukowa Sekcji Paleontologicznej PTG, Abstrakty, Poznań, September 21–23, , pp. 25–26.

Chrząstek, A. and Nowicka, N. 2021. Trace fossils and depositional environments of the middle Turonian sandstones in the Upper Nysa Kłodzka Graben (Sudetes, Poland) revisited. Geological Quarterly, 65, 10.

Closs, H. 1922. Der Gebirgsbau Schlesiens und die Stellung seiner Bodenschätze. Gebrüder Borntraeger, Berlin, 8°, ss. VIII, 107 p.

Dathe, E. and Petrascheck, W. 1933. Geologische Übersichtskarte des niederschlesich-böhmischen Beckens, 1: 100 000. Mittleiungan der Geologischen Gesellschaft in Wien, Band XXVI. Lith. Anst. V. Leop. Kraatz (Gez. V.J. Nowak 1911); Berlin.

Don, J. 1996. The Late Cretaceous Nysa Graben: implications for Mesozoic–Cenozoic fault-block tectonics of the Sudetes. Zeitschrift für Geologische Wissenschaften, 24, 317–324.

Don, B. and Don, J. 1960. Notes on the origin of the Nysa Graben. Acta Geologica Polonica, 10, 71–106.

Don, J. and Wojewoda J. 2004. Tectonics of the Upper Nysa Kłodzka Graben: Contentious Issues. Acta Geodynamica et Geomaterialia, 1, 173–178.

Don, J. and Wojewoda, J. 2005. Tektonika rowu górnej

Nysy Kłodzkiej – sporne problem – odpowiedź. Przegląd Geologiczny, 53, 212–221.

Don, J. and Gotowała, R. 2008a. Tectonic evolution of the late Cretaceous Nysa Kłodzka Graben, Sudetes, SW Poland. Geologia Sudetica, 40, 51–63.

Don, J. and Gotowała, R. 2008b. Tectonic map of the Nysa Kłodzka Graben (Sudetes). In: Don, J. and Gotowała, R. (Eds), Tectonic evolution of the late Cretaceous Nysa Kłodzka Graben, Sudetes, SW Poland. Geologia Sudetica, 40, insert 1:50 000.

Don, J., Skacel, J. and Gotowała, R. 2003. Geological map of the Śnieżnik Metamorphic Unit, Staré Město Zone and Velké Vrbno Dome. In: J., Don., Skacel, J. and Gotowała, R. (Eds), The boundary zone of the East and West Sudetes on the 1:50 000 scale geological map of the Velké Vrbno, Staré Město and Śnieżnik Metamorphic Units. Geologia Sudetica, 35, insert 1:100 000.

Dornbos, S.Q., Noffke, N. and Hagadorn, J.W. 2007. Mat-decay features. In: J. Schieber, P.K. Bose, P.G. Eriksson, S. Banerjee, S. Sarkar, W. Altermann and O. Catuneau (Eds), Atlas of Microbial Mat Features Preserved within the Clastic Rock Record, pp. 106–110. Elsevier; Amsterdam.

Dumanowski, B. 1961. Forms of spherical cavities in the Stołowe Mountains (Heuscheur Gebirge). Acta Universitatis Vratislaviensis, Ser. B, 8, 123–137. [In Polish with English summary]

Dziedzic, K. 1996. Two-stage origin of the Hercynian volcanics in the Sudetes, SW Poland. Neues Jahrbuch für Geologie und Paläontologie Abhandlungen, 199, 65–87.

Ellis, P.G. and McClay, K.R. 1988. Listric extensional fault systems – results of analogue model experiments. Basin Research, 1, 55–70.

Grygar, R. and Jelínek, J. 2003. Upper Morava and Nysa Pull-apart Grabens: Implication for Neotectonic Dextral Transtension on Sudetic Faults System. Geolines, 16, 35–36.

Halamski, A.T. 2013. Latest Cretaceous leaf floras from southern Poland and western Ukraine. Acta Palaeontologica Polonica, 58, 407–443.

Halamski, A. T., Kvaček, J. and Svobodová, M. 2018. Fossil mega- and microflora from the Březno Beds s.s. (Bohemian Cretaceous Basin, Coniacian). Review of Palaeobotany and Palynology, 253, 123–138.

Halamski, A. T., Kvaček, J., Svobodová, M., Durska, E. and Heřmanová, Z. 2020. Late Cretaceous mega-, meso-, and microfloras from Lower Silesia. Acta Palaeontologica Polonica, 65, 811–878.

Holub, V. 1972. Permian of the Bohemian Massif. In: Falke, H. (Ed.), Rotliegendes Essays on European Lower Permian, 137–188. E. J. Brill.

Holub, V. and Tásler, R. 1974. Mladší paleozoikum a spodní trias v podloží české křídové pánve. In: Malkovský, M. (Ed.), Geologie české křídové pánve a jejího podloží, pp. 72–100. Ústřední Ústav Geologický; Praha.

Janeček, T. 2015. Paleontological evaluation of the locality Štíty in the Šumperk district (Bohemian Cretaceous Basin). Bechelor Thesis, Palacký Universityin Olomouc, Faculty of Science, Department of Geology, 75 pp. [In Czech with English summary]

Jerzykiewicz, T. 1967. Significance of the cross-bedding for the paleogeography of the Upper Cretaceous sedimentary basin of the North Bohemia, Saxony and Sudetes. Bulletin of the Polish Academy of Sciences, Earth Sciences, Série Géologie et Géographie, 15, 63 p.

Jerzykiewicz, T. 1968a. Sedymentacja górnych piaskowców ciosowych niecki śródsudeckiej (górna kreda). Geologia Sudetica, 4, 409–462.

Jerzykiewicz, T. 1968b. Uwagi o genezie i orientacji ciosu w skałach górnokredowych niecki śródsudeckiej. Geologia Sudetica, 4, 465–478.

Jerzykiewicz, T. 1969. Old palaeontological evidence of the stratigraphic position of the youngest Upper Cretaceous sandstones (Góry Stołowe, Middle Sudetes). Bulletin of the Polish Academy of Sciences, Earth Sciences, Série Géologie et Géographie, 17, 173–170.

Jerzykiewicz, T. 1970. The Upper Cretaceous turbidite sequence in the Sudetes (south-western Poland). Bulletin of the Polish Academy of Sciences, Earth Sciences, Série Géologie et Géographie, 18, 149–159.

Jerzykiewicz, T. 1971. A flysch-littoral succession in the Sudetic Upper Cretaceous. Acta Geologica Polonica, 21, 165–200.

Jerzykiewicz, T. and Wojewoda, J. 1986. The Radków and Szczeliniec sandstones: An example of giant foresets on a tectonically controlled shelf of the Bohemian Cretaceous Basin (Central Europe). In: Knight, R.J. and McLean, J.R. (Eds), Shelf Sands and Sandstones. Canadian Society of Petroleum Geologists, Memoir, 11, 1–35.

Kauffman, E.G. 1978. An outline of Middle Cretaceous marine history and inoceramid biostratigraphy in the Bohemian basin, Czechoslovakia. Annales du Muséum national d'histoire naturelle de Nice, 4.13, 1–12.

Kędzierski, M. 2002. Stratygrafia i paleobiogeografia osadów kredy opolskiej i dolnych warstw idzikowskich na podstawie nanoplanktonu wapiennego. PhD Thesis, Jagiellonian University; Kraków.

Klein, V. and Soukup, J. 1966. The Bohemian Cretaceous Basin. In: Zoubek, V. (Ed.), Regional Geology of Czechoslovakia, Part I, The Bohemian Massif. Prague: Czechoslovak Academy of Sciences, 487–512.

Klein, V., Müller, V. and Valečka, J. 1979. Lithofazielle und paläogeographische Entwicklung des Böhmischen Kreidebeckens. Aspekte der Kreide Europas. IUGS Series A, 6, 435–446.

Knaust, D. 2017. Atlas of Trace Fossils in Well Core: Appearance, Taxonomy and Interpretation. Springer, 271 p.

Knaust, D. 2021a. Rosselichnidae ifam. nov.: burrows with concentric, spiral or eccentric lamination. Papers in Palaeontology, 7, 1847–1875.

Knaust, D. 2021b. The paradoxical ichnotaxonomy of *Thalassinoides paradoxicus*: a name of different meanings. Paläontologische Zeitschrift, 95, 179–186.

Kodym, O. (Ed.) 1967. Geological Map of Czechoslovakia. Ústřední ústav geologický; Praha.

Komuda, J. and Don, J. 1964. Brachyantyklina Bystrzycy Klodzkiej. Acta Geologica Polonica, 14, 169–174.

Kurowski L. 1998. Fluvial sedimentology of the Biały Kamień Formation (Upper Carboniferous, Sudetes, Poland). Geologia Sudetica, 31, 69–77.

Kvaček, J., Halamski, A.T., Svobodová, M. and Durska, E. 2015. Coniacian flora of the Sudetes (south-western Poland): Palaeoecological and palaeoclimatic interpretations. Palaeogeography, Palaeoclimatology, Palaeoecology, 436, 178–187.

Lankrejer, A.C. and Littke, R. 1997. Tectonic evolution of the Intra Sudetic Basin (SW Poland). Implications from basin analysis and subsidence history. Terra Nostra, (Deutsche Forschungs Gemeinschaft) Abstracts of the 6th Kolloquim of the DFG Schwerpunkt programm "Orogene Processe". Juelich, February 1997.

Laurin, J. and Uličný, D. 2004. Controls on a shallow-water hemipelagic carbonate system adjacent to a siliciclastic margin: example from Late Turonian of Central Europe. Journal of Sedimentary Research, 74, 697–717.

Leszczyński, S. 2010. Coniacian–?Santonian paralic sedimentation in the Rakowice Małe area of the North Sudetic Basin, SW Poland: sedimentary facies, ichnological record and palaeogeographical reconstruction of an evolving marine embayment. Annales Societatis Geologorum Poloniae, 80, 1–24.

Leszczyński, S. and Nemec, W. 2020. Sedimentation in a synclinal shallow-marine embayment: Coniacian of the North Sudetic Synclinorium, SW Poland. The Depositional Record, 6, 144–161.

Luo, M., Shi, G.R. and Lee, S. 2020. Stacked *Parahaentzschelinia* ichnofabrics from the Lower Permian of the southern Sydney Basin. Palaeogeography, Palaeoclimatology, Palaeoecology, 541, 109538.

Maltman, A. 1994. The Geological Deformation of Sediments. Chapman and Hall.

Martin-Chivelet, J., Palma, R.M., Lopez-Gomez, J. and Kietzmann, D.A. 2011. Earthquake-induced soft-sediment deformation structures in Upper Jurassic open-marine microbialites (Neuquen Basin, Argentina). Sedimentary Geology, 235, 210–221.

Mikuláš, R. and Prouza, V. 1999. The Cretaceous biogenic structures created in Triassic sandstones (Devět křížů at Červený Kostelec, NE Bohemia, Czech Republic). VéstnÍk Českého Geologického Ústavu, 74, 335–342.

Miller, K.G., Sugarman, P.J., Browning, J.V., Kominz, M.A., Hernández, J.C., Olsson, R.K., Wright, J.D., Feigenson, M.D. and Van Sickel, W. 2003. Late Cretaceous chronology of large, rapid sea-level changes: glacioeustasy during the greenhouse world. Geology, 31, 585–588.

Miller, K.G., Kominz, M.A., Browning, J.V., Wright, J.D., Mountain, G.S., Katz, M.E., Sugarman, P.J., Cramer, B.S., Christie-Blick, N. and Pekar, S.F. 2005. The Phanerozoic record of global sea-level change. Science, 310, 1293–1298.

Moretti, M., Alfaro, P., Caselles, O. and Canas, J.A. 1999. Modelling seismites with a digital shaking table. Tectonophysics, 304, 369–383.

Nara, M. 2002. Crowded *Rosselia socialis* in Pleistocene inner shelf deposits: benthic paleoecology during rapid sea-level rise. Palaios, 17, 268–276.

Nara, M. 2007. *Rosselia socialis*: a dwelling structure of a probable terebellid polychaete. Lethaia, 28, 171–178.

Naylor, M.A., Mandl, G. and Sijpesteijn, C.H.K. 1986. Fault geometries in basement-induced wrench faulting under different initial stress states. Journal of Structural Geology, 8, 737–752.

Nemec, W. 1984. Wałbrzych beds (Lower Namurian) in the Wałbrzych Basin: an alluvial sedimentation in coal-basin. Geologia Sudetica, 19, 7–73.

Nemec, W., Porębski, S.J. and Teisseyre, A.K. 1982. Explanatory notes to the lithotectonic molasse profile of the Intra-Sudetic Basin, Polish part (Sudety Mis., Carboniferous–Permian). Veroff, Zentralinst, Phys. Erde AdW DDR, 66, 207–278.

Ollier, C.D. 1978. Induced fracture and granite landforms. Zeitschrift für Geomorphologie, Neue Folge, 22, 3, 249–257.

Pachucki, C. 1957. O stratygrafii i litologii kredy w rowie Nysy Kłodzkiej. Annales Universitatis Mariae Curie-Sklodowska, 12, 1–55.

Pokorný, R. 2008. *Funalichnus*, a new ichnogenus and its type ichnospecies *Funalichnus strangulatus* (Fritsch 1883), Upper Cretaceous of the Bohemian Cretaceous Basin, Czech Republic. Ichnos, 15, 51–58.

Porada, H. and Bouougri, E. 2007. "Wrinkle structures" – a critical review. In: Schieber, J. Bose, P.K., Eriksson,P.G. , Banerjee, S., Sarkar, S., Altermann, W. and Catuneau, O. (Eds), Atlas of Micro Clastic Rock Record, 135–144. Elsevier; Amsterdam.

Raczyński, P. 1997. Stanowisko 5 (Stary Waliszów) [Stop 5. Stary Waliszów]. In: Wojewoda, J. (Ed.), Obszary źrodlowe. Zapis w osadach. VI Krajowe Spotkanie Sedymentologów, 26–28.09.1997, Lewin Kłodzki. WIND Wrocław, 123–124.

Radwański, S. 1966. Upper Cretaceous Facies and Faunas in the Central Part of the Sudety Mts. (summary). Annales de la Société Géologique de Pologne, 36, 99–119.

Radwański, S. 1968. Górnokredowe osady w Sudetach i wpływ tektoniki na ich sedymentację. Kwartalnik Geologiczny, 12, 607–617.

Radwański, S. 1975. Kreda Sudetów Środkowych w Świetle wyników nowych otworów wiertniczych. Biuletyn Instytutu Geologicznego, 287, 2–56.

Reynolds, R. and McIlroy, D. 2017. Three-dimensional morphological analysis of a Parahaentzschelinia-like trace fossil. Papers in Palaeontology, 3 (2), 241–258.

Rode, K. 1936. Die Schichtenfolge der Kreide im Neissegraben. Zentralblatt für Mineralogie B, 3, 109–118.

Rotnicka, J. 1997. Wykształcenie facjalne tzw. margli plenerskich na południowych zboczach Gór Stołowych (Sudety, kreda górna). In: "Obszary Źródłowe; Zapis w Osadach", J. Wojewoda (Ed.), Materiały VI Spotkania Sedymentologów, Lewin Kłodzki, 26–28 September 1997, Abstracts.

Schultz, S., MacEachern, J.A., Catuneanu, O. and Dashtgard, S.E. 2020. Coeval deposition of transgressive and normal regressive stratal packages in a structurally controlled area of the Viking Formation, central Alberta, Canada. Sedimentology, 67, 2974–3002.

Scupin, H. 1935. Die stratigraphischen Beziehungen der mittel- und nordsudetischen Kreide. Zeitschrift der Deutschen Geologischen Gesellschaft. 87, 523–538.

Sobczyk, A, Danišík, M., Aleksandrowski, P. and Anczkiewicz, A. 2015. Post-Variscan cooling history of the central Western Sudetes (NE Bohemian Massif, Poland) constrained by apatite fission-track and zircon (U-Th)/He thermochronology. Tectonophysics, 649, 47–57.

Sobczyk, A., Sobel, E.R. and Georgieva, V. 2020. Meso-Cenozoic cooling and exhumation history of the Orlica–Śnieżnik Dome (Sudetes, NE Bohemian Massif, Central Europe): Insights from apatite fission–track thermochronometry. Terra Nova, 32, 122–133.

Sobczyk A. and Szczygieł, J. 2021. Paleostress reconstruction of faults recorded in the Niedźwiedzia Cave (Sudetes): insights into Alpine intraplate tectonic of NE Bohemian Massif. International Journal of Earth Sciences (Geologische Rundschau), 110, 833–847.

Sokalski D., Wojewoda J. and Kowalski A. 2020. Epigenetic and Induced Fractures from the Radków Bluff (Stołowe Mountains) Documented with Terrestrial Laser Scanner – Structural Implications. Book of Abstracts, XX Conference of PhD Students and Young Scientists, October 14–16, 2020.

Taj, R.J., Aref, M.A.M. and Schreiber, B.C. 2014. The influence of microbial mats on the formation of sand volcanoes and mounds in the Red Sea coastal plain, south Jeddah, Saudi Arabia. Sedimentary Geology, 311, 60–74.

Tásler, R. 1961. Prehled geologie permokarbonu a spodniho triasu. In: Svoboda, J. and Chaloupsky, J. (Eds), Vysvetlivky kprehledne geolicke mape CSSR. Ústřední Ústav Geologický, Praha.

Tásler, R. 1966. Triassic. In: Svoboda, J. et al. (Eds), Regional Geology of Czechoslovakia, part I: the Bohemian Massif, 481–483. Publishing House of the Czechoslovakia Academy of Sciences, Prague. [In Czech with English summary]

Tásler, R. (Ed.) 1979. Geologie české části vnitrosudetské pánve. Ústřední ústav geologický, Praha, 292 p.

Teisseyre, A.K. 1966. Dolnokarboński wulkanizm w najniższym kulmie NE części niecki środsudeckiej (On the lower Carboniferous volcanism of the Intrasudetic Basin: new data about eruptive and pyroclastic rocks). Acta Geologica Polonica, 16, 445–475. [In Polish, with English summary]

Teisseyre, A.K. 1968. The Lower Carboniferous of the Intrasudetic Basin: a study in sedimentary petrology and basin analysis. Geologia Sudetica, 4, 221–298.

Teisseyre, A.K. 1973. Carboniferous fans and fanglomerates in the Central Sudetes 1: Marginal faults, downfaulting and sedimentation. Bulletin of the Polish Academy of Sciences, Earth Sciences, Série Sciences de la Terre, 21, 147–155.

Teisseyre, A.K. 1975. Sedimentology and palaeogeography of the Kulm alluvial fans in the western Intrasudetic Basin (Central Sudetes, SW Poland). Geologia Sudetica, 9, 5–135.

Teisseyre, A.K. and Teisseyre, J., 1969. Faulting and sedimentation on the north-western margin of the Intrasudetic Basin. Bulletin of the Polish Academy of Sciences, Earth Sciences, Série Sciences de la Terre, 17, 41–48.

Teisseyre, B. 1972a. Zespół dolnoturońskiej mikrofauny z Krzeszowa. Acta Geologica Polonica, 22, 71–81.

Teisseyre, B. 1972b. Mikrofauna strefy Inoceramus labiatus w środkowych Sudtach. Prace Naukowe Instytutu Geotechniki, Politechnika Wrocławska, 11, 70–81.

Teisseyre, B. 1975. Poziomy mikrofaunistyczne w osadach górnej kredy niecki śródsudeckiej w świetle analizy dendrytu zmienności. Kom. Instytutu Geotechniki, Politechnika Wrocławska, 12 p.

Trzęsiok, D., Krzykawski, T., Niedźwiedzki, R., Brom, K., Gorzelak, P. and Salamon, M.A. 2014. Palaeoenvironment of the Upper Cretaceous (Coniacian) concretions-bearing Lagerstätten from Poland. Palaeogeography, Palaeoclimatology, Palaeoecology, 401, 154–165.

Uličný, D. 1997. Sedimentation in a reactivated, intracontinental strike-slip fault zone: the Bohemian Cretaceous Basin, Central Europe. Gaea heidelbergensis, 3, Abstracts, 18th IAS Regional European Meeting, Heidelberg, 347.

Uličný, D. 2001. Depositional systems and sequence stratigraphy of coarse-grained deltas in a shallow-marine, strike-slip setting: the Bohemian Cretaceous Basin, Czech Republic. Sedimentology, 48, 599–628.

Uličný, D. 2004. A drying-upward aeolian system of the Bohdašín Formation (Early Triassic), Sudetes of NE Czech Republic: record of seasonality and long-

term palaeoclimate change. Sedimentary Geology, 167, 17–39.

Uličný, D., Nichols, G. and Waltham, D. 2002. Role of initial depth at basin margins in sequence architecture: field examples and computer models. Basin Research, 14, 347–360.

Uličný, D., Špičáková, L. and Čech, S. 2003. Changes in depositional style of an intra-continental strike-slip basin in response to shifting activity of basement fault zones: Cenomanian of the Bohemian Cretaceous Basin. GeoLines, 16, 133–148.

Uličný, D., Laurin, J. and Čech, S. 2009a. Controls on clastic sequence geometries in a shallow-marine, transtensional basin: the Bohemian Cretaceous Basin, Czech Republic. Sedimentology, 56, 1077–1114.

Uličný, D., Špičáková, L., Grygar, R., Svobodova, M., Čech, S. and Laurin, J. 2009b. Palaeodrainage systems at the basal unconformity of the Bohemian Cretaceous basin: roles of inherited fault systems and basement lithology during the onset of basin filling. Bulletin of Geosciences, 84, 577–610.

Vakarelov, B.K., Bhattacharya, J.P. and Nebrigic, D.D. 2006. Importance of high-frequency tectonic sequences during greenhouse times of Earth history. Geology, 34, 797–800.

Valečka, J. 1979. Paleogeografie a litofaciálnívývoj severozápadní části české křídovépánve. Věstník Ústředního Ústavu Geologického, 33, 47–81.

Valečka, J. 1984. Storm-surge versus turbidite origin of the Coniacian to Santonian sediments in the eastern part of the Bohemian Cretaceous Basin. Geologische Rundschau, 113, 651–682.

Valečka, J. 1989. Sedimentology, stratigraphy and cyclicity of the Jizera Formation (Middle–Upper Turonian) in the Děčín area (N. Bohemia). Věstník Ústředního Ústavu Geologického, 64, 77–90.

Valečka, J. and Skoček, V. 1991. Late Cretaceous lithoevents in the Bohemian Cretaceous Basin, Czechoslovakia. Cretaceous Research, 12, 561–577.

Vejlupek, M. 1986. Strukturni stavba police a svatonovicko-hronovske panve. Věstník Ústředního ústavu geologického. 61, 139–148

Voigt, T. 1996. Sea-level changes during Late Cenomanian and Early Turonian in the Saxonian Cretaceous Basin. Mitteilungen den Geologisch-Paläontologisches Institut, Universität Hamburg, 77, 275–290.

Walaszczyk, I. 2000. Inoceramid bivalves at the Turonian/Coniacian boundary: biostratigraphy, events and diversity trend. Acta Geologica Polonica, 50, 421–430.

Walaszczyk, I. and Cobban, W.A. 2006. Palaeontology and biostratigraphy of the Middle–Upper Coniacian and Santonian inoceramids of the US Western Interior. Acta Geologica Polonica, 56, 241–348.

Wilmsen, M. and Niebuhr, B. 2014. The rosetted trace fossil *Dactyloidites ottoi* (Geinitz, 1849) from the Cenomanian (Upper Cretaceous) of Saxony and Bavaria (Germany): ichnotaxonomic remarks and palaeoenvironmental implications. Paläontologische Zeitschrift, 88, 123–138.

Wojewoda, J. 1986. Fault scarp induced shelf sand bodies in Upper Cretaceous of the Intrasudetic Basin. In: Teisseyr,e A.K. (Ed.), 7 JAS Regional Meeting Guidebook, Excursion A-T, 1–30.

Wojewoda, J. 1987. Seismotectonically induced sediments and structures in the Upper Cretaceous sandstones of the Intrasudetic Basin. Przegląd Geologiczny 4, 169–175.

Wojewoda, J. 1997. Upper Cretaceous littoral-to-shelf succession in the Intrasudetic Basin and Nysa Trough, Sudety Mts. In: Wojewoda, J. (Ed.), Obszary Źródłowe: Zapis w Osadach. Tom I, 81–96. WIND; Wrocław.

Wojewoda, J. 2003. "Gilbert Type Delta" versus "Accumulation Terraces" models and their application to middle Turonian–early Coniacian sedimentary setting in the Intrasudetic Basin: A discussion. Geolines, 16, 109–111.

Wojewoda, J. 2007. Neotectonic Aspect of the Intrasudetic Shear Zone. Acta Geodynamica et Geomaterialia, 4, 1–11.

Wojewoda, J. 2007a. Palaeogeography and tectonic evolution of the Žernov–Nachod–Kudowa sedimentary area. In: 5th Meeting of the Central European Tectonic Studies Group (CETEG'5), April 11–14.04.2007, Tepla.

Wojewoda, J. 2007b. Žďárky–Pstrążna Dome – dextral strike-slip fault related structure at the eastern termination of the Poříčí–Hronov Fault Zone (Sudetes, Góry Stołowe Mts.). In: 5th Meeting of the Central European Tectonic Studies Group (CETEG'5), April 11–14.04.2007, Tepla.

Wojewoda, J. 2007c. Neotectonic aspect of the Intrasudetic Shear Zone. Acta Geodynamica et Geomaterialia, 4, 1–11.

Wojewoda, J. 2007d. Perm basenu Nachodu. Sedimentologica, 1, 85–99.

Wojewoda, J. 2007e. The Czerwona Woda Creek: A tectonically controlled mountain river basin. On recent geodynamics of the Sudety Mts. and adjacent areas, 8th Czech–Polish Workoshop, Kłodzko, 29–31.03.2007. pp. 34–35. [In Polish]

Wojewoda, J. 2008a. Post-Variscan evolution of the Poříčí–Hronov zone. 9th Czech–Polish Workshop on Recent Geodynamics of the Sudeten and Adjacent Areas, 12–15.11.2008, Náchod, Abstracts, 27–28.

Wojewoda, J. 2008b. Poříčí–Hronov strike-slip zone related structures. 9th Czech–Polish Workshop on Recent Geodynamics of the Sudeten and Adjacent Areas, 12–15.11.2008, Náchod, Abstracts, 29–30.

Wojewoda, J. 2009. Žďarky–Pstrążna Dome: a strike-slip fault-related structure at the eastern termina-

tion of the Poříčí–Hronov Fault Zone (Sudetes). Acta Geodynamica et Geomaterialia, 6, 273–290.

Wojewoda, J. 2011. Extensional development of the sudetic basins. SEDIMENT 2011: Archives of the Earth System, Abstracts, pp. 101–103. June 23–26, Leipzig, Germany.

Wojewoda, J. 2011. Stołowe Mountains Geo-attractions – a geological guide to the Table Mountains National Park. Wydawnictwo PNGS, 70 pp. [In Polish]

Wojewoda J. 2012. Joints in Cretaceous sandstones of the Góry Stołowe Mountains: tectonic and non-tectonic. In: 13th Czech–Polish Workshop on Recent Geodynamics of the Sudety Mts. and Adjacent Areas, November 20–22, Wrocław–Pawłowice, Poland, pp. 57–58. [In Polish]

Wojewoda, J. 2019. The Intrasudetic Basins and Synclinorium in the extensional model of the Sudetes evolution – environmental and paleogeographic schemes. In: 20th Czech–Polish Workshop on Recent Geodynamics of the Sudeten and the Adjacent Areas, Jakuszyce, October 25–27th, pp. 23–28.

Wojewoda, J. 2020. Borderland geo-attractions – Stołowe Mountains and Broumowskie Walls. B. Kokot vel Kokociński, Nowa Ruda, 300 pp. [In Polish and Czech]

Wojewoda, J. and Mastalerz, K. 1989. Cklimate evolution, allo- and autocyclicity of sedimentation: an example from the Permo-Carboniferous continental deposits of the Sudetes, SW Poland. Przegląd Geologiczny, 37, 173–180. [In Polish with English summary]

Wojewoda, J. and Mastalerz, K. 1989. Ewolucja klimatu oraz allocykliczność i autocykliczność sedy-mentacji na przykładzie osadów kontynentalnych górnego karbonu i permu w Sudetach. Przegląd Geologiczny, 432, pp. 173–180.

Wojewoda, J. and Ollier, C. 2013. Weathering induced fractures, examples from the Góry Stołowe Mts. In: Krobicki, M. and Feldman-Olszewska, A. (Eds), Głębokomorska sedymentacja fliszowa, sedymentologiczne aspekty historii basenów karpackich. POKOS 5'2013: V Polska Konferencja Sedymentologiczna, Żywiec, 16–19.05.2013. Warszawa, Państwowy Instytut Geologiczny-Państwowy Instytut Badawczy, abstrakty, 57–58. [In Polish]

Wojewoda, J. and Kowalski, A. 2016. The role of the South-Sudetic Shear Zone in the evolution of the Sudetes. In: Wojewoda, J. and Kowalski, A. (Eds), Przewodnik do Wycieczek Kongresowych, wycieczka 2.3, pp. 21–43. [In Polish]

Wojewoda, J., Koszela, St. and Aleksandrowski, P. 2010. A kilometre-scale low-angle detachment related to strike-slip faulting in upper Cretaceous mudstones of the Table Mountains (Central Sudetes, SW Poland). In: 8th Meeting of the Central European Tectonic Group Studies (CETeG), 22–25 April 2010, p. 127.

Wojewoda, J., Białek, D., Bucha, M., Głuszyński, A., Gotowała, R., Krawczewski, J. and Schutty, B. 2011. Geology of the Góry Stołowe National Park – selected issues. In: Chodak, T., Kabała, C., Kaszubkiewicz, J., Migoń, P., Wojewoda, J. (Eds), Geoekologiczne Warunki Środowiska Przyrodniczego Parku Narodowego Gór Stołowych. WIND, Wrocław, pp. 53–96. [in Polish]

Wojewoda, J., Rauch, M. and Kowalski, A. 2016. Synsedimentary seismotectonic features in Triassic and Cretaceous sediments of the Intrasudetic Basin (U Devìti krížù locality) – regional implications. Geological Quarterly, 2016, 60, 355–364.

Wołkowicz, S. 1988. On the sedimentation of the Lower Permian Walchia Schales from Ratno Dolne (Intra-Sudetic Depression). Przegląd Geologiczny, 36, 214–218. [In Polish with English summary]

Xiao, I.L. and Suppe, J. 1992. Origin of rollover. Bulletin of the American Association of Petroleum Geologists, 76, 509–529.

Ziółkowska, M., Wojewoda, J. and Zimmerle, W. 1992. The boreal "Flammen: mergel" lithofacies in the Lower Saxony Basin (Germany) as compared with corresponding rocks in the Intrasudetic Basin (Poland). Abstract. Fifth International Cretaceous Symposium, Hamburg, 1–3.

11TH INTERNATIONAL
CRETACEOUS
SYMPOSIUM
Warsaw, Poland, 2022

CRETACEOUS DEEP-SEA FACIES, STRATIGRAPHY, AND ICHNOLOGY IN THE POLISH FLYSCH CARPATHIANS

Alfred Uchman | Mateusz Szczęch

Faculty of Geography and Geology, Institute of Geological Sciences, Jagiellonian University, Gronostajowa 3a, PL-30-387 Kraków, Poland; e-mails: alfred.uchman@.uj.edu.pl; mateusz.szczech@uj.edu.pl

ABSTRACT

Thick and variable series of flysch deposits of the Outer Carpathians offer a good insight in deep-sea deposition and palaeoenvironments during the Cretaceous. Their stratigraphy has improved in the latest decades even if the stratigraphic tools (mainly microfossils) available are generally difficult to work with. The Carpathian flysch is known from its trace fossils, which are abundant and diverse in some formations. More and more Cretaceous events have been recognized.

THE FLYSCH CARPATHIANS IN POLAND AND THEIR CRETACEOUS FORMATIONS

The Flysch Carpathians in Poland (also known as the Outer Carpathians) are a part of the Western Carpathians located north of the Pieniny Klippen Belt. They are built of several imbricated nappes, detached from their substrate and forming an accretionary wedge, and originated in the Miocene during the Alpine orogeny (e.g., Oszczypko et al. 2015). To the north, the nappes are overthrusted on Miocene deposits of the Carpathian Foredeep, which developed on different units of the flexurally bended European platform. The nappes are composed of folds and thrust sheets containing very thick, variably deep-sea, mostly gravity-flow dominated Cretaceous–Paleogene deposits. Each nappe is characterized by a specific series of deposits that originated in interconnected sub-basins and/or facies zones within the Western Tethys. At least in the Late Cretaceous–Eocene, these were distinctly separate, as suggested by differences in the facies represented. The sedimentary material was supplied from both the surrounding areas and intrabasinal elevations known as cordillieras. From south to north, the Magura, Dukla, Silesian, Subsilesian, and Skole nappes have been distinguished. The tectogenesis of the Polish Carpathians is complex and, in several aspects, quite ambiguous (see Książkiewicz 1977a; Golonka and Picha 2006; Oszczypko 2006; Kuśmierek and Baran 2016; Golonka et al. 2019; and references therein).

The Polish Flysch Carpathians are a classic area for investigations on the sedimentary structures of turbiditic deposits (Książkiewicz 1954; Dżułyński and Ślączka 1958; Dżułyński et al. 1959; Dżułyński 1963, 1996; Dżułyński and Walton 1963), the paleogeography of flysch deposits (Książkiewicz 1956, 1962), deep-sea ichnology (Książkiewicz 1977b; Uchman 1998), and agglutinated benthic foraminifers (e.g., the Cretaceous–Paleogene agglutinated foraminiferal zonations of Geroch and Nowak (1984)). Nevertheless, the nature of the rather small, isolated outcrops are problematic in attempts to better recognize depositional systems on broader scales. As such, the accuracy of stratigraphic recognition is generally low because, for the most part, imprecise tools are all that are available. The present excursion will visit selected Cretaceous deposits in the Silesian, Subsilesian, and Magura nappes (Fig. 1).

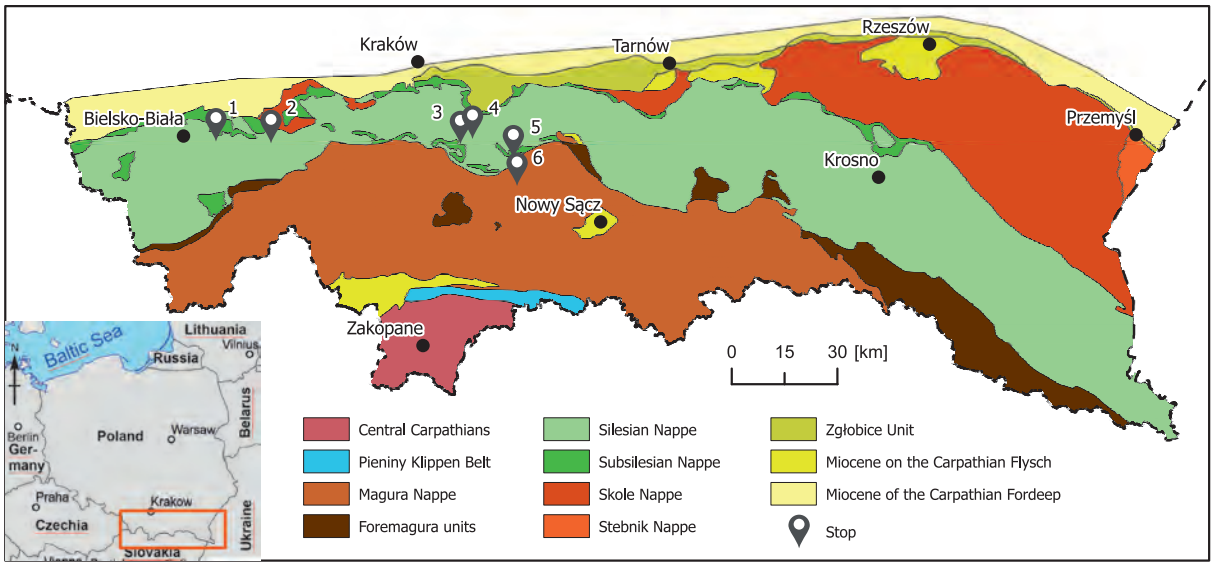

Fig. 1. Geological map of the Polish Carpathians, with visited localities marked.

Silesian Nappe

The Silesian Nappe is a huge tectonic unit running through the whole arc of the Western Carpathians and a large part of the Eastern Carpathians. It contains the most complete sedimentary succession in the Flysch Carpathians, ranging from the late Tithonian through the Cretaceous (Fig. 2) to the Miocene. The Late Jurassic–Early Cretaceous interval was deposited during the post-rifting thermal stage. In this extensional stage of development, the basin is referred to as the Proto-Silesian Basin, and was probably a part of the Severin–Moldavidic Basin, which is also represented in other units of the Eastern Carpathians (e.g., Ślączka et al. 2006; Golonka et al. 2008). In the western part of the Polish Flysch Carpathians and in Moravia (Czech Republic), the opening of the basin is marked by small intrusions (sills and dykes) of teschenites, which are basic rocks containing plagioclase, augite, biotite, analicite, and chlorites. The lithostratigraphy of the Cretaceous in the Silesian Nappe is a matter of active debate, and has yet to be uniformly formalized and unified (Golonka et al. 2008).

The Vendryně Formation or **the Lower Cieszyn Shale (Tithonian–Berriasian)** is a 300 m thick unit composed of grey marly mudstones, marls, and lutitic limestones intercalated with debris flow bodies of gravelly mudstones con-

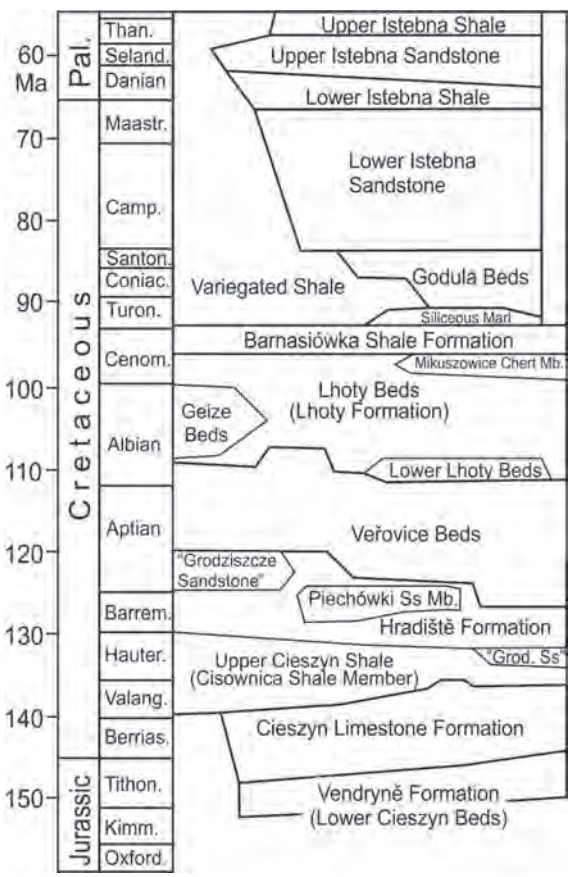

Fig. 2. Stratigraphic scheme of Late Jurassic–Cretaceous lithostratigraphic units in the Silesian Nappe in the Polish Carpathians, based on Vašíček et al. 2010, and references therein.

taining marl and limestone olistholithes (e.g., Słomka 1986; Górniak 2015). These deposits contain a mixture of microfossils and, to a limited degree, macrofossils from different marine environments (Bieda et al. 1963; Szydło 1997; Szydło and Jugowiec 1999).

The Cieszyn Limestone (upper Tithonian–Berriasian or upper Tithonian–upper Valanginian), 100–250 m thick, is dominated by commonly sandy, turbiditic calcarenites and calcilutites interbedded with marly shales. In some areas, conglomerate beds and calcarenites with components redeposited from shallow-marine platforms are present (Matyszkiewicz and Słomka 1994.)

The Upper Cieszyn Beds or **the Cisownica Shale Member (Valanginian–Hauterivian** or **Hauterivian** only**)**, ~300 m thick, is dominated by dark grey to black marly mudstones interlayered with numerous, very thin to thin layers (1–3 cm) of mostly cross-laminated, turbiditic, fine-grained calcareous sandstones, rare sandy limestones, and locally sideritic claystones (e.g., Burtan 1978). The sandstones display sharp erosive bases and transitional gradations to the overlying mudstones. These deposits are interpreted as turbiditic sandstone-mudstone couplets capped by hemipelagic mudstones. They are similar to the turbiditic facies C2.3 of Pickering et al. (1986), but the muddy portion is thicker in the investigated deposits (for facies by Pickering et al. used in this guidebook see Table 1). The Valanginian–Hauterivian age assessment is based on benthic foraminifers (Geroch and Nowak, 1963; Nowak 1968). According to Olszewska et al. (2008), the underlying Cieszyn Limestone extends, at a minimum, until the end of the Valanginian, which largely limits the Upper Cieszyn Beds to the Hauterivian. The sandstone turbidites were transported from the northwest and deposited above the calcite compensation depth (CCD). The Upper Cieszyn Beds are presented at Poznachowice Górne (Stop 3), where the approx. 200 m-thick section is the most expanded in the Polish Carpathians. The Cisownica Shale Member (Golonka et al. 2008) also embraces the lower part of the Hradiště Beds of previous authors [see below].

The Hradiště Formation = Hradiště (Grodziszcze) Beds (upper Hauterivian–middle Barremian – locally **lower Aptian),** 95–140 m thick, is represented by grey marly shales alternating with rare, thin, calcareous sandstone beds and marlstones. Locally, sandstone beds can be more frequent. In some areas, these facies are replaced by thick-bedded calcareous sandstones and debris-flow deposits containing exotic pebbles and blocks; this latter grouping were traditionally distinguished as the Grodziszcze Sandstone, which has subsequently been re-named the Piechówki Sandstone Member of the Hradište Formation (Golonka et al. 2008). In most exposures, the Hradiště Formation is Barremian, but has also been dated as lower Aptian in the eastern Polish Carpathians (Stępina section; Szymakowska 1977). In the Bielsko-Biała region, the deposition of the Hradište Formation ceased in the middle Barremian (Gedl 2003). The Hradiště Formation is presented at Poznachowice Górne (Stop 3).

The Veřovice Shale or **Veřovice Formation (Barremian–middle Albian),** approximately 180–500 m thick (Książkiewicz 1951), is composed of prevailing dark grey or black, mostly non-calcareous mudstones and siltstones (exceptionally, calcareous in the lower part of the unit), which are irregularly intercalated by thin- to medium-bedded fine-grained sandstones and contain sideritic concretions. Horizontal lamination occurs locally in the shales. The sandstones display ripple cross-lamination. The sandstone beds were probably deposited by episodic bottom currents. The absence of

Facies	Facies description	Interpretation
C2.1	Very thick/thick-bedded sand-mud couplets: very thick/thick-bedded sand-mud couplets, with well developed normal grading and commonly Tabc divisions.	Deposition from high-concentration turbidity current.
C2.2	Medium-bedded sand-mud couplets: medium-bedded sand-mud couplets, with well developed normal grading and commonly Tbcd divisions.	Deposition from high-concentration turbidity current.
C2.3	Thin-bedded, sand-mud couplets: thin-bedded sand-mud couplets, with well developed normal grading and commonly Tbcde divisions.	Deposition from low concentration turbidity current.

Table 1. Facies by Pickering et al. (1986) used herein.

$CaCO_3$ in the shales suggests deposition below the CCD. Moreover, lower bathyal depths have been inferred based of foraminifers (Szydło, 1997). Geochemical and organic matter analyses indicate both high plant detritus input from adjacent lands and high phytoplankton production (Gucwa and Wieser 1980; Wójcik-Tabol and Ślączka 2015). The Veřovice Shale has been dated to the Barremian–earliest Albian (Geroch and Nowak 1963; Szydło 1996, 1997) or, more broadly, the Barremian–Aptian (e.g., Szymakowska 1981; Olszewska 1997). In the Andrychów region, Veřovice Shale sedimentation terminated in the early Albian, while in the Bielsko-Biała region it ranges from the late Barremian to the late Aptian (Gedl 2003). In the western part of the Silesian Unit (Czech Republic), the Veřovice Shale is confined to the upper Aptian (Skupien, 2003) and is distinguished as the non-calcareous, 200–500 m thick Veřovice Formation (Golonka et al. 2008). According to Słomka et al. (2006), the thickness of the Veřovice Shale in the Polish Carpathians is stable and ranges from 180 to 250 m. Golonka et al. (2008) proposed limiting the Veřovice Formation to the non-calcareous black shales of the upper Aptian. According to these authors, the older, at least partly calcareous black shales in the Polish Carpathians previously considered to be part of the Veřovice Shale should be ascribed, rather, to the Hradište Formation. The Veřovice Shale is presented at Kozy and at Zagórnik (Stop 1 and Stop 2), where about the uppermost 70 m of the unit are exposed (Cieszkowski et al. 2001).

The Lhoty (Lgota) Beds or **the Lhoty Formation (Albian–middle Cenomanian)**, 300–350 m thick, is dominated by thin- and medium-bedded turbiditic sandstones and greenish grey, spotty mudstones (the dark spots are cross sections of trace fossils visible on parting surfaces). Locally, thick-bedded sandstones occur in the lower part of this unit, and spongiolithic cherts (Mikuszowice Chert) in the upper part. The Lhoty Beds have been subdivided into the Lower Lhoty Beds, the Middle Lhoty Beds (which constitute the vast majority of the Lhoty Beds in the Silesian Nappe) and the Upper Lhoty Beds or the Mikuszowice Chert. The locally occurring Lower Lhoty Beds, generally 80 m thick, are composed of thick-bedded, commonly amalgamated sandstones, channelized in the upper part (facies C2.1, C2.2 of Pickering et al. 1986), and interbedded with packages of thin- to medium-bedded, commonly graded turbidites. This unit is characterised by thickening-up trends (channelized depositional lobes?).

The Middle Lhoty Beds are 220 m thick in the Kozy quarry (Stop 1), and dominated by thin- and medium-bedded, mostly fine-grained turbiditic sandstones with well-developed Bouma (1962) intervals and interbedded dark grey to green mudstones; the sandstone/mudstone ratio is approximately 1:1 (Unrug 1959). Locally, isolated thick sandstone beds are present. Facies C2.3 of Pickering et al. (1986) prevails. Lenticular, mainly cross-laminated beds of fine-grained, well-sorted sandstone intercalated in shales have been interpreted as tractionites (Unrug 1959, 1977). Upper bathyal depths are proposed on the basis of foraminiferids (Książkiewicz 1975), but deposition below the CCD is suggested due to the presence of non-calcareous hemipelagites atop turbidite-hemipelagite rhythms. The Middle Lhoty Beds were likely deposited in distal, locally proximal depositional lobes and fan fringe settings.

The Upper Lhoty Beds (Mikuszowice Chert) are 50 m thick and only locally present. They consist of thin-bedded (rarely medium-bedded) sandstones that contain a considerable amount of biogenic silica, mainly as opal and chalcedony cement. In some beds, silica predominates and forms spongiolite chert bands. The sandstones are regularly interbedded with mudstones. Facies C2.3 of Pickering et al. (1986) prevails. In the northern marginal part of the Silesian Unit, the Lhoty Beds are replaced by the Geize Beds, which consist mainly of thick-bedded siliceous sandstones with spongiolites.

The Lhoty Beds were dated to the Albian–?Cenomanian (Geroch and Nowak 1963), but a middle Cenomanian age at the top of this unit was provided on the basis of foraminiferids and radiolarians (Bąk et al. 2001) and dinocysts (Gedl 2001; see also data from Jaminski 1995). The Lhoty Beds are presented in the Kozy and Rzyki sections (Stop 1 and Stop 2).

In the stratotype area, the **Barnasiówka Radiolarian Shale Formation (upper Cenomanian–lower Turonian)** consists of (1) a lower, 10 m-thick interval of thin-bedded silty and sandy turbidites (partly calcareous) interbedded with non-calcareous green and subordi-

nate black shales, (2) a middle interval, 2.2 m thick, with organic-rich black shales intercalated with green shales and bentonites – an equivalent of the Bonarelli Horizon – and (3) an upper interval, 1.2 m thick, with green and red siliceous-manganiferrous shales, including two Fe-Mn horizons and a single organic-rich black shale (Bąk et al. 2001). The stratigraphy of this formation is based on foraminifers, radiolarians, and carbon isotope data; it belongs to the *Whiteinella archaeocretacea* Zone (Bąk et al. 2001, 2005; Bąk, 2007). The lower and middle intervals correspond to the Ocean Anoxic Event 2 (OAE-2) $d^{13}C$ excursion, and the upper interval (transitional to the Godula Beds) belongs to the earliest Turonian post-excursion interval. The Cenomanian–Turonian boundary is placed within the 0.9 m-thick interval from the base of the first Fe-Mn layer to the base of the thin, organic-rich shale, directly underlying the second Fe-Mn layer (Bąk 2007).

The Siliceous Marl (Turonian) is a few metre-thick, exclusively local unit composed of turbiditic light grey or beige, thin-bedded siliceous marlstones, limestones and sandy marlstones. The beds show normal grading, with sharp bases. Their lower part is usually sandy. The upper part of the beds is strongly bioturbated, with well visible trace fossils, mainly *Chondrites* (Cieszkowski et al. 2003). The Siliceous Marls is presented in the Rzyki section (Stop 2).

The Godula Beds (Turonian–Santonian), 400–600 m thick in the Beskid Mały range (Książkiewicz 1951), commonly contain thick-bedded sandstones and conglomerates apart from the dominant thin-bedded flysch. These are interpreted as non-channelized sediments, together with the channel and interchannel facies of deep-sea fans and depositional-lobe facies in the eastern part of the Beskid Mały range. To the east, they are sometimes replaced by variegated shales with a younger base (Słomka 1995).

The Istebna Formation (Campanian–Paleocene) (*sensu* Menčík 1983; Wójcik et al. 1996; Picha et al. 2006), also known as the Istebna Beds in the Polish part of the Outer Western Carpathians, is up to 2100 m thick, and crops out across large areas of the Silesian Nappe (Unrug 1963; Menčík and Tyráček 1985; Żytko et al. 1989). It is subdivided into the Lower Istebna Beds and the Upper Istebna Beds, with further subdivision of the latter unit into the Lower Istebna Shale, the Upper Istebna Sandstone, and the Upper Istebna Shale (cf. Burtan 1937; Burtanówna et al. 1937; Burtan 1973). These subdivisions are distinct in the stratotype area in the Beskid Śląski Mountains. To the east in the Beskid Mały Mountains, the Lower Istebna Shale and the Upper Istebna Sandstone pinch out locally, so the remaining subdivisions are indistinguishable and, as such, merged (Książkiewicz 1951).

The Istebna Formation is dated to the lower Campanian–Danian (Hanzlíková 1972). However, according to Skupien and Mohamed (2008), its lower boundary ranges from the end of the Campanian to, most likely, the beginning of the Maastrichtian. Microfossils and rare macrofossils are indicative of a Campanian–Paleocene age in the Beskid Śląski Mountains (e.g., Geroch 1960; Wagner 2008). The boundary between the Lower Istebna Beds and the Upper Istebna Beds is located close to the Cretaceous–Paleogene boundary (Bieda et al. 1963; Nescieruk and Szydło 2003).

The Lower Istebna Beds (Campanian–Maastrichtian), 600–1600 m thick, are composed mainly of thick-bedded, mainly medium- to coarse-grained, locally conglomeratic sandstones. They are mostly poorly sorted oligomictic quartz arenites, arkoses, or greywackes (Kamieński et al. 1967, Bromowicz et al. 1976; Bromowicz 2001), which are dirty white with rusty spots, pale yellow, rusty cream, or brownish in colour. The sandstones are highly porous, poorly cemented with clay minerals and, locally, with silica. In some beds, stronger concretionary cementation is present. Bed thicknesses regularly attain 5 m or, rarely, are even greater. Commonly, these beds are amalgamated and with erosive, sometimes (i.e., not rarely) channelized bases. The thick-bedded sandstones can be ascribed to a few lithofacies, including sandy conglomerates, sandstones, and sandstones with mudstones, and rarely to sedimentary deformed deposits (Strzeboński 2003). Some of these beds and/or bed packages are interbedded by thin layers of laminated sandy mudstones with abundant plant detritus or thin-bedded turbiditic sandstones (Unrug 1963). Moreover, sandstone-mudstone, mudstone, and gravelly mudstone facies asso-

ciations can be distinguished (e.g., Unrug 1963; Menčík 1983; Strzeboński 2005, 2015, 2022). In some sections, "*Inoceramian*-type" packages of thin- and medium-bedded calcareous turbiditic sandstones and shales, up to 150 m, occur (Teysseyre 1947; Skoczylas-Ciszewska and Kamieński 1959).

The thick-bedded sandstones originated from non-turbulent gravitational, sandy-debrite, or turbiditic flows and were mainly deposited in the channel and overchannel, and rarely in depositional lobe areas, with regards to the classical fan system (Mutti and Ricci Lucchi 1972). However, they are referred to a siliciclastic ramp or apron that formed in close proximity to its clastic material source (Strzeboński 2003, 2005, 2015, 2022). The thinner sandstone beds are mostly turbidites. The source was situated on the Silesian Ridge (the so-called Silesian Cordilliera or Silesian Ridge) rimming the Silesian Basin from the south (Książkiewicz 1962; Unrug 1963, 1968; Ślączka 1986; Strzeboński 2003, 2015). The driver of source activity can be explained by either eustatic sea level fall and/or tectonic elevation of the Silesian Ridge. Axial transportation from west to east, and even from the northwest, was also present, the latter probably forced by the basin morphology. Gravity-driven, clastic material flows were partially stopped and rebounded from the slope of the Subsilesian elevation/slope, which bordered the basin from the north (Książkiewicz 1962; Unrug 1963 1968; Ślączka 1986; Ślączka et al. 2006). In the Moravskoslezské Beskydy Mountains (Czech Republic), the clastic material of the Istebna Formation was additionally transported from the northwest and north-northwest, probably from the Baška Ridge, which is the westernmost elevated part of the Subsilesian zone, or from the southeast margin of the Bohemian Massif (Menčík 1983; Birkenmajer 1985; Słomka 1995). The Lower Istebna Beds are presented in the Dąbie–Stradomka river section (Stop 4).

Subsilesian Nappe

The Subsilesian Nappe is a composite structure that usually appears on the surface in narrow zones between the Silesian Nappe and the Magura or Skole nappes, or in tectonic windows close to the margins of the Magura and Silesian nappes. It contains Cretaceous–Paleogene deposits, mainly variable marls that are usually strongly tectonized and poorly exposed. Paleogeographically, it is located at an elevation between the Skole and the Silesian basins (Węglówka Ridge) and/or on the slopes of the Silesian Basin. Locally, the ridge(s) supplied clastic material to the basins (Ślączka et al. 2006; Słomka et al. 2006). The deposits of the Subsilesian nappe are laterally variable, and their correlation remains insufficient.

The **Upper Cieszyn Beds (Valanginian–Hauterivian), Hradiště (Grodziszcze) Beds (upper Hauterivian–middle Barremian)** and **the Veřovice Shale (Barremian–middle Albian), and the Lhoty Beds (Albian–Cenomanian)** are the same as in the Silesian Nappe (see previous chapter), because they were deposited in the same Proto-Silesian Basin in the rifting stage of development.

The Jasienica (Fucoid) Marl (Cenomanian), ~15 m thick, is composed of dark grey to light grey and greenish grey, thin-bedded, locally silicified "spotty" marlstones, intercalated with rare, commonly discontinuous thin beds and laminae of medium-grained sandstones and occasional mm-thick mudstone laminae. The marlstones contain sand and silt grains of quartz, light mica, glauconite, and carbonates, together with foraminifera tests, rare echinoderm spines, and dispersed carbonized plant detritus. The topmost part of the Jasienica Marl contains black shales, interpreted as a temporal equivalent of the Bonarelli Level deposited during OAE-2. The Jasienica Marl was distinguished as the "fucoid marls" or "spotty marls" by Skoczylas-Ciszewska (1960) and interpreted as pelagic and hemipelagic deposits (Uchman et al. 2013). The Jasienica Marl is presented in Nowe Rybie (Stop 5).

The Żegocina Marl (upper Turonian–lower Coniacian–?lower Campanian), up to 15 m thick, is represented by creamy, light greenish, hard, partly silicified, thinly to medium bedded marlstones (Skoczylas-Ciszewska 1960) with rare, discontinuous, thin intercalations of medium-grained sandstones and mudstones. The extent of silicification increases towards the top. It is poorly bioturbated, mostly with *Chondrites*, *Planolites*, and *Thalassinoides*. The age assignment is based on calcareous nan-

noplankton (Kędzierski et al. 2012); Jugowiec-Nazarkiewicz and Jankowski (2001) identified lower Campanian calcareous nannoplankton in some outcrops. The Żegocina Marl is presented in Nowe Rybie (Stop 5).

The Węglówka Marl (lower Coniacian–Paleocene?), up to 70 m thick, is a succession of variegated, mostly reddish, and to a lesser extent greenish, mostly massive marls. The marls are bioturbated, but trace fossils are poorly visible. Some intervals display *Zoophycos*, *Chondrites,* and *Planolites*.

The Frydek Marl (Campanian–Maastrichtian), at least 100 m thick, is composed of grey and dark grey marls intercalated with rare single sandstone beds or packages, as well as with debris flow muddy conglomerates with exotic blocks of crystalline and sedimentary rocks. Lenses and beds of sideritic dolomites are also present (Skoczylas-Ciszewska 1956). Chronostratigraphic determinations are based on foraminifers and calcareous nannoplankton (Brandys 2000; Bielawska 2002; Jugowiec-Nazarkiewicz 2007).

The Rybie Sandstone (Campanian–Maastrichtian–?Paleocene), up to 650 m thick, is composed of grey, yellow weathering, thin-, medium- to thick-bedded glauconitic sandstones intercalated with grey shales and conglomerates. In the lower part, they contain abundant rose feldspar supplied from crystalline rocks. Horizons of conglomerates and debris flow deposits with exotic pebbles and blocks (e.g., Jurassic limestones, Carboniferous coal) are locally present (Skoczylas-Ciszewska 1956). The sandstones form isolated lithosomes, deposited mostly in slope gullies or channels and in lobes at their termination. Jugowiec-Nazarkiewicz and Jankowski (2001) suggested a Campanian age of this unit on the basis of calcareous nannoplankton, but it is unclear if this assemblage is *in situ*. The **Rajbrot Sandstone** (Skoczylas-Ciszewska, 1956) is a more or less coeval unit of similar lithology, but its beds are thinner. Its relationship to the Rybie Sandstone is unclear. Thin-bedded shales and sandstones from an isolated locality in the western part of the Polish Carpathians, distinguished as the **Pisarzowice Beds** (?Cenomanian–Turonian–?Coniacian), about 50 m thick, lie below the Frydek Marl (Liszkowa and Nowak 1960), but otherwise are still poorly known.

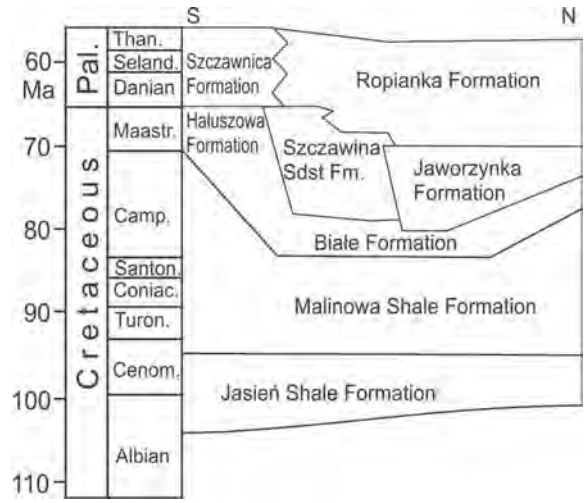

Fig. 3. Stratigraphic scheme of Late Jurassic–Cretaceous lithostratigraphic units in the Magura Nappe in the Polish Carpathians (based on Oszczypko et al. 2005).

Magura Nappe

The Magura Nappe is the southernmost large tectonic unit of the Polish Outer Carpathians. The mid-Cretaceous to lowermost Miocene flysch-dominated deposits of this nappe accumulated in the long-lived Magura Basin (e.g., Oszczypko 1992). The older (Jurassic–Lower Cretaceous) deposits of the basin are involved in the Pieniny Klippen Belt. Traditionally, the Santonian–Paleocene formations are known as the Inoceramian Beds or the Ropianka Formation. However, in the last two decades, these deposits have been subdivided into several formations, and the Ropianka Formation is formally limited to the upper Inoceramian Beds (Fig. 3).

The Jasień Formation (Albian–Cenomanian) is exposed only locally. It is at least 15 m thick and composed of strongly tectonized, bioturbated (with *Planolites* and *Chondrites*), green and olive green, non-calcareous mudstones (Oszczypko et al. 2005).

The Malinowa Formation (Turonian–late Santonian), 50–100 m thick, is composed of red, non-calcareous mudstones intercalated with

non-calcareous green mudstones and rare sandstone beds. The frequency of intercalations increases towards the top (Oszczypko et al. 2005). This is a prime example of deep-sea red beds.

The Hałuszowa Formation (**late Santonian–Campanian),** 100 m thick, is dominated by grey turbiditic marls with intercalations of thin- and medium-bedded turbiditic sandstones and red marls (Oszczypko et al. 2005).

The Białe Formation (early Campanian–early Maastrichtian), up to 100 m thick, is composed of thin- to medium-bedded, very fine-grained, calcareous, turbiditic sandstones intercalated by grey-bluish and grey-yellowish or greenish and yellowish calcareous mudstones and siltstones. In the middle and upper parts of the formation, several packages, each a few metres thick, of thin- to thick-bedded sandstones and marls, with rare intercalations of red shales and marls, are present (Oszczypko et al. 1991). The uppermost portion of the formation contains thin to medium beds of turbiditic calcilutites (Cieszkowski et al. 1989). The marly intercalations contain abundant *Nereites irregularis* (Schafhäutl). Generally, this formation exhibits coarsening and thickening upwards trends in exposed sections (Oszczypko et al. 2005).

The Jaworzynka Formation (middle Campanian–early Maastrichtian), 200 m thick, is composed of thick- to very thick-bedded, green-grey, non-calcareous sandstones (with biotite) and fine-grained conglomerates intercalated by grey-greenish, non-calcareous shales in its lowest quarter. Higher up, thick-bedded, medium- to fine-grained muscovitic sandstones are present. The lower part displays paleotransport from the southeast, and the upper part from the west-northwest and west (Oszczypko et al. 2005).

The Szczawina Sandstone Formation (middle Campanian–early Paleocene), up to 350 m thick, is dominated by thick-bedded, grey-green, coarse- to fine-grained, muscovitic, calcareous sandstones with thin intercalations of green, black, locally red shales and thin- to medium-bedded sandstones. In some areas, a 50–80 m-thick succession of thin-bedded turbidites within the formation is distinguished as the Maastrichtian **Krzysztonów Member** (Oszczypko et al. 2005).

The Ropianka Formation (Maastrichtian–Paleocene) is up to 250 m. In the lower part, it is composed of grey or greenish, turbiditic, thin- to medium-bedded flysch deposits, consisting of fine- to very fine-grained, calcareous, muscovitic sandstones intercalated with grey or greenish calcareous or non-calcareous mudstones or marlstones. Intercalations of thick-bedded, coarse- to medium-grained sandstones and red, calcareous shales are present. In the upper part of the formation, dark-grey, medium-bedded, very fine-grained, non-calcareous sandstones containing glauconite and biotite are present. The uppermost part of the formation is characterized by dark grey, thin-bedded turbidites intercalated with light grey mudstones. The Ropianka Formation is presented in the Słopnice–Słopniczanka river section (Stop 6).

In its northern zones, the higher part of the Magura Nappe succession contains **the Variegated Shale (Łabowa Shale Formation; lower Eocene or lower–middle Eocene),** which is mainly composed of reddish and greenish, muddy to clayey shales (e.g., Książkiewicz 1962; Oszczypko 1991; Birkenmajer and Oszczypko 1992; Oszczypko et al. 2005), a type of deep-sea red bed similar those found in the Alps, the Apennines, and the Basque Basin. They are nearly or totally carbonate-free (Leszczyński and Uchman 1991), hemipelagic or diluted, mainly thin-bedded turbiditic deposits. In the southern part, thin- to medium-bedded turbiditic deposits are present (e.g., the Szczawnica Formation). The upper Middle Eocene and Oligocene part of the succession is dominated by the thick-bedded deposits of the Magura Group. The youngest deposits are dated to the lowest Miocene.

Dukla Nappe

This nappe is exposed in the southeastern part of the Polish Carpathians (from where it extends to Slovakia and Ukraine), in some tectonic windows in the Magura Nappe, and locally in the front of this nappe. The vast majority, however, is covered by the Magura Nappe. The Dukla Nappe is not on the excursion route.

The oldest deposits in the Dukla Nappe are the **Łupków Beds (?Santonian–Maastrichtian)**, 900 m thick, which contain dark grey, rarely brownish, marly mudstones and siltstones intercalated by dark grey, thin-bedded, fine-grained calcareous sandstones. Rarely, grey marlstone beds are present. They transition upwards to the **Cisna Beds (Maastrichtian–Paleocene)**, which are up to 1200 m thick. They are dominated by coarse-grained, locally fine conglomeratic, calcareous greywacke sandstones, which are micaceous in the upper part. Moreover, they are intercalated by dark grey mudstones and siltstones interbedded by thin-bedded, laminated sandstones. In the western part of the nappe, the Łupków and Cisna Beds lose their individuality and are collectively referred to as the **Inoceramian Beds**, which are 1200 m thick. These, in turn show a thickening up trend and more frequent light grey mudstones. All of these divisions are mostly turbiditic.

Younger divisions include the Majdan Beds (Paleocene), Hieroglyphic Beds (Paleocene–Eocene), Przybyszów Beds (middle Eocene), Green Shale (upper Eocene), Globigerina Marl (topmost Eocene), Menilitic Beds (Oligocene), Krosno Beds (Oligocene), Podgrybowskie Marl (Oligocene), and the Grybów Shale (Oligocene). All are deep-sea deposits, mostly turbiditic or hemipelagic (Ślączka 1971).

Skole Nappe

The Skole Nappe is the most external tectonic unit in the northern Carpathians that contains Cretaceous deposits. It is located on the northeast bend of the Carpathian orogenic arc in Poland and Ukraine (Jankowski et al. 2004) and is composed of deep-marine, Lower Cretaceous to Lower Miocene deposits that accumulated in the Skole Basin, the fill of which was folded and thrust northward during the Miocene (e.g., Gągała et al. *2012*). Deposits of this nappe are not presented during the excursion.

Sedimentation in the Skole Nappe started in the **Hauterivian** with mostly dark mudstones (**the Bełwin Mudstone** and **the Spas Shale**), which pass into **Cenomanian** dark-greenish shales with radiolarites (**Dołhe Radiolarian Shale**) (Gucik 1963). In the **Turonian**, changes in the tectonic regime – from extensional to compressional – in the Skole Basin and its northern borderland initiated the flysch-type sedimentation of the Ropianka Formation.

The Ropianka Formation or **the Inoceramian Beds (Upper Cretaceous–Paleocene)** is 1500 m thick and occupies a large part of the Skole Nappe (e.g., Kotlarczyk 1978, 1979; see also Bromowicz 1974; Kotlarczyk et al. 1988; Leszczyński et al. 1995; Ślączka and Miziołek 1995). It is subdivided into four members (Kotlarczyk 1978), each of which starts with calcareous "flysch" facies and ends with "normal flysch" facies (Kotlarczyk 1978, 1988). In the past decade, the Ropianka Formation was the subject of several, mostly stratigraphic investigations (e.g., Leszczyński et al. 1995; Gasiński and Uchman 2009, 2011; Gasiński et al. 2013; Salata and Uchman 2013; Kędzierski et al. *2015*; Łapcik et al. *2016*; Kowalczewska and Gasiński 2018; Łapcik 2018; Waśkowska et al. 2019; Wierzbicki and Kędzierski 2020; Slimani et al. 2021).

The **Cisowa Member** (**Turonian–lower Campanian**) is exposed, but can be distinguished only in the Cisowa IG-1 borehole (Wdowiarz et al. 1974).

The **Wiar Member** (**lower Campanian–lower Maastrichtian**), along with typical turbiditic deposits, contains the "Fucoid Marl" (Bromowicz 1974; Kotlarczyk 1978).

The **Leszczyny Member** (**lower Maastrichtian–lower Paleocene**), along with typical turbiditic deposits, contains conglomerates containing exotic pebbles, as reported by Wdowiarz (1949), Bromowicz (1974), Kotlarczyk (1978) and Dżułyński et al. (1979). Moreover, it contains the Baculites Marl (Węgierka Marl), developed as 1) olistoliths of light marls, 2) bedded marls, and 3) sandy debris flow sediments with blocks of limestones and marls (Burzewski 1966; Kotlarczyk 1978; Geroch et al. 1979). It is associated with conglomerates containing exotic material and large olistoliths of Tithonian limestones that occur south of Przemyśl (Bukowy and Geroch 1957; Kotlarczyk 1988). Maastrichtian pebble mudstones and conglomerates with exotic materials are distinguished as the Makówka Slump Debris (Kotlarczyk 1978, 1988; Dżułyński et al.

1979; Malata 2001). In the Wiar and Leszczyny members, a turbiditic system was recognized; it contains channelized depositional lobes, which transit to non-channelized lobes (Łapcik 2019). In this member, the Cretaceous–Paleogene boundary is confined to narrow intervals on the basis of planktonic foraminifers (Gasiński and Uchman 2011), but some discrepancies with dating based on calcareous nannoplankton and dinocysts do exist (Kędzierski et al. 2015).

The **Wola Korzeniecka Member** (**Paleocene**) is composed of thin-bedded flysch. The non-calcareous shales of this member suggest a deepening of the Skole Basin (Malata and Poprawa 2006) in transition to the overlying **Variegated Shale Formation** (**Eocene**; Rajchel 1990; Leszczyński and Uchman 1991; Bąk et al. 1997; Barwicz-Piskorz and Rajchel 2012) and the younger **Hieroglyphic Formation** (**Eocene**; Rajchel 1990). The Oligocene to early Miocene is represented by the Menilite Formation and Krosno Formation

FIELD STOPS

Stop 1:
Kozy – abandoned quarry. Lower Cretaceous of the Silesian Nappe
(*Alfred Uchman, Mateusz Szczęch*)

The stop is located at the base of the Beskid Mały range in the western part of the Polish Flysch Carpathians (Fig. 4). The abandoned quarry at Kozy (now partly a recreation area; GPS coordinates: N 49° 49.978'; E 19° 09.875') contains a thick portion of the Silesian Nappe succession. In the lower part, a higher portion of the Veřovice Shale (Barremian–lowermost Albian) is exposed, mainly along the roads leading to the higher levels of the quarry. It

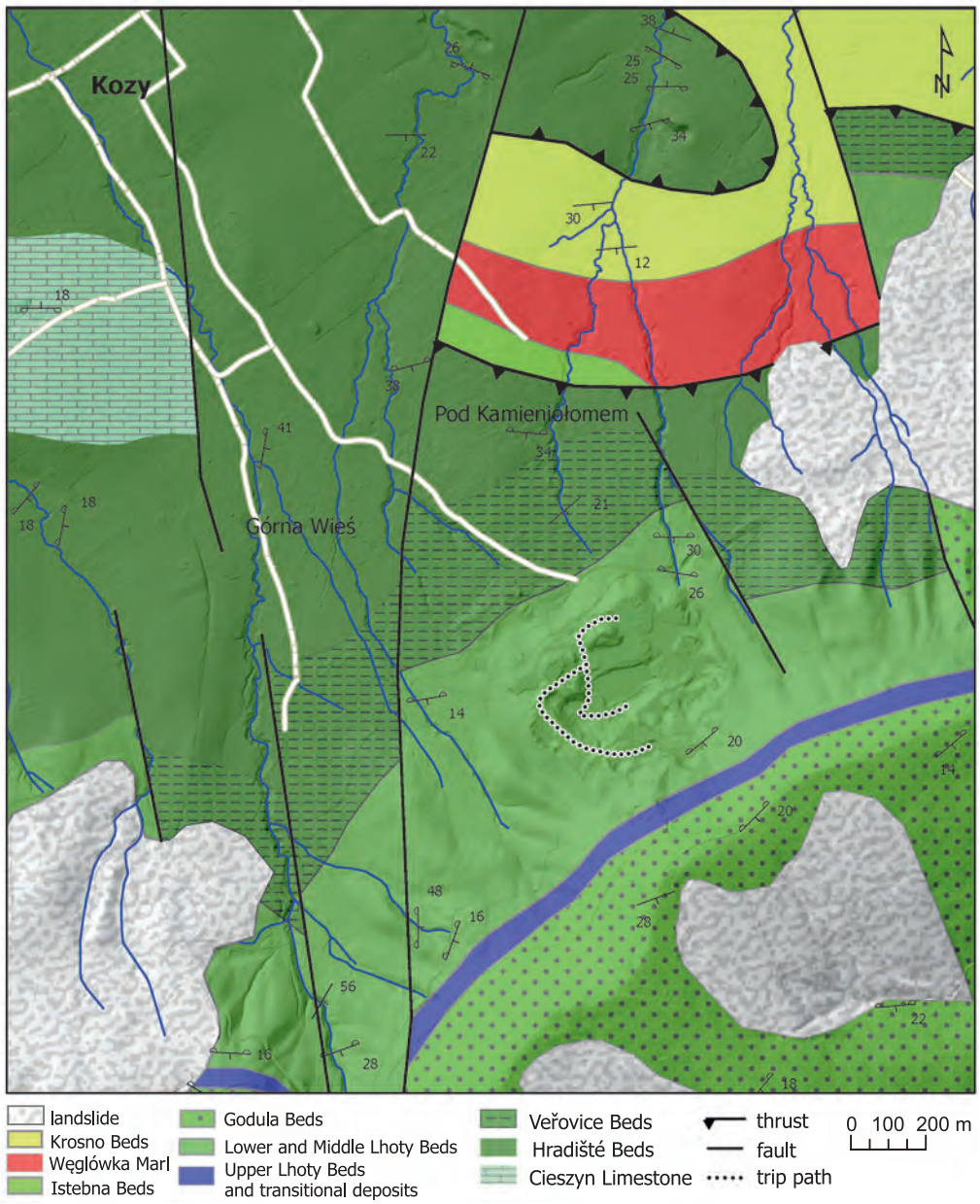

Fig. 4. Geological map of Kozy quarry (Stop 1) in the Silesian Nappe, based on Nešcieruk and Wójcik (2014, 2018).

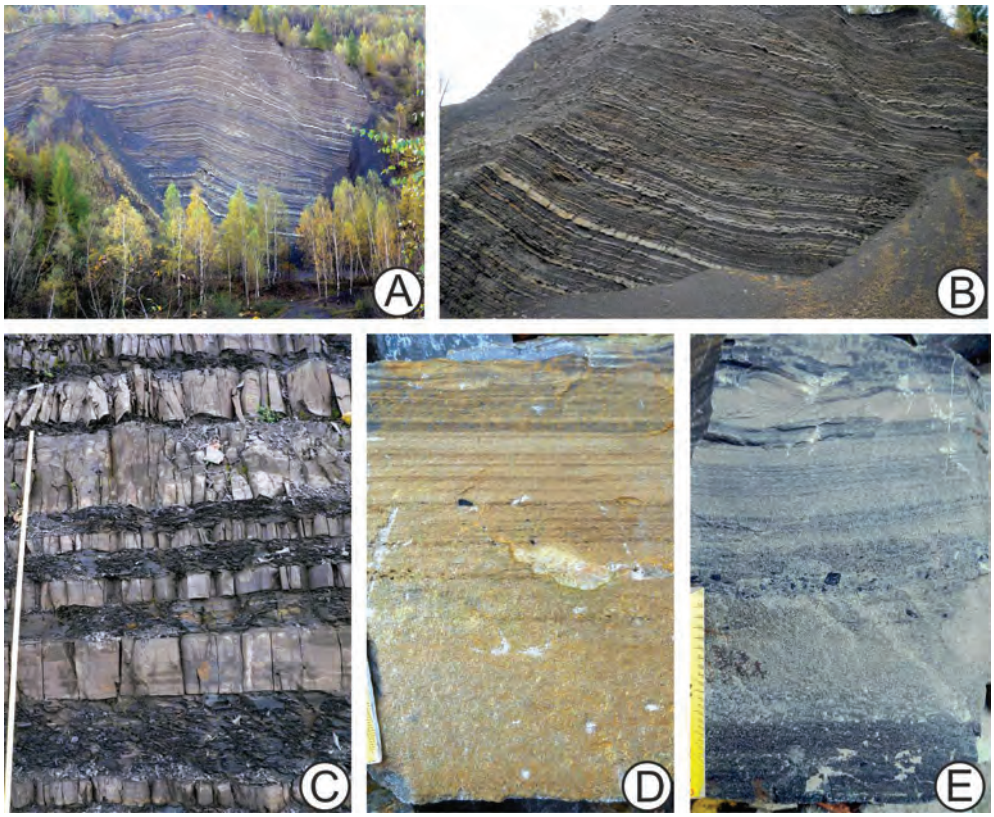

Fig. 5. The Lhoty Beds in Kozy quarry. **A, B** – General view of the Middle Lhoty Beds outcrops. **C** – Sandstone beds intercalated with siltstones and mudstones. **D, E** – Ta, Tb, and Tc Bouma intervals in two beds. In E, coal clasts between Ta and Tb.

is composed mostly of dark grey and black non-calcareous mudstones and siltstones, with intercalations of thin-bedded sandstones. The topmost part contains the dinocyst *Litosphaeridium arundum* Davey, which has a lowest known occurrence in the mid-Albian (Gedl 2003). The Veřovice Shale will be presented in more detail at the next stop.

The main part of the quarry is occupied by the Lhoty Beds (Albian–middle Cenomanian). It is 220 m thick in the area, of which 150 m is exposed in the quarry (Unrug 1959). The lower part, up to the lake level, is an equivalent of the Lower Lhoty Beds, which are sandier than the higher, substantially thicker Middle Lhoty Beds. The deposits of the latter are composed of thin- and medium-bedded, mostly silicified fine-grained turbiditic sandstones with well-developed Bouma intervals (Fig. 5), and several non-turbiditic banded sandstone beds. Thick sandstone beds are rare. Individual beds generally have the same thickness at outcrop scale, commonly at distances of more than 100 m. Only some beds have variable thickness or pinch out on outcrop scale. In general, thinning and thickening trends are not recognized, but intervals with thicker and thinner beds are present; this is suggestive of an accretionary mode of deposition compensated by subsidence. The sedimentary material (mainly quartz, but also feldspar or coal debris) has been supplied from the west and southwest.

In the equivalent of the Lower Lhoty Beds, the dinocyst *Apteodinum maculatum grande* (Cookson and Heughes) points to an upper Albian age assignment (Gedl, 2003). Non-calcareous, greenish and grey shales contain poorly diverse trace fossils, mainly *Chondrites targionii* (Fig. 6A), *Thalassinoides* isp. (Fig. 6B), *Planolites beverleyensis* (Fig. 6B), *P. montanus,* rarely *Scolicia strozzii* (Fig. 6C), and ?*Rhizocorallium* isp. (Fig. 6D).

The highest part of the quarry (c. 43 m) is occupied by an equivalent of the Upper Lhoty Beds, the Barnasiówka Radiolarian Shale Formation, and the Siliceous Marl. However,

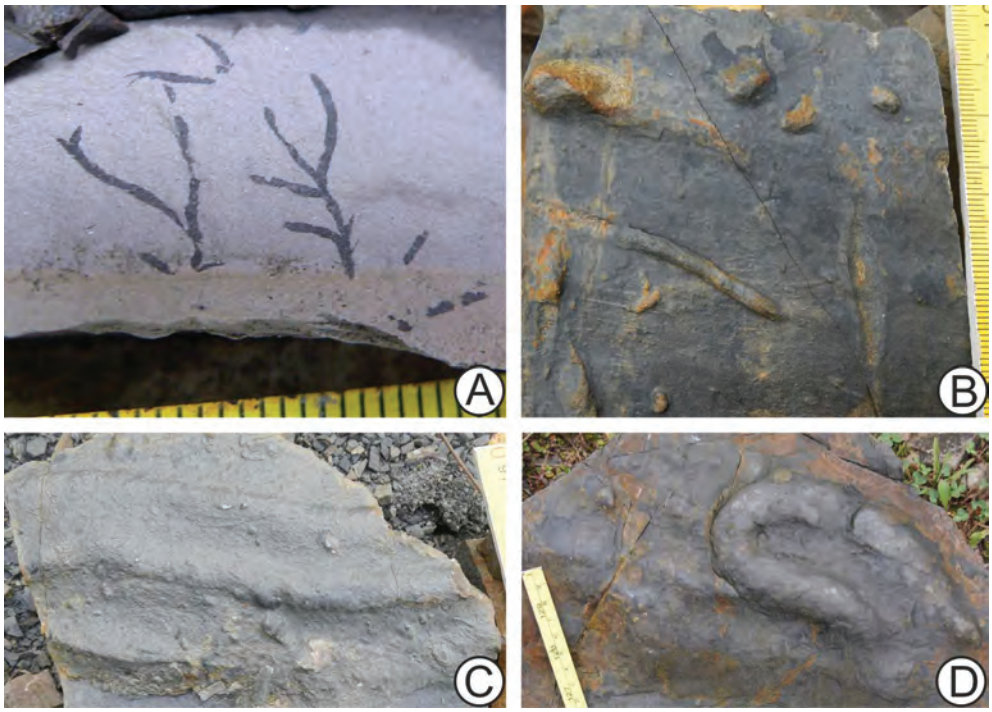

Fig. 6. Trace fossils in the Lhoty Beds in Kozy quarry. **A** – *Chondrites targionii*, endichnion in mudstones. **B** – *Planolites beverleyensis* (thinner ridges) and ?*Thalassinoides* isp. (larger mounds and ridges). Hypichnia on a sandstone bed. **C** – *Scolicia strozzii*, hypichnion on sandstone bed. **D** – ?*Rhizocorallium* isp., hypichnion on sandstone bed.

these units cannot be distinguished at Kozy, because the lithological features of these units are absent or marginally expressed. Here, this is a thin-bedded flysch with very fine- and fine-grained turbiditic sandstones and grey marly mudstones, marls or silicified marls. Most of the beds initiate with fine-grained sandstones, which pass into silicified marls and marly mudstones at the top. These deposits contain the trace fossils *Chondrites intricatus*, *Ch, targionii, Planolites beverleyensis*, *P. montanus*, *Thalassinoides* isp., *Ch. affinis*, *Trichichnus linearis*, *Taenidium* isp., and *Pilichnus dichotomus*. Their age is uncertain, although at least in the upper part it is supposed to be lower Turonian. If so, depositional equivalents of the Bonarelli Level should be exposed, but no macroscopic evidence for OAE-2 has been observed.

Just above the quarry, thick beds of glauconitic, locally conglomeratic sandstones belonging to the lowest part of the Godula Beds (Turonian–Santonian) are poorly exposed in the forest. In addition to quartz, they contain chert and limestone clasts.

Stop 2:
Zagórnik and Rzyki–Wieprzówka river section. Lower–Upper Cretaceous of the Silesian Nappe

(*Alfred Uchman, Piotr Łapcik, Mateusz Szczęch*)

The section is located at the foot of the Beskid Mały range in the western part of the Silesian Nappe (Figs 1, 7–9). It was presented by Cieszkowski et al. (2001, 2003) and Uchman and Cieszkowski (2008a, b) on previous excursions. In the lowest part of section (starting point GPS coordinates: N 49° 50' 00.6''; E 19° 22' 16.9''; ±6 m), the upper part (~32 m thick) of the Veřovice Shale is exposed along the incised river channel. The lower part of the Veřovice Shale is covered by fluvial gravel and mudstones behind a system of ?Holocene faults. The beds are slightly folded and generally dip towards the south. They are sliced by several small faults and thrusts that disrupt the continuity of the section but do not disrupt the stratigraphic order.

The Veřovice Beds are prevailingly com-

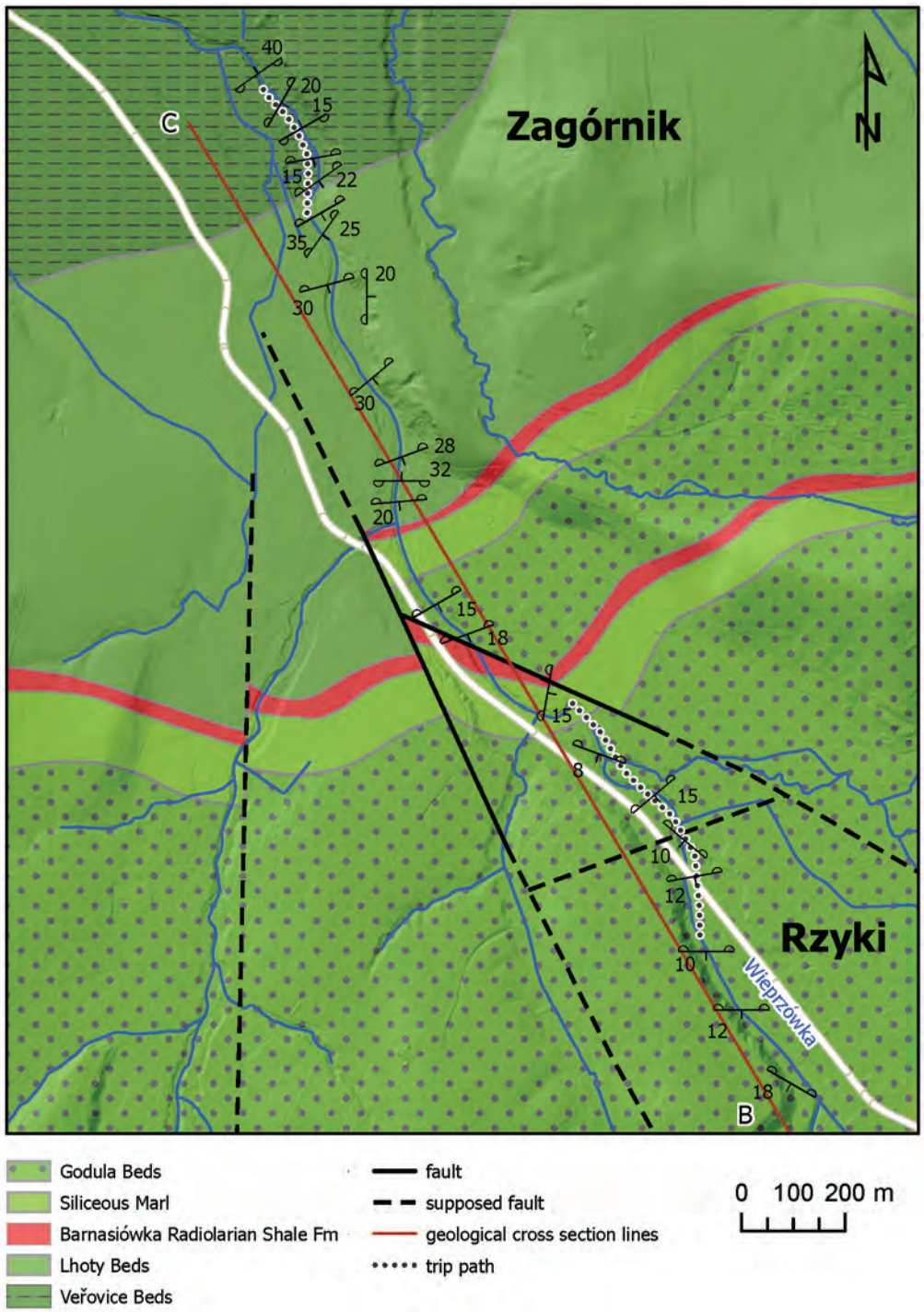

Fig. 7. Geological map of the Rzyki section (Stop 2) in the Silesian Nappe, based on Uchman and Cieszkowski (2008a, b). B–C – part of geological cross section line for section on Fig. 8.

posed of dark grey and black, non-calcareous, partly siliceous mudstones and siltstones, with a considerable contribution of heterolithic deposits. They are irregularly intercalated by thin- to medium-bedded fine-grained sandstones (Figs 10, 11). All the lithologies are subdivided into facies (Table 2). The sandstones are horizontally laminated and/or ripple cross-lam-

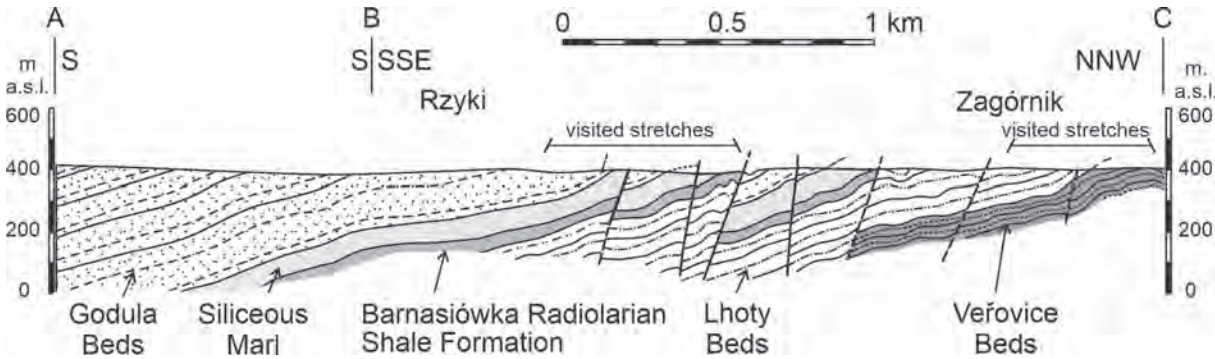

Fig. 8. Cross section along the Wieprzówka river (modified after Uchman and Cieszkowski 2008a).

inated. In places, there are ferruginous concretions. More or less sandy packages can be distinguished in the section. These deposits are considered basin plain facies with periods of bottom current activity (Uchman and Cieszkowski 2008; Waśkowska et al. 2009); here, they are assigned to basin plain and lower slope deposits. The presence of turbidites together with a variety of heterolithic deposits (mostly of turbulent and transient turbulent nature; see Baas et al. 2016 and references therein) indicates that the local seafloor was relatively dynamic, with erosional and depositional influences from different types of sediment gravity flows (Fig. 11). Contributions from contourites (see Strzeboński et al. 2009) and hyperpycnites are not excluded.

In the presented locality, the dinocyst *Cerbia tabulata* from the uppermost part of the Veřovice Shale points to the lowest Albian (Gedl 2003). Based on the foraminifer assemblage and the non-calcareous character of sediments, deposition in the lower bathyal depth is suggested (Książkiewicz 1975; Szydło 1997). The dark mudstones are organic-rich sediments supplied with plant detritus from adjacent lands and, occasionally, by high phytoplankton production, where TOC reaches ~4% (Strzeboński et al. 2009; Pavluš and Skupien 2014; Wójcik-Tabol and Ślączka 2015). These would be easily considered an example of Lower Cretaceous anoxic deposits (e.g., Bralower et al. 1994), such as these related to the early Aptian Selli event (OAE 1a) or the early Albian Paquier event (OAE 1b), but exact stratigraphic assignment is problematic, and there is no evidence of improved oxygenation between two distinct packages of

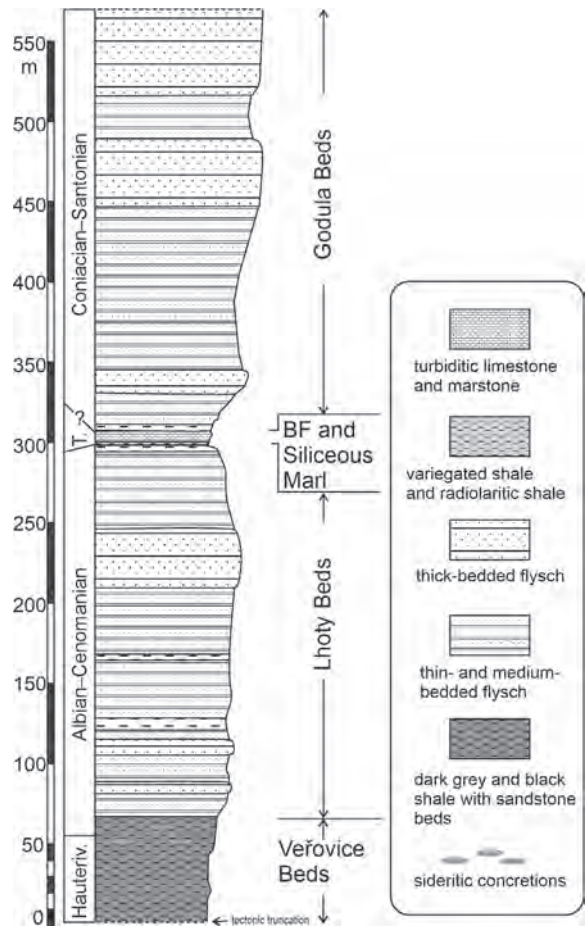

Fig. 9. Generalized stratigraphic column of the area (modified after Uchman andCieszkowski, 2008a).

anoxic deposits which could be tied to these events. According to Wójcik-Tabol and Ślączka (2015), deposits associated with OAE 1b are present in the transition to the overlying Lhoty Beds based on the carbon isotope anomaly

Facies name	Grain size	Bed thickness	Description	Depositional processes
Facies F1: Massive graded and ungraded sandstone	Non-calcareous and fine- to coarse-grained sandstone	2.5 to 80 cm, mean ~18.3 cm	Tabular sharp erosional bases, load features, and sole marks. Massive, graded to ungraded. Amalgamation and abrupt grain size brakes. Rare intraformational mudclasts (concentrated to the basal and/or top part of the massive bed).	Non-tractional dumping of sediment suspension from a highly concentrated flow with turbulent or transient turbulent nature
Facies F2: Structured sandstone	Non-calcareous fine- to coarse-grained sandstone	<1 to 60.5 cm thick, mean ~6.4 cm (thickness changes and lateral pinch-outs)	Sharp, frequently erosional bottoms with sole marks (mostly trace fossils and flute marks). Planar parallel stratification (more abundant in thicker beds), ripple cross-lamination, climbing ripples, wavy lamination, convolutions, and plastic deformation. Rare mudclasts. Trace fossils: mostly *Ophiomorpha*, *Thalassinoides*, and rarely *Protovirgularia*, *Phycosiphon* and *Palaeophycus*.	Turbulent or transient turbulent currents, which allowed the formation of various traction sedimentary structures. Referred to as low-density turbidites. The high rate of bed aggradation resulted in climbing ripple lamination and sediment deformation due to escape of pore water
Facies F3: Banded division	Fine- to medium-grained sandstone	1.5 to 41 cm, mean ~11.7 cm	Tabular sharp bottoms with sole marks. Distinctive black bands and laminae (mostly dark mudstone aggregates and coalified plant detritus) intercalated with yellowish to whitish sand, which may show planar parallel lamination, ripple cross-lamination or be massive. The bands and laminae are from 1 mm up to a few cm thick. Both proportions and thickness of intercalated bands may change in one banded division, and either may dominate. Plastic deformations and interbed load structures (mostly loaded ripples at the top of the bed) are abundant.	1) the banding formed in the upper-stage plane-bed regime and tractional reworking beneath mud-laden transitional plug flows (Stevenson et al. 2020), or 2) repetitive autocyclic formation and *en masse* freezing of cohesive traction carpets due to the settling of flocculated mud and entrapped coaly detritus, with the intervening episodes of tractional sand deposition.
Facies F4: Muddy chaotic sandstone	poorly sorted, muddy sandstone (fine- to medium-grained) to sandy mudstone	14.5 to 300 cm, mean ~153.6 cm	Sharp contact with underlying deposits, mostly without signs of erosion. Massive, non-graded beds. Clasts (up to 30x10 cm) of non-calcareous black and poorly calcareous grey mudstones are scattered in the matrix. Some larger clasts show bedding, which correspond to intercalations of facies F2, F5, F6, and F7.	Deposits of laminar and cohesive flows. The appearance of partly bedded intervals, represents various stages of a mass-movement transformation from slump into debris flow.
Facies F5: Dunes and lag deposits	Fine- to coarse-grained sandstone and conglomerate	The maximum height of the bedforms is up to 15 cm	Distinctive bedform morphology with regular lateral thickness changes. Mostly flat bottom, but loads and sole marks are not uncommon. Wavelengths range from a few tens of centimetres up to 250 cm; however rarely can be traced for longer distances to obtain detailed data. Massive or poorly cross-stratified with imbricated grains.	Sustained and turbulent traction currents. Varieties of bedform size and grain size reflect the dynamic of the local sea floor with bypass of gravity flows of different sizes and speed. Conglomeratic deposits of F5 – lag deposits, contrasting with the fine-grained surrounding deposits.

Facies F6: Black mudstones	Non-calcareous, dark mudstones and silty-sandy mudstones (due to diagenesis, some beds are brownish, rusty-orange, light greyish and whitish)	<1 cm and 60 cm, mean ~3 cm	Gradational, or rarely sharp lower boundaries, and mainly are sharply overlain by other facies. Pyrite mineralization and sideritic concretions.Mainly massive, macroscopically non-stratified, with rare silt and very fine sand laminae. Part of the dark mudstone shows spotted ichnofabric, which is poorly visible due to their dark colour. Trace fossils: *Chondrites*, *Planolites*, *Ophiomorpha*?, *Thalassinoides*?, rarely *Protovirgularia*, *Phycosiphon*, and *Palaeophycus.*	More clayey mudstone is considered as hemipelagic deposits, whereas silty and sandy mudstone (especially occurring above facies F1, F2, F3 and F7) with vague laminae is most likely of dilute low-density turbiditic origin. More chaotic sandy-silty mudstone with suspended larger grains – deposits of laminar flows (e.g., fluid mud).
Facies F7: Grey mudstones	Non-calcareous to very poorly calcareous; light grey, greenish and bluish-white mudstones	<1 cm to 15 cm, mean 2.5 cm	Gradational to sharp lower boundaries. Mainly massive (homogenised by bioturbation), macroscopically non-stratified. Mainly spotted ichnofabric, *Chondrites*, *Planolites Ophiomorpha*?, *Thalassinoides*?, rarely *Protovirgularia*, *Phycosiphon*, *Palaeophycus,* and *Alcyonidiopsis* isp.	Hemipelagic 'background' sedimentation below or near the local lysocline.
Facies F8: Siltstone	Yellowish and whitish siltstone, may contain a small contribution of very fine-grained sand	0.1 to 5 cm thick, mean ~0.7 cm	Sharp and flat lower surfaces, with small trace fossils. Sharp to gradual and flat to uneven top. Graded (on the microscale) to ungraded and structureless. Rare planar parallel lamination, low-angle lamination, and cross-lamination, locally with mud drapes. Sedimentary structures may be plastically deformed by the escape of water into the wavy or more chaotic laminae.	Product of fine-grained dilute and fully turbulent sediment gravity flows or lower transitional plug flows. During such deposition, silt-sized grains were freely settled out of suspension, and traction structures were formed.

Table 2. Facies description and interpretation.

(low $\delta^{13}C$ values). However, an improvement in oxygenation is clear therein (see below). Anoxic conditions in the Veřovice Shale can only be partially confirmed by ichnological data (Uchman 2001b, 2004). Most deposits are barren of trace fossils and show primary lamination. However, bioturbated horizons less than 1 cm thick occur locally at the top of some sedimentary events, and are slightly lighter in colour. They contain *Phycosiphon incertum* (Fig. 12B), very small *Chondrites intricatus* and *Ch. targionii* (Fig. 12C)*, Planolites* isp., and *Palaeophycus* isp., which are the dominant ichnotaxa. Locally, *Thalassinoides* isp. can be seen. The bivalve burrows *Protovirgularia pennata* and *P. obliterata* are locally common (Fig. 12D) and occur in a few centimetre thick zone below *Chondrites*. Common *Protovirgularia* is unusual. The presence of *Protovirgularia* in the lowest tier – distinctly below *Chondrites* – suggests that it was produced by chemosymbiotic bivalves that could burrow in anoxic sediment, like the solemyacid bivalve *Solemya* (Seilacher 1990) and some lucinid and thyasirid bivalves (Powell et al. 1998, and references therein). The Early Cretaceous anoxic events probably delayed the colonization of deep-sea floor environments by the irregular echinoids responsible for the production of *Scolicia* (Tchoumatchenco and Uchman 2001), which is absent in the Veřovice Shale and older Carpathian formations. Thus, the trace fossil association at Zagórnik was putatively influenced by global phenomena related to the Cretaceous anoxic events.

About 160 m upstream of the starting point, the transition to the Lhoty Beds can be observed in a ~5.5–6 m thick package of beds. The first thin layers of green-grey bioturbated non-calcareous mudstone shales occur here:

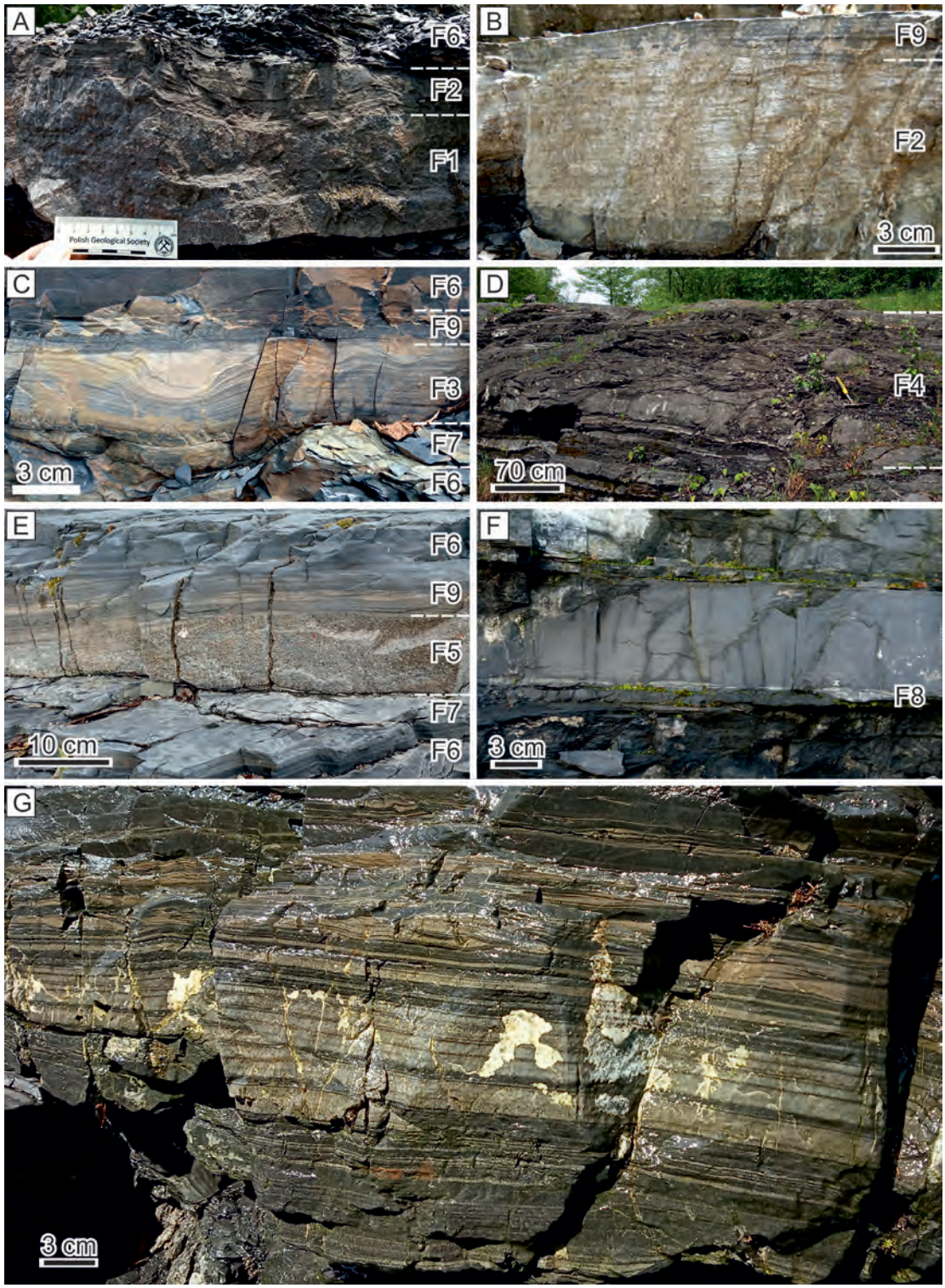

Fig. 10. Representative photographs of sedimentary facies F1–F9 in the Veřovice Shale and Lhoty Beds. **A** – Massive sandstone (F1) capped by planar-parallel laminated division (F2) passing into dark mudstone (F6). **B** – Planar-parallel and ripple cross-laminated sandstone (F2) capped with heterolithic deposits (F9). **C** – Muddy interval (F6 and F7) passing into banded sandstone with loaded ripples at the top (F3) and heterolithic deposits (F9). **D** – Debritic muddy sandstone with mudclasts (F4) in the Lhoty Beds. **E** – Coarse-grained dune bedform (F5) with heterolithic top (F6) in the Lhoty Beds. **F** – Lenticular silty bedforms (F8). **G** – Stack of heterolithic deposits (F9).

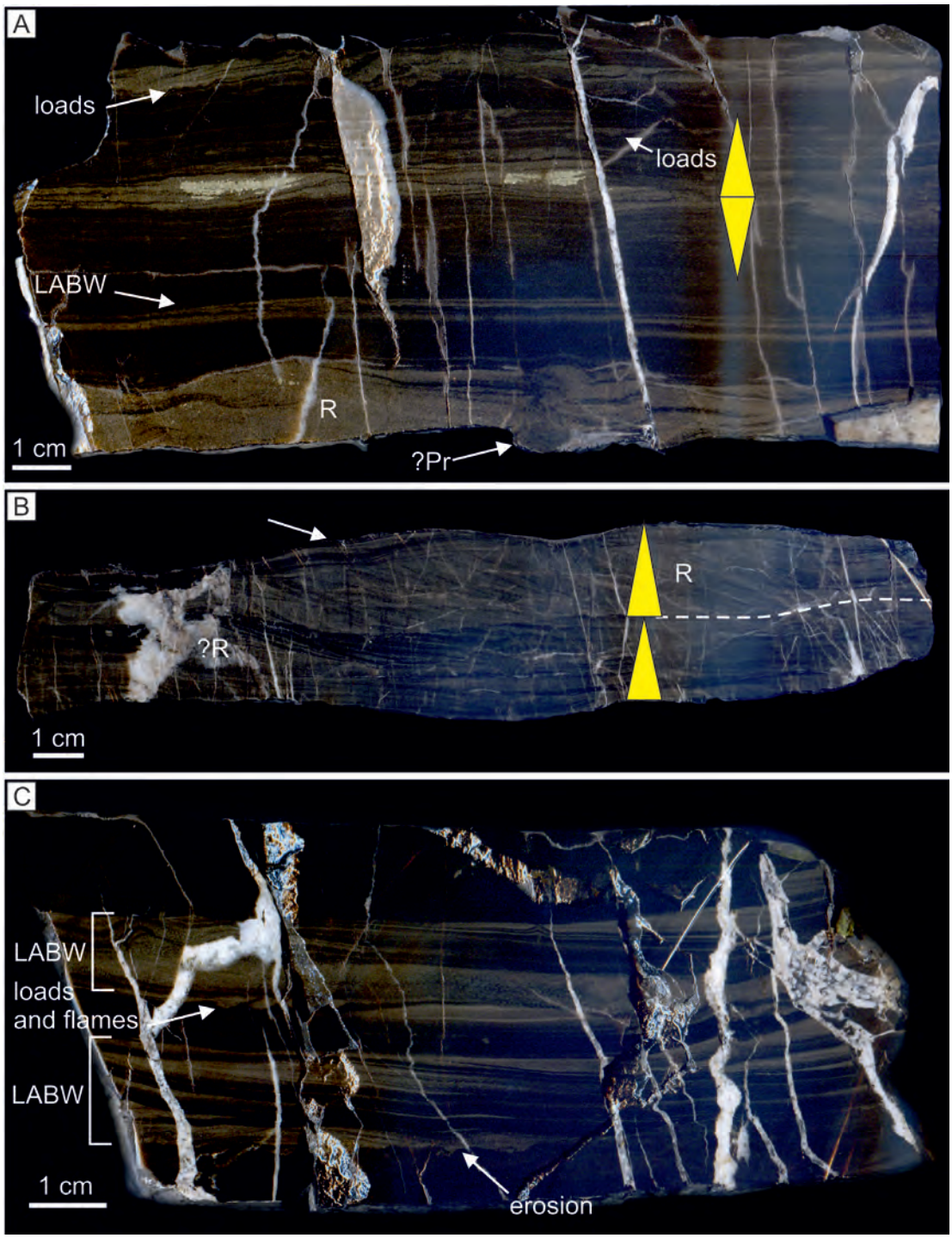

Fig. 11. Cut surfaces of heterolithic deposits (F9). **A** – Partly homogenised ripples (R) with mud drapes and a trace fossil of ?*Protovirgularia* isp. (?Pr) with stack of climbing low-amplitude bed-waves (LABW) at the top. In the middle of the picture, heterolithic deposits show symmetrical grain-size trends (potential hyperpycnal flow deposits). The top of the picture represents strongly deformed heterolithic deposits with load structures. **B** – Two cycles of waning flow. At the bottom, heterolithic deposits with low angle lamination, and small ripples with mud drapes (?R) superimposed with ripples (R) with small lenticular bedforms (white arrow) at the top. Note the internal erosional surface marked with a dashed line, which may represent maximum flow velocity during one event of a hyperpycnal flow. **C** – Stack of low-angle laminated heterolithic deposits interpreted as low-amplitude bed-waves (LABW). Note the erosional surface at the bottom of the picture and loading in the middle of the picture.

Fig. 12. Outcrops and trace fossils of the Veřovice Shale in the Rzyki section. **A** – Upstream view of the section. **B** – *Phycosiphon incertum*. **C** – *Chondrites targionii*. **D** – *Protovirgularia obliterata*.

their frequency and the contribution of sandstones gradually increases upsection. Above and below the first green-grey layer, siderite concretions are spaced at an interval of about 1.5 m (Figs 13, 14). *Phycosiphon incertum* is abundant. This interval represents the beginning of oceanic circulation recovery and improved sea-floor oxygenation (Uchman and Cieszkowski 2008; Strzeboński et al. 2009; Wójcik-Tabol and Ślączka 2015). Improved seafloor ventilation after the deposition of the Veřovice Shale may be related to the late Aptian drop in global temperature (Scott 1995; Price et al. 1998), which might have accelerated oceanic circulation. However, if so, there was some delay in seafloor ventilation in the area presented.

Typical deposits of the Lhoty Beds begin with intercalated thin-bedded sandstones (non-calcareous quartz arenites with whitish, greyish, yellowish and rusty orange colours), black and greenish-grey mudstones, and heterolithic deposits, which in total are ~73 m thick. Upsection, the contribution and thickness of the sandstone beds gradually increase in a ~50 m thick interval dominated by medium- to thick-bedded sandstones. This gradual thickening and increase in the contribution of sandstone is interpreted as the progradation of a depositional lobe complex. Sedimentary succesion of the Lhoty Beds shows numerous autocyclic shifts between sedimentary subenvironments of the depositional lobe (lobe off-axis, fringe, and distal fringe).

A late Albian age 12 m above the base of the Lhoty Beds has been determined *via* dinocysts, while the whole formation ranges up to the middle Cenomanian (Cieszkowski et al. 2003). Based on foraminifers, the Lhoty Formation represents deposition in an upper bathyal setting (Książkiewicz 1975), but deposition below the CCD is suggested due to the

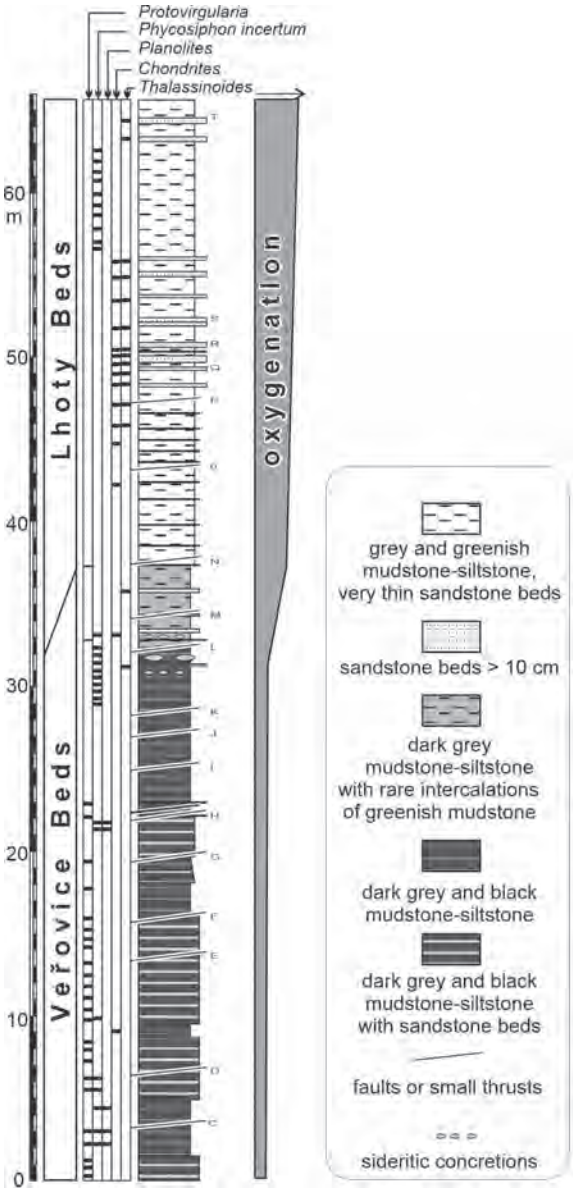

Fig. 13. Stratigraphic log of the transitional interval between the Veřovice Shale and Lhoty Beds (modified after Uchman and Cieszkowski, 2008a).

presence of non-calcareous hemipelagites at the top of turbidite-hemipelagite rhythms.

Bioturbated greenish mudstones occur at the top of turbidite-hemipelagite couplets. Fine- and medium-grained sandstone layers, up to 35 cm thick, are more frequent upsection, and display typical Bouma intervals that point to their turbiditic origin. Structured sandstone and banded sandstone facies (see Stevenson et al. 2020) prevail. This part of the section continues for about 120 m and termi-

Fig. 14. Greenish bioturbated layers alternating with grey layers at the transition between the Veřovice Shale and Lhoty Beds.

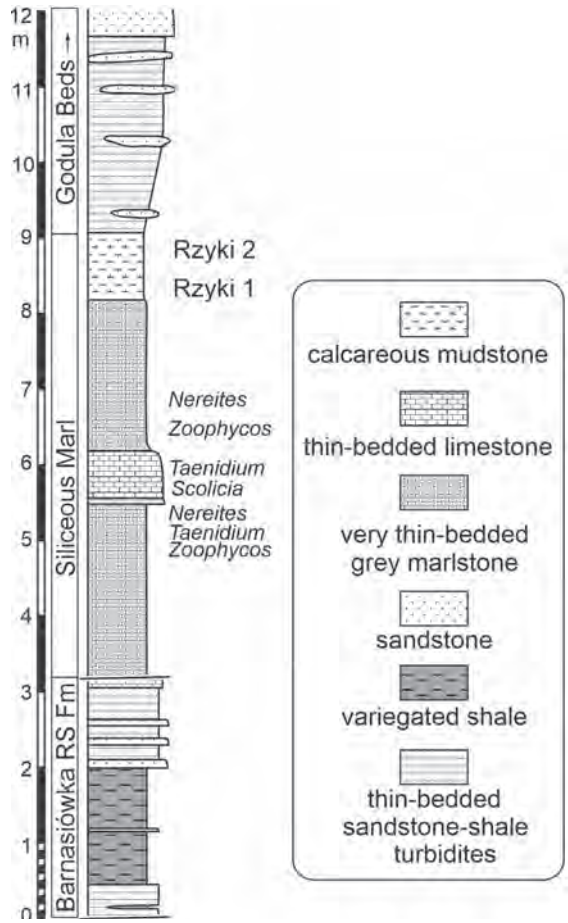

Fig. 15. Stratigraphic log of the Siliceous Marl in the Rzyki section (modified after Uchman and Cieszkowski 2008b).

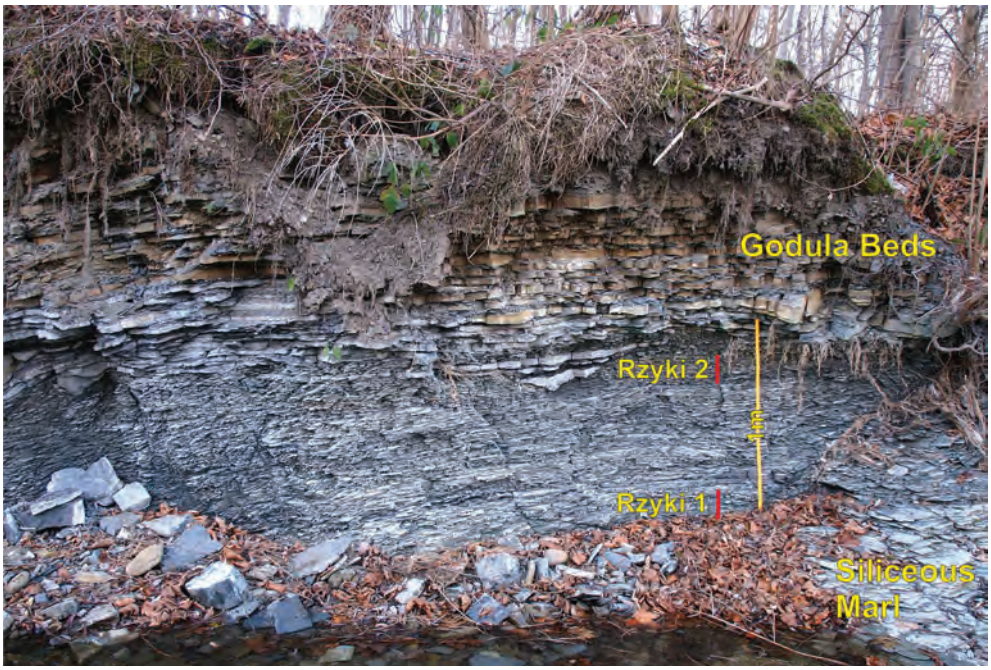

Fig. 16. Outcrop of the transition between the Siliceous Marl and the Godula Beds, with microfaunal samples indicated.

nates where the Lhoty Beds are partly covered. Upsection, the Lhoty Beds continue for at least ~120–150 m.

Most of the green-grey shales in the Lhoty Beds contain *Planolites, Chondrites*, and *Thalassinoides* against a totally bioturbated background. Such an ichnofabric is indicative of generally improved oxygenation. *Phycosiphon incertum* is still present in the lower part of the Lhoty Beds, but is less common in the middle and upper parts. *Protovirgularia* is very rare. Bioturbation extends to the top of turbiditic sandstones, where *Thalassinoides* is abundant in some beds. Questionable *Zoophycos* isp. and *Nereites* isp. have been found in the uppermost part of the section. The soles of turbidites in the Lhoty Beds contain very few trace fossils, and those present are commonly semi-reliefs of *Thalassinoides* and *Planolites*. "*Arthrophycus*" *tenuis* is present in some beds. Graphoglyptids are absent. The oldest occurrence of *Scolicia* in the Flysch Carpathians is noted here (Książkiewicz 1970, 1977b). Rarely, below turbidites, shales are dark grey or black and trace fossils or other signs of bioturbation are absent. There is no evidence of significant erosion. This is indicative of short anoxic events; however, the oxygenation of the sediments in the Lhoty Beds was generally much more pervasive than in the underlying Veřovice Shale.

A kilometre upstream, above some tectonic disturbances, a package of thin-bedded flysch (Godula Beds?), and a stretch covered by alluvia, both the Cenomanian variegated mudstones and radiolarites of the Barnasiówka Radiolarian Shale Formation and the Siliceous Marl are present (starting point GPS coordinates: N 49° 49' 18.7''; E 19° 22' 48.6''; ±5 m; Fig. 15). The Barnasiówka Radiolarian Shale Formation (upper Cenomanian–lower Turonian) is very reduced here, at least partly due to tectonic truncation, and is mostly (in some years, completely) covered by river debris. The section is tectonically disturbed by faults and small thrusts. Depending on the state of exposure, greenish-grey, siliceous, thin-bedded flysch deposits (~0.45 m) are visible. These are overlain by a 1.6 m thick package of red and green variegated shales, which in turn are overlain by about a metre thick package of thin-bedded sandstone-shale turbidites (Fig. 17A). OAE-2 deposits are expected downsection, but they are tectonically truncated or covered.

The Siliceous Marl is exposed on the riverbanks (Fig. 17B). It occurs above the Barnasiówka Radiolarian Shale Formation, and below the Godula Beds (Turonian–Santonian)

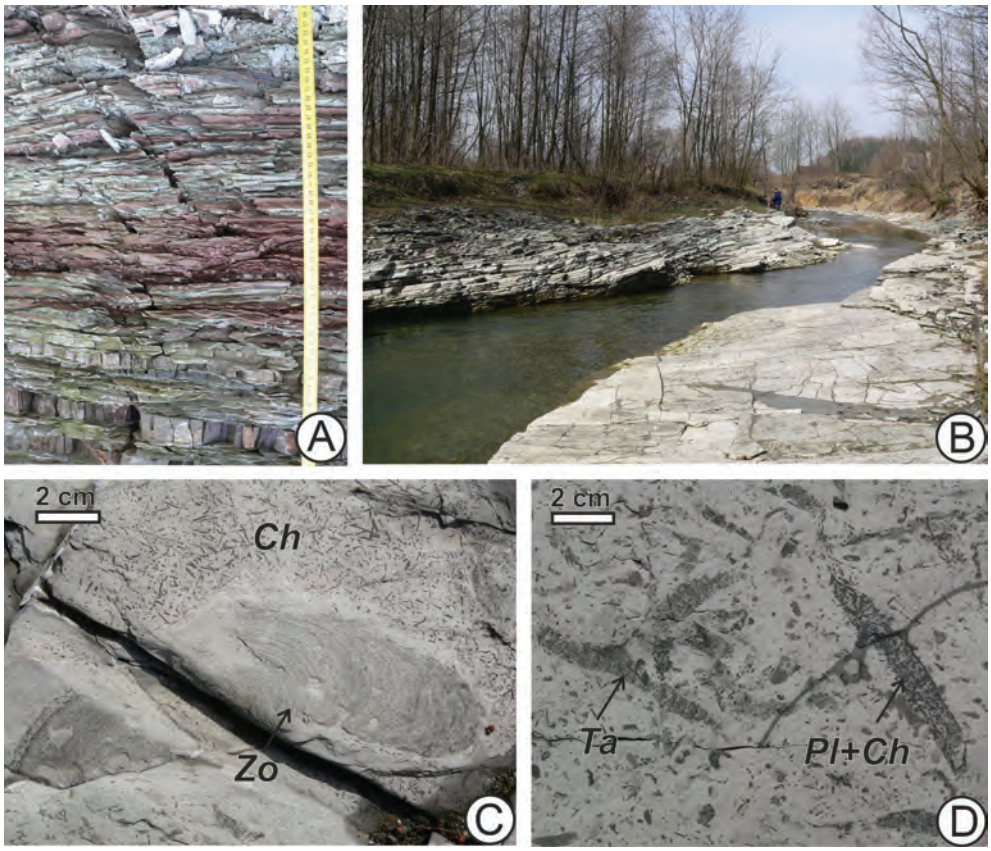

Fig. 17. Outcrop of the Barnasiówka Radiolarian Shale Formation (**A**), the Siliceous Marl (**B**), and some trace fossils from the Siliceous Marl (**C, D**). *Ta – Taenidium dieslingi, Planolites* reworked with *Chondrites* (*Pl+Ch*), *Zoophycos* isp. (*Zo*), and *Chondrites intricatus* (*Ch*).

(Fig. 15). The Siliceous Marl is composed of thin-bedded marls with a limestone package in the lower and middle parts, which together are 5.1 m thick. Upstream, the transition to the overlying Godula Beds is observed. The marls pass into grey, calcareous, thin-bedded shales (about 1 m), overlain by thin-bedded, shale-sandstone turbidites with lenses of thicker sandstones, which already belong to the Godula Beds (Fig. 16).

The Siliceous Marl has been described in the nearby valley (Kaczyna section; Alexandrowicz and Lalik 1999), and later in the studied section (Cieszkowski et al. 2001). Its age has been determined to be middle/late Turonian–early Coniacian (Gedl 2001; Cieszkowski et al. 2001, 2003) on the basis of dinocysts, or to the early Turonian–early Coniacian on the basis of poorly preserved calcareous nannofossils (Kędzierski in Cieszkowski et al. 2001, 2003). In the lower part of the marlstone-limestone complex, *Inoceramus* ex gr. *lamarcki* Parkinson has been found. This bivalve is typical of the upper middle Turonian and the upper Turonian, but is also present in the Coniacian (I. Walaszczyk, pers. comm. 2003). In the metre-thick package transitional to the Godula Beds, a lower sample (Rzyki 1, Fig. 16) contains the foraminifers cf. *Whiteinella* sp. (Turonian–Santonian), dominating agglutinated tubular forms, *Karrerulina conversa*, *Arenobulimmina* sp., and single radiolarians. The higher sample (Rzyki 2, Fig. 16) contains silicified dominant agglutinated tubular forms, *Dendrohrya* sp., an individual ?*Hedbergella* sp., *Heterohelix* sp., and fragments of *Verneulinoides* sp., *Plectina* sp., and *Glomospira* sp. All these microfossils are suggestive of a Turonian–?Coniacian age (determinations by Lucyna Bobrek 2022).

The first ichnological studies of this unit were provided by Cieszkowski et al. (2001, 2003). The limestones and marlstones show abundant trace fossils dominated by *Chondrites intricatus* (Fig. 17C) and *Planolites* isp. (Fig. 17D). *Zoophycos*

Fig. 18. Outcrops of the Godula Beds. A. Thick-bedded flysch in the lower part of the Godula Beds. B. Thin-bedded flysch above the bridge.

isp. (Fig. 17C), *Scolicia* isp., *Taenidium dieslingi* (Fig. 17D), *Gyrophyllites* isp., *Phymatoderma* isp., and *Nereites* isp. are less common. The deep tiers are occupied by *Chondrites* and *Zoophycos*. Some individual beds are deeply bioturbated. *Nereites* isp. is rare. Only one graphoglyptid, represented by a specimen of *Desmograpton* isp., was found. Frequently, *Planolites* fillings are reworked with *Chondrites* (Fig. 17C). According to ichnological data, pore water oxygenation was similar to or slightly better than in the Lhoty Beds. There is no evidence of anoxia.

Post-depositional trace fossils of the fodinichnia, pascichnia, and chemichnia prevail in the presented section, similar to the Holovnia Siliceous Marls (Turonian–lower Santonian) of the Skole Nappe (eastern Polish Flysch Carpathians; Leszczyński 2003) and other Late Cretaceous marly flysch deposits of the Alps (Uchman, 1999) and Apennines (Uchman, 2007). In general, ichnodiversity in Cretaceous–Cenozoic calcareous and mixed siliciclastic-calcareous flysch deposits is lower than in siliciclastic flysch deposits (Uchman 1999, 2007), mainly due to the reduced diversity of pre-depositional trace fossils. This is probably due to preservational conditions. For preservation of pre-depositional, shallow-tier trace fossils, especially graphoglyptids, delicate erosion is necessary for the exhumation of burrow systems before casting on the sole of a turbiditic sandstone. Particles of marly oozes mostly consist of coccospheres and foraminifer tests, which are porous and have a large surface compared to their weight (so, therefore, have a much higher buoyancy than siliciclastic grains). Consequently, turbiditic currents of marly mud are less energetic (lighter) than turbiditic currents of siliciclastic mud and are therefore unable to scour the sea floor as deeply. Thus, marly turbidites are less able to exhume shallow burrow systems and cast

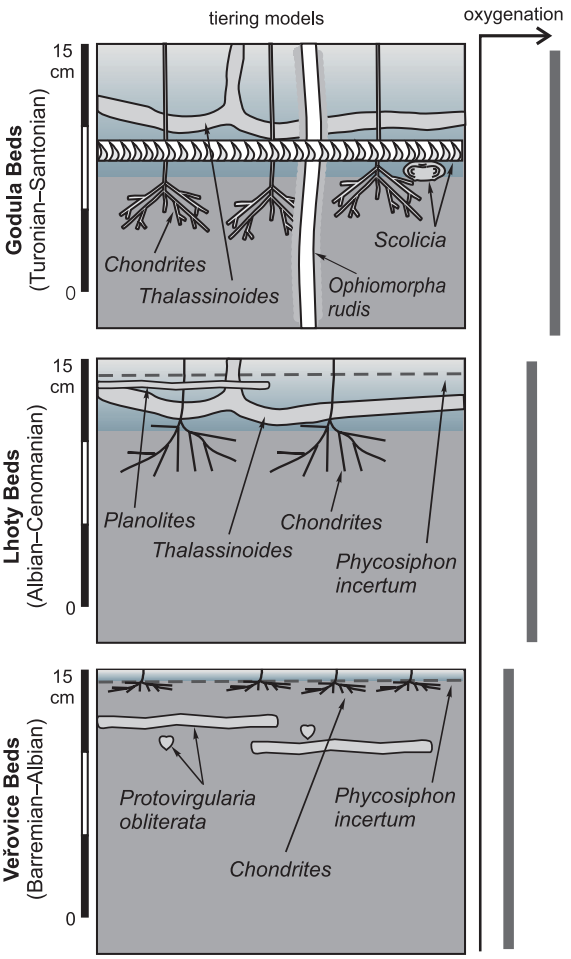

Fig. 19. Changes in tiering patterns and oxygenation in the Veřovice Shale, Lhoty Beds, and Godula Beds (based on Uchman 2004).

them on turbiditic soles. Therefore, the shallow-tier ichnofauna, though diverse in siliciclastic turbidites, are underrepresented in calcareous flysch (Uchman 1999, 2007). Moreover, the slower settling of very fine carbonate bioclastic grains in carbonate turbidites, lasting for up to several months, can influence infauna that construct open burrow systems (Miller et al. 2004) and are not adapted for permanent settling of fine particles. Additionally, the soles are commonly built of sediments finer than sand. In conjunction, all these factors can reduce trace fossil diversity.

Upriver (GPS coordinates: N 49° 49' 15.1''; E 19° 22' 52.5''; ±5 m), the lowermost part of the Godula Beds (Turonian–Santonian) is exposed. Here, it begins with a thick-bedded siliciclastic flysch with grey-greenish non-calcareous mudstone shales intercalated with thin- to medium-bedded, fine- to medium-grained sandstone shale flysch (Fig. 18A). Some sandstone beds display Bouma divisions. Some beds appear as convex down lenses; these were deposited in small channels. Higher in the section, an at least 140 m-thick succession of thin-bedded and shaley flysch with intercalations of medium beds is exposed (Fig. 18B). It transitions to "normal" thin- and medium-bedded sandstone shale turbidites (at least 150 thick), and even higher up to thick-bedded sandstones, which underlie the northern slopes of the Beskid Mały range. In the presented section, the base can be dated to the late Turonian and Santonian according to biostratigraphical data from the Siliceous Marl.

In the riverbed about 40 m above the bridge of the main road to the centre of the village of Rzyki (GPS coordinates: N 49° 49' 07.6''; E 19° 23' 00.6''; ±7 m), a few beds containing full reliefs of *Scolicia*, *Chondrites intricatus*, and *Planolites* outcrop. An approximately 15 m-thick section crops out here in a cliff on the western side of the valley. The mudstones of the Godula Beds are completely bioturbated in 2–3 cm thick layers at the top of the turbidite-hemipelagite couplets. More trace fossils can be found on the soles of turbiditic sandstones, including graphoglyptids (for example, *Cosmorhaphe* a few metres above the contact with the Siliceous Marl). In general, "*Arthrophycus*" *tenuis*, *Ophiomorpha annulata*, and *Scolicia* are locally common in the Godula

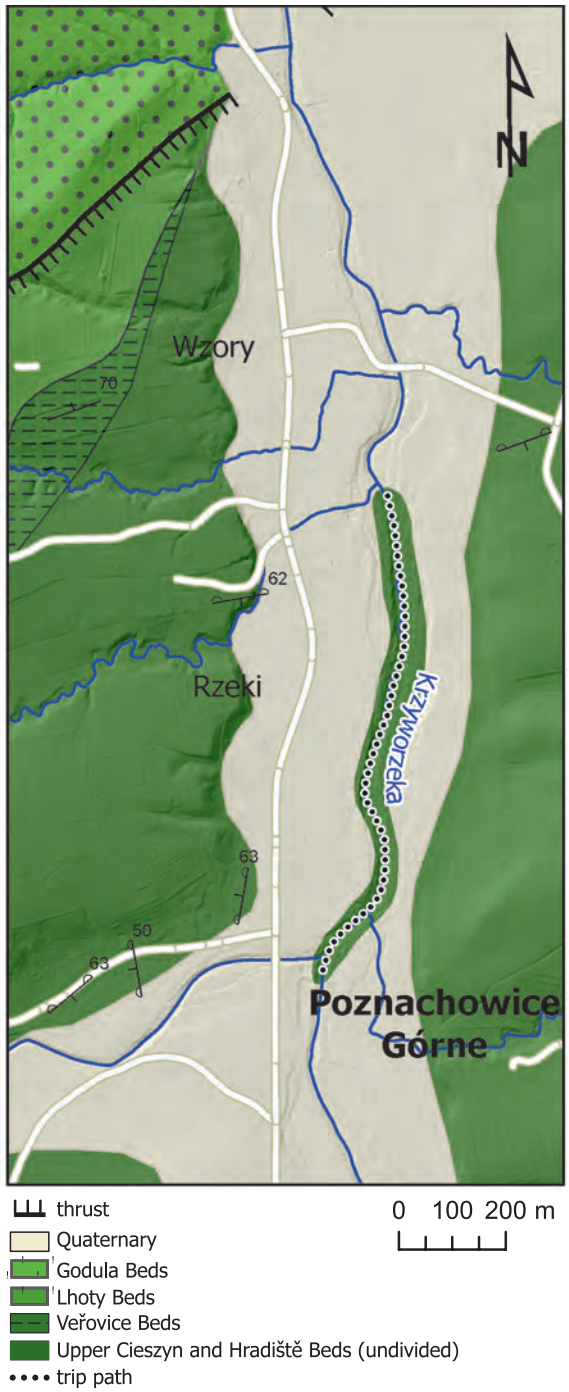

Fig. 20. Geological map of Poznachowice Górne (Stop 3) in the Silesian Nappe, based on Wójcik (2017) and Burtan (1977).

Beds. The latter two ichnotaxa represent deep burrowers.

Changes in the trace fossil assemblages in the presented section are well correlated with ichnodiversity. The Veřovice Beds contain

5 ichnogenera, the Middle Lhoty Beds 15 ichnogenera, and the Godula Beds 26 ichnogenera (Uchman 2004). Additionally, an increase in tiering pattern complexity is observed in the same stratigraphic order (Fig. 19). This is reflective of general changes in deep-sea trace fossil assemblages during the Early Cretaceous and after the Cenomanian–Turonian anoxic event (OAE-2) (Uchman 2001b).

Stop 3: Poznachowice Górne–Krzyworzeka river section. Lower Cretaceous of the Silesian Nappe

(*Alfred Uchman, Mateusz Szczęch*)

The Krzyworzeka river section, located between the villages of Poznachowice Górne and Czasław (Fig. 20), contains mostly the very thin- and thin-bedded facies of the Upper Cieszyn Beds (Valanginian–Hauterivian) and the Hradište Beds (upper Hauterivian–middle Barremian), which are undivided in this area because of poor lithological contrast (Burtan 1954, 1966a, b, 1974). In this region, the Veřovice Shale is tectonically reduced. Lower Cretaceous deposits occur in several small, imbricated thrust slices close to the northern margin of the Wiśniowa Tectonic Window, which belongs to the Subsilesian Unit. The observed deposits are dominated by dark grey to black marly mudstones interlayered with numerous, very thin to thin layers of mostly cross-laminated fine-grained sandstones, rare sandy limestones, and local siderite claystones (e.g., Burtan 1978; Fig. 21A–E). The sandstones show sharp erosive bases and transitional gradations to overlying mudstones. These deposits are interpreted as turbiditic sandstone-mudstone couplets capped by hemipelagic mudstones. They are similar to the turbiditic facies C2.3 of Pickering et al. (1986), but the muddy part is thicker in the investigated deposits than in this facies model. Locally, convex-down lenses of coarse- to medium-grained calcareous sandstones are present. They show erosive bases and steep angles on one side, and gently pinch out on the opposite side (Fig. 21F). They are interpreted as fillings of shallow meandering channels (Uchman 2008a).

Burtan (1978, 1984) used the term Hradište Beds to refer only to the thick-bedded flysch occurring as lenses within thin-bedded deposits with the same general lithotype as the Upper Cieszyn Beds. They contain conglomerates and exotic blocks, which can be interpreted as debris-flow deposits. These deposits are older than the Barremian Piechówki Sandstone Member (Golonka et al. 2008) and were assumed as Hauterivian (Burtan 1978, p. 25) on the basis of *Lamellaptychus* at nearby Wiśniowa and Raciechowice–Wolica (Gąsiorowski 1960). Krajewski and Urbaniak (1964, p. 120) mentioned the occurrence of *Aptychus* in the Hradište Beds in Poznachowice Dolne in a tributary stream of the Krzyworzeka River, and undetermined Anthozoa and an ammonite of the genus *Crioceras* from the Hradište Beds on an unnamed hill at the foot of nearby Grodzisko Mount. Szymakowska (1981) showed a few sites with ammonites in the Poznachowice Dolne region on a general geological map of the Polish Carpathians but unfortunately without any closer data on the localities and determinations. Downriver, in two separate sites not visited during this excursion, the ammonites *Teschenites subflucticulus* Reboulet and *Criosarasinella mandovi* Thieuloy were found: microfossils were subsequently analysed from the same samples (Vašíèek et al. 2010). *T. subflucticulus* is diagnostic of the late Valanginian *Furcillata* Zone, but the co-occurring calcareous nannoplankton are consistent with the late Hauterivian–late Barremian, and the dinocysts with the late Hauterivian. *C. mandovi* also points to the late Valanginian *Furcillata* Zone, and this is consistent with the nannoplankton data (early Valanginian–early Barremian) but dinocysts are suggestive of the late Hauterivian. The preservation of the ammonites and the sedimentary characteristics of their host beds exclude redeposition. The age difference of almost 3 Ma remains a dilemma (Vašíček et al. 2010). Near the *C. mandovi* site, calcareous nannoplankton from the Valanginian–Hauterivian boundary interval was analysed in a series of beds in which packages of lighter and darker mudstones occur. In general, the dark grey mudstones contained more Boreal taxa, while the light grey mudstones reflect more Tethyan taxa. This is demonstrative of periodic changes in surface water circulations (Kędzierski and Ochabska 2012).

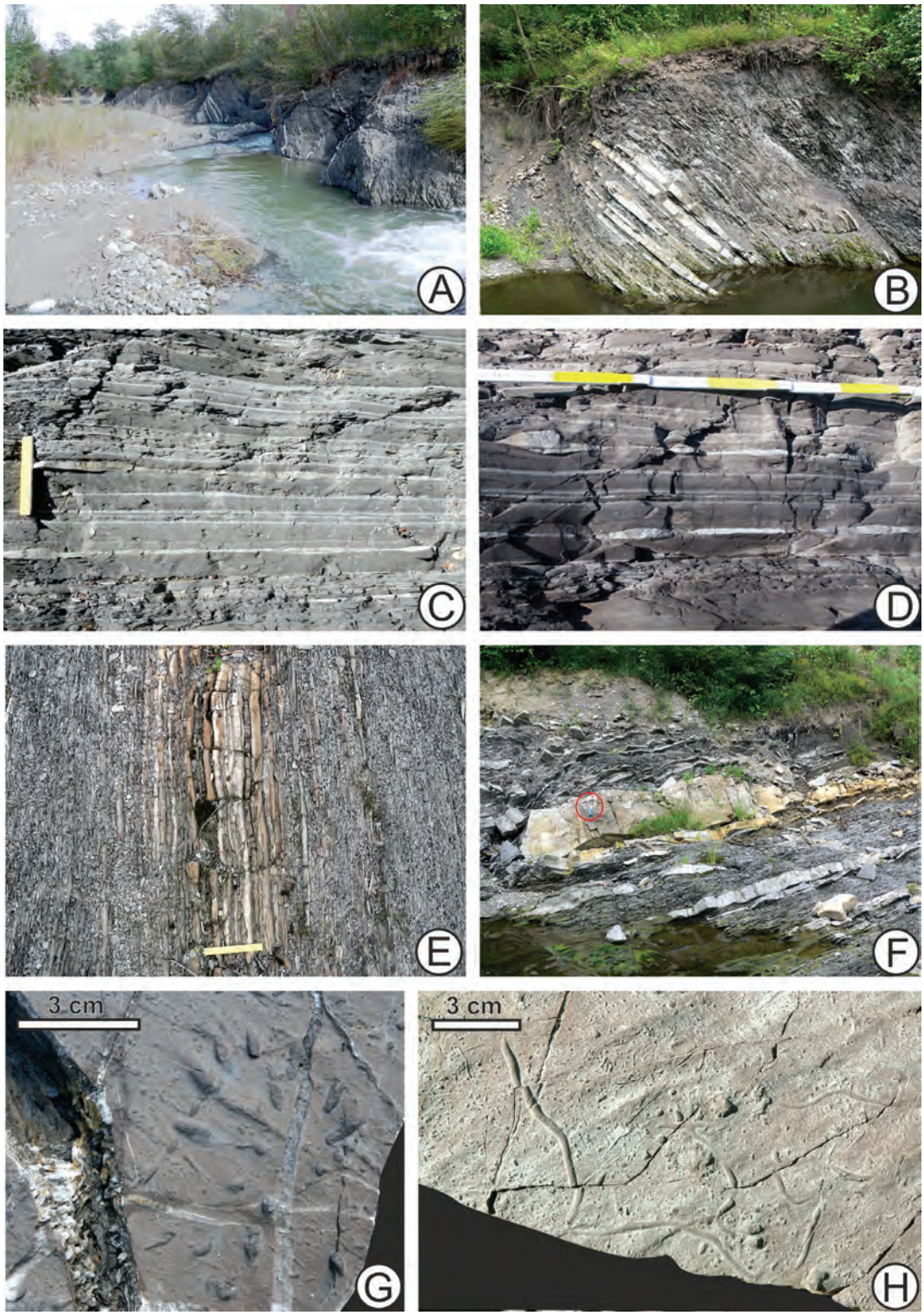

Fig. 21. Facies and trace fossils of the Lower Cretaceous deposits in the Krzyworzeka section. **A** – View of outcrops. B. Outcrop with a package of thicker sandstone beds. **C** – Light grey, very thin siltstone-mudstone depositional rhythms, scale = 10 cm. **D** – Dark grey, very thin-bedded, very fine-grained sandstone/siltstone-mudstone depositional rhythms. **E** – Package of very thin-bedded sandstones within siltstone-mudstone dominated deposits; scale = 10 cm. **F** – Asymmetric sandstone channel fill (overturned; circled hammer for scale). **G** – *Lorenzinia nowaki*. H. *Megagrapton submontanum*.

Trace fossils of the presented deposits are relatively abundant and diverse. Most are preserved in semi- or full-relief on the lower surfaces of turbiditic sandstones. *Chondrites intricatus, Helminthopsis abeli, H. hieroglyphica, H. tenuis*, and *Planolites* are the most abundant ichnotaxa. Among the diverse graphoglyptids, *Belorhaphe zickzack*, *Lorenzinia nowaki* (Fig. 21E), *Paleodictyon strozzii,* and *Megagrapton submontanum* (Fig. 21H) can be found. The common occurrence of *Protovirgularia* isp. is characteristic. Other trace fossils (*Chondrites targionii, Gordia* isp., *Phycodes bilix, Phycodes* isp., *Protovirgularia pennata, Thalassinoides* isp.) are rare. A totally bioturbated light layer (spotty layers *sensu* Uchman 1999) occurs at the top of dark turbidite-hemipelagite couplets. Most of the couplets are less than 1 cm thick, and the spotty layer is ~3 mm thick. This layer contains mostly *Planolites* crosscut by very thin *Chondrites* overprinting a totally bioturbated background. In at least a few beds, the spotty layer does not occur at all. The trace fossil assemblage points to the deep-sea Paleodictyon ichnosubfacies of the Nereites ichnofacies (Uchman 2008a).

Stop 4:
Dąbie–Stradomka river section. Upper Cretaceous of the Silesian Nappe (*Alfred Uchman, Oliwia Kowalczewska, Mateusz Szczęch*)

This section starts on the right bank of the river (GPS coordinates: N 49° 49 720'; E 20° 10.301'; ±3 m) and ends below the damaged bridge (Fig. 23). It is about 106 m thick and covers the upper Lower Istebna Sandstone (Fig. 22). The lower part of the section is composed of mud-dominated turbidites (Fig. 24A) intercalated with debris flow pebbly mudstones (Fig. 24B, C) and thick-bedded sandstone packages. Most of the mud-dominated turbidites start from ripple cross-bedded sandstones and pass through siltstones to grey, calcareous mudstones. The mudstones are much more prevalent than sandstones. They have metre-scale thicknesses in the lower part, and are distinctly thinner (i.e., decimetre-scale thickness) upsection. Some mudstones are greenish at the very top. The debris flow pebbly mudstone beds are graded, composed mainly of sand and mud mixed in changing proportions. They contain fragments of grey, rarely black sandstone beds, dark grey and black mudclasts, and quartz pebbles that float in the matrix. Plastically deformed thin-bedded flysch packages are present. The thickest debris flow beds reach about 10 m. The thick-bedded sandstone packages are similar to those in the upper part of the section (see below). These deposits accumulated at the base of the slope due to debris flows and turbidites originating from remobilization slope muds (cf. Strzeboński 2022).

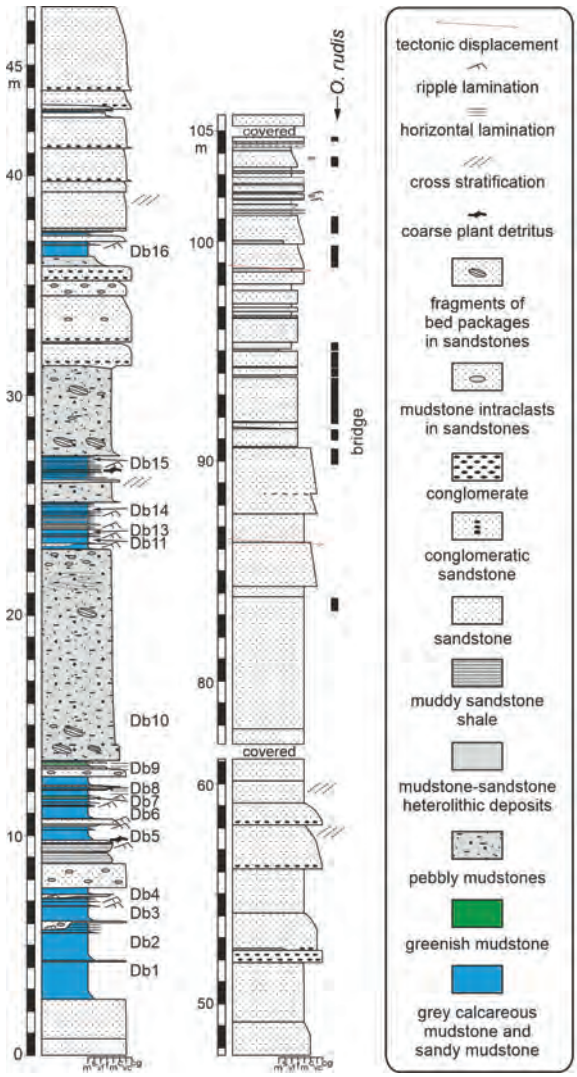

Fig. 22. Section of the Lower Istebna Beds in the Dąbie section.

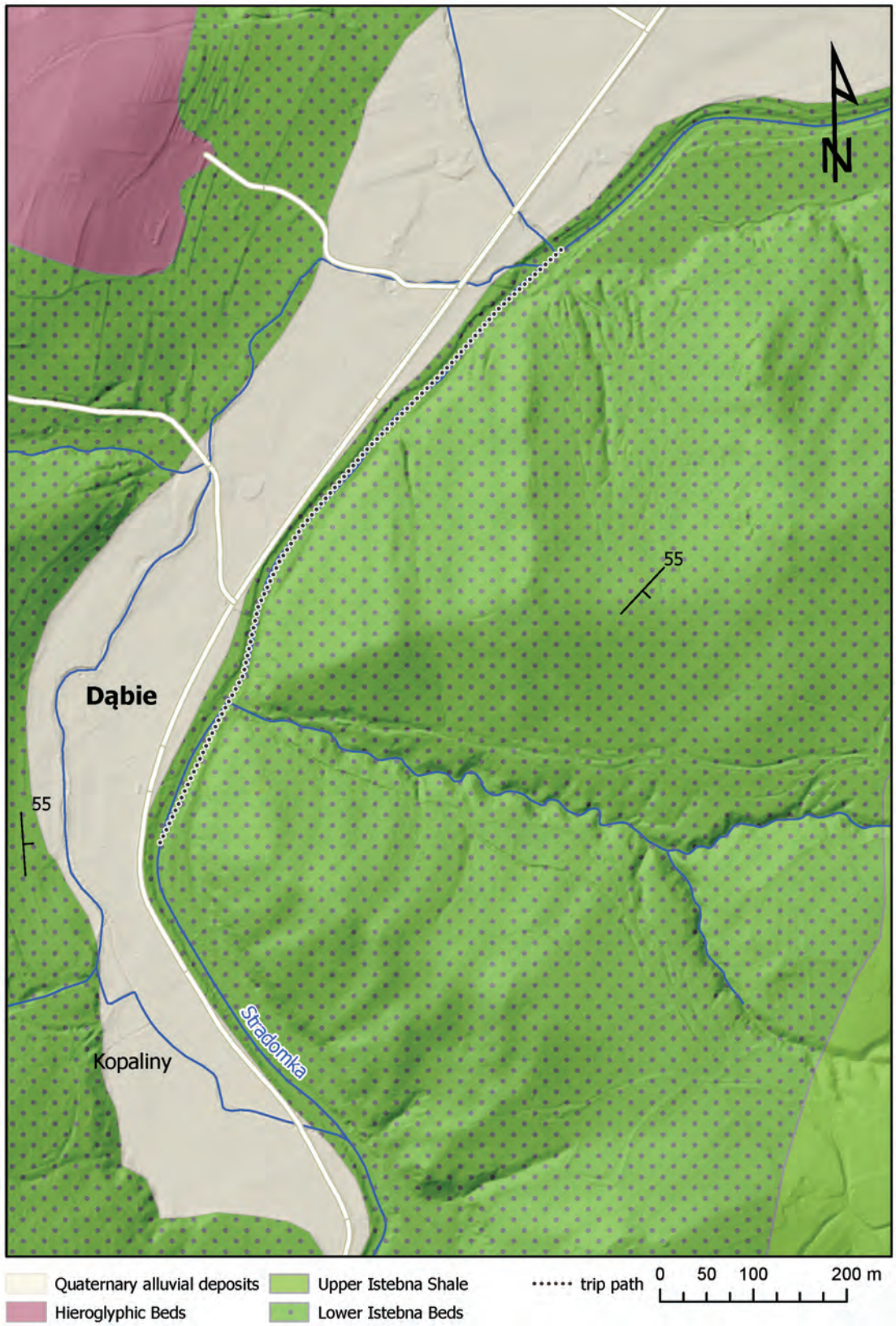

Fig. 23. Geological map of Dąbie (Stop 4) in the Silesian Nappe, based on Burtan (1977).

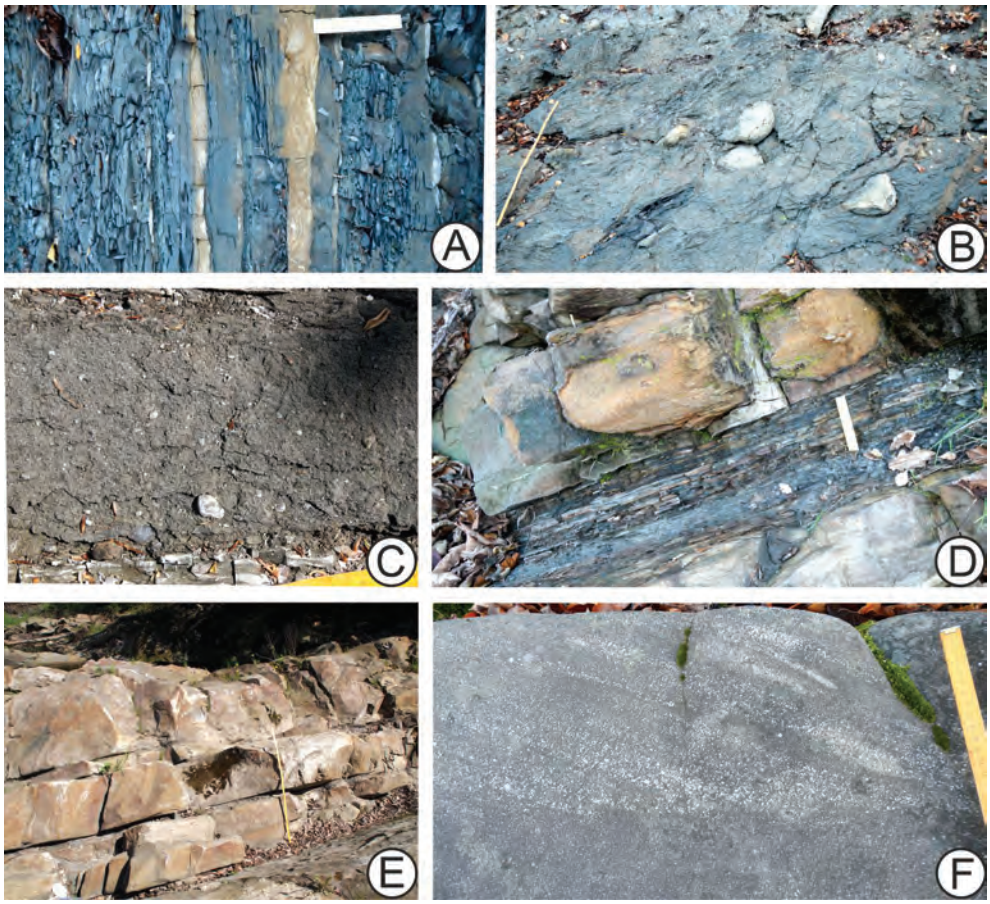

Fig. 24. Selected facies features of the Lower Istebna Beds in the Dąbie section. **A** – Mud-dominated turbidites. **B** – Pebbly mudstone debris flows with sandstone blocks; measurement stick is 1 m long. **C** – Pebbly mudstone debris flows. **D** – Package of heterolithic deposits between thick sandstone beds; scale = 10 cm. **E** – Thick sandstone beds, measurement stick is 1 m long. **F** – Cross bedding in the upper part of a thick sandstone bed.

The upper part of the section is composed of thick-bedded, in places conglomeratic sandstones (Fig. 24E), a single fine conglomerate bed, and thin beds of sandstones and sandstone-heterolithic deposits in the top part. The sandstone grains are mainly quartz, but include a high percentage of feldspar and lithoclasts. Their beds are usually graded, some with cross bedding in the upper parts (Fig. 24F). Conglomerates and conglomeratic sandstones contain pebbles composed of quartz, lydites, metamorphic rocks, and rarely sandstones or other rocks. The heterolithic deposits are composed of very thin-bedded sandstones, siltstones, and mudstones in variable proportions (Fig. 24F). They are bioturbated and rich in fine carbonized plant detritus (Fig. 25D). Most thin-bedded sandstones are ripple-cross or parallel laminated. It is probable that the thick-bedded sandstone beds are sandy debrites, supplied from the south and accumulated in the form of ramps and aprons (cf. Strzeboński 2015, 2022).

Calcareous mudstone samples contain benthic and planktonic foraminifers, including the epipelagic *Planohetereohelix* sp., *Muricohedbergella* sp., and *Globigerinelloides* sp., as well as the bathypelagic *Globotruncana* sp., *Globotruncanella* sp., and *Globotruncanita* sp. Small, epipelagic forms are more common than bathypelagic forms. Calcareous benthic foraminifera are small and usually belong to the trochospiral morphogroup. *Globotruncanella petaloidea* (Gandolfi), present in sample Db16, is a Maastrichtian species. *Globotruncanita* sp., present in sample Db6, is a purely Late Cretaceous species. The epipelagic forms are also typical for the Late Creta-

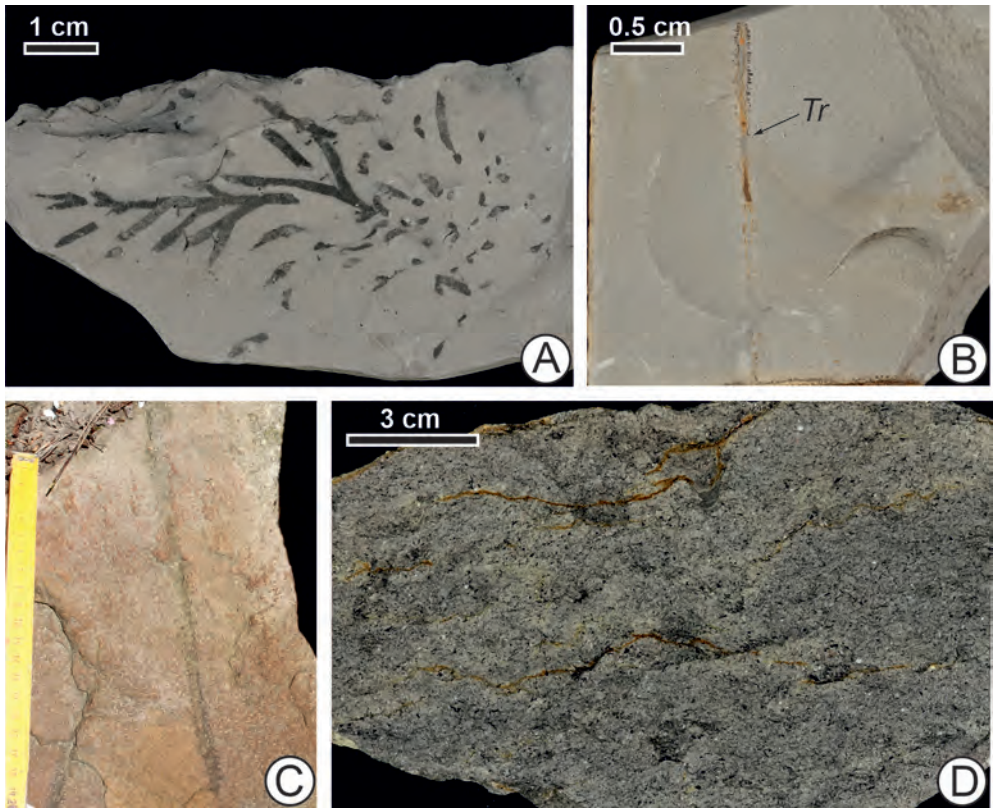

Fig. 25. Ichnological features of the Lower Istebna Beds in the Dąbie section. **A** – *Chondrites targionii* in turbiditic marly mudstones. **B** – *Trichichnus* isp. in turbiditic marly mudstones. **C** – *Ophiomorpha rudis* crossing a sandstone bed. **D** – Muddy sandstone rich in plant detritus and bioturbated with *Ophiomorpha rudis*. Horizontal cutting surface.

ceous. Agglutinated foraminifera of the deep water agglutinated foraminifera (DWAF) assemblage are also present; the tubular forms of this assemblage are often pyritized. In some samples, diatoms, echinoderm spines, and sponge spicules are present.

The muddy turbidites contain *Chondrites targionii* (Fig. 25A), *Trichichnus* isp. (Fig. 25B), and *Planolites* isp. In some sandstone beds, mostly in the upper part of the section, *Ophiomorpha rudis* (Fig. 25C) is present; its burrow system is composed of oblique to vertical shafts crossing the beds and horizontal, irregular mazes concentrated close to bedding or amalgamation planes, mostly in heterolithic deposits rich in plant detritus. The burrows are 1–2 cm in diameter, and can be up to a metre long. Unrug (1963) briefly discussed them as vertical burrows that pass downward into horizontal systems on the soles of thick beds. Książkiewicz (1977b) named them *Sabularia rudis,* which was later included in *Ophiomorpha* (Uchman 1995, 1998). The dominant occurrence of *Ophiomorpha rudis*, as observed here, is typical of the *Ophiomorpha rudis* ichnofacies (Uchman 2001a), which is characteristic of thick sandstone flysch, mostly in channel and proximal depositional lobe facies.

Other trace fossils are rarely present in the Lower Istebna Beds. Unrug (1963) mentioned the occurrence of *Spirorhaphe* and *Cosmorhaphe,* but the latter ichnogenus has never been found again in this unit. The impoverished Paleodictyon ichnosubfacies of the Nereites ichnofacies is present in packages of the medium- and thin-bedded flysch deposits sandwiched between the thick- and very thick-bedded sandstones of the Lower Istebna Beds; they contain *Chondrites* isp., *Phycosiphon incertum*, *Planolites* isp., *"Arthrophycus" strictus*, *Thalassinoides* isp., *Ophiomorpha annulata*, *O. rudis*, *Scolicia strozzii,* and *Helminthorhaphe flexuosa* (Rajchel and Uchman, 2012).

Stop 5:
Nowe Rybie – side road section. Cretaceous of the Subsilesian Unit

(*Alfred Uchman, Paweł Zegadło, Mateusz Szczęch*)

The section in Nowe Rybie (Fig. 26) is located within the Żegocina Tectonic Window of the Lanckorona–Żegocina Zone, part of the Subsilesian Unit/Nappe. The Late Cretaceous deposits of the unit accumulated on the intrabasinal Sub-Silesian Ridge and the slope of the Silesian Basin (Oszczypko et al. 2008). The first transect runs at the bottom of a deep gorge with a small stream and a waterfall. The other transect runs along the nearly parallel main road.

The first transect starts with an isolated outcrop of the Veřovice Shale (a few metres thick), which represents the rift Proto-Silesian Basin (Fig. 27). Above a considerable break, about 3.5 m of the Jasienica (Fucoid) Marl (Cenomanian–Turonian) can be observed along the stream. It is composed of dark grey to light grey and greenish grey, thin-bedded spotty marls, which are rarely intercalated by medium-grained sandstones and mudstones to marly claystones. Some beds are slightly silicified. In the uppermost part of this unit, a 2.8 cm layer of light greenish mudstone is overlain by 20 cm of black non-calcareous shale with a green claystone lamina at the top. This, in turn, is overlain by a metre of black, distorted non-calcareous shales. They represent the Bonarelli Level (OAE-2), which is incomplete here due to tectonic dislocation at the boundary between lithologically different rocks (Uchman et al. 2013). The black shales are not bioturbated and contain abundant, black, opaque, equidimensional phytoclasts and amorphous organic matter indicative of anoxia and high productivity (Radmacher and Uchman 2020).

Upsection, red, variegated, partly silicified marls crop out. Their lowest part shows two ferromanganeous layers, characterised by irregular lamination and concentrically laminated nodules (Fig. 28D). According to foraminifer, nannofossil, and microfacies data, the Cenomanian–Turonian boundary is located within a narrow interval between the Bonarelli Level and the ferruginous level (Kędzierski et al. 2012). Pelagic and hemipelagic sedimentation on a middle slope is interpreted for the lower part of the section, according to the benthic and planktonic foraminiferal associations (Machaniec et al. 2005).

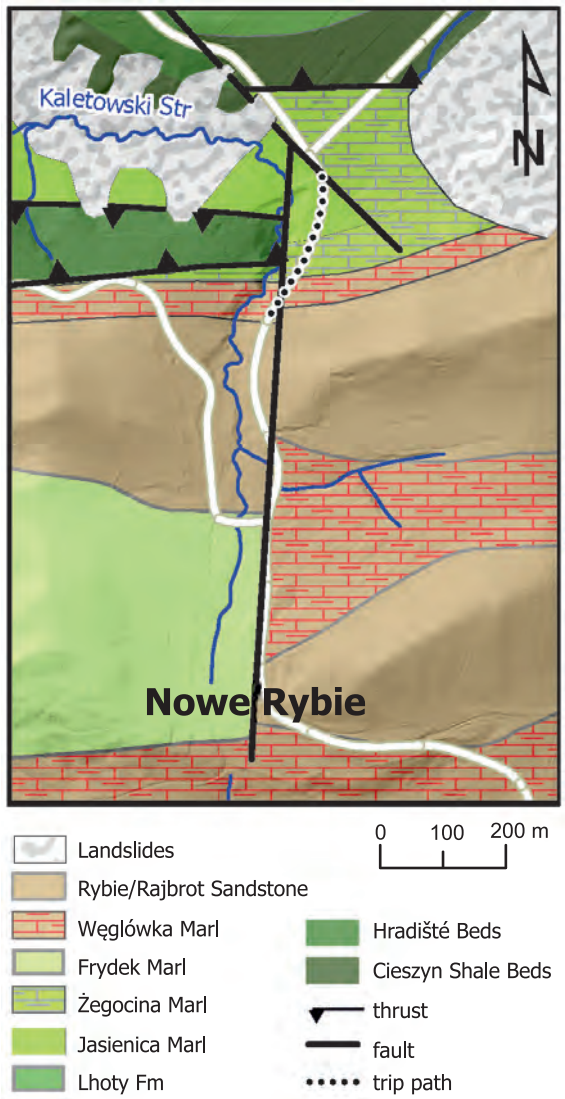

Fig. 26. Geological map of Nowe Rybie (Stop 5) in the Subsilesian Nappe, based on Wójcik et al. (2016).

The Jasienica Marl contains both smaller and larger *Chondrites, Planolites, Palaeophycus, Thalassinoides, Alcyonidiopsis,* and *Zoophycos*, which occur on a totally bioturbated background (Fig. 28A–C). According to the distribution of trace fossils, the section has been subdivided into four intervals, of which intervals 2 and 3 are separated by the Bonarelli Level. The first interval, middle–upper Cenomanian in age (Kędzierski et al. 2012), was deposited

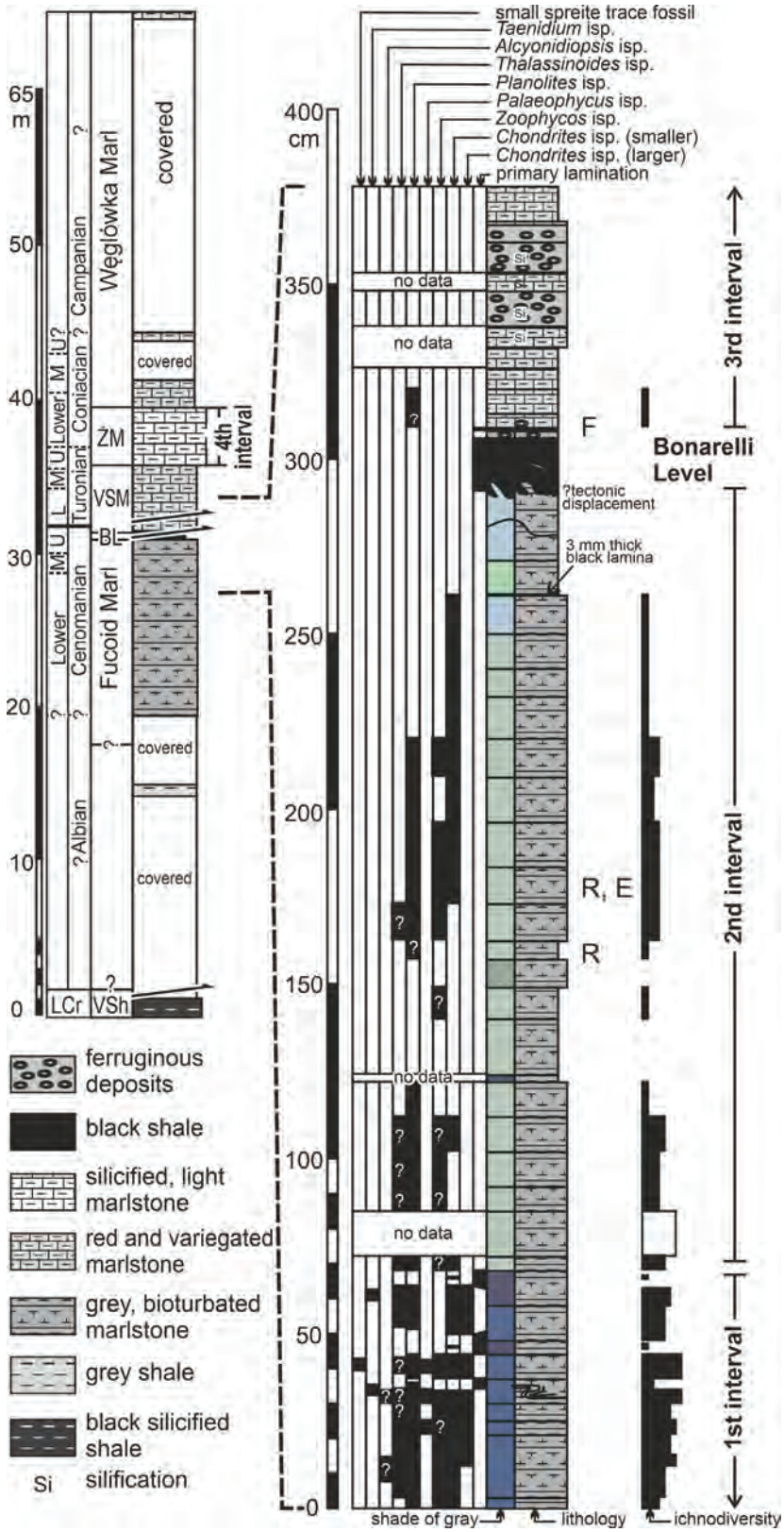

Fig. 27. Section of the first transect in the Nowe Rybie section (modified after Uchman et al. 2013). R – horizon with radiolaria, E – horizon with pelagic crinoids, F – horizon with thin bivalve shells (filaments).

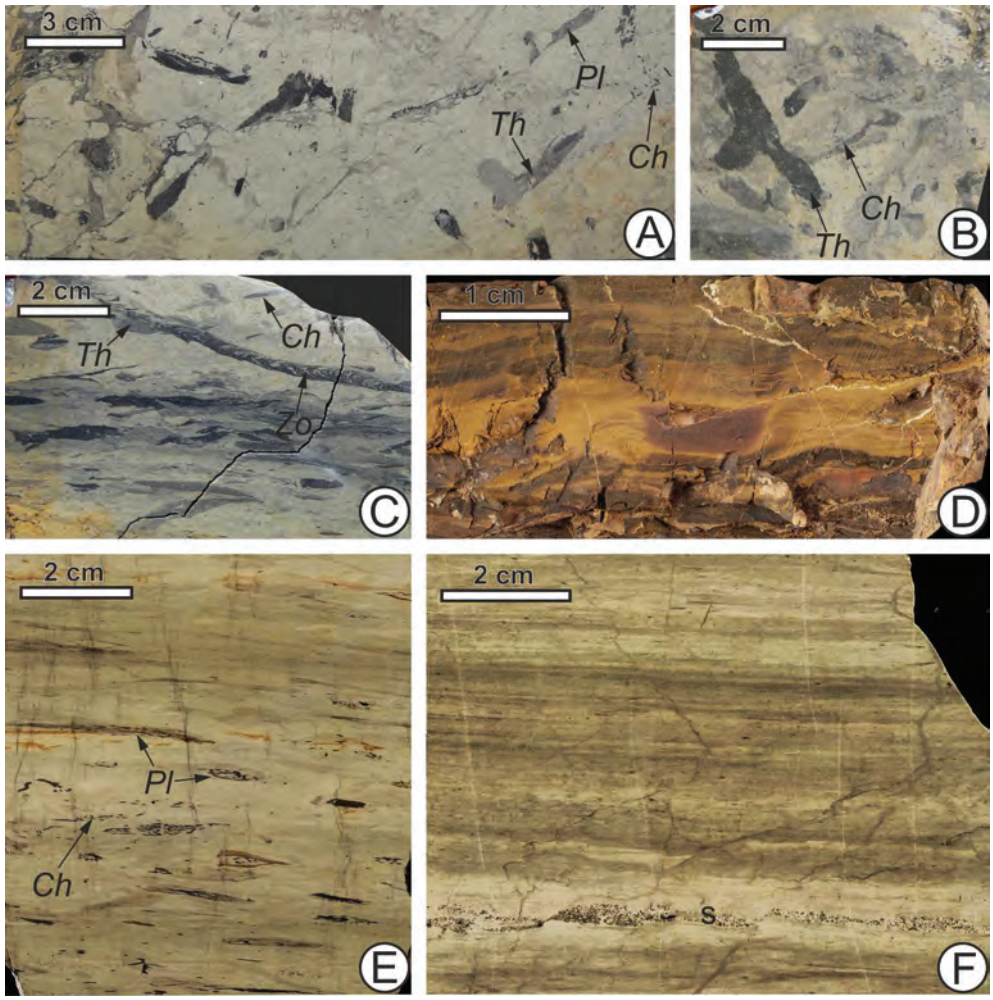

Fig. 28. Ichnofabrics of the Jasienica (Fucoid) Marl (**A**–**C**), the ferruginous bed above the Bonarelli Level (**D**), and the Żegocina Marl (**E**, **F**). *Ch – Chondrites, Pl – Planolites, Th – Thalassinoides, Zo – Zoophycos*, s – sandstone lamina. A and B are horizontal; C–F are vertical wetted cutting surfaces.

in an oxic to mesotrophic environment suitable for epifauna and shallow to deep infauna, except for short anoxic events represented by dark grey marls with primary lamination; these anoxic events occurred before OAE-2 (Uchman et al. 2013). They are also known from other deep-sea sections in the Carpathians (Silesian Unit) and in the Betic Cordillera (Uchman et al. 2008; Rodríguez-Tovar and Uchman 2011; Rodríguez-Tovar et al. 2009a, b). The abundance and diversity of trace fossils decrease upwards in the interval. This is suggestive of an evolution towards less oxic, mesotrophic, and ultimately eutrophic conditions on the sea floor (Uchman et al. 2013).

In the second interval (upper Cenomanian; Kędzierski et al. 2012), the abundance and diversity of trace fossils are considerably lower than in the first interval. Micropaleontological data suggest a significant deterioration of paleoenvironmental conditions (Kędzierski et al. 2012). It seems that this is not a consequence of reduced oxygenation, because organic matter concentrations are lower than in the first interval and the sediments are bioturbated, but rather that environmental stress resulted from extreme oligotrophy (Uchman et al. 2013). In this interval, two horizons with abundant radiolaria are recognized; the second is accompanied by abundant pelagic crinoids (roveacrinids). The abundant occurrence of these microfossils are considered to be bioevents (Kędzierski et al. 2012).

The third interval (Turonian; Kędzierski et

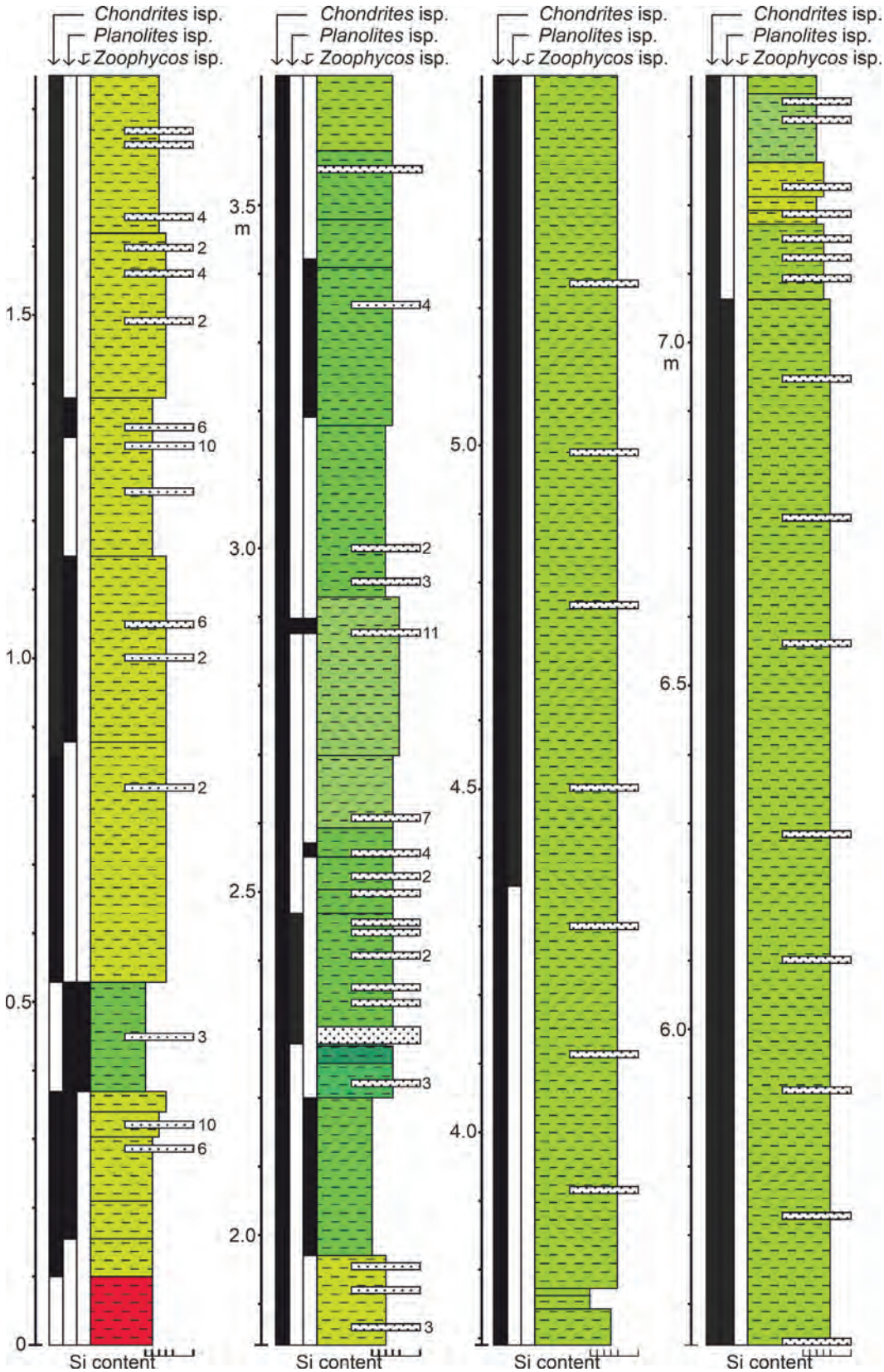

Fig. 29. Section of the Żegocina Marl along the road in the Nowe Rybie section.

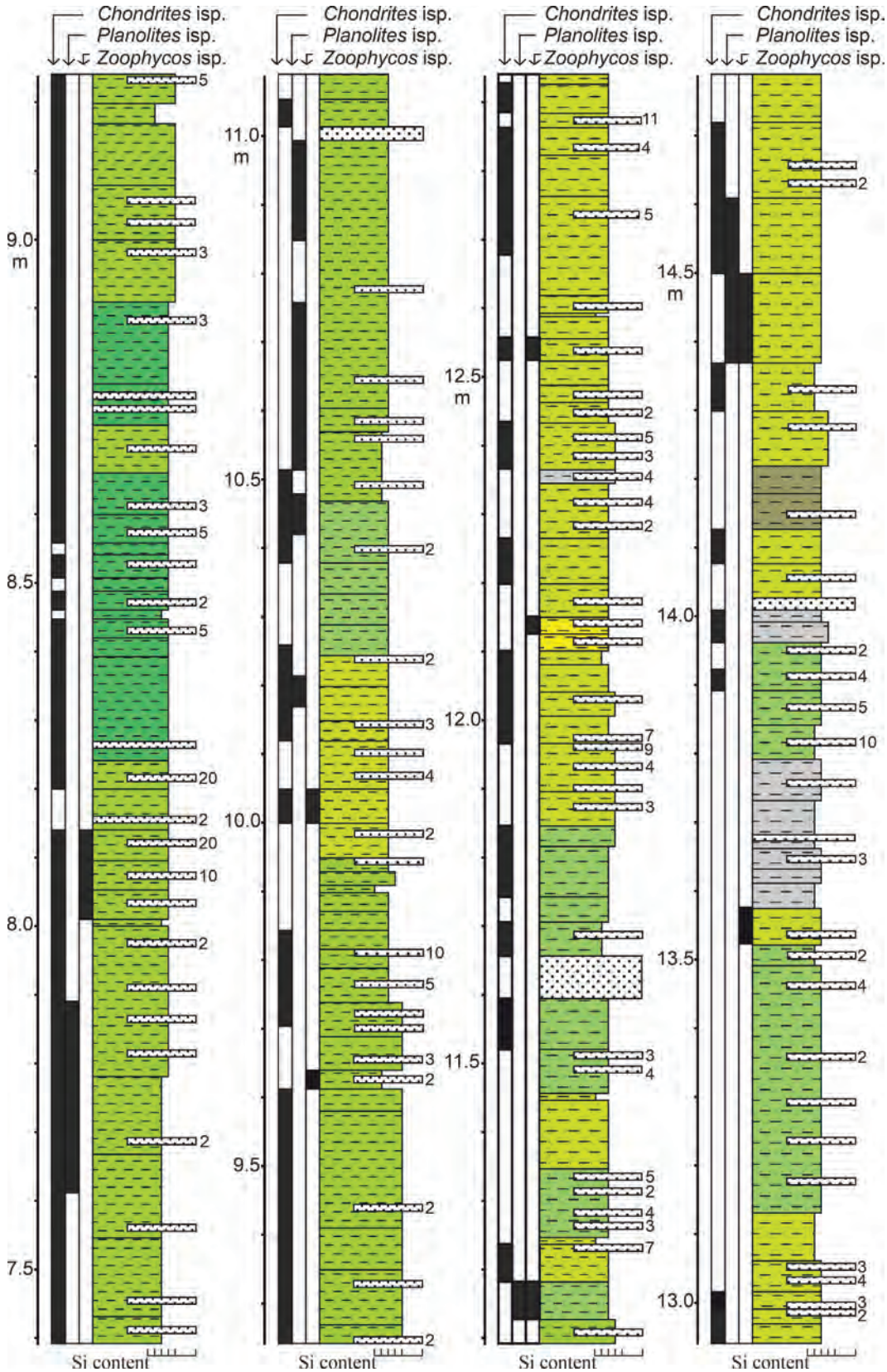

Fig. 29. (*continued.*)

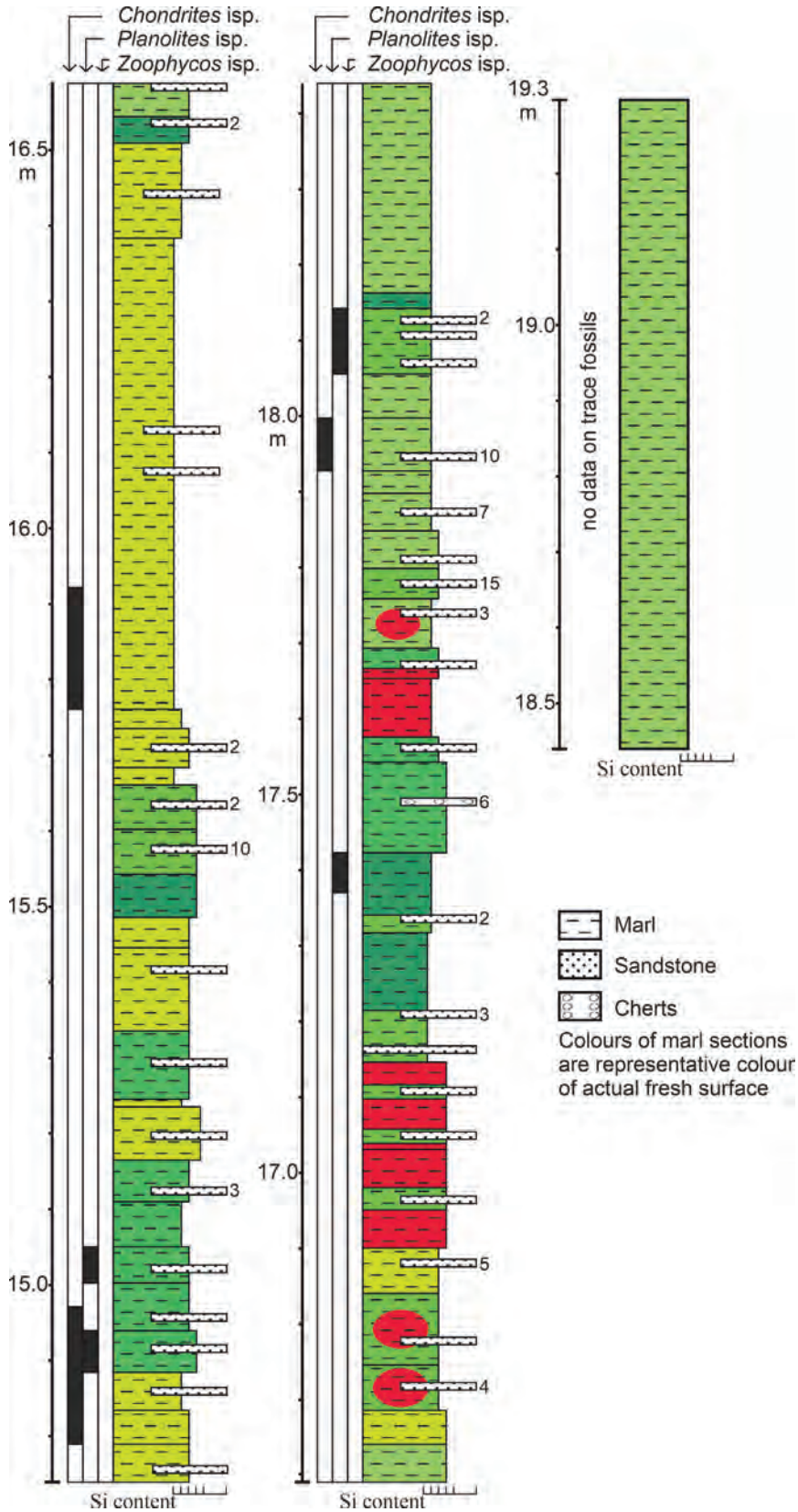

Fig. 29. (*continued.*)

al. 2012) is located above the black shales of the Bonarelli Level and is characterised by low organic matter concentrations, sedimentation rates, and degrees of bioturbation (Uchman et al. 2013). Kędzierski et al. (2012) suggested that high-nutrient and oxygen-depleted conditions existed in the upper water column – but not necessarily on the sea floor, where extreme oxygenation and oligotrophy were possible (Uchman et al. 2013). An increase in oligotrophic conditions from the top of interval 2 to the base of interval 3 (except for the Bonarelli Level), with (i) hyperoligotrophic and oxic conditions and (ii) highly oxidized conditions in intervals 2 and 3, respectively, was confirmed by investigations of dinocysts and palynofacies: dinocysts, mostly from the *Spiniferites* group, occur exclusively in the first interval (Radmacher and Uchman 2020). At the base of this interval, thin bivalve shells (filaments) occur (Kędzierski et al. 2012).

The fourth interval refers to the Żegocina Marl (upper Turonian–lower Coniacian), which crops out in the waterfall. Its thickness, only 5.5 m here, seems to be tectonically reduced in the lower part, because its thickness in the second transect (a hundred metres away) is three times greater. The Żegocina Marl is composed of bedded, silicified, creamy to light greenish or rose (only in the topmost part) lutitic marls with rare, usually discontinuous, very thin layers or laminae of medium- to coarse-grained sandstones. The hardness of the marls fluctuates. Rare cherts can occur in the upper part. They are bioturbated, but the trace fossil diversity is very low (*Chondrites*, *Planolites*, rare *Thalassinoides* and *Zoophycos*). Commonly, *Planolites* is preferentially reworked with *Chondrites* (Fig. 28E). In some beds, diffused lamination expressed by colour differences is present (Fig. 28F). Within the laminae, bioturbation structures are visible; in such horizons, the bioturbation was very shallow. In the second transect along the road, the Żegocina Marls section is more complete (Fig. 29).

Above the Żegocina Marl, the Węglówka Marl (upper Coniacian–Campanian–?Paleocene) can be observed in small, temporary outcrops of weathering debris. It is composed of red to green soft, massive marls: these are bioturbated, but their trace fossils are very poorly visible. It seems that bioturbation in the Żegocina and Węglówka marls was continuous and very shallow, mainly in soupy near-surface sediment unsuitable for the preservation of trace fossils. This demonstrates that the favourable conditions from before OAE 2 had not yet returned.

The second transect (on the road; Fig. 29) starts with the Jasienica Marl (~15 m), transitional beds (~5 m) containing grey, rose and greenish marls of variable hardness, and the Żegocina Marl (~12.3 m). The Bonarelli level is missing here; it is probably tectonically sheered. Above the Węglówka Marl, the Rybie Sandstone (?Paleocene–Eocene) is poorly exposed along the road escarpment. It is at least 50 m thick and composed of turbiditic sandstone beds of variable thickness, intercalated with light grey shales. The sandstones, at least in the lower part, are rich in rose feldspar. Small coal clasts are present. Among the trace fossils, *Ophiomorpha annulata* and *Ophiomorpha rudis* were noted. The sandstones contain exotic pebbles and form isolated bodies in the area.

Stop 6: Słopnice–Słopniczanka river section. Upper Cretaceous of the Magura Nappe (*Alfred Uchman, Oliwia Kowalczewska, Mateusz Szczęch*)

Three thrust sheets with beds dipping generally to the north, and a syncline, containing the Ropianka Formation (Campanian–Paleocene), variegated shales of the Łabowa Shale Formation (Eocene), and the Beloveža Formation (Eocene) crop out along the Słopniczanka river at Słopnice toward Zamieście. They belong to the Rača Zone of the Magura Nappe. Their tectonics was elucidated by Konon (1996). The present route crosses them from south to north (Fig. 30).

The Ropianka Formation (Maastrichtian–Paleocene) can be observed in the Łopień Syncline (GPS coordinates: N 49° 42' 40.4''; E 20° 20' 45.1''; ±5 m). Upstream, the lower part of the Ropianka Formation crops out. It contains a folded and thrusted package of grey, thin, medium, and thick beds of mostly fine-grained, micaceous, calcareous, quartz-dominated sandstones intercalated with grey marlstones and grey calcareous siltstone and

mudstones. Most of the beds are turbidites, and some show Bouma intervals. There are some beds of mud-dominated debris flow deposits. Upriver, the thick-bedded muscovitic sandstones on either side of the bridge of a local road may already belong to the upper Szczawina Formation (middle Campanian–Paleocene).

A series of samples taken from the mudstones in this part of the section, and in the next portion belonging to the Ropianka Formation, contain uniformly preserved foraminifers of DWAF assemblages typical of the bathyal-abyssal depths. At least 50% of the samples contain tubular agglutinated forms, which mostly represent suspension feeders. These include *Bathysiphon* sp., *Nothia* sp., *Rhabdammina* sp. and *Rhizammina* sp. Other common taxa include *Trochamminoides* sp., *Paratrochamminoides* sp., *Caudammina* sp., *Saccammina* sp., *Placentammina* sp., and *Glomospira* sp. Less common, but continuously present in the section, are *Recurvoides* sp., *Rzehakina* sp., *Ammodiscus* sp., *Ammosphaeroidina* sp., *Reophax* sp., *Subreophax* sp., and *Karrerulina* sp. Almost of these have poor stratigraphic resolution, ranging from the Campanian up to the Eocene or Oligocene. However, in a couple of samples, *Annectina grzybowskii* (Jurkiewicz), *Hormosina velascoensis* (Cushman), and *Rzehakina epigona* (Rzehak) are present, which together with the presence of *Rzehakina inclusa* (Grzybowski), *Caudammina excelsa* (Dylążanka), and *Caudammina ovula* (Grzybowski) may indicate the uppermost part of the *Rz. inclusa* Zone *sensu* Olszewska (1997). This is supported by the co-occurrence of *Rz. inclusa* and *Rz. fissistomata*. While the latter is regarded as a marker for the Paleocene, it may already appear in the Maastrichtian. As such, these samples can be ascribed to the upper Maastrichtian.

The section is rich in trace fossils, as presented by Uchman (2008b) and Uchman and Wetzel (2017). In the grey, thin- and medium-bedded, micaceous sandstones intercalated with grey calcareous siltstones and mudstones, *Chondrites, Planolites, Phycosiphon incertum, Nereites irregularis, Tubulichnium rectum* (Fig. 31A), *Zoophycos*, and rarely *Desmograpton* isp., and *Cladichnus fisheri* have been found in the southern segment of the section. Downriver, a thin- to medium-bedded, over-

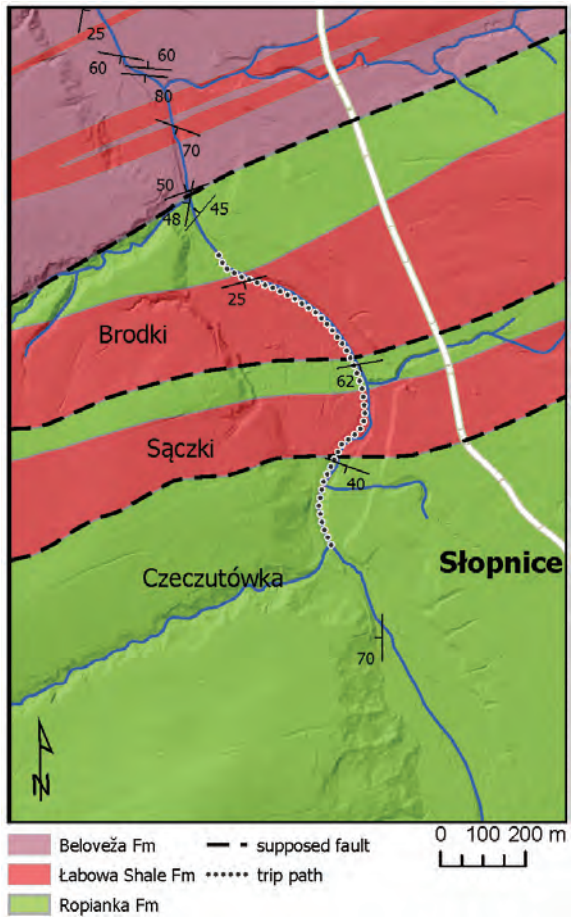

Fig. 30. Geological map of Słopnice (Stop 6) in the Magura Nappe, based on Uchman (2008b).

turned flysch can be observed. It contains *Chondrites intricatus, Ch. targionii, Phycosiphon incertum, Nereites irregularis, Zoophycos* isp., *Tubulichnium rectum, Ophiomorpha oraviense, Planolites* isp., *?Rhizocorallium* isp., *Thalassinoides, Gordia* isp., *Helminthopsis* isp. *Chondrorhaphe bifida, Acanthorhaphe delicatula, Helicolithus sampelayoi, Fascisichnium* isp., *Urohelminthoida appendiculata, Belorhaphe zigzag, Paleodictyon strozzii* (Fig. 31B), *Desmograpton* isp., *Glockerichnus alata, Spirophycus bicornis* (Fig. 31C), *Scolicia prisca,* and *Scolicia strozzii*. The large foraminifer *Arthrodendron,* which is built of chains of chambers, is common in a package of beds. *Bathysiphon* sp. is present as well. The trace fossil assemblage is typical of the Paleodictyon ichnosubfacies of the Nereites ichnofacies.

Downriver, a tectonically reduced slice of the variegated shales (Łabowa Shale For-

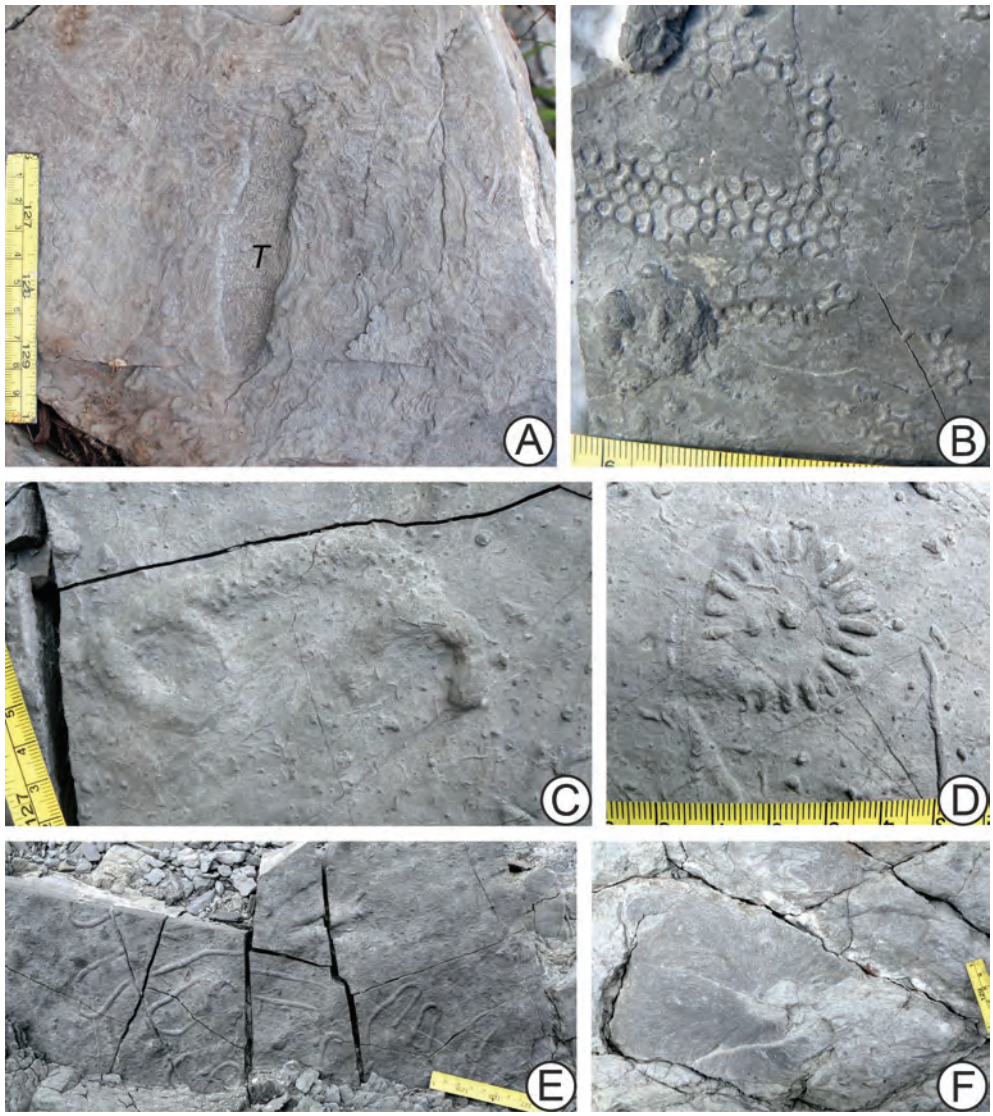

Fig. 31. Selected trace fossils from the Ropianka Formation. **A** – *Tubulichnium rectum* (*T*) and *Nereites irregularis*. **B** – *Paleodictyon strozzii*. **C** – *Spirophycus bicornis*. **D** – *Lorenzinia carpathica*. **E** – *Helminthorhaphe magna*. **F** – *Zoophycos* isp.

mation) of the Sączki Thrust Sheet can be observed (GPS coordinates: N 49° 42' 45.2''; E 20° 20' 46.6''; ±5 m). In this section, the variegated shales are deeply bioturbated. The shales, and sandstones within them, contain *Scolicia* isp., *Planolites* isp., *Avetoichnus luisae*, *Halopoa* isp., *Nereites*, and ?*Thalassinoides*. This suggests that the original organic matter content in the sediment was high enough to maintain the burrowing community, regardless of the very low organic carbon content at present (Wetzel and Uchman 2018).

Further down the river, the thin- to medium-bedded flysch of the Ropianka Formation (up to GPS coordinates: N 49° 42' 47.6''; E 20° 20' 45.4''; ±6 m) crop out. The trace fossils *Spirorhaphe* isp., *Cosmorhaphe sinuosa, Lorenzinia carpathica* (Fig. 31D), *Helminthorhaphe magna* (type locality; Fig. 31E), *Ubinia* isp., *Halimedides* isp., *Ptychoplasma vagans, Chondrites intricatus, Ch. targionii, Phycosiphon incertum, Nereites irregularis, Scolicia strozzii, Spirophycus bicornis,* and "*Arthrophycus*" *strictus,* and the macroforaminifer *Arthrodendron*, have been found here.

Walking downriver, the Variegated Shale of the Brodki Thrust Sheet crop out for about 350 m (up to GPS coordinates: N 49° 42' 54.4''; E 20° 20' 30.5''; ±5 m). Turbiditic beds are very com-

mon in the shales. Among the trace fossils, *Planolites* and locally *Scolicia* are common.

Downriver a package of thin-to medium bedded flysch deposits can be observed on the western bank of the river, probably representing the Beloveža Formation (Eocene). Below, thin- to thick-bedded flysch of the Ropianka Formation crop out (up to GPS coordinates: N 49° 43' 00.5''; E 20° 20' 26.5''; ±5 m) and the Variegated Shale can be seen again. The Ropianka Formation outcrops end with thick sandstone beds intercalated with thin- and medium-bedded flysch. The sandstones are calcareous and micaceous. In the thin and medium beds, *Lorenzinia carpathica, Lorenzinia nowaki, Urohelminthoida dertonensis, Helminthorhaphe flexuosa, H. japonica*, *Spirorhaphe* isp., *Ubinia* isp., *Megagrapton irregulare*, *Acanthorhaphe delicatula, Chondrorhaphe bifida*, *Ophiomorpha annulata, O. rudis, Taenidium* isp., *Nereites irregularis, Phycosiphon incertum, Tubulichnium incertum, Rotundusichnium zumayense, Zoophycos* isp. (Fig. 31F), and *Scolicia* isp. have been found. The large-chambered foraminifer *Arthrodendron* can be found rarely.

REFERENCES

Alexandrowicz, W.P. and Lalik, W. 1999. Granica między warstwami lgockimi i godulskimi w północnej części Beskidu Małego. Zeszyty Naukowe AGH, Geologia, 25, 107–123.

Barwicz-Piskorz, W. and Rajchel, J. 2012. Radiolarian and agglutinated foraminiferal biostratigraphy of the Paleogene deep-water deposits on the north ern mar gin of the Carpathian Tethys (Skole Unit). Geological Quarterly, 56, 1–24.

Bąk, K. 2007. Environmental changes around the Cenomanian–Turonian boundary in a marginal part of the Outer Carpathian Basin expressed by microfacies, microfossils and chemical records in the Skole Nappe (Poland). Annales Societatis Geologorum Poloniae, 77, 39–67.

Bąk, K., Bąk, M. and Paul, Z. 2001. Barnasiówka Radiolarian Shale Formation – a new lithostratigraphic unit in the Upper Cenomanian–lowermost Turonian of the Polish Outer Carpathians (Silesian Series). Annales Societatis Geologorum Poloniae, 71, 75–103.

Bąk, M., Bąk, K. and Ciurej, A. 2005. Mid-Cretaceous spicule-rich turbidites in the Silesian Nappe of the Polish Outer Carpathians: radiolarian and foraminiferal biostratigraphy. Geological Quarterly, 49, 275–290.

Bąk, K., Bąk, M., Geroch, S. and Manecki, M. 1997. Biostratigraphy and paleoenvironmental analysis of benthic foraminiferal and radiolarians in Paleogene Variegated Shales in the Skole Unit, Polish Flysch Carpathians. Annales Societatis Geologorum Poloniae, 67, 135–154.

Baas, J.H., Best, J.L. and Peakall, J. 2016. Predicting bedforms and primary current stratification in cohesive mixtures of mud and sand. Journal of the Geological Society, 173, 12–45.

Bieda, F., Geroch, S., Koszarski, L., Książkiewicz, M. and Żytko, K. 1963. Stratigraphie des Karpates externes polonaises. Biuletyn Instytutu Geologicznego, 181, 1–210.

Bielawska, J., 2002. Paleoecological remarks about the late Cretaceous foraminiferids from the Frydek-type marls (Subsilesian Unit, Polish Outer Carpathians). Geologica Carpathica, 53, special issue on CD.

Birkenmajer, K. 1985. Fourth Day. In: Birkenmajer, K. (Ed.), Main Geotraverse of the Polish Carpathians (Cracow–Zakopane). Guide to Excursion 2, XIII Congress of the Carpatho-Balkan Geological Association, Cracow, Poland, 90–136. Wydawnictwa Geologiczne; Warszawa.

Birkenmajer, K. and Oszczypko, N. 1988. New lithostratigraphic standard for the Paleogene of the Magura Flysch Basin (southern part). Bulletin of the Polish Academy of Sciences, Earth Sciences, 36, 253–259.

Bralower, T.J., Arthur, M.A., Leckie, R.M., Sliter, W.V., Allard, D.J. and Schlanger, S.O. 1994. Timing and paleoceanography of oceanic dysoxia/anoxia in the late Barremian to early Aptian (Early Cretaceous). Palaios, 9, 335–369.

Brandys, J. 2000. Biostratigraphy and paleoecology of the Upper Cretaceous Frydek-type marls from the Rajbrot tectonic window (Polish Flysch Carpathians). Slovak Geological Magazine, 6, 218–219.

Bromowicz, J. 1974. Facial variability and lithological character of Inoceramian Beds of the Skole Nappe between Rzeszów and Przemyśl. Prace Geologiczne, Polska Akademia Nauk, Oddział w Krakowie, Komisja Nauk Geologicznych, 84, 1–83. [In Polish, with English summary]

Bromowicz, J. 2001. Application of the building stones of the Cracow area for the masonry reconstructions – evaluation of perspectives. Gospodarka Surowcami Mineralnymi, 17, 5–73. [In Polish, with English abstract]

Bromowicz, J. Gucik, S., Magiera, J., Moroz-Kopczynska, M., Nowak, T.W. and Peszat, C. 1976. Piaskowce karpackie, ich znaczenie surowcowe i perspektywy wykorzystania. Zeszyty Naukowe AGH, Geologia, 2, 3–94.

Bukowy, S. and Geroch, S. 1957. On the age of exotic conglomerates at Kruhel Wielki near Przemyśl (Carpathians). Rocznik Polskiego Towarzystwa Geologicznego, 26, 297–329. [In Polish, with English summary]

Burtan, J. 1937. Stratigraphie des Schlesischen Beskiden. Bulletin International de l'Académie Polonaise des Sciences et des Lettres de Cracovie, Clasee des Sciences Mathématiques et Naturelles Série A: 1936, 195–209.

Burtan, J. 1954. Szczegółowa Mapa Geologiczna Polski, 1: 50 000, Arkusz M34-77A Wieliczka. Instytut Geologiczny.

Burtan, J. 1966a. Szczegółowa Mapa Geologiczna Polski, 1: 50 000, Arkusz M34-77A Wieliczka. Instytut Geologiczny.

Burtan, J. 1966b. Szczegółowa Mapa Geologiczna Polski, 1: 50 000, Arkusz M34-77C Mszana Dolna. Instytut Geologiczny.

Burtan, J. 1973. Explanations to Detailed Geological Map of Poland, 1: 50.000, Wisła (1028). Wydawnictwa Geologiczne, Warszawa. [In Polish]

Burtan, J. 1974. Szczegółowa Mapa Geologiczna Polski, 1: 50 000, Arkusz 1016 Mszana Dolna. Instytut Geologiczny.

Burtan, J. 1977. Szczegółowa Mapa Geologiczna Polski w skali 1:50 000, arkusz Mszana Dolna (1016). Wydawnictwa Geologiczne.

Burtan, J. 1978. Objaśnienia do Szczegółowej Mapy Geologicznej Polski. Arkusz Mszana Dolna (1016), 1: 50 000, 70. Wydawnictwa Geologiczne, Warszawa. [In Polish]

Burtan, J. 1984. Tektonika Karpat fliszowych na południe od Wieliczki. Biuletyn Instytutu Geologicznego, 340, 5–19.

Burtanówna, J., Konior, K. and Książkiewicz, M. 1937. Mapa geologiczna Karpat Śląskich w skali 1:50 000 (z objaśnieniami). Wydawnictwo Śląskie, Polska Akademia Umiejętności; Kraków. [In Polish, French summary]

Burzewski, W. 1966. Baculites marls on the lithostratigraphy background of the upper Inoceramian Beds of the Skiba Carpathians. Zeszyty Naukowe AGH, Geologia, 7, 89–115. [In Polish]

Cieszkowski, M., Oszczypko, N. and Zuchiewicz, W. 1989. Upper Cretaceous siliciclastic-carbonate turbidites at Szczawa, Magura Nappe, West Carpathians, Poland. Bulletin of Polish Academy of Sciences, Earth Sciences, 37, 231–245.

Cieszkowski, M., Gedl, E., Ślączka, A. and Uchman, A. 2001. Stop C2 – Rzyki Village. In: Cieszkowski, M. and Ślączka, A. Silesian and Subsilesian units. 12th Meeting of the Association of European Geological Societies and LXXII Zjazd Polskiego Towarzystwa Geologicznego, Field Trip Guide. Państwowy Instytut Geologiczny, Kraków, pp. 115–118.

Cieszkowski, M., Gedl, E. and Uchman, A. 2003. Stop 3. Zagórnik–Rzyki villages. In: Ber, A. and Alexandrowicz, Z. (Eds), Geological Heritage Concept, Conservation and Protection Policy in Central Europe, 3–4 October 2003, Cracow, Poland. Abstracts and Field Trip Guide-Book, pp. 86–90. Polish Geological Institute; Warsaw.

Dżułyński, S. 1963. Directional structures in flysch. Studia Geologica Polonica, 12, 1–136.

Dżułyński, S. 1996. Erosional and deformational structures in single sedimentary beds: A genetic commentary. Annales Societatis Geologorum Poloniae, 66, 101–189.

Dżułyński, S., Książkiewicz, M. and Kuenen, P.H. 1959. Turbidites in flysch of the Polish Carpathians. Bulletin of the Geological Society of America, 70, 1089–1118.

Dżułyński, S. and Ślączka, A. 1958. Directional structures and sedimentation of the Krosno Beds. Rocznik Polskiego Towarzystwa Geologicznego, 28, 205–260.

Dżułyński, S., Kotlarczyk, J. and Ney, R. 1979. Submarine mass movements in the Skole Basin. In: Kotlarczyk, J. (Ed.), Poziomy z olistostromami w Karpatach przemyskich. Materiały Terenowej Naukowej Konferencji w Przemyślu: Stratygrafia formacji z Ropianki (fm), 17–27. Powielarnia AGH; Przemyśl.

Dżułyński, S. and Walton, E. K. 1963. Experimental production of sole markings. Transaction of the Edinburgh Geological Society, 19, 279–305.

Gągała, Ł., Vergés, J., Saura, E., Malata, T., Ringenbach, J.C., Werner, P. and Krzywiec, P. 2012. Architecture and orogenic evolution of the northeastern Outer Carpathians from cross-section balancing and forward modelling. Tectonophysics, 532, 223–241.

Gasiński, M.A. and Uchman, A. 2009. Latest Maastrichtian foraminiferal assemblages from the Husów region, Skole Nappe, Polish Flysch Carpathians. Geologica Carpathica, 60, 283–294.

Gasiński, M.A. and Uchman, A. 2011. The Cretaceous–Paleogene boundary in turbiditic deposits identified to the bed: a case study from the Skole Nappe, Polish Carpathians. Geologica Carpathica, 62, 333–343.

Gasiński, M.A., Olshtynska, A. and Uchman. 2013. Late Maastrichtian foraminiferids and diatoms from the Ropianka Formation, Skole Nappe, Polish Carpathians: a case study from the Chmielnik-Grabówka section. Acta Geologica Polonica, 63, 515–525.

Gąsiorowski, S. 1960. Two faunas Aptychi from the Grodischt sandstones. Bulletin de l'Académie Polonaise Sciences. Série Ciences Géologiques et Géographiques, 8, 131–135.

Gedl, E. 2001. Late Cretaceous dinocysts of the siliceous limestones from Rzyki (Silesian Nappe, western Outer Carpathians, Poland). Biuletyn Państwowego Instytutu Geologicznego, 396, 48–49.

Gedl, E. 2003. Biostratygrafia i paleoekologia warstw wierzowskich i lgockich jednostki śląskiej polskich Karpat fliszowych na zachód od Raby w świetle badań palinologicznych, 246. Unpublished Ph.D. thesis, Jagiellonian University.

Geroch, S. 1960. Microfaunal assemblages from the Cretaceous and Paleogene Silesian Unit in the Beskid Śląski Mts. Bulletin of the Geological Institute, 153, 7–138. [In Polish, English summary]

Geroch, S. and Nowak, W. 1963. Profil dolnej kredy

śląskiej w Lipniku koło Bielska. Rocznik Polskiego Towarzystwa Geologicznego, 32, 241–264.

Geroch, S. and Nowak, W. 1984. Proposal of zonation for the Late Tithonian–Late Eocene based upon arenaceous foraminifera from the Outer Carpathians, Poland. In: Oertli (Ed.), Benthos '83: 2nd International Symposium on Benthic Foraminifera (Pau, France), 225–239. Elf-Aquitaine, ESSO REP and Total CFP; Pau and Bordeaux.

Geroch, S., Krysowska-Iwaszkiewicz, M., Michalik, M., Prochazka, K., Radomski, A., Radwański, Z., Unrug, Z., Unrug, R. and Wieczorek, J. 1979. Sedimentation of the Węgierka marls. Rocznik Polskiego Towarzystwa Geologicznego, 49, 105–133. [In Polish, with English summary]

de Gibert, J.M., Arbues, P., Puig, M. and Marzo, M. 2001. Ichnological signatures of turbidite channels from the Eocene Ainsa slope complex (Spanish Pyrenees). American Association of Petroleum Geologists 2001 Annual Meeting, Denver, Colorado, United States, June 3–6, 2001, Expanded Abstracts, p. 71.

Golonka, J. and Picha, F.J. 2006. The Carpathians and their foreland: Geology and hydrocarbon resources. AAPG Memoir, 84, 259–291.

Golonka, J., Vašíček, Z., Skupien, P., Waśkowska-Oliwa, A., Krobicki, M., Cieszkowski, M., Ślączka, A. and Słomka, T. 2008. Lithostratigraphy of the Upper Jurassic and Lower Cretaceous deposits of the western part of the Outer Carpathians (discussion proposition). Geologia, 34, 9–31. [In Polish, with English summary]

Górniak, K. 2015. High-resolution petrography of marls from Goleszów (Polish Outer Carpathians, Upper Jurassic Vendryně Formation). Geological Quarterly, 59, 135–144.

Gucik, S. 1963. Profil kredy dolnej z Bełwina w Karpatach przemyskich. Kwartalnik Geologiczny, 7, 257–268.

Gucwa, I. and Wieser, T. 1980. Geochemia i mineralogia skał osadowych fliszu karpackiego zasobnych w materię organiczną. Polska Akademia Nauk – Oddział w Karkowie, Prace Mineralogiczne, 69, 3–43.

Hanzlíková, E. 1972. Carpathian Upper Cretaceous Foraminifera of Moravia (Turonian–Maastrichtian). Rozpravy Ústředního ústavu geologického, 39, 1–160.

Jaminski, J. 1995. The mid-Cretaceous palaeoenvironmental conditions in the Polish Carpathians – a palynological approach. Review of Palaeobotany and Palynology, 87, 43–50.

Jankowski, L., Kopciowski, R. and Rytko, W. (Eds) 2004. Geological Map of the Outer Carpathians; Borderlands of Poland, Ukraine and Slovakia, 1: 200 000. Publication Dep. of Polish Geological Institute; Warsaw.

Jugowiec-Nazarkiewicz, M. 2007. Nanoplankton wapienny górnokredowych facji pelagicznych jednostki podśląskiej Polskich Karpat Fliszowych (Calcareous nannoplankton from Upper Cretaceous pelagic facies of the Subsilesian Unit, Polish Outer Carpathians). Biuletyn Państwowego Instytutu Geologicznego, 426, 53–90.

Jugowiec-Nazarkiewicz, M. and Jankowski, L. 2001. Nannoplankton biostratigraphy of the Żegocina marls; a new aspect of the geologic setting of the Lanckorona-Żegocina zone. Przegląd Geologiczny, 49, 1186–1190. [In Polish, with English summary]

Kamieński, M., Peszat, C. and Rutkowski, J. 1967. Petrographic variability of the Carpathian sandstones and the problem of sandstone classification. Rocznik Polskiego Towarzystwa Geologicznego, 37, 499–508. [In Polish, with English summary]

Kędzierski, M., Machaniec, E., Rodríguez-Tovar, F.J. and Uchman, A. 2012. Bio-events, foraminiferal and nannofossil biostratigraphy of the Cenomanian/Turonian boundary interval in the Subsilesian Nappe, Rybie section, Polish Carpathians. Cretaceous Research, 35, 181–198.

Kędzierski, M., Gasiński, M. A. and Uchman, A. 2015. Last occurrence of *Abathomphalus mayaroensis* (Bolli) foraminiferid index of the Cretaceous Paleogene boundary: the calcareous nannofossil proof. Geologica Carpathica, 66, 181–195.

Kędzierski, M. and Ochabska, A. 2012. Calcareous nannofossil biostratigraphy and sedimentary environment of Valanginian–Hauterivian rhythmites (Silesian Nappe, Polish Carpathians). Annales Societatis Geologorum Poloniae, 82, 225–237.

Konon, A. 1996. Tektonika góry Łopień (Beskid Wyspowy). Przegląd Geologiczny, 44, 1195–1198.

Kotlarczyk, J. 1978. Stratigraphy of the Ropianka Formation or of Inoceramian Beds in the Skole Unit of the Flysch Carpathians. Prace Geologiczne, Polska Akad. Nauk, Oddział w Krakowie, Komisja Nauk Geologicznych, 108, 1–82. [In Polish, with English summary]

Kotlarczyk, J., Pękala, K. and Gucik, S. (Eds). 1988. Karpaty Przemyskie. Przewodnik 59 Zjazdu Polskiego Towarzystwa Geologicznego, Przemyśl, 16–18.IX.1988, 298. Wydawnictwo Akademii Górniczo-Hutniczej; Kraków.

Kotlarczyk, J. 1979. Stratigraphy of the Ropianka Formation of the Skole unit. Materiały Terenowej Konferencji Naukowej w Przemyślu, Przemyśl, 28–29 czerwca 1979 r. Sekcja Sedymentologiczna Polskiego Towarzystwa Geologicznego, Kraków, 7–16. [In Polish]

Kotlarczyk, J. 1988. Outline of the stratigraphy of the marginal tectonic units of the Carpathian orogen In: Kotlarczyk, J., Pękala, K. and Gucik, S. (Eds), Przewodnik 59 Zjazdu Polskiego Towarzystwa Geologicznego, Karpaty Przemyskie, 16–18 września 1988, 23–62. Wydawnictwo AGH; Kraków. [In Polish]

Kowalczewska, O. and Gasiński, M.A. 2018. Late Cretaceous foraminiferids from sections in the Zabratówka area (Skole Nappe, Outer Carpathians, Poland). Annales Societatis Geologorum Poloniae, 88, 71–85.

Krajewski, S. and Urbaniak, J. 1964. Wielokomórkowe znaleziska fauny w północnych Karpatach fliszowych, część I. Wielokomórkowce. Biuletyn Instytutu Geologicznego, 179, 1–188.

Książkiewicz, M. 1951. Objaśnienia do Arkusza Wadowice. Państwowy Instytut Geologiczny, Warszawa, 283 pp.

Książkiewicz, M. 1954. Graded bedding and lamination in the Carpathian flysch. Rocznik Polskiego Towarzystwa Geologicznego, 22, 399–449.

Książkiewicz, M. 1956. Geology of the Northern Carpathians. Geologische Rundschau, 45, 369–411.

Książkiewicz, M. (Ed.). 1962. Geological Atlas of Poland. Stratigraphic and facial problems. Fascicle 13 – Cretaceous and Early Tertiary in the Polish External Carpathians, 1: 600,000. Państwowy Instytut Geologii; Warszawa.

Książkiewicz, M. 1970. Observations on the ichnofauna of the Polish Carpathians. In: Crimes, T.P. and Harper, J.C. (Eds), Trace fossils. Geological Journal, Special Issue, 3, 283–322.

Książkiewicz, M. 1975. Bathymetry of the Carpathian Flysch basin. Acta Geologica Polonica, 25, 309–367.

Książkiewicz, M. 1977a. The tectonics of the Carpathians. In: Geology of Poland, v. 4: Tectonics. Geological Institute, Warszawa, pp. 476–669.

Książkiewicz, M. 1977b. Trace fossils in the flysch of the Polish Carpathians. Palaeontologia Polonica, 36, 1–208.

Kuśmierek, J. and Baran, U. 2016. Structure and tectonic evolution of the NE segment of the Polish-Ukrainian Carpathians during the Late Cenozoic: subsurface cross-sections and palinspastic models. Geologica Carpathica, 67, 347 – 370

Łapcik, P. 2018. Sedimentary processes and architecture of Upper Cretaceous deep-sea channel deposits: A case from the Skole Nappe, Polish Outer Carpathians. Geologica Carpathica, 69, 71–88.

Łapcik, P. 2019. Facies anatomy of a progradational submarine channelized lobe complex: semi-quantitativeanalysis of the Ropianka Formation (Campanian–Paleocene) in Hucisko Jawornickie section, Skole Nappe, Polish Carpathians. Acta Geologica Polonica, 69, 111–141.

Łapcik, P., Kowal-Kasprzyk, J. and Uchman, A. 2016. Deep-sea mass-flow sediments and their exotic blocks from the Ropianka Formation (Campanian–Paleocene) in the Skole Nappe: a case study of the Wola Rafałowska section (SE Poland). Geological Quarterly, 60, 301–319.

Leszczyński, S. 2003. Bioturbation structures in the Holovnia Siliceous Marls (Turonian–Lower Santonian) in Rybotycze (Polish Carpathians). Annales Societatis Geologorum Poloniae, 73, 103–122.

Leszczyński, S. and Uchman, A. 1991. To the origin of variegated shales. Geologica Carpathica, 42, 279–289.

Leszczyński, S., Malik, K. and Kędzierski, M. 1995. New data on lithofacies and stratigraphy of the Siliceous and Fucoid marl of the Skole Nappe (Cretaceous, Polish Carpathians). Annales Societatis Geologorum Poloniae, 65, 43–62. [In Polish, with English summary.]

Liszkowa, J. and Nowak, W. 1960. The Subsilesian series in the Bielsko Carpathians (The Frydek Subsilesian series). Kwartalnik Geologiczny, 4, 510–529. [In Polish, with English summary]

Machaniec, E., Gasiński, M.A., Ślączka, A. and Leśniak, T. 2005. A Middle Cenomanian foraminiferal assemblage from the Nowe Rybie section (Żegocina Tectonic Window, Subsilesian Unit, Polish Outer Carpathians). Studia Geologica Polonica, 124, 249–258.

Malata, T. 2001. The Skole Unit east of Rzeszów. Posiedzenia Naukowe Państwowego Instytutu Geologii, 57 (9), 60–63. [In Polish].

Matyszkiewicz, J. and Słomka, T. 1994. Organodetrital conglomerates with ooids in the Cieszyn Limestone (Tithonian–Berriasian) of the Polish Flysch Carpathians and their palaeogeographic significance. Annales Societatis Geologorum Poloniae, 63, 211–248.

Menčík, E. (Ed.) 1983. Geology of the Moravskoslezské Beskydy Mts. and Podbeskydská pahorkatina Upland. Ustredni Ústav Geologicky; Praha. [In Czech, with English summary]

Menčík, E. and Tyráček, J. (Eds) 1985. Synoptic Geological Map of the Beskydy Mts. and the Podbeskydská Pahorkatina Upland, 1: 100.000. Czech Geological Office, Geological Survey; Prague.

Miller, W., III, Stefani, C. and Grandesso, P. 2004. Alternation of ecologic regimes in a deep-marine carbonate basin: calciturbidite trace fossils from the Cretaceous Scaglia Rossa, northeastern Italy. Palaeogeography, Palaeoclimatology, Palaeoecology, 204, 317–330.

Mutti, E. and Ricci Lucchi, F. 1972. Le toribiditi dell'Appennino settentrionale: introduzione all'analisi di facies. Società Geologica Italiana Memorie, 11, 161–199.

Nescieruk, P. and Szydło, A. 2003. Pozycja warstw istebniańskich w Beskidzie Morawsko-Śląskim. Posiedzenia Naukowe Państwowego Instytutu Geologicznego, 60, 67–68.

Nescieruk, P. and Wójcik, A. 2014. Szczegółowa Mapa Geologiczna Polski w skali 1:50 000, arkusz Bielsko-Biała (1012). Państwowy Instytut Geologiczny – Państwowy Instytut Badawczy.

Nieścieruk, P. and Wójcik, A. 2018. Szczegółowa Mapa Geologiczna Polski w skali 1:50 000, arkusz Kęty (993). Państwowy Instytut Geologiczny – Państwowy Instytut Badawczy.

Nowak, W. 1968. Stomiosphaerids of the Cieszyn Beds (Kimmeridgian–Hauterivian) in the Polish Silesia and their stratigraphical value. Summary. Annales Societatis Geologorum Poloniae, 38, 275–328.

Olszewska, B. 1997. Foraminiferal biostratigraphy of the

Polish Outer Carpathians, a record of basin geohistory. Annales Societatis Geologorum Poloniae, 67, 325–337.

Olszewska, B., Szydło, A., Jugowiec-Nazarkiewicz, M. and Nescieruk, P. 2008. Integrated biostratigraphy of carbonate deposits of the Cieszyn Beds in the Polish Western Carpathians. Geologia, 34, 33–59. [In Polish, with English summary]

Oszczypko, N. 1991. Stratigraphy of the Palaeogene deposits of the Bystrica Subunit (Magura Nappe, Polish Outer Carpathians). Bulletin of the Polish Academy of Sciences, Earth Sciences, 39, 415–431.

Oszczypko, N. 2006. Powstanie i rozwój polskiej części zapadliska przedkarpackiego (Development of the Polish sector of the Carpathian Foredeep). Przegląd Geologiczny, 54 (5), 396–403.

Oszczypko, N., Malata, E., Bąk, K., Kędzierski, M. and Oszczypko-Clowes, M. 2005. Lithostratigraphy and biostratigraphy of the Upper Albian–Lower/Middle Eocene flysch deposits in the Bystrica and Rača subunits of the Magura Nappe (Beskid Wyspowy and Gorce ranges; Poland). Annales Societatis Geologorum Poloniae, 75, 27–69.

Oszczypko, N., Malata, E., Bąk, K., Kędzierski, M. and Oszczypko-Clowes, M. 2005. Lithostratigraphy and biostratigraphy of the Upper Albian–Lower/Middle Eocene flysch deposits in the Bystrica and Rača subunits of the Magura Nappe (Beskid Wyspowy and Gorce Ranges; Poland). Annales Societatis Geologorum Poloniae, 75, 27–69.

Oszczypko, N., Ślączka, A. and Żytko, K. 2008. Tectonic subdivision of Poland: Polish Outer Carpathians and their foredeep. Przegląd Geologiczny, 56, 927–935.

Oszczypko, N., Ślączka, A., Oszczypko-Clowes, A. and Olszewska, B. 2015. Where was the Magura Ocean. Acta Geologica Polonica, 65, 319–344.

Picha, F.J., Stráník, Z. and Krejčí, O. 2006. Geology and hydrocarbon re-sources of the Outer West Carpathians and their foreland, Czech Republic. In: Golonka, J. and Picha, F. (Eds), The Carpathians and their foreland: Geology and hydrocarbon resources. AAPG Memoir, 84, 49–175.

Pickering, K., Stow, D., Watson, M. and Hiscott, R. 1986. Deep-water facies, processes and models: a review and classification scheme for modern and ancient sediments. Earth-Science Reviews, 23, 75–174.

Powell, E.N., Callendar, W.R. and Stanton, R.J., Jr. 1998. Can shallow- and deep-water chemoautotrophic and heterotrophic communities be discriminated in fossil record? Palaeogeography, Palaeoclimatology, Palaeoecology, 144, 85–114.

Price, G.D., Valdes, P.J. and Sellwood, B.W. 1998. A comparison of GCM simulated Cretaceous 'greenhouse' and 'icehouse' climates: implications for the sedimentary record. Palaeogeography, Palaeoclimatology, Palaeoecology, 142, 123–138.

Rajchel, J. 1990. Lithostratigraphy of the Upper Paleocene and Eocene deposits in the Skole Unit. Zeszyty Naukowe AGH, Geologia, 48, 1–112. [In Polish, with English summary]

Rajchel, J. and Uchman, A. 2012. Ichnology of Upper Cretaceous deep-sea thick-bedded flysch sandstones: Lower Istebna Beds, Silesian Unit (Outer Carpathians, southern Poland). Geologica Carpathica, 63, 107–120.

Radmacher, W. and Uchman, A. 2020. Oxygen as a factor controlling palynological record: An example from the Cenomanian–Turonian transition in the Rybie section, Polish Carpathians. Marine and Petroleum Geology, 112, 104067. https://doi.org/10.1016/j.marpetgeo.2019.104067

Rodríguez-Tovar, F.-J., Uchman, A., Martín-Algarra, A. and O'Dogherty, L. 2009a. Nutrient spatial variation during intrabasinal upwelling at the Cenomanian–Turonian oceanic anoxic event in the westernmost Tethys: an ichnological and facies approach. Sedimentary Geology, 215, 83–93.

Rodríguez-Tovar, F.-J., Uchman, A. and Martín-Algarra, A. 2009b. Oceanic Anoxic Event at the Cenomanian–Turonian boundary interval (OAE-2): ichnological approach from the Betic Cordillera, southern Spain. Lethaia, 42, 407–417.

Rodríguez-Tovar, F.J. and Uchman, A. 2011. Ichnological data as a useful tool for deep-sea environmental characterization: a brief overview and an application to recognition of small-scale oxygenation changes during the Cenomanian–Turonian anoxic event. Geo-Marine Letters, 31, 525–536.

Salata, D. and Uchman, A. 2013. Conventional and high-resolution heavy mineral analyses applied to flysch deposits: comparative provenance studies of the Ropianka (Upper Cretaceous–Paleocene) and Menilite (Oligocene) formations (Skole Nappe, Polish Carpathians). Geological Quarterly, 57, 649–664.

Scott, R.W. 1995. Global environmental controls on Cretaceous reefal ecosystems. Palaeogeography, Palaeoclimatology, Palaeoecology, 119, 187–199.

Seilacher, A. 1990. Aberrations in bivalve evolution related to photo- and chemosymbiosis. Historical Biology, 3, 289–311.

Seilacher, A. and Seilacher-Drexler, E. 1994. Bivalvian trace fossils: A lesson from actuopaleontology. Courier Forschungsinstitut Senckenberg, 169, 5–15.

Skoczylas-Ciszewska, K. and Kamieński, M. 1959. O facji inoceramowej warstw istebniańskich Pogórza Wiśnicko-Rożnowskiego. Kwartalnik Geologiczny, 3, 977–995.

Skoczylas-Ciszewska, K. 1960. Geology of the Żegocina Zone (Western Flysch Carpathians). Acta Geologica Polonica, 10, 485–591.

Skupien, P. 2003. A summary of palynological results of the study of the lower part of the Silesian Unit (Czech part of the Outer Western Carpathians. Sborník vìdeckých prací Vysoké školy báòské –

Technické univerzity Ostrava, řada hornickogeologická, Monografie, 8, 107–116.

Skupien, P. and Mohamed, O. 2008. Campanian to Maastrichtian palynofacies and dinoflagellate cysts of the Silesian Unit, Outer Western Carpathians, Czech Republic. Bulletin of Geosciences, 83, 207–224.

Ślączka, A. 1971. Geology of the Dukla unit. Prace Instytutu Geologicznego, 63, 1–97. [In Polish, with English summary]

Ślączka, A. (Ed.). 1986. Atlas of paleotransport of detrital sediments in the Carpathian-Balkan Mountain System. Part II: Cenomanian–Senonian. The Hungarian Geological Institute; Budapest.

Ślączka. A. and Miziołek. M. 1995. Geological setting of Ropianka Beds in Ropianka (Polish Carpathians). Annales Societatis Geologorum Poloniae, 65, 29–41.

Ślączka, A., Kruglow, S., Golonka, J., Oszczypko, N. and Popadyuk, I. 2006. The general geology of the Outer Carpathians, Poland, Slovakia, and Ukraine. In: Picha, F. and Golonka, J. (Eds), The Carpathians and their foreland: Geology and hydrocarbon resources. American Association of Petroleum Geologists, Memoir, 84, 221–258.

Slimani, H., M'Hamdi, A., Uchman, A., Gasiński, M.A., Guédé, K.É. and Mahbouba, I. 2021. Dinoflagellate cyst biostratigraphy of Upper Cretaceous turbiditic deposits from a part of the Bąkowiec section in the Skole Nappe (Outer Carpathians, southern Poland). Cretaceous Research, 123, 104780, https://doi.org/10.1016/j.cretres.2021.104780

Słomka, T. 1986. Submarine mass movement deposits in Lower Silesia shales. Zeszyty Naukowe AGH, Geologia, 12, 25–35. [In Polish, with English summary]

Słomka, T. 1995. Deep-marine siliciclastic sedimentation of the Godula Beds, Carpathians. Polska Adademia Nauk – Oddział w Krakowie, Prace Geologiczne, 139, 7–132. [In Polish, with English summary]

Słomka, T., Malata, T., Leśniak, T., Oszczypko, N. and Poprawa, P. 2006. Evolution of Silesian and Subsilesian basins. In: Oszczypko, N., Uchman, A. and Malata, E. (Eds), Palaeotectonic Evolution of the Outer Carpathian and Pieniny Klippen Belt Basins, 111–126. Jagiellonian University, Institute of Geological Sciences; Kraków. [In Polish, with English summary]

Stevenson, C.J., Peakall, J., Hodgson, D.M., Bell, D. and Privat, A. 2020. T_B or not T_B: Banding in turbidite sandstones. Journal of Sedimentary Research, 90, 821–842.

Strzeboński, P. 2005. Cohesive debrites of the Istebna Beds (Upper Senonian–Paleocene) west of the Skawa River. Kwartalnik AGH, Geologia, 31, 201–224.

Strzeboński, P. 2003. Sedymentacja warstw istebniańskich (górny senon–paleocen) zachodniej części serii śląskiej Karpat. Sprawozdanie z Posiedzeń Komisji Nauk Geologicznych Polskiej Akademii Nauk, Oddział Kraków, 47, 1–5.

Strzeboński, P. 2015. Late Cretaceous–Early Paleogene sandy-to-gravelly debris flows and their sediments in the Silesian Ba sin of the Al pine Tethys (Western Outer Carpathians, Istebna Formation). Geological Quarterly, 59, 195–214.

Strzeboński, P. 2022. Contrasting styles of siliciclastic flysch sedimentation in the Upper Cretaceous of the Silesian Unit, Outer Western Carpathians: sedimentology and genetic implications. Annales Societatis Geologorum Poloniae, 92, 159–180.

Strzeboński, P., Golonka, J., Waśkowska, A., Krobicki, M., Słomka, T., Skupen, P., Vašíček, Z. 2009. Utwory formacji wierzowskiej na tle wczesnokredowych warunków sedymentacji w zachodniej części basenu protośląskiego (Morawy, Republika Czeska). Geologia, 35, 31–38.

Szydło, A. 1996. Charakterystyka mikropaleontologiczna utworów dolnej kredy z rejonu Bielska-Białej i Żywca. Posiedzenia Naukowe Państwowego Instytutu Geologicznego, 52, 67–68.

Szydło, A. 1997. Biostratigraphical and palaeoecological significance of small foraminiferal assemblages of the Silesian (Cieszyn) Unit, Western Carpathians. Annales Societatis Geologorum Poloniae, 64, 325–337.

Szydło, A. and Jugowiec, M. 1999. Foraminifera and calcareous nannoplankton assemblages from ?Tithonian–Neocomian "Cieszyn Beds" (Silesian Unit, Polish Western Carpathians). Geologica Carpathica, 50, 203–211.

Szymakowska, F. 1977. Stratigraphy of the Wierzowice Beds from Stępina–Cieszyn area (central Polish Carpathians) on the basis of ammonites. Kwartalnik Geologiczny, 21, 279–290. [In Polish, with English summary]

Szymakowska, F. 1981. Stratygrafia osadów kredy dolnej fliszowych Karpat Zewnętrznych na podstawie amonitów. Biuletyn Instytutu Geologicznego, 33, 57–65.

Teysseyre, H. 1947. Budowa geologiczna okolic Węglówki (Geology of Węglówka region). Nafta, 3 (5–9), 146–149, 185–190, 220–224, 258–261.

Tchoumatchenco, P. and Uchman, A. 2001. The oldest deep-sea *Ophiomorpha* and *Scolicia* and associated trace fossils from the Upper Jurassic–Lower Cretaceous deep-water turbidite deposits of SW Bulgaria. Palaeogeography, Palaeoclimatology, Palaeoecology, 169, 85–99.

Uchman, A. 1991a. Trace fossils of the Inoceramian beds and the Szczawnica Formation in the Krynica and Bystrzyca Zones of the Magura Nappe. Przegląd Geologiczny, 39, 207–212. [In Polish]

Uchman, A. 1995. Taxonomy and palaeoecology of flysch trace fossils: The Marnoso-arenacea Formation and associated facies (Miocene, Northern Apennines, Italy). Beringeria, 15, 3–115.

Uchman, A. 1998. Taxonomy and ethology of flysch trace fossils: A revision of the Marian Książkiewicz collec-

tion and studies of complementary material. Annales Societatis Geologorum Poloniae, 68, 105–218.

Uchman, A. 1999. Ichnology of the Rhenodanubian Flysch (Lower Cretaceous–Eocene) in Austria and Germany. Beringeria, 25, 65–171.

Uchman, A. 2001a. Eocene flysch trace fossils from the Hecho Group of the Pyrenees, northern Spain. Beringeria, 28, 3–41.

Uchman, A. 2001b. Ichnological record of oxygenation changes in the Lower Cretaceous flysch deposits of the Silesian Unit, Polish Carpathians. In: Zuchiewicz, W. (Ed.), Carpathians Palaeogeography and Geodynamics: A Multidisciplinary Approach, 1^{2t}h Meeting of the Association of European Geological Societies, MAEGS 2001, Kraków, Poland, 8–15 September, 2001, Abstracts. Biuletyn Państwowego Instytutu Geologicznego, 396, 159–160.

Uchman, A. 2004. Deep-sea trace fossils controlled by palaeo-oxygenation and deposition: an example from the Lower Cretaceous dark flysch deposits of the Silesian Unit, Carpathians, Poland. Fossils and Strata, 51, 39–57.

Uchman, A. 2007. Deep-sea ichnology: development of major concepts. In: Miller, W., III (Ed.), Trace Fossils Concepts, Problems, Prospects, 248–267. Elsevier; Amsterdam.

Uchman, A. 2008a. Stop 13 – Poznachowice Dolne–Upper Cieszyn Beds and Grodziszcze Beds (Valanginian–Hauterivian) – ichnology of very thin turbidites. In: Pieńkowski, G. and Uchman, A. (Eds), Ichnological Sites of Poland; The Holy Cross Mountains and the Carpathian Flysch; The Second International Congress on Ichnology, Cracow, Poland, August 29–September 8, 2008; Pre-Congress and Post-Congress Field Trip Guidebook, 140–141. Polish Geological Institute; Warszawa.

Uchman, A. 2008b. Stop 11 – Słopnice–Ropianka Formation (Senonian–Palaeocene) and Variegated Shale (Eocene). In: Pieńkowski, G. and Uchman, A. (Eds), Ichnological Sites of Poland; The Holy Cross Mountains and the Carpathian Flysch; The Second International Congress on Ichnology, Cracow, Poland, August 29–September 8, 2008; Pre-Congress and Post-Congress Field Trip Guidebook, 136–138. Polish Geological Institute; Warszawa.

Uchman, A., Bąk, K. and Rodríguez-Tovar, F.J. 2008. Ichnological record of deep-sea palaeoenvironmental changes around the Oceanic Anoxic Event 2 (Cenomanian–Turonian boundary): an example from the Barnasiówka section, Polish Outer Carpathians. Palaeogeography, Palaeoclimatology, Palaeoecology, 262, 61–71.

Uchman, A. and Cieszkowski, M. 2008a. Stop 1 – Zagórnik – the Veřovice Beds and their transition to the Lgota Beds: ichnology of Early Cretaceous black flysch deposits. In: Pieńkowski, G. and Uchman, A. (Eds), Ichnological Sites of Poland; The Holy Cross Mountains and the Carpathian Flysch; The Second International Congress on Ichnology, Cracow, Poland, August 29–September 8, 2008; Pre-Congress and Post-Congress Field Trip Guidebook, 99–104. Polish Geological Institute; Warszawa.

Uchman, A. and Cieszkowski, M. 2008b. Stop 2 – Rzyki – Siliceous Marl and the lowermost part of the Godula Beds: ichnology of the calcareous turbidites. In: Pieńkowski, G. and Uchman, A. (Eds), Ichnological Sites of Poland; The Holy Cross Mountains and the Carpathian Flysch; The Second International Congress on Ichnology, Cracow, Poland, August 29–September 8, 2008; Pre-Congress and Post-Congress Field Trip Guidebook, 104–109. Polish Geological Institute; Warszawa.

Uchman, A., Rodríguez-Tovar, F.J., Machaniec, E. and Kędzierski, M. 2013. Ichnological characteristics of Late Cretaceous hemipelagic and pelagic sediments in a submarine high around the OAE-2 event: a case from the Rybie section, Polish Carpathians. Palaeogeography, Palaeoclimatology, Palaeoecology, 370, 222–231.

Uchman, A. and Wetzel, A. 2017. Hidden subsurface garden on own faeces – the trace fossil *Tubulichnium rectum* (Fischer-Ooster, 1858) from the Cretaceous–Palaeogene deep-sea sediments. Palaeontologia Electronica, 20.2.40A: 1–18. palaeo-electronica.org/content/2017/1968-tubulichnium-deep-sea-trace

Unrug, R. 1959. On the sedimentation of the Logota beds (Bielsko area, Western Carpathians). Rocznik Polskiego Towarzystwa Geologicznego, 29, 197–225.

Unrug, R. 1963. Istebna Beds – a fluxoturbidity formation in the Carpathian Flysch. Rocznik Polskiego Towarzystwa Geologicznego, 33, 49–92.

Unrug, R. 1968. The Silesian cordillera as a source of clastic material of the flysch sandstone of the Beskid Śląski and Beskid Wysoki Ranges (Polish Western Carpathians). Rocznik Polskiego Towarzystwa Geologicznego, 38, 81–164. [In Polish, with English summary]

Unrug, R. 1977, Ancient deep-sea traction currents deposits in the Lgota beds (Albian) of the Carpathian Flysch. Rocznik Polskiego Towarzystwa Geologicznego, 47, 355–370.

Vašíček, Z., Gedl, E., Kędzierski, M. and Uchman, A. 2010. Two ammonites from the Early Cretaceous deep-sea sediments of the Silesian Nappe, Polish Carpathians, and stratigraphic problems resulted from micropalaeontological dating of their sites. Annales Societatis Geologorum Poloniae, 80, 25–37.

Wagner, R. (Ed.). 2008. Tabela stratygraficzna Polski. Karpaty. Polish Geological Institute; Warszawa.

Waśkowska, A., Golonka, J., Strzeboński, P., Krobicki, M., Słomka, T., Vašíček, Z., Skupen, P. 2009. Early Cretaceous deposits of the proto-Silesian Basin in Polish-Czech Flysch Carpathians. Geologia, 35, 39–47. [In Polish, with English abstract]

Waśkowska, A., Joniec, A., Kotlarczyk, J. and Siwek, P. 2019. The Late Cretaceous Fucoid Marl of the Ropianka Formation in the Kąkolówka Structure (Skole Nappe, Outer Carpathians, Poland) – lithology and foraminiferal biostratigraphy. Annales Societatis Geologorum Poloniae, 89, 259–284.

Wetzel, A. and Uchman, A. 2018. The former presence of organic matter caused its later absence: Burndown of organic matter in oceanic red beds enhanced by bioturbation (Eocene Variegated Shale, Carpathians). Sedimentology, 65, 1504–1519. doi: 10.1111/sed.12436

Wdowiarz, S. 1949. Structure géologique des Karpates Marginales au sud-est de Rzeszów. Biuletyn Państwowego Instytutu Geologicznego, 11, 1–51.

Wierzbicki, A. and Kędzierski, M. 2020. Maastrichtian climate changes – the calcareous nannofossil record from flysch deposits of the Outer Carpathians. Annales Societatis Geologorum Poloniae, 90, 447–462.

Wójcik, A. 2017. Szczegółowa Mapa Geologiczna Polski w skali 1: 50 000, arkusz Wieliczka (997). Państwowy Instytut Geologiczny – Państwowy Instytut Badawczy.

Wójcik, A., Czerwiec, J. and Krawczyk M. 2016. Szczegółowa Mapa Geologiczna Polski w skali 1: 50 000, arkusz Limanowa (1017). Państwowy Instytut Geologiczny – Państwowy Instytut Badawczy.

Wójcik, A., Kopciowski, R., Malata, T., Marciniec, P. and Nescieruk, P. 1996. Proposition of the division of lithostratigraphic units of the Polish Outer Carpathians. In: Przewodnik 57 Zjazdu Polskiego Towarzystwa Geologicznego, Szczyrk, 6–9 czerwca 1996. PTG, Kraków, 209–215. [In Polish]

Wójcik, K. 1907. Exotica fliszowe Kruhela Wielkiego koło Przemyśla. Sprawozdanie Komisyi Fizyograficznej Akademii Umiejętności w Krakowie, 42, 3–24.

Wójcik-Tabol, P. and Ślączka, A. 2015. Are Early Cretaceous environmental changes recorded in deposits of the western part of the Silesian Nappe? A geochemical approach. Palaeogeography, Palaeoclimatology, Palaeoecology, 417, 293–308.

Żytko, K., Zając, R., Gucik, S., Ryłko, W., Oszczypko, N., Garlicka, I., Nemčok, J., Eliáš, M., Menčík, E. and Stráník, Z. 1989. Map of the tectonic element of the Western Outer Carpathians and their foreland. In: Poprawa, D. and Nemčok, J. (Eds), Geological Atlas of the Western Outer Carpathians and their Foreland, 1: 500,000. Państwowy Instytut Geologiczny; Warszawa, GÚDŠ; Bratislava, ÚÚG; Praha.

11TH INTERNATIONAL
CRETACEOUS
SYMPOSIUM
Warsaw, Poland, 2022

FROM SHALLOW TO DEEP MARINE DEPOSITIONAL ENVIRONMENTS OF THE CRETACEOUS NORTHWESTERN TETHYS – A RECORD OF ALPINE SYSTEM DIFFERENTIATION IN THE POLISH CARPATHIANS

Jacek Grabowski (coordinator)[1]| Krzysztof Bąk[2]| Marta Bąk[3]| Michał Krobicki[3]| Damian Lodowski[1,4]| Alfred Uchman[5]| Jan Golonka[3]| Zbigniew Górny[3]| Jan Hejnar[6]| Jolanta Iwańczuk[1]| Barbara Olszewska[7]| Nestor Oszczypko[5]| Dorota Salata[5]| Andrzej Wierzbowski[4]| Patrycja Wójcik-Tabol[5]

1| Polish Geological Institute – National Research Institute, Rakowiecka 4, 00-975 Warszawa, Poland;

e-mails: jacek.grabowski@pgi.gov.pl; damian.lodowski@pgi.gov.pl; jolanta.iwanczuk@pgi.gov.pl

2| Faculty of Exact and Natural Sciences, Pedagogical University of Krakow, Podchorążych 2, 30-084 Kraków, Poland; e-mail: krzysztof.bak@up.krakow.pl

3| Faculty of Geology, Geophysics and Environmental Protection, AGH University of Science and Technology, Al. Mickiewicza 30, Kraków 30-059, Poland; e-mails: martabak@agh.edu.pl; krobicki@agh.edu.pl; górny.zbigniew.agh@gmail.com; jgolonka@agh.edu.pl

4| Faculty of Geology, University of Warsaw, Żwirki i Wigury 93, 02-089 Warszawa, Poland; e-mails: damian.lodowski@uw.edu.pl; awwierzb@uw.edu.pl

5| Faculty of Geography and Geology, Institute of Geological Sciences, Jagiellonian University, Gronostajowa 3a, 30-387 Kraków, Poland; e-mails: alfred.uchman@uj.edu.pl; nestor.oszczypko@uj.edu.pl; dorota.salata@uj.edu.pl; p.wojcik-tabol@uj.edu.pl

6| Institute of Geological Sciences, Polish Academy of Sciences, Senacka 1, 31-002 Kraków, Poland; e-mail: ndhejnar@cyfronet.pl

7| Polish Geological Institute – National Research Institute, Carpathian Branch, Skrzatów 1, 31-560 Kraków, Poland; e-mail: barbara.olszewska@pgi.gov.pl

ABSTRACT

The Western Carpathians represent a fold-and-thrust belt that forms the northernmost European Alpides in the Czech Republic, Slovakia, and Poland. They consist of an older range, known as the Inner or Central Carpathians, and a younger range, the Outer or Flysch Carpathians, separated by the Pieniny Klippen Belt. The Inner Carpathians are formed of thick- and thin-skinned nappes thrusted in the Late Jurassic and Cretaceous, while the exclusively thin-skinned nappes of the Outer Carpathians originated during the Cenozoic. Both Cretaceous and Neogene tectonic phases affected the Pieniny Klippen Belt. Cretaceous deposits are present in each of the three tectonic domains, representing a variety of environments spanning from pelagic carbonates, hemipelagic marlstones, and flysch-type terrigenous sediments to *Urgonian*-type platform carbonates.

INTRODUCTION

(*Jan Golonka and Michał Krobicki*)

The Carpathians form a great mountain arc that stretches more than 1,300 km, from the Vienna Forest to the Iron Gate on the Danube (Fig. 1). To the west, the Carpathians are linked to the eastern Alps, and to the east they pass into the Balkan chain. Traditionally, the Carpathians are subdivided into the Western and Eastern Carpathians. The Western Carpathians consist of an older range, known as the **Inner** or **Central** Carpathians, and a younger range, known as the **Outer** or **Flysch** Carpathians. They are separated by the **Pieniny Klippen Belt**, a strongly tectonized structure, about 600 km long and 1–20 km wide, stretching from Vienna to Romania (Figs 1, 2).

The Outer Carpathians are built of a stack of thin-skinned nappes and thrust sheets capturing different lithostratigraphic units and tectonic structures. The Outer Carpathians nappes were thrusted onto the European Plate (Figs 3, 4). The **Inner Carpathian** basement is composed of continental crust of Hercynian (Variscan) age, with a Carboniferous–Cenozoic sedimentary cover. In the Late Cretaceous, the dominantly Mesozoic sedimentary sequences were folded and thrust into a series of thick and thin-skinned nappes. The Hercynian basement and Mesozoic nappes are unconformably covered by mid-Eocene–Oligocene continental to deep-marine deposits and Early–Middle Miocene marine and terrestrial (continental) molasses. The deposits of **the Pieniny Klippen Belt**

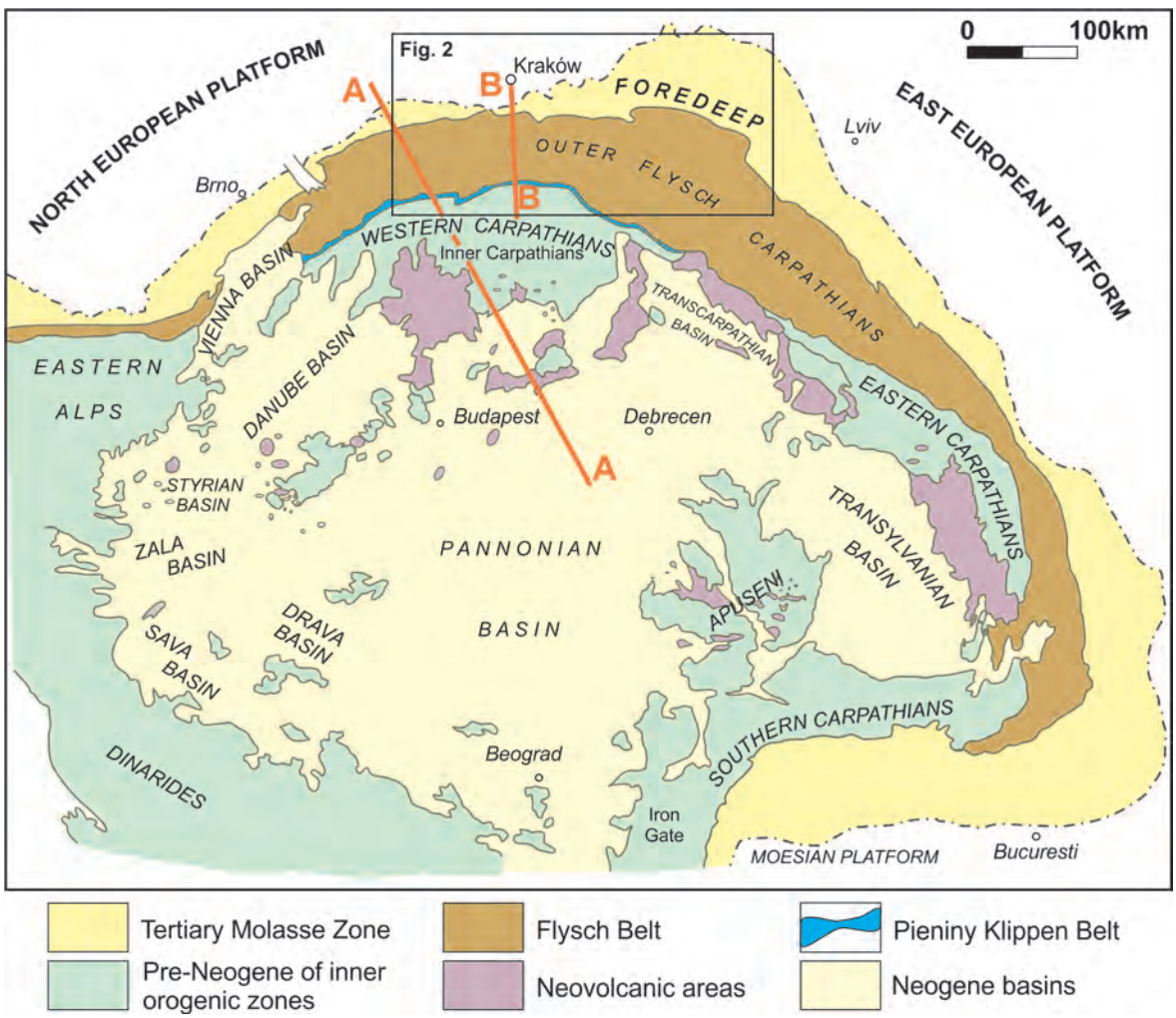

Fig. 1. Tectonic sketch map of the Alpine-Carpathian-Pannonian-Dinaride basin system (modified after Plašienka et al. 2000). A-A and B-B – location of cross-sections (see Figs 3 and 4 respectively).

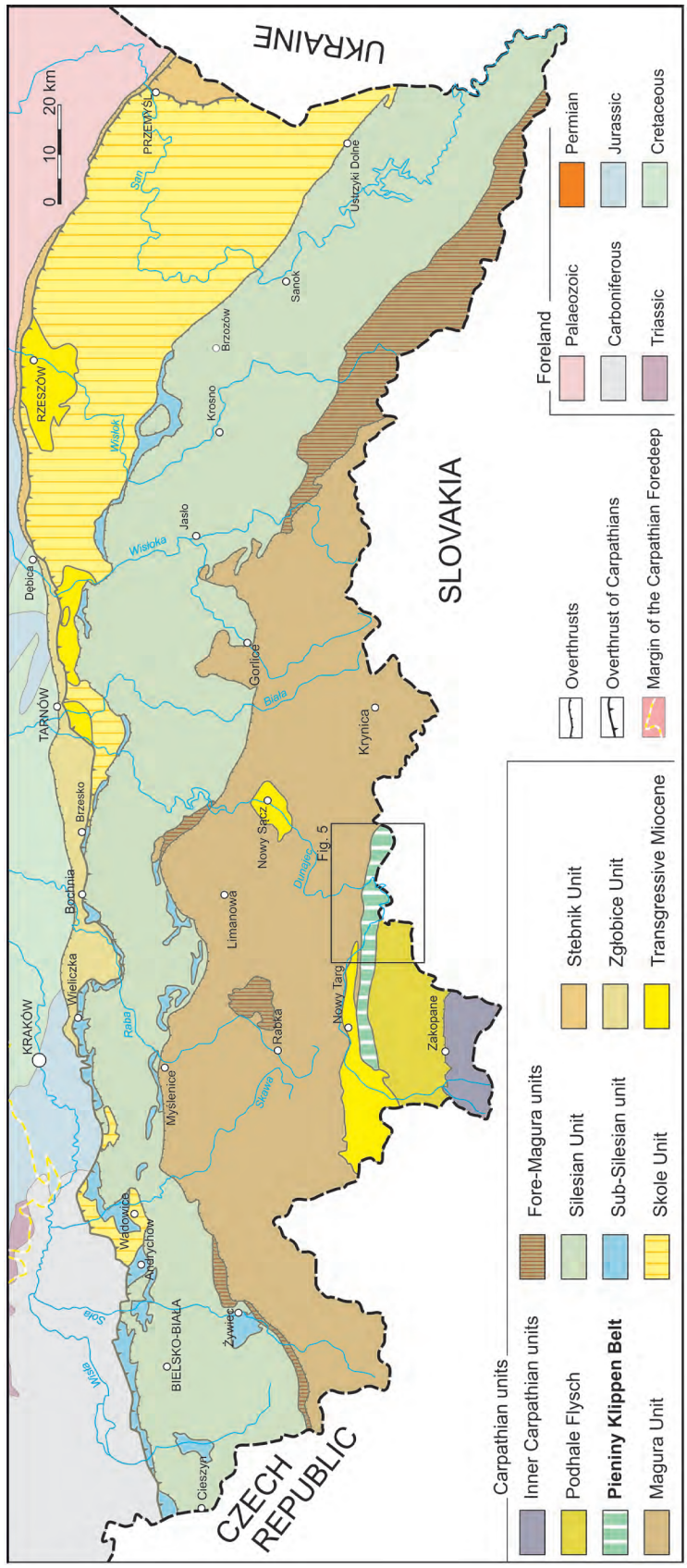

Fig. 2. Geological map of the Polish Carpathians (simplified after Żytko et al. 1989).

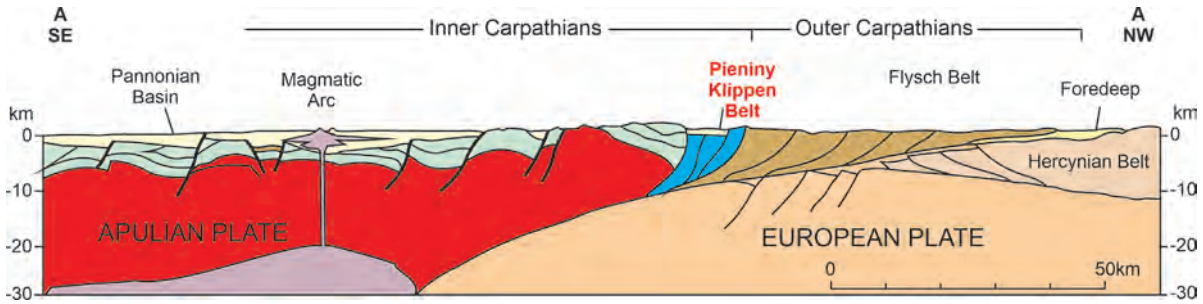

Fig. 3. Generalized cross-section across the Carpathian-Pannonian region (from Picha 1996).

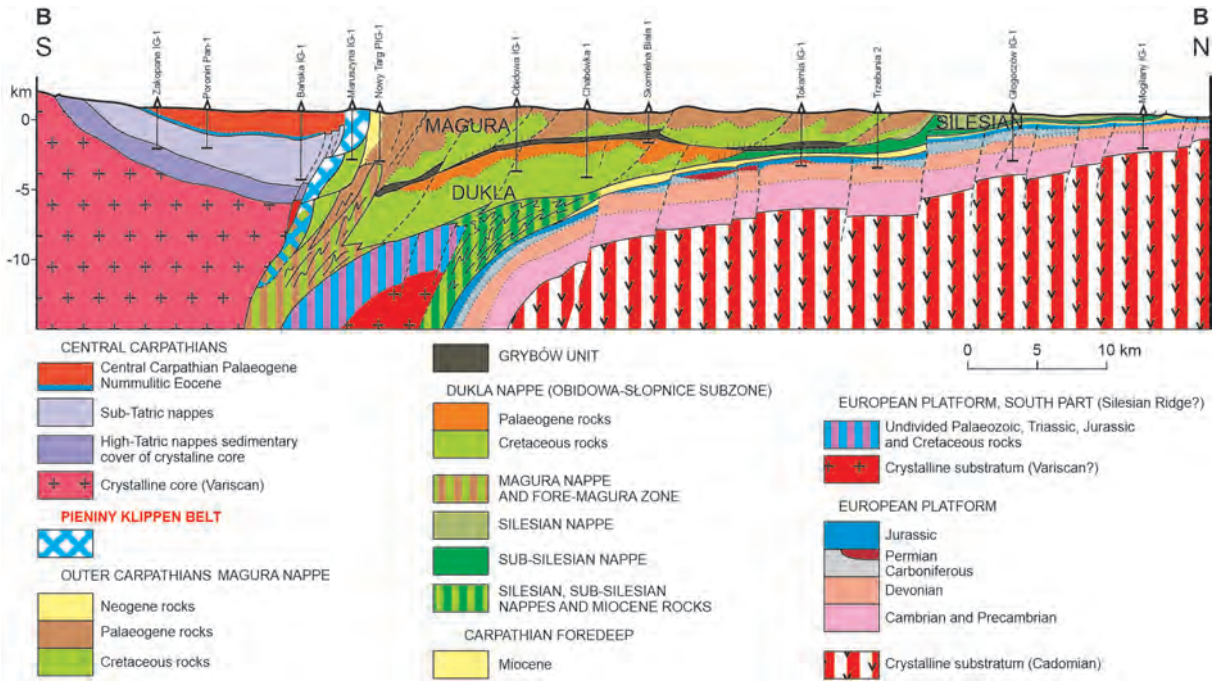

Fig. 4. Generalized cross-section across the Outer Carpathians, Pieniny Klippen Belt and northern part of the Tatra Mts (Inner Carpathians) (after Golonka and Krobicki 2006).

originated in the oceanic Penninic realm of the Alpine Tethys (e.g., Săndulescu 1988; Birkenmajer 1986; Oszczypko 1992; Stampfli 2001; Plašienka 2018), which developed between the Inner Carpathian-Eastern Alpine terrane (Apulian Plate in Fig. 3) and the European Plate.

REGIONAL STRUCTURE

Outer Flysch Carpathians

(*Jan Golonka and Michał Krobicki*)

The Outer Flysch Carpathians are composed of a stack of nappes and thrust sheets spread along the Carpathians, mainly built of continuous flysch sequences up to 6 km thick, capturing the Jurassic to Early Miocene. All of the Outer Carpathian nappes are overthrust onto the southern part of the European Platform and covered by autochthonous Miocene deposits of the Carpathian Foredeep over at least 70 km (Fig. 3). During overthrusting, the northern Carpathians nappes were uprooted from the basement; only their basinal parts are preserved. A narrow zone of folded Miocene deposits developed along the frontal Carpathian thrust, constituting the Zgłobice-Wieliczka Unit in the Northern Carpathians (Fig. 2). From lowest to highest, the nappe succession is as follows (concordant to our trip – from north to

south): the Skole (Skiba) Nappe (mainly present in the easternmost West Carpathians), the Subsilesian Nappe, the Silesian Nappe, the Fore-Magura nappe group, and the Magura Nappe. Here, we only discuss the main units.

The **Subsilesian Nappe** tectonically underlies the Silesian Nappe. In the western sector of the West Carpathians, both nappes thrust over Miocene molasse of the Carpathian Foredeep; in the eastern sector, they thrust over the Skole Nappe. This nappe consists Upper Cretaceous–Paleogene flysch deposits.

The **Silesian Nappe** occupies the central Outer Carpathians, pinching out below the most internal nappes. The sedimentary facies of the Silesian Nappe represent a continuous succession from the Late Jurassic to the Early Miocene. The oldest Silesian Nappe sediments are only known in the Moravian and Silesian areas in the Western Carpathians, and are represented by Kimmeridgian–Lower Tithonian dark grey calcareous mudstones (Lower Cieszyn Shale). The Silesian and Subsilesian basins were connected during their deposition.

The **Magura Nappe** is the innermost – and largest – tectonic unit of the Western Carpathians, thrust over various units of the Fore-Magura nappe group and the Silesian Nappe. To the south, it is in tectonic contact with the Pieniny Klippen Belt, which separates it from the Inner Carpathians. The oldest Jurassic–Lower Cretaceous rocks are only found in the part of the Magura Basin that was incorporated into the Pieniny Klippen Belt (i.e., the Grajcarek Unit) (Birkenmajer 1977).

The Outer Carpathian rift developed in association with the beginning of calcareous flysch sedimentation (the Cieszyn beds). The Western Carpathian Silesian Basin probably extended into the Eastern Carpathians (Sinaia or "black flysch") and to the Southern Carpathian Severin Zone (Săndulescu 1988). Remnants of carbonate platforms (Olszewska and Wieczorek 2001) with reefs (*Štramberk*-type limestones) along the margin of the Silesian Basin resulted from the regional fragmentation of the European platform. The Silesian Ridge (an exotic cordillera) separated the Silesian and Magura basins (Golonka et al. 2003). During the late Tithonian and Early Cretaceous opening of the western Silesian Basin, alkaline magma (teschenite association rocks) intruded the flysch deposits (Lucińska-Anczkiewicz et al. 2002).

Pieniny Klippen Belt (PKB)
(*Michał Krobicki and Jan Golonka*)

The Pieniny Klippen Belt (Fig. 5, PKB) is composed of several successions of mainly deep and shallow-water limestones, covering the Early Jurassic to Late Cretaceous (Andrusov et al. 1973; Birkenmajer 1977, 1986, 1988; Mišík 1994; Golonka and Krobicki 2004) (Figs 6, 7).

During the Jurassic and Cretaceous, the submarine Czorsztyn Ridge (= "pelagic swell" of Mišík 1994, mainly the Czorsztyn Succession) and surrounding zones formed an elongated structure within the Pieniny Klippen Basin, with dominantly pelagic sedimentation styles (Birkenmajer 1977, 1986; Mišík 1994; Michalík and Reháková 1995; Aubrecht et al. 1997; Golonka and Krobicki 2001, 2004). A palinspastic reconstruction of the PKB Basin suggests the occurrence of a submarine ridge during the entire Jurassic and Cretaceous. This elongated Czorsztyn Ridge separated the Pieniny and Magura basins in the Carpathian part of the northernmost Tethys Ocean (Fig. 8). Its SW-NE orientation and location within the Tethys Ocean is supported by palaeomagnetic data, sedimentary sequence relationships, and palaeoclimate (see discussion in Golonka and Krobicki 2001; see also Lewandowski et al. 2005; Grabowski et al. 2008). The Pieniny and Magura basins were dominated by pelagic sedimentation. The deepest part of the PKB Basin is well-documented by deep water Jurassic–Early Cretaceous deposits (radiolarites and pelagic *Maiolica*-type cherty limestones) of the Branisko and Pieniny successions (1986; Golonka and Sikora 1981; Golonka and Krobicki 2004; Krobicki et al. 2006). The transitional, shallower sequences, which primarily occupied slopes between the deepest basinal units and the Czorsztyn Ridge, are known as the Czertezik and Niedzica successions; the shallowest zone is captured by the Czorsztyn Succession, which primarily occupied the southeastern slope of the Czorsztyn Ridge (Birkenmajer 1986; Golonka and Krobicki 2004; Krobicki and Golonka 2006).

The present-day limits of the PKB are strictly tectonic. They may be characterized as (sub)vertical faults and shear zones (Figs 3, 4), along which a strong reduction of the original sedimentary basins took place (Birkenmajer 1986; Golonka and Krobicki 2006; Krobicki and

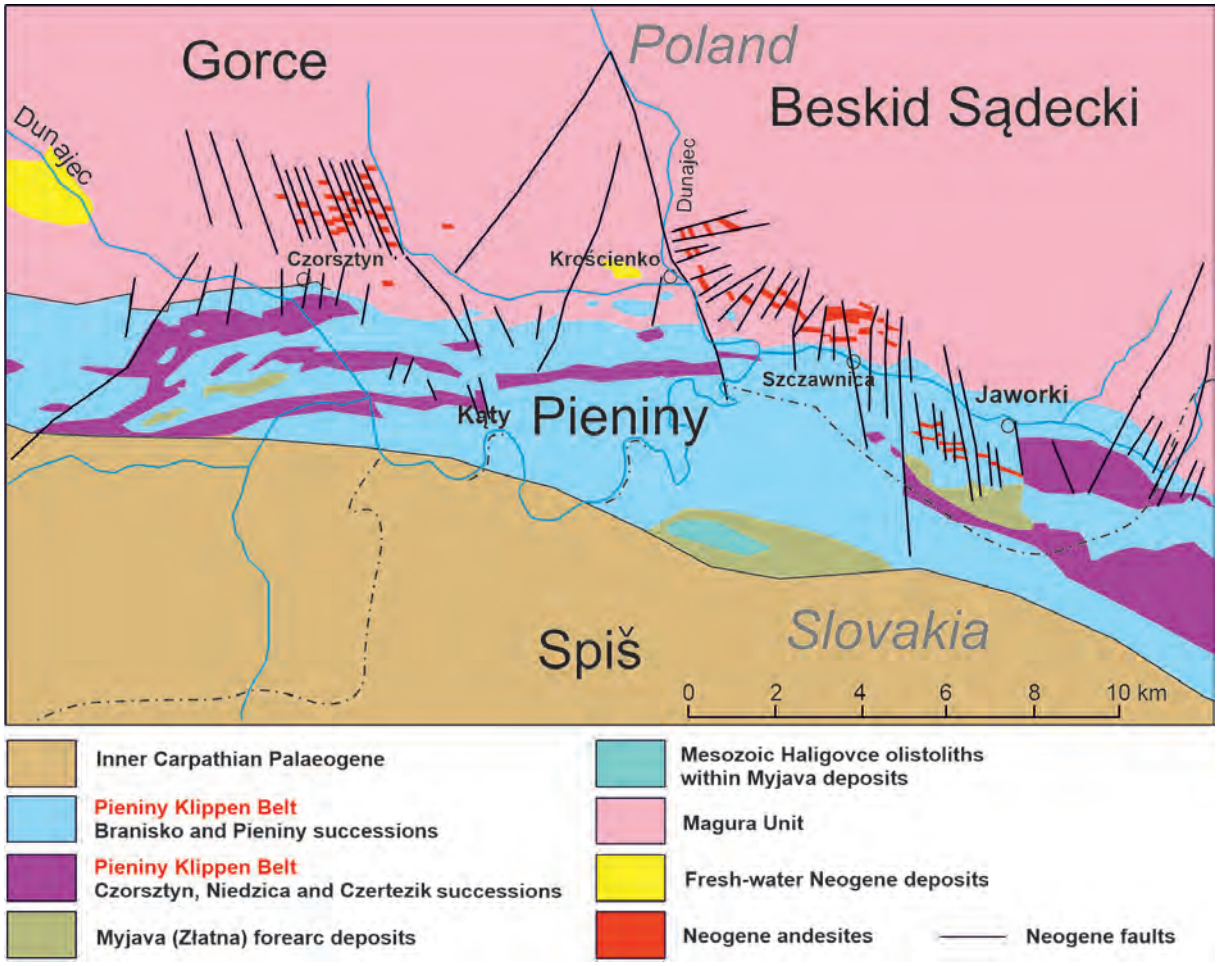

Fig. 5. Geological sketch of the Pieniny Klippen Belt (Polish sector) and surrounding regions (simplified after Birkenmajer 1979).

Golonka 2006). In the PKB, different tectonic components, strike-slip and thrust faults, toe-thrusts, and olistostromes were chaotically mixed, giving rise to the present-day mélange character of the PKB, where individual tectonic units are difficult to distinguish.

The **earliest stage** of the PKB development is documented by exotic Triassic limestone pebbles in the Cretaceous–Tertiary flysch of the PKB (Birkenmajer et al. 1990) and the Outer Carpathian Flysch (Magura Unit, see Soták 1986).

The **oldest Jurassic** rocks, known only from the Ukrainian and Slovakian parts of the PKB (Krobicki et al. 2003; Schlögl et al. 2004; Wierzbowski et al. 2012, 2021), consist of various *Gresten*-like clastic sediments with intercalations of *Gresten*-like dark/black fossiliferous limestones with brachiopods and grypheoids (?Hettangian–?Sinemurian) (Schlögl et al. 2004, with literature). Subsequently, Pliensbachian–Lower Bajocian *Bositra* (*Posidonia*) black shales with spherosiderites, as seen in Homole Gorge (Stop 2), and dark marls and spotty limestones of the widespread Tethyan *Fleckenkalk/Fleckenmergel* facies, indicate oxygen-depleted conditions (Fig. 6). One of the most rapid changes in sedimentation styles and palaeoenvironments within the PKB basins occurred during the late Early Bajocian, when well-oxygenated multicoloured crinoidal limestones replaced dark and black sedimentation. The origin of the aforementioned Czorsztyn Ridge was connected to this Bajocian post-rift geotectonic reorganization (Golonka et al. 2003; Krobicki 2006, 2009).

The deposition of red nodular *Ammonitico*

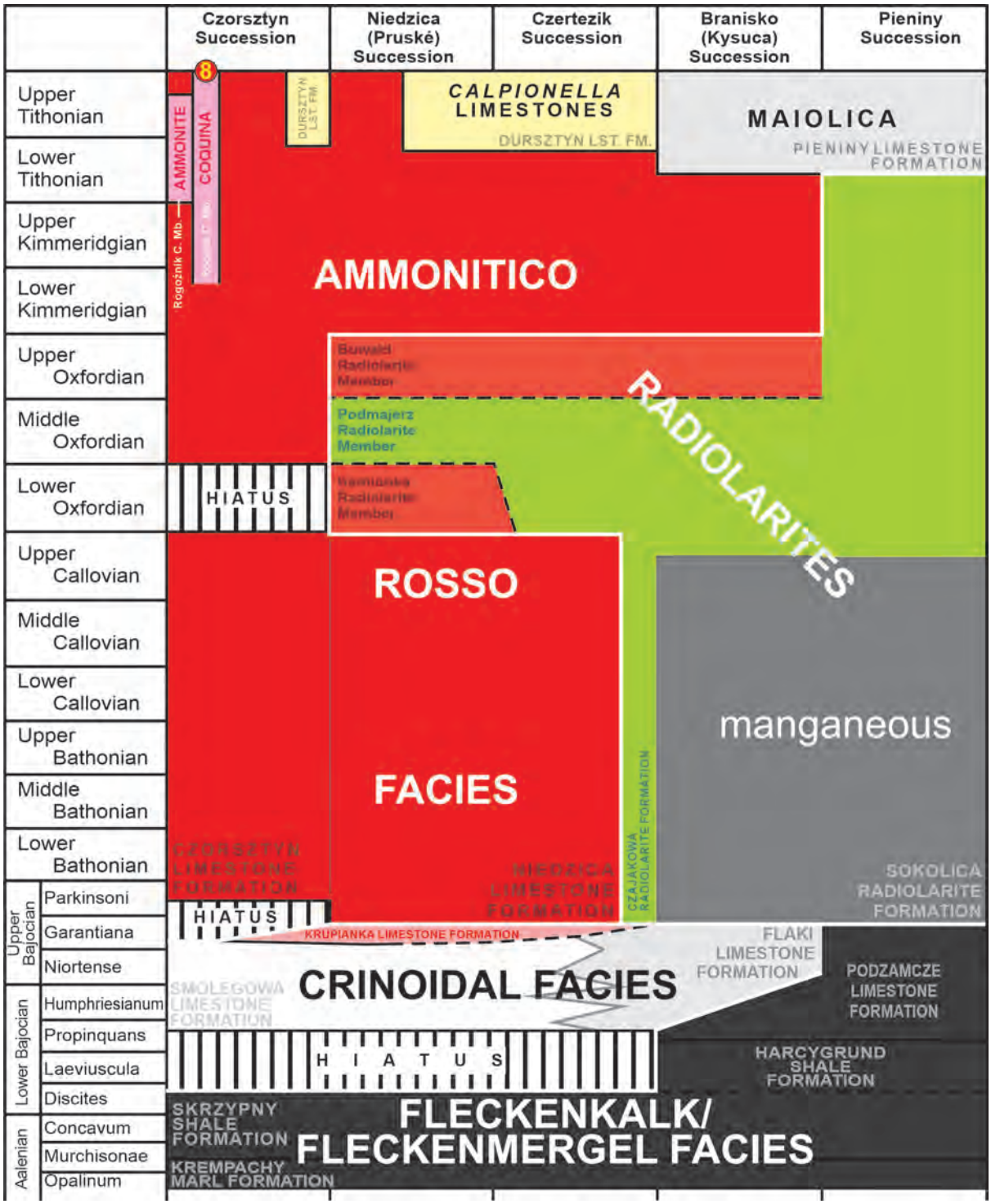

Fig. 6. Stratigraphical correlation between Jurassic lithofacies (lithostratigraphic units; after Birkenmajer 1977) of the Pieniny Klippen Belt successions (after Wierzbowski et al. 2004; supplemented by Krobicki and Wierzbowski 2004), with field excursion locality context marked.

Rosso-type limestones starting in the latest Bajocian was due to Meso-Cimmerian vertical movements, which led to subsidence on the Czorsztyn Ridge and produced tectonically differentiated blocks (e.g., Birkenmajer 1986; Aubrecht et al. 1997; Wierzbowski et al. 1999;

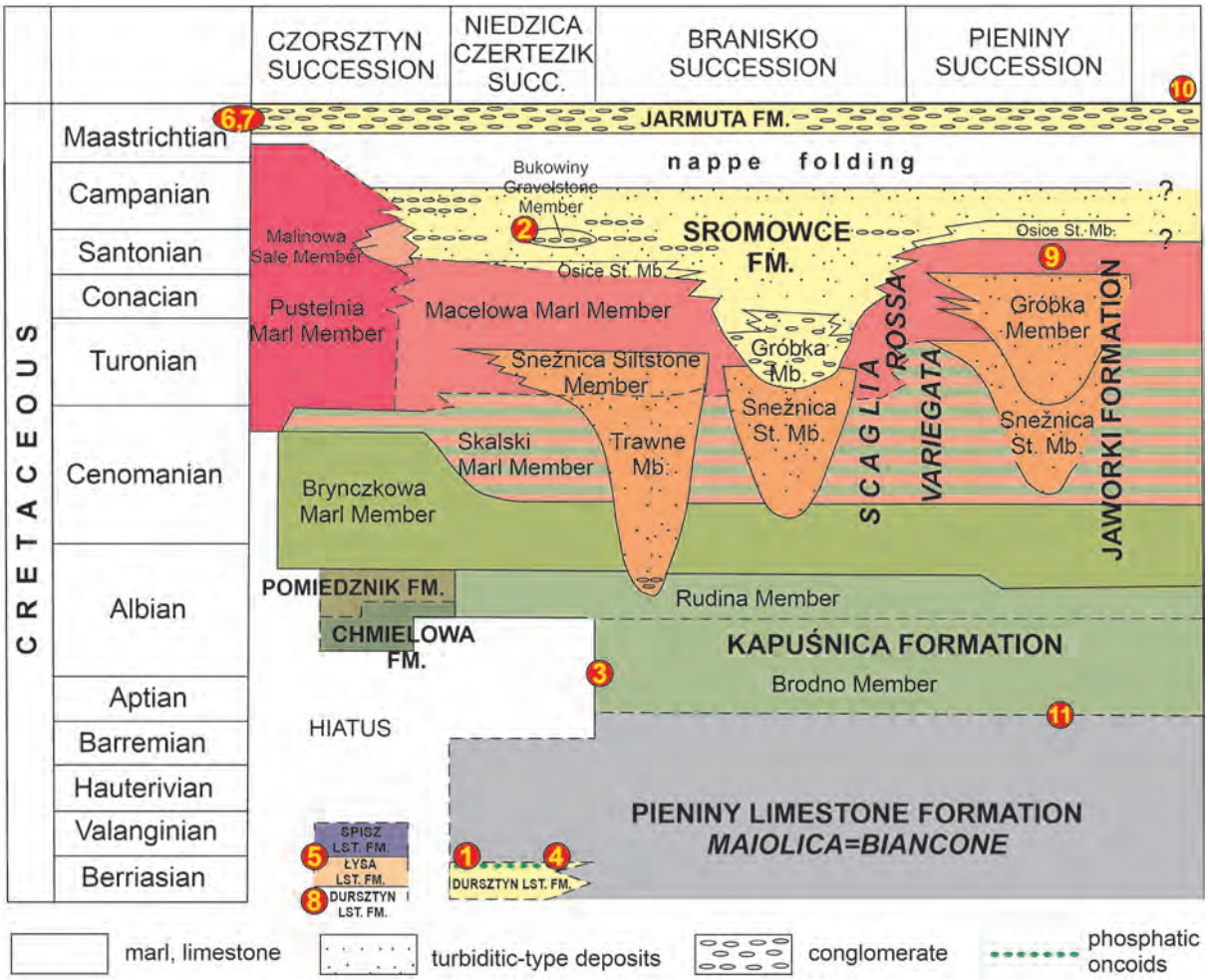

Fig. 7. Detailed Cretaceous stratigraphy of the Czorsztyn, Niedzica, Czertezik, Branisko and Pieniny successions in the Pieniny Klippen Belt in Poland (simplified from Birkenmajer and Jednorowska 1987), with field excursion locality context marked.

Aubrecht 2001; Krobicki 2006; Krobicki and Golonka 2006).

The **Late Jurassic** (Oxfordian–Kimmeridgian) of the PKB reflects the strongest facies differentiation, with mixed siliceous-carbonate sedimentation. *Ammonitico Rosso*-type limestones mostly occured on sea bottom elevations (i.e., the Czorsztyn Ridge and its slopes), whereas the deposition of radiolarites (Birkenmajer 1977, 1986) took place in deeper bordering basins. The main phase of this facies differentiation, involving mixed siliceous-carbonate sedimentation (among other sedimentation styles) took place later, largely during the Oxfordian. The greatest depths are captured by widespread Oxfordian radiolarites, which occur in all basinal successions except for the shallowest zone (Czorsztyn Succession). Indeed, Oxfordian radiolarites are typical for the transitional (Niedzica and Czertezik successions) and strictly basinal parts of the basin (Branisko and Pieniny successions).

During the **latest Jurassic–Early Cretaceous** (Tithonian–Berriasian), the Czorsztyn Succession included hemipelagic to pelagic, medium-depth organogenic carbonates: for instance, white and creamy *Calpionella*-bearing limestones. Several tectonic horsts and grabens formed, rejuvenating some older Eo- and Meso-Cimmerian faults (Birkenmajer 1986; Krobicki 1996). These features resulted from intensive Neo-Cimmerian tectonic movements, causing the formation and destruction of submarine tectonic horsts in the Carpathian basins. They are documented by facies diversification, condensed beds and hardgrounds with ferro-

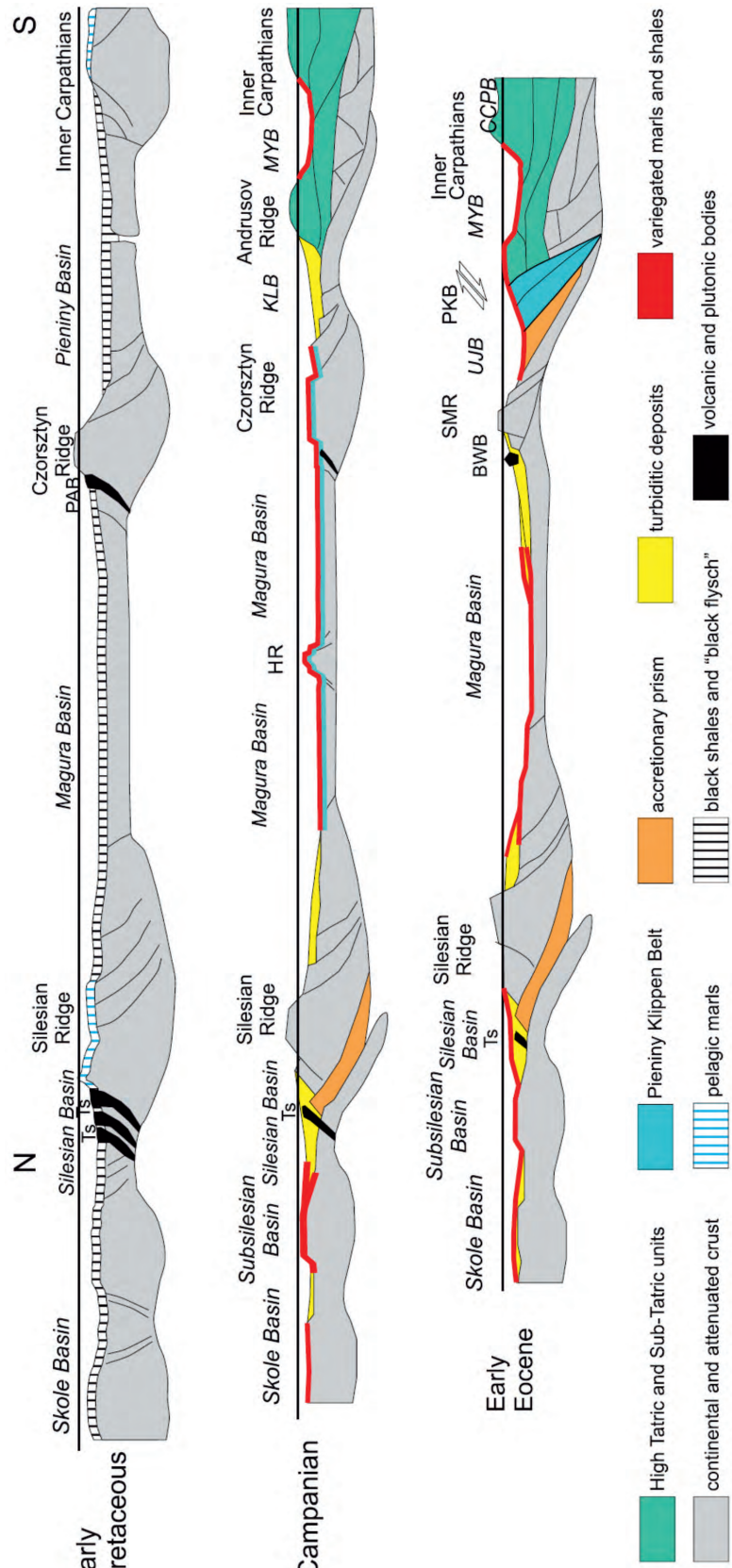

Fig. 8. Early Cretaceous–Early Eocene palinspastic evolutionary model for the Magura Basin, not to scale (based on Oszczypko 2006 and Oszczypko et al. 2012, modified). CCPB – Central Carpathian Paleogene Basin, HR – Hluk Ridge, UJB – Ujak Basin, KLB – Klape Basin, MYB – Myjava Basin, PKB – Pieniny Klippen Belt, SMR – South Magura Ridge, Ts – teschenites, PAB – Pieniny alkaline basalts, BWB – Biata Woda basaltic block.

manganese-rich crusts and/or nodules, sedimentary-stratigraphic hiatuses, sedimentary breccias, and/or neptunian dykes. Additionally, palaeogeographical and palaeoclimatological evidence (e.g., phosphate deposits) suggest the presence of an upwelling zone in the northern Tethys (Golonka and Krobicki 2001). Within deeper successions (mainly the Branisko and Pieniny successions), *Maiolica*-type (= *Biancone*) cherty limestone facies were deposited contemporaneously. *Maiolica*-type limestones constitute a famous, widespread Tethyan facies well-known from both the Alpine and the Apennine regions (Wieczorek 1988). In the western Tethys, this facies mainly originated in deep basins (above the calcite compensation depth, but below the aragonite compensation depth), but could also be deposited on submarine elevations or drowned platforms. Around the Jurassic/Cretaceous boundary, *Maiolica*-type limestones are particularily widespread, reflecting the greatest degree of facies unification (Wieczorek 1988). These white-grey, well-bedded, calpionellid-bearing micritic limestones now compose the highest parts of the Pieniny Mountains (e.g., Trzy Korony Mountains, Sokolica Mountain, and so forth) (Figs 6, 7).

Late Cretaceous pelagic deposits developed as *Scaglia Rossa* pelagic, foraminiferal, multicoloured green/variegated/red marl deposits (= *Couches Rouge* = *Capas Rojas*) during the third and last depositional episode of PKB evolution (Birkenmajer 1986, 1988; Bąk 2000), with sedimentary facies unified within all successions (Albian–Coniacian). These are overlain by flysch and/or flyschoidal facies (Santonian–Campanian) (e.g., Birkenmajer 1986; Birkenmajer and Jednorowska 1987b; Birkenmajer and Gasiński 1992; Mišík 1994; Aubrecht et al. 1997; Bąk, K. 1998; Bąk, M. 1999). During this syn-orogenic stage, the flyschoidal deposits developed as submarine turbiditic wedges, fans, and canyon fills (Radwański 1978; Birkenmajer 1986), with several episodes of debris flows with numerous exotic pebbles (Late Albian–Early Campanian) (Fig. 7).

The PKB closed during the **Cretaceous/Paleocene** transition, as a consequence of strong Late Cretaceous (Subhercynian and Laramian) thrust-folding (Birkenmajer 1977, 1986, 1988): here, the northward folding of successive nappes composed of Jurassic–Cretaceous deposits took place. Simultaneously with Laramian nappe folding, the uppermost Cretaceous (Maastrichtian) fresh-water and marine molasse containing exotic material formed: the Paleocene flysch constitutes a continuation of this sedimentary event. They unconformably cover the klippen nappes previously folded, and form the Klippen Mantle. Subsequently, the klippen nappes and Klippen Mantle were folded together somewhat later.

The second tectonic episode was connected with strong Savian and Styrian compression (**Early** and **Middle Miocene**, respectively), when the Cretaceous nappes, the Klippen Mantle, and younger Paleogene deposits were refolded together (Birkenmajer 1986) and the transverse strike-slip fault system originated. A clearly visible effect of the several tectonic folding and deformational phases within the PKB is the geomorphologic development of tectonically isolated klippes of hard Jurassic and Cretaceous rocks, surrounded by softer shales, marls, and flysch. The process of megabrecciation and megaboudinage is regionally clear, with the PKB forming a very narrow tectonic structure between the Inner Carpathians on the south and the Outer (Flysch) Carpathians on the north; the PKB constitutes a melange in the suture zone between the Inner Carpathian-Alpine range, the Alcapa terrane, and the North European plate. Finally, a strike-slip fault system developed with the eastward movement of the Alcapa plate.

The final important event in the PKB was **Middle Miocene (Sarmatian)** volcanism, represented by calc-alkaline andesite dykes and sills that mainly cut through the Paleogene flysch of the Outer Carpathians, Magura Nappe, dating radiometrically (Birkenmajer and Pécskay 2000a; Anczkiewicz and Anczkiewicz 2016). They form the Pieniny Andesitic Line (PAL) (Fig. 5).

Tatra Mountains (*Alfred Uchman*)

The Tatra Mountains are part of the Inner Western Carpathians, located south of the PKB (Fig. 2). This part of the Carpathians – the Slovakian Block – is characterized by uplifted crystalline massifs covered by Upper Carboniferous–Mesozoic sedimentary rocks, and depressions filled by Paleogene and Neogene deposits. The crystalline massif of the Tatra Mountains is part of the Variscan

system (e.g. Gawęda et al. 2017) involved in the Alpine structures. It is built of ?Late Proterozoic–Lower Paleozoic metamorphic rocks intruded by Carboniferous granitoids. In the Late Cretaceous (Turonian), the crystalline massifs and their cover were overthrusted by nappes dominated by Tethyan Mesozoic sedimentary rocks (e.g. Kotański 1961; Jurewicz 2005; Plašienka 2018) belonging to different tectonic-sedimentary zones (the Tatricum, Fatricum, and Hronicum domains). The post-tectonic Upper Cretaceous *Gosau*-type deposits are poorly developed, and their presence in the Tatra Mountains is doubtful. Subsequnetly, this area was covered by Eocene–Oligocene continental and shallow- to deep-marine deposits (Podhale Flysch, Fig. 2, e.g. Gedl 2000). Cenozoic uplifting (e.g. Śmigielski et al. 2016) and rotation (e.g. Jurewicz 2005) induced a generally northern dip direction in the autochthonous and allochthonous units in the Tatra Mountains. The presence of several thrust sheets belonging to different domains resulted in a complex mosaic geological structure of the sedimentary part of the Tatra Mountains. The nappes were first recognized in the Carpathians at the beginning of the 20th century.

The sedimentary rocks of the Tatra Mountains mostly include Triassic, Jurassic, and Cretaceous strata that originated in the Tethys Ocean and show considerable variability in facies development (Figs 9, 10). Differences between rocks in particular nappes and the autochthonous cover are the basis for distinguishing the High-Tatric units (Tatricum Domain; autochthonous and allochthonous), the Lower Sub-Tatric (Krížna) Nappe (Fatricum Domain) and the Upper Sub-Tatric (Choč) Nappe (Hronicum Domain) (e.g. Lefeld et al. 1985; Jach et al. 2014). The deposits of the Krížna Nappe accumulated south of the High-Tatric units, representing deposits of a Jurassic–Cretaceous deeper sea. The Choč Nappe is the most southern tectonic-facies domain in the Tatra Mountains.

High-Tatric series (Tatricum Domain) (Fig. 9)

?Permian–Triassic: The oldest sedimentary rocks in the Tatra Mountains are only known from poorly exposed occurrences in the eastern part of the Tatra Mountains in Slovakia (the slopes of Jagnięcy Wierch Mountain). They consist of conglomerates that rest directly on weathered granitoids of the crystalline core, and represent the continental *Verrucano* facies. As such, they have been ascribed to the Permian. A much more extensive area is occupied by the Lower Triassic (Induan–?Lower Olenekian) red quartzitic sandstones of the Lúžna Formation, which are fluvial subtropical semidesert continental sediments (e.g. Jach et al. 2014). In the upper part, they pass into marginal marine non-calcareous mudstones with sandstone, dolomite, and dolomitic shale beds (Werfenian Beds). The upper Olenekian is represented by dolomites and mudstones deposited in a shallow, commonly hypersaline sea. In the Middle Triassic, limestones and rarely dolomites, up to 600 m thick, originated in a warm, shallow sea on a carbonate platform (e.g. Jaglarz and Szulc 2003). They form crags and cliffs in many places in the Tatra Mountains. In the Late Triassic (Carnian–Norian), continental red mudstones with sandstone and conglomerate beds of the Carpathian Keuper are the major constituent (e.g. Rychliński 2008). Locally, they are replaced by (1) grey mudstones with sandstone beds containing remains of the youngest Triassic flora, or by (2) shallow marine laminated dolomites and limestones. In places, a considerable thickness of Middle Triassic rocks was removed by continental erosion during the Late Triassic, and by marine erosion at a later date.

Jurassic: The Triassic deposits are covered by highly laterally variable sandstones, locally limestones, and spiculites of the Lower Jurassic Dudziniec Formation, which fill synsedimentary tectonic depressions formed in the partly eroded Triassic rocks of the High-Tatric autochthon as a consequence of Early Jurassic rifting in the Western Tethys (e.g. Jezierska and Łuczyński 2016). Lower Jurassic deposits are absent in places. The Middle Jurassic (Bajocian) is represented by light grey and pinkish crinoidal limestones of the Smolegowa Limestone Formation, which were deposited on the shelf. They are covered by condensed crinoidal, ferruginous, and nodular Bathonian limestones, which also occur in neptunian dykes (e.g. Łuczyński 2021). The pelagic grey and pink pelitic, oncoidal-peloidal, locally nodular limestones of the Raptawicka

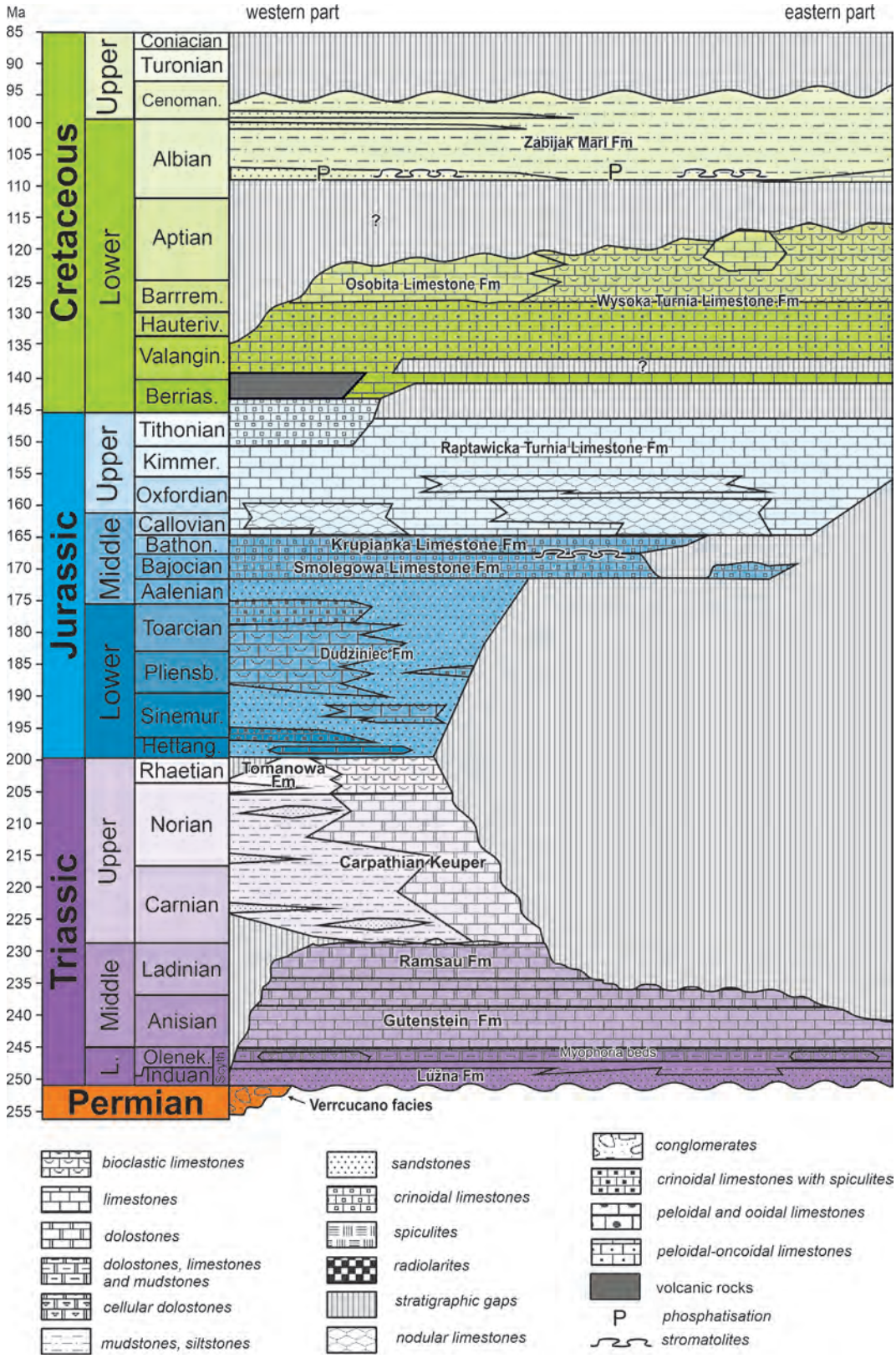

Fig. 9. Simplified lithostratigraphic scheme of the Mesozoic and Permian succession in the Tatricum Domain, Tatra Mountains (modified after Uchman 2014; Lefeld et al. 1985).

Turnia Limestone Formation occupy the higher part of the succession. They were traditionally assigned to the Callovian–Hauterivian (Lefeld et al. 1985); however, new data indicate that they might not be younger than Tithonian, and a stratigraphical gap occurs at the Jurassic/Cretaceous boundary in some sections of the Tatricum domain (Lodowski et al. 2022).

Cretaceous: Shallow-marine sandy limestones with the brachiopod *Pygope diphya*, limburgite tuffites, and lavas (Tithonian–Berriasian) occur locally in the westernmost part of the Tatra Mountains (Osobita Mountain, Slovakia). The Valanginian–Hauterivian sediments are not well documented, and are probably represented by crinoidal and bioclastic limestones of the newly defined Giewont Member (lower part of the Wysoka Turnia Limestone Formation, Lodowski et al. 2022). The upper part of the Wysoka Turnia Formation (Barremian–Aptian–lowest Albian?) is commonly called the *Urgonian* and is comparable to the Schrattenkalk Formation from the North Calcareous Alps. It is composed of organodetrital, shallow-marine platform, creamy limestones, and reef breccias with numerous fossils (Lefeld 1968; Masse and Uchman 1997). The platform sloped to the south. West of Dolina Kościeliska valley, the Wysoka Turnia Limestone Formation is replaced by the Osobita Limestone Formation, which is composed of dark grey micritic limestones with silica layers (cherts). The carbonate platform of the Wysoka Turnia Limestone Formation was emergent, most probably in the late Aptian and early Albian, and later drowned due to the large mid-Cretaceous transgression, much like many contemporaneous platforms globally.

At this point, a rapid deepening occured, and the sedimentation rate quickly dropped. Condensed, commonly glauconitic limestones with hardgrounds, pelagic stromatolites, and phosphatic oncoids formed locally. They mark the beginning of the Zabijak Marlstone Formation (Albian–Cenomanian–?Lower Turonian), which is dominated by dark grey, grey, and yellowish marls and mudstones, and sandstones in the higher part (Lefeld et al. 1985; Krajewski 2003; Bąk and Bąk 2013). The sedimentation of these deposits resulted from suspension flows (turbiditic currents). Hala Pisana glade in Dolina Kościeliska valley is eroded through these soft deposits. They are the youngest rocks of the High-Tatric series in the Tatra Mountains.

Krížna Nappe (Fatricum Domain) (Fig. 10)

Triassic: The Krížna Nappe (Lower Sub-Tatric) section begins with red and white quartzitic sandstones, similar to those of the High-Tatric series, but much less widespread and interpreted as largely continental sediments, transitioning to marine in the upper part. They are covered by variable Induan–?lower Olenekian dolomites, including the *Rauwacken*-type dark grey limestones, black and green shales, and locally conglomerates, all deposited in a shallow, hypersaline sea (e.g. Rychliński and Szulc 2005). The overlying Anisian–Ladinian dolomites and limestones, a few hundred metres thick, were deposited on a carbonate ramp that emerged and karstified in the Carnian. They are covered by violet and green shales with dolomitic concretions, sandstones, and conglomerate beds of the Carpathian Keuper (upper Carnian–Norian). The Rhaetian Fatra Formation is composed of shallow-marine bedded limestones, marly shales, and dolomites, some beds of which are quite fossiliferous (e.g. Michalik et al. 2007).

Jurassic: The Rhaetian Fatra Formation passes diachronically into the Kopieniec Formation (Sinemurian), which is composed of shelf grey marly mudstones, sandstones, and dark limestones (e.g. Michalik et al. 2007). Above, the shallow-marine quartzitic sandstones of the Koperszady Sandstone Formation occur in the eastern part of the Tatra Mountains. The higher part of the section is occupied by spotty limestones and marls (*Fleckenmergel* facies) of the Sołtysia Marl Formation (Sinemurian–lower Pliensbachian, and up to the Middle Jurassic, in the western and eastern Tatra Mountains, respectively, e.g. Iwańczuk et al. 2012). In the western part of the Tatra Mountains, these deposits are overlain by spiculites (upper Pliensbachian), and these in turn by crinoidal limestones (lower Toarcian), locally with manganese ores related to hot submarine springs. They pass upward into red, nodular, partly marly limestones with ammonites (Toarcian), with ferruginous macrooncoids marking condensation. Higher up, limestones with the bivalve *Bositra* occur (Jach 2007). They pass up-

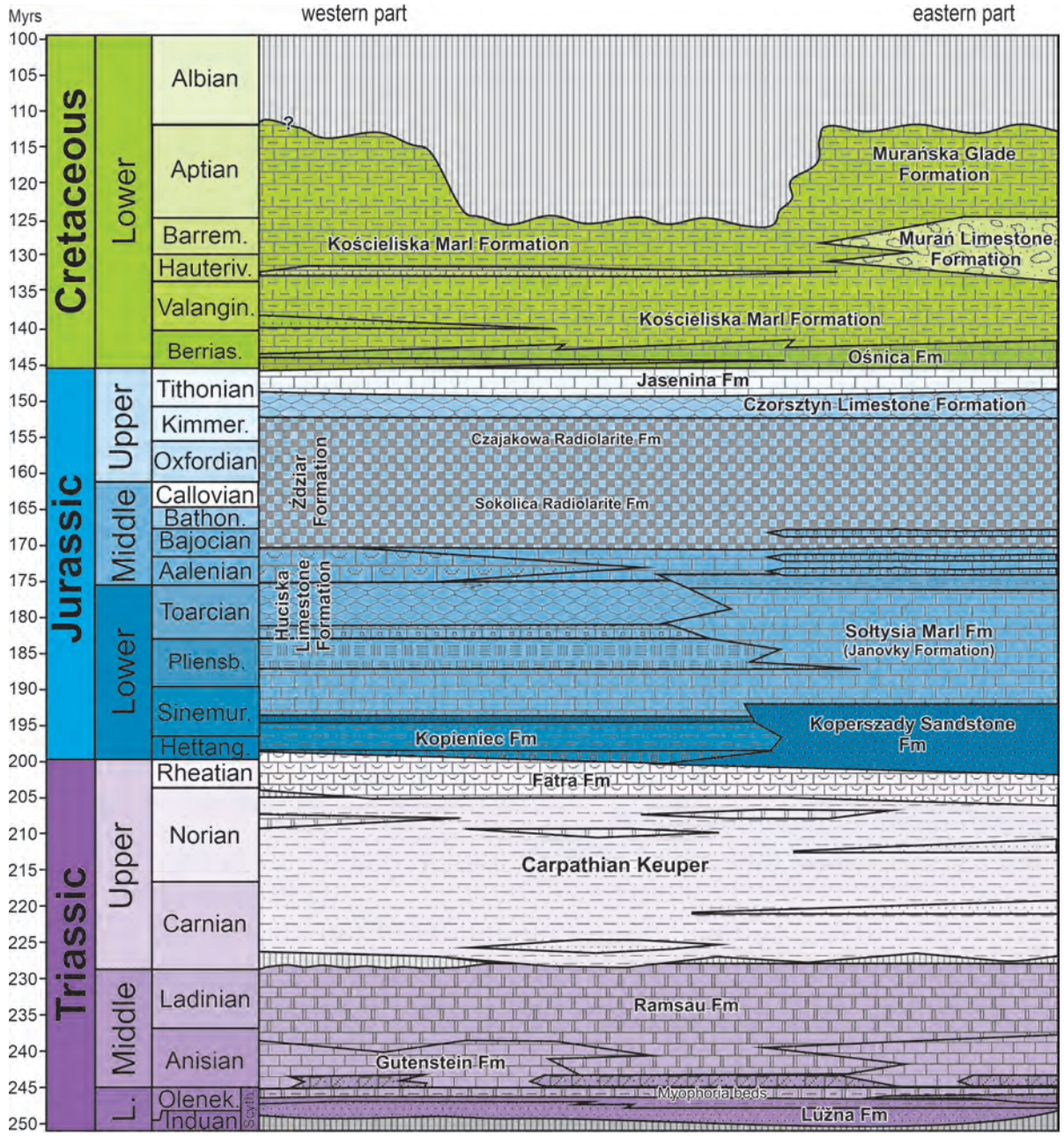

Fig. 10. Simplified lithostratigraphic scheme of the Fatricum Mesozoic succession (after Uchman 2014; Lefeld et al. 1985). Explanations the same as in Fig. 9).

ward into the green and red radiolarites and radiolaritic limestones of the Ždiar Formation (middle Bathonian–upper Kimmeridgian), deposited near the calcium carbonate compensation depth. In turn, these are covered by red nodular or platy limestones (upper Kimmeridgian–lower Tithonian, Jach et al. 2019). Younger deep-sea deposits belong to the Jasenina Formation (Lower Tithonian–lowermost Berriasian), which is composed of marls interbedded with olive grey micritic limestones that are silicified in the upper part (Grabowski and Pszczółkowski 2006).

Cretaceous: Cretaceous rocks of the Krížna Nappe begin with pelitic limestones of the highest Jasenina Formation and the Osnica Formation (Berriasian, Grabowski and Pszczół-

kowski 2006; Grabowski et al. 2013). These limestones pass upward into dark grey bioturbated marls and marly shales with sandstone beds and limestone beds (including crinoidal limestones), which are collectively distinguished as the Kościeliska Marl Formation (topmost Berriasian–Aptian; Pszczółkowski 2003a, b). Above the Kościeliska Marl Formation, the Muráň Limestone Formation (Hauterivian–Barremian) is distinguished in the eastern part of the Tatra Mountains (Lefeld 1974; Pszczółkowski 2003a, b; Gedl et al. 2007). It is composed of a few dozen metres of organodetrital limestones, which were at least partly deposited by turbiditic currents and as olistoliths. They are overlain by marls with olistoliths, assigned to the Muránská Lúka Formation (Aptian–lowermost Albian).

Choč Nappe (Hronicum Domain)

Triassic: Deposits of the Choč Nappe (Upper Sub-Tatric) are only known from fragmentary occurrences along the western part of the northern margin of the Tatra Mountains (Gaździcka et al. 2009). The oldest deposits of the Choč Nappe are upper Anisian dolomites and micritic, locally laminated limestones of the Anisian Gutenstein Limestone. They are overlain by grey dolomites of the Ramsau Dolomite (upper Anisian–Ladinian). All of these deposits originated in a warm and shallow sea. Deeper sea deposits are represented by the Reifling Limestone, composed of grey, silicified, nodular limestones with fossils. They are interbedded by grey mudstones and marls of the Partnach Beds. At the western end of the Tatra Mountains, younger black, bedded limestones with black shale beds belong to the Svarin Beds. The Upper Triassic is also represented here by sandstones and shales of the Lunz Beds (middle Carnian). The widely distributed Wetterstein Dolomite (upper Ladinian–Carnian) is formed by light, massive dolomites, and in places also by limestones. They originated on a carbonate platform, on its slope with reefs and bioherms, and later in a shallow lagoon. A higher stratigraphic position is occupied by the Hauptdolomit (Carnian–Norian), which is composed of grey, medium- and thick-bedded dolomicrites and dolosparites intercalated by dark grey clayey shales. The Rhaetian is represented by diverse, fossil-bearing limestones and is distinguished as the Norovica Formation.

Jurassic: Jurassic rocks from the Choč Nappe only crop out in the Dolina Kościeliska valley region. They are dominated by diverse crinoidal, crinoidal-shelly, crinoidal with spiculites, and peloidal limestones of the Lower Jurassic. They are laterally very variable, pointing to large differences in sea floor depth over short distances (e.g. Uchman 1993). Sea floor elevations and depressions, largely related to block tectonics, were common during the Early Jurassic in several areas of the Tethys Ocean. The youngest strata are red limestones, which might belong to the Middle Jurassic. The younger rocks of the Choč Nappe were probably eroded.

Paleogene deposits

Paleogene deposits discordantly cover the folded and overthrusted rocks of the Tatricum, Fatricum, and Hronicum domains. They covered land with partly denudated relief, and start with conglomerates locally deposited on land, but mainly in a shallow sea. They are covered by dolomitic sandstones, commonly with numerous tests of large benthic foraminifers, mainly nummulites, which lived in a shallow and warm sea (e.g. Roniewicz 1969). The Eocene deposits contain tuffite layers that originated from volcanic ash falls. By the end of the Eocene, the sea was deeper, and sedimentation of marls, algal-nummulitic limestones, and conglomerates with nummulites took place. In the Oligocene, these pass into the deep-sea mudstones and turbiditic sandstones of the Podhale Flysch, which compose the foot of the Tatra Mountains and the largest part of the Podhale region (e.g. Gedl 2000). The Tatra Mountains were completely buried under a few kilometers of Eocene and Oligocene deposits. During a new phase of tectonic movements in the Miocene, the Tatra Mountains were elevated and their rocks exhumed by erosion (e.g. Anczkiewicz et al. 2015; Śmigielski et al. 2016).

FIELD STOPS

The field trip starts in Kraków and leads southward to the Carpathians. In the vicinity of Kraków, Mesozoic rocks of the North European Plate are exposed. The platform is dissected by numerous faults into several horsts and grabens. The grabens are filled with Miocene molasse deposits, while horsts elevate Upper Jurassic and locally Upper Cretaceous rocks. These rocks are mainly represented by Oxfordian cyanobacterial-sponge buildups with associated nodular, chalky, and micritic limestones (Matyszkiewicz 1997). By crossing the bridge on the Vistula River, we can observe Wawel Hill, with Wawel Royal Castle at the top. Wawel Hill is composed of white-weathering Upper Oxfordian (Bifurcatus Zone – A. Wierzbowski, personal communications) massive limestones. These limestones are horst-elevated and shaped by karst phenomena. To the south, the road crosses the Carpathian Foredeep filled with Miocene molasse deposits. The hydrosulphuric mineral water springs are related to the Miocene deposits (Cieszkowski and Ślączka 2001). After a few kilometers, the route passes over the frontal thrust-faults of the Outer Carpathian flysch belt.

Before arriving to Kościeliska Valley, the first stop of the excursion, we stop on the southern slopes of Gubałówka Range, located just north of the Tatras. This provides a viewpoint with a panorama of the northern slopes of the Tatra Mountains. The highest mounts, on the horizon, are mostly built of metamorphic and magmatic rocks of the crystalline core. In the middle, some are formed by Triassic–Cretaceous rocks of the autochthonous and allochthonous High-Tatric units (Tatricum Domain). The lower mounts in the foreground are composed of several thrust sheets containing Triassic–Cretaceous deposits of the Krížna Nappe (Fatricum Domain), and on the western side partly of the Choč Nappe (Hronicum Domain).

This viewpoint is located on Oligocene flysch deposits of the Podhale Flysch Sunclinorium (part of the Inner Carpathian Paleogene). Toward the Tatra Mountains, these deposits are less sandy (the shale-dominated Zakopane Beds). Therefore, a morphological moat developed in front of the mountains. They are underlain by Eocene nummulitic limestones, sandstones, and conglomerates exposed in the entrance to the valleys and on the slopes of the first mountains in the Tatra Mountains. In the higher parts of the mountains, post-glacial morphology can be observed.

Stop 1: Tatra Mountains

Kościeliska Valley: Geological traverse through the main tectonic units of the Tatra Mountains (Fig. 11).

The walking excursion starts from the entrance to Kościeliska Valley (northern slope of the Tatra Mountains), and crosses the main units of the Tatra Mountains that contain sedimentary rocks (Figs 11C, 12). This guidebook is focused on the Cretaceous formations, but brief descriptions also refer to the passing Jurassic and Triassic rocks.

Stop. 1: P1. Kiry: Lower part of the Inner Carpathian Paleogene *(Alfred Uchman)*

In the first 800 m of the route, the Inner Carpathian Paleogene succession can be observed, dipping monoclinally to the north. From the top, the succession contains 1) nummulitic limestone of the Borové Formation (Middle Eocene: late Lutetian–Priabonian), 2) dolomitic sandstone (Bartonian), 3) grey conglomerates and 4) red conglomerates. The conglomerates were deposited in a fan delta followed by shelf clastic and carbonate ramp deposits. The succession rapidly transitions to the mostly Oligocene–?Miocene turbiditic deposits of the Podhale Basin, which are 2500 m thick. The increasing sandstone contribution in these deposits influences the morphology of the southern part of the Podhale Basin (to the north, outside of the Tatra Mountains). The basal part of the Inner Carpathian Paleogene truncates erosionally folded and thrusted units of the Tatra Mountains. Clasts in the conglomerates, mainly carbonates, are derived almost exclusively from sedimentary rocks of the Hronicum and Fatricum domains.

Stop. 1: P2. Brama Kantaka (Niżna Brama Kościeliska): Lower Jurassic of the Hronicum Domain, Choč Nappe. *(Alfred Uchman)*

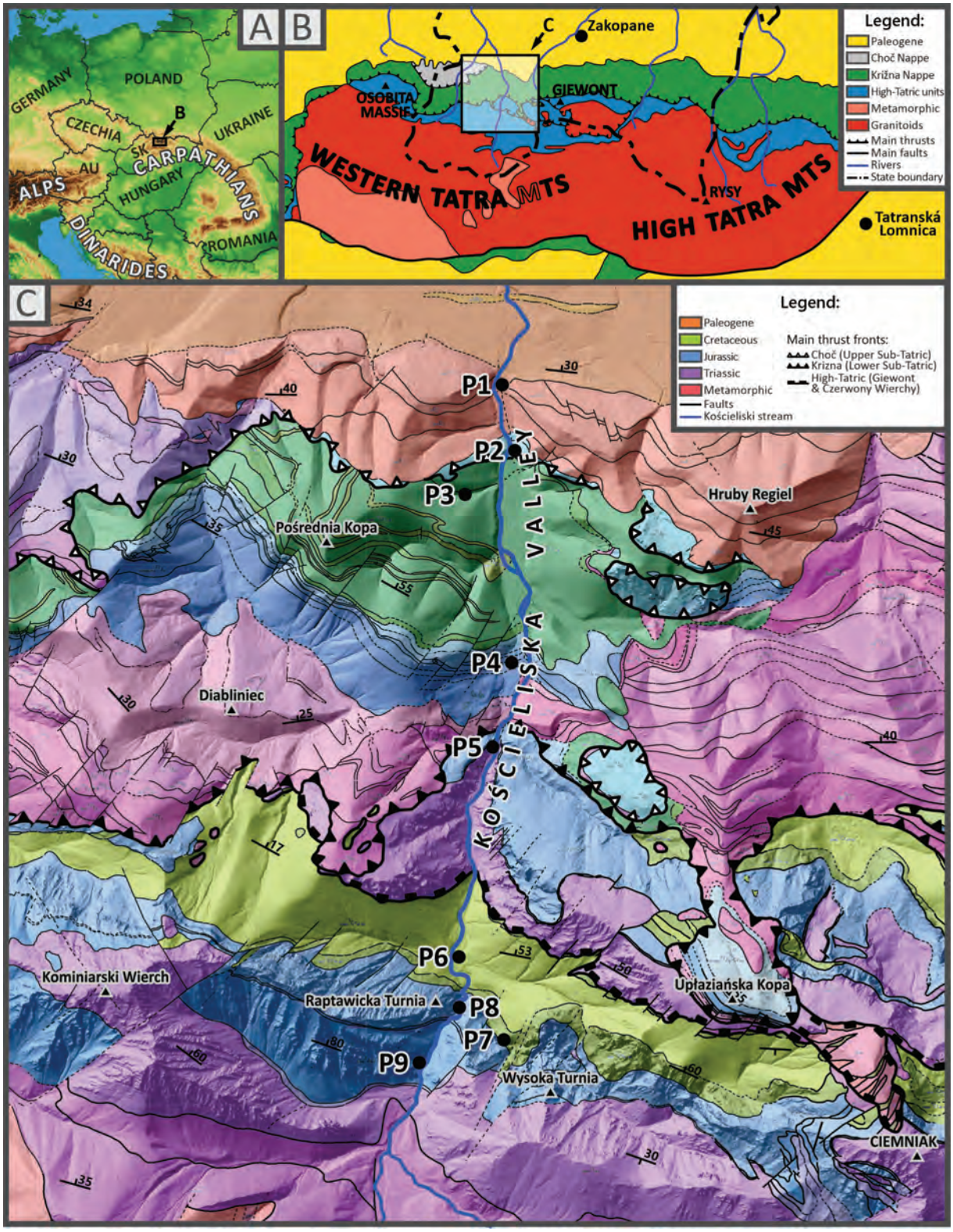

Fig. 11. A – Geographic location of the Tatra Mountains; B – Generalized geological map of the Tatra Mountains; C – Geological map of the Kościeliska Valley area (after Bac Moszaszwili et al. 1979), with observation points (P1 through P9) of stop 1.

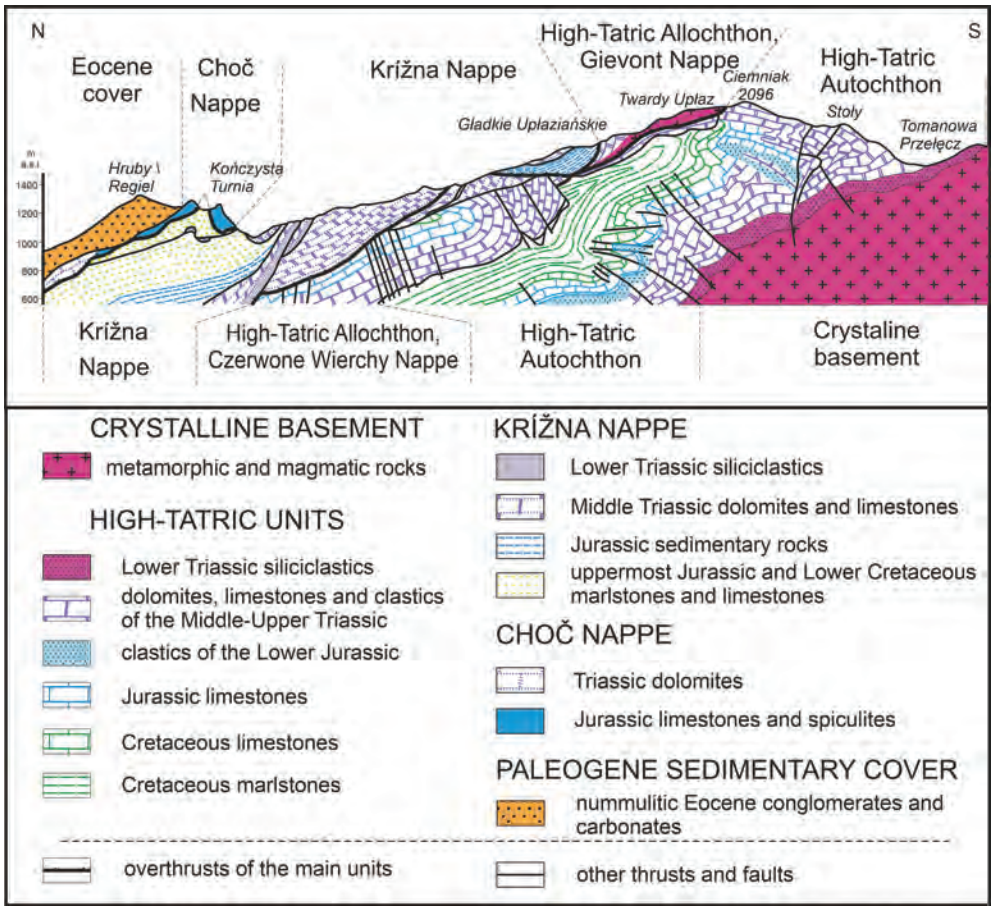

Fig. 12. Cross section along the eastern slope of Kościeliska Valley (after Bac-Moszaszwili et al. 1979, with modifications after Uchman 2014 and further changes).

The distinct narrowing of the valley forms a natural rocky gate built of Lower Jurassic carbonates of the Choč Nappe (Miętusia Formation, Brama Kantaka Thrust Sheet, Hronicum Domain), which are here overturned, strongly tectonized, and truncated from the north by Paleogene erosion. The stratigraphic succession is dominated by massive crinoidal limestones (Pliensbachian–?Toarcian) covering peloidal-cortoidal limestones (?upper Sinemurian; *Bahamian*-type facies), which are only present on the western side of the rocky gate. The crinoidal limestones interfinger with silicified crinoidal calcarenites containing spiculitic cherts and crinoidal calcarenites with brachiopods (*Hierlatz* facies). Further east, possibly Middle Jurassic red calcilutites are present in neptunian dykes crossing rocks of the thrust sheet. The sedimentary succession is referred to the "horst-und-graben" topography, which resulted from rifting in the Western Tethys.

Stop. 1: P3. Wyżnia Kira Kościeliska glade and Wściekły Gully: Kościeliska Marl Formation (Berriasian–Aptian–?Albian). *(Alfred Uchman, Jacek Grabowski, Jolanta Iwańczuk, Patrycja Wójcik-Tabol)*

After crossing the rocky gate of Brama Kantaka, the valley stretches distinctly. The widening is mostly developed on the marlstones of the Kościeliska Marl Formation (Berriasian–Aptian–?Albian), which are present in at least two, and probably three thrust sheets belonging to the Bobrowiec "Partial" Nappe, part of the Krížna Nappe. This formation – and the entire Krížna Nappe – represents the Fatricum Domain. The onset of terrigenous delivery in the Late Berriasian may be regarded as a regional event within the Krížna succession, as it also occurs in the Slovak part of the Central Western Carpathians (e.g., Grabowski et al. 2010). It can be followed in a similar stratigraphic position in many Western Tethys sec-

tions: for instance, the Northern Calcareous Alps, the Western Balkans, and Western Cuba (Grabowski and Sobień 2015).

Within the upper Valanginian marls of the Kościeliska Marl Formation, a complete $\delta^{13}C$ record of the Weissart event was documented (Pszczółkowski et al. 2010; see also Kuhn et al. 2005). $\delta^{13}C$ values quickly increase from below 1‰ up to 2.15‰ close to the lower–upper Valanginian boundary. The event occurs in a marly interval and is not marked by any black shale deposition, similar to other Tethyan sections where anoxic sediments do not occur within the anomaly interval (e.g., Westermann et al. 2010). An integrated palaeoenvironmental study of the Kryta section is in progress, comprising detailed magnetic susceptibility logging and geochemical investigations.

The thickness of the Kościeliska Marl Formation reaches ca. 100 m, but in the Kościeliska Valley it is at least triplicated due to tectonic deformation. Poor exposures and monotonous lithology have prevented better recognition of the tectonic structure. The upper part of the formation is presented in Wściekły Gully (in Polish: Wściekły Żleb, meaning "furious gully"), which is a V-shaped side valley from the west. The Cretaceous deposits dip monoclinally to the north within the Bobrowiec Thrust Sheet (Figs 13, 14A, B).

At the entrance to the gully, a few metres thick, locally silicified grey crinoidal calcarenite outcrops. In places, it contains cherts (Fig. 14E). The calcarenite is considered an equivalent of the Muráň Limestone Formation of the eastern part of the Tatra Mountains (Belianske Tatry), where it reaches 200 m. Here, a few packages of calcarenite interbedded with calcilutites and marlstones crop out on the northern slope of the gully (Fig. 14C). In this part of the Tatra Mountains, they are distinguished as the Muráň Limestone Member of the Kościeliska Marl Formation. The calcarenitic material was redeposited from a carbonate platform to the basin, alongside marly sedimentation. In the presented locality, the Muráň Limestone Member is dated to early late Hauterivian on the basis of dinocysts (Gedl et al. 2007).

Looking up the gully, light grey, grey, or dark grey marly calcilutites, marlstones, and rarely calcilutites can be observed in the lower part of the gully, stratigraphically below the calcarenite (Fig. 14A, B). They belong to the Wściekły Żleb Member, which has been dated as upper Hauterivian (Pszczółkowski 2003) or lower Hauterivian (Gedl et al. 2007). The lower Hauterivian age is confirmed by the ammonite *Olcostephanus densicostatus* (Wegner) (determination by Zdeněk Vašíček, 2022) found in debris at the bottom of the gully (Fig. 14G). This ammonite ranges from the upper Valanginian to the lower Hauterivian; it was also found in the nearby Lejowa Valley along with *Spitidiscus* cf.

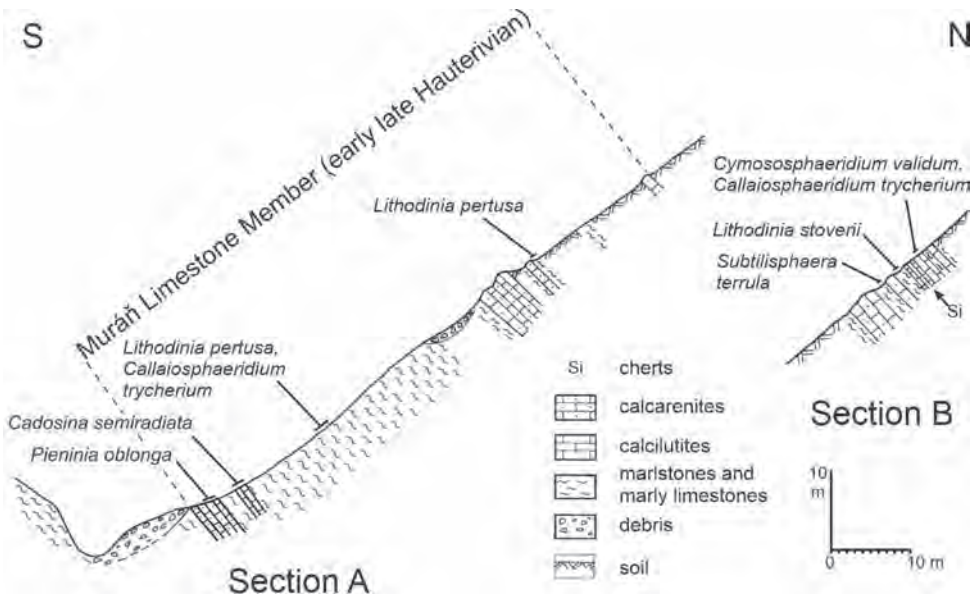

Fig. 13. Cross sections along the northern slope of Wściekły Żleb gully (modified after Gedl et al. 1997).

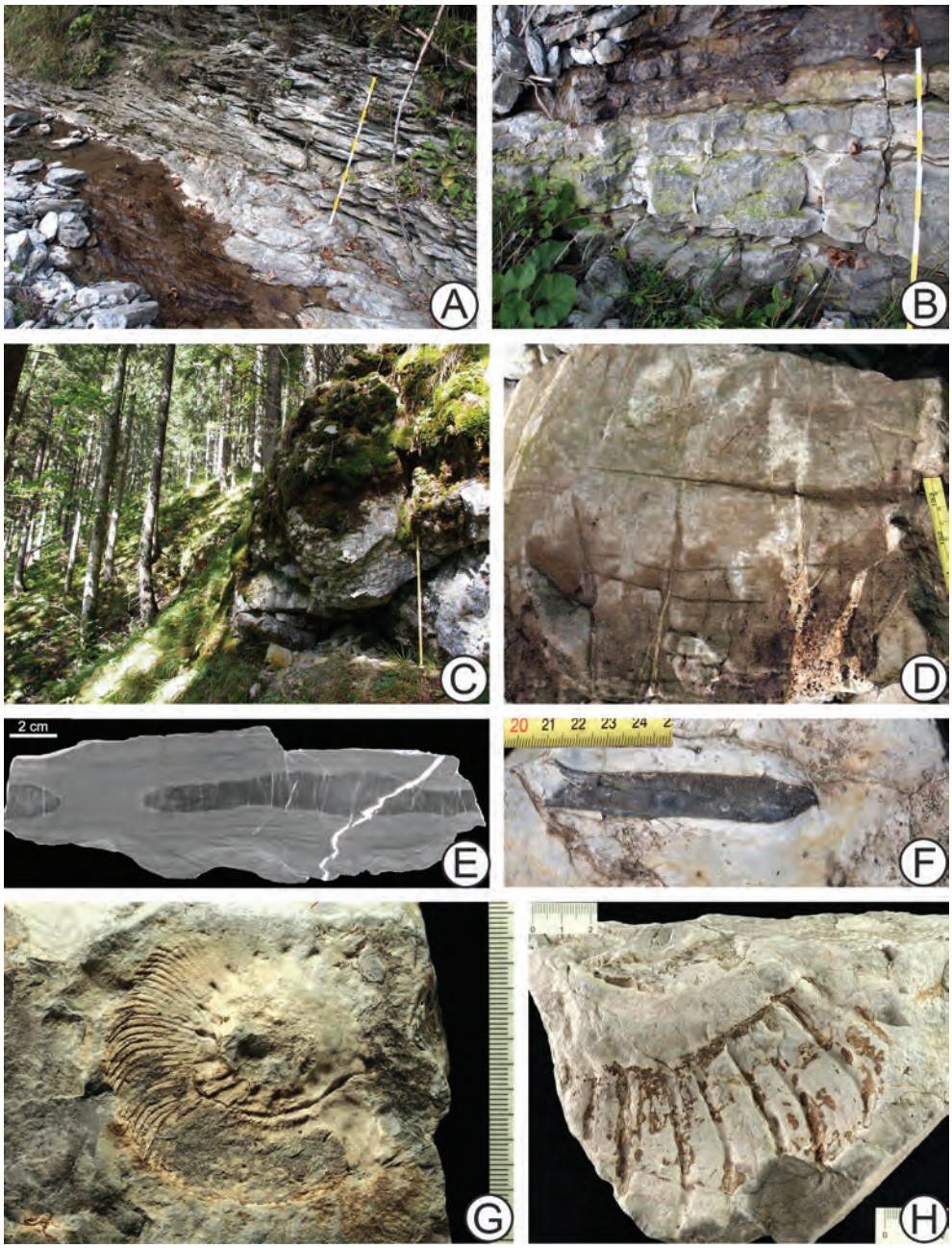

Fig. 14. The Kościeliska Marl Formation in Wściekły Żleb gully. A, B – Outcrop at the bottom of the gully. C – Crag built of calcarenites of the Muráň Limestone Member. D – Block of sandstone from the Kryta Member. E – Chert in the calcarenites of the Muráň Limestone Member. F – Belemnite in a loose block from the Wściekły Żleb Member. G – *Olcostephanus densicostatus* (Wegner) (determination by Zdeněk Vašíček 2022) from a loose block, Wściekły Żleb Member. H – Fragment of an undetermined ammonite from a loose block, Wściekły Żleb Member.

cankovi Vašíček and Michalík, *Criosarasinella* cf. *subheterocostata* Reboulet, *Crioceratites primitivus* Reboulet, *Crioceratites coniferus* Busnardo in Busnardo et al., and the aptychus *Didayilamellaptychus seranonis* (Coquand) (Vašíček et al. 2020). Calcareous nannoplankton investigations along Kościeliska Valley point to the Valanginian–early Aptian, although a local, problematic Aptian–Albian age exists in one sample (Kędzierski and Uchman 1997). The Aptian age (L. cabri Zone) was determined in a parallel gully further north based on foramin-

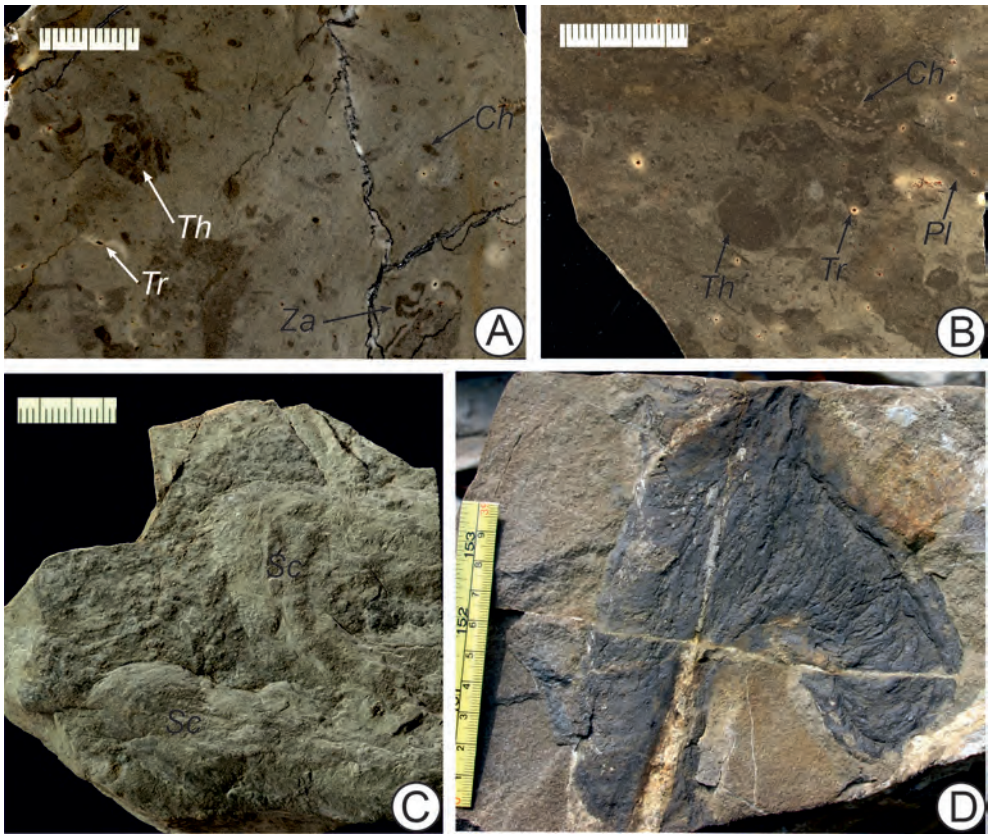

Fig. 15. Trace fossils and bioturbation structures in the Kościeliska Marl Formation in Wściekły Żleb gully. A, B – Polished and wet slabs from the Wściekły Żleb Member; *Ch – Chondrites, Pl – Planolites, Th – Thalassinoides, Tr – Trichichnus, Za – Zavitokichnus*. C – *Scolicia* isp. (*Sc*), Wściekły Żleb Member. D – *Zoophycos* isp. in a sandstone block of the Kryta Member.

ifers and *Nannoconus* species (Pszczółkowski 2015). Lower Cretaceous ammonites, belemnites, aptychi, brachiopods, and bivalves were listed by Wigilew (1914), and Lefeld (1974) illustrated some of them and supplemented the palaeontological inventory.

The lutitic carbonate rocks are strongly bioturbated, with no primary lamination observed. *Trichichnus, Chondrites, Planolites*, and *Thalassinoides* (Fig. 15A, B) are the most commonly observed trace fossils. *Taenidium, Palaeophycus, ?Teichichnus, ?Skolithos, Scolicia, Zavitokichnus,* and *Zoophycos* are rare. The trace fossils show a characteristic tiering pattern, with *Trichichnus, Chondrites, Planolites,* and *Thalassinoides* from the deepest to the shallowest tier (Fig. 16; Uchman 1997, and additional data). The fine-grained lithology, complete bioturbation, and trace fossils belonging to the impoverished *Zoophycos* ichnofacies point to a basinal environment beyond the shelf.

On the southern slopes, a few fine-grained calcareous sandstone beds occur (Fig. 14D), belonging to the Kryta Member (middle lower Valanginian). They occupy a higher stratigraphic position than the Furkaska Member (uppermost Berriasian–Valanginian), which is the lowest member of the Kościeliska Marls Formation. Sandstone blocks are observed among debris at the bottom of the gully. The sandstones are mainly medium-grained lithic and arkosic arenites, although hybridic arenites also occur (Świerczewska and Pszczółkowski 1997). Magnetic separation revealed that Cr-spinels are an important component of the sandstones. The sandstones occur in similar stratigraphic position in the Oravice area of Slovakia, just 6–7 km west of our locality. The Oravice event has been named after the eponymous area (Reháková 2000; Pszczółkowski 2003a, b). According to Reháková (2000), the Oravice event took place in the uppermost Calpionellites Zone, correlated with the Pertransiens ammonite Zone.

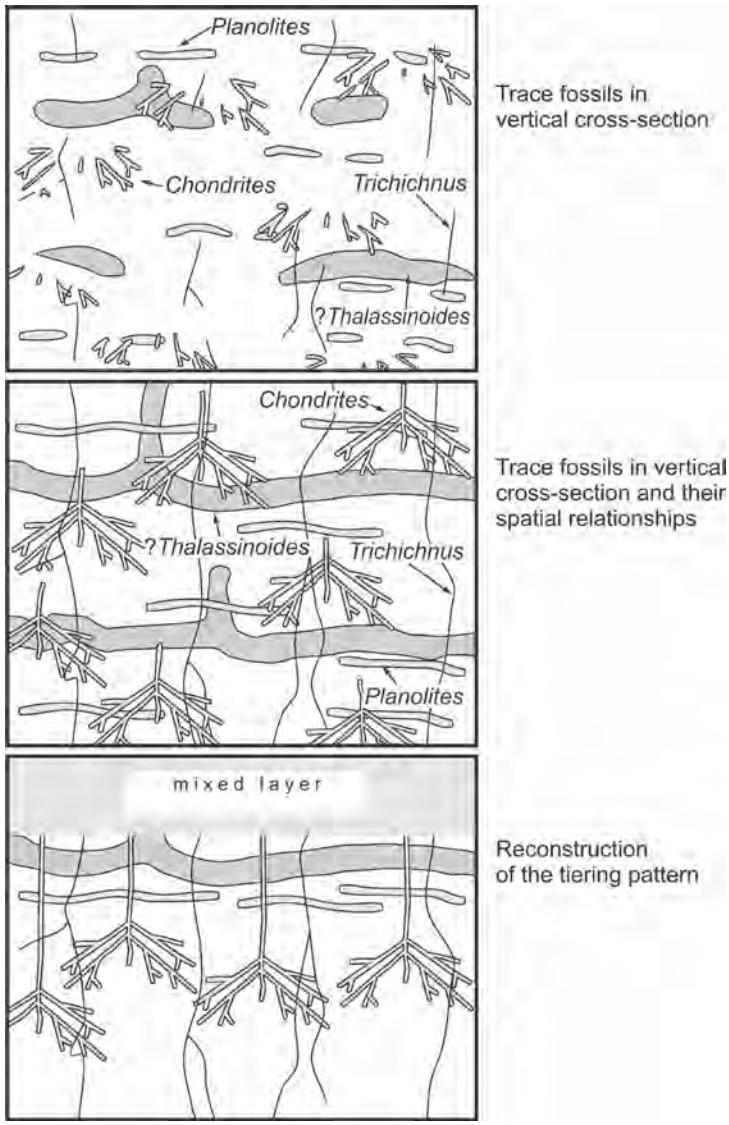

Fig. 16. Tiering pattern from the Kościeliska Marl Formation (changed after Uchman 1997).

Pszczółkowski (2003a) dated the sandstones for the upper Calpionellites Zone and the lowermost Tintinopsella Zone (higher Lower Valanginian).

Rocks of the Meliata suture zone, situated to the (present-day) east and/or southeast of the Zliechov Basin (Slovakia), were probably the clastic sediment source (Vašiček et al. 1994). Within the Calpionellites Zone, the sedimentation rate is estimated at 20–28 m/Ma.

Analysis of macerals from marly samples in the Wściekły Żleb Gully and outcrops at the entrance to Miętusia Valley show the presence of vitrinite (45%), liptinite (40%), and intertinite (15%). The liptinite is derived from non-humifiable plant matter and lipid-rich algae (Taylor et al. 1998), collectively relatively hydrogen-rich remains. Vitrinite is derived from humic matter, and its optical features and chemical composition generally fall between liptinite and inertinite. Inertinite includes macerals of diverse origin: tissues with preserved structural details, detrital fragments, and charred amorphous material. Inertinite is characterized by a high carbon content and a low oxygen and hydrogen content. The macerals suggest open-marine conditions, as supported by a low organic detritus content. Scarce organic debris (mainly oxidized land plant particles accompanied by non-fluorescent amorphous organic matter)

suggests deposition occurred under aerobic conditions.

Stop 1: P4. Path to Przysłop Kominiarski: Upper Jurassic succession of the Fatricum Domain. (*Alfred Uchman*)

This stop shows the middle portion of the stratigraphic succession of the Bobrowiec Thrust Sheet. As in the former stop, the beds dip monoclinally to the north. A few creamy and light grey calcilutite beds crop out on the turning point of the path, belonging to the *Maiolica*-type facies. It is not clear whether they belong to the uppermost Jasenina Formation (Lower Tithonian–lowermost Berriasian) or to the Osnica Formation (Berriasian), which underlies and passes gradually into the Kościeliska Marl Formation.

Approximately 200 m from the beginning of the path, a row of crags built mainly of greenish and reddish calcareous radiolarites and radiolarian limestones can be observed from a distance. Their blocks have fallen close to the path and are accessible for direct observation. The radiolarites belong to the Ždiar Formation (middle Bathonian–upper Kimmeridgian). They are covered by platy and nodular limestones (upper Kimmeridgian–Lower Tithonian). The radiolarites contain aptychi but not ammonite shells, suggestive of deposition between the calcite compensation depth and the aragonite compensation depth. The higher stratigraphic position is occupied by olive grey calcilutites of the aforementioned Jasenina Formation (Lower Tithonian–lowermost Berriasian).

Stop 1: P5. Brama Kraszewskiego and the stretch of the valley up to Owczy Gully before Pisana Glade: Jurassic and Triassic succession of the allochthonous High-Tatric Unit (Tatricum Domain). (*Alfred Uchman*)

The distinct narrowing of the valley (Brama Kraszewskiego) forms a natural rocky gate in Jurassic limestones of the allochthonous Czerwone Wierchy Fold (the Organy "Unit"). The beds dip monoclinally to the north. Stratigraphically, from the top we can observe grey and reddish pelagic calcilutites with microfacies containing *Saccocoma* and *Globochaete alpina*. With a stratigraphic gap (the Bathonian condensed limestone is missing), they rest on a few metres thick, shallow marine Bajosian crinoidal limestone. These, in turn, cover Middle Triassic massive and bedded dolomites that can observed at a distance of a kilometre.

Stop 1: P6. Owczy Gully and Pisana Glade: Stratigraphy and palaeogeographic events in the Albian–Turonian of the Hightatric Succession. (*Krzysztof Bąk and Marta Bąk*)

The stratigraphy of the lowermost Zabijak Formation (glauconitic, phosphatic, and echinodermal-foraminiferal limestones; Żeleźniak Member) is based on ammonites and mollusks (Uhlig 1897; Passendorfer 1930; Marcinowski and Wiedman 1985, 1990; Vašiček 1997), and partly carbon isotope data (Bąk K. et al. 2016a) and planktonic foraminifers (Bąk K. 2015; Bąk K. et al. 2016a, 2018). Macrofossils enable a placement of the Albian transgression in the Tatric area in the *Douvilleiceras mammillatum–Hoplites dentatus* Chrone.

Planktonic foraminifers document the age of intrabasinal tectonic movements within the Tatric platform (Ku Stawku Bed) as middle Albian (?*Ticinella primula* Zone). The demise of this carbonate platform is placed in the *Planomalina buxtorfii–Parathalmanninella appenninica* Zone, corresponding to the upper *Mortoniceras inflatum* ammonite Zone. It is related to the positive $\delta^{13}C_{carb}$ excursion of Oceanic Anoxic Event 1d.

The middle and upper parts of these sediments (marlstones, siltstones, and sandstones; Kamienne and Pisana members) have been mainly studied using foraminifers (Kušik 1959; Čulova and Andrusov 1964; Olszewska and Wieczorek 1995; Bąk K. and Bąk M. 2013; Bąk K. 2015; Bąk K. et al. 2016a, b), and to a limited extent radiolarian and carbon isotope data (Bąk K. et al. 2016b). Together, they indicate continuous hemipelagic and flysch sedimentation under neritic and upper bathyal depths from the *Planomalina buxtorfii–Parathalmanninella appenninica* Zone (latest Albian) through the *Helvetoglobotruncana helvetica* Zone (Middle Turonian); however, the Cenomanian–Turonian transition has not yet been documented in this area. The youngest Cenomanian succession in the Zabijak Formation corresponds to an interval preceding OAE2, exemplified by a negative $\delta^{13}C_{carb}$ excursion (part of the *Rotalipora cushmani* Zone). Data about the Early–Middle Turonian planktonic foraminiferal assemblages are restricted to a short note about the

occurrence of *Marginotruncana renzi* (Gandolfi) in the Zabijak Formation.

Stop 1: P7. Lower part of Kraków Gorge and surroundings: Wysoka Turnia Formation (Hauterivian–Albian) of the High-Tatric autochthonous succession (Tatric Domain). (*Alfred Uchman*)

At the beginning of the path to Kraków Gorge (just south of the second bridge on Kościeliski Stream; eastern side of the valley), 6 m of dark grey calcilutites overlie at least 4.5 m of dark grey calcarenites. This section is probably incomplete at the top. They belong to the Osobita Limestone Formation, which replaces the platform limestones of the Wysoka Turnia Formation (Barremian–Aptian–earliest Albian?) starting from the bottom of Kościeliska Valley to the west, where they are thicker and silicified. The calcilutites cropping out in the valley contain crinoid debris, benthic foraminifers (single orbitolinids are present), and rarely mollusc shell debris. The calcarenites are dominated by crinoid debris and contain mollusc shell debris (fragments of rudists?), benthic foraminifers (single orbitolinids are present), bryozoans, *Crescentiella*, and algae. The bioclasts are partly micritized.

The path runs to the lower part of Kraków Gorge, which formed in tectonized rocks of the High-Tatric autochthonous succession, probably under thick snow cover during the latest glaciation. At the entrance, c. 12 m of dark grey calcilutites belonging to the Osobita Limestone Formation are available. The walls of the gorge are mainly built of pelagic limestone of the Raptawicka Turnia Limestone Formation. Krakow Gorge is wider in a segment where the tectonically inserted Zabijak Marl Formation crop out. The route runs along touristic paths and passes through the short, inclined, Smocza Jama Cave, which is open to both sides.

Above Smocza Jama Cave, the path runs on the eastern slope of the valley, above which there are a few crags mainly built of massive, light grey calcarenite of the Wysoka Turnia Formation (Barremian–Aptian–lowest Albian?). Better outcrops of this formation are in the higher part of Kraków Gorge, but unfortunately are not easily accessible.

The Wysoka Turnia Formation consists of massive or poorly bedded creamy calcarenites, up to 90 m thick. Only in some places can recognizable bioclasts be observed on weathered surfaces, mainly consisting of thick-shelled bivalves, mostly ostreids (some bored with *Entobia* isp.) and rarely small rudists, gastropods, and rarely corals. In thin section, the limestones are mainly grainstones dominated by echinoderm and shell debris, with orbitiolinids, other benthic calcareous foraminifers, and *Crescentiella* ("*Tubiphytes*") (Fig. 17). The stratigraphic age is based on orbitiolinids, dasyclads (Passendorfer 1930; Lefeld 1968; Masse and Uchman 1997) and the rudist *Horiopleura* cf. *baylei* (Coquand) (Masse and Uchman 1997). In the allochthonous Giewont Nappe, the topmost part of the Wysoka Turnia Formation is dated to the end Barremian or early Aptian, while in the autochthonous part it extends up to the end of the Aptian and probably to the earliest Albian (Masse and Uchman 1997). The corals include *Axosmilia* sp., *Calamophylliopsis fotisalensis* (Bendukidze), *Eugyra lanckoronensis* Morycowa, *Microsolena distefanoi* (Prever), and *Procladocora* sp. (Morycowa and Lefeld 1966; Morycowa 1968). Foraminifera are represented by *Charentia cuvillieri* Neumann, *Dictyoconus pachymarginalis* Schroeder, *Meandrospira* cf. *washitensis* Loeblich & Tappan, *Nubecularia* sp., *Orbitolina* (*Mesorbitolina*) *texana* (Roemer), *Sabaudia minuta* (Hofker), and *Vercorsella scarcellai* (De Castro). Algae are represented by *Archaeolithothamnium* sp., *Boueina* cf. *globosa* Dragastan et al., *Carpathoporella fontis* (Patrulius), *Genotella* cf. *pfenderae* (Konishi & Epis), *Neomeris* sp., *Polystrata alba* Pfender, and *Solenopora urgoniana* Pfender. *Pieninia oblonga* Borza & Mišík is also present (Masse and Uchman 1997).

Walking down the slope built of the Zabijak Formation, small outcrops are present along a small creek. Along the path, we can observe Middle Triassic limestone blocks of the High Tatric allochthonous unit.

Stop 1: P8. Raptawicka Gate: Jurassic/Cretaceous boundary interval in the High-Tatric succession. (*Damian Lodowski*)

The Raptawicka Gate is located in the middle of Kościeliska Valley, ca. 4 km south of its mouth (Fig. 18). The gate is built of the topmost Jurassic and basal Cretaceous rocks of the High-Tatric autochthonous sedimentary

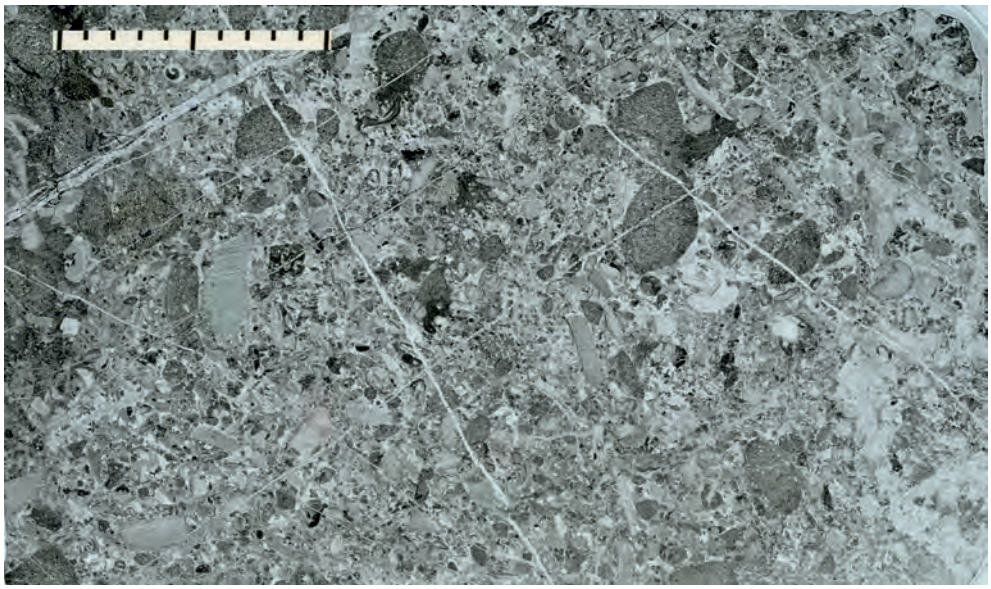

Fig. 17. Thin section of a grainstone from the top part of the Wysoka Turnia Formation. Echinoderm debris is predominant, and orbitolinids are abundant.

Fig. 18. Raptawicka Turnia Limestone Formation at Raptawicka Gate.

cover. These are dark gray cyanoid limestones of the Raptawicka Turnia Limestone Formation (Tithonian) and the overlying lighter calcarenites of the Giewont Member of the Wysoka Turnia Limestone Formation (?Valanginian–Hauterivian; Lodowski et al. 2022; see also

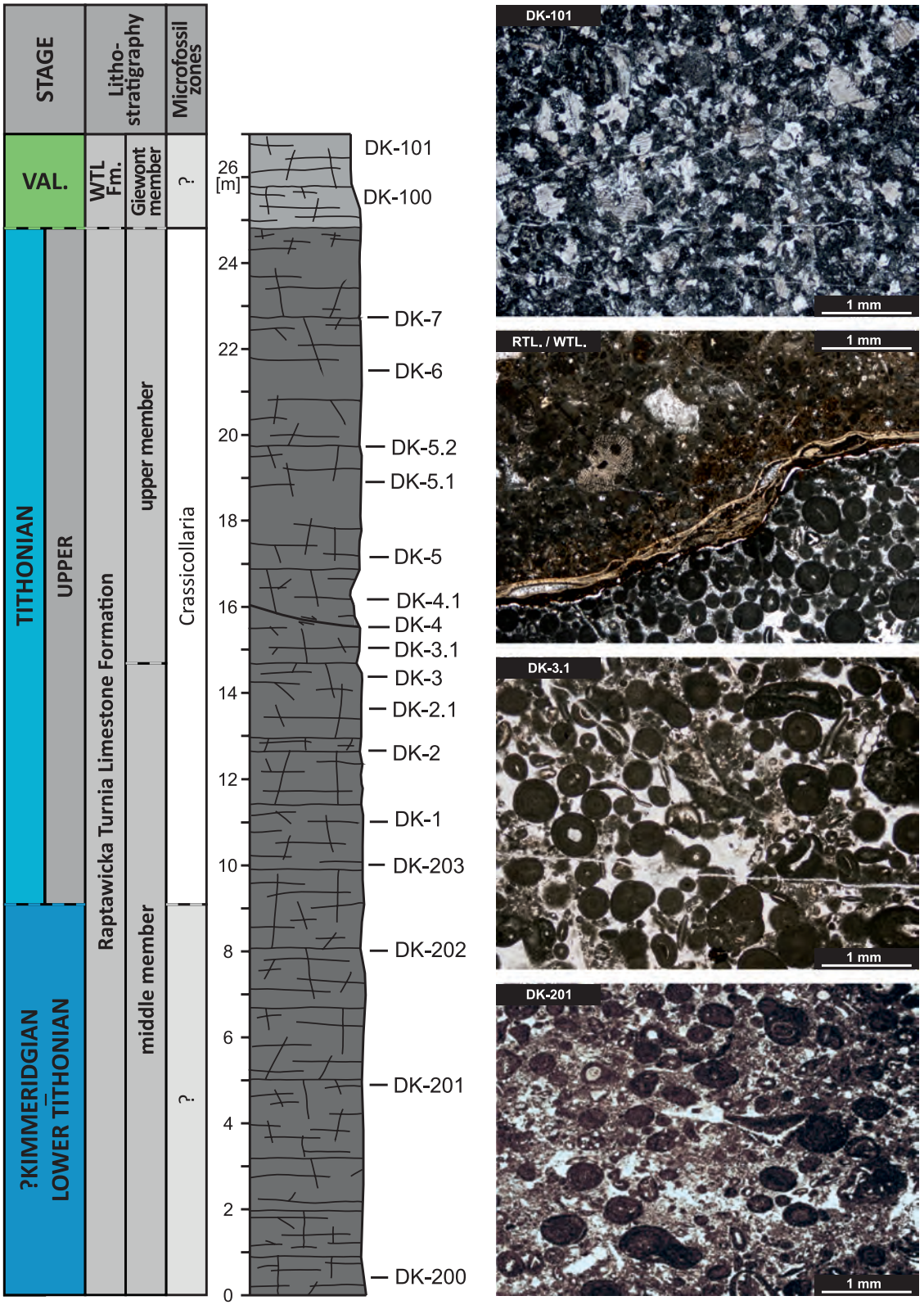

Fig. 19. Stratigraphy and microfacies of the Raptawicka Gate section (modified after Lodowski et al. 2022 and A. Pszczółkowski, unpublished data). RTL/WTL – boundary between the Raptawicka Turnia and Wysoka Turnia Limestone Formations in the Giewont section; WTL Fm. – Wysoka Turnia Limestone Formation; VAL – Valanginian.

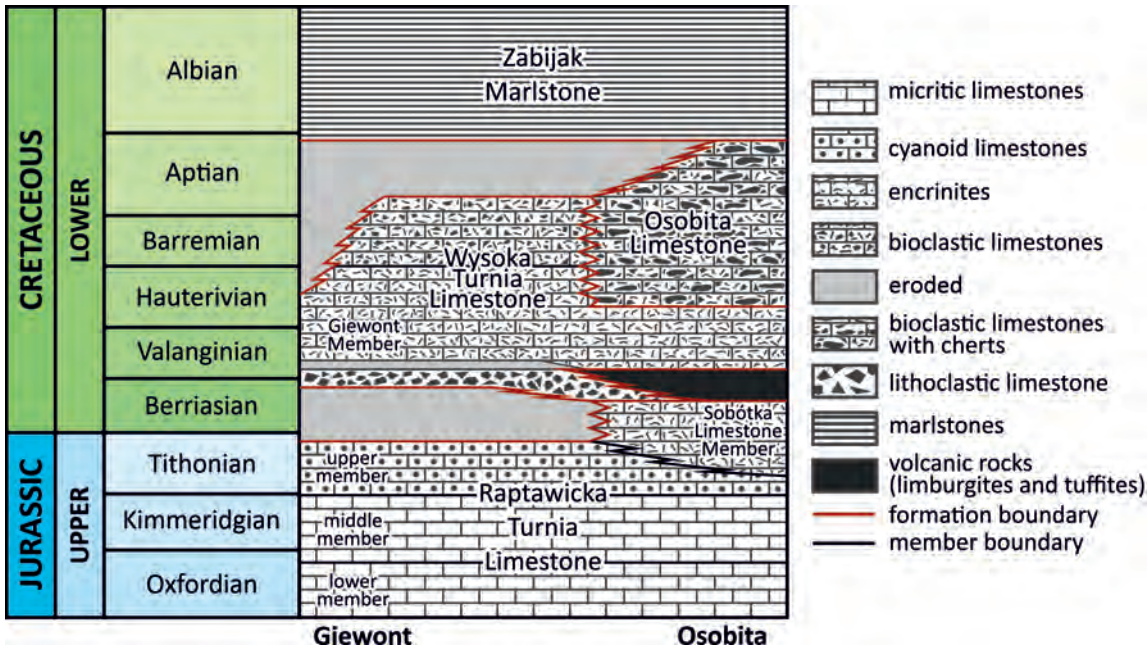

Fig. 20. Lithostratigraphy of the High-Tatric succession. Modified after Uchman (2014) and Lodowski et al. (2022).

Lefeld et al. 1985) (Fig. 19). The contact between the Raptawicka Turnia Limestone and the Wysoka Turnia Limestone formations has never been documented in this location. According to Lodowski et al. (2022) and based on their studies in the equivalent Giewont Unit (one of the High-Tatric nappes), this contact is erosive and occurs in the upper Tithonian (Figs 19, 20).

The stratigraphy of the uppermost Jurassic–basal Cretaceous of the High-Tatric succession is not straightforward. Although the uppermost Jurassic rocks contain stratigraphically important microfossils, such as calcareous dinocysts and calpionellids (e.g., Pszczółkowski et al. 2016; Lodowski et al. 2022), these are badly preserved. The biostratigraphy of the lower Cretaceous is even more problematic (Lodowski et al. 2022).

That being said, the biostratigraphy of the High-Tatric succession is additionally reinforced by correlation of the stable carbon isotope curve with data from other Western Tethyan sections. The most characteristic feature is a drop in $\delta^{13}C$ values across the Kimmeridgian–Tithonian transition, from ca. 2.5 to 1.8‰. Elevated values (2–2.5‰) relative to the Tithonian within the calcarenites of the Wysoka Turnia Limestone Formation point to their late Valanginian age (Lodowski et al. 2022) (Fig. 21). From this point of view, the question remains whether the peak of the upper Valanginian carbon isotope excursion (the 'Weissert event'; see, e.g., Price et al. 2016) can be observed in the High-Tatric succession (or not, for instance due to a hiatus).

The Jurassic–Cretaceous boundary interval in the High-Tatric succession records several palaeoenvironmentally important trends and events with tectonic, eustatic, and climatic implications. Microfacies analyses revealed that late Kimmeridgian microoncoid (= cyanoid) bearing wackestones disappear near the Kimmeridgian/Tithonian boundary, replaced by pseudonodular limestones. Cyanoids reappear in the lower Tithonian and become the dominant rock component in the uppermost lower Tithonian; besides increasing in abundance, it is worth noting they become increasing coarser and spherical upwards (Fig. 21). Ultimately, the upper Tithonian is cut by an erosive surface on which a hardground crust developed (Fig. 19); above, lithoclastic limestones and calcarenites occur. Such a record indicates that maximum sedimentation depths were reached during the Kimmeridgian/Tithonian transition, whereas a secular shallowing trend characterized almost the entire Tithonian–(?)

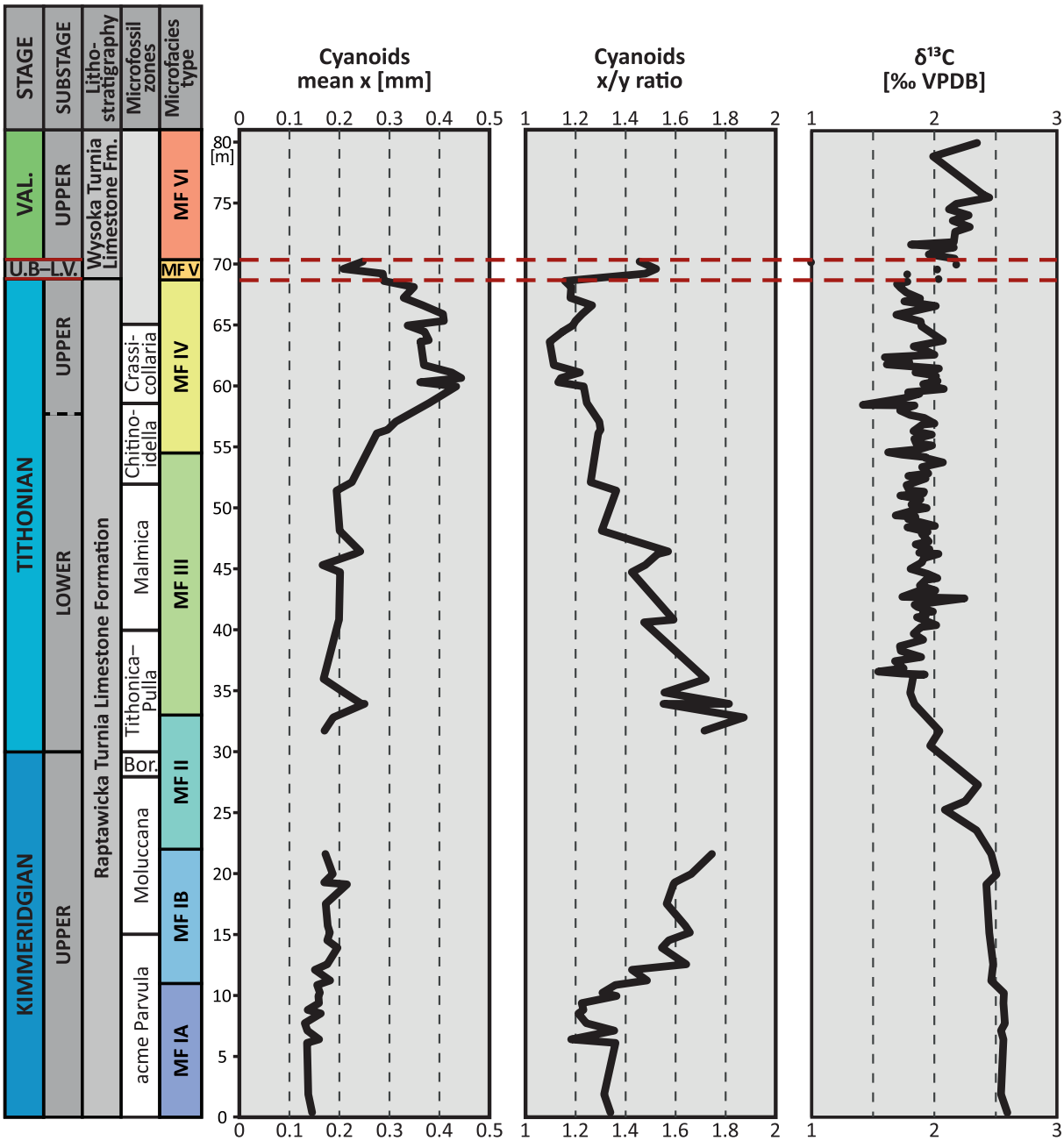

Fig. 21. Microfacies, cyanoid morphometrics, and stable carbon isotopes of the High-Tatric succession (modified after Lodowski and Grabowski, in review).

Berriasian. Due to the presumably large altitude of this palaeobathymetric turnover, Lodowski and Grabowski (in review) interpreted it as resulting predominantly from tectonic uplift (see also Madzin et al. 2014); however, the possibility of a compounding effect from long-term sea-level fall (e.g., Hardenbol et al. 1998) was noted.

The High-Tatric succession was also investigated with regards to palaeoredox conditions, variations in palaeoproductivity(nutrient)-related trace metals, and palaeoclimate evolution, the latter via various terrestrial detrital input proxies. From the elemental geochemistry point of view, the most characteristic feature of the Jurassic–Cretaceous transition in the High-Tatric succession is a relatively narrow in-

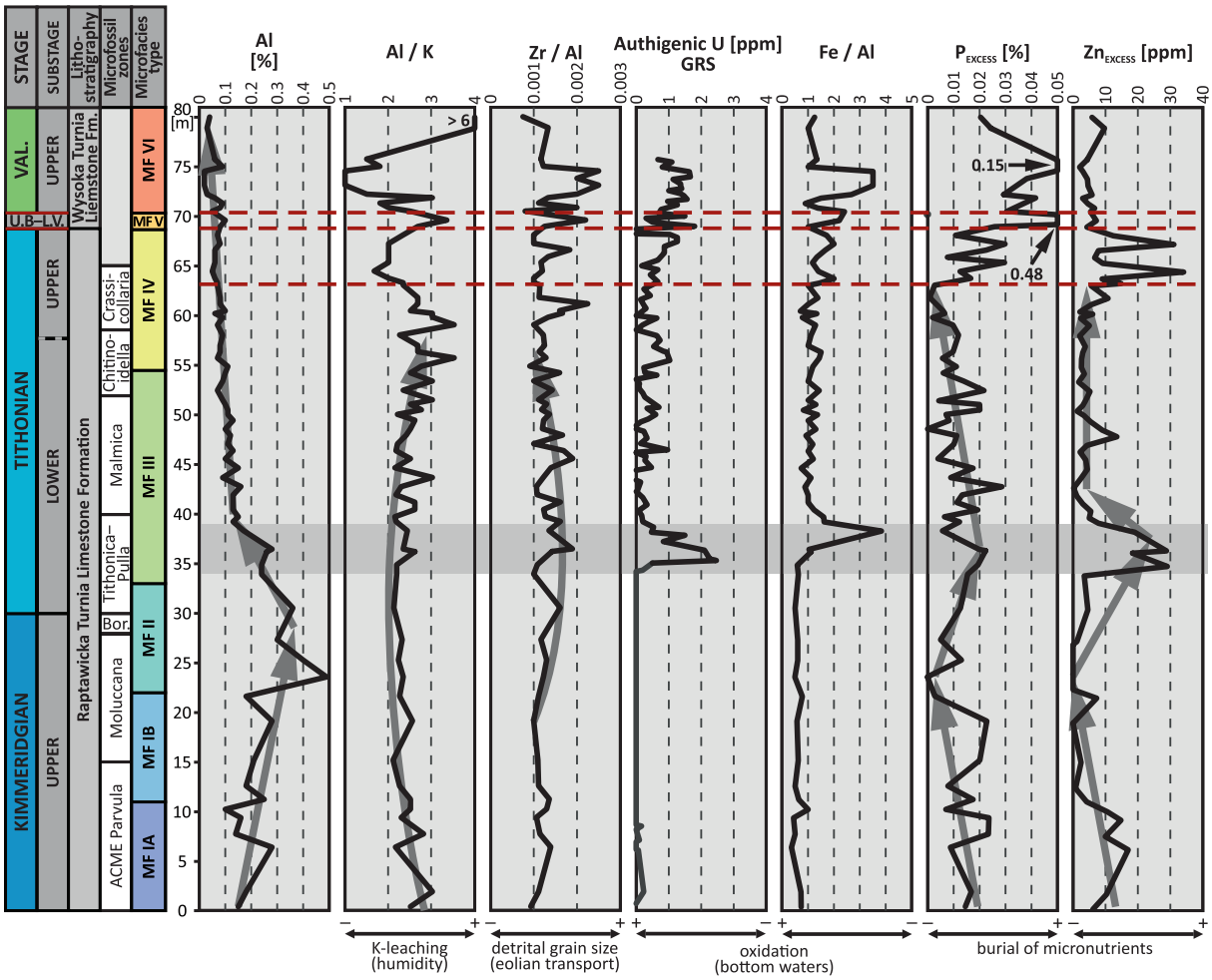

Fig. 22. Selected geochemical indices in the upper Kimmeridgian–upper Valanginian of the High-Tatric succession. Gray belt indicates a euxinic interval. Modified after Lodowski and Grabowski (in review).

terval within the lower Tithonian beds in which major peaks in seafloor euxinia proxies (e.g., Authigenic U, Fe/Al; e.g., Algeo and Liu 2020) (Fig. 22) are observed. Importantly, this phenomenon correlates with a significant increase in nutrient-style trace metal contributions, such as P and Zn; moreover, a similar relation is also observed within the upper Tithonian beds (Lodowski and Grabowski, in review) (Fig. 22). This implies that seafloor hypoxia and increased trace metal burial took place at the same time; consequently, a common mechanism that can explain both processes must be considered.

During the latest Jurassic, the South Tatric Ridge area was subjected to very limited, yet measurable lithogenic influx. The upper Kimmeridgian accounts for the maximum – and relatively stable – clastic fraction contribution. Above, a stratigraphic decline is observed through the entire Tithonian and Lower Cretaceous, which implies the prolonged isolated palaeogeographic setting of this area. Interestingly, both Al/K, for which elevated values are commonly interpreted as indicative of K-leaching (typical for a humid climate mode; e.g., Wei et al. 2006), as well as Zr/Al, which approximates the intensity of eolian transport (e.g., Schnetger et al. 2000), point to a relatively humid late Kimmeridgian, aridization during the latest Kimmeridgian–earliest Tithonian, a relatively humid late early–early late Tithonian, and another arid climate mode during the late Tithonian.

The record described above provides a coherent picture of the latest Jurassic palaeoenvironment of the High-Tatric deposition zone,

with climate playing a major controlling role. Progressive aridization during the Late Jurassic can also be indirectly traced in the neighboring Zliechov and Pieniny basins. There, siliceous (=radiolarite) type sedimentation was replaced by carbonate deposition by the end of the Kimmeridgian (Jach and Rehaková 2019; Bąk et al. 2019). Consequently, the earliest and late Tithonian euxinic events in the High-Tatric succession are considered to be connected with reduced efficiency of the monsoonal upwelling process (e.g., De Wever et al. 2014; see also Golonka and Krobicki 2001), which eventually led to (?limited) stratification. A simultaneous increase in trace metal accumulation (Fig. 22) is a direct result of this process: reduced water-column mixing also affected the nutrient shuttle (uptake) system, enabling their incorporation into sediments (Lodowski and Grabowski, in review). As the mid-Tithonian was characterized by more a humid climate, the monsoonal upwelling returned, driving water column mixing, seafloor oxidation, and increased nutrient shuttle efficiency (Fig. 22). Beyond the Tithonian, terrestrial detrital input proxies indicate a humid climate during the late Berriasian–early Valanginian and the latest Valanginian, whereas an arid mode characterized the early late Valanginian (Fig. 22). Importantly, all the described trends are coherent with the literature, and can be correlated with other Western Tethyan and northern European successions (e.g., Hesselbo et al. 2009; Föllmi 2012; for more, see Lodowski and Grabowski, in review).

Stop 1: P9. From Brama Raptawicka to the Ornak mountain hut: Dudziniec Formation (Lower Jurassic). (*Alfred Uchman*)

The route runs through the valley along a narrowed stretch. Here, the Dudziniec Formation (Lower Jurassic) crops out. It is composed mostly of calcareous, locally silicified, poorly sorted medium- to very coarse-grained sandstones. Quartz and dolomite pebbles are locally present. In places, they pass into sandy limestones. The age assignment of these deposits is based on stratigraphic position and brachiopods, including spiriferinids. The lithologies are quite variable over short distances. The thickness of the Dudziniec Formation is variable, from maximal values of about 400 m thick in Kościeliska Valley to 0 m in some areas. This is related to the rifting in the Western Tethys, which broke the crust into elevated and depressed blocks.

The road leads to the mountain hut through the last glacial moraine system, as manifested morphologically and by large blocks of crystalline rocks. The mountain hut "Ornak" is a good place to see the upper part of the Kościeliska Valley, which is mainly built of metamorphic rocks (mostly gneisses) of the crystalline core. The valley shows a U-shaped cross section typical of post-glacial landscapes.

To the west, the deep Iwaniacka Pass is visible. Its southern slopes are built of Olenekian (Werfenian) quartzitic fluvial sandstones, which rest on the crystalline basement. They pass into red and variegated mudstones followed by dolomitic marls, cavernous dolomites, and breccias of the upper Olenekian. These marginal marine deposits compose the lower part of the pass. In the northern slopes of the pass, Middle Triassic limestones and dolomites – deposits of a carbonate ramp – crop out. The Triassic succession can be partially observed from "Ornak".

Stop 2: Pieniny Klippen Belt

Stop 2: P1. Homole Gorge near Jaworki village: nappe structure in the Pieniny Klippen Belt. (*Michał Krobicki*)

The famous Homole Gorge cuts through the Homole tectonic block south of Jaworki village (Fig. 23). There is a variety of opinions on the origin of this block, including an autochthonous position within the Czorsztyn Ridge (e.g., Birkenmajer 1986), a nappe thrust over the other tectonic units (e.g., Jurewicz 1997, 2005), and an olistolithic origin (Cieszkowski and Golonka 2006). In Homole Gorge, a near 100 m thick white crinoidal limestone succession, assigned to the Smolegowa Limestone Formation of the Czorsztyn Succession, is exposed (Birkenmajer 1977) (Figs 24, 25). These limestones are overlain by red crinoidal limestones of the Krupianka Limestone Formation and *Ammonitico Rosso*-type nodular limestones of the Czorsztyn Limestone Formation, which reach maximum 20 m thickness. Both the Smolegowa and Krupianka formations are Bajocian (Middle Jurassic),

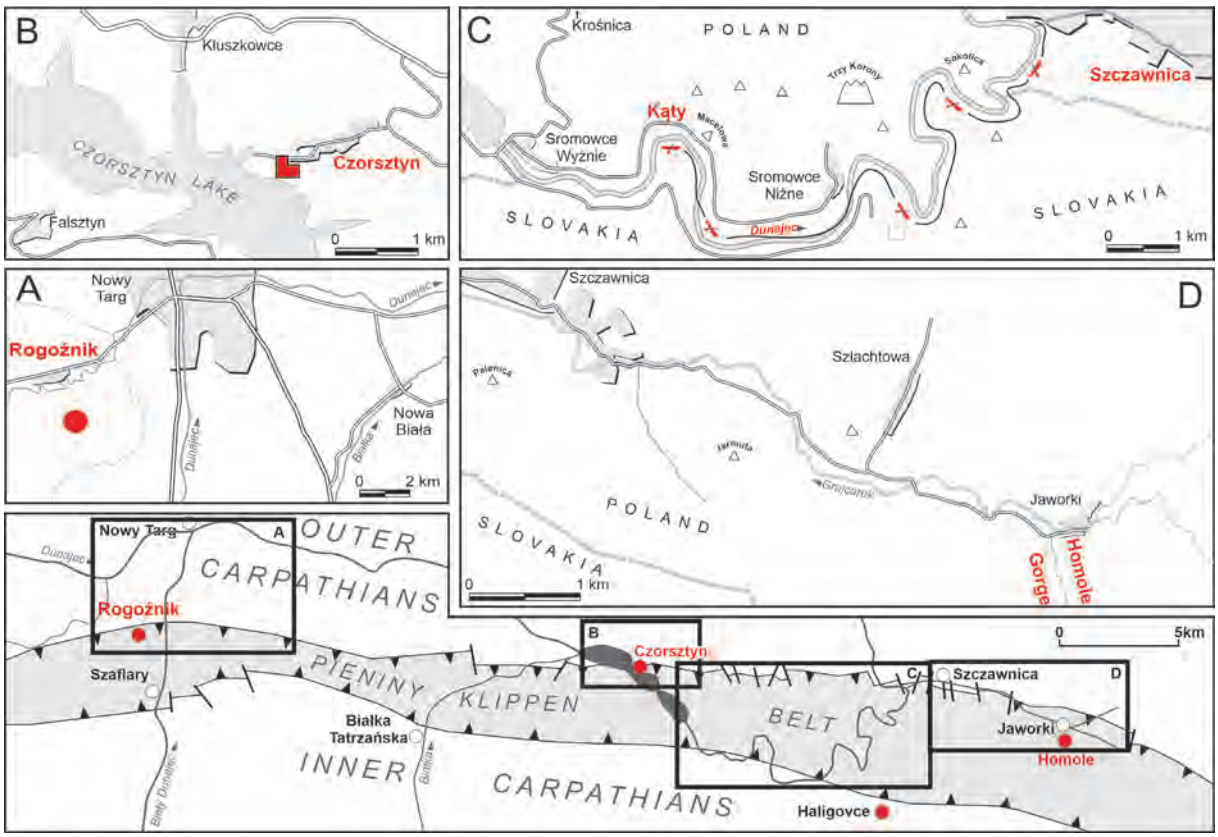

Fig. 23. Polish part of the Pieniny Klippen Belt and the locations of excursion stops.

whereas the condensed nodular limestones of the *Ammonitico Rosso* facies (Czorsztyn Limestone Formation) represent the Middle Jurassic to Early Cretaceous. The decrease of pelagic sedimentation rates took place during the late Middle–Late Jurassic, as recorded by the deepening-upward sequence. The famous Pieniny Klippen Belt tectonic fold and thrust structure can be observed in Czajakowa Skała in the upper part of Homole Gorge (Birkenmajer 1970,) (Fig. 24). Here, the Niedzica Nappe is thrust over the thick Czorsztyn Unit. Several beds representing red nodular *Ammonitico Rosso*-type limestones of the Niedzica Limestone Formation and Czorsztyn Limestone Formation as well as intercalated radiolarites of the Czajakowa Radiolarite Formation are strongly tectonically disturbed, forming an overturned fold (Birkenmajer 1970; Jurewicz 1994). The type locality of the Czajakowa Radiolarite Formation occurs within this klippe. The Czajakowa Skała also captures a complete sequence of the Jurassic deposits of the Niedzica Succession (Birkenmajer 1977; Wierzbowski et al. 1999). The oldest deposits are black and grey marly shales with spherosiderite concretions, belonging to the Skrzypny Shale Formation (Birkenmajer 1977; Tyszka 1994), are exposed here. While small outcrops of these black shales occur below the Czajakowa Skała Klippe within local landslides, the best outcrops of these rocks within the Pieniny Klippen Belt in Poland occur in Krupianka stream, which runs westwards through Homole Gorge. Their thickness reaches 4–5 metres. The shales contain abundant spherosiderites and sometimes perfectly preserved ammonites. The ammonite fauna indicates the black shales were latest Aalenian and/or earliest Bajocian (Middle Jurassic) age, representing oxygen-depleted facies of the *Fleckenmergel*-type. These deposits are overlain by yellowish-greyish-red and dark cherry-greenish crinoidal limestones. The contact between the black shales and crinoidal limestones is sharp and irregular. An ammonite

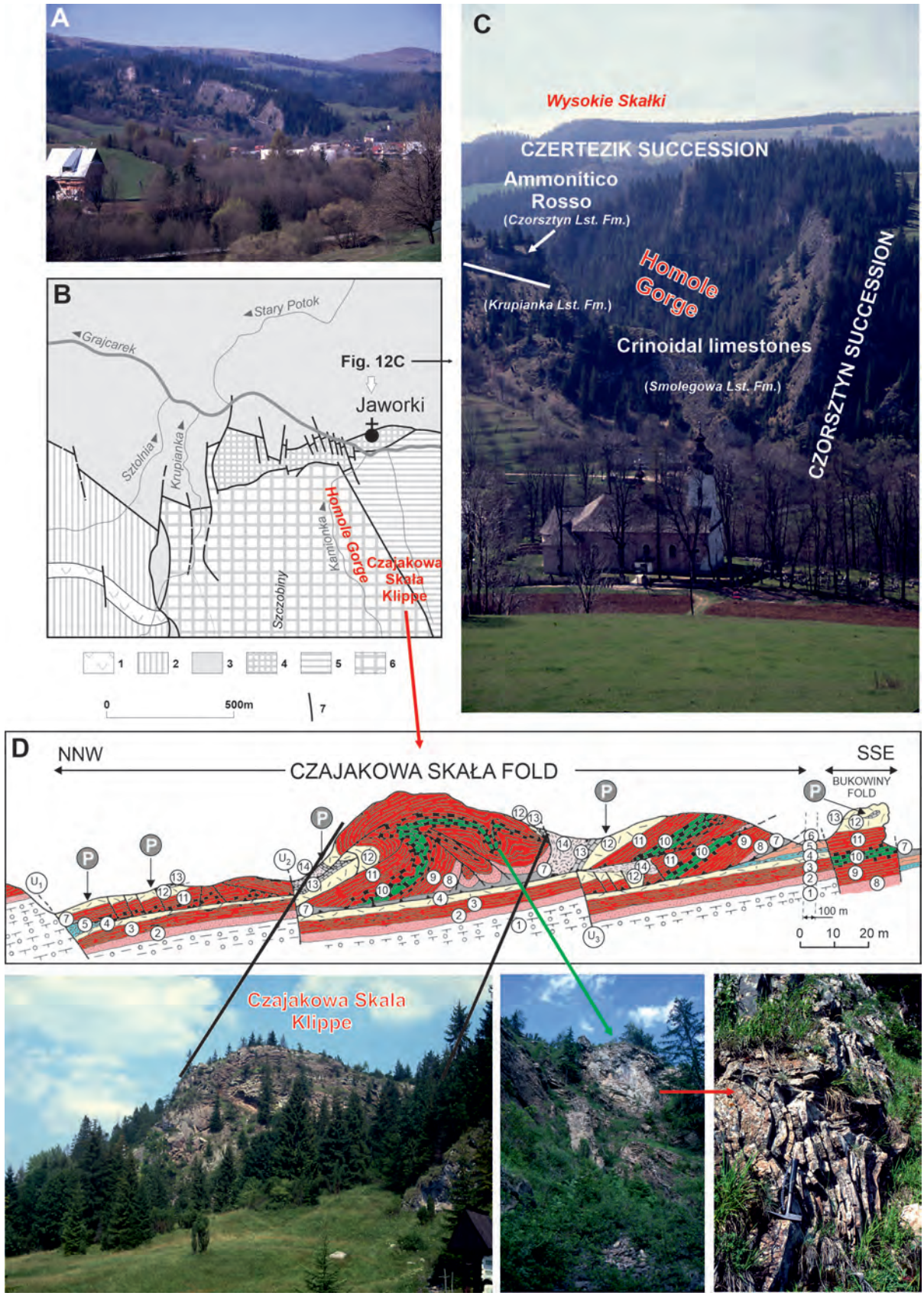
A
B
Stary Potok
Grajcarek
Fig. 12C
Jaworki
Sztolnia
Krupianka
Kamionka
Homole Gorge
Czajakowa Skała Klippe
Szczoblny
1
2
3
4
5
6
7
0
500m
C
Wysokie Skałki
CZERTEZIK SUCCESSION
Ammonitico Rosso
(Czorsztyn Lst. Fm.)
(Krupianka Lst. Fm.)
Homole Gorge
Crinoidal limestones
(Smolegowa Lst. Fm.)
CZORSZTYN SUCCESSION
D
NNW
CZAJAKOWA SKAŁA FOLD
SSE
BUKOWINY FOLD
100 m
0 10 20 m
Czajakowa Skała Klippe

← Fig. 24. **A** – General panoramic view of the Jaworki area. **B** – Tectonic sketch of the Homole block, northern part (after Birkenmajer 1970, 1983); 1 – andesite intrusion (Middle Miocene: Sarmatian); 2 – autochthonous Magura-type Paleogene; 3 – Grajcarek Unit (Magura Succession); 4 – Czorsztyn Unit (Czorsztyn Succession); 5 – Skalski Stream depression (Niedzica Nappe–Niedzica Succession); 6 – Homole block (Czorsztyn Unit with overthrust Niedzica and Branisko nappes); 7 – strike-slip faults. **C** – Entrance to Homole Gorge. **D** – Czajakowa Skała and Bukowiny Fold (after Birkenmajer 1970; modified by Jurewicz 1994); Czorsztyn Succession: 1 – Smolegowa Limestone Formation (white crinoidal limestones); 2 – Krupianka Limestone Formation (red crinoidal limestones); 3 – Czorsztyn Limestone Formation (red nodular *Ammonitico Rosso*-type limestones); 4 – Dursztyn Limestone Formation (pink and white *Callpionella* limestones); 5 – Pomiedznik Formation (marly limestones); 6 – Jaworki Formation (variegated marls); Niedzica Succession: 7 – Krempachy Marl and Skrzypny Shale formations (*Fleckenmergel*-type grey and black spotty marls/shales, sometime with spherosiderite concretions in the latter formation); 8 – Smolegowa Limestone Formation (green-red crinoidal limestones); 9 – Niedzica Limestone Formation (red nodular *Ammonitico Rosso*-type limestones); 10 – Czajakowa Radiolarite Formation (red and green radiolarites); 11 – Czorsztyn Limestone Formation (red nodular *Ammonitico Rosso*-type limestones); 12 – Dursztyn Limestone Formation (red and white *Callpionella* limestones); 13 – Pieniny Limestone Formation (white and grey cherty *Maiolica*-type limestones); 14 – Kapuśnica Formation (greenish spotty limestones). P – Location of phosphate deposits on the top surface of the Sobótka Limestone Member of the Dursztyn Limestone Formation (formal units after Birkenmajer 1977; after Krobicki and Golonka 2008a).

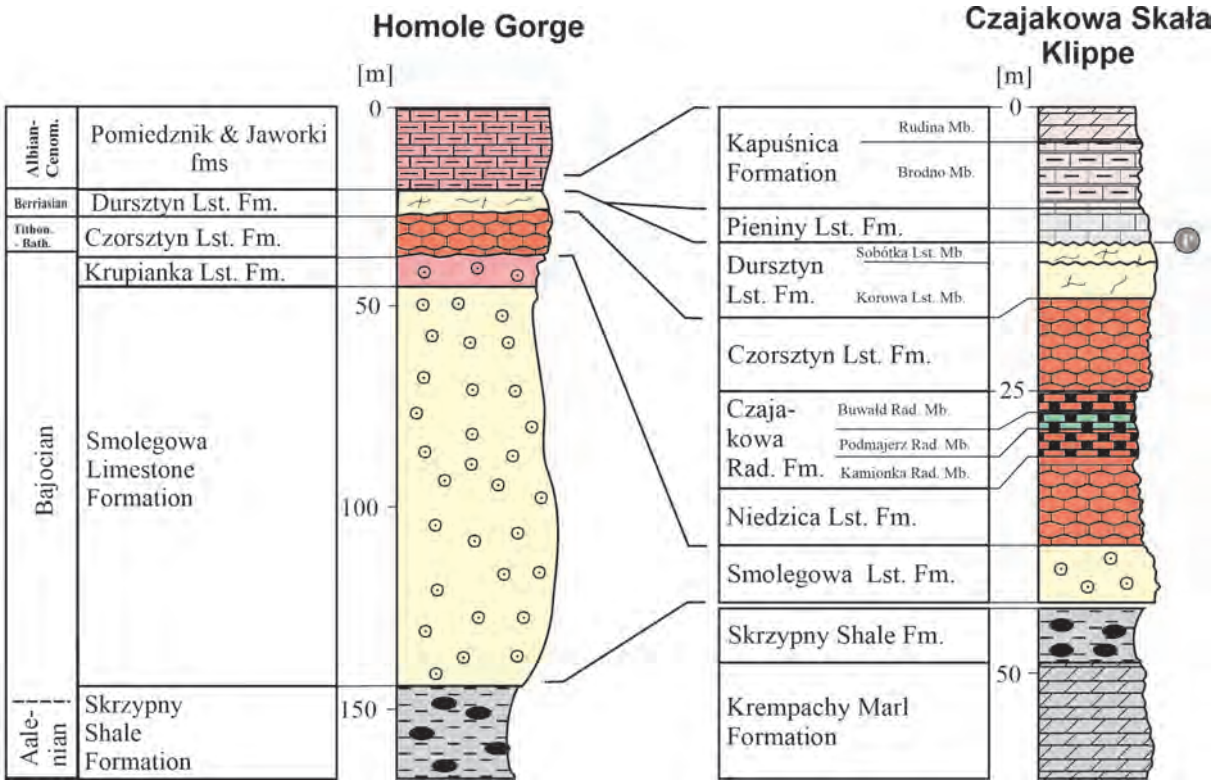

Fig. 25. Lithostratigraphical columns of the Czorsztyn Succession of Homole Gorge (left) and the Niedzica Succession of Czajakowa Skała klippe (right) (after Birkenmajer 1977; modified; after Krobicki and Golonka 2008a).

fauna was found in the lowermost crinoidal limestones of the Smolegowa Limestone Formation; these very precise biostratigraphical data suggest a hiatus between the black shales and crinoidal limestones, spanning the Laeviuscula and part of the Propinquans ammonite Zones of the Lower Bajocian (Middle Jurassic) (Krobicki and Wierzbowski 2004; Krobicki 2006). The Cretaceous strata are the youngest part of this sequence, and the Lower Cretaceous (Berriasian) deposits capture an extremely interesting phosphatic event (large phosphatic macrooncoid pavements) (Fig. 7), indicative of contemporaneous upwelling currents in the Pieniny Klippen Basin.

Stop 2: P2. Skalski stream near Jaworki village: Upper Cretaceous deposits with exotics. (*Michał Krobicki and Barbara Olszewska*)

The Upper Cretaceous and Paleogene

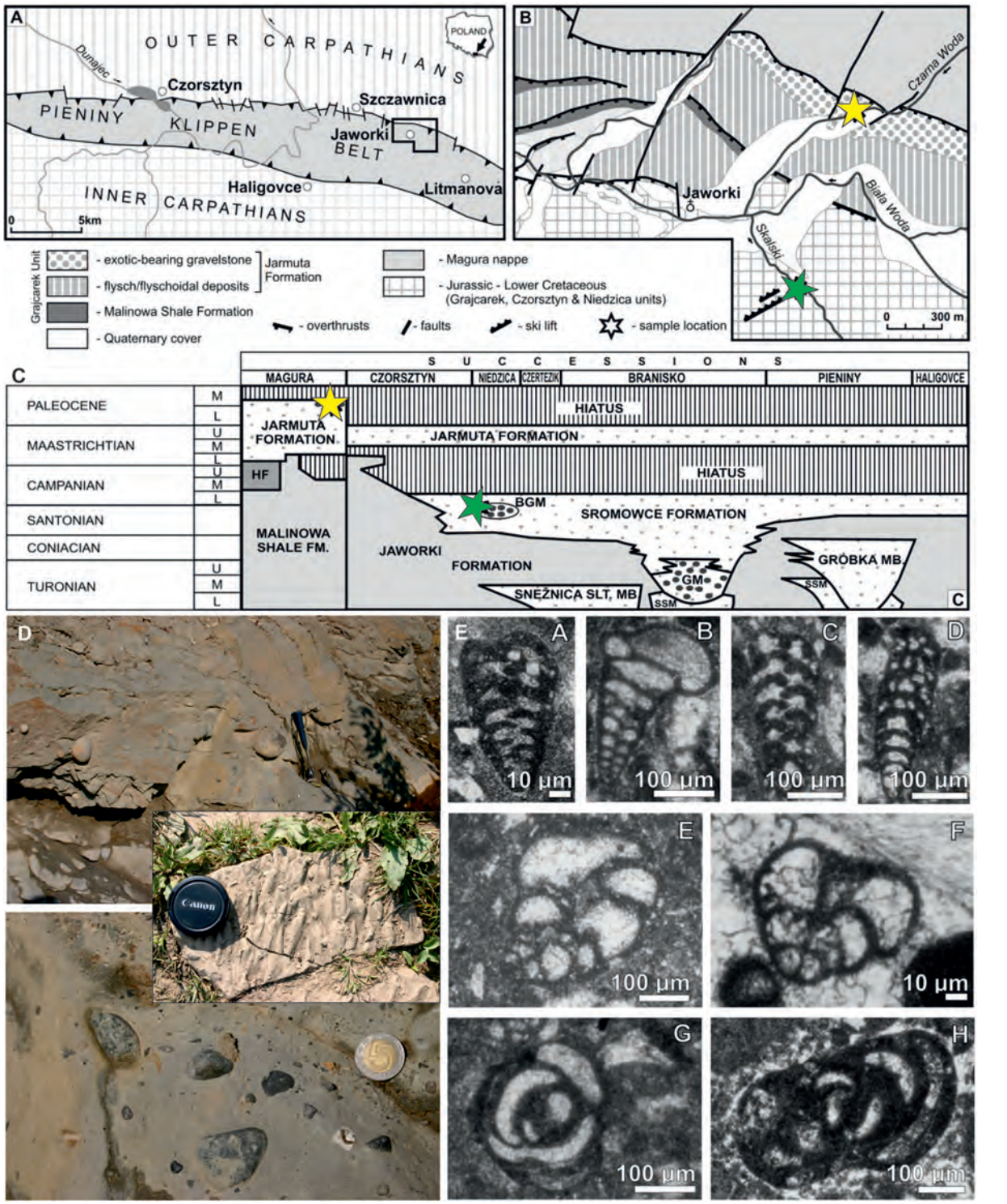

Fig. 26. Skalski stream section near Jaworki village. Location of the section on (**A**) a geological map of the Pieniny Klippen Belt and (**B**) a map of the Jaworki area. **C** – Chronostratigraphic position of the Bukowiny Gravelstone Member of the Sromowce Formation of the Niedzica Succession and the Jarmuta Formation of the Grajcarek Unit in the vicinity of Jaworki village (simplified after Birkenmajer and Dudziak, 1991; chronostratigraphy of lithostratigraphical units after Birkenmajer and Jednorowska 1987; Birkenmajer and Oszczypko 1989; Bąk 1998, simplified and modified following Wierzbowski et al. 2004); HF – Hałuszowa Formation, BGM – Bukowiny Gravelstone Member, SSM – Snežnica Siltstone Member, GM – Gróbka Member, black dots – pebble bearing gravelstones with exotic material, stars – sample locations described in text; **D** – view of the →

exotic-bearing gravelstones of the Pieniny Klippen Belt are linked with flysch/flyschoidal sequences of the Sromowce Formation and the Jarmuta Formation, respectively (Birkenmajer 1977). These exotic rocks are useful for reconstructing the basement and sedimentary cover of source areas (Birkenmajer 1988). The present outcrop is located in Skalski stream, below the lower ski lift station (see Birkenmajer and Lefeld 1969; Birkenmajer 1977, 1988; Radwański 1978; Birkenmajer and Wieser 1990; Birkenmajer et al. 1990). Lower Cretaceous *Urgonian*-type exotic rocks are often found within such gravelstones. For example, *Urgonian* limestone exotics are found in the uppermost Santonian pebbly mudstone of the Bukowiny Gravelstone Member (Jednorowska 1981), which represents a submarine slump, in the middle of the Sromowce Formation of the Niedzica Succession (Birkenmajer 1977; Birkenmajer and Jednorowska 1987) (Fig. 26).

The *Urgonian* is a characteristic shallow-water carbonate facies that formed along the northern Tethyan shelf from the Barremian to the Late Albian; it is worth noting that this facies extended into the area of the future Carpathian orogen (Lefeld 1968, 1988; Masse and Uchman 1997). In the Inner Carpathians, the *Urgonian* facies is represented in the High-Tatric units of the Tatra Mountains (Lefeld 1968) and in the Manín Unit of Váh Valley (Mišík 1990). In the PKB, the *Urgonian*-like facies occurs in the Haligovce Nappe (Birkenmajer 1959) and as exotic pebbles in the Upper Cretaceous Sromowce Formation and the Upper Cretaceous–Paleocene Jarmuta Formation (Birkenmajer and Lefeld 1969; Birkenmajer 1970, 1977, 1986; Birkenmajer and Wieser 1990). In the Outer Carpathians, *Urgonian*-type limestones exclusively occur as exotic pebbles in younger deposits (Birkenmajer and Lefeld 1969; Birkenmajer 1970, 1973, 1977; Oszczypko 1975; Burtan et al. 1984). So far, micropalaeontological investigations of these limestones have been limited to orbitolinid determination (but see remarks in Mišík 1990; Krobicki and Olszewska 2004, 2005). Foraminiferal assemblages of *Urgonian*-type limestones contain many stratigraphically significant larger and smaller foraminifera species. They span the Hauterivian–Albian, predominantly the Barremian to Early Aptian. Planktonic foraminifera (*Hedbergella*, *Heterohelix*, *Favusella*), tintinnids (*Colomiella* cf. *recta* Bonet), and calcareous dinocysts ("Calcispheres") [*Crustocadosina semiradiata* (Wanner)] are sporadic. The tintinnids (*Colomiella* cf. *recta* Bonet) and planktonic foraminifera [*Heterohelix* aff. *moremani* (Cushman)] do, however, suggest a younger age (Reháková and Michalík 1997).

Additionally, magmatic/sub-volcanic, well-rounded exotic pebbles occur here. The exotics are represented by granitic and andesitic rocks (andesite, basaltic andesite, basaltic trachyandesite, trachyandesite, and rhyolitic pebbles, and rare dacite, tephrite, trachybasaltic, and basaltic pebbles): several have been radiometrically dated by the U-Pb SHRIMP $^{206}Pb/^{238}U$ method as 266.0±1.6, 266.4±1.8, 268.8±1.9 and 269.7±1.8 Ma (Guadalupian) (Poprawa et al. 2013; Krobicki et al. 2018). The SHRIMP data and geochemical character of the exotic pebbles suggest a uniform source rock (most probably Inner Carpathians), possibly connected with the Middle Permian subduction of oceanic crust and the formation of a magmatic arc. As such, the investigated exotics are not related with the Early Cretaceous subduction of the oceanic crust and do not represent the so-called Exotic Andrusov Ridge, as postulated earlier (e.g., Birkenmajer 1988).

Stop 2: P3. Bereśnik Hill near Jaworki village: mid-Cretaceous pelagic shell beds, Late Cretaceous deposits and inversion structure. (*Michał Krobicki*)

Pelagic deposits of the Albian/Cenomanian transition mainly occur in the Kapuśnica and Jaworki formations. The Kapuśnica Formation (Upper Aptian–Albian) is represented by dark-grey shales, grey-blue and green marly shales with intercalations of light-grey pelitic spotty (also cherty) limestones, rare fine-grained turbidite sandstone intercalations, and a few black radiolarian shale layers. The lower part of the Jaworki Formation, the Brynczkowa Marl

Bukowiny Gravelstone Member of the Sromowce Formation in Skalski stream; **E** – Foraminifers of the *Urgonian* limestones: A – *Praechrysalidina infracretacea* Luperto Sinni (vertical section); B – *Praedorothia praeoxycona* (Moullade) (longitudinal section); C, D – ?*Pseudotextulariella scarsellai* (de Castro) (longitudinal sections); E – *Pfenderina* cf. *janae* Neagu (longitudinal section); F – *Pfenderina aureliae* Neagu (vertical section); G – *Pseudonummuloculina aurigerica* Calvez (oblique section); H – *Pseudonummuloculina aurigerica* Calvez (sub-axial section).

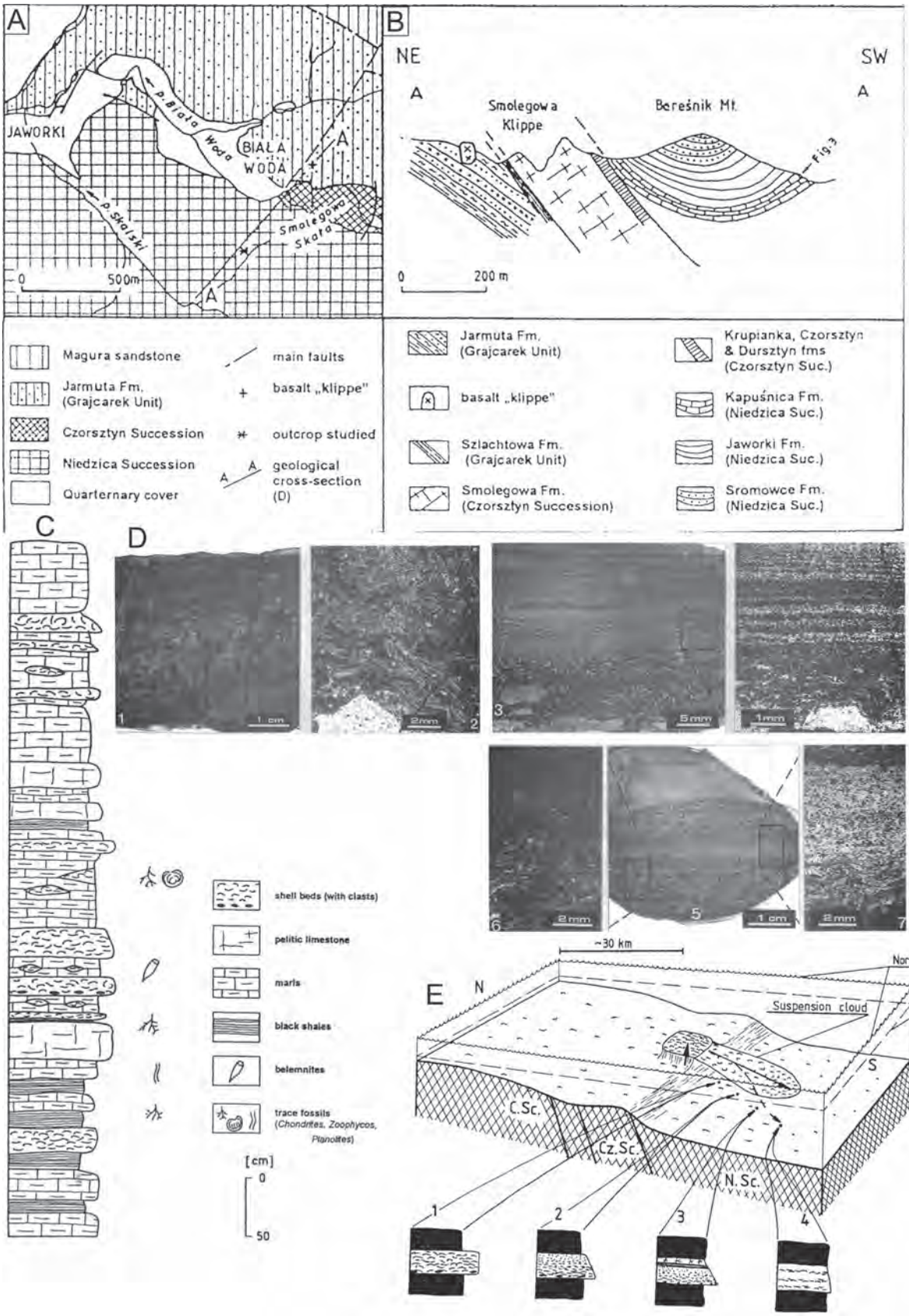
A
JAWORKI
BIAŁA WODA
Smolegowa Skała
0
500m
B
NE
SW
Smolegowa Klippe
Bereśnik Mt.
Fig.3
0
200 m
Magura sandstone
Jarmuta Fm. (Grajcarek Unit)
Czorsztyn Succession
Niedzica Succession
Quarternary cover
main faults
basalt „klippe"
outcrop studied
geological cross-section (D)
Jarmuta Fm. (Grajcarek Unit)
basalt „klippe"
Szlachtowa Fm. (Grajcarek Unit)
Smolegowa Fm. (Czorsztyn Succession)
Krupianka, Czorsztyn & Dursztyn fms (Czorsztyn Suc.)
Kapuśnica Fm. (Niedzica Suc.)
Jaworki Fm. (Niedzica Suc.)
Sromowce Fm. (Niedzica Suc.)
C
D
1 cm
2mm
5mm
1mm
shell beds (with clasts)
pelitic limestone
marls
black shales
belemnites
trace fossils (Chondrites, Zoophycos, Planolites)
[cm]
0
50
E
~30 km
N
Norm
Suspension cloud
S
C.Sc.
Cz.Sc.
N.Sc.
1
2
3
4

Member (Upper Albian–Lower Cenomanian), is represented by pelagic green marls, marly shales, and marly limestones with siliciclastic turbidite wedges (i.e., Trawne Member, Snežnica Siltstone Member) (Fig. 7), and some radiolarian black shale layers. Seven local foraminiferal zones have been recognised in the Upper Albian through Cenomanian (Gasiński 1988), corresponding to four standard zones (Birkenmajer and Jednorowska 1987). Belemnites, ammonites, and pelecypods are very rare (see Kokoszynska and Birkenmajer 1956). Shell beds occur in the Niedzica Succession and represent the Upper Albian through Lower Cenomanian (foraminiferal palaeobathymetric association B1 of Gasiński (Gasiński 1991; Birkenmajer and Gasiński 1992)). These Albian–Cenomanian shell beds are exposed in a right bank tributary of Skalski Stream, about 1.5 km southeast of Jaworki village (Krobicki 1995) (Fig. 27). A section 7.5 m thick is seen in the steep stream bank. The section exposes mostly green and green-grey hard marls, spotty marly limestones, and shales (cherry red-grey at some places), with subordinate intercalations of green spotty pelitic limestones and shell beds. Some beds are boudinaged. The shell beds occur as layers and lenses varying in thickness from about 0.5 to 20 cm. They are built almost exclusively of small thin-shelled bivalves of the genus *Aucellina*. The shells are dismembered and severly crushed, and many are also deformed by compaction, as shown by broken shells whose fragments have remained in place. Unbroken shells are preserved in the lower parts of some shell beds. Abundant and well-preserved tests of (mainly) planktonic foraminifera are present together with the bivalve shells; other fossils include small, indeterminable, spiny bivalve pieces and echinoderm fragments. The shell beds are nearly monospecific (paucispecific *sensu* Kidwell et al. 1986). Belemnites and single *Aucellina* shells are very rare in the accompanying marls and marly limestones, which do, however, contain abundant trace fossils, represented mainly by *Chondrites*, *Zoophycos*, and *Planolites*-like burrows. The sedimentary features of these deposits are indicative of deep-water pelagic deposition. Soft-substratum conditions are suggested by both body fossils (*Aucellina* shells) and trace fossils (dominantly deposit-feeders), the latter indicative of low energy bottom waters. The foraminiferal assemblages are characteristic of a middle slope (Gasiński 1991; Birkenmajer and Gasiński 1992). In contrast, the skeletal accumulations represent high-energy events. Shell beds occur widely in different carbonate or mixed clastic/carbonate shallow-marine settings, both ancient (e.g., Aigner 1985; Fürsich and Oschmann 1986) and modern (e.g., Davies et al. 1989). Most shell beds formed above storm wave base, and skeletal accumulations formed below are rare (Kidwell et al. 1986, fig. 5). Widely occurring pelagic bivalve turbidites in the Alpine-Mediterranean region are an exception (e.g., Bernoulli and Jenkyns 1974).

The upper part of Bereśnik Hill is composed of Late Cretaceous *Scaglia Rossa* deposits, again overlain by the flysch-type Sromowce Formation with exotics in a local inversion structure.

Stop 2: P4. Biała Woda valley (near Brysztan Klippe): Berriasian phosphatic structures. (*Michał Krobicki*)

This stop presents the Jurassic/Cretaceous boundary sequences exposed in natural outcrops of the Niedzica Succession in the eastern part of the Polish PKB. The Dursztyn Limestone Formation, subdivided into the Korowa Limestone Member and the Sobótka Limestone Member (Birkenmajer 1977), represents the Tithonian/Berriasian boundary strata of the Niedzica Succession. In the vicinity of Niedzica, the Niedzica Succession forms isolated tectonic wedges, strongly folded together with Upper Cretaceous marly deposits of the Czorsztyn Succession. East of Jaworki (Fig. 5) the Niedzica Succession occurs as a

← Fig. 27. Bereśnik hill near Jaworki village. **A** – Geological sketch-map of the vicinity of Jaworki (simplified after Birkenmajer 1979); **B** – Geological cross-section in Biała Woda valley (after Krobicki 1995); **C** – The Kapuśnica Formation section with *Aucellina* shell beds, in the the Skalski Stream tributary; **D** – Various *Aucellina* shell bed types, Kapuśnica Formation of the Niedzica Succession; **E** – Generalised model for the origin of various types of storm-generated shell beds. C.Sc. – Czorsztyn Succession; Cz.Sc. – Czertezik Succession; N.Sc. – Niedzica Succession. Type of shell beds: 1 – densely packed, homogenous shell beds, in some cases with clasts, sharply delimited from marl or pelitic limestone beds; 2 – graded shell beds with clasts at base; 3 – sequences starting from small clasts and shell lag at base, passing through graded, laminated, and finally bioturbated at the top; 4 – thin shell accumulations in silty marls and limestones (after Krobicki 1995).

large sheet (nappe) thrust over the Czorsztyn Succession. The outcrops expose white, massive, micritic limestone that grades upwards into thin-bedded, micritic limestone with abundant bioclasts (crinoids, brachiopods, ammonites, small gastropods), assigned to the Sobótka Limestone Member. At the top of this member, a 10–20 cm thick layer composed of green, phosphorite-rich micritic limestone occurs. At this level, large (8–10 cm) phosphatic macrooncoids form an oncolitic pavement (see Krobicki 1993, 1994, 1996). On bedding surfaces, large ammonites (up to 30 cm in diameter) are visible. The rock is strongly fractured; Fe-Mn crusts cover the irregular surfaces of the sedimentary discontinuity (Figs 7, 28). The PKB rock record suggests that upwelling was present in the earliest Cretaceous. The

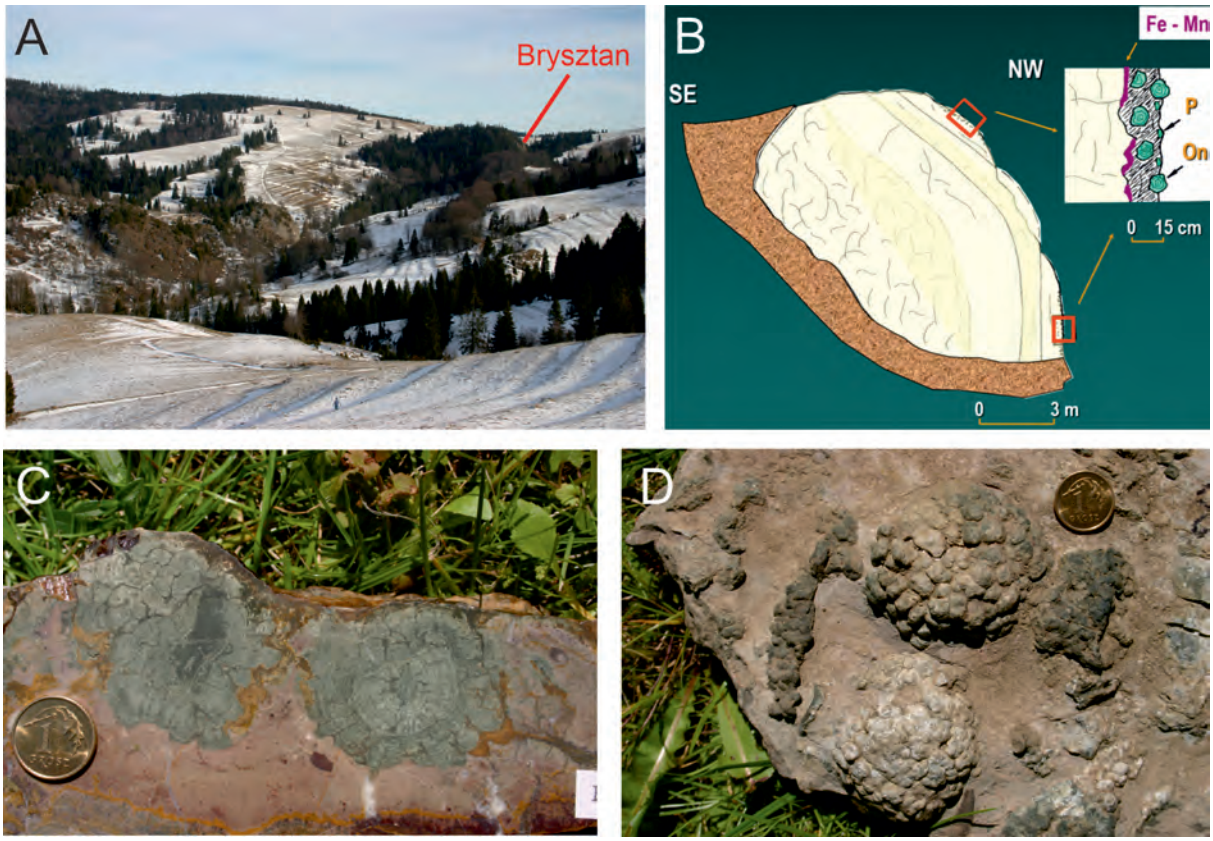

Fig. 28. Biała Woda-Brysztan section. **A** – General view; **B** – outcrop of the Dursztyn Limestone Formation, Sobótka Limestone Member (Berriasian), Niedzica Succession. Inset: top of last bed (after Krobicki 1993, 1994): Fe-Mn – Fe-Mn crusts, P – phosphorites, On – phosphatic macrooncoids; **C**, **D** – phosphatic macrooncoids.

Fig. 29. Palaeoenvironmental position of phosphatic deposits: **A** – Czajakowa Skała and Bukowiny folds, western wall of Homole Gorge near Jaworki (geology after Birkenmajer 1970; modified by Jurewicz 1994) [for explanations to the cross section, see Figure 24]. **B** – Sedimentation model on the intraoceanic Czorsztyn pelagic swell in the Berriasian, with influences of Neo-Cimmerian tectonic movements and upwelling currents (modified after Krobicki 1996): 1 – Rogoźnik Coquina Member (Dursztyn Limestone Formation: A – sparitic coquina, B – micritic coquina); 2 – Czorsztyn Limestone Formation (*Ammonitico Rosso* facies); 3 – Sobótka Limestone Member (Dursztyn Limestone Formation); 4, 5 – Łysa Limestone Formation (4 – Harbatowa Limestone Member, 5 – Walentowa Breccia Member); successions: C – Czorsztyn, N – Niedzica, Cz – Czertezik; **C**, **D** – Palaeoenvironments, wind directions, and upwelling zones of the Carpathian area during the Tithonian–Berriasian (palaeogeography modified after Golonka et al. 2003): C – summer Northern Hemisphere, B – winter Northern Hemisphere: 1 – mountains/highlands (tectonically active), 2 – topographically medium-low (tectonically inactive, non-depositional), 3 – undifferentiated terrestrial, 4 – coastal, transitional, marginal marine, 5 – shallow marine, shelf, 6 – slope, 7 – deep ocean basin with sediments (continental, transitional, or oceanic crust), 8 – deep ocean basin with little to no sediments (primarily oceanic crust), 9 – wind directions, 10 – upwelling zone; abbreviations of oceans and plates names: Bl – Balcans, Br – Briançonnais terrane, Bu – Bucovinian terrane, Cr – Czorsztyn Ridge, EA – Eastern Alps, Hv – Helvetic zone, IC – Inner Carpathians, Li – Ligurian (Piemont) Ocean, Me – Meliata suture, Mg – Magura Basin, Mo – Moesia Plate, PKB – Pieniny Klippen Belt Basin, RD – Rheno-Danubian Basin, Rh – Rhodopes, SC – Silesian Ridge (cordillera), Si – Siret, Sl – Silesian Basin, Ti – Tisa Plate, Vl – Valais Trough. →

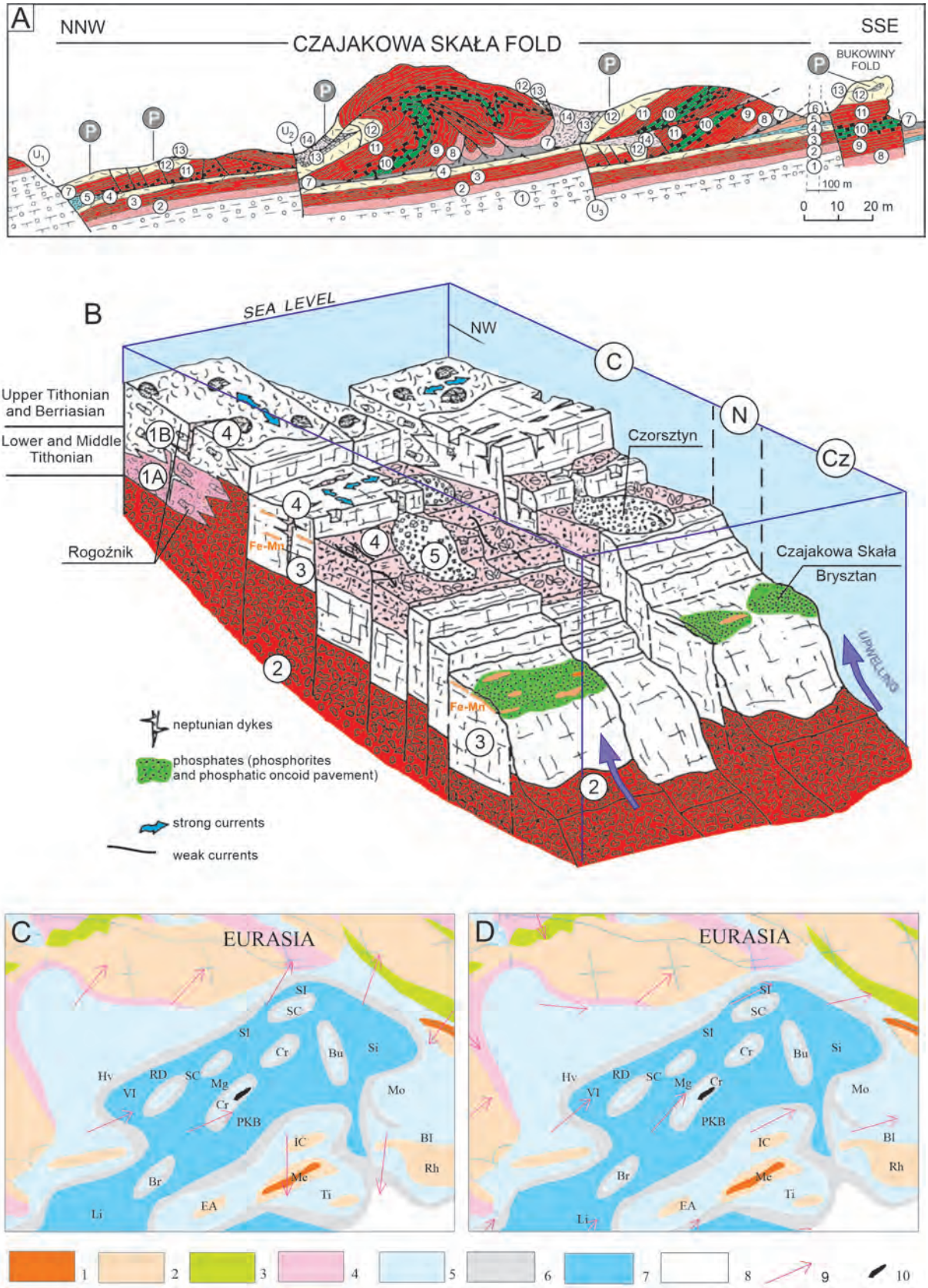
A
NNW
CZAJAKOWA SKAŁA FOLD
SSE
BUKOWINY FOLD
100 m
0 10 20 m
B
SEA LEVEL
NW
Upper Tithonian and Berriasian
Lower and Middle Tithonian
1B
1A
Rogoźnik
Fe-Mn
C
N
Cz
Czorsztyn
Czajakowa Skała
Brysztan
UPWELLING
neptunian dykes
phosphates (phosphorites and phosphatic oncoid pavement)
strong currents
weak currents
C
EURASIA
D
EURASIA
Hv
VI
RD
SC
Mg
Cr
PKB
Sl
Cr
Bu
Si
Mo
IC
Mc
Ti
Br
Li
EA
BI
Rh

inception of upwelling may be associated with the timing of tectonic reorganisation. Tectonic movements generated shallow platforms and islands along the NE-SW trending ridges between the main part of the Tethys and the Eurasian Platform. Palaeoclimate modelling (Golonka and Krobicki 2001) (Fig. 29) suggests that prevailing wind directions in the Jurassic–Cretaceous of the Circum-Carpathian Tethys area were north-northeast, parallel to the ridges. Upwelling may have been induced at the southeastern margin of the ridges. This style of oceanic circulation is often recorded in a specific depositional association. Given the extremely high biological productivity associated with upwelling, these generally include mainly biogenic rocks with high organic matter, silica, and phosphate (in various forms) contents, and deposits with elevated abundances of selected trace elements. The coincidence of these factors in a given palaeogeographical situation might help to reconstruct the palaeoceanographical conditions of a specific upwelling circulation style. Upwelling areas are marine regions in which masses of cold, nutrient-rich seawater is lifted from ocean depths towards more shallow zones, most often situated along continent margins. In turn, nutrient-rich water circulation facilitated zoo- and phytoplankton growth. At the lowest trophic level, organic productivity must have been very high, as benthic organisms flourished along the several hundred kilometres-long intraoceanic Czorsztyn pelagic swell. At the same time – that is, the Tithonian–Berriasian boundary interval – a microplankton (mainly calpionellid) explosion occured in the Western Carpathians sedimentary basins, triggered by palaeogeographic changes related to Neo-Cimmerian tectonics (Reháková and Michalík 1994). The presence of phosphate-rich deposits (phosphorites, microbial phosphate structures, macrooncoids) in the Berriasian deposits of the Niedzica Succession, which in a palinspastic reconstruction represents a shelf-edge/slope boundary, supports this idea (Fig. 29).

Stop 2: P5. Biała Woda valley (waterfall): Berriasian crinoidal limestones, synsedimentary breccias and Valanginian crinoidal limestones. (*Michał Krobicki and Andrzej Wierzbowski*)

In the formal lithostratigraphic subdivision of the PKB (Birkenmajer 1977), the uppermost Jurassic–lowermost Cretaceous of the Czorsztyn Succession is represented by the Dursztyn Limestone Formation, the Łysa Limestone Formation, and the Spisz Limestone Formation (Fig. 7). The age of the Spisz Limestone Formation, the youngest Neocomian unit of the Czorsztyn Succession in the Pieniny Klippen Belt, was previously poorly known. The formation was generally attributed to the Hauterivian; however, in places such as the Biała Woda Valley section, it was assumed to be older, as indicated by aptychi considered diagnostic for the Berriasian–Valanginian (cf. Birkenmajer 1977). Wierzbowski (1994), Krobicki (1996), and Krobicki and Wierzbowski (1996) proved that the lowermost Spisz Limestone Formation reveals signs of stratigraphic condensation, containing ammonites characteristic of the Early Valanginian and, locally, the early Late Valanginian.

The sections studied in the Biała Woda Valley are located in its western (left) bank, at the waterfall (see Figs 30, 31). The sequence of the deposits corresponds strictly to that exposed at the waterfall, in the eastern (right) bank of the valley. The oldest deposit in section A (Fig. 31) is a grey and grey-brown breccia consisting of angular limestone clasts several millimeters in diameter. The clasts are calcareous mudstones with abundant calpionellids, mostly *Calpionella alpina* Lorenz and *Globochaete*. This breccia bed (the "lower breccia bed" of Birkenmajer 1963) is exposed at the normal level of the stream. Its base is not exposed, but at a minimum its total thickness exceeds 0.4 m; according to Birkenmajer (1963), it is at least 1.6 m thick. The succeeding bed, about 1.0 m thick, is a crinoid-brachiopod limestone. Still younger is another breccia bed ("upper breccia bed"), 0.2 m thick, very similar in lithology to that at the base of the section. At the present time, the discussed part of the section is now referred to the Walentowa Breccia Member of the Łysa Limestone Formation (denoted as WBM in Fig. 31; comp. Birkenmajer 1977). The corresponding deposits of the Biała Woda waterfall section were attributed by Birkenmajer (1977, fig. 30A) to the Harbatowa Limestone Member ("lower breccia bed" and the crinoid-brachiopod limestone bed) and to the

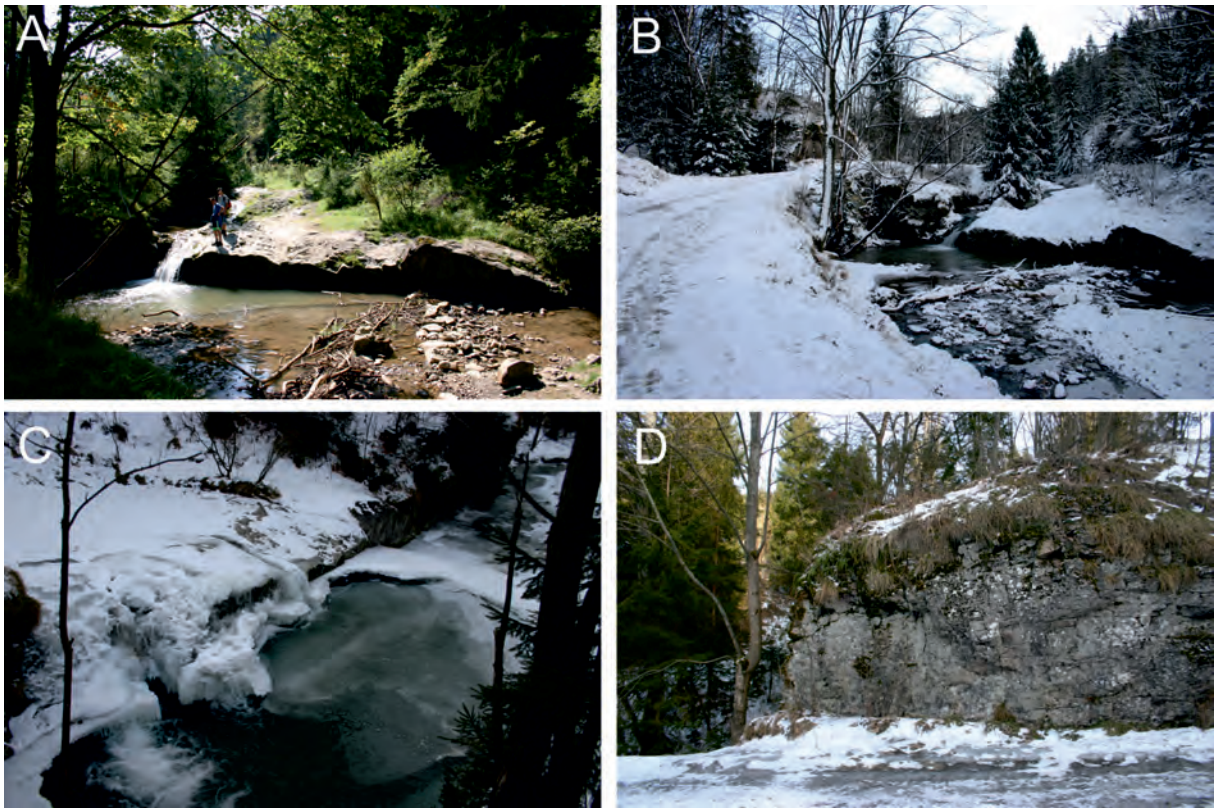

Fig. 30. Waterfall outcrop in Biała Woda valley (Berriasian–Valanginian limestones) during (**A**) summer and (**B**–**D**) winter.

Walentowa Breccia Bed ("upper breccia bed") of the Łysa Limestone Formation. The overlying beds, numbered 1–4 in section A and 3–4 in section B (Fig. 31), 3.65 m thick, consist of brown, red-brown, and red-violet-brown crinoid-brachiopod limestones. They are packstones and grainstones with abundant crinoid ossicles (up to 5 mm diameter), brachiopod shells and, less commonly, benthic foraminifera tests. Poorly preserved ammonites (Phylloceratacеae and Berriasellinae) and aptychi are also found. The ammonites, brachiopods, and calpionellids, including *Calpionellopsis* sp., *Tintinnopsella carpathica* (Murgeanu and Filipescu), and *Remaniella* sp., are indicative of the Late Berriasian. These deposits were originally attributed to the lower Spisz Limestone Formation by Birkenmajer (1963, 1977). In fact, they are almost identical in their lithological development and stratigraphic position to the Kosarzyska Limestone Member of the Łysa Limestone Formation and should be correlated with that unit (Krobicki and Wierzbowski 1996; comp. Wierzbowski and Remane 1992; Wierzbowski 1994). These sections in the Biała Woda Valley yielded lowermost Cretaceous brachiopods. These brachiopods were collected bed by bed, starting from the crinoid-brachiopod limestones of the Walentowa Breccia Member of the Łysa Limestone Formation and proceeding to the middle of the Spisz Limestone Formation (bed 5). The brachiopod shells are variously preserved; they are almost always disarticulated and strongly fragmented, often forming brachiopod shell pavements (particularly within bed 3a). Only about 20% of the specimens are completely preserved; the remaining ones occur as single valves, generally still suitable for specific identification. The degree of disarticulation depends on the size of individuals, with big irregular pygopids (genus *Pygope*) typically found as single valves. Isometric brachiopods [e.g., *Zittelina wahlenbergi* (Zejszner) and *Lacunosella hoheneggeri* (Suess)] often occur as complete shells. Within the Walentowa Breccia Member, pygopids dominate [*Pygope janitor* (Pictet); *Nucleata nucleata*

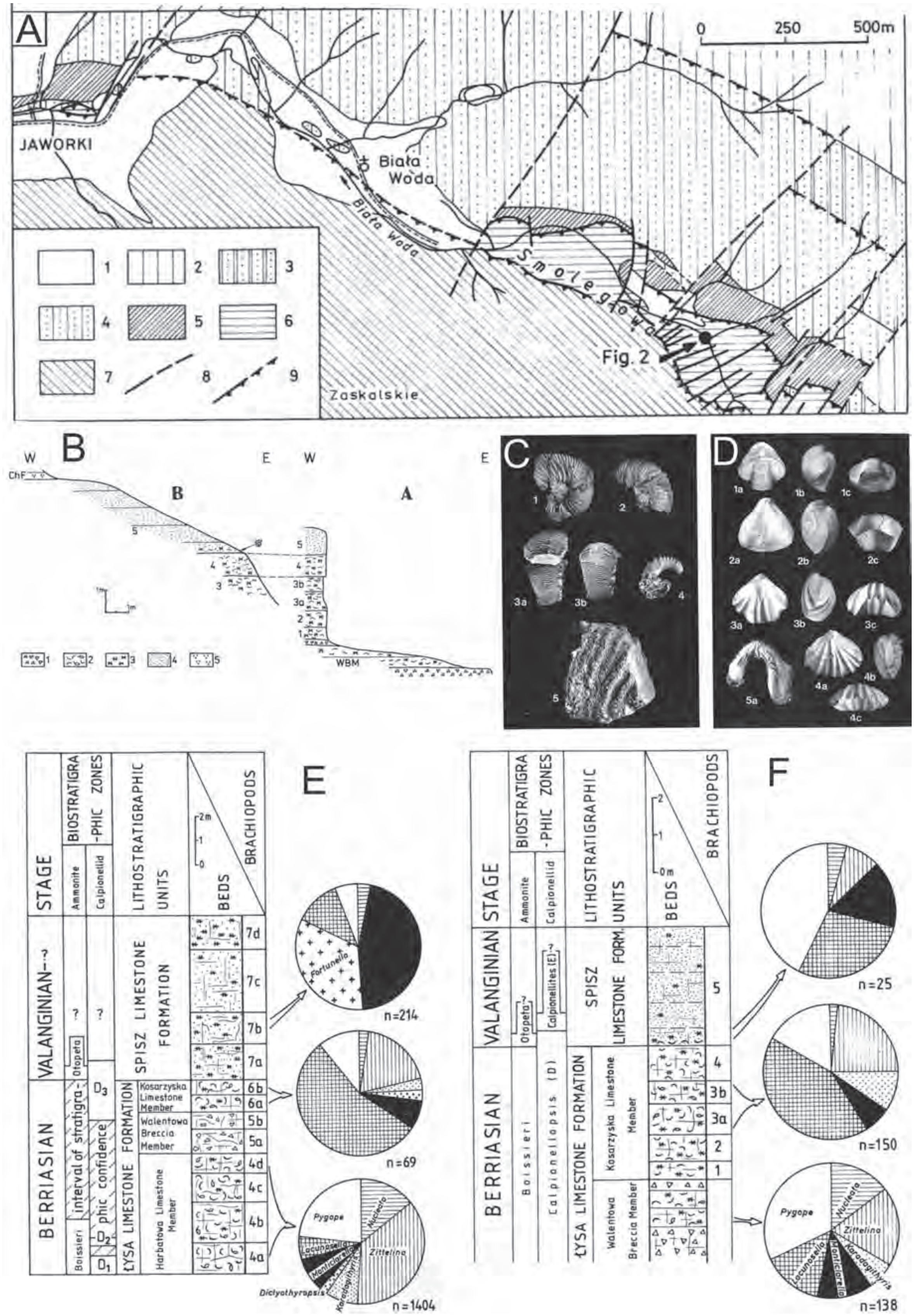
A
0
250
500m
JAWORKI
Biała Woda
Biała Woda
Smolegowa
Fig. 2
Zaskalskie
1
2
3
4
5
6
7
8
9
B
W
E
W
E
ChF
B
A
WBM
C
D
E
STAGE
BIOSTRATIGRAPHIC ZONES
Ammonite
Calpionellid
LITHOSTRATIGRAPHIC UNITS
BEDS
BRACHIOPODS
VALANGINIAN--?
BERRIASIAN
Boissieri
Otopeta
interval of stratigraphic confidence
D3
D2
D1
SPISZ LIMESTONE FORMATION
ŁYSA LIMESTONE FORMATION
Kosarzyska Limestone Member
Walentowa Breccia Member
Harbatowa Limestone Member
7d
7c
7b
7a
6b
6a
5b
5a
4d
4c
4b
4a
Fortunella
n=214
n=69
Pygope
Nucleata
Zittelina
Lacunosella
Monticlarella
Karadagithyris
Dictyothyropsis
n=1404
F
STAGE
BIOSTRATIGRAPHIC ZONES
Ammonite
Calpionellid
LITHOSTRATIGRAPHIC UNITS
BEDS
BRACHIOPODS
VALANGINIAN
BERRIASIAN
Otopeta
Calpionellites (E)
Boissieri
Calpionellopsis (D)
SPISZ LIMESTONE FORM.
ŁYSA LIMESTONE FORMATION
Kosarzyska Limestone Member
Walentowa Breccia Member
5
4
3b
3a
2
1
n=25
n=150
Pygope
Nucleata
Zittelina
Lacunosella
Monticlarella
Karadagithyris
n=138

(Schlotheim)], followed in abundance by rhynchonellids [*Lacunosella hoheneggeri* (Suess); *Monticlarella capillata* (Zittel)] and dallinids [*Zittelina wahlenbergi* (Zejszner); *Z. pinguicula* (Zittel)], and *Karadagithyris bilimeki* (Suess)]. This brachiopod assemblage occurs in the crinoid-brachiopod bed immediately above the "lower breccia bed" (Krobicki and Wierzbowski 1996). In younger beds, represented by the Kosarzyska Limestone Member, numerous brachiopods occur mainly within bed 3, where rhynchonellids dominate [*Lacunosella hoheneggeri* (Suess); *L. zeuschneri* (Zittel), *Monticlarella agassizi* (Zejszner)], accompanied by *Zittelina wahienbergi* (Zejszner) or pygopids [*Pygope janitor* (Pictet) and *P. diphya* (Colonna), *Nucleata nucleata* (Schlotheim)] and *Karadagithyris bilimeki* (Suess) (Krobicki and Wierzbowski 1996).

In contrast, brachiopods are infrequent in the Spisz Limestone Formation (Krobicki 1994, 1995). They were collected from four sections: Korowa Skała Klippe, Falsztyn-Pomiedznik, Czorsztyn-Sobótka Klippe (Fig. 32), and the Biała Woda waterfall (Krobicki 1996). The dominant brachiopod species in the Spisz Limestone Formation assemblages are the same as those in Tithonian and Berriasian strata (Barczyk 1971, 1972a, b, 1979a, b; Krobicki 1994). A very sparse brachiopod fauna (25 specimens) was found in the lowermost part of bed 5: *Monticlarella agassizi* (Zejszner), *Lacunosella hoheneggeri* (Suess), *L. zeuschneri* (Zittel), *Pygope* cf. *janitor* (Pictet), *Nucleata* ex gr. *nucleata* (Schiotheim), and *Zittelina wahlenbergi* (Zejszner). The stratigraphic usage of single brachiopod species is limited, except for those of the genus *Fortunella* (Czorszty-Sobótka outcrop). However, the Valanginian brachiopod assemblages are useful for ecostratigraphy, and comparisons of the Late Berriasian and Valanginian assemblages from the Pieniny Klippen Belt show they are also useful for palaeoenvironmental reconstructions.

Stop 2: P6. Biała Woda valley: mid-Cretaceous basaltic olistolith. (*Nestor Oszczypko, Michał Krobicki and Dorota Salata*)

A block of basalt a few meters in diameter has long been known from Biała Woda valley (Figs 8, 33) (Horwitz and Rabowski 1929; Birkenmajer 1979). This olistolith occurs within conglomerates of the Jarmuta Formation (Maastrichtian–Paleocene) belonging to the Grajcarek Succession (Birkenmajer and Wieser 1990 and references therein). The radiometric age (K-Ar) of this basalt was determined as 140±8 Ma, which roughly corresponds to the Jurassic–Cretaceous boundary (Birkenmajer and Wieser 1990). More recent radiometric dating by Birkenmajer and Pécskay (2000b) for both columnar and platy-jointed varieties of the basalt gave ages of 110±4.2 Ma and 120±4.5 Ma, respectively, equivalent to the Barremian–Albian interval. The basalt has geochemical features of intraplate alkali basalts (Oszczypko et al. 2012). and geochemically resembles two olistoliths in the Proč Formation in eastern Slovakia (Spišiak and Sýkora 2009). The Early Cretaceous volcanism at the northern edge of the Pieniny Klippen Belt was probably related to the opening of the Magura Basin, although this theory is still under discussion (Oszczypko and Oszczypko-

← Fig. 31. Position of the investigated outcrops and geological sketch-map of the Pieniny Klippen Belt in the vicinity of Jaworki and Biała Woda Valley (**A**) (after Birkenmajer, 1979, simplified): 1 – Quaternary deposits; 2, 3 – Magura Nappe (Paleogene: 2 – Magura Formation; 3 – Szczawnica Formation); 4, 5 – Grajcarek Unit (4 – Upper Cretaceous; 5 – Lower Cretaceous–Jurassic); 6 – Czorsztyn Succession (Jurassic–Cretaceous) 7 – Niedzica Succession (Jurassic–Cretaceous); 8 – more important dislocations. 9 – northern and southern tectonic boundaries of the Pieniny Klippen Belt; **B** – Geological sections in the Biała Woda Valley at waterfall (the distance between sections A and B is about 25 m) (after Krobicki and Wierzbowski, 1996). Lithostratigraphy: Łysa Limestone Formation (WBM – Walentowa Breccia Member, beds 1–4 Kosarzyska Limestone Member); Spisz Limestone Formation (bed 5); Chmielowa Formation (ChF). Lithology: 1 – breccias; 2 – brachiopod limestones; 3 – crinoid calcarenites; 4 – fine-grained limestones consisting mostly of crinoid and shell debris; 5 – micritic limestones, *Hedbergella* microfacies; ammonite finds indicated; **C**, **D** – ammonites (C) and brachiopods (D) of the Berriasian and Valanginian age (**C**: 1, 2 – *Jeanihieuloyiles* sp., Upper Valanginian; 3 – *Olcostephanus* sp., Lower Valanginian; 4 – *Rodighieroites* sp., Upper Valanginian; 5 — ?*Dicostella* sp., Upper Valanginian; **D**: 1 – *Zittelina pinguicula* (Zittel); Upper Berriasian; 2 – *Zittelina wahlenbergi* (Zejszner); Upper Berriasian; 3 – *Lacunosella hoheneggeri* (Suess); Upper Berriasian; 4 – *L. zeuschneri* (Zittel); Lower Valanginian; 5 – *Pygope janitor* (Pictet); Upper Berriasian; **E, F** – comparison between brachiopod assemblages in Berriasian–Valanginian strata (E – Czorsztyn-Sobótka Klippe and F – Biała Woda Valley). Lithostratigraphic units after Birkenmajer (1977); stratigraphy and numbering of beds in Czorsztyn-Sobótka after Wierzbowski and Remane (1992); brachiopod pie charts after Krobicki (1994, 1996) and Krobicki and Wierzbowski (1996).

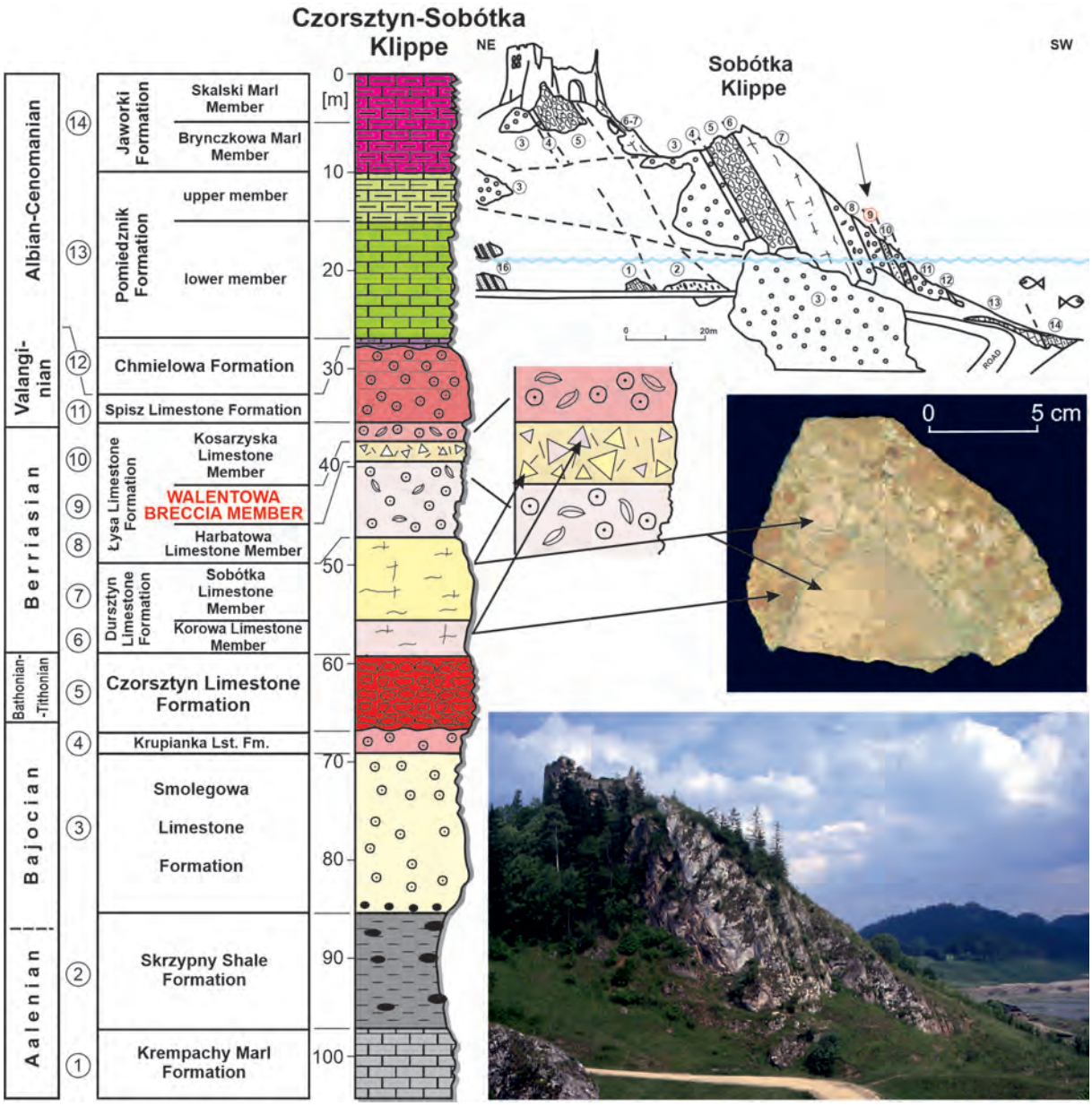

Fig. 32. The Czorsztyn Succession of the Czorsztyn-Sobótka section (after Birkenmajer 1977), with the position of the Walentowa Breccia Member of the Łysa Limestone Formation, and a panoramic, illustrative cross-section of Czorsztyn Castle over artificial Czorsztyn Lake (right-upper). Lower-right photograph shows a view of Sobótka Klippe in 1992 (modified after Birkenmajer 1963, 1979).

Clowes 2009). Traditionally an Early/Middle Jurassic age, coeval with the opening of the Ligurian–Penninic Ocean, has been accepted (see Birkenmajer 1986; Oszczypko 1992,; Golonka et al. 2003; Oszczypko et al. 2012).

Stop 2: P7. Czarna Woda valley: exotic-bearing debris flow with *Urgonian*-type clasts (Fig. 34). (*Michał Krobicki and Barbara Olszewska*)

The presented outcrop occurs in Czarna Woda stream north of Jaworki village. There, a Middle Paleocene (lower NP 5 zone – Birkenmajer and Dudziak 1991) pebbly mudstone belonging to the uppermost Jarmuta Formation of the Grajcarek Unit crops out. It represents a pebble-bearing submarine slump. Exotic pebbles are very well rounded, consisting of both magmatic/metamorphic (e.g.,

Fig. 33. Basaltic olistolith in Biała Woda Valley.

granitoids, gneisses, quartzites) and sedimentary rocks (multicoloured sandstones, oolitic limestones, dark bivalve coquinas, dolostones, etc.) (see also Birkenmajer et al. 1987). *Urgonian* limestone pebbles are a significant component of exotic assemblages and represent different kinds of carbonate platform environments (cf. Mišík 1990). They contain microfossils comparable with the *Urgonian*-type facies known from the peri-Mediterranean Tethys. A rich assemblage of characteristic microfossils – *Archalveolina reicheli* (de Castro), *Palorbitolina lenticularis* (Blumenbach), *Mesorbitolina subconcava* (Leymerie), *Praeorbitolina cormyi* Schroeder, *Pseudonummuloculina aurigerica* Calvez, and *Simpliorbitolina manasi* Ciry and Rat – confirm the stratigraphical and palaeoenvironmental connection of the microfossil assemblages with classical *Urgonian*-type, shallow-water carbonate sedimentation (Krobicki and Olszewska 2005) (for additional description, see Stop 2/3). Additionally, magmatic/sub-volcanic exotic pebbles occur here and are represented by granitic and andesitic-type rocks (mainly andesite, basaltic andesite, basaltic trachyandesite, trachyandesite and rhyolitic pebbles). The radiometric dates of these exotics, by the U-Pb SHRIMP $^{206}Pb/^{238}U$ method, are Guadalupian (Poprawa et al. 2013; Krobicki et al. 2018). The source area of these exotics is most probably the Inner Carpathians, and they have been connected with Middle Permian oceanic crust subduction and magmatic arc origin as mentioned above.

Stop 2: P8. Rogoźnik: Tithonian/Berriasian ammonite-brachiopod coquina. (*Michał Krobicki, Jan Golonka and Andrzej Wierzbowski*)

The Czorsztyn Succession of the PKB is best exposed at Rogoźnik Klippe, Homole Gorge, and Czorsztyn Castle. The Rogoźnik (or Rogoża) klippen lies within the nature reserve located south of the village of Rogoźnik and Wielki Rogoźnik stream (**this is a protected area – please do not hammer the rocks**). The locality comprises a small klippe and a neighboring abandoned quarry (Figs 23, 35–37). The former is the type locality of the

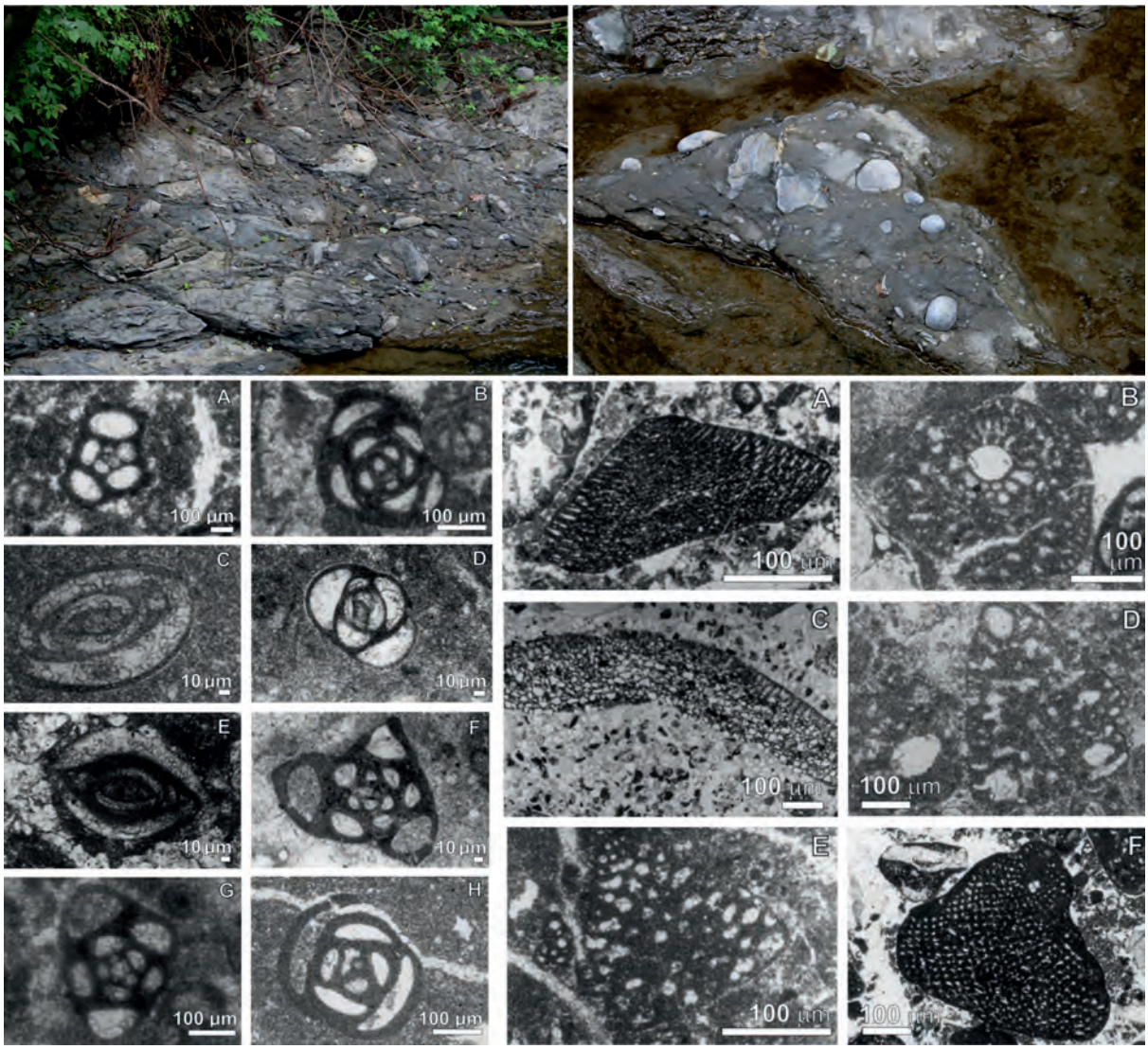

Fig. 34. Gravelstones with *Urgonian* exotics (Czarna Woda Valley; Paleocene of the Jarmuta Formation after Birkenmajer and Jednorowska 1987; Birkenmajer et al. 1987, in contrast to Oszczypko et al. 2020, who interpreted them as Miocene of the Kremna Formation) and their foraminifers (after Krobicki and Olszewska 2005); **left two columns**: A – *Moesiloculina histri* (Neagu) (transverse section); B – *Scythiloculina bancilai* Neagu (transverse section); C – *Istriloculina elliptica* (Iovcheva) (vertical section); D – *Istriloculina elliptica* (Iovcheva) (transverse section); E – *Rumanoloculina pseudominima* (Bartenstein and Kovatcheva) (veritcal section); F – *Rumanoloculina pseudominima* (Bartenstein and Kovatcheva) (transverse section); G – *Rumanoloculina ponticuli* Neagu (transverse section); H – *Istriloculina alimanensis* Neagu (transverse section); **right two columns**: A – *Palorbitolina lenticularis* (Blumenbach) (axial section); B – *Palorbitolina lenticularis* (Blumenbach) (oblique section cutting the embryonic apparatus); C – *Mesorbitolina subconcava* (Leymerie) (axial section); D – *Neorbitolinopsis conulus* (Douville) (axial section); E – *Simpliorbitolina manasi* Ciry et Rat (axial section); F – *Praeorbitolina cormyi* Schroeder (axial section)

Rogoźnik Coquina Member; the latter of the Rogoża Coquina Member (Birkenmajer 1977). Both lithostratigraphic units constitute a special Upper Jurassic ammonite coquina-type development markedly different from coeval nodular limestones, which are especially well represented in the Czorsztyn Succession of the PKB (cf. Kutek and Wierzbowski 1986). The klippen at Rogoźnik village is well known as the richest Upper Jurassic ammonite locality in the PKB, with very detailed biostratigraphic documentation (Kutek and Wierzbowski 1986; Wierzbowski et al. 2006), and with a rich brachiopod fauna as well (Krobicki 1994; Wierzbowski et al. 2006). The ammonite succession (Fig. 37) extends from the Lower

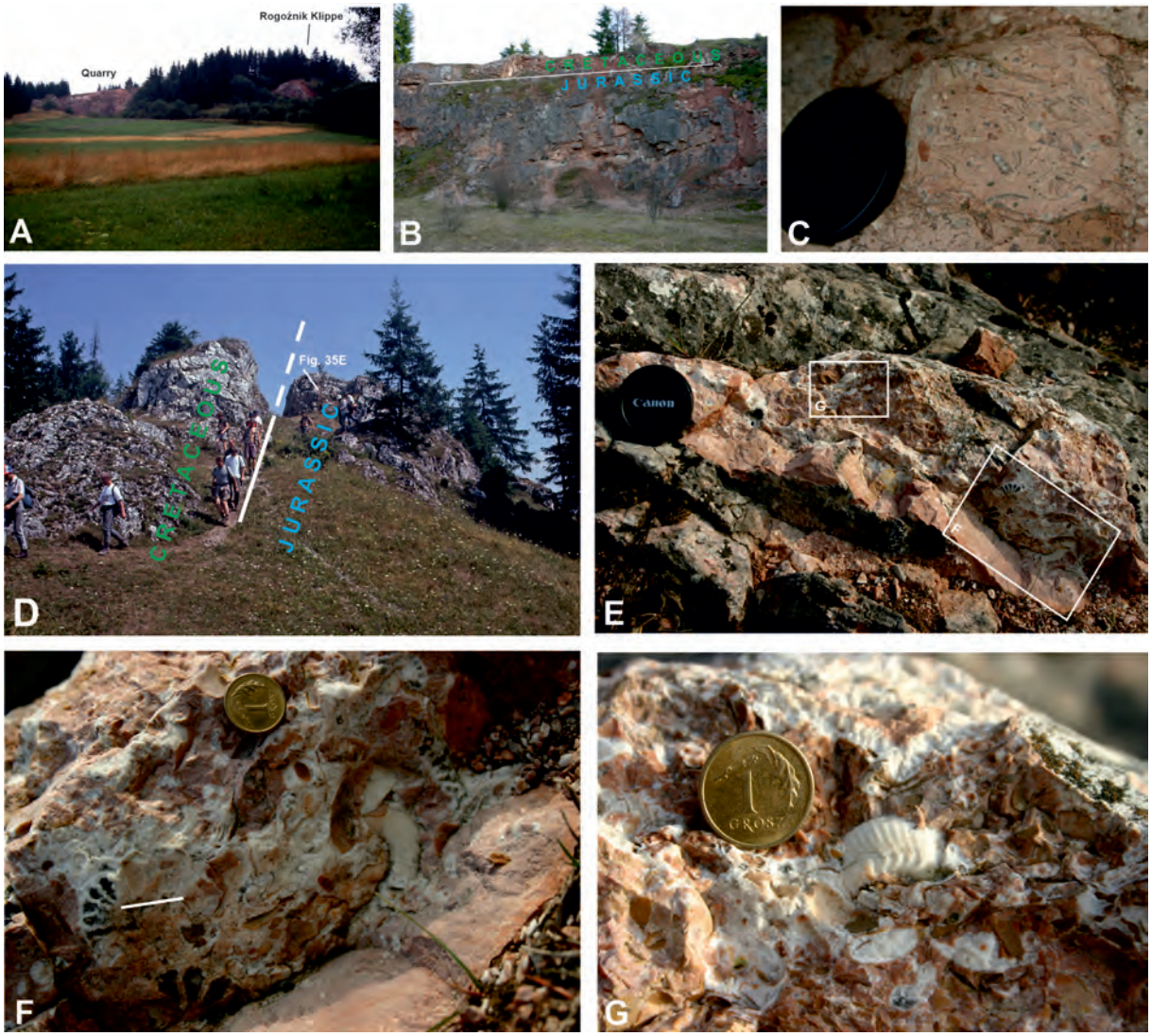

Fig. 35. **A**, **B** – Abandoned quarry in Rogoźnik. **C** – Micritic ammonite coquina (Rogoźnik Coquina Member of the Czorsztyn Limestone Formation). **D** – Rogoźnik Klippen above this quarry, with the Jurassic–Cretaceous boundary marked. **E**–**G** – Ammonite sparry coquina, full of ammonites usually filled by sparry calcite, of the Rogoża Coquina Member of the Czorsztyn Limestone Formation, with (**G**) typical ornamentation of uppermost Jurassic *Simocosmoceras* (after Krobicki and Golonka 2008).

Tithonian up to the lowermost Berriasian. The Rogoźnik Coquina Member consist of pink to reddish coquinas with voids filled with white sparry calcite and numerous fossils: mostly ammonites and their debris, aptychi, brachiopods, and crinoid fragments, and less commonly gastropods, echinoids, bivalves, solitary corals, sponges, and fish teeth.

In the studied section of the Rogoźnik Coquina Member, the Lower–Middle Tithonian brachiopod fauna distinctly differs from the Upper Tithonian–Berriasian one (Fig. 38) (Krobicki 1994). The comparatively high percentage of both rhynchonellids (*Lacunosella*) and the dallinid *Dictyothyropsis* in the Upper Tithonian–Berriasian brachiopod assemblages suggests that these strata apparently record a shallower depositional environment compared to the Lower–Middle Tithonian part of the section.

The differences between the Lower–Middle Tithonian and Upper Tithonian–Berriasian brachiopod assemblages in this section clearly reflect changing palaeoenvironmental conditions. One of the most consequential brachiopod faunal turnovers is the replacement of a

dominantly pygopid s.l. assemblage (*Pygope* and *Nucleata*, Lower–Middle Tithonian) by a "shallow-water" assemblage with important contributions from rhynchonellids (*Lacunosella*) and the dallinid *Dictyothyropsis* (Upper Tithonian–Berriasian) (Fig. 38). Changes in brachiopod fauna assemblages may be employed to determine palaeoecological conditions based on an analysis of given taxa in successive lithofacies, which in turn may be dependent on the palaeogeographic position of specific facies in the palinspastic reconstruction of the Pieniny Klippen Belt. In this sense, the main diagnostic features are the presence of rhynchonellids (genus *Lacunosella*), the dallinid *Dictyothyropsis tatrica*, and a qualitative trend in the occurrence of pygopids s.l. (*Pygope* and *Nucleata*). Rhynchonellids *(Lacunosella hoheneggeri* and *L. zeuschneri*) commonly occur in shallow-water, reef-like Tithonian–Lower Valanginian sediments (the *Štramberk* limestones) of the Outer Carpathian basins (Nekvasilová 1977). *Lacunosella hoheneggeri* was regarded by Ager (1965) as typical of sublittoral zones. A few *Dictyothyropsis tatrica* specimens also have equivalents in the *Štramberk* limestones (Barczyk 1979, 1991). Pygopids s.s. have been usually interpreted as deep-water organisms (Ager 1976). Dieni and Middlemiss (1981) described an abundant collection of these brachiopods from the Venetian Alps, from pelagic limestones of the *Maiolica* facies that are the facial equivalent of the cherty limestones of the Branisko and Pieniny successions (Pieniny Limestone Formation). Recently, it was sug-

Fig. 36. Southeastern wall of Rogoźnik quarry with sample location and biostratigraphical interpretation (after Reháková and Wierzbowski 2005).

Fig. 37. A – The Rogoźnik Klippen. B – Cross section of the Rogoźnik Klippen. C – Ammonite ranges and biostratigraphy of the Rogoźnik succession (after Kutek and Wierzbowski 1986; modified). →

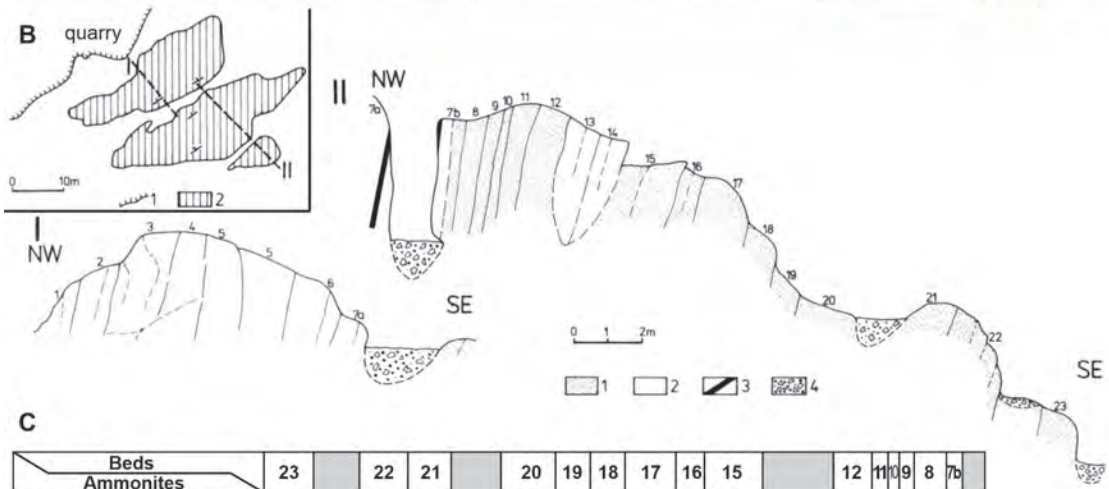

C

Beds / Ammonites	23		22	21		20	19	18	17	16	15		12	11	10	9	8	7b
Hybonoticeras mundulum (Opp.)																		
Schaireiria neoburgensis (Opp.)																		
Aspidoceras cf. zeuschneri Zit.																		
Aspidoceras cf rogoznicense (Zeusch.)																		
Aspidoceras spp																		
Sutneria asema (Opp.)																		
Simocosmoceras simum (Opp.)																		
Simocosmoceras cf. adversum (Opp.)																		
Simocosmoceras cattuloi (Zit)																		
Richterella spp																		
Parapallasioceras ex gr. contiguus (Cat.)																		
Simoceras (Simoceras) spp																		
Haploceras staszyci (Zeusch.)-elimatum(Opp.)																		
Haploceras cf. verruciferum (Men.)																		
Haploceras tomephorum Zit.																		
Haploceras carachtheis (Zeusch.)																		
Glochiceras lithographicum (Opp.)																		
Pseudolissoceras spp																		
Semiformiceras semiforme (Opp.)																		
Semiformiceras fallauxi (Opp.)																		
Semiformiceras birkenmajeri K & W																		
Semiformiceras spp																		
Taramelliceras cf. waageni (Zit.)																		
Streblites folgariacus (Opp.)																		
Cyertosiceras collegialis (Opp.)																		
Protancyloceras guembeli (Opp.)																		
Protancyloceras passendorferi sp.n.																		
Protancyloceras gracile (Opp.)																		
Ammonites Zones	hybonotum					darwini	darwini and/or semiforme			semiforme				fallauxi				

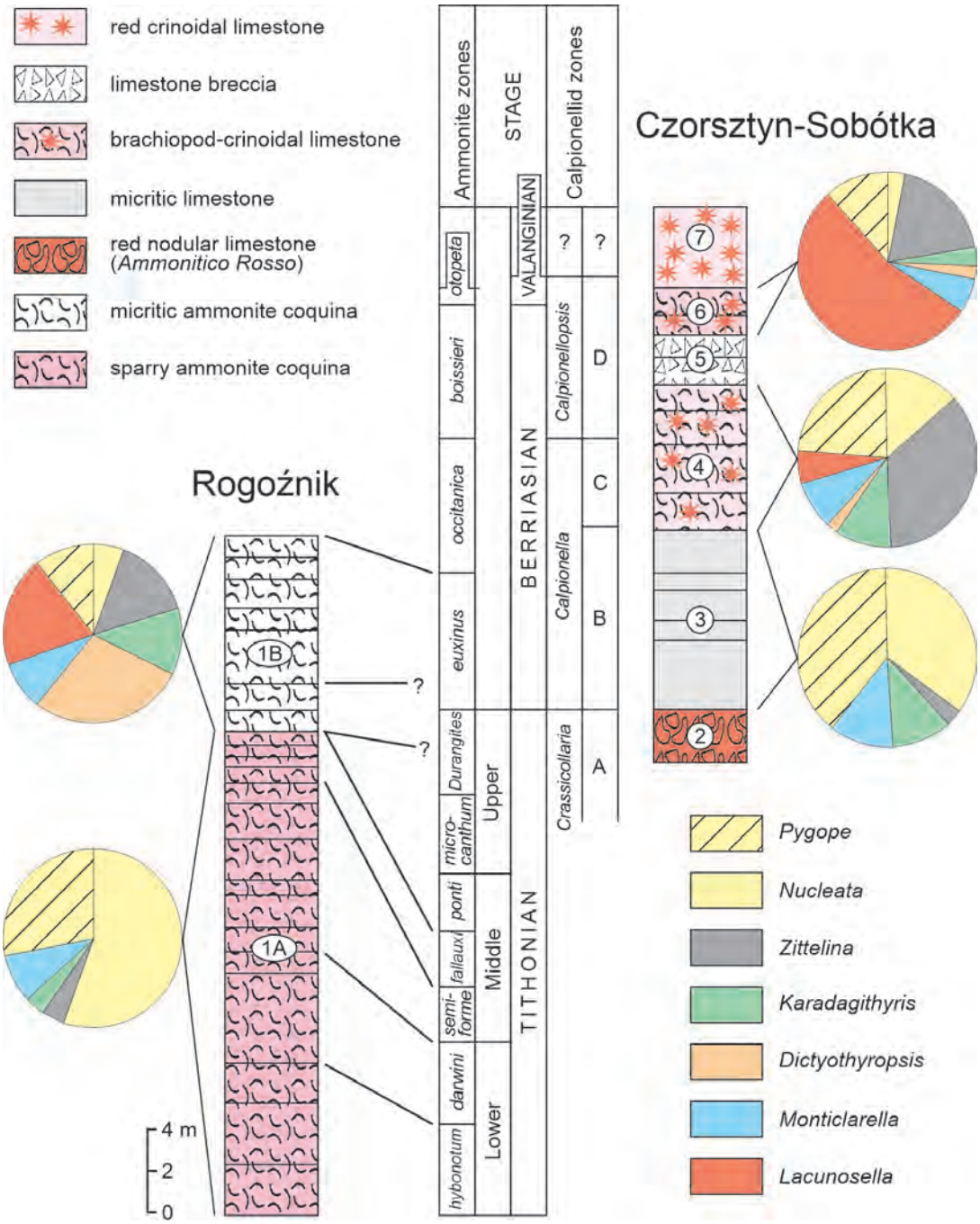

Fig. 38. Correlation of the Tithonian–Berriasian of the Rogoźnik Klippen and Czorsztyn-Sobótka section with brachiopod assemblage pie charts (modified after Krobicki 1996; stratigraphy after Kutek and Wierzbowski 1986 and Wierzbowski and Remane 1992; lithostratigraphy after Birkenmajer 1977): 1 – Rogoźnik Coquina Member (Czorsztyn Limestone Formation) (A – red sparitic coquina, B – white micritic coquina); 2 – Czorsztyn Limestone Formation; 3 – Sobótka Limestone Member (Dursztyn Limestone Formation) (white *Calpionella* limestone); 4–6 – Łysa Limestone Formation (4 – Harbatowa Limestone Member, 5 – Walentowa Breccia Member, 6 – Kosarzyska Limestone Member); 7 – Spisz Limestone Formation.

gested that pygopids s.s. could also occupy shallow waters atop seamounts (?Czorsztyn pelagic swell) (Ager 1993).

In the Czorsztyn Succession, abundant *Lacunosella* suggests a generally shallower depositional environment relative to those

strata in which rhynchonellids are rare or absent. Alternative, an increasing percentage of pygopids s.l. in the assemblage suggests deeper environments. Usually, if *Lacunosella* representatives constitute about 25% of the assemblage, both *Pygope* and *Nucleata* are subordinate and *vice versa*.

Stop 2: P9. Sromowce: Upper Cretaceous *Scaglia Rossa* with clastics. (*Michał Krobicki and Jan Golonka*)

Strongly folded Jurassic–Cretaceous strata are visible along the road from Sromowce Wyżne to Sromowce Niżne on the southern slope of Mount Macelowa, close to the Dunajec River, where the Pieniny Succession is overturned. The oldest Oxfordian radiolarites occupy the topmost part of Mount Macelowa (on its northern slope), gray cherty limestones of the *Maiolica* facies (Pieniny Limestone Formation) occupy the transitional position, and in the topographically lowest position Late Cretaceous *Globotruncana*-bearing marls of the *Scaglia Rossa*-type are present (Birkenmajer 1977; Bąk 1998, 2000). Previously, this unit was named the Jaworki Marl Formation (Birkenmajer 1977), but after the discovery of several siliciclastic intercalations (flysch-flyschoid/turbidite wedges) within it (e.g., Snežnica Siltstone Member, Gróbka Member, Osice Siltstone Member; see Birkenmajer and Jednorowska 1987) (Fig. 7), Birkenmajer (1987) revised the formal lithostratigraphy, renaming it the Jaworki Formation. Fig. 7 depicts Birkenmajer and Jednorowska's (1987) ideas about the Cretaceous lithostratigraphy of the Pieniny Mountains. It is certainly controversial; note that the Gróbka Member was assigned to two different formations and the position of the Trawne Member is quite speculative (Golonka and Sikora 1981). Pelagic red marls and marly limestones with grayish intercalations of calcareous sandstones and siltstones of a distal turbiditic origin predominate in this outcrop (Figs 39, 40). This is the youngest part of the multicolored (green-variegated-red) globotruncanid marls of the Macelowa Marl Member of the Jaworki Formation, with good Upper Cretaceous foraminiferal biozonation (*Dicarinella concavata–D. asymmetrica* zones, Upper Coniacian–Santonian) (Bąk 1998, 2000). These deposits originated during the final evolutionary episode of the Pieniny Basin, when the overall unification of sedimentary facies occurred. The *Scaglia Rossa*-type facies (= *Couches Rouge* = *Capas Rojas*) represented by the Jaworki Formation – which were widespread in the Late Cretaceous Tethyan Ocean – indicates open connections throughout the Northern Tethys.

Stop 2: P10. Haligovce and Lipnik: Paleocene reefs after the K/Pg mass extinction (Fig. 41). (*Michał Krobicki*)

Within the Paleogene flysch near the villages of Haligovce and Lipnik, there are large blocks of Paleocene olistolithic limestones, the oldest deposits of the Pieniny Paleogene (Scheibner 1968; Potfaj 2002; Krobicki et al. 2004; Buček and Köhler 2017). Palaeontological and microfacies analyses revealed the presence of numerous corals, red algae, and foraminifera, and to a lesser extent bryozoans, serpulids, fragments of bivalves, brachiopods, echinoderms, and sponges, and sporadically sponge spicules. Analysis of coral colonies revealed nine colonial scleractinian species (*Asirocoenia*, ?*Acropora*, *Goniopora*, *Actinacis*, *Rhizangia*, *Orbignygyra*, *Favites*, *Oculina*, and ?*Rabdophylliopsis*) (Krobicki et al. 2004), but no solitary corals. The corals are often coated with red algae, most commonly Corallinaecae but also Peyssonneliaceae (*Polystrata alba*). The foraminifers are represented by large encrusting agglutinating (e.g., *Haddonia* sp.) and calcareous forms. Other characteristic foraminifera include: *Marssonella lodoensis* Israelsky, *Anomalina* cf. *rubiginosa* (Cushman), *Cibicides* cf. *succedens* (Brotzen), and *Pararotalia* sp. The described corals most closely resemble the Paleocene coral assemblages from the Danian–Thanetian of Slovenia (Turnśek and Drobne 1998) and Italy (Vecsei and Moussavian 1997), exhibiting recovery of reef ecosystems after the K/Pg crisis. However, the Paleogene algal limestones in the Polish Carpathians are not indicative of a reef environment. According to the Paleocene palaeogeographic evolution of this area, the PKB closed due to the collision of the Central Carpathians terranes with the Czorsztyn Ridge (Birkenmajer 1986, 1988). The Adria, Eastern Alps, and Inner Carpathians terranes continued their movement northward. The Paleocene subsidence of the Magura Basin


POLAND
SLOVAKIA
Szczawnica
Sokolica
Trzy Korony
Sobczański Gorge
Mnichy
Facimiech
Kąty
Macelowa Góra
Dunajec
Sromowce Średnie
Sromowce Niżne
Červený Kláštor
Haligovce
A
B
C
D
E
Trzy Korony
Trzy Korony
Sokolica
0
20 cm

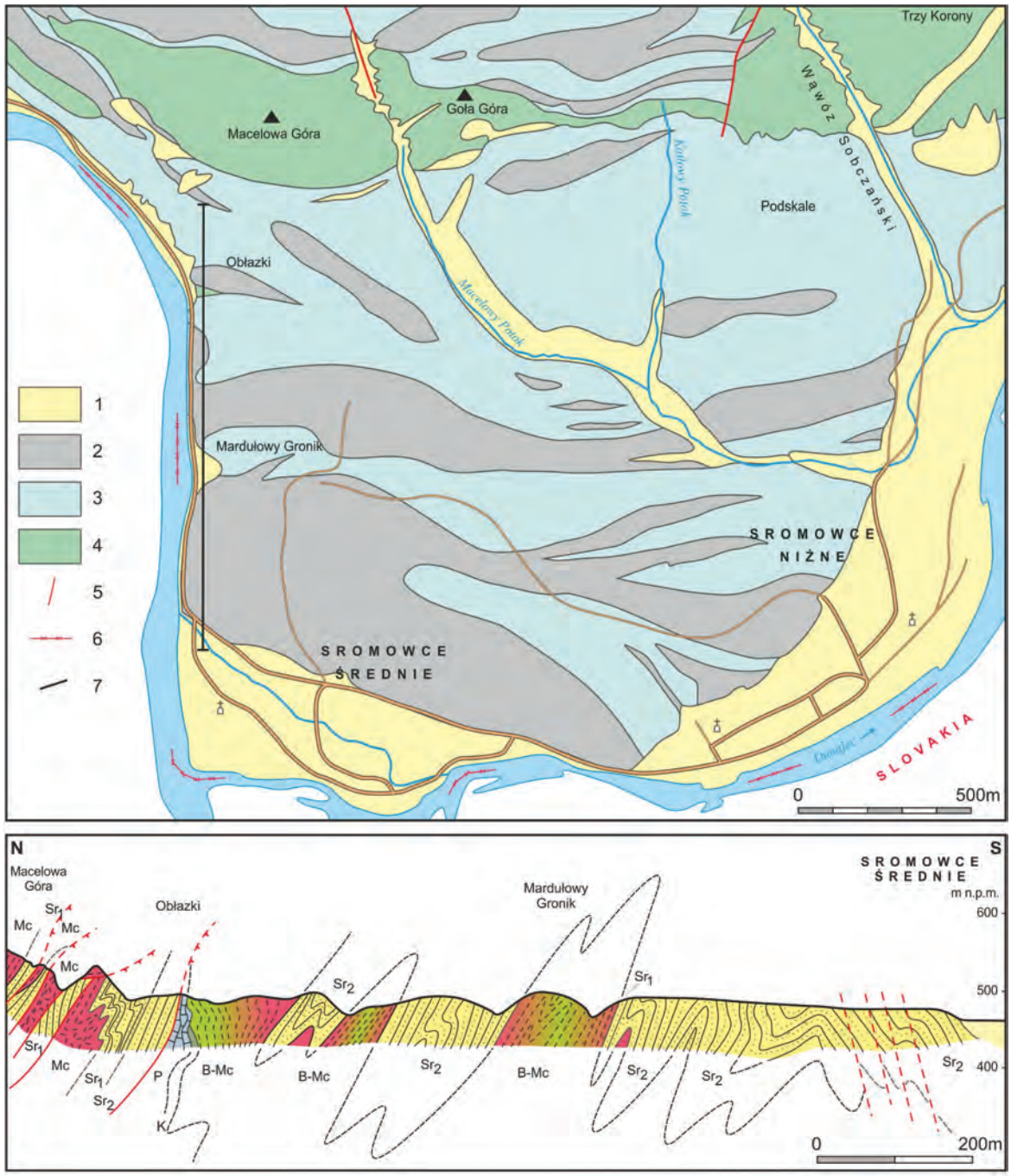

Fig. 40. Geological map of the vicinity of Sromowce (simplified after Horwitz 1963; Birkenmajer and Jednorowska 1984) and geological cross-section: 1 – Quaternary; 2 – Sromowce Formation; 3 – Jaworki Formation, partly Kapuśnica Formation; 4 – Pieniny Limestone Formation, partly also Czajakowa Radiolarite Formation; 5 – faults; 6 – national border; 7 – geological cross-section (below); P – Pieniny Limestone Formation (grey cherty limestones); K – Kapuśnica Formation (green spotty marls); B-Mc – Jaworki Formation (Brynczkowa, Skalski and Macelowa Marl members – green, variegated, and red marls respectively); Sr – Sromowce Formation (Sr1 – Osice Siltstone Member; Sr2 – flysch) (after Golonka et al. 2018)

← Fig. 39. Aerial view of the central Pieniny Mountains and Dunajec River Gorge with photograph locations: **A** – Upper Cretaceous red marls of the *Scaglia Rossa*-type facies of the Macelowa Marl Member of the Jaworki Formation (Macelowa Mountain); **B** – close to the beginning of rafting in Sromowce-Kąty harbor in the Pieniny Mountains, boat full of tourists; **C** – Trzy Korony Mountains, built of (**D**) *Maiolica*-type well-bedded cherty limestones of the Pieniny Limestone Formation, usually strongly tectonically folded; **E** – Sokolica Mountain over the Dunajec River Gorge (after Krobicki and Golonka 2008)

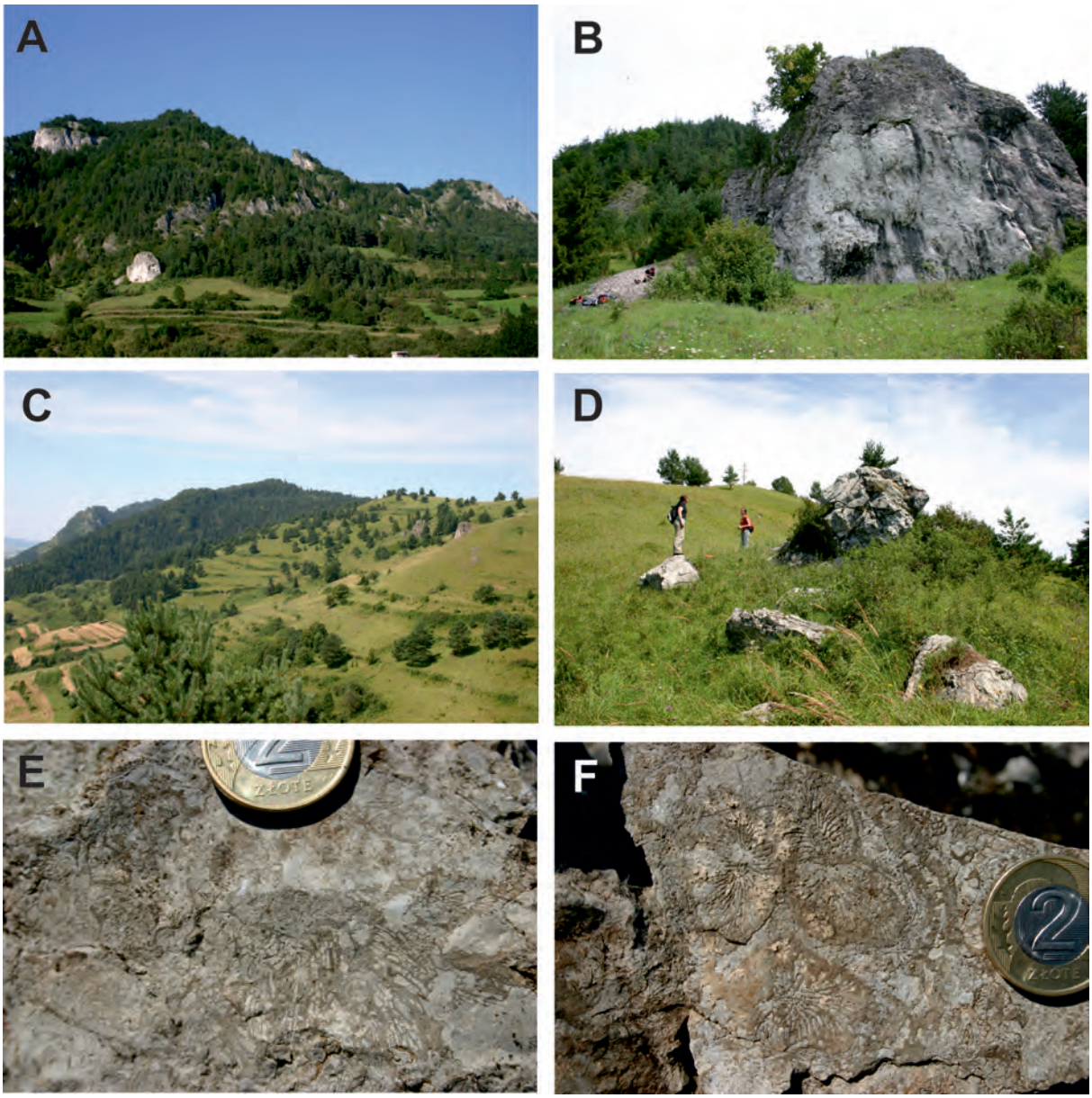

Fig. 41. The (**A**–**C**) Haligovce Klippen and (**C**, **D**) the Lipnik Klippen, with olistoliths of (**E**, **F**) Paleocene coral-bearing limestones of the Kambühel limestones.

was associated with the shift of the subduction zone north of the Czorsztyn Ridge. In the Paleocene, the Alcapa superterrane formed by combining the Eastern Alps, Tisza, and Inner Carpathians blocks, along with other small terranes. The aforementioned Paleocene reefs (Scheibner 1968; Köhler el at. 1993; Buček and Köhler 2017) formed in the shallowest zones of the basin, and isolated occurrences are also known from the Eastern Alps (near Kambühel near Ternitz in Austria, the stratotype of the Kambühel limestones; Faupl et at. 1987) and across western Slovakia (Scheibner 1968; Köhler et al. 1993) through to Haligovce (Scheibner 1968; Potfaj 2002; Krobicki et al. 2004; Buček and Köhler 2017).

Stop 2: P11. Červený Kláštor: *Maiolica*-type limestones with resedimentation events. (*Michał Krobicki, Jan Hejnar* and *Jan Golonka*)

In the vicinity of Červený Kláštor, the Pieniny Limestone Formation (*Maiolica*-type

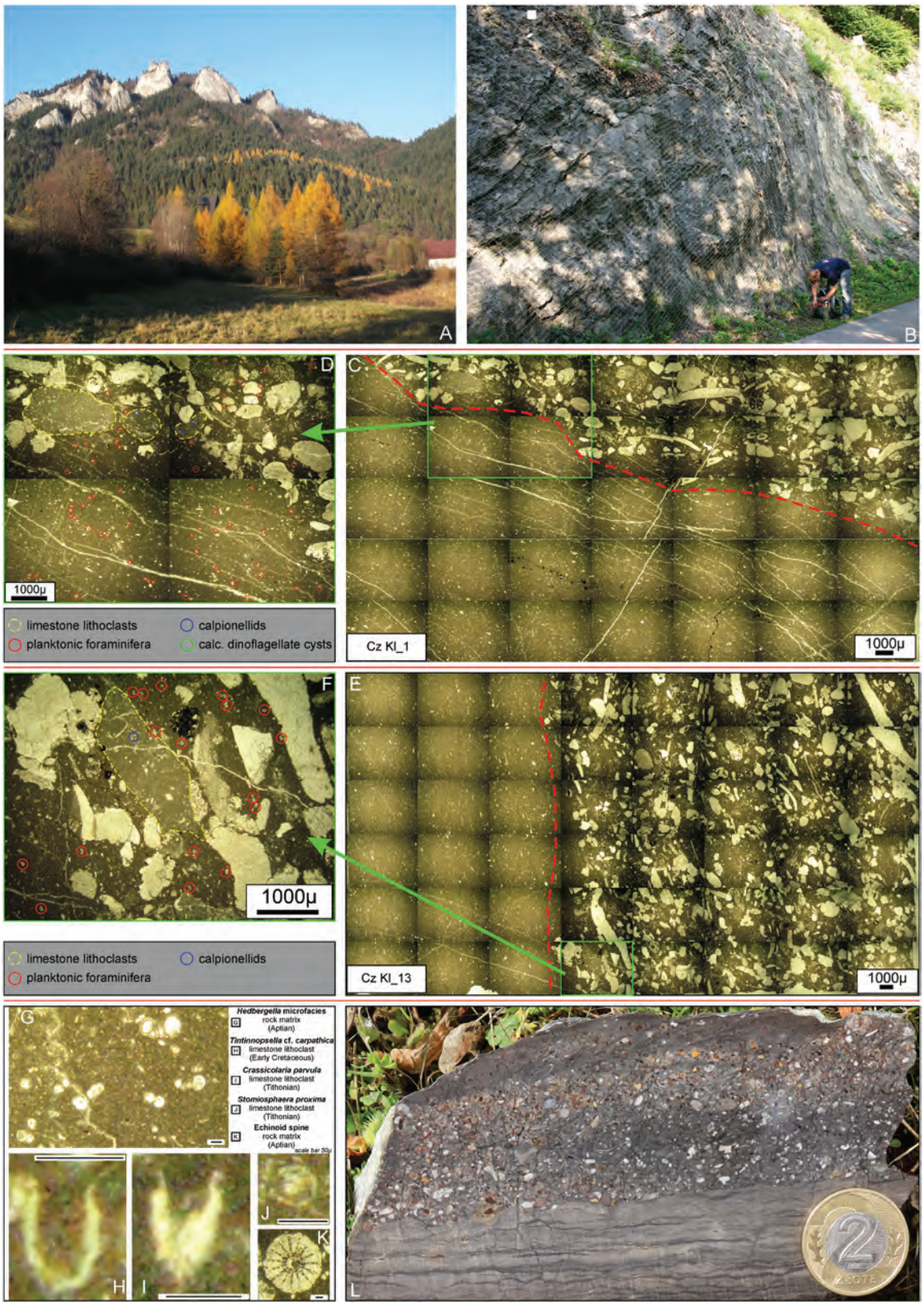

Fig. 42. **A** – The Trzy Korony (Three Crowns) Mountains. **B** – Červený Kláštor – general view; **C**, **E** – thin-sections of contact between micritic limestones and fine-grained limestones (see also slab – **L**) with microfossils (**D**, **F**–**K**).

facies, which also builds the Trzy Korony/Three Crowns – see Fig. 42A) of the Pieniny Succession dominates, developed as thin-bedded cherty limestones, intercalated with marly limestones with fine-grained litho- and bio-clasts (Fig. 42B, C, L). These intercalations may belong to the Kapuśnica Formation, which usually lies above micritic *Maiolica*-type limestones, and in this outcrop is the transition zone for this style of pelagic sedimentation. However, biostratigraphically these are of mid-Cretaceous age (Fig. 7).

In the presented section, biostratigraphic research focused on microfossil assemblages (Borza 1969; Reháková 2000; Fekete et al. 2017) (Fig. 42D–K); tintinnids, calcareous dinoflagellate cysts, and planktonic foraminifera have the most stratigraphic significance in studies of Creataceous pelagic carbonate facies. Together with radiolarians, sponges and *Globochete alpina* they form the major microfacies/microfossil associations. They range from the Berriasian to Albian, providing high-resolution biostratigraphic zonation.

Micropalaeontological thin section investigations demonstrated microfacies dominated by planktonic foraminifera (*Hedbergella*) present in the rock matrix. The abundant occurrence of the genus *Hedbergella*, accompanied by radiolarians, sponges, rare, poorly preserved tintinids, and sporadic calcareous dinoflagellate cysts, corresponds to the Aptian Stage. The predominance of planktonic foraminifera coinciding with the nannoconid crisis has been linked to the Lower Aptian Selli and Konhora (Reháková 2000) events.

The litho- and bioclasts observed in thin section are poorly rounded and sorted, and frequently crumbled. Lithoclasts are mainly represented by cherts and limestones, whereas the bioclasts are dominated by crinoids. The limestone lithoclasts show a clearly distinct assemblage of microfossils relative to the rock matrix. Micropalaeontological study of limestone lithoclasts confirmed the presence of Late Jurassic (Tithonian) and Early Cretaceous (Berriasian–Valanginian) microfossils (calpionellids and calcareous dinoflagellate cysts). The sedimentological features of the studied beds suggeset they capture one of the first episodes of mid-Cretaceous resedimentation within the PKB basin, with pelagic sedimentation.

Stop: 3:
Outer Flysch Carpathians

Stop 3: P1. Barnasiówka section: sedimentary response of the deep marginal Carpathian basin to sea level variation and palaoceanographic events during late Albian–Early Turonian (*Marta Bąk, Krzysztof Bąk and Zbigniew Górny*)

Outstanding outcrops of the upper Albian–lower Turonian succession – the Barnasiówka-Jasienica and Barnasiówka-Ostra Góra sections – occur in the southern Silesian Nappe of the Polish Outer Carpathians, within the Lanckorona-Żegocina tectonic zone (Fig. 43). There, the Albian–Turonian (?Coniacian) rocks create the narrow Barnasiówka Ridge, situated in the southwestern part of the Wieliczka Foothills. The presented section, consisting of flysch and hemipelagic facies, is located in an active quarry.

The results presented here are based on our research over the past two decades in this quarry and neighboring areas, which have been – and still are being – expanded as rock exploitation progresses. These include a diversity of topics, including biostratigraphy, chemostratigraphy, and a wide spectrum of

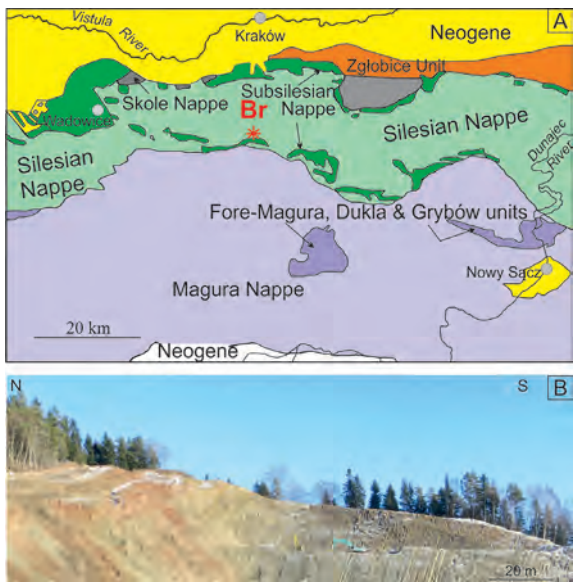

Fig. 43. **A** – Geological sketch-map of the middle Western Outer Carpathians (Poland) (supplemented after Oszczypko et al. 2005) showing the location of the excursion locality in the Silesian Nappe (Barnasiówka-Jasienica quarry – Br). **B** – Photograph of the Cenomanian–Turonian succession in the Barnasiówka-Jasienica quarry.

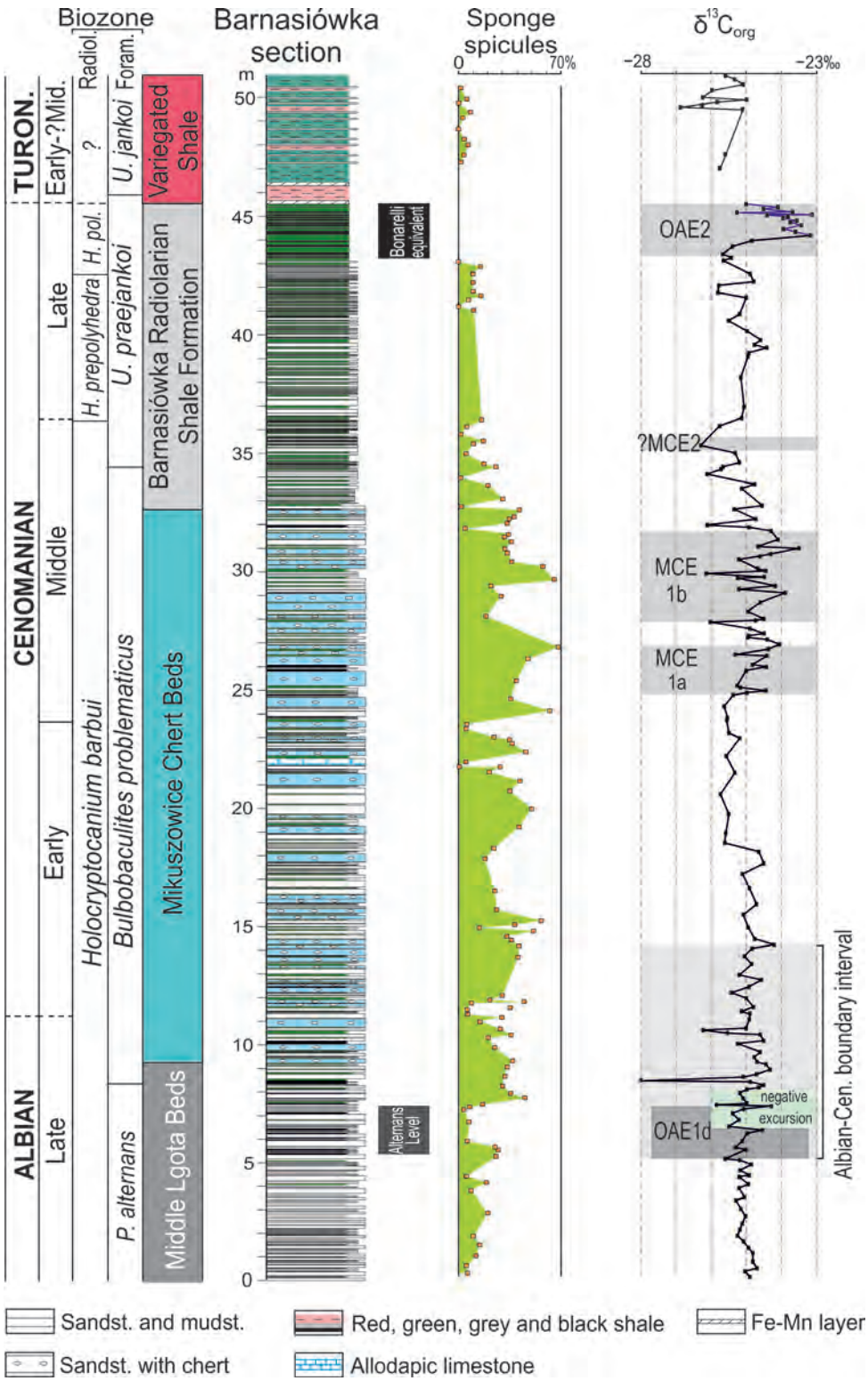

Fig. 44. Lithological log of the Barnasiówka section (Silesian Nappe, Western Outer Carpathians), plotted against relative sponge spicule abundance from spiculites in the turbidite sandstones and the $\delta^{13}C_{org}$ curve (supplemented from Bąk M et al., in review). Abbreviations: Tur – Turonian; Var. Sh. –variegated shale (non-calcareous hemipelagic red and green siliceous claystones); Bonar. – Bonarelli-equivalent Level; H. pol. – *Hemicryptocapsa polyhedra*, OAE – oceanic anoxic event; MCE – mid-Cenomanian Event.

palaeontological (including microfacies), petrographic, and geochemical analyses, with a particular focus on palaeoceanographic and palaeoenvironmental issues (Fig. 44). A special feature of these studies was their high sampling resolution, necessary due to the relatively low sediment accumulation rate from the late Albian through the early Turonian, ca. 3–8 mm/kyr, with a hiatal interval during the latest Cenomanian–earliest Turonian.

The upper Albian–lower Turonian stratigraphy presented here (Fig. 44) is based on radiolarians (Bąk, M. 2000, 2004, 2011), agglutinated foraminifera (Bąk K. et al. 2001), and carbon isotope data (Bąk K. 2007a; Bąk M. 2011; Bąk M. et al. 2022). Planktonic foraminifers represent redeposited specimens containing mainly hedbergellids, which are not diagnostic for biostratigraphy (Bąk K. 2007a; Bąk M. et al. 2011; Górny et al. 2022).

Microfossils and $\delta^{13}C_{org}$ data indicate continuous hemipelagic and flysch sedimentation in the Silesian Basin from the uppermost *Plectorecurvoides alternans* Zone (late Albian) through the lower *Uvigerinammina jankoi* Zone (early Turonian). Two radiolarian zones, the *Hemicryptocapsa prepolyhedra* and *H. polyhedra* zones, provide good documentation of the Late Cenomanian; however, the Cenomanian–Turonian boundary is not recognised in this area due to hiatuses, as reflected in the precipitation of the Fe-Mn layer with macronodules.

The position of the Albian–Cenomanian boundary was interpreted using the $\delta^{13}C_{org}$ curve (Bąk M. et al., in press), and correlation with curves from the Rose Creek Pit Upper Core (Richey et al. 2018) and Mont Risou (Gale et al. 1996). It lies in the lower Mikuszowice Chert Beds (ca. 2 m above its base).

The upper Albian–lower Turonian facies in this section contain two organic-rich sediment "horizons". The first, the Alternans Level, is the local expression of Oceanic Anoxic Event 1d (Bąk M. et al., in press). The second, a Bonarelli-equivallent Level, coincides with OAE2 (Bąk K. 2007a). The $\delta^{13}C_{org}$ data also enable the recognition of the Mid-Cenomanian Event (MCE Ia and MCE Ib) in the the upper Mikuszowice Chert Beds (Bąk M. et al., in press). This carbon-isotopic event, however, does not coincide with the accumulation of organic-rich facies, except in its lower part (i.e., within MCE Ia).

REFERENCES

Ager, D.V. 1976. The nature of the fossil record. Proccedings of the Geological Association, 87, 131–160.

Ager, D.V. 1993. Mesozoic brachiopods and seamounts. In: Palfy, J and Vörös, A. (Eds), Mesozoic Brachiopods of Alpine Europe, 11–13. Budapest.

Aigner, T. 1985. Storm Depositional System. Dynamic Stratigraphy in Modem and Ancient Shallow-Marine Sequences, 174 p. Springer; Berlin–Heidelberg.

Algeo, T.J. and Liu, J. 2020. A re-assessment of elemental proxies for paleoredox analysis. Chemical Geology, 540, 119549.

Anczkiewicz, A.A., Danisik, M. and Środoń, J. 2015. Multiple low-temperature thermochronology constraints on exhumation of the Tatra Mountains: new implications for the complex evolution of the Western Carpathians in the Cenozoic. Tectonics, doi: 10.1002/2015TC003952.

Anczkiewicz, A.A. and Anczkiewicz, R. 2016. U-Pb zircon geochronology and anomalous Sr-Nd-Hf isotope systematics of late orogenic andesites: Pieniny Klippen Belt, Western Carpathians, South Poland. Chemical Geology, 427, 1–16.

Andrusov, D. 1953. Étude géologique de la zone des Klippes internes des Carpathes Occidentales. IV & V. Geologicke Práce Slovenskej Akademie Vied a Úmiejetnosti, 34, 1–149.

Andrusov, D., Bystrický, J. and Fusán, O. 1973. Outline of the structure of the West Carpathians. Guide book. X Congress CBGA, 44 p. GÚDŠ, Bratislava.

Aubrecht, R. 2001. New occurrences of the Krasín Breccia (Pieniny Klippen Belt, West Carpathians): indication of Middle Jurassic synsedimentary tectonics. Acta Geologica Universita Comenianae, 56, 35–56.

Aubrecht, R., Mišík, M. and Sýkora, M. 1997. Jurassic synrift sedimentation on the Czorsztyn Swell of the Pieniny Klippen Belt in Western Slovakia. In: Plašienka, D., Hók, J., Vozár, J. and Ellecko, M. (Eds), Alpine evolution of the Western Carpathians and related areas, 53–64, Dionýz Stur Publisher; Bratislava.

Bac-Moszaszwili, M., Burchardt, J., Głazek, J., Iwanow, A., Jaroszewski, W., Kotański, Z., Lefeld, J., Mastella, L., Ozimkowski, W., Roniewicz, P., Skupiński, A. and Westwalewicz-Mogilska, E. 1979. Mapa Geologiczna Tatr Polskich (Geological Map of the Polish Tatra), 1:300 000. Wydawnictwa Geologiczne; Warszawa.

Barczyk, W. 1972a. Some representatives of the family Pygopidae (Brachiopoda) from the Tithonian of the Pieniny Klippen Belt. Acta Geologica Polonica, 22, 3, 507–513.

Barczyk, W. 1972b. On the representatives of the genus *Nucleata* Quenstedt (Brachiopoda) from the Tithonian and Berriasian of the environs of Czorsztyn, Poland. Prace Muzeum Ziemi, 20, 151–160.

Barczyk, W. 1979a. Rhynchonellid brachiopods from the

Upper Tithonian and Lower Berriasian of the Pieniny Klippen Belt. Acta Geologica Polonica, 29, 5, 1–58.

Barczyk, W. 1979b. Brachiopods from the Jurassic/Cretaceous boundary of Rogoźnik and Czorsztyn in the Pieniny Klippen Belt. Acta Geologica Polonica, 29, 207–214.

Barczyk, W. 1991. Succession of the Tithonian to Berriasian brachiopod faunas at Rogoźnik, Pieniny Klippen Belt. Acta Geologica Polonica, 41, 1–2, 101–107.

Bąk, K. 1998. Foraminiferal biostratigraphy of the Upper Cretaceous red deep water deposits in the Pieniny Klippen Belt, Carpathians, Poland. Studia Geologica Polonica, 111, 7–92.

Bąk, K. 2000. Biostratigraphy of deep-water agglutinated Foraminifera in Scaglia Rossa-type deposits of the Pieniny Klippen Belt, Carpathians, Poland. In: Hart, M.B., Kaminski, M.A. and Smart, C.W. (Eds), Proceedings of the Fifth International Workshop on Agglutinated Foraminifera, 15–41. Grzybowski Foundation Special Publication, 7; Kraków.

Bąk, K. 2007a. Deep-water facies succession around the Cenomanian–Turonian boundary in the Outer Carpathian Basin: Sedimentary, biotic and chemical records in the Silesian Nappe, Poland. Palaeogeography, Palaeoclimatology, Palaeoecology, 248, 255–290.

Bąk, K. 2015. Late Albian foraminifera from record of carbonate platform drowning on the Tatric Ridge, a part of the Carpathian domain: stratigraphic and palaeoenvironmental inferences. Carpathian Journal of Earth and Environmental Sciences, 10, 237–250.

Bąk, K. and Bąk, M. 2013. Late Albian through Cenomanian foraminiferal assemblage from the youngest deposits of Tatra Mountains, Central Western Carpathians; biostratigraphical and palaeoecological aspects. Acta Geologica Polonica, 63, 223–237.

Bąk, K., Bąk, M. and Paul, Z. 2001. Barnasiówka Radiolarian Shale Formation – a new lithostratigraphic unit in the Upper Cenomanian–lowermost Turonian of the Polish Outer Carpathians (Silesian Series). Annales Societatis Geologorum Poloniae, 71, 75–103.

Bąk K., Fabiańska, M., Bąk, M., Misz-Kennan, M., Zielińska M., Dulemba, P., Bryndal, T. and Naglik, B. 2016a. Organic matter in upper Albian marine sediments in the High-Tatric units, central western Carpathians related to Oceanic Anoxic Event 1d – geochemistry, microfacies and palynology. Palaeogeography, Palaeoclimatology, Palaeoecology, 453, 212–227.

Bąk, K., Bąk, M. Dulemba, P., Okoński, S. 2016b. Late Cenomanian environmental conditions at the submerged Tatric Ridge, Central Western Carpathians during the period preceding Oceanic Anoxic Event 2 – A palaeontological and isotopic approach. Cretaceous Research, 63, 95–112.

Bąk, K., Kowalczyk, J., Wolska, A., Bąk, M. and Natkaniec-Nowak, L. 2018. Iron and silica enrichments in the Middle Albian neptunian dykes from the High-Tatric Unit, Central Western Carpathians: an indication of hydrothermal activity for an extensional tectonic regime. Geological Magazine, 155, 1–19.

Bąk, M. 1999. Cretaceous Radiolaria from the Pieniny Succession, Pieniny Klippen Belt, Polish Carpathians. Studia Geologica Polonica, 115, 91–115.

Bąk, M. 2000. Radiolaria from the Upper Cenomanian–Lower Turonian deposits of the Silesian Unit (Polish Flysch Carpathians). Geologica Carpathica. 51, 309–324.

Bąk, M. 2004. Radiolarian biostratigraphy of the Upper Cenomanian–Lower Turonian deposits in the Subsilesian Nappe (Outer Western Carpathians). Geologica Carpathica, 55, 239–250.

Bąk, M. 2011. Tethyan radiolarians at the Cenomanian–Turonian Anoxic Event from the Apennines (Umbria-Marche) and the Outer Carpathians: Palaeoecological and palaeoenvironmental implications. Studia Geologica Polonica, 134, 1–279.

Bąk, M., Bąk, K. and Ciurej, A. 2011. Palaeoenvironmental signal from the microfossils record in the Mikuszowice Cherts of the Silesian Nappe, Polish Outer Carpathians. In: Bąk, M., Kaminski, M.A. and Waśkowska, A. (eds), Integrating microfossil records from the oceans and epicontinental seas. Grzybowski Foundation Special Publication, 17, 15–25.

Bąk, M., Bąk, K. and Górny, Z. 2022. Timing of mass redeposition of sponge spicules from the peri-Tethyan shelf into the deep Carpathian basin and their relation to mid-Cretaceous global sea level changes. Geological Society of America Bulletin. https://doi.org/10.1130/B36178.1

Bernoulli, D. and Jenkyns, H.C. 1974. Alpine, Mediterranean and central Atlantic Mesozoic facies in relation to the early evolution of the Tethys. In: Dott, R.H. Jr. and Shaver, R.H. (Eds), Modern and Ancient Geosynclinal Sedimentation. SEPM Society for Sedimentary Geology, Special Publications, 19, 129–160.

Birkenmajer, K. 1959. Significance of the Haligovce Klippe for the geology of the Pieniny Klippen Belt (Carpathians). Rocznik Polskiego Towarzystwa Geologicznego, 29, 1, 73–88. [In Polish, English summary]

Birkenmajer, K. 1963. Stratigraphy and palaeogeography of the Czorsztyn series (Pieniny Klippen Belt, Carpathians) in Poland. Studia Geologica Polonica, 9, 1–380. [In Polish, English summary]

Birkenmajer, K. 1970. Pre-Eocene fold structures in the Pieniny Klippen Belt (Carpathians) of Poland. Studia Geologica Polonica, 31, 7–77. [In Polish, English summary]

Birkenmajer, K. 1973. Lower Cretaceous. Pieniny Klippen Belt (in Polish). In: Sokołowski, S. (Ed), Budowa Geologiczna Polski. I, Stratygrafia. cz 2. Mezozoik, 674–679. Wydawnictwa Geologiczne; Warszawa.

Birkenmajer, K. 1977. Jurassic and Cretaceous lithostratigraphic units of the Pieniny Klippen Belt, Carpathians, Poland. Studia Geologica Polonica, 45, 1–158.

Birkenmajer, K. 1979. Przewodnik geologiczny po pieninskim pasie skałkowym, 237 pp. Wydawnictwa Geologiczne; Warszawa.

Birkenmajer, K. 1986. Stages of structural evolution of the Pieniny Klippen Belt, Carpathians. Studia Geologica Polonica, 88, 7–32.

Birkenmajer, K. 1987. The Trawne Member (Upper Albian–Upper Cenomanian) – a flysch development in the Branisko Nappe, Pieniny Klippen Belt, Carpathians. Studia Geologica Polonica, 92, 29–40.

Birkenmajer, K. 1988. Exotic Andrusov Ridge: its role in plate-tectonic evolution of the West Carpathian Foldbelt. Studia Geologica Polonica, 91, 7–37.

Birkenmajer, K. and Dudziak, J. 1991. Middle to Late Palaeocene Nannoplankton Zones in the Jarmuta Formation, Pieniny Klippen Belt, Carpathians. Bulletin of the Polish Academy of Sciences, Earth Sciences, 39, 47–54.

Birkenmajer, K. and Gasiński, M.A. 1992. Albian and Cenomanian palaeobathymetry in the Pieniny Klippen Belt Basin, Polish Carpathians. Cretaceous Research, 13, 479–485.

Birkenmajer, K. and Jednorowska, A. 1983. Upper Cretaceous stratigraphy of the Branisko Nappe at Sromowce Wyżne, Pieniny Klippen Belt of Poland. Studia Geologica Polonica, 77, 7–26.

Birkenmajer, K. and Jednorowska, A. 1984. Upper Cretaceous stratigraphy in the Pieniny Nappe at Sromowce Niżne, Pieniny Klippen Belt, Carpathians, Poland. Studia Geologica Polonica, 83, 25–50.

Birkenmajer, K. and Jednorowska, A. 1987a. Upper Cretaceous and Lower Palaeogene deposits at Maruszyna, Pieniny Klippen Belt of Poland. Studia Geologica Polonica, 77, 27–33.

Birkenmajer, K. and Jednorowska, A. 1987b. Late Cretaceous foraminiferal biostratigraphy of the Pieniny Klippen Belt (Carpathians, Poland). Studia Geologica Polonica, 92, 7–28.

Birkenmajer, K. and Lefeld, J., 1969. Exotic Urgonian limestones from the Pieniny Klippen Belt of Poland. Bulletin de l'Academie Polonaise des Sciences, Serie sciences géologie et géographie, 17, 13–15.

Birkenmajer, K. and Oszczypko, N. 1989. Cretaceous and Palaeogene lithostratigraphic units of the Magura nappe, Krynica subunit, Carpathians. Annales Societatis Geologorum Poloniae, 59, 145–181.

Birkenmajer, K. and Pécskay, Z. 2000a. K-Ar dating of the Miocene andesite intrusions, Pieniny Mts, West Carpathians, Poland: a supplement. Studia Geologica Polonica, 117, 7–25.

Birkenmajer, K. and Pécskay, Z. 2000b. Early Cretaceous K-Ar age of a large basalt olistolith at Biała Woda, Pieniny Klippen Belt, West Carpathians, Poland. Studia Geologica Polonica, 117, 27–35.

Birkenmajer, K. and Wieser, T. 1990. Exotic rock fragments from the Upper Cretaceous deposits near Jaworki, Pieniny Klippen Belt, Carpathians, Poland. Studia Geologica Polonica, 97, 7–67.

Birkenmajer, K., Dudziak, J., Jednorowska, A. and Kutyba, J. 1987. Foraminiferal-nannoplankton evidence for Maastrichtian and Paleocene ages of the Jarmuta Formation: its bearing on dating Laramian orogeny in the Pieniny Klippen Belt, Carpathians. Bulletin of the Polish Academy of Sciences, Earth Sciences, 35, 287–298.

Birkenmajer, K., Kozur, H. and Mock, R. 1990. Exotic Triassic pelagic limestone pebbles from the Pieniny Klippen Belt of Poland: a further evidence for Early Mesozoic rifting in West Carpathians. Annales Societatis Geologorum Poloniae, 60, 3–44.

Borza, K. 1969. Die Mikrofazies und Mikrofossilien des Oberjuras und der Unterkreide der Klippenzone der Westkarpaten, 130 p. Editory House of the Slovak Academy of Science; Bratislava.

Burtan, J., Chowaniec, J. and Golonka, J. 1984. Preliminary results of studies on exotic carbonate rocks in the western part of the Polish Flysch Carpathians. Biuletyn Instytutu Geologicznego, 346, 147–159. [In Polish, English summary]

Buček, S. and Köhler, E. 2017. Palaeocene reef complex of the Western Carpathians. Slovak Geological Magazine, 17, 1, 3–163.

Cieszkowski, M. and Golonka, J. 2006. Olistostroms as indicators of the geodynamic process (Northern Carpathians). Geolines, 20, 27–28.

Cieszkowski, M. and Ślączka, A. 2001. Silesian and Subsilesian Units. In: Birkenmajer, K. and Krobicki, M. (Eds), 12th meeting of the Association of European Geological Societies; 10–15 September 2001, Kraków: Carpathian palaeogeography and geodynamics: a multidisciplinary approach; field trip guide, 109–113. Polish Geological Institute; Kraków.

Cúlová, V. and Andrusov, D. 1964. Précision de l'âge de la formation des nappes de recouvrement des Carpathes Occidentales Centrales. Geologický Sbornik, 15, 253.

Davies, D.J., Powell, E.N. and Stanton, R.J. Jr. 1989: Taphonomic signature as a function of environmental process: shells and shell beds in a hurricane-influenced inlet on the Texas coast. Palaeogeography, Palaeoclimatology, Palaeoecology, 72, 317–356.

De Wever, P., O'Dogherty, L. and Goričan, Š. 2014. Monsoon as a cause of radiolarite in the Tethyan realm. Comptes Rendus Geoscience, 346, 287–297.

Dieni, I. and Middlemiss, F.A. 1981. Pygopid brachiopods from the Venetian Alps. Bolletino Societatis Paleontologia Italiana, 20, 19–48.

Faupl, P., Pober, E. and Wagreich, M. 1987. Facies development of the Gosau Group of the eastern parts of the Northern Calcareous Alps during the Cretaceous and Paleogene. In: Flügel, F.E.W. and Faupl, P. (Eds) Geodynarnics of the Eastern Alps, 142–155. Vienna.

Fekete, K., Sotak, J., Boorova, D., Lintnerova, O., Michalik, J. and Grabowski, J. 2017. An Albian demise of the carbonate platform in the Manin Unit (Western Carpathians, Slovakia). Geologica Carpathica, 68, 385–402.

Föllmi, K.B. 2012. Early Cretaceous life, climate and anoxia. Cretaceous Research, 35, 230–257.

Fürsich, F.T. and Oschmann, W. 1986. Storm shell beds of *Nanogyra virgula* in the upper Jurassic of France. Neues Jahrbuch für Geologie und Paläontologie, Abhandlungen, 172, 141–161.

Gale, A.S., Kennedy, W.J., Burnett, J.A., Caron, M. and Kidd, B.E. 1996. The late Albian to early Cenomanian succession at Mont Risou near Rosans (Drome, SE France): An integrated study (ammonites, inoceramids, planktonic foraminifera, nannofossils, oxygen and carbon isotopes). Cretaceous Research, 17, 515–606.

Gasiński, M.A. 1988. Foraminiferal biostratigraphy of the Albian and Cenomanian sediments in the Polish part of the Pieniny Klippen Belt, Carpathian Mountains. Cretaceous Research, 9, 217–247.

Gasiński, M.A. 1991. Albian and Cenomanian palaeobathymetry of the Pieniny Klippen Belt Basin (Polish Carpathians) based on foraminifers. Bulletin of the Polish Academy of Sciences, Earth Sciences, 39, 1–11.

Gawęda, A., Burda, J., Golonka, J., Klötzli, U., Chew, D., Szopa, K. and Wiedenbeck, M. 2017. The evolution of Eastern Tornquist-Paleoasian Ocean and subsequent Continental collision: a case study from the Western Tatra Mts, Central West Carpathians, Poland. Gondwana Research, 48, 134–152.

Gaździcka, E., Gaździcki, A., Filipczak, K. and Uchman, A. 2009. Upper Sub-Tatric (Choč) Nappe between the Lejowa and Chochołowska valleys in the Tatra Mountains.Przegląd Geologiczny, 57, 56–63.

Gedl P. 2000. Biostratigraphy and palaeoenvironment of the Podhale Palaeogene (Inner Carpathians, Poland) in the light of palynological studies, p. I and II. Studia Geologica Polonica, 117, 69–154, 155–303.

Gedl, E., Kołodziej, B. and Uchman, A. 2007. Muráň Limestone Member (Upper Hauterivian) of the Kościeliska Marl Formation, Polish Western Tatra Mts: dinocyst biostratigraphy and microfacies analysis. Studia Geologica Polonica, 127, 119–137.

Golonka, J. and Krobicki, M. 2001. Upwelling regime in the Carpathian Tethys: a Jurassic–Cretaceous palaeogeographic and paleoclimatic perspective. Geological Quarterly, 45, 15–32.

Golonka, J. and Krobicki, M. 2004. Jurassic paleogeography of the Pieniny and Outer Carpathian basins. Rivista Italiana di Paleontologia e Stratigrafia, 110, 5–14.

Golonka, J. and Krobicki, M. 2006. Field trip A – From Tethyan to Platform Facies. Outer Carpathians. In: Wierzbowski, A., Aubrecht, R., Golonka, J., Gutowski, J., Krobicki, M., Matyja, B.A, Pieńkowski, G. and Uchman, A. (Eds), Jurassic of Poland and adjacent Slovakian Carpathians. Field trip guidebook, 11–15. 7th International Congress on the Jurassic System, 6–18 September 2006, Kraków, Poland.

Golonka, J. and Sikora, W. 1981. Microfacies of the Jurassic and Lower Cretaceous sedimentarily thinned deposits of the Pieniny Klippen Belt in Poland. Biuletyn Instytutu Geologicznego, 31, 7–37. [In Polish, English summary]

Golonka, J., Krobicki, M., Oszczypko, N., Ślączka, A. and Słomka, T. 2003. Geodynamic evolution and paleogeography of the Polish Carpathians and adjacent areas during Neo-Cimmerian and preceding events (latest Triassic–earliest Cretaceous). In: McCann, T. and Saintot, A. (Eds), Tracing Tectonic Deformation Using the Sedimentary Record, 208, 138–158. Geological Society, Special Publication; London.

Górny, Z., Bąk, M., Bąk, K. and Strzeboński, P.A. 2022. Planktonic biota constituents responses to global sea-level changes recorded in the uppermost Albian to middle Cenomanian deep-water facies of the Outer Carpathians. Minerals, 12, 152.

Grabowski, J. and Pszczółkowski, A. 2006. Magneto- and biostratigraphy of the Tithonian–Berriasian pelagic sediments in the Tatra Mts (central Western Carpathians, Poland): sedimentary and rock magnetic changes at the Jurassic/Cretaceous boundary. Cretacoeus Research. 27, 398–417.

Grabowski, J., Schnyder, J., Sobień, K., Koptiková, L., Krzemiński, L., Pszczółkowski, A., Hejnar, J. and Schnabl, P. 2013. Magnetic susceptibility and spectra gamma logs in the Tithonian–Berriasian pelagic carbonates in the Tatra Mts (Western Carpathians, Poland): palaeoenvironmental changes at the Jurassic/Cretaceous boundary. Cretaceous Research, 43, 1–17.

Grabowski, J., Krobicki, M. and Sobień, K. 2008. New palaeomagnetic results from the Polish part of the Pieniny Klippen Belt, Carpathians – evidence for the palaeogeographic position of the Czorsztyn Ridge in the Mesozoic. Geological Quarterly, 52, 31–44.

Grabowski, J., Michalík, J., Pszczółkowski, A. and Lintnerová, O., 2010. Magneto- and isotope stratigraphy around the Jurassic/Cretaceous boundary in the Vysoka unit (Male Karpaty Mountains): correlations and tectonic implications. Geologica Carpathica, 61, 309–326.

Grabowski, J. and Sobień, K. 2015. Variation of clastic input in the Berriasian of the Lower Sub-Tatric (Križna) succession in the Tatra Mts (Central Western Carpathians, Poland) – data from magnetic susceptibility and inorganic geochemistry. Annales Societatis Geologorum Poloniae, 85, 139–150.

Hardenbol, J., Thierry, J., Harley, M.B., Jacquin, Th., de Graciansky, P.-C. and Vail, P.R. 1998. Mesozoic and

Cenozoic sequence chronostratigraphic framework of European basins. Appendix. SEPM Special Publication, 160, 763–786.

Horwitz, L. and Rabowski, F. 1929. Excursion dans les Piénines (Karpates polonaises) de la Sociéte Géologique Polonaise (18–21 V 1929). Annales Societatis Geologorum Poloniae, 6, 109–155. [In Polish, French summary].

Iwańczuk, J., Iwanow, A. and Wierzbowski, A. 2012. Lower Jurassic to lower Middle Jurassic succession at Kopy Sołtysie and Płaczliwa Skała in the eastern Tatra Mts (Western Carpathians): stratigraphy, facies and ammonites. Volumina Jurassica, 11, 19–58.

Jach, R. 2007. Bositra limestones : a step towards radiolarites : case study from the Tatra Mountains. Annales Societatis Geologorum Poloniae, 77, 161–170.

Jach, R., Rychliński, T. and Uchman, A. (red). 2014. Skały osadowe Tatr, 278 pp. Tatrzański Park Narodowy; Zakopane.

Jach, R. and Rehákova, D. 2019. Middle to Late Jurassic carbonate-biosiliceous sedimentation and palaeoenvironment in the Tethyan Fatricum domain, Krížna Nappe, Tatra Mts, Western Carpathians. Annales Societatis Geologorum Poloniae, 89, 1–46.

Jaglarz, P. and Szulc, J. 2003. Middle Triassic evolution of the Tatricum sedimentary basin: an attempt of sequence stratigraphy to the Wierchowa Unit in the Polish Tatra Mountains. Annales Societatis Geologorum Poloniae, 73, 169–182.

Jezierska, A. and Łuczyński, P. 2016. Jurassic unconformities in the High-Tatric succession. Geological Quarterly, 60, 273–290.

Jurewicz, E. 1994. Structural analysis of the Pieniny Klippen Belt at Jaworki, Carpathians, Poland. Studia Geologica Polonica, 7–87. [In Polish, English summary]

Jurewicz, E. 1997. The contact between the Pieniny Klippen Belt and Magura Unit (the Małe Pieniny Mts.). Geological Quarterly, 41, 315–326.

Jurewicz, E. 2005. Geodynamic evolution of the Tatra Mts. and the Pieniny Klippen Belt (Western Carpathians): problems and comments. Acta Geologica Polonica, 3, 295–338.

Kędzierski, M. and Uchman, A. 1997. Age and palaeoenvironment of the Kościeliska Marl Formation (Lower Cretaceous) in the Tatra Mountains, Poland: preliminary results. Annales Societatis Geologorum Poloniae, 67, 237–247.

Kidwell, S.M., Fürsich, F.T. and Aigner, T. 1986. Conceptual framework for the analysis and classification of fossil concentrations. Palaios, 1, 3, 228–238.

Kokoszyńska, B. and Birkenmajer, K. 1956. Albian fauna of the Niedzica Series from the Klippen Belt of the Pieniny Mountains. Acta Geologica Polonica, 6, 371–380. [In Polish]

Kotanski, Z. 1961. Tektogeneza i rekonstrukcja paleogeografii pasma wierchowego w Tatrach. Acta Geologica Polonica, 11, 187–476.

Köhler, E., Salaj, J. and Bućek, S. 1993. Paleogeographical development of the Myjava sedimentary area (Western Slovakia) during the existence of the Paleocene reef complex. Geologica Carpathica, 44, 373–380.

Krajewski, K. 2003. Facies development and lithostratigraphy of Hightatric mid-Cretaceous (Zabijak Formation) in the Polish Tatra Mountains. Studia Geologica Polonica, 121, 81–158.

Krobicki, M. 1993. Tithonian–Berriasian brachiopods in the Niedzica Succession of the Pieniny Klippen Belt (Polish Carpathians): paleoecological and paleobiogeographical implications. In: Pálfy, J. and Vörös, A. (Eds), Mesozoic Brachiopods of Alpine Europe, 69–77. Budapest.

Krobicki, M. 1994. Stratigraphic significance and palaeoecology of the Tithonian–Berriasian brachiopods in the Pieniny Klippen Belt, Carpathians, Poland. Studia Geologica Polonica, 106, 89–156.

Krobicki, M. 1995. Storm-generated shell beds in pelagic Albian–Cenomanian sediments, Pieniny Klippen Belt, Carpathians. Geologica Carpathica, 46, 277–284.

Krobicki, M. 1996. Neo-Cimmerian uplift of intraoceanic Czorsztyn pelagic swell (Pieniny Klippen Belt, Polish Carpathians) indicated by the change of brachiopod assemblages. In: Riccardi, A.C. (Ed.), Advances in Jurassic Research. GeoResearch Forum, 1–2, 255–264.

Krobicki, M. 2006. Field trip A – From Tethyan to Platform Facies. Outer Carpathians. Stop A5 – Falsztyn-Czorsztyn Succession (Aalenian–Bajocian). In: Wierzbowski, A., Aubrecht, R., Golonka, J., Gutowski, J., Krobicki, M., Matyja, B.A, Pieńkowski, G. and Uchman, A. (Eds). Jurassic of Poland and adjacent Slovakian Carpathians. Field trip guidebook. 7th International Congress on the Jurassic System, 6–18 September 2006, Kraków, Poland, 39–41. Warszawa.

Krobicki, M. 2009. Bajocian synsedimentary tectonics and its significance in Jurassic evolution of the Pieniny Klippen Belt. Geologia (kwartalnik AGH), 35, 65–78. [In Polish, English summary]

Krobicki, M. and Golonka, J. 2006. Pieniny Klippen Belt. In: Wierzbowski, A., Aubrecht, R., Golonka, J., Gutowski, J., Krobicki, M., Matyja, B.A, Pieńkowski, G. and Uchman, A. (Eds). Jurassic of Poland and adjacent Slovakian Carpathians. Field trip guidebook. 7th International Congress on the Jurassic System, 6–18 September 2006, Kraków, Poland, 15–22. Warszawa.

Krobicki, M. and Golonka, J. 2008. Geological history of the Pieniny Klippen Belt and Middle Jurassic black shales as one of the oldest deposits of this region – stratigraphical position and palaeoenvironmental significance. Geoturystyka, 2, 13, 3–18.

Krobicki, M. and Olszewska, B. 2004. Foraminifers from calcareous exotics of the Urgonian facies in the Upper Cretaceous and Palaeogene deposits of the Pi-

eniny Klippen Belt, Poland (in Polish). In: Krobicki, M. (Ed.), Egzotyki karpackie – znaczenie w rekonstrukcjach paleogeograficzno-geotektonicznych. Ogólnopolskie seminarium, 13 grudnia 2004, 43–45. Kraków.

Krobicki, M. and Olszewska, B. 2005. Urgonian-type microfossils in exotic pebbles of the Late Cretaceous and Palaeogene gravelstones from the Sromowce and Jarmuta formations (Pieniny Klippen Belt, Polish Carpathians). Studia Geologica Polonica, 124, 215–235.

Krobicki, M. and Wierzbowski, A. 1996. New data on stratigraphy of the Spisz Limestone Formation (Valanginian) and the brachiopod succession in the lowermost Cretaceous of the Pieniny Klippen Belt, Carpathians, Poland. Studia Geologica Polonica, 109, 53–67.

Krobicki, M. and Wierzbowski, A. 2004. Stratigraphic position of the Bajocian crinoidal limestones and their palaeogeographic significance in evolution of the Pieniny Klippen Belt. Tomy Jurajskie, 2, 69–82. [In Polish, English summary]

Krobicki, M., Kruglov, S.S., Matyja, B.A., Wierzbowski, A., Aubrecht, R., Bubniak, A. and Bubniak, I. 2003. Relation between Jurassic Klippen successions in the Polish and Ukrainian parts of the Pieniny Klippen Belt. Mineralia Slovaca, 35, 56–58.

Krobicki, M., Golonka, J., Kołodziej, B., Olszewska, B., Oszczypko, N., Słomka, T., Tragelehn, H. and Wieczorek, J. 2004. Paleoceńskie olistolity wapieni koralowo-glonowych rejonu Haligowiec (pieniński pas skałkowy, Słowacja). In: Krobicki, M. (Ed.), Egzotyki karpackie – znaczenie w rekonstrukcjach paleogeograficzno-geotektonicznych. Ogólnopolskie seminarium, 13 grudnia 2004, 53–55. Kraków.

Krobicki, M., Poprawa, P. and Golonka, J. 2006. Early Jurassic–Late Cretaceous evolution of the Pieniny Klippen Basin indicated by tectonic subsidence analysis. In: Oszczypko, N., Uchman, A. and Malata, E. (Eds), Palaeotectonic evolution of the Outer Carpathian and Pieniny Klippen Belt Basins, 165–178. Instytut Nauk Geologicznych UJ; Kraków. [In Polish]

Krobicki, M., Poprawa, P., Nejbert, K., Armstrong, R. and Pecskay, Z. 2018. New geochemical and geochronological data of magmatic and sub-volcanic exotic rocks from the Late Cretaceous and Paleogene gravelstones (Pieniny Klippen Belt, Carpathians, Poland). In: Šujan, M., Csibri, T., Kiss, P. and Rybár, S. (Eds), Environmental, Structural and Stratigraphical Evolution of the Western Carpathians, Abstract Book, 11th ESSEWECA Conference, 29th–30th November 2018, 54–55. Bratislava.

Kuhn, O., Weissert, H., Föllmi, K.B. and Hennig, S. 2005. Altered carbon cycling and trace metal enrichment during the Late Valanginian and Early Hauterivian. Eclogae Geologicae Helveticae, 98, 333–344.

Kušik, R. 1959. Litologia sedimentarnych serii uzemia Orawic. Geologický Sbornik, 10, 203–222.

Kutek, J. and Wierzbowski, A. 1986. A new account on the Upper Jurassic stratigraphy and ammonites of the Czorsztyn succession, Pieniny Klippen Belt. Acta Geologica Polonica, 36, 289–316.

Lefeld, J. 1968. Stratigraphy and paleogeography of the High-Tatric Lower Cretaceous in the Tatra Mountains. Studia Geologica Polonica, 24, 1–115.

Lefeld, J. 1974. Middle–Upper Jurassic and Lower Cretaceous biostratigraphy and sedimentology of the Sub-Tatric succession in the Tatra Mts (Western Carpathians). Acta Geologica Polonica, 24, 277–364.

Lefeld, J. 1988. Urgonian formation in the Carpathians. In: Nairn, E.M. (Ed) Evolution of the northern margin of Tethys: the results of the IGCP Project 198. Mémoires de la Sociéte Géologique de France, Nouvelle serie, 154, 141–145.

Lefeld, J., Gaździcki, A., Iwanow, A., Krajewski, K. and Wójcik, K. 1985. Jurassic and Cretaceous lithostratigraphic units of the Tatra Mountains. Studia Geologica Polonica, 84, 7–93.

Lewandowski, M., Krobicki, M., Matyja, B.A. and Wierzbowski, A. 2005. Palaeogeographic evolution of the Pieniny Klippen Basin using stratigraphic and palaeomagnetic data from the Veliky Kamenets section (Carpathians, Ukraine). Palaeogeography, Palaeoclimatology, Palaeoecology, 216, 53–72.

Lodowski, D.G. and Grabowski, J. In review. Tracing the latest Jurassic–earliest Cretaceous paleoenvironment evolution in carbonates: a case study of the Giewont succession (Central Western Carpathians, Poland). Sedimentology.

Lodowski, D.G., Pszczółkowski, A., Wilamowski, A. and Grabowski, J. 2022. Jurassic–Cretaceous transition in the High-Tatric succession (Giewont Unit, Western Tatra Mts, Poland): integrated stratigraphy and microfacies. Acta Geologica Polonica, 72, 107–135.

Lucińska-Anczkiewicz, A., Villa, I.M., Anczkiewicz, R. and Ślączka, A. 2002. $^{40}Ar/^{39}Ar$ dating of alkaline lamprophyres from the Polish Western Carpathians. Geologica Carpathica, 53, 45–52.

Łuczyński, P. 2021. Early and Middle Jurassic tectonically controlled deposition in the High-Tatric succession (Tatricum), Tatra Mountains, southern Poland: a review. Geological Quarterly, 65.

Madzin, J., Sýkora, M. and Soták, J. 2014. Stratigraphic position of alkaline volcanic rocks in the autochtonous cover of the High-Tatric Unit (Western Tatra Mts., Central Western Carpathians, Slovakia). Geological Quarterly, 58, 163–180.

Marcinowski, R. and Wiedman, J. 1985. The Albian ammonite fauna of Poland and its paleogeographical significance. Acta Geologica Polonica, 35, 199–219.

Marcinowski, R. and Wiedman, J. 1990. The Albian ammonites of Poland. Paleontologia Polonica, 50, 1–94.

Masse, J.-P. and Uchman, A. 1997. New biostratigraphic data on the Early Cretaceous platform carbonates of the Tatra Mountains, Western Carpathians, Poland. Cretaceous Research, 18, 713–729.

Matyszkiewicz, J. 1997. Microfacies, sedimentation and some aspects of diagenesis of Upper Jurassic sediments from the elevated part of the Northern peri-Tethyan Shelf: a comparative study on the Lochen area (Schwäbische Alb) and the Cracow area (Cracow-Wieluń Upland, Poland). Berliner Geowissenschaftliche Abhandlungen, E21, 1–111.

Michalík, J. and Reháková, D. 1995. Sedimentary records of Early Cretaceous tectonic activity in the Alpine-Carpathian region. Slovak Geological Magazine, 2, 159–164.

Michalík, J., Lintnerová O., Gaździcki, A. and Soták, J. 2007. Record of environmental changes in the Triassic–Jurassic boundary interval in the Zliechov Basin, Western Carpathians. Palaeogeography, Palaeoclimatology, Palaeoecology, 244, 71–88.

Mišík, M. 1990. Urgonian facies in the West Carpathians. Knihovnièka Zemního plynu a nafty, 9a, 25–54.

Mišík, M. 1994. The Czorsztyn submarine ridge (Jurassic–Lower Cretaceous, Pieniny Klippen Belt): an example of a pelagic swell. Mitteilungen Österreichiche Geologische Gessellsaft, 86, 133–140.

Mišík, M., Sikora, M., Mock, R. and Jablonský, J. 1991. Paleogene Proć conglomerate of the Klippen Belt in the West Carpathians material from the Neopieninic Exotic Ridge. Acta Geologica et Geogrąfica Universitae Comenianae, Geologia, 46, 9–101.

Morycowa, E. 1966. Koralowce wapieni urgońskich serii wierchowej Tatr polskich (Les Madréporaires des calcaires urgoniensis de la série haut-tatrique dans le Tatra polonais). Rocznik Polskiego Towarzystwa Geologicznego, 36, 519–542.

Nekvasilová, O. 1977. Rhynchonellida (Brachiopoda) from the Lower of Štramberk (Czechoslovakia). Sbornik Geologickych Ved, Paleontologia, 19, 45–76.

Olszewska, B. and Wieczorek, J. 1995. Preliminry report on foraminifers from the youngest (middle Cretaceous) deposits of the Tatra Mts (Western Carpathians). In: Annual Assembly of IGCP Project No. 362, Tethyan and Boreal Cretaceous, Museum of Natural History, Maastricht 17–18.09.1995, Programme and abstracts, 61–62. Maastricht.

Oszczypko, N. 1975. Exotic rocks in the Palaeogene of the Magura nappe between the Dunajec and Poprad Rivers (Carpathians, Poland). Rocznik Polskiego Towarzystwa Geologicznego, 45, 403–431. [In Polish, English summary]

Oszczypko, N. 1992. Late Cretaceous through Paleogene evolution of Magura Basin. Geologica Carpathica, 43, 333–338.

Oszczypko, N. 2006. Late Jurassic–Miocene evolution of the Outer Carpathian fold-and-thrust belt and its foredeep basin (Western Carpathians, Poland). Geological Quarterly, 50 (1), 169–194.

Oszczypko, N., Malata, E., Bąk, K., Kędzierski, M. and Oszczypko-Clowes, M. 2005. Lithostratigraphy, biostratigraphy and palaeoenvironment of the Upper Albian–Lower/Middle Eocene flysch deposits in the Beskid Wyspowy and Gorce Ranges; Polish Outer Carpathians, Magura Nappe; Bystrica and Rača subunits. Annales Societatis Geologorum Poloniae, 75, 27–69.

Oszczypko, N. and Oszczypko-Clowes, M. 2009. Stages in the Magura Basin: a case study of the Polish sector (Western Carpathians). Geodinamica Acta, 22, 83–100.

Oszczypko, N., Salata, D. and Krobicki, M. 2012. Early Cretaceous intra-plate volcanism in the Pieniny Klippen Belt – a case study of the Velykyi Kamenets'/Vilkhivchyk (Ukraine) and the Biała Woda (Poland) sections. Geological Quarterly, 56, 629–648.

Oszczypko, N., Oszczypko-Clowes, M. and Olszewska, B. 2020. Geological setting and lithological inventory of the Czarna Woda conglomerates (Magura Nappe, Polish Outer Carpathians). Acta Geologica Polonica, 70, 397–418.

Passendorfer, E. 1930. Studjum stratygraficzne i paleontologiczne and kredą serji wierchowej w Tatrach (Étude stratigraphique et paléontologique du Crétacé de la séroe hau-tatrique dans les Tatras). Prace Państwowego Instytutu Geologii, 2, 548–667 (1–327).

Picha, F.J. 1996. Exploring for hydrocarbons under thrust belts a challenging new frontier in the Carpathians and elsewhere. American Association of Petroleum Geologists Bulletin, 89, 1547–1564.

Plašienka, D., Grecula, P., Putiš, M., Kováč, M. and Hovorka, D. 2000. Evolution and structure of the Western Carpathians: an overview. In: Grecula, P., Hovorka, D. and Putiš, M. (Eds), Geological evolution of the Western Carpathians, 1–24. Geocomplex; Bratislava.

Plašienka D. 2018. Continuity and episodicity in the early Alpine tectonic evolution of the Western Carpathians: how large-scale processes are expressed by the orogenic architecture and rock record data. Tectonics, 37, 2029–2079.

Poprawa, P., Krobicki, M., Nejbert, K., Armstrong, R. and Pecskay, Z. 2013. Egzotyki skał magmowych ze żwirowców ilastych kredy i paleocenu pienińskiego pasa skałkowego – nowe dane geochemiczne i geochronologiczne (U-Pb SHRIMP i K/Ar). In: Krobicki, M. and Feldman-Olszewska, A. (Eds), V Polska Konferencja Sedymentologiczna POKOS 5'2013, Głębokomorska sedymentacja fliszowa, Sedymentologiczne aspekty historii basenów karpackich; 16–19.05.2013 Żywiec, Abstrakty referatów i posterów oraz artykuły, Przewodnik do wycieczek, 211–214.

Potfaj, M. 2002. The saddle between Haligovce and Lesnica. Guide to geological excursions. XIIth Congress Carpathian-Balkan Geological Association., Bratislava, Slovak Republic, Bratislava: appendix.

Price, G.D., Főzy, I. and Pálfy, J. 2016. Carbon cycle history through the Jurassic–Cretaceous boundary: A

new global $\delta^{13}C$ stack. Palaeogeography, Palaeoclimatology, Palaeoecology, 451, 46–61.

Pszczółkowski, A. 2003a. Kościeliska Marl Formation (Lower Cretaceous) in the Polish Western Tatra Mountains: lithostratigraphy and microfossil zones. Studia Geologica Polonica, 121, 7–50.

Pszczółkowski, A. 2003b. Tithonian–Hauterivian events from the lower Subtatric succession of the Tatra Mts (Western Carpathians) in the framework of calpionellid stratigraphy (southern Poland). Przegląd Geologiczny, 51, 987–994 [in Polish with English summary].

Pszczółkowski, A. 2015. Aptian foraminiferal stratigraphy and *Nannoconus* assemblages from the Kopka section (Western Tatra Mountains, Poland). Annales Societatis Geologorum Poloniae, 85, 123–138.

Pszczółkowski, A., Grabowski, J., Michalík, J. and Sobień, K. 2010. Latest Berriasian–Hauterivian carbon isotope stratigraphy and magnetic susceptibility: new data from three West Carpathian sections of Poland and Slovakia. In: Granier, B. (Ed.), STRATI 2010 Abstracts. 4th French Congress on Stratigraphy, 194–195. Paris.

Pszczółkowski, A., Grabowski, J. and Wilamowski, A. 2016. Integrated biostratigraphy and carbon isotope stratigraphy of the Upper Jurassic shallow water carbonates of the High-Tatric Unit (Mały Giewont area, Western Tatra Mountains, Poland). Geological Quarterly, 60, 893–918.

Radwański, Z. 1978. Sedimentary environment of the Sromowce Formation flysch deposits (Upper Cretaceous) of the Pieniny Klippen Belt, Carpathians, Poland. Studia Geologica Polonica, 57, 7–86. [in Polish, English summary]

Reháková, D. 2000. Evolution and distribution of the Late Jurassic and Early Cretaceous calcareous dinoflagellates recorded in the Western Carpathian pelagic carbonate facies. Mineralia Slovaca, 32, 79–88.

Reháková, D. and Michalík, J. 1997. Evolution and distribution of calpionellids – the most characteristic constitutents of Lower Cretaceous Tethyan microplankton. Cretaceous Research, 18, 493–504.

Reháková, D. and Wierzbowski, A. 2005. Microfacies, and stratigraphic position of the Upper Jurassic Rogoża Coquinas at Rogoźnik, Pieniny Klippen Belt, Carpathians. Tomy Jurajskie, 3, 15–27.

Richey, J.D., Upchurch, G.R., Montañez, I.P., Lomax, B.H., Suarez, M.B., Crout, N.M., Joeckel, R.M., Ludvigson, G.A. and Smith, J.J. 2018. Changes in CO_2 during Ocean Anoxic Event 1d indicate similarities to other carbon cycle perturbations. Earth and Planetary Science Letters, 491, 172–182.

Roniewicz, P. 1969. Sedymentacja eocenu numulitowego Tatr. Acta Geologica Polonica, 19, 503–608.

Rychliński, T. 2008. Facies development and sedimentary environments of the Carpathian Keuper deposits from the Tatra Mountains, Poland and Slovakia. Annales Societatis Geologorum Poloniae, 78, 1–18.

Rychliński, T. and Szulc, J. 2005. Facies and sedimentary environments of the upper Scythian–Carnian succession from the Belanske Tatry Mountains, Slovakia. Annales Societatis Geologorum Poloniae, 75, 155–169.

Săndulescu, M. 1988. Cenozoic Tectonic History of the Carpathians, In: Royden, L. and Horváth, F. (Eds), The Pannonian Basin: A study in basin evolution. American Association of Petroleum Geology, Memoire, 45, 17–25.

Scheibner, E. 1968. Contribution to the knowledge of the Paleogene reef-complexes of the Myjava Hričov-Haligovka zone (West Carpathians). Mitteilungen Bayerischen Palaontologie und historische Geologie, 8, 67–97.

Schlögl, J., Rakús, M., Krobicki, M., Matyja, B.A., Wierzbowski, A., Aubrecht, R., Sitár, V. and Józsa, Š. 2004. Beňatina Klippe – lithostratigraphy, biostratigraphy, palaeontology of the Jurassic and Lower Cretaceous deposits (Pieniny Klippen Belt, Western Carpathians, Slovakia). Slovak Geological Magazine, 10, 241–262.

Schnetger, B., Brumsack, H.-J., Schale, H., Hinrichs, J. and Dittert, L. 2000. Geochemical characteristics of deep-sea sediments from the Arabian Sea: a high-resolution study. Deep-Sea Research II, 47, 2735–2768.

Soták, J. 1986. Stratigraphy and typlogy of the Upper Triassic development in outer units in the West Carpathians (reconstructions from redeposites localised in the Silesian Cordillera area). Knihovnicka Zemny Plyn a Nafta, 31, 1–53.

Spišiak, J. and Sýkora, D. 2009. Geochemistry and mineralogy of the Hanigovce basalts – the Proc (Jarmuta) beds. In: Jurkovic, L., Slaninka, I. and Durža, O. (Eds), Symposium of the State Geological Institute of Dionýz Štur, 106–109. Bratislava.

Stampfli, G.M. (Ed.) 2001. Geology of the western Swiss alps – a guide book. Mémoires de Géologie (Lausanne), 361, 1–195.

Ślączka, A. and Kaminski, M.A. 1998. A Guidebook to excursions in the Polish Carpathians: Field Trips for Geoscientists, 173 p. Grzybowski Foundation, Special Publication, 6. Kraków.

Ślączka, A., Kruglow, S., Golonka, J., Oszczypko, N. and Popadyuk, I. 2006. The General Geology of the Outer Carpathians, Poland, Slovakia, and Ukraine. In: Picha, F. and Golonka, J. (Eds), The Carpathians and their foreland: Geology and hydrocarbon resources: American Association of Petroleum Geologists, Memoir, 84, 1–70.

Śmigielski, M., Sinclair, H.D., Stuart, F.M., Persano, C. and Krzywiec, P. 2016. Exhumation history of the Tatra Mountains, Western Carpathians, constrained by low-temperature thermochronology. Tectonics, 10.1002/2015TC003855.

Świerczewska, A. and Pszczółkowski, A. 1997. Skład i

pochodzenie materiału detrytycznego piaskowców ogniwa z Krytej (Kreda dolna, Tatry). In: Wojewoda, J. (Ed.), Obszary Źródłowe: Zapis w Osadach. Materiały Konferencyjne. VI Krajowe Spotkanie Sedymentologów. Lewin Kłodzki, 26–28.09.1997: 55–56. Wind; Wrocław.

Turnšek, D. and Drobne, K. 1998. Paleocene corals from the northern Adriatic platform. In Hottinger, L. and Drobne, K. (Eds.), Paleogene Shallow Benthos of the Tethys 2. Dela-Opera SAZU 4. Razprave, Slovenian Academy of Science and Arts, Ljubljana, 32, 129–154.

Tyszka, J. 1994. Response of Middle Jurassic benthic foraminiferal morphogroups to disoxic/oxic conditions in the Pieniny Klippen Basin, Polish Carpathians. Palaeogeography, Palaeoclimatology, Palaeoecology, 110, 55–81.

Tyszka, J. 2001. Microfossil assemblages as bathymetric indicators of the Toarcian/Aalenian "Fleckenmergel"-facies in the Carpathian Pieniny Klippen Belt. Geologica Carpathica, 52, 147–158.

Vašíček, Z. 1997. Ammonite stratigraphy of the pre-Albian Lower Cretaceous formations of the Western Carpathians (Czech and Slovak republics). Geologica Carpathica, 48, 231–242.

Vašíček, Z., Błażejowski, B., Gaździcki, A., Król, M., Lefeld, J., Skupien, P. and Wierzbowski, A. 2020. Early Cretaceous ammonites and dinoflagellates from the Western Tatra Mountains, Poland. Acta Palaeontologica Polonica 65, 4, 799–810.

Vecsei, A. and Moussavian, E. 1997. Paleocene reefs on the Maiella Platform Margin, Italy: an example of the effects of the Cretaceous/Tertiary boundary events on reefs and carbonate platforms. Facies, 36, 123–140.

Uchman, A. 1993. Lower Jurassic carbonate sedimentation controlled by tilted blocks in the Choč Unit in the Tatra Mts, Poland. Zentralblatt für Geol und Paläontol., 1, 875–883

Uchman, A. 1997. Paleoenvironment of the Cretaceous marlstones in the Polish Tatra Mts. in the light of ichnological researches. Przegląd Geologiczny, 45, 10, 1018–1023. Warszawa [In Polish, English summary].

Uchman, A. 2014. Przedmowa. In: Jach, R., Rychliński, T. and Uchman, A. (Eds), Skały osadowe Tatr (Sedimentary Rocks of the Tatra Mountains). Tatrzański Park Narodowy, Zakopane, p. 11.

Uhlig, V. 1897. Geologie des Tatragebirges. II. Tektonik des Tatragebirges. III. Geologische Gesicht des Tatragebirges. IV. Beiträge zur Oberflächengeologie. Denkschriften der Akademie der Wissenschaften, Mathematisch-Naturwissenschaftliche Klasse, 68, 43–140.

Wei, G., Li, X.-H., Liu, Y., Shao, L. and Liang, X. 2006. Geochemical record of chemical weathering and monsoon climate change since the early Miocene in the South China. Paleoceanography, 21, PA4214. DOI: 10.1029/2006pa001300.

Westermann, S., Föllmi, K.B., Adatte, T., Matera, V., Schnyder, J., Fleitmann, D., Fiet, N., Ploch, I. and Duchamp-Alphonse, S. 2010. The Valanginian $\delta^{13}C$ excursion may not be an expression of a global anoxic event. Earth and Planetary Science Letters, 290: 118–131.

Wieczorek, J. 1988. Maiolica – A unique facies of the Western Tethys. Annales Societatis Geologorum Poloniae, 58, 255–276.

Wierzbowski, A. 1994. Late Middle Jurassic to earliest Cretaceous stratigraphy and microfacies of the Czorsztyn Succession in the Spisz area, Pieniny Klippen Belt, Poland. Acta Geologica Polonica, 44, 3–4, 223–249.

Wierzbowski, A. and Remane, J. 1992. The ammonite and calpionellid stratigraphy of the Berriasian and lowermost Valanginian in the Pieniny Klippen Belt (Carpathians, Poland). Eclogae geologice Helvetiae, 85, 3, 871–891.

Wierzbowski, A., Jaworska, M. and Krobicki, M. 1999. Jurassic (Upper Bajocian–lowest Oxfordian) ammonitico rosso facies in the Pieniny Klippen Belt, Carpathians, Poland, its fauna, age, microfacies and sedimentary environment. Studia Geologica Polonica, 115, 7–74.

Wierzbowski, A., Aubrecht, R., Krobicki, M., Matyja, B.A. and Schlögl, J. 2004. Stratigraphy and palaeogeographic position of the Jurassic Czertezik Succession, Pieniny Klippen Belt (Western Carpathians) of Poland and Eastern Slovakia. Annales Societatis Geologorum Poloniae, 74, 237–256.

Wierzbowski, A., Aubrecht, R., Golonka, J., Gutowski, J., Krobicki, M., Matyja, B.A, Pieńkowski, G. and Uchman, A. (Eds). 2006. Jurassic of Poland and adjacent Slovakian Carpathians. Field trip guidebook. 7th International Congress on the Jurassic System, 6–18 September 2006, Kraków, Poland, 3–235.

Wierzbowski, A., Krobicki, M. and Matyja, B.A. 2012. The stratigraphy and palaeogeographic position of the Jurassic successions of the Priborzhavske-Perechin Zone in the Pieniny Klippen Belt of the Transcarpathian Ukraine. Volumina Jurassica, 10, 25–60.

Wigilew [Vigilev], B. 1914. Neokom reglowy w Tatrach (Das subtatrische Neokom in der Tatra). Polska Akademia Umiejętności, Sprawozdania Komisji Fizjograficznej, 48, 42–46.

Żytko, K., Zając, R., Gucik, S., Ryłko, W., Oszczypko, N., Garlicka, I., Nemčok, J., Eliáš, M., Menčik, E. and Stránik, Z. 1989. Map of the tectonic elements of the Western Outer Carpathians and their foreland. In: Poprawa, D. and Nemčok, J. (Eds), Geological Atlas of the Western Outer Carpathians and their Foreland. Państwowy Instytut Geologiczny, Warszawa; GUDŠ, Bratislava; Uug, Praha.

11TH INTERNATIONAL
CRETACEOUS
SYMPOSIUM
Warsaw, Poland, 2022

THE JURASSIC–CRETACEOUS TRANSITION IN THE WESTERN CARPATHIANS

Jacek Grabowski[1]| Damian Lodowski[1,2]| Jozef Michalík[3]| Daniela Reháková[4]| Ottilia Szives[5]| Špela Goričan[6]| Ottilia Lintnerová[4]| Eva Halásová[4]| Lilian Švabenická[7]| Kamil Fekete[8]| Daniela Boorova[8]

1| Polish Geological Institute – National Research Institute, Rakowiecka 4, 00-975 Warszawa, Poland; e-mail: jacek.grabowski@pgi.gov.pl; damian.lodowski@pgi.gov.pl

2| Faculty of Geology, University of Warsaw, Żwirki i Wigury 93,02-089 Warszawa, Poland; e-mail: damian.lodowski@uw.edu.pl

3| Earth Science Institute of the Slovak Academy of Sciences, Dúbravská cesta 9, 840 05, Bratislava, Slovakia; e-mail: Jozef.Michalik@savba.sk

4| Faculty of Natural Sciences, Department of Geology and Paleontology, Mlynska Dolina, Ilkovičova 6, 842 15 Bratislava, Slovakia; e-mails: daniela.rehakova@uniba.sk; ottilia.lintnerova@uniba.sk; eva.halasova@uniba.sk

5| Department of Palaeontology and Geology, Hungarian Natural History Museum, 1431 Budapest, Pf. 137, Hungary; e-mail: szives.ottilia@nhmus.hu

6| Ivan Rakovec Institute of Paleontology, Research Centre of the Slovenian Academy of Sciences and Arts, Novi trg 2, 1000 Ljubljana, Slovenia; e-mail: spela@zrc.sazu.si

7| Czech Geological Survey, Klarov 131/3, 118 21 Prague, Czech republic; e-mail: lilian.svabenicka@geology.cz

8| State Geological Institute of Dionýz Štúr, Mlynská dolina 1, 817 04 Bratislava, Slovakia; e-mails: kamil.fekete@geology.sk; daniela.boorova@geology.sk

ABSTRACT

A set of high-resolution bio- (calpionellid, calcareous dinocyst, calcareous nannofossil), magneto-, chemo- ($\delta^{13}C$), and cyclostratigraphic techniques, in addition to sedimentological, rock magnetic, and geochemical observations, enable precise local and regional correlations in selected Jurassic–Cretaceous boundary sections within the Pieniny Klippen Belt and Transdanubian Range of the Western Carpathians. Four sections (Brodno and Snežnica in the Pieniny Klippen Belt; Hárskút and Lókút in the Transdanubian Range), while variable in facies and lithologic characteristics, depict a consistent bioevent scheme as well as corresponding paleoenvironmental attributes, including lithogenic input fluxes and $\delta^{13}C$ trends. Preliminary interpretations indicate that these might have been related to latest Jurassic–earliest Cretaceous climatic perturbations that affected a vast part of the western Tethyan domain.

INTRODUCTION

The position of the Jurassic/Cretaceous (J/K) boundary poises a longstanding problem: indeed, it is the last system boundary that has not been fixed yet. Since 1975 (Énay 2020), the base of the Berriasian Stage has served as the leading nominee for the boundary between the Jurassic and Cretaceous Systems. In 2016, the Berriasian Working Group voted to designate the acme event of *Calpionella alpina*, a marker of the base of the Alpina Subzone, as the primary marker for the Tithonian/Berriasian (T/B) boundary (Wimbledon et al. 2020). However, even in the Tethys, calpionellids are not the only critical faunal elements in the Late Jurassic and Early Cretaceous: ammonites, calcareous dinocysts, and nannofossils have significant scientific – and historical – importance for characterizing the J/K transition interval (Reháková and

Michalík 1997; Frau et al. 2016a, b, c; Casellato and Erba 2021; Szives and Főzy 2022). In addition to the classical paleontological criteria for placing stage or system boundaries, independent methods, including magneto-, chemo-, climate-, and cyclostratigraphy, may provide important data for supraregional correlation (see Deconinck 1993; Schnyder et al. 2006; Grabowski et al. 2010, 2017; Schnabl et al. 2015; Price et al. 2016; Galloway et al. 2020).

One of the major purposes of the GSSP Program is the collection of data from complete sections that could serve as candidate stage boundary stratotypes. A diverse variety of regional stratotypes can provide continuous records of sedimentation and biotic events across the Jurassic/Cretaceous boundary, enabling a precise evaluation of all proxies necessary for an exact designation of the boundary location.

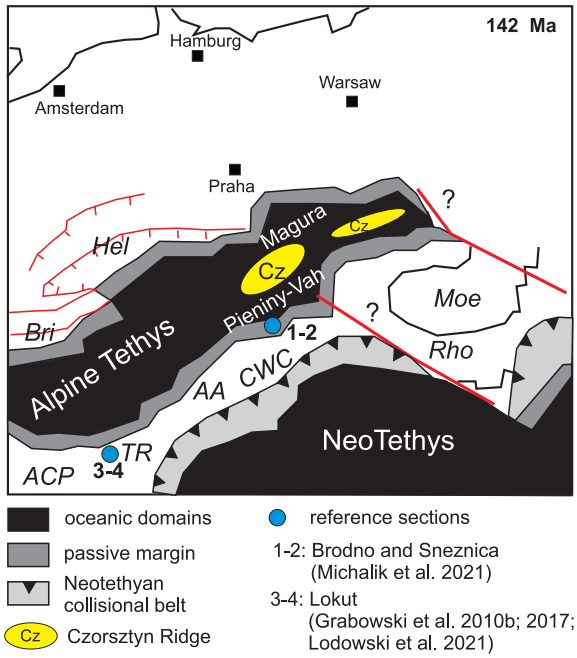

Fig. 1. Simplified paleogeographic sketch of the Alpine – Carpathian area in the Berriasian (modified after Stampfli and Hochard 2009; Grabowski et al. 2019), and schematic position of the sections visited during the excursion. AA – Austroalpine Units, ACP – Adriatic Carbonate Platform, Bri – Brianconnais, CWC – Central Western Carpathians, Cz – Czorsztyn Ridge, Hel – Helvetic Unit, Moe – Moesian Platform, Rho – Rhodopes, TR – Transdanubian Mountains. Note that the northeast termination of the Alpine Tethys was probably not blind (note the question marks), and the ocean continued towards the southeast between the CWC and Moesia-Rhodopes, connecting with the NeoTethys (Golonka et al. 2005).

TITHONIAN/BERRIASIAN SECTIONS IN THE PIENINY KLIPPEN BELT (SLOVAKIA) AND TRANSDANUBIAN MTS (HUNGARY)

(Jozef Michalík, Ottilia Szives, Damian Lodowski and Jacek Grabowski)

The Pieniny Klippen Belt and Transdanubian Mountains were situated on the southern margin of the Alpine Tethys (Ligurian–Penninic–Vahic Ocean; Fig. 1). The facies development of the Jurassic/Cretaceous transition in both domains is quite similar to that of other Western Tethyan basins (e.g., Bernoulli and Jenkyns 2009; Jach and Reháková 2019). The Oxfordian and lower Kimmeridgian are represented by radiolarites and radiolarian limestones. Red nodular limestones (*Ammonitico Rosso*) typically occur in the upper Kimmeridgian and lower Tithonian. During the late Tithonian and Berriasian, the sedimentation rate of calcareous micro- and nannoskeleton-derived "planktonic rain" accelerated, producing whitish pelagic sediments of the *Maiolica* type.

In the Western Carpathians, the Brodno section (Michalík et al. 1990, 2009, 2021; Houša et al. 1996a, b) has been proposed as the regional J/K boundary stratotype. Due to some gaps in its stratigraphic record (for instance, missing index ammonites, and somewhat reduced thickness), complementary J/K boundary successions have been recently studied in the Central Carpathians, including the Strážovce section (Borza 1984; Michalík et al. 1990) and the Hlboča section (Grabowski et al. 2010). Additional research has been undertaken in the Pośrednie sections in the Tatra Mountains (Grabowski and Pszczółkowski 2006; Grabowski et al. 2013), as well as in the Ukrainian part of the Pieniny Klippen Belt (Grabowski et al. 2019).

Our field trip will demonstrate the J/K boundary sequence in two pelagic limestone sections of the Slovakian part of the Pieniny Klippen Belt (stops 1 and 2).

The Transdanubian Range Unit covers the majority of northwest Hungary, encompassing the area north of Lake Balaton and west of the Danube River (Figs 2, 23). Together

Fig. 2. Field trip route marked on the general topographic map of the Western Carpathians.

with the Zagorje–Mid-Transdanubian and the Bükk Units, it constitutes part of the Pelso Composite Unit, formed during the Late Cretaceous–Early Paleogene collision of these microterranes. In turn, the Pelso, along with the Austroalpine, Penninic and Western Carpathian Units, was amalgamated during the Paleogene–early Miocene tectonic reorganization of the Alpine–Carpathian domain into the present-day ALCAPA composite terrane. The Transdanubian Range itself is composed of a few low (up to 757 m a.s.l.) mountain ranges made of slightly metamorphosed Variscan basement and unconformably overlying Alpine sequences (Szederkényi et al. 2013), providing a record of the transitional zone between the Austroalpine and South Alpine Zones (e.g., Haas and Péró 2004; Csontos and Vörös 2004).

During the Late Jurassic, the Transdanubian Range was characterized by large-scale basin-and-horst architecture, with typically pelagic sedimentation prevailing in basins and non-deposition or condensation zones on horsts (Vörös and Galácz 1998). In connection with the progressive closure of the Neotethys, uplift in its marginal zones (e.g., Gawlick et al. 2009; Missoni and Gawlick 2011) resulted in the division of the Transdanubian Range into two basins: the Gerecse Basin in the northeast and the Bakony Basin in the south (see below and Fig. 23). The former, proximal to the collision zone, was dominated by fine-grained siliciclastic and argillite sedimentation, whereas in the distal Bakony Basin pelagic carbonates and siliceous oozes were deposited. The two basins were separated by a submarine elevation (forebulge), on which limited condensed carbonate sedimentation took place (Fülöp 1964; Tari 1994; Lodowski et al. 2022). Recently, new bio- and magnetostratigraphic and geochemical investigations were carried out on some Hungarian sections, namely Lókút (Grabowski et al. 2010, 2017; Lodowski et al. 2022), Hárskút (HK-12 and HK-12/a) (Lodowski et al. 2022), and the Szilas Ravine. Geochemical research was previously performed on HK-12 by Főzy et al. (2010) and on HK-II and Lókút LH-I by Price et al. (2016). Very recently, ammonite collecting at HK-12/a clarified the ammonite biostratigraphy of the section (Szives and Főzy 2022).

The two localities visited during this field trip (stops 3 and 4) are located in the central

Bakony Mountains. They provide a record of the marginal parts of the Bakony Basin (the Lókút succession, of the external "Zirc Basin") and the swell facies (Hárskút succession). The Upper Jurassic–Lower Cretaceous sedimentary sequence of the Bakony Mountains initiates with Oxfordian radiolarites of the Lókút Radiolarite Formation. These are followed by the Kimmeridgian–mid-Tithonian *Ammonitico Rosso*-type limestones of the Pálihálás Formation and the upper Tithonian–Berriasian *Maiolica*-type Szentivánhegy Limestone Formation. In the northeast part of the Bakony Basin, the Szentivánhegy Limestone Formation is covered by the crinoid-rich Valanginian–Hauterivian Borzavar Limestone Formation, which towards the south is gradually replaced by marly limestones of the Mogyorósdomb Limestone Formation, which in the south Bakony constitutes the entire Tithonian–Hauterivian. The top of the Bakony Basin succession is represented by the Hauterivian–Barremian marls of the Sümeg Marl Formation, which are capped and sealed by a slight angular unconformity (Fülöp 1964; Haas 1995; Szederkényi et al. 2013; Lodowski et al. 2022).

FIELD STOPS

Stop 1:
Brodno section

(Jozef Michalík, Daniela Reháková, Otília Lintnerová, Eva Halásová, Kamil Fekete, Jacek Grabowski and Damian Lodowski)

The Brodno section is situated in an abandoned quarry on the eastern side of the narrow straits of the Kysuca River Valley, known as the "Kysuca Gate", north of Žilina (49° 16' 03.2" N, 18° 45' 12.7" E) (Michalík et al. 2009; Fig. 3). It yields a record of hemipelagic marine sedimentation in a marginal zone (the Pieniny Klippen Belt) of the Outer Western Carpathians. The lithology, fossil record and stratigraphy were studied by Andrusov (1938, 1950, 1959), Scheibner (1961, 1962, 1967), Borza (1969), Scheibner and Scheibnerová (1969), and Samuel et al. (1988). A more detailed description of Upper Jurassic and Lower Cretaceous litho- and biostratigraphy was provided by Michalík et al. (1990), Reháková and Michalík (1992), and Vašíček et al. (1992). Houša et al. (1996) introduced the magnetostratigraphy of the Jurassic/Cretaceous boundary beds and correlated it with microbiostratigraphic data.

The results of an integrated biostratigraphic study using three microplankton groups (calpionellids, calcareous dinoflagellates, and nannofossils) and stable isotope ($\delta^{18}O$, $\delta^{13}C$) chemostratigraphy in the Brodno section were discussed by Michalík et al. (2009, 2021). This section was proposed as the West Carpathian regional J/K boundary stratotype. Although the Brodno section lacks an ammonite record, it does represent a continuously well-exposed, biostratigraphically documented succession, at least by the standards of the West Carpathian region. The distribution of stratigraphically important planktonic organisms

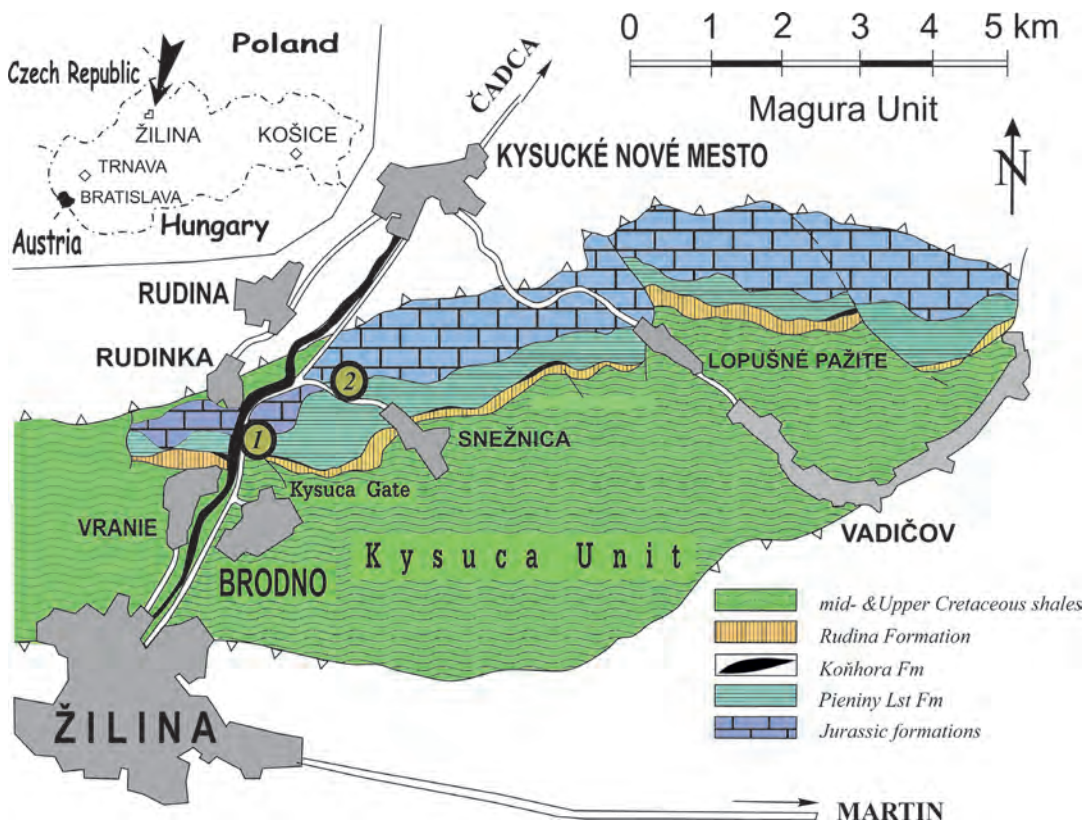

Fig. 3. Location of the Brodno (1) and Snežnica (2) sections in the Kysuca Gate, north of Žilina.

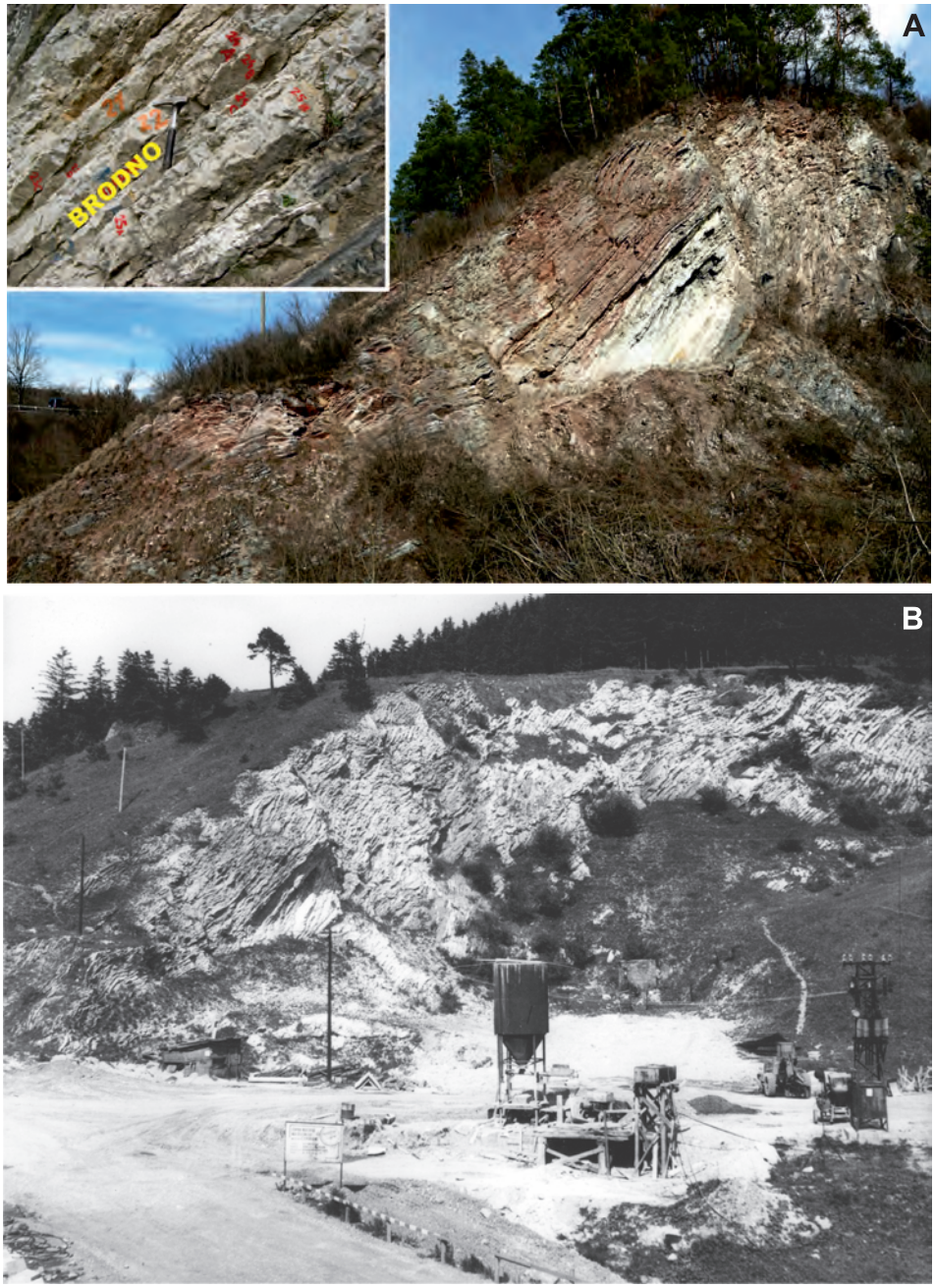

Fig. 4. A. Brodno Quarry at the foot of Brodnianka Hill – a general view of the Western Carpathian J/K boundary stratotype. The sequence is overturned: the left, upper side of the rock wall captures the Czorsztyn Limestone Formation, and the right side is formed by the Pieniny Limestone Formation. Upper left: a detailed view of the Jurassic/Cretaceous boundary interval with the Brodno (M19n1r) magnetosubchrone in the lowermost Berriasian. B. Historical photo of Brodno Quarry from the 1960s. Archive of Dimitry Andrusov.

reveal several coeval calpionellid and nannofossil bioevents in the Jurassic/Cretaceous boundary pelagic carbonate sequence. Stable isotope data underline environmental changes during the studied interval.

The succession starts with red nodular marly limestones of the *Ammonitico Rosso* lithofacies, known as the Czorsztyn Limestone Formation (Birkenmajer 1977; Fig. 4). As in many other Tethyan areas, Late Jurassic sedimentation rates in the Pieniny Klippen Basin were low. On the basis of magnetostratigraphy,

sediment accumulation rates were estimated to be 1–2 m/Ma (Grabowski and Pszczółkowski 2006; Michalík et al. 2021). In an analysis of Milankovitch frequency band periodicity in the Spanish Rio Argos section, Hoedemaeker and Lereveld (1995) situated sequence boundaries at the base of marly interbeds. In a similar vein, Schlager (2005) suggested that siliciclastics may be found in all system tracts, as they are a common constituent of basinal lowstand fans ("reciprocal sedimentation"). On the contrary, Michalík (2007) argued that the character of lowstand deposits strongly depends on the lithological composition of the emergent shoreline. As the Lower Cretaceous lowstand sequences in the West Carpathians were mostly supplied by carbonate platform-derived calcitic debris, they consisted of fine-detrital (grain size, of course, depending on proximity to shoreline) limestone beds.

Sedimentary environment and sequence architecture

According to the analysis of microfacies distribution (see Michalík 2007), several cyclic microfacies repetitions were recognized in part of the sequence on the left side of the quarry wall (Fig. 4). These cycles are 0.5 to 1.6 m thick. Considering an average sedimentary rate of 2 mm/ka, which is derived from microbiostratigraphic and magnetostratigraphic analysis, their duration should be roughly 400 kilo-years (800 or 2,400 ka, respectively). As phenomena demonstrating cycle condensation and amalgamation are generally common in this facies, these oscillations evidently were characteristic of long eccentricity Milankovich cycles. Cycle architecture seems to have been controlled by eustatic sea-level change. The sequence is arranged into inexpressive low frequency (40 ka, i.e., obliquity) cycles expressed by alternations of limestone layers and more marly insertions. The origin of these cycles was probably driven by climatic (humidity-driven) oscillations. The biostratigraphic boundaries are usually not identical to sequence boundaries; instead, biostratigraphic boundaries are usually located within the highstand of the underlying cycle (Fig. 5).

1. The lowermost cycle (beds L51 to L58) consists of pale greenish to rose-colored limestones (*Saccocoma* to *Globochaete* wackestones) with microfossils (*Cadosina parvula*, *Stomiosphaera moluccana*, *Cadosina semiradiata semiradiata*, *Colomisphaera pulla*, and *Carpistomiosphaera tithonica*) documenting the lower Tithonian Pulla and Tithonica Zones. The last, thickest and most micritic layer (L58) represents highstand conditions close to the end of magnetochron M22n.

2. The second cycle, thin-bedded nodular to brecciated pale greenish limestones (wackestone to packstone) with red cherts and marly interlaminae (beds L59 to L67), is terminated by the thicker layer L68, constituting the highstand. *Saccocoma* and *Globochaete alpina* predominate over crinoid ossicles, bivalve and aptychi fragments, ostracod shells, foraminifera tests, calcified radiolarians, and dinoflagellates of the lower Tithonian Malmica Zone association. The calcareous nannofossil assemblage from the L52–L68 interval is dominated by *Conusphaera mexicana mexicana*, *Conusphaera mexicana minor*, *Cyclagelosphaera margerelii*, *Cyclagelosphaera deflandrei*, *Watznaueria barnesiae*, and *Watznaueria manivitae*.

3. The lower part (beds L69 to L74) of the third cycle consists of radiolarian–globochaetid wackestone and packstone. Acme accumulations of thick-walled *Cadosina semiradiata semiradiata* (L69) and *Cadosina semiradiata fusca* (Semiradiata Acme Zone) accompanied by abundant *Conusphaera* may be a proxy of increasing sea surface temperatures. The middle part (beds L75 to L79) of the cycle is formed by rose-gray biomicrite of the radiolarian–*Saccocoma*–*Globochaete* microfacies (packstone and wackestone). Calcareous dinoflagellate cysts and early calpionellid forms (Fig. 5) are indicative of the Dobeni Subzone of the uppermost lower Tithonian Chitinoidella Zone. The upper part (beds L80 to L89) of the cycle consists of marly nodular to brecciated limestones with marly interlaminae. The occurrence of *Chitinoidella boneti*, *Borziella slovenica*, *Dobeniella tithonica*, *Dobeniella cubensis*, and *Dobeniella bermudezi* characterizes the Boneti Subzone of the Chitinoidella Zone. Calcareous nannofossils obtained from L69 to L96 were assigned to the Polycostella beckmannii Subzone (NJ 20-B) within the middle Tithonian, in magnetochrones M21n to M20n2n. The assemblages of the lower part of this interval are dominated by *Conusphaera mexicana mexicana*, accompanied by *Conusphaera mexicana*

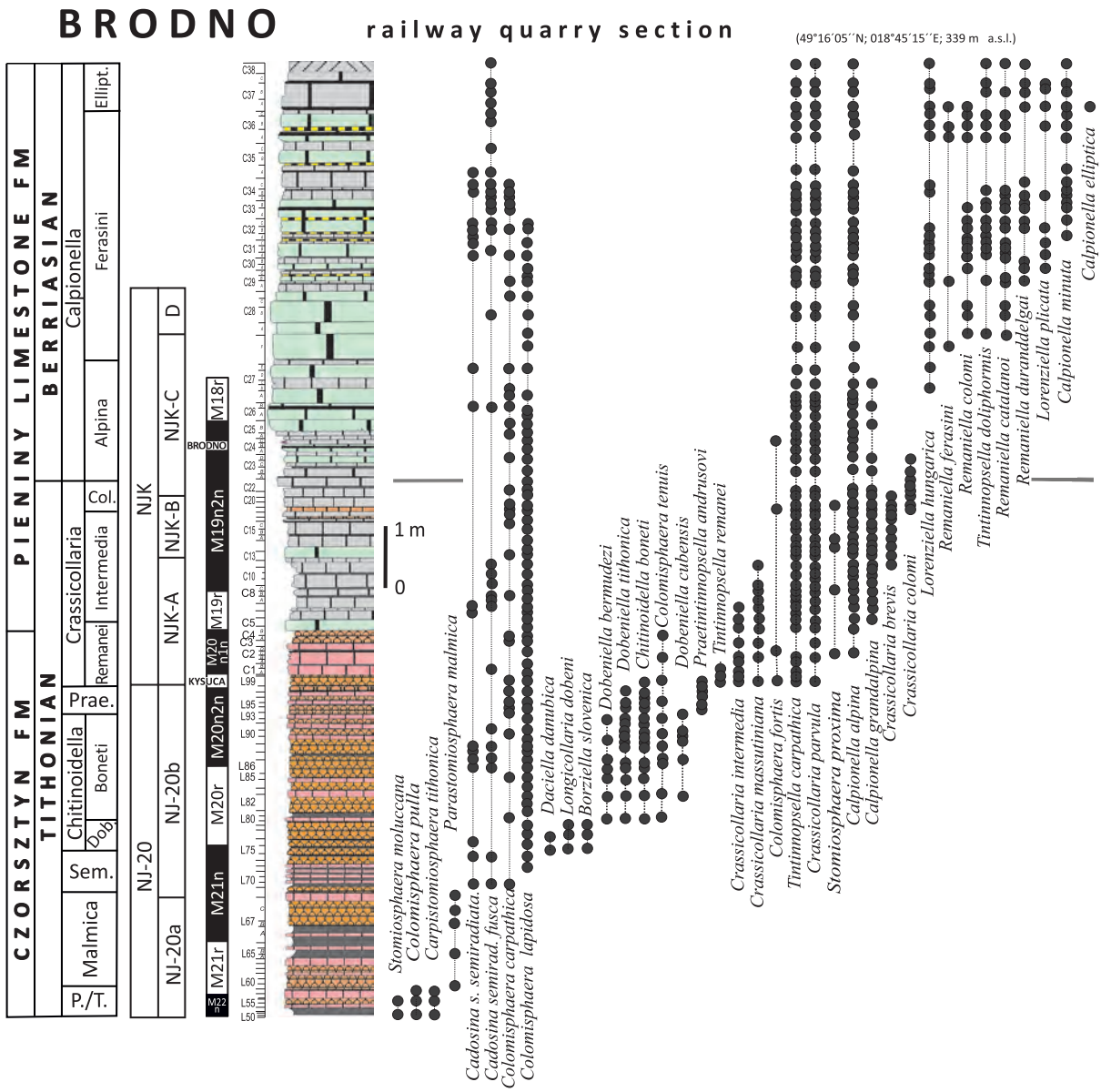

Fig. 5. Lithological log of the studied Brodno sequence, calpionellid and calcareous dinoflagellate distribution, and calcareous nanofossil zonation (after Michalík et al. 2009, 2021). Abbreviations: P./T. – Pulla/Tithonica; Sem. – Semidardiata; Dob – Dobeni; Prae – Praetintinnopsella; Col. – Colomi; Ellipt. – Elliptica.

minor, *Watznaueria barnesiae,* and *Watznaueria manivitae*. The nannolitic form of *Polycostella beckmannii* is abundant in beds L77–L83. *Discorhabdus ignotus* and *Zeugrhabdotus erectus* occur less frequently.

4. The fourth cycle (L90 to L98) is represented by a pale, bedded, indistinctly nodular biomicrite limestone complex. Radiolarian–*Saccocoma*–*Globochaete* wackestones, and locally silicified *Saccocoma*–radiolarian biomicrites contain *Colomisphaera tenuis*, *Schizosphaerella minutissima* and *Colomisphaera carpathica*. *Chitinoidella boneti*, *Dobeniella tithonica*, *Dobeniella bermudezi* and transitional early hyaline *Praetintinnopsella andrusovi* characterize the uppermost Boneti Subzone (Chitinoidella Zone) and the passage into the upper Tithonian Praetintinnopsella Zone.

5. The fifth cycle begin at the base of bed L99 (Kysuca Subzone, magnetosubchrone M20n1r). Each limestone layer (4 to 20 cm thick) is separated by thin (2 to 40 mm) marly interlaminae.

Biomicrite wackestones with *Crassicollaria–Globochaete*–radiolarian microfacies contain *Crassicollaria intermedia*, which predominates over *Crassicollaria massutiniana*, *Crassicollaria parvula*, *Calpionela alpina*, *Calpionella grandalpina, Tintinnopsella remanei* and *Tintinnopsella carpathica*. The calcareous dinoflagellate association is composed of *Colomisphaera minutissima*, *Colomisphaera carpathica*, *Cadosina semiradiata semiradiata*, *Cadosina semiradiata fusca* and *Stomiosphaerina proxima*. The calpionellid index association is indicative of the upper Tithonian Remanei Subzone of the Crassicollaria Zone. Samples L98 to C26 were attributed to the Microstaurus chiastius Zone (NJK). The first occurrence (FO) of *Helenea chiastia* and *Hexalithus noeliae* indicates the upper Tithonian Hexalithus noeliae Subzone (NJK-A). The abundance of Watznaueriaceae coccoliths (*Watznaueria barnesiae, Watznaueria manivitae*) fluctuates between 25–80%, and that of *Cyclagelosphaera margerelii* between 3–20%; *Discorhabdus ignotus* and *Zeugrhabdotus erectus* are abundant (up to 10%) in bed C1B. The last occurrence (LO) of *Polycostella beckmannii* in sample C4A is characteristic of the upper Tithonian.

6. The sixth cycle (C14–C16) is composed of well-bedded, pale *Maiolica* limestones (*Crassicollaria–Globochaete* biomicrite and radiolarian–*Crassicollaria* wackstone) with thin (up to 2 cm) marly interbeds. Small *Crassicollaria brevis* dominates over *Calpionella grandalpina*, *Calpionella alpina*, *Crassicollaria parvula* and *Tintinnopsella carpathica.* Their association with the calcareous dinoflagellates *Schizosphaerella minutissima*, *Colomisphaera carpathica,* and *Stomiosphaerina proxima* characterize the Intermedia Subzone of the upper Tithonian Crassicollaria Zone. Here, the FO of *Nannoconus infans* (C13) and *Nannoconus wintereri* (C17) have been recorded.

7. Bedded pale gray biomicrite wackestone to packstone (C17–C22) with thin (up to 2 cm) marly interbeds, consisting of the crassicollarian–globochaete and radiolarian–globochaete–crassicollarian microfacies. Common *Globochaete* with *Crassicollaria parvula* and *Calpionella grandalpina* predominates over *Crassicollaria colomi*. *Calpionella alpina*, *Tintinnopsella carpathica*, and *Tintinnopsella doliphormis* are frequent. Dinoflagellate taxa include *Colomisphaera lapidosa*, *Colomisphaera carpathica*, *Colomisphaera fortis*, and *Stomiosphaerina proxima*. The presence of *Crassicollaria colomi* indicates the Colomi Subzone of the Crassicollaria Zone. One specimen of *Cruciellipsis cuvillieri* was found in C20, close to the FO of *Nannoconus wintereri.*

8. A well-bedded pale gray biomicritic wackestone, capturing the calpionellid–globochaete microfacies, with thin (up to 1 cm) marly insertions (C23A–C25A) dominated by small spherical *Calpionella alpina*. *Crassicollaria parvula*, *Crassicollaria colomi*, *Calpionella grandalpina* and *Tintinnopsella carpathica* are less frequent. The base of the Alpina Subzone of the Calpionella Standard Zone was identified in bed C24A. The Brodno Magnetosubchron (M19n1r) is located in layer C24B.

9. Well-bedded pale biomicritic wackestone, with *Calpionella–Globochaete* and *Calpionella*–radiolarian microfacies (C25B-27E). *Globochaete alpina* dominates over *Crassicollaria parvula*, *Tintinnopsella carpathica*, *Cadosina semiradiata fusca* and *Cadosina semiradiata semiradiata*. The microbreccia layers contain small limestone clasts with Tithonian microfossils.

10. A complex with anomalously thick (20–48 cm) layers of biomicritic *Calpionella* wackestone (C28A–C29A), terminated by a submarine slump. Small sphaerical *C. alpina* still dominate. The FO of *Nannoconus steinmanni minor*, along with an increase in the abundance and diversity of nannoconids, in bed C28 enables the placement of the base of the eponymous Subzone, which is correlated with the lowermost Berriasian. The start of the nannoconid bloom is indicated by the FO of *N. steinmanni minor*, *Nannoconus globulus minor* and *Nannoconus kamptneri minor*, accompanied by *Conusphaera mexicana mexicana*, *Cyclagelosphaera deflandrei*, *Cyclagelosphaera margerelii*, *Diazomatholithus lehmannii*, *Discorhabdus ignotus*, *Watznaueria barnesiae*, *Watznaueria britannica*, *Watznaueria manivitae*, and *Zeugrhabdotus embergeri.*

11. Thick-bedded cherty limestones with radiolarian–*Calpionella* microfacies (C29B–C38). Radiolarians are dispersed in the wackestone, but additionally are also concentrated in six 4–6 cm thick radiolarite layers. The FO of *Remaniella ferasini* in the overlying thick bedded cherty *Maiolica* limestones marks the base of the Ferasini Subzone of the standard Calpionella Zone.

Carbonate, C_{org}, and gamma ray spectrometry data

Organic matter concentrations in cycles 1 to 5 of the lower Tithonian (0.15 to 0.25%) gradually decrease upwards in each cycle (Fig. 6). The highest organic matter concentration was observed at the beginning of cycle 4 (bed L93). The lowest concentrations were attained just below the J/K boundary, in the upper parts of cycles 5 to 8 (at the base of the Pieniny Limestone Formation). In contrast, the calcium carbonate content gradually increases upwards (from 85% to 97%), with a restrained minimum in the 6th cycle at the base of the Pieniny Limestone Formation (Fig. 6). This increase in carbonate content aligns well with the emergence of nannoconids in the section. Preliminary gamma ray spectrometric (GRS) logging results confirm a relatively enhanced terrigenous input (Th and K content) in the lower part of the section, corresponding to the Czorsztyn Limestone Formation (i.e., to the base of magnetozone M19r). The upper part of the section reveals generally low, but fluctuating, terrigenous input (Fig. 7).

Stable carbon and oxygen isotopes

Globally, bulk micritic carbonate carbon isotope curves in J/K boundary sequences show smooth trends resulting from equilibrated bio-productivity and organic matter burial rates (Weissert and Channell 1989; Weissert and Lini 1991; Weissert and Mohr 1996; Gröcke et al. 2003; Tremolada et al. 2006). In the Brodno sequence, the $\delta^{13}C$ values (L90–C27: 1.45‰) ranges between 1.3‰ and 1.5‰ (VPDB) (Fig. 6).

The lowermost cycle (up to L58), part of the Czorsztyn Limestone Formation (*Ammonitico Rosso* facies), contains slightly elevated $\delta^{13}C$ values (1.46–1.73‰). In the second, third and fourth cycle, $\delta^{13}C$ values gradually decrease, reaching the lowest value in L98 (1.28‰). The only small positive excursion occurs in L79 (1.51‰), corresponding to the *Polycostella* peak. Rhythmic fluctuations during the gradual rise of average $\delta^{13}C$ values in the 4th to 6th cycle (start of the *Maiolica* facies at the base of the Pieniny Limestone Formation) probably reflect the rhythmic character of the rock sequence due to sea-level oscillations (Fig. 6). A much wider range of $\delta^{13}C$ values (1.33–1.55‰) is recognized in the 7th cycle, immediately below the J/K boundary level, with a general decreasing trend. Finally, $\delta^{13}C$ values in cycles above the J/K boundary increase yet again.

The authentic character of the $\delta^{13}C$ record is underlined by relatively high and conservative $\delta^{18}O$ values (–2.29‰ to –0.88‰). Oxygen isotope fractionation is markedly sensitive to temperature and salinity variations in seawater. As such, carbonate $\delta^{18}O$ values could reflect these environmental proxies, in combination with records from micro- and nannofossils (Price et al. 1998; Gröcke et al. 2003; Hay et al. 2006; Tremolada et al. 2006).

Interpretation of absolute sea-water temperature from $\delta^{18}O$ bulk rock data must be treated with caution (Michalík et al. 2021). The average $\delta^{18}O$ value in the Brodno section is –1.62‰ (VSMOW). According to Michalík et al (2009), the $\delta^{18}O$ values less than average (–1.85‰ to –2.29‰) in the 2nd cycle could reflect a relatively warm episode during the Early Tithonian, with temperature changes of roughly 2–3˚C. Positive excursions in cycles 3 and 4 (approximately –1.5‰) might indicate progressive temperature decline (nearly 2–3˚C), which is more or less correlatable with the emergence of *Polycostella*. Higher, a positive $\delta^{18}O$ excursion (bed C3) may have been driven by factors other than only cooler temperatures. This positive $\delta^{18}O$ event was not only preceeded by a fall in *Polycostella* abundance, but also accompanied by shifts in the abundance of *Watznaueria* and *Cyclagelosphaera* that could indicate changes in water composition: for instance, salinity or eutrophication. Around the J/K boundary (cycles 6, 7, and 8), more negative $\delta^{18}O$ values (-1.5‰ to -2.6‰) are suggestive of a temperature increase. Stable isotope analyses are also consistent with a modest cooling of earliest Berriasian surface waters.

The data obtained might indicate that seawater temperature ranged between 15.5–21.3˚C, when the isotopic composition of seawater ($\delta^{18}O_{SW}$) is assumed to be – 1.0‰, a value deemed appropriate for the ice-free, post-Jurassic world (Gröcke et al. 2003). These values fit the 14–21˚C temperature interval calculated by Price et al. (1998, 2000) and Gröcke et al. (2003) for the Kimmeridgian–Tithonian of the northern Tethys. However, these relatively large (5–6˚C) temperature fluctations seem unrealistic. It was recently suggested that $\delta^{18}O$

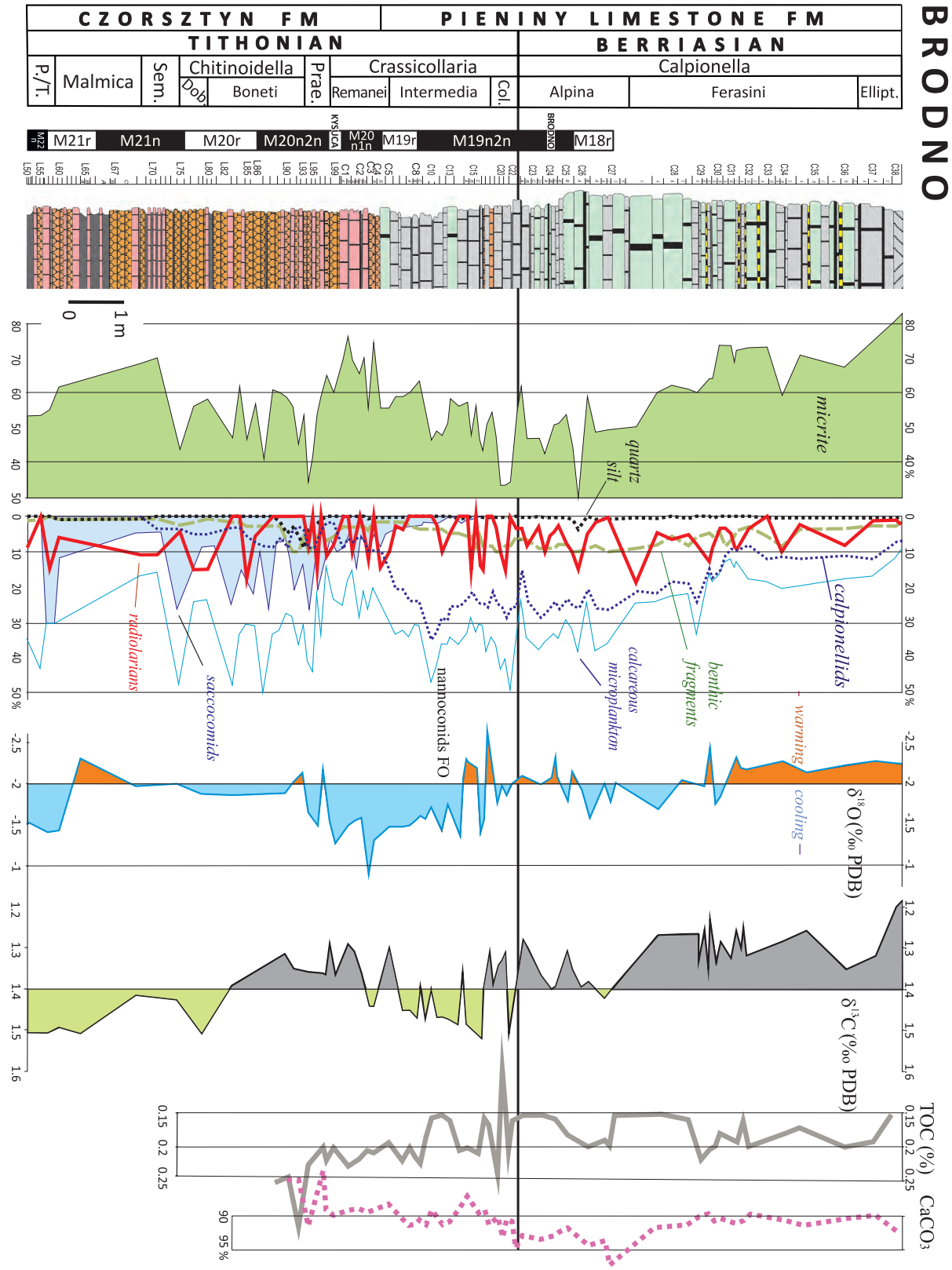

Fig. 6. Lithological column of the studied Brodno sequence, magnetostratigraphy, quantitative representation of allochems in microfacies, $\delta^{18}O$ and $\delta^{13}C$ chemostratigraphy, and carbon geochemistry.

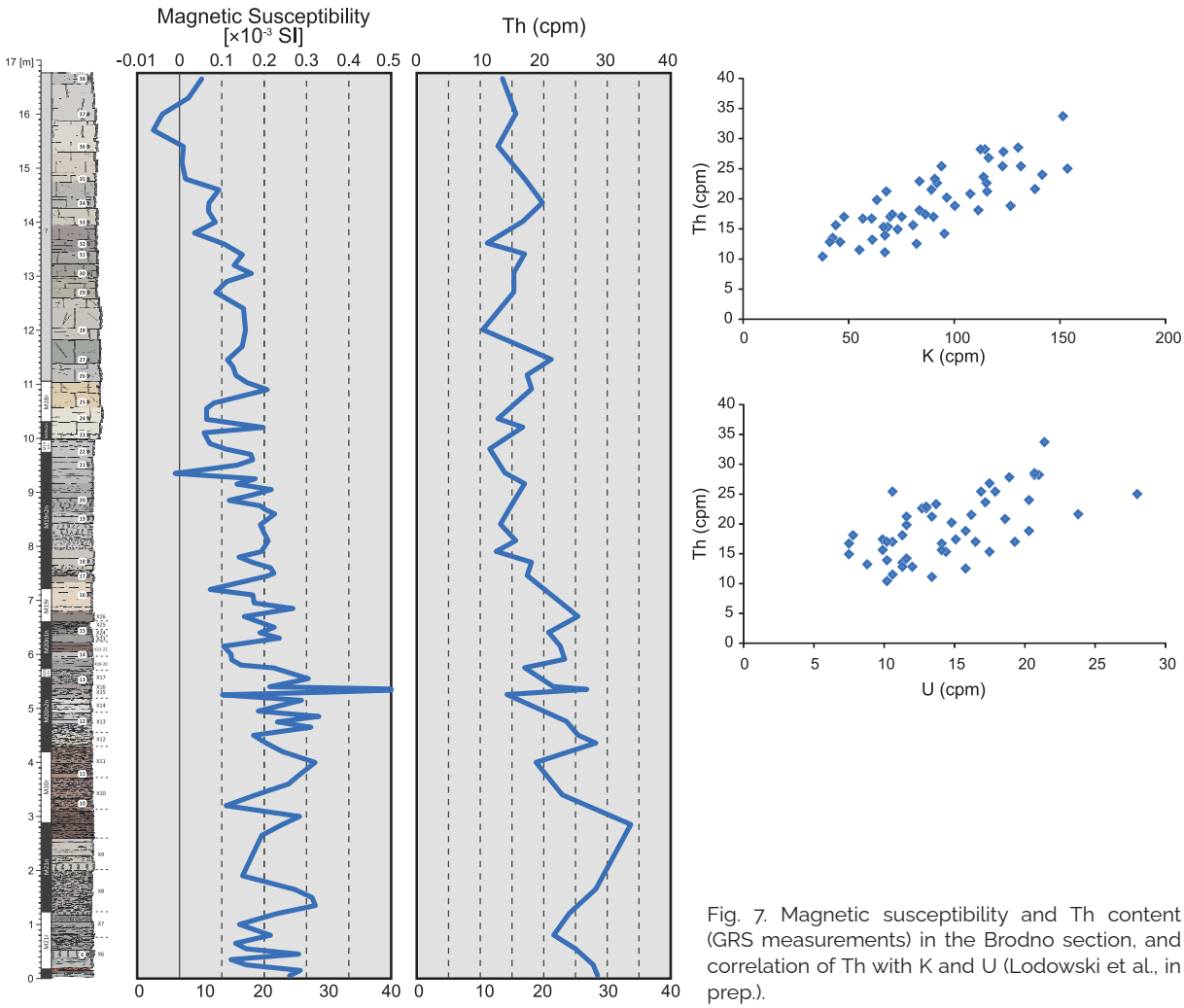

Fig. 7. Magnetic susceptibility and Th content (GRS measurements) in the Brodno section, and correlation of Th with K and U (Lodowski et al., in prep.).

record in the lower part of the Brodno section (up to M20n1r magnetosubchrone) is affected either by low resolution sampling or some diagenetic alterations (Michalík et al. 2021). Part of this apparent temperature fall could conceivably be attributed to decreases in surface-water salinity (see also Tremolada et al. 2006). $\delta^{18}O$ values indicate that the uppermost Tithonian deposits were formed during a relatively cold interval (18.5°C, on average) temporarily interrupted by warm episodes; however, in general it was a rather arid period (Fig. 6). This is, additionally, documented by monotonous $\delta^{13}C$ values and low organic carbon abundances. The late Tithonian cooling was followed by limited warming in the latest Tithonian and the earliest Berriasian. Short term $\delta^{18}O$ fluctations might be indicative of temperature and salinity changes, and the invasion of warm water (or, alternatively, the stagnation of cold water inputs) into the basin around the J/K boundary interval: this is furthermore documented by nannoconid blooms and their definitive diversification, accompanied by depletion of the calpionellid association.

Magnetostratigraphy and correlation with the Global Polarity Time Scale (GPTS)

According to Houša et al. (1999), in the Brodno section the base of the standard Crassicollaria Zone lies approximately in the middle of Magnetozone M20n. The base of the standard Calpionella Zone – that is, the Jurassic/Cretaceous boundary – lies in the middle part of Magnetochron M19n (in their solution 2), be-

tween beds C15A and C15B. These authors correlated their data from the Brodno section with sections in northern Italy (Foza), central Italy (Val Bosso), and Spain (Rio Argos). Pszczółkowski et al. (2005) identified the NJK-c Subzone within the upper Tithonian Nannoconus wintereri Subzone. Grabowski and Pszczółkowski (2006) located the Jurassic/Cretaceous boundary (between calpionellid biozones A and B of Remane 1971; Remane et al. 1986) within Magnetochron M19n, below the Brodno (M19n-1r) Subchron. Ogg and Lowrie (1986) placed the J/K boundary close to the base of the Grandis Zone (~ top of the Jacobi Zone and correlated it with the base of Magnetochron M18r.

The interval immediately above the base of the Beriasella privasensis Zone (= M17r/M17n, between Elliptica and Cadischiana calpionellid Subzones, formerly B and C subzones; Galbrun 1985; Grabowski 2011) is typical of a drowning event (Gawlick and Schlagintweit 2006), with synsedimentary slumpings (Hoedemaeker and Leereveld 1995), kaolinite (Schnyder et al. 2005), and phosphate- or iridium enrichment (Zakharov et al. 1996). The latter may even be associated with the Mjølnir (Dypvik et al. 2006), Shatsky Rise, and/or Morokweng impact craters (Koberl et al. 1997; Mahoney et al. 2005; Tremolada et al. 2006).

Stop 2:
Snežnica section

(*Jozef Michalík, Daniela Reháková, Otília Lintnerová, Špela Goričan, Jacek Grabowski, Damian Lodowski, Lilian Švábenická, Kamil Fekete and Daniela Boorova*)

The section is exposed in a hundred meter tall wall of a freshly abandoned quarry (N 49° 16' 14.35"; E 18° 46' 31.18") on the steep southeastern slope of Snežnica hill (Figs 3, 8). It is located above and to the left of the local road to Snežnica village. Below, the Upper Jurassic–Lower Cretaceous boundary interval is documented. In total, 117 samples were thin-sectioned for microfacies analyses and documentation of stratigraphically important calcareous microfossil successions – that is, calpionellids, calcareous dinoflagellates and radiolarians. So far, calcareous nannofossils have been studied from several pilot samples (Table 1).

Microfacies, calpionellid, and calcareous dinocyst zonations

Lithofacies were interpreted following Dunham (1962), and standard microfacies types (SMFs) and facies zones (FZs) were deter-

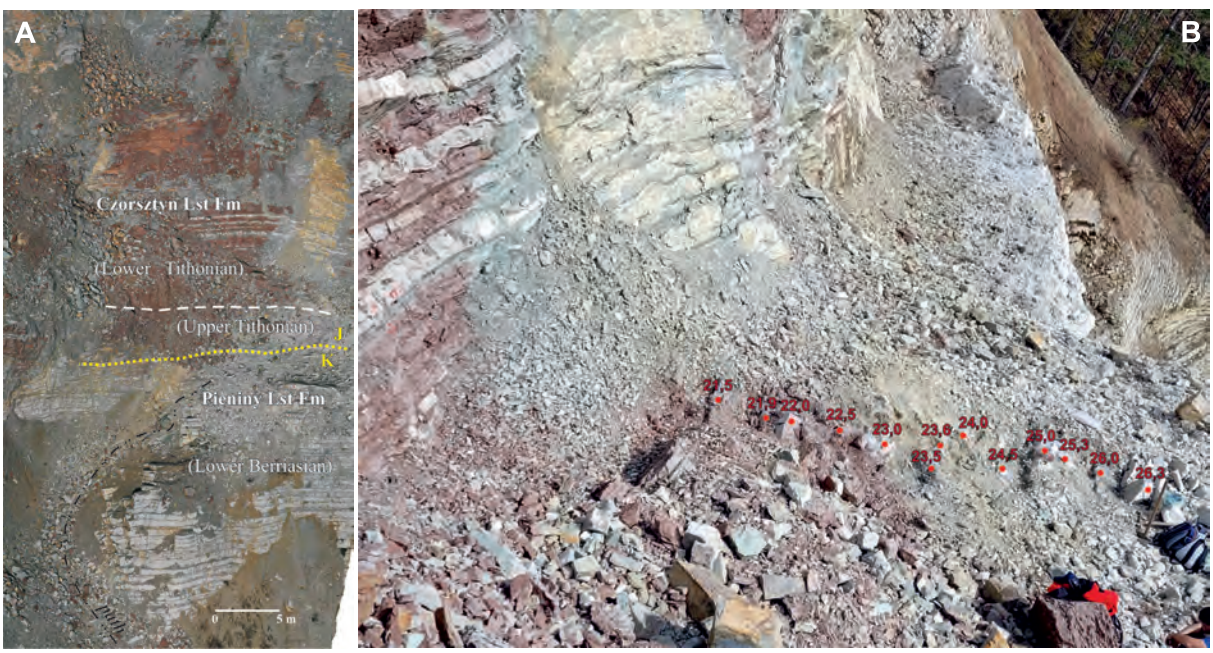

Fig. 8. A. Aerial view of the Snežnica quarry with the studied J/K section indicated. Photo by M. Marciš and K. Fekete. B. Detailed view of the Snežnica quarry with detailed documentation of the J/K boundary interval. Photo by K. Fekete.

Sněžnica	Casellato and Erba 2021		Sample No.	*Faviconus multicolumnatus*	*Conusphaera mexicana minor*	*Cyclagelosphaera argoensis*	*Polycostella beckmannii*	*Nannoconus* sp.	*Conusphaera mexicana mexicana*	*Nannoconus compressus*	*Zeugrhabdotus cooperi*	*Nannoconus globulus minor*	*Watznaueria cynthae*	*Zeugrhabdotus embergerii*	*Nannoconus erbae*	*Nannoconus wintereri*	*Nannoconus globulus globulus*	*Retacapsa surirella*	*Nannoconus kamptneri minor*	*Nannoconus steinmanii minor*	*Umbria granulosa granulosa*	*Nannoconus steinmanii steinmanii*
			48.1 m											ER						ER		
			47.1 m			ER		ER				ER						ER	ER		ER	
			46.1 m					ER				ER							ER	ER		
			45.8 m top					VR	ER			ER			ER			ER	ER	ER		
			45.1 m base			ER									?				ER			ER
			44.7 m					ER														
	NC1		43.1 m			ER		VR	ER			VR							ER	ER		
			42.4 m																			
			41.6 m top			ER		VR	ER		ER	VR							ER	ER	f	ER
			41.0 m base					ER				ER	ER									
			40.6 m top					ER				ER							ER		ER	?
Umbria granulosa granulosa			40.4 m base			ER						ER				f	ER		ER			ER
FO *N. steinmannii steinmannii*			39.6 m			cf.		ER	?			ER							ER		fER	ER
			38.9 m									ER	ER						ER?			
		b	37.9 m top									ER										
			37.3 m base			ER		ER				ER	ER				ER			ER		
N. kamptneri/steinmannii minor			36.6 m top			ER		ER				ER					ER		ER?			
			36.1 m base					ER	ER			ER										
			35.0 m									ER	ER		ER							
			34.1 m			ER						ER										
			32.8 m			ER		ER	ER		ER	ER	?									
			32.5 m top					ER	VR			ER					ER					
	NC0		32.0 m base			f		ER	ER			ER			?							
			31.4 m					ER	ER			ER	ER									
			30.4 m top			f			ER													
		a	30.0 m base						VR													
			29.9 m top			ER			ER			ER			?f							
			29.0 m base			ER			R			ER										
			28.0 m																			
			27.8 m top			f			ER				ER									
LO *P. beckmannii*			27.1 m base				ER	ER	R				ER									
Retacapsa surirella			26.5 m top			ER		ER	ER			VR	ER				ER	ER				
alpina acme			26.3 m base																			
FO *N. wintereri, N. globulus globulus*			25.9 m top			ER						ER	ER		?	cf.						
FO *W. cynthae*			25.6 m middle		ER	cf.			ER				ER	ER								
	NJT17		25.2 m base				?	?		?		?										
FO *N. globulus minor*			24.3 m top			?						?										
			24.0 m base			?			ER													
			23.9 m top					?	ER													
			23.0 m base		ER				VR													
			22.0 m						ER													
			21,0 m						ER													
LO *F. multicolumnatus*			20,0 m	VR					VR													
			19.00 m		ER	ER	VR		R		ER											
			18.0 m		ER		ER		VR													
FO *Z. cooperii*			17.0 m		ER		VR	?	R		ER											
			16.0 m						ER													
FO *C. mex. mex. s.s., N. compressus*			15.2 m		ER				VR	ER												
			14.2 m	ER	ER	ER	R	ER														
FO *P. beckmannii*			13.1 m	VR	ER	ER	R															
	NJT15a		11.9 m																			
FO *C. mexicana minor*			11.1 m	VR	cf.																	
			10.0 m	VR																		
			9.6 m																			
			8.0 m																			
	NJT14		7.3 m																			
FO *F. multicolumnatus*			6.0 m	ER	?																	
			5.0 m																			
F. multicolumnatus fragment			4.9 m	f?																		
			3.6 m																			
			2.0 m																			
			1.0 m																			

Table 1. Distribution of calcareous nannofossil taxa and biostratigrpahic correlation in the Snežnica section. Main events are highlighted in gray. Nannofossil events according to Casellato and Erba (2021). In brown - red nodular limestones (Czorsztyn Fm), in blue – calpionellid limestones (Pieniny Fm). Frequency of taxa: R = rare (8-6 specimens in slide), VR – very rare (5–3 specimens in slide), ER – extremely rare (1–2 specimens in slide), cf – confer., ? – questionable, f – fragment.

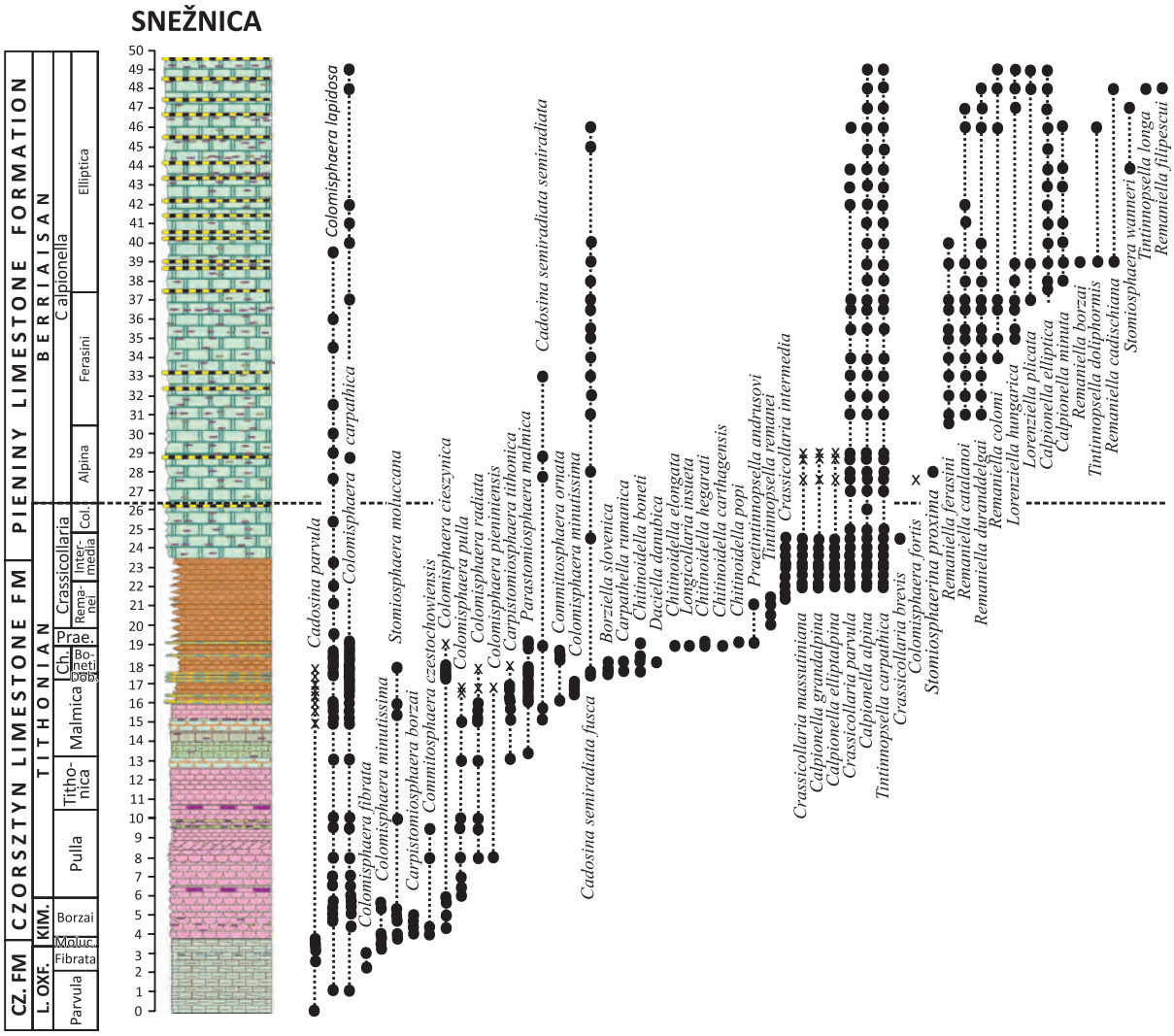

Fig. 9. Lithological log of the Snežnica section, with distribution and zonation of calpionellids and calcareous dinoflagellates. Abbreviations: CZ. FM – Czajakowa Formation; L. OXF. – Lower Oxfordian; KIM. – Kimmeridgian; Moluc. – Moluccana; Ch. – Chitinoidella; Dob. – Dobeni; Prae. – Praetintinnopsella; Col. – Colomi.

mined as proposed by Wilson (1975) and modified by Flügel (2004). Microfacies types SMF 2, SMF 3 and SMF 4 were recognized, characterizing a basin slope depositional environment (FZ 3–4). The calpionellid zonation of Reháková and Michalík (1997) and calcareous dinoflagellate zonation *sensu* Reháková (2000) were applied. The limestone sequence studied in the Snežnica section is constrained by a calcareous dinoflagellate succession to the upper Oxfordian (Parvula Zone) to the lower Tithonian (Malmica Zone); above, a continuous calpionellid succession extends through the upper lower Tithonian (Chitinoidella Zone, Dobeni Subzone) to the late Early Berriasian (standard Calpionella Zone, Elliptica Subzone; Fig. 9).

Upper Oxfordian Parvula Zone (*sensu* Reháková 2000): Grey laminated siliceous limestones of *Bositra*, *Bositra*–radiolaria–spiculite, and spiculite microfacies (packstone, passing locally to wackestone; SMF 2).

Upper Oxfordian Fibrata Zone (*sensu* Reháková 2000): Grey-brown laminated detrital siliceous limestones of the *Bositra*–spiculite and *Bositra* microfacies (packstone; SMF 2), with pyrite accumulations on the surface and

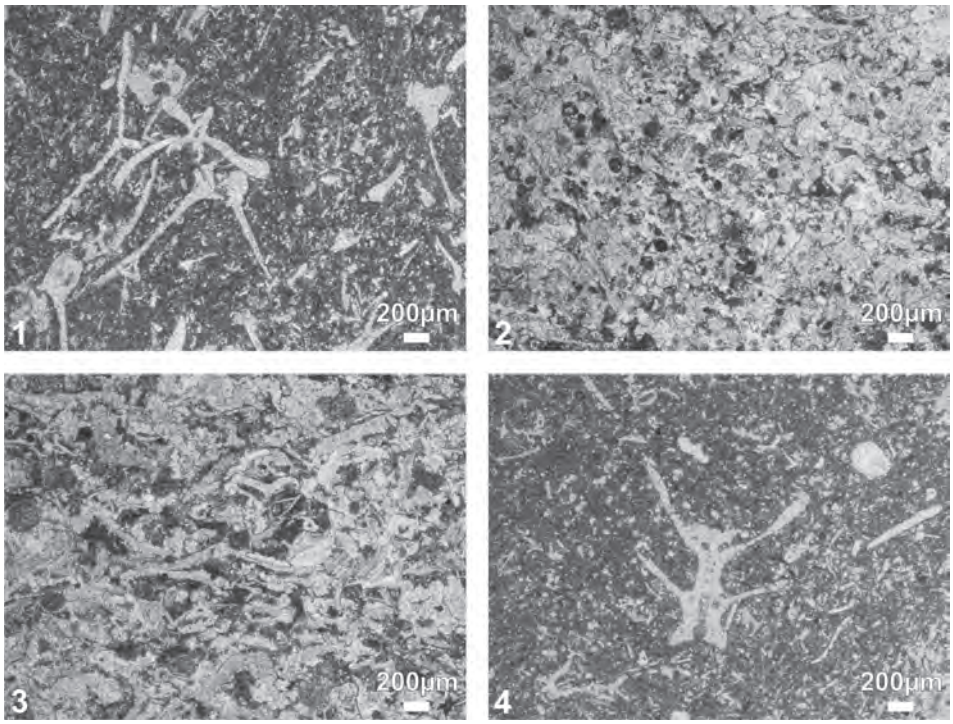

Fig. 10. Upper Jurassic microfacies in the Snežnica section: 1. *Saccocoma–Globochaete* wackestone to packstone. Sample Sn 15; 2. Pelbioclastic *Saccocoma* packstone. Sample Sn 16.3; 3. *Saccocoma* packstone. Sample Sn 17.3; 4. *Saccocoma–Globochaete* wackestone. Sample Sn 19.2.

chert nodules. Locally graded and sorted *Bositra* filaments are dominant over radiolarians, sponge spicules, rare crinoids, aptychi, and cysts of *Cadosina parvula, Colomisphaera fibrata*, and *Colomisphaera minutissima*.

Lower Kimmeridgian Parvula Acme Zone (*sensu* Reháková 2000): Brown laminated and bioturbated biomicrite limestone (wackestone; SMF 2–3), with small *Bositra* filaments, crinoid columnalia and aptychi, *Cadosina parvula*, and *Colomisphaera minutissima*. Slightly recrystallized matrix contains pyrite nests.

Upper(?) Kimmeridgian Moluccana Zone (Nowak 1976): Pinkish-gray fine-grained limestone separated by thin clay laminae, with belemnites and abundant pyrite. Biomicrite (wackestone, SMF 2–3) is bioturbated, with laminae rich in resedimented bioclasts (abundant *Cadosina parvula*). The microfossils are represented by *Bositra* filaments, crinoids (also *Saccocoma* sp.), aptychi, and cysts of *Stomiosphaera moluccana* and *Colomisphaera minutissima*.

Upper Kimmeridgian Borzai Zone (Nowak 1976): Reddish-brown and brown nodular limestone, composed of biomicrite of the *Saccocoma*–radiolarian or *Saccocoma* microfacies (packstone; SMF 2) and laminated biomicrite of the *Saccocoma–Globochaete* microfacies (packstone or wackestone; SMF 2–3; Fig. 10). *Saccocoma* sp. dominates over *Globochaete alpina* spores, fragments of aptychi, filaments, ostracods, foraminifera with calcitic tests, crinoid ossicles and columnalia, and cysts of *Carpistomiosphaera borzai*, *Colomisphaera lapidosa*, *Colomisphaera carpathica, Colomisphaera cieszynica, Colomisphaera minutissima*, *Commitosphaera czestochowiensis, Stomiosphaera moluccana*, *Stomiosphaera* sp. and *Cadosina parvula.* Some bioclasts bear microborings. A few samples contain a fine siliciclastic admixture (quartz grains and muscovite). The matrix is sometimes affected by slight dolomitization; stylolites and fractures are frequently impregnated by Fe hydroxides. The slightly recrystallized matrix contains scattered pyrite cubes (locally, forming nests). On the base of the *Saccocoma* elements analyzed, in

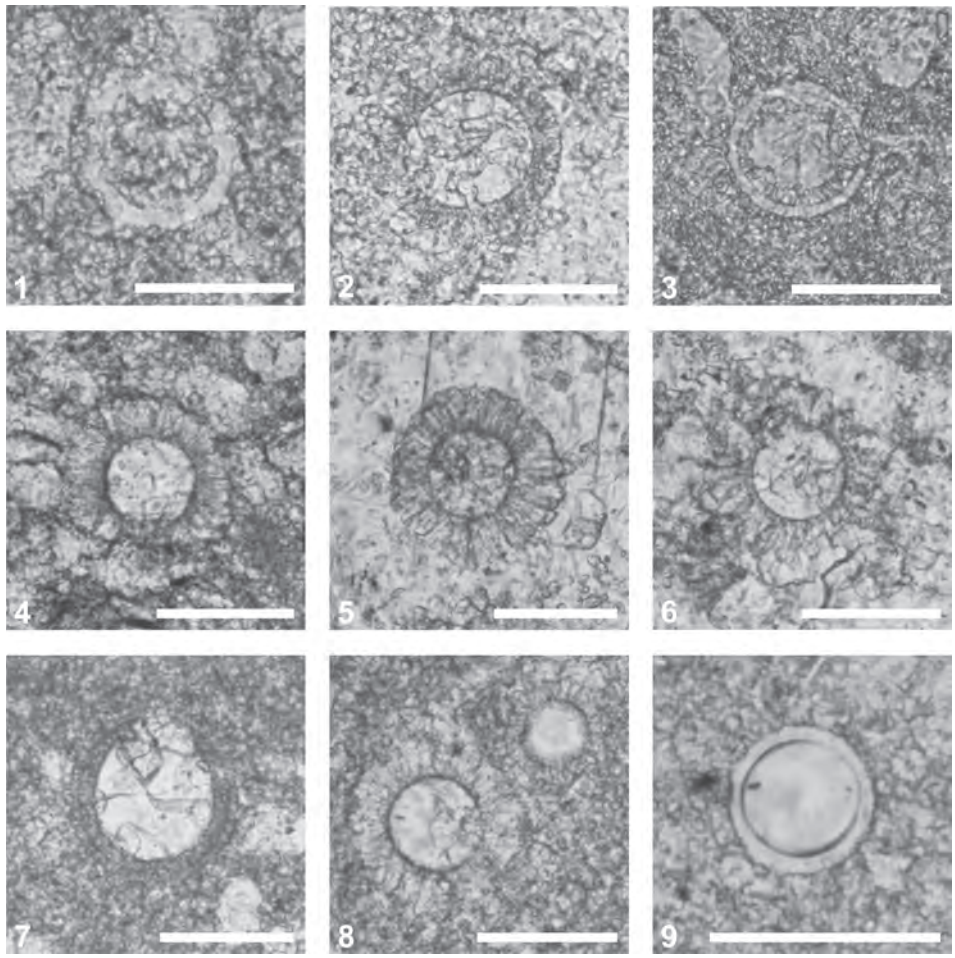

Fig. 11. Lower Tithonian dinoflagellate cysts from the Snežnica section: 1. *Stomiosphaera moluccana*, Sn 10; 2. *Carpistomiosphaera tithonica*, Sn 15; 3. *Parastomiosphaera malmica*, Sn 13.3; 4. *Colomisphaera carpathica* (Borza), Sn 15.4; 5. *Colomisphaera cieszynica*, Sn 17.3; 6. *Committosphaera ornata*, Sn 18.1; 7. *Cadosina semiradiata semiradiata*, Sn 20.5; 8. *Colomisphaera carpathica* and *Colomisphaera lapidosa*, Sn 28.9; 9. *Cadosina semiradiata fusca*, Sn 43.5. Scale bar is 50 μm.

this section it seems that the lower Tithonian S-3: Sacoccoma Zone *sensu* Benzaggagh et al. (2015) starts slightly earlier than previously recognized.

Lower Tithonian Pulla Zone (Reháková 2000): Thin-bedded reddish-brown and brown nodular or pseudo-nodular limestones (locally with greenish nodules) and slightly laminated siliceous limestones with stratiform cherts. Laminated, locally bioturbated biomicrite packstone of the *Globochaete–Saccocoma* microfacies hosts abundant belemnites, and locally passes to wackestone (SMF 2–3). *Saccocoma* sp. and *Globochaete alpina* are prevalent among bioclasts and are accompanied by less frequent filaments, ostracods, bivalves, foraminifera (*Lenticulina* sp., *Spirilina* sp.), crinoids (*Pentacrinus* sp.), aptychi, calcified radiolarians and cysts of *Colomisphaera pulla, Colomisphaera lapidosa, Colomisphaera cieszynica, Colomisphaera carpathica, Colomisphaera radiata, Colomisphaera pieniniensis* and *Committosphaera czestochowiensis.* Bioclasts are locally phosphatized; some are silicified.

Lower Tithonian Tithonica Zone (*sensu* Lakova et al. 1999): Greenish-gray fine-grained limestones with cherty layers, thin-bedded gray laminated limestones, reddish-brown nodular and pseudo nodular limestones with chert nodules and ammonite molds. They are biomicritic, locally laminated packstone or wackestone of

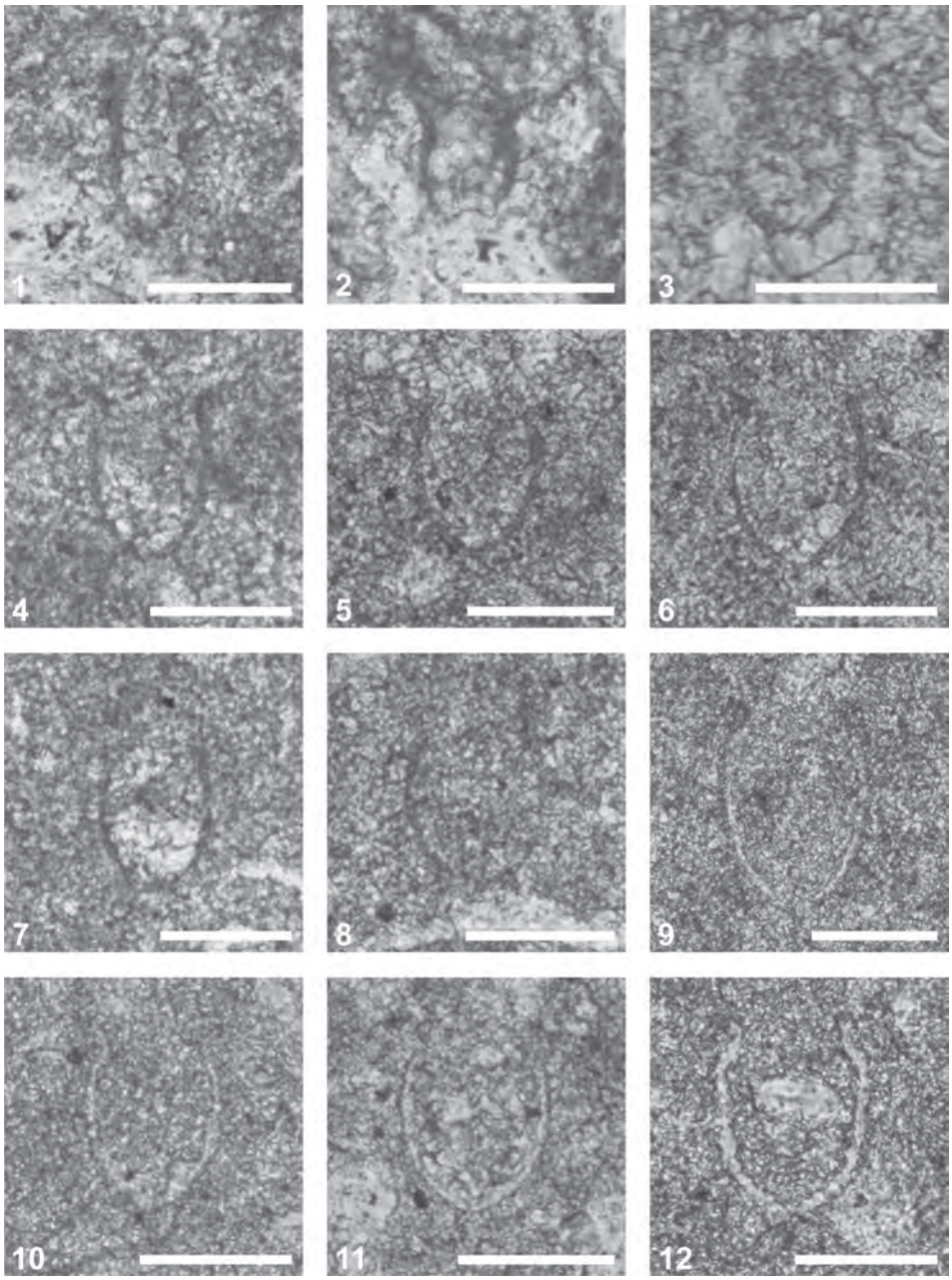

Fig. 12. Upper lower to upper Tithonian chitinoidellids and calpionellids from the Snežnica section: 1. *Longicollaria dobeni*, Sn 18; 2. *Borziella slovenica*, Sn 18.1; 3. *Dobeniella cubensis*, Sn 18.1; 4. *Chitinoidella boneti*, Sn 20.5; 5. *Chitinoidella hegarati*, Sn 21; 6. *Chitinoidella popi*, Sn 21; 7–8. *Longicollaria insueta*, Sn 20.5; 9–10. *Praetintinnopsella andrusovi*, Sn 21; Sn 21.4; 11. *Tintinnopsella remanei*, Sn 21.4; 12. *Crassicollaria* aff. *intermedia*, Sn 21.4. Scale bar is 50 μm.

the *Saccocoma–Globochaete* microfacies (SMF 2–3). Besides the dominant *Saccocoma* sp. and *Globochaeta alpina,* these deposits contain crinoid columnalia, foraminifera, *Spirilina* sp., aptychi, calcified radiolarians (locally filled by chalcedony), sponge spicules, and cysts of *Colomisphaera tithonica, Colomisphaera pulla, Colomisphaera lapidosa, Colomisphaera carpathica, Colomisphaera radiata, Cadosina semiradiata semiradiata, Cadosina parvula,* and *Stomiosphaera moluccana* (Fig. 11). Some bioclasts are phosphatized or silicified. The packstone matrix has rich stylolites and scattered pyrite, and is slightly recrystallized.

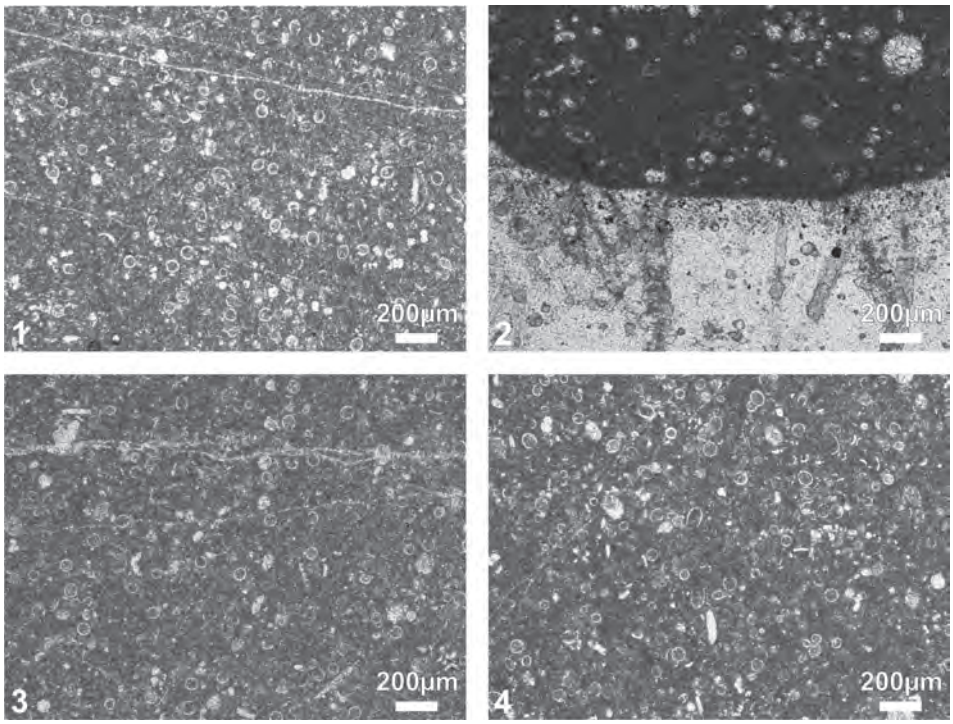

Fig. 13. Upper Jurassic–Early Cretaceous microfacies in the Snežnica section: 1. *Calpionella–Globochaete* wackestone, Colomi Subzone, Crassicollaria Zone, Sn 24; 2. Chert layer in radiolarian–*Calpionella* wackestone – onset of the Alpina Subzone, Calpionella Zone; J/K boundary interval, Sn 26.3; 3. *Calpionella–Globochaete* wackestone – onset of the Alpina Subzone, Calpionella Zone; J/K boundary interval, Sn 26.3; 4. *Calpionella–Globochaete* wackestone, Remaniella Subzone, Calpionella Zone, Sn 36.5.

Lower Tithonian Malmica Zone (*sensu* Nowak, 1968): Reddish-brown and brown nodular and pseudo-nodular limestones with local thin clayey intercalations, and light gray fine-grained (allodapic) limestones with brown cherts. Pelbiomicrite, bioturbated wackestone and subordinate packstone of the *Globochaete–Saccocoma* microfacies, and packstone of the *Saccocoma* microfacies were recognized, representing SMF 2 and SMF 4. *Saccocoma* sp. and *Globochaete alpina* spores are still dominant, and are accompanied by fragments of ostracods, bivalves, foraminifera, aptychi, echinoids, and cysts of frequent *Parastomiosphaera malmica* (Fig. 11) and rare *Colomisphaera carpathica*, *Colomisphaera minutissima, Colomisphaera lapidosa*, *Colomisphaera pieniniensis, Colomisphaera pulla*, *Committosphaera ornata, Cadosina semiradiata semiradiata*, *Cadosina semiradiata fusca*, *Cadosina parvula*, *Carpistomiosphaera tithonica*, *Colomisphaera radiata*, *Stomiosphaera moluccana,* and *Stomiosphaera* sp. In several layers (Sn 14.3, 16.1, and Sn 17), bioclasts are arranged chaotically. Matrix and bioclasts are locally silicified. Based on analysed *Saccocoma* elements, this interval could be correlatable with the Saccocoma S4 Zone (Benzaggagh et al. 2015) or with the Darwini – Semiforme ammonite Zone.

Lower Tithonian Chitinoidella Zone, Dobeni Subzone (*sensu* Grandesso 1977 and Borza 1984): Pale green fine-grained limestones: pelbiomicrite, laminated (locally with graded allochems) packstone of the *Saccocoma*, *Globochaete–Saccocoma*, and *Saccocoma–* crinoidal microfacies (SMF 2, 3, and 4), with chert nodules. *Saccocoma* sp. is dominant over *Globochaete alpina*, crinoid columnalia, and rare foraminifera, aptychi, bivalve fragments, and microgranular calpionellids. *Borziella slovenica*, *Colomisphaera carpathica, Colomisphaera cieszynica*, and *Parastomiosphaera malmica* cysts prevail over redeposited *Carpistomiosphaera tithonica, Cadosina parvula*, and *Colomisphaera radiata* cysts.

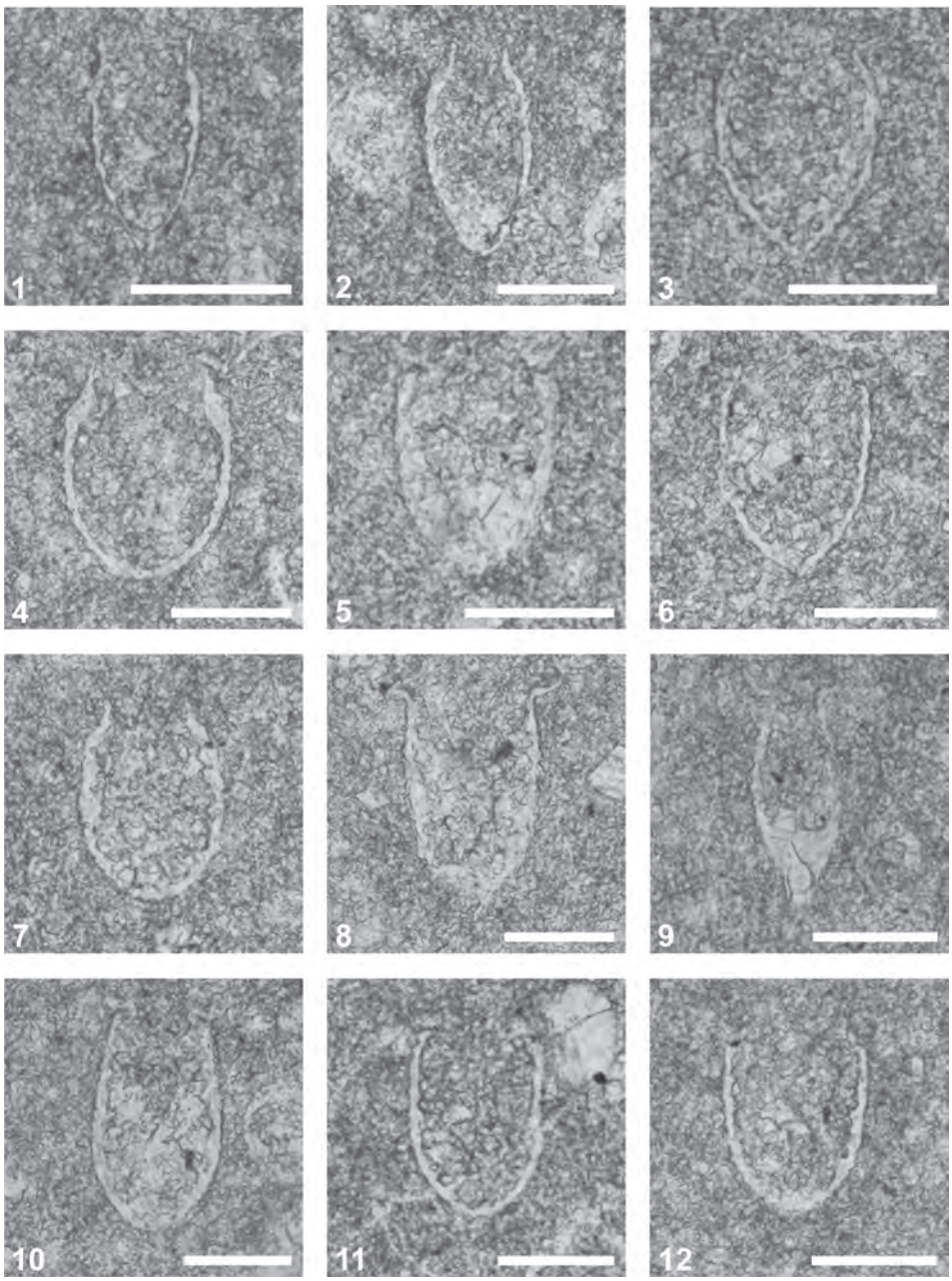

Fig. 14. Upper Tithonian–Lower Berriasian calpionellids from the Snežnica section: 1. *Crassicollaria parvula*, Sn 25; 2. *Crassicollaria colomi*, Sn 36.5; 3. *Tintinopsella doliphormis*, Sn 31.5; 4. *Calpionella alpina*, Sn 35.5; 5. *Remaniella ferasini*, Sn 33; 6. *Remaniella colomi*, Sn 35; 7. *Calpionella elliptica*, Sn 44.5; 8. *Tintinopsella longa*, Sn 44.5; 9. *Tintinopsella subacuta*, Sn 45.5; 10. *Remaniella cadischiana*, Sn 39; 11. *Remaniella borzai*, Sn 39.5; 12. *Remaniella duranddelgai*, Sn 39.5. Scale bar is 50 μm.

Late Tithonian Chitinoidella Zone, Boneti Subzone (*sensu Grandesso 1977 and Borza 1984)*: Reddish-brown and brown nodular limestones with thin marly layers, pale gray to green fine-grained (allodapic) limestones composed of slightly bioturbated, locally laminated biomicrite with graded bioclasts. Packestone and wackestone, locally passing to packstone or *Globochaete–Saccocoma/* pelbiomicrite wackestone with synsedimentary erosion-supported intraclasts and extraclasts (SMF 2, 3 and 4). *Globochaete alpina* and *Saccocoma* sp. are dominant over crinoids, bivalves, ostracods, aptychi, juvenile ammo-

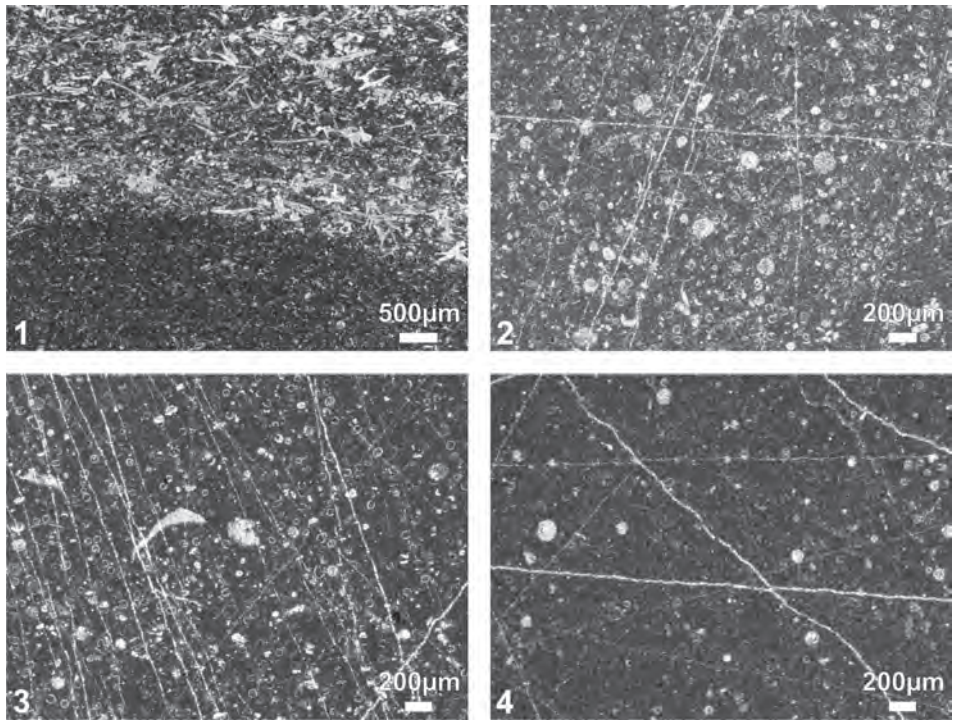

Fig. 15. Late Jurassic–Early Cretaceous microfacies in the Snežnica section: 1. Laminated *Saccocoma–Globochaete* wackestone to packstone with rare calcified radiolarians, Sn 14, 2. Radiolarian–*Calpionella* wackestone, Alpina Subzone, Calpionella Zone, Sn 28; 3. Radiolarian–*Calpionella* wackestone, Alpina Subzone, Calpionella Zone, Sn 29; 4. *Calpionella*–radiolarian wackestone, Elliptica Subzone, Calpionella Zone, Sn 44.

nites, calcified radiolarians, sponge spicules, crinoids, foraminifera tests, *Colomisphaera carpathica, Colomisphaera lapidosa, Colomisphaera cieszynica, Parastomiosphaera malmica, Stomiosphaera moluccana, Colomisphaera radiata, Committosphaera ornata, Committosphaera czestochowiensis*, *Cadosina semiradiata semiradiata,* and *Cadosina semiradiata fusca* cysts, and microgranular loricae of *Borziella slovenica, Carpathella rumanica, Chitinoidella boneti, Daciella danubica, Longicollaria insueta, Chitinoidella elongata, Chitinoidella hegarati, Chitinoidella carthagensis*, and *Popiella oblongata* (Fig. 12).

Upper Tithonian Praetintinnopsella Zone (Grandesso, 1977): Reddish-brown and brown nodular limestone (locally with greenish gray nodules) with beds of fine-grained allodapic limestone. Biomicrite, bioturbated *Saccocoma*–radiolarian–*Globochaete* wackestone with nests composed of *Saccocoma* packstone or biomicrite wackestone, *Globochaete–Saccocoma* packstone, pelbiomicrite *Globochaete–Saccocoma* crinoidal packstone, and *Globochaete*–radiolarian wackestone (SMF 3 and SMF 4). Strata contain frequent *G. alpina*, *Saccocoma* sp., and locally also abundant calcified radiolarians, sponge spicules, and rare ostracods, bivalves, aptychi *Laevaptychus* sp., crinoids, foraminifera test fragments (*Spirilina* sp., *Lenticulina* sp.), cysts of *Colomisphaera lapidosa*, *Colomisphaera cieszynica, Colomisphaera carpathica*, *Colomisphaera sp.*, *Cadosina semiradiata semiradiata*, *Cadosina semiradiata fusca*, and *Parastomiosphaera malmica*, and loricae of *Praetintinnopsella andrusovi*, *Chitinoidella boneti*, *Chitinoidella hegarati*, and *Chitinoidella popi*.

Upper Tithonian Crassicollaria Zone, Remanei Subzone (Remane et al. 1986): Reddish-brown and brown nodular limestones. Biomicrite wackestone or packstone of the *Saccocoma–Globochaete* and radiolarian–*Saccocoma–Globochaete* microfacies (SMF 3), locally with synsedimentary erosion-supported intraclasts. *Globochaete alpina*, *Saccocoma* sp., and calcified radiolarians dominate over fragments of ostracods, bivalves, apty-

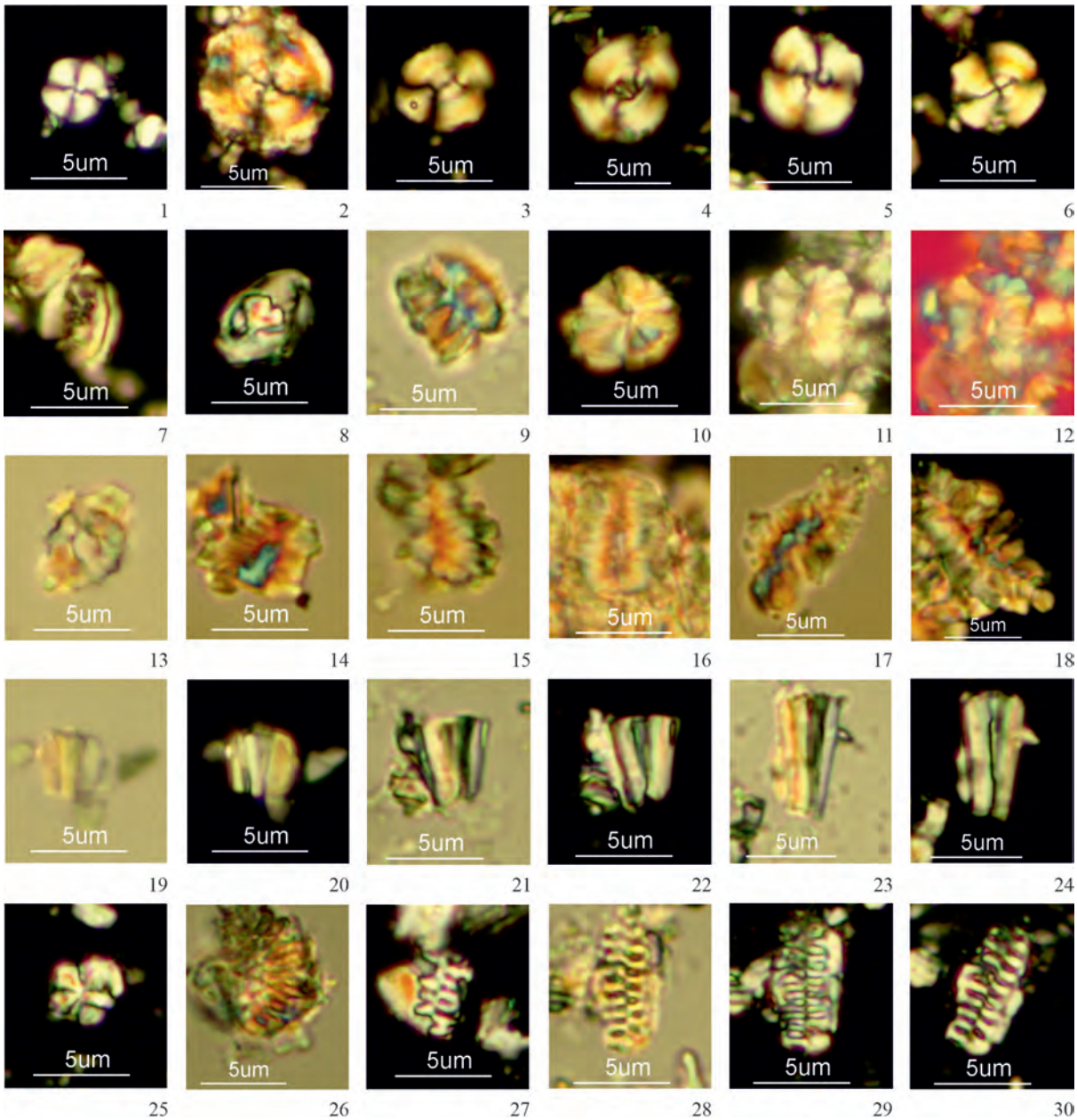

Fig. 16. Calcareous nannofossils in the Snežnica section. 1 – *Cyclagelosphaera margerelli*, 28.0 m; 2 – *Cyclagelosphaera argoensis*, 43.1 m; 3 – *Watznaueria communis*, 37.3 m; 4 – *Watznaueria britannica*, 40.4 m; 5 – *Watznaueria cynthae*, 31.4 m; 6 – *Watznaueria barnesiae*, 35.0 m; 7 – *Umbria granulosa granulosa*, 40.6 m; 8 – *Zeugrhabdotus cooperi*, 17.0 m; 9 – *Nannoconus compressus*, 15.2 m; 10 – *Nannoconus* sp., 26.5 m; 11, 12 – *Nannoconus erbae*, 25.9 m; 13 – *Nannoconus globulus minor*, 24.3 m; 14 – *Nannoconus* cf. *wintereri*, 40.4 m; 15 – *Nannoconus steinmannii minor*, 37.3 m; 16 – *Nannoconus kamptneri minor*, 40.4 m; 17, 18 – *Nannoconus steinmannii steinmannii*, 39.6 m (17) and 41.6 m (18); 19–22 – *Conusphaera mexicana minor*, 35.1 m (19, 20) and 35.0 m (21, 22); 23, 24 – *Conusphaera mexicana mexicana*, 15.2 m, 25 – *Polycostella beckmannii*, 13.1 m; 26 – *Faviconus* cf. *multicolumnatus*, 10.0 m; 27–30 – *Faviconus multicolumnatus*, 10.0 m (27), 11.1 m (28–30). Images in cross-polarized light; except 9, 13–17, 19, 21, 23 and 28 which are in plane-polarized light; and 12 – in gypsum plate.

chi, juvenile ammonites, crinoids, and foraminifera, cysts of *Colomisphaera lapidosa* and *Colomisphaera carpathica*, rare (and the first) fully hyaline loricae of *Tintinnopsella remanei*, *Calpionella alpina*, and *Crassicollaria intermedia* and the last *Praetintinnopsella andrusovi*.

Radiolarian taxa / Samples	UAZ95	14.00	28.90	44.50
Angulobracchia heteroporata Steiger				X
Angulobracchia mediopulvilla Steiger				X
Angulobracchia? portmanni Baumgartner	13–22			X
Arcanicapsa spp.			X	X
Archaeodictyomitra apiarium (Rüst)	8–22	X	X	X
Archaeospongoprunum patricki Jud	13–22			X
Cinguloturris cylindra Kemkin and Rudenko	12–17	X		
Crococapsa accincta (Steiger)		X		
Crococapsa pseudouterculus (Aita)		X	X	
Cryptamphorella dumitricai Schaaf		X		X
Deviatus diamphidius (Foreman)	8–14			X
Dicerosaturnalis gratiosus Dumitrica and Hungerbühler				X
Dicerosaturnalis trizonalis (Rüst)		X	X	X
Doliocapsa doliolum (Aita)		X		
Emiluvia chica Foreman	3–18	X		X
Eucyrtidiellum pyramis (Aita)	12–13	X		
Halesium palmatum Dumitrica				X
Hemicryptocapsa capita Tan	17–18		X	
Hemicryptocapsa carpathica (Dumitrica)	7–11			X
Hiscocapsa? altiforamina (Tumanda)	18–21			aff.
Hiscocapsa kaminogoensis (Aita)		cf.	cf.	
Hsuum raricostatum Jud	13–15		X	X
Mirifusus dianae (Karrer) s.l.	7–20			X
Neorelumbra buwaydahensis Kiessling		cf.		
Neorelumbra tippitae Kiessling		cf.		cf.
Obesacapsula cetia (Foreman)	10–17			X
Obesacapsula rusconensis Baumgartner	13–19		cf.	X
Obesacapsula verbana (Parona)	11–20		cf.	X
Pantanellium berriasianum Baumgartner	13–15	X		
Pantanellium squinaboli (Tan)	11–22	X	X	X
Parapodocapsa amphitreptera (Foreman)	9–18	X		
Parapodocapsa furcata Steiger	13–16		X	X
Praeparvicingula cosmoconica (Foreman)	13–22		X	X
Protunuma japonicus Matsuoka and Yao	7–12	cf.		
Pseudocrucella? elisabethae (Rüst)	13–22			X
Pseudodictyomitra carpatica (Lozyniak)	11–21	X		X
Pseudoeucyrtis? fusus Jud	13–17			X
Pseudoxitus gifuensis (Mizutani)	11–16		X	
Spinosicapsa aff. *coronata* Steiger *sensu* Baumgartner et al. (1995b)	11–20	X		X
Spinosicapsa milloti (Schaaf)	13–19			X
Spinosicapsa triacantha (Fischli)				X
Svinitzium depressum (Baumgartner)	13–18		cf.	cf.
Tethysetta boesii (Parona)	9–22	X		X
Thanarla patricki (Kocher)		X		
Triactoma kellumi Pessagno and Yang		X		
Tritrabs ewingi (Pessagno)	4–22			X
Xitus robustus Wu			X	
Zhamoidellum sp. A *sensu* Goričan (1994)		X	cf.	
AU Zones of Baumgartner et al. (1995a)		**12–13**	**13–15**	
Zones according to Matsuoka (1995)		***Pseudodictyomitra carpatica* Zone**		

Table 2. Radiolarian species in the Snežnica section. The second column gives the zonal ranges of the species according to Baumgartner et al. (1995a). The zonal assignment according to Baumgartner et al. (1995a) and Matsuoka (1995) is shown in the bottom rows.

Upper Tithonian Crassicollaria Zone, Intermedia Subzone (Remane et al. 1986): Reddish-brown and brown nodular, thin-bedded *Maiolica*-type limestones. Biomicrite and bioturbated wackestone of the *Calpionella–Globochaete* microfacies (SMF 3; Fig. 13). *Saccocoma* sp. rapidly decreases in abundance. The main bioclasts are *Globochaete alpina*, calcified radiolarians, bivalves, ostracods, aptychi, juvenile ammonites, foraminifera (*Spirillina* sp., *Lenticulina* sp.), agglutinated foraminifera (*Protomarsonella* sp.), cysts of *Colomisphaera lapidosa*, and loricae of *Crassicollaria intermedia*, *Crassicollaria massutiniana*, *Crassicollaria parvula*, *Calpionella alpina*, *Calpionella grandalpina*, *Calpionella elliptalpina*, and rare *Tintinnopsella carpathica*.

Upper Tithonian Crassicollaria Zone, Colomi Subzone (Pop 1994): Thin-bedded *Maiolica* limestone with dark gray chert nodules. Biomicrite wackestone of the *Calpionella–Globochaete* microfacies (SMF 3). Bioclasts are spores of *G. alpina*, loricae of *Crassicollaria parvula* (Fig. 14) dominant over *Crassicollaria massutiniana*, *Calpionella grandalpina*, *Calpionella alpina*, *Tintinnopsella carpathica* and *Cadosina semiradiata semiradiata* cysts, and fragments of ostracods, crinoid columnalia, aptychi, and foraminifera (*Lenticulina* sp., *Spirillina* sp.).

Lower Berriasian Calpionella Zone, Alpina Subzone (*sensu* Pop 1974; Remane et al. 1986): Pale, regularly thin-bedded *Maiolica*-type limestone with dark gray chert nodules. Biomicrite wackestones of the *Calpionella–Globochaete*–radiolarian microfacies (SMF 3 and 4; Figs 13, 15, 16). Small spherical forms of *Calpionella alpina* dominate over rare *Crassicollaria parvula* and *Tintinnopsella carpathica*. There are also common calcified radiolarians, *G. alpina* spores, rare cysts of *Colomisphaera lapidosa* and *Stomiosphaerina proxima*, aptychi fragments, bivalves, ostracods, crinoids, ophiurids, foraminifera, and sponge spicules. Some beds contain an increasing amount of deposited bioclasts, including calpionellids like *Calpionella grandalpina*, *Calpionella elliptalpina*, and *Crassicollaria massutiniana*, the cysts *Cadosina semiradiata semiradiata*, *Cadosina semiradiata fusca*, and *Colomisphaera fortis*, and *Saccocoma* sp.

Lower Berriasian Calpionella Zone, Ferasini Subzone (Pop 1994): Pale, regularly thin-bedded *Maiolica*-type limestone with dark gray chert nodules and stratiform chert layers. Biomicrite wackestone of the *Calpionella–Globochaete*–radiolarian microfacies and bioturbated wackestone of the *Calpionella*–radiolarian microfacies (SMF 3; Fig. 13). *Calpionella alpina* together with *Globochaete alpina* and calcified radiolarians dominate. They are accompanied by fragments of bivalves, crinoids, ophiurioids, aptychi, foraminifera, the calpionellids *Remaniella ferasini*, *Remaniella catalanoi*, *Remaniella duranddelgai*, *Remaniella colomi, Lorenziella hungarica*, *Lorenziella plicata*, *Crassicollaria parvula,* and *Tintinnopsella carpathica*, and cysts of *Colomisphaera lapidosa, Stomiosphaerina proxima, Cadosina semiradiata fusca*, and *Cadosina semiradiata semiradiata.* At the base of the zone in sample Sn-30.5, a few Tithonian calpionellid species and *Saccocoma* sp. fragments were documented.

Middle Berriasian Calpionella Zone, Elliptica Subzone (Pop 1974): Pale, regularly thin-bedded *Maiolica*-type limestone with dark gray chert nodules and stratiform chert layers. Biomicrite wackestone of the *Calpionella*–radiolarian microfacies (SMF 3). Calpionellids and calcified radiolarians prevail in the microfacies. *Calpionella alpina*, *Calpionella elliptica*, *Calpionella minuta*, *Calpionella* sp., *Crassicollaria parvula*, *Tintinnopsella carpathica*, *Tintinnopsella doliphormis*, *Lorenziella hungarica*, *Lorenziella plicata, Remaniella ferasini*, *Remaniella catalanoi*, *Remaniella duranddelgai*, *Remaniella colomi*, *Remaniella cadischiana, Remaniella borzai,*

Fig. 17. Radiolarians from the Snežnica section, Sn-14: 1, 2. *Dicerosaturnalis trizonalis*; 3. *Pantanellium squinaboli*; 4. *Pantanellium berriasianum*; 5. *Triactoma kellumi*; 6. *Emiluvia chica*; 7. *Spinosicapsa* aff. *coronata*; 8. *Parapodocapsa amphitreptera*; 9. Cryptamphorella *dumitricai*; 10a–b, 11. *Zhamoidellum* sp. A; 10a–b: lateral and antapical view of the same specimen; 12, 13. *Crococapsa pseudouterculus*; 14. *Crococapsa accincta*; 15. *Hiscocapsa* cf. *kaminogoensis*; 16a–b, 17. *Doliocapsa doliolum*; 16a–b: lateral and antapical view of the same specimen.; 18. *Cinguloturris cylindra*; 19. *Cinguloturris* sp.; 20. *Xitus* sp.; 21. *Neorelumbra* cf. *buwaydahensis*; 22. *Neorelumbra* cf. *tippitae*; 23, 24. *Eucyrtidiellum pyramis*; 25, 26. *Tethysetta boesii*; 27, 28. *Praeparvicingula* spp.; 29. *Pseudodictyomitra carpatica*; 30, 31. *Pseudodictyomitra* spp.; 32–36. *Archaeodictyomitra apiarium*; 37. *Thanarla patricki*; 38. *Protunuma* cf. *japonicus*. Magnification: 5; 125x (scale bar 120 μm); 1–4, 6–8, 18–22, 25–29, 31–36, 38: 150x (scale bar 100 μm); 9–17, 23–24, 30, 37: 200x (scale bar 75 μm). →

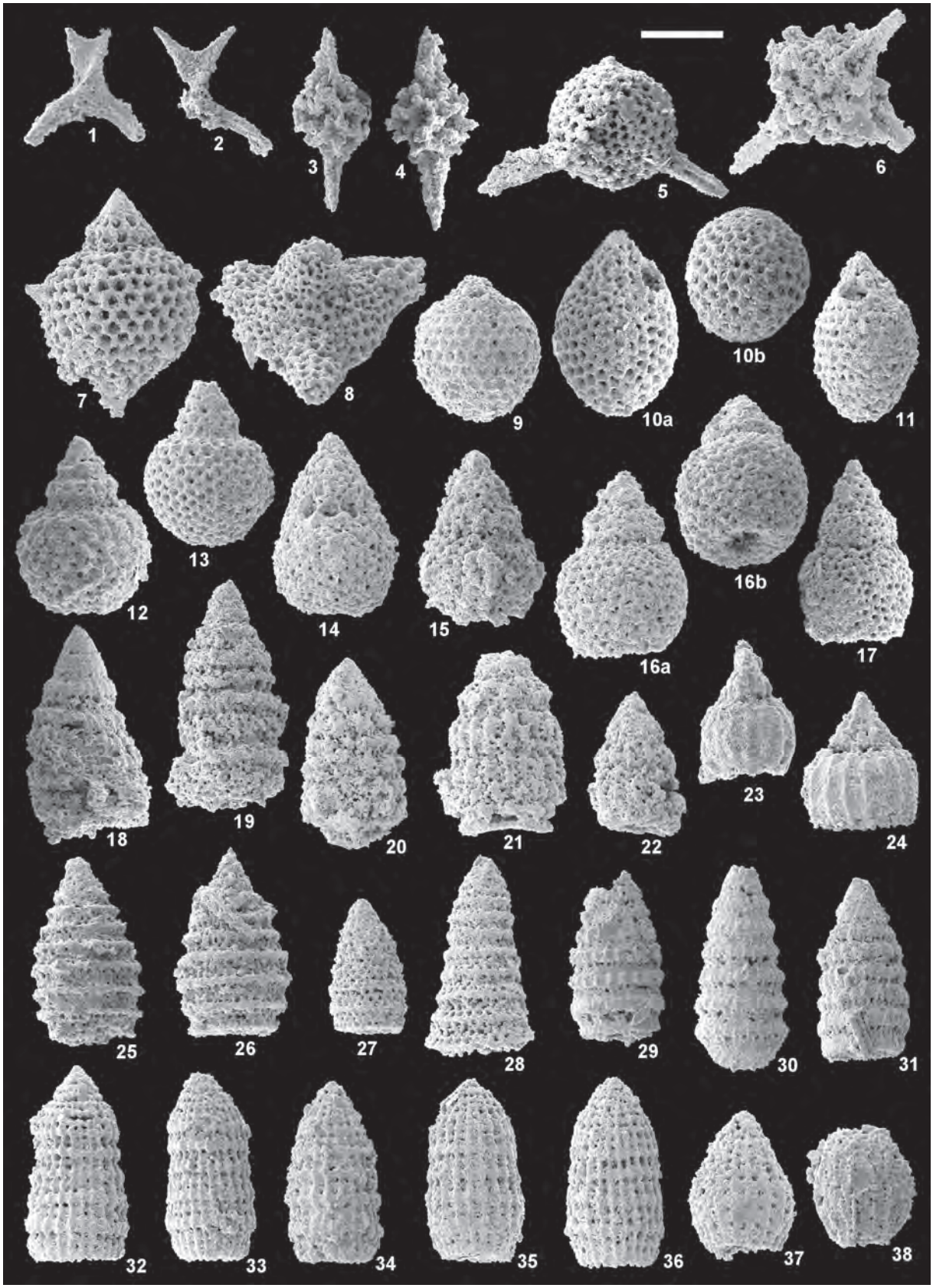
1
2
3
4
5
6
7
8
9
10a
10b
11
12
13
14
15
16a
16b
17
18
19
20
21
22
23
24
25
26
27
28
29
30
31
32
33
34
35
36
37
38

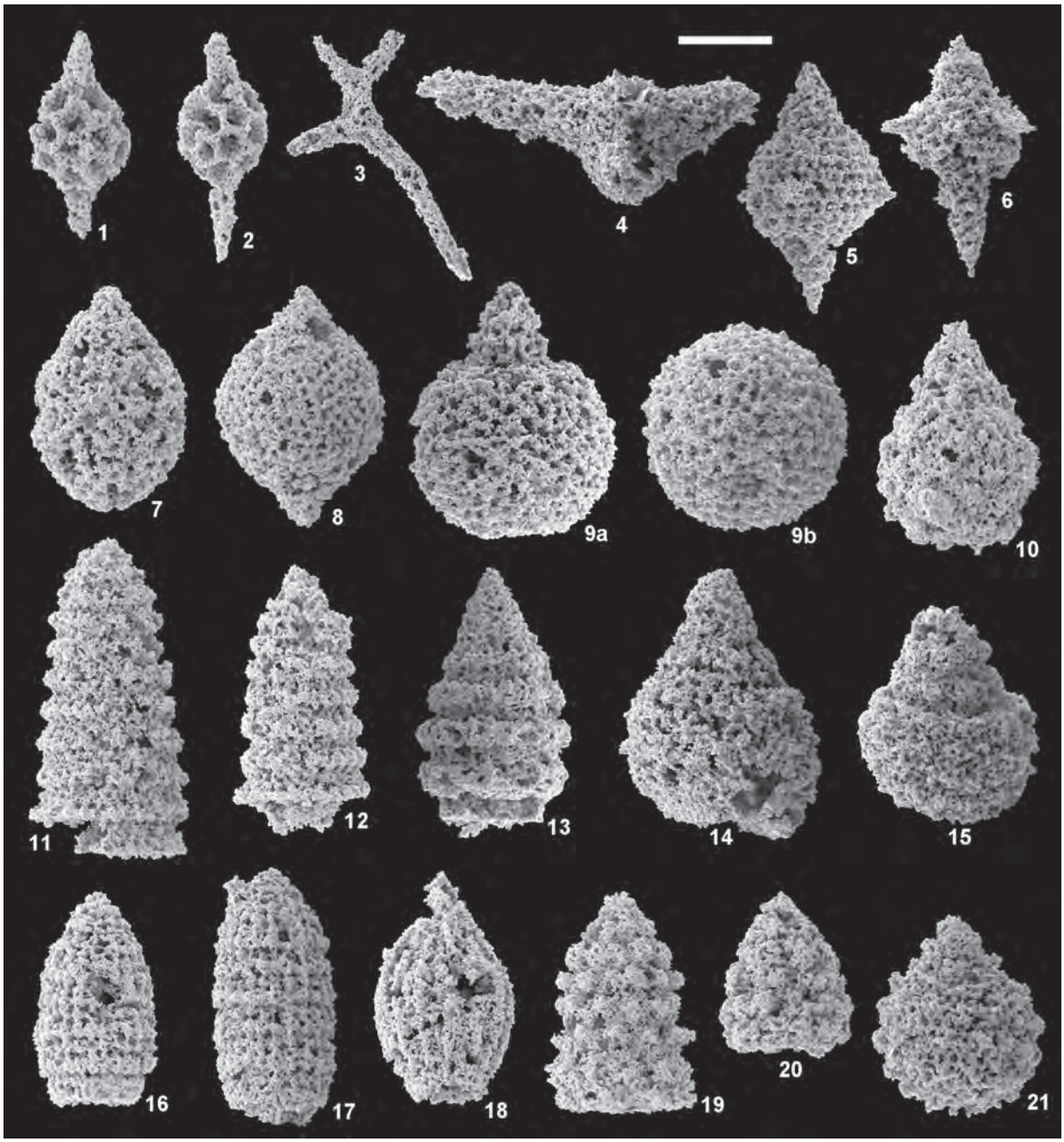

Fig. 18. Radiolarians from the Snežnica section, Sn-28.9: 1, 2. *Pantanellium squinaboli*; 3. *Dicerosaturnalis trizonalis*; 4. *Parapodocapsa furcata*; 5, 6. *Spinosicapsa* spp.; 7. *Zhamoidellum* sp.; 8. *Hemicryptocapsa capita*; 9a–b. *Crococapsa pseudouterculus*; lateral and antapical view of the same specimen; 10. *Hiscocapsa* cf. *kaminogoensis*; 11, 12. *Praeparvicingula cosmoconica*; 13. *Svinitzium* cf. *depressum*; 14. *Obesacapsula* cf. *verbana*; 15. *Obesacapsula* cf. *rusconensis*; 16, 17. *Archaeodictyomitra apiarium*; 18. *Hsuum raricostatum*; 19. *Xitus robustus*; 20. *Pseudoxitus gifuensis*; 21. *Arcanicapsa* sp. Magnification: 15: 100x (scale bar 150 μm); 1–6, 11–12, 14, 16–21: 150x (scale bar 100 μm); 7–10, 13: 200x (scale bar 75 μm).

Remaniella filipescui, cysts of *Colomisphaera lapidosa*, *Colomisphaera carpathica, Stomiosphaera moluccana*, *Stomiosphaera wanneri*, *Stomiosphaera* sp., *Cadosina semiradiata fusca*, calcite walled foraminifera (*Spirillina* sp., *Lenticulina* sp., *Nodosaria* sp., and *Patelina subcretacea*), fragments of agglutinated foraminifera, and infrequent fragments of bivalves, echinoids, crinoids, aptychi, ostracods, and ophiuroids were determined.

Calcareous nannofossils and nannofossil zonation

The abundance and preservation of calcareous nannofossils is highly dependent on lithology. In the Czorsztyn Limestone Formation, the nodular limestones of the *Ammonitico Rosso* facies provide poor and fragmented nannofossils (1–5 specimens per 10 microscopic fields of view), with relatively high species diversity. In contrast, the biomicritic limestones of the Pieniny Limestone Formation contain an extremely poor nannofossil record (1 specimen per 10–20 microscopic fields of views). The genera *Watznaueria* and *Cyclagelosphaera* are quantitatively predominant, together composing about 90–95% of the assemblage. This phenomenon is probably indicative of intense nannofossil dissolution (Roth and Krumbach 1986) in both formations. Therefore, the observed assemblages do not reflect the original calcareous nannoflora. That being said, nannofossil marker species, especially nannoconids, have been occassionally found.

Rare nannofossil occurrences in the lowermost part of the section do not enable precise biostratigraphic interpretation. That being acknowledged, fragments (4.9 m) and whole specimens (6.0 m) of *Faviconus multicolumnatus* reflect Zone NJT14 (Kimmeridgian). The NJT15a Subzone (lower Tithonian) is demonstrated by the FO of *Conusphaera mexicana minor* (11.1 m). The interval from the FO of *Polycostella beckmannii* (13.1 m) to the FO of *Nannoconus globulus minor* (24.3 m) captures Zones NJT15b and NJT16, and so is correlated with the upper lower Tithonian. The FO of *Nannoconus globulus minor* indicates Zone NJT17a (upper Tithonian). A fragment of the stratigraphically significant marker species *Nannoconus wintereri* (25.9 m), accompanied by *N. globulus globulus*, allows correlation with Zone NC0, the base of the Berriasian. The *Calpionella alpina* acme event, which defines the Tithonian–Berriasian boundary, is detected just above 26 m (Reháková in Michalík et al. 2021).

Nannoconus steinmannii/kamptneri minor (36.6 m) and *Umbria granulosa grahulosa* (39.6 m) indicate Zone NC0b (lowermost Berriasian). The FO of *N. steinmannii steinmannii* (40.4 m) defines the base of Zone NC1 (upper lower Berriasian).

Radiolarians and radiolarian zonation

Of the thirteen samples treated for radiolaria, three were productive (14.00 m, 28.90 m, and 44.50 m). Moderately well-preserved radiolarians were obtained from samples 14.00 and 44.50, while sample 28.90 yielded poorly preserved radiolarians. All radiolarians were found in limestone; none could be extracted from chert nodules. The species inventory of the productive samples is listed in Table 2 and illustrated in Figs 17–20.

According to the zonation of Baumgartner et al. (1995a), sample 14.00 is assigned to UAZs 12–13, as suggested by *Cinguloturris cylindra* and *Eucyrtidiellum pyramis* (Table 2). Samples 28.90 and 44.50 are assigned to UAZs 13–15 based on *Hsuum raricostatum* and the species denoted above, which have FADs in UAZ 13. *Hemicryptocapsa carpathica*, which ocurred in sample 44.50, was restricted to the Jurassic in the zonation of Baumgartner et al. (1995a) (see Table 1), but later it was also found in the Berriasian (Matsuoka 1998). According to the zonation established by Matsuoka (1995), all three samples belong to the rather long Pseudodictyomitra carpatica Zone. This zonal assignment is suggested by the presence of *Pseudodictyomitra carpatica* (Table 2) and the absence of *Cecrops septemporatus*, the evolutionary first appearance datum of which defines the top of this zone. Here, we note that available radiolarian zonations are rather crude across the Jurassic/Cretaceous boundary. A group of radiolarian researchers is intensely working on refining radiolarian biochronology through the Tithonian–Berriasian interval. Two objectives exist – to include a great variety of species in a future composite range chart (e.g., O'Dogherty et al. 2018) and to carry out high resolution sampling in key J/K boundary sections (e.g., Matsuoka et al. 2021).

Stable carbon and oxygen isotopes, magnetic susceptibility, and gamma ray spectrometry

As described above, sequences of *Ammonitico Rosso* and *Maiolica*-style facies are characterized by a long-term carbon isotope trend without significant carbon isotope excursions (see Michalík et al. 2009, 2016; Michalík and Reháková 2011). $\delta^{13}C$ values gradually de-

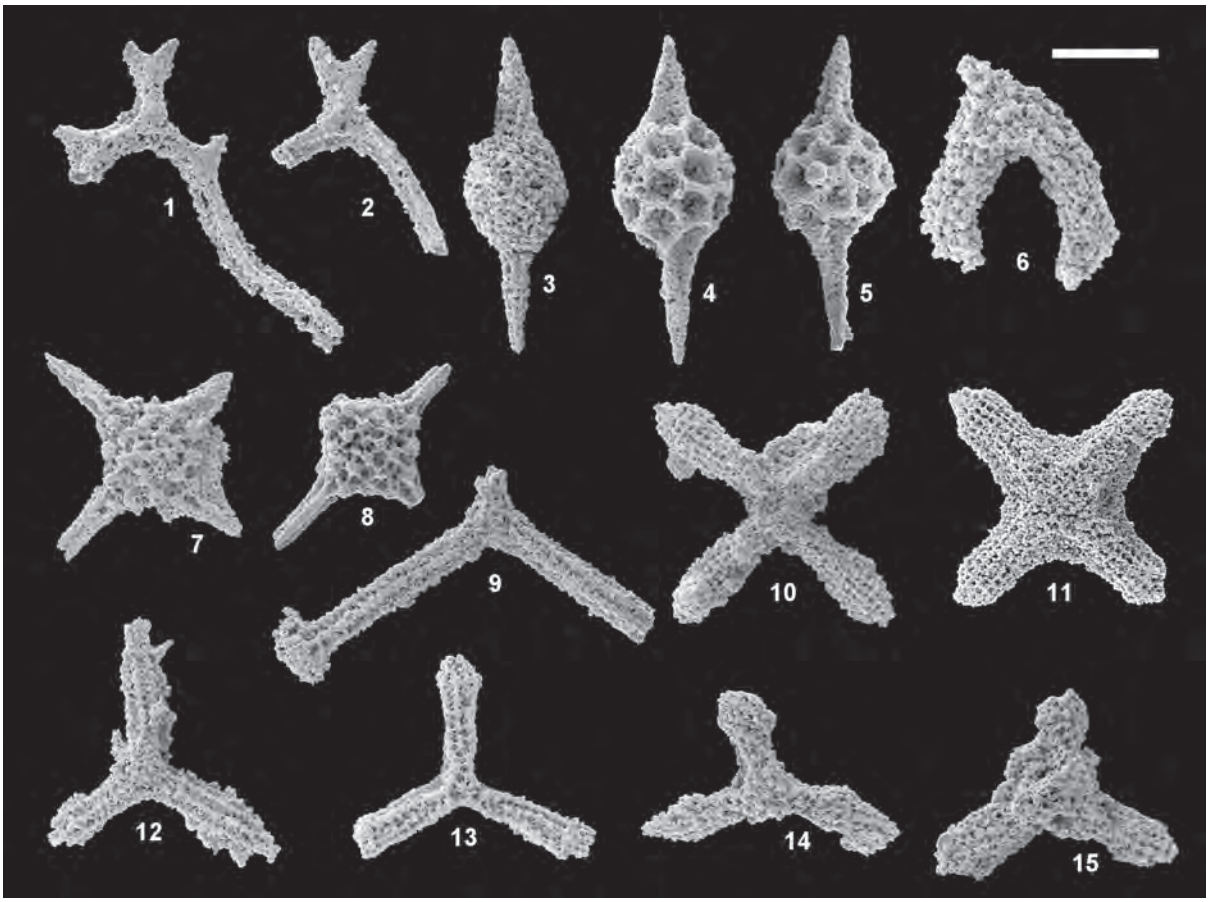

Fig. 19. Spumellarian radiolarians from the Snežnica section, Sn-44.5: 1. *Dicerosaturnalis gratiosus*; 2. *Dicerosaturnalis trizonalis*; 3. *Archaeospongoprunum patricki*; 4, 5. *Pantanellium squinaboli*; 6. *Deviatus diamphidius*; 7, 8. *Emiluvia chica*; 9. *Tritrabs ewingi*; 10, 11. *Pseudocrucella? elisabethae*; 12. *Halesium palmatum*; 13. *Angulobracchia heteroporata*; 14. *Angulobracchia? portmanni*; 15. *Angulobracchia mediopulvilla*. Magnification: 7–15: 100x (scale bar 150 μm); 1–6: 150x (scale bar 100 μm).

creased from about +3‰ in the late Oxfordian to around +1‰ in the late Tithonian; these relatively stable values persisted throughout the whole Berriasian. In the Snežnica section (Fig. 21), $\delta^{13}C$ data ranged from 1.013‰ to 2.040‰, confirming that the $\delta^{13}C$ trend indicates decelerated seawater carbon cycling (Weissert and Channell 1989; Price et al. 2016). Similar curves have been documented in the majority of sections on the Tethyan margin (Michalík et al. 2021). In the J/K boundary interval, an increase of seawater temperature (approximately 2–4˚C) has been suggested on the basis of $\delta^{18}O$ trends in the Brodno and Strapkova sections (Michalík et al. 2009, 2016). However, these results should be interpreted with a degree of caution. Pelagic carbonate sediment is largely derived from planktonic skeletons (i.e., nannofossils, calpionellids, and so forth), and so its original $\delta^{18}O$ values will be influenced by local conditions, especially by precipitation rates and of surface water evaporitization; these are especially pertinent in the arid climate of the Early Berriasian. The wide range (–6‰ to +1‰) and high-frequency variability of $\delta^{18}O$ values in the Brodno and Strapkova sections seems to be the result of both seawater salinity variations and short time sedimentary cycles during the J/K boundary. The decrease of $\delta^{18}O$ values from the Intermedia/Colomi boundary interval to the base of the Alpina Subzone is indicative of sustained warming. Large, positive $\delta^{18}O$ shifts may reflect evaporation-related, early diagenetic factors and short time eustatic fluctuations. A few short, and one longer, progressive increases of $\delta^{18}O$ values in the Alpina and Ferasini Subzones may represent a slight cooling trend. The oxygen isotopic composition of

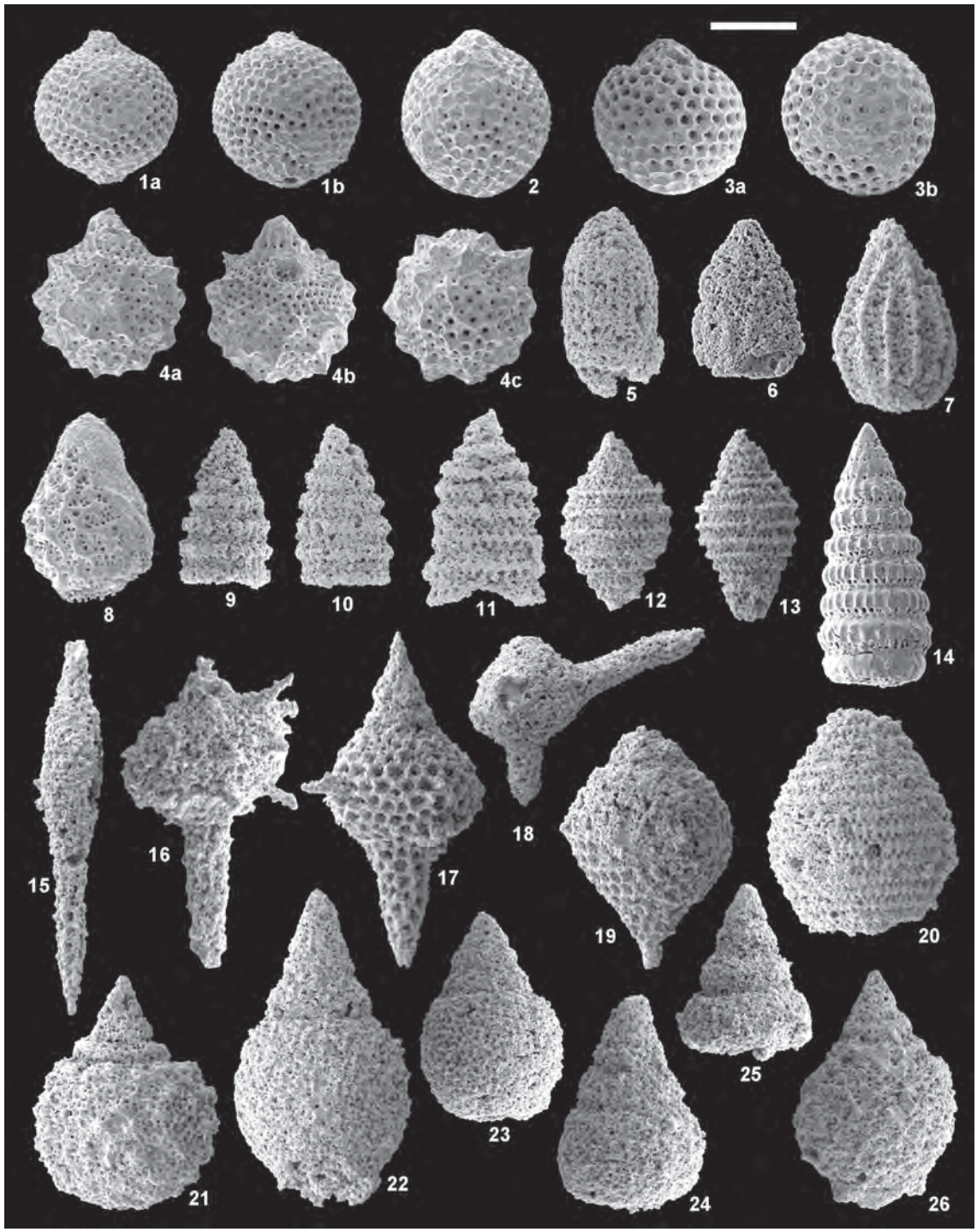

Fig. 20. Nassellarian radiolarians from the Snežnica section, Sn-44.5. 1a–b. *Hemicryptocapsa carpathica*; 2, 3a–b. *Cryptamphorella dumitricai*; 3a–b: lateral and antapical view of the same specimen; 4a–c. *Arcanicapsa* sp. Lateral (a), apical (b) and antapical view (c) of the same specimen; 5. *Archaeodictyomitra apiarium*; 6. *Neorelumbra* cf. *tippitae*; 7. *Hsuum raricostatum*; 8. *Hiscocapsa?* aff. *altiforamina*; 9, 10. *Svinitzium* cf. *depressum*; 11. *Praeparvicingula cosmoconica*; 12, 13. *Tethysetta boesii*; 14. *Pseudodictyomitra carpatica*; 15. *Pseudoeucyrtis? fusus*; 16. *Spinosicapsa milloti*; 17. *Spinosicapsa triacantha*; 18. *Parapodocapsa furcata*; 19. *Spinosicapsa* aff. *coronata sensu* Baumgartner et al. (1995b); 20. *Mirifusus dianae* s.l.; 21. *Obesacapsula cetia*; 22–25. *Obesacapsula verbana*; 26. *Obesacapsula rusconensis*. Magnification: 12– 13, 19–26: 100x (scale bar 150 μm); 5–7, 9–11, 14, 15–18: 150x (scale bar 100 μm); 2–4, 8, 14: 200x (scale bar 75 μm); 1a–b: 250x (scale bar 60 μm). Specimens in figs. 1–4, 8, and 14 are pyritized.

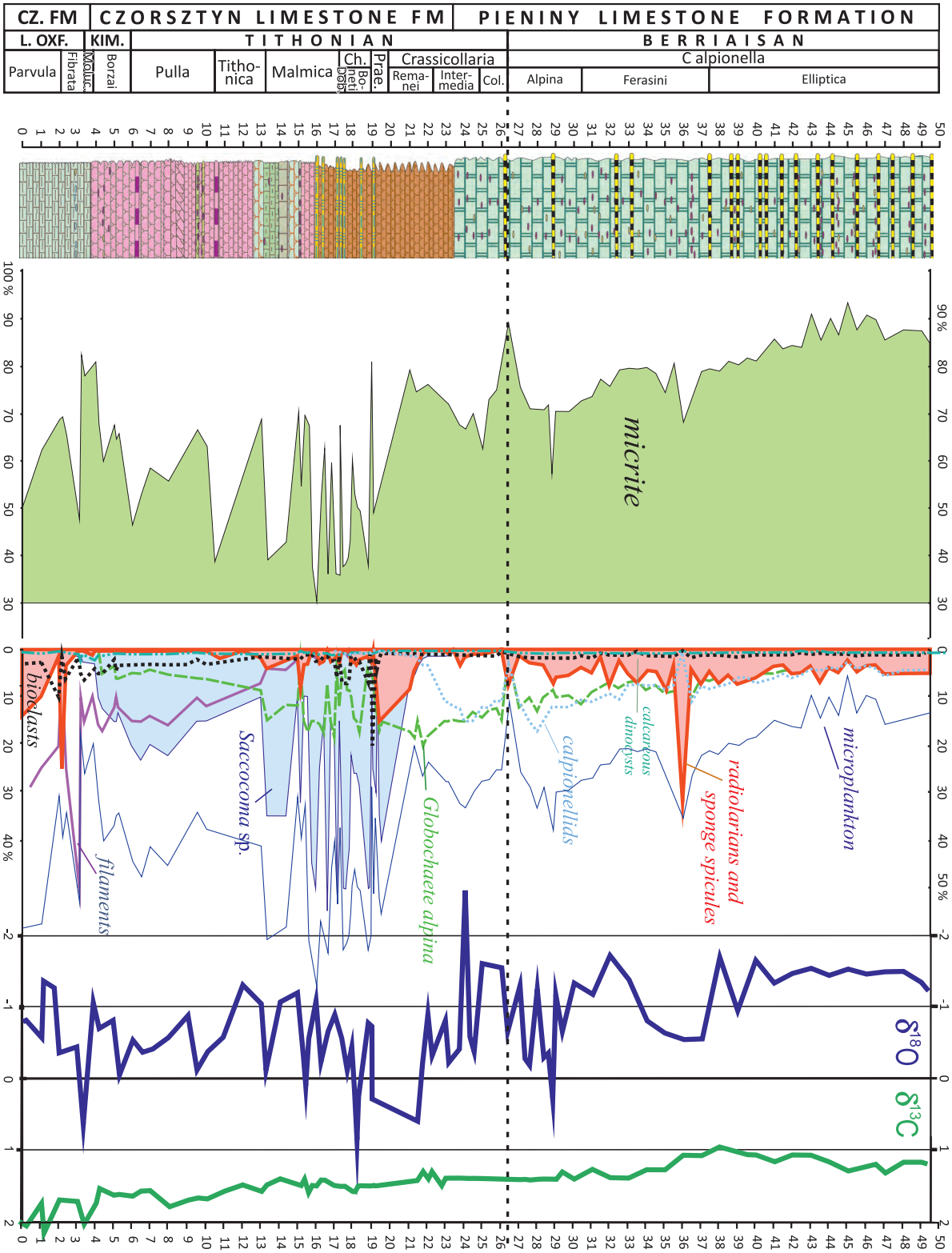

Fig. 21. Lithological column of the Snežnica sequence, quantitative representation of allochems in microfacies, calpionellid and calcareous dinocyst zonations, and $\delta^{18}O$ and $\delta^{13}C$ chemostratigraphy. Abbreviations: CZ. FM – Czajakowa Formation; L. OXF. – Lower Oxfordian; KIM. – Kimmeridgian; Moluc. – Moluccana; Ch. – Chitinoidella; Dob. – Dobeni; Prae. – Praetintinnopsella; Col. – Colomi.

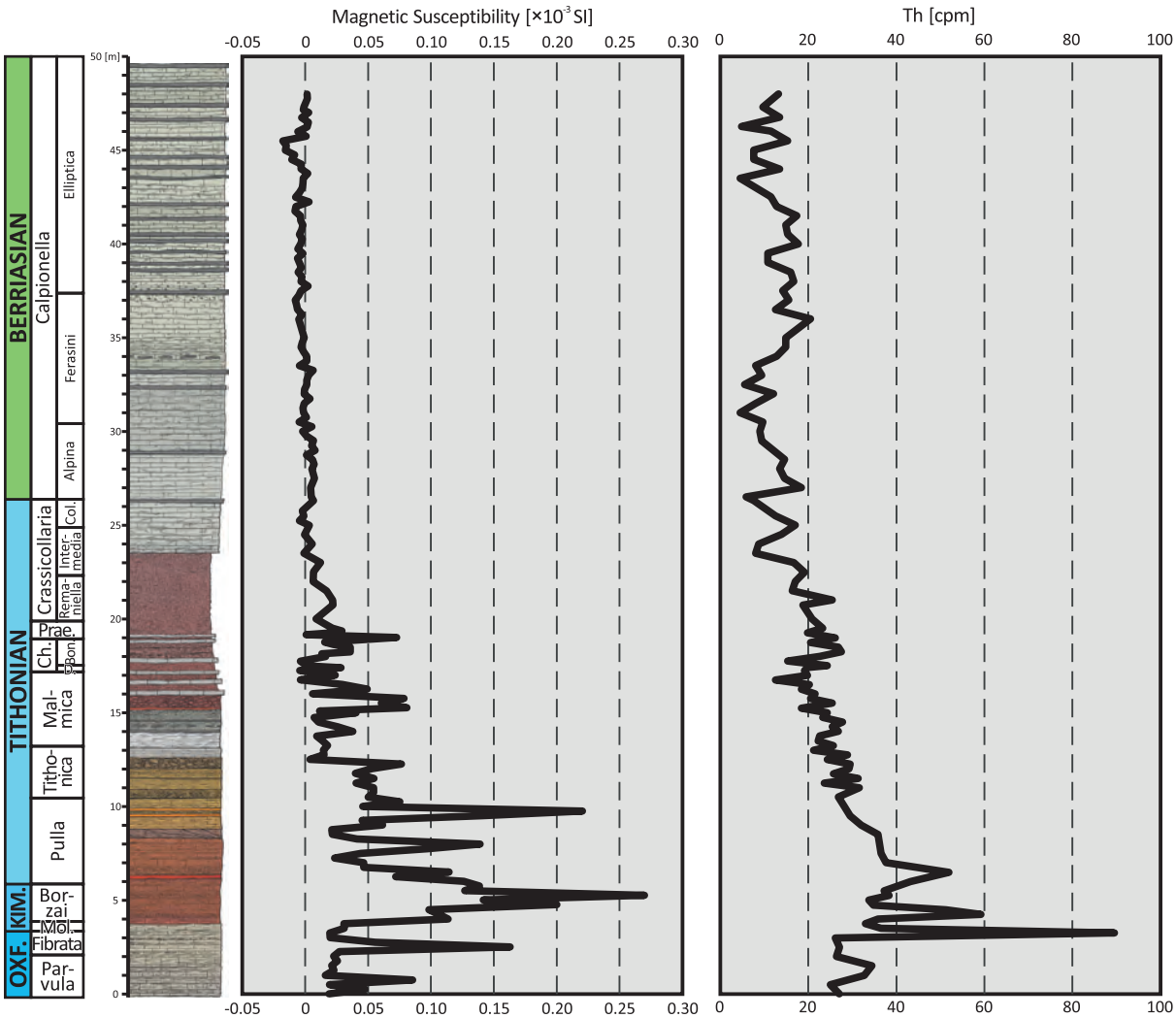

Fig. 22. Magnetic susceptibility and Th content (from GRS measurements) in the Snežnica section (Lodowski et al. in preparation). Abbreviations: OXF. – Oxfordian; KIM. – Kimmeridgian; Mol. – Mollucana; Ch. – Chitinoidella; D. – Dobeni; Bon. – Boneti; Prae. – Praetintinnopsella; Col. – Colomi.

pelagic carbonates could be also influenced by meteoric groundwater released from aquifers to basins during eustatic sea-level drop (Haq 2014; Price et al. 2016). The $\delta^{18}O$ distribution within the sections suggests that large lateral variation of water salinity and composition likely existed.

Magnetic susceptibility and Th concentrations reveal long-term decreasing trends, with maximum values in the Kimmeridgian and lowermost Tithonian (Fig. 22). These trends conform to increases in micrite and calcareous micro- and nannoplankton contributions (Fig. 21), and so are concordant with the Brodno section (Fig. 7).

Stop 3:
Lókút

(*Damian Lodowski and Ottilia Szives*)

The Lokut section (N 47° 12' 15", E 17° 52' 54") is located at the top of the Lokut Hills, on the eastern edge of Lókút village (Figs 23, 24). At its base, ?Oxfordian radiolarites are overlain by ca. 6 m thick? uppermost Oxfordian–lower Tithonian red nodular limestones, biostratigraphically constrained by ammonites (Vígh 1984). Above, in ca. 6 m of upper Tithonian–lowermost Berriasian beds, the nodular structure gradually disappears, ultimately replaced by creamy *Maiolica*-type limestones of early

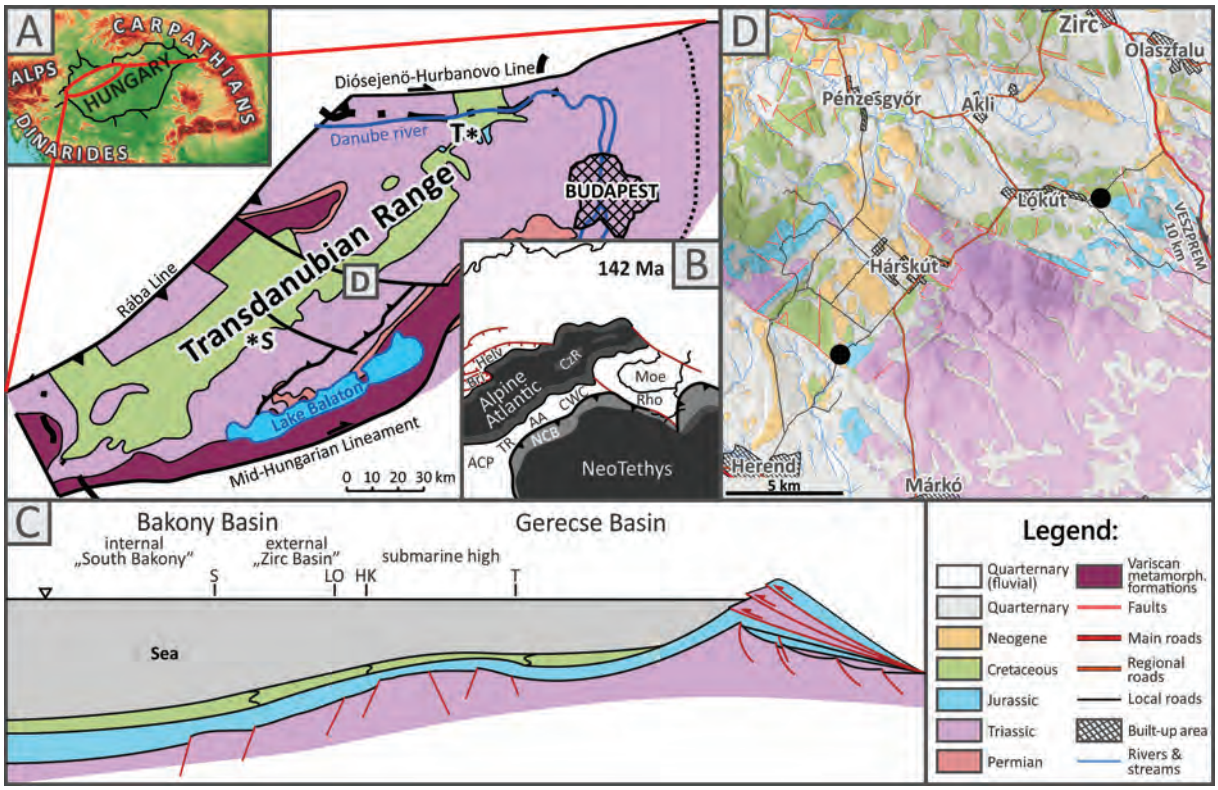

Fig. 23. Geological setting of the Transdanubian Range. A) Simplified pre-Cenozoic map of the Transdanubian Range. B) Simplified paleogeographic map of the circum-Carpathian region during the Berriasian (modified after Stampfli and Hochard, 2009; see Fig. 1). C) Conceptual paleobathymetric cross-section through the latest Jurassic–earliest Cretaceous structure of the Transdanubian Range. D) Geological map in the vicinity of Hárskút and Lókút. Modified after Lodowski et al. (2022).

Berriasian age. The top of the lower Berriasian, which is at least 11 m thick, is not observed (Fig. 25). Magneto- and biostratigraphy (calcareous dinocysts, calpionellids, and nannofossils) of the Tithonian–lower Berriasian interval were investigated in detail by Grabowski et al. (2010, 2017) and Lodowski et al. (2022), whilst Szives and Főzy (2022) have attempted to update the ammonite zonation of the Lókút succession. Chemostratigraphic calibration ($\delta^{13}C$) was provided by Price et al. (2016), Grabowski et al. (2017), and Lodowski et al. (2022), depicting the Kimmeridgian–Tithonian decreasing trend, a minimum near the Tithonian/Berriasian boundary, and relatively stable – although slightly higher – values above (Fig. 25).

The Lókút succession allow to track the vanishing of the saccocomids. These planktic crinoids dominated the lower–lower upper Tithonian packstones; they begin to disappear within magnetozone M20n1n and are absent above, where nearly microfossil-barren wackestones occur (Figs 25, 26). The nannofossil calcification events (NCEs; see Casellato 2009) have also been documented within the succession. The elder NCE I is observed within the upper lower/lowermost upper Tithonian beds, whereas the uppermost Tithonian–lowermost Berriasian captures the younger NCE II (IIA and IIB) (Lodowski et al. 2022).

Precise stratigraphic control enabled sedimentation rate calculations, which revealed that sedimentation rates increased through the Tithonian, from ca. 1 m/Ma during the early Tithonian magnetochron M21r to 7 m/Ma during the earliest Berriasian M18r, and generally decreased above (Fig. 25; Lodowski et al. 2022). These observations, along with terrestrial detrital input data (Grabowski et al. 2017; Lodowski et al. 2022), confirmed that during the latest Jurassic–earliest Cretaceous the lithogenic influx to Lókút continually decreased (Al on Fig. 25). This trend has been interpreted as an effect of progressive aridization, linked with increasing inefficent inland weathering (Lodowski et al. 2022).

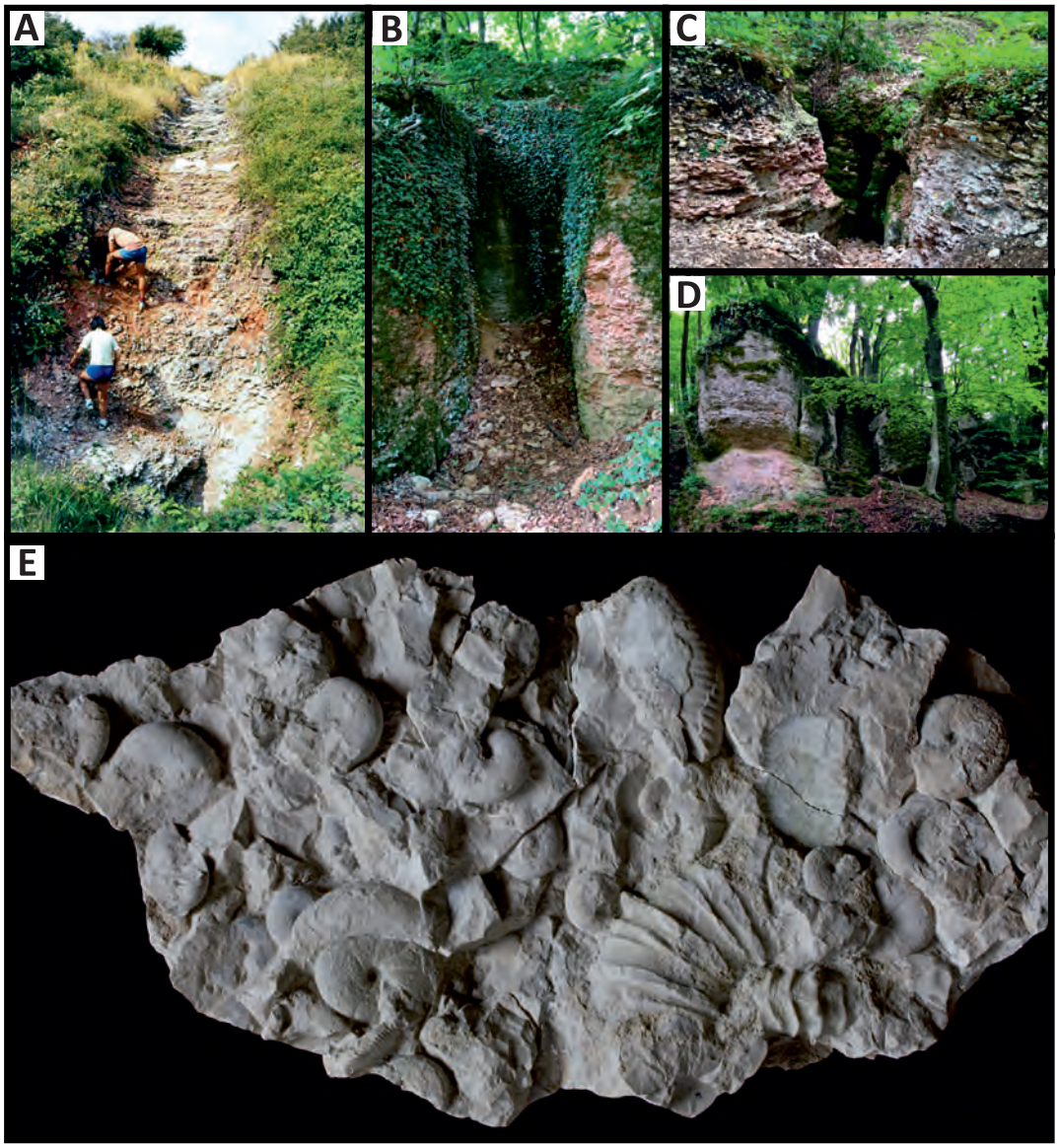

Fig. 24. Transdanubian Range sections visited during this field excursion. A – Lókút LO-I (LH-I); B – Hárskút HK-12/a; C – Hárskút HK-12; and D – Hárskút HK-II; E – Piece of Maiolica-type limestone, packed with ammonites, from the condensed Valanginian Bed 10 of the HK-12 section.

Geochemical investigations in the Lókút succession (Grabowski et al. 2017; Lodowski et al. 2022; Szives et al. 2022) generally depict oxic bottom waters conditions. However, a trend towards positive values of authigenic (non-detrital) U leading into the Berriasian is perceptible (Fig. 28), which may suggest worsening seafloor ventilation. In turn, amongst paleoproductivity-related trace elements, the P_{EXCESS} contribution increases notably through the upper Tithonian and remain relatively elevated in the lower Berriasian. In contrast, a secular increase in Ba_{EXCESS} is observed through the entire Tithonian–lower Berriasian (Fig. 28). This phenomenon will be considered in detail while discussing the Hárskút sections.

Stop 4: Hárskút

(*Damian Lodowski and Ottilia Szives*)

The Upper Jurassic–Lower Cretaceous of the Habrskut succession (N47° 9' 58", E 17°

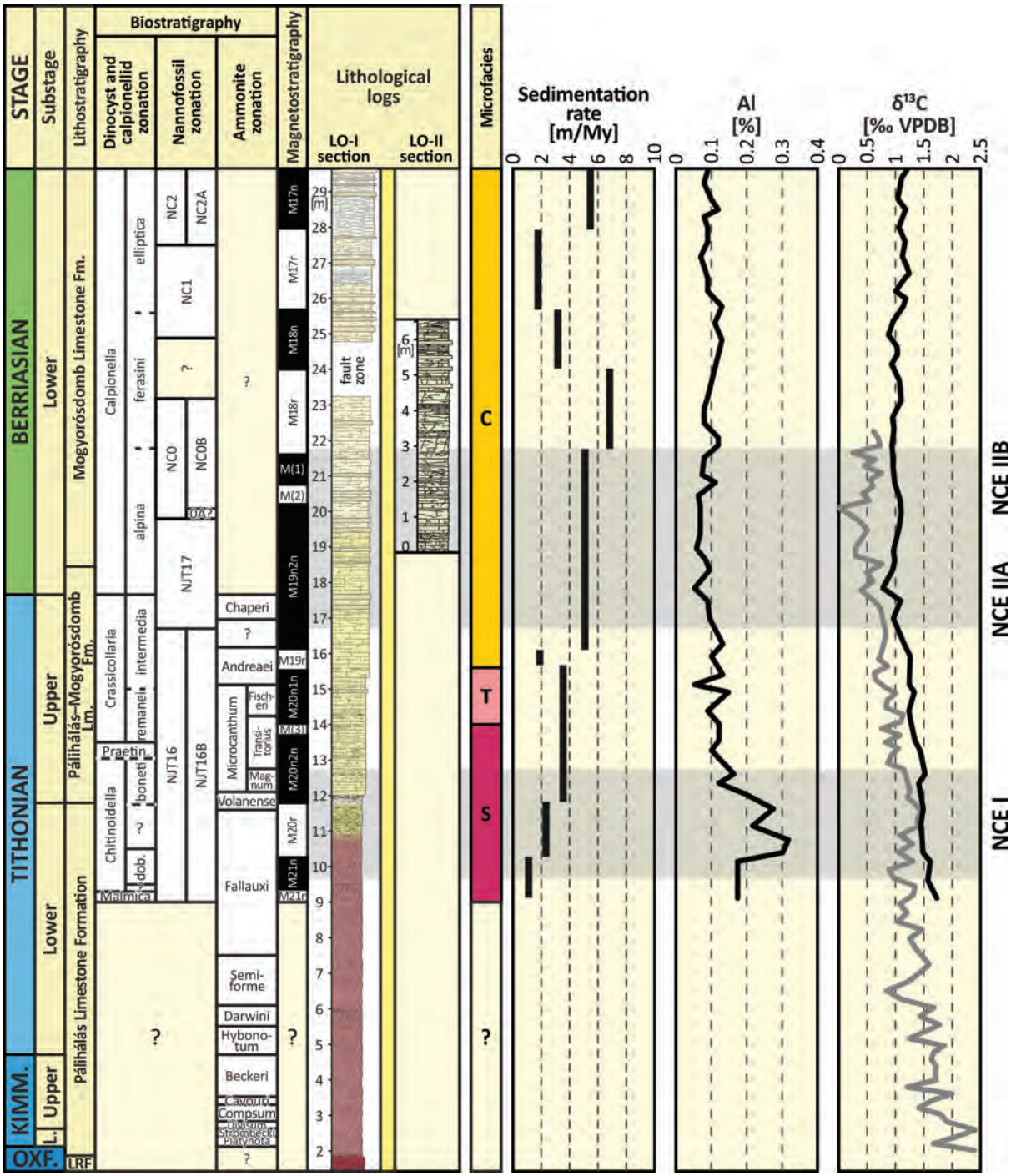

Fig. 25. Stratigraphy, sedimentation rates, Al concentrations, and stable carbon isotopes in the Lókút composite section. Microfossil and nannofossil stratigraphy and magnetostratigraphy after Grabowski et al. (2017) and Lodowski et al. (2022). Ammonite stratigraphy combined from Vígh (1984) and Szives and Főzy (2022). $\delta^{13}C$ curves after Price et al. (2016; gray) and Lodowski et al. (2022; black). Sedimentation rates as calculated by Lodowski et al. (2022). Abbreviations: LRF – Lókút Radiolarite Formation. Explanations: S – *Saccocoma* microfacies; T – transitional microfacies; C – Calpionellid wackestones; M(1) – M19n1n; M(2) – M19n1r; M(3) – M20n1r, NCA - nannofossil calcification event.

47' 11") can be observed in several outcrops (HK-12, HK-12/a, HK-II) in the forest south-west of Hárskút (Figs 23 and 24). As in Lókút, the base of the succession is constituted of

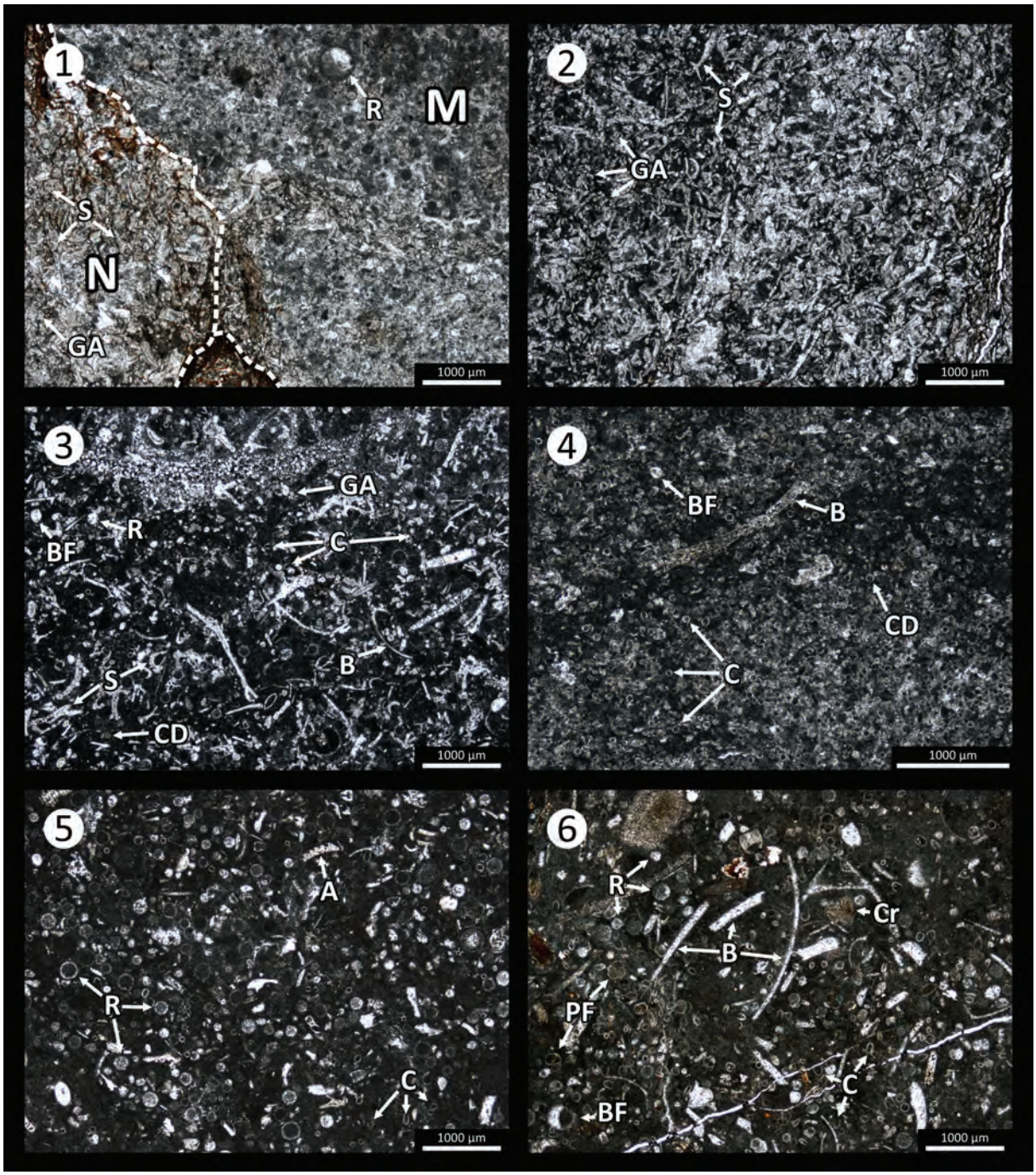

Fig. 26. Microfacies (MF) of the Lókút and Hárskút sections. 1–2: *Saccocoma* dominated packstone (1: lower Tithonian; 2: upper Tithonian of the HK-12/a section); 3: transitional MF (upper Tithonian of the HK-12/a section); 4–5: calpionellid dominated wackstone/packstone with radiolarians (4: lower Berriasian of the LO-I section; 5 – upper Berriasian of the HK-12 section); 6: bioclastic wackestone/packstone (lower Valanginian of the HK-12 section). Abbreviations: B – bivalve; BF – benthic foraminifera; C – calpionellid; CD – calcareous dinoflagellate; Cr – crinoid trochite; GA – *Globochaete alpina*; M – matrix; N – nodule; PF – planktonic foraminifera; R – radiolaria; S – *Saccocoma*.

Oxfordian radiolarites. These are followed by Kimmeridgian–mid-upper Tithonian nodular limestones and upper Tithonian–upper Berriasian pelitic limestones. Intriguingly, the *Ammonitico Rosso* facies reappears in the upper Berriasian–lowermost Valanginian, one

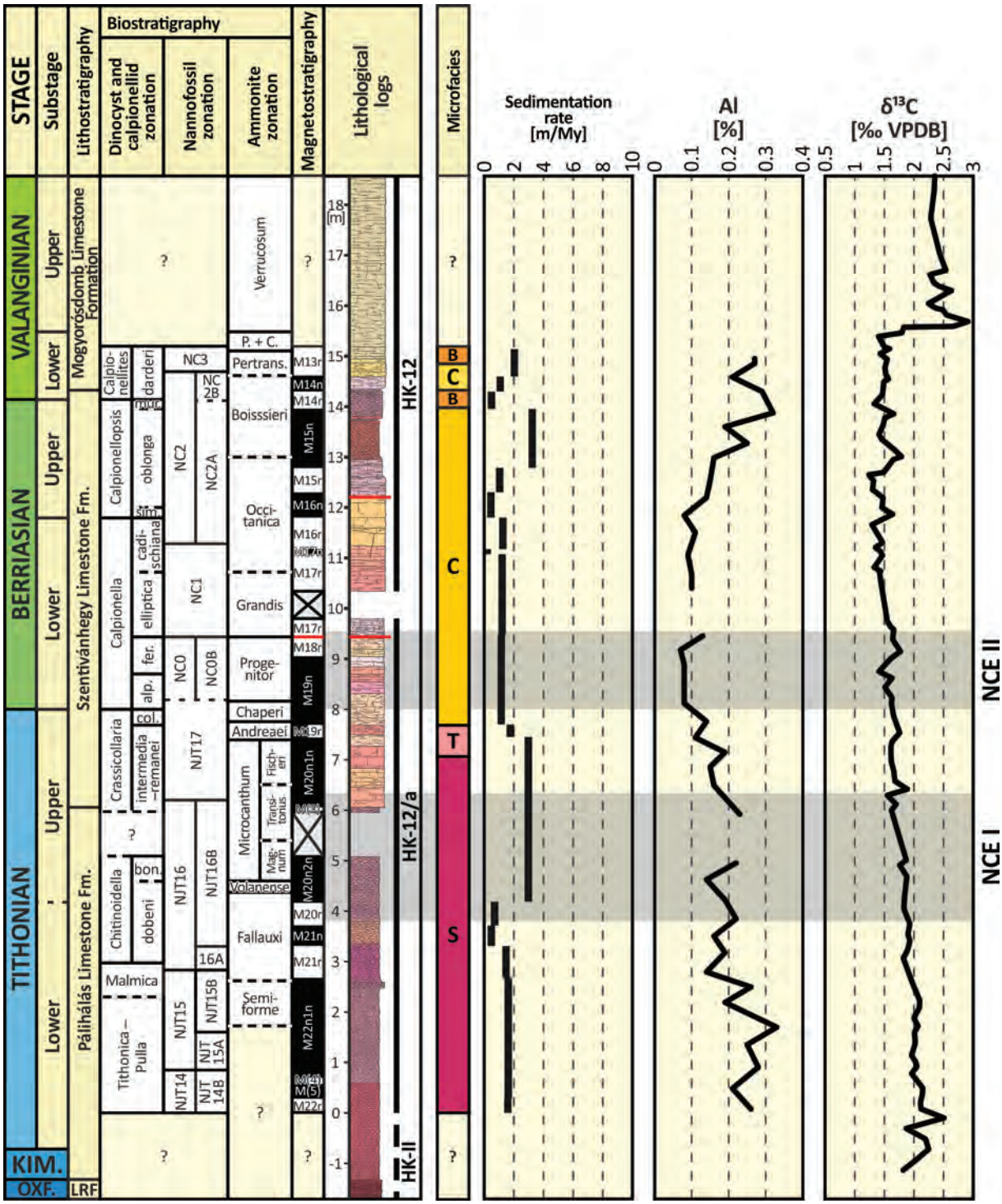

Fig. 27. Stratigraphy, sedimentation rates, Al concentrations, and $\delta^{13}C$ chemostratigraphy in the Hárskút composite section. Micro- and nannofossil zonation and magnetostratigraphy after Lodowski et al. (2022). Ammonite stratigraphy combined from Főzy et al. (2010) and Szives and Főzy (2022). $\delta^{13}C$ curve after Főzy et al. (2010; Valanginian of the HK-12 section), Price et al. (2016; HK-II section), and Lodowski et al. (2022; HK-12/a section and Berriasian of the HK-12 section). Sedimentation rates as calculated by Lodowski et al. (2022). Abbreviations: KIM. – Kimmeridgian; OXF. – Oxfordian; LRF – Lókút Radiolarite Formation; Pertrans. – Pertransiens; P. + C. – Pertransiens + Campylotoxus; bon. – boneti; col. – colomi; fer. – ferasini; sim. – simplex; mur. – murgeanui. Explanations: S – *Saccocoma* microfacies; T – transitional microfacies; C – Calpionellid wackestones; B – bioclastic wackestones/packstones. Red lines on lithological log – hiatuses/condensation

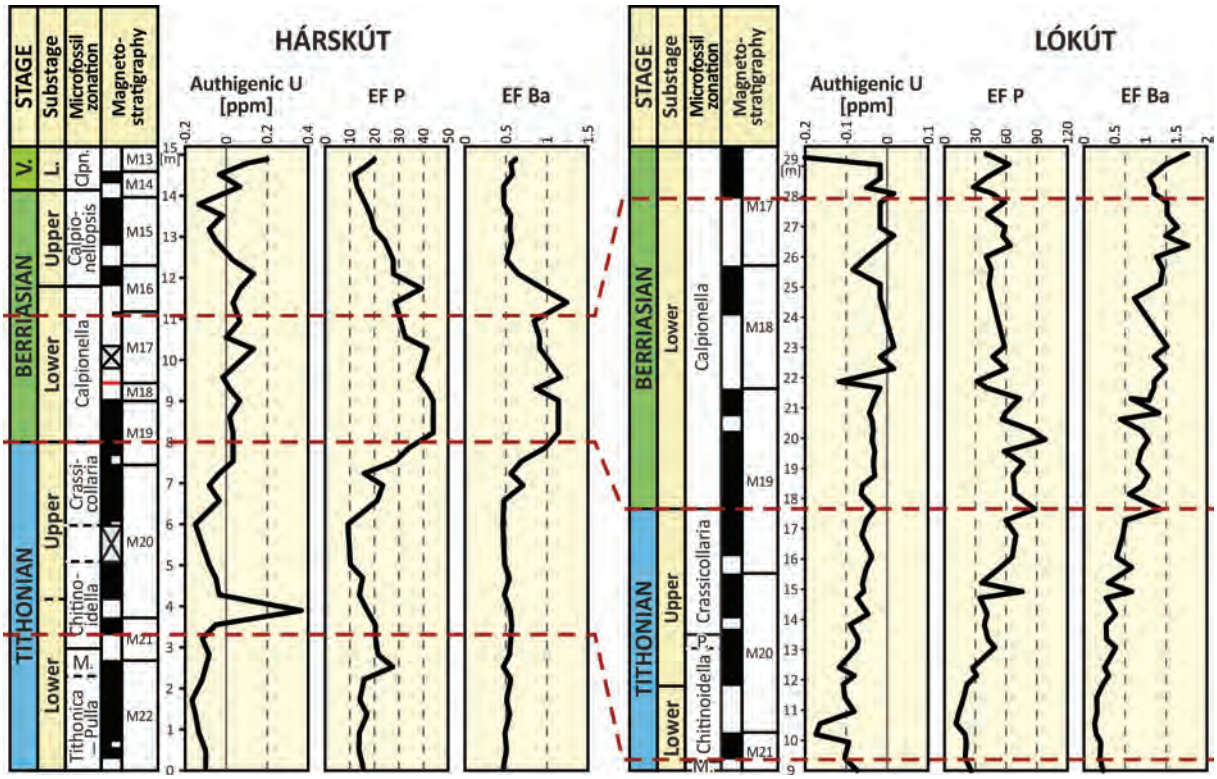

Fig. 28. Authigenic U, P_{EXCESS} and Ba_{EXCESS} in the Hárskút and Lókút sections.

of the youngest reports of this facies recognized to date (compare with Cecca et al. 1992, Lukeneder 2011). The uppermost strata seen in this area are Valanginian *Maiolica*-type limestones and Hauterivian marls (Főzy et al. 2010; Lodowski et al. 2022).

The high-resolution magneto- and biostratigraphic study of Lodowski et al. (2022) in the HK-12 and HK-12/a sections enabled the recognition of two hiatal/condensation zones: the lower Berriasian, spanning the entire M18n magnetozone, and the upper Berriasian, covering the majority of magnetozone M16n (Fig. 27). Using ammonites, Szives and Főzy (2022) postulated two additional discontinuities: the lower at the lower/upper Tithonian boundary and the higher within the upper Tithonian Crassicollaria calpionellid Zone (Fig. 27). These discoveries are reasonable given the relatively elevated paleobathymetric setting of the Hárskút succession, in which bottom currents might have periodically swept out unlithified sediments, resulting in condensations and/or hiatuses.

$\delta^{13}C$ curves from the Hárskút sections (Fig. 27; Főzy et al. 2010; Price et al. 2016; Lodowski et al. 2022) decline upsection, from ca. 2‰ near the Kimmeridgian/Tithonian boundary to ca. 1.25‰ near the lower/upper Berriasian transition. In the upper Berriasian–lower Valanginian, values remain relatively stable. In the lowermost upper Valanginian, an outstanding peak to near 3‰ is interpreted as the "Weissert" carbon isotope event (Főzy et al. 2010). After an initial decrease to ca. 2.3‰, the late Valanginian exhibits stable $\delta^{13}C$ values, and another decreasing trend is characteristic of the uppermost Valanginian–Hauterivian.

Like the Lókút succession, the Hárskút sections enable us to track the sedimentary turnover connected with the disappearance of *Saccocoma*-dominated microfacies (Figs 26, 27). The microfacies succession is very similar: lower–upper Tithonian crinoidal packstones, transitional microfacies, and uppermost Tithonian–Berriasian wackestones. However, the disappearance of *Saccocoma* itself was slightly shifted in time between the localities: in Hárskút, the transitional microfacies also covers magnetozone M19r.

It is nothworthy that the NCE horizons known from Lókút (Grabowski et al. 2017; Lodowski et al. 2022) were also documented in Hárskút; although slightly shifted between localities (especially NCE I; compare Fig. 25 and Fig. 27), their ranges are correlative. Attention is also drawn to the fact that the demise of the *Saccocoma* microfacies lies between NCE I and NCE II in both successions. This suggests that the changes contributing to NCEs, such as climate, atmospheric pCO_2, and Mg/Ca ratios (e.g., Bornemann et al. 2003; Tremolada et al. 2006; Casellato 2009), may have also been important for saccocomids.

Sedimentation rates obtained from magnetostratigraphic data generally suggest very low to low rates of deposition (below 4 m/Ma, usually ca. 1m/Ma), with local highs (e.g., within magnetozone M15n). Consequently, the Tithonian decreasing lithogenic influx trend recognized in the Lókút succession has also been documented in Hárskút. Interestingly, the upper Berriasian captures increased clastic contribution, which also remains elevated within the lower Valanginian (Fig. 27). This phenomenon was interpreted by Lodowski et al. (2022) as associated with tectonic re-activation in the Neotethyan Collision Belt (accretionary prism at the northwest rim of the Neotethys; Missoni and Gawlick 2010), which also resulted in the onset of mixed siliciclastic-carbonate sedimentation in the Gerecse Basin (Fodor et al. 2013).

Corresponding patterns to Lókút are observed in paleoredox proxies and trace elements (Fig. 28). The most characteristic is in the uppermost Tithonian–lowermost upper Berriasian interval, where Authigenic U, P_{EXCESS} and Ba_{EXCESS} all display elevated values. Beyond this interval, a decreasing trend occurs in the lower/upper Tithonian transition, and an increasing trend is observed within the lower Valanginian. This phenomenon was recently interpreted as connected with paleoenvironmental perturbations, primarily related to Tithonian–Berriasian climate change (Szives et al. 2022). In this case, the onset of an arid climate mode during the late Tithonian (e.g., Grabowski et al. 2017) should have resulted in less intense monsoonal circulation, affecting monsoonal upwelling processes (e.g., De Wever 2014), and ultimately leading to reduced water column mixing and (stronger) stratification. Under these conditions, seafloor ventilation become less efficient, leading to the accumulation of Authigenic U. Accordingly, restricted mixing in the upper ocean affected the nutrient shuttle system, allowing for the burial of more micronutrient-type elements (P_{EXCESS} and Ba_{EXCESS} on Fig. 28) than under the 'normal' mixed state.

REFERENCES

Aita, Y. and Okada, H. 1986. Radiolarians and calcareous nannofossils from the uppermost Jurassic and lower Cretaceous strata of Japan and Tethyan regions. Micropaleontology, 32, 97–128.

Andreini, G., Caracuel, J.E. and Parisi, G. 2007. Calpionellid biostratigraphy of the Upper Tithonian–Upper Valanginian interval in Western Sicily (Italy). Swiss Journal of Geosciences, 100, 179–198.

Andrusov, D. 1938. Geological research of the inner Klippen Belt in Western Carpathians III. Rozpravy Státního geologického ústavu Československé republiky 9, 1–135. [In Czech]

Andrusov, D. 1950. The Klippen Belt between Vlára River and Žilina. Geologicky Zbornik SAV, 1, 288–292. [In Slovak]

Andrusov, D. 1959. Geology of the Czechoslovakian Carpathians II, 1–375. Vydavateľstvo SAV**;** Bratislava. [In Slovak]

Baumgartner, P.O., Bartolini, A., Carter, E.S., Conti, M., Cortese, G., Danelian, T., De Wever, P., Dumitrica, P., Dumitrica-Jud, R., Goričan, Š., Guex, J., Hull, D.M., Kito, N., Marcucci, M., Matsuoka, A., Murchey, B., O'Dogherty, L., Savary, J., Vishnevskaya, V., Widz, D. and Yao, A. 1995a. Middle Jurassic to Early Cretaceous radiolarian biochronology of Tethys based on Unitary Associations. In: Baumgartner, P.O., O'Dogherty, L., Goričan, Š., Urquhart, E., Pillevuit, A. and De Wever, P. (Eds), Middle Jurassic to Lower Cretaceous Radiolaria of Tethys: Occurrences, Systematics, Biochronology. Mémoires de Géologie (Lausanne), 23, 1013–1048.

Baumgartner, P.O., O'Dogherty, L., Goričan, Š., Dumitrica-Jud, R., Dumitrica, P., Pillevuit, A., Urquhart, E., Matsuoka, A., Danelian, T., Bartolini, A., Carter, E.S., De Wever, P., Kito, N., Marcucci, M. and Steiger, T. 1995b. Radiolarian catalogue and systematics of Middle Jurassic to Early Cretaceous Tethyan genera and species. In: Baumgartner, P.O., O'Dogherty, L., Goričan, Š., Urquhart, E., Pillevuit, A. and De Wever, P. (Eds), Middle Jurassic to Lower Cretaceous Radiolaria of Tethys: Occurrences, Systematics, Biochronology. Mémoires de Géologie (Lausanne), 23, 37–685.

Benzaggagh, M., Homberg, C., Schnyder, J. and Ben Abdesselam-Mahdaoui, S.B. 2015. Description et biozonation des sections de crinoïdes saccocomidés

du Jurassique supérieur (Oxfordien–Tithonien) du domaine téthysien occidental. Annales de Paléontologie, 101, 95–117.

Bernoulli, D. and Jenkyns, H.C. 2009. Ancient oceans and continental margins of the Alpine-Mediterranean Tethys: deciphering clues from Mesozoic pelagic sediments and ophiolites. Sedimentology, 56, 149–190.

Birkenmajer, K. 1977. Jurassic and Cretaceous lithostratigraphic units of the Pieniny Klippen Belt, Carpathians, Poland. Studia Geologica Polonica, 45, 1–158.

Borza, K. 1969. Die Mikrofazies und Mikrofossilien des Oberjuras und Unterkreide der Klippenzone der Westkarpaten, 1–124. Vydavateľstvo SAV; Bratislava.

Borza, K. 1984. The Upper Jurassic–Lower Cretaceous parabiostratigraphic scale on the basis of Tintinninae, Cadosinidae, Stomiosphaeridae, Calcisphaerulidae and other microfossils from the West Carpathians. Geologicky Zbornik, 35, 539–550.

Boughdiri, M., Sallouhi, H., Maâlaoui, K., Soussi, M. and Cordey, F. 2006. Calpionellid zonation of the Jurassic – Cretaceous transition in north Atlasic Tunisia. Updated Upper Jurassic stratigraphy of the 'Tunisian Trough' and regional correlations. Comptes Rendus Geoscience, 338, 1250–1259.

Bragin, V.Yu., Dzyuba, O.S., Kazansky, A.Yu. and Shurygin, B.N. 2013. New data on the magnetostratigraphy of the Jurassic–Cretaceous boundary interval, Nordvik Peninsula (northern East Siberia). Russian Geology and Geophysics, 54, 335–348.

Bralower, T.J., Monechi, S. and Thierstein, H.R. 1989. Calcareous nannofossils zonation of the Jurassic–Cretaceous boundary interval and correlations with the Geomagnetic Polarity Timescale. Marine Micropaleontology, 14, 153–235.

Casellato, C.E. 2009. Causes and consequences of calcareous nannoplankton evolution in the Late Jurassic: implications for biogeochronology, biocalcification and ocean chemistry, 122 p. Ph.D. Thesis, Universita degli Studi di Milano; Milan.

Casellato, C.E. 2010. Calcareous nannofossil biostratigraphy of Upper Callovian–Lower Berriasian successions from the Southern Alps, North Italy. Rivista Italiana di Paleontologia e Stratigrafia, 16, 357–404.

Casellato, C.E. and Erba, E. 2021. Reliability of calcareous nannofossil events in the Tithonian–early Berriasian time interval: implications for a revised high resolution zonation. Cretaceous Research, 117, 104611.

Cecca, F., Fourcade, E. and Azéma, J. 1992. The disappearance of the "Ammonitico Rosso". Palaeogeography, Palaeoclimatology, Palaeoecology, 99, 55–70.

Csontos, L. and Vörös, A. 2004. Mesozoic plate tectonic reconstruction of the Carpathian region. Palaeogeography, Palaeoclimatology, Palaeoecology, 210, 1–56.

Deconinck, J.-F. 1993. Clay mineralogy of the Late Tithonian – Berriasian deep sea carbonates of the Vocontian trough (SE France), relationship with sequence stratigraphy. Bulletin des Centres de Recherches Exploration – Production, Elf Aquitaine, 17, 223–234.

Dypvik, H., Gudlaugsson, S.T., Tsikalas, F., Attrep, M. Jr., Ferrell, R.E. Jr., Krinsley, D.H., Mörk, A., Faleide, J.I. and Nagy, J. 1996. Mjölnir structure: An impact crater in the Barents Sea. Geology, 24, 779–882.

Dunham, R.J. 1962. Classification of carbonate rocks according to depositional texture. In: Ham, W.E. (Ed.), Classification of carbonate rocks – a symposium. American Association of Petroleum Geologists Memoir, 1, 108–121.

Elbra, T., Reháková, D., Schnabl, P., Čížková, K., Pruner, P., Kdýr, Š., Bubík, M., Svobodová, A. and Švábenická, L. 2018. Magneto- and biostratigraphy across the Jurassic–Cretaceous boundary in the Kurovice section, Western Carpathians, Czech Republic. Cretaceous Research, 89, 211–223.

Elbra, T., Schnabl, P., Čížková, K., Pruner P., Kdýr, Š., Grabowski, J., Reháková, D., Svobodová, A., Frau, C. and Wimbledon, W.A.P. 2018. Palaeo-and rock magnetic investigations across Jurassic-Cretaceous boundary at St Bertrand's Spring, Drôme, France – Applications to magnetostratigraphy. Studia Geophysica et Geodaetica, 62, 323–338.

Enay, R. 2020. The Jurassic/Cretaceous is an impasse. Why do not go back to Oppel's 1865 original and historic definition of the Tithonian? Cretaceous Research, 106, 104241.

Flügel, E. 2004. Microfacies of Carbonate Rocks. Springer-Verlag; Berlin. 976 p.

Fodor, L., Sztanó, O. and Kövér, S. 2013. Mesozoic deformation of the northern Transdanubian Range (Gerecse and Vértes Hills). Acta Mineralogica-Petrographica, 31, 1–52.

Főzy, I., Janssen, N.M.M., Price, G.D., Knauer, J. and Pálfy, J. 2010. Integrated isotope and biostratigraphy of a Lower Cretaceous section from the Bakony Mountains (Transdanubian Range, Hungary): A new Tethyan record of the Weissert event. Cretaceous Research, 31, 525–545.

Frau, C., Bulot, L.G., Reháková, D. and Wimbledon, W.A.P. 2016a. Revision of the ammonite index species *Berriasella jacobi* Mazenot, 1939 and its consequences for the biostratigraphy of the Berriasian Stage. Cretaceous Research, 66, 94–114.

Frau, C., Bulot, L.G. and Wimbledon, W.A.P. 2016b. Systematic paleontology of the Perisphinctoidea in the J/K boundary interval at Le Chouet (Drome, France), and its implications for biostratigraphy. Acta Geologica Polonica, 66**,** 175–204.

Frau, C., Bulot, L.G., Wimbledon, W.A.P. and Ifrim, C. 2016c. Upper Tithonian ammonites (Himalayitidae Spath, 1925 and Neocomitidae Salfeld, 1921) from Charens (Drome, France). Geologica Carpathica, 67, 543–559.

Fülöp, J. 1964. A Bakony hegység alsó-kréta (berriazi–apti) képződményei (Unterkreide [Berrias-Apt] Bildungen des Bakonygebirges). Geologica Hungarica Series Geologia, 13, 194 p.

Galbrun, B. 1985. Magnetostratigraphy of the Berriasian stratotype section (Berrias, France). Earth and Planetary Science Letters, 74, 130–136.

Galloway, J.G., Vickers, M., Price, G.D., Poulton, T.P., Grasby, S.E., Hadlari, T., Beauchamp, B., Sulphur, K. 2020. Finding the VOICE: organic carbon isotope chemostratigraphy of the Late Jurassic–Early Cretaceous of Arctic Canada. Geological Magazine, 157, 1643–1657.

Gawlick, H.-J. and Schlagintweit, F. 2006. Berriasian drowning of the Plassen carbonate platform at the type-locality and its bearing on the early Eoalpine orogenic dynamics in the Northern Calcareous Alps (Austria). International Journal of Earth Sciences, 95, 451–462.

Gawlick, H.-J., Missoni, S., Schlagintweit, F., Suzuki, H., Frisch, W., Krystyn, L., Blau, J. and Lein, R. 2009. Jurassic Tectonostratigraphy of the Austroalpine Domain. Journal of Alpine Geology, 50, 1–152.

Golonka, J., Gahagan, L., Krobicki, M., Marko, F., Oszczypko, N. and Ślączka, A. 2006. Plate tectonic evolution and paleogeography of the Circum–Carpathian region. In: Golonka, J. and Picha, F. (Eds), The Carpathians: Geology and Hydrocarbon Resources. American Association of Petroleum Geologists Memoir, 84, 11–46.

Goričan, Š. 1994. Jurassic and Cretaceous radiolarian biostratigraphy and sedimentary evolution of the Budva Zone (Dinarides, Montenegro). Mémoires de Géologie (Lausanne), 18, 1–177.

Grabowski, J. 2011. Magnetostratigraphy of the Jurassic/Cretaceous boundary interval in the Western Tethys and its correlations with other regions: a review. Volumina Jurassica, 9, 105–128.

Grabowski, J. and Pszczółkowski, A. 2006. Magneto-and biostratigraphy of the Tithonian–Berriasian pelagic sediments in the Tatra Mountains (central Western Carpathians, Poland): sedimentary and rock magnetic changes at the Jurassic/Cretaceous boundary. Cretaceous Research, 27, 398–417.

Grabowski, J., Michalík, J., Szaniawski, R. and Grotek, I. 2009. Synthrusting remagnetization of the Krížna Nappe: high resolution palaeo-and rock magnetic study in the Strážovce section, Strážovske vrchy Mts, Central West Carpathians (Slovakia). Acta Geologica Polonica, 59, 137–155.

Grabowski, J., Michalík, J., Pszczółkowski, A. and Lintnerová, O. 2010a. Magneto- and isotope stratigraphy around the Jurassic/Cretaceous boundary in the Vysoká Unit (Male Karpaty Mountains): correlations and tectonic implications. Geologica Carpathica, 61, 309–326.

Grabowski, J., Haas, J., Márton, E. and Pszczółkowski, A. 2010b. Magneto- and biostratigraphy of the Jurassic/Cretaceous boundary in the Lókút section (Transdanubian range, Hungary). Studia Geophysica et Geodaetica, 54, 1–26.

Grabowski, J., Schnyder, J., Sobień, K., Koptiková, L., Krzemiński, L., Pszczółkowski, A., Hejnar, J. and Schnabl, P. 2013. Magnetic susceptibility and spectra gamma logs in the Tithonian– Berriasian pelagic carbonates in the Tatra Mts (Western Carpathians, Poland): palaeoenvironmental changes at the Jurassic/Cretaceous boundary. Cretaceous Research, 27, 398–417.

Grabowski, J., Lakova, I., Schnabl, P., Sobień, K. and Petrova, S. 2014. Berriasian bio-and magnetostratigraphy and magnetic susceptibility of the Barlya section (Western Balkan Unit, Bulgaria) – preliminary results. Volumina Jurassica, 12, 185–194.

Grabowski, J., Bakhmutov, V., Kdýr, Š., Krobicki, M., Pruner, P., Reháková, D., Schnabl, P., Stoykova, K. and Wierzbowski, H. 2019. Integrated stratigraphy and palaeoenvironmental interpretation of the Upper Kimmeridgian to Lower Berriasian pelagic sequences of the Velykyi Kamienets section (Pieniny Klippen Belt, Ukraine). Palaeogeography, Palaeoclimatology, Palaeoecology, 532, 109216.

Guzhikov, A.Yu., Arkadiev, V.V., Baraboshkin, E.Yu., Bagaeva, I., Piskunov, V.K., Rud´ko S.V., Perminov, V.A. and Manikin, A.G. 2012. New sedimentological, bio-, and magnetostratigraphic data on the Jurassic–Cretaceous boundary interval of Eastern Crimea/Feodosiya). Stratigraphy and Geological Correlation 20, 261–294.

Grandesso, P. 1977. Gli strati a Precalpionellidi del Titoniano e I loro raporti con il Rosso Ammonitico Veneto. Memoire di Scienze Geologiche, 32, 1–15.

Gröcke, D.R., Price, G.D., Ruffell, A.H., Mutterlose, J. and Baraboshkin, E. 2003. Isotopic evidence for Late Jurassic–Early Cretaceous climate change. Palaeogeography, Palaeoclimatology, Palaeoecology, 202, 97–118.

Haas, J. 1995. Magyarország földtana (Geology of Hungary), 119 p. Eötvös Kiadó; Budapest.

Haas, J. and Péró, C. 2004. Mesozoic evolution of the Tisza Mega-unit. International Journal of Earth Sciences, 93, 297–313.

Haq, B. U. 2014. Cretaceous eustasy revisited. Global and Planetary Change, 113, 44–58.

Haško, J. 1978. The Orava Unit – new unit of the Klippen Belt, Western Carpathians. Geologické práce, Správy 70, 115–121 [In Slovak].

Hay, W.W., Migdisov, A., Balukhovsky, A.N., Wold, Ch.N., Flögel, S. and Söding, E. 2006. Evaporites and the salinity of the ocean during the Phanerozoic: Implications for climate, ocean circulation and life. Palaeogeography, Palaeoclimatology, Palaeoecology 240, 3–46.

Hoedemaeker, P.J. and Leereveld, H. 1995. Biostratig-

raphy and sequence stratigraphy of the Berriasian–lowest Aptian (Lower Cretaceous) of the Rio Argos succession, Caravaca, SE Spain. Cretaceous Research, 16, 195–230.

Hoedemaeker, J.P., Janssen, N. M. M., Casellato, C. E., Gardin, S., Reháková, D. and Jamrichová, M. 2016. Jurassic–Cretaceous boundary in the Río Argos succession (Caravaca, SE Spain). Integrated biostratigraphy of section Z along the Barranco de Tollo. Revue de Paleobiologie, 35, 111–247.

Houša, V., Krs, M., Krsová, M. and Pruner, P. 1996. Magnetostratigraphic and micro-paleontological investigations along the Jurassic–Cretaceous boundary strata, Brodno near Žilina (Western Slovakia). Geologica Carpathica, 47, 135–151.

Houša, V., Krs, M., Krsová, M., Man, O., Pruner, P. and Venhodová, D. 1999. High-resolution magnetostratigraphy and micropaleontology across the J/K boundary strata at Brodno near Žilina, western Slovakia: summary of results. Cretaceous Research, 20, 699–717.

Houša, V., Krs, M., Man, O., Pruner, P., Venhodová, D., Cecca, F., Nardi, G. and Piscitello, M. 2004. Combined magnetostratigraphic, palaeomagnetic and calpionellid investigations across the Jurassic/Cretaceous boundary strata in the Bosso Valley, Umbria, central Italy. Cretaceous Research, 25, 771–785.

Houša, V., Pruner, P., Zakharov, V.A., Košťák, M., Chadima, M., Rogov, M.A., Šlechta, S. and Mazuch, M. 2007. Boreal – Tethyan correlation of the Jurassic / Cretaceous boundary interval by palaeoenvironments and palaeoceanography changes across the J/K boundary magneto-and biostratigraphy. Stratigraphy and Geological Geological Correlation, 15, 297–309.

Hori, N. 1999. Latest Jurassic radiolarians from the northeastern part of the Torinoko Block, Yamizo Mountains, central Japan. Science Reports of the Institute of Geoscience, University of Tsukuba, Section B (Geological Sciences), 20, 47–114.

Koeberl, C., Armstrong, R. A. and Reynold, W.U. 1997. Morokweng, South Africa: A large impact structure of Jurassic–Cretaceous boundary age. Geology, 25, 731–734.

Kowal-Kasprzyk, J. and Reháková, D. 2019. A morphometric analysis of loricae of the genus *Calpionella* and its significance for the Jurassic/Cretaceous boundary interpretation. Newsletters on Stratigraphy, 52, 33–54.

Lakova, I. and Petrova, S. 2013. Towards a standard Tithonian to Valanginian calpionellid zonation of the Tethyan Realm. Acta Geologica Polonica, 63, 201–221.

Lakova, I., Stoykova, K. and Ivanova, D. 1999. Calpionellid, nannofossils and calcareous dinocyst bioevents and integrated biochronology of the Tithonian to Valanginian in the West Balkan Mountains, Bulgaria. Geologica Carpathica, 50, 151–168.

Lodowski, D.G., Pszczółkowski, A., Szives, O., Főzy, I. and Grabowski, J. 2022. Jurassic – Cretaceous transition in the Transdanubian Range (Hungary): integrated stratigraphy and paleomagnetic study of the Hárskút and Lókút sections. Newsletters on Stratigraphy, 55, 99–135.

López-Martínez, R., Barragán, R., Reháková, D. and Cobiella-Reguera, J.L. 2013. Calpionellid distribution and microfacies across the Jurassic/Cretaceous boundary in western Cuba (Sierra de los Óreganos). Geologica Carpathica, 64, 195–208.

López-Martínez, R., Barragán, R. and Reháková, D. 2015. Calpionellid biostratigraphy across the Jurassic/Cretaceous boundary in San José de Iturbide, Nuevo León, north-eastern Mexico. Geological Quarterly, 59, 581–592.

Lukeneder, A., Halásová, E., Kroh, A., Mayrhofer, S., Pruner, P., Reháková, D., Schnabl, P., Spovieri, M. and Wagreich M. 2010. High resolution stratigraphy of the Jurassic–Cretaceous boundary interval in the Gresten Klippenbelt (Austria). Geologica Carpathica, 61, 365–381.

Lukeneder, A. 2011. The Biancone and Rosso Ammonitico facies of the northern Trento Plateau (Dolomites, Southern Alps, Italy). Annalen des naturhistorischen Museums in Wien, Serie A, 113, 9–33.

Mahoney, J.J., Duncan, R.A., Tejada, M.L.G., Sager, W.W. and Bralower, T.J. 2005. Jurassic–Cretaceous boundary age and mid-ocean-ridge type mantle source for Shatsky Ridge. Geology, 33, 185–188.

Márton, E. 1986. The problems of correlation between magnetozones and calpionellid zones in Late Jurassic–Early Cretaceous sections. Acta Geologica Hungarica, 29, 125–131.

Matsuoka, A. 1995. Jurassic and Lower Cretaceous radiolarian zonation in Japan and in the western Pacific. The Island Arc, 4, 140–153.

Matsuoka, A. 1998. Faunal composition of earliest Cretaceous (Berriasian) radiolaria from the Mariana Trench in the western Pacific. News of Osaka Micropaleontologists, special volume, 11, 165–187.

Matsuoka, A., Xin, L., Chiari, M. and Bertinelli, A. 2020. Radiolarian occurrences from the Jurassic–Cretaceous transition beds in the Maiolica Formation of the Bosso Valley section, Northern Apennines, central Italy. Cretaceous Research, 114, 104500.

Michalík, J. 1994. Notes on the paleogeography and paleotectonics of the Western Carpathian area during the Mesozoic. Mitteilungen der Österreichischen Geologischen Gesellschaft, 86, 101–110.

Michalík, J. 2007. Rock record and microfacies indicators of the Jurassic/Lower Cretaceous pull-apart development of the Zliechov Basin, central Western Carpathians. Geologica Carpathica, 58, 443–453.

Michalík, J., Reháková, D. and Peterčáková M. 1990. To the stratigraphy of Jurassic–Cretaceous boundary beds in the Kysuca sequence of the West Carpath-

ian Klippen Belt, Brodno section near Žilina. Zemní Plyn a Nafta, 9b, 57–71.

Michalík, J., Reháková, D., Hladíková, J. and Lintnerová, O. 1995. Lithological and biological indicators of orbital changes in Tithonian and Lower Cretaceous sequence, Western Carpathians, Slovakia. Geologica Carpathica, 46, 161–174.

Michalík, J., Lintnerová, O., Bak, M., Skupien, P., Soták, J., Halásová, E. and Boorová, D. 2008. Sedimentary, biological and isotopic record of Early Aptian paleoclimatic event in the Pieniny Klippen Belt, Slovak Western Carpathians. Cretaceous Research, 29, 871–892.

Michalík, J., Reháková, D., Halásová, E. and Lintnerová O. 2009. The Brodno section – a potential regional stratotype of the Jurassic/ Cretaceous boundary (Western Carpathians). Geologica Carpathica, 60, 213–232.

Michalík, J. and Reháková, D. 2011. Possible markers of the Jurassic/Cretaceous boundary in the Mediterranean Tethys: A review and state of art. Geoscience Frontiers, 2, 475–490.

Michalík, J., Reháková, D., Grabowski, J., Lintnerová, O., Svobodová, A., Schlögl, J., Sobień, K. and Schnabl, P. 2016. Stratigraphy, plankton communities, and magnetic proxies at the Jurassic/Cretaceous boundary in the Pieniny Klippen Belt (Western Carpathians, Slovakia). Geologica Carpathica, 67, 303–328.

Michalík, J., Grabowski, J., Lintnerová, O., Reháková, D., Kdýr, Š. and Schnabl, P. 2021. Jurassic – Cretaceous boundary record in the Carpathian sedimentary sequences. Cretaceous Research, 118, 1–19.

Missoni, S. and Gawlick, H.-J. 2011. Evidence for Jurassic subduction from the Northern Calcareous Alps (Berchtesgaden; Austroalpine, Germany). International Journal of Earth Sciences, 100, 1605–1631.

Von Mojsisovics, E. 1867. Umgebung von Rogoźnik und Czorsztyn. Nördliche Tatra-Thäler. Verhandlungen der k.k. Geologischen Reichsanstalt, 10, 212–214.

Nowak, W. 1976. *Parastomiosphaera malmica* (Borza) z Karpat polskich i jej znaczenie dla korelacji utworów dolnego tytonu. Rocznik Polskiego Towarzystwa Geologicznego, 46, 89–134.

O'Dogherty, L., Carter, E.S., Dumitrica, P., Goričan, Š., De Wever, P., Bandini, A.N., Baumgartner, P.O. and Matsuoka, A. 2009. Catalogue of Mesozoic radiolarian genera. Part 2: Jurassic– Cretaceous. Geodiversitas, 31, 271–356.

O'Dogherty, L., Goričan, Š., Baumgartner, P.O., Matsuoka, A. and Chiari, M. 2018. Catalogue of Tithonian–Berriasian radiolarians. JK2018 International Symposium, Abstract Volume, Museum d'Histoire naturelle de Genève, 64–65.

Ogg, J.G. and Lowrie, W. 1986. Magnetostratigraphy of the Jurassic–Cretaceous boundary. Geology, 14, 547–550.

Ogg, J.G., Hasenyager, R.W., Wimbledon, W.A., Channell, J.E.T. and Bralower, T.J. 1991. Magnetostratigraphy of the Jurassic–Cretaceous boundary interval – Tethyan and English faunal realms. Cretaceous Research, 12, 455–482.

Pop, G. 1974. Les zones des Calpionelles Tithonique–Valanginiens du silon de Resita (Carpates meridionales). Revue Roumaine de Géologie Géophysique et Géographie: Série de géologie, 18, 109–125.

Pop, G. 1994. Calpionellid evolutive events and their use in biostratigraphy. Romanian Journal of Stratigraphy, 76, 7–24.

Price, G.D., Valdes, P.J. and Selwood, B.W. 1998. A comparison of GCM simulated Cretaceous "greenhouse" and "icehouse" climate: implication for the sedimentary record. Palaeogeography, Palaeoclimatology, Palaeoecology, 142, 123–138.

Price, G.D., Ruffell, A.H., Jones, C.E., Kalin, R.M. and Mutterlose, J. 2000. Isotopic evidence for temperature variation during the Early Cretaceous (late Ryazanian-mid-Hauterivian). Journal of the Geological Society, 157, 335–343.

Price, G.D., Főzy, I. and Palfy, J. 2016. Carbon cycle history through the Jurassic–Cretaceous boundary: a new global $\delta^{13}C$ stack. Palaeogeography, Palaeoclimatology, Palaeoecology, 451, 46–61.

Pruner, P., Houša, V., Oloriz, F., Košťák, M., Man, O., Schnabl, P., Venhodová, D., Tavera J.M. and Mazuch, M. 2010. High-resolution magnetostratigraphy and biostratigraphic zonation of the Jurassic/Cretaceous boundary strata in the Puerto Escano section (southern Spain). Cretaceous Research, 31, 192–206.

Pszczółkowski, A., Delgado, D.G. and Gil, S.G. 2005. Calpionellid and nannoconid stratigraphy and microfacies of limestones at the Tithonian–Berriasian boundary in the Sierra del Infierno (Western Cuba). Annales Societatis Geologorum Poloniae, 75, 1–16.

Reháková, D. 2000. Evolution and distribution of the Late Jurassic and Early Cretaceous calcareous dinoflagellates recorded in the Western Carpathians pelagic carbonate facies. Mineralia Slovaca, 32, 79–88.

Reháková, D. and Michalík, J. 1992. Correlation of Jurassic–Cretaceous boundary beds in West Carpathian profiles. Földtani Közlöny, 122, 51–66.

Reháková, D. and Michalík, J. 1994. Abundance and distribution of late Jurassic–Early Cretaceous microplankton in Western Carpathians. Geobios, 27, 135–156.

Reháková, D. and Michalík, J. 1997. Evolution and distribution of calpionellids – the most characteristic constituents of Lower Cretaceous Tethyan microplankton. Cretaceous Research, 18, 493–504.

Reháková, D., Halásová, E. and Lukeneder, A. 2009. The Jurassic–Cretaceous boundary in the Gresten Klippenbelt (Nutzhof, Lower Austria): Implications for micro- and nannofacies analysis. Annalen des Naturhistorischen Museums in Wien, 110A, 345–381.

Remane, J. 1971. Les calpionelles, protozoaires planc-

toniques des mers mésogéennes de l'Epoque Secondaire. Annales Guébhard, 47, 1–25.

Remane, J. 1986. Calpionellids and the Jurassic–Cretaceous boundary. Acta Geologica Hungarica, 29, 15–26.

Remane, J., Borza, K., Nagy, I., Bakalova-Ivanova, D., Knauer, J., Pop, G. and Tardi-Filácz, E. 1986. Agreement on the subdivision of the standard calpionellid zones defined at the 2nd Planktonic Conference Roma 1970. Acta Geologica Hungarica, 29, 5–14.

Samuel, O., Gašparíková, V. and Ondrejíčková, A. 1988. Microbiostratigraphic correlation of the Lower and Middle Cretaceous sequences of the western part of the Klippen Belt, 1–60. MS thesis, Geological Institute of Dionýz Štúr, Bratislava.

Satolli, S., Turtu, A., and Donatelli, U. 2015. Magnetostratigraphy of the Salto del Cieco section (Northern Appenines, Italy) from the Pliensbachian to Jurassic/Cretaceous boundary. Newsletters on Stratigraphy, 48, 153–177.

Scheibner, E. 1961. Mesozoic of the Pieniny Klippen Belt. In: Excursion guide of 12th Congress of Czecho-Slovakian Mineralogical and Geological Association, Ser. B – Mesozoic. 71–79. [In Slovak]

Scheibner, E. 1962. Some new knowledge from Klippen Belt in Slovakia. Geologické Práce, Správy 62, 233–238.

Scheibner, E. 1967. Carpathian Klippen Belt. In: Buday, T. et al. (Eds), Regional geology of ČSSR, Part II: the West Carpathians, Academia Praha, 7–105.

Scheibner, E. and Scheibnerová, V. 1969. Type profile of the Kysuca Sequence (unit), (Pieniny Klippen Belt, Carpathians). Věstník Ústředního ústavu geologického, 44, 339–349.

Schlager, W. 2005. Carbonate sedimentology and sequence stratigraphy. SEPM Concepts in Sedimentology and Paleontology, 8, 1–200.

Schnabl P., Pruner, P. and Wimbledon, W.A.P. 2015. A review of magnetostratigraphic results from the Tithonian – Berriasian of Nordvik (Siberia) and possible biostratigraphic constraints. Geologica Carpathica, 66, 489–498.

Schnyder, J., Gorin, G., Soussi, M., Baudin, F. and Deconinck, J.F. 2005. Enregistredment de la variation climatique au passage Jurassique/Crétacé sur la marge sud de la Téthys: mineralogie des argiles et palynofacies de la coupe du Jebel meloussi (Tunisie Centrale, Formation Sidi Kralif). Bulletin de la Société géologique de France, 176, 2, 171–182.

Schnyder, J., Ruffel. A., Deconinck, J.-F. and Baudin, F. 2006. Conjuctive use of spectral gamma-ray logs and clay mineralogy in defining late Jurassic–early Cretaceous paleoclimate change (Dorset, U.K.) Palaeogeography, Palaeoclimatology, Palaeoecology, 229, 303–320.

Stampfli, G.M and Hochard, C. 2009. Plate tectonics of the Alpine realm. In: Murphy, J.B., Keppie, J.D. and Hynes, A.J. (Eds), Ancient orogens and modern analogues. Geological Society London, Special Publications, 327, 89–111.

Steiger, T. 1992. Systematik, Stratigraphie und Palökologie der Radiolarien des Oberjura-Unterkreide-Grenzbereiches im Osterhorn-Tirolikum (Nördliche Kalkalpen, Salzburg und Bayern). Zitteliana, 19, 3–188.

Svobodová, A. and Košťák, M. 2016. Calcareous nannofossils of the Jurassic–Cretaceous boundary strata in the Puerto Escaño section (southern Spain) – biostratigraphy and palaeoecology. Geologica Carpathica, 67, 223–238.

Svobodová, A., Švábenická, L., Reháková, D., Svobodová, M., Skupien, P., Elbra, T. and Schnabl, P. 2019. The Jurassic/Cretaceous and high resolution biostratigraphy of the pelagic sequences of the Kurovice section (Outer Western Carpathians, the northern Tethyan margin). Geologica Carpathica 70, 153–182.

Szederkényi, T., Kovács, S., Haas, J. and Nagymarosy, A. 2013. Geology and History of Evolution of the ALCAPA Mega-Unit. In: Hass, J. (Ed.), Geology of Hungary. 1–103. Springer; Heidelberg, New York, Dordrecht, London.

Szives, O. and Főzy, I. 2022. Towards the ammonite zonation of the Jurassic/Cretaceous transition: new data from ammonitico rosso/biancone sections of the Transdanubian Range (Hungary). Newsletters on Stratigraphy, 55, 385–426.

Szives, O., Lodowski, D.G., Grabowski, J., Vörös, A., Szinger, B., Price, G. and Főzy, I. 2022. The Jurassic/Cretaceous transition in the Bakony Basin. In: Főzy, I. (Ed.), Late Jurassic–Early Cretaceous fauna, biostratigraphy and paleotectonic evolution in the Bakony Mountains (Transdanubian Range, Hungary). Institute of Geosciences, University of Szeged, GeoLitera Publishing House.

Tari, G. 1994. Alpine tectonics of the Pannonian Basin (Ph. D. thesis), 510 p. Rice University; Houston, Texas.

Tremolada, F., Bornemann, A., Bralower, T., Koeberl, C. and van de Schootbrugge, B. 2006. Paleoceanographic changes across the Jurassic/Cretaceous Boundary: the calcareous phytoplankton response. Earth and Planetary Science Letters, 241, 361–371.

Vašíček, Z., Reháková, D., Michalík, J., Peterčáková, M. and Halásová, E. 1992. Ammonites, aptychi, nanno-and microplankton from the Lower Cretaceous Pieniny Formation in the "Kysuca Gate" near Žilina (Western Carpathian Klippen Belt, Kysuca Unit). Západné Karpaty, Séria Paleontológia, 16, 43–57.

Vígh, G. 1984. Die biostratigraphische Auswertung einiger Ammoniten-Faunen aus dem Tithon des Bakonygebirges sowie aus dem Tithon–Berrias des Gerecsegebirges. Annals of the Hungarian Geological Institute, 67, 210 p.

Weissert, H. and Channell, J.E.T. 1989. Tethyan carbonate carbon isotope stratigraphy across the Juras-

sic–Cretaceous boundary: an indicator of decelerated global carbon cycling? Paleoceanography, 4, 483–494.

Weissert, H. and Lini, A. 1991. Ice Age interludes during the time of Cretaceous Greenhouse Climate? In: Müller, D.W., McKenzie, J.A. and Weissert, H. (Eds), Controversies in modern geology, 173–191. Academic Press.

Weissert, H. and Mohr, H. 1996. Late Jurassic climate and its impact on carbon cycling. Palaeogeography, Palaeoclimatology, Palaeoecology, 122, 27–43.

Wilson, J.L. 1975. Carbonate facies in geologic history, 471 pp. Springer; Berlin.

Wimbledon, W.A.P., Reháková, D., Pszczółkowski, A. Casellato, C.E., Halásová, E., Frau, C., Bulot, L.G., Grabowski, J., Sobień, K., Pruner, P., Schnabl, P. and Čížková, K. 2013. An account of the bio- and magnetostratigraphy of the upper Tithonian–lower Berriasian interval at Le Chouet, Drôme (SE France). Geologica Carpathica, 64, 437–400.

Wimbledon, W.A.P., Reháková, D., Svobodová, A., Elbra, T., Schnabl, P., Pruner, P., Šifnerová, K., Kdýr, Š., Dzyuba, O., Schnyder, J., Galbrun, B., Košťák, M., Vaňková, L., Copestake, P., Hunt, C.O., Riccardi, A., Poulton, T.P., Bulot, L.G., Frau, C. and de Lena, L. 2020. The proposal of a GSSP for the Berriasian Stage (Cretaceous System): part 1. Volumina Jurassica, 18, 53–106.

Young, J.R., Bown, P.R. and Lees, J.A. 2013. Nannotax3 website (Eds), International Nannoplankton Association. February 2018. URL: http://ina.tmsoc.org/Nannotax3

Zakharov, V.A., Bown, P. and Rawson, F. 1996. The Berriasian Stage and the Jurassic–Cretaceous Boundary. Bulletin de l'Institut royal des Sciences naturelles de Belgique, Sciences de la Terre 66, suppl., 7–10.

Zakharov, V.A., Rogov, M.A., Dzyuba, O.S., Žák, K., Košťák, M., Pruner, P., Skupien, P., Chadima, M., Mazuch, M. and Nikitenko, B.L. 2014. Palaeoenvironments and palaeoceanography changes across the Jurassic/Cretaceous boundary in the Arctic realm: case study of the Nordvik section (north Siberia, Russia). Polar Research, 33, 19714.

11TH INTERNATIONAL

CRETACEOUS SYMPOSIUM

Warsaw, Poland, 2022

Organised by:

UNIVERSITY OF WARSAW

WYDZIAŁ GEOLOGII

Co-organised by:

INSTYTUT PALEOBIOLOGII POLSKA AKADEMIA NAUK

ING PAN

UNIWERSYTET JAGIELLOŃSKI W KRAKOWIE

PAŃSTWOWY INSTYTUT GEOLOGICZNY PAŃSTWOWY INSTYTUT BADAWCZY

WGGiOŚ

Gmina Siedliszcze gościnni z natury

Muzeum Nadwiślańskie w Kazimierzu Dolnym Oddział Przyrodniczy

Under the auspices of:

Subcommission on Cretaceous Stratigraphy